COLOR ATLAS OF CLINICAL HEMATOLOGY

COLOR ATLAS OF CLINICAL HEMATOLOGY

Molecular and Cellular Basis of Disease

FIFTH EDITION

A. Victor Hoffbrand
Emeritus Professor of Haematology, University College London
London, UK

Paresh Vyas
Professor of Haematology
Honorary Consultant Haematologist and Group Leader, MRC Molecular Haematology Unit, University of Oxford
Oxford, UK

Elías Campo
Senior Consultant, Haematopathology Unit, Hospital Clinic of Barcelona;
Professor of Anatomical Pathology, University of Barcelona
Barcelona, Spain

Torsten Haferlach
MLL Münchner Leukämielabor GmbH
Munich, Germany

Keith Gomez
Consultant Haematologist
Royal Free Hospital NHS Foundation Trust
London, UK

WILEY Blackwell

This edition first published 2019

Edition History
Churchill-Livingstone (1987); Mosby-Wolfe (1994); Mosby (2000); Mosby Elsevier (2009)

Registered Offices
John Wiley & Sons, Inc., 111 River Street, Hoboken, NJ 07030, USA
John Wiley & Sons Ltd, The Atrium, Southern Gate, Chichester, West Sussex, PO19 8SQ, UK

Editorial Office
9600 Garsington Road, Oxford, OX4 2DQ, UK

For details of our global editorial offices, customer services, and more information about Wiley products visit us at www.wiley.com.

Wiley also publishes its books in a variety of electronic formats and by print-on-demand. Some content that appears in standard print versions of this book may not be available in other formats.

A catalogue record for this book is available from the Library of Congress and the British Library.

9781119057017

Cover images: Courtesy of Victor Hoffbrand, Thomas Wagner, Torsten Haferlach, and Keith Gomez;
background image: Courtesy of Elías Campo
Cover design by Wiley

Set in 10/11pt Adobe Garamond by SPi Global, Pondicherry, India

10 9 8 7 6 5 4 3 2 1

CONTENTS

PREFACE

In the 9 years since the fourth edition of this *Color Atlas of Clinical Hematology* was published, tremendous advances have been made in the understanding of the pathogenesis of blood diseases. This is mainly due to the application of new molecular genetic techniques, including next-generation sequencing, to reveal the variants of DNA that underlie many of these inherited and acquired diseases. The World Health Organization (WHO) has incorporated this new knowledge in the 2016 Revised Classification of the Lymphoid and Myeloid Neoplasms. This Classification has been adopted in Chapters 13–24 of the present fifth edition of the *Atlas*. These cover the clinical and microscopic appearances and the immunologic, cytogenetic, and molecular genetic abnormalities that underlie these diseases. The references to the WHO 2016 Classification are:

- Swerdlow SH, Campo E, Pileri S, et al. The revision of the World Health Organisation classification of lymphoid neoplasms. *Blood* 2016;127:2375–2390.
- Arber DA, Orazi A, Hasserjian R, et al. The 2016 revision to the World Health Organization classification of myeloid neoplasms and acute leukemia. *Blood* 2016;127:2391–2405.
- Swerdlow SH, Campo E, Harris NL, et al., eds. *WHO Classification of Tumours of Haematopoietic and Lymphoid Tissues*, revised 4th edn. International Agency for Research on Cancer, Lyon, 2017.

The first three chapters of the new edition of the *Atlas*, written as previously by Paresh Vyas, are aimed at providing the reader with an understanding of normal cell machinery and of the molecular basis for such processes as DNA and cell replication, RNA species, trafficking and splicing, protein synthesis, transcription factors, growth factor signal transduction, epigenetics, cell differentiation, autophagy, and apoptosis. The subsequent 29 chapters describe and illustrate how these processes are disturbed in the various diseases of the bone marrow, blood, and lymphoid systems. Treatment is not usually described, except in Chapter 29 on thrombosis, but the *Atlas* includes diagrams which show the various points in the biochemical pathways where many of the new targeted therapies act.

Four new authors, all internationally renowned hematologists and pathologists, have updated the various sections of the book. Elías Campo (Barcelona), one of the lead authors of the WHO (2016) Classification, has rewritten the six chapters dealing with the lymphoid neoplasms. Torsten Haferlach (Munich) has added a new section explaining and illustrating the molecular techniques used for the diagnosis of the hematologic neoplasms. He has also collaborated substantially in rewriting the six chapters describing and illustrating the myeloid neoplasms. Keith Gomez (UK) has updated the text and added new illustrations and tables for the four chapters dealing with normal platelets, normal blood coagulation, and the bleeding and thrombotic disorders. Stefano Pileri (Bologna), also a lead author of the WHO 2016 Classification, has updated the chapter on histiocytic diseases. I am grateful to all four of these distinguished colleagues for taking on the task of bringing the chapters so expertly up to date despite their other heavy commitments.

While welcoming these new authors, I wish to express an enormous professional and personal tribute to John Pettit, who co-authored all four of the previous editions of the *Atlas*. John joined me at the Royal Free Hospital in 1975 when the Department of Haematology was in its infancy. We were confronted for the first time in our careers with teaching undergraduate medical students. We collaborated in writing handouts for the students as teaching aids. These were expanded to become a new undergraduate textbook, *Essential Haematology*, first published in 1980 by Blackwell Scientific.

In 1976 John and I set about collecting photographs of interesting clinical and microscopic appearances of blood diseases and assembled these as a new atlas, *Clinical Haematology Illustrated*. This was published in 1987 by Gower Medical Publishing. John returned from London to his native New Zealand in 1977 but we subsequently collaborated by mail and fax. John spent at least a week every year in London so we could work together on new editions of both books.

John was a great teacher as well as first class laboratory and clinical hematologist. His clear style of writing in succinct sentences, combined with his beautiful simple line diagrams and well-chosen clinical and microscope images of the highest quality, has contributed substantially to the success of both books. John retired from authorship of *Essential Haematology* after the fifth edition and of this *Atlas* after the fourth 2009 edition, but his major influence on style and content of both books, as well as the superb images he acquired for them, remain.

John Pettit

We are grateful to our new publishers Wiley Blackwell for their unstinting support and especially to Claire Bonnett and Magenta Styles in encouraging and supporting this pan-European team of authors and to Jennifer Seward in expertly editing all our manuscripts and assembling the book, including artwork, to a standard in which it could be published. We hope the book in its printed and electronic forms can be used as previously as an illustrated encyclopedia of normal blood and bone marrow processes and of blood diseases.

Victor Hoffbrand
London, 2018

CHAPTER

MOLECULAR BIOLOGY OF THE CELL

1

The aim of the first chapter is to provide a primer covering our understanding of the basic molecular and cellular processes of the cell, which inform a scientific understanding of hematologic diseases.

COMPARTMENTALIZATION OF THE CELL

A central evolutionary advance was the compartmentalization of cells, as shown in Fig. 1.1. The cell is bounded by a complex cell membrane that allows regulation of molecules into and out of the cell. Within the cytoplasm a number of different organelles perform key functions. For example, as described later in this chapter, mitochondria are critical for adenosine triphosphate (ATP) generation and heme biosynthesis. Proteins are translated from amino acids and undergo post-translational modification in the Golgi complex and rough endoplasmic reticulum. Depending on the cell type, there are specialized structures within the cytoplasm that allow the cell to perform its specialized role.

THE NUCLEUS

As we focus in on the nucleus, it is clear that it is also bounded by a specialized nuclear envelope and membrane (Fig. 1.2). Entry and exit out of the nucleus is regulated by nuclear pores. Within the nucleus, deoxyribonucleic acid (DNA) is tightly packaged by proteins and the DNA/protein complex is known as chromatin. Chromatin has different appearances under light or electron microscopes. When DNA is tightly packaged (and the genes more likely to be not expressed), it is known as heterochromatin. Under the light/electron microscope it appears darker. When DNA is less tightly packaged it is called euchromatin and is lighter in appearance. The other visible structure within the nucleus, in some cells, is the nucleolus, where ribosomal genes are transcribed and assembly of the ribosome takes place (as discussed later).

The DNA in the nucleus is distributed among 22 pairs of autosomal chromosomes (numbered 1–22, in order of size) and two sex chromosomes (Fig. 1.3A). When cells are in the metaphase phase of the cell cycle, chromosomes condense and can be visualized by a technique called karyotyping. Chromosomes are divided into two arms: a short arm, termed

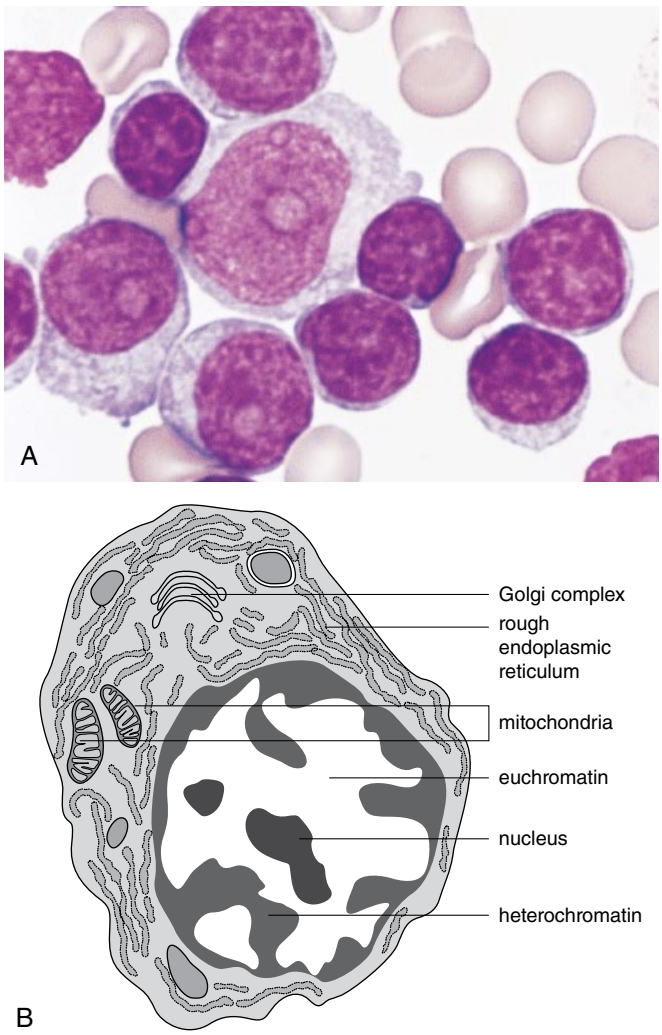

Fig. 1.1. A, Photomicrograph showing the morphology of many cells with prominent nucleoli, in this case, B cells. **B,** A schematic representation of the intracellular composition as visualized by electron microscopy. The nucleus is composed of euchromatin, which is less condensed, paler, and more transcriptionally active, and heterochromatin, which is more condensed, darker, and less transcriptionally active. In cytoplasm subcellular organelles including mitochondria, rough endoplasmic reticulum, and the Golgi complex are shown. The function of these organelles is discussed later. (Courtesy of Professor JV Melo.)

Color Atlas of Clinical Hematology: Molecular and Cellular Basis of Disease, Fifth Edition. A. Victor Hoffbrand, Paresh Vyas, Elías Campo, Torsten Haferlach, and Keith Gomez

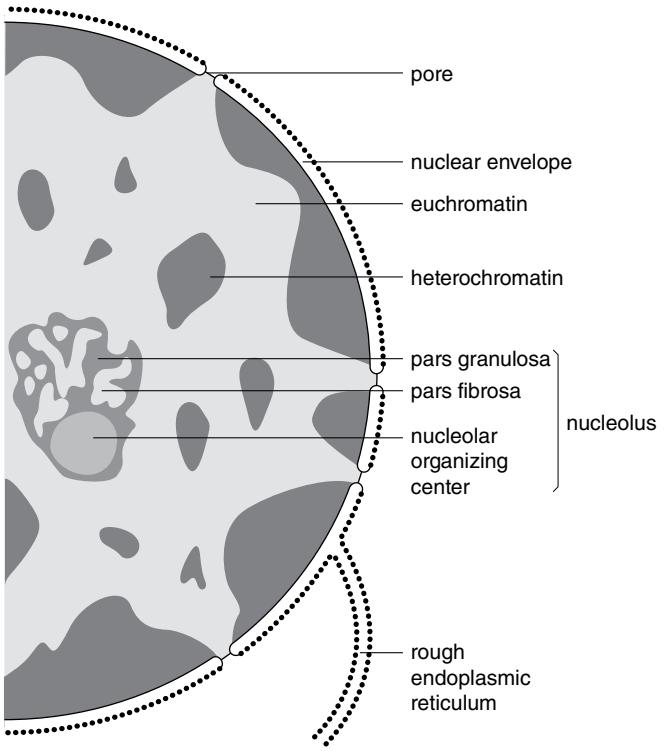

Fig. 1.2. Schematic representation of a portion of the nucleus. The nucleus is highly compartmentalized, containing specialized structures. The nucleolus is composed of a pars granulosa, a pars fibrosa, and a nucleolar organizing center and makes transfer RNA. The nucleus is bounded by a nuclear envelope that is lined by rough endoplasmic reticulum. There is controlled entry and exit into the nucleus via nuclear pores.

p, and a longer arm, q. The region where the chromosomes join is termed the centromere. Chromosomes are further subdivided into light and dark bands (depending on how they stain with the Giemsa dye) (Fig. 1.3B). When cells are not in metaphase, chromosomes are more diffusely spread through the nucleus. Most current evidence suggests that the chromosomes occupy discrete territories (chromosomal territories) within a nucleus (Fig. 1.3C). These territories need not be contiguous and can be shared with other chromosomes. However, there are still many aspects of how chromosomes are organized that remain unclear. For example, what constrains chromosomes to territories and how do territories affect gene regulation? Recent work suggests that within chromosomal territories chromatin exists in topologically associated domains (TADs) and that actively expressed genes along the chromosome and possibly even from different chromosomes may congregate in specialized structures where RNA is made from (transcribed) from genes. This process is called transcription and the specialized structures are known as transcription factories (see later).

The sequencing of the human genome was a landmark in biology. It allowed all the human genes arrayed along the chromosomes to be catalogued (Table 1.1). Genes are divided into protein-coding genes (of which there are ~21 000), genes that encode different types of RNA (e.g. ribosomal RNA, micro-RNAs, small nuclear RNA), and RNA moieties that are not translated into a functional protein or RNA (pseudogenes). The genome also dedicates sequence to other RNA species that do not make protein but that regulate either transcription or the production of protein from RNA (a process known as translation). These RNA sequences include micro-RNAs, long and

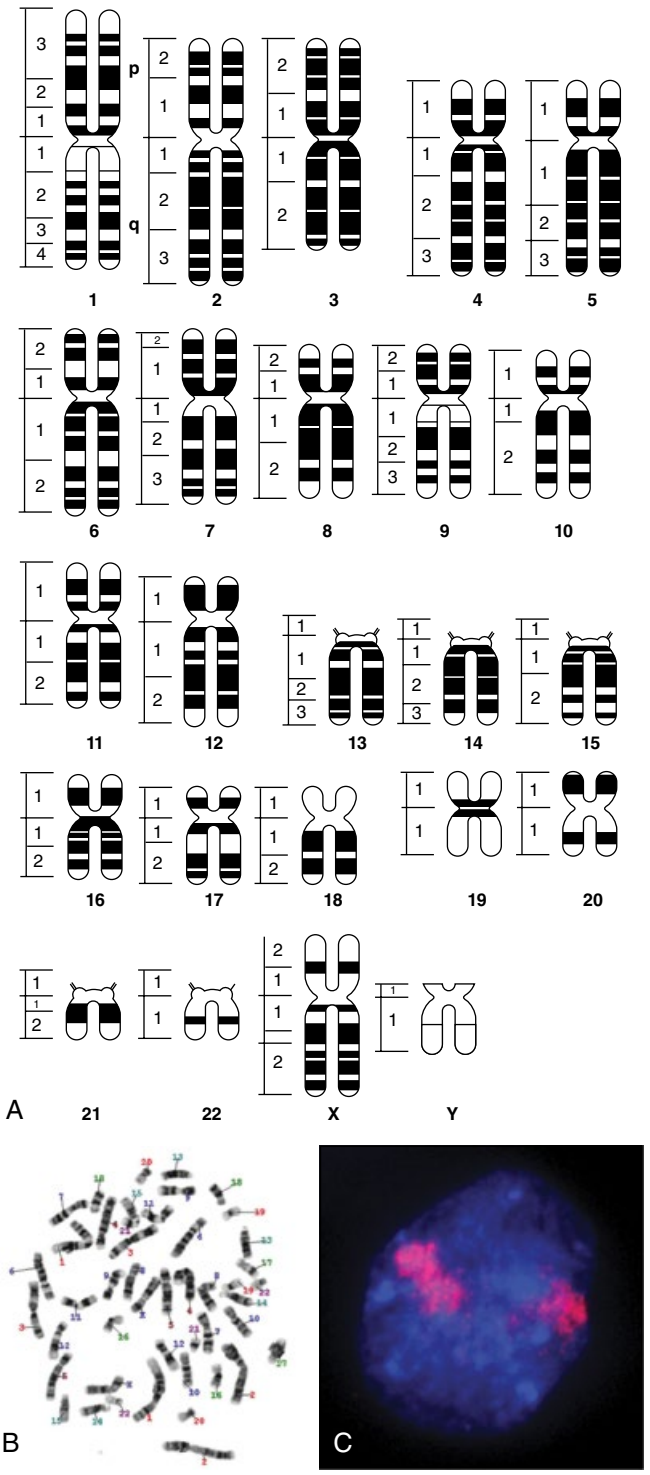

Fig. 1.3. A, DNA in the human nucleus is organized into 46 chromosomes. There are two copies of chromosomes 1–22 with two sex chromosomes (XX or XY). Each chromosome is divided into a short arm (p) and a long arm (q) and then subdivided into major numeric subsections. For example, the short arm of chromosome 1 (1p) has three subsections and the long arm (1q) has four subsections. **B,** The gross subdivision of chromosome can be visualized by Giemsa staining of chromosomes that have been subject to brief proteolytic cleavage. (B, Courtesy of Professor H Lodish.) **C,** Within an interphase nucleus chromosomes occupy discrete territories. The figure shows the territory occupied by chromosome 11 (red color) in a primary erythroblast. (C, Courtesy of Jo Green and Dr. Veronica Buckle.)

TABLE 1.1. ALL THE GENES AND OPEN READING FRAMES IN THE HUMAN GENOME HAVE BEEN CHARACTERIZED FROM THE SEQUENCING OF THE HUMAN GENOME. THIS TABLE SHOWS THE SIZE OF EACH CHROMOSOME (IN MEGABASES) AND NUMBER OF GENES AND PSEUDOGENES ON EACH CHROMOSOME.

Chromosome number	Size (Mb)	Gene	Pseudogene
1	248.96	5,078	1,372
2	242.19	3,862	1,166
3	198.3	2,971	887
4	190.22	2,441	799
5	181.54	2,578	766
6	170.81	3,000	876
7	159.35	2,774	896
8	145.14	2,152	661
9	138.4	2,262	702
10	133.8	2,174	631
11	135.09	2,920	835
12	133.28	2,521	680
13	114.36	1,381	477
14	107.04	2,055	583
15	101.99	1,814	555
16	90.34	1,920	451
17	83.26	2,432	541
18	80.37	988	295
19	58.62	2,481	514
20	64.44	1,349	329
21	46.71	756	202
22	50.82	1,172	348
X	156.04	2,158	859
Y	57.23	577	395
MT	0.016569	37	–

short noncoding RNAs. There are also sequences dedicated to regulating transcription of individual genes or banks of genes; these are called promoters and enhancers. This provides a primary description of our genetic makeup. The characterization of the human genome is still being refined as we understand more about how genes are organized and how transcriptional expression and protein translation is controlled.

Genes themselves are composed of DNA, which is made up of four nucleotides. Each nucleotide consists of a phosphate group linked by a phosphoester bond to a pentose sugar molecule (ribose) that lacks a hydroxyl group (thus it is deoxyribose), which is then attached to one of four heterocyclic carbon- and nitrogen-containing organic rings: adenine (A), cytosine (C), guanine (G) and thymidine (T). C and T are known as pyrimidines and A and G as purines. These are then linked together into polynucleotides via phosphoester bonds. As James Watson and Francis Crick correctly proposed, these are organized into two associated antiparallel polynucleotide strands that have a 5′ to 3′ direction and form a double helix. The strands are held in register by base-pairing between the two strands such that each A is paired with a T via two hydrogen bonds and each C with a G via three hydrogen bonds. Hydrophobic and van der Waals interactions combine with the thousands of hydrogen bonds to give the double helix great stability. In the common "B" form, the helix is right handed and makes a complete turn every 3.4 nm (about 10 base pairs) (Fig. 1.4A,B). The space between the strands creates a major and minor groove. In low humidity, DNA can adopt a more compact form with 11 base pairs per helical turn ("A" form) (Fig. 1.4C). Finally, short stretches of DNA composed of alternate purines and pyrimidines can form an alternate stacked Z structure.

GENE TRANSCRIPTION AND MESSENGER RNA TRANSLATION: THE PRODUCTION AND JOURNEY OF mRNA

A copy of the DNA of genes is transcribed into RNA by transcription in the nucleus. RNA is processed and transported into the cytoplasm. RNA corresponding to protein genes is then translated in the cytoplasm. Not surprisingly, these processes are very complex, affording opportunities for the cell to exquisitely regulate the complement of proteins made but also vulnerable to errors that lead to disease.

Genes are transcribed by one of three different RNA polymerases (RNA Pol I, II, and III). RNA Pol II transcribes most protein-coding genes. The remaining genes are transcribed by RNA Pol I and III. These include genes encoding ribosomal RNAs (makes ribosomes, see later), small nuclear RNAs (involved in processing RNA in a process called splicing, see later), and some transfer RNAs (involved in protein translation, see later). Pol I- and Pol II-transcribed genes will not be discussed in detail further in this book. However, it is important to remember that in a typical rapidly growing mammalian cell, ~80% of total RNA is ribosomal RNA and ~15% is transfer RNA.

When RNA is transcribed, a gene is said to be "expressed." Transcription of each gene begins at the 5′ end of the gene at its transcriptional start site (TSS) (Fig. 1.5). For any one gene the TSSs can either be single or multiple over several neighboring nucleotides. The DNA sequence 5′ of the gene helps to regulate transcription and is known as the promoter. This sequence works with other sequences (called regulatory sequences or *cis*-elements, see later) to provide finely tuned control over the amount of mRNA produced. In Chapter 9 the regulatory sequences involved in globin gene expression are described.

The body of the gene is segmented into exons separated by intervening sequences (introns). The exonic sequence is divided into protein-coding and noncoding sequences. RNA Pol II makes a RNA copy of the whole of the gene (primary transcript). This RNA species is then processed within the nucleus. As the nascent elongating primary transcript is produced a 5′ 7-methylguanine cap is added to the 5′ end to protect the RNA from enzymatic degradation. In addition, as nascent RNA transcript (heterogeneous RNA [hnRNA]) emerges from the RNA Pol II, it is sheathed in a large set of nuclear proteins in structures called heterogeneous ribonuclear particles (hnRNPs). hnRNP-associated proteins are important for transport of the RNA species and probably aid in the processing of RNA. Once the primary transcript is made, the 3′ end of the transcript is recognized by a protein complex that includes an enzyme called an endonuclease that cleaves the RNA transcript to produce a 3′

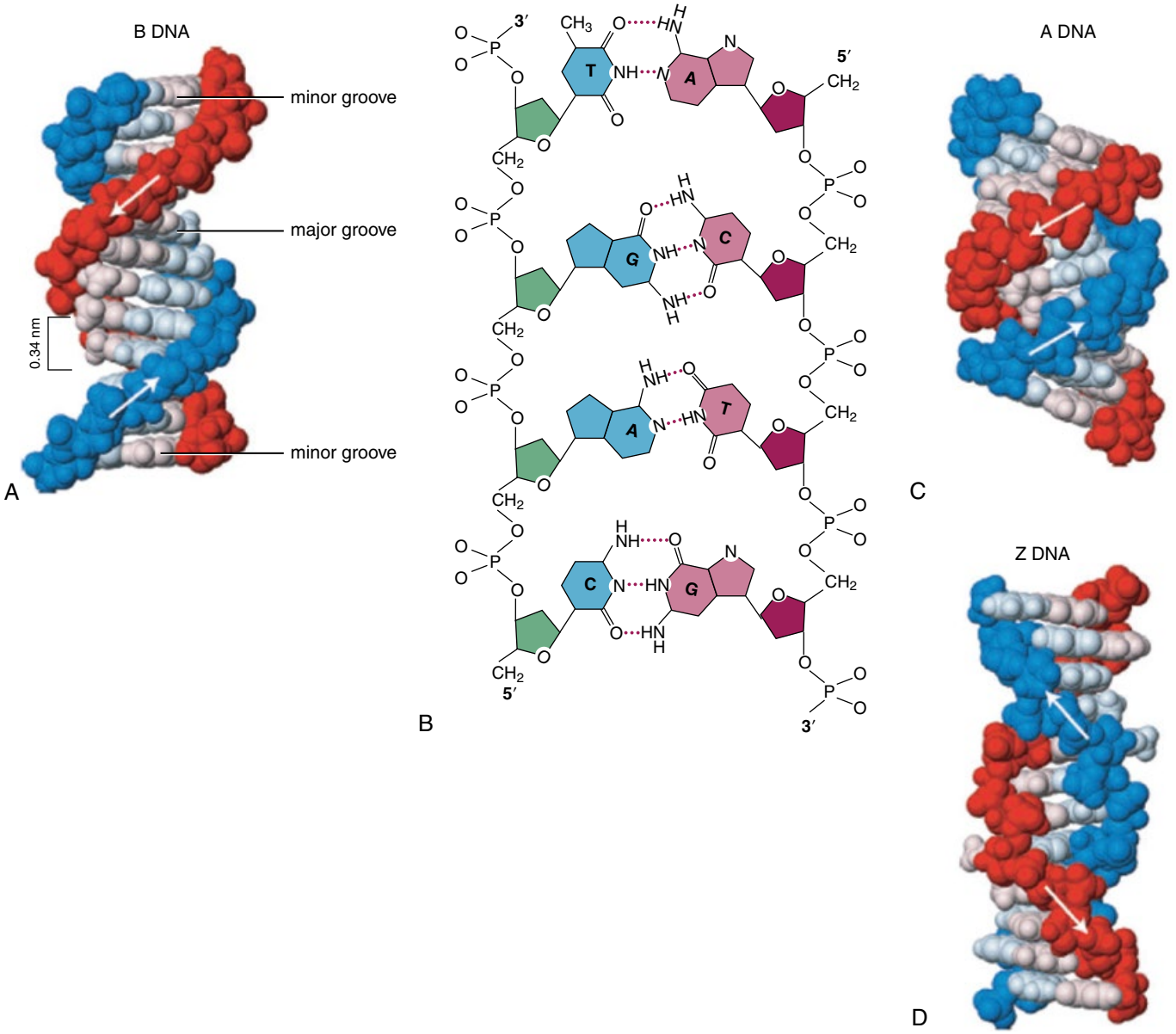

Fig. 1.4. Models of various structures adopted by DNA. **A,** Space-filling model of the "B" form of DNA. This is the common form of DNA, with a helical turn every 10 base pairs. The major and minor grooves are visible. **B,** Stick model shows that DNA is composed of a sugar phosphate backbone with the bases ("A," "C," "G," and "T") pointing inward (blue and light brown). **C,** More compact "A" form of DNA with 11 bases pairs per helical turn. **D,** "Z" form of DNA is a left-handed helix. (Courtesy of Professor H Lodish.)

end of the RNA. This then allows the enzyme polyadenylate polymerase to attach a homo-polymeric string of A residues to the 3′ end of the transcript called the poly-A tail. Increasing recent evidence suggests that the processes of transcription initiation, elongation by RNA Pol II, and 3′ end processing may be co-regulated.

The introns are then spliced out to form the mature mRNA species (a simplified version of this process is presented in Fig. 1.6). Splicing is an elaborate process that involves a large number of steps catalyzed by a splicing complex (or spliceosome), which contains small nuclear RNAs (snRNAs) and proteins, and that produces small nuclear ribonuclear particles (snRNPs). It is estimated that over 100 proteins are involved in splicing. At first approximation, this process is probably as complex as regulation of transcriptional initiation and translation. One reason why a cell invests this degree of effort into splicing is that it allows a cell to generate multiple different mRNA species from a single gene, contributing to the biological complexity that an organism can achieve from a limited gene set. However, the genes encoding proteins controlling splicing can acquire mutations and the mutant proteins may cause aberrant splicing, leading to hematologic diseases. One important part of splicing is that the two nucleotides that lie in the intron and mark the boundary of an exon–intron are almost always invariant (Fig. 1.6). Thus, the 5′ end of the intron is usually marked by the dinucleotide "GU" whereas the 3′ end has "AG."

Like hnRNA, mRNA is wrapped in chaperone proteins to form mRNPs (messenger ribonuclear particles) that are exported from the nucleus through a water-impermeable phospholipid bilayer, the nuclear envelope that is studded with proteins and pores (Figs. 1.7 and 1.8). The nuclear pore complex (NPC) is a large structure (~125 million Da), about 30 times the size of the ribosome. It is made of multiple copies of a large number (~100)

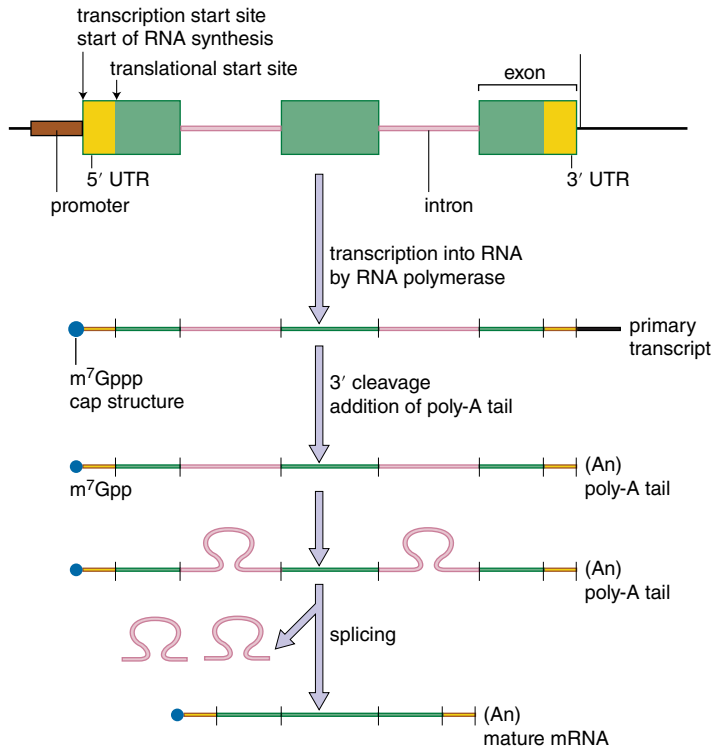

Fig. 1.5. Most genes encoding proteins are first transcribed into mature messenger RNA (mRNA) via multiple steps. *Top*, Genes are divided into exons (shown as boxes) separated by introns (shown as pink lines). Preceding the transcribed region is a promoter region (brown box) that helps regulate transcription timing and rate. A transcriptional initiation site marks the beginning of transcription. The beginning and end of the transcribed regions are usually not translated into protein and are known as the 5′ and 3′ untranslated regions (UTRs) (depicted as yellow boxes). Translated areas are shown as green boxes. The whole gene from the transcriptional start site is transcribed by RNA polymerase to make a primary transcript. This has a specialized cap structure at its 5′ end to protect the transcript from degradation. The 3′ end of the transcript is then cleaved and a tail of "A" nucleotide residues (known as a poly-A tail, "An") is added at the 3′ end of the transcript (to protect the end from degradation). Then the introns loop out (see later for details) and are spliced out to create the mRNA moiety.

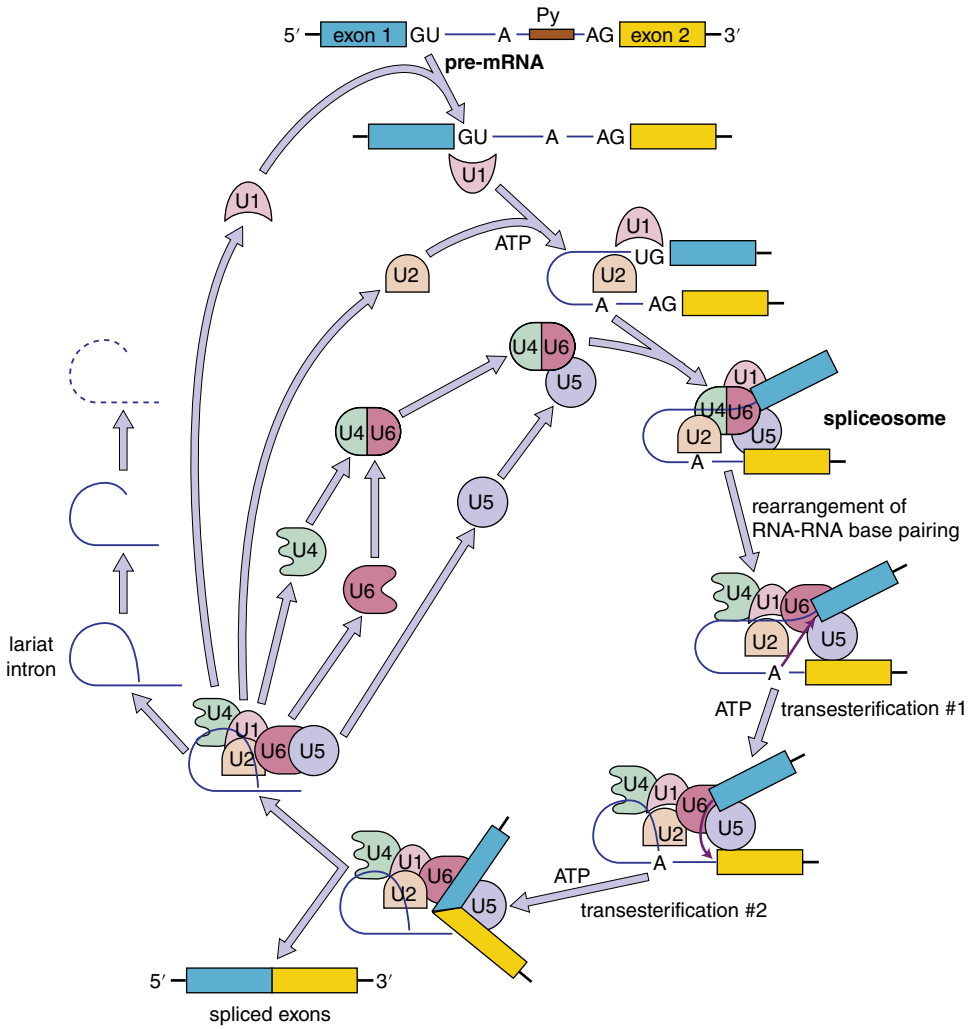

Fig. 1.6. Detail of splicing out of introns coordinated by splicing small nuclear ribonuclear protein particles (snRNPs) U1, U2, and U4–U6. U1 and U2 snRNPs associate with unspliced transcript in an ordered sequence at specific nucleotides ("GU") at the 5′ intron–exon boundary and a pyrimidine tract (Py) near an "A" nucleotide known as the branch point. U4–U6 then assemble, catalyzing an ATP-dependent rearrangement of RNA base-pairing structure. The snRNPs then catalyze two transesterification reactions that allow the exons to join. The intervening intron forms a lariat structure that is degraded. The snRNPs are recycled. Mutation in genes controlling splicing are recurrently detected in myeloid malignancies (Chapters 13 and 15).

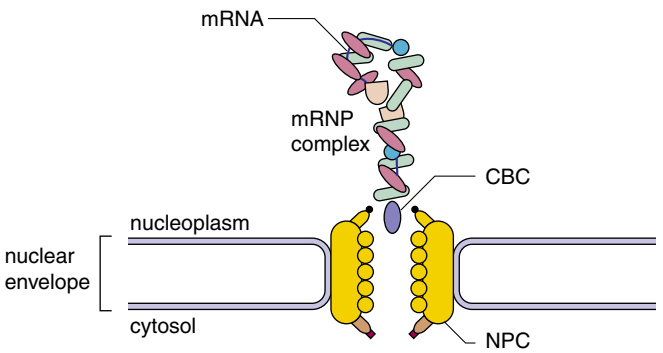

Fig. 1.7. Nascent primary transcripts and mRNAs are associated with nuclear proteins to form heterogeneous ribonuclear protein particles (hnRNPs). Some of these hnRNPs help transport mRNA out of the nucleus. The 5′ end of the mRNA–hnRNP complex (mRNP) associates with a cap-binding complex (CBC) that is exported through a specialized nuclear pore complex (NPC). Some of the hnRNPs remain in the nucleus and are recycled. The mRNA then interacts with cytosolic mRNP-binding proteins that escort the mRNP to ribosomes to be translated. mRNP export is an active, controlled, and coordinated process.

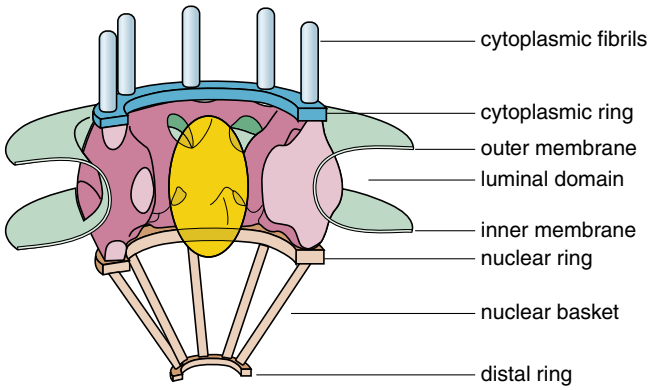

Fig. 1.8. Detailed schematic view of a eukaryotic nuclear pore complex. It is a highly ordered structure that is embedded in the nuclear and cytosolic membranes.

of proteins. It has a ring-basket structure. The ring points into the nucleus and filaments that form a basket. The structure is then embedded in the nuclear envelope. mRNPs are exported to the cytoplasm in a GTP-dependent process through the NPC. It is facilitated by a subset of RNP proteins that contain amino acid sequences functioning as nuclear export signals (NES). Similarly, proteins made in the cytosol have to be imported into the nucleus through NPCs. Such proteins often, but not always, have nuclear localization signal sequences (NLS).

Once in the cytoplasm, mRNA is covered by cytosolic proteins. The stability of mRNAs is variable and can be regulated. This can help determine the amount of mRNA available for protein synthesis.

Just as large macromolecular machines are required to make DNA and mRNA, proteins are translated from mRNA in a large structure called a ribosome. The details of translation are described in Fig. 1.9. The large and small ribosomal subunits, with the aid of specific translational initiation proteins (factors), locate the translational start site, which is usually the first codon (the three RNA nucleotides) for the amino acid methionine, in an ATP- and GTP-dependent process. As codons are composed of triplets of mRNA nucleotides, there are three different reading frames or ways in which mRNA triplets can be read by the ribosome. The frame that is selected is defined by the position of the start codon. Once engaged, the ribosome moves along the mRNA and sequentially adds amino acids to the growing peptide chain by recognizing sequential triplets of mRNA nucleotides (codons) (Fig. 1.9B). The amino acid added to the peptide is defined by the RNA codon selected and, as shown in Fig. 1.10, there is a code for how the different RNA codons specify particular amino acids. Of note, certain RNA codons specify "stop" signals (as well as a start signal, see above) that cause peptide chain termination. In eukaryotic cells (i.e. organisms with cells that have internal compartments, such as mammalian cells), multiple ribosomes commonly engage and concurrently translate a single mRNA to form a circular polysome to increase the efficiency of protein translation. As ribosomes finish translation at the 3′ end, the subunits quickly reassemble to reinitiate synthesis at the 5′ end of the mRNA.

Nascent peptide chains have to be properly folded, and amino acids modified and then either directed to the right cellular compartments or labeled for export. Proteins with a specific signal sequence direct the ribosome to the endoplasmic reticulum where protein synthesis is completed and peptides are directed to the Golgi complex and sorted for different destinations (the secretory pathway) (Figs. 1.11 and 1.12). In other cases, proteins complete synthesis in cytosolic ribosomes and are directed to other compartments (the nucleus, mitochondria, peroxisome). The transport of proteins depends on signal sequences (e.g. a nuclear localization signal) and interaction with specific receptor/transport proteins.

DNA MUTATIONS CAN ALTER PROTEIN SYNTHESIS BY A NUMBER OF MECHANISMS

Changes in a DNA sequence are called variants. Sometimes changing the DNA sequence can have deleterious consequences, in which case the variant is known as a mutation. DNA mutations occur at a variety of places in the gene locus and can cause aberrant mRNA and protein production (Fig. 1.13). For example, point nucleotide substitutions in the coding sequence (Fig. 1.13) can cause either an amino acid substitution (missense mutation) or introduce a stop codon (nonsense mutation). Deletions or additions of nucleotides (other than in multiples of three nucleotides) can cause an alteration in the reading frame (frameshift mutation). In addition to mutations in the coding sequence, mutations can also occur in the promoter (or other distal *cis*-regulatory elements) to alter transcription; in the invariant splice acceptor donor sites in the intron at the intron–exon boundary to affect splicing; or in sequences that control 3′ end processing (poly-A addition sites) and 5′ end processing (addition of the cap site) (Fig. 1.14). The whole spectrum of these mutations is exemplified in the germline in the β-globin gene in β-thalassemia (see Chapter 9) or, to a lesser extent, in acquired mutations in FMS-like tyrosine kinase 3 (*FLT3*) in acute myeloid leukemia (AML) (Fig. 1.15) (see Chapter 13).

TRANSCRIPTIONAL CONTROL OF GENE EXPRESSION

One major level of control of protein production is by regulating mRNA transcription. For any gene, expression is regulated by regulatory DNA sequences (*cis*-elements), proteins (transcription

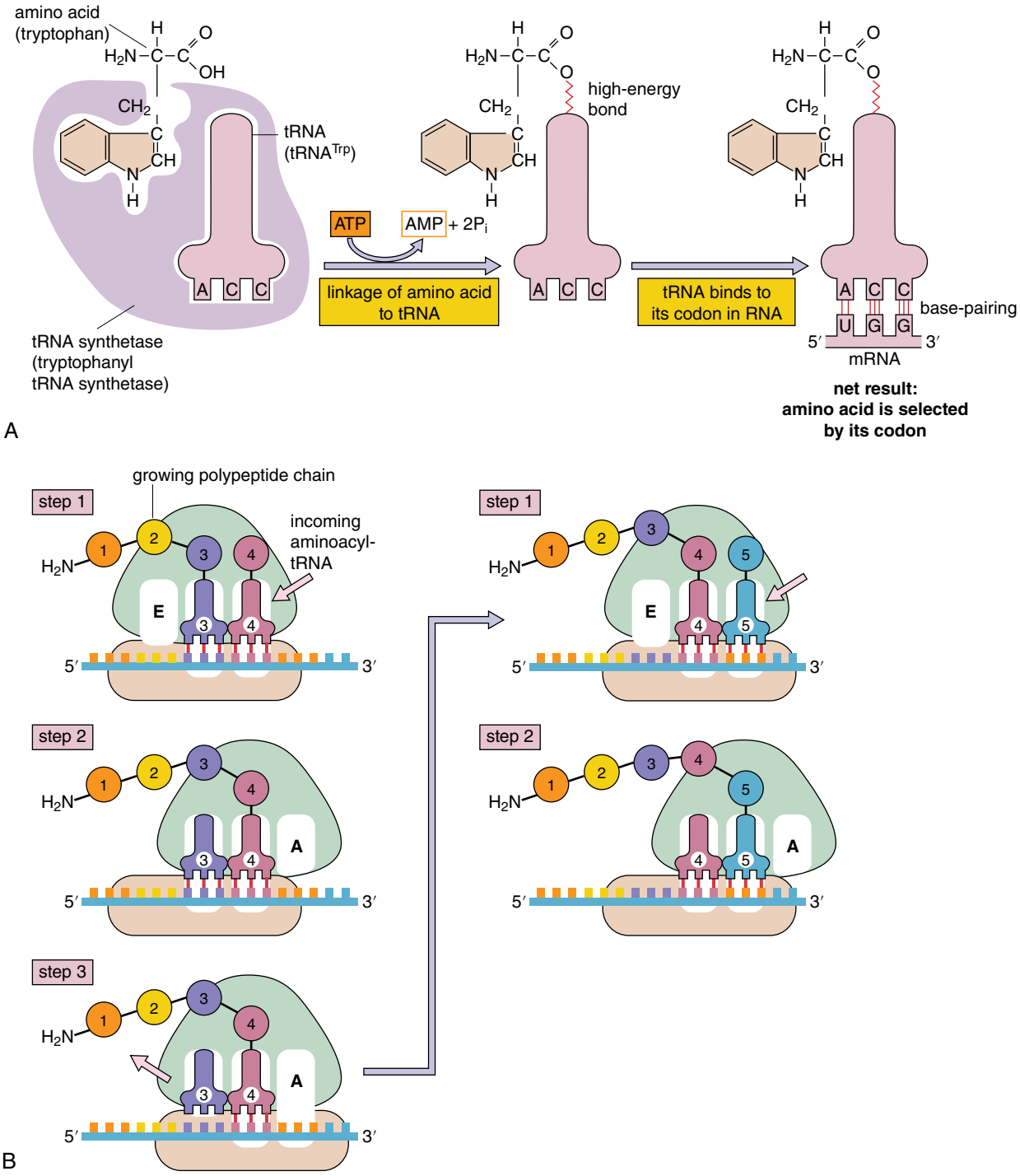

Fig. 1.9. Messenger RNA is translated into proteins. **A,** mRNAs docked in the ribosome interact with transfer RNAs (tRNAs) that bind amino acids. Different amino acids bind specific tRNA molecules. Here, the amino acid tryptophan is coupled to a specific $tRNA^{Trp}$ by an adapter aminoacyl-tRNA synthetase in an ATP-dependent reaction. The triple RNA nucleotide "ACC" sequence in the $tRNA^{Trp}$ (anticodon sequence) then base pairs to a triple RNA sequence "UGG" (codon) in mRNA. Thus the amino acid is selected by specific codon–anticodon recognition. **B,** To form an elongating protein polypeptide in a ribosome from mRNA, amino acids are added sequentially as specific tRNAs are recruited by codon–anticodon base-pairing. In this figure, in *step 1* on the left-hand side, amino acids 1, 2, and 3 have already been added. Amino acid is docked (via the specific tRNA) next to amino acid 3. In *step 2*, amino acid 4 is bound to amino acid 3 and a new tRNA-docking position ("A") is available for the next tRNA to dock. In *step 3*, mRNA moves along and is opposite position "A" and the tRNA that brought in amino acid 3 is ejected. These steps are then repeated on the right-hand side to allow docking of tRNA that brings in amino acid 5, which is added to the growing polypeptide chain.

factors and transcriptional cofactors) that regulate the transcription of the gene by binding either directly, or indirectly, to *cis*-element. Finally, as DNA is very tightly packed to accommodate it into the nucleus, *cis*-elements and the genes themselves have to be "unpacked" to allow the genes to be expressed. Regulation of gene expression through control of packing and unpacking of DNA is known as epigenetic regulation of gene expression. We discuss it in more detail later.

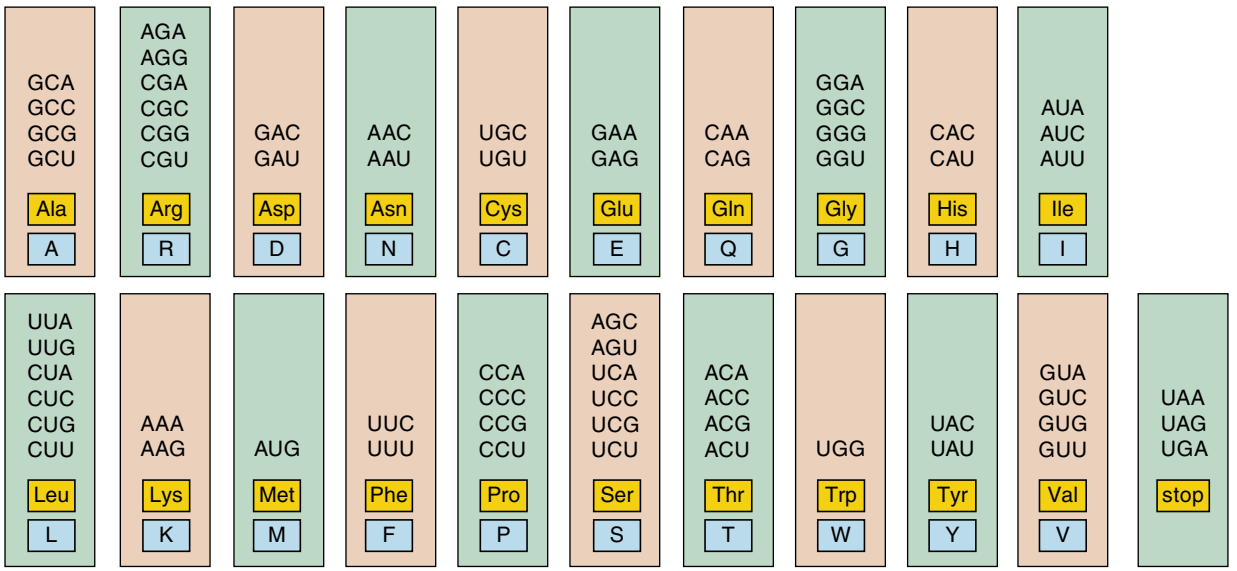

Fig. 1.10. Different RNA codons are used to code for amino acids. *Top left*, For example, the amino acid alanine (three-letter code Ala [yellow box] and one-letter code A [blue box]) is coded by the codons "GCA," "GCC," "GCG," and "GCU." The codons "UAA," "UAG," and "UGA" bring a halt to addition of amino acids and are known as stop codons.

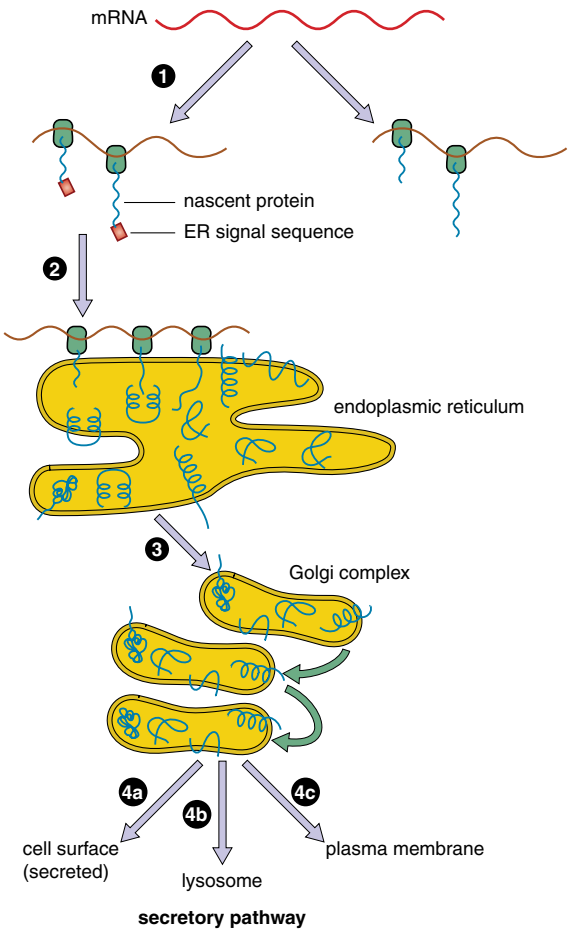

Fig. 1.11. Newly synthesized proteins are folded and post-translationally modified in the rough endoplasmic reticulum and the Golgi apparatus. *Step 1*, Ribosomes (green rectangles) synthesize polypeptide chains (blue lines) from an mRNA template (red line). Proteins with a signal sequence (pink square) are taken up by the rough endoplasmic reticulum, where translation is completed. Proteins without a signal sequence complete translation in the cytosol on free ribosomes. *Step 2*, In the rough endoplasmic reticulum the proteins are folded and post-translationally modified. *Step 3*, They are transferred to the Golgi via transport vesicles. *Step 4a,b,c*, The folded protein is then sorted for onward transport.

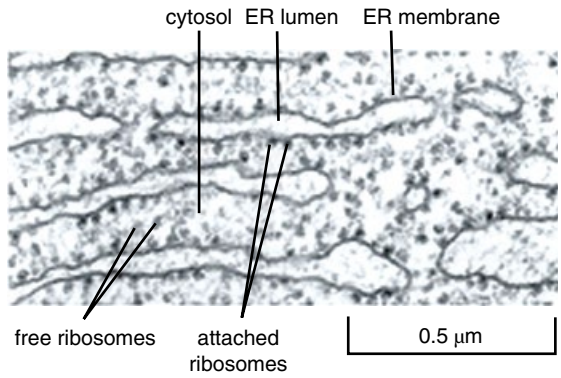

Fig. 1.12. Electron micrograph of ribosomes attached to the rough endoplasmic reticulum in a pancreatic cell.

CIS-ELEMENTS AND TRANSCRIPTION FACTORS

Figure 1.16 shows that *cis*-elements can be located near to the gene. For example, the promoter defines the location of transcription start site(s) and the directionality of transcription. The *cis*-elements can also be located at distance from the gene and can either promote (enhancer) or repress (silencer) transcription. The *cis*-elements are composed of multiple binding sites for transcription factors (TFs). Thus, the *cis*-element acts as a docking site for multiple DNA-binding TFs that in turn tether other TFs and cofactors that do not bind DNA.

Like many other proteins, TFs have a modular structure. For example, DNA-binding TFs such as MAX have a domain called the basic region (b) that binds DNA and an adjacent region, the helix-loop-helix (HLH) motif that interacts with other TFs and cofactors (Fig. 1.17). These domains allow TFs to be organized into families that share similar amino acid sequences and structural domains. Thus, MAX is part of the bHLH TF family. TFs in a common family often bind similar ~6–10 DNA base pair sequences (binding sites) and bind with similar protein partners.

Once TFs and cofactors bind *cis*-elements proximal and distal to the gene most, some but not all, evidence suggests that the *cis*-elements come together by looping out intervening DNA

(Figs. 1.18 and 1.19). Either before or after looping, the complex of TFs and cofactors recruits RNA Pol II containing preinitiation complex. RNA Pol II is then phosphorylated on a specific domain (the C-terminal domain) that allows RNA Pol II to disengage from the preinitiation complex and elongate the RNA chain as it proceeds along the gene.

Study of hematopoietic genes has contributed significantly to our understanding of eukaryotic gene expression. Examples include the α and β globin gene loci (Fig. 1.20). In the β-globin locus, multiple closely spaced distal *cis*-elements combine to form a specific type of enhancer known as a locus control region (LCR). TFs and cofactors are bound at the LCR and even more distal *cis*-elements are thought to bind together by looping out intervening DNA and promote transcription of different globin genes in a developmental stage-specific manner.

Wild-type sequences

amino acid	N-Phe	Arg	Trp	Ile	Ala	Asn-C
mRNA	5′-UUU	CGA	UGG	AUA	GCC	AAU-3′
DNA	3′-AAA	GCT	ACC	TAT	CGG	TTA-5′
	5′-TTT	CGA	TGG	ATA	GCC	AAT-3′

Missense

3′-AAT	GCT	ACC	TAT	CGG	TTA-5′
5′-TTA	CGA	TGG	ATA	GCC	AAT-3′
N-Leu	Arg	Trp	Ile	Ala	Asn-C

Nonsense

3′-AAA	GCT	ATC	TAT	CGG	TTA-5′
5′-TTT	CGA	TAG	ATA	GCC	AAT-3′
N-Phe	Arg	Stop			

Frameshift by addition

3′-AAA	GCT	ACC	ATA	TCG	GTT A-5′
5′-TTT	CGA	TGG	TAT	AGC	CAA T-3′
N-Phe	Arg	Trp	Tyr	Ser	Gln

Frameshift by deletion

GCTA
CGAT

3′-AAA	CGT	ATC	GGT	TA-5′
5′-TTT	GGA	TAG	CCA	AT-3′
N-Phe	Gly	Stop		

Fig. 1.13. Changes in coding parts of the DNA sequence of a gene can alter the protein produced. In this example, the wild-type (normal) protein and corresponding mRNA and DNA sequences are shown at the top. Point mutations that change the amino acid encoded in the protein are known as missense mutations. Here a "T" to "A" change in the DNA (reading 5′ to 3′) alters the protein sequence from phenylalanine (Phe) to leucine (Leu). On occasion the amino acid change can alter protein function. *Below*, The point change ("C" to "A") introduces a stop codon. This is a nonsense mutation. *Below*, If nucleotide/nucleotides is/are added (the nucleotide "T") or deleted ("CGAT"), this alters the reading frame (the order in which the triplets of nucleotides are read as codons) and alters protein sequence. This is a frameshift mutation. Nonsense and frameshift mutations usually have a more profound effect on protein sequence.

CHROMATIN AND EPIGENETIC CONTROL OF GENE EXPRESSION

DNA is highly packaged in a nucleus. For a TF to gain access to a short DNA sequence in a particular *cis*-element of an individual gene, the chromatin associated with that sequence has to be specifically unpacked (Figs. 1.21–1.23). Metaphase chromosomes are progressively unpackaged via intermediate states (Fig. 1.22) called chromosome territories that are poorly defined to transcriptional activation domains (see next paragraph) to a 30 nm chromatin fiber. These higher order structures are gradually being understood, as new, remarkable techniques, such as high-resolution electron microscopy and genome-wide molecular mapping

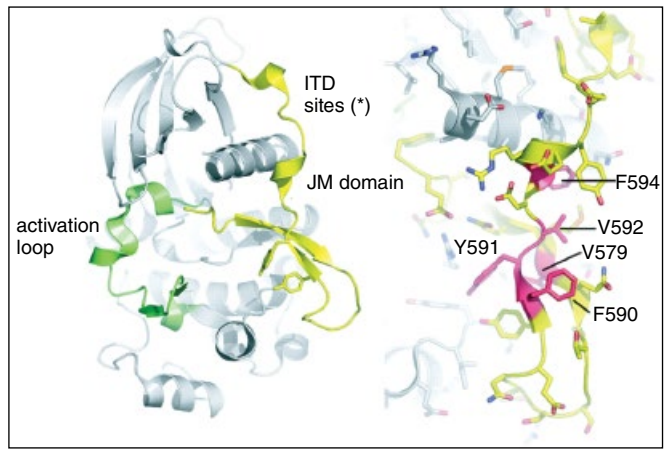

Fig. 1.15. Ribbon model of the crystal structure of the FMS-like tyrosine kinase 3 (FLT3) domain (with green activation loop and yellow juxtamembrane [JM] domain). The positions of internal tandem duplications (ITDs) in the JM domain, leading to FLT3 activation, are indicated. *Right*, Close view of the mutation sites in the JM domain (yellow). The structure is shown as a ribbon backbone, with side-chains as colored sticks.

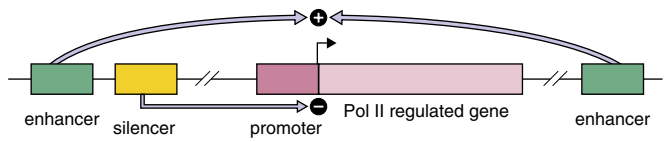

Fig. 1.16. Regulation of genes transcribed by RNA polymerase II is controlled by multiple DNA sequences (*cis*-elements). Here, the gene is regulated by proximal sequences—a promoter that abuts the transcriptional initiation site (arrow) and distal sequences that function to both enhance (enhancers) and repress (silencers) gene expression.

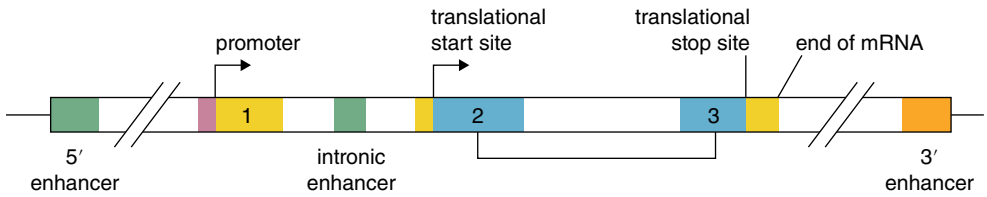

Fig. 1.14. Schematic representation of a gene locus. On the left is the 5′ end of the locus and an enhancer is shown as a green box, the promoter as a pink box, and the transcriptional start site as a arrow. This gene has three exons and the exons are shown as boxes. Noncoding portions of exon are in yellow and coding portions of exons are in blue. Exon 2 and 3 have both noncoding and coding regions. The translational start site is indicated. The gene also has a 3′ enhancer shown in orange.

of long-range chromatin interactions, are deployed to visualize these structures. The 30 nm chromatin fiber is composed of fibrils of DNA wrapped around nucleosomes (composed of histone octamer – two units each of H2A, H2B, H3, and H4) and finally to naked DNA. Histone octamers can include variant histones, of which there are a number, for example, H2A.Bbd, H2A.X, H3.1, H3.2, H3.3, and H3.X. H3.Y, that serve diverse roles in DNA replication and transcription of DNA into RNA.

TADs describe an intermediate level of chromatin packing where tens of kilobases to megabases, DNA, and chromatin

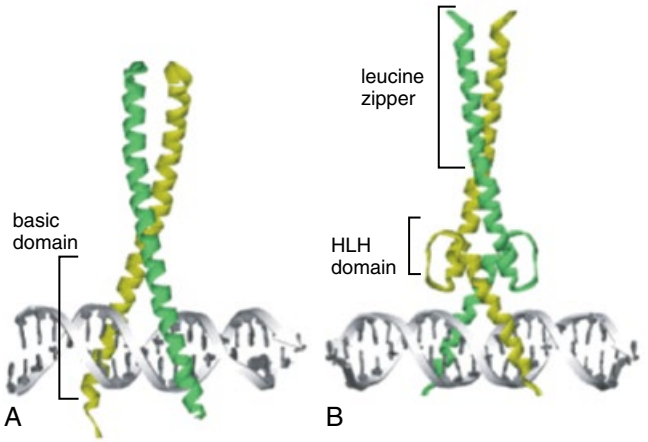

Fig. 1.17. A, Crystal structure of two transcription factors (green shades) shows the intimate contact between the basic residues (basic domain) and specific sequences in the major groove of DNA (white double helix). The two TFs then interact with each other via helical structures that are rich in leucine residues (leucine zipper domains). Thus these TFs contain bzip domains. **B,** Crystal structure of two TFs (green shades) that bind the major groove of DNA (white shade) via basic residues (basic domain). Immediately following this domain are helix-loop-helix domains (HLH) followed by leucine zipper regions. Therefore these TFs have bHLH domains with leucine zippers.

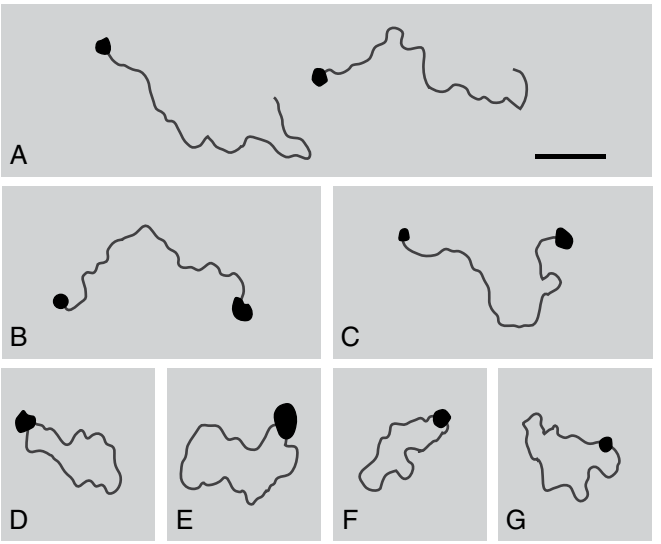

Fig. 1.19. Looping between *cis*-elements can be visualized. **A,** Schematic representation of an electron micrograph of the transcription factor Sp1 (shown as a black spot) bound to a cognate binding site at one end of DNA (irregular line). **B** and **C,** Two cognate DNA-binding sites were engineered at either end of the DNA fragment. **D–G,** Over time, Sp1 bound to the ends of the DNA self-associated and looped the intervening DNA out.

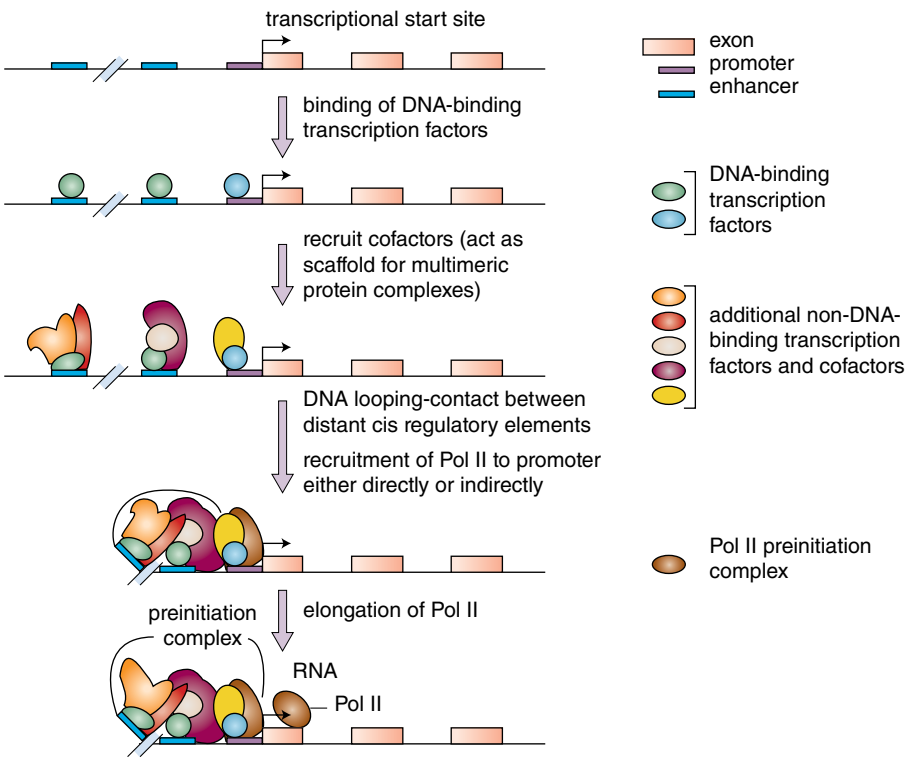

Fig. 1.18. Gene expression is controlled by transcription factors that bind *cis*-elements. DNA-binding TFs binding to *cis*-elements then recruit cofactors and other transcriptional regulators. It is also likely that DNA-binding TFs and non-DNA-binding TFs/cofactors may form preformed complexes that bind directly to DNA. Binding of RNA polymerase II, the preinitiation complex, and DNA looping between different *cis*-elements triggers transcription and elongation of polymerase II along the gene.

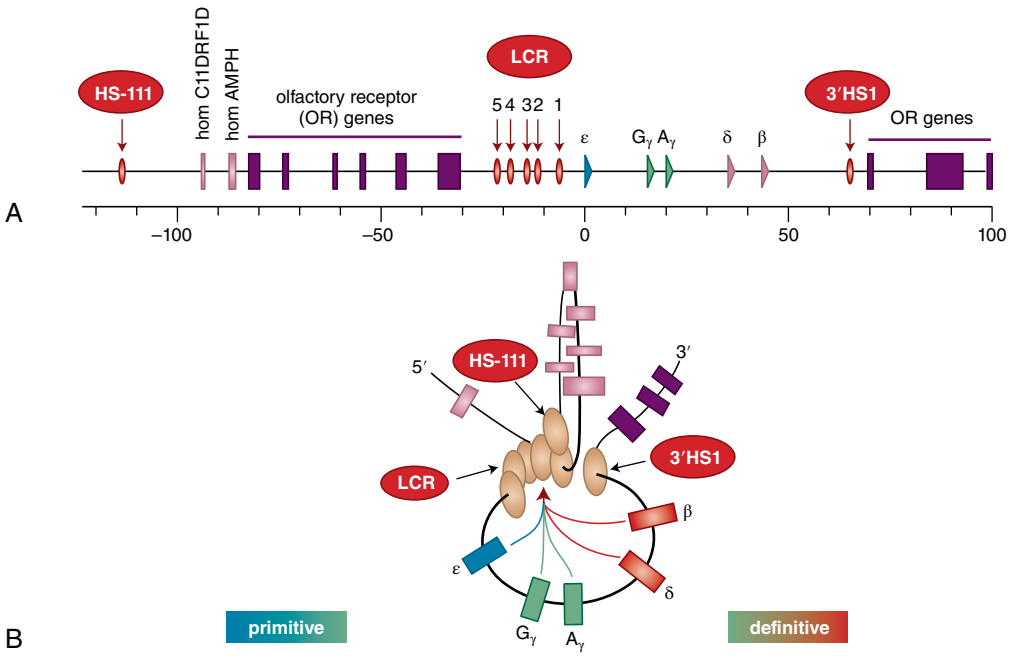

Fig. 1.20. The *cis*-elements that regulate gene expression can be distributed over a large area and can be complex. One of the best-studied gene loci is the human β-globin gene cluster on chromosome 11. **A,** There are five genes in the β-globin gene cluster (ε, Gγ,Aγ, δ, and β, depicted as arrowheads). At the 5′ of the gene cluster there are five *cis*-elements (numbered 1 to 5, marked by arrows and collectively termed the locus control region, LCR). Two more *cis*-elements are located 111 kilobases 5′ (HS-111) and approximately 65 kilobases 3′ (3′HS1). The whole β-globin domain (genes and *cis*-elements) is embedded in the midst of a bank of olfactory receptor (OR) genes (purple blocks) and two other genes (pink blocks). The scale below the locus is in kilobases. **B,** In a nucleus, current evidence supports a model where all the β-globin cluster *cis*-elements physically interact (even though widely dispersed) with each other and with a β-like globin gene. Embryonic ε globin is expressed first (in primitive red cells), then the fetal γ genes, and finally the adult δ- and β-globin genes (both in definitive red cells).

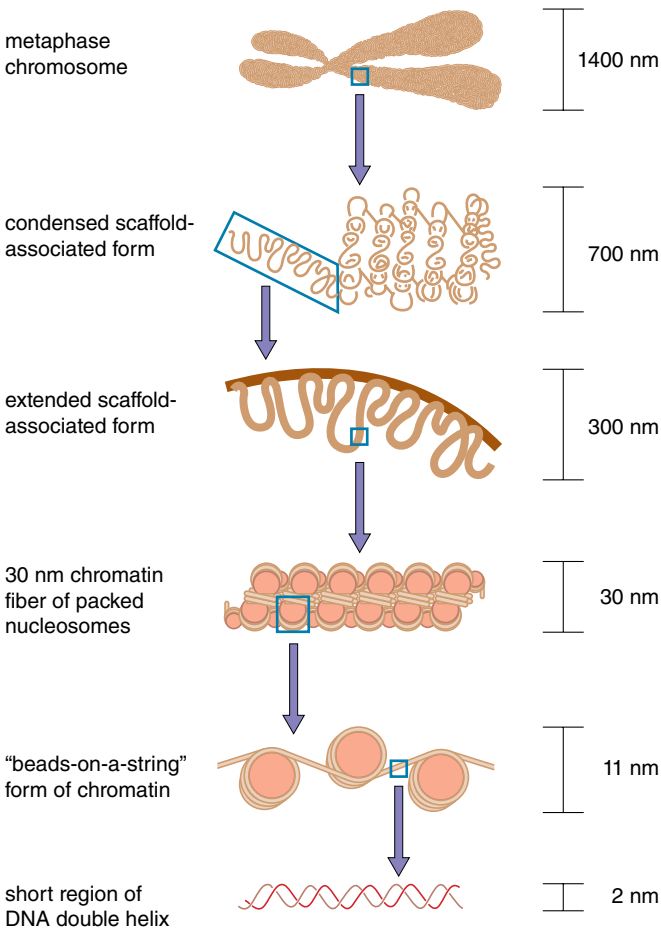

proteins are organized into spatial domains (Fig. 1.22C,D). Within each TAD there usually lie a number of genes and the DNA sequences that regulate those genes. The whole point of a TAD is that it segments chromatin such that all the DNA sequences capable of regulating genes usually function within the TAD they are located in (Fig. 1.22D–E). Thus, TAD boundaries help delimit the extent over which DNA sequences that regulate gene expression can function. TAD boundaries are marked by proteins called cohesins, and a protein called CTCF (CCCTC-binding factor). Thus, abnormalities in cohesin and CTCF have the potential to disrupt TAD boundaries and alter gene expression. Importantly, mutations in cohesins and CTCF are recurrently present in hematologic malignancies, especially myeloid blood cancers (AML and myelodysplastic syndromes).

Regulation of the selective packing or unpacking of chromatin affords another level at which control on gene expression can be exerted. Control of expression of specific

Fig. 1.21. Genes do not exist as naked DNA in the nucleus but are highly packaged. This figure shows that when metaphase chromosomes are unpackaged they are composed of fibrils of chromatin and may be associated with nuclear structures (one example that has been suggested is nuclear scaffolds that are often attached to nuclear membranes). When further unpacked, these chromatin fibrils are composed of 30 nm chromatin fibers, which in turn are composed of DNA wrapped around histone protein octamers called nucleosomes. When the 30 nm fiber is unwrapped the nucleosomes are linked by intervening DNA (like beads on a string). Nucleosomes can be temporarily shifted (remodeled) to expose naked DNA. The exact physical structure of higher order chromatin structure (30 nm fiber and higher orders of packaging) is unclear. Regulating the wrapping and unwrapping of DNA also affords a layer of regulation on controlling which genes are expressed (unwrapped) and which are not (wrapped).

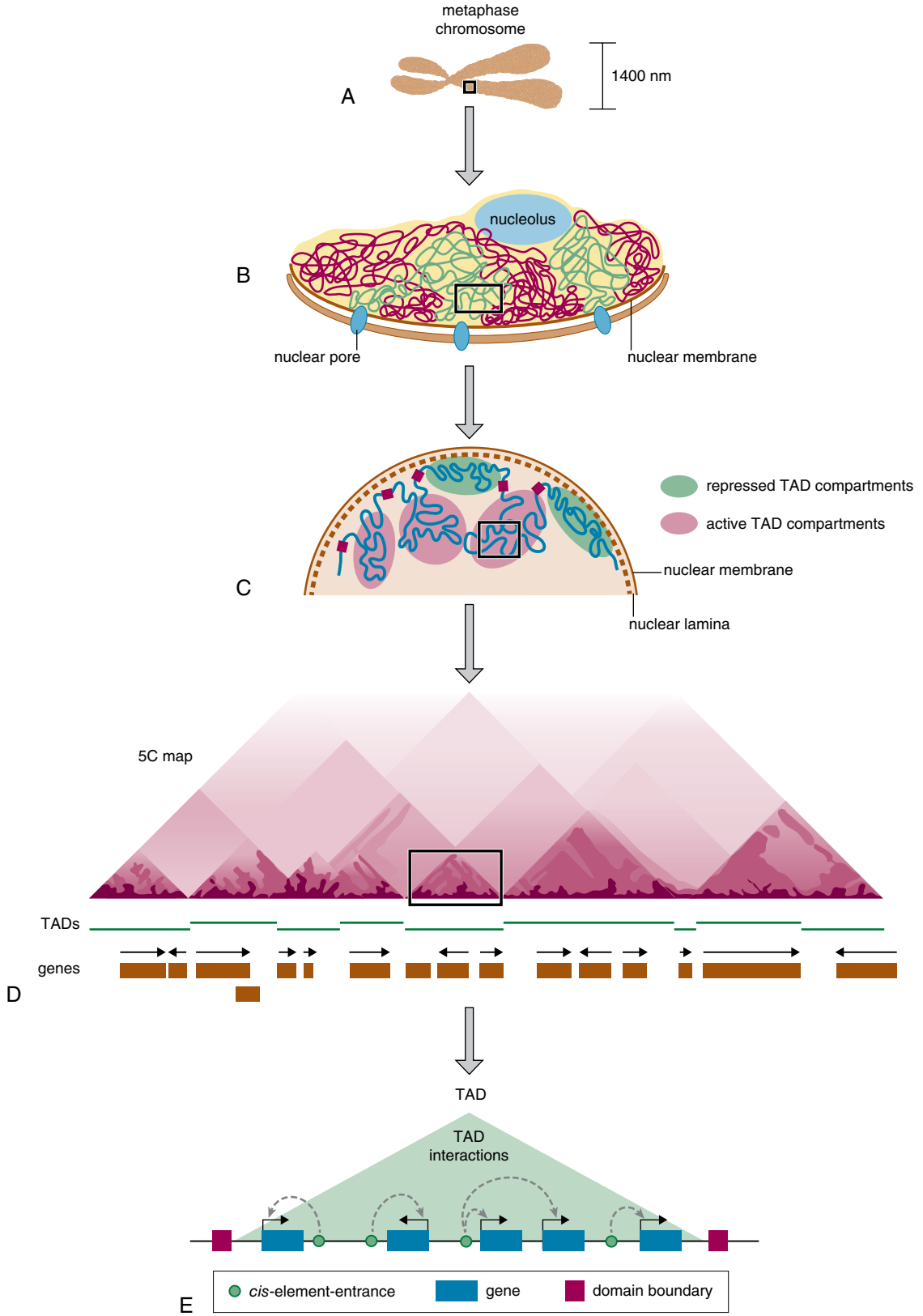

Fig. 1.22. Schematic representation of how DNA-encoding genes and the chromatin that coats genetic loci are packaged and unpackaged to allow selective gene expression. **A,** A metaphase chromosome and portion of the chromosome is examined in more detail in part B. **B,** Portion of chromosome composed of poorly defined chromatin fibers (irregular red and green lines that extend from the nuclear membrane into the nucleus) arranged into a number of chromosomal territories. The territories are shown in red and green. Genes encoding ribosomal RNAs are located in the nucleolus. Nuclear pores allow communication to the cytoplasm. **C,** Portion of chromosomal territory composed of a number of chromatin fibers that are arranged into topologically associated domains (TADs). Some are actively transcribed (pink) and some are repressed (green). Boundaries between TADs are shown as red squares. **D,** A number of TADs shown in greater detail by a technique called five-dimensional chromatin conformation capture (5C). This technique maps physical interactions within TADs and between TADs (shown as triangles). The stronger the interaction the darker the shade of color of the triangle. *Below*, Nine TADs of varying lengths are shown as lines. Under each TAD are a number of genes. Each gene is composed of exons (small vertical lines) and introns (space between lines with arrows). The arrows indicate the direction in which the gene is transcribed. **E,** Closer view of a TAD. The TAD boundaries are shown as red squares. There are five genes within the TAD (blue boxes). The arrows at the ends of each gene indicate the direction of transcription (5′ to 3′). The green circles indicate *cis*-elements that control transcriptional expression of the gene. Note, one *cis*-element may control expression of more than one gene.

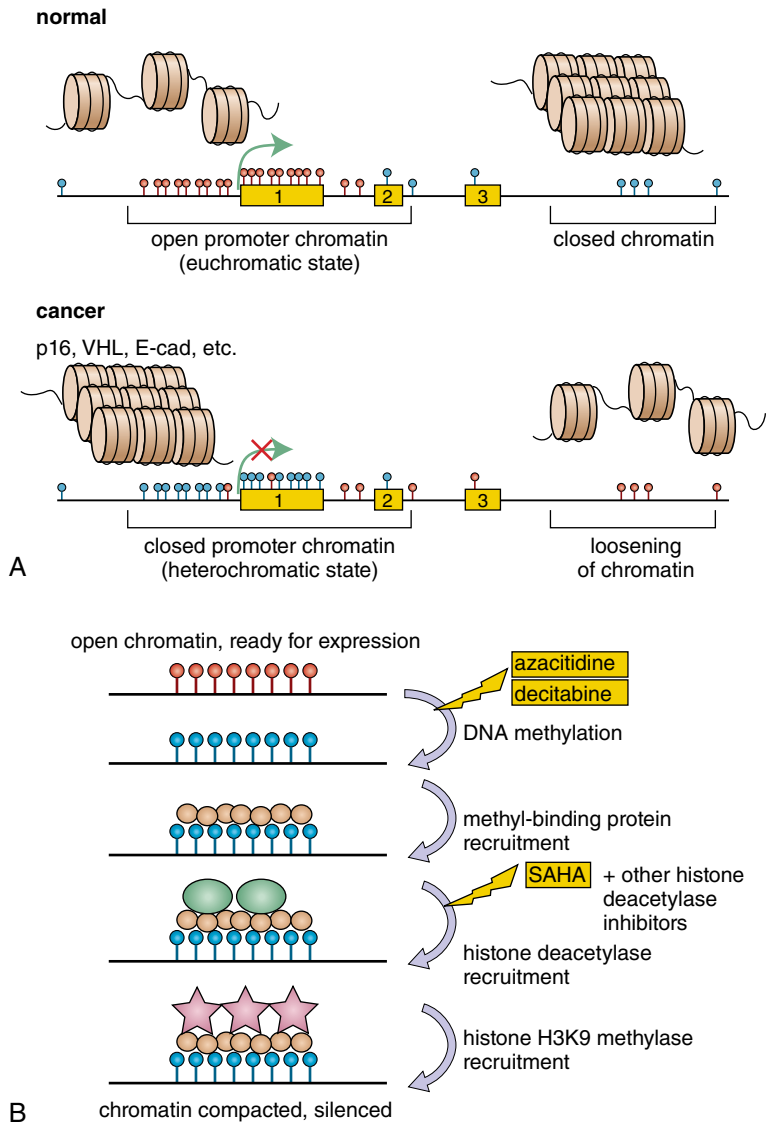

Fig. 1.23. A, Genes are in yellow boxes. Unwrapped genes (1) are in an open chromatin, euchromatic state. These genes have unmethylated CpG DNA residues (shown as pink lollipops) and are transcribed (green arrow). Genes that are not transcribed (2 and 3) often have methylated CpG residues (blue lollipops). Closed chromatin is shown as closely packaged nucleosomes. In cancer, gene expression is often inappropriate, and this is reflected in the changed chromatin structure. Thus genes such as p16, VHL, and E-cadherin (E-cad) are not transcribed. CpG residues are methylated and the chromatin is in a closed conformation. **B,** The transition from an open to a closed chromatin state occurs via multiple steps that can be targeted by drugs. *Top*, A gene locus is in an open chromatin conformation and the dinucleotide CpGs are not methylated (pink lollipops). DNA can then be methylated (blue lollipops). This can be inhibited by DNA methyltransferase inhibitors that are used in clinical practice (azacitidine and decitabine). Methyl CpG-binding protein (brown circles) is recruited to methylated DNA and this is thought to facilitate binding of histone deacetylases and histone H3K9 and H3K27 methylases. Acetylated histones are associated with open chromatin and facilitate transcription, whereas deacetylated histones and histone H3 methylated at residue lysine (K) 9 and K27 are associated with closed chromatin and transcriptional repression. A number of drugs in clinical use inhibit histone deacetylases. These include sodium valproate, SAHA, and MGCD0103.

genes by regulation of the state of chromatin is not encoded in DNA of the gene and thus is termed epigenetic regulation of gene expression. Huge advances have been made in our understanding of the epigenetic regulation and chromatin structure and its influence on gene expression both in normal cells and to a lesser extent in diseases such as some of the hematologic malignancies (Fig. 1.23).

Regulation of the selective packing or unpacking of chromatin affords another level at which control on gene expression can be exerted. Control of expression of specific genes by regulation of the state of chromatin is not encoded in DNA of the gene and thus is termed epigenetic regulation of gene expression. Huge advances have been made in our understanding of the epigenetic regulation and chromatin structure and its influence on gene expression both in normal cells and to a lesser extent in diseases such as some of the hematologic malignancies (Fig. 1.23). This is exemplified in Fig. 1.23A, where the *cis*-elements that regulate expression of a key gene are shown in either an open chromatin conformation, allowing access to TFs and expression of the gene, or in a closed chromatin conformation (where gene expression is repressed). The normal chromatin state at key genes that control cell fate (e.g. growth, self-renewal, and differentiation) can be altered in a pathogenic manner in cancer.

This increased knowledge has led to the development of a new class of therapies for hematologic disease. To understand how these drugs may work in outline, it is helpful to consider epigenetic regulation of gene expression in a little more detail.

Control of packing is principally mediated by histones and methylation of DNA at the dinucleotide CpG (Fig. 1.23A,B). Histones can be post-translationally modified (acetylated, phosphorylated, methylated, or ubiquinated) at multiple residues by a large number of enzymes in a complex manner (Fig. 1.24). The complex and varying nature of the post-translational histone modifications (or histone marks) for any segment of chromatin is known as the "histone code" for that segment. Some of the histone marks cause the chromatin to be less tightly packed and activate gene expression. Consequently they are known as activating marks. Examples of activating marks include acetylation of histone H3 and H4, such as trimethylation of histone H3 at lysine residue 36 (me3H3K36) and H3 at lysine residue 4 (me3H3K4). Conversely, some marks are known as repressive marks as they cause the chromatin to become more tightly packed, repressing gene expression. Examples of repressive marks include trimethylation of histone H3 at lysine residue 9 (me3H3K9) and trimethylation of histone H3 at lysine residue 27 (me3H3K27). Both activating and repressive marks are laid down on chromatin regionally

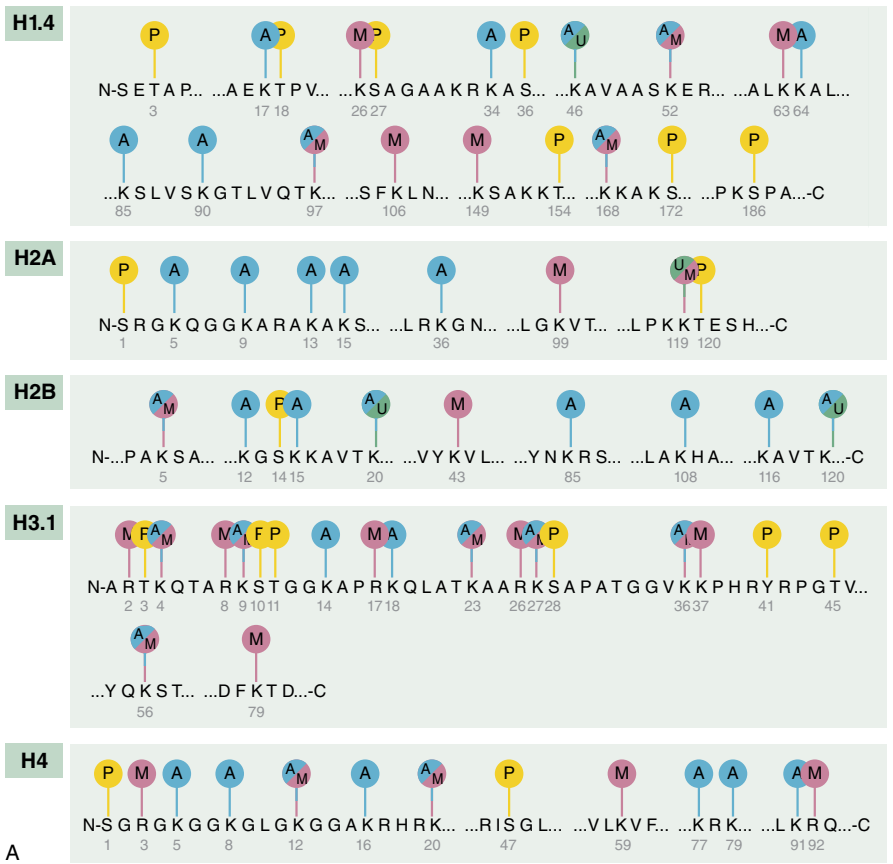

A

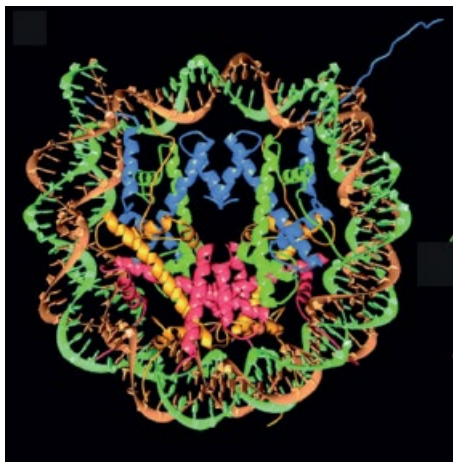
B

Fig. 1.24. A, All histones are subject to post-transcriptional modifications, which mainly occur in histone tails. The amino acid sequence (as a single-letter code) is shown from histones H1.4, H2A, H2B, H3.1, and H4. The numbers below the single-letter code refer to the position of the amino acid. The main post-transcriptional modifications are depicted in this figure: A, acetylation (blue), M, methylation (red), P, phosphorylation (yellow), and U, ubiquitination (green). Some amino acid can be subject to more than one type of modification. Source: Portela A, Esteller M. *Nat Biotechnol* 2010;28:1057–1068. Reproduced with permission of Springer Nature. **B,** The view is down the DNA superhelix axis of a nucleosome core particle showing ribbon traces for the 146 base pair DNA phosphodiester backbones (green and brown) and eight histone protein main chains (blue: H3; green: H4; yellow: H2A; red: H2B. Source: Luger K, et al. *Nature* 1997;389:251–260. Reproduced with permission of Springer Nature.

in a very precise manner. The activating mark me3H3K4 is only seen at promoters, whereas me3H3K36 is present at enhancers. Similarly, the repressive mark me3H3K27 is seen at heterochromatin. Regional localization of histone marks allows identification of promoters and enhancers.

The histone-modifying enzymes are called "writers" as they "write" or impart a series of post-translational modification to histones. The histone marks imparted by writers allow chromatin to interact with a large number of chromatin-associated proteins called "readers." Finally, histone marks can be removed by other enzymes and these are known as "erasers." Reader, writer, and eraser proteins have modules (or domains) that "write," "read," and "erase" the histone code. All these proteins are grouped into families based on the modules that "write" or "read" or "erase" (Fig. 1.25). Recurrent mutations in the genes encoding these histone-modifying proteins are often seen in blood diseases.

Similarly, CpG dinucleotides can be methylated by DNA methyltransferases (DNMT) (Fig. 1.26). There are two broad classes of DNMTs: DNMT3A and DNMT3B are de novo methylases whereas DNMT1 maintains methylated DNA through DNA replication. Demethylation of DNA occurs by a very complex set of enzymatic reactions as shown in Fig. 1.26. These precise details of methylation are important as the proteins involved in DNA methylation and demethylation are often mutated in hematologic malignancies, pointing to the importance of this process for normal hematopoiesis.

Methylation of DNA is associated with more highly packaged DNA and repression of gene expression. Methylation of CpG residues promotes binding of methyl CpG-binding proteins (MeCPs). This in turn facilitates binding of writers and readers of repressive histone marks such as histone deacetylases (Fig. 1.23). Drugs that inhibit DNA methyltransferases (e.g. azacitidine and decitabine) and writers of repressive (e.g. vorinostat or pabinostat) would potentially reverse the repression of genes, especially those that promote differentiation of malignant cells (Fig. 1.23).

TRANSCRIPTION FACTORS, CONTROL OF GENE EXPRESSION, AND LINEAGE COMMITMENT

A cardinal event in the differentiation of a lineage-specific cell is the elaboration of a lineage-specific program of gene expression (Fig. 1.27). Expression of lineage-specific genes, as of all genes, is dependent on *cis*-elements and TFs (see earlier). These TFs can either be widely expressed or have a restricted pattern of expression. For example, there is a small of subset of TFs that are principally or exclusively expressed in blood cells. It is the action of these hematopoietic TFs that are critical in directing hematopoietic-specific gene expression. One such hematopoietic TF is GATA1. GATA1 is expressed in erythroid cells and megakaryocytes as well as eosinophils and mast cells. In all these cell

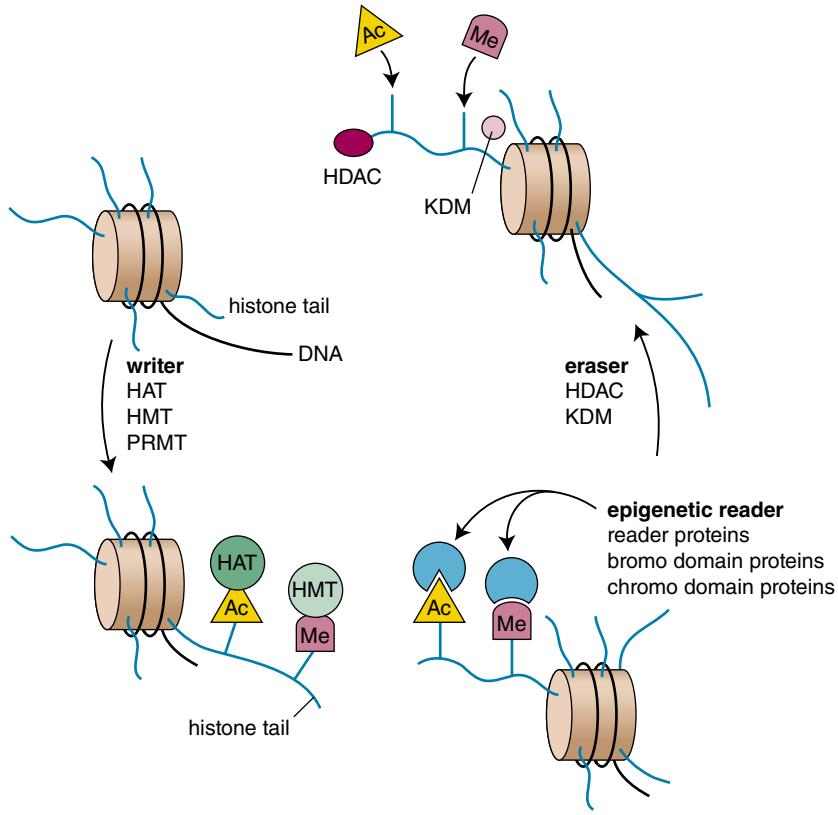

Fig. 1.25. Epigenetic regulation is a dynamic process. Proteins called epigenetic writers, such as histone acetyltransferases (HATs), histone methyltransferases (HMTs), and protein arginine methyltransferases (PRMTs), modify histones with post-translational modifications (known as epigenetic marks) on amino acid residues on histone tails. These post-translational modifications are recognized by proteins called epigenetic readers. They have amino acide domains called bromo domains and chromo domains that bind to these epigenetic marks. The post-translational modifications on histones are removed by proteins called epigenetic erasers, such as histone deacetylases (HDACs) and lysine demethylases (KDMs), that catalyze the removal of epigenetic marks. Addition and removal of these post-translational modifications of histone tails leads to the addition and/or removal of other marks in a highly complicated histone code. Together, histone modifications regulate various DNA-dependent processes, including transcription, DNA replication, and DNA repair. Source: Katrina J, et al. *Nat Rev Drug Discov* 2014;13:673–691. Reproduced with permission of Springer Nature.

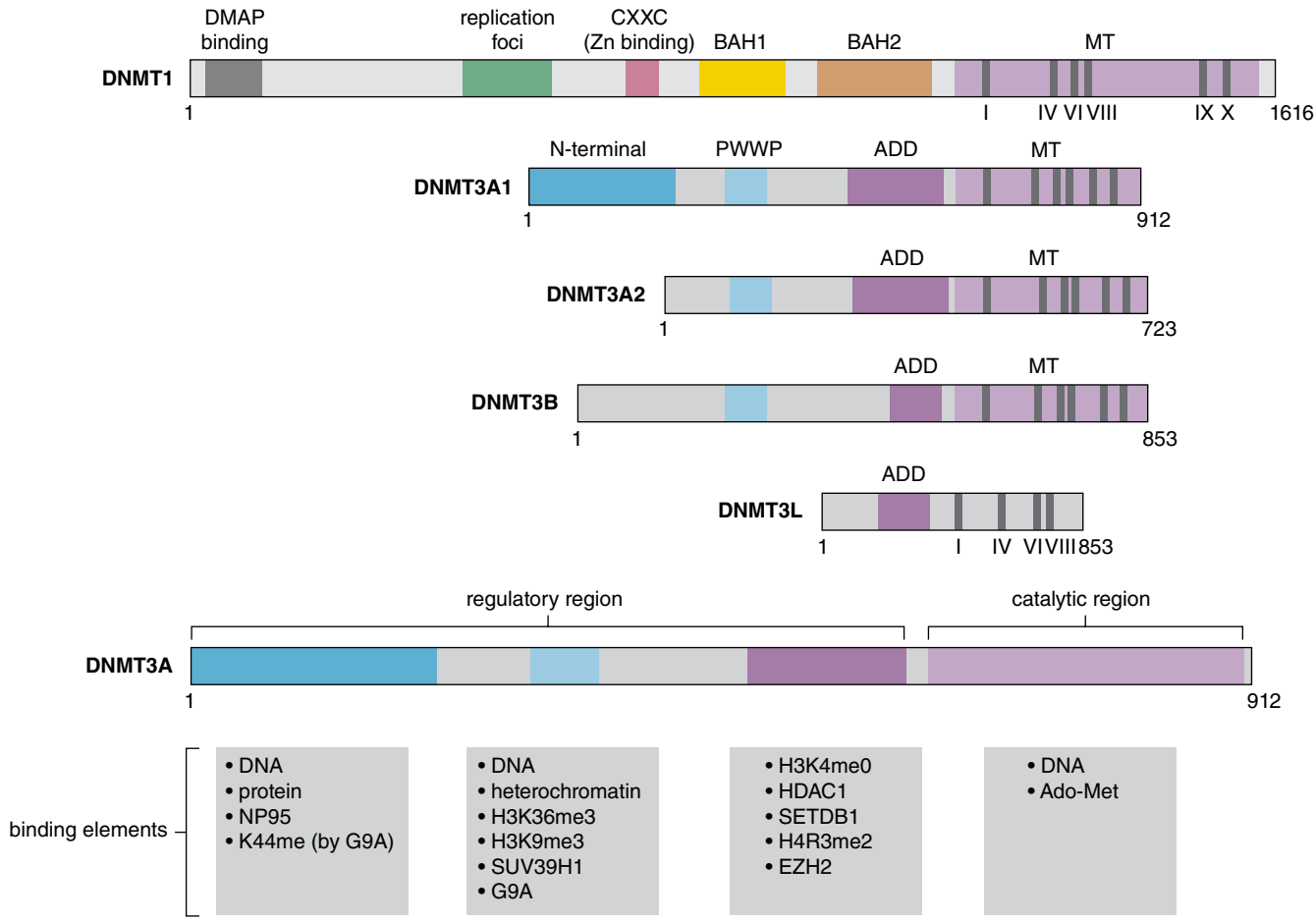

Fig. 1.26. DNA methyltransferase 1 (DNMT1), DNMT3A1, DNMT3A2, DNMT3B, DNMT3-like (DNMT3L), and major DNMT3A splice isoforms are depicted as boxes. Protein length is indicated as number of amino acids at the end of each protein. Each DNMT3A protein isoform has a modular structure, being composed of a mixture of protein domains. Each domain performs a different function. Domain abbreviations: ADD, ATRX-DNMT3-DNMT3L (related to the plant homology [PHD]-like domain of regulator ATRX); BAH, bromo adjacent homology domain; DMAP, DNMT1-associated protein; PWWP, Pro-Trp-Trp-Pro. MT is the catalytic methyltransferase domain, and I, IV, VI, IX, and X are motifs in the catalytic domain: motif I allows the binding of the methyl group donor AdoMet (*S*-adenosyl methionine). Motifs I and X are for cofactor binding and motifs VIII and IX are for DNA binding. The catalysis of DNA methylation occurs at the IV, VI, and VIII motifs. Source: Yang L, et al. *Nat Rev Cancer* 2015;15:152–165. Reproduced with permission of Springer Nature.

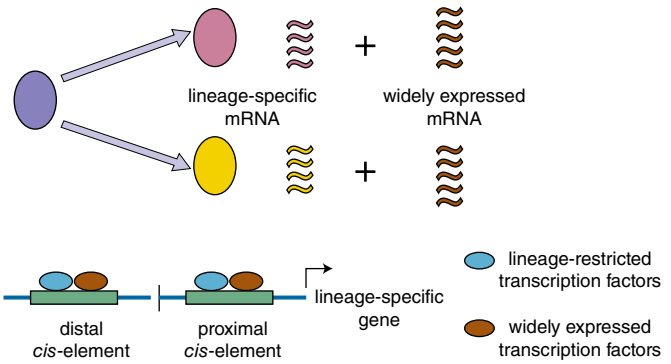

Fig. 1.27. A cardinal event in lineage specification is the expression of a program of lineage-specific gene expression. A multipotential cell (blue) differentiates into cells of two different lineages (pink and yellow). Although the phenotype of any cell, including cells of a specific lineage, is the sum of the lineage-specific and widely expressed RNAs, the specific phenotype of a lineage is a function of the lineage-specific RNAs. *Below*, Expression of a lineage-specific gene is controlled by DNA sequences (*cis*-elements) and widely expressed and lineage-restricted transcription factors. Thus, ultimately, one important element in regulating lineage specification is the complement of lineage-restricted TFs that are expressed and the transcriptional networks they control.

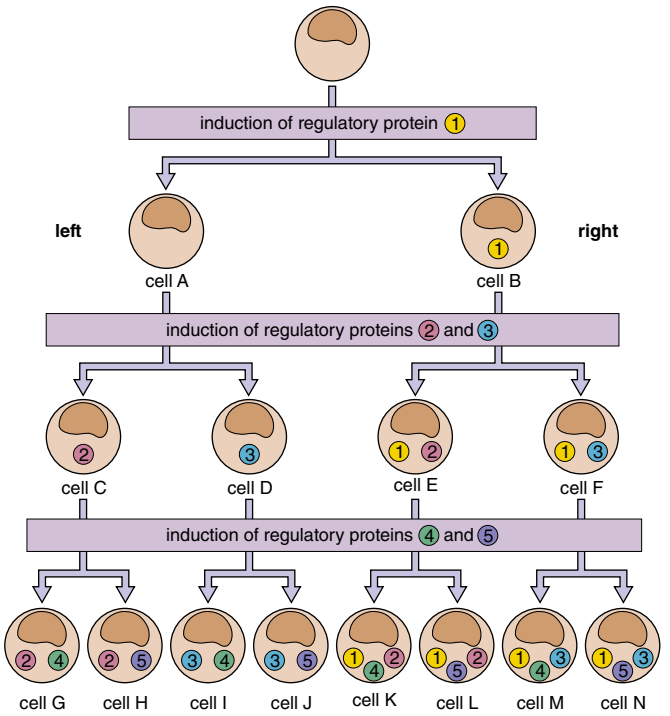

Fig. 1.28. This simplified diagram illustrates the principle that combinations of a limited number of critical regulatory proteins can generate different cell types (lineages) during development and adult life. Thus, in the embryonic life, the cell at the apex of the hierarchy and all its progeny divide asymmetrically such that the cell on the left always produces an even-numbered regulatory protein whereas the cell on the right produces an odd-numbered protein. The protein complement produced by a cell is then perpetuated by its progeny (cellular memory). In this simplistic scenario, five different regulatory proteins generate eight cell types (G to N). With continuation of this scheme, 10 000 cell types would be generated by only 25 different gene regulatory proteins.

types, it is critically required for expression of most of the genes associated with terminal maturation. Extrapolating this more broadly to hematopoiesis, accumulating evidence suggests that a small subset of critical hematopoietic TFs generate all blood cells by working in a combinatorial manner to direct lineage-specific programs of expression (Fig. 1.28). These TFs are not only crucial for normal blood cell programs but the genes encoding them are often a target of acquired mutation that leads to hematologic malignancy.

MICRO-RNAs

Over the last few decades a previously unrecognized class of RNAs, micro-RNAs (miRNAs), have been shown to play important biological roles in controlling expression of proteins in normal cells (Fig. 1.29). Micro-RNAs are encoded by RNA Pol II-transcribed genes to produce pre-miRNAs. These are processed initially in the nucleus and then in the cytoplasm. Here, mature 22 base pair miRNAs bind principally to the untranslated regions of mRNA transcripts leading either to mRNA degradation or repression of translation of mRNAs.

REGULATORY NONCODING RNAs

A relatively new class of RNA molecules have recently been shown to control gene expression and are collectively termed noncoding RNAs (ncRNAs). These include Piwi RNA (piRNAs) (Fig. 1.30A) and long noncoding RNAs (lncRNAs) (Fig. 1.30B). piRNAs are 26–31 nucleotides long and collectively are the most abundant ncRNAs in animal cells. Their roles are still being discerned in hematopoiesis and more generally in control of RNA and protein expression. To date, their clearest role is in epigenetic and translational silencing retrotransposons. The lncRNAs are the largest class of ncRNAs, usually between 200 and 400 nucleotides. It is estimated that there are 10 000–60 000 lncRNAs, a number far greater than protein-encoding mRNAs. The postulated roles of lncRNAs are set out in Fig. 1.30B. Some of these have been shown biochemically in cells and others *in vitro*.

Functional analysis of lncRNAs is in its infancy. It will be quite some time before we fully understand their physiological role and contribution to pathology. But it is likely that they will modulate a cell's response to its environment and in that regard contribute to the complexity of biological responses seen in hematopoiesis. This is likely become a very active area of research.

DNA REPLICATION AND TELOMERES

Every time a human cell divides, its 6 billion base pairs have to be faithfully replicated. This extraordinary task is accomplished daily in billions of cells, for the most part without deleterious consequence. When a cell enters the phase in cell cycle (S, synthesis phase, see later) where the genome is replicated, replication is initiated at multiple areas in the genome called replication foci. DNA replication then proceeds in a semiconservative manner, meaning that the two DNA strands in a double helix separate, are individually replicated, and the resulting two double helices segregate into daughter cells (Fig. 1.31). Thus, each daughter cell has a strand of newly synthesized DNA and a strand from the parental cell. Given that DNA polymerase, the enzyme that replicates DNA, does so in a 5′ to 3′ manner, only one strand is replicated continuously (the leading strand) whereas the other strand has to be replicated in short fragments (Okazaki fragments) (Fig. 1.31B,C). For the lagging strand a number of additional steps are required to ligate the discontinuous Okazaki

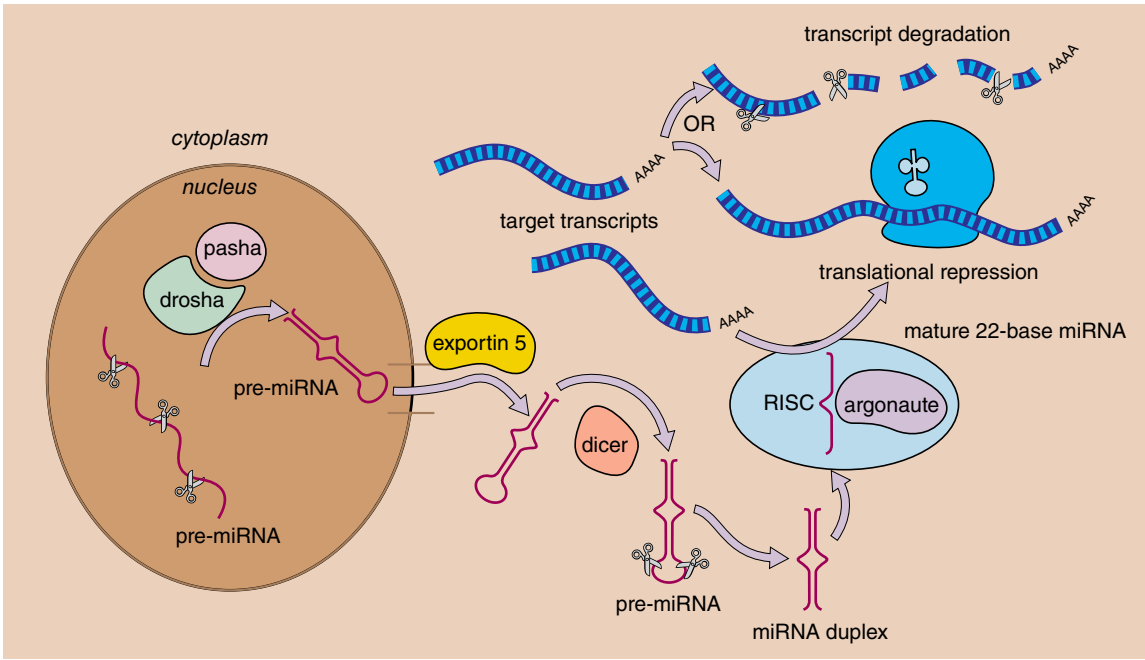

Fig. 1.29. An important class of molecules that regulates gene expression are micro-RNAs (miRNAS). A simplified diagram illustrates how miRNAs are produced and how they regulate miRNA and protein levels. Most miRNAs are expressed from RNA polymerase II-regulated genes as pre-miRNAs. This is cleaved by a nuclear RNase III Drosha and its partner protein DGCR8 Pasha into 50–80 base pair stem–loop pre-miRNAs. These pre-miRNAs are actively exported with the help of exportin-5 into the cytoplasm, where another nuclease, Dicer, excises them into 20–24 base pair mature miRNA duplexes. One of the two miRNA strands is then bound by the multiprotein complex called RNA-induced silencing complex (RISC), which contains, among other proteins, the protein argonaute (RISC/Argonaute). This strand can then repress gene expression by binding to mRNAs by partial sequence complementarity. Binding of mature miRNAs can either inhibit translation of mRNAs or target the mRNA for degradation.

fragments into a continuous DNA strand. DNA synthesized from multiple foci is then ligated together.

One special problem created by the semiconservative mode of DNA replication is the replication of the lagging DNA strand at the ends of chromosomes (Fig. 1.32). This is overcome by having repetitive sequences (called telomeres) at the ends of chromosomes that decrease with each round of replication. For cells that need to self-renew and maintain a high proliferative potential (e.g. germ and other stem cells), the enzyme telomerase can extend the repetitive sequences and compensate for loss at replication. Telomerase is a specialized ribonuclear protein complex composed of a RNA component called TERC that binds to the end of the leading strand and this is replicated by a specialized reverse transcriptase that is also a component of telomerase, called TERT. Loss of telomerase function leads to progressive telomere shortening and this can have catastrophic consequences for cell viability and can lead to transformation of the cell (Fig. 1.33). The degree of maintenance of telomeres determines the number of generations a cell can produce and is often increased above normal in malignant cells. This is discussed further in Chapter 12, where the importance of telomeres in human is elegantly demonstrated by acquired and germline mutations in the patients with dyskeratosis congenita and aplastic anemia.

MUTATIONS AND HOW THEY RESULT IN DISEASE

During DNA replication, errors in fidelity can lead to single base changes (Fig. 1.34A) that will create allele-specific changes in DNA sequence composition that are known as single-nucleotide polymorphism (SNPs) or single-nucleotide variants (SNVs).

If SNVs occur in coding sequence they can either be silent or result in mutation with a functional consequence (Fig. 1.34B). The single-nucleotide missense substitution of a T to G in the sixth codon of the β-globin gene that changes a glutamic acid to valine to produce a βs globin allele (a sickle β-globin allele) is an example of a pathogenic SNP. Due to selective pressure, multiple such functional missense mutations can be detected, even in a single gene such as β-globin or G6PD (Fig 1.34C) (see Chapter 8), producing a large of number of alleles associated with disease.

When SNVs occur in nongeneic parts of the genome they can either have no consequence or potentially alter the regulation of a key gene if the SNV occurs in *cis*-elements (promoters or enhancers) or creates a new *cis*-element, thereby altering the DNA binding of TFs, leading to altered gene expression (Fig. 1.34D). One example of this is mutations that promote expression of the TF SCL/TAL1 or c-myc by promoting its aberrant expression in T-cell acute lymphoblastic leukemia. More examples like this are now coming to light from SNV association studies.

DNA replication errors can also lead to translocation of chromosomes (Fig. 1.35). This is one of the most common karyotypic abnormalities in hematologic malignancy, which affects the expression of the gene either quantitatively (especially frequent in acute lymphoblastic leukemia) or qualitatively. Pathologically important translocations often lead to production of fusion transcripts where the genes at the sites of translocation produce proteins of altered function. For example, BCR-ABL in chronic myeloid leukemia, PML-RARA in acute promyelocytic leukemia (APML or AMLM3), or PBX-EHA in pre B-ALL (see Chapters 13 and 14). Translocation can also cause disease by altering gene expression with pathologic consequences by

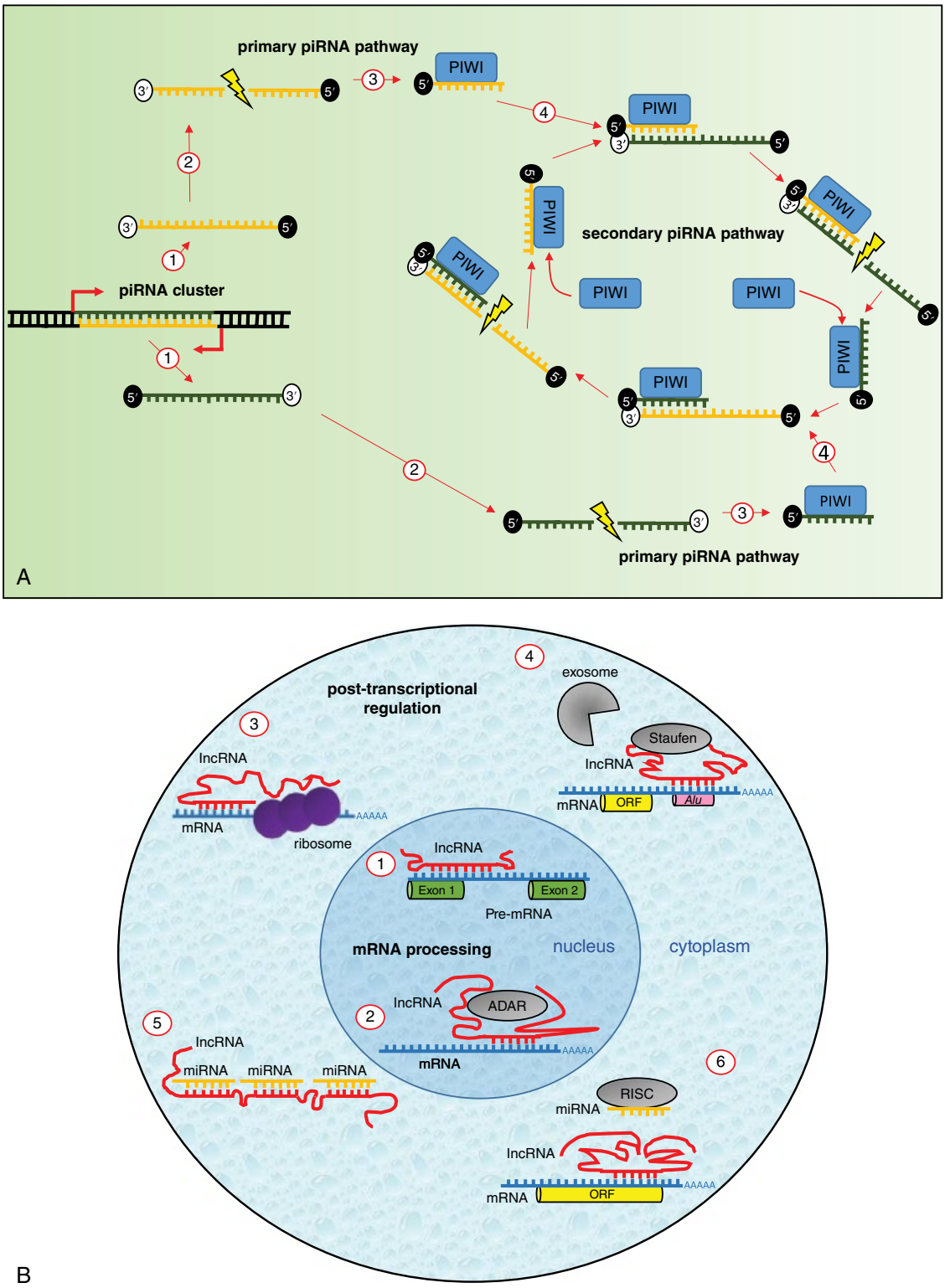

Fig 1.30. A, PIWI proteins and piRNAs regulate expression of genes and transposons at both transcriptional and post-transcriptional levels. *Step 1*, Sense and antisense piRNA precursor transcripts are transcribed from piRNA clusters in the nucleus. *Step 2*, piRNA precursor transcripts are exported to the cytoplasm and processed by the primary biogenesis pathway to generate mature sense piRNAs. *Step 3*, Mature piRNAs consisting of the 5′ end of the precursor then associate with PIWI proteins to enter the secondary piRNA pathway. *Step 4*, The PIWI:piRNA complexes associate with the complementary sequence in unprocessed precursor piRNA (or transposons and protein-coding transcripts) and mediate cleavage. The resulting cleaved 5′ end of the piRNA precursors is taken up by another PIWI protein and the precursor (or transposon or protein-coding transcript) is silenced. This process is known as the ping-pong cycle. PIWI–piRNA complexes interact with polysomes; mRNA cap-binding complex (CBC), P-body components, and piRNAs are mapped to the 3′ UTR of mRNAs. The PIWI–piRNA complexes can enter the nucleus and regulate gene transcription through epigenetic mechanisms including heterochromatin formation and DNA methylation. **B,** The roles of lncRNA in mRNA processing and post-transcriptional regulation. Within the nucleus, lncRNA modulates mRNA processing in one of two ways: (1) mRNA is bound at regions overlapping exon:intron boundaries. (2) lncRNA recruits mRNA-editing enzymes, such as adenosine deaminase (ADAR), to complementary mRNA sequences. In the cytoplasm, lncRNA regulates post-transcriptional events through at least four distinct mechanisms: (3) Recruitment of post-transcriptional machinery to mRNA due to possession of sequence-specific domains, such as SIN EB2 repeat elements that have affinity for ribosomes. (4) lncRNAs that contain Alu repeat elements associate with Alu elements in the 3′ UTR of mRNA, which recruits Staufen to induce mRNA degradation via RNA exosomes. (5) Linear or circular lncRNAs can serve as molecular sponges to sequester miRNAs from their target sequences. (6) lncRNAs can mask sequences in mRNA that would serve as targets for miRNAs bound to RNA-induced silencing complex (RISC). Source: Wilkes MC, et al. *Mol Genet Metab* 2017;122(3):28–38. Reproduced with permission of Elsevier.

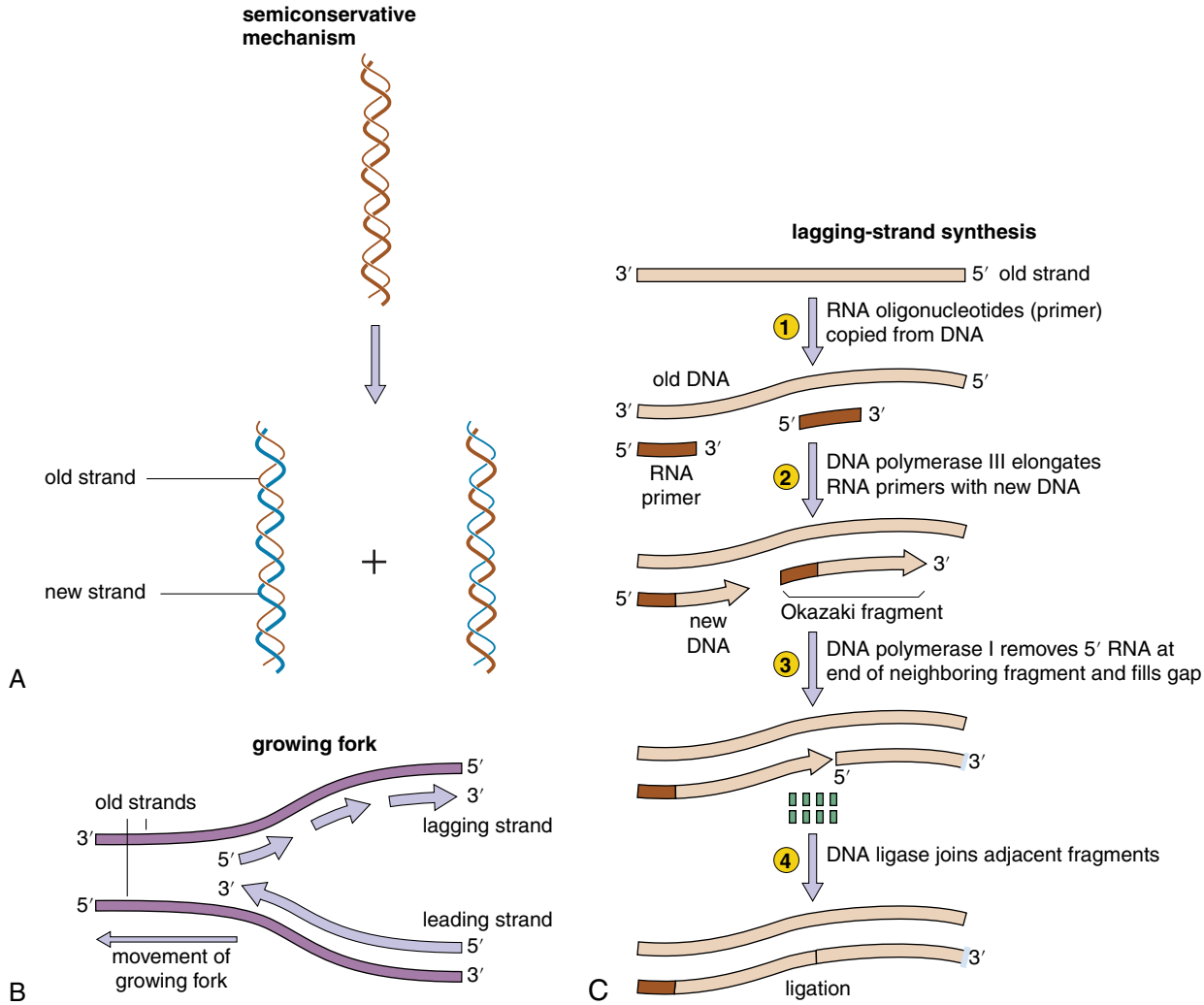

Fig. 1.31. DNA replication is semiconservative. **A,** The parental DNA is composed of two strands. During replication each parental strand acts as a template for replication, and thus progeny strands contain one new strand and one old strand. **B,** DNA replication is initiated at origins of replication, and as replication proceeds the parental strands separate and a replication fork forms. DNA is synthesized from a 5′ to 3′ direction, and this creates two types of strands of newly replicated DNA. One strand, called a leading strand, is continuously synthesized by DNA polymerase III by sequential addition of deoxyribonucleotides in the same direction as the movement of the replication fork (the bottom strand in this figure). In contrast, the other newly synthesized strand is made discontinuously (top strand) and is known as the lagging strand. **C,** Synthesis of the lagging strand requires multiple steps. First, multiple RNA oligonucleotides (primers) are synthesized from parental DNA strand templates. These serve to prime synthesis of fragments (called Okazaki fragments) of the new (lagging) strand. DNA polymerase I then removes the RNA primers, fills in the gaps with DNA, and finally DNA ligase joins adjacent DNA fragments.

altering the cell fate of hematopoietic stem/progenitor cells (Fig. 1.36). Control of cell fate is more extensively discussed in Chapters 2 and 3.

CELL CYCLE

One critical determinant of cell fate is whether cells enter the cell cycle. Although much is known about the molecular controls and cell biology of the cell cycle, we are still unearthing the complexity of how decisions are made on whether cell cycles are linked with external cues, the cellular history of the cell, and the cell compartment a cell is in (i.e. stem cell or progenitor cell).

The cell cycle is divided into phases (Fig. 1.37A and C). There is cyclic synthesis of DNA (S phase), a pause known as G_2, followed by chromosome condensation, nuclear envelope breakdown and chromosome segregation. This leads to chromosome decondensation, nuclear envelope reformation and cytokinesis terminating in separation of two daughter cells (mitosis or M phase). A critical set of proteins that control passage through cell cycle are the cyclins, the expression of which differs throughout the cell cycle by periodic changes in synthesis and degradation (Fig. 1.37B). They activate a set of protein kinases (CDKs) (Fig. 1.37B), which then phosphorylate various proteins. Phosphorylation of the retinoblastoma susceptibility gene product RB prevents RB from blocking the TFs (e.g. E2F), which is essential for transition from the G_1 to the S phase of the cell cycle. The cyclin/CDK complexes are regulated by inhibitors. Thus, cyclin D–CDK4 and cyclin D–CDK6 complexes are inhibited by a 16 kDa protein encoded by the *INK4a* gene and a 15 kDa protein encoded by the *INK4b* gene, inhibiting progress from mid to late G_1.

The *TP53* gene codes for a 53 kDa transcription control factor that mediates a block in the cell cycle at the G_1–S phase boundary).

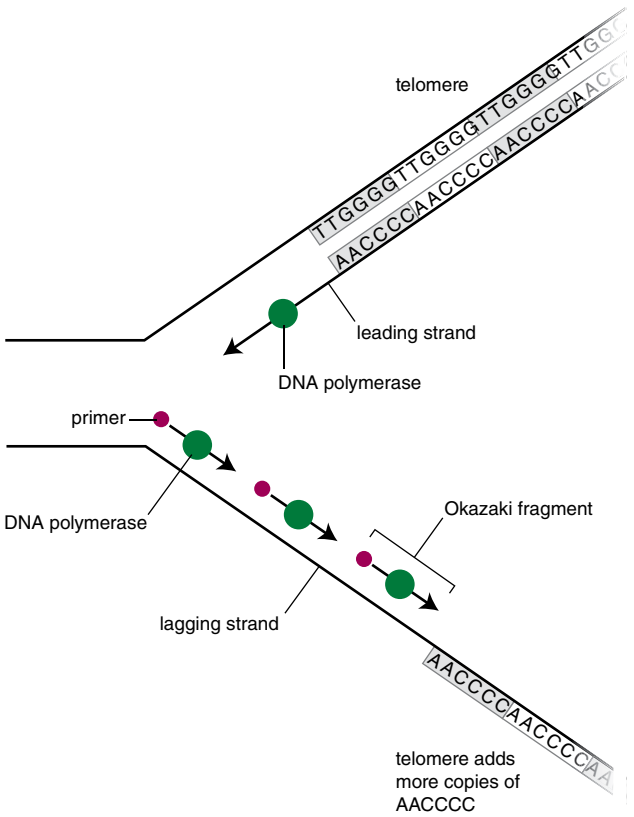

Fig. 1.32. Replication of the ends of chromosomes requires specialized structures called telomeres. Telomeres are DNA sequences composed of a motif that is repeated. In humans the repeat DNA motif is "TTGGGG" on one strand and "AACCCC" on the other. The leading strand is shown on the upper fork. The DNA polymerase (green circle) is replicating DNA. On the lagging strand a primer sequence allows short Okazaki fragments to be made. The telomere is then replicated on both strands by a specialized RNA–protein complex called telomerase.

This is mediated by a p21 cyclin CDK inhibitor, p21CIPI. Expression of p53 is induced by DNA damage that results from radiation or drugs. The cell is therefore held up in G_1 to allow the cell to repair the damage. If the damage is extensive, p53 induces apoptosis by increased expression of proapoptotic gene *BAX*. This is not the only example of how progression through cell cycle and response to external cues (in this case DNA damage) are linked with another cell fate choice option, namely apoptosis.

APOPTOSIS

Cell death can occur by necrosis or by a physiologically active mechanism (apoptosis, programmed cell death) (Fig. 1.38). Necrosis occurs in response to ischemia, chemical trauma, or hyperthermia. It affects many adjacent cells, and is characterized by cell swelling, with early loss of plasma membrane integrity and swelling of organelles and nucleus. There is usually an inflammatory infiltrate of phagocytic cells in response to spillage of cell contents into surrounding space.

Programmed cell death occurs by an active process that requires calcium ions. Nuclear condensation, nuclear fragmentation, and cytoplasmic vacuolation occur early, with later changes in the organelles and plasma membrane (Fig. 1.39). Apoptosis also involves digestion of cell DNA by an endonuclease to produce on a gel a ladder of regular bands 180 base pairs apart. Cleavage occurs by double-stranded breaks on linker regions between nucleosomes. The final part of the apoptosis pathway involves caspase enzymes. The executioner caspase 3 cleaves a restricted set of cellular proteins, including polyadenosine diphosphate–ribose polymerase, laminin, and gelsolin (Fig. 1.39). Caspase 3 is activated by caspase 9. This in turn is activated by the apoptotic protease 1 (APAF-1), which itself is activated by cytochrome *c*. Cytochrome *c* is released from mitochondria when the proapoptotic protein BAX is in excess and forms homodimers. Cells are protected from apoptosis by BCL-2, which binds to BAX and

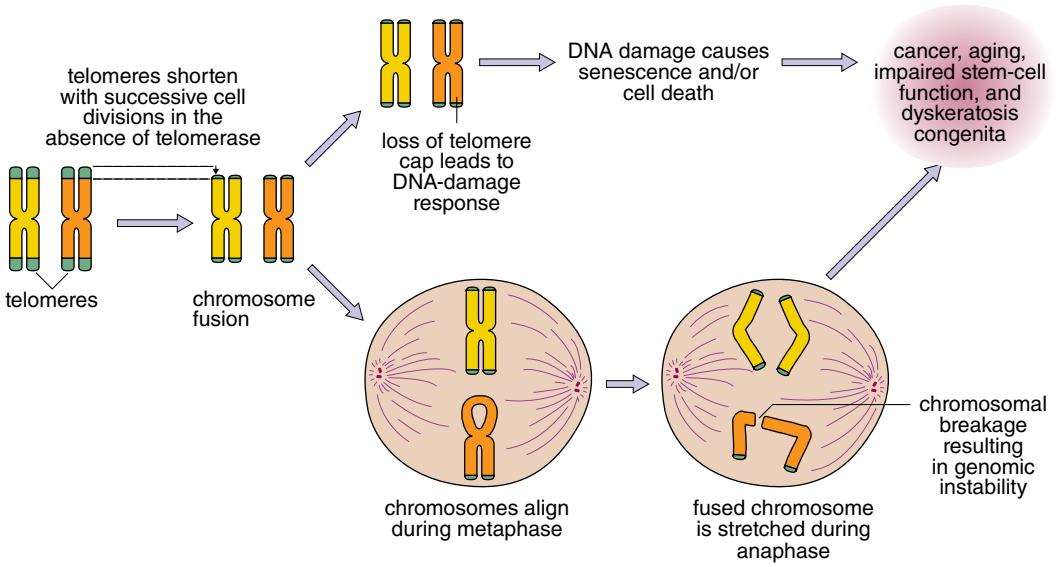

Fig. 1.33. The enzyme complex telomerase is essential for maintaining telomere length, and this is critical for chromosomal and cell viability. Lack of telomerase activity leads to telomere shortening with successive cell division. This can activate DNA damage responses and lead to cell senescence and cell death. Alternatively, telomere shortening can precipitate chromosomal fusion, and genomic instability. A specific condition associated with impaired telomerase activity is dyskeratosis congenita (see Chapter 12), in which children and young adults can have hematopoietic stem cell failure and leukemia. More generally, impaired telomere function has been implicated in many cancers and aging.

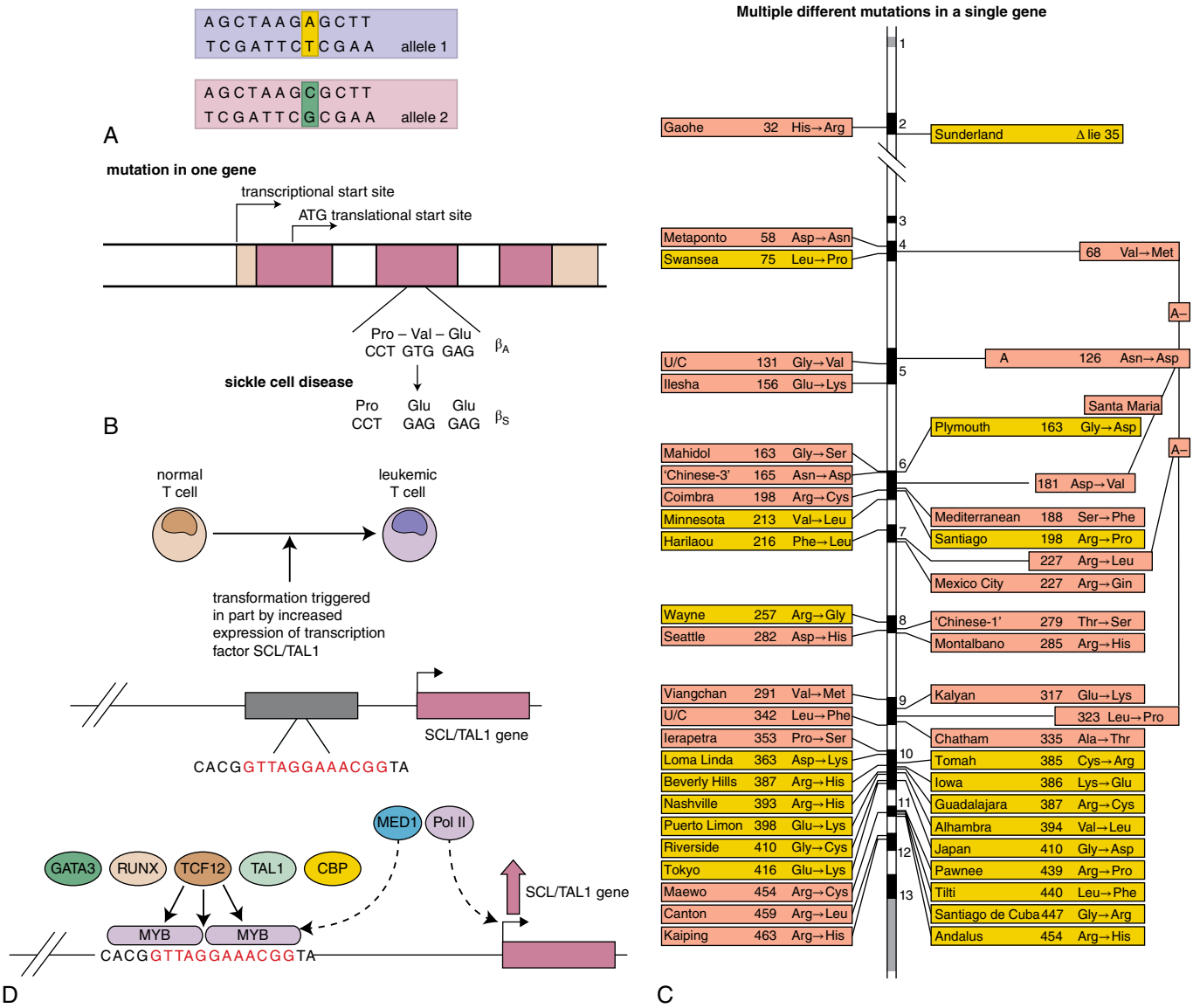

Fig 1.34. Errors in DNA replication or the maintenance of the methylated state of CpG residues can change DNA sequence. **A,** When the DNA sequence change occurs at single nucleotide it is known as a single-nucleotide polymorphism (SNP). In this example, the "A" residue on allele 1 is changed to a "C" residue on allele 2. **B,** When SNP occurs in a coding sequence it can alter the protein sequence. In this example, a "T" residue at the sixth codon in exon 2 of the human β-globin gene is changed to an "A" residue. This changes a valine (val) to glutamic acid (glu). This results in a β-sickle allele. In the homozygous state this causes sickle cell disease (see Chapter 9). **C,** Mutations can occur at multiple positions in the gene. In the glucose-6-phosphate dehydrogenase (*G6PD*) gene, many different mutations cause G6PD deficiency. These may cause drug sensitivity (pink) or more rarely chronic nonspherocytic hemolytic anemia (NSHA) (yellow). The exons are shown as black bands except exon 1, which is noncoding and shown in gray. Source: C, Adapted with permission from Vulliamy TJ et al. Molecular basis of glucose-6-phosphate dehydrogenase deficiency. *Trends Genet* 1992;8:138–143. **D,** Nucleotide changes can also occur in DNA sequences that control RNA expression of a gene. In this example, the gene encoding the important blood transcription factor SCL/TAL1 is shown as a pink box on the left. 5′ of the gene a sequence "GTTAGGAAACGG" has been erroneously inserted (shown as pink letters) and this creates a new binding site for transcription factor MYB. MYB, in turn, attracts the additional transcription factors GATA3, RUNX1, TCF12, TAL1 itself, and CBP. This transcription factor complex works with the general transcription factor MED1 and RNA polymerase II (Pol II) to increase transcription of SCL/TAL1, which is oncogenic. This situation is seen in human T-cell acute lymphoblastic leukemia (see Chapter 14). Source: Vulliamy TJ, et al. *Trends Genet* 1992;8:138–143. Reproduced with permission of Elsevier.

thereby inhibits cytochrome *c* release and caspase activation. Apoptosis is promoted by BAD, which forms heterodimers with BCL-2. Apoptosis may also be stimulated by direct DNA damage (e.g. by radiation or drugs) or by withdrawal of a growth factor (e.g. interleukin 3 [IL-3]). When IL-3 is present it promotes cell survival in IL-3-responsive cells by stimulating protein kinase B to phosphorylate BAD, thus preventing its association with BCL-2.

ORGANELLES IN CELLS

MITOCHONDRIA

Mitochondria are complex organelles that are the main sites of ATP production (Fig. 1.40A,B) during aerobic metabolism, important for heme biosynthesis (see Chapter 5) and finally play a role in apoptosis. They are among the largest organelles and can comprise up to 25% of the cellular volume. They are

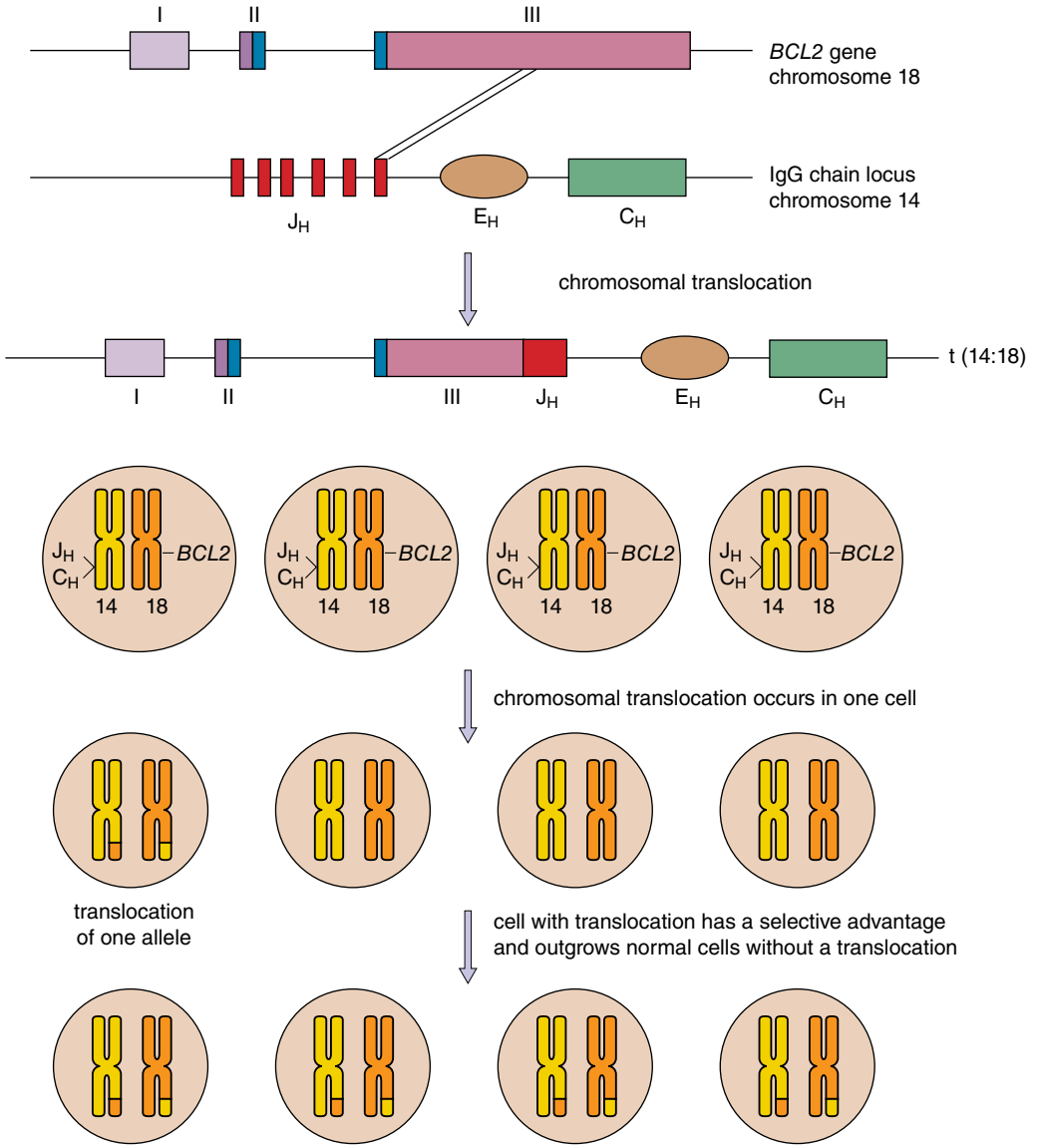

Fig. 1.35. Chromosomal translocation can lead to disease-causing mutation. In this example, the *BCL2* gene on chromosome 18 is involved in a translocation with the Ig heavy chain locus on chromosome 14. In this case the translocation breakpoints are inside the genes and give rise to a fusion transcript. Acquisition of this translocation provides a selective advantage to cells.

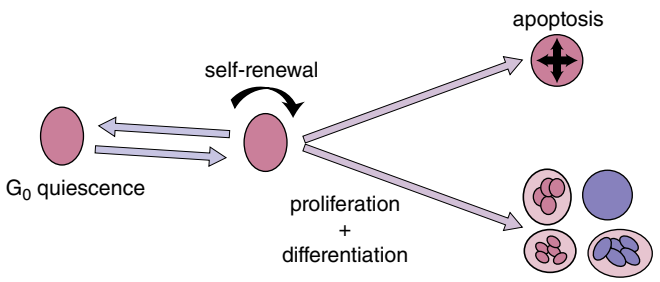

Fig. 1.36. Schematic showing the cell fate choices available to a hematopoietic stem/progenitor cell.

composed of two structurally and functionally distinct inner and outer membranes. The inner membrane has a large number of invaginations or cristae that protrude into the central space or matrix of the mitochondria. The complex biochemical pathways that produce ATP from aerobic metabolism of glucose (via pyruvate produced by the glycolytic pathway) can result in up to 34 molecules of ATP for every molecule of glucose. This involves phosphorylation and oxidation. Fatty acids can also be metabolized to CO_2 to generate ATP. Metabolism of pyruvate and fatty acids generates NADH and $FADH_2$ molecules that are oxidized to NAD^+ and FAD, and the resulting protons are pumped across the inner mitochondrial membrane. ATP generation is powered by the resulting proton-motive force. Thus, it is easy to see why mitochondria are required to provide energy for a cell.

LINK BETWEEN METABOLISM AND GENE EXPRESSION

It is being increasingly appreciated that cellular energetics is a vital consideration in the maintenance of tumor cell viability. This is as true for blood cancers as for other cancers. At least two broad mechanisms operate. First, by-products of

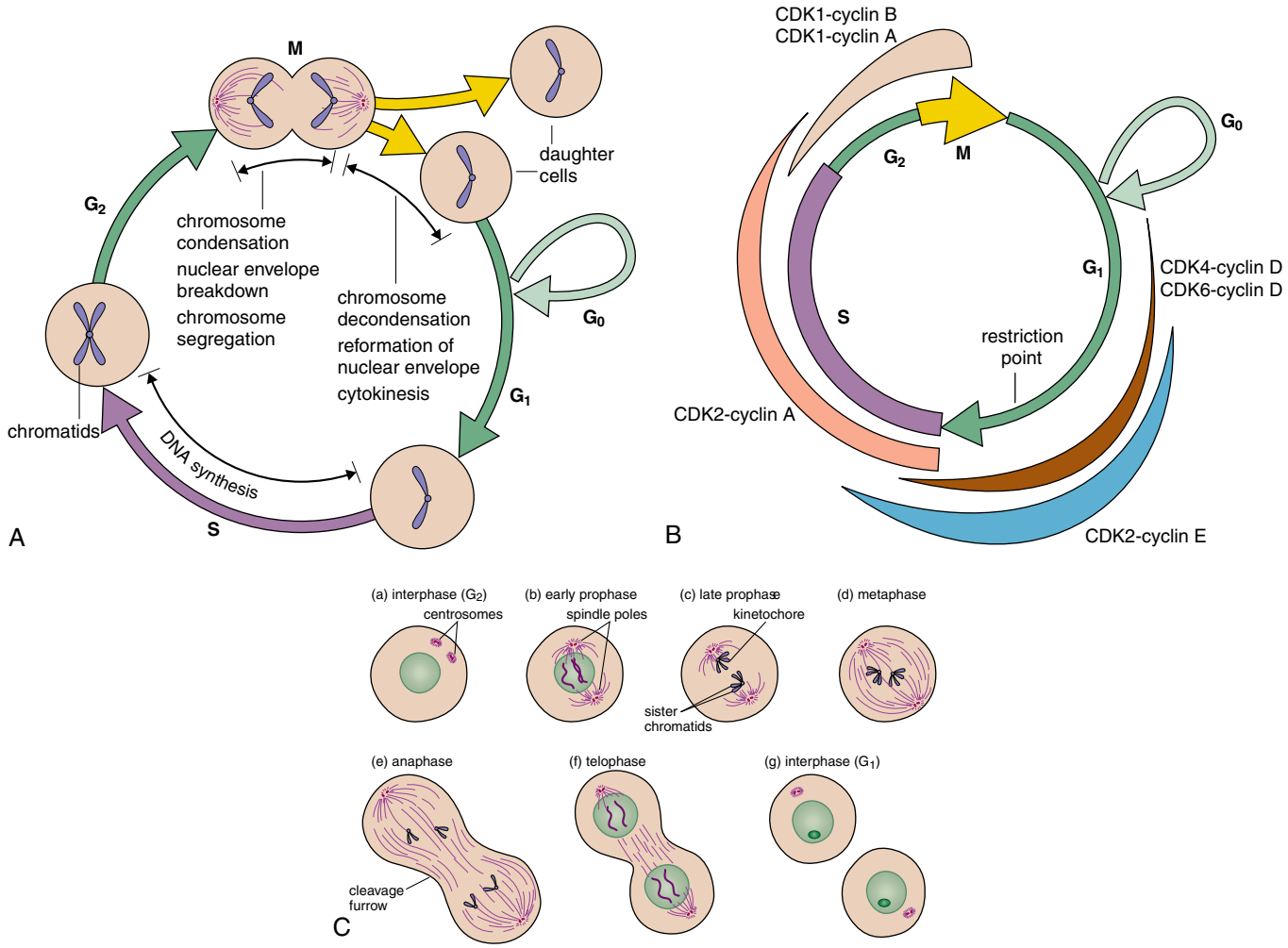

Fig. 1.37. A, Schematic representation of the cell cycle. Quiescent cells ("G_0") enter the cycle in "G_1" and progress to synthesize DNA in the "S" phase. In the G_2 phase cells have 4*n* DNA content and this leads to mitosis "M." The G_1, S, and G_2 phases collectively are known as interphase. Although chromosomes are condensed only in mitosis, they are shown here in condensed form throughout the cell cycle to emphasize the numbers of chromosomes at different stages in the cell cycle. **B,** Passage through the cell cycle is, in part, regulated by proteins that themselves cycle. These include the cycle-dependent kinases (CDKs) that are physically associated (i.e. are a complex) with proteins that regulate them, called cyclins. Different combinations of CDKs and cyclins are required to progress through different stages of the cell cycle. Thus CDK2–cyclin E complex is important in G_1. Critical regulatory points in the cell cycle are called restriction points, and the location of the G_1 restriction point is shown. **C,** During the cell cycle a key facet is the proper separation of sister chromatids (generated in "S" phase). (a) In late G_2, structures called centrioles are replicated. (b) In early prophase, chromosomes and associated centrioles move to cell poles. Now the chromosomes start to condense and can be seen as threads. The nuclear membrane begins to disaggregate. (c) In late prophase, chromosome condensation is complete. The chromosome centromeres are visible, and they progressively move to the pole and microtubular spindle fibers connect the centromeres to the poles of the cell. (d) In metaphase, chromosomes move to the cell equatorial plane. (e) In anaphase, the sister chromatids separate into independent chromosomes. Each centromere is connected to the pole by a spindle fiber and moves to the pole. Simultaneously, the cell elongates. Cytokinesis begins and cleavage furrows appear. (f) In telophase, new nuclear membranes are seen and chromosomal decondensation starts. The cells now reenter G_1 and interphase. (g) Interphase.

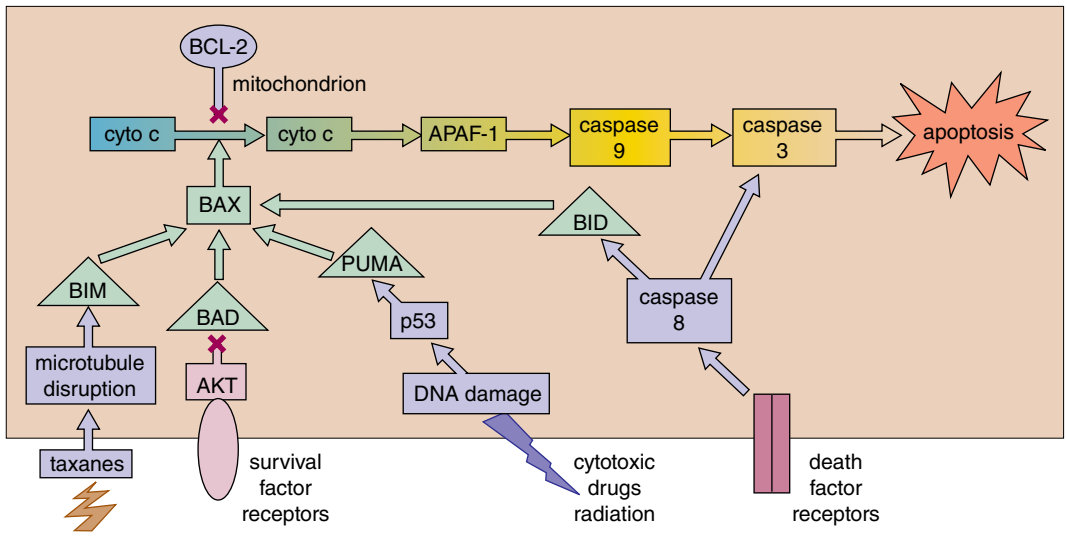

Fig. 1.38. This simplified diagram shows key elements of the pathways that lead to caspase 3 activation and apoptosis. A number of stimuli can activate the pathway. See text for details.

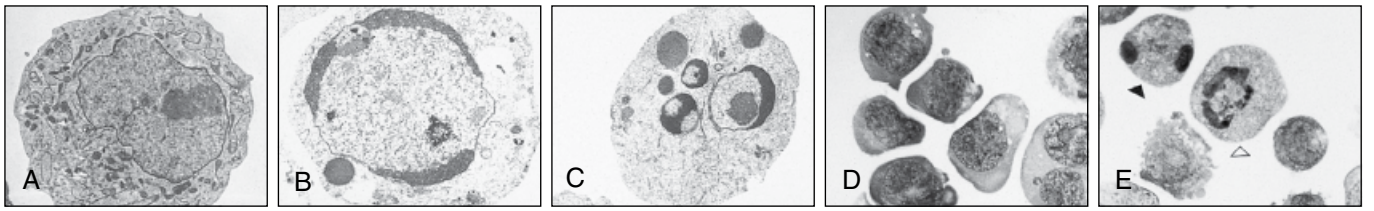

Fig. 1.39. Apoptosis: **(A–C)** electron microscopic and **(D, E)** light microscopic appearances. **A,** Normal K562 cell line. **B,** Early apoptotic cell showing chromatin condensation at the nuclear periphery. **C,** Later apoptotic cell showing both chromatin condensation and nuclear fragmentation. **D,** Normal K562 cell line. **E,** Early apoptotic cell (open arrowhead) with peripheral chromatin condensation and late apoptotic cell (solid arrowhead) with both chromatin condensation and nuclear fragmentation. Source: Riordan FA, et al. *Oncogene* 1998;16:1533–1542. Reproduced with permission from Springer Nature.

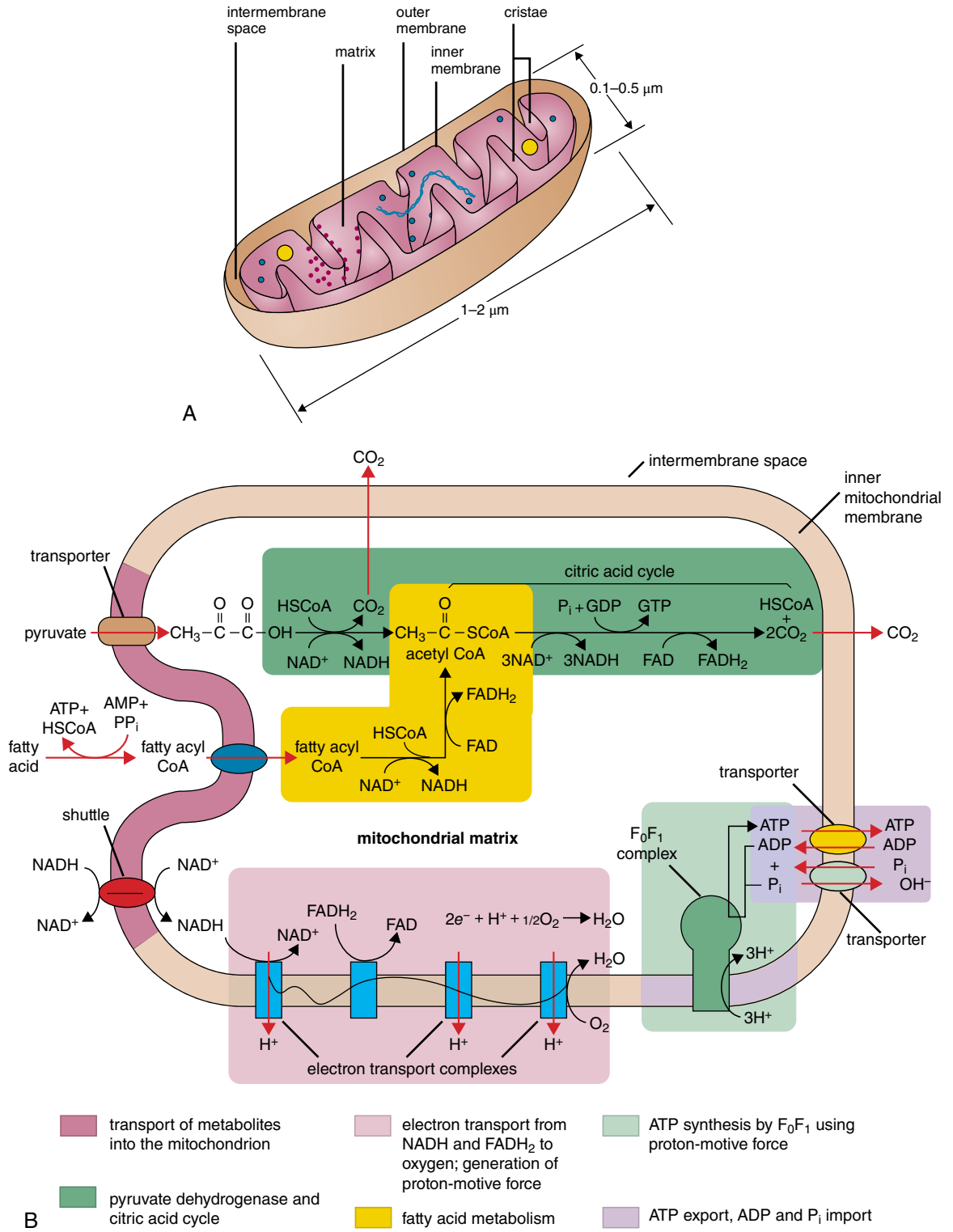

Fig. 1.40. A, Three-dimensional schematic diagram of a mitochondron cut longitudinally. The ATP-producing complexes (F_0F_1, red cell dots) are located on the inner membrane protruding inward. Mitochondrial DNA (blue), ribosomes (blue circles), and granules (yellow dots) are shown. **B,** Summary of aerobic oxidation of pyruvate illustrates some of the complexity of the biochemistry within the mitochondria.

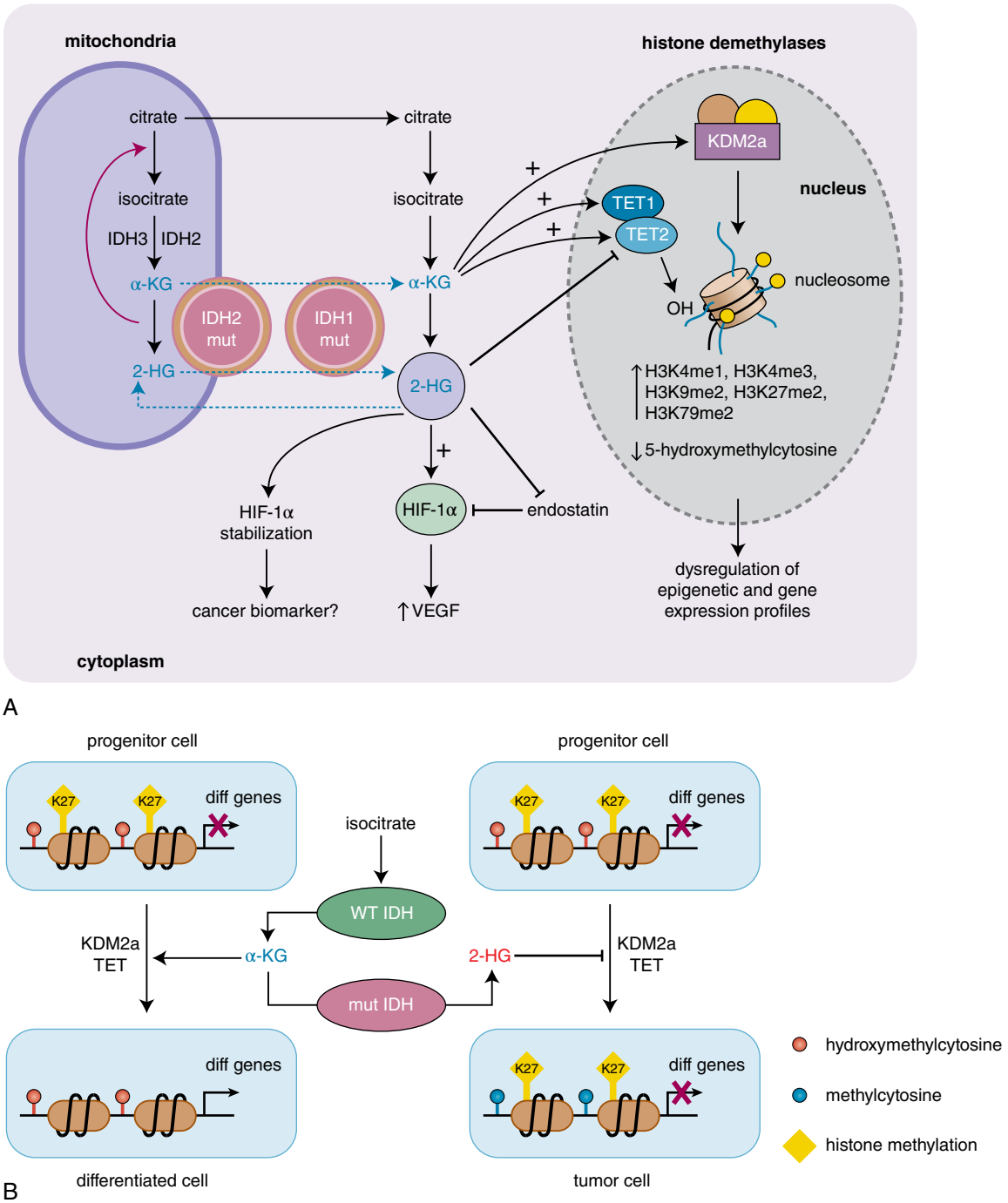

Fig 1.41. Cellular energetics and gene expression are linked. Here, we show one example of this. **A,** As part of the Krebs cycle, citrate is converted to isocitrate, which in turn is converted to α-ketoglutarate (α-KG) by the enzymes isocitrate dehydrogenase (IDH). There are three isoforms of IDH (IDH1, IDH2, and IDH3). IDH2 and IDH3 are located in the mitochrondria and IDH1 is cytoplasmic. α-KG is a required cofactor for the enzymes that modify histones (e.g. histone demethylases KDM2a) and demethylate DNA (TET1 and TET2). Mutations in IDH1 and IDH2 are found in myeloid cancer (see Chapter 14). Mutant IDH1 and IDH2 convert α-KG to the oncometabolite 2-hydroxyglutarate (2-HG). 2-HG inhibits histone demethylases and TET1 and TE2, thus antagonizes α-KG function. Furthermore, 2-HG promotes a cell's adaption to hypoxia (often seen in cancers) by promoting expression of HIF-1α. **B,** This deregulates histone and DNA methylation, alters gene expression, and promotes oncogenesis by stalling differentiation and promoting proliferation. A progenitor cell is shown on top on both left- and right-hand sides. Normally, α-KG would activate histone demethylase KDM2A and DNA TET demethylases. This removes methyl groups on histone H3K27 (which repress transcription) and keep cytosine residues as either cytosine or hydroxymethylcytosine. Both these epigenetic marks are permissive for transcription allowing expression of genes, for example those associated with differentiation. In contrast, 2-HG blocks TET and KDM2A enzymes, resulting in continued histone H3K27 methylation and cytosine residues being methylated. Both of these epigenetic marks repress expression of genes required for differentiation and lead to differentiation block, which a hallmark of blood cancers.

metabolism control gene expression (Fig. 1.41). An example here is that 2-ketoglutarate, an intermediate of the citric acid cycle, is an essential cofactor of enzymes that regulate DNA methylation and histone modification. Similarly amino acid metabolism provides the methyl donors for DNA and histone methylation. The proteins mediating the links between metabolism and gene expression are mutated in blood diseases (see Chapter 13).

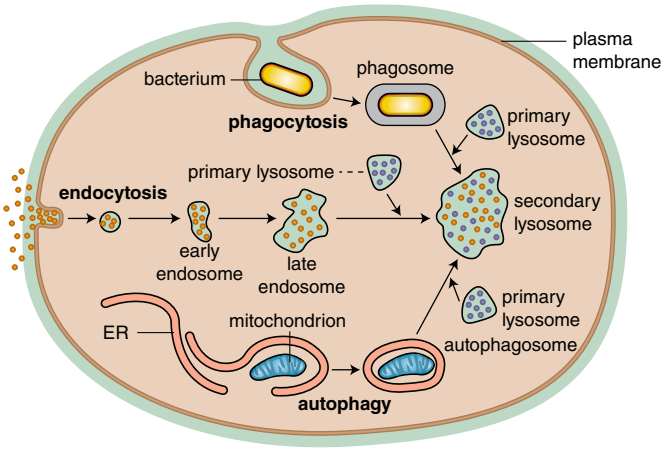

Fig. 1.42. Lysosomes degrade ingested extracellular particles (e.g. bacteria) and intracellular particles. Three main pathways deliver material to lysosomes: phagocytosis, endocytosis, and autophagy

REMOVAL OF CIRCULATING AND CELLULAR DEBRIS BY LYSOSOMES

Lysosomes are closed intracellular compartments composed of a single membrane that are responsible for degrading intracellular components no longer required for the cell's metabolism. Material is mostly taken up by a lysosome by three routes: phagocytosis, endocytosis, and autophagy (Fig. 1.42). Phagocytosis is when material is taken up into a membrane-bound phagosome. Endocytosis is the process by which small portions of the plasma membrane invaginate to form a small membrane-bound vesicle (endosomes). The endosomes is then combined with a primary lysosome to create a secondary lysosome. Secondary lysosomes can also form when primary lysosomes fuse with phagosomes. Finally, aged mitochondria are removed by a process known as autophagy, in which an autophagosome combines with a primary lysosome to make a secondary lysosome.

Lysosomes then release enzymes (termed acid hydrolases) that work at acid pH to denature the lysosome contents (e.g. proteins). There is an ATP-dependent pump that generates the acid pH and lysosomal enzymes work best in acid (pH 4.8) conditions and not in neutral cytosolic pH.

PROTEIN UBIQUITINATION

Ubiquitin (ubiquitous immunopoietic peptide) is a highly conserved 76-amino-acid 8.5 kDa peptide that is used to mark proteins for destruction. Ubiquinated proteins are targeted to the proteosome, which cleaves ubiquitin-tagged proteins in an ATP-dependent process to yield peptides and intact ubiquitin. Ubiquitin is added by a conjugating enzyme (ubiquitinating complex). First, ubiquitin is activated and bound to the enzyme E1 and then is transferred to the enzyme E2. E2 binds the ubiquitin ligases E3 (there are many different types of E3 ligase) (Fig. 1.43). The protein targeted for destruction is recognized by internal sequences. Successive conjugations of ubquitin moieties (at least four) usually to a lysine residue are required for proteosome targeting. The ubiquitin–proteosome pathway is a central process in controlling protein turnover in the cell. There are several hematologic diseases associated with this pathway, including forms of Fanconi anemia (mutations in genes for a large E3 ligase) and von Hippel–Lindau disease (mutations in genes for another E3 ligase). Furthermore, a widely used class of drugs in blood cancers (called ImiDs or CelMods) attach to ubiquitin E3 ligase to mark specific proteins for destruction (see Chapter 21).

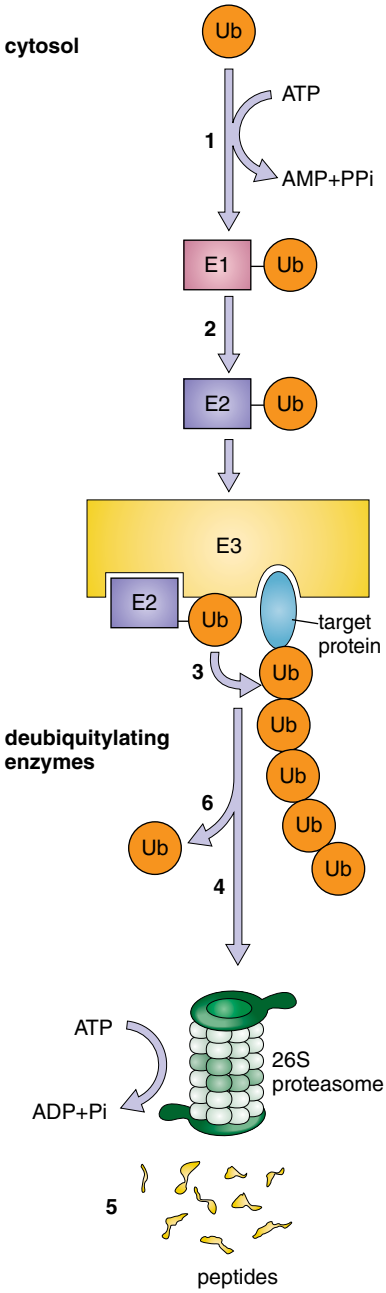

Fig. 1.43. Proteosomal degradation of cellular protein. Ubiquitin (Ub) is added to enzyme E1 (ubiquitin-activating enzyme) in an ATP-dependent process (1). Ubiquitin is transferred to protein E2 (ubiquitin–carrier protein) (2). This is then complexed to ubquitin ligase (3). E3 binds E2/ubiquitin and the target protein destined for destruction. This allows ubiquitin to be transferred to the polyubiquitin chain on the target protein. The polyubiquitinated protein is then proteolyzed in a 26S proteosome in an ATP-dependent process.

CHAPTER

2

HEMATOPOIESIS

SITES OF HEMATOPOIESIS

Hematopoiesis is the process by which blood cells are made. This occurs in waves and at multiple discrete anatomical sites that change through development (Fig. 2.1). In humans, as in other vertebrates, blood development occurs in three successive waves (Fig. 2.2). The first two waves (1 and 2) take place in the extraembryonic yolk sac and give rise to transient blood populations. The third wave (3) develops in the ventral wall of the intraembryonic dorsal aorta (Fig. 2.3) and gives rise to hematopoietic stem progenitor cells (HSPCs), providing the organism with lifelong blood production. Wave 1 produces primitive red blood cells (expressing embryonic globins) (Chapter 9) that deliver oxygen to tissues in the rapidly growing embryo, megakaryocytes, and macrophages (Fig. 2.4). Waves 2 and 3 give rise to definitive multipotent erythro-myeloid progenitors (EMPs) in the yolk sac and HSPCs in the dorsal aorta, respectively. Additional hematopoietic activity can also be detected in the embryo in the umbilical arteries, allantosis, and placenta. It is still a matter of much debate whether HSPCs arise from the dorsal aorta in the embryo proper or by colonization from the yolk sac. It is also unclear if HSPCs from the dorsal aorta migrate and colonize the other embryonic sites or whether they arise de novo at these other sites.

Waves 2 and 3 produce a highly specialized endothelium, referred to as hemogenic endothelium, from which HSPCs bud in a process known as the endothelial-to-hematopoietic transition (EHT) (Fig. 2.5). This is consistent with the hypothesis, first framed 100 years ago, of an endothelial origin for blood cells. EMPs and HSPCs subsequently migrate to and differentiate in the fetal liver, spleen, thymus, and ultimately bone marrow (Fig. 2.1).

It is thought that dorsal aorta hematopoietic stem cells (HSCs) (or possibly yolk sac HSCs) migrate to the fetal liver. In the fetal liver, expansion and differentiation of HSCs allows for development of definitive red cells, myeloid cells, and lymphoid cells (T cells that develop in the thymus and B cells in the marrow).

Bone marrow also contains cells other than blood cells. In development, blood cells arise from mesoderm (Fig. 2.6A). Meosderm contains many different lineages including blood, cardiac, and paraxial (muscle, cartilage, fat, and fibroblastic stroma cells). Thus, bone marrow (with its mesodermal origins) contains multipotential cells that are poorly defined called mesenchymal stem cells (MSCs) that can produce a variety of

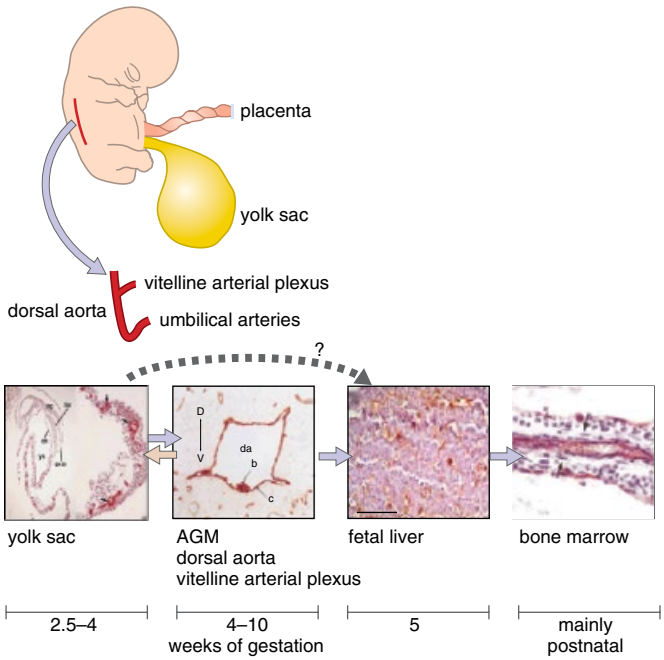

Fig. 2.1. Changing anatomic locations of hematopoiesis through development. Hematopoiesis is initially detected in the extraembryonic yolk sac in a region known as the aorta–gonad mesonephros (AGM) in the embryo, the placenta, the umbilical arteries, and vitelline vessels. It then shifts to the fetal liver and finally to the bone marrow. See text for further details.

mesenchymal cell types: osteoblasts (to make bone), chrondocytes (to make cartilage), connective and synovial tissue (to make tendon), and possibly skeletal muscle (Fig. 2.6B–E). There is active research into these and other mesoendodermal bone marrow cell populations as they provide the prospect that bone marrow could be used to purify and expand these populations for therapeutic benefit.

ROAD MAPS OF HEMATOPOIESIS

CELLULAR PATHWAYS AS HSCs DIFFERENTIATE INTO TERMINALLY MATURE CELLS

At the apex of hematopoiesis HSCs sustain all the hematopoietic lineages throughout the lifetime of the individual. Considerable progress has been made over the last few decades in prospectively

Color Atlas of Clinical Hematology: Molecular and Cellular Basis of Disease, Fifth Edition. A. Victor Hoffbrand, Paresh Vyas, Elías Campo, Torsten Haferlach, and Keith Gomez

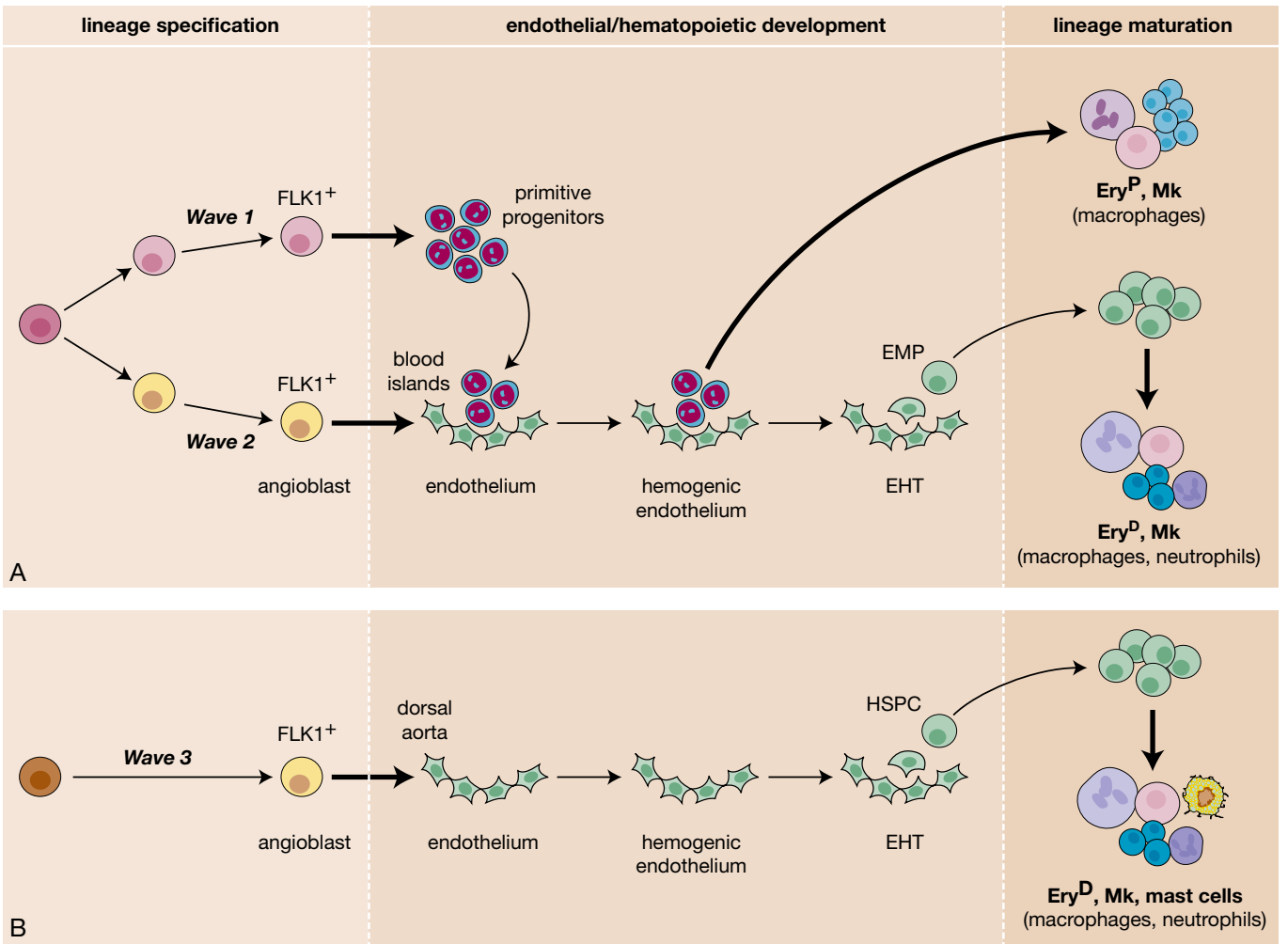

Fig. 2.2. There are three waves of hematopoiesis during development. **A,** There is a common origin for waves 1 and 2 in the epiblast, primitive streak, and early lateral plate mesoderm where cells acquire the cell surface receptor FLK1. This binds to vascular endothelial growth factor that promotes endothelial and hematopoietic specification in early mesoderm. Wave 1 FLK1+ cells give rise to embryonic primitive progenitors (top) and the endothelial cells (bottom) that give rise to the blood islands of the yolk sac. These blood islands provide a niche for the yolk sac blood-forming cells. There are two types of blood-forming cells. Primitive progenitors (from Wave 1) give rise to primitive erythroid cells (Ery^P), megakaryocytes (Mk), and macrophages. Wave 2 cells that form the yolk sac endothelium differentiate into blood-forming cells through a process called endothelial-to-hematopoietic transition (EHT). These Wave 2 hematopoietic cells are called definitive erythro-myeloid progenitors (EMPs). EMPs migrate to the fetal liver to give rise to definitive erythroid cells (Ery^D), Mk, and myeloid cells (macrophages and neutrophils). **B,** A third wave of hematopoiesis from FLK1+ cells also originates from the epiblast, primitive streak and early lateral plate mesoderm. But here FLK1+ cells migrate from the endothelial cell layer of the ventral wall dorsal aorta. Again these cells undergo an EHT to form definitive hematopoietic stem progenitor cells (HSPCs) that migrate to the fetal liver. These cells sustain lifelong myeloid and lymphoid hematopoiesis. Thus, during development there is a very close association between specification and maturation of blood cells and endothelial cells of blood vessels. Source: Porcher C, et al. *Blood* 2017;129(15):2051–2060.

isolating HSCs and the different downstream multipotential progenitors (MPPs) and unilineage progenitors from humans and rodents. These studies allowed isolation of populations of cells of defined functionality and made it easier to dissect the relationships between different blood cell populations. This is essential in describing the cellular basis of normal hematopoiesis and in turn is critical when trying to understand how cells in hematologic diseases arise by genetic and epigenetic change from normal hematopoietic cells.

Central to the isolation of HSCs and MPPs has been the identification of combinations of cell surface markers that allow separation of HSCs, MPPs, and unilineage progenitors by fluorescence-activated cell sorting (FACS). Figure 2.7 schematically illustrates how HSCs (and progenitors) are isolated and tested for function. Hematopoietic tissues are isolated, cells disassociated, and then labeled with panels of fluorescently conjugated antibodies. The cell populations can then be analyzed and separated on an FACS sorter. For example, human HSC populations express the cell surface antigen CD34. CD34 cells comprise around 1% of the bone marrow mononuclear cell population. Within CD34+ cells, HSCs principally reside in the CD38– population, which are only 5–8% of the CD34 population. Within the CD34+CD38– population, HSCs are enriched in cell populations that express the cell surface marker CD90+ and do not express CD45RA. This progressive purification scheme allows greater and greater enrichment of a cell population with HSC activity.

These highly purified populations can then be tested functionally in in vitro assays that serve as surrogate assays for stem/early progenitor cells, such as long-term culture-initiating cell assay and cobblestone-area-forming assay. The most stringent test for stem cell activity is the ability of a cell population

to serially engraft a whole animal and produce all hematopoietic cells. For human cells, this has involved transplanting cell populations into immunodeficient mice (such as NSG mice or newer more "humanized" mouse models such as MISTRG mice) that will allow human cells to engraft. More recently, engraftment has been tested in mice with implanted humanized ossicles to more accurately mimic the human bone marrow niche. Although there are limitations with this assay, it is considered the "gold standard" assay. Progenitor activity of populations can be tested either in vitro in colony (Fig. 2.8) or liquid culture assays or in vivo in xenograft studies.

These studies have allowed the construction of roadmaps of the cellular intermediates as an HSC differentiates into mature, terminally differentiated blood cells (Fig. 2.9). These cellular intermediates have distinctive expression of cell surface antigens (immunophenotypes). The HSPC pool is itself heterogeneous. The work on cellular intermediates has been driven forward with single-cell interrogation of cell populations using better in vitro and in vivo assays of stem/progenitor function and continuous imaging of all the cell progeny of a single HSPC. This work is uncovering the complexity of the cellular hierarchies and it is likely that over the next few years our appreciation of cellular hematopoiesis will undergo further revision. Figure 2.9A shows the hierarchy as it was understood in 2017 and Fig. 2.9B is a revised version of that hierarchy in 2018. It is also important to bear in mind that some of the information about these cellular

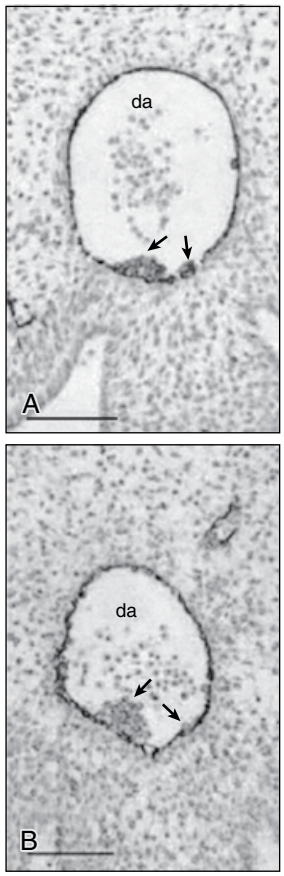

Fig. 2.3. Yolk sac blood islands in a human fetus. **A,** Transverse section in a three-somite human embryo (21 days) at the truncal level stained with anti-CD34 antibody. Paired dorsal aorta (da) ventrolateral to the neural tube (nt) and above the yolk sac (ys) and blood islands (bi). **B,** Higher magnification of a solid hemangioblastic mesodermal cluster of CD34-expressing cells in a blood island of the yolk sac (brown). Source: Tavian M, et al. *Development* 1999;126:793–803. Reproduced with permission of the Company of Biologists Ltd.

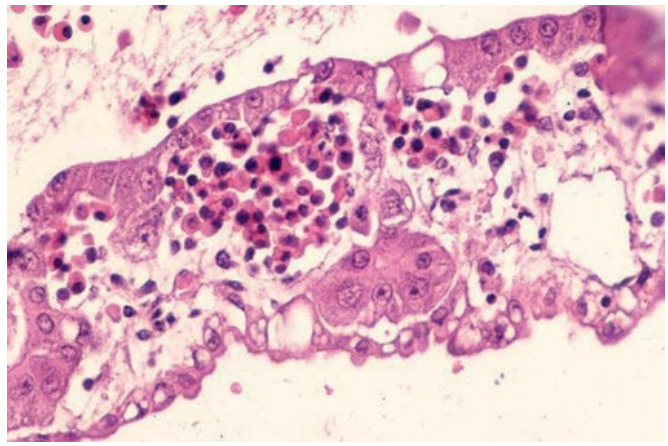

Fig. 2.4. Angioblastic blood islands form in the yolk sac (18 days) and trophoblast (19 days). The figure shows erythropoiesis in the yolk sac. Source: http://www.brown.edu/Courses/Digital_Path/systemic_path/heme/hemeyolk.html

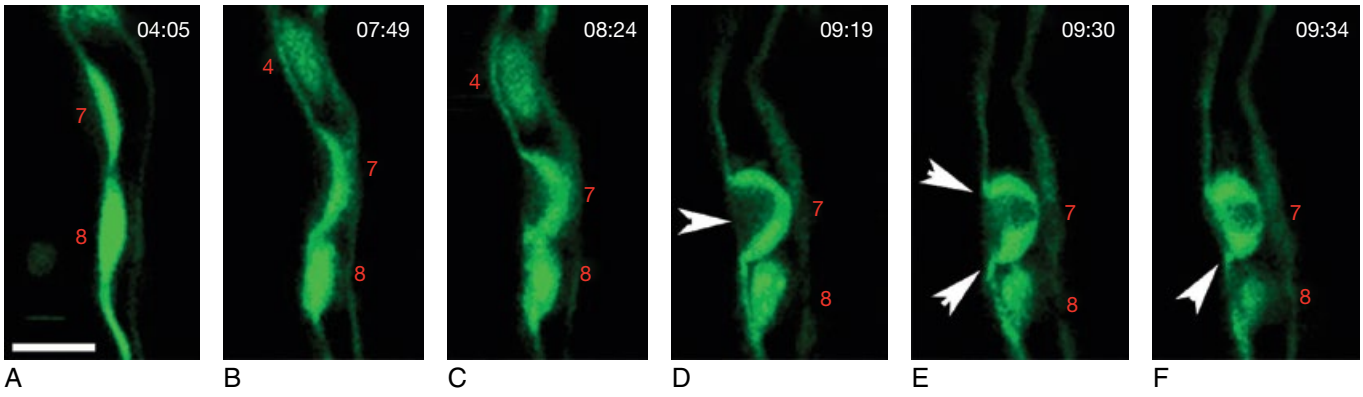

Fig. 2.5. A–F, Time lapse confocal microscopy showing how endothelial cells exit from the aortic floor into the subaortic space to become hematopoietic cells. White numbers indicate recording time in hours and minutes. Aortic cells undergoing endothelial-to-hematopoietic transition (EHT) are numbered in red. Arrowheads in **(D)** show the thin line evidencing the joining of the lateral neighbors of the exiting cell, whereas arrowheads in **(E)** and **(F)** show the remaining focal attachment sites to the budding hematopoietic stem cell to its rostral rostral and caudal neighbors. Scale bar, 10 mm. Source: Kissa K, Herbome P. *Nature* 2010;464:112–115. Reproduced with permission of Springer Nature.

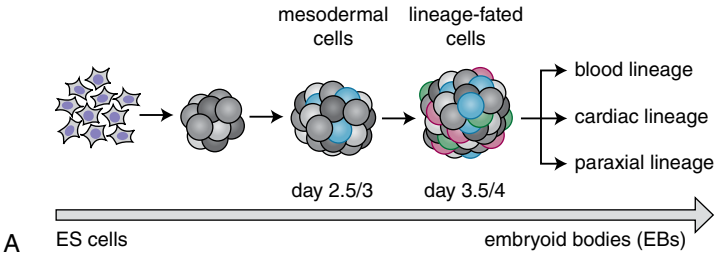

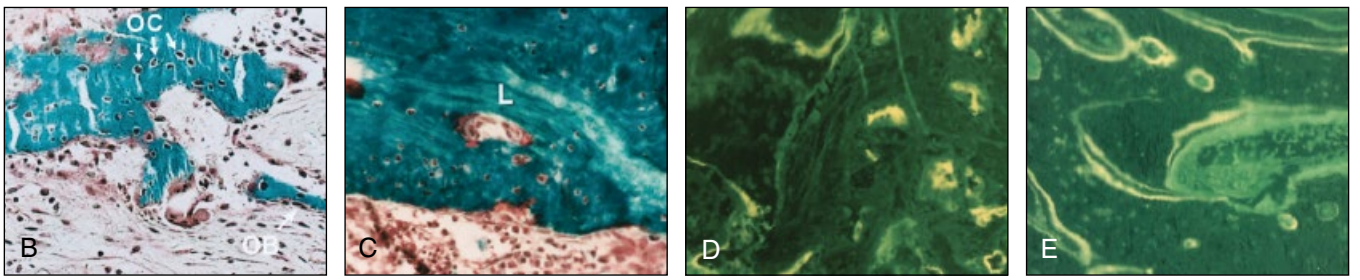

Fig. 2.6. A, Mesoderm is one of the three germ layers (together with ectoderm and endoderm) and is patterned early in development. It contains cells that will give rise to many lineages, including blood, cardiac, and paraxial lineages. **B–E,** Differentiation of mesenchymal stem cells (MSCs) in culture: **(B)** undifferentiated human MSCs; **(C)** bone formation by osteoblasts and osteocytes into which human MSCs have differentiated when grown on ceramic tubes and placed in severe combined immunodeficiency mice; **(D)** cartilage derived from human MSCs grown from a cell platelet; **(E)** rabbit MSCs form tendon when placed in a ruptured tendon sheath. Source: A, Provided courtesy of Professor Catherine Porcher; B–E, Gerson SL. *Nature Med* 1999;5:262–264. Reproduced with permission from Springer Nature.

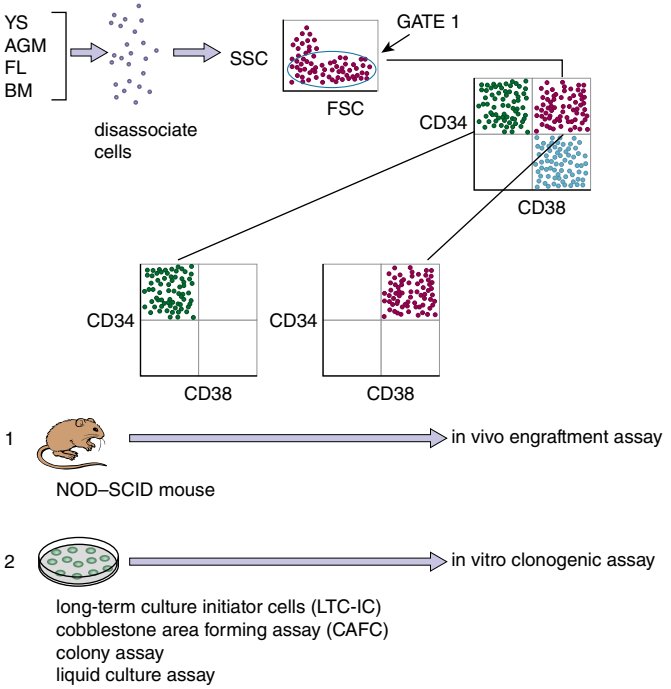

Fig. 2.7. This shows how hematopoietic stem cells can be isolated from different sources. Cells are initially disassociated and stained with multiple antibodies. They are then analyzed and then sorted using fluorescence-activated cell sorting (FACS). Here mononuclear live cells are separated in Gate 1. These live cells are then analyzed for CD34 and CD38 expression. Those live cells that are CD34+CD38− are enriched for stem cell potential. Further purification can be undertaken on the basis of additional cell surface markers such as CD90 (Thy1), SLAM markers, and N-cadherin. To test the functionality of isolated (sorted) cells, the cells can be tested in in vivo assays (transplanted into immunodeficient mice such as the NOD-SCID mouse model) and in vitro in long-term culture (long-term culture-initiating cell culture assay and cobblestone-area-forming assay), clonogenic colony assays, and liquid culture assays. YS, yolk sac; AGM, aorta–gonad mesonephros; FL, fetal liver; BM, bone marrow; SSC, side scatter; FSC, forward scatter.

pathways comes from studies in rodents and not all the findings in rodents may apply human hematopoiesis.

In mice, different HSCs sustain hematopoiesis for variable periods of time. Some HSCs enter hematopoiesis more quickly, then fail to sustain blood production over the long term, whereas others produce blood cells after a delay and sustain hematopoiesis for the lifetime of the animal. In addition, different HSCs contribute to different blood lineages; some HSCs are biased to producing myeloid cells only, some to platelets, yet others to lymphoid cells, and some give more balanced blood cell production.

Downstream of HSCs the pathways of differentiation are still under debate. One model suggests that HSCs give rise to multiple multipotential progenitor cells (MPPs) capable of giving rise to all blood cells but lacking stem cell function with the ability to serially transplant mice. It is increasingly clear that erythroid cells and megakaryocytes differentiate through a distinct set of progenitors from the rest of the lympho-myeloid cells. Bipotential megakaryocyte–erythroid progenitors have been identified that give rise to unipotential erythroid and megakaryocyte progenitors. Multipotential lympho-myeloid progenitors are likely to be very rare and they most likely give rise to more restricted bipotential and unipotential myeloid and lymphoid progenitors (Fig. 2.9B).

It is also clear that genetic changes (such as mutations) or epigenetic changes, either in disease states or experimentally induced, can alter the progress of cells through these compartments. This can allow abnormal, or accelerated, or reverse differentiation. In the past the dogma has suggested that differentiation can only proceed in one direction, but we are now discovering that the whole process of hematopoiesis has a lot more plasticity than was realized.

Once specified, HSPCs have a number of cell fate options (Fig. 2.10A). The key features of HSCs are their ability to self renew throughout the lifetime of the individual and maintain their multipotentiality. Most of the time they remain quiescent and are in G_0 of the cell cycle. If they divide, they can undergo

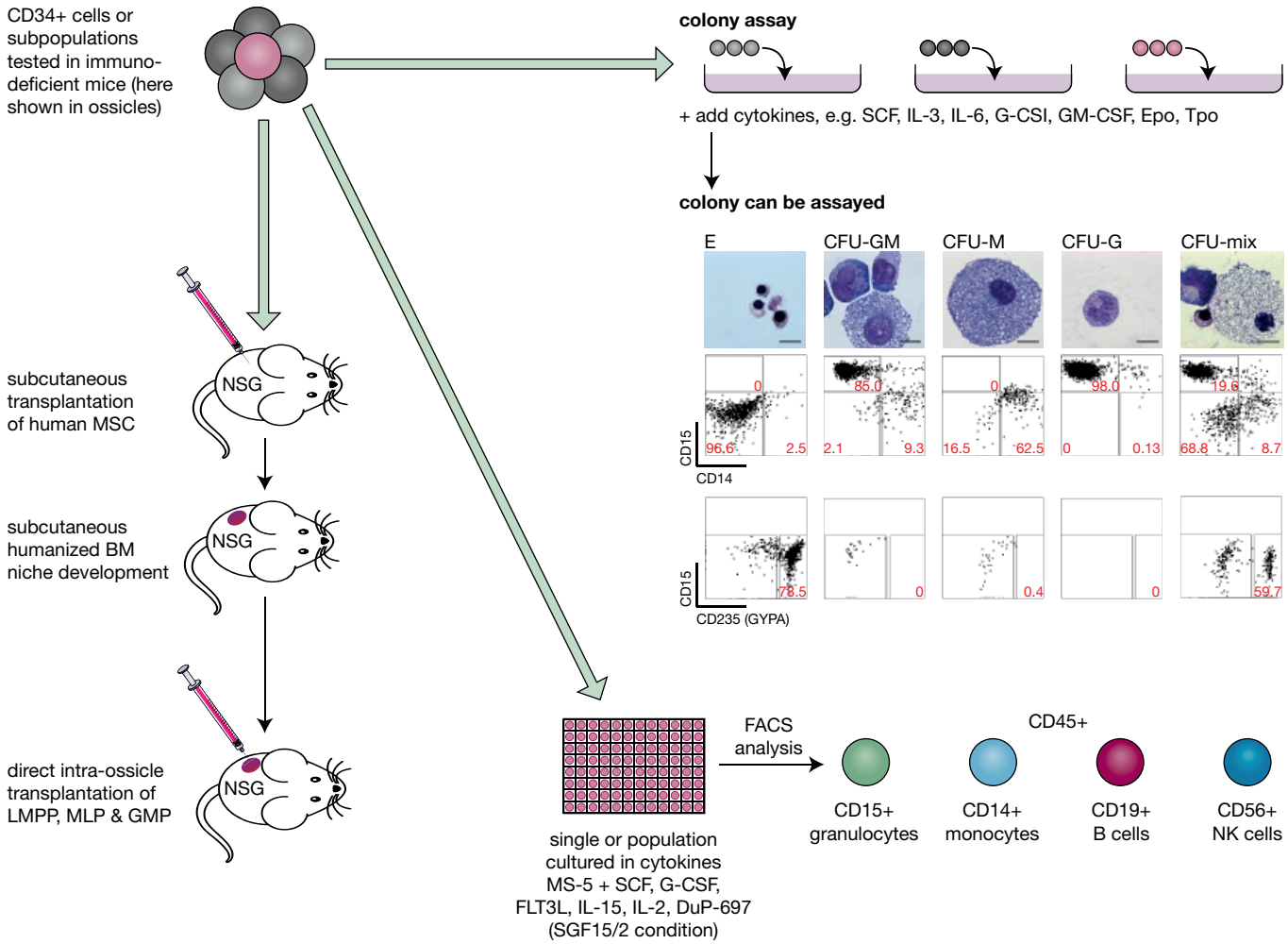

Fig. 2.8. Human hematopoietic CD34+ progenitor function can be tested in vivo (in immunodeficient mice) or in vitro in colony assays or in liquid culture. On the left, progenitor function is currently best tested in vivo by creating "humanized" bone marrow ossicles in immunodeficient mice (the NSG strain of immunodeficient mice is shown here). Humanized ossicles are created by culturing human mesenchymal stem cells (MSCs) within a scaffold (e.g. Matrigel). These are then implanted subcutaneously in mice and over some weeks they ossify and vascularize, creating a bone-like structure with human bone marrow (BM) mesenchymal cells within it. The mature blood cells produced are then tested by fluorescence-activated cell sorting (FACS)-purified human progenitors by injecting them into the humanized ossicle and then harvesting the ossicle some days or weeks later. LMPP, lymphoid-primed multipotential progenitor; MLP, multipotential lymphoid progenitor; GMP, granulocyte–macrophage progenitor. On the right, FACS-purified human progenitor cells are put into semi-solid (jelly like) media and each single progenitor cells produces a cellular colony. Below are shown May–Grünwald–Giemsa-stained cells from an erythroid colony (E) (mature red cells) that are CD14−CD15−CD235A+ (glycophorin A) by FACs analysis (see below); a granulocyte–macrophage colony (CFU-GM) (myelocytes/macrophage) that are CD15+ or CD14+ or CD14+CD15+; a macrophage colony (CFU-M) (macrophage) that are CD14+; a granulocyte colony (CFU-G) (granulocyte) that are CD15+; a mixed myeloid–erythroid colony (CFU-mix) (myelocytes/macrophage/red cells) that are CD15+ or CD14+ or CD14+CD15+ or CD235A+. On the right at the bottom, single human CD34+ progenitors or populations of CD34+ progenitor cells are cultured in single wells in a culture dish with cytokines such as stem cell factor (SCF), granulocyte colony-stimulating factor (G-CSF) Fms-like tyrosine 3 ligand (FLT3L), interleukin 15 (IL-15), interleukin 2 (IL-2) and DuP-697, and a marrow stromal cell layer (MS-5). The cells produced can then be assayed by FACS or morphologically.

three types of cell division. In the first, they can generate two more HSCs. This type of division promotes expansion of HSC numbers at the expense of differentiation and ultimate production of lineage-affiliated cells. If this was the only type of HSC cell division, it would lead to cytopenias from arrested differentiation, a situation akin to hematopoietic malignancy. Second, HSCs can divide asymmetrically to produce an HSC and a more differentiated progeny that will eventually give rise to one or more lineages. This is a "balanced division," maintaining HSC numbers but allowing blood cell production. Third, HSCs can divide symmetrically to produce two differentiated progeny. If this was the only type of cell division undertaken by HSC, it would lead to exhaustion of HSCs and eventually aplasia. Finally, HSCs can undergo apoptosis. The sum of all the HSC cell fate divisions determines the quality and quantity of HSC activity.

As HSCs differentiate into progenitors and then terminal mature cells, the cell fate options available to them change (Fig. 2.10B). Progenitors have reduced self-renewal potential and this further declines with differentiation. In contrast to HSCs, progenitors spend much less time in G_0 and are highly proliferative. They provide much of the amplification in cell numbers required to satisfy the enormous daily demand for blood cells. In an adult human, ~10^{10} new blood cells are made daily. Finally, as progenitors enter terminal differentiation, the proliferative capacity is slowly lost and cells enter progressively more restricted pathways of differentiation that eventually lead to unilineage differentiation. Terminally mature cells are often postmitotic (e.g. red cells and granulocytes) and express the proteins required for function of terminally mature cells.

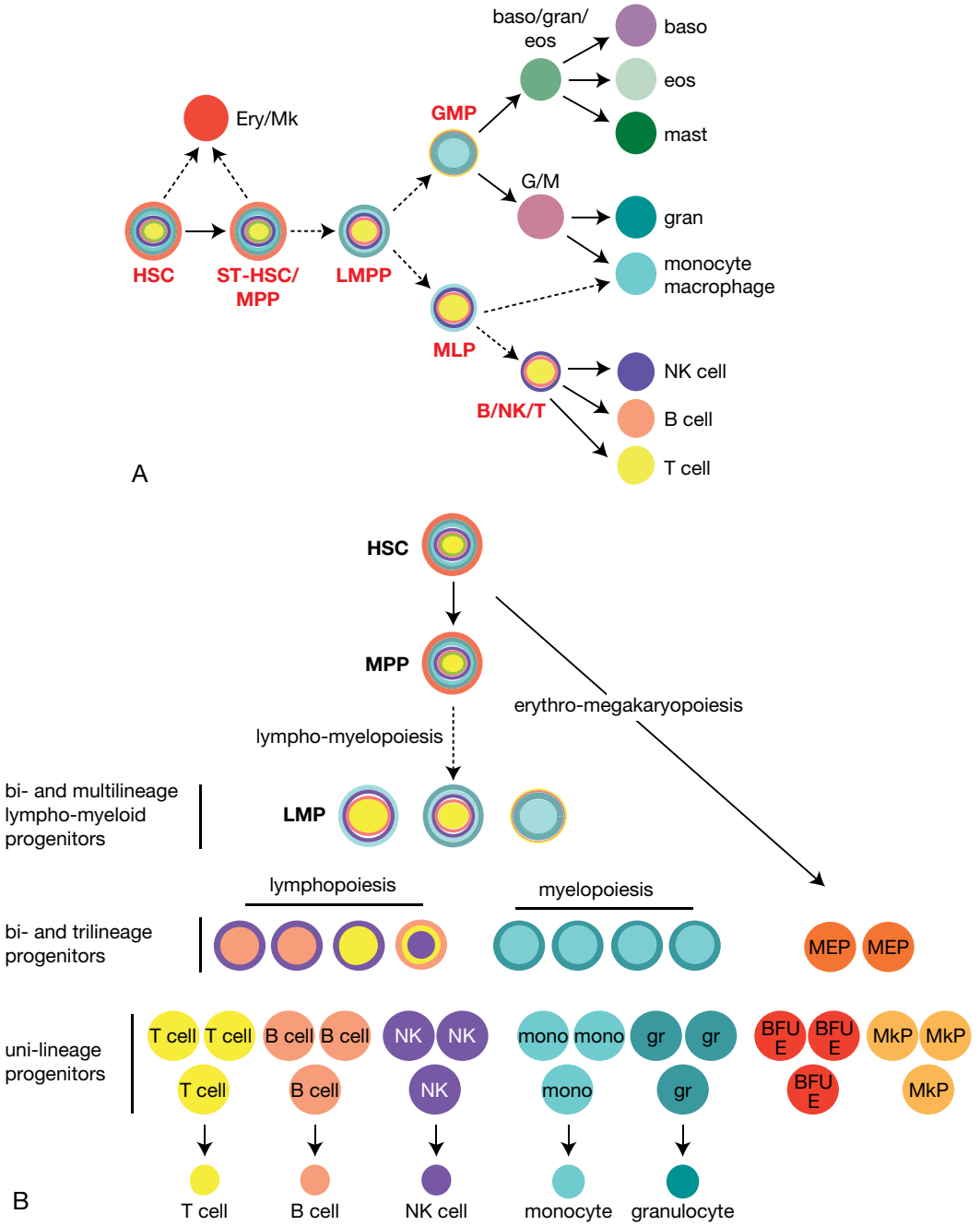

Fig. 2.9. Schematic representations of cellular hierarchy of human hematopoiesis. **A,** Until recently, hematopoiesis was thought to be organized as shown in this panel. Hematopoietic stem cell (HSCs) give rise to multipotential HSCs (also known as multipotential progenitors, MPPs) that lack long-term self-renewal potential. The erythroid and megakaryocyte lineages (Ery/Mk) most likely derive from HSCs and MPPs. Downstream of MPPs are lymphoid-primed multipotential progenitors (LMPPs) that then differentiate into granulocyte–macrophage progenitors (GMPs), which terminally differentiate into mature myeloid cells (basophils, eosinophils, mast cells, granulocytes, and monocyte macrophages). LMPPs also differentiation into multipotential lymphoid progenitors (MLPs) that differentiate into natural killer cells, B cells, and T cells. The color of each stem/progenitor cell reflects the cell lineages it produces. **B,** Recent evidence shows the differentiation pathway in **(A)** to be incorrect. Downstream of the MPPs lie lymphoid–myeloid progenitors (LMPs). These give rise to a diverse bi- and trilineage progenitors and then unilineage progenitors that then terminally differentiate.

TRANSCRIPTIONAL CONTROL OF HEMATOPOIESIS

A crucial class of proteins that help to control hematopoiesis are the transcription factors (TFs) (see Chapter 1), which are expressed either exclusively in blood cells or have restricted tissue-specific patterns of expression. The function of these critical factors has often come to light as the genes encoding them have acquired mutations in hematologic diseases such as lymphoma and leukemia (see Chapters 13 and 14). Their importance is also underscored by the conserved role they play in hematopoiesis through evolution. Over the last two decades, this attribute has allowed the function of TFs to be investigated extensively in animal models, in which the genes encoding critical TFs have been deleted, modified, overexpressed, and misexpressed. A summary of the site of action of some of these

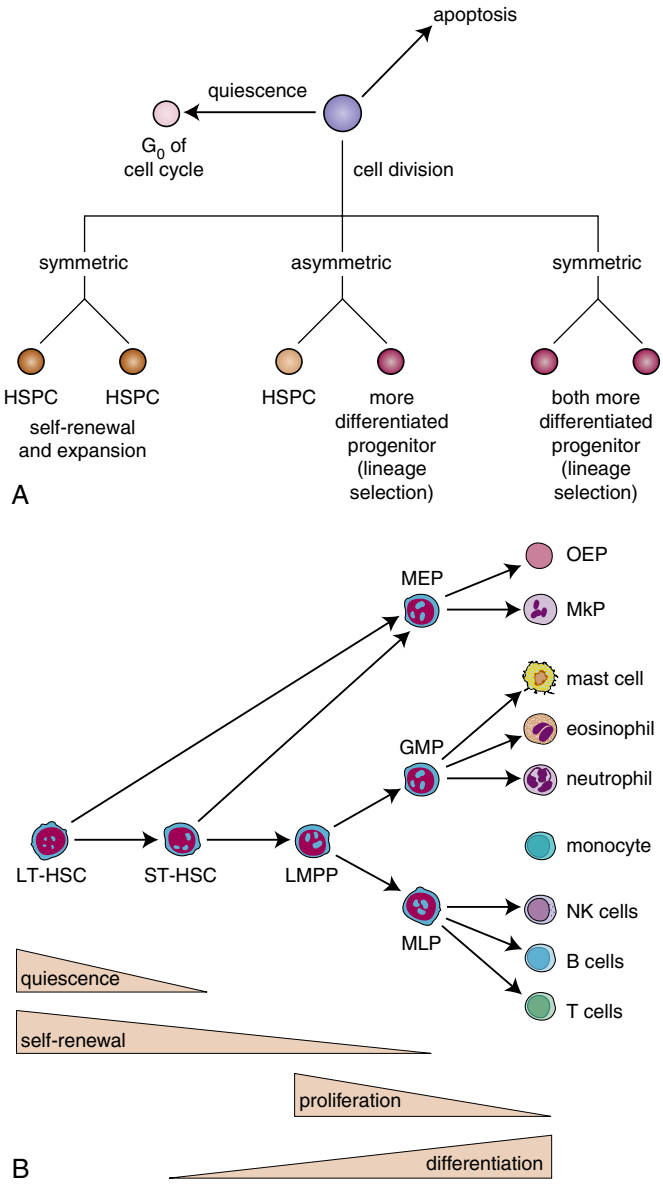

Fig. 2.10. A, Simplified schematic showing the cell fate choices open to a hematopoietic stem progenitor cell (HSPC). Cells can either be quiescent, or undergo apoptosis or divide. Cell division can either be symmetrical self-renewing cell division (the two daughter cells have the same potential as the parental cell), asymmetrical (daughter cells produce one cell with the same potential as the parental cell and one cell that is more differentiated), or symmetrical differentiation cell division (the two daughter cells are more differentiated than the parental cell). **B,** The cell fate choices taken by an HSPC at different stages of hematopoietic differentiation. Hematopoietic stem cells (HSCs) are mainly quiescent and self renew (either through symmetrical self-renewal or asymmetric division), progenitors are highly proliferative, have less self-renewal, and are more likely to differentiate (i.e. more likely to have symmetrical differentiation divisions or asymmetrical divisions). As cells terminally mature the focus is on divisions that lead to terminal differentiation (symmetrical differentiation divisions) and exit from the cell cycle, finally leading to apoptosis. LT-HSC, long-term hematopoietic stem cell; ST-HSC, short-term hematopoietic stem cell; LMPP, lymphoid-primed multipotential progenitors; MEP, megakaryocyte–erythroid progenitor; GMP, granulocyte–macrophage progenitors; MLP, multipotential lymphoid progenitors; MEP, megakaryocyte–erythroid progenitor; MkP, megakaryocyte progenitor.

TFs is shown in Fig. 2.11. Although a complete description of the function of these proteins is not possible here, some of the key points that arise from these studies are as follows:

- TFs are divided into families that have similar proteins domains.
- They often bind DNA and interact with other proteins (other TFs and proteins that control transcription) via specific domains.
- TFs work in combinations to both activate and repress the expression of a large number of genes.
- TFs are required at discrete stages of hematopoiesis and any one TF often functions at multiple stages within one lineage and can function in more than one lineage.
- Ultimately, TFs work in complicated networks that can be modeled much like semiconductor/computing networks. TFs work in negative feedback loops, feedforward loops, and cross-antagonistic loops to mention just three such types of interaction.
- The function of TFs helps regulate the cell's potential to make blood cells of different lineages, proliferate, undergo apoptosis, and self renew.

More specifically, the TFs SCL/TAL1 and LMO2 are required to specify HSCs from mesoderm; RUNX1 (AML1) specifies HSCs from hemogenic endothelium; and RUNX1, TAL1, TEL1, MLL, and GATA2 are required to maintain stem cells once they have been specified. In myelopoiesis, the TFs PU.1, the C/EBP family (C/EBPα and C/EBPε), GFI-1, EGR-1, and NAB2 all promote the granulocyte–macrophage lineage programs. GATA2 is required in stem/early progenitor cells but is also required for mast cells and in the early phases of megakaryocyte–erythroid lineage maturation and late stages of megakaryocyte differentiation. Working with GATA2 to promote erythropoiesis and megakaryopoiesis are GATA1, FOG1, SCL, KLF4, p45NF-E2, and Fli-1. In early lymphoiesis, the TF Ikaros is required. In B lymphopoiesis, the TFs E2A (and its family members), EBF, and PAX5 are required, and finally, the TF BLIMP1 is necessary for plasma cell formation. In T-cell maturation, Notch signaling activates the TF CSL, which works with the TFs RUNX1, GATA3, T-BET, NFATc, and FOXP3.

Of note, the TF SCL/TAL1, MLL, RUNX1, LMO2, PU.1, C/EBPα, PAX5, E2A, GATA2, and GATA1 are all implicated in the pathogenesis of human leukemia.

THE HEMATOPOIETIC NICHE

It has been long appreciated that HSPCs require specialized anatomical locations called niches to survive and exercise their cell fate options. Niches are likely to exist in all hematopoietic organs. Most of the work has concentrated on the bone marrow niche and lessons have been learnt from a number of organisms, especially mice. In the niche a number of extrinsic inputs influence hematopoietic cells (Fig. 2.12). The niche consists of a physical architecture: the cells surrounding hematopoietic cells (such as stromal cells, adiopocytes, endothelial and perivascular cells of the vasculature and osteoblasts) and the extracellular matrix (Table 2.1 and Fig. 2.13). Humoral inputs include cytokines. Paracrine signaling inputs (molecules that act over a short range) include chemokines, such as CXCL12 that interacts with the receptor CXCR4 on hematopoietic cells, soluble WNT (Wingless-related) proteins, NOTCH modulators, fibroblast

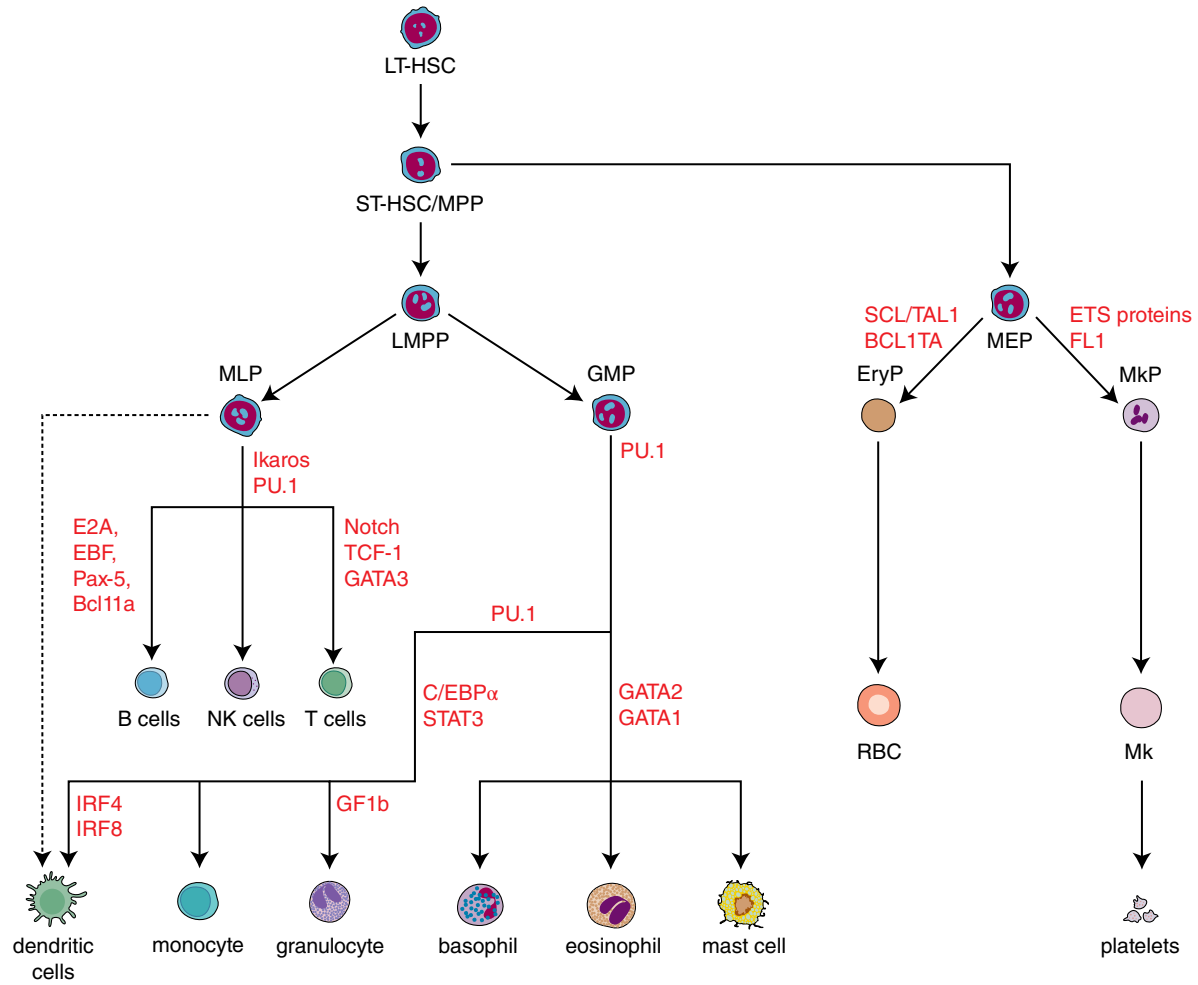

Fig. 2.11. Schematic representation of hematopoiesis and where key hematopoietic-specific transcription factors (TFs) have nonredundant functions as revealed by gene deletion studies in mice. Thus, for example, the TFs GATA2, RUNX1, SCL/TAL1, LMO2, and ETV6 are all critically required in hematopoietic stem cells (HSCs), and loss of function of these genes causes a block hematopoietic differentiation at the HSC level, showing they are required for HSC function. Similarly, the other TFs shown downstream of HSC are required later in hematopoiesis at the stages where the TFs are shown. LT-HSC, long-term hematopoietic stem cell; ST-HSC, short-term hematopoietic stem cell; MPP, multipotential progenitors; LMPP, lymphoid-primed multipotential progenitor; MLP, multipotential lymphoid progenitor; GMP, granulocyte–macrophage progenitor; MEP, megakaryocyte–erythroid progenitor; Ery^{p}, erythroid progenitor; MkP, megakaryocyte progenitor.

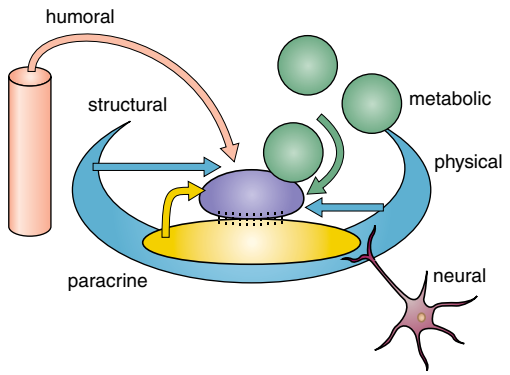

Fig. 2.12. Stem cells are thought to reside in specialized regions of the bone marrow, or "niches." The factors that regulate stem cell biology include the architectural space, physical engagement of the cell membrane with tethering molecules on neighboring cells or surfaces, signaling interactions at the interface of the stem cell and its niche, paracrine and endocrine signals from local or distant sources, neural inputs, and metabolic products of tissue activity. Source: Scadden DT. *Nature* 2006;441:1075–1079. Reproduced with permission from Springer Nature.

TABLE 2.1. HEMATOPOIESIS DEPENDS ON THESE STROMAL CELLS AND EXTRACELLULAR MATRIX

Cells	Extracellular matrix/bone
Macrophages	Fibronectin
Fibroblasts	Hemonectin
Reticulum ("blanket") cells	Laminin
Fat cells	Collagen
Endothelial cells	Proteoglycans (acid mucopolysaccharides; e.g. chondroitin, heparan)

growth factors (FGFs), and members of the Hedgehog family (Fig. 2.14). The roles of cytokines, paracrine factors and the downstream signaling pathways in hematopoiesis are discussed in Chapters 1 and 3.

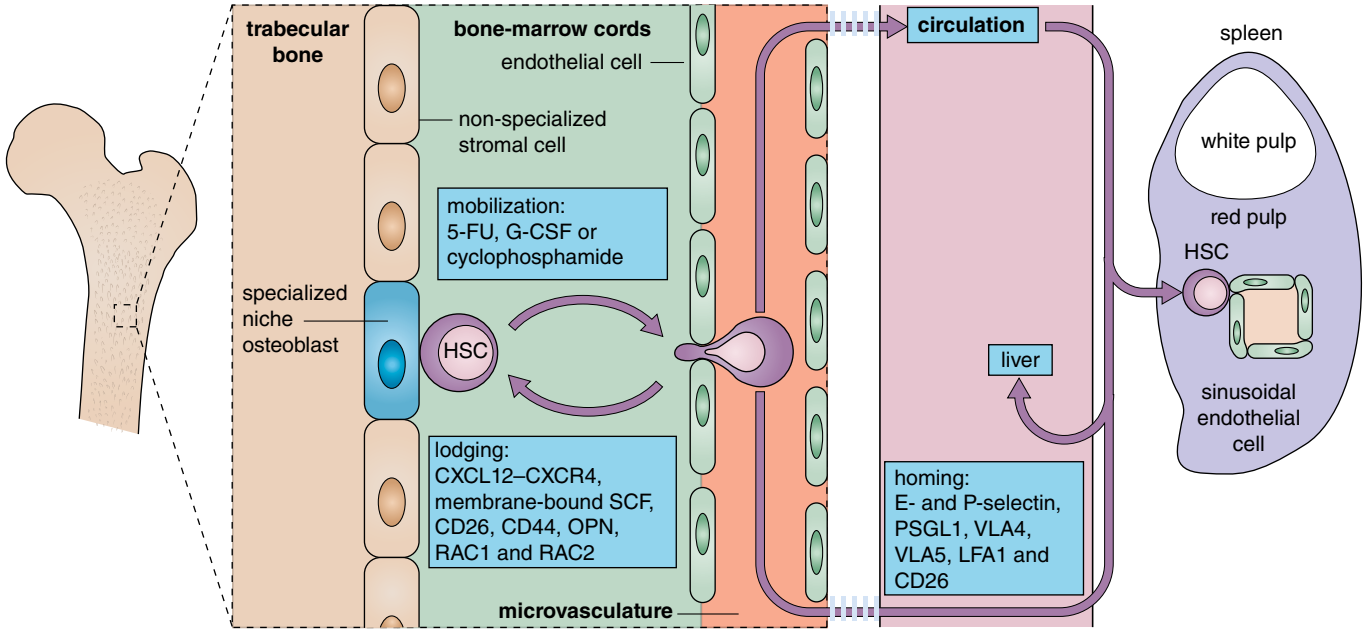

Fig. 2.13. Mobilization, homing, and lodging. Schematic diagram showing some of the factors involved in these processes. Hematopoietic stem cells (HSCs) bound to the niche are mobilized into peripheral blood by growth factor therapy (G-CSF) or chemotherapy (cyclophosphamide or other regimens). Once in the bloodstream they migrate to all hematopoietic organs, including the spleen (as shown). They home to the bone marrow and bind to a number of cell surface molecules, including endothelial- (E-) and platelet- (P-)selectin, P-selectin glycoprotein ligand 1 (PSGL1), very late antigen 4 (VLA4) and VLA5, and lymphocyte function-associated antigen 1 (LFA1). After entering the marrow they lodge in the niche, a process that is regulated by membrane-bound stem cell factor (SCF), CXC-chemokine ligand 12 (CXCL12) and its receptor CXC-chemokine receptor 4 (CXCR4), osteopontin (OPN), hyaluronic acids, and their corresponding receptors. Source: Wilson A, Trumpp A. *Nat Rev Immunol* 2006;6:93–106. Reproduced with permission from Springer Nature.

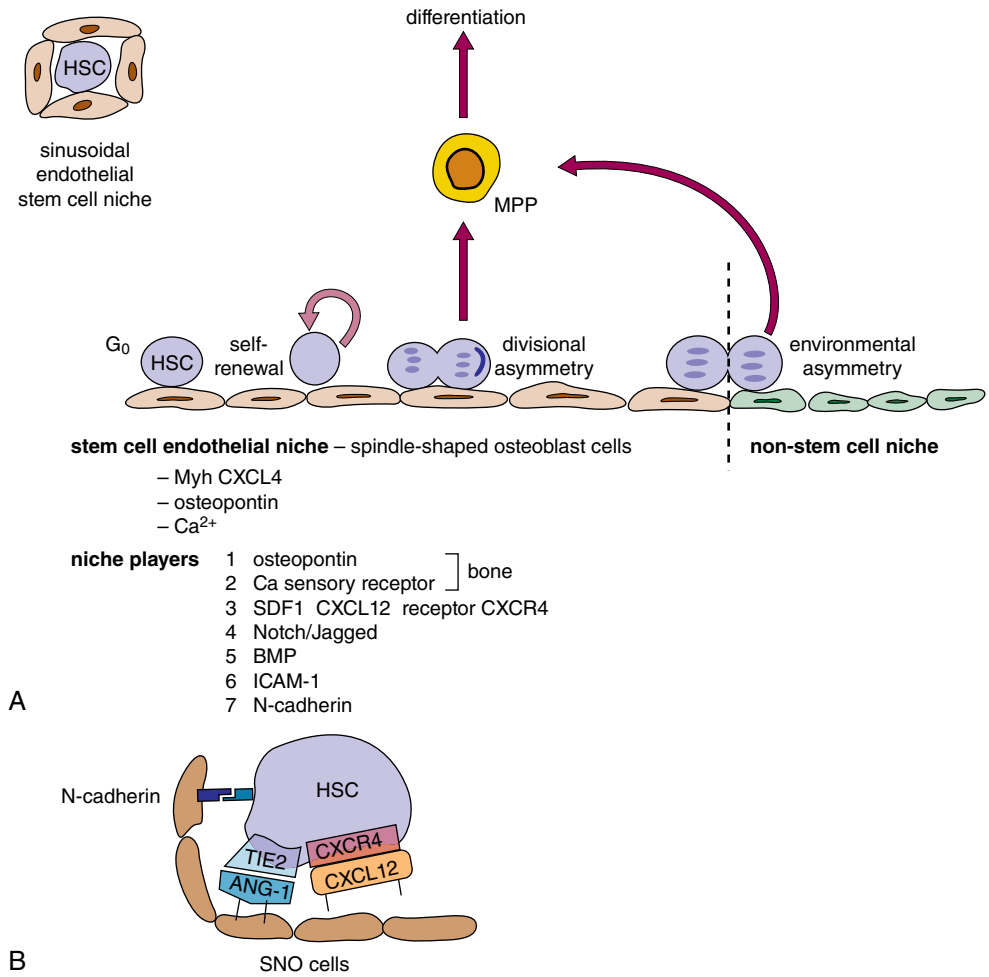

Fig. 2.14. A, The bone marrow niche, which, in part, consists of sinusoidal endothelial cells, helps control hematopoietic stem cell (HSC) fate. HSCs can be in G_0 or can enter the cell cycle to divide symmetrically or asymmetrically (divisional asymmetry) to self renew and/or to produce more differentiated cells such as multipotential progenitors (MPPs). HSCs can also migrate into and out of the niche (environmental asymmetry). The components of the niche (niche players) are listed below. **B,** An HSC anchored into the niche via TIE2/TEK binding to its ligand angiopoietin-1 (ANG-1) on sinusoidal endothelial cells (SNO cells) and CXC-chemokine ligand 12 (CXCL12) on SNO cells binding to its receptor CXCR4.

More recently it has begun to be appreciated that metabolic inputs (such as ionic calcium levels regulated in part by surrounding osteoblasts) and neural inputs (signaling from the autonomic nervous system) may also regulate hematopoietic stem/early progenitor behavior. The regulation of stem/progenitor cells is in part controlled by cell–cell contacts that are mediated by cell surface adhesion molecules that regulate the interaction of hematopoietic cells with surrounding niche cells and are important in the retention and release of HSPCs. This is important in controlling the trafficking of HSPCs both normally and in situations such as therapeutic stem/progenitor cell mobilization (Fig. 2.14).

In addition to the marrow niche there are likely to be other niches that we know even less about. For example, in development the fetal liver is a critical site of hematopoiesis and it is likely the niche here will be different from that in the bone marrow. In addition, there is increasing work studying how modifying the niche may modify the nature of the cell divisions (symmetrical-versus-asymmetric, Fig. 2.9) that HSCs undergo (Fig. 2.11A).

CHAPTER

GROWTH FACTOR SIGNALING

3

Blood cells, like other cells, receive signals that influence how they proliferate, differentiate and apoptose (i.e. the cell fate choice blood cells make). These signals also affect the functions of mature cells and are involved in the amplification of leukocytes in response to infection, red cells in response to anemia, and platelets in response to thrombocytopenia. In this chapter we review the biology of the signaling ligands, the receptors they interact with, and aspects of how these signals are transduced by cells. There are families of signaling pathways that share features in common. Often a signaling molecule will act at more than one stage in hematopoiesis and have different effects at different stages of hematopoiesis.

Signaling inputs can be transmitted in a number of different ways (Fig. 3.1). Cytokines or growth factors are released systemically into the bloodstream by organs (e.g. the kidneys that release erythropoietin or the liver that produces thrombopoietin) or other bone marrow cells: stromal cells (fibroblasts and endothelial cells), lymphocytes, and macrophages. Hematopoietic cytokines include colony-stimulating factors (CSFs), interleukins (ILs), specific families of growth factors such as transforming growth factor β, Notch pathway factors, chemokines, toll-like factors, and interferons (IFNs). Signaling molecules can also act more locally, for example, just within the bone marrow. These molecules can target cells at long range or just affect target cells nearby (paracrine), for example within a local niche (see Chapter 2). In some cases, paracrine signaling requires cell-to-cell contact. Finally, cells can release signaling molecules that regulate their own behavior (autocrine signaling).

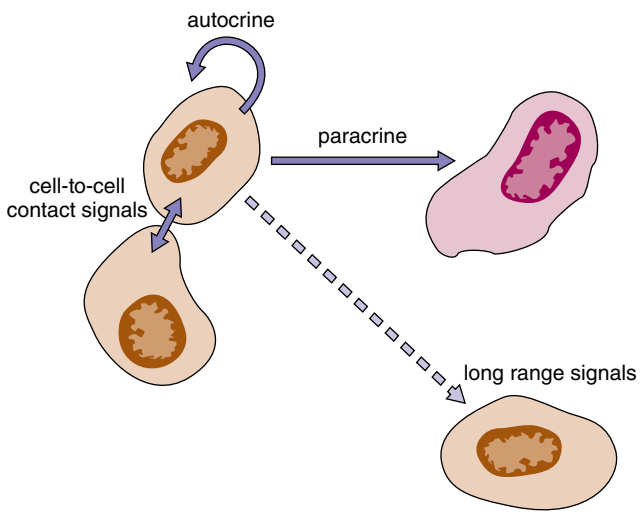

Fig. 3.1. Cells receive signals by a number of means. Cells can signal to themselves (autocrine), by cell-to-cell contact (juxtacrine), via short-range signals (paracrine), and via long-range signals.

SIGNALING AT DIFFERENT STAGES OF HEMATOPOIESIS

One way of demonstrating which cytokines, growth factors, and local signaling molecules function at different stages of hematopoiesis is by documenting the different complements of cell surface receptors that detect and respond to external signaling molecules in stem/progenitor and mature blood cells (Fig. 3.2).

In vitro culture systems have shown that whilst some cytokines support lineage-specific lineages, others affect multiple lineages. This has led to the notion that like hematopoiesis itself, signaling molecules (including cytokines) can be arranged in a hierarchical manner. Some, like stem cell factor (SCF, that binds the receptor c-KIT), FMS-like tyrosine kinase 3 (FLT3), thrombopoietin (TPO), and interleukin 3 (IL-3) act on hematopoietic stem cells (HSCs) and multipotential cells. Others have a more restricted action and act on specific lineages. Examples include erythropoietin (EPO) (functions on erythroid cells), TPO (important for megakaryocytes), granulocyte CSF (G-CSF) (required for neutrophils), granulocyte–macrophage CSF (GM-CSF) (promotes granulocyte and monocyte production), IL-5 (central cytokine for eosinophils), and IL-4, IFNγ, and IL-7 (required for lymphocytes). The actions of different cytokines and signaling molecules on all the different cell intermediates in granulopoiesis (Fig. 3.3), erythropoiesis (Fig. 3.4), megakaryopoiesis, and lymphopoiesis (Fig. 3.5) are shown.

Some of the complexity of the signaling interplay between hematopoietic cells and cells in their microenvironment is shown in Fig. 3.6. Endotoxin stimulates monocytes to release IL-1 and tumor necrosis factor (TNF) that in turn induces marrow stromal cells, (fibroblasts, endothelial cells), as well as T lymphocytes and macrophages, to produce a number of cytokines.

However, over time, and with increasingly refined analysis of genetically modified animal models, it has become apparent that cytokines such as TPO, G-CSF, and GM-CSF can regulate stem/progenitor cells as well as lineage-specific cells. Furthermore, it is likely some of these cytokines will have effects outside hematopoiesis.

Color Atlas of Clinical Hematology: Molecular and Cellular Basis of Disease, Fifth Edition. A. Victor Hoffbrand, Paresh Vyas, Elías Campo, Torsten Haferlach, and Keith Gomez

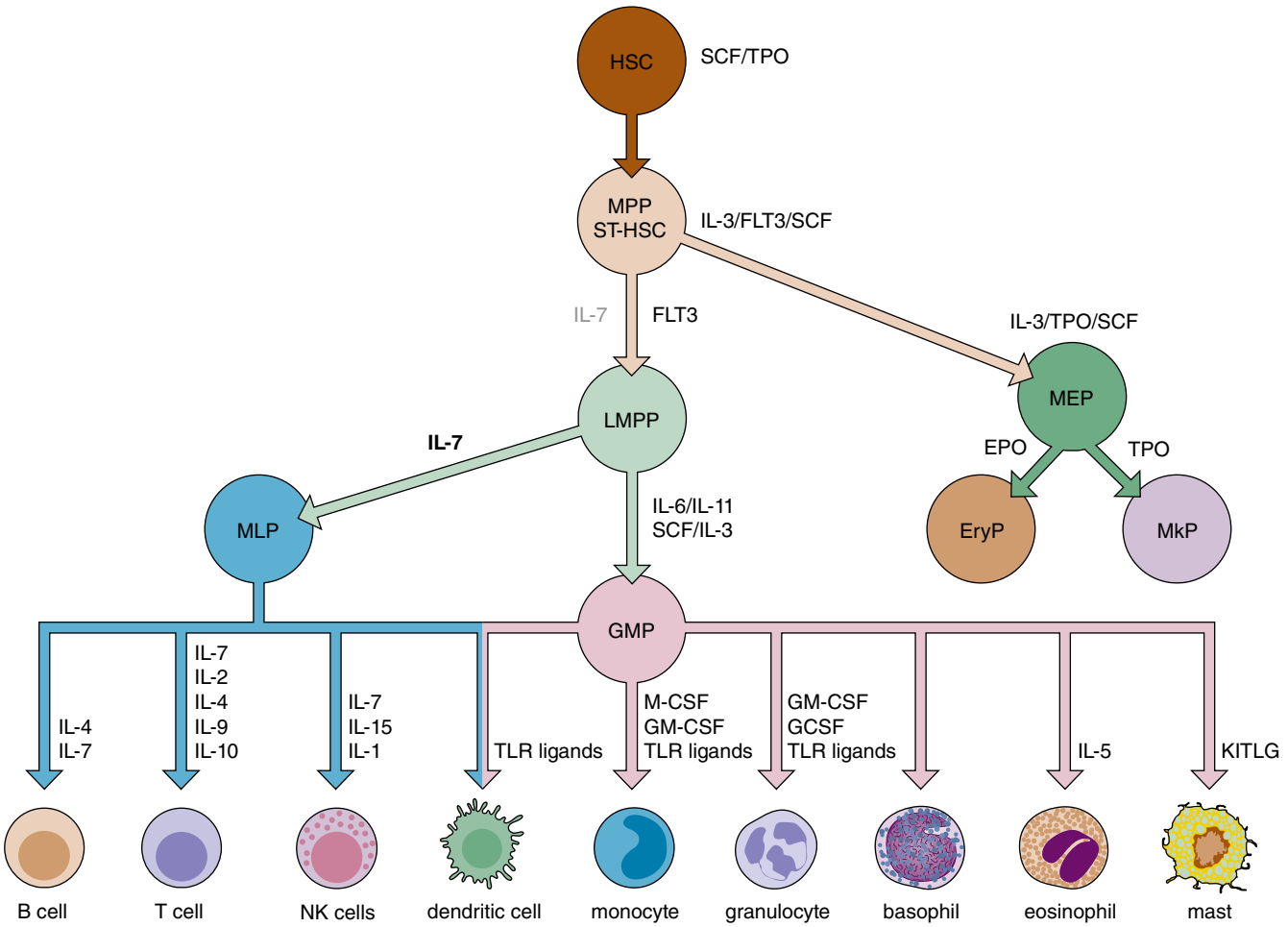

Fig. 3.2. Some of the main cytokines acting on hematopoietic stem cells (HSCs) and progenitor cells. MPP, short-term HSC/multipotential progenitor; LMPP, lymphoid-primed multipotential progenitor; MLP, multipotential lymphoid progenitor; GMP, granulocyte–macrophage progenitor, MEP, megakaryocyte–erythroid progenitor; EryP, erythroid progenitor; MkP, megakaryocyte progenitor; SCF, stem cell factor; TPO, thrombopoietin, FLT3, FMS-like tyrosine kinase 3; IL, interleukin (specific interleukins have a specific numeral); EPO, erythropoietin, GM-CSF, granulocyte–macrophage colony-stimulating factor, M-CSF, macrophage/monocyte colony-stimulating factor; G-CSF, granulocyte colony-stimulating factor; TLR, toll-like receptor.

For example, EPO is thought to protect central nervous system neurons against hypoxic stress. The pleiotropic effects of cytokines are likely due to cell-specific cytokine receptor expression, the availability of cytokines, synergistic interactions between cytokines, and the differential attenuation of cytokine signals in a cell type-specific manner by negative regulators such as the SOCS (suppressor of cytokine signaling) proteins. Importantly, identification of cytokines such as EPO and G-CSF has led to their use therapeutically to increase erythrocyte and neutrophil production, respectively, in bone marrow transplantation and treatment of congenital and acquired cytopenias. They are also used to mobilize multipotent progenitors into the peripheral blood to improve the harvest of these cells prior to autologous stem cell transplantation.

CYTOKINE RECEPTORS

The cytokines bind to their receptors with high picomolar affinity, leading to receptor homodimerization (e.g. erythropoietin receptor, EPOR) or heterodimerization/oligomerization of receptor subunits (e.g. IL-2 receptor) or induction of a conformational change in preformed receptor dimers (EPOR), resulting in the activation of downstream signaling pathways.

Cytokine receptors are divided into a number of families (Fig. 3.7). Receptors can be composed of dimers of a single receptor chain (Fig. 3.7A). Examples include erythropoietin receptor (EPOR), thrombopoietin receptor (MPL) and granulocyte colony stimulating factor receptor (G-CSFR). Alternatively, receptors can be heterodimeric, with a common signaling subunit and a unique ligand-binding chain. There are three categories of receptor here. One group of hematopoietic receptors share a common 130 kDa glycoprotein signaling subunit (gp130) (Fig. 3.7B). They include IL-6 receptor (IL-6Rα/gp130), IL-11 receptor (IL-11Rα/gp130), IL-12 receptor (IL-12Rα/gp130), leukemia inhibitory factor receptor (LIFRβ/gp130), and oncostatin M receptor (OSMRα/gp130). The second heterodimeric group of receptors share a common 140 kDa β-chain (Figs. 3.7C and 3.8). These include IL-3 receptor (IL-3Rα/gp140), IL-5 receptor (IL-5Rα/gp140), and granulocyte–macrophage colony-stimulating factor receptor (GM-CSFRα/gp140). Finally, some receptors share a common γc-chain (Fig. 3.7C) and include the IL-2 receptor (IL-2Rα/β/γc), IL-4 receptor (IL-4Rα/γc), IL-7 receptor (IL-7Rα/γc), IL-9 receptor (IL-9Rα/γc), IL-13 receptor IL-13Rα/γc), IL-15 receptor (IL-15Rα/γc), and IL-21 receptor (IL-21Rα/γc).

All these homodimeric and heterodimeric receptor groups constitute the type 1 cytokine receptor family. They share four

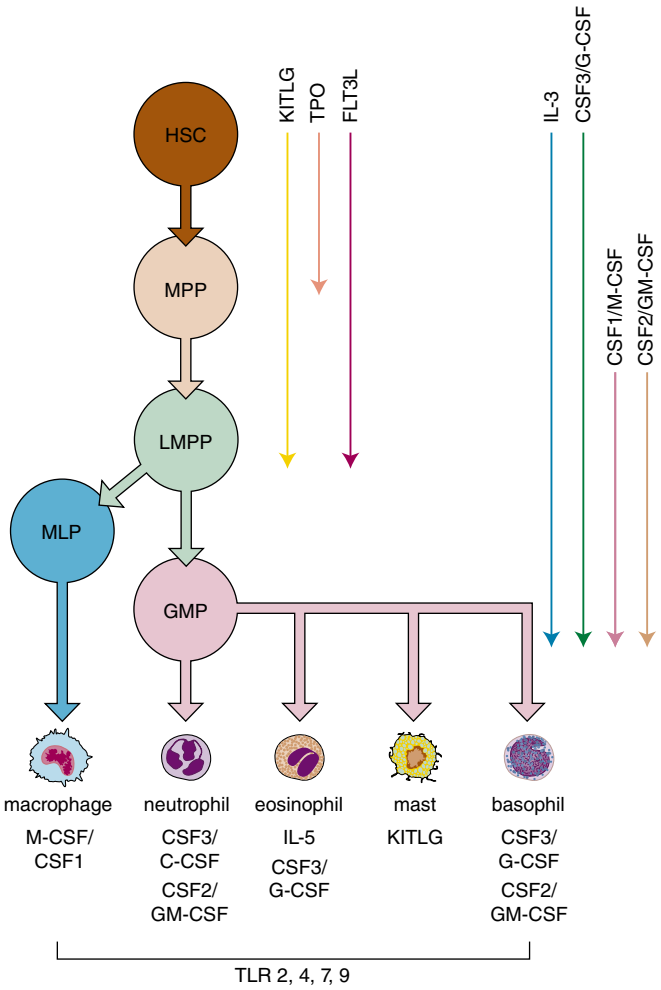

Fig. 3.3. The cytokines that act on the sequence of myeloid progenitors and granulocytic cells that differentiate from a hematopoietic stem cell (HSC). Abbreviations of cytokines as in Fig. 3.2. The action of cytokines on HSCs and progenitor cells is shown as arrows on the right. The cytokines required during terminal differentiation is shown below the mature cells. See text for details. KITLG, Kit ligand.

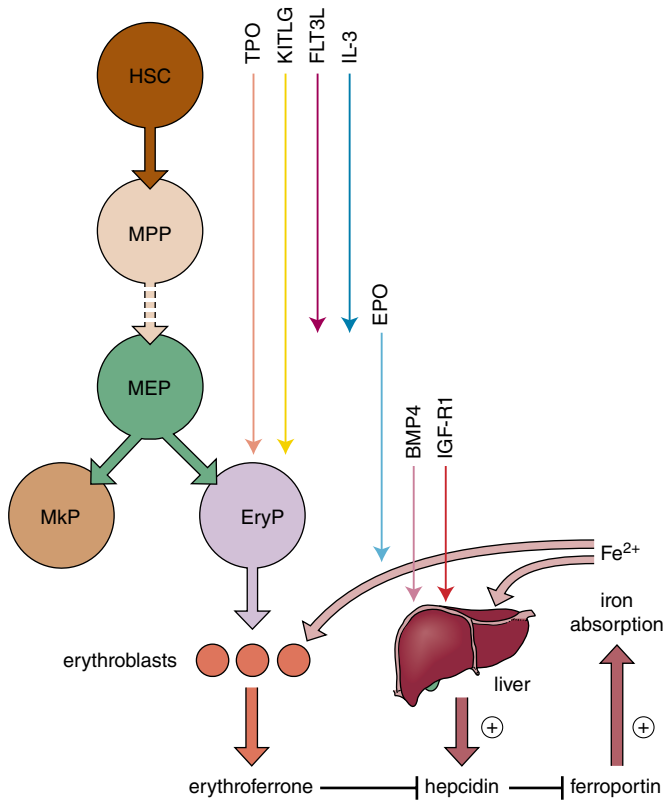

Fig. 3.4. The growth factors that act on the sequence of erythroid progenitors and differentiated erythroid cells (erythroblasts) that differentiate from a hematopoietic stem cell (HSC). Abbreviations of cytokines as Fig. 3.2. BMP4, bone morphogenetic protein 4; IGFR-1, insulin-like growth factor receptor 1. Erythroblasts produces erythroferrone that blocks hepcidin. Hepcidin antagonizes ferroportin, which promotes iron absorption. By blocking hepcidin, erythroferrone promotes ferroportin expression and thus iron absorption, ensuring that erythroblasts can access iron.

conserved cysteine residues, a tryptophan-serine-X-tryptophan-serine motif (WSXWS motif), and fibronectin type III domains in the extracellular part of the receptor. They also share a conserved membrane-proximal intracytoplasmic domain called the Box1/Box2 domain that is important for signaling upon ligand binding.

A separate class of receptors, the type 2 family, includes the receptors for IFNα/β and IFNγ (Fig. 3.7D). These receptors are composed of two distinct subunits (IFNR1/IFNR2). They contain Box1/Box2 domains but lack the WSXWS motif.

SIGNALING PATHWAYS DOWNSTREAM OF RECEPTORS

Once a ligand has engaged a receptor an intricate series of complex molecular events transduce the signal to effect changes in nuclear gene expression. Below, we give examples of these pathways. These are often drawn as linear pathways. However, it is important to remember that any one ligand/receptor pair often signal through more than one intracellular signaling pathway. Moreover, if multiple ligand/receptor pairs are "seen" by a cell, then a complex interaction between pathways is likely to occur in a cell. This is hard to accurately document, is often not shown in textbooks, and is likely to determine the in vivo consequences of hematopoietic cells interacting with extrinsic signaling molecules.

WNT PATHWAY

An example of an important signaling pathway for HSC self-renewal is the evolutionarily conserved canonical Wnt (Wingless-related) pathway that acts both in development and in adult homeostasis (Fig. 3.9). Multiple Wnt ligands engage their cognate receptor complex, consisting of a serpentine receptor of the Frizzled family and a member of the low-density lipoprotein (LDL) receptor family, LRP5/6. When the receptor is occupied, the receptor binds the cytoplasmic scaffold protein Axin and the Axin-binding protein Dishevelled. Axin/Dishevelled then inhibit a protein-destruction complex that contains the tumor suppressor protein adenomatous polyposis coli (APC) and the kinase GSK3-β (glycogen synthetase kinase 3 β). β-Catenin then accumulates in the cytoplasm and is transported into the nucleus. Here it binds the DNA-binding transcription factor TCF/LEF proteins. The β-catenin/TCF/LEF complex can then activate target genes. Target gene expression leads to HSC expansion and altered HSC function.

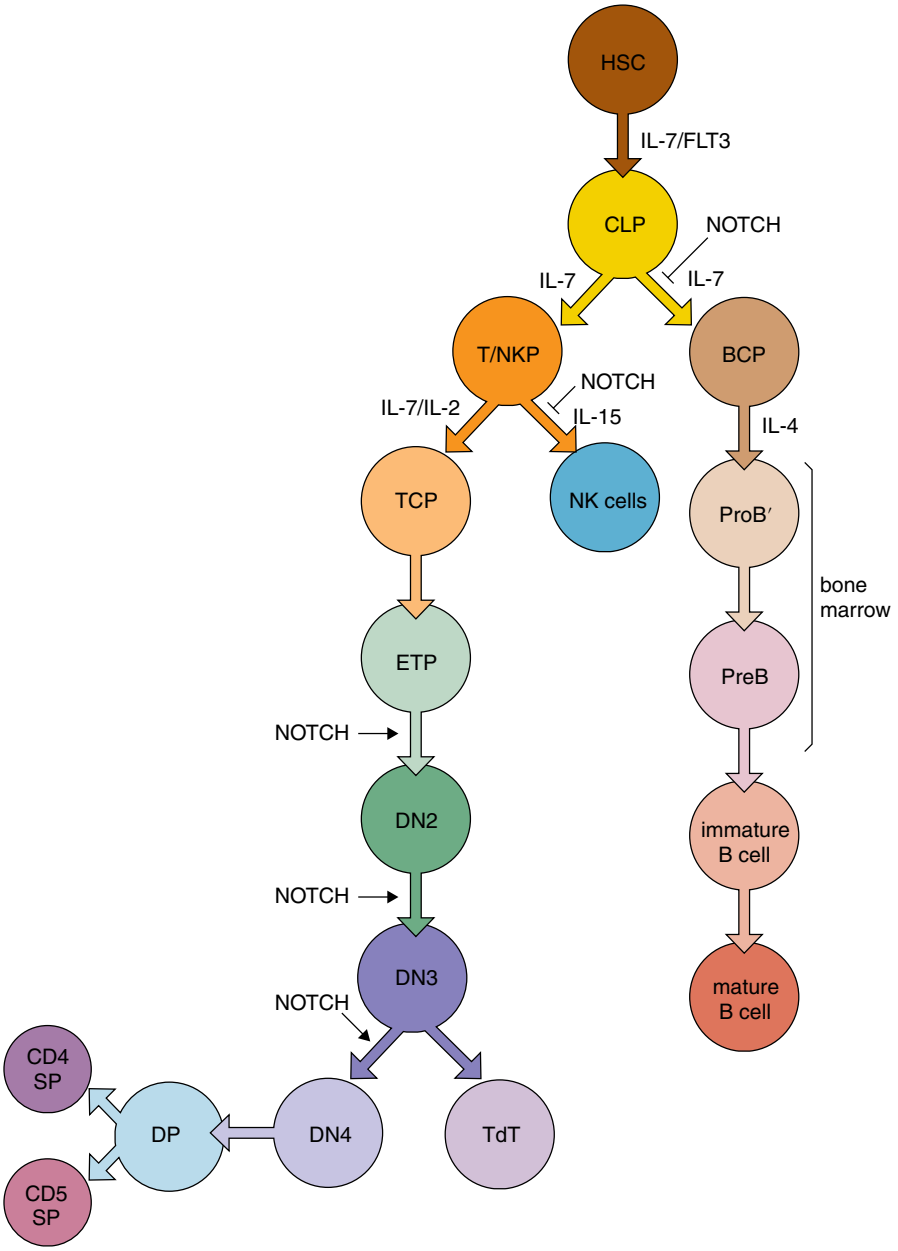

Fig. 3.5. The cytokines that act on the sequence of lymphocyte progenitors and differentiated lymphocytes that differentiate from a hematopoietic stem cell (HSC). T/NKP, T and NK cell progenitor; TCP, T-cell progenitor; ETP, early thymic progenitor; DN2, DN3, DN4, different types of double negative D42 CD82 T cells; DP, double positive CD41 CD81 T cells; SP, single positive T cell; BCP, B-cell progenitor; NK, natural killer cell; TdT, terminal deoxynucleotidyl transferase.

When the receptor is not engaged, the β-catenin is phosphorylated on conserved serine and threonine residues. Phosphorylated β-catenin is then ubiqutinated and degraded by a proteosome. Thus, β-catenin is not able to accumulate. Without β-catenin, LEF/TCF represses gene transcription. This leads to decreased ability of HSCs to repopulate hematopoiesis in vivo. In addition to the canonical Wnt signaling, Wnt also signals via a noncanonical calcium pathway and the c-Jun kinase pathway.

CYTOKINE SIGNALING PATHWAYS

Interaction of cytokines with the ligand-binding receptor subunit initiates oligomerization (see earlier) with other receptor subunits. This triggers a web of intracellular signaling pathways that have distinct but also intercommunicating components (Fig. 3.10). The common finding of leukemia-associated mutations in these signaling pathways have suggested that they may be a required class mutation for leukemogenesis (see Chapter 12).

Common to most pathways are changes in protein phosphorylation on tyrosine, serine, and threonine residues (catalyzed by tyrosine and serine/threonine kinases, respectively). In some cases (e.g. the receptors for SCF, M-CSF) the intracellular domain of the receptor acts as a tyrosine kinase, which phosphorylates itself on tyrosine residues following ligand binding. In all cases, the receptors activate important kinase pathways including the phosphatidylinositol 3-kinase (PI3K) pathway (Figs. 3.10 and 3.11), the three mitogen-activated protein kinase pathways (MAPK) [extracellular-signal regulated kinase (ERK), c-Jun N-terminal kinases/stress-activated protein kinases (JNK/SAPK), and p38 MAPK] (Figs. 3.10 and 3.12), and the Janus-activated kinases (JAK) (Figs. 3.10 and 3.13). Other important signal transduction components include the STAT proteins (signal transducers of activation and transcription) that principally, but not exclusively, are activated by the JAK kinases.

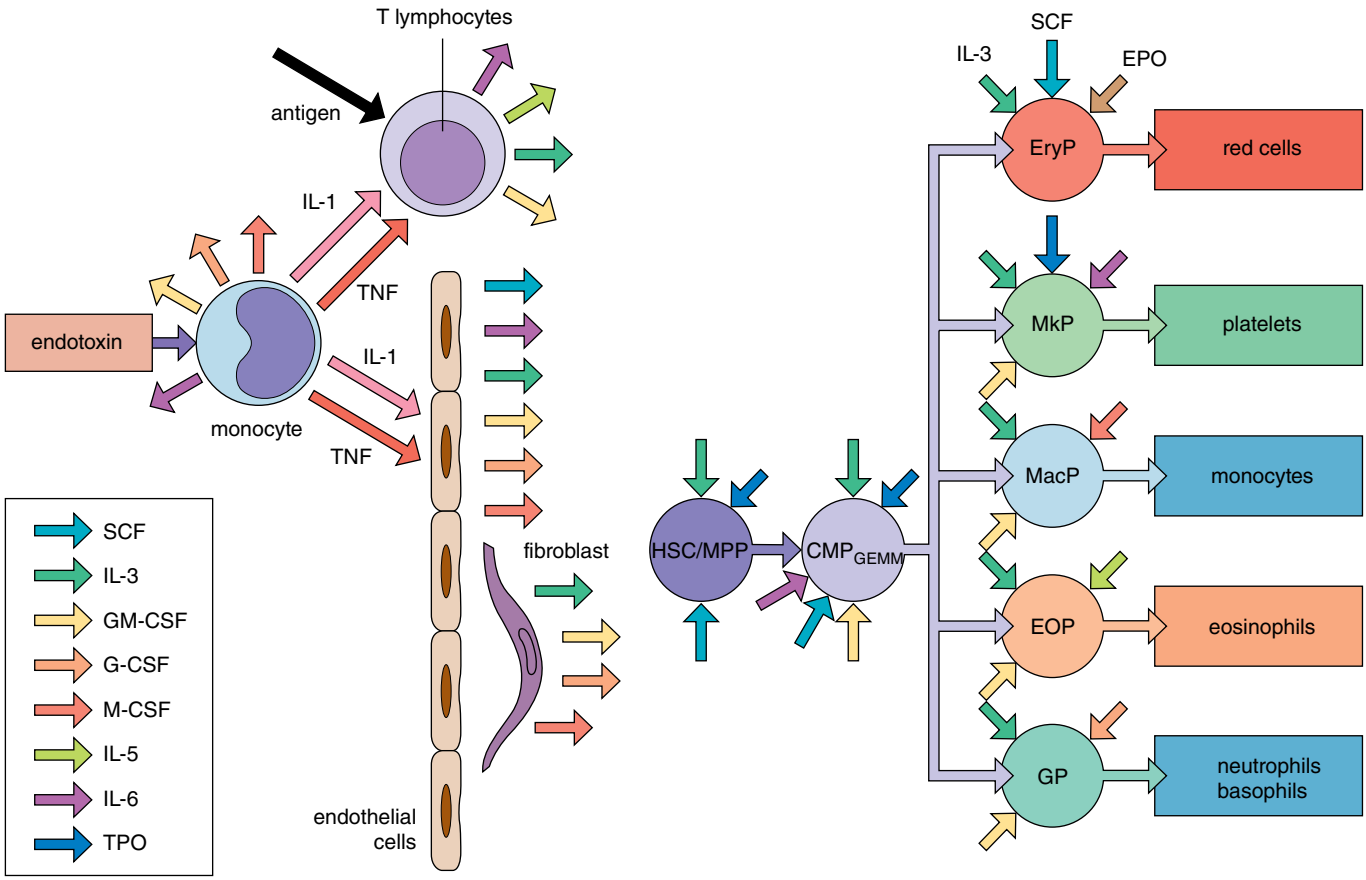

Fig. 3.6. Regulation of hematopoiesis. Pathways of stimulation of leukopoiesis by endotoxin (e.g. from infection). It is likely that endothelial and fibroblast cells release basal quantities of GM-CSF and G-CSF in the normal resting state and that this is enhanced substantially by the monokines TNF and IL-1 released in response to infection. Also, IL-1 and TNF stimulate T cells, and antigen may stimulate T cells directly. The action of IL-3 on human hematopoietic stem cells has not been proved. Abbreviations of cytokines as Fig. 3.2. MacP, monocyte progenitor; GP, granulocyte progenitor.

THE RAS/MAP KINASE PATHWAY

The RAS/MAP kinase pathway (Figs. 3.11 and 3.12) has been one of the most intensively studied signal transduction pathways. Phosphotyrosine residues on receptors bind signal-transducing proteins that contain SRC homology 2 (SH2) domains, such as GAB1/SHC (Fig. 3.12). These in turn bind a complex of proteins that includes Grb2 and SOS. This leads to conversion of p21/RAS-GDP to p21/RAS-GTP at the cell membrane. Farnesylation (i.e. a posttranslational modification consisting of the transfer of an isoprenoid moiety to the C-terminus of the protein) is required for localization of RAS to the cell membrane. Binding of RAS to the cell membrane is essential for function, including activation of downstream effectors, in the MAP kinase pathway, and it is a prerequisite for its transforming activity. Farnesylation is inhibited by farnesyl transferase inhibitors that are under investigation therapeutically in leukemia.

$p21^{RAS}$-GTP phosphorylates and activates the kinase RAF1, which in turn phosphorylates a series of MAP kinases (ERKs) that have major roles in transmitting the signal to the nucleus and activating transcription factors. In one related but separate pathway, the enzyme phospholipase Cγ (PLCγ), which cleaves phosphatidylinositol bisphosphate, is activated to break down membrane lipid, releasing two secondary messengers, diacylglycerol (DG) and inositol trisphosphate (IP3; Fig. 3.11). Activation of PLCγ occurs by binding to phosphotyrosine residues of the activated receptor (Fig. 3.11). The enzyme protein kinase C (PKC) is activated by DG and, in turn, phosphorylates proteins mainly on threonine and serine residues. Release of intracellular calcium ions is caused by IP3. The exact way in which these two biochemical changes subsequently cause signal transduction to the nucleus is unclear.

PHOSPHATIDYLINOSITOL 3-KINASE PATHWAY

PI3K is also activated by binding to activated receptor. It phosphorylates inositol lipids in the cell membrane. Together with phosphoinositide-dependent protein kinase-1 (PDK-1) it then phosphorylates protein kinase B (also known as AKT), which can then interact with the RAF/MAPK pathway (Figs. 3.10 and 3.11). Constitutive deregulated activation of this pathway has been shown to be oncogenic in human malignancy.

JAK-STAT PATHWAY

For those receptors that do not possess inherent protein kinase activity, the JAK-STAT system links cell surface receptors with transcription factor genes. The JAK kinase family includes JAK1, JAK2, JAK3, and TYK2. They are cytoplasmic molecules of 130 kDa and possess a conserved region at the N-terminal end, a kinase-like domain (JH2 domain), and a tyrosine kinase domain (JH1 domain) at the C-terminal end (Figs. 3.10, 3.13 and 3.14). The JAK kinases are activated by ligand binding and receptor

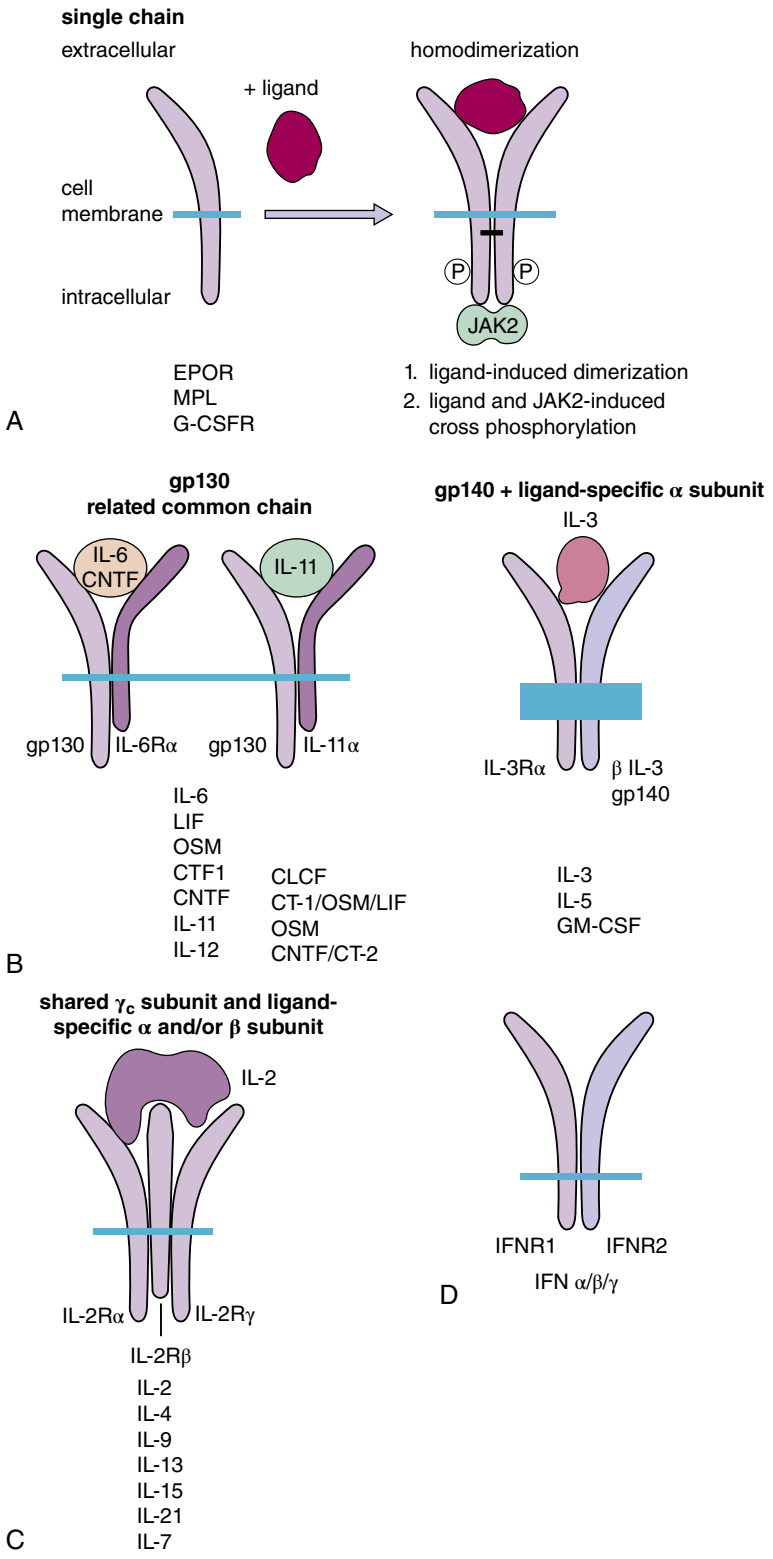

Fig. 3.7. A, EPO, TPO, and G-CSF receptors are all single-chain polypeptides that have an extracellular/transmembrane and intracellular portions *(left)*. On binding ligand, the receptor chains homodimerize, and recruit the downstream signal transduction molecule, the kinase JAK2, leading to cross-phosphorylation of the receptor chains and JAK2 *(right)*. MPL, thrombo protein receptor; G-CSFR, G-CSF receptor. **B,** IL-6, LIF (leukemia-inhibitory factor), OSM (oncostatin M), CTF1 (cardiotrophin 1), CNTF (ciliary neurotrophic factor), IL-11, and IL-12 bind a unique receptor-specific chain that is complexed to a common chain called gp130. The combination of the unique receptor-specific chain and gp130 creates a high-affinity receptor *(left)*. The cytokines IL-3, IL-5, and GM-CSF also bind a heterodimeric receptor, composed of a unique receptor-specific chain (the α chain of the receptor) that is complexed to a common chain called gp140. The genes encoding the unique chain are *IL3RA* (for IL-3 receptor), *IL5RA* (for IL-5 receptor), and *CSF2RA* (for GM-CSF receptor) *(right)*. **C,** Many interleukins (as indicated in the diagram) bind either a heterodimeric or heterotrimeric receptor that shares a common γ chain. **D,** Interferons α, β, and γ bind a heterodimeric receptor composed of two subunits. Interferons α and β bind the same receptor (genes encoding the polypeptides are called *IFNAR1* and *IFNAR2*), whereas interferon γ binds a receptor with a similar structure but composed of related but distinct polypeptides encoded by the genes *IFNGR1* and *IFNGR2*.

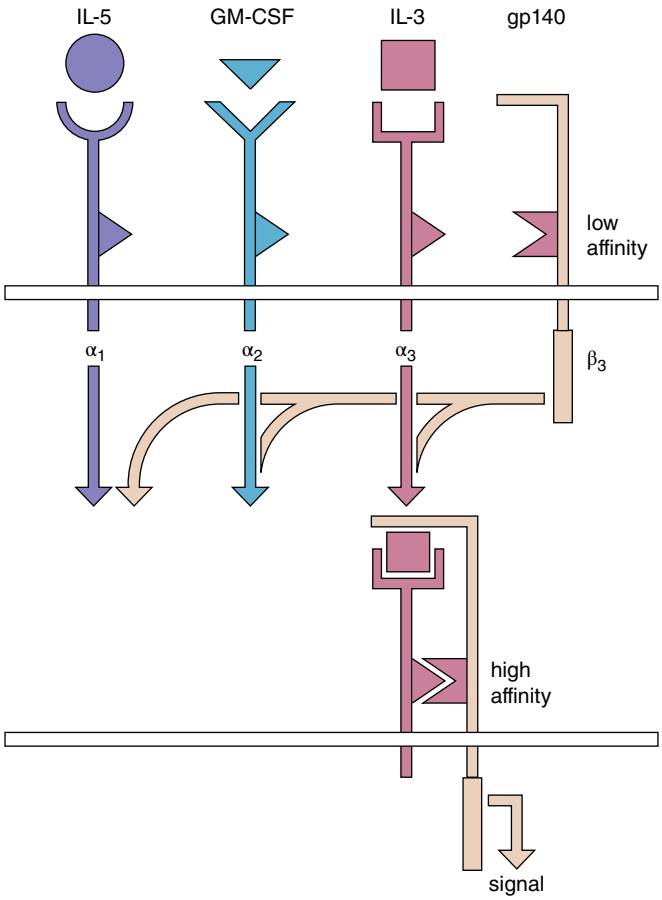

Fig. 3.8. Receptors for GM-CSF, IL-3, and IL-5: structures. These have different α-chains but a common β-chain (gp140) that, after binding to the α-chain in the presence of the growth factor, forms a high-affinity receptor and is subsequently responsible for signal transduction to the cell interior. Source: Nicola NA, Metcalf D. *Cell* 1991;67:1–4. Reproduced with permission of Elsevier.

dimerization. Box1 and Box2, conserved regions on the cytokine receptor intracytoplasmic regions, are involved in binding and activation of JAKs. The JAK kinases then phosphorylate tyrosine residues in latent cytokine transcription factors, the STATs. The STATs are DNA-binding proteins of 80–100 kDa with an SH2 domain and tyrosine phosphorylation sites at the C-terminal end (Figs. 3.13 and 3.14). The activated STATs form

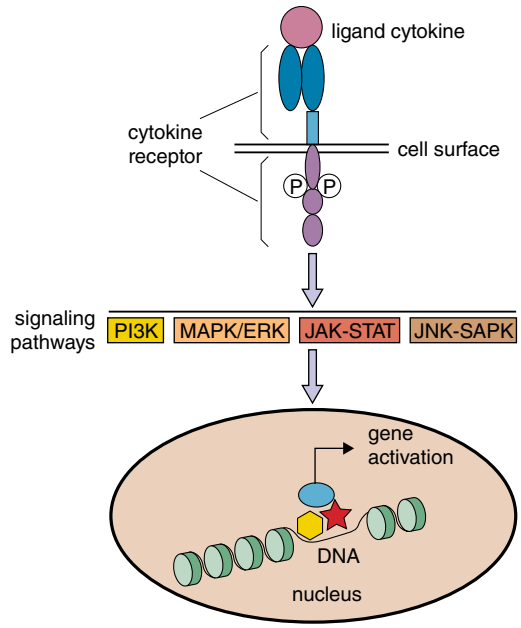

Fig. 3.10. Binding of cytokines to cytokine receptors leads to activation of intracellular signaling pathways (PI3K, MAPK/ERK, JAK-STAT, JNK-SAPK) that transmit messages from the cytoplasm to the nucleus where gene transcription is modulated. Ultimately this affects cell fate choice, cell cycle, and apoptosis machinery.

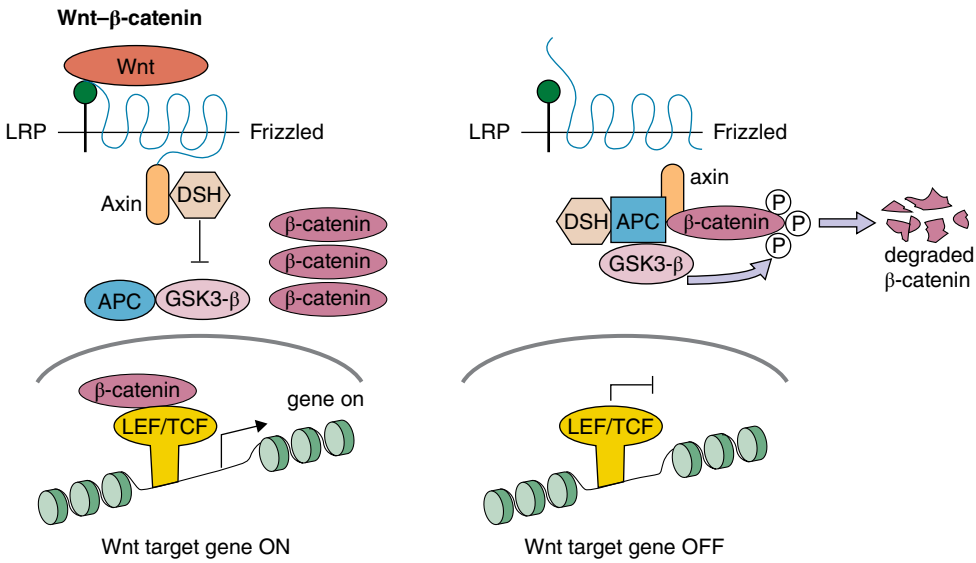

Fig. 3.9. Schematic pathway of the Wnt–Frizzled receptor. On the left, when Wnt is bound to its receptor – a heterodimer of Frizzled and its partner LRP – the receptor binds the Axin 1/Dishevelled (DSH) complex. This complex inhibits *APC* (adenomatous polyposis coli gene) and the kinase GSK3-β (glycogen synthase kinase 3 β). When GSK3-β is inhibited, it fails to phosphorylate β-catenin, and β-catenin can then accumulate. β-Catenin then translocates into the nucleus and binds to the transcription factor LEF/TCF. β-Catenin/LEF/TCF then activates gene expression (Wnt target gene is "on"). On the right, when LRP/Frizzled are not engaged by Wnt, DSH/APC/Axin/GSK3-β forms an active complex that phosphorylates β-catenin. Phosphorylated β-catenin is then targeted for proteolysis, and LEF/TCF fails to activate Wnt target genes.

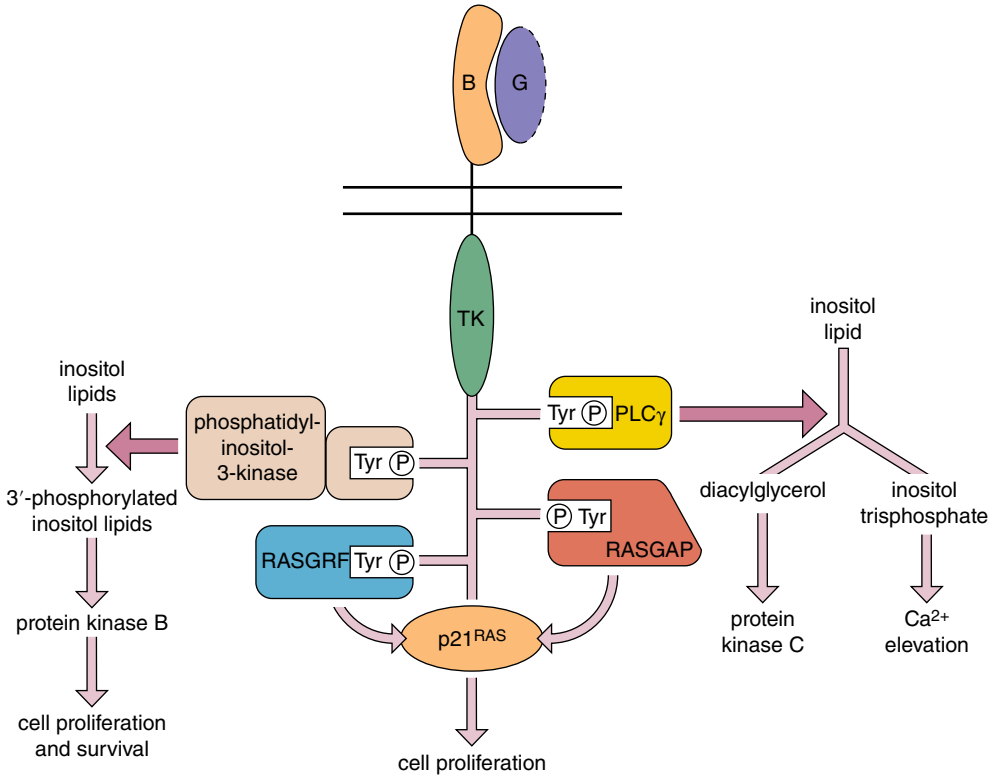

Fig. 3.11. SH2 domain-containing proteins bind to activated tyrosine phosphorylated growth factor receptors. For clarity, only one partner of the receptor dimer is shown. PLCγ, phospholipase Cγ; RASGAP, RAS GTPase-activating protein; RASGRF, guanine nucleotide-releasing factor. Source: Wickremasinghe RG, Hoffbrand AV. The molecular basis of leukaemia and lymphoma. In: Hoffbrand AV, et al., eds. Postgraduate Haematology, 4th edn. Butterworth-Heinemann, 1999, pp. 354–372. Reproduced with permission of Elsevier.

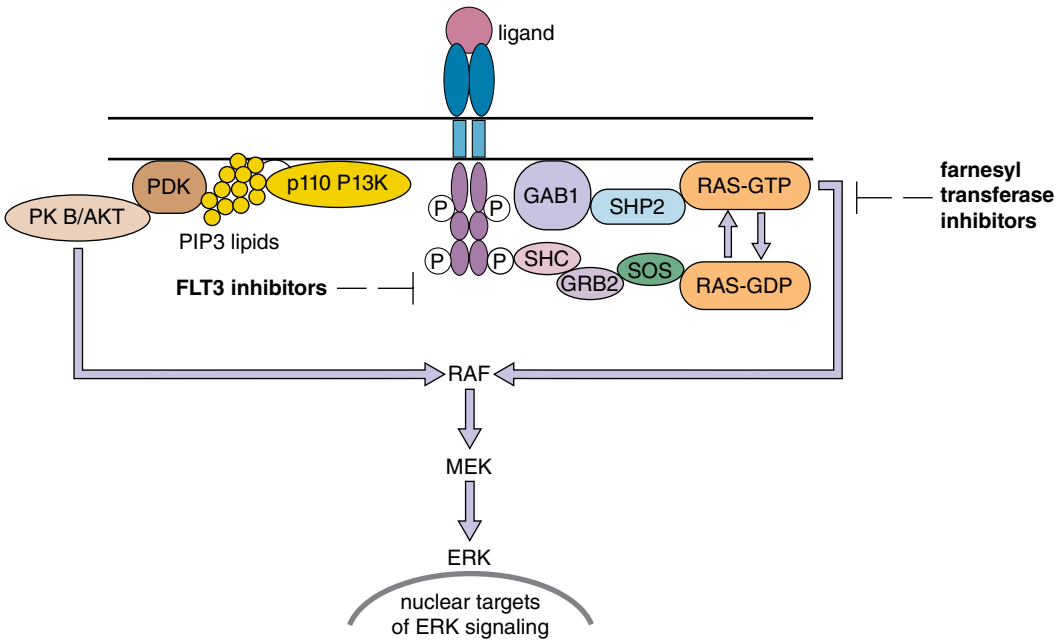

Fig. 3.12. Simplified relationship between the RAS and PI3K pathways. After binding of ligand to the receptor the intracellular membrane becomes phosphorylated. This then binds a series of proteins that activates the RAS pathway via either the SH-containing adapter protein Shc (Src homology 2 domain containing transforming protein), GRB2 (growth factor receptor-bound protein 2), SOS (Son of Sevenless), and GAB1 (GRB2-associated binding protein 1). This leads to production of RAS-GTP that activates RAF1, which is a MAP kinase kinase kinase (MAP3K). RAF1 can also be activated by the phosphoinositol 3-kinase pathway via membrane-bound p110 PI3K and PDK, which activates protein kinase B (PK B/AKT). PK B then activates RAF1. RAF1 phosphorylates MEK1/2 kinase, which phosphorylates ERK1/2 kinase. This leads to activation of nuclear ERK1/2 targets. The RAS pathway can be targeted by farnesyl transferase inhibitors (such as tipfarnib). Also shown: the receptor itself can be targeted, and in this case an FLT3 receptor is targeted by FLT3 inhibitors. (See also Chapters 13 and 14.)

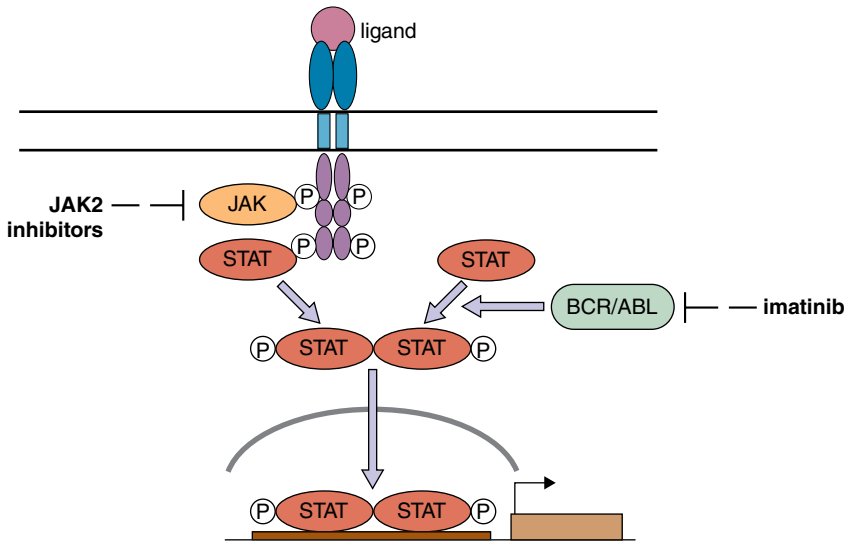

Fig. 3.13. The JAK-STAT pathway. Ligand binding leads to receptor dimerization, cross-phosphorylation of the receptor JAK, and STAT binding and phosphorylation of STAT proteins. Phospho-STAT proteins translocate to the nucleus where they bind critical DNA sequences to modulate gene expression. The modes of action of JAK2 inhibitors and imatinib are shown.

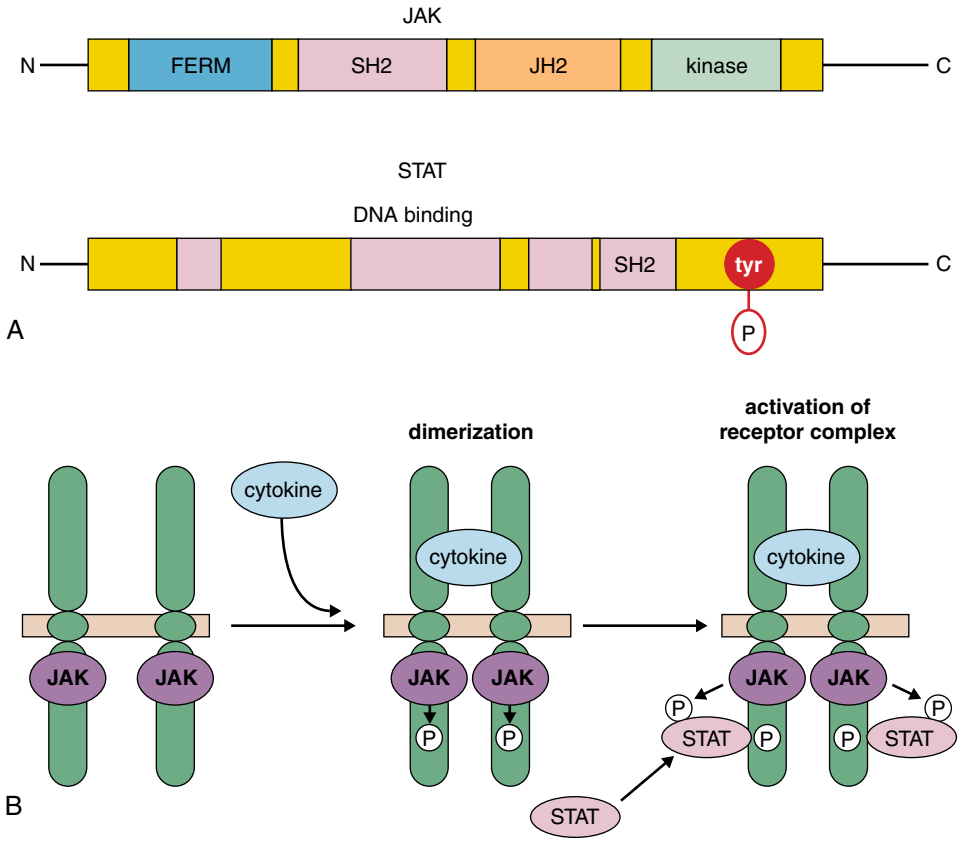

Fig. 3.14. A, Schematic structure of domains within the JAK protein (in this case JAK2 is shown). There are four domains: the FERM domain (required for binding to EPOR and other receptors), the SH2 domain (a protein interaction module), the JH2 domain (regulates activity of the kinase domain), and finally the kinase domain. **B,** The steps that lead to activation of the JAK-STAT pathway after binding of cytokine to the receptor. (See also Chapter 15.)

a homo- or heterodimers and translocate to the nucleus, where they bind to specific DNA motifs, positive promoter elements for cytokine-responsive genes. In addition to STAT activation, JAK kinases also phosphorylate additional proteins, including insulin-receptor substrate 1 and 2 (IRS-1, IRS-12) and GAB2. The resultant phosphotyrosine residues serve as binding sites for SH2 domain-containing proteins, which activate signaling pathways that lead to ERK activation.

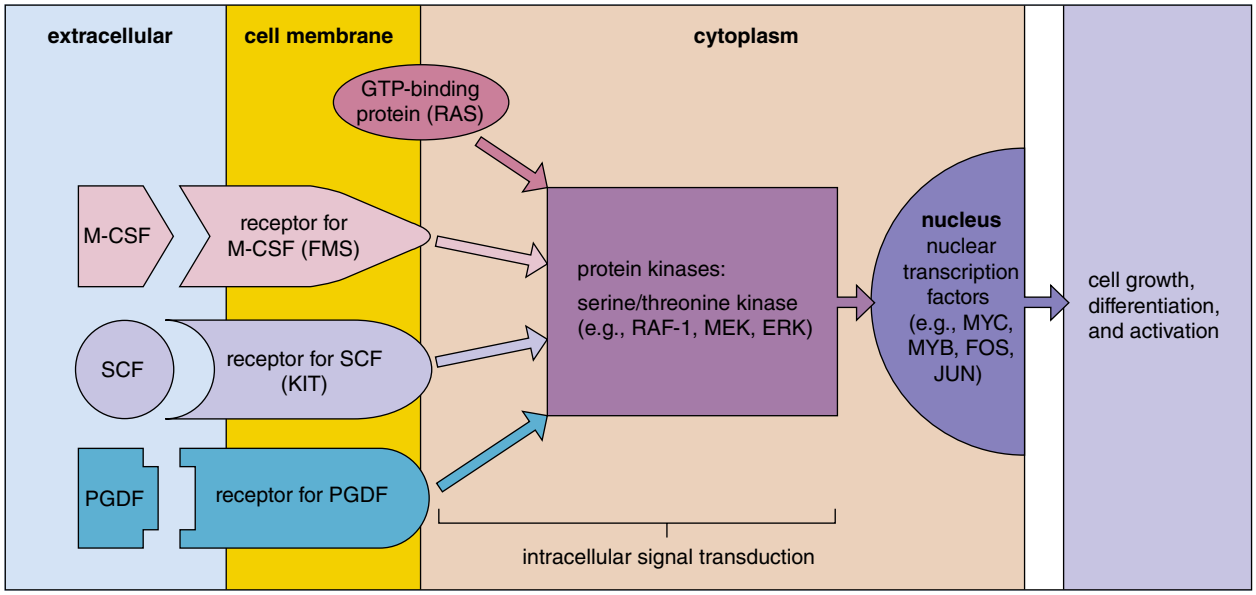

Fig. 3.15. Cellular proto-oncogene products: examples of those that act at different stages of the pathways that transduce growth signals from the cell membrane to the nucleus. Abbreviations of cytokines as in Fig. 3.2.

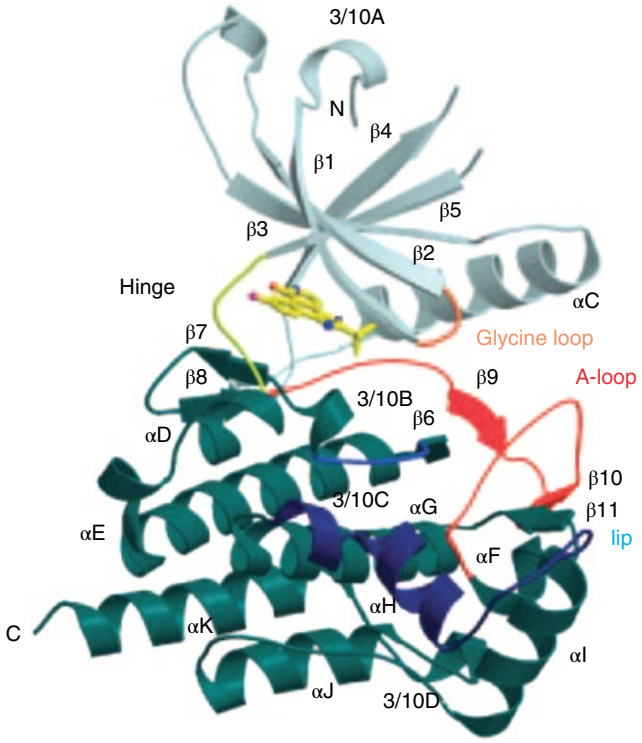

Fig. 3.16. Overview of the crystal structure of the JAK2 kinase domain. The kinase domain is divided into an N-terminal portion (gray) and a C-terminal region (green) linked by a hinge (yellow). The catalytic region (blue) and activation loop (red) are centrally important for kinase activity. Structural studies such as these are important to design targeted therapies for diseases in which there is constitutively active JAK signaling.

MUTATIONS IN SIGNALING COMPONENTS LEADING TO CLONAL HEMATOLOGIC DISORDERS

In hematologic malignancies, mutations are present in genes regulating intracellular signaling. These include cytokine receptors (e.g. mutations in *FLT3* and *KIT* genes in acute myeloid leukemia, AML), intracellular signaling components (*JAK2* mutations in myeloproliferative disorders, T-cell acute lymphoblastic leukemia, Down syndrome acute lymphoblastic leukemia, constitutive activation of ABL kinase by the *BCR-ABL* fusion gene in chronic myeloid leukemia, mutations in *RAS*, *PTP11* genes in AML and myelodysplasia) (Fig. 3.15). Given the high frequency of such mutations and the fact that these mutations often deregulate enzymatic kinase function that is usually tightly controlled, much effort has gone into solving crystal structures of components of signaling pathways. In Fig. 3.16 the crystal structure of the JAK2 kinase domain is shown. These studies are important to help development of novel, potentially less toxic, targeted specific kinase inhibitors.

CHAPTER

4

ERYTHROPOIESIS AND EXAMINATION OF THE PERIPHERAL BLOOD AND BONE MARROW

ERYTHROPOIESIS

Every day the human bone marrow makes approximately 10^{10} new blood cells, the bulk of them mature erythrocytes, in a process called erythropoiesis. Rare hematopoietic stem cells (HSCs) enter cell cycle and commit to the myeloid lineage. A hierarchy of progenitors with erythroid potential (CFU-GEMM, MEP, BFU-E, and CFU-E) are then progressively amplified in number and enter the cell cycle more actively to produce mature red cells (Figs. 4.1 and 4.2). Growth factors (see Fig. 3.4) and key transcription factors are essential (Figs 2.11 and 4.2). The nuclear and cytoplasmic changes, their relative frequency in adult bone marrow, and their percentage in the cycle of hematopoietic progenitor and precursor cells as an HSC differentiates into erythroid cells are shown in Fig. 4.1. During terminal erythroid maturation, erythroid precursors (erythroblasts) mature through morphologically distinct maturation stages.

The main function of red cells is to carry oxygen to the tissues and return carbon dioxide from the tissues to the lungs. Hemoglobin is the critical protein constituent of red cells that is responsible for this gaseous exchange. The principal adult hemoglobin molecule (HbA) has a molecular weight of 68 000. It consists of α- and β-globin polypeptide chains (α_2, β_2). Each globin polypeptide chain has its own heme group that coordinates an iron molecule. The metabolism of iron and heme synthesis is set out in Chapter 5.

Control of erythroid production is principally regulated by varying the production of the cytokine erythropoietin (EPO). This is a 34–39 kDa protein (when fully glycosylated) secreted predominantly by the peritubular interstitial cells of the kidney,

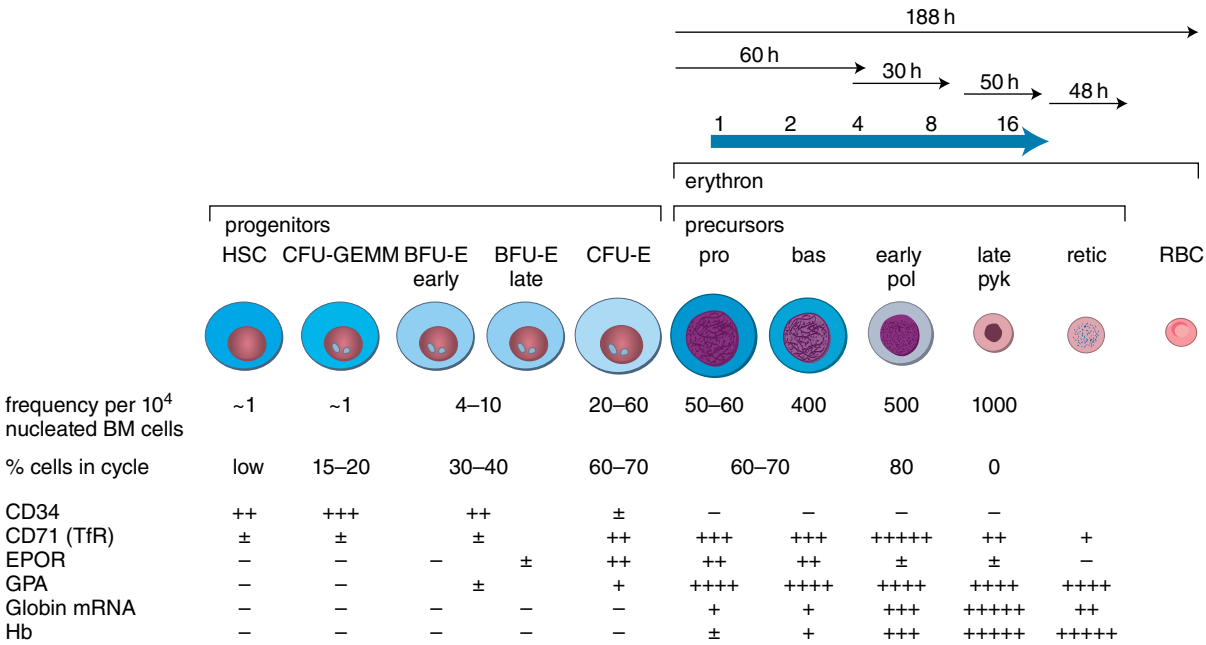

Fig. 4.1. The progression of cells through erythropoiesis from hematopoietic stem cells (HSCs) through multipotential myeloid cells (CFU-GEMM), to the earliest unilineage erythroid cells. Burst colony-forming erythroid cell (BFU-E), colony-forming erythroid (CFU-E), to maturing erythroblasts (proerythroblasts [pro], basophilic erythroblasts [bas], early polychromatic erythroblasts [early pol], late pyknotic erythroblasts [pyk]), finally to enucleated reticulated cells (retic) and mature erythrocytes (RBCs). CD36, CD45, α_4-integrin (CD49d), and band 3 are also expressed during various stages of erythropoiesis. GPA, glycophorin A (CD235a); TfR, transferrin receptor; BM, bone marrow. (Courtesy of Professor DR Higgs.)

Color Atlas of Clinical Hematology: Molecular and Cellular Basis of Disease, Fifth Edition. A. Victor Hoffbrand, Paresh Vyas, Elías Campo, Torsten Haferlach, and Keith Gomez

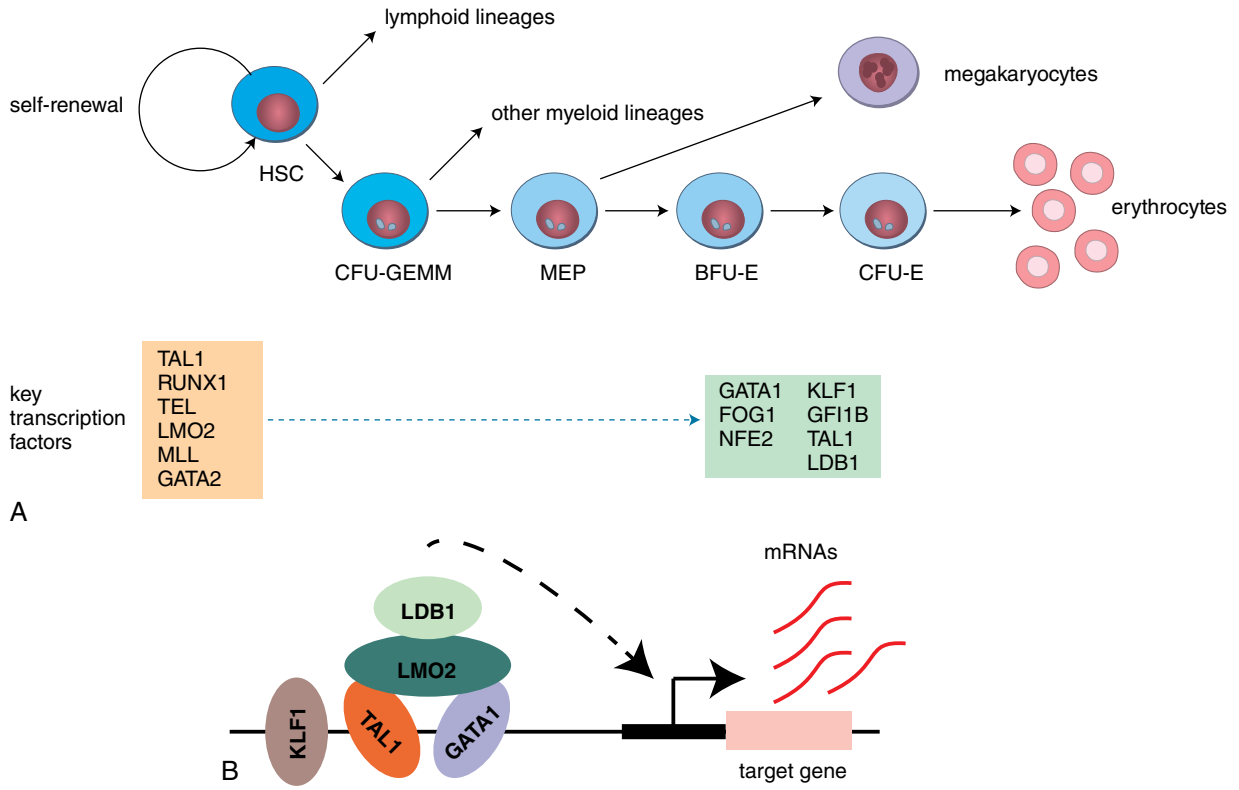

Fig. 4.2. A, Summary of some steps in self-renewal, lineage specification, and differentiation of hematopoietic stem cells to red cells. Some of the key transcription factors involved in this process are summarized beneath the diagram. HSC, hematopoietic stem cell; CFU-GEMM, colony-forming unit–granulocyte–erythrocyte monocyte megakaryocyte; MEP, megakaryocyte–erythroid progenitor; BFU-E, burst-forming unit–erythroid; CFU-E, colony-forming unit–erythroid; TEL, translocation Ets leukemia; LMO2, LIM domain only 2; MLL, mixed lineage leukemia; GATA1, GATA-binding factor 1; GATA2, GATA-binding factor 2; FOG, friend of GATA; NFE2, nuclear factor erythroid-derived 2; KLF1, Kruppel-like factor 1 (erythroid); GFI1B, growth factor-independent 1B; TAL1, T-cell acute lymphoblastic leukemia 1. Source: Hoffbrand AV, et al., eds. *Postgraduate Haematology*, 7th edn. John Wiley & Sons, 2016. Reproduced with permission of John Wiley & Sons. **B,** The core erythroid network (CEN) of transcription factors (TFs) is composed of the DNA-binding TFs (GATA1, TAL1 and KLF1) and the non-DNA-binding TFs (LDB1 and LMO2). The CEN loops from enhancers to promoters to activate target gene expression. TFs in the CEN may interact with other TFs at subsets of regulatory elements to enhance or repress expression of target genes. Source: *Br J Haematol* 2016;173:206–218. Reproduced with permission of John Wiley & Sons.

which also express platelet-derived growth factor receptor beta and neuroglial antigen 2 (Fig. 4.3). Small amounts of EPO are also made in adult liver and in brain cells (predominantly pericytes but also neurons, glial cells, and endothelial cells). EPO stimulates erythropoiesis largely at the committed CFU-E stage. A proportion of BFU-E progenitors and more mature cells (up to the reticulocyte stage) also have erythropoietin receptors (EPORs) and are sensitive to EPO. The action of EPO is to increase the overall red cell mass leading to increased hemoglobin production.

EPO secretion by the kidneys is regulated by an autocrine/paracrine system. Blood oxygen tension is sensed by peritubular interstitial cells in the kidney and, to a lesser extent, by hepatocytes. This is influenced by a number of factors, such as atmospheric oxygen, cardiopulmonary function, renal blood flow, hemoglobin concentration, and oxygen dissociation curve. At high oxygen tension a family of oxygen-sensitive prolyl hydroxylase enzymes hydroxylate the transcription factor HIF-1α (hypoxia-inducible factor α) on prolyl residues (Fig. 4.4). This leads to ubiquitination of HIF-1α by an ubiquitin ligase complex that contains the tumor suppressor von Hippel–Lindau protein (VHL). Ubiquitinated HIF-1α is then degraded. Lower levels of HIF-1α lead to lower transcription of EPO in renal mesangial cells. By contrast, in response to hypoxia caused, for example, by anemia or high altitude, the prolyl hydroxylases are inhibited and HIF-1α levels are high, and this upregulates EPO production. High iron levels also upregulate HIF levels (Fig. 4.4).

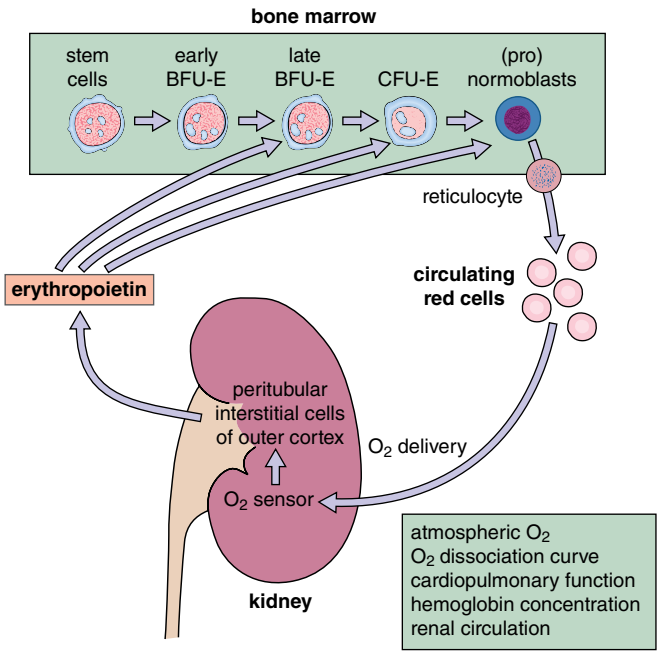

Fig. 4.3. Red cell production is controlled, in part, by serum erythropoietin levels. Erythropoietin is produced by the kidney, which senses blood oxygen levels. Decreased oxygen tension leads to increased erythropoietin production. Erythropoietin promotes survival of BFU-E and downstream erythroid cellular intermediates.

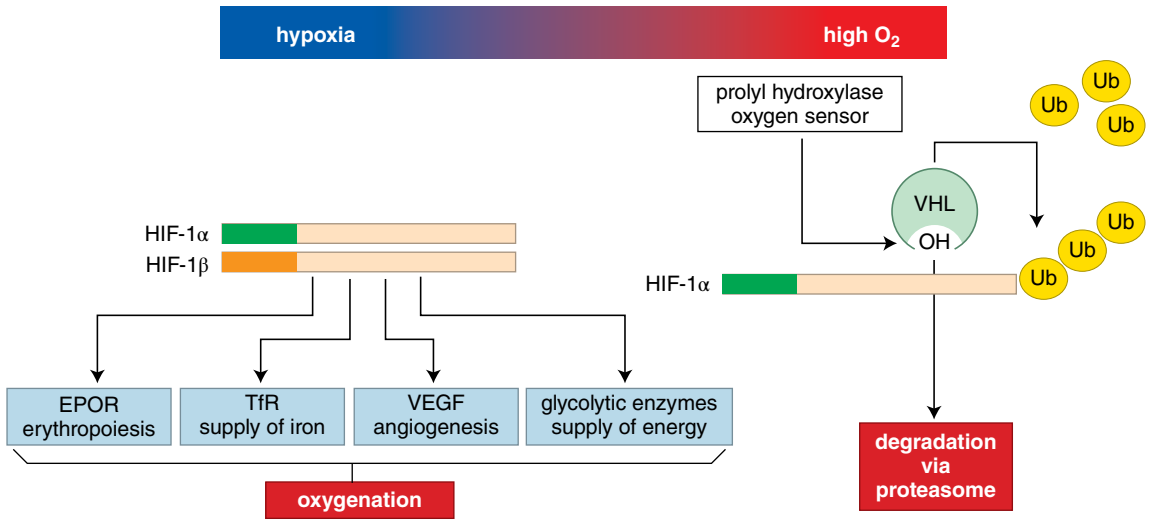

Fig. 4.4. The oxygen-sensing system. Ub, ubiquitination; VHL, von Hippel–Lindau protein; HIF, hypoxia-inducible factor. VHL is an E3 ubiquitin ligase. In the context of normal oxygenation, HIF-1α is hydroxylated, providing a binding site for VHL, which ubiquitinates it, thereby targeting it for degradation by the proteasome. At low oxygen tension, hydroxylation cannot occur and VHL cannot bind and ubiquitinate HIF-1α, the half-life of which is therefore greatly increased. As a result, HIF-1 is able to carry out its function as a transcription factor, upregulating the expression of its target genes, such as EPOR, TfR, VEGF, and glycolytic enzymes in response to hypoxia. Source: Hoffbrand AV, et al., eds. *Postgraduate Haematology*, 7th edn. John Wiley & Sons, 2016. Reproduced with permission of John Wiley & Sons.

Germline mutations of the EPOR (associated with low or normal plasma EPO levels) and of VHL (Chuvash VHL mutation and other VHL mutations, associated with a high plasma EPO level) are causes of familial erythrocytosis.

EXAMINATION OF PERIPHERAL BLOOD AND THE BONE MARROW

The usual initial diagnostic approach to blood disorders is blood counting (Table 4.1) and blood film examination and, if required, examination of the cytology and histology of the bone marrow (Table 4.2). Blood films are usually spread on glass slides and stained, like bone marrow aspirates, with one of the Romanowsky stains (e.g. May-Grünwald–Giemsa or Wright's) (Fig. 4.5). Bone marrow aspirates provide films on which the cytologic details of developing cells can be examined (Fig. 4.6A–C). The proportions of different cells are assessed, appearances of the individual cells noted, and a search made for the presence of cells foreign to the normal marrow, such as metastatic deposits of carcinoma. The aspirate is also stained by Perls' reaction to assess iron stores and iron in developing erythroblasts (see Fig. 5.17). Bone marrow trephine biopsies produce cores of bone and marrow, which are decalcified and processed for histologic assessment (Figs. 4.7–4.9). The trephine provides an excellent sample for examination of marrow architecture and cellularity. It is the most reliable method of detecting marrow infiltrates. Immunohistochemistry is valuable in identifying change in cell composition of the marrow and the presence of abnormal cells.

TABLE 4.1. NORMAL BLOOD COUNT

Hemoglobin (Hb)	Male	13.5–17.5 g/dL
	Female	11.5–15.5 g/dL
Red cells (RBC; erythrocytes	Male	4.5–6.5/L
	Female	$3.9–5.6 \times 10^{12}$/L
Packed cell volume (PCV; hematocrit)	Male	40–50%
	Female	36–48%
Mean corpuscular volume (MCV)		80–95 fL
Mean corpuscular hemoglobin (MCH)		27–34 pg
Mean corpuscular hemoglobin concentration (MCHC)		30–35 g/dL
Reticulocytes		0.5–2.0%; $50–60 \times 10^9$/L
White cells (WBC; leukocytes)	Total	$4.0–11.0 \times 10^9$/L
	Neutrophils	$2.5–7.5 \times 10^9$/L
	Lymphocytes	$1.5–3.5 \times 10^9$/L
	Monocytes	$0.2–0.8 \times 10^9$/L
	Eosinophils	$0.04–0.44 \times 10^9$/L
	Basophils	$0.01–0.1 \times 10^9$/L
Platelets		$150–400 \times 10^9$/L

ERYTHROID CELLS IN THE BONE MARROW AND PERIPHERAL BLOOD

During terminal erythroid maturation, erythroid precursors (erythroblasts) mature through morphologically distinct maturation stages. The earliest recognizable erythroid cell in the marrow is the proerythroblast, a large cell with dark blue cytoplasm and a primitive nuclear chromatin pattern (Fig. 4.10). The more differentiated erythroblasts are progressively smaller and contain increasing amounts of hemoglobin, to give a polychromatic cytoplasm; the nuclear chromatin becomes progressively more condensed. Basophilic (early), polychromatic (intermediate), and pyknotic (late) stages of erythroblast development are recognized (Figs. 4.11 and 4.12). Kinetic studies have identified four cell cycles between the proerythroblast and the late nondividing erythroblast (Fig. 4.12C). In the marrow, erythroblasts are associated closely with their supportive macrophages and so are in "nests" (Fig. 4.13). These tend to be in the center of the

TABLE 4.2. PERCENTAGE OF CELLS OF VARIOUS CATEGORIES IN BONE MARROW FILMS

Cells		Observed range (%)	95% range (mean)
Blast cells		0.0–3.2	0.0–3.0 (1.4)
Promyelocytes		3.6–13.2	3.2–12.4 (7.8)
Neutrophil myelocytes		4.0–21.4	3.7–10.0 (7.6)
Eosinophil myelocytes		0.0–5.0	0.0–2.8 (1.3)
Metamyelocytes		1.0–7.0	2.3–5.9 (4.1)
Neutrophils	Males	21.0–45.6*	21.9–42.3 (32.1)
	Females	29.6–46.6*	28.8–45.9 (37.4)
Eosinophils		0.4–4.2	0.3–4.2 (2.2)
Eosinophils plus eosinophil myelocytes		0.9–7.4	0.7–6.3 (3.5)
Basophils		0.0–0.8	0.0–0.4 (0.1)
Erythroblasts	Males	18.0–39.4*	16.2–40.1 (28.1)
	Females	14.0–31.8*	13.0–32.0 (22.5)
Lymphocytes		4.6–22.6	6.0–20.0 (13.1)
Plasma cells		0.0–1.4	0.0–1.2 (0.6)
Manocytes		0.0–3.2	0.0–2.6 (1.3)
Macrophages		0.0–1.8	0.0–1.3 (0.4)
Myeloid: erythroid ratio	Males	1.1–4.0†	1.1–4.1 (2.1)
	Females	1.6–5.4†	1.6–5.2 (2.8)

Significance of difference between men and women: *$P < 0.001$; †$P < 0.01$.

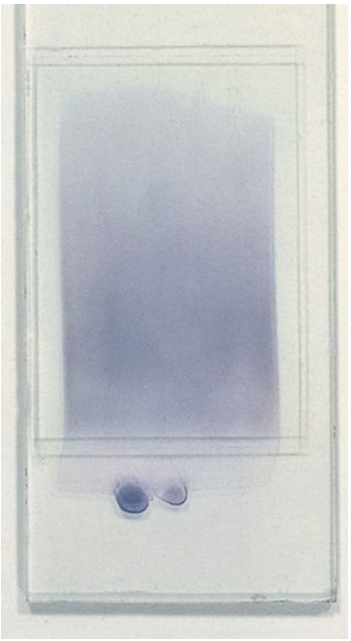

Fig. 4.5. Peripheral blood film: Glass slide of a well-spread blood film stained by the May-Grünwald–Giemsa technique.

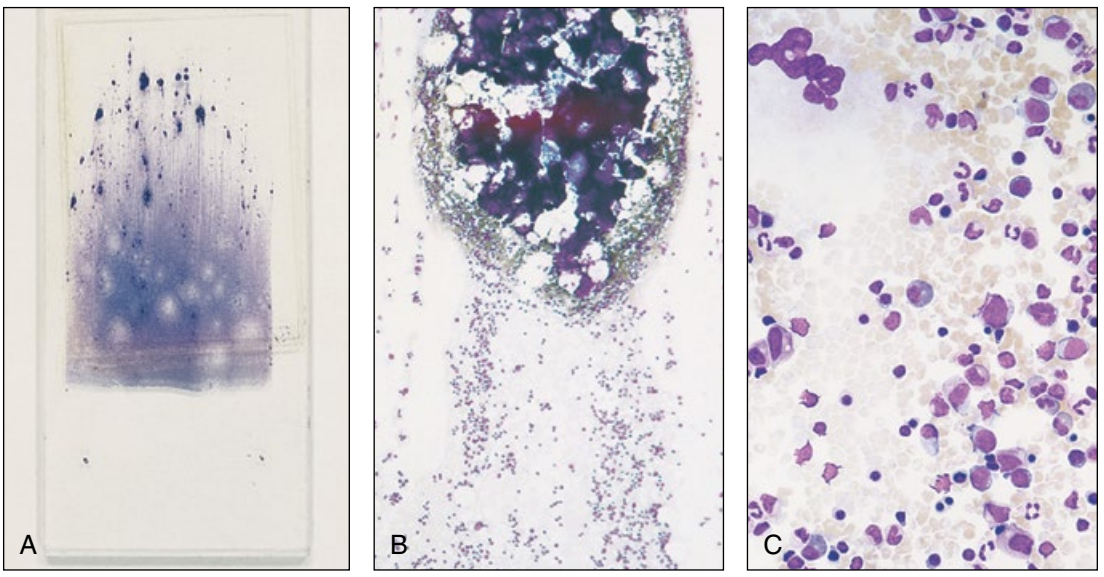

Fig. 4.6. A, Bone marrow aspirate: This normal aspirate has been spread, allowed to dry, and stained by the May-Grünwald–Giemsa technique. Bone marrow fragments are clearly visible at the tail end of the smear. **B,** Normal marrow fragment and cell trails: the marrow fragment contains hematopoietic cells, supporting reticuloendothelial cells and some fat spaces. During the spreading procedure, representative cells of each hematopoietic cell line spill out into "trails" behind the marrow fragments. **C,** Higher magnification.

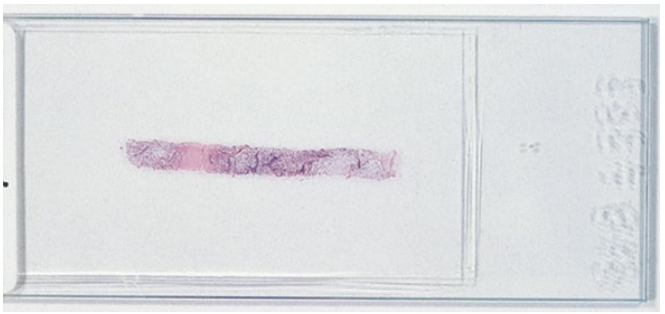

Fig. 4.7. Normal trephine biopsy: Gross appearance of a section prepared from a trephine biopsy of the posterior iliac crest. (H&E stain.)

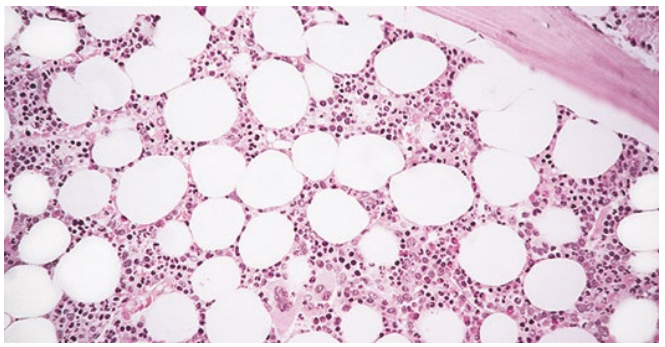

Fig. 4.8. Normal trephine biopsy: representative histology taken from the posterior iliac crest. Approximately half the intertrabecular space is occupied by hematopoietic tissue and half by fat. H & E stain.

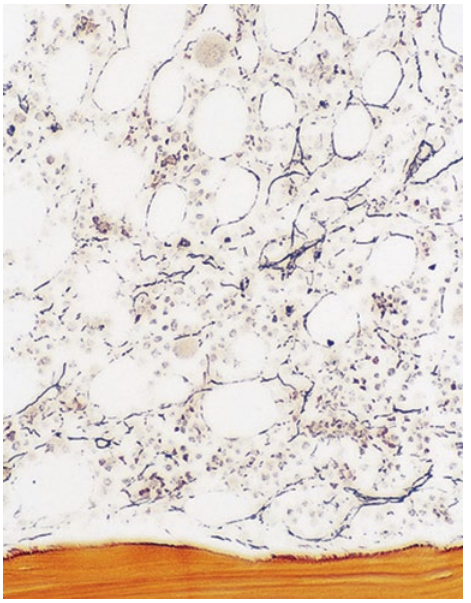

Fig. 4.9. Normal trephine biopsy: the reticulin fibers are thin and delicate, and form a network around the hematopoietic cells. Silver impregnation stain.

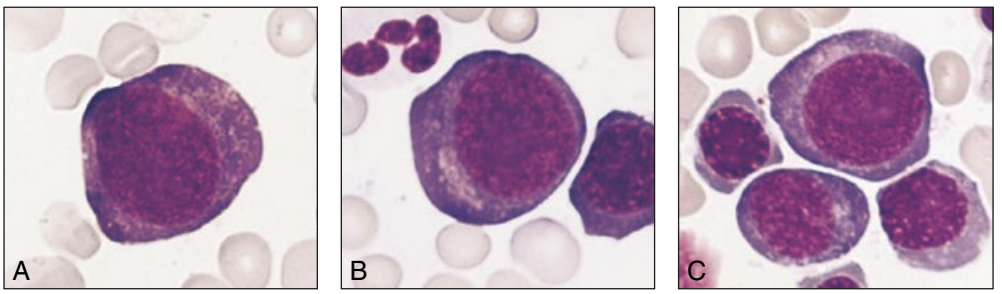

Fig. 4.10. Erythropoiesis. **A–C,** Proerythroblasts and smaller basophilic and polychromatic erythroblasts.

hematopoietic tissue close to blood vessels and away from the bone trabeculae.

Finally, through a process that is probably an erythroid-specific variant of apoptosis, the nucleus is enucleated to produce a reticulocyte that still contains messenger ribonucleic acid (mRNA) capable of synthesizing hemoglobin and stains with supravital stains (Fig. 4.14). This cell spends 1–2 days in the marrow and then a further 1–2 days in the peripheral blood and spleen, when the RNA is completely lost and an orthochromatic or pink-staining erythrocyte (red blood cell [RBC]) results. The mature red cell contains little or no mRNA.

In adults in normal steady-state conditions, only reticulocytes and red cells are present in peripheral blood. Red cells in normal peripheral blood are circular and fairly uniform in size with a mean cell diameter of 8 µm. For successful gaseous exchange, the flexible biconcave red cell, 8 µm in diameter, has to pass through the microcirculation, whose diameter is only 3.5 µm. In the ideal part of the blood film for examination, which is where the red cells are just beginning to touch and overlap, their biconcave shape produces a central pallor. Only mild variations in size (anisocytosis) and shape (poikilocytosis) are seen (Fig. 4.15).

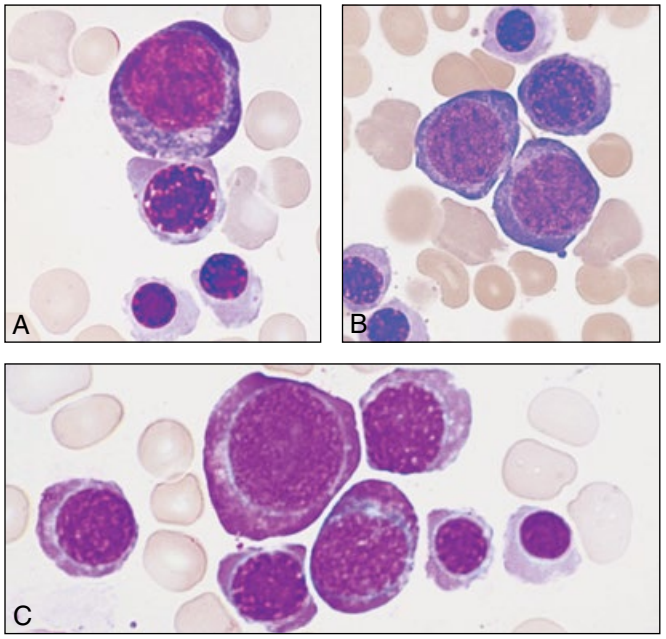

Fig. 4.11. Erythropoiesis. **A,** From top to bottom: basophilic, polychromatic, and two pyknotic erythroblasts. **B,C,** further examples of basophilic, polychromatic, and pyknotic erythroblasts.

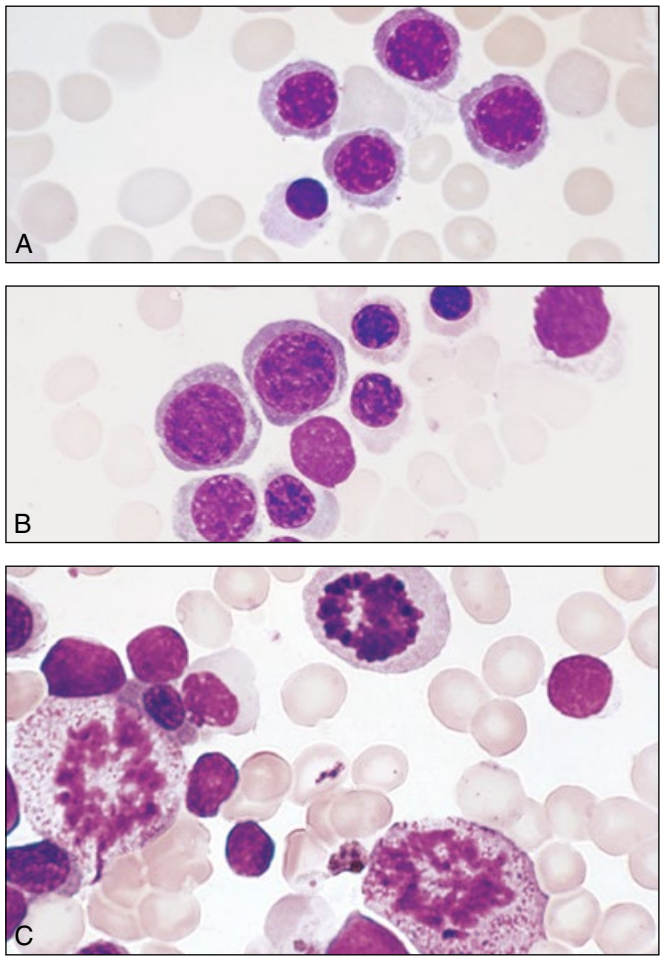

Fig. 4.12. Erythropoiesis. **A,B,** Polychromatic and pyknotic erythroblasts. **C,** Mitotic figures: three cells, a late basophilic erythroblast (upper field), and two myelocytes, in metaphase. Only a small fraction of the cells seen in normal marrow are undergoing mitosis.

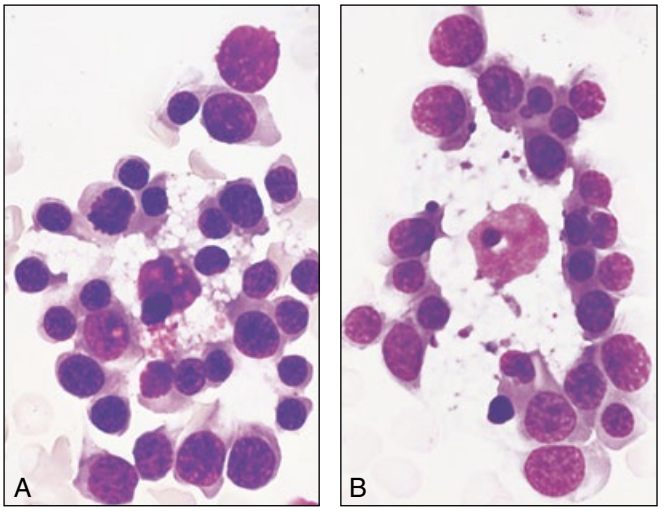

Fig. 4.13. Erythroblast–macrophage nests. **A,B,** Erythroblasts in tight clusters around central macrophages with lipid-laden cytoplasm. It is thought this close proximity in an erythroid "nest" may help erythroblasts to access macrophage iron.

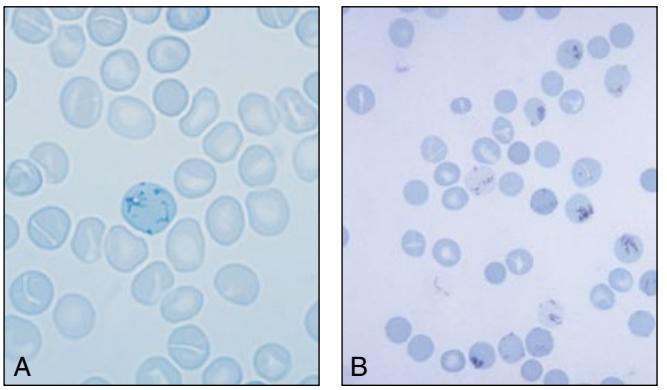

Fig. 4.14. Reticulocytes. Reticular material (precipitated RNA and protein) is shown clearly **(A)** in normal blood by supravital staining with new methylene blue, and **(B)** in autoimmune hemolytic anemia.

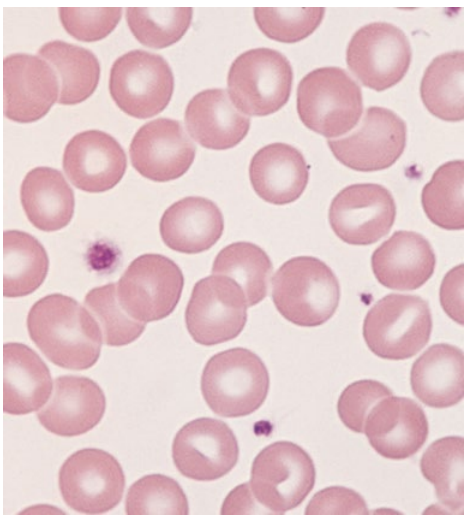

Fig. 4.15. Normal red cells are mean 8 μm in diameter with minor variations in size and shape. The majority show a central pale area of diminished staining. Platelets, 1–3 μm across, are also evident.

CHAPTER

HYPOCHROMIC ANEMIAS

5

Anemia is common throughout the world, with a global prevalence estimated in 2010 as 32.9% (Fig. 5.1). It causes substantial disability, estimated in 2010 as 8.4% of the disability from all conditions. It is more common in females than males in most regions and age groups. Anemia is most common in Sub-Saharan Africa and South Asia. Iron deficiency is the most common cause but the other hypochromic anemias, the anemia of chronic disorders, and the thalassemias are also major contributors. The hypochromic anemias are characterized by hypochromic cells in the peripheral blood with a mean cell hemoglobin (MCH) of <27 pg. The cells are also usually microcytic, with a mean cell volume (MCV) of <80 fL.

Hypochromasia is caused by failure of hemoglobin synthesis, the mechanism of which is shown in Fig. 5.2. This failure occurs most commonly as a result of iron deficiency, but it may also arise from an acquired block in iron metabolism, as in the anemia of chronic disorders and in rare congenital disorders of proteins involved in iron metabolism, causing failure of protoporphyrin and heme synthesis (e.g. sideroblastic anemias); from failure of globin synthesis (e.g. thalassemias) (see Chapter 9); or from crystallization of hemoglobin in some of the other hemoglobin disorders (e.g. hemoglobin C) (see Chapter 9). Lead inhibits both heme and globin synthesis and may cause a hypochromic anemia, but it also causes hemolysis, probably because of failure of RNA breakdown.

IRON METABOLISM

Most body iron present in hemoglobin is found in circulating red cells (Fig. 5.3). The macrophages of the reticuloendothelial system recognize senescent red cells which they internalize and degrade. They release iron from the phagolysosome into the cytosol via the NRAMP1 protein (Fig. 5.4). Heme may be transported from the phagolysosome into the cytosol by the heme transporter HRG1 and then iron released by the heme oxygenase HMOX1. Some heme is also directly exported by FLVCR1 to adjacent erythroblasts. The macrophages either store iron released

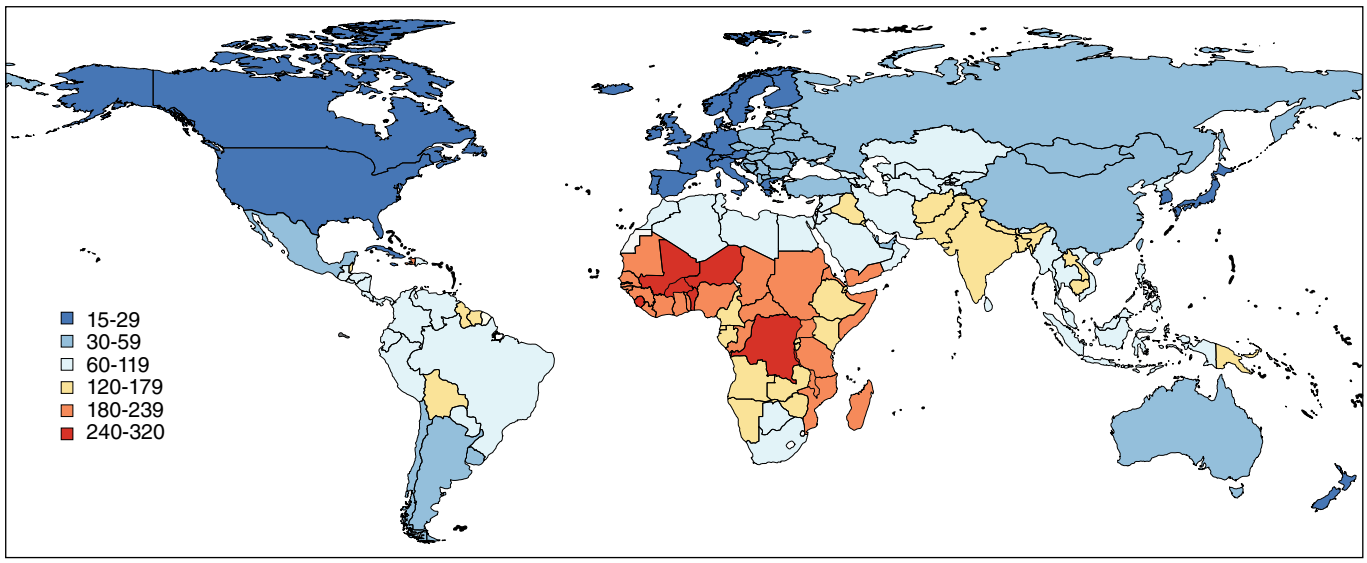

Fig. 5.1. Total years of life lived with disability (YLD) per 10 000 population in 2010, all ages, resulting from all causes of anemia by country. Source: Kassebaum NJ, et al. *Blood* 2014;123(5):615–624.

Color Atlas of Clinical Hematology: Molecular and Cellular Basis of Disease, Fifth Edition. A. Victor Hoffbrand, Paresh Vyas, Elías Campo, Torsten Haferlach, and Keith Gomez

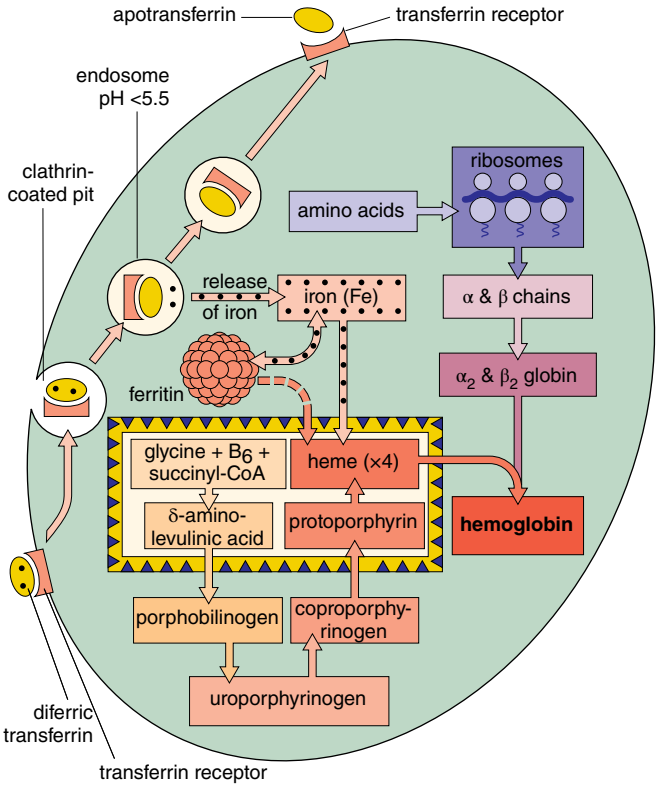

Fig. 5.2. Hemoglobin synthesis in the developing red cell: Iron enters the cell with transferrin and is combined with protoporphyrin, synthesized largely from glycine and succinyl CoA in mitochondria, to form heme. One molecule of heme attaches to one of the globin polypeptide chains to form a unit of hemoglobin, and one hemoglobin molecule is made up of four hemoglobin units. Transferrin, together with its receptor, enters the cell by receptor-mediated endocytosis. Iron is released by a fall in pH, and the apotransferrin and receptor are recycled to plasma and membrane, respectively. Hypochromic anemias arise from lack of iron or failure of heme synthesis for other reasons.

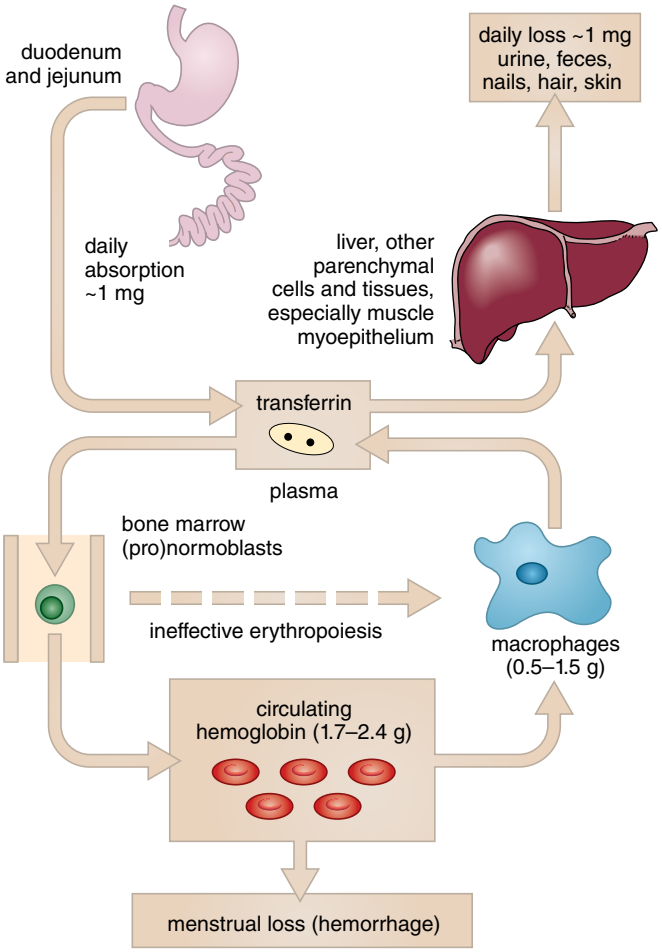

Fig. 5.3. Iron metabolism: Normal iron content of circulating hemoglobin and macrophages is indicated, as well as the approximate amount of iron absorbed and lost from the body each day.

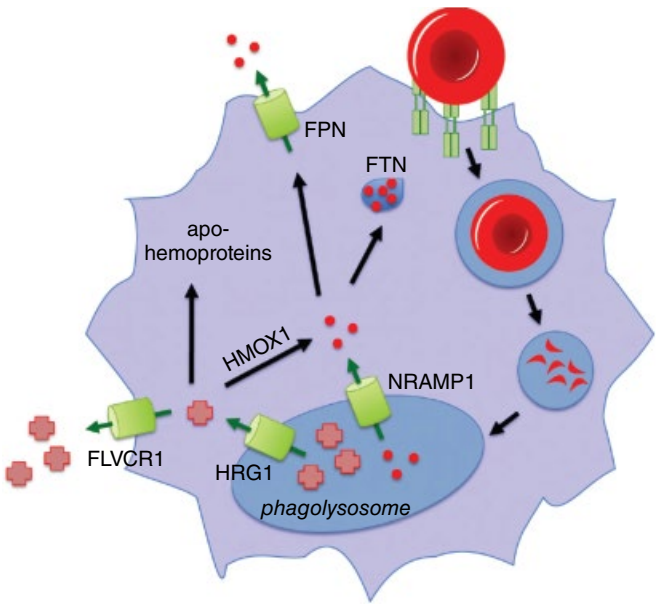

Fig. 5.4. Iron metabolism. Iron is released from phagolysosomes in macrophages and exported into the cytosol by NRAMP1 or released as heme by the transporter HRG1 and then either oxidized to iron by heme oxidase (HMOX1) or exported from the macrophage directly to erythroblasts by the membrane-bound heme exporter FLVCR1. Some heme may also be attached directly to heme apoproteins. Iron in the cytosol enters ferritin or is exported from the cell by ferroportin (FPN). Source: Korolnek T, Hamza I. *Blood* 2015;125:2893–2897.

from hemoglobin as ferritin and hemosiderin or transport iron via ferroportin to plasma, where it attaches to transferrin. This takes it to tissues with transferrin receptors, especially the bone marrow, where the iron is incorporated by erythroid cells into hemoglobin. There is a small loss of iron each day in urine, feces, skin, and nails and in menstruating females via blood. This loss (1–2 mg daily) is replaced by iron absorbed from the diet.

IRON ABSORPTION

Entry of inorganic iron into the duodenal enterocyte is via the protein receptor DMT-1 (divalent metal transporter 1) (Fig. 5.5). Levels of DMT-1 are regulated by the iron-responsive element (IRE) mechanism, iron deficiency leading to increased DMT-1. Exit of iron into portal plasma is controlled by ferroportin. The levels of this protein are regulated by hepcidin, which is discussed next. Heme iron is absorbed via a heme receptor at the cell surface, heme being subsequently digested by heme oxygenase and other enzymes and its iron released in the enterocyte.

HEPCIDIN

Hepcidin is a large polypeptide produced by the liver that controls iron metabolism by inhibiting its absorption and release from macrophages (Fig. 5.6A). Hepcidin causes degradation of the messenger RNA (mRNA) for ferroportin, a protein that promotes iron release from enterocytes into portal plasma and from macrophages into peripheral blood. Synthesis of hepcidin is controlled by three proteins: HFE, hemojuvelin (HJV), and transferrin receptor 2 (TFR2) (Fig 5.6B). Low levels of HFE or HJV or low iron saturation of TFR2 or of matriptase-2 (see later) lead to reduced hepcidin levels, resulting in increased iron absorption. SMAD1/5/8, which, after phosphorylation by the HJV/BMP6 complex, transfers to the nucleus, binds BMP4. This complex acts on the promoter to increase hepcidin synthesis.

Interleukin 6 (IL-6), IL-1, and IL-22, produced in response to inflammation, stimulate hepcidin production. On the other hand, anoxia via erythropoietin, proteins identified as erythroferrone, GDF15, and TWSG1 produced by erythroblasts, all downregulate hepcidin secretion. Matriptase-2, coded for by the gene TMPRSS6 on chromosome 22q, is a transmembrane serine protease in liver and other tissues. It is responsible for downregulating hepcidin transcription when iron stores are depleted. It does this by cleaving the membrane protein HJV, one of the coreceptors (with HFE and TFR2) for the bone morphogenic receptor complex, which initiates hepcidin transcription and synthesis. Recent evidence suggests that the toll-like receptors TLR2 and TLR6 on macrophages may degrade ferroportin independently of hepcidin. These receptors may be activated by bacterial lipoproteins. It is also suggested that in response to iron status liver sinusoidal endothelial cells produce BMP2 and BMP6, which in a paracrine fashion stimulate hepcidin synthesis (Fig. 5.6B).

Increased erythropoiesis, especially ineffective erythropoiesis, causes a fall in plasma hepcidin due to increased release of erythroferrone or similar proteins from erythroblasts, which inhibit hepcidin synthesis. Iron deficiency causes a rise in matriptase-2 and a rise in TF saturation, which both result in a fall in plasma hepcidin level.

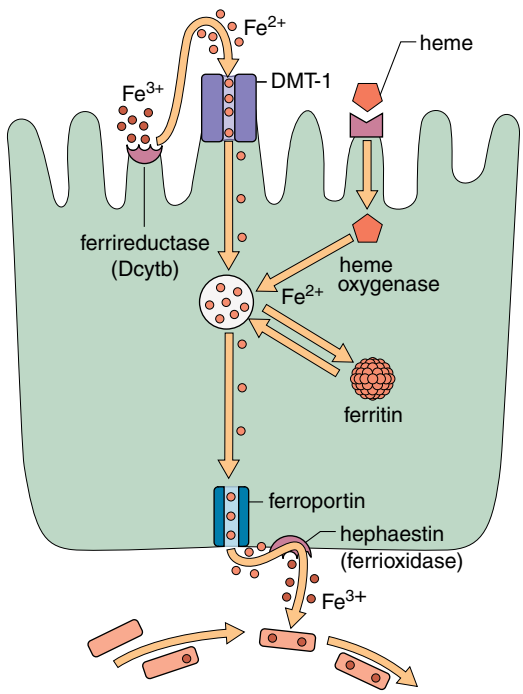

Fig. 5.5. Iron absorption: Inorganic iron is reduced to the Fe^{2+} form and transported into the cell by DMT-1 and out by ferroportin. It is reoxidized to Fe^{3+} as it exits the enterocyte. Heme iron is now thought to be absorbed by a separate receptor.

IRON HOMEOSTASIS

Metabolism of iron in body cells involves similar proteins to those involved in iron absorption (Fig. 5.7). Iron uptake via the transferrin receptor, intracellular storage of iron in ferritin, the incorporation of iron into heme in mitochondria and the hypoxia-inducible factor HIF-2α are all coordinated in response to iron supply at the transcriptional and translational levels. This is achieved partly by the presence of IREs located in the upstream untranslated regions of the mRNAs for ferritin, ferroportin, *m*-aconitase, HIF-2α, and the erythroid heme synthetic enzyme δ-aminolevulinic acid synthase (ALA-S) or, in the downstream untranslated region, mRNAs for transferrin receptor 1 (TFR1) and the iron transporter DMT-1 (Fig. 5.8). HIF-2α directly regulates transcription of several iron transport and release genes in the duodenum, high HIF-2α levels enhancing iron absorption. The IREs consist of both a double-stranded stem and a single-stranded loop RNA structure. Iron regulatory proteins (IRPs) bind to IRE and exist in two isoforms, IRP1 and IRP2. Increased iron levels result in conversion of IRP1 to an iron–sulfur cluster, containing acotinase, which lacks IRE-binding activity. Increased iron also leads to degradation of IRP2. Low levels of iron have the opposite effects.

IRON-DEFICIENCY ANEMIA

Iron deficiency usually results from hemorrhage because most body iron is present in circulatory hemoglobin. The symptoms of iron deficiency are caused by anemia (if sufficiently severe), as well as damage to epithelial tissues in some cases. Symptoms of the underlying disease may also be present. On rare occasions, a patient has a bizarre craving to eat items such as ice, chalk, or paper. This is known as "pica." In infants, impairment of

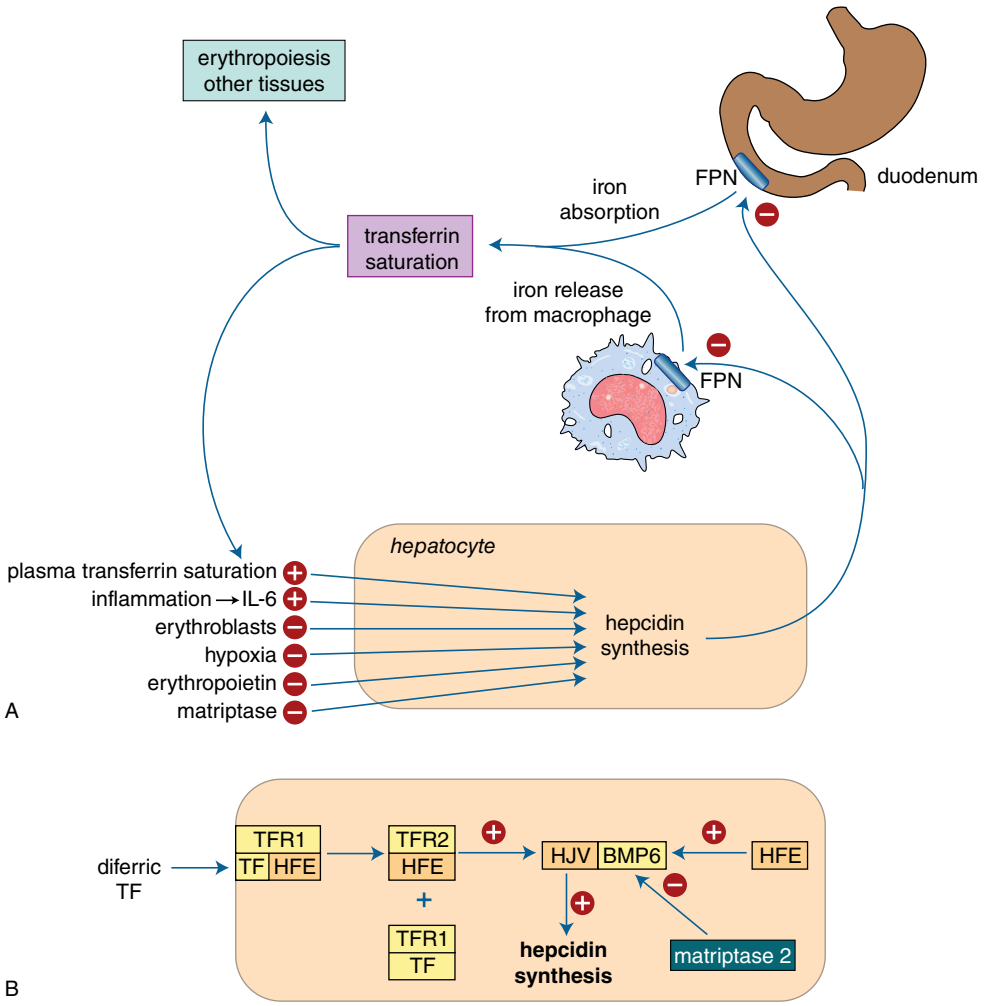

Fig. 5.6. A, Hepcidin reduces iron absorption and release from macrophages by stimulating degradation of ferroportin. Its synthesis is increased by transferrin saturation and inflammation but reduced by increased erythropoiesis, erythropoietin, hypoxia, and matriptase. **B,** The proposed mechanism by which the degree of transferrin saturation by iron affects hepcidin synthesis. BMP, bone morphogenetic protein; HJV, hemojuvelin; TFR1 and 2, transferrin receptors 1 and 2. BMP stimulates hepcidin synthesis and this is enhanced by HJV binding to BMP. Diferric transferrin competes with TFR1 for binding of HFE. The more diferric transferrin, the less TRF1 is bound to HFE and the more HFE is available to bind to TFR2. The HFE/TFR2 complex promotes HJV binding to BMP and so promotes hepcidin synthesis. Low concentrations of diferric transferrin, as in iron defciency, allow HFE binding to TFR1, reducing the amount of HFE able to bind TFR2 and thus reducing HJV binding to BMP and so reducing hepcidin secretion. HFE also enhances BMP expression directly but mutated HFE inhibits its expression. Source: Hoffbrand AV, et al. Hoffbrand's Essential Haematology, 7th edn. Wiley-Blackwell, 2015. Reproduced with permission of John Wiley & Sons.

psychomotor development and cognitive function may occur, especially in the first 2 years of life.

A patient with iron-deficiency anemia may show pallor of the mucous membranes, which is usually only recognized clinically if the hemoglobin is less than about 9.0 g/dL. Pallor of the conjunctivae, lips, palm creases, and nail beds are also seen (Figs. 5.9 and 5.10). Skin color, however, is not a reliable sign of anemia because it depends on the state of the skin circulation, as well as on the hemoglobin content of the blood. A patient's nails are frequently ridged and brittle (Fig. 5.10) or may show spoon nails, known as koilonychia (Fig. 5.11). There may be angular cheilosis (stomatitis; cracking at the corners of the mouth), especially in those with badly fitting false teeth (Fig. 5.12).

In severe cases, especially in older patients, an atrophic glossitis with loss of filiform papillae may be present (Fig. 5.13).

There may also be dysphagia resulting from postcricoid webs (Plummer–Vinson or Paterson–Kelly syndrome), especially in middle-aged women.

The biochemical explanation for these epithelial cell abnormalities is unclear; they may be related to a reduction in heme-containing enzymes (e.g. cytochromes, cytochrome *c* oxidase, succinic dehydrogenase, catalase, peroxidase, ribonucleotide reductase, xanthine oxidase, and aconitase). When anemia is very severe and of rapid onset, there may be retinal hemorrhages (Fig. 5.14).

BLOOD AND BONE MARROW APPEARANCES

A blood film shows the presence of hypochromic microcytic red cells (Fig. 5.15A,B) with abnormally shaped cells ("pencil" or cigar-shaped poikilocytes) and occasional target cells. The severity of both the blood film changes and the fall in MCH and MCV is related to the degree of anemia. Platelet count is often raised, particularly if hemorrhage is occurring.

Bone marrow is of normal cellularity, sometimes with normoblastic hyperplasia, and the developing erythroblasts show

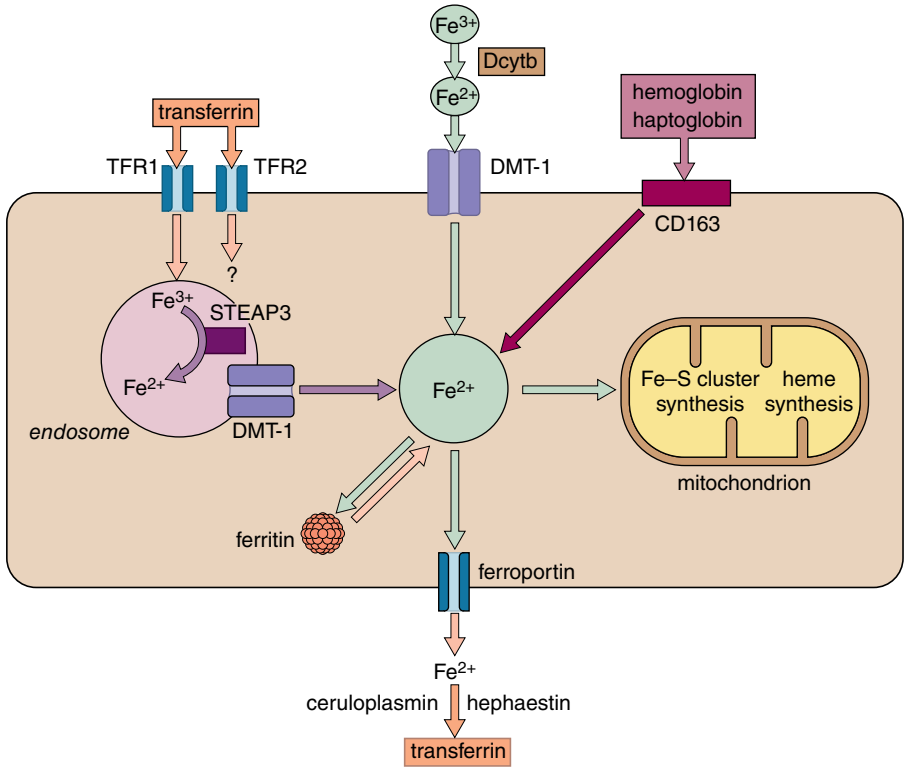

Fig. 5.7. Cellular iron metabolism: Similar proteins are involved as in iron absorption. STEAP3 is an intracellular ferrireductase. Dcytb is also a ferrireductase. TFR, Transferrin receptor. New data show PCBP1, an iron chaperone, delivers iron to ferritin and a cargo protein, NCOA4, directs ferritin to phagosomes for degradation. FLCVR (not shown) is a protein which exports heme iron from the cell. Mitoferrin (not shown) is involved in the transport of iron into the mitochondrion. Source: Hentze MW, et al. *Cell* 2004;117:285–297. Reproduced with permission of Elsevier.

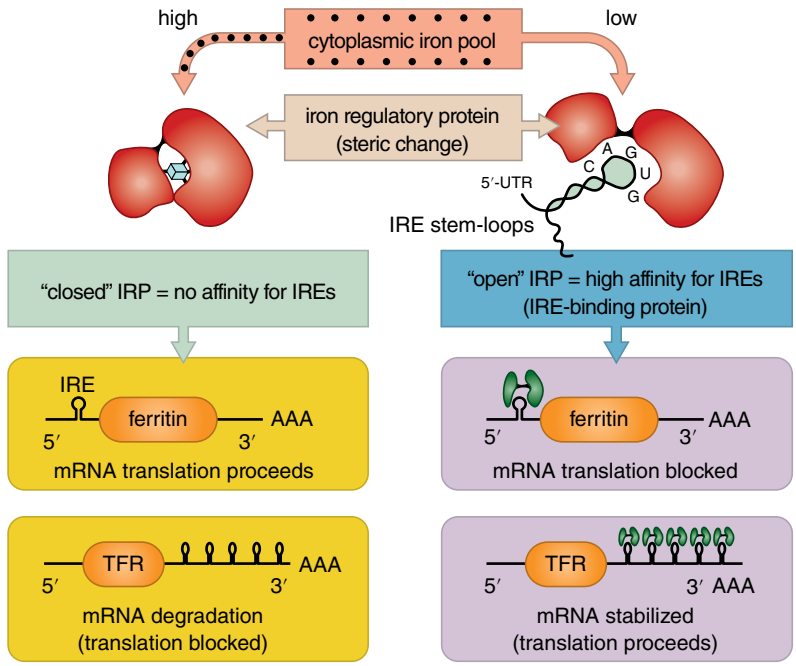

Fig. 5.8. Cellular iron homeostasis: The synthesis of transferrin receptor (TFR), DMT-1, ferritin, erythroid δ-aminolevulinic acid synthase (ALA-S), ferroportin, HIF-2α, and *m*-acotinase is regulated at the level of RNA translation by cytoplasmic iron regulatory proteins (IRP). These proteins can bind to mRNAs that contain a stem and loop structure—an iron-responsive element (IRE). When iron is plentiful, it has a low affinity for IRE, resulting in less transferrin receptor and DMT-1 but more ferritin, erythroid ALA-S, ferroportin, HIF-2α, and *m*-acotinase synthesis. When iron supply is low, binding to the IRE is increased, with increased synthesis of transferrin receptor and DMT-1 and less ferritin, ALA-S, ferroportin, HIF-2α, and *m*-acotinase synthesis. (Courtesy of Dr. D Girelli.)

a ragged vacuolated cytoplasm (Fig. 5.16). Whereas normal bone marrow shows iron in macrophages and a few scattered siderotic granules in erythroblasts on Perls' staining, in iron deficiency there is a complete absence of iron stores and of siderotic granules in developing erythroblasts (Fig. 5.17).

CAUSES OF IRON DEFICIENCY

The causes of iron-deficiency anemia are listed in Table 5.1. About two-thirds of body iron is circulating in red cells as hemoglobin, 1 liter of blood containing about 500 mg of iron. The next biggest store, which varies between 0 and 2 g, is within

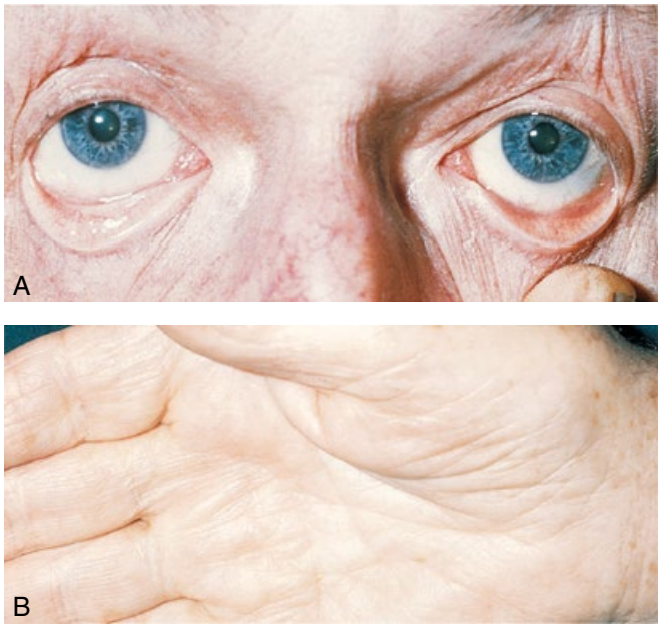

Fig. 5.9. Iron-deficiency anemia. **A,** Pallor of conjunctival mucosa. Mucous membrane pallor becomes clinically apparent when the hemoglobin concentration is below 9 g/dL. **B,** Pallor of palmar skin creases.

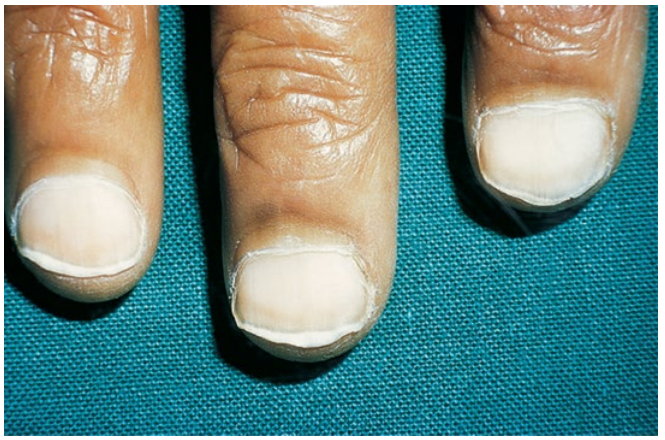

Fig. 5.10. Iron-deficiency anemia causing marked pallor of the nail beds in a dark-skinned patient. The nails are flattened.

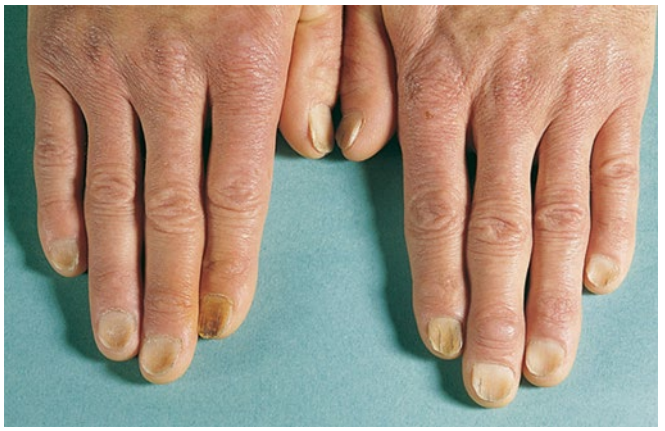

Fig. 5.11. Iron-deficiency anemia: Koilonychia caused by iron deficiency. The nails are concave, ridged, and brittle. This patient's anemia had been rapidly corrected by blood transfusion before an operation for cecal carcinoma. The cause of the nail changes in iron deficiency is uncertain but may be related to the iron requirement of many enzymes present in epithelial and other cells. (Courtesy of Dr. SM Knowles.)

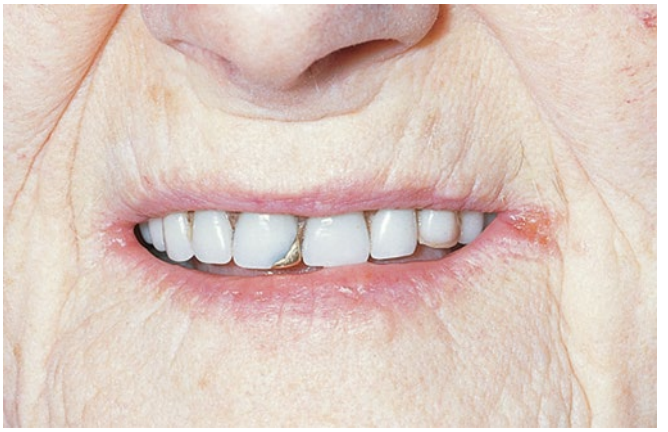

Fig. 5.12. Iron-deficiency anemia: Angular cheilosis. There is fissuring and ulceration at the corners of the mouth. The biochemical mechanism is uncertain but may be similar to that for nail, mucosal, and pharyngeal changes.

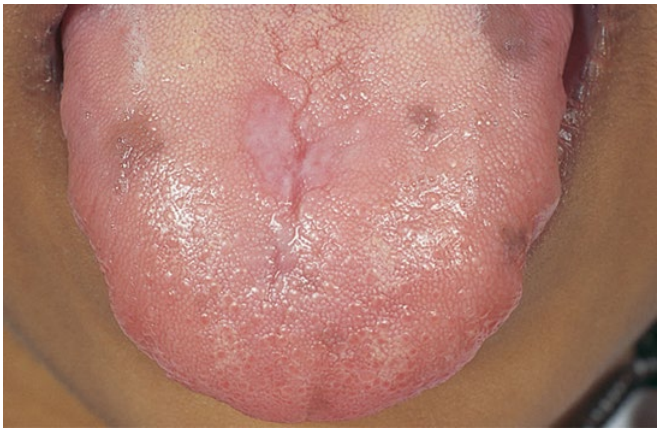

Fig. 5.13. Iron-deficiency anemia: Glossitis due to iron-deficiency anemia. The bald, fissured appearance of the tongue is caused by flattening and loss of papillae.

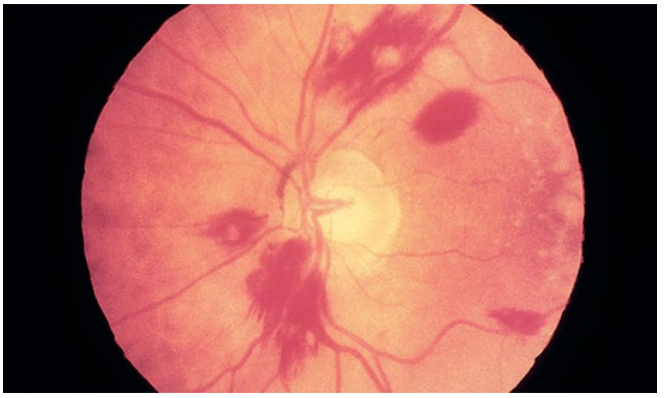

Fig. 5.14. Iron-deficiency anemia: Multiple retinal hemorrhages in a 25-year-old woman with chronic iron deficiency because of severe hemorrhage (menorrhagia; Hb, 2.5 g/dL). These appearances may occur in other severe anemias.

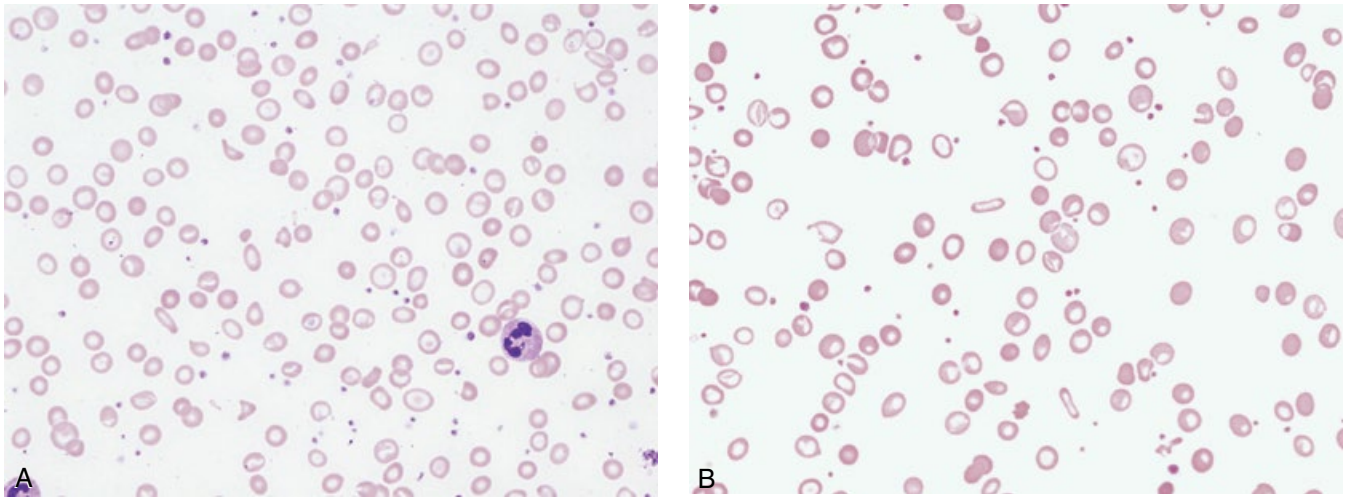

Fig. 5.15. A, Iron-deficiency anemia: Low-power view of peripheral blood film. The red cells are hypochromic and microcytic. Some poikilocytes are present, including thin elongated ("pencil") cells and occasional target cells. Platelets are plentiful. Hb, 7.5 g/dL. **B,** Iron-deficiency anemia: Low-power peripheral blood film taken during therapy with oral iron. There is a dimorphic population of hypochromic microcytic cells and target cells and well-hemoglobinized cells of normal size, but there are some large polychromatic cells (newly formed well-hemoglobinized reticulocytes).

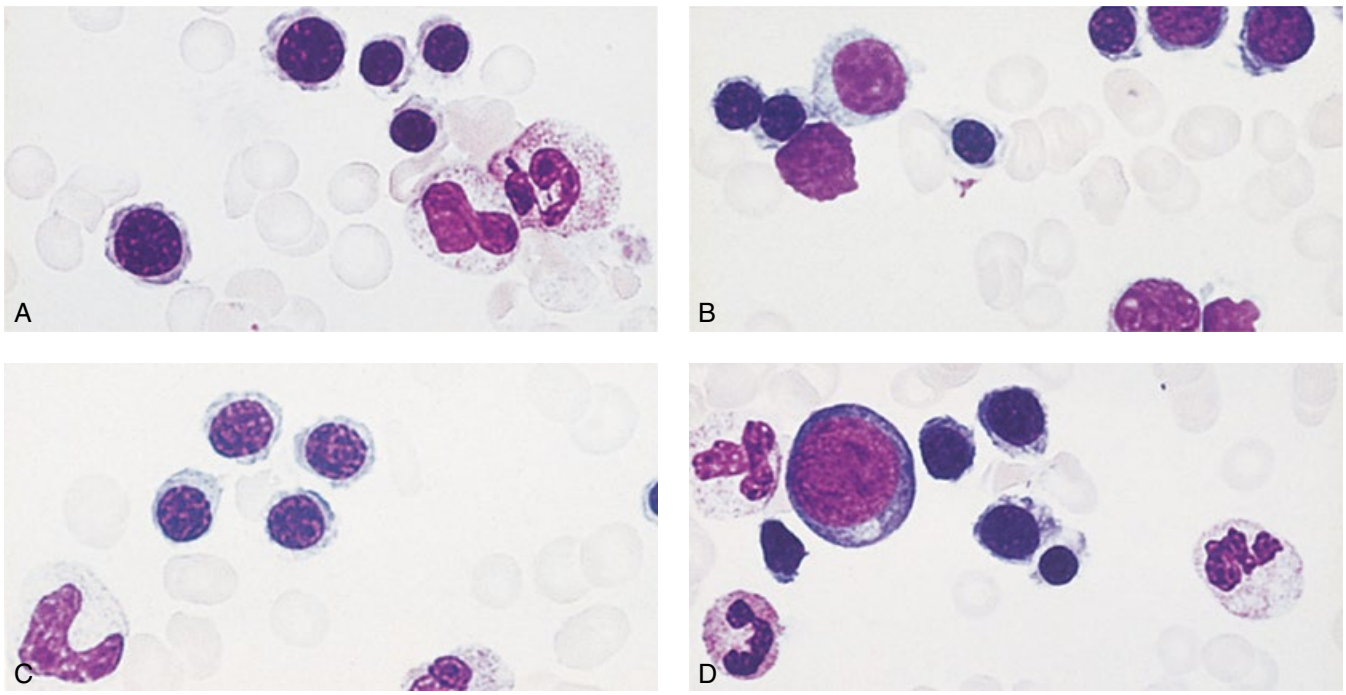

Fig. 5.16. Iron-deficiency anemia: Bone marrow aspirate. **A–D,** The cytoplasm of polychromatic and pyknotic erythroblasts is scanty, vacuolated, and irregular in outline. This type of erythropoiesis has been described as "micronormoblastic."

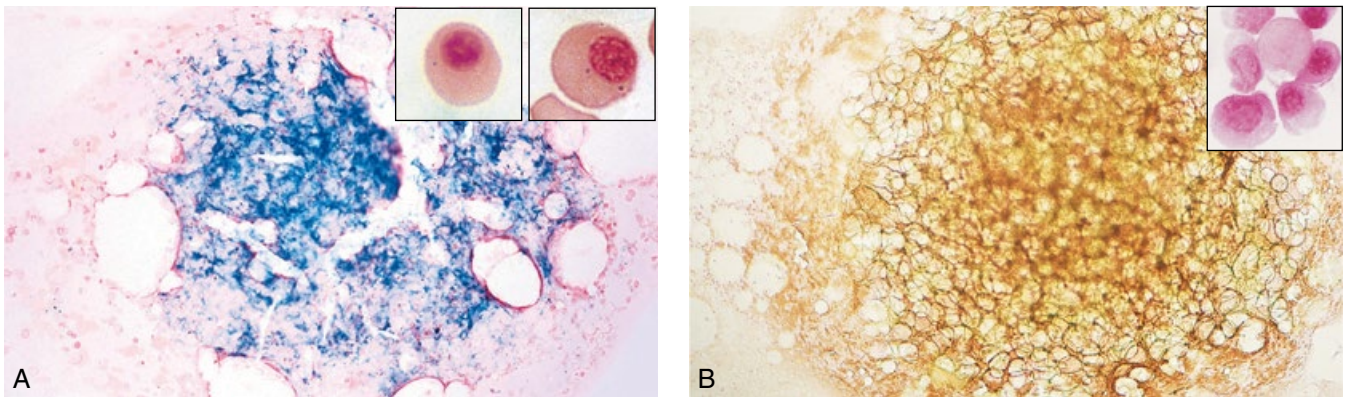

Fig. 5.17. Iron-deficiency anemia: Perls' stain with methyl red counterstain. **A,** Low-power view of normal bone marrow aspirate showing blue staining (iron) in macrophages and (inset, high power) siderotic granules in developing erythroblasts. **B,** Absence of blue staining (iron) in marrow fragment and (inset) of siderotic granules in erythroblasts.

TABLE 5.1. CAUSES OF IRON-DEFICIENCY ANEMIA

Hemorrhage
Gastrointestinal
Hiatus hernia
Esophageal varices
Peptic ulcer
Aspirin, glucocorticoids, NSAIDs ingestion
Hookworm
Schistosomiasis
Neoplasm
Ulcerative colitis
Telangiectasia
Angiodysplasia
Diverticulosis
Hemorrhoids
Pulmonary
Pulmonary hemosiderosis
Uterine
Menorrhagia
Ante- and postpartum
Renal tract
Hematuria
Chronic dialysis
Self-induced
Transfer to fetus
Pregnancy
Infancy
Hemosiderinuria
Chronic intravascular hemolysis
Paroxysmal nocturnal hemoglobinuria
Heart valve hemolysis
Malabsorption
Atrophic gastritis
Gluten-induced enteropathy
Gastrectomy
Bariatric surgery
Duodenal bypass
H. pylori infection
Poor diet
Poor-quality diet, especially if mostly vegetable
Infants fed on cows' milk with late weaning

NSAID, nonsteroidal anti-inflammatory drug.

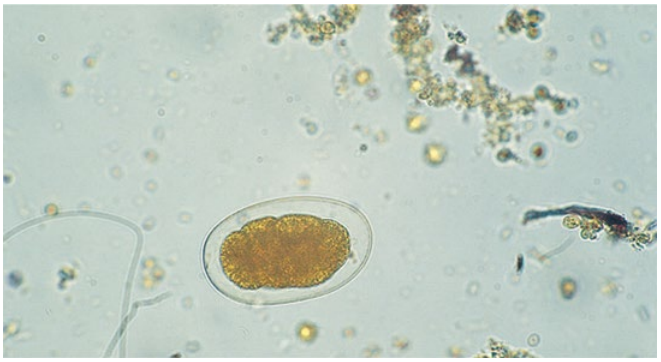

Fig. 5.18. Iron-deficiency anemia: An ovum of the hookworm, *Ancylostoma duodenale*, a frequent cause of iron-deficiency anemia in many parts of the world. Blood loss and therefore severity of anemia are related to the degree of parasitization.

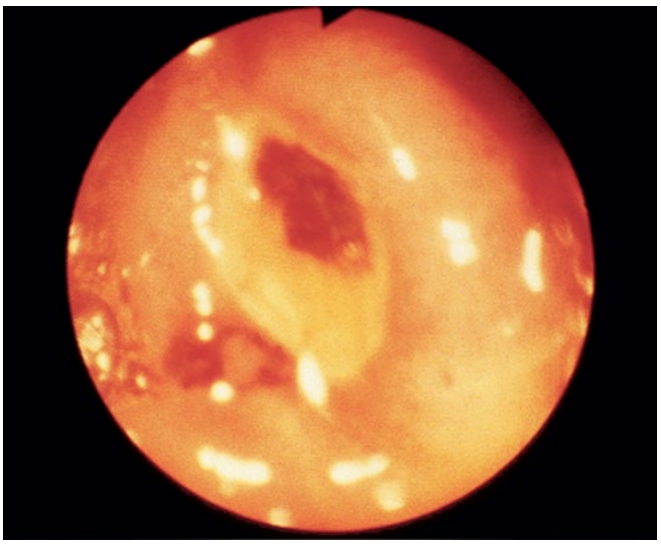

Fig. 5.19. Iron-deficiency anemia: Endoscopic appearance of a bleeding duodenal ulcer in a 45-year-old man with symptoms of anemia. (Courtesy of Professor RE Pounder.)

the macrophages of the reticuloendothelial system in the form of the storage proteins hemosiderin (visible on light microscopy) and ferritin (seen only by electron microscopy). The absence of iron stores, with a fall below normal in serum iron and serum ferritin and a rise in total iron-binding capacity (transferrin) but without anemia and without a fall in red cell indices, is termed latent iron deficiency. Iron in myoglobin and a variety of enzymes make up the rest of the body iron.

Daily iron losses and, thus, requirements for iron in adults are normally small in relation to body stores, about 1 mg daily in men and postmenopausal women, and 1.5–3.9 mg in menstruating women. Requirements are also increased in children (to provide for growth and increase in red cell mass) and during pregnancy (for transfer to the fetus).

Iron deficiency is usually the result of hemorrhage. In women, menorrhagia or repeated pregnancy without iron supplementation is a frequent cause. In men and postmenopausal women, iron deficiency is usually caused by chronic gastrointestinal blood loss. The most common causes in many countries in Africa are hookworm infestation (Fig. 5.18) and intestinal schistosomiasis. In Western countries iron deficiency is often the result of bleeding from hiatus hernia, peptic ulceration (Fig. 5.19), chronic aspirin ingestion, colonic or cecal carcinoma (Fig. 5.20), angiodysplasia (Fig. 5.21), or hemorrhoids. Rare causes of iron deficiency are pulmonary hemosiderosis (Fig. 5.22), chronic intravascular hemolysis (as in paroxysmal nocturnal hemoglobinuria), and self-inflicted venesection.

A normal Western diet contains 10–15 mg of iron daily, of which 5–10% is absorbed. Iron absorption is increased in iron deficiency but reduced by some food substances, such as phytates and phosphates. Poor dietary intake of iron, as is common in some developing countries, may be the sole cause of iron deficiency if present for many years. However, more often poor diet provides a background of reduced iron stores on which other causes of iron deficiency, such as heavy menstrual loss or increased requirements for pregnancy or for growth in infants and children, may lead to iron-deficiency anemia.

Malabsorption alone is an unusual cause of iron deficiency. Even in patients with atrophic gastritis or gluten-induced enteropathy, loss resulting from an increased turnover of cells and exudation of transferrin iron may be as important as the malabsorption. Following gastrectomy, the two main factors are blood loss and malabsorption, which is more marked for food iron than for inorganic iron.

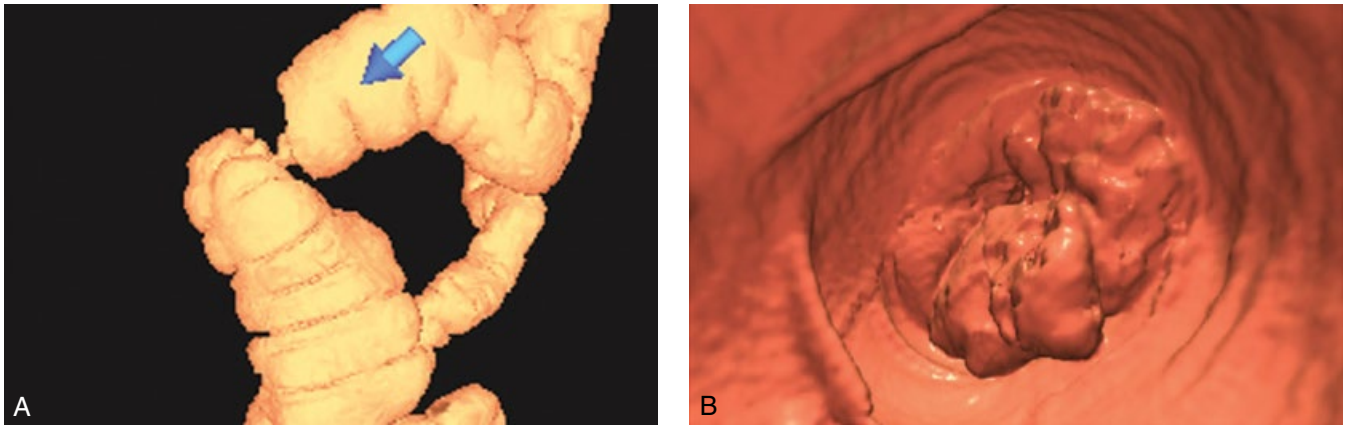

Fig. 5.20. Iron-deficiency anemia. **A,** Virtual colonoscopy: annular ("apple-core") narrowing of the colon due to adenocarcinoma 126 cm from the anal verge. **B,** Luminal views reveal fungating adenocarcinoma (same case as **B**). (Courtesy of Dr. J Bell.)

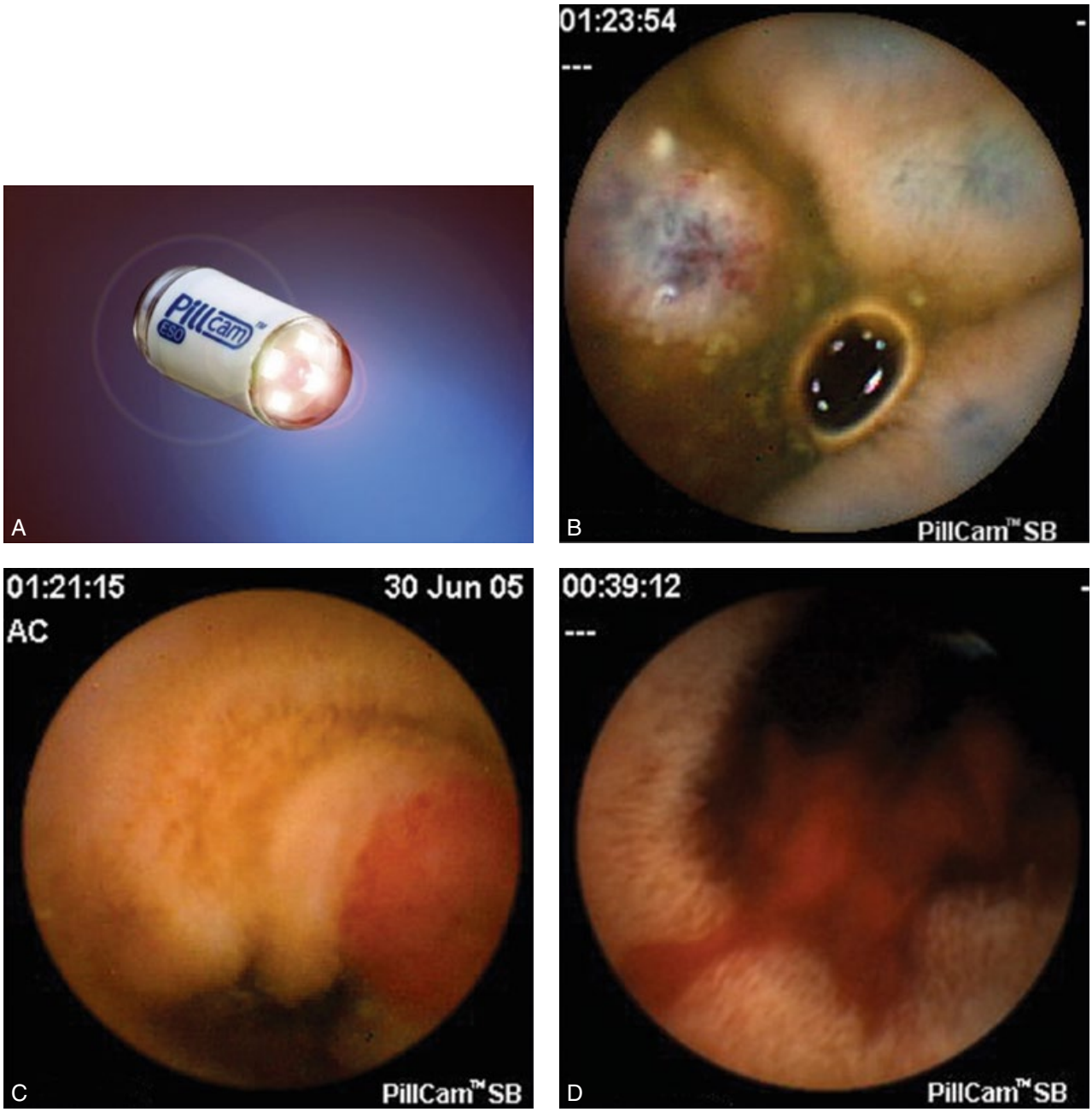

Fig. 5.21. Iron-deficiency anemia. **A,** Pill camera. This is swallowed and transmits images to a camera worn as a belt. The camera is not reused. **B,** Pill camera image shows bleeding angioma present in small intestine. **C,** Angiodysplasia present in small intestine. **D,** Angiodysplasia bleeding in small intestine. (Courtesy of Professor O Epstein and Dr. M Caplin.)

IRON-REFRACTORY IRON-DEFICIENCY ANEMIA (IRIDA)

The most frequent cause of this rare hypochromic, microcytic anemia is homozygous or doubly heterozygous mutations in the matriptase-2 gene. The mutations, usually single nucleotide variations, include multiple intronic variants in some, combined with exonic polymorphisms, the most common of which is *V737A*. Typically there is a moderately severe anemia (hemoglobin 6.0–9.0 g/dL) and severe microcytosis (MCV 45–65 fL). Low serum iron and very low percentage saturation of the iron-binding capacity (<5%) is seen. Serum hepcidin levels are inappropriately high and serum ferritin levels normal. The anemia is refractory or shows a suboptimal response to oral iron but may incompletely and transiently respond to parenteral iron. IRIDA may improve in adulthood.

A similar anemia occurs with homozygous or doubly heterozygous mutations of DMT-1, presumably due to its involvement in iron release from endosomes (see Fig. 5.5). Mutations in the transferrin gene and caeruloplasmin gene (which result in failure of ferrioxidase activity) are other causes of IRIDA.

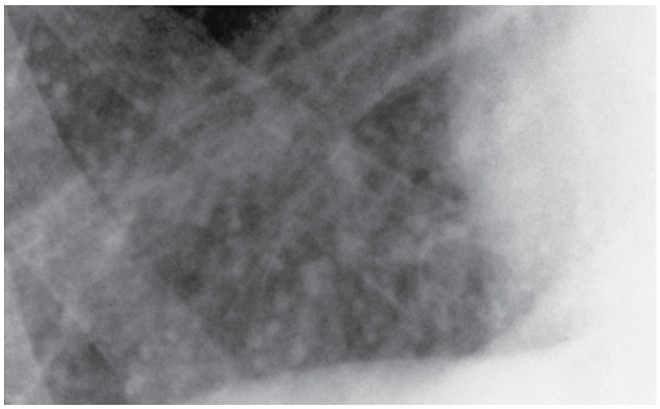

Fig. 5.22. Iron-deficiency anemia: Chest radiograph showing diffuse mottled appearance caused by pulmonary hemosiderosis. The lesions consist of aggregates of iron-laden macrophages with surrounding fibrosis. (Courtesy of Dr. R Dick.)

SIDEROBLASTIC ANEMIA

Sideroblastic anemia is characterized by the presence of ring sideroblasts (>15% of erythroblasts) in the bone marrow (Fig. 5.23). The iron is deposited in the mitochondria of the erythroblasts (Fig. 5.24). The erythroblasts show cytoplasmic vacuolation that differs from that in iron deficiency or in β-thalassemia major (Fig. 5.25). The marrow is usually hypercellular with erythroid hyperplasia. Sideroblastic anemia is caused by congenital or acquired faults in heme synthesis, mitochondrial iron metabolism (Fig. 5.26), the mitochondrial respiratory chain, or iron–sulfur cluster formation (Fig. 5.27). Iron–sulfur (Fe–S) clusters are cofactors linked usually by cysteine residues to certain proteins. They are required by mitochondrial enzymes involved in electron transport and other mitochondrial enzymes (Fig. 5.7), and also by some cytosolic enzymes, such as IRP1 (see Fig. 5.8). 2Fe–2S, 3Fe–4S, and 4Fe–4S are the most frequent of these clusters in nature (Fig. 5.27). Their assembly is complex and defects in this process cause a wide range of clinical abnormalities, including sideroblastic anemia.

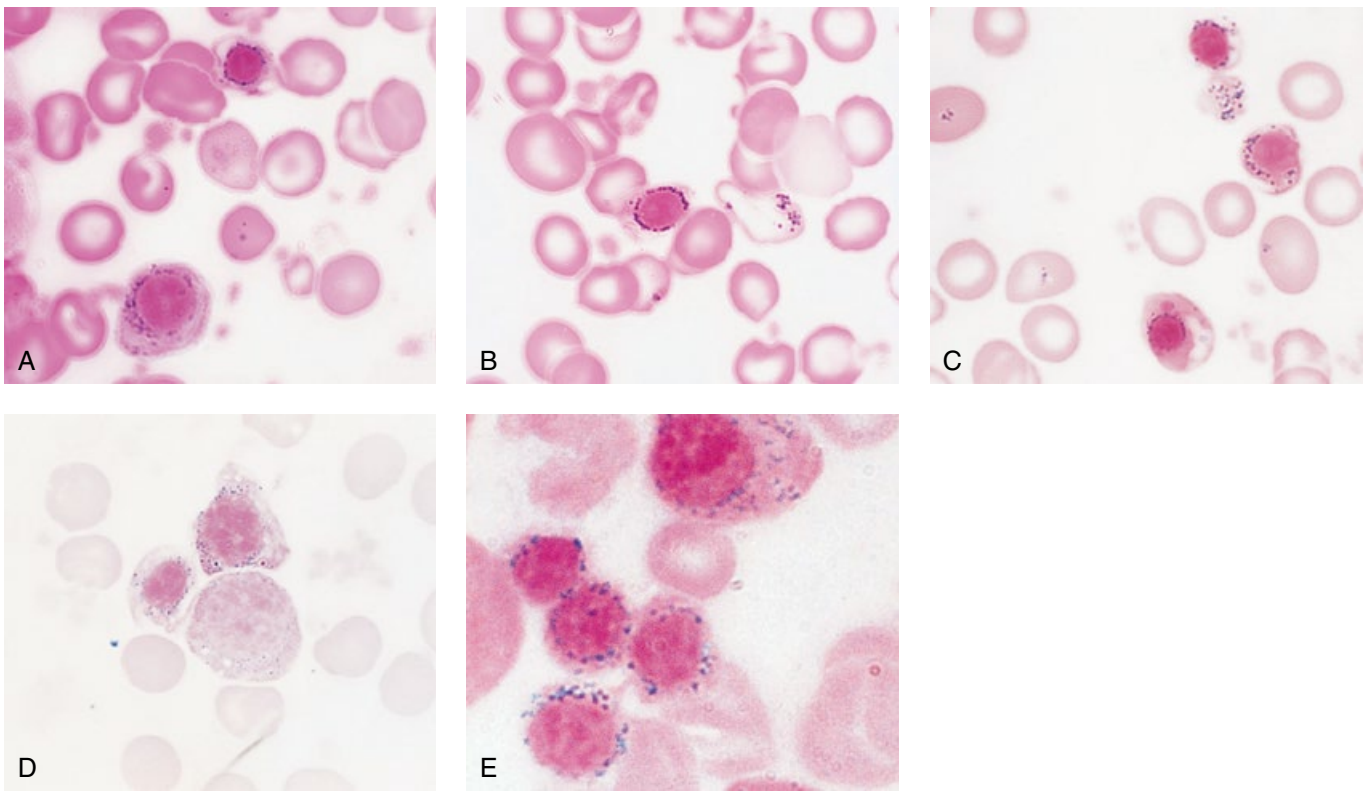

Fig. 5.23. Sideroblastic anemia. **A–E,** Bone marrow aspirate showing erythroblasts with complete or nearly complete rings (or collars) of iron granules around their nuclei. The rings are best seen in late erythroblasts but in severe cases also occur in the earliest recognizable erythroblasts. (Perls' stain.)

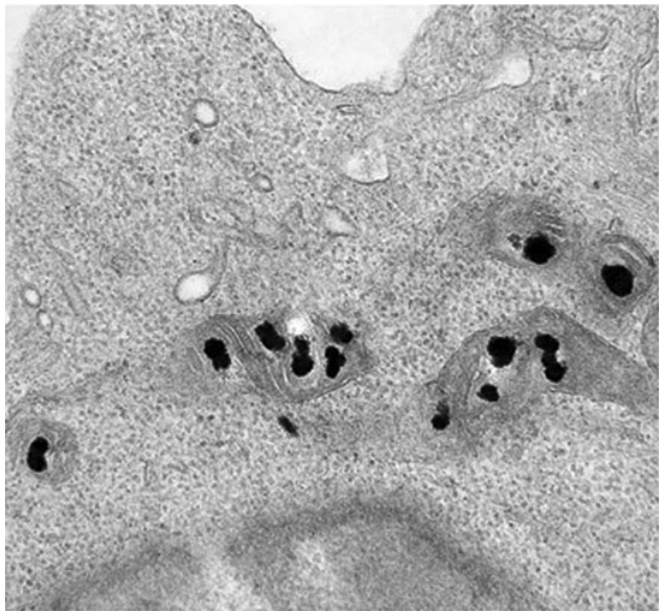

Fig. 5.24. Hereditary sideroblastic anemia: Electron microscopy of erythroblast showing iron-laden mitochondria. Source: Haworth C, et al. *Br J Hematol* 1982;50:549–561. Reproduced with permission of John Wiley & Sons. (Courtesy of Professor SN Wickramasinghe.)

Sideroblastic anemia is classified into congenital and acquired types; the acquired type is further subdivided into primary and secondary types, including some types associated with other bone marrow disorders (Table 5.2). In the secondary types, the proportion of ring sideroblasts is usually <15% and the anemia is due to other causes.

CONGENITAL SIDEROBLASTIC ANEMIA

X-LINKED

The congenital type usually occurs with sex-linked pattern of inheritance.. The blood film is hypochromic and microcytic, or dimorphic of varying severity (Fig. 5.28). Pappenheimer bodies are frequent in the peripheral blood red cells after splenectomy in either the congenital or acquired forms. The bone marrow usually shows erythroid hyperplasia associated with ineffective erythropoiesis. Heavy iron loading may occur if blood transfusions have been given (Fig. 5.29).

The following mutations have been identified in different cases (Table 5.2):

- *Erythroid δ-aminolevulinic acid synthase (ALA-S2)*: The most frequent cause of congenital sideroblastic anemia is mutation in the gene on the X chromosome coding for the erythroid-specific enzyme ALA-S2

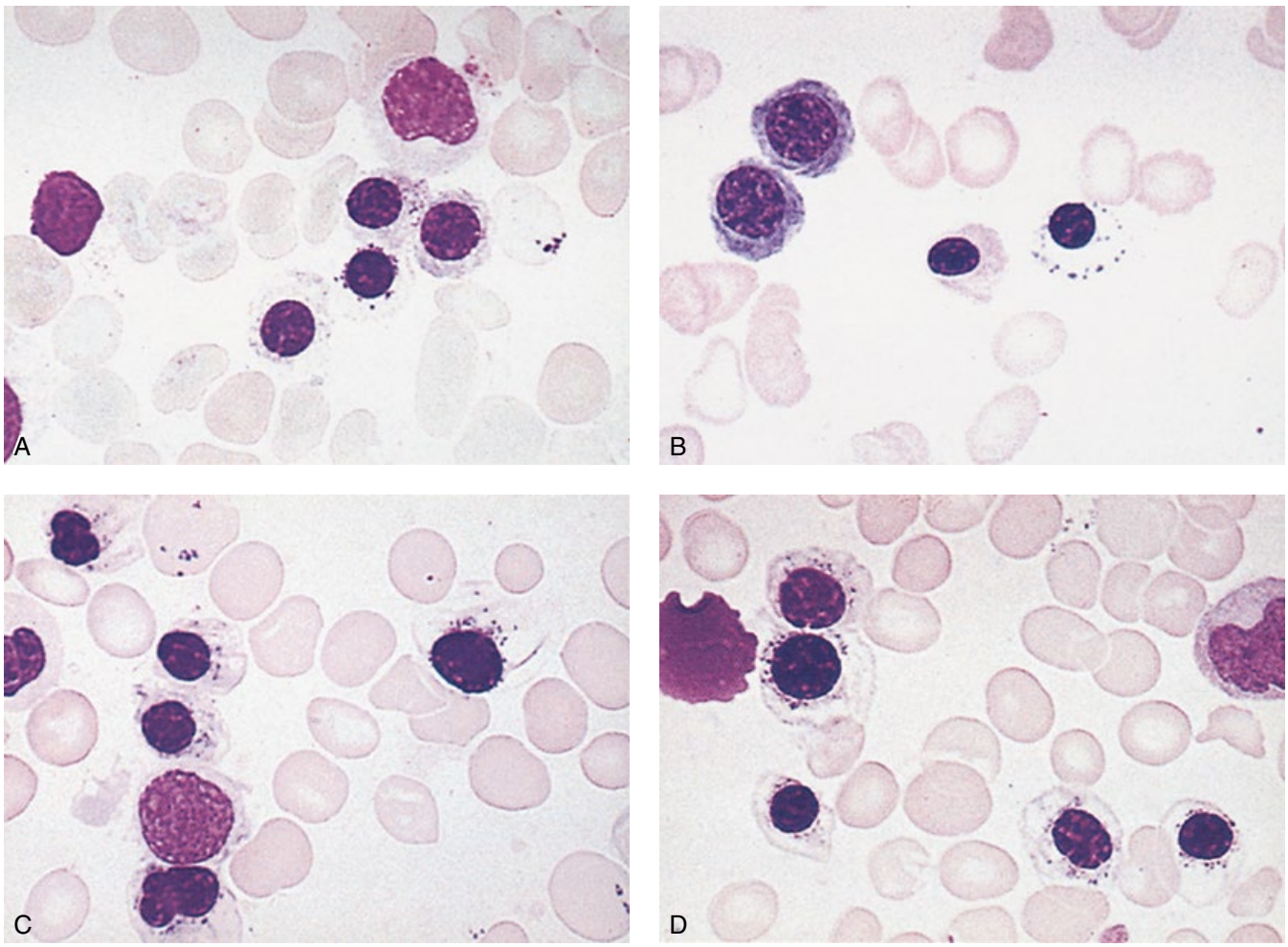

Fig. 5.25. Refractory anemia with ring sideroblasts. **A–D,** Bone marrow aspirate showing vacuolation of erythroblasts with intact cytoplasmic margins. In some cells the vacuoles are surrounded by heavily stained cytoplasmic granules (punctate basophilia). Contrast the appearances with those in iron-deficiency anemia (see Fig. 5.16) and thalassemia major (see Fig. 9.19).

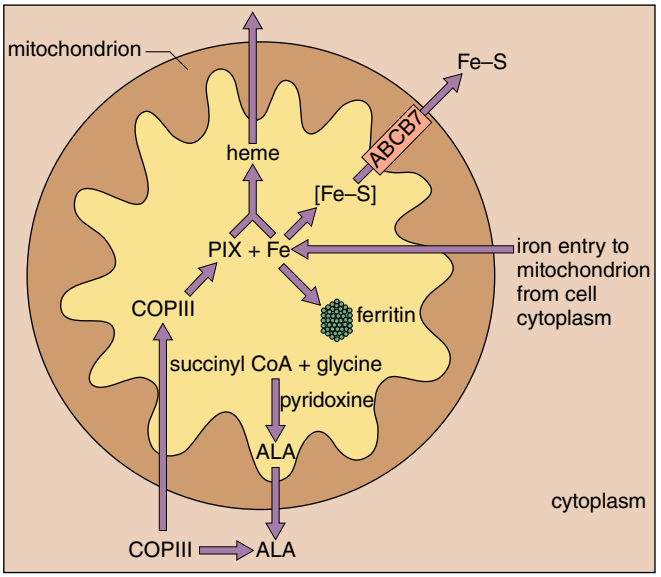

Fig. 5.26. Mitochondrial iron metabolism. ALA, δ-aminolevulinic acid; CoA, coenzyme A; COP, coproporphyrin; Fe–S, iron–sulfur cluster; PIX, protoporphyrin IX.

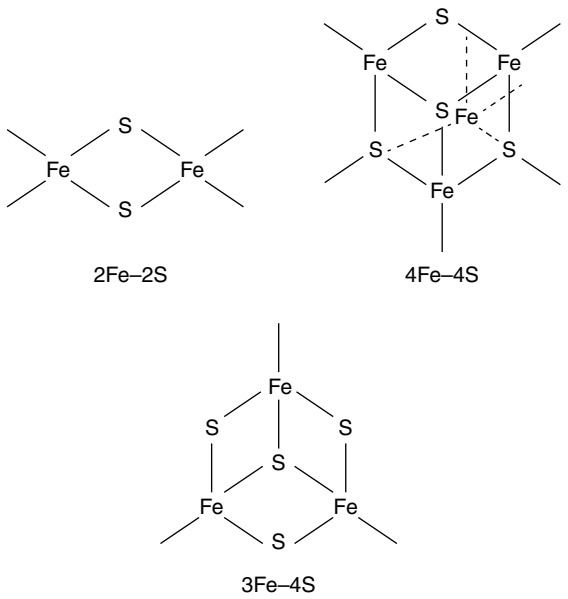

Fig. 5.27. Iron–sulfur clusters. The most frequent in nature are 2Fe–2S, 3Fe–4S, and 4Fe–4S. Fe–S clusters are cofactors ligated to certain proteins, mainly in mitochondria where they are involved in electron transport, regulation sensings, and DNA repair. Their assembly is complex and defects in the process can cause a wide range of clinical abnormalities. The cytoplasmic protein IRP1 has an Fe–S cluster.

(Fig. 5.30). This usually affects males and manifests in the third decade of life. Women are rarely affected. Manifestation in both sexes in old age has been described. The mutations identified have been missense, affecting exons 5–11 (Fig. 5.30). Pyridoxine responsiveness correlates with mutations affecting exon 9, the region that codes for the pyridoxal-5-phosphate-binding site. Exon 5 may also code for sequences involved in pyridoxal-5-phosphate binding.

- *ABCB7*: Mutations of this gene usually cause an X-linked sideroblastic anemia with ataxia. ABCB7 is an ATP-binding cassette protein involved in transport of iron–sulfur clusters from the mitochondria (see Fig. 5.26). There is usually nonprogressive ataxia.
- *NDUFB11*: This gene codes for a mitochondrial respiratory complex 1-associated protein. The gene is on the X chromosome. The mutation p.93del has been reported in five males with normocytic sideroblastic anemia. Lactic acidosis and a myopathy may be present.

TABLE 5.2. CLASSIFICATION OF SIDEROBLASTIC ANEMIA

Genetic
X-Linked
Erythroid δ-aminolevulinic acid synthase (ALA-S2) (see Fig. 5.30)
Sideroblastic anemia with ataxia (gene *ABCB7*, an ATP-binding cassette protein)
NDUFB11 (mitochondrial respiratory chain protein)
Mitochondrial
Mitochondrial amino acid carrier protein SLC25A38
Mitochondrial respiratory enzyme mutations, e.g. Pearson, Kearns–Sayre syndromes
YARS2 (gene coding for mitochondrial tyrosyl-tRNA synthase)
Autosomal
Glutaredoxin 5
Erythropoietic protoporphyria (gene ferrochetalase)
Thiamine-responsive megaloblastic and sideroblastic anemia (gene *SLC19A2* encoding the thiamine transporter THTR-1, e.g. DIDMOAD syndrome)
Other rare forms (see text)
With B-cell immune deficiency (gene unknown)
Acquired
Primary
Myelodysplastic syndromes
Secondary
Associated with malignant marrow disorders, such as acute myeloid leukemia, polycythemia vera, myelofibrosis, and myeloma
Drugs (isoniazid, pyrizinamide, cycloserine, chloramphenicol, penicillamine, fusidic acid)
Toxins (lead, alcohol)
Megaloblastic anemia, hemolytic anemia, pregnancy, rheumatoid arthritis, carcinoma

MITOCHONDRIAL DNA MUTATIONS

SLC25A38 is an erythroid-specific inner mitochondrial transport protein for amino acids. Sideroblastic anemia occurs with homozygous or compound heterozygote defects. Mutations occur throughout the gene.

Pearson and Kearns–Sayre syndromes result from a defect in one or more enzymes in the mitochondrial respiratory chain generating ATP (Fig. 5.31). Pearson syndrome consists of neutropenia, thrombocytopenia, sideroblastic anemia, exocrine pancreatic dysfunction, and hepatic dysfunction. It is caused by deletion (or even more rarely duplication) of sections of mitochondrial DNA. Vacuolation of marrow erythroid and myeloid precursors may be seen (Fig. 5.32). The syndrome may be accompanied by neurologic and muscle disorders. In Kearns–Sayre syndrome the brain, spinal cord, and peripheral nerves are usually affected.

The electron microscopy of a skeletal muscle biopsy of a 42-year-old man with the combination of congenital sideroblastic anemia and a proximal myopathy are shown in Fig. 5.33.

The skeletal muscle biopsy shows crystalline deposits in mitochondria. The exact defect was unclear despite analysis of ALA-S and mitochondrial DNA.

Myopathy, lactic acidosis, and sideroblastic anemia 2 (MLASA2) may result from homozygous or doubly heterozygous mutations of *YARS2*, the gene coding for mitochondrial tyrosyl-tRNA. This syndrome may also result from mutations in the gene for pseudo-uridine synthase 1.

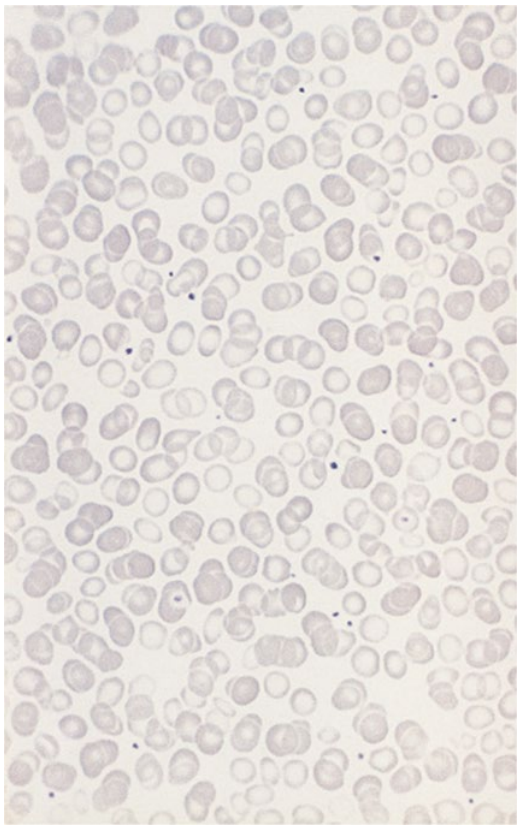

Fig. 5.28. Sideroblastic anemia (hereditary): Peripheral blood film from a 19-year-old man shows a dimorphic anemia with a mixture of poorly hemoglobinized microcytic cells and well-hemoglobinized normocytic cells (Hb, 11.5 g/dL; MCV, 78 fL; MCH, 22.3 pg).

AUTOSOMAL

- *Glutaredoxin (GLRX) 5*: This enzyme is needed for Fe–S cluster synthesis. It is required for IRP1 synthesis and thus for ALA-S2 translation. Homozygous or doubly heterozygous mutation of the gene is a very rare cause of sideroblastic anemia.
- *Ferrochelatase*: Mutations in the gene for ferrochelatase cause erythropoietic protoporphyria (see Chapter 6). The defect in heme synthesis is usually associated with a mild hypochromic, microcytic anemia. In some but not all cases ring sideroblasts have been identified in the bone marrow.
- *Thiamine-responsive megaloblastic and sideroblastic anemia*: This results from a defect in thiamine phosphorylation due to mutation of the gene *SLC19A2* on chromosome 1q23.3 encoding the thiamine transporter THTR-I. The megaloblastic anemia is thought to result from failure of ribose 5-phosphate synthesis. Thiamine is involved in synthesis of succinyl CoA, a substrate for ALA-S2, which explains the defective heme synthesis and ring sideroblast formation. DIDMOAD (Wolfram) syndrome consists of diabetes insipidus, diabetes mellitus, optic atrophy, and sensorineural deafness. It may be accompanied by megaloblastic and sideroblastic anemia, in some cases responding to thiamine. The patient in Fig. 5.34 resembles one with the DIDMOAD syndrome most closely. A less common triad of thiamine-responsive megaloblastic anemia, diabetes mellitus, and sensorineural deafness has been described.
- *Germline mutations of other genes*: *SCL19A2* and *TRNT1* have been described in rare cases of sideroblastic anemia.

In refractory anemia with ring sideroblasts (primary acquired sideroblastic anemia), there is usually macrocytosis and gross anisocytosis and poikilocytosis. The erythroblasts appear megaloblastic in about 50% of cases. This disease is classified as a type of myelodysplasia and is discussed in Chapter 15.

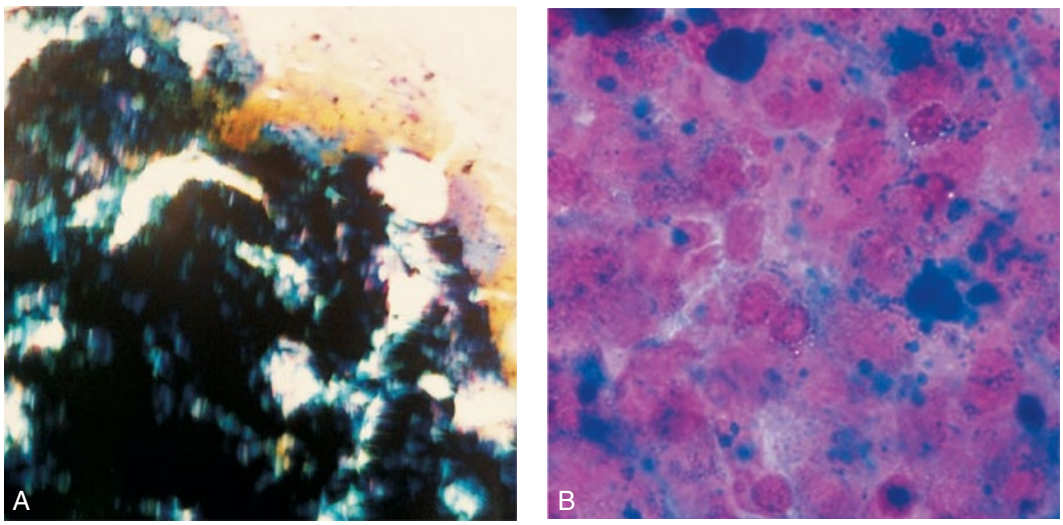

Fig. 5.29. Sideroblastic anemia (hereditary). **A,** Bone marrow fragments stained for iron show a gross increase in iron in a patient who had been transfused for many years before the diagnosis was made. Treatment with pyridoxine allowed a satisfactory rise in hemoglobin, enabling subsequent venesections for reduction of iron overload. **B,** High-power view shows multiple ring sideroblasts and increased iron (hemosiderin) in macrophages.

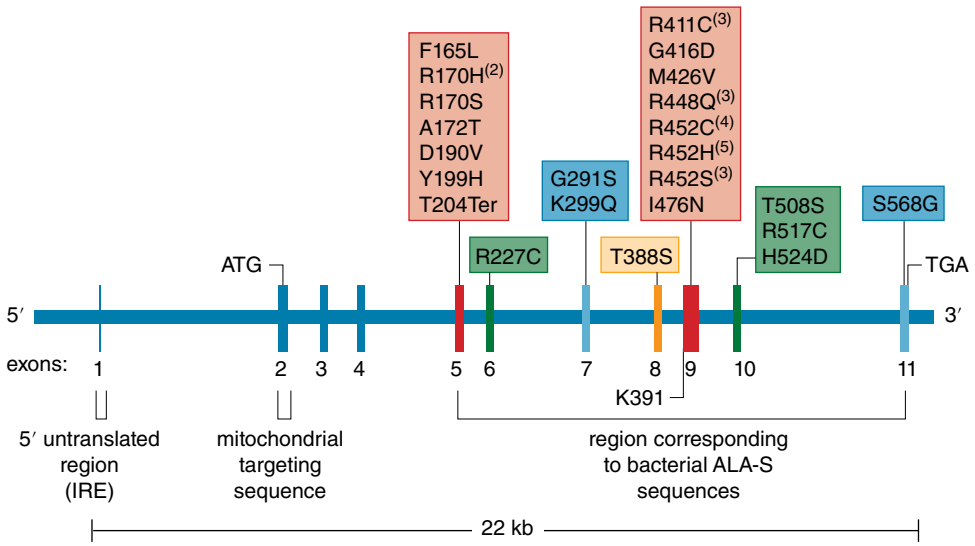

Fig. 5.30. Sideroblastic anemia: Mutations in the δ-aminolevulinic acid synthase (ALA-S) gene in patients with X-linked sideroblastic anemia. IRE, Iron-responsive element. The superscript numbers in parentheses refer to the number of cases described at the time of writing. (Courtesy of Professor DF Bishop.)

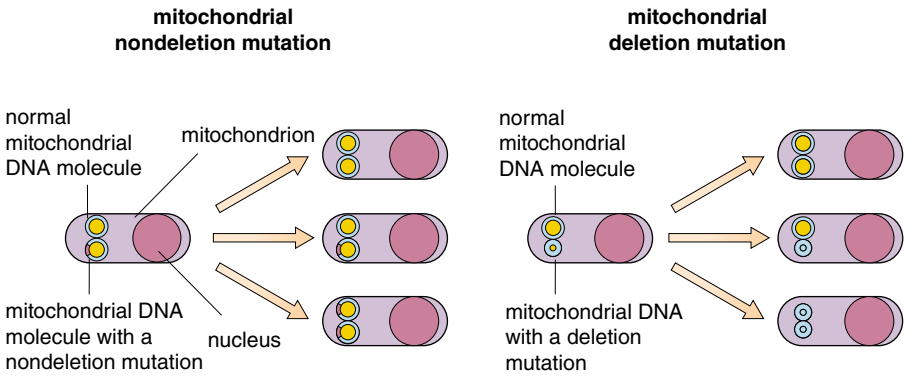

Fig. 5.31. Mitochondrial DNA consists of a circular loop of DNA coding for enzymes in the mitochondrial respiratory chain. It is inherited from the cytoplasm of the maternal ovum. Multiple copies (50–1000) are present in each cell. The relative proportions of a mutant (deletional or nondeletional) and wild-type mitochondrial DNA that occur in the individual cells of a particular tissue determine the phenotype when a mitochondrial defect is inherited.

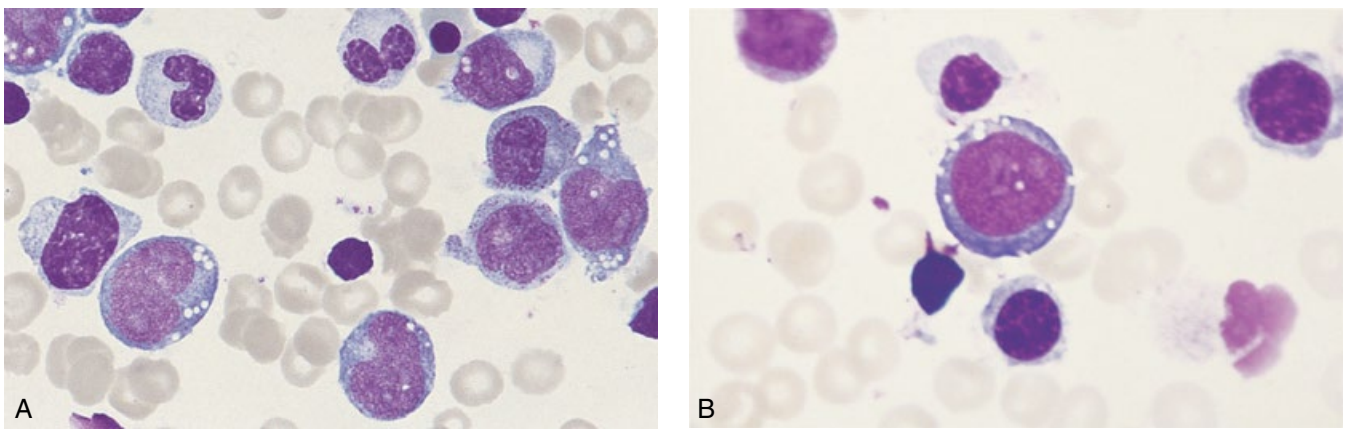

Fig. 5.32. Congenital sideroblastic anemia. **A,** Bone marrow of a baby with Pearson syndrome showing vacuolated proerythroblasts and dysplastic neutrophils. **B,** Bone marrow of a 42-year-old man with congenital sideroblastic anemia showing vacuolation of blast cells.

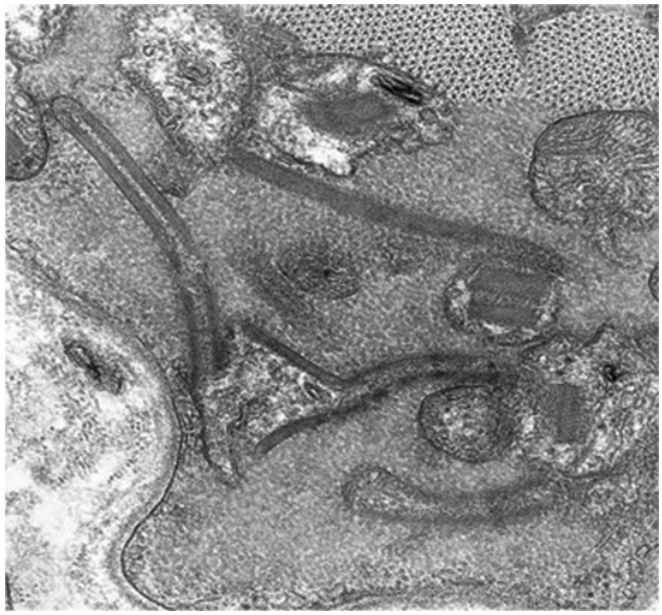

Fig. 5.33. Congenital sideroblastic anemia: Electron micrograph of skeletal muscle of a 42-year-old man showing bizarrely shaped mitochondria with abnormal cristae and intramitochondrial paracrystalline inclusions. The changes are typical of a mitochondrial respiratory chain defect. (Courtesy of Professor AHV Schapira.)

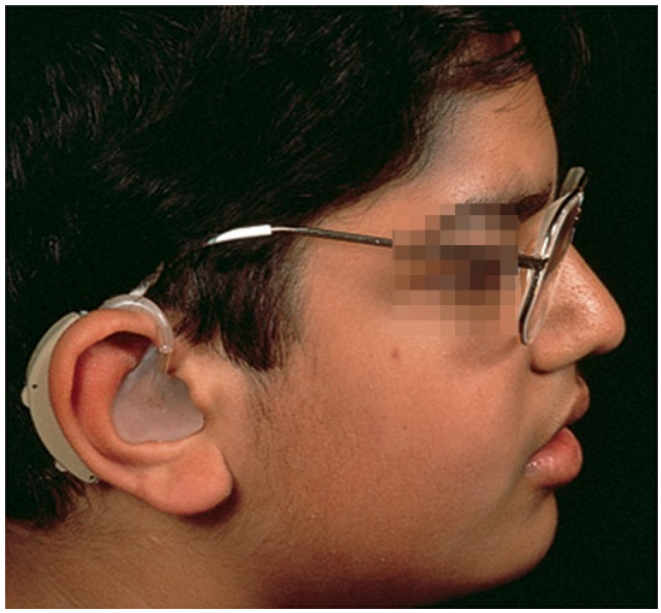

Fig. 5.34. Sideroblastic anemia: An 11-year-old boy with congenital deafness, optic atrophy, diabetes mellitus, and megaloblastic and sideroblastic anemia (a variant of DIDMOAD syndrome). His older sister showed the same syndrome, but in her case the anemia responded to thiamine. In this patient the anemia was refractory to thiamine, pyridoxine, and folic acid, and regular blood transfusions were needed. (Courtesy of Dr. JZ Wimperis.)

In myelodysplasia with ring sideroblasts, there are usually mutations in the gene *SF3B1* involved in splicing. The mutation causes misrecognition of 3′ splice sites, resulting in aberrant mRNA transcripts. The genes *ABCB7*, *PPOX* (encoding protoporphyrin oxidase), and *TMEM14C* (encoding an inner mitochondrial membrane protein required for porphyrin transport) are all downregulated in *SF3B1*-mutated cells.

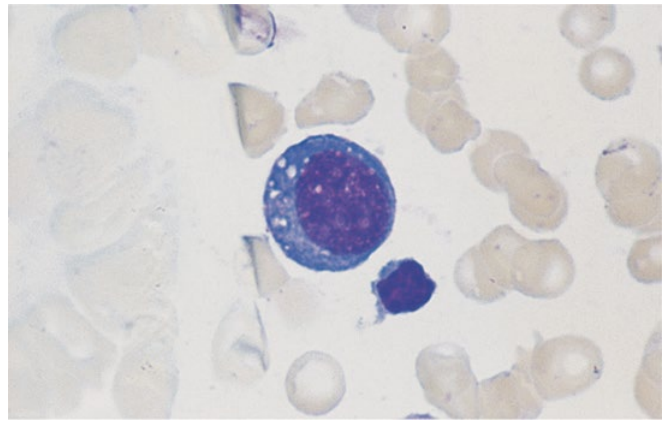

Fig. 5.35. Alcohol-related bone marrow toxicity: Vacuolation of a pronormoblast can be seen.

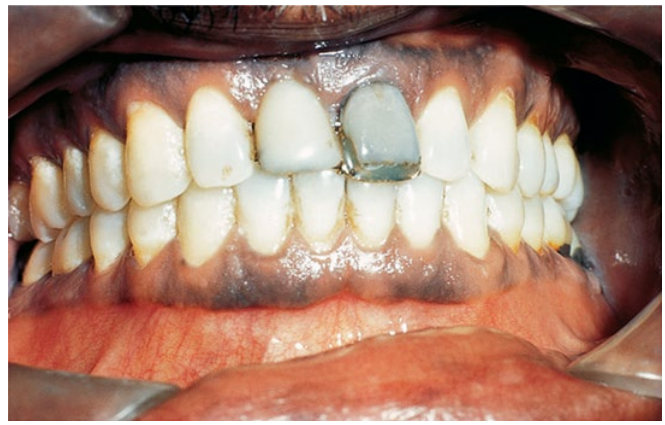

Fig. 5.36. Lead poisoning: A lead line in the gums of a young man with abdominal colic. The poisoning was from prolonged occupational exposure to molten lead.

ALCOHOL

Excessive ingestion of alcohol may cause a variety of hematologic abnormalities, including macrocytosis, megaloblastic and sideroblastic changes. In some cases vacuolation of erythroblasts is apparent (Fig. 5.35).

LEAD POISONING

Clinically, lead poisoning causes abdominal colic and constipation, a peripheral neuropathy, and anemia. Two important enzymes in heme synthesis, δ-aminolevulinic acid dehydratase and ferrochelatase, are inhibited. There may be a lead line visible in the gums (Fig. 5.36), marked punctate basophilia in the peripheral blood (Fig. 5.37A), a mild hypochromic anemia with hemolysis, and ring sideroblasts in the marrow (Fig. 5.37B). Lead poisoning may result from excessive exposure to lead paint or to lead in industry. It may also occur because of ingestion of herbal medicines containing excess lead. The punctate basophilia is caused by aggregates of undegraded RNA, a result of inhibition of the enzyme pyrimidine 5′-nucleotidase (Table 5.3).

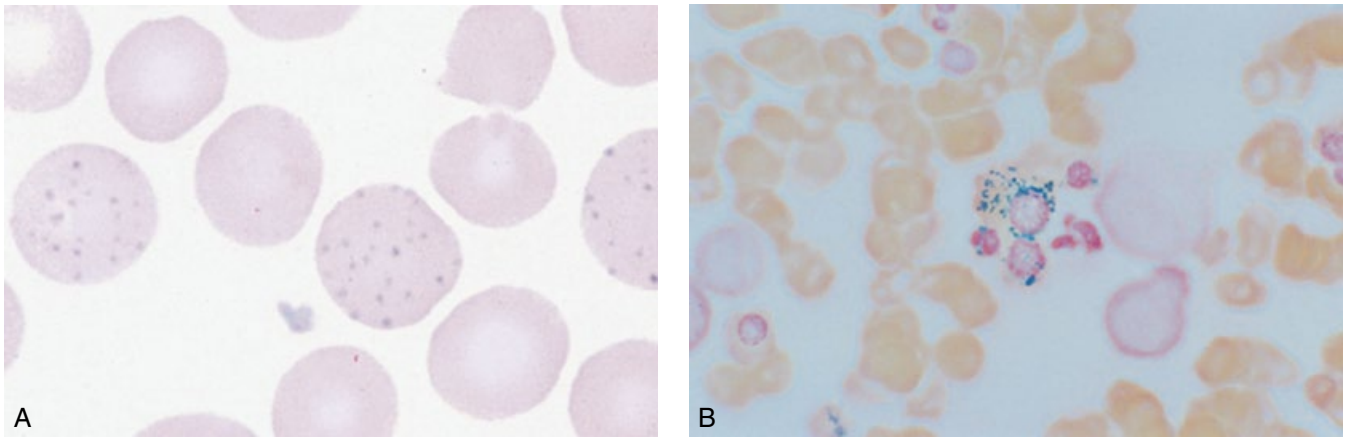

Fig. 5.37. Lead poisoning. **A,** Peripheral blood film showing punctate basophilia. This is caused by precipitates of undegraded RNA, the result of inhibition by lead of pyrimidine 5′-nucleotidase, one of the enzymes responsible for RNA degradation. Similar appearances occur in hereditary pyrimidine 5′-nucleotidase deficiency (see Fig. 8.23). **B,** Bone marrow aspirate showing coarse siderotic granules in a ring around the nucleus of an erythroblast. (Perls' stain.)

TABLE 5.3. PUNCTATE BASOPHILIA: CAUSES

Thalassemia (α and β)
Acquired sideroblastic anemia and other myelodysplasias
Lead poisoning
Severe megaloblastic anemia
Pyrimidine 5′-nucleotidase deficiency
Congenital dyserythropoietic anemia

DIFFERENTIAL DIAGNOSIS OF HYPOCHROMIC MICROCYTIC ANEMIAS

The causes of hypochromic microcytic anemia include iron deficiency, thalassemias, and other genetic disorders of hemoglobin, the anemia of chronic disorders, IRIDA, sideroblastic anemia, and lead poisoning (Table 5.4). These causes may be differentiated by special tests, including measurement of serum iron, total iron-binding capacity, or serum ferritin; by hemoglobin electrophoresis or high-performance liquid chromatography (HPLC) examination; or, if necessary, by DNA analysis. Bone marrow examination is necessary to diagnose sideroblastic anemia. In thalassemia trait, the disorders may be suspected from the presence of a high red cell count (more than 5.5×10^{12}/L) with low MCV and MCH values (see Chapter 9). Serum hepcidin is raised in chronic inflammation or malignancy but low in iron deficiency.

TABLE 5.4. DIFFERENTIAL DIAGNOSIS OF HYPOCHROMIC MICROCYTIC ANEMIA

	Iron deficiency	Chronic inflammation or malignancy	Thalassemia trait (α or β)	Sideroblastic anemia	IRIDA
MCV MCH	Reduced in relation to severity of anemia	Normal or mild reduction	Reduced: very low for degree of anemia	Usually low in congenital type but MCV often raised in acquired type	Reduced[a]
Serum iron	Reduced	Reduced	Normal	Raised	Reduced[b]
TIBC	Raised	Reduced	Normal	Normal	Reduced
Serum ferritin	Reduced	Normal or raised	Normal	Raised	Raised
Serum hepcidin	Reduced	Raised	Normal	?	Raised
Bone marrow iron stores	Absent	Present	Present	Present	Present
Erythroblast iron	Absent	Absent	Present	Ring forms	Absent
Hemoglobin electrophoresis	Normal	Normal	HbA_2 raised in β form	Normal	Normal

MCV, mean cell volume; MCH, mean cell hemoglobin; TIBC, total iron-binding capacity; IRIDA, iron-refractory iron-deficiency anemia.

[a] Very low (MCV 45–65 fL).

[b] % saturation <5%.

CHAPTER

THE PORPHYRIAS AND IRON OVERLOAD

6

Porphyrins are essential components of hemoglobin- and heme-containing enzymes. Table 6.1A shows the pathways of porphyrin synthesis and the diseases that result from inherited or acquired abnormalities in the pathway. The two main types of inherited defect of porphyrin synthesis that are associated with light sensitivity and also affect the hematopoietic system are congenital erythropoietic porphyria (CEP, also known as Günther disease) and congenital erythropoietic protoporphyria (CEPP). They are classified among the cutaneous porphyrias (Table 6.1B). Acute porphyrias (which are not associated with hematologic abnormalities) present with episodes of abdominal pain, vomiting, peripheral neuropathy, and mental changes. Fits and hyponatremia may also occur. These symptoms are largely due to the effect of the porphyrin excess on the central, peripheral, and autonomic nervous systems. Attacks may be triggered by alcohol, prescribed drugs, hormonal changes, and stress. There is an excess of porphobilinogen in the urine.

CONGENITAL ERYTHROPOIETIC PORPHYRIA

Inherited as an autosomal recessive trait, CEP is characterized by excessive production of uroporphyrinogen I, which forms the pigments uroporphyrin I and coproporphyrin I. There is deficiency of the heme synthetic enzyme uroporphyrin III cosynthase located on chromosome 10q25.2-26.3. The most frequent

TABLE 6.1A. PORPHYRIN METABOLISM

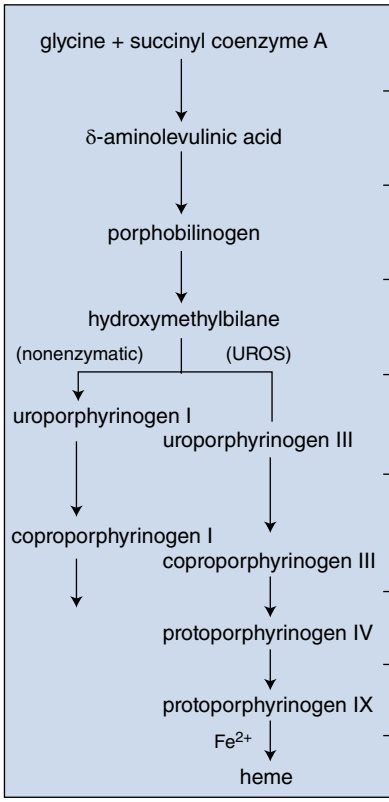

Enzyme	Disease	Type	Symptoms	Products
ALAS2	X-linked sideroblastic anemia	Erythroid	Microcytic anemia	Sideroblasts
ALAD	ALA dehyratase porphyria	Hepatic	Neurovisceral	Urinary ALA
HMBS	Acute intermittent porphyria	Hepatic	Neurovisceral	Urinary ALA, PBG
UROS	Congenital erythropoietic porphyria	Erythropoietic	Photosensitivity Hemolytic anemia	Urinary and red blood cell Uroporphyrinogen I, coproporphyrinogen I
UROD	Porphyria cutanea tarda Hepatoerythropoietic porphyria	Hepatic/ erythropoietic	Photosensitivity Hemolytic anemia	7-C porphyrin, fecal isocoproporphyrin
CPOX	Hereditary coproporphyria	Hepatic photosensitivity	Neurovisceral, coproporphyrin	Urinary ALA, porphobilinogen,
PPOX	Variegate porphyria	Hepatic	Neurovisceral, photosensitivity	Urinary ALA, porphobilinogen, fecal protoporphyrin
FECH	Erythropoietic protoporphyria	Erythropoietic	Photosensitivity	Red blood cell protoporphyrin, fecal protoporphyrin

AR, Autosomal recessive; AD, autosomal dominant; XL, X-linked.
Source: Sassa S. *Br J Haematol* 2006;135:282–292.

Color Atlas of Clinical Hematology: Molecular and Cellular Basis of Disease, Fifth Edition. A. Victor Hoffbrand, Paresh Vyas, Elías Campo, Torsten Haferlach, and Keith Gomez

TABLE 6.1B. MODE OF INHERITANCE, ENZYME DEFECT, AND CLINICAL PRESENTATION IN THE ACUTE AND CUTANEOUS PORPHYRIAS

	Inheritance	Gene/enzyme	Clinical presentation	
			Acute attacks	Skin symptoms (both)
Acute porphyrias				
ALA dehydratase deficiency porphyria	AR	*ALAD*/ALA dehydratase	100%	None
Acute intermittent porphyria	AD	*HMBS*/Hydroxymethylbilane synthase	100%	None
Hereditary coproporphyria	AD	*CPOX*/Coproporphyrinogen oxidase	>95%	<5% (20–30%)
Variegate porphyria	AD	*PPOX*/Protoporphyrinogen oxidase	40%	60% (20%)
Cutaneous porphyrias				
Porphyria cutanea tarda	AD[a]	*UROD*/Uroporphyrinogen decarboxylase	None	100%
Congenital erythropoietic porphyria	AR	*UROS*/Uroporphyrinogen synthase	None	100%
Erythropoietic protoporphyria	AR	*FECH*/Ferrochelatase	None	100%
X-linked erythropoietic protoporphyria	XL	ALAS2/ALA synthase 2	None	100%

AR, Autosomal recessive; AD, autosomal dominant; XL, X-linked.
[a] 20% inherited, 80% acquired.
Source: Stein PE, et al. *Br J Haematol* 2017;176:527–538. Reproduced with permission of John Wiley & Sons.

genetic mutation is C73R, which, when homozygous, results in <1% of normal enzyme activity. The plasma and erythrocytes contain excessive quantities of uroporphyrin I, coproporphyrin I, and protoporphyrin.

Patients present with bullous ulcerating lesions of light-exposed skin that are prone to infection and hirsutism (Fig. 6.1). Hemolytic anemia is usual and associated, as in this patient, with splenomegaly. The urine is red and fluorescent (Fig. 6.2), and the bones and teeth are discolored and also fluorescent (Fig. 6.3). The nucleated red cells fluoresce when exposed to ultraviolet light (Fig. 6.4).

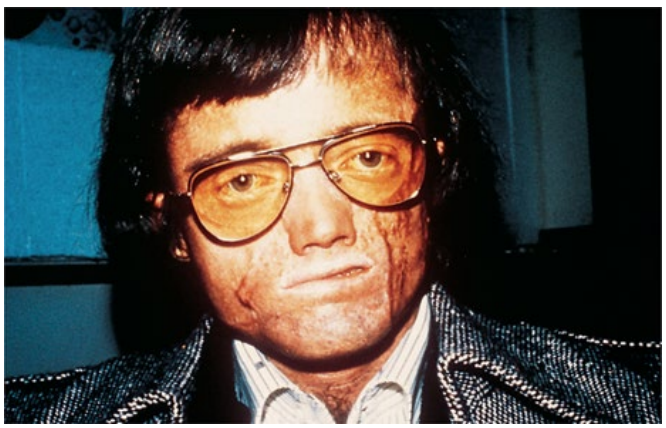

Fig. 6.1. Congenital erythropoietic porphyria: This 22-year-old man was first diagnosed with this condition (Günther disease) at 6 years of age, although skin changes had been noted from 2 years of age, especially in the summer. Blistering and susceptibility to mechanical injury were found on exposed areas of skin and led to damage to the extremities, including the nose, ears, and hands. He has erythrodontia, splenomegaly, and increased erythropoiesis, with red cells that fluoresce. Hemolysis increased with age and was associated with reticulocytosis. In this case, increased activity of ALA-S and decreased activity of uroporphyrinogen cosynthase were demonstrated, with increased excretion of uroporphyrin I and coproporphyrin I in the urine, together with increased concentrations of these porphyrins in erythrocytes and plasma. (Courtesy of Dr. MR Moore.)

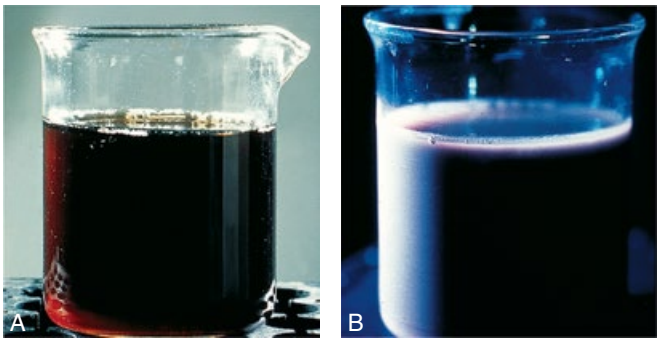

Fig. 6.2. Congenital erythropoietic porphyria: **A,** Urine sample in daylight. **B,** Urine sample in ultraviolet light. (Courtesy of Dr. MR Moore.)

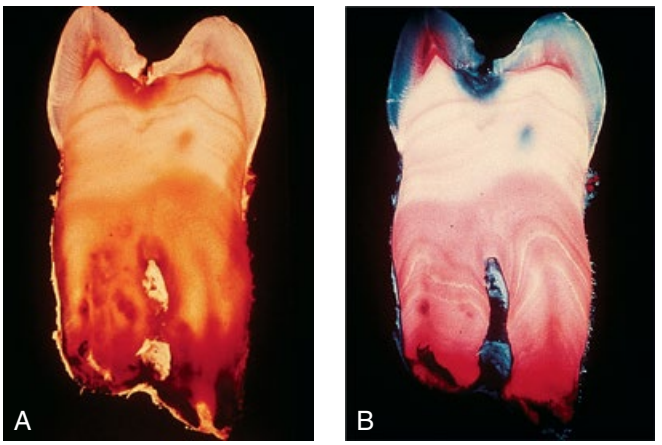

Fig. 6.3. Congenital erythropoietic porphyria: **A,** Molar tooth in ordinary light, with brown discoloration, **B,** In ultraviolet light, with fluorescence most marked in the cortical bone. (Courtesy of Dr. MR Moore.)

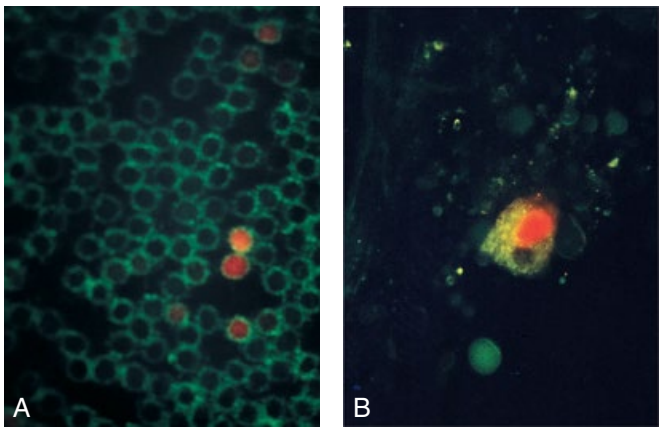

Fig. 6.4. Congenital erythropoietic porphyria: **A,** Peripheral blood film. **B,** Bone marrow aspirate viewed in ultraviolet light show nuclear fluorescence of erythroblasts caused by the presence of large amounts of uroporphyrin I. (Courtesy of Dr. I Magnus.)

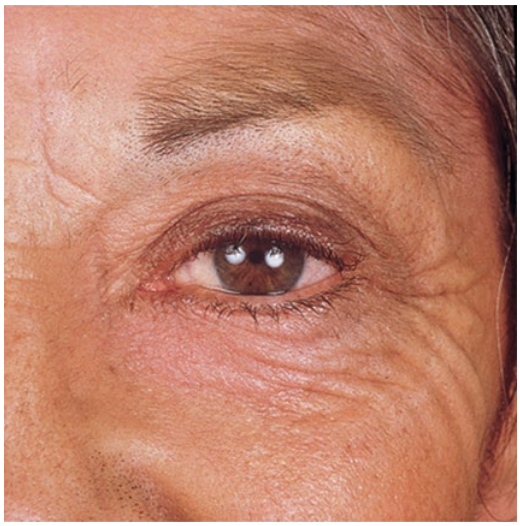

Fig. 6.5. Porphyria cutanea tarda: This 55-year-old woman had bullous eruptions on exposed skin surfaces. (Courtesy of Professor M Rustin.)

For comparison, a patient with the much more frequent porphyria cutanea tarda is shown in Fig. 6.5. A bullous eruption occurs on exposure to sunlight. There is a defect of hepatic uroporphyrinogen decarboxylase, which may be genetic or acquired as a result of alcohol, iron, or estrogen in excess. Iron loading may be a result as well as a cause of the syndrome.

CONGENITAL ERYTHROPOIETIC PROTOPORPHYRIA

In CEPP, which is inherited as an autosomal dominant disease, the underlying defect is one of ferrochelatase (heme synthase, chromosome 18q22), the final enzyme in heme synthesis. There is excess production of protoporphyrin, which accumulates in erythrocytes, the liver, and other tissues. The erythroblasts fluoresce when exposed to ultraviolet light. They may show ring sideroblasts.

Patients with CEPP are also light sensitive and develop pruritus, pain, swelling, and reddening of the skin. The urine and teeth are of normal color and nonfluorescent, and hemolytic anemia is not present. Cholestasis, hepatitis, and cirrhosis may lead to death from liver failure.

IRON OVERLOAD

GENETIC HEMOCHROMATOSIS

The main causes of increased storage of iron are listed in Table 6.2. Transfusional iron overload is discussed in detail in conjunction with thalassemia major in Chapter 9, and porphyria cutanea tarda was discussed previously in this chapter. The genetic basis for most cases of genetic hemochromatosis has now been established (Table 6.3), and these diseases are discussed briefly here.

The clinical features of the most common type of genetic hemochromatosis are largely similar to those of transfusional iron overload and include hyperpigmentation of the skin due to melanin deposition (Fig. 6.6) and endocrine abnormalities: diabetes mellitus; gonadal, pituitary, thyroid, and parathyroid dysfunction. Liver parenchymal iron overload is invariable (Fig. 6.7), and fibrosis, cirrhosis, and hepatocellular carcinoma may develop, particularly if viral hepatitis is also present. Computed tomography (CT) scans (Fig. 6.8) can be used to diagnose and measure liver iron overload. Magnetic resonance imaging (MRI) is now preferred to measure both liver and cardiac iron (Fig. 6.9). T_2^* measures the speed of relaxation of the tissue after a magnetic field: the more rapid the relaxation, the higher the iron content (see Chapter 9). A cardiomyopathy may occur with arrhythmia, pericarditis, or congestive heart failure. An asymmetric arthropathy principally affecting the distal interphalangeal joints with calcium pyrophosphate deposition is characteristic of genetic hemochromatosis (Fig. 6.10) and is not seen in transfusional iron overload.

The gene *HFE*, which is responsible for the most common type of genetic hemochromatosis (type I), is located on the short arm of chromosome 6p22.2. HFE is one of the proteins controlling synthesis of hepcidin (Chapter 5). The HLA class 1-like gene *HFE* is located 3 mb telomeric to the HLA-A locus.

TABLE 6.2. CAUSES OF IRON OVERLOAD

Increased iron absorption
From diets of normal iron content
Primary (genetic) hemochromatosis
Iron-loading anemia (refractory anemias with increased bone marrow erythroid cells)
Chronic liver disease (cirrhosis, porto-caval shunt)
Porphyria cutanea tarda
Rare congenital defects (atransferrinemia, aceruloplasminemia, Friedreich ataxia, hyperferritinemia with autosomal dominant congenital cataracts, other diseases)
From diets with increased iron content
African diet overload[a]
Medicinal iron
Transfusional iron overload
Rare congenital defects, see Table 6.4

[a] A genetic abnormality may play a role.

TABLE 6.3. CLASSIFICATION OF HEREDITARY HEMOCHROMATOSIS

Type	Gene	Inheritance and phenotype	Severity	Incidence
1	*HFE*	AR, parenchymal iron overload	Highly variable	Common
2 (juvenile)	Hemojuvelin (*HFE2*)	AR, parenchymal iron overload	Severe	Rare
	Hepcidin (*HAMP*)	AR, parenchymal iron overload	Severe	Rare
3	*TFR2*	AR, parenchymal iron overload	Variable	Rare
4a	Ferroportin (*SLC40A1*)	AD, RE iron	Variable	Rare
4b	Ferroportin (mutations in binding site for hepcidin)	AD, parenchymal iron overload	Severe	Rare

AD, Autosomal dominant; AR, autosomal recessive; RE, reticuloendothelial.
Source: Hoffbrand AV, et al. *Postgraduate Haematology,* 7th edn. JohnWiley & Sons, 2016. Reproduced with permission of John Wiley & Sons.

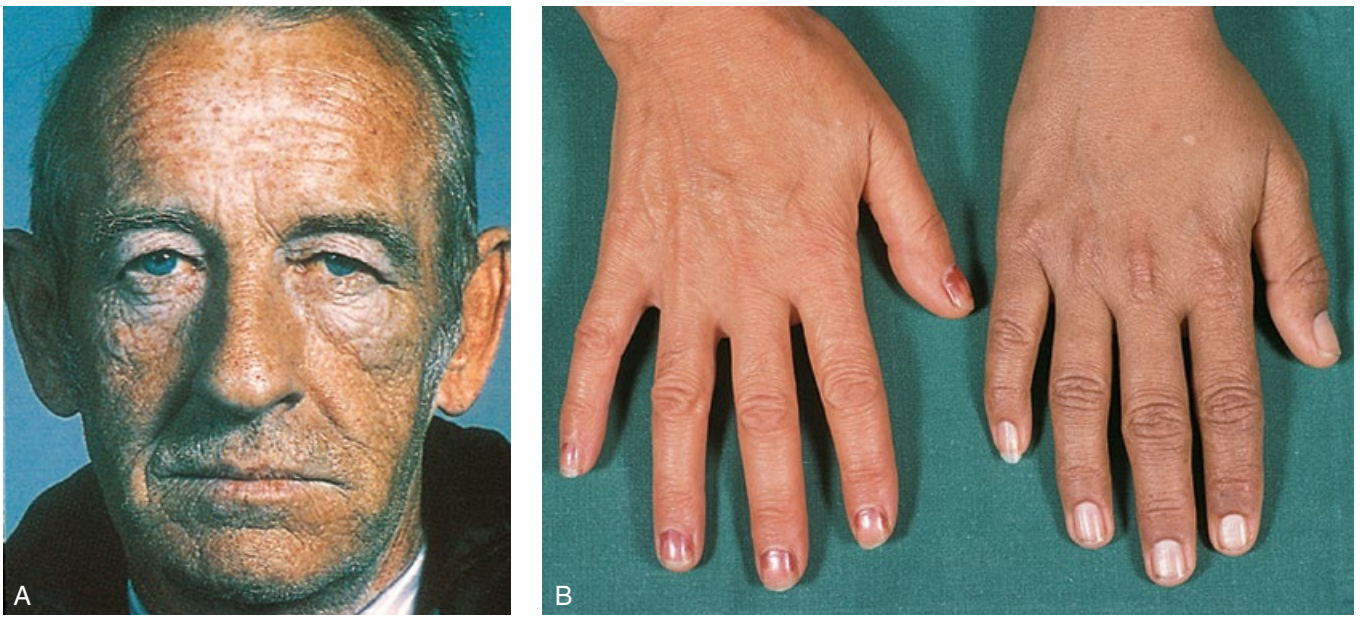

Fig. 6.6. Genetic hemochromatosis Type 1. **A,** The appearance of an adult male patient with genetic hemochromatosis is shown. Note the characteristic bronze appearance. The hyperpigmentation results from melanin deposition in the skin. The patient also showed hepatic cirrhosis and diabetes mellitus. (Courtesy of Dr. R Britt.) **B,** For comparison, the hand *(on the right)* of a 16-year-old patient with thalassemia major shows heavy melanin pigmentation; in contrast, his mother's hand *(on the left)* shows normal coloration.

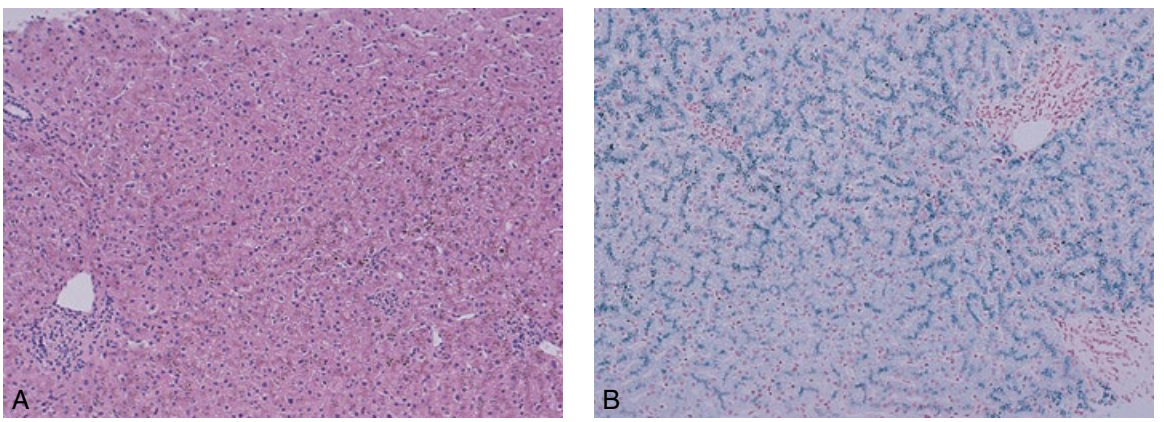

Fig. 6.7. Genetic hemochromatosis. **A,** Needle biopsy of the liver in a 30-year-old woman. H&E stain showing normal architecture with golden brown deposits (hemosiderin) in parenchymal cells. **B,** Perls' stain confirming heavy siderosis of parenchymal cells with sparing of Kupffer cells.

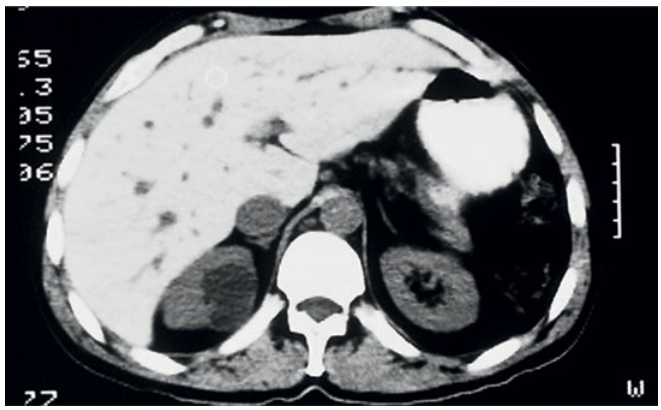

Fig. 6.8. Genetic hemochromatosis: Axial computed tomography (CT) scan showing increased density of the liver caused by iron overload. The patient, a 50-year-old man, has diabetes mellitus and also pyruvate kinase deficiency, for which splenectomy had been performed.

It contains seven exons and the putative protein structure is shown in Fig. 6.11. A homozygous missense G to A mutation at nucleotide 845 resulting in a cysteine to tyrosine substitution at amino acid 282 has been found in 83–100% of cases of genetic hemochromatosis in most series studied. About a quarter of all men but only 1% of women homozygous for the mutation show iron overload-related disease. A second mutation, C to G in exon 2, results in a histidine to aspartic acid substitution at amino acid 63, and a small percentage of genetic hemochromatosis patients are compound heterozygotes. Other rarer mutations of HFE underlie other cases of genetic hemochromatosis.

In rare cases, genetic hemochromatosis can result from genetic defects of hemojuvelin (HJV) (1q21.2) and hepcidin (19q13.1) itself (genetic hemochromatosis type 2), in which case the clinical presentation is usually earlier in life and more severe, often with an iron-induced cardiomyopathy (Table 6.3). Transferrin receptor type 2 mutation may also cause genetic hemochromatosis (type 3). The clinical presentation is usually

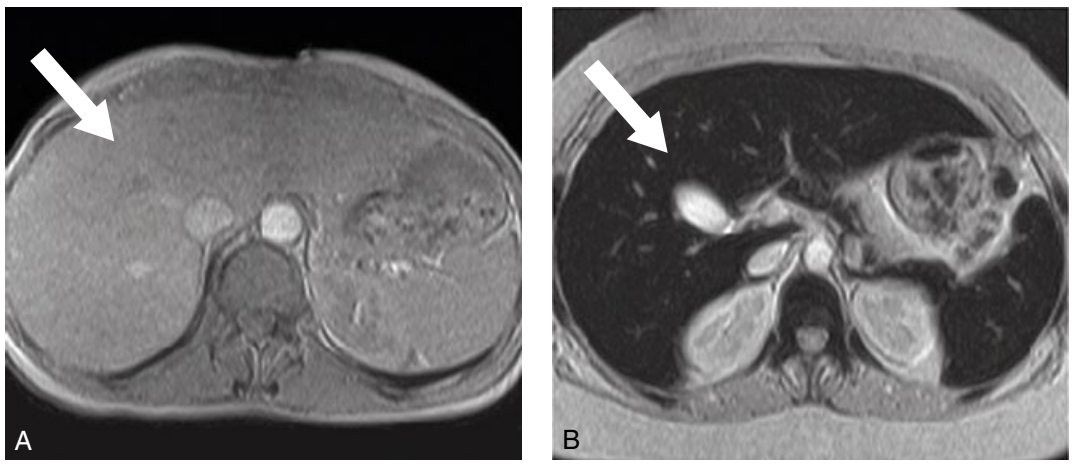

Fig. 6.9. Transfusional iron overload: T_2* magnetic resonance imaging appearances of liver and spleen **(B)** compared with normal **(A)**. (Courtesy of Professor DJ Pennell.)

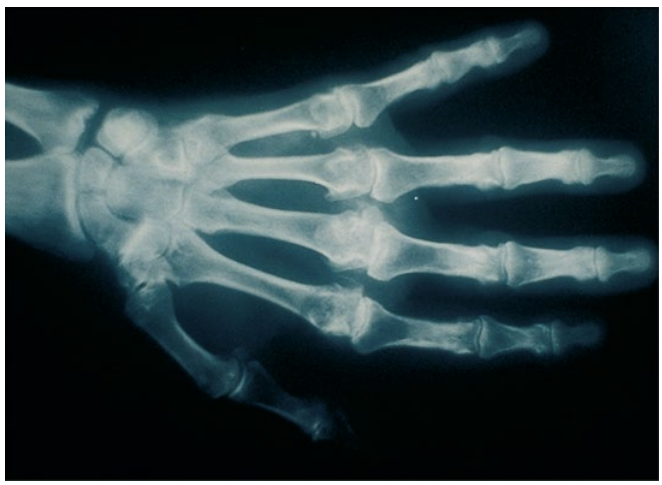

Fig. 6.10. Genetic hemochromatosis: Radiograph of a hand showing degenerative arthritis (caused by calcium pyrophosphate deposition) affecting the interphalangeal joints.

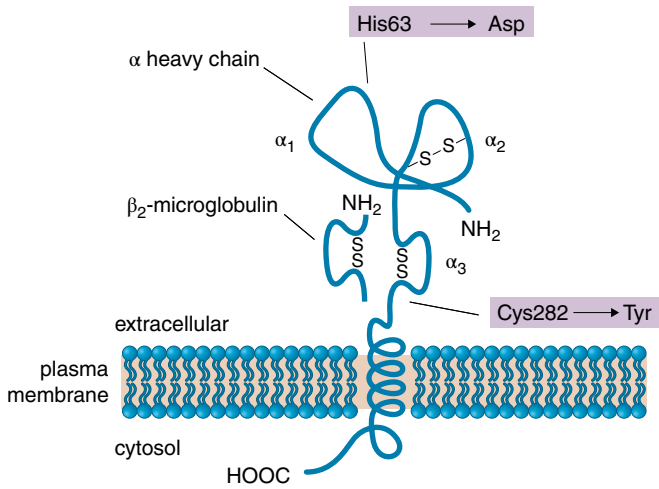

Fig. 6.11. Genetic hemochromatosis: Hypothetical model of the protein derived from the *HFE* gene based on its homology to the HLA class I molecule. The sites of the mutations found in primary hemochromatosis are shown. Source: Feder JN, et al. *Nat Genet* 1996;13:399–408. Reproduced with permission of Springer Nature.

later than in type 2 disease. In types 1–3 genetic hemochromatosis the serum hepcidin is low. There is iron accumulation in parenchymal cells and a raised serum ferritin, but macrophage iron is usually, but not always, normal (Fig. 6.12). Mutations of the ferroportin gene *SLC11A3* are classified as GH type 4. There is, however, phenotypic variation depending on the mutation involved, parenchymal iron loading occurring when the mutations are in the hepcidin-binding site of the gene (Type 4b) and reticuloendothelial loading, predominantly, as in Fig. 6.12, when the mutations are elsewhere in the gene (Type 4a).

Management of genetic hemochromatosis consists of venesection to remove iron and appropriate treatment for dysfunction of damaged organs. For patients presenting in heart failure or with an arrhythmia due to a cardiomyopathy, iron chelation with continuous intravenous desferrioxamine and oral deferiprone is the most rapid treatment to reverse the cardiac damage.

RARE CAUSES OF IRON OVERLOAD

Porphyria cutanea tarda (see Fig. 6.5) is associated with iron loading in the liver. In the rare autosomal recessive disorder atransferrinemia, there is a microcytic, hypochromic anemia with excess iron deposition in the reticuloendothelial cells (Table 6.4). In aceruloplasminemia, which is also autosomal recessive, retinal and basal ganglia degeneration occurs with iron loading in the liver, pancreas, brain, and other organs. Serum iron is low, total body iron content normal, and serum ferritin raised. Iron overload and sideroblastic anemia resulting from a genetic defect in an iron–sulfur cluster protein, glutaredoxin 5, has been described (see Chapter 5). Mutation of *DMT1* (see also Chapter 5) results in a hypochromic microcytic anemia with liver iron overload. This could be due to increased upregulation of the heme-iron absorption pathway, bypassing the *DMT1* defect in the intestine. Friedreich ataxia manifests in middle age with spinocerebellar ataxia and a cardiomyopathy. There is a mutation in the gene for frataxin, a mitochondrial protein. This leads to a decrease in biosynthesis of iron–sulfur clusters and heme and in oxidative damage to mitochondrial DNA, proteins, and membranes. Excess iron deposition is found in the heart.

HEREDITARY HYPERFERRITINEMIA WITH AUTOSOMAL DOMINANT CONGENITAL CATARACT SYNDROME

Hereditary hyperferritinemia cataract syndrome (HHCS) manifests with early-onset cataract (caused by ferritin deposition in the lens; Fig. 6.13) and elevated serum ferritin (1000–2500 μg/L).

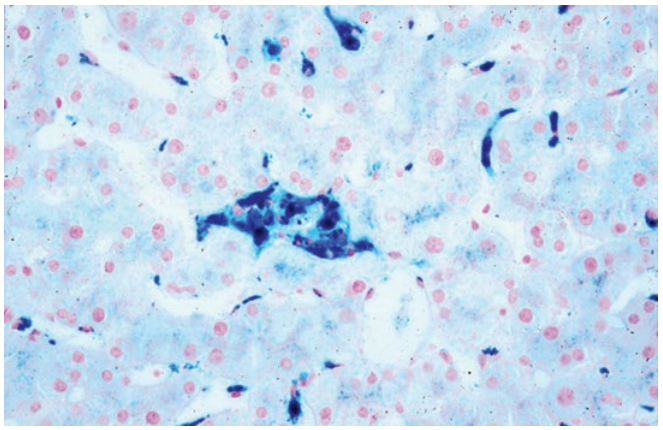

Fig. 6.12. Genetic hemochromatosis, type 4a: Ferroportin defect. Iron is increased in the reticuloendothelial (Kupffer) cells but not usually in parenchymal cells unless the underlying mutations are in the hepcidin-binding site of the gene. (Courtesy of Dr. J Dooley.)

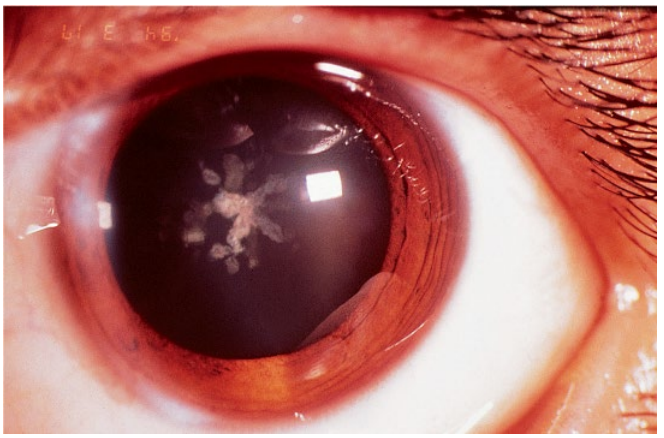

Fig. 6.13. Hereditary hyperferritinemia cataract syndrome: The "starring" lens opacity is characteristic. (Courtesy of Dr. D Girelli and Professor R Corrocher.)

TABLE 6.4. RARE CAUSES OF IRON OVERLOAD

Disease	Inheritance	Gene	Clinical features
Hypotransferrinemia	AR	*TF*	Anemia, iron overload
Aceruloplasminemia	AR	*CP*	Anemia, iron overload
DMT1 defects	AR	*SLC11A2*	Anemia, iron overload, neurological symptoms
Friedreich ataxia	AR	Frataxin	Spino-cerebellar ataxia, cardiomyopathy
Hyperferritinemia cataract	AD	L-ferritin	Bilateral cataracts
Hemochromatosis	AD	H-ferritin	Iron overload
Hemochromatosis, sideroblastic anemia	AR	Glutaredoxin 5	Iron overload
Neonatal hemochromatosis	?	?	Liver failure, iron overload

AD, Autosomal dominant; AR, autosomal recessive.
Source: Camaschella C. *Blood* 2005;106:3710–3717. Reproduced with permission of *Blood: Journal of the American Society.*

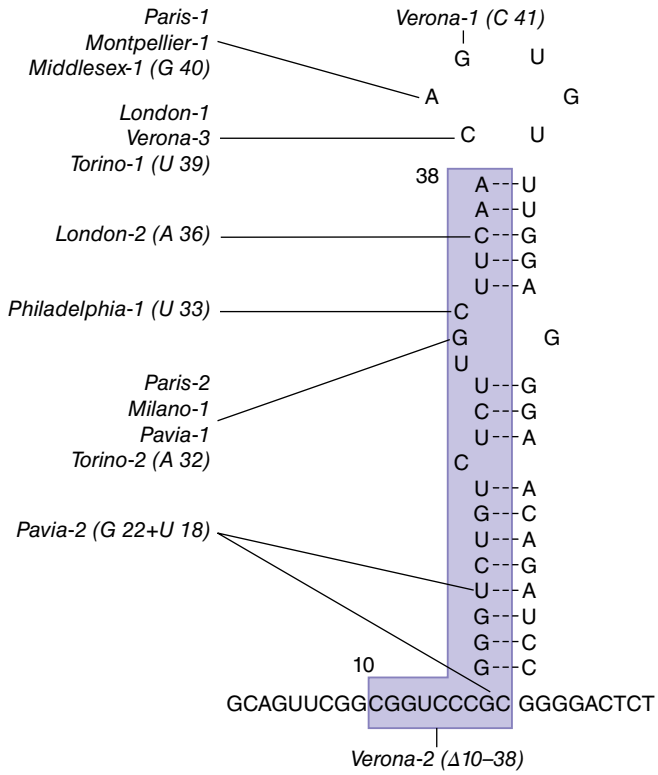

Fig. 6.14. Hereditary hyperferritinemia cataract syndrome: Representation of the iron-response element (IRE) located in the 5′ untranslated region (UTR) of L-ferritin mRNA and of the mutations associated with HHCS showing evidence for genetic heterogeneity of the disease. (Courtesy of Dr. D Girelli and Professor R Corrocher.)

Serum ferritin, normally composed of molecules with either light (L; molecular weight 19 kDa, coded for on chromosome 19q13.3–13.4) or heavy (H; molecular weight 21 kDa, coded for on chromosome 11q13) subunits (24 in total), is of L type only, the type mainly found in normal tissues of iron storage (e.g. liver and spleen). The H type is dominant in organs, not normally iron storage sites (e.g. heart). There are mutations in the iron-response element (IRE) of the L-ferritin mRNA (Fig. 6.14) that affect its binding to the iron-regulatory protein (IRP). Iron stores, serum iron, and transferrin levels are normal.

CHAPTER

7 MEGALOBLASTIC ANEMIAS

The megaloblastic anemias are a group of disorders characterized by a macrocytic blood picture and megaloblastic erythropoiesis. The causes are listed in Table 7.1. The underlying biochemical defect appears to be a fault in DNA synthesis, which may result from a lesion at some point in pyrimidine or purine synthesis or from inhibition of DNA polymerization. The anemia is usually caused by deficiency of vitamin B_{12} (cobalamin, referred to simply as B_{12} hereafter) or folate. In most cases the site of the biochemical defect in DNA synthesis is known. In some types, however, particularly in myeloblastic leukemia and myelodysplasia in which megaloblastic changes are unresponsive to B_{12} and folate therapy, the exact site of the defect remains obscure.

B_{12} is involved in only two reactions in human tissues (Figs. 7.1 and 7.2), whereas folate coenzymes are involved in many reactions involving one carbon unit transfer. The roles of B_{12} and folate in DNA biosynthesis are shown in Fig. 7.1. Folate deficiency affects thymidylate synthesis, a rate-limiting step in pyrimidine synthesis, because a folate coenzyme, 5,10-methylenetetrahydrofolate polyglutamate, is necessary for this reaction. Folate coenzymes are also required in two reactions in purine synthesis, but these are not normally considered rate limiting for DNA synthesis in humans.

B_{12} is not required directly for DNA synthesis. It is needed as methylcobalamin to convert 5-methyltetrahydrofolate (methyl-THF),

TABLE 7.1. CAUSES OF MEGALOBLASTIC ANEMIA

Vitamin B_{12} deficiency	Excess losses	**Abnormalities of vitamin B_{12} metabolism**
Inadequate diet	Dialysis	*Congenital*
Veganism	Congestive heart failure	Transcobalamin II deficiency
Maternal deficiency	Drugs	Homocystinuria with methylmalonic aciduria
Malabsorption	Anticonvulsants	*Acquired*
Gastric	Barbiturates	Nitrous oxide anesthesia
Pernicious anemia, acquired (autoimmune), and congenital, IF deficiency partial, or total gastrectomy	Mixed	**Abnormalities of folate metabolism**
Intestinal	Alcohol	*Congenital*
Stagnant-loop syndrome (e.g. jejunal diverticulosis, ileocolic fistulae)	Liver disease	Inborn errors (e.g. 5-methyltetrahydrofolate transferase deficiency)
Chronic tropical sprue	Malabsorption	*Acquired*
Ileal resection and Crohn disease	Gluten-induced enteropathy	Antifolate drugs (e.g. methotrexate, pyrimethamine)
Congenital-specific malabsorption with proteinuria (Imerslund–Gräsbeck)	Dermatitis herpetiformis	**Abnormalities of DNA synthesis**
Fish tapeworm	Tropical sprue	*Congenital*
Drugs (e.g. metformin)	Congenital specific	Orotic aciduria
Folate deficiency	Systemic infections	Lesch–Nyhan syndrome
Inadequate diet	Increased utilization	Dyserythropoietic anemia
Poverty	Pregnancy	Thiamine-responsive
Institutions	Prematurity	*Acquired*
Goats' milk	Excess marrow turnover (e.g. in hemolytic anemias)	Drugs (e.g. hydroxyurea, cytosine arabinoside, 6-mercaptopurine, 5-azacytidine)
Special diets	Malignancy (e.g. myeloma, carcinoma)	
	Inflammatory disease (e.g. Crohn disease, rheumatoid arthritis, widespread eczema)	

IF, intrinsic factor.

Color Atlas of Clinical Hematology: Molecular and Cellular Basis of Disease, Fifth Edition. A. Victor Hoffbrand, Paresh Vyas, Elías Campo, Torsten Haferlach, and Keith Gomez

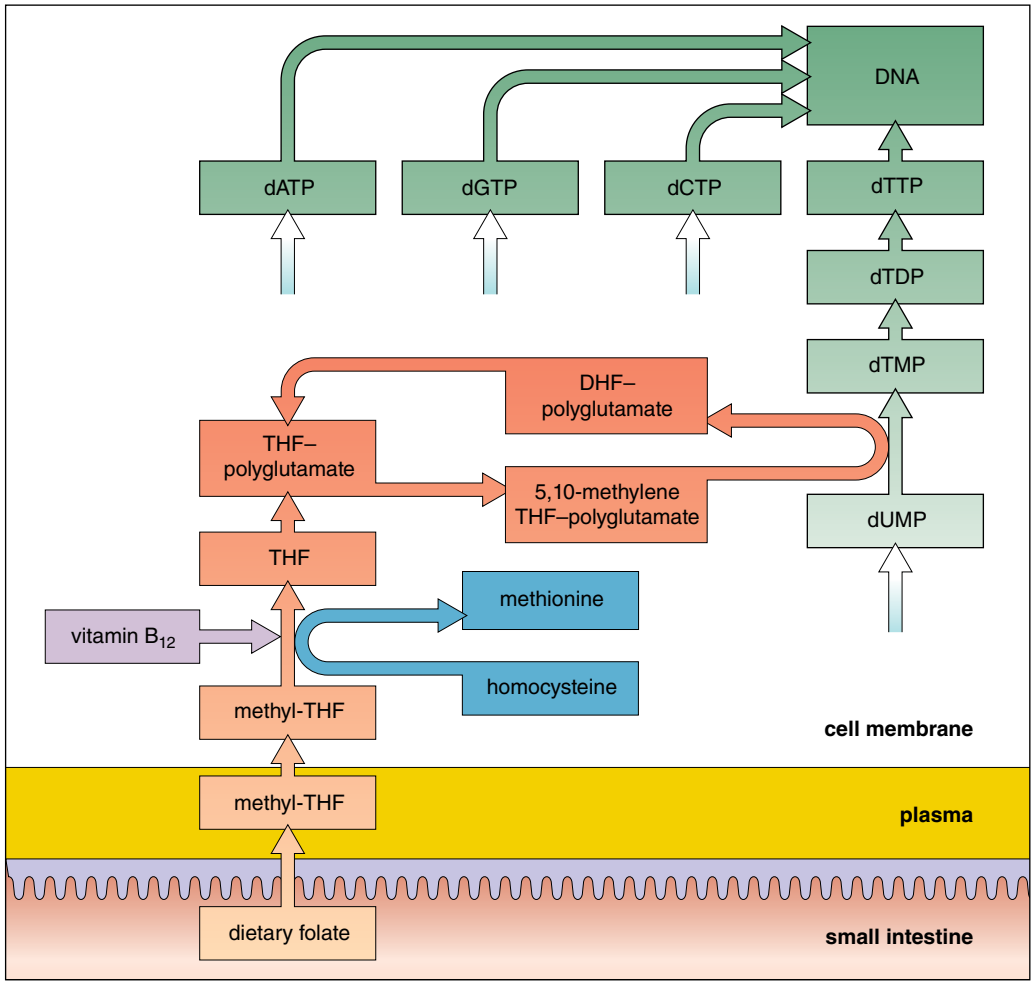

Fig. 7.1. Megaloblastic anemia: suggested roles of B_{12} and folate in DNA biosynthesis. ATP, Adenosine triphosphate; CTP, cytosine triphosphate; d, deoxyribose; DHF, dihydrofolate; GTP, guanosine triphosphate; TDP, thymidine diphosphate; THF, tetrahydrofolate; TMP, thymidine monophosphate; TTP, thymidine triphosphate; UMP, uridine monophosphate.

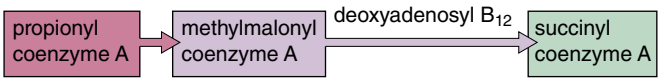

Fig. 7.2. Megaloblastic anemia: Deoxyadenosyl B_{12} acts as a coenzyme in the conversion of L-methylmalonyl coenzyme A to succinyl coenzyme A.

which enters cells from plasma, into other folate coenzyme forms (including all the polyglutamate derivatives) through its involvement in the methionine synthase reaction in which homocysteine is methylated to methionine. In this reaction the removal of the methyl group from methyl-THF forms THF, which can be converted into folate polyglutamates by the addition of glutamate moieties. Methyl-THF cannot act as a substrate for the enzyme responsible for polyglutamate formation. The role of folate in the metabolism of homocysteine is also shown in Fig. 7.9.

B_{12} in food is released from protein binding by proteolytic enzymes and attached to a so-called R-binder (Fig. 7.3). B_{12} is released from this binding by pancreatic enzymes and transferred to intrinsic factor (IF) secreted by the parietal cells of the stomach. B_{12} in bile also attaches to intrinsic factor. Intrinsic factor-bound B_{12} is carried to the ileum, where it attaches to specific receptors formed by a cubilin/amnion complex; the IF is digested and B_{12} appears in the portal blood attached to a polypeptide protein, transcobalamin II. In peripheral blood, most B_{12} is attached to the glycoprotein transcobalamin I (derived from granulocytes, monocytes, and their precursors), but it is transcobalamin II that is responsible for delivery of the vitamin to the tissues.

Dietary folate is deconjugated to the monoglutamate form, fully reduced, and methylated in the upper intestinal epithelial cells so that it is all absorbed in the form of methyl-THF (see Fig. 7.1).

CLINICAL FEATURES

Megaloblastic anemia is usually of insidious onset, progressing so slowly that the patient has time to adapt. A patient may therefore not seek treatment until the anemia is quite severe, unless diagnosed early through an incidental blood examination for other reasons. There is jaundice of varying degree in combination with anemia, giving the patient's skin a lemon-yellow tint (Fig. 7.4). The jaundice is caused by unconjugated bilirubin produced in excess because of severe intramedullary death of nucleated red cell precursors (ineffective erythropoiesis) with reticuloendothelial breakdown of their hemoglobin. A marked rise in serum lactate dehydrogenase concentration also occurs because of excessive cell breakdown.

Severe cases show features of intravascular breakdown of hemoglobin with methemalbuminemia and hemosiderinuria.

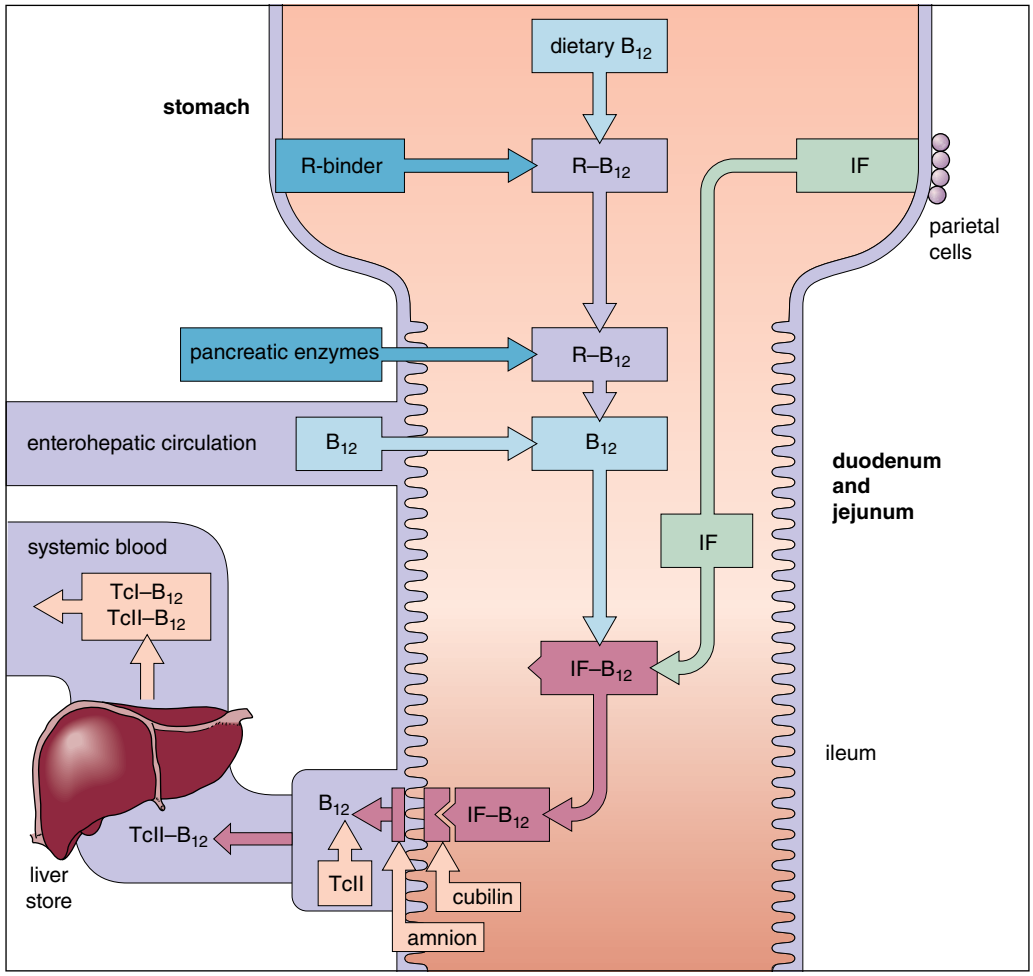

Fig. 7.3. Megaloblastic anemia: Absorption of B_{12}. IF, intrinsic factor; R, R-binder; TcI, transcobalamin I; TcII, transcobalamin II.

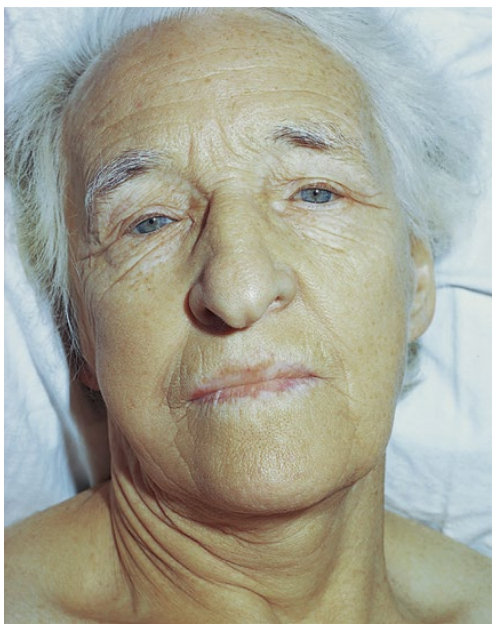

Fig. 7.4. Megaloblastic anemia: Typical lemon-yellow appearance of a 69-year-old woman with pernicious anemia and severe megaloblastic anemia. (Hb, 7.0 g/dL; MCV, 132 fL.) The color is from the combination of pallor (from anemia) and jaundice (from ineffective erythropoiesis).

Pancytopenia often occurs. The white cell and platelet counts are rarely as low as in severe aplastic anemia.

Disordered proliferation of the epithelial cell surfaces gives rise to glossitis (Fig. 7.5) and angular cheilosis (Fig. 7.6) and can also be seen microscopically in the buccal, bronchial, bladder, and cervical mucosae.

In a small proportion of cases, melanin pigmentation of the skin is present. A neuropathy of varying severity may occur with B_{12} deficiency, such as subacute combined degeneration of the spinal cord that includes posterior and lateral column demyelination (Fig. 7.7) and peripheral or optic neuropathy. The patient has bilaterally symmetric symptoms that are usually most marked in the lower limbs and comprise tingling, unsteadiness of gait, falling over in the dark, altered sensation, and reduced strength. Visual and psychiatric disturbances are less frequent.

Folic acid therapy before conception and in early pregnancy has been shown to reduce the incidence of babies with neural tube defect (NTD). The lesions may be spina bifida (Fig. 7.8), anencephaly, or encephalocele. This occurs even if the mother is not folate deficient, as assessed hematologically or by serum or red cell folate (although the lower the serum folate or B_{12} or red cell folate, the higher the incidence, even when the levels are in the accepted normal range). An association between NTD and a common mutation (nucleotide 677C → T) in the gene for the enzyme 5,10-methylene-THF reductase (Fig. 7.9) has been

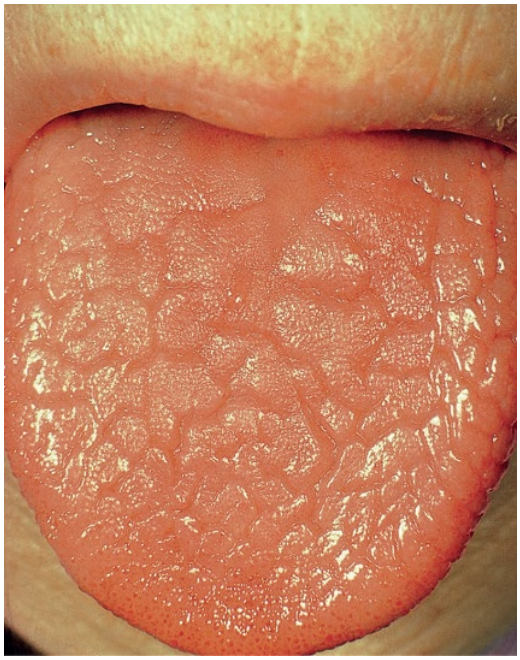

Fig. 7.5. Megaloblastic anemia: Glossitis caused by B_{12} deficiency in a 55-year-old woman with untreated pernicious anemia. The tongue is beefy red and painful, particularly with hot and acidic foods. An identical appearance occurs in folate deficiency because of impaired DNA synthesis in the mucosal epithelium.

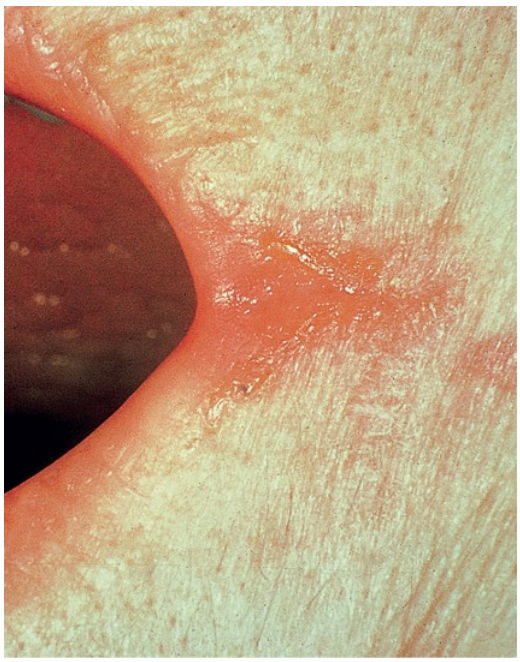

Fig. 7.6. Megaloblastic anemia: Angular cheilosis (same patient as in Fig. 7.5). This is also thought to result from impaired proliferation of epithelial cells. It is unusual for this abnormality to be so marked.

found. The mutated enzyme is thermolabile. It is considered that prophylactic folic acid overcomes this or other as yet unidentified abnormalities of folate or B_{12} metabolism. The mutation is associated with a raised homocysteine level. Folate or B_{12} deficiency aggravates the tendency for a rise in homocysteine level to occur in maternal plasma. It is unclear exactly how disturbed homocysteine metabolism leads to NTD.

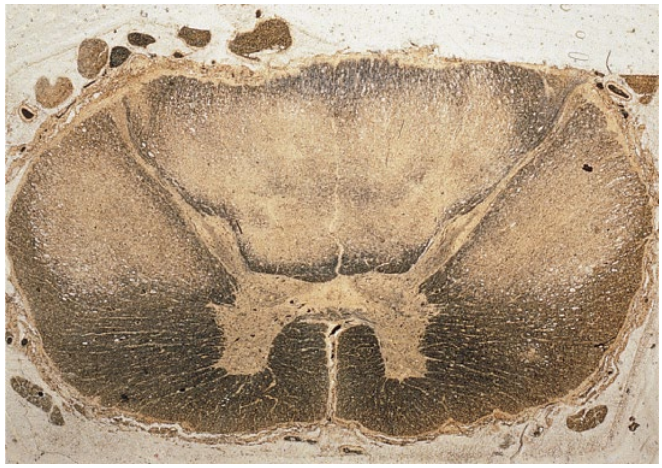

Fig. 7.7. Pernicious anemia: Cross-section of spinal cord of a patient with severe B_{12} neuropathy who died (subacute combined degeneration of the spinal cord). There is demyelination of the lateral (pyramidal) and posterior columns (Weigert–Pal stain).

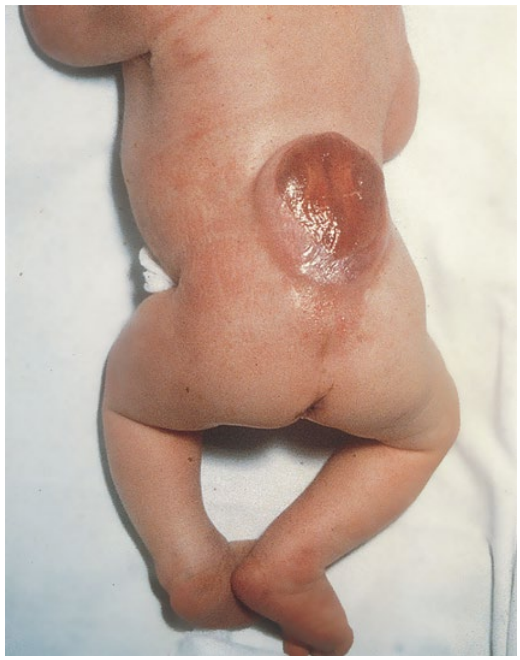

Fig. 7.8. Baby with spina bifida. (Courtesy of Professor CJ Schorah.)

Raised plasma homocysteine levels are also associated with an increased incidence of arterial and venous thrombosis (see Chapter 29). The levels may be raised because of B_{12}, folate, or vitamin B_6 deficiency or through smoking or excess alcohol consumption. The levels are higher in males and postmenopausal women than in premenopausal women or those on hormone replacement therapy, and rise with age. Congenital homocystinuria that results from an inherited defect of one of three enzymes, cystathionine synthase, methionine synthase, or 5,10-methylene-THF reductase (see Fig. 7.9) is associated with the onset of cardiovascular disease in childhood or early adult life.

BLOOD COUNT AND BLOOD FILM APPEARANCES

The blood film shows oval macrocytes, fragmented cells, poikilocytes of varying shapes (Figs. 7.10 and 7.11), and hypersegmented

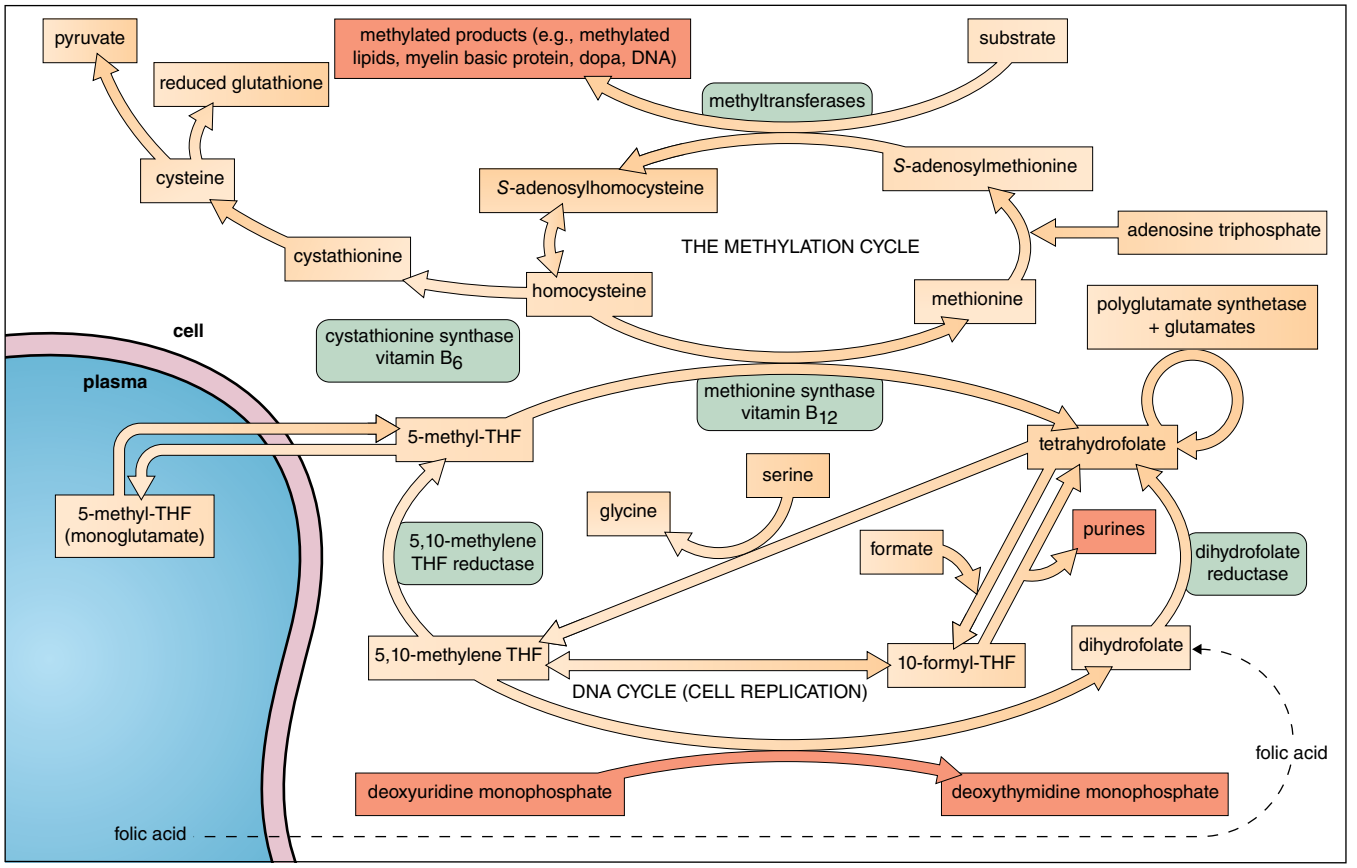

Fig. 7.9. The role of folate coenzymes and vitamins B_{12} and B_6 in the metabolism of homocysteine and in DNA synthesis. (Courtesy of Professor J Scott.)

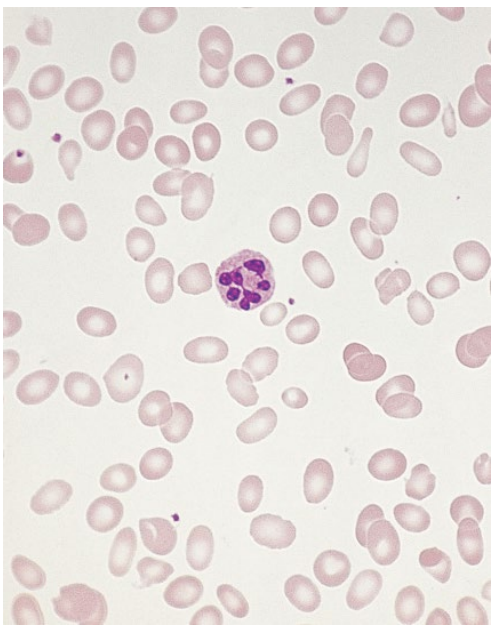

Fig. 7.10. Megaloblastic anemia: peripheral blood film in a severe case, showing oval macrocytes, marked anisocytosis, and poikilocytosis. There is a neutrophil with a hypersegmented nucleus (more than five lobes). (Hb, 5.1 g/dL; MCV, 129 fL.)

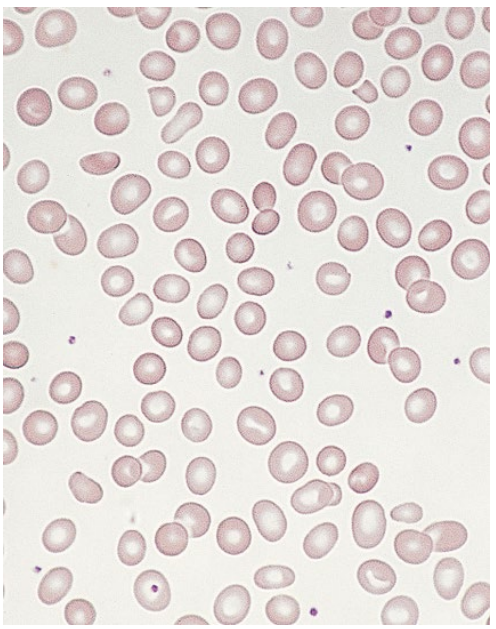

Fig. 7.11. Megaloblastic anemia: peripheral blood film in a mild case showing moderate red cell macrocytosis, anisocytosis, and poikilocytosis. (Hb, 10.5 g/dL; MCV, 112 fL.)

neutrophils showing more than five nuclear lobes, some of which may be macropolycytes (Figs. 7.10 and 7.12). The severity of these changes depends on the degree of anemia. In the most anemic patients, megaloblasts may circulate because of extramedullary hematopoiesis in the liver and spleen (Fig. 7.13). Cabot rings, which are acidophilic and arginine rich and contain nonhemoglobin iron, may also be seen (Fig. 7.13, *inset*). If the spleen has been removed, as with a gastrectomy, or has atrophied, as in 15%

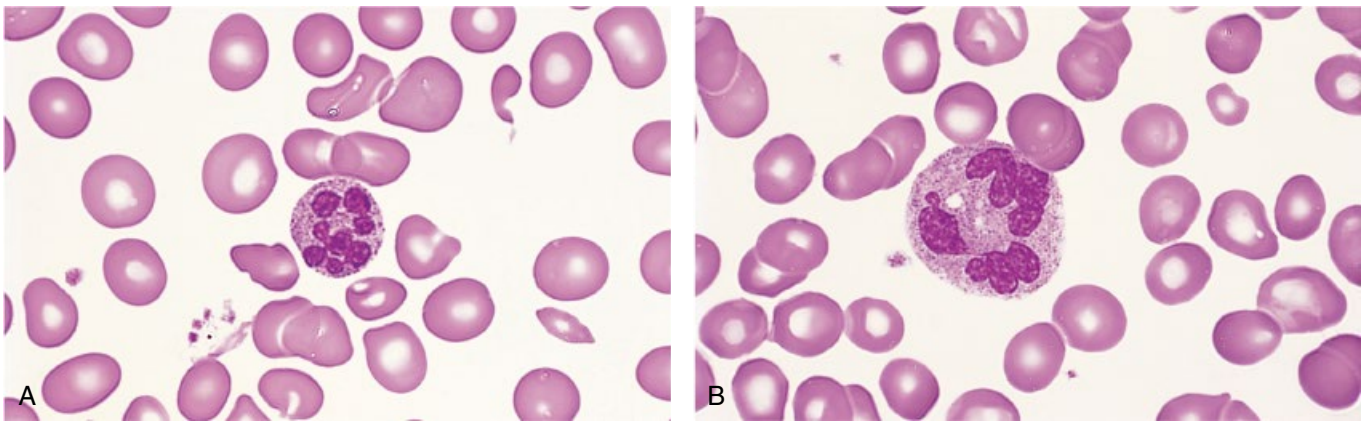

Fig. 7.12. Megaloblastic anemia: Higher power views. **A,** Hypersegmented neutrophil. **B,** Hyperdiploid neutrophil or "macropolycyte."

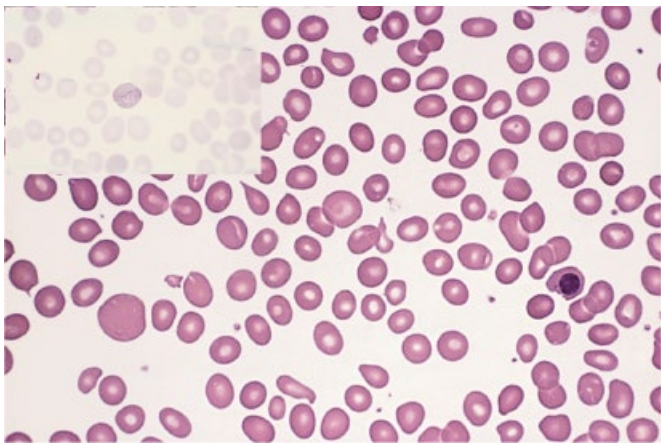

Fig. 7.13. Megaloblastic anemia: Peripheral blood film in a severe case showing a circulating orthochromatic nucleated red cell. The presence of such circulating megaloblasts may be the result of extramedullary hemopoiesis in the spleen and liver. *Inset,* A Cabot ring, which is occasionally seen in the peripheral blood in severe megaloblastic anemia.

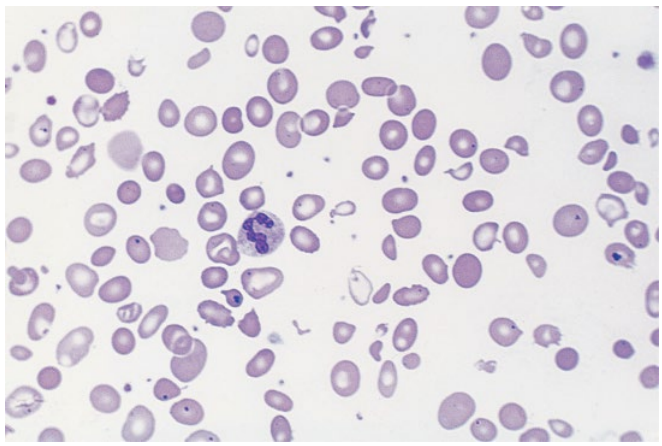

Fig. 7.14. Megaloblastic anemia and splenic atrophy: Peripheral blood film showing Howell–Jolly bodies (DNA remnants) and Pappenheimer bodies (iron- and protein-containing bodies). The patient had severe folate deficiency and splenic atrophy caused by adult celiac disease.

of adult cases with gluten-induced enteropathy (adult celiac disease), changes caused by hyposplenism in the peripheral blood are particularly marked (Fig. 7.14). In some extremely anemic patients, the mean cell volume is normal because of excessive fragmentation of red cells.

BONE MARROW APPEARANCES

In severe cases, the bone marrow is markedly hypercellular with a relative increase in early erythroblasts caused by death of later cells (Fig. 7.15). The myeloid-to-erythroid ratio may be reversed, with an excess of erythroid precursors. Developing erythroblasts show asynchrony of nuclear and cytoplasmic maturation, the nucleus retaining an open, lacy, or stippled appearance while the cytoplasm matures and hemoglobinizes normally. The developing (nucleated) red cells also show a variety of dyserythropoietic features with an excess of multinucleate cells, nuclear bridging, and Howell–Jolly bodies. Dying cells are also present (Fig. 7.16).

Giant and abnormally shaped metamyelocytes are found (Fig. 7.17) and the megakaryocytes show hypersegmented nuclei with an open chromatin network (Fig. 7.18).

In milder cases, megaloblastic changes in the red cell precursors are only identified in late erythroblasts with mild asynchrony of nuclear-cytoplasmic development (Fig. 7.19). This is termed mild, transitional, or intermediate megaloblastic change.

Where iron deficiency and megaloblastic anemia coexist, a dimorphic anemia occurs with two red cell populations in the peripheral blood, one of well-hemoglobinized macrocytes and the other of hypochromic microcytes (Fig. 7.20A). Megaloblastic changes may be masked in the erythroblasts, even though giant metamyelocytes are seen in the bone marrow (Fig. 7.20B). In patients with normal iron stores, there is usually excessive iron granulation of erythroblasts. In some cases, especially in association with alcohol, ring sideroblasts are frequent but disappear with appropriate therapy.

CAUSES OF MEGALOBLASTIC ANEMIA

VITAMIN B_{12} DEFICIENCY

Because B_{12} is stored in amounts of 2–3 mg, and daily losses and requirements are 1–2 µg, it takes 2–4 years for B_{12} deficiency to develop from dietary lack or malabsorption. Deficiency resulting from excessive losses or breakdown of B_{12} has not been described. The anesthetic gas nitrous oxide may rapidly inactivate body B_{12}

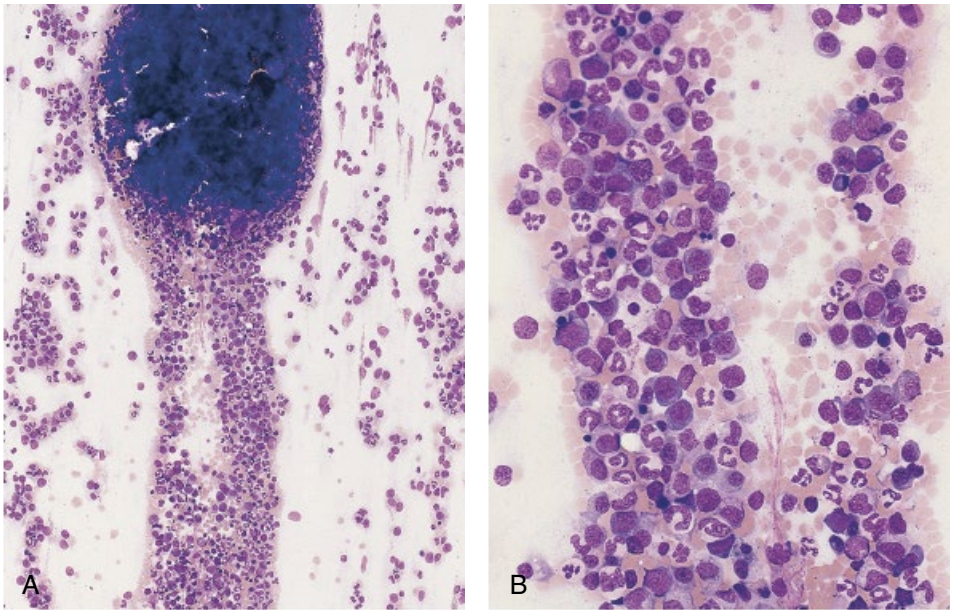

Fig. 7.15. Megaloblastic anemia. **A,** Low-power view of bone marrow fragments showing an increased cellularity with loss of fat spaces. **B,** Higher power view of cell trails showing accumulation of early cells, an increased proportion of erythroid precursors, and the presence of giant metamyelocytes and hypersegmented neutrophils.

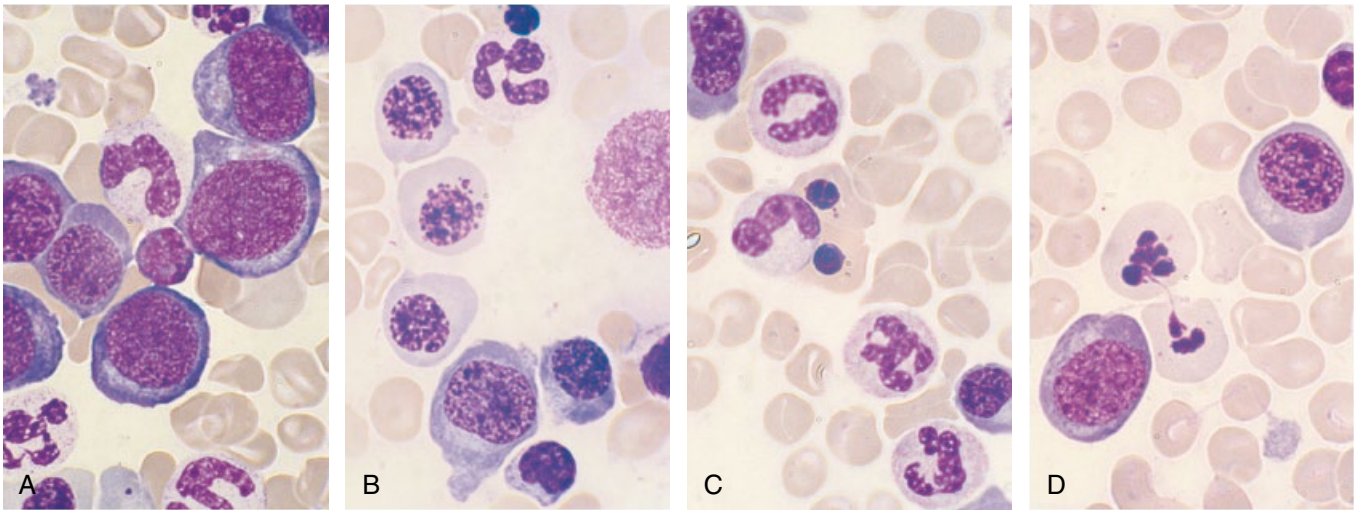

Fig. 7.16. Megaloblastic anemia: High-power views. **A,** Accumulation of early cells, mainly promegaloblasts. **B,** Megaloblasts at all stages (the nuclei have primitive open [lacy] chromatin patterns despite maturation of the cytoplasm with hemoglobinization [pink staining] and two cells have nuclear [DNA] fragments [Howell–Jolly bodies] in their cytoplasm). **C,** Two late megaloblasts with fully orthochromatic (pink staining) cytoplasm (two large band-form neutrophils are also present). **D,** The central orthochromatic cells have karyorrhectic pyknotic nuclei linked by a thin chromatin bridge.

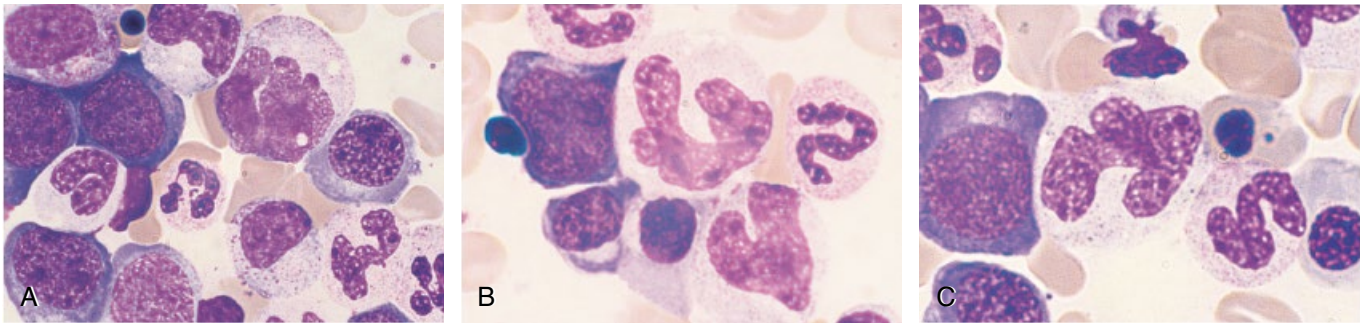

Fig. 7.17. Megaloblastic anemia. **A–C,** High-power views showing a number of giant abnormally shaped metamyelocytes.

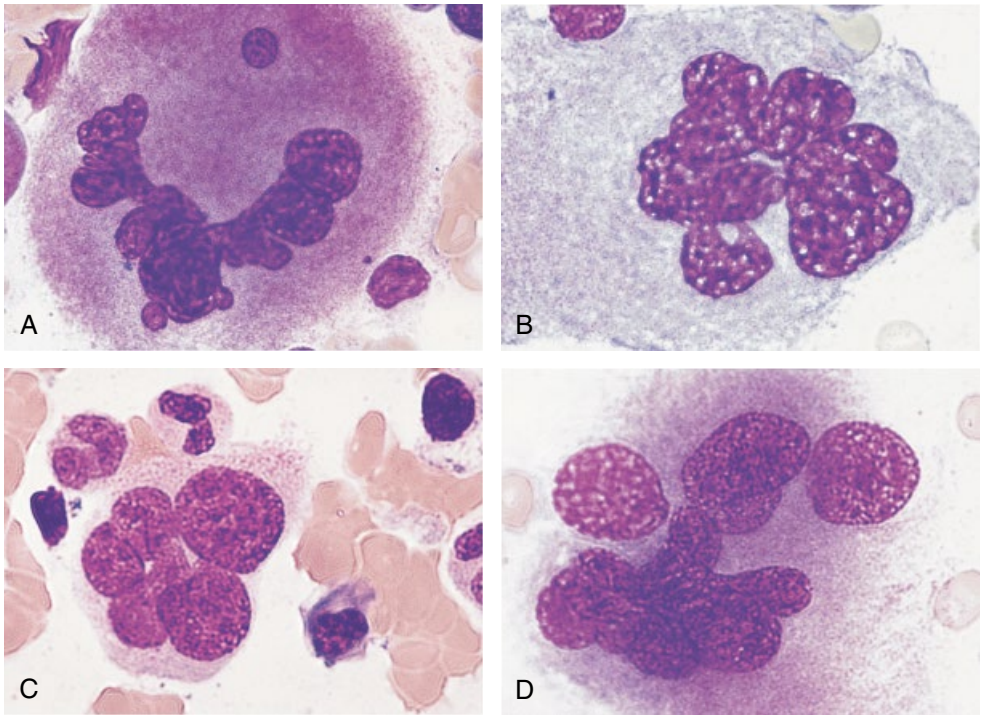

Fig. 7.18. Megaloblastic anemia: Megakaryocytes of variable maturity. **A–D,** All show nuclei with abnormal open chromatin patterns.

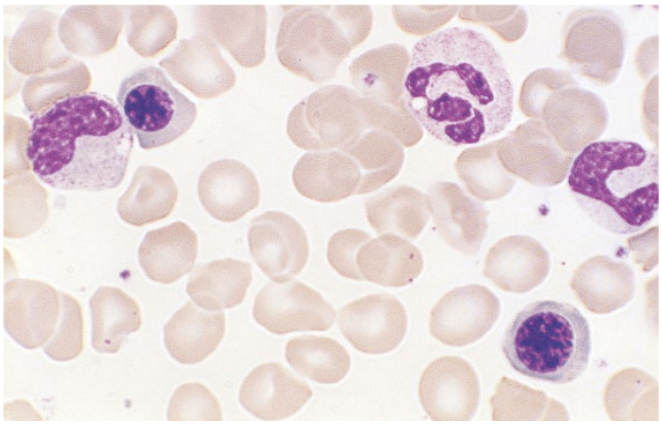

Fig. 7.19. Megaloblastic anemia: Mild marrow changes in B_{12} deficiency following partial gastrectomy. The nucleated red cells show mild asynchrony of nuclear-cytoplasmic development with delay of nuclear maturation *(lower right)*. Iron stores were present. (Hb, 12.4 g/dL; MCV, 105 fL; serum B_{12}, 80 ng/L [normal, 160–925 ng/L]; serum folate, 10.3 µg/L [normal, 6.0–21.0 µg/L].)

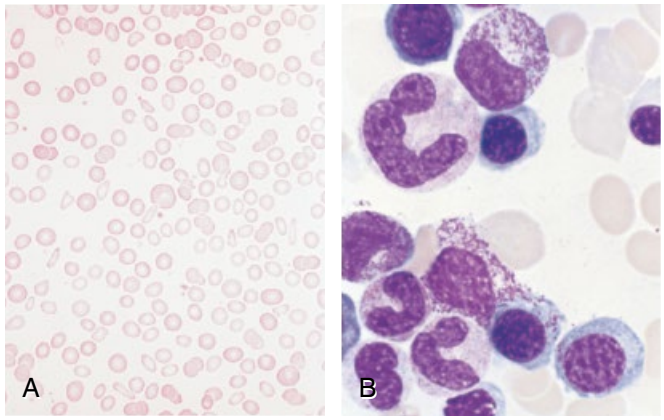

Fig. 7.20. Megaloblastic anemia. **A,** Dimorphic peripheral blood film in iron and B_{12} deficiencies following partial gastrectomy. There is a mixed population of microcytic hypochromic cells and well-hemoglobinized macrocytes. (Hb, 8.0 g/dL; MCV, 87 fL; MCH, 27 pg.) **B,** In the bone marrow aspirate from the same case, giant metamyelocytes are present but megaloblastic changes in the erythroblasts are masked.

from the fully reduced cobalamin I state to the oxidized cobalamin II and cobalamin III forms. If exposure is prolonged, megaloblastic changes occur (Fig. 7.21).

Whereas folate occurs in most foods, including fruit, vegetables, and cereals, as well as animal products, B_{12} occurs only in foods of animal origin. A vegan diet may lead to B_{12} deficiency. Liver has the highest concentration of both folate and B_{12} because it is the main storage organ.

Although not necessarily associated with severe anemia, severe B_{12} deficiency, assessed by serum B_{12} levels, may cause demyelination of the posterior and lateral columns of the spinal cord (see Fig. 7.7). It is often associated with a peripheral neuropathy and is found more frequently in males than in females. In contrast, pernicious anemia, the most common cause of severe B_{12} deficiency, is more common in females.

Addisonian pernicious anemia is the dominant cause of B_{12} deficiency in Western countries. Although particularly common in northern Europe, it occurs in all ethnic groups and countries. It is associated with early graying of the hair (Fig. 7.22), vitiligo (Fig. 7.22), and thyroid disorders (Fig. 7.23), as well as with other organ-specific autoimmune diseases, such as Addison disease and hypoparathyroidism. Specific variants of the gene *NALP1* on chromosome 17p13 coding for NACHT leucine-rich repeat protein 1, a regulator of the innate immune system, show association with vitiligo and autoimmune diseases, including pernicious anemia. There is gastric atrophy (Fig. 7.24) with achlorhydria. Parietal cell autoantibodies are present in the serum of 90% of patients and IF autoantibodies in 50%. Gastric carcinoma develops two to three times more frequently than in control populations.

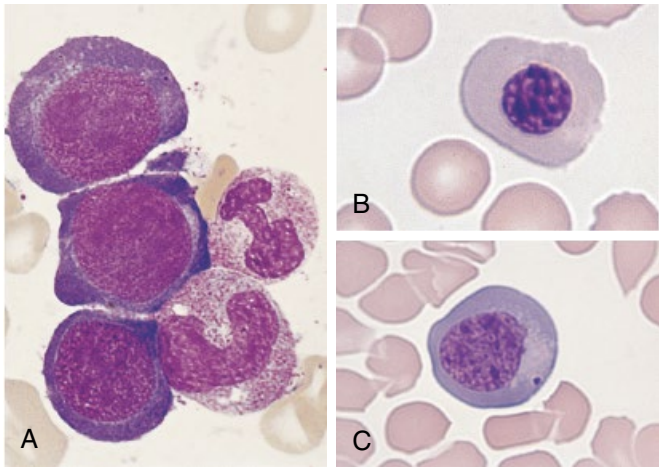

Fig. 7.21. B_{12} oxidation. **A–C,** Bone marrow aspirate showing megaloblasts in a patient receiving prolonged nitrous oxide anesthesia in intensive care following cardiac surgery.

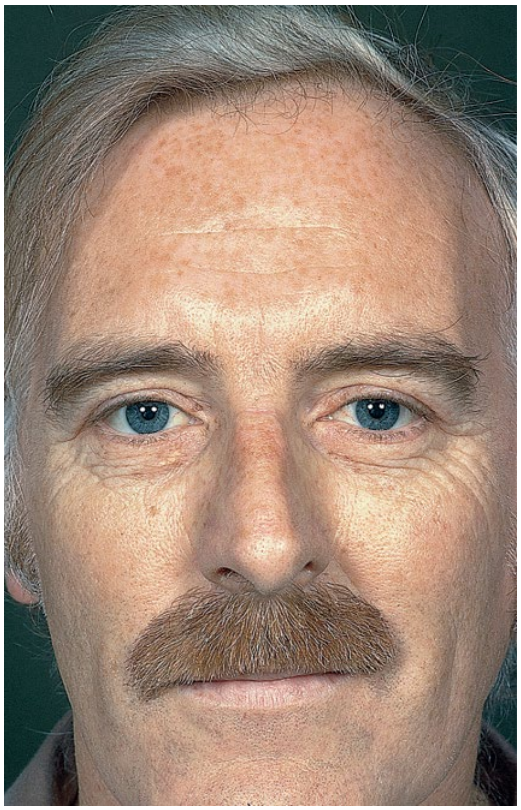

Fig. 7.22. Pernicious anemia: This 38-year-old man shows premature graying and has blue eyes and vitiligo, three features that are more common in patients with pernicious anemia than in control subjects.

Small intestinal causes of B_{12} deficiency include the stagnant-loop syndrome, ileocolic fistula, and ileal resection.

FOLATE DEFICIENCY

Because adult daily requirements of folate are about 100 µg, body stores (10–15 mg) are sufficient for only a few months, a period that can be reduced in conditions of increased turnover and, hence, breakdown of folates.

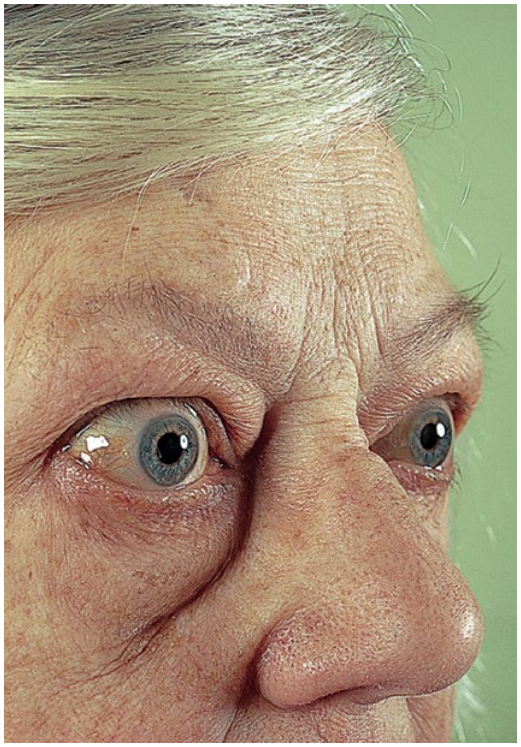

Fig. 7.23. Pernicious anemia: Exophthalmic ophthalmoplegia in a patient who developed myxoedema while receiving maintenance B_{12} therapy. She had presented with megaloblastic anemia 6 years earlier.

Folate deficiency may result from inadequate dietary intake or malabsorption, as in gluten-induced enteropathy (celiac disease) (Figs. 7.25 and 7.26) and tropical sprue (Fig. 7.27).

Dermatitis herpetiformis is associated with gluten-induced enteropathy and, hence, with folate deficiency. The duodenal mucosa may show only mild changes (e.g. infiltration of the mucosal epithelium by lymphocytes) (Fig. 7.28). The most common cause of deficiency used to be pregnancy, when folate requirements rise from the normal 100 µg daily to about 350 µg daily. However, the incidence of this complication is now reduced with prophylactic folic acid therapy. Other causes of increased folate utilization include diseases with increased bone marrow or other cell turnover (see Table 7.1). The excessive demands for folate in these conditions, combined with poor dietary intake, may lead to megaloblastic anemia.

ABNORMALITIES OF VITAMIN B_{12} OR FOLATE METABOLISM

These abnormalities may be inherited or acquired. Transcobalamin II deficiency is an autosomal recessive inherited trait leading, in the homozygous state, to megaloblastic anemia caused by failure of B_{12} transport into bone marrow and other cells. It usually manifests in the first few months of life.

Rare abnormalities of intracellular B_{12} metabolism are usually, but not always, associated with megaloblastic anemia (Fig. 7.29). A number of rare abnormalities of folate metabolism have been described, and megaloblastic anemia may also arise during therapy with the antifolate drugs that inhibit dihydrofolate reductase, such as methotrexate or pyrimethamine.

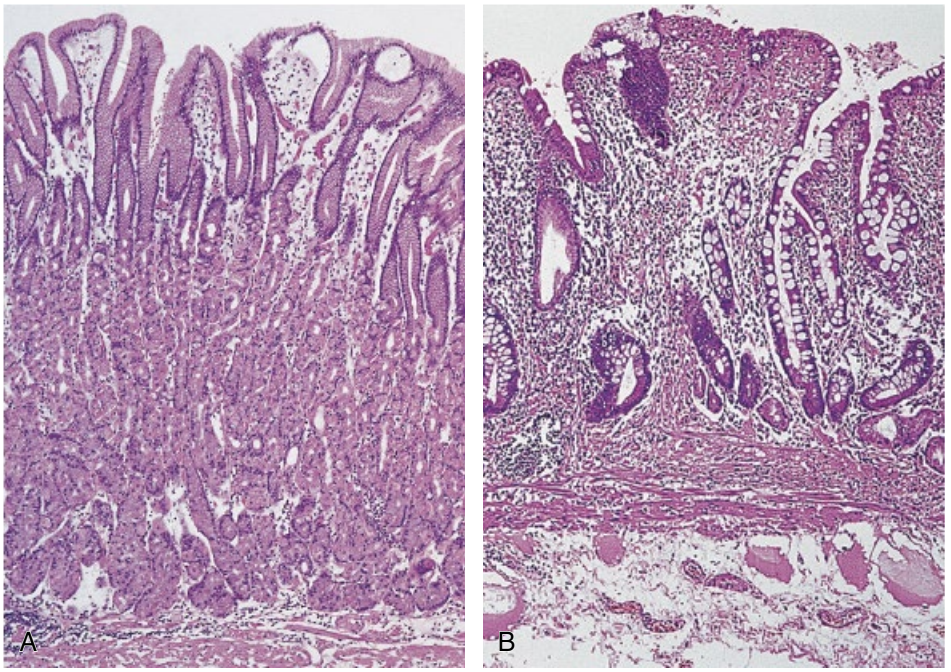

Fig. 7.24.. Pernicious anemia: Sections of stomach. **A,** Normal. **B,** In pernicious anemia. There is atrophy of all coats, loss of gastric glands and parietal cells, and infiltration of the lamina propria by lymphocytes and plasma cells. (Courtesy of Dr. JE McLaughlin.)

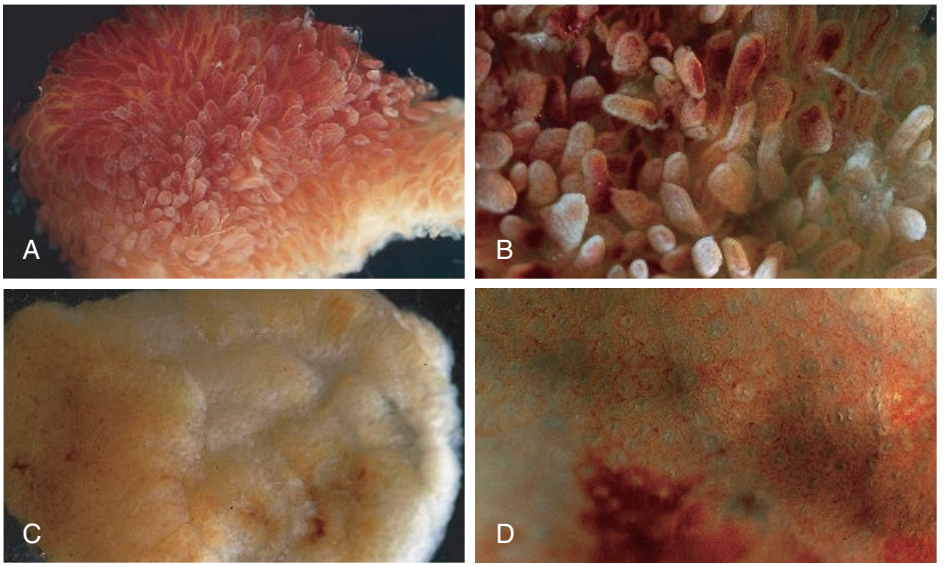

Fig. 7.25. Adult celiac disease: Low- and medium-power dissecting microscope views of jejunal biopsies. **A, B,** Normal villi in finger and leaf patterns. **C, D,** Abnormal mosaic pattern with obvious crypt openings. (Courtesy of Dr. JS Stewart.)

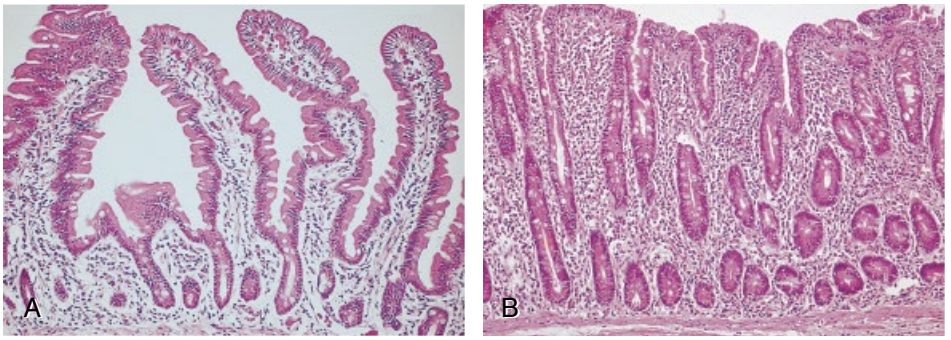

Fig. 7.26. Celiac disease: Histologic sections of jejunal biopsies. **A,** Normal mucosa with finger-like villi. **B,** Subtotal villous atrophy with absence of villi and hypertrophy of the mucosal crypts. (Courtesy of Dr. A Price.)

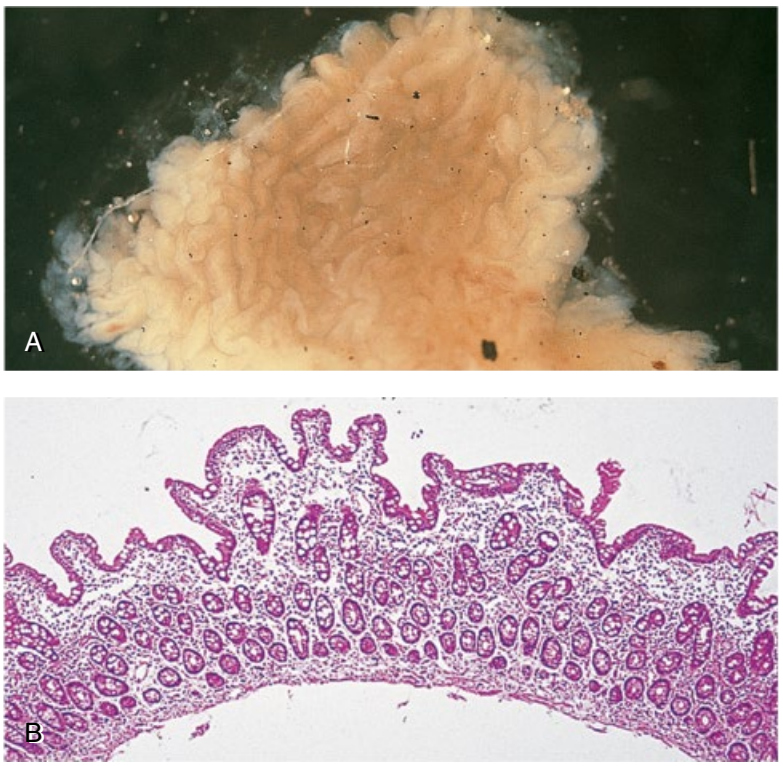

Fig. 7.27. Tropical sprue: Jejunal biopsy. **A,** Dissecting microscope appearance showing typical convoluted mucosal pattern. **B,** Partial villous atrophy. (Courtesy of Professor V Chadwick.)

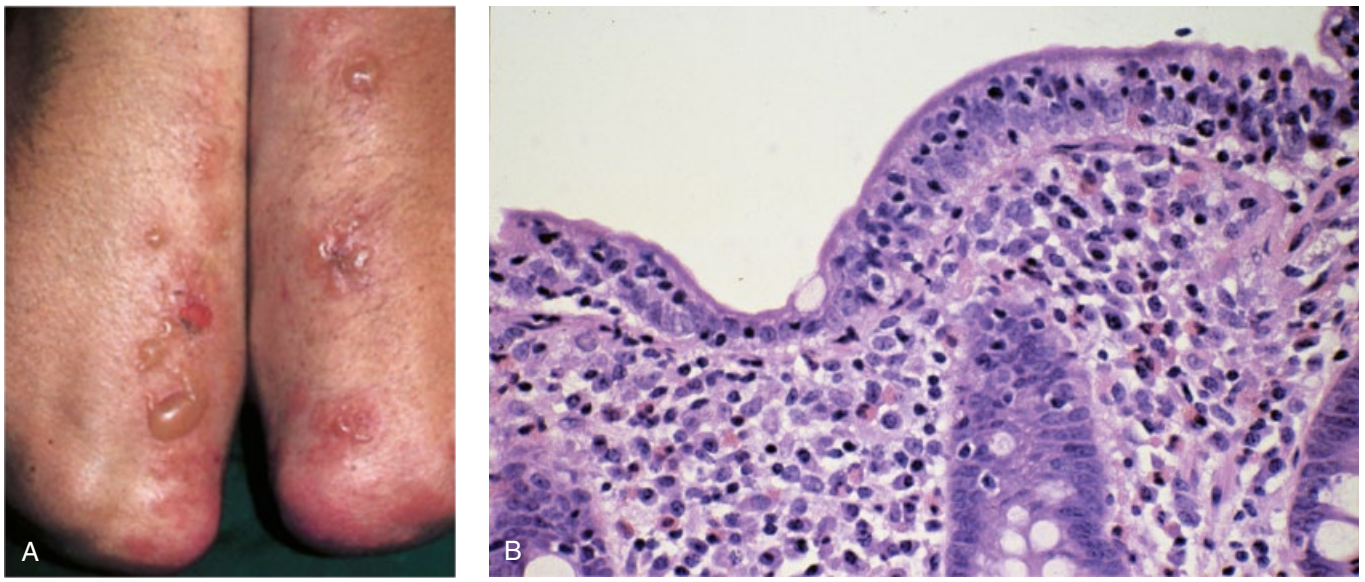

Fig. 7.28. Dermatitis herpetiformis. **A,** Typical appearance of blisters on the extensor surfaces of the arms. This skin condition is associated with gluten-induced enteropathy and folate deficiency. **B,** Duodenal biopsy showing intraepithelial lymphocytes. (Courtesy of Professor L Fry.)

OTHER CAUSES

Megaloblastic anemia as a result of antimetabolite chemotherapy with, for example, hydroxyurea or cytosine arabinoside shows similar morphologic features to those that result from B_{12} or folate deficiencies. However, dyserythropoietic changes are often more marked.

In acute myeloid leukemia of the erythroblastic type or in myelodysplasia, megaloblastic changes are usually confined to the erythroid series. Giant metamyelocytes, hypersegmented polymorphs and other changes in leukopoiesis, or megakaryocytes seen in B_{12} or folate deficiency are not present.

Rare inborn errors of metabolism other than those affecting B_{12} or folate metabolism, such as orotic aciduria in which there is a fault in pyrimidine synthesis, may also result in megaloblastic anemia (Fig. 7.30). A defect in thiamine phosphorylation may

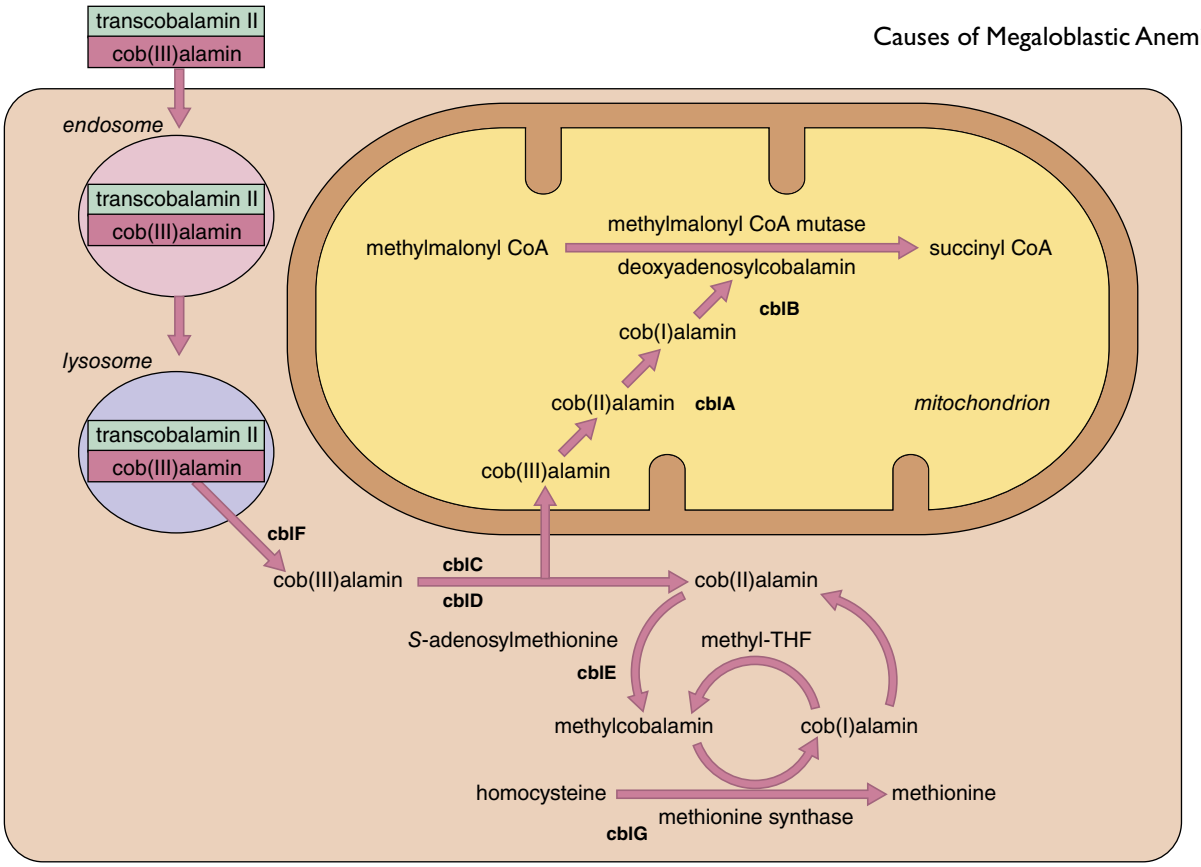

Fig. 7.29. Inborn errors of cobalamin (cbl, B_{12}) metabolism. Cob(III)alamin, cob(II)alamin, and cob(I)alamin are the cobalt in cobalamin in its trivalent, divalent, or monovalent oxidation state (cblA to cblG, sites of inborn errors in cobalamin metabolism). THF, Tetrahydrofolate. Source: Rosenblatt DS. Inborn errors of folate and cobalamin metabolism. In: Carmel R, Jacobsen DW, eds. *Homocysteine in Health and Disease*, Cambridge University Press, 2001, p. 249. Reproduced with permission from Cambridge University Press.

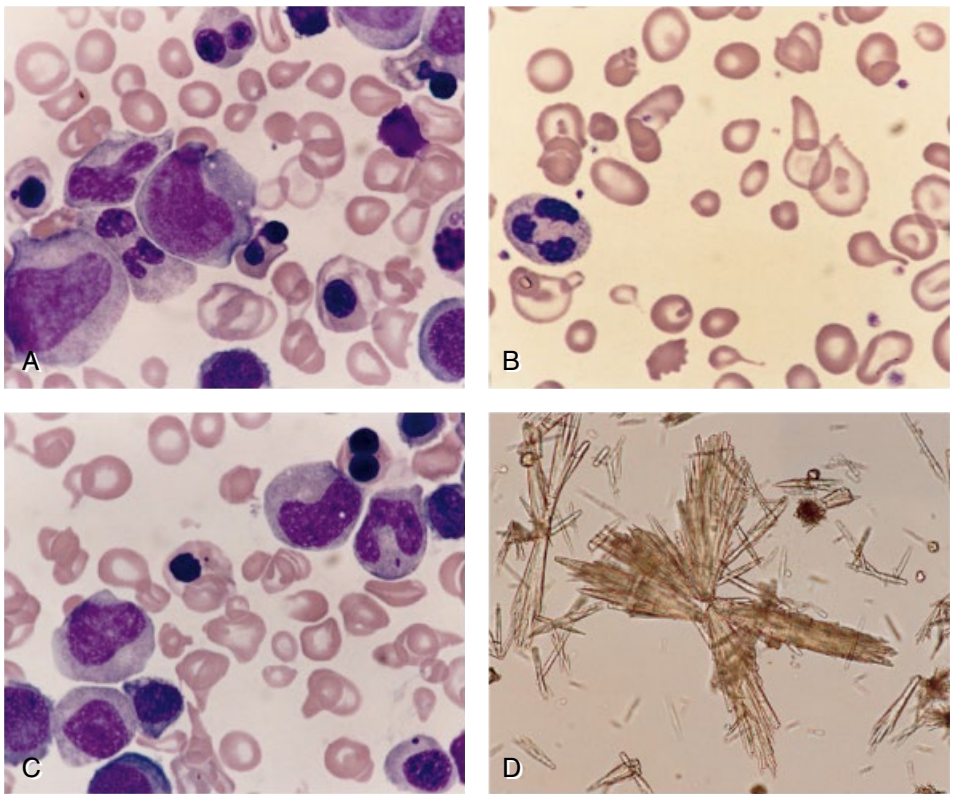

Fig. 7.30. Orotic aciduria: Female who presented at six months with anemia (Hb, 6.0 g/dL; MCV, 110 fL) and normal white cell and platelet counts. The serum B_{12} and folate levels were normal. **A, C,** Bone marrow shows megaloblastic erythropoiesis with a binucleate cell, Howell–Jolly body formation, and giant metamyelocytes. **B,** The peripheral blood film shows marked anisocytosis and poikilocytosis with macrocytic and microcytic cells. **D,** Crystals of orotic acid are present in the urine. The child responded hematologically to treatment with uridine 50 mg/kg daily orally with a reduction in orotic acid excretion. (Courtesy of Dr. J Price.)

TABLE 7.2. CAUSES OF MACROCYTOSIS, OTHER THAN MEGALOBLASTIC ANEMIA

Alcohol
Liver disease
Hypothyroidism
Myelodysplasia, including acquired sideroblastic anemia
Aplastic anemia and red cell aplasia
Raised reticulocyte count
Hypoxia
Myeloma and other paraproteinemias
Cytotoxic drugs
Pregnancy

lead to megaloblastic and sideroblastic anemia responding to thiamine. This is discussed in Chapter 5.

Macrocytosis may be caused by a number of marrow disorders that disturb erythropoiesis, cause lipid deposition on the red cell membrane, or affect red cell size by other mechanisms (Table 7.2). When the cause is alcohol excess, the mean cell volume (MCV) is often raised, even though the hemoglobin level is normal.

CHAPTER

8

HEMOLYTIC ANEMIAS

The dominant cause of the anemia in hemolytic anemias is an increased rate of red cell destruction. This is usually extravascular (taking place in the macrophages of the reticuloendothelial system, as in normal individuals), although in some types of acute or chronic hemolysis red cell destruction occurs intravascularly (Fig. 8.1). The clinical and laboratory features differ according to whether the main site of destruction is extravascular or intravascular.

In addition to the clinical feature of pallor, many patients show mild fluctuating jaundice and splenomegaly. Increased bilirubin production may result in pigment gallstones (Fig. 8.2).

Laboratory findings in hemolytic anemia include raised unconjugated serum bilirubin and increased fecal stercobilinogen and urinary urobilinogen from accelerated red cell destruction. Serum haptoglobins are absent. Reticulocytosis (Fig. 8.3A) and bone marrow erythroid hyperplasia are the result of compensatory increases in red cell production. Characteristic changes in red cell morphology

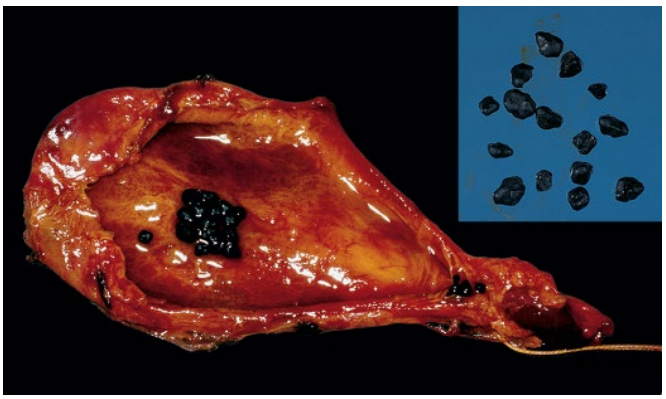

Fig. 8.2. Thalassemia major: Opened gallbladder and its bilirubin gallstones *(inset)*.

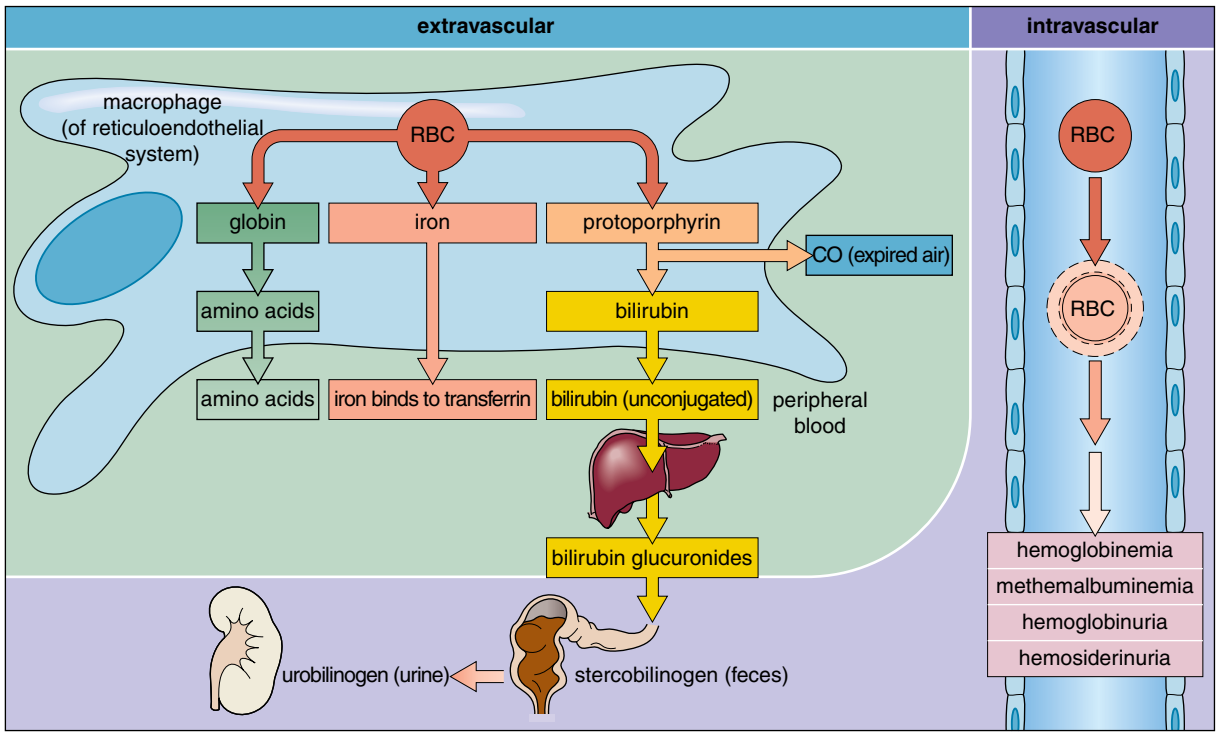

Fig. 8.1. Hemolytic anemia: Extravascular and intravascular mechanisms of red blood cell (RBC) breakdown.

Color Atlas of Clinical Hematology: Molecular and Cellular Basis of Disease, Fifth Edition. A. Victor Hoffbrand, Paresh Vyas, Elías Campo, Torsten Haferlach, and Keith Gomez

occur in a number of hemolytic anemias and, in the most severe, the peripheral blood film shows red cell polychromasia (caused by reticulocytosis) and occasional erythroblasts (Fig. 8.3B).

In those anemias caused by oxidant damage to hemoglobin and other red cell proteins, Heinz bodies may be found in reticulocyte preparations (Fig. 8.4). Intravascular red cell destruction is accompanied by hemoglobinemia, hemoglobinuria (Fig. 8.5), plasma methemoglobinemia, methemalbuminemia, and hemosiderinuria (Fig. 8.6). Jaundice is less common. Causes of intravascular hemolysis are listed in Table 8.1.

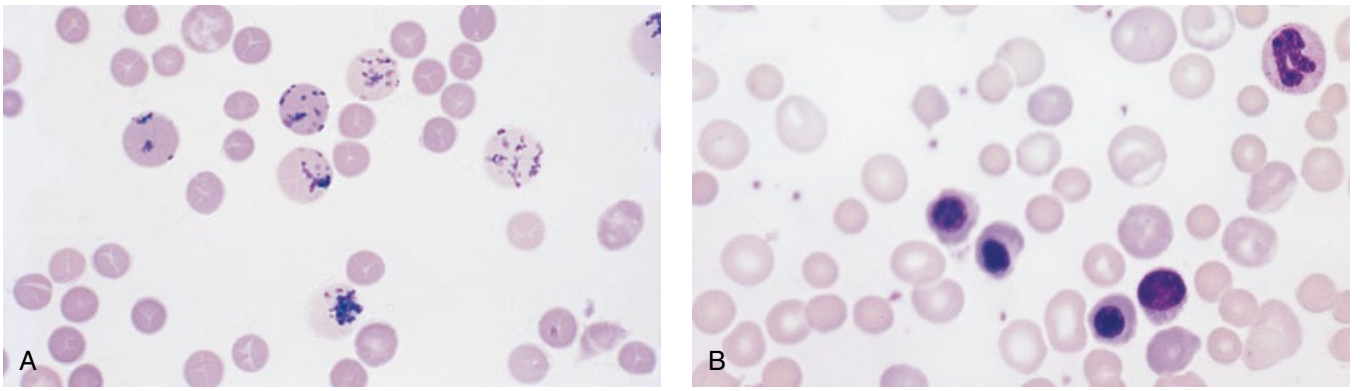

Fig. 8.3. Hemolytic anemia. **A,** Reticulocytosis. Reticular (precipitated RNA) material is seen in the larger cells. New methylene blue stain (Giemsa counterstain). **B,** Autoimmune hemolytic anemia. Peripheral blood film showing erythroblasts, spherocytosis, and polychromasia.

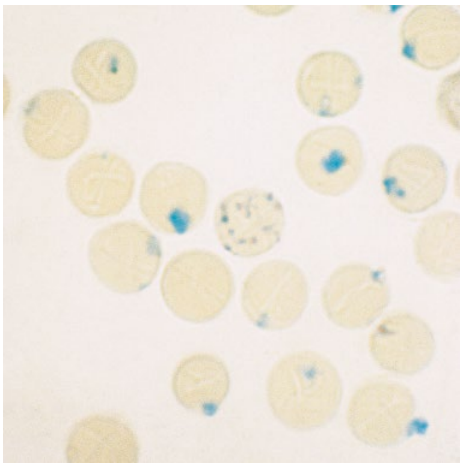

Fig. 8.4. Deficiency of glucose-6-phosphate dehydrogenase: Peripheral blood film showing Heinz bodies in red cells and a single reticulocyte. (Supravital new methylene blue stain.)

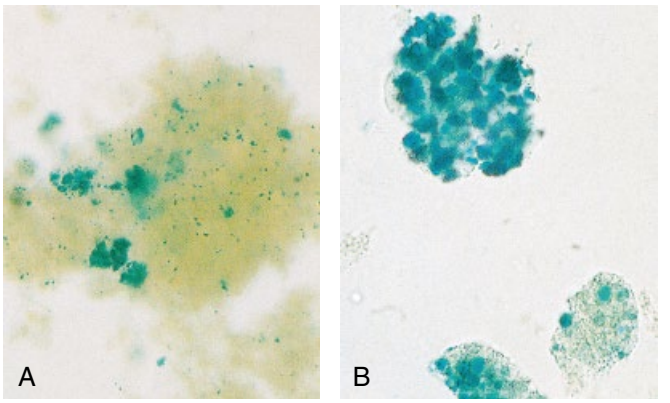

Fig. 8.6. Intravascular hemolysis in paroxysmal nocturnal hemoglobinuria (PNH). Hemosiderinuria. **A,** Prussian blue-positive material seen in urinary deposit. **B,** At higher magnification in individual renal tubular cells (Perls' stain).

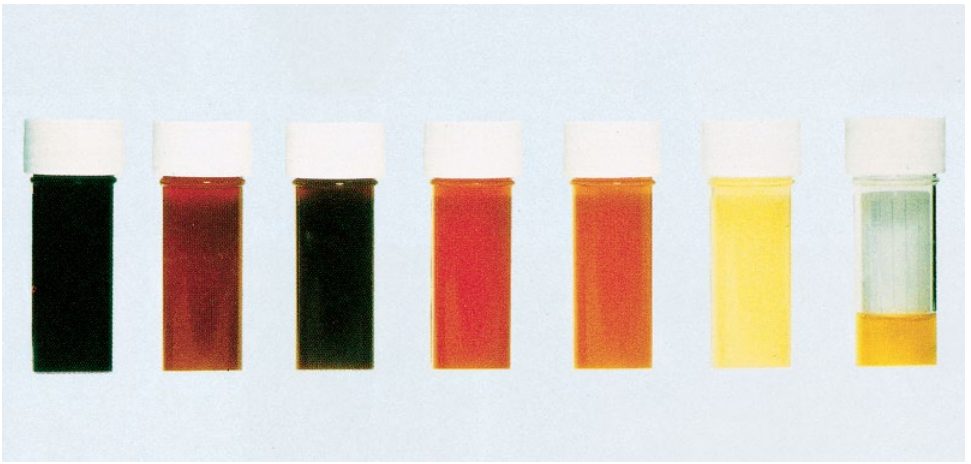

Fig. 8.5. Glucose-6-phosphate dehydrogenase deficiency: Urine samples showing hemoglobinuria of decreasing severity following an episode of acute intravascular hemolysis.

HEREDITARY HEMOLYTIC ANEMIA

The hereditary hemolytic anemias are usually the result of intrinsic red cell defects. A simplified classification is shown in Table 8.2. Thalassemia and other genetic disorders of hemoglobin are discussed in Chapter 9.

NORMAL RED CELL MEMBRANE

Normal red cell membrane consists of a phospholipid bilayer, with hydrophilic phosphate residues on the external and inner surfaces and nonpolar fatty acid side-chains projecting into the center (Fig. 8.7). The bilayer also contains a variable proportion of cholesterol. Proteins may be either transmembrane integral proteins, for example, band 3 and glycophorins A or B, or peripheral (extrinsic) proteins, such as spectrin, actin, and bands 2.1 (ankyrin), 4.1, and 4.2, which form a scaffolding structure on the inner surface of the membrane. The band numbers refer to the Coomassie blue bands on sodium dodecyl sulfate plus polyacrylamide gel electrophoresis (SDS-PAGE; Fig. 8.8).

The phospholipids or proteins on the external surface may carry sugars that determine blood groups or may act as viral receptors. Spectrin consists of two forms, α and β, joined to form a heterodimer with a hairpin structure. The protein 2.1 (ankyrin) binds the spectrin β-chains to band 3, a large integral membrane protein, while the tail end of spectrin binds to protein 4.1, thus forming spectrin tetramers. Protein 4.1 also binds to glycophorin A or aminophospholipids to serve as secondary attachment sites of the cytoskeleton to the inner surface of the bilayer.

RED CELL BLOOD GROUP ANTIGENS

The red cell plasma membrane contains a large number of different antigens. Many of these have sugar residues attached to membrane proteins or lipids. The structure of the most important antigens, those of the ABO system, is discussed in Chapter 32.

TABLE 8.1. CAUSES OF INTRAVASCULAR HEMOLYSIS

Mismatched blood transfusion (usually ABO)
G6PD deficiency with oxidant stress (e.g., drugs, fava beans, infections)
Red cell fragmentation syndromes
Some autoimmune hemolytic anemias
Some drug-induced hemolytic anemias: direct action (e.g. dapsone, salazopyrine) and immune complex types (e.g. phenacetin, quinidine, diclofenac)
Paroxysmal nocturnal hemoglobinuria
Unstable hemoglobins
Chemicals (e.g. sodium chlorate, nitrates, arsine)
Severe burns
Infections (e.g. *Clostridium perfringens*, malaria, babesiosis, bartonellosis, dengue fever)
Snake and spider bites

G6PD, Glucose-6-phosphate dehydrogenase.

TABLE 8.2. CAUSES OF HEREDITARY HEMOLYTIC ANEMIA

Membrane defects	Metabolic defects	Hemoglobin defects
Hereditary spherocytosis	Deficiency of: pyruvate kinase	Defective synthesis (e.g. thalassemia α or β)
Hereditary elliptocytosis	triose phosphate isomerase	Abnormal variants (e.g. HbS, HbC, unstable)
Hereditary stomatocytosis	pyrimidine 5-nucleotidase	
Southeast Asian ovalocytosis	glucose-6-phosphate dehydrogenase	
	glutathione synthase	

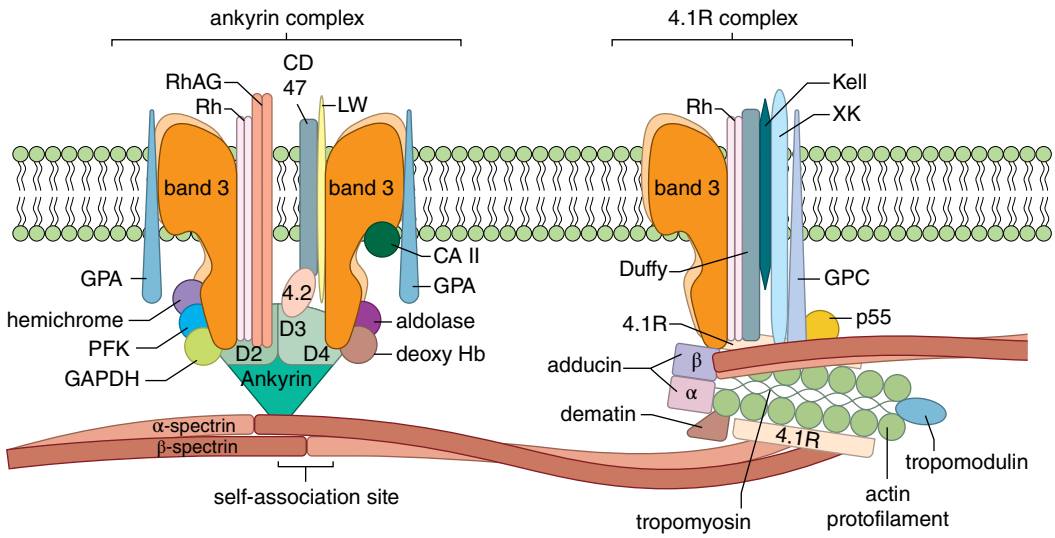

Fig. 8.7. Schematic model of the structural organization of the red cell membrane. The membrane is a composite structure in which the lipid bilayer is linked to the spectrin-based membrane skeleton. The linking of the lipid bilayer to the membrane skeleton is mediated by band 3–ankyrin–protein 4.2–β-spectrin interactions and by glycophorin C–protein 4.1R interaction (vertical interactions). The horizontal interactions in the spectrin network involve spectrin dimer–dimer interaction and spectrin–actin–protein 4.1 interaction. RhAG, Rhesus antigen; GPA, glycophorin A; PFK, phosphofructokinase; GAPDH, glyceraldehyde-3-phosphate dehydrogenase; GPC, glycophorin C. Source: Hoffbrand AV, et al. *Postgraduate Haematology*, 7th edn. John Wiley & Sons, 2016. Reproduced with permission of John Wiley & Sons.

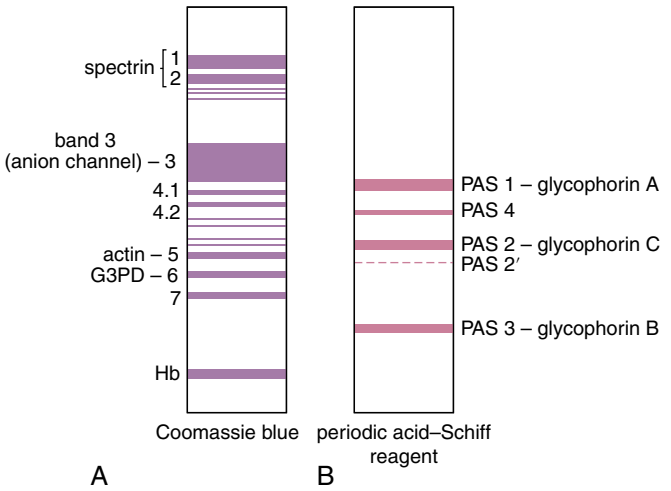

Fig. 8.8. Red cell membrane: Separation of proteins by electrophoresis in sodium dodecyl sulfate (SDS) gels. **A,** Staining for protein. **B,** Staining for carbohydrate. Source: Contreras M, Lubenko A. Immunohematology: introduction. In: Hoffbrand AV, et al., eds. *Postgraduate Hematology*, 4th edn. Butterworth-Heinemann, 1999. Reproduced with permission of Elsevier.

TABLE 8.3. CAUSES OF HEREDITARY SPHEROCYTOSIS, HEREDITARY ELLIPTOCYTOSIS, AND SOUTHEAST ASIAN OVALOCYTOSIS

Hereditary spherocytosis (vertical interactions)	Hereditary elliptocytosis (horizontal interactions)
Ankyrin deficiency (45%)	Spectrin abnormalities
Amino acid substitution	α Chain defects (80%)
Frameshift and nonsense mutations	β Chain defects (5%)
δ Untranslated region/promoter mutations	Protein 4.1 deficiency (15%)
Splicing defects	Southeast Asian ovalocytosis (band 3 defect; deletion of nine amino acids at junction of cytoplasmic and transmembrane domains)
Gene deletions	
Balanced translocations	
Spectrin deficiency	
α Chain defects (rare)	
β Chain defects (30%)	
Pallidin (protein 4.2) abnormalities (5%)	
Band 3 deficiency (20%)	

The figures given in parentheses indicate the approximate percentages of patients with hereditary spherocytosis or hereditary elliptocytosis with that abnormality.

There are over 600 different antigens. The best characterized are listed in Table 32.1. Blood group antigens are important in blood transfusion, and autoantibodies may be directed against them in autoimmune hemolytic anemias (e.g. against specific Rhesus antigens in warm-type autoimmune hemolytic anemia, and against the i antigen in infectious mononucleosis).

HEREDITARY SPHEROCYTOSIS

The red blood cell membrane disorders are divided into two groups: structural defects and altered permeability. The most common to cause an hemolytic anemia is hereditary spherocytosis. This may result from a variety of abnormalities of the cytoskeletal proteins involved in vertical interactions of the red cell membrane. Defects of ankyrin (45%), β-spectrin (30%) or α-spectrin (rarely) band 3 (20%) or protein 4.2 (5%) have been described in various kindreds (Table 8.3). The mutations (e.g. in ankyrin) can be amino acid substitutions, frameshift, nonsense, splicing defects, gene deletions, mutations in untranslated and promoter regions and translocations. The cells are excessively permeable to sodium influx. Glycolysis and ATP turnover are increased. The marrow produces red cells of normal biconcave shape, but these lose membrane during passage through the spleen and the rest of the reticuloendothelial system. The resultant rigid and spherical cells have a shortened life span, the spleen being the principal organ of red cell destruction.

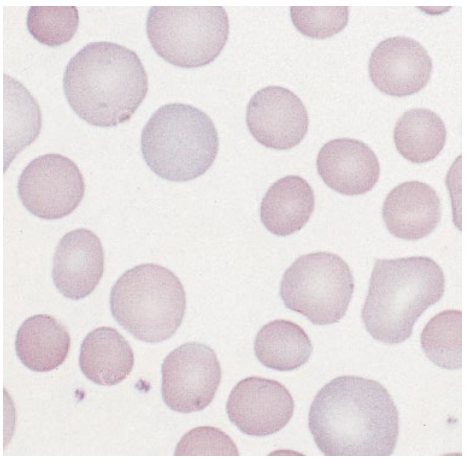

Fig. 8.9. Hereditary spherocytosis: peripheral blood film showing smaller spherocytes among larger polychromatic red cells.

The condition is usually characterized by a dominant inheritance pattern. Typically, anemia, jaundice, and splenomegaly are present. The blood film shows microspherocytes (Fig. 8.9), and red cell osmotic fragility is characteristically increased (Fig. 8.10A).

In most patients (92%) with hereditary spherocytosis there is loss of Rh-related membrane proteins and fluorescence activated cell sorting (FACS) screening shows reduced binding of eosin-labeled maleimide (Fig. 8.10B). Less-sensitive tests include osmotic fragility, and acidified glycerol lysis. The blood film in many of hereditary spherocytosis patients with band 3 deficiency may show mushroom-shaped "pincered" red cells (Fig. 8.11). Splenectomy produces a considerable improvement in red cell survival and is associated with a rise in hemoglobin levels to normal.

HEREDITARY ELLIPTOCYTOSIS

The characteristic feature in hereditary elliptocytosis is the presence of elongated red cells in the peripheral blood (Fig. 8.12). A number of inherited protein defects that affect horizontal red blood cell membrane interactions, especially of α-spectrin (80%) or β-spectrin (5%) or band 4.1 (15%), may produce this condition (see Table 8.3). A defective spectrin dimer–dimer interaction results in an increased proportion of dimers in relation to spectrin tetramers. The clinical expression in heterozygotes (elliptocytosis trait) is variable: although some have anemia and splenomegaly, the majority have only minimal or no reduction in red cell survival with little or no anemia. The inheritance is dominant. In rare patients homozygous for a mutation in the gene for α-spectrin, *SPTA1*, and occasional heterozygotes, there is severe anemia with marked hemolysis and splenomegaly and bizarre red cell morphology termed pyropoikilocytosis (Fig. 8.13).

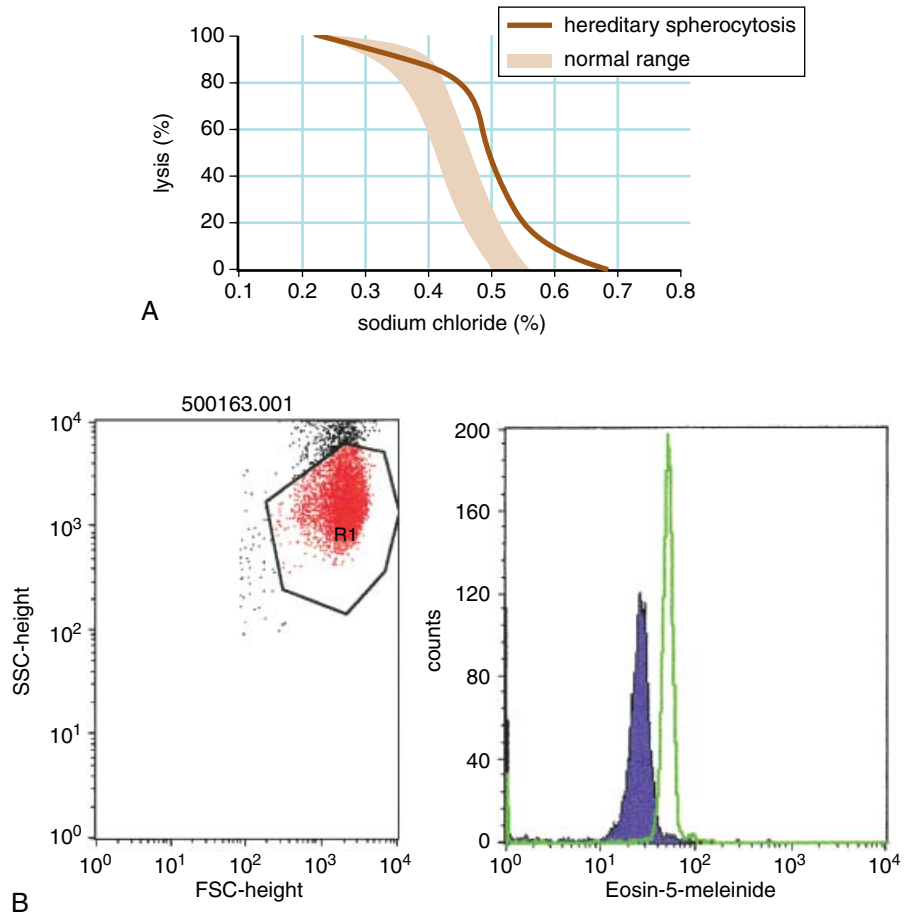

Fig. 8.10. A, Osmotic fragility test: Comparison of red cell lysis in severe hereditary spherocytosis and in normal blood. The curve is shifted to the right of the normal range, but a tail of osmotically resistant cells (reticulocytes) is present. **B,** Hereditary spherocytosis: Fluorescence overlay plot of eosin-5-maleimide (EMA) screening test. In hereditary spherocytosis (purple histogram) there is reduced binding of EMA due to reduced levels of band 3 membrane protein. The histogram of normal EMA-treated cells is shown in green. Normal control set to mean cell fluorescence (MCF) of 53. Patient shows MCF of 24.9.

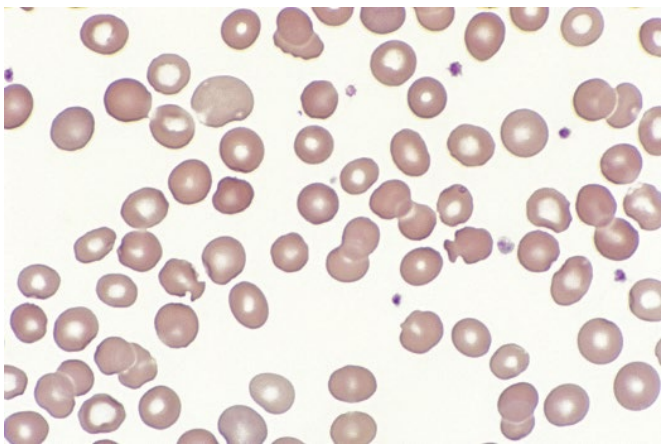

Fig. 8.11. Hereditary spherocytosis: Blood film in band 3 deficiency. In addition to spherocytes, two "mushroom" or "pincered" cells are shown.

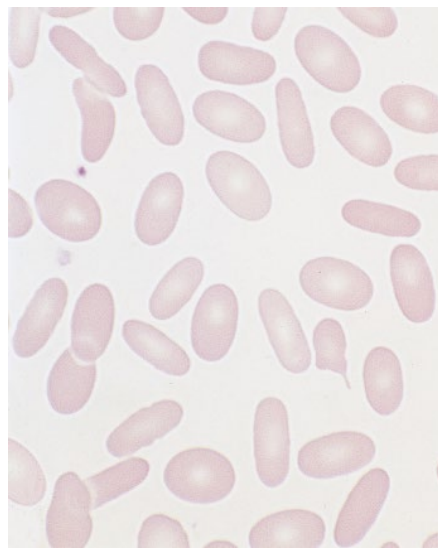

Fig. 8.12. Hereditary elliptocytosis: Blood film showing characteristic elliptical red cells.

Southeast Asian Ovalocytosis (Stomatocytic Hereditary Elliptocytosis)

Southeast Asian ovalocytosis (Fig. 8.14) is an asymptomatic trait found in 5–25% of people in some coastal areas of New Guinea, Indonesia, the Philippines, southern Thailand, and Malaysia. Newborns may show a hemolytic anemia. There is a nine-amino-acid deletion at the junction of the cytoplasmic and transmembrane domains of band 3. The inheritance is autosomal dominant. Homozygosity is probably lethal but one homozygous case with a severe hemolytic anemia in utero and tubular acidosis has been reported. Band 3 is also expressed in

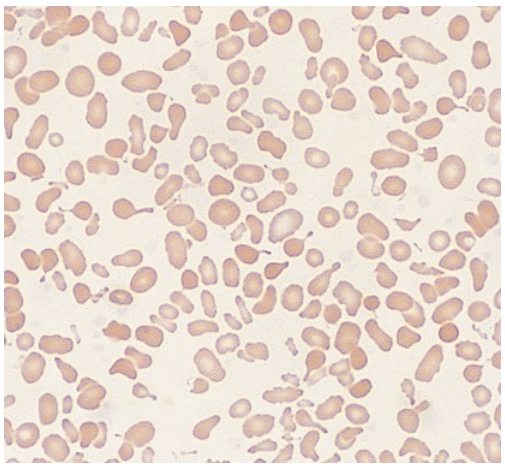

Fig. 8.13. Hereditary pyropoikilocytosis: Blood film showing red cell anisocytosis, microspherocytosis, and micropoikilocytosis. (Mean cell volume, 61 fL.)

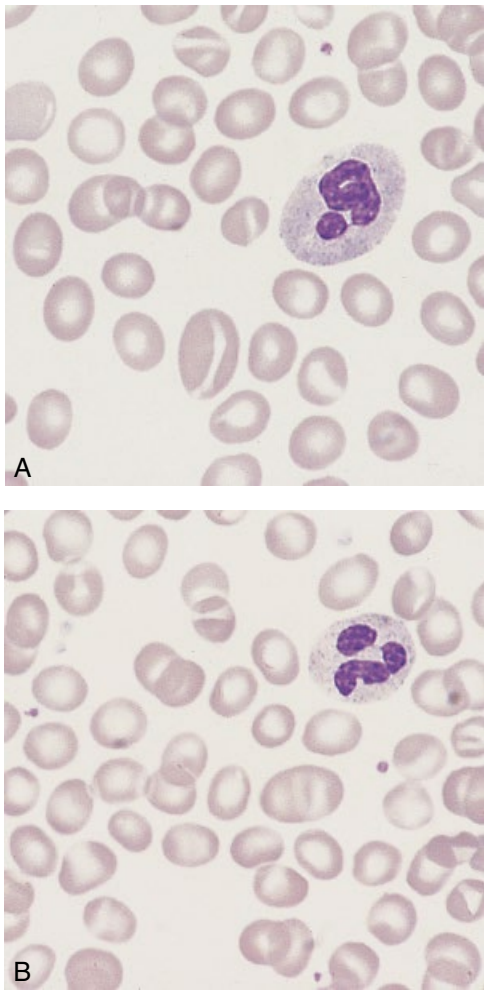

Fig. 8.14. Southeast Asian ovalocytosis. **A, B,** Peripheral blood films showing ovalocytes and stomatocytes, some with a longitudinal or Y-shaped slit and others with a transverse ridge. The red cell membrane is rigid, conferring resistance to malaria. The cells may form abnormal rouleaux and have reduced deformability. The genetic defect is in band 3 protein in which there is deletion of nine amino acids and which binds tightly to ankyrin. (Courtesy of Professor Barbara Bain.)

the kidneys. People with heterozygosity are relatively protected from malaria.

Other Rare Inherited Defects of the Red Cell Membrane

Other rare inherited defects of the red cell membrane include hereditary stomatocytosis (Fig. 8.15) and familial pseudohyperkalemia, and acanthocytosis associated with neurological syndromes (Fig. 8.16). Hereditary stomatocytosis is divided into overhydrated and dehydrated (xerocytosis) types. Both are due to alteration of membrane permeability to the cations Na^+ and K^+ with disturbance of the red blood cell cation content and cell volume. Overhydrated hereditary stomatocytosis is a rare autosomal dominant hemolytic anemia in which increased membrane sodium permeability is associated with mutation of *SCLA1* (band 3), *GLUT1* (glucose transporter), or the ammonium transporter Rh type A. Stomatin levels are low or absent but seems a marker for another gene defect as no abnormalities of the stomatin-encoding gene have been found in patients with the condition. Cryohydrocytosis is a syndrome with normal red cells at 37°C but swelling of the cells when at room temperature.

Dehydrated hereditary stomatocytosis or xerocytosis is more frequent with a wider range of phenotype from asymptomatic to severe hemolysis. It is usually due to a dominant mutation in either the gene *PIEZO1* for the piezo-type ion channel component 1 or more rarely of the gene *KCNN4* coding for the so-called Gardos channel, a Ca^{2+}-dependent potassium channel (see Fig. 8.7). Gain-of-function mutations of the gene *SLC4A1* coding for band 3 may also cause xerocytosis by changing band 3 from an anion exchanger to a cation transporter. Stomatocytes are rare or absent from the blood film in dehydrated hereditary stomatocytosis but poikilocytes and echinocytes are frequent.

Phytosterolemia (sitosterolemia) is an autosomal recessive condition resulting from mutation in either the *ABCG5* or the *ABCG8* gene, in which there is excessive absorption of dietary sterols including plant sterols. As a result there is formation of xanthomas and premature atherosclerosis. The blood film, which shows the combination of large platelets and stomatocytosis, is critical in making the diagnosis (Fig. 8.15B). Often the platelet count is reduced. Diagnosis is important because of premature vascular disease and because patients who are misdiagnosed have sometimes been treated with corticosteroids or splenectomy.

Familial pseudohyperkalemia is due to gain-of-function mutations in the gene for the ABCB6 cation transporter, which cause cause excess leakage of potassium into plasma from the familial pseudohyperkalemia red blood cells at the low temperatures at which blood for transfusion is stored.

Neuro-acanthocytosis includes four syndromes (see Table 8.4). Two of these – choreo-acanthocytosis and the McLeod phenotype – are shown in Fig. 8.16. The syndromes include movement disorders linked to atrophy of the basal ganglia and acanthocytosis of red cells with normal β-lipoproteins. The common link between the neurological and erythroid abnormalities is a fault in cell membranes.

NORMAL RED CELL METABOLISM

Normal red cells maintain themselves in a physiologic state for about 120 days by metabolizing glucose through the glycolytic (Embden–Meyerhof) and pentose phosphate (hexose monophosphate shunt) pathways (Fig. 8.17). In this way the cells are able to generate the energy needed to maintain cell shape and flexibility, as well as cation and water content through the action of sodium and calcium pumps. Although ATP acts as an energy store, it may also act as a substitute for 2,3-diphosphoglycerate

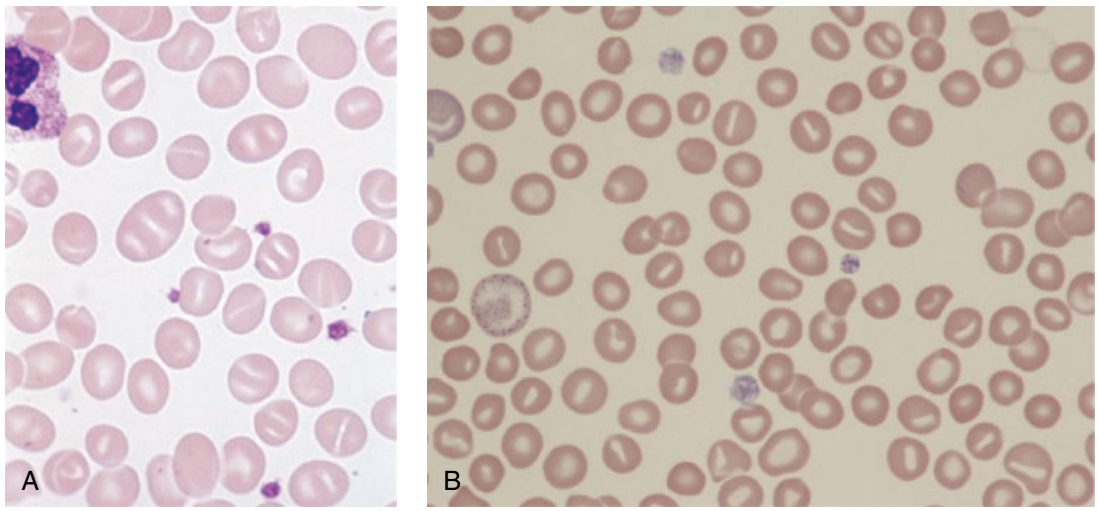

Fig. 8.15. A, Hereditary stomatocytosis: Peripheral blood film showing many cells with the characteristic loosely folded appearance of the membrane. The membrane has increased passive permeability allowing excess sodium entry. **B,** Phytosterolemia (sitosterolemia) in a 12-year-old Iranian boy. His parents were first cousins and he was known to have β-thalassemia heterozygosity. The blood film showed microcytosis and basophilic stippling, consistent with the known β-thalassemia trait. However, there was a combination of stomatocytes and large platelets. The diagnosis of phytosterolemia was confirmed by measurement of plasma lipids. There was an increase of cholesterol and triglycerides, but in addition plant sterols were strikingly increased: campesterol 1008 lmol/L (normal range 0–56), stigmasterol 31 lmol/L (normal zero), sitosterol 1324 lmol/L (0–41), fucosterol 187 lmol/L (zero), and stigmastanol 124 lmol/L (zero). Investigation of the patient's brother showed the same condition. The patient was commenced on therapy with ezetimibe, a sterol pump inhibitor that reduces absorption of plant sterols. Source: B, Bain BJ, Chakravorty S (2016) *Am J Hematol* 2016;91:643. Reproduced with permission of John Wiley & Sons. (Courtesy Professor Barbara Bain.)

TABLE 8.4. CHARACTERISTICS OF CONDITIONS CATEGORIZED AS NEURO-ACANTHOCYTOSIS

Syndrome	Mutated gene and inheritance	Clinicopathological features
Choreo-acanthocytosis	*VPS13A*, autosomal recessive	Adult-onset progressive neurodegeneration, myopathy, often epilepsy
McLeod phenotype	*KX*, X-linked recessive	Adult-onset progressive neurodegeneration, myopathy, cardiomyopathy, weak or absent expression of Kell antigens
Huntington-like disease 2a	*JPH3*, autosomal dominant	Adult-onset progressive neurodegeneration
Pantothenate-kinase-associated neurodegeneration[a]	*PANK2*, autosomal recessive	Childhood-onset progressive neurodegeneration, pallidal degeneration, sometimes retinitis pigmentosa

[a] Some cases have acanthocytes.
Source: Bain BJ, Bain PG. *Am J Hematol* 2013;88:712. Reproduced with permission of John Wiley & Sons.

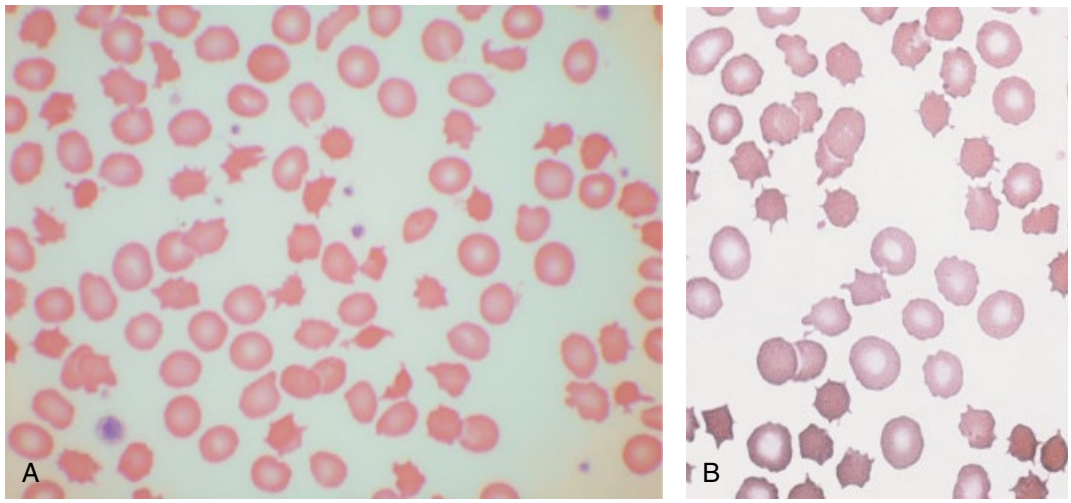

Fig. 8.16. A, Choreo-acanthocytosis: Blood film of a 38-year-old female with involuntary facial and eye movements, dysphagia, dysarthria, and chorea. (Courtesy of Professor Barbara Bain.) **B,** McLeod phenotype: Peripheral blood film showing marked acanthocytosis of red cells associated with the rare McLeod blood group. There is lack of the Kell antigen precursor (XK), the gene for which is on the X chromosome. The hemolytic anemia may be associated with a myopathy or peripheral neuropathy. Alloimmunization to the Kell antigen occurs if transfusion of red cells is given.

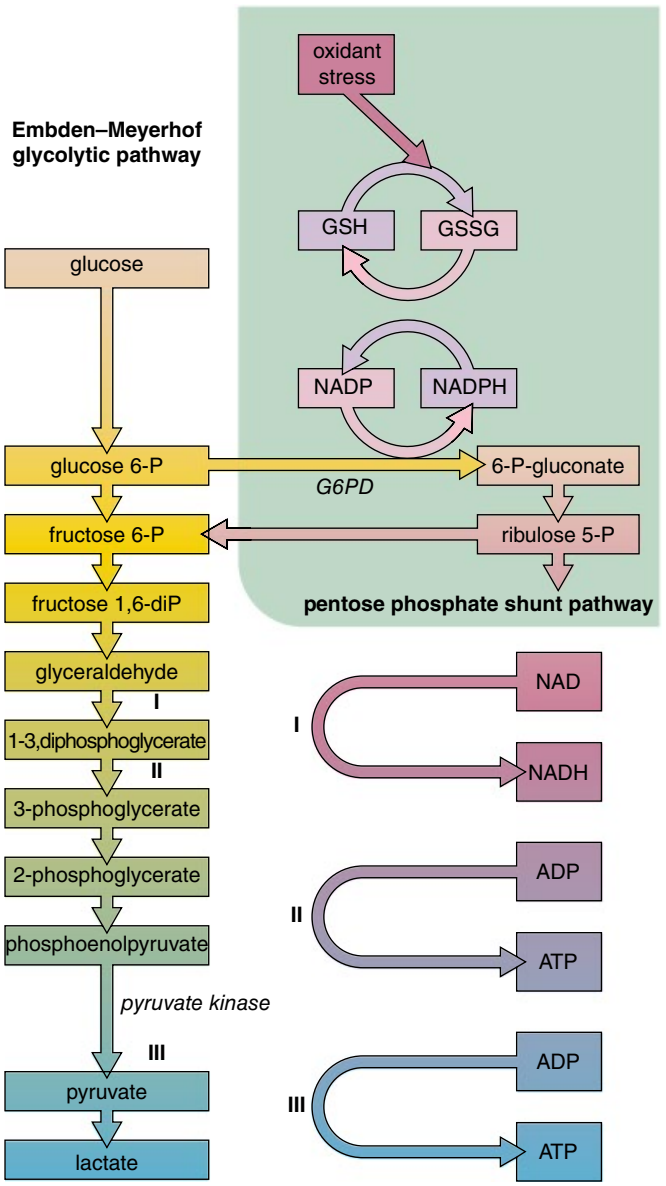

Fig. 8.17. Normal red cell metabolism: Embden–Meyerhof (glycolytic) and pentose phosphate (hexose monophosphate shunt) pathways.ADP,Adenosine diphosphate; GSH, reduced glutathione; GSSG, oxidized glutathione; P, phosphate; for other abbreviations see text.

(2,3-DPG) in maintaining the position of the oxygen dissociation curve. The most abundant red cell phosphate, 2,3-DPG is generated by the Rapoport–Luebering shunt of the glycolytic pathway (Fig. 8.18). The higher the 2,3-DPG content of red cells, the more easily is oxygen liberated from hemoglobin. Reducing power is also generated as the reduced forms of nicotinamide-adenine dinucleotide (NADH) and NAD phosphate (NADPH) and reduced glutathione (GSH), which protect the membrane, hemoglobin, and other cell structures from oxidant damage. Red cells have limited purine and pyrimidine metabolism (e.g. breakdown of ribosomal RNA).

HEMOLYTIC ANEMIAS ASSOCIATED WITH INHERITED DEFECTS OF ENZYMES

Hemolytic anemias may occur with inherited defects of enzymes involved in red cell metabolism. Glucose-6-phosphate

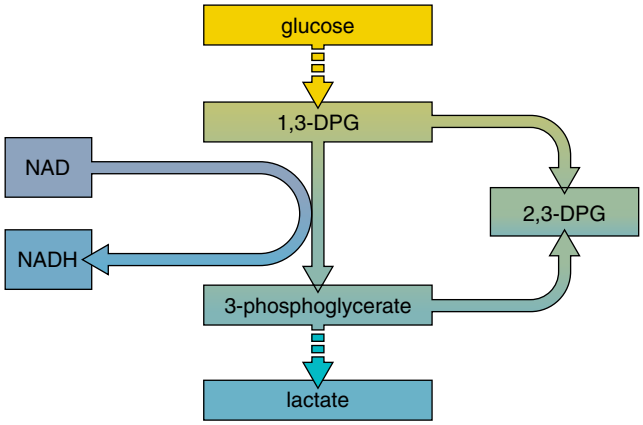

Fig. 8.18. Normal red cell metabolism:The Rapoport–Luebering shunt pathway for maintenance of red cell 2,3-diphosphoglycerate (2,3-DPG) levels.

TABLE 8.5. WORLD HEALTH ORGANIZATION CLASSIFICATION OF GLUCOSE-6-PHOSPHATE DEHYDROGENASE VARIANTS AND DEFICIENCY

Class	Enzyme activity (% normal)	Examples	Clinical effects
I	Severe (usually <20)	Santiago de Cuba (Gly447Arg)	Chronic nonspherocytic hemolytic anemia, acute exacerbations
II	<10	Mediterranean (Ser188Phe)	Favism, drug-induced hemolytic anemia, neonatal jaundice
		Canton (Arg459Leu)	
		Orissa (Ala44Gly)	
III	Moderate (>10, <60)	A– (Val68Met; Asn126Asp)	Drug-induced hemolytic anemia, neonatal jaundice
IV	100	B (wild type)	None
		A+ (Asn126Asp)	None

dehydrogenase (G6PD) deficiency (Tables 8.5 and 8.6) affects many millions worldwide, and the glycolytic and nucleotide enzyme deficiencies listed in Table 8.7 are all rare causes of hemolytic anemia.

Glucose-6-Phosphate Dehydrogenase Deficiency

G6PD is a "housekeeping gene" needed in all cells. Deficiency affects the red cells most severely, perhaps because they have no alternative source of NADPH and as a result of their long non-nucleated life span. The activity of G6PD diminishes as red cells age. The normal G6PD enzyme is genetically polymorphic and the most common form is type B. In Africa, up to 40% of the population carry an electrophoretically different normal form, type A, due to a common mutation at asparagine 126 to aspartate.

Many of the >400 hundred inherited variants of the enzyme due to 186 gene mutations (Fig. 8.19) show less activity than normal. Worldwide, 400 million people are thought to be deficient (Fig. 8.20). The World Health Organization has classified

TABLE 8.6. GLUCOSE-6-PHOSPHATE DEHYDROGENASE DEFICIENCY: DRUGS THAT CAUSE HEMOLYTIC ANEMIA IN ASSOCIATION WITH G6PD DEFICIENCY, AND THOSE THAT CAN BE GIVEN SAFELY TO PEOPLE WITH G6PD DEFICIENCY WITHOUT NONSPHEROCYTIC HEMOLYTIC ANEMIA (NSHA)

Drugs that may cause hemolytic anemia in people with G6PD deficiency	Drugs that can be given safely in therapeutic doses to people with G6PD deficiency without NSHA
Antimalarials Pyrimethamine with sulfadoxine (Fansidar) Pyrimethamine with dapsone (Maloprim) Primaquine ? Chloroquine *Sulfonamides* Sulfamethoxazole Some other sulfonamides *Sulfones* Dapsone Thiazolesulfone *Other antibacterial compounds* Nitrofurans Nalidixic acid *Anthelmintics* β-Naphthol *Miscellaneous* ? Vitamin K Naphthalene (moth balls) Methylene blue Doxorubicin	Ascorbic acid Aspirin Colchicine Isoniazid Menadiol Phenytoin Probenecid Procainamide Pyrimethamine Quinidine Quinine Trimethoprim

? – there is some dispute with these compounds.
G6PD, Glucose-6-phosphate dehydrogenase; NSHA, nonspherocytic hemolytic anemia.
Source: Beutler E. *N Engl J Med* 1991;324:169–178. Reproduced with permission of Massachusetts Medical Society: *The New England Journal of Medicine*.

TABLE 8.7. GLYCOLYTIC AND NUCLEOTIDE ENZYME DEFECTS ASSOCIATED WITH CONGENITAL NONSPHEROCYTIC HEMOLYTIC ANEMIA

Glycolytic enzyme disorders[a,b]
Pyruvate kinase (>90% of all cases)
Glycose phosphate isomerase
Hexokinase
Phosphofructokinase
Aldolase (extremely rare)
Triosephosphate isomerase
Phosphoglycerate kinase
Nucleotide enzyme disorders[a]
Pyrimidine 5′-nucleotidase
Adenylate kinase (extremely rare)
Adenosine deaminase excess

[a] Almost all are autosomal recessive with carriers hematologically normal.
[b] Some types are associated with neurological defects and/or myopathy.

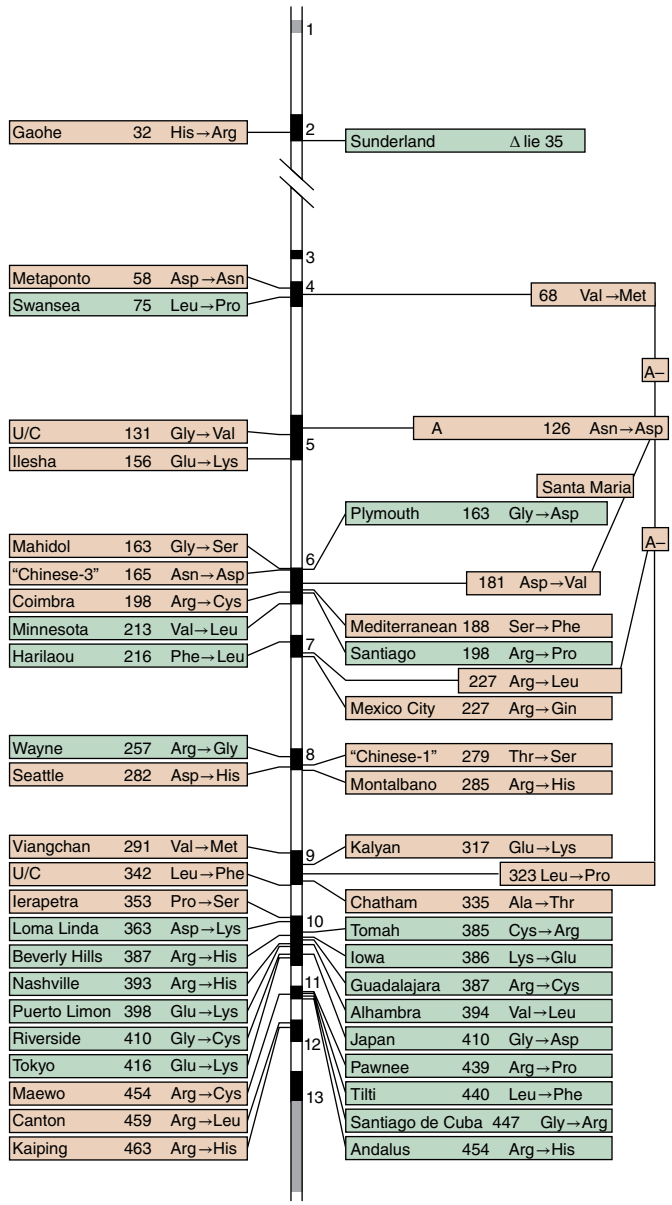

Fig. 8.19. Glucose-6-phosphate dehydrogenase (G6PD) deficiency: Some of the G6PD mutations that may cause drug sensitivity (green) or, more rarely, chronic nonspherocytic hemolytic anemia (NSHA) (orange). The exons are shown in black bands, except exon 1, which is noncoding and shown in gray. Source: Vulliamy TJ, et al. *Trends Genet* 1992;8:138–143. Reproduced with permission of Elsevier.

G6PD variants on the extent of the enzyme deficiency and on the severity of hemolysis (see Table 8.5):

- Class I: severe deficiency associated with nonspherocytic hemolytic anemia (NSHA)
- Class II: less than 10% activity; includes the common Mediterranean and Asian variants not associated with NSHA
- Class III: 10–60% of activity; includes the common A– form
- Class IV: normal activity
- Class V: increased activity.

Variants of the final two groups are of no clinical significance. The most frequent clinical syndrome is acute intravascular hemolysis caused by oxidant stress, drugs (Table 8.6), or fava beans

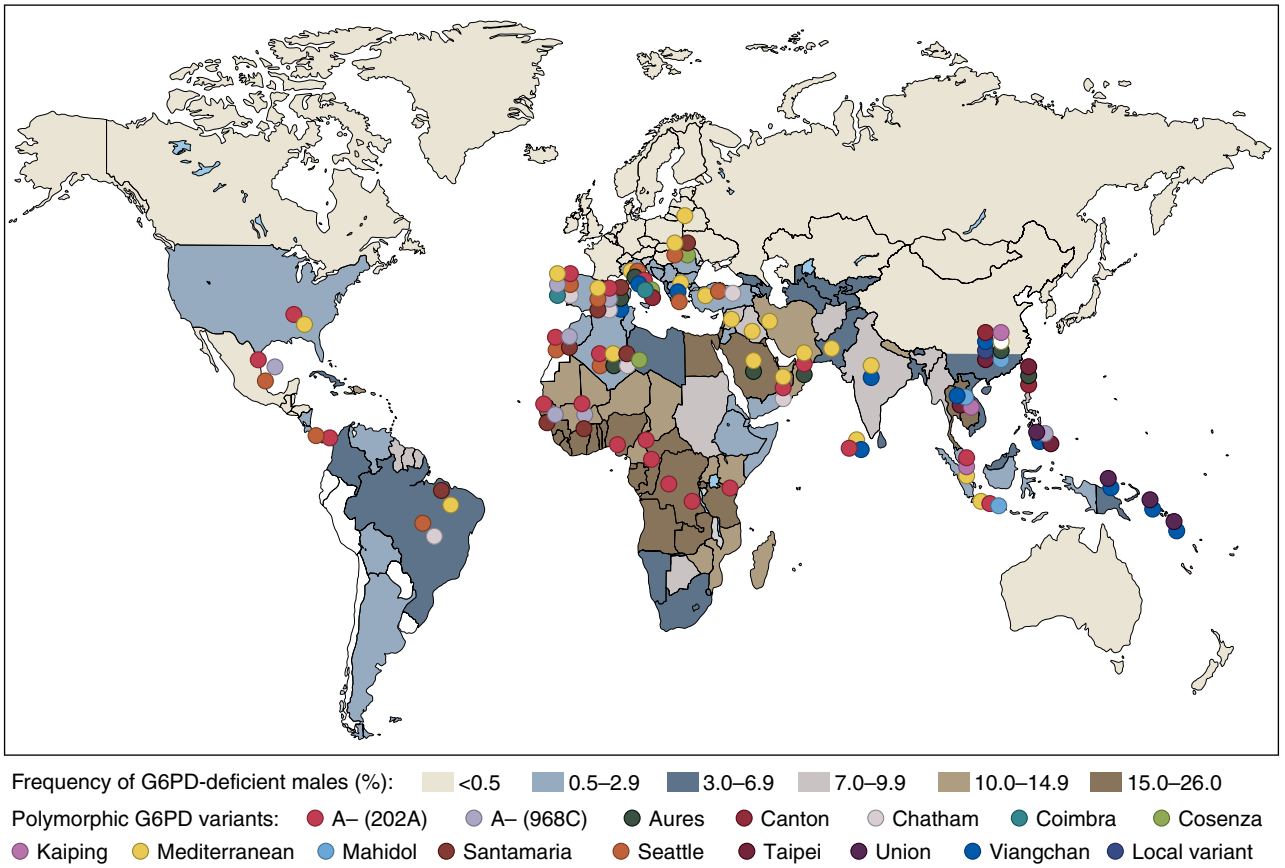

Fig. 8.20. World distribution of polymorphic glucose-6-phosphate dehydrogenase-deficient mutants. The different shadings indicate the frequency of the G6PD-deficient phenotype in the respective population. Based on Figure 4 in Luzzatto L, Nannelli C, Notaro R. *Hematol Oncol Clin North Am* 2016; 30: 373–393.

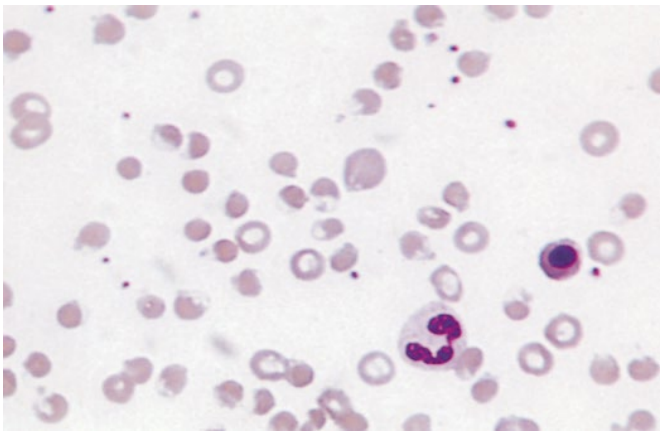

Fig. 8.21. Glucose-6-phosphate dehydrogenase deficiency: Peripheral blood film following acute oxidant drug-induced hemolysis shows an erythroblast and damaged red cells, including irregularly contracted "blister" and "bite" cells.

or occurring during severe infection, diabetic ketoacidosis, or hepatitis. Patients who develop hemolysis all have a biochemical G6PD level <30%. Marked changes occur in red cell morphology (Fig. 8.21) with Heinz bodies (see Fig. 8.4) and hemoglobinuria (see Fig. 8.5). Neonatal jaundice may also occur, and the most severe defects result in a chronic NSHA.

The gene is located on the X chromosome and is fully expressed in males, but only one X chromosome is active in each female cell. As a result of X-chromosome inactivation, female heterozygotes for G6PD deficiency have two populations of cells (on average 50% of each), either with or without the enzyme. Because G6PD deficiency confers protection against *Plasmodium falciparum* malaria, it has a high frequency in areas of the world where malaria is or was common. Rarely, lack of G6PD may be responsible for decreased leukocyte function and for hyperbilirubinemia in some patients with neonatal jaundice or viral hepatitis.

Pyruvate Kinase Deficiency

Pyruvate kinase deficiency is the most frequently encountered hemolytic anemia due to an inherited defect in the Embden–Meyerhof glycolytic pathway. The majority of patients have red cells that show no particular diagnostic features (Fig. 8.22A), although "prickle" cells may be found, especially following splenectomy (Fig. 8.22B). The postsplenectomy reticulocyte count is often very high. The diagnosis is made by a specific enzyme assay.

Pyrimidine 5-Nucleotidase Deficiency

This rare congenital hemolytic anemia is associated with basophilic stippling of the red cells (Fig. 8.23) caused by abnormal residual RNA. This enzyme normally catalyzes the hydrolytic dephosphorylation of pyrimidine 5′-ribose monophosphates to freely diffusible pyrimidine nucleosides, an important step in the breakdown of RNA at the reticulocyte stage. The enzyme is also inhibited by lead.

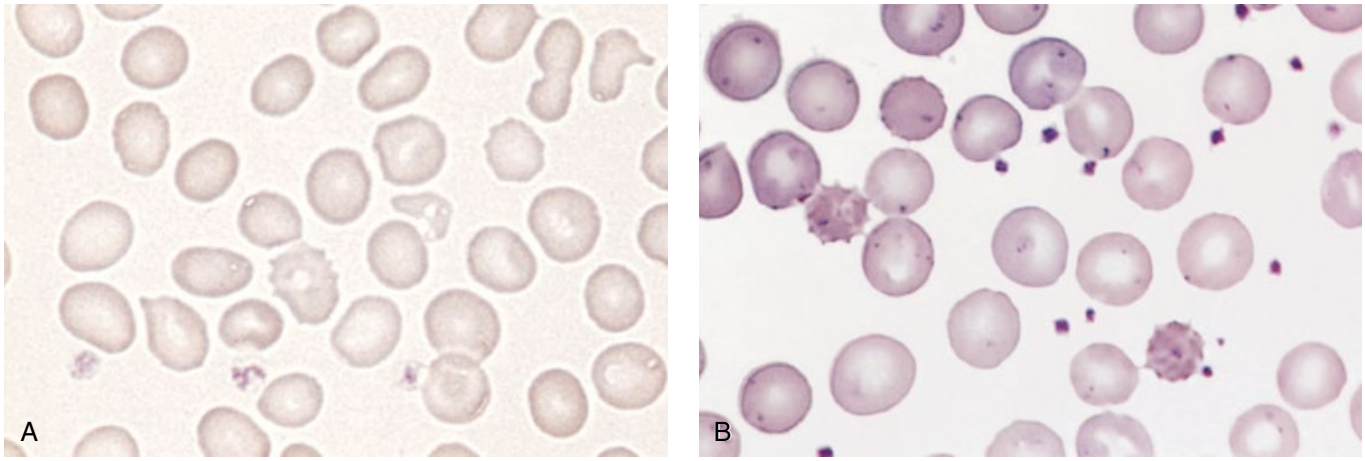

Fig. 8.22. Pyruvate kinase deficiency: **A,** Peripheral blood film presplenectomy shows red cell anisocytosis and poikilocytosis. **B,** Peripheral blood film postsplenectomy with two small echinocytes or "prickle" cells.

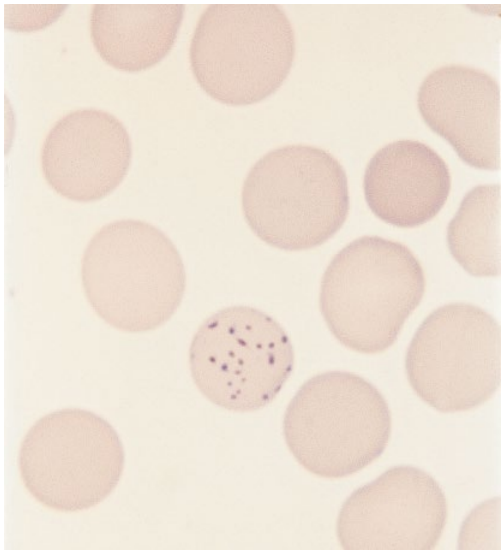

Fig. 8.23. Pyrimidine 5-nucleotidase deficiency: Peripheral blood film showing basophilic stippling in the central red cell.

TABLE 8.8. CAUSES OF ACQUIRED HEMOLYTIC ANEMIA

Immune
Autoimmune hemolytic anemia
Drug-induced immune hemolytic anemia
Isommune
Hemolytic transfusion reaction
Hemolytic disease of the newborn
Red cell fragmentation syndrome
Hypersplenism
Paroxysmal nocturnal hemoglobinuria
Secondary
Renal disease, liver disease, etc.
Miscellaneous
Chemicals
Drugs
Infections
Toxins
Wilson disease

ACQUIRED HEMOLYTIC ANEMIA

The majority of acquired hemolytic anemias are caused by extracorpuscular or environmental changes. A simplified classification is given in Table 8.8.

AUTOIMMUNE HEMOLYTIC ANEMIAS

Autoimmune hemolytic anemias are characterized by a positive direct Coombs' (antiglobulin) test (Fig. 8.24) and are divided into "warm" and "cold" types, according to whether the antibody reacts better with red cells at 37°C or at 4°C. These acquired disorders occur at any age and produce hemolytic anemias of varying severity, often with associated disease (Table 8.9). In the warm type, the peripheral blood usually shows marked red cell spherocytosis (Fig. 8.25). In the cold type, cold agglutinin disease, the antibodies are usually immunoglobulin M (IgM) and may be associated with intravascular hemolysis. The IgM is typically monoclonal in the primary form of the condition or where there is an underlying lymphoproliferative disease

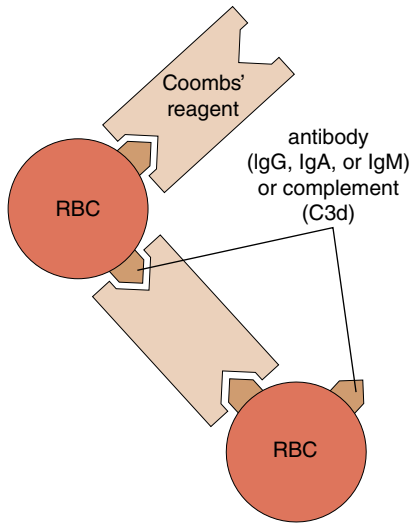

Fig. 8.24. Direct antiglobulin (Coombs') test. The Coombs' reagent may be broad spectrum or specifically directed against IgG, IgM, IgA, or complement (C3d). The test is positive if the red cells agglutinate. RBC, red blood cell.

TABLE 8.9. CAUSES OF AUTOIMMUNE HEMOLYTIC ANEMIA

Warm AIHA
Primary
Secondary
Neoplasia (CLL, lymphoma, solid organ, e.g. thymoma, carcinoma, ovarian dermoid cyst)
Infection (e.g. hepatitis C, HIV, CMV, VZV, pneumococcal infection, leishmaniasis, tuberculosis)
Immune dysregulation
Connective tissue disorders (e.g. SLE, Sjögren syndrome, scleroderma)
Ulcerative colitis, PBC, sarcoidosis
Post-transplantation
Immune deficiency syndromes (e.g. CVID)
Drug-induced (cephalosporins, β-lactamase inhibitors, diclofenac)
Other (pregnancy, diphtheria–pertussis–tetanus vaccination)
Cold AIHA
Cold hemagglutinin disease
Primary
Secondary
Malignancy (e.g. CLL, NHL, solid organ)
Infection (e.g. mycoplasma pneumonia, viral infections including IM)
Autoimmune disease
Post-allogeneic HSCT
Paroxysmal cold hemoglobinuria
Primary
Secondary
Infection (e.g. adenovirus, influenza A, syphilis, CMV, IM, VZV, measles, mumps, malaria, *Escherichia coli*) Legionnaires' disease
Mixed type AIHA
Primary
Secondary
Lymphoma, SLE, infection

AIHA, autoimmune hemolytic anemia; CLL, chronic lymphocytic leukemia; CMV, cytomegalovirus; CVID, common variable immunodeficiency; HIV, human immunodeficienc y virus; HSCT, hematopoietic stem cell transplantation; IM, infectious mononucleosis; NHL, non-Hodgkin lymphoma; PBC, primary biliary cirrhosis; SLE, systemic lupus erythematosus; VZV, varicella zoster virus.
Source: Adapted from Hill QA, et al. and the British Society for Haematology Guidelines (2017), *Br J Haematol* 2017;177:208–220.

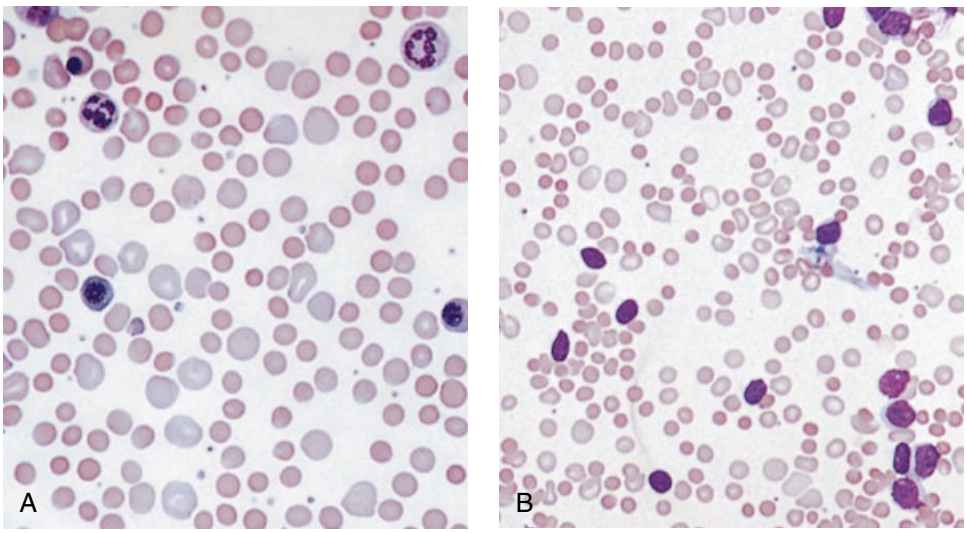

Fig. 8.25. Autoimmune hemolytic anemia: **A,** Peripheral blood film showing erythroblasts, polychromatic macrocytes, and marked spherocytosis. **B,** With associated chronic lymphocytic leukemia: Peripheral blood film showing red cell polychromasia spherocytosis and increased numbers of lymphocytes.

but polyclonal post infection. In the primary form, a disease of older adults, there are usually nodules of clonal lymphocytes in the bone marrow which, unlike those in lymphoplasmacytic lymphoma, are MYD88 negative. Cytogenetic abnormalities reported include trisomies 3 and 12 and the t(8;22) mutation. It may be indolent for many years or transform into an aggressive lymphoma. The red cells become coated with IgM directed against the I antigen or, typically in infectious mononucleosis, the i antigen in the peripheral parts of the circulation. This binds complement C3b, which remains on the cells as C3d when the IgM dissociates and when the red cells return to the warmer central parts of the circulation. The macrophages of the reticuloendothelial system ingest the C3d-coated cells. Marked autoagglutination of red cells may be seen in the blood film (Fig. 8.26). In many patients, the hemolysis is aggravated by cold weather, and it is often associated with acrocyanosis (purplish skin discoloration) or Raynaud phenomenon (Fig. 8.27).

Paroxysmal cold hemoglobinuria is a rare syndrome of acute intravascular hemolysis after exposure to the cold. It is due to an IgG (Donath Landsteiner) antibody with specificity for the P blood group antigens which binds to red cells in the cold but binds complement to lyse red cells at 37°C. It is usually transient following a viral infection.

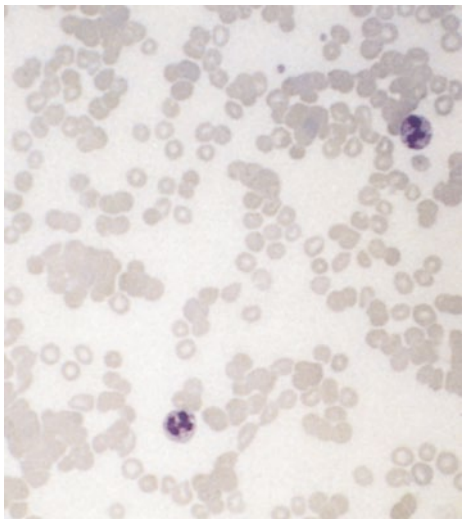

Fig. 8.26. Autoimmune hemolytic anemia (cold type): peripheral blood film showing autoagglutination of red cells.

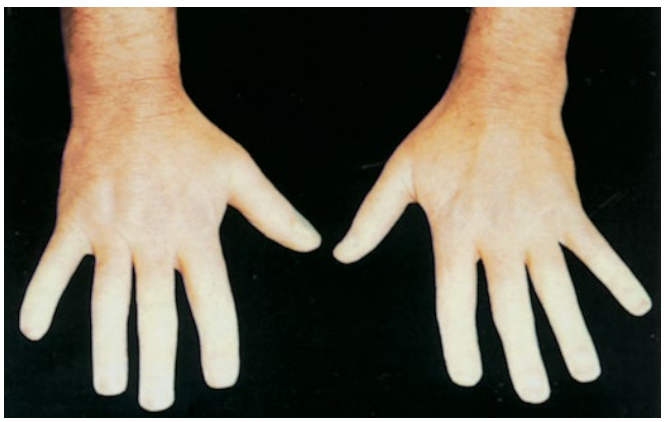

Fig. 8.27. Autoimmune hemolytic anemia (cold type): Raynaud phenomenon manifested by marked pallor of the fingers.

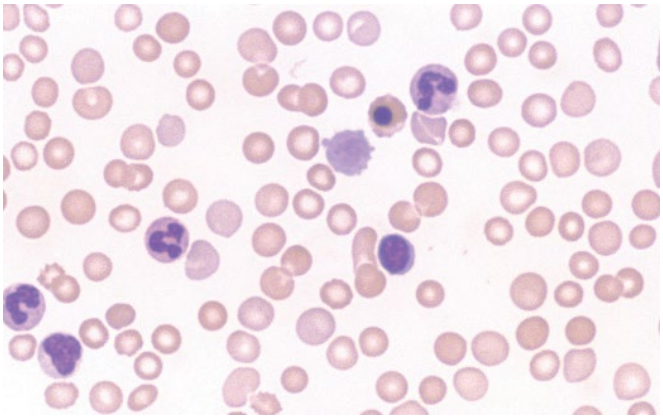

Fig. 8.28. Evans syndrome: The blood film shows an erythroblast, red cell spherocytosis, polychromasia, and a solitary giant platelet.

In warm autoimmune hemolytic anemia, high-dose corticosteroids often achieve a remission. Rituximab, other immunosuppressive drugs, such as mycophenolate mofetil, azathioprine, or cyclophosphamide, and splenectomy may be of value in those who do not respond satisfactorily. Patients with chronic cold autoimmune hemolytic anemia should avoid the cold, and may benefit from therapy with rituximab, bendamustine, fludarabine, purine analogs, and proteasome inhibitors or alkylating drugs.

EVANS SYNDROME

In Evans syndrome, patients with autoimmune hemolytic anemia also have an autoimmune thrombocytopenia. The blood film shows features of both conditions (Fig. 8.28). There is often an associated illness (e.g. lymphoproliferative disease or immunodeficiency).

DRUG-INDUCED IMMUNE HEMOLYTIC ANEMIA

Drugs cause immune hemolytic anemia by three mechanisms: antibodies may be directed against a red cell membrane–drug complex (e.g. with penicillin,cephalosporins, tolbutamide); there may be deposition of a protein–antibody–drug complex on the red cell surface (e.g. with quinidine, stibophen, rifampicin); or occasionally an autoimmune process is involved, as with methyldopa, cladribine, fludarabine, or levodopa.

ISOIMMUNE HEMOLYTIC ANEMIA

Severe hemolysis follows transfusion of incompatible blood, particularly if the blood is of the wrong ABO group. There may be massive intravascular hemolysis, and the blood film usually shows both autoagglutination and spherocytosis (Fig. 8.29). The other major cause of isoimmune hemolytic anemia is hemolytic disease of the newborn, which may result from a number of different maternofetal blood group incompatibilities (Table 8.10 and Figs. 8.30 and 8.31); see also Chapter 32).

RED CELL FRAGMENTATION SYNDROMES

The causes of red cell fragmentation syndrome are listed in Table 8.11. Fragmentation arises from direct damage to red cells, either on abnormal surfaces such as heart valves, or vascular

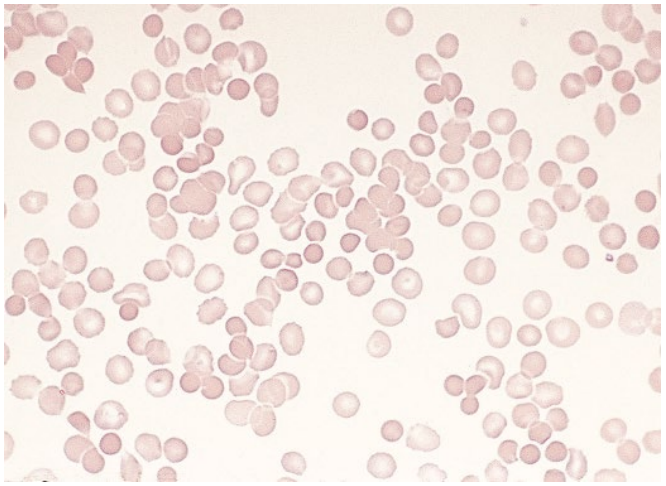

Fig. 8.29. ABO incompatibility transfusion reaction: Peripheral blood film showing red cell autoagglutination and spherocytosis.

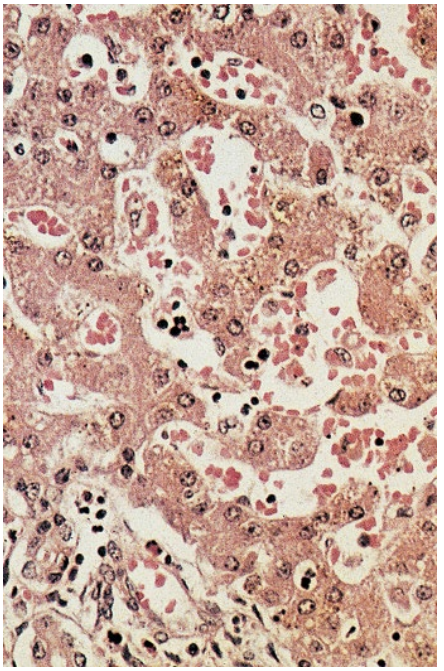

Fig. 8.30. RhD hemolytic disease of the newborn (erythroblastosis fetalis): Peripheral blood film from an infant born with severe anemia showing large numbers of erythroblasts, red cell polychromasia, and anisocytosis.

TABLE 8.10. ISOIMMUNE HEMOLYTIC ANEMIA: THE MAIN BLOOD GROUP SYSTEMS AND THEIR ASSOCIATION WITH HEMOLYTIC DISEASE IN THE NEWBORN

Blood group system	Frequency of antibodies	Hemolytic disease of newborn
ABO	Very common	Causal
Rh	Common	Causal
Kell	Occasional	Causal
Duffy	Occasional	Causal
Kidd	Occasional	Causal
Lutheran	Rare	Causal
Lewis	Rare	Not causal
P	Rare	Not causal
MNSs	Rare	Not causal
Ii	Rare	Not causal

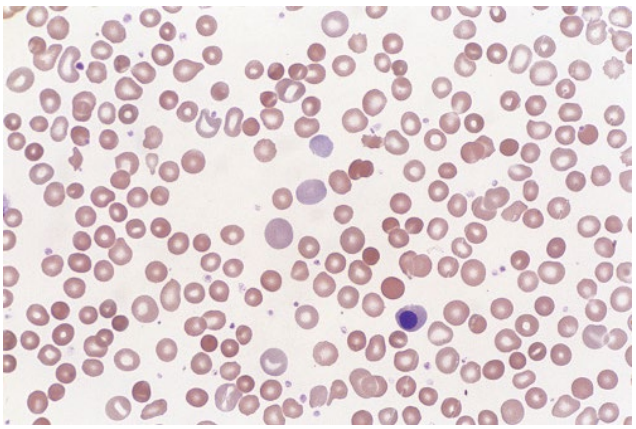

Fig. 8.31. Hemolytic disease of the newborn resulting from ABO incompatibility. The blood film shows an erythroblast, red cell polychromasia, and spherocytosis.

malformations or changes in the microcirculation such as fibrin shearing in disseminated intravascular coagulation, vasculitis, and endothelial damage. Blood film changes in patients with mucin-secreting adenocarcinoma, thrombotic thrombocytopenic purpura, hemolytic–uremic syndrome, and Gram-negative septicemia are shown in Figs. 8.32 and 8.33.

SECONDARY HEMOLYTIC ANEMIAS

In a number of systemic disorders, hemolysis may contribute to observed anemia. In renal failure there may be crenated cells (echinocytes), including "burr" cells and acanthocytes (Fig. 8.34; see also Fig. 30.30). Red cell targeting is a feature of the hemolysis associated with liver disease, and with severe liver failure, there is often marked hemolysis with prominent red cell acanthocytosis (see Fig. 30.33).

TABLE 8.11. CAUSES OF FRAGMENTATION HEMOLYSIS

Cardiac hemolysis
Prosthetic heart valves
Patches, grafts
Paraprosthetic or perivalvular leaks
Arteriovenous malformations
Kasabach–Merritt syndrome
Malignant hemangioendotheliomas
Microangiopathic
TTP, HUS
Malignant disease
Vasculitis
Preeclampsia, HELLP
Renal vascular disorders
Disseminated intravascular coagulation

HELLP, Hemolysis, elevated liver enzymes low platelets; HUS, hemolytic–uremic syndrome; TTP, thrombotic thrombocytopenic purpura.

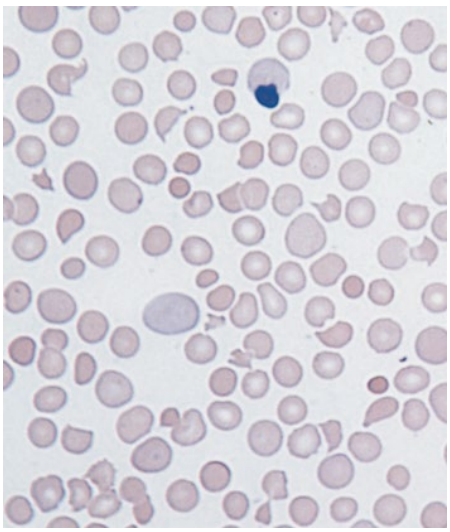

Fig. 8.32. Red cell fragmentation syndrome: Peripheral blood film showing polychromatic and fragmented red cells in thrombotic thrombocytopenic purpura.

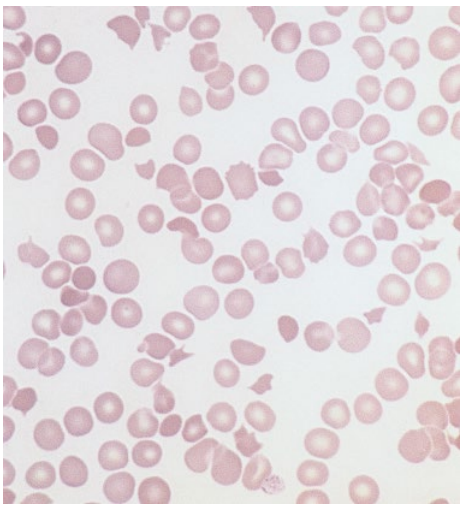

Fig. 8.33. Red cell fragmentation syndrome: Peripheral blood film in Gram-negative septicemia, showing red cell polychromasia, microspherocytes, and fragmentation.

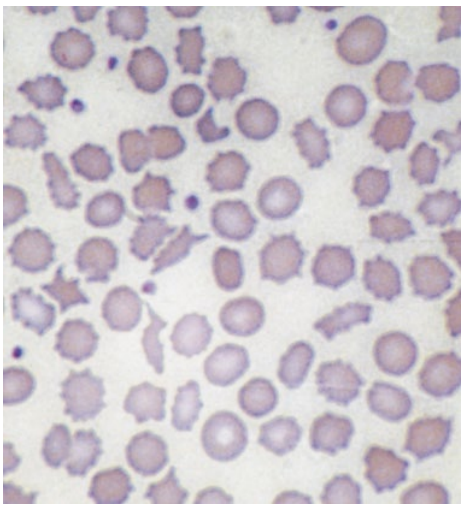

Fig. 8.34. Chronic renal failure: Peripheral blood film showing red cell changes, including "burr" cells and acanthocytes (coarse crenated cells).

PAROXYSMAL NOCTURNAL HEMOGLOBINURIA

In paroxysmal nocturnal hemoglobinuria (PNH), an acquired clonal disorder, the bone marrow produces red cells with defective cell membranes that are particularly sensitive to lysis by complement. There is chronic intravascular hemolysis with hemoglobinuria and hemosiderinuria (see Fig. 8.6). The defect that results in complement sensitivity is in the formation of phosphatidylinositol, which anchors a number of proteins via an intervening glycan structure to the cell membrane (Fig. 8.35). The proteins anchored by glycosylphosphatidylinositol (GPI) include membrane inhibitor of reactive lysis (MIRL = CD59), decay accelerating factor (DAF = CD55), and C8-binding protein (C8B). These three proteins all react with complement. Leukocyte function antigen (LAF-3 = CD58), acetylcholinesterase, alkaline phosphatase, and low-affinity immunoglobulin G (IgG) receptor (FcRIII) are also deficient (Fig. 8.36). Lack of MIRL appears to be responsible for the undue sensitivity to complement. The enzyme α-1,6-*N*-acetylglucosaminyltransferase is the enzyme involved in synthesis of the GPI anchor that is missing or defective because of different types of mutations in the *PIGA* (phosphatidylinositol glycan complementation class A) gene. The enzyme complex transfers *N*-acetylglucosamine from uridine diphosphate-*N*-acetylglucosamine to phosphatidylinositol. The *PIGA* gene is located on the X chromosome (Xp22.1) so each somatic cell, male or female, has only one active copy. The mutation rate for the gene is similar to that

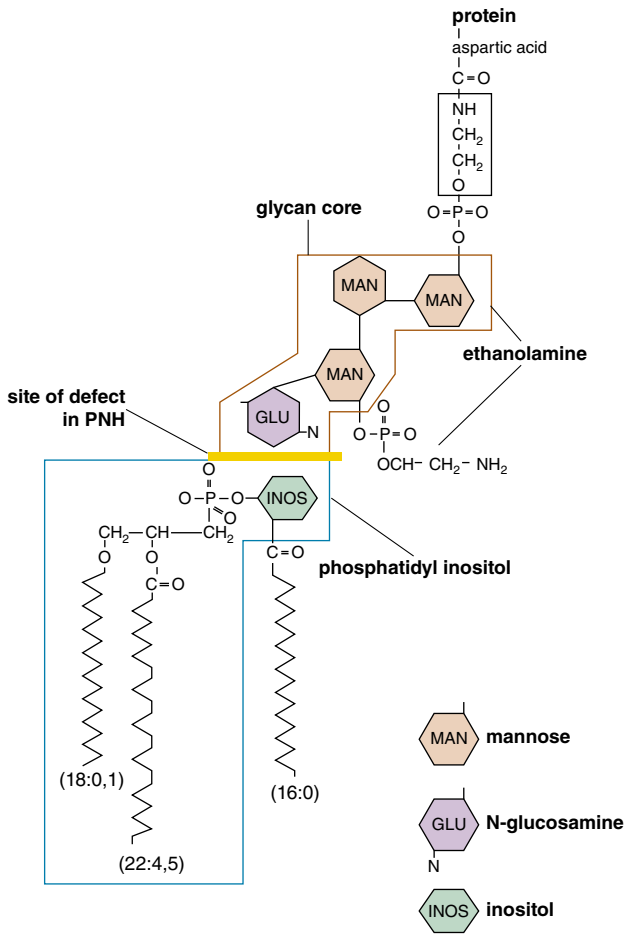

Fig. 8.35. The glycosylphosphatidylinositol (GPI) anchor: The structure and site of the defect in paroxysmal nocturnal hemoglobinuria. (Courtesy of Professor Wendell Rosse.)

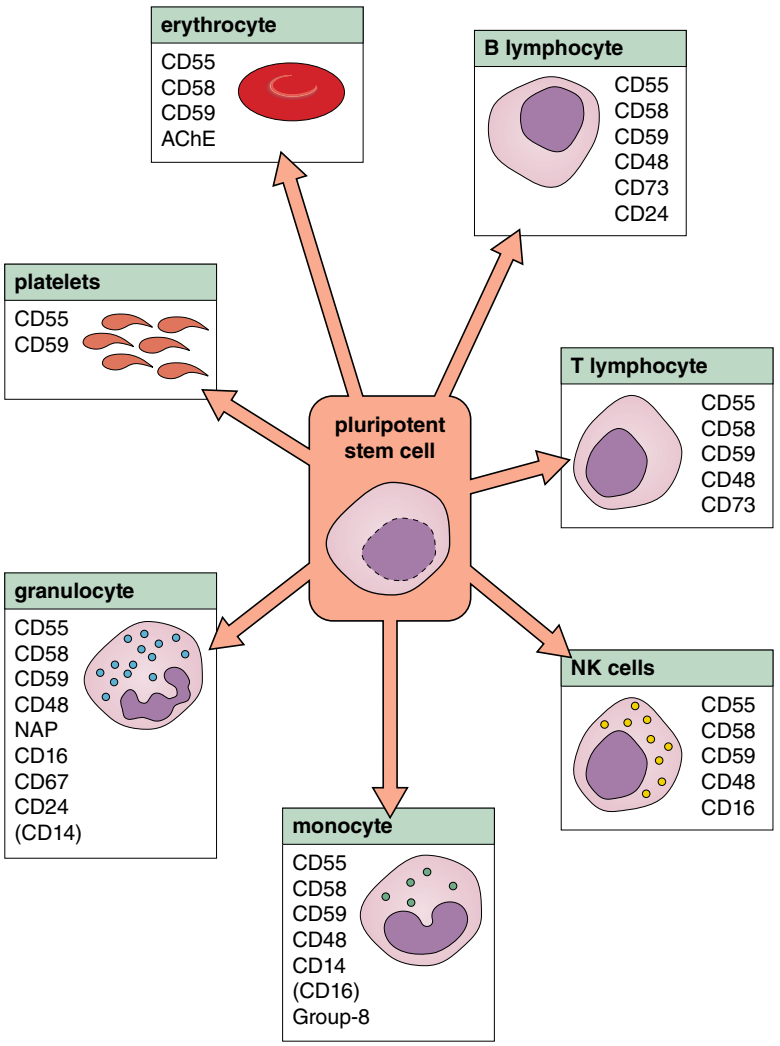

Fig. 8.36. Expression of GPI-linked molecules on the surface of blood cells. AChE, acetylcholinesterase; CD16, FcRIII low-affinity receptor for IgG; CD55, DAF (see text); CD59, MIRL (see text); Group-8, monocyte activation antigen; NAP, alkaline phosphatase. Source: Rotoli B, et al. *Blood Rev* 1993;7:75–86. Reproduced with permission from Elsevier.

for other genes. The reason why GPI-deficient clones expand could be due to second genetic events or because of a growth advantage on the background of marrow hypoplasia.

The patients often develop iron deficiency. The bone marrow tends to be hypocellular and the reticulocyte count is lower than in other hemolytic anemias of equal severity. The white cell and platelet counts are also often low. Many patients develop recurrent venous thromboses. Occasionally patients have the Budd–Chiari syndrome. Flow cytometry of red cells and granulocytes using anti-CD59 provides an accurate estimate of the size of the PNH cell population. Eculizumab, a humanized antibody that blocks the activation of the complement protein C5 and the terminal membrane attack phase of complement action, is effective in controlling hemolysis in patients with PNH who are transfusion dependent and in reducing thrombotic episodes.

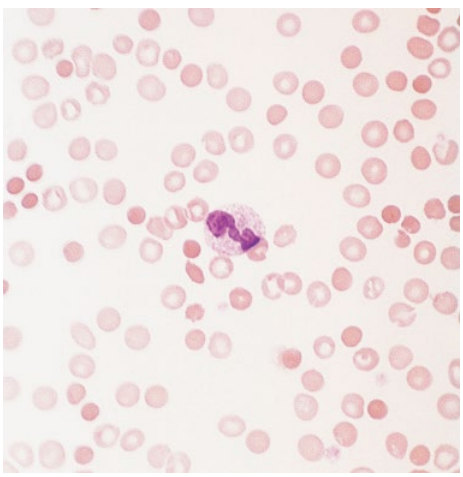

Fig. 8.37. Hemolytic anemia in clostridial septicemia: Peripheral blood film showing red cell spherocytosis.

OTHER HEMOLYTIC ANEMIAS

Severe hemolytic anemia may be found during clostridial septicemia (Fig. 8.37) and in other infections, including malaria and bartonellemia (see Chapter 31). Hemolytic anemias may also be caused by extensive burns (Fig. 8.38), chemical poisoning, and snake and spider bites. Overdose with oxidizing drugs, such as sulfasalazine (Fig. 8.39) or dapsone (Fig. 8.40), may also cause severe hemolysis. Wilson disease is also a cause of hemolysis, thought to result from oxidant damage to red cells caused by excess copper (Fig. 8.41).

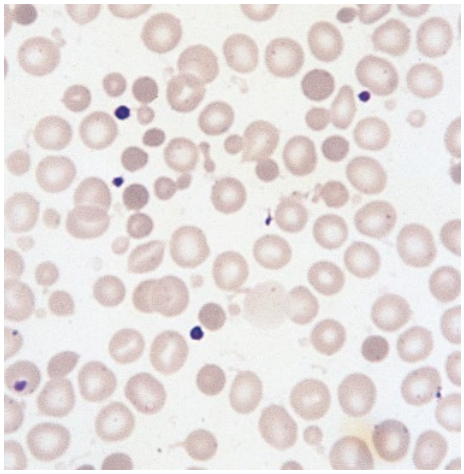

Fig. 8.38. Hemolytic anemia following extensive burns: Peripheral blood film showing microspherocytes, ghost cells, cells with membrane projections, and "dumbbell" forms.

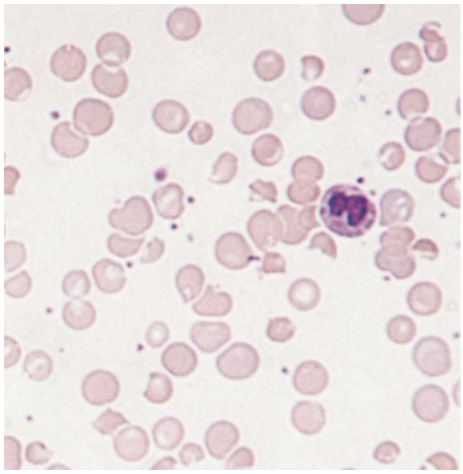

Fig. 8.39. Drug-induced hemolytic anemia: Peripheral blood film associated with overdose of sulfasalazine. The red cells show polychromasia, irregular contraction, and some fragmentation.

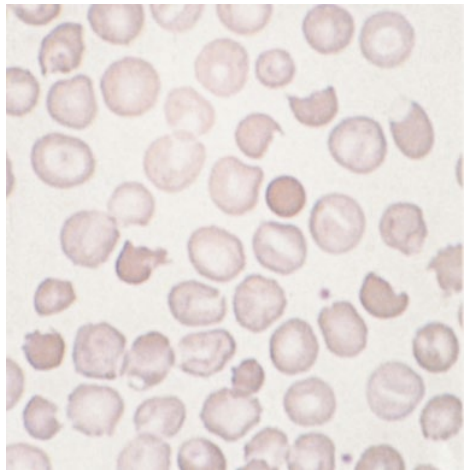

Fig. 8.40. Drug-induced hemolytic anemia: Peripheral blood film in a case associated with high-dosage dapsone therapy for dermatitis herpetiformis. The red cells show irregular contraction, target cells, and cells with "bites" out of the membrane. There is a single "blister" cell in the lower central area of the field.

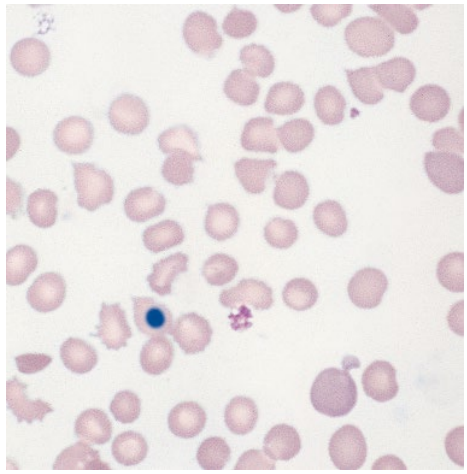

Fig. 8.41. Hemolytic anemia in Wilson disease: Peripheral blood film showing polychromasia, spur cells (acanthocytes), and a normoblast. (Courtesy of Dr. R Britt.)

CHAPTER

9 GENETIC DISORDERS OF HEMOGLOBIN

THALASSEMIA

Globin synthesis depends on two gene clusters situated on chromosomes 11 and 16 (Fig. 9.1). Different hemoglobins dominate in the embryo, fetus, and adult (Fig. 9.2). Each globin gene includes three coding regions, or exons, and two noncoding regions, called intervening sequences or introns. Globin molecules are synthesized from the appropriate genes via an RNA transcript. The genes all show two boxes, TATA and CCAAT, in the 5′ region, closely upstream in the flanking region, and further upstream sequences GGGGTG and CACCC. These all have important regulatory functions. They are promoter sequences involved in the initiation of transcription. At the 3′ noncoding region, there is a sequence AATAAA, which is the signal for the

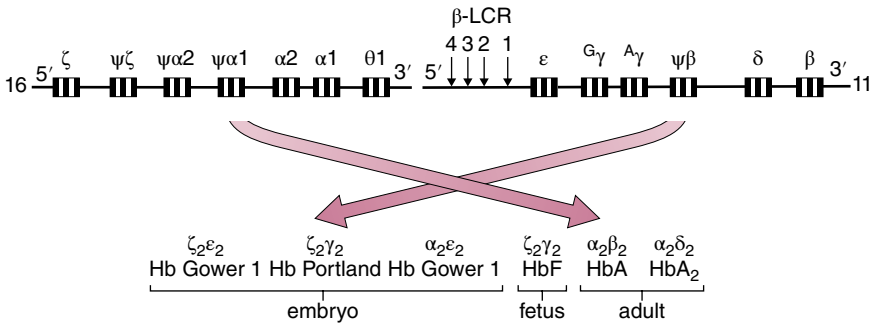

Fig. 9.1. Synthesis of hemoglobin: Organization of the clusters of genes and their coding regions (exons, in black) for globin chain synthesis on chromosomes 11 and 16; noncoding regions (introns) occur between the exons. Gγ and Aγ are forms of the γ-globin gene that codes for glutamic acid or alanine at position 136. LCR, Locus control region. Source: Weatherall DJ. Genetic disorders of haemoglobin. In: Hoffbrand AV, et al. *Postgraduate Haematology*, 4th edn. Butterworth-Heinemann, 1999, pp. 91–119. Reproduced with permission of Elsevier.

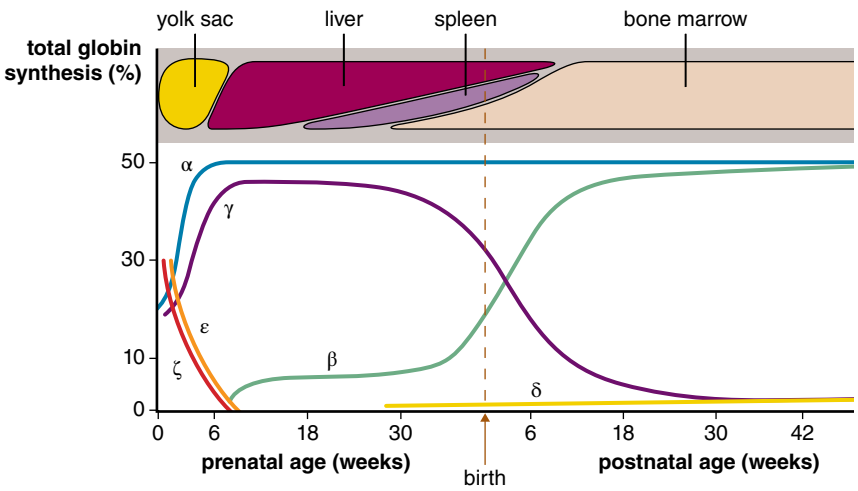

Fig. 9.2. Synthesis of hemoglobin: Sites of globin chain synthesis in the embryo, fetus, and adult. Source: Hoffbrand AV, Pettit JE. *Essential Haematology*, 3rd edn. Blackwell Scientific, 1993. Reproduced with permission from John Wiley & Sons.

Color Atlas of Clinical Hematology: Molecular and Cellular Basis of Disease, Fifth Edition. A. Victor Hoffbrand, Paresh Vyas, Elías Campo, Torsten Haferlach, and Keith Gomez

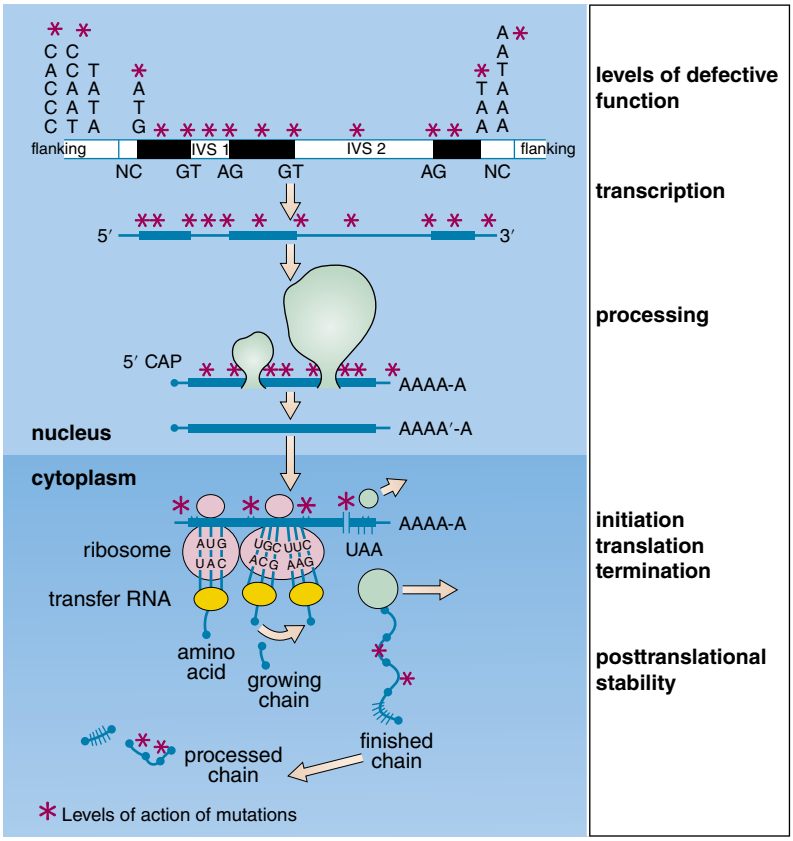

Fig. 9.3. Synthesis of hemoglobin: Stages in the synthesis of β-globin from DNA to the final polypeptide chain. A, Adenine; C, cytosine; G, guanine; IVS, intervening sequence; T, thymine; U, uracil. Source: Weatherall DJ. Genetic disorders of haemoglobin. In: Hoffbrand AV, et al. *Postgraduate Haematology*, 4th edn. Butterworth-Heinemann, 1999, pp. 91–119. Reproduced with permission of Elsevier.

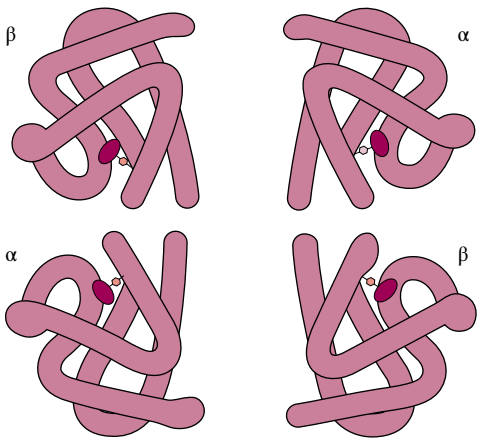

Fig. 9.4. Synthesis of hemoglobin: The hemoglobin tetramer – in this example, HbA.

messenger RNA (mRNA) to be cleaved (Fig. 9.3). Upstream of the β-globin cluster, there is a key regulatory region, the locus control region (LCR) (see Fig. 9.1), which performs two functions. It allows the β-globin cluster to transform from a transcriptionally inactive closed chromatin formation to an open transcriptionally active form. It also enhances transcription from the β-globin gene cluster. To do this, it binds erythroid-specific (e.g. GATA-1, NF-E2) and ubiquitous *trans*-acting factors. The α-globin clusters also include an LCR-like region designated HS40, but it differs from the β-LCR. Following transcription, the RNA is processed (spliced) to remove redundant RNA derived from introns situated within the coding part of each gene (Fig. 9.3). The exon–intron junctions have the sequence GT at their 5′ end and AG at their 3′ end. These sequences are essential for correct splicing. The messenger is modified by addition of a CAP (start site for RNA transcription) structure at the 5′ end and a series of adenylic acid residues (the poly-A tail) at the 3′ end. The processed message moves to the cytoplasm, attaches to ribosomes, and acts as a template for the addition of appropriate amino acids via their transfer RNAs. The amino acids link up to form the final polypeptide chain.

Each molecule of hemoglobin consists of four globin chains (Fig. 9.4). In normal adults, hemoglobin (Hb) A (α_2,β_2) forms 96–97% of the hemoglobin. The thalassemias are a group of disorders in which the underlying abnormality is reduced synthesis of either the α or β chains of hemoglobin A (Table 9.1, Fig. 9.5). The global distribution of thalassemia and the frequency of different mutations in Mediterranean populations are shown in Fig. 9.6.

β-Thalassemia is divided into three types:

- A homozygous (major) form, in which there is complete or almost complete absence of β-globin chain synthesis
- A heterozygous (minor) or trait form, in which synthesis of only one β chain is reduced
- A clinically intermediate form, which can be a mild form of homozygous β-thalassemia, the result of interaction of β-thalassemia with other genetic disorders of hemoglobin synthesis, or an unusually severe form of β-thalassemia trait (see Table 9.2).

In general, β-thalassemias are the result of point mutations in or near the globin genes that cause, for example, defective transcription, processing of RNA, translation or post-translation stability or splicing; internal intervening sequence (IVS); cryptic splice site; CAP and polyadenylation site changes or premature stop codons, nonsense lesions, and frameshift; and initiation site

TABLE 9.1. CLASSIFICATION OF THE THALASSEMIA DISORDERS: CLINICAL, α-THALASSEMIAS, AND β-THALASSEMIAS

Classification of thalassemias I: Clinical

Thalassemia major
Transfusion-dependent homozygous β^0-thalassemia
Homozygous β^+-thalassemia (some types)

Thalassemia intermedia
Mild forms of compound β^+ α^+ β^0/β^+ thalassemia
Hemoglobin Lepore syndromes
Homozygous δβ-thalassemia and hereditary persistence of fetal hemoglobin
Combinations of α- and β^+-thalassemias
Heterozygous β-thalassemia with triplicated α genes
Dominant β-thalassemia
Heterozygosity for β-thalassemia and β-chain variants (e.g. HbE/β-thalassemia)
Hemoglobin H disease

Thalassemia minor
β^0-Thalassemia trait
δβ-Thalassemia trait
Hereditary persistence of fetal hemoglobin
β^+-Thalassemia trait
α^0-Thalassemia trait
α^+-Thalassemia trait

Classification of thalassemias II: α-Thalassemias

Designation	Haplotype	Heterozygous	Homozygous
α^0-Thalassemia	– – /	α^0-Thalassemia; MCH, MCV low	Hydrops fetalis
Dysfunctional α-thalassemia	– α^0/	α^0-Thalassemia; MCH, MCV low	Hydrops fetalis
α^+-Thalassemia	– α/	α^+-Thalassemia; minimal, if any, hematologic abnormality	As heterozygous α^0-thalassemia
Nondeletion α-thalassemia	α α/	Variable	HbH disease in some cases
Hb Constant Spring (CS)		0.5–1% HbCS	More severe than heterozygous α^0-thalassemia
The combination of α^0-thalassemia (or dysfunctional α-thalassemia) and α^+-thalassemia gives rise to HbH disease			

Classification of thalassemias III: β-Thalassemias

Type	Heterozygous	Homozygous
β^0	Thalassemia minor; HbA_2 >3.5%	Thalassemia major; HbF 98%; HbA_2 2%; no HbA
β^+	Thalassemia minor; HbA_2 >3.5%	Thalassemia major or intermedia; HbF 70%–80%; HbA 10%–20%; HbA_2 variable
δβ hereditary persistence of fetal hemoglobin	Thalassemia minor; HbF >5%–20%; HbA_2 normal or low	Thalassemia intermedia; HbF 100%
Hb Lepore	Thalassemia minor; HbA >80–90%; Hb Lepore 10%; HbA_2 reduced	Thalassemia major or intermedia; HbF 80%; Hb Lepore 10%–20%; HbA, HbA_2 absent

Hb, hemoglobin; MCH, mean cell hemoglobin; MCV, mean cell volume.

changes (Fig. 9.7). Gene deletion may also cause β-thalassemias (Fig. 9.8) but is more common in the α-thalassemias. Over 400 different genetic lesions have been detected in the β-thalassemias.

β-Thalassemia results in unbalanced synthesis of β chains and non-β (α and γ) chains. The greater the degree of imbalance, the more severe the anemia. Unpaired α chains pair and precipitate in the developing red cell, leading to ineffective erythropoiesis (Fig. 9.9).

β-THALASSEMIA MAJOR

The clinical features of β-thalassemia major result from a severe anemia combined with an intense increase in erythropoiesis, largely ineffective, with excessive bone marrow activity and extramedullary hematopoiesis. In the poorly transfused patient, there is expansion of the flat bones of the face and skull (Figs. 9.10–9.13) and expansion of the marrow in all bones (Fig. 9.14). There may be gross osteoporosis and premature fusion of the epiphyses (Fig. 9.15). Even in well-transfused and well-chelated patients, osteoporosis is frequent (Figs. 9.16), especially in males and in association with diabetes mellitus and failure of spontaneous puberty. Polymorphisms in the genes for the estrogen receptor, vitamin D receptor, collagen type α1 and transforming growth factor β1 (TGF-β1) are all involved in determining bone mass. Spontaneous fractures may occur. Another feature is enlargement of the liver and spleen, mainly because of extramedullary erythropoiesis but also from excessive breakdown of red cells and iron overload.

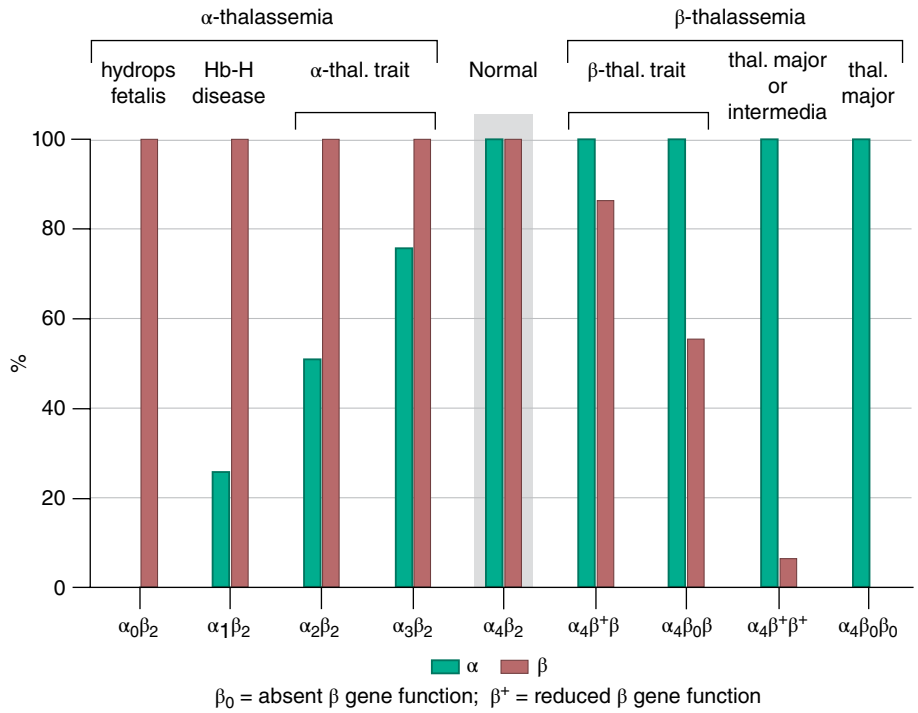

Fig. 9.5. Ratio of α:β chain synthesis in the different α- and β-thalassemias. Source: Mehta AB, Hoffbrand AV. *Haematology at a Glance*. Blackwell Publishing, 2014. Reproduced with permission of John Wiley & Sons.

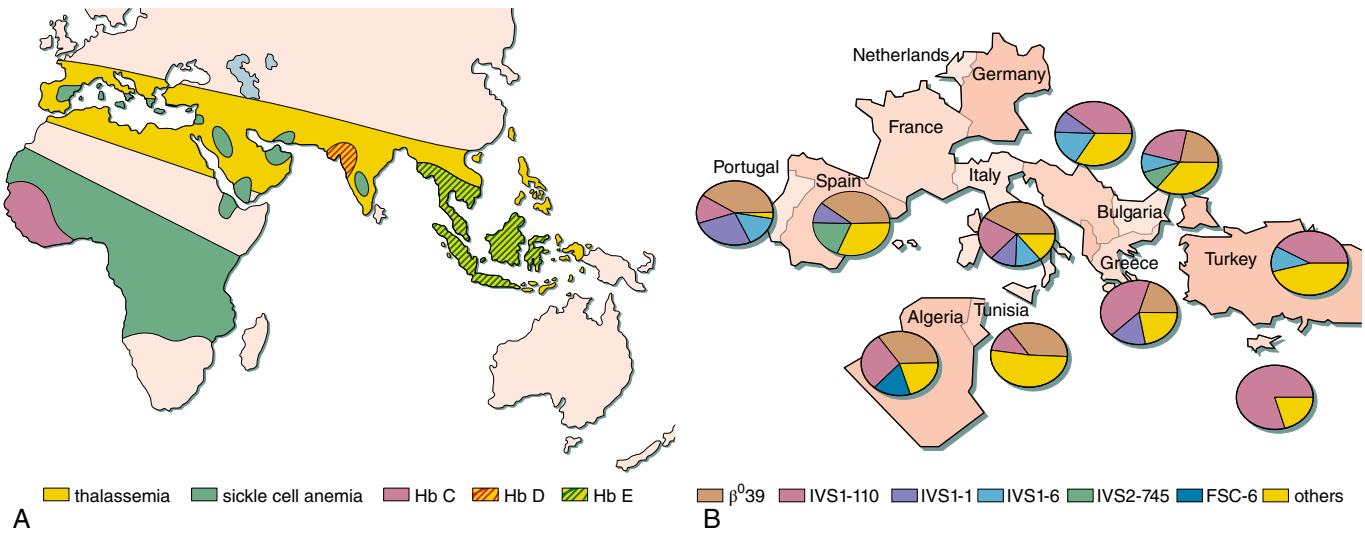

Fig. 9.6. Distribution of thalassemia disorders. **A,** The geographic distribution of thalassemia, sickle cell anemia, and the other common hemoglobin disorders. It is likely that the carriers of these disorders have a selective advantage against malaria compared with normal individuals. The disorders are also found in other parts of the world where emigrants from areas of higher incidence have settled. **B,** Frequency of different mutations of β-thalassemia in Mediterranean at-risk populations. 1, 6, 39, 110, 745, Mutations of corresponding codons; FSC-6, frameshift mutation 6; IVS1, IVS2, introns 1 or 2 of β-globin gene. (Courtesy of Professor Anthony Cao.)

The peripheral blood in the poorly transfused patient shows the presence of hypochromic cells, target cells, and nucleated red cells (Fig. 9.17). Following splenectomy, red cell inclusions increase (e.g. iron granules and Howell–Jolly bodies) and the platelet count is high (Fig. 9.18). The bone marrow shows red cell hyperplasia with pink-staining inclusions of precipitated α-globin chains in the cytoplasm of erythroblasts (Fig. 9.19). Many of the erythroblasts die in the marrow and are digested by macrophages. There is increased iron in the macrophages and increased iron granules in developing erythroblasts (Fig. 9.20).

Much of the bone abnormality can be prevented by regular transfusions from the age of presentation (usually six months) to maintain the hemoglobin at all times at a level above 9–10 g/dL. However, these regular transfusions, together with increased iron absorption, lead to iron overload. Each unit of blood contains 200–250 mg of iron. After 50 units have been transfused, or earlier in children, siderosis develops, with increased pigmentation

TABLE 9.2. CAUSES OF β-THALASSEMIA INTERMEDIA

Mild forms of β-thalassemia
Homozygosity for mild β^+-thalassemia alleles
Compound heterozygosity for two mild β^+-thalassemia alleles
Compound heterozygosity for a mild and more severe β-thalassemia allele

Inheritance of α- and β-thalassemia
β^+-thalassemia with α^0-thalassemia (– –/αα)
or with α^+-thalassemia (–α/αα or –α/–α)
β^+-thalassemia with genotype of HbH disease (– –/–α)

β-Thalassemia with elevated γ-chain synthesis
Homozygous β-thalassemia with heterocellular HPFH
Homozygous β-thalassemia with Gγ or Aγ promoter mutations
Compound heterozygosity for β-thalassemia and deletion forms of HPFH

Coinheritance of HbF quantitative trait loci
Linked: Xmn1-G (raised) γ polymorphism
Unlinked: *BC11A* gene (chromosome 2), *HBS1L-MYB* intergenic polymorphisms (chromosome 6q) *KLF1* variants

Compound heterozygosity for β-thalassemia and β-chain variants
HbE/β-thalassemia
Other interactions with rare β-chain variants

Heterozygous β-thalassemia with triplicated or quadruplicated α-chain genes (ααα or αααα globin complexes)

Dominant forms of β-thalassemia

Interactions of β- and $(\delta\beta)^+$- or $(\delta\beta)^0$-thalassemia

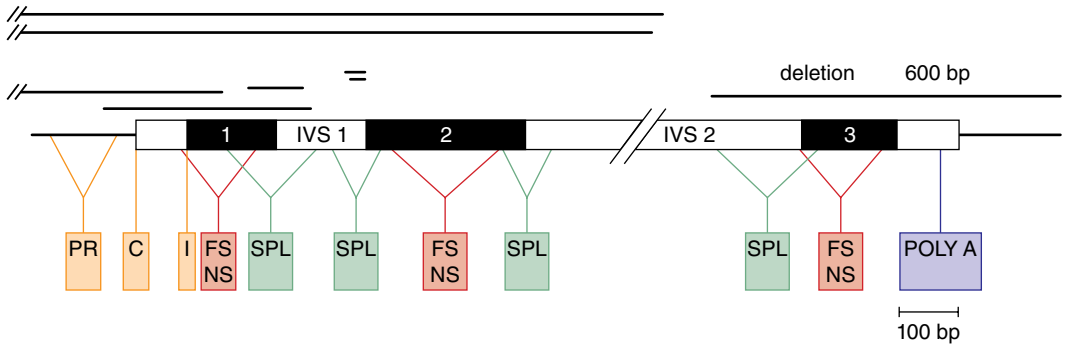

Fig. 9.7. β-Thalassemia: The classes of mutations that underlie β-thalassemia. The 600 base pair deletion may also cause β-thalassemia. Other rare deletions may occur that affect the β-globin gene, the β and δ genes, or the γ, δ, and β genes (see Fig. 9.8). C, CAP site; FS, frameshift; I, initiation codon; NS, nonsense (premature chain termination) mutation; POLY A, poly-A addition site mutation; PR, promoter; SPL, splicing mutation. (Courtesy of Professor DJ Weatherall.)

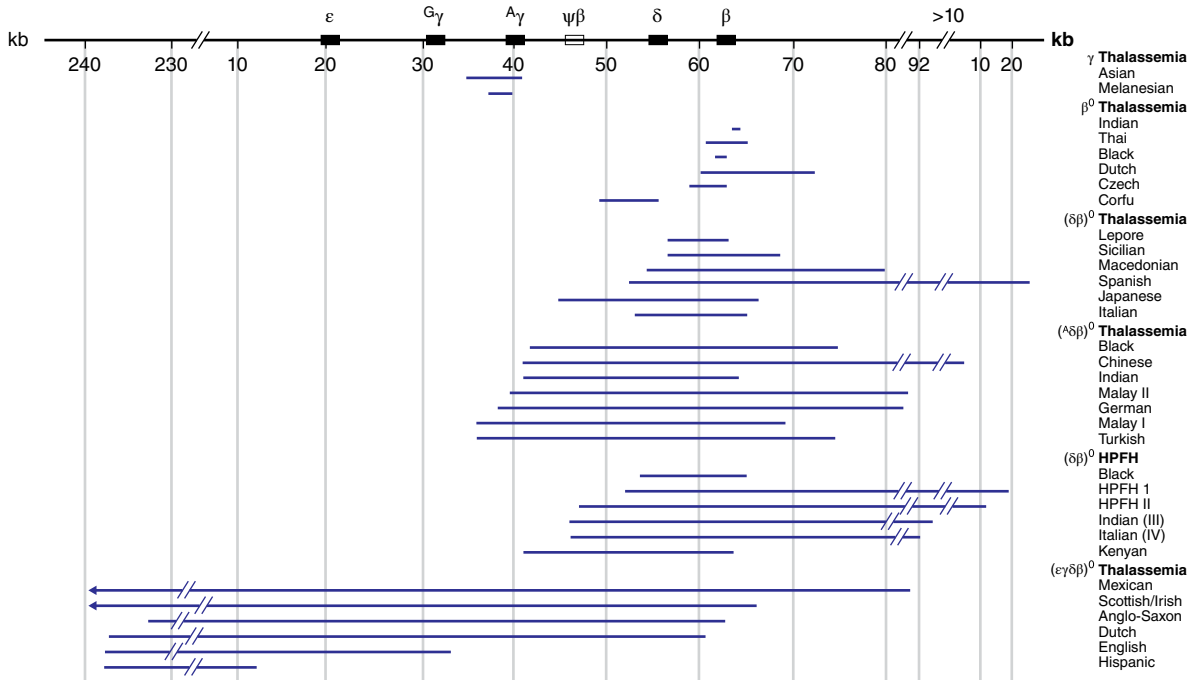

Fig. 9.8. β-Thalassemia: The deletions that underlie δβ- and εγδβ-thalassemias and hereditary persistence of fetal hemoglobin. Source: Weatherall DJ. Genetic disorders of haemoglobin. In: Hoffbrand AV, et al. *Postgraduate Haematology*, 5th edn. Blackwell Publishing, 2005, pp. 85–103. Reproduced with permission from John Wiley & Sons.

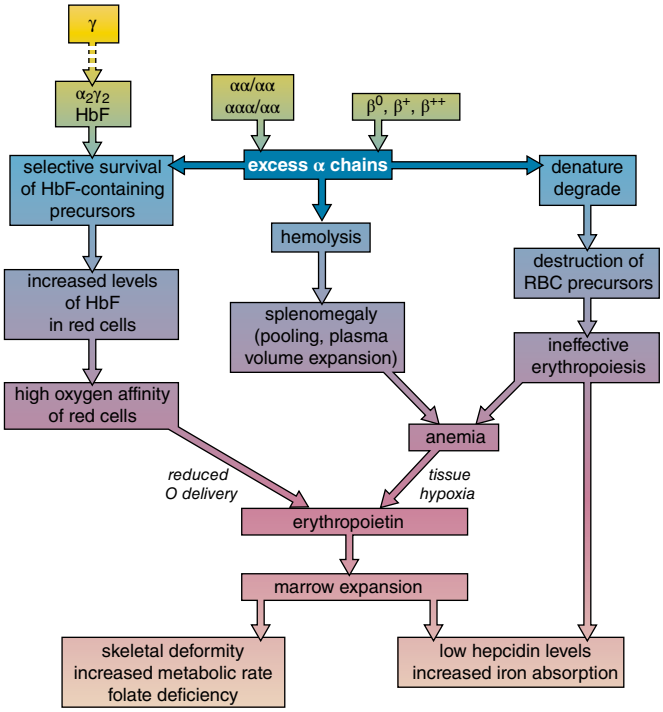

Fig. 9.9. Pathophysiology of β-thalassemia. Source: Weatherall DJ. Genetic disorders of haemoglobin. In: Hoffbrand AV, et al. *Postgraduate Haematology*, 5th edn. Blackwell Publishing, 2005, pp. 85–103. Reproduced with permission from John Wiley & Sons.

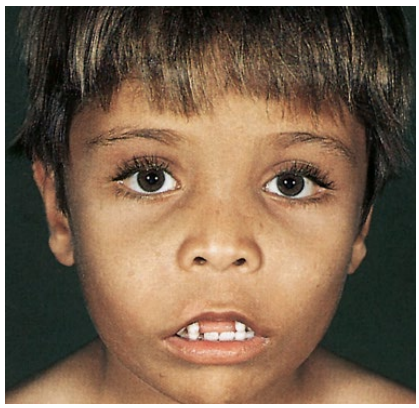

Fig. 9.10. β-Thalassemia major: Characteristic facies of a 7-year-old Middle Eastern boy include prominent maxilla and widening of the bridge of the nose. There is also marked bossing of the frontal and parietal bones and zygomata.

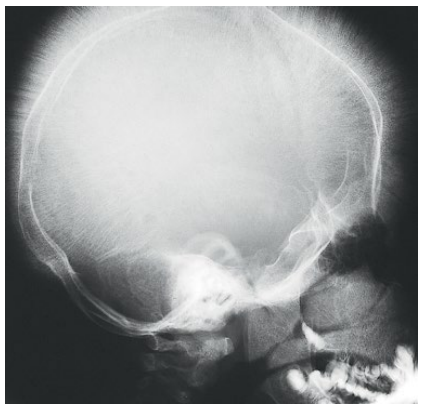

Fig. 9.11. β-Thalassemia major: Lateral radiograph of the skull (same case as shown in Fig. 9.10) shows the typical "hair-on-end" appearance, with thinning of the cortical bone and widening of the marrow cavity.

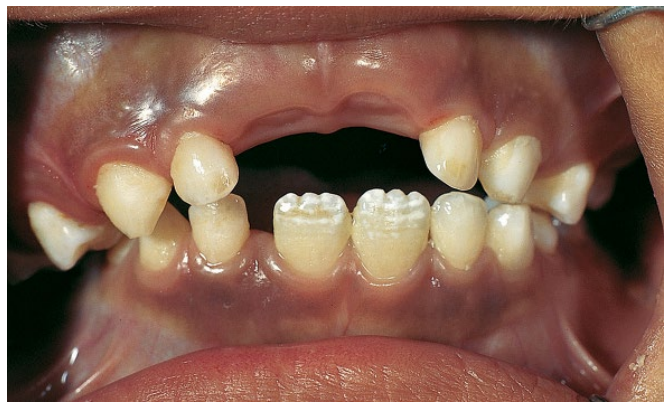

Fig. 9.12. β-Thalassemia major: The teeth (same case as shown in Fig. 9.10) are splayed because of widening of the maxilla and mandible.

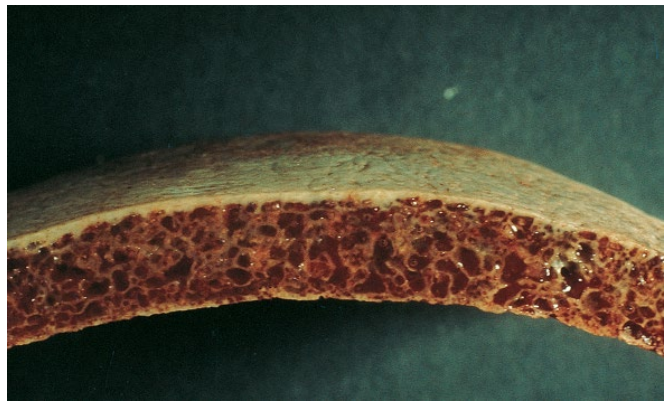

Fig. 9.13. β-Thalassemia major: Section through the skull at necropsy shows marked thinning of the cortices and an open porotic cancellous bone. The mahogany brown color results from extensive iron deposition (hemosiderin), in the marrow. (Courtesy of Dr. PG Bullough and Dr. VJ Vigorita.)

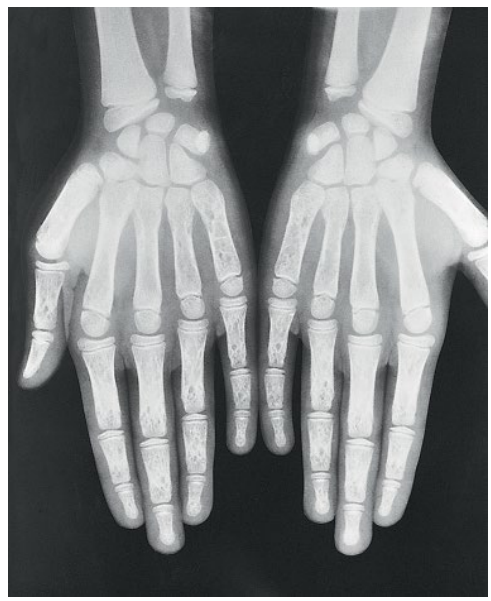

Fig. 9.14. β-Thalassemia major: Radiograph of the hands of an undertransfused 7-year-old child. Thinning of the cortical bone results from expansion of the marrow space.

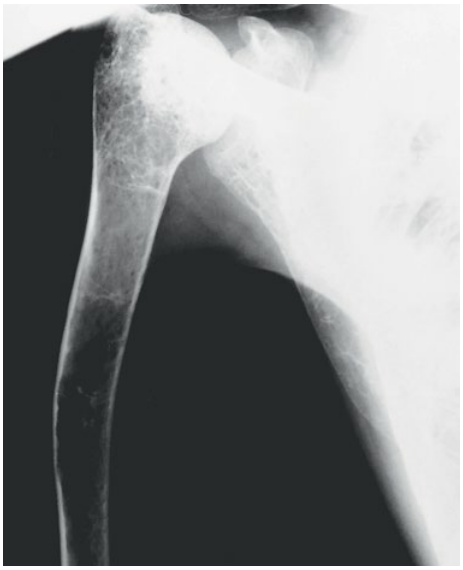

Fig. 9.15. β-Thalassemia major: Severe osteoporosis and premature fusion of humeral epiphysis in an undertransfused patient. Osteoporosis is more common in males, in patients with diabetes mellitus, and in those with failed puberty. (Courtesy of Dr. B Wonke.)

of skin exposed to light and susceptibility to infection (Fig. 9.21), reduced growth, and delayed sexual development and puberty. Iron overload is also a result of increased iron absorption because hepcidin levels are low due to increased production of proteins by erythroblasts, which inhibit hepcidin synthesis (Fig. 5.6).

Bone development is delayed and abnormal (Figs. 9.22–9.24). Damage due to iron overloading occurs in the liver (Figs. 9.25 and 9.26) and myocardium (Figs. 9.27). Measurement of iron in the heart, liver, and other organs is carried out by T_2* magnetic resonance imaging (T_2* MRI). This can detect cardiac iron excess before functional tests reveal cardiac damage (Fig. 9.28). MRI studies show that the degree of iron loading in the liver and heart may not parallel each other (Fig. 9.29). There is also damage to the endocrine organs, including the pancreas (Fig. 9.30), hypothalamus, pituitary, thyroid, and parathyroids (Fig. 9.31).

Iron overload may, however, be substantially reduced by iron chelation therapy. This may be achieved by daily subcutaneous desferrioxamine infusions. The orally active iron chelators deferiprone and deferasirox are now increasingly used.

Complications of desferrioxamine therapy may include ototoxicity with high tone deafness, retinal damage (Fig. 9.32), and, in children, pseudorickets, causing changes in the bones

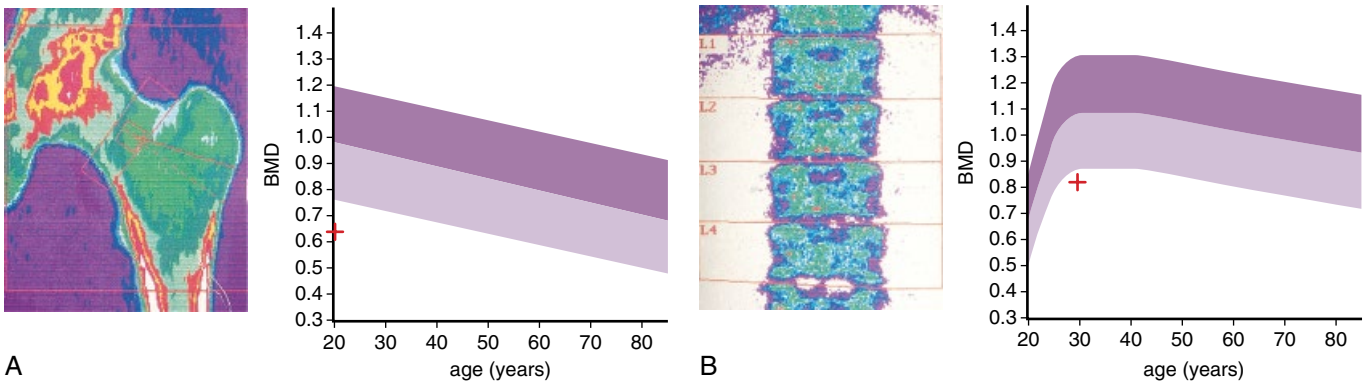

Fig. 9.16. β-Thalassemia major: Bone density scans of hip **(A)** and lumbar vertebrae **(B)**. The bands represent 1.5 standard deviation above and below the mean age-specific bone mineral density (BMD). The red crosses indicate the patient's results. (Courtesy of Dr. B Wonke.)

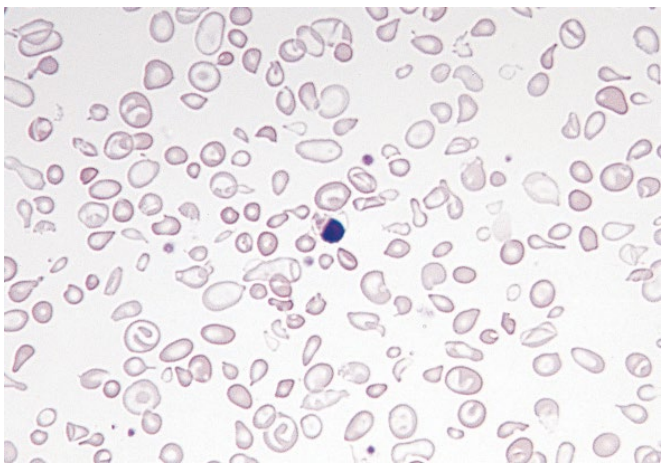

Fig. 9.17. β-Thalassemia major: Peripheral blood film showing prominent hypochromic microcytic cells, target cells, and an erythroblast. Some normochromic cells are present from a previous blood transfusion.

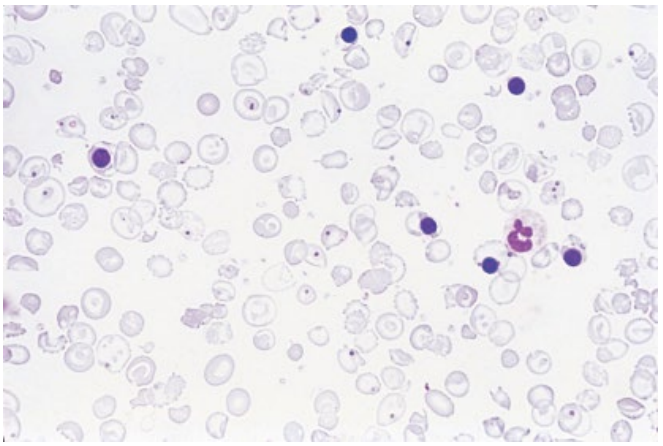

Fig. 9.18. β-Thalassemia major: Peripheral blood film after splenectomy in which hypochromic cells, target cells, and erythroblasts are prominent. Pappenheimer and Howell–Jolly bodies are also seen, and the platelet count is raised.

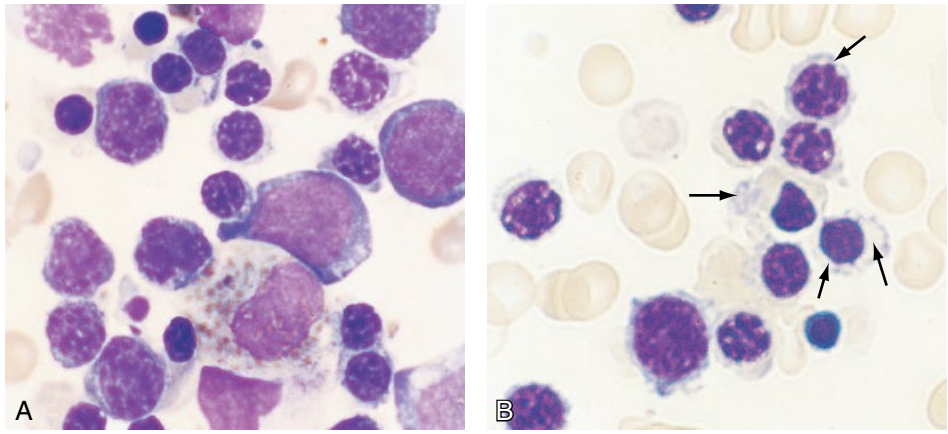

Fig. 9.19. β-Thalassemia major: Bone marrow aspirates. **A,** Marked erythroid hyperplasia and erythroblasts with vacuolated cytoplasm; degenerate forms and a macrophage that contains pigment are present. **B,** Erythroblasts with pink-staining cytoplasmic inclusions ("hemoglobin lakes," arrows) and precipitates of excess α-globin chains.

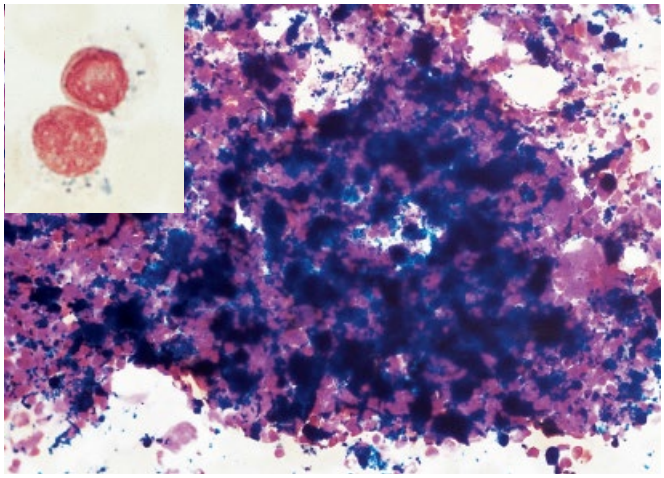

Fig. 9.20. β-Thalassemia major: Low-power view of bone marrow fragment showing grossly increased iron stores, largely contained in macrophages as hemosiderin and (seen on electron microscopy) as ferritin. Bone marrow erythroblasts show prominent coarse iron granules *(inset)*. (Perls' stain.)

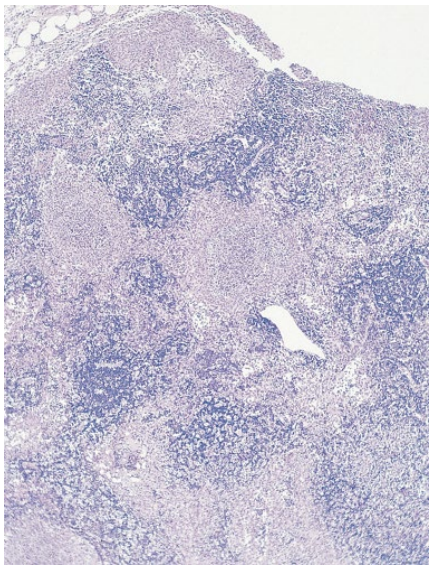

Fig. 9.21. β-Thalassemia major: Mesenteric adenitis caused by *Yersinia enterocolitica* infection. The lymph node contains large numbers of granulomas with central necrosis. In keeping with the severity of the disease, the necrosis is more marked than that usually seen. The infection is particularly common in patients with iron overload. (Courtesy of Dr. J Dyson.)

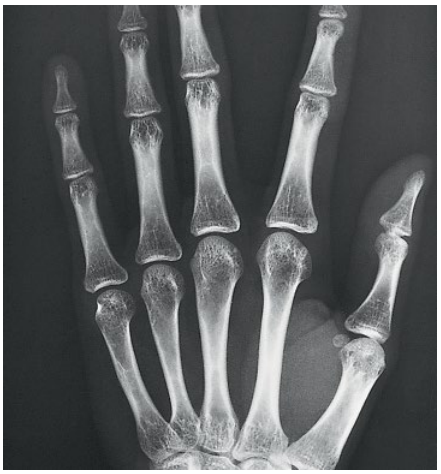

Fig. 9.22. β-Thalassemia major: Radiograph of the hand of a 19-year-old man. The estimated bone age is 14 years and there is failure of epiphyseal closure. Widening of the marrow cavity and thinning of trabeculae and cortex are also seen.

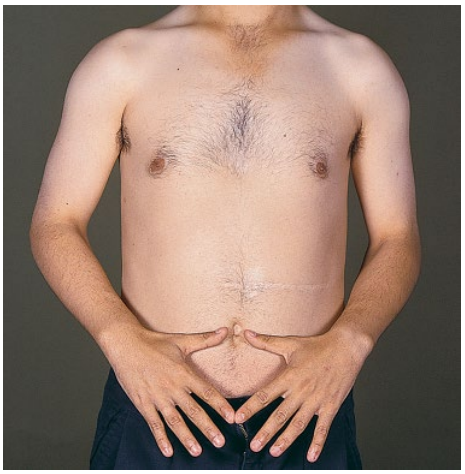

Fig. 9.23. β-Thalassemia major: Shortening of the upper arms because of premature epiphyseal closure of the humeral heads.

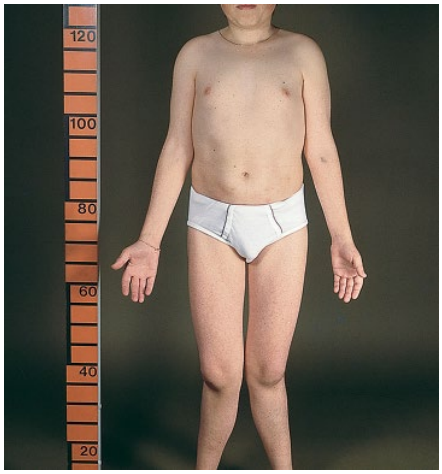

Fig. 9.24. β-Thalassemia major: Genu valgum deformity.

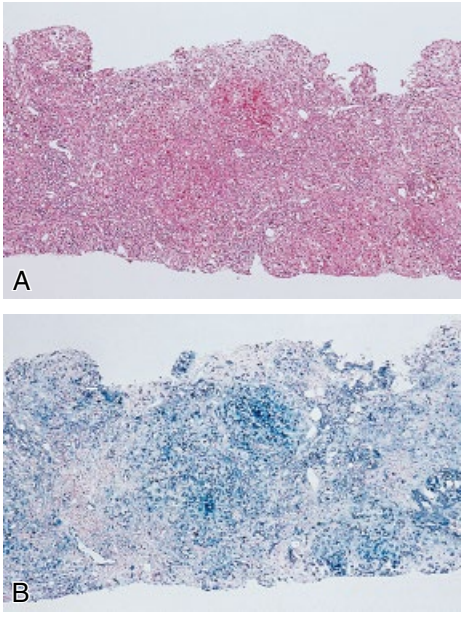

Fig. 9.25. β-Thalassemia major. **A,** Needle biopsy of the liver showing disturbances of normal architecture with fibrosis in portal tracts and nodular regeneration of hepatic parenchymal cells. (H&E.) **B,** Grade IV siderosis with iron deposition in the hepatic parenchymal cells, bile duct epithelium, macrophages, and fibroblasts. (Perls' stain.)

(Fig. 9.33), or spinal platyspondyly in some cases with intervertebral calcification (Fig. 9.34), which may be accompanied by reduced growth. Alternative orally acting iron chelators include 1,2-dimethyl-3-hydroxypyrid-4-one (deferiprone) and deferasirox (Fig. 9.35). Deferiprone is usually given three times daily. Side effects that have occurred include agranulocytosis, joint pains or effusions, and (rarely) zinc deficiency (Fig. 9.36). Deferasirox, which is given only once daily, causes mainly fecal iron excretion. Side effects include skin rashes and renal dysfunction.

Splenectomy may be needed to reduce transfusion requirements. Other supportive measures include folic acid, hepatitis immunization, and pneumococcal, hemophilus, and meningococcal immunization, plus regular prophylactic penicillin. Hormonal replacement therapy is needed in some cases, and calcium, vitamin D, and bisphosphonates for osteoporosis. Thalassemia major may also be cured by stem cell transplantation.

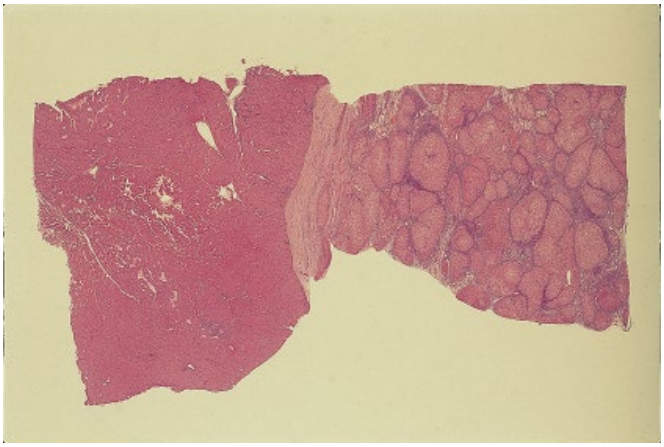

Fig. 9.26. β-Thalassemia major: Postmortem section taken from the liver of a 27-year-old male patient dying of hepatocellular carcinoma (on the *left*), with preexisting hepatic cirrhosis (on the *right*) and hepatitis C infection. (Courtesy of Dr. B Wonke.)

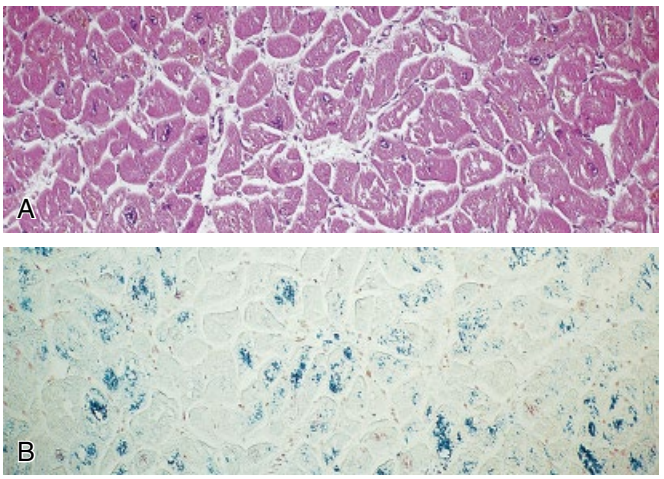

Fig. 9.27. β-Thalassemia major: Postmortem sections of myocardium seen by H&E **(A)** and Perls' staining **(B)**.The individual muscle fibers contain heavy deposits of iron pigment. In transfusional iron overload, iron deposition is most marked in the left ventricle (shown here) and interventricular septum.

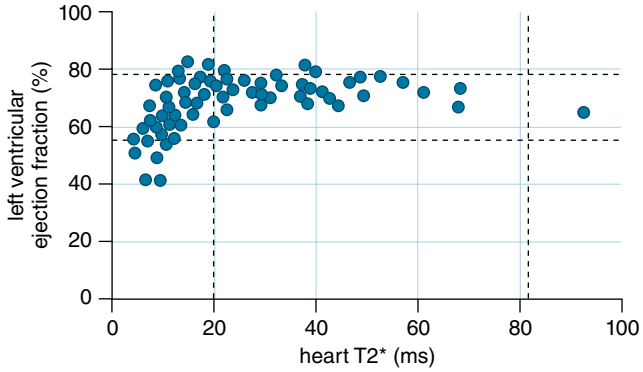

Fig. 9.28. Relationships of myocardial T_2* and left ventricular ejection fraction (LVEF) in patients with thalassemia major and iron overload. A T_2* relaxation time of <20 ms shows cardiac iron loading and <10 ms that this is severe. Some patients with T_2* <20 ms have subnormal LVEF, whereas in others this is normal. Source: Anderson LJ, et al. *Eur Heart J* 2001;22: 2171–2179. Reproduced with permission of Oxford University Press.

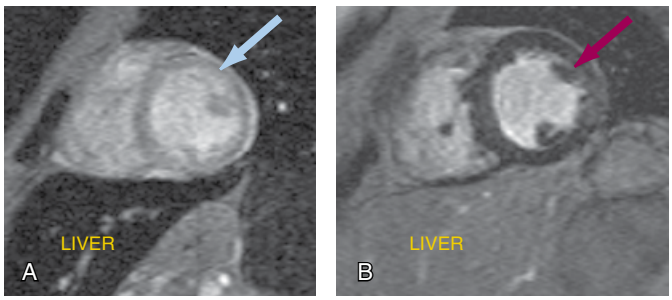

Fig. 9.29. T_2* MRI studies. Lack of correlation between heart and liver iron. **A,** Liver iron overload, myocardial iron appears normal. **B,** Myocardial iron overload, liver iron appears normal. For normal appearances see Fig. 6.9. (Courtesy of Professor DJ Pennell.)

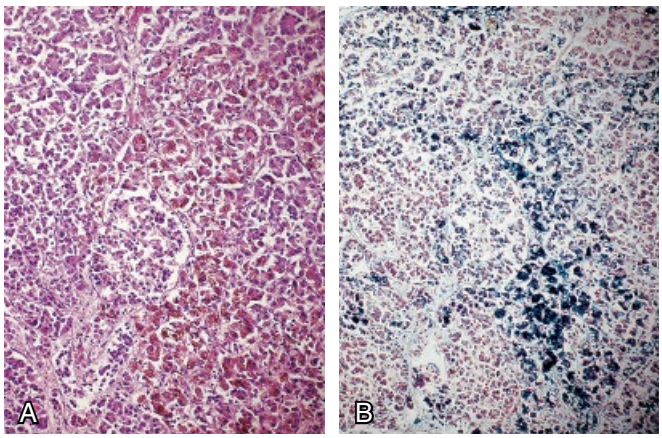

Fig. 9.30. β-Thalassemia major: Postmortem sections of pancreas. **A,** Pigment (hemosiderin and lipofuscin) in acinar cells, macrophages, and connective tissue, with less obvious pigment in the islet cells. (H&E.) **B,** Gross iron (hemosiderin) deposits in all cell types, particularly marked in the acinar cells. (Perls' stain.)

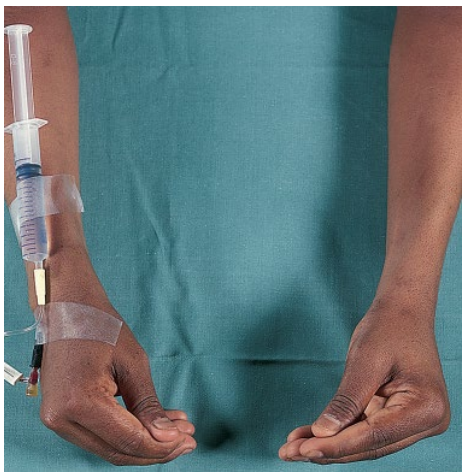

Fig. 9.31. β-Thalassemia major: Tetany (Trousseau sign) as a result of hypoparathyroidism caused by transfusional iron overload. An infusion of calcium is in progress. (Courtesy of Dr. B Wonke.)

β-THALASSEMIA INTERMEDIA (NONTRANSFUSION-DEPENDENT THALASSEMIA)

The causes of β-thalassemia intermedia (also termed nontransfusion-dependent thalassemia) are listed in Table 9.2. One form results from homozygous hemoglobin Lepore (Fig. 9.37) or heterozygous Lepore in conjunction with another β-chain abnormally. β-Thalassemia intermedia is compatible with normal growth and development (Fig. 9.38) but is characterized by bone deformities (Figs. 9.38 and 9.39), extramedullary hematopoiesis (Fig. 9.39), and iron overload. Ankle ulcers (Fig. 9.40), probably the result of anoxia caused by anemia and stasis of the local circulation, may arise as in thalassemia major, sickle cell anemia, and other hemolytic anemias.

Iron overload in thalassemia intermedia occurs because of increased absorption and blood transfusion and is treated by chelation. Luspatercept, a drug which acts as a ligand trap for GDF11 and other TGF-β family ligands is under trial for treatment. It is aimed at reducing ineffective erythropoiesis and promoting terminal differentiation of erythroblasts. Early results indicate that it raises the hemoglobin, reduces transfusion needs, and reduces iron loading.

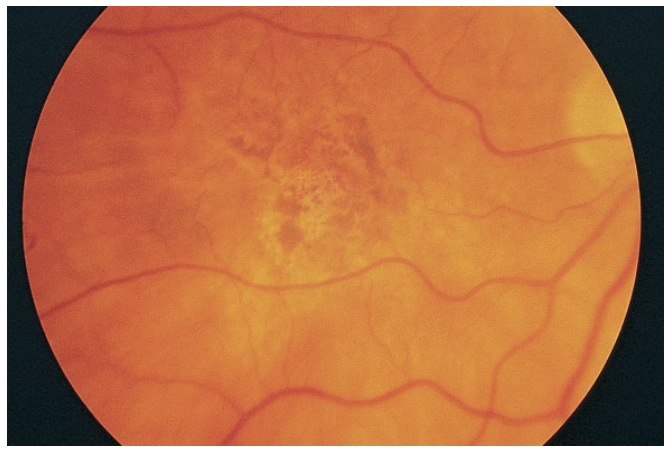

Fig. 9.32. Desferrioxamine toxicity: Optic fundus of a 78-year-old man with primary acquired sideroblastic anemia (myelodysplasia) and transfusional iron overload receiving desferrioxamine (2 g) subcutaneously daily and intravenously with blood transfusions. He complained of night blindness and loss of visual acuity. There is degeneration with hyperpigmentation of the macula.

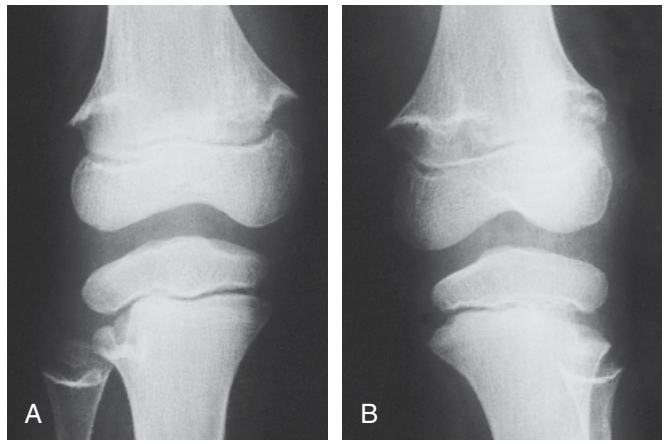

Fig. 9.33. Desferrioxamine toxicity. **A, B,** Pseudorickets in the knees of a child with β-thalassemia major who is receiving desferrioxamine therapy. There is flaring of the metaphyses and poor mineralization of the distal metaphyses with normal epiphyses. (Courtesy of Dr.V DeSanctis.)

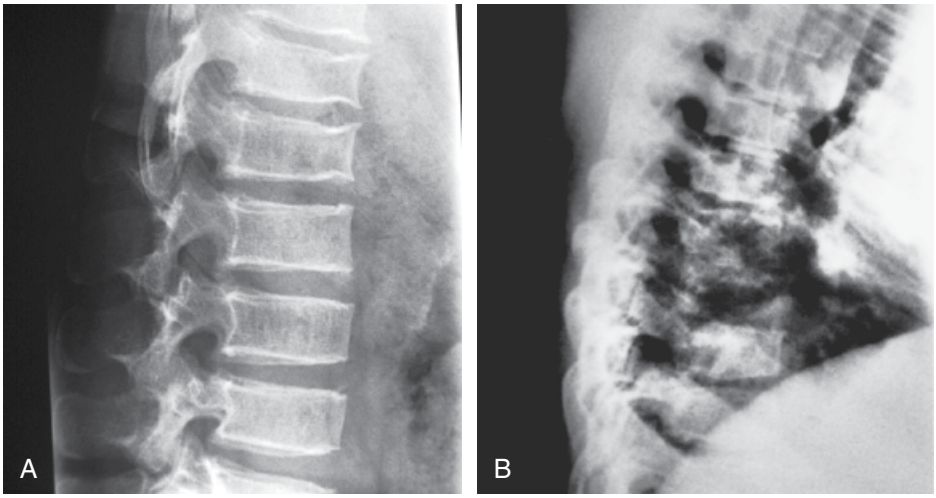

Fig. 9.34. Desferrioxamine toxicity: Platyspondyly of the spine. (Courtesy of Dr. P Tyler and *British Journal of Radiology* and of Dr. B Wonke.)

Fig. 9.35. Myelodysplastic syndrome: Urine samples without (yellow) and with chelation therapy for transfusional iron overload. Subcutaneous desferrioxamine has resulted in orange urine, whereas oral deferiprone has resulted in a darker, red urine.

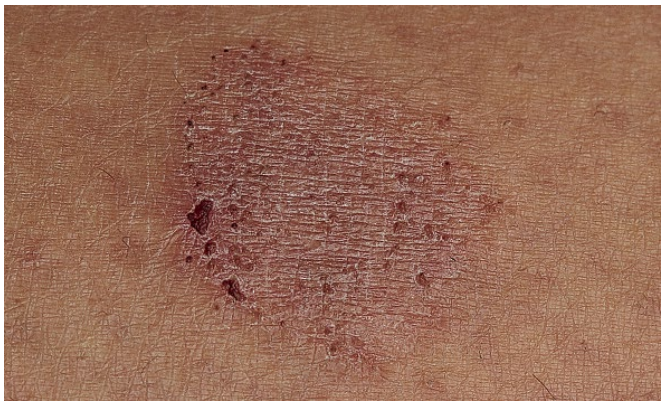

Fig. 9.36. Oral iron chelation: Zinc deficiency causing raised, dry, itchy scaling patch in a patient receiving deferiprone (L1) long term.

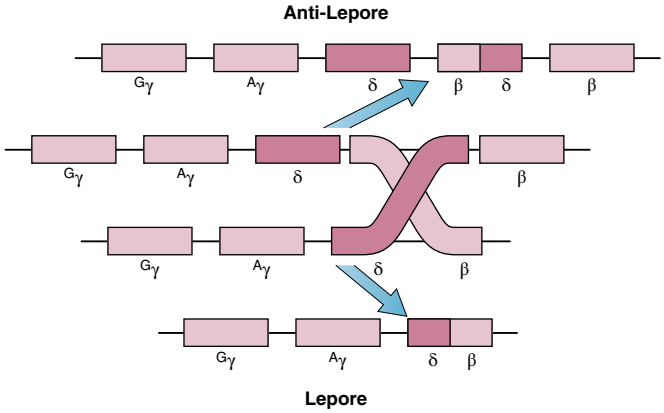

Fig. 9.37. Structure of hemoglobin Lepore and anti-Lepore, hemoglobin Kenya and anti-Kenya. These structural abnormalities are caused by crossing over of the δ- or γ- and β-globin genes at meiosis.

Fig. 9.38. β-Thalassemia intermedia: This 29-year-old Cypriot patient received occasional blood transfusions, with her hemoglobin ranging between 6.5 and 9.0 g/dL. She displays a thalassemic facies with marked maxillary expansion and also developed pigment gallstones. She has normal sexual development and fertility, as shown by her 2-year-old son.

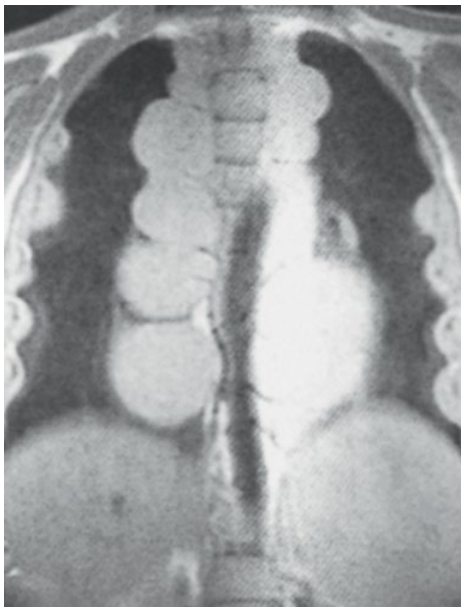

Fig. 9.39. β-Thalassemia intermedia: MRI scan from a 42-year-old Turkish patient with bossing of the skull bones, maxillary expansion, and splenomegaly (Hb, 9.7 g/dL; mean cell volume [MCV], 78 fL; mean cell hemoglobin [MCH], 23.5 pg; hemoglobin electrophoresis: HbF, 98%; HbA_2, 2.0%). The scan shows masses of extramedullary hematopoietic tissue arising from the ribs and in the paravertebral region without encroachment of the spinal cord.

β-THALASSEMIA TRAIT

In β-thalassemia trait there is a hypochromic microcytic blood picture with a high red cell count (>5.5×10^{12}/L; Fig. 9.41) and raised HbA_2 percentage on hemoglobin electrophoresis.

β-THALASSEMIA WITH A DOMINANT PHENOTYPE

β-Thalassemia with a dominant phenotype refers to a subgroup of β-thalassemias that result in a thalassemia intermedia phenotype in individuals who have inherited only a single copy of the abnormal β gene. Usually mutations affect exon 3 of the β-globin gene (Fig. 9.42). There is production of long unstable β-globin gene protein, which, together with excess α chains, produces inclusions in normoblasts and red cells. The clinical features are those of a severe dyserythropoietic anemia associated with splenomegaly. The inclusion bodies are seen in the bone marrow and in peripheral red cells after splenectomy (Fig. 9.43).

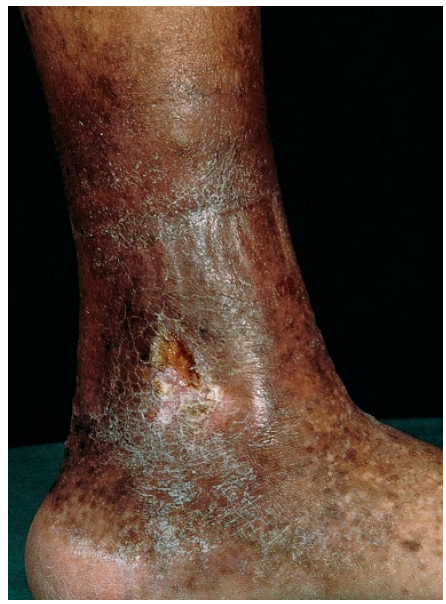

Fig. 9.40. β-Thalassemia intermedia: Ankle ulcer above the lateral malleolus.

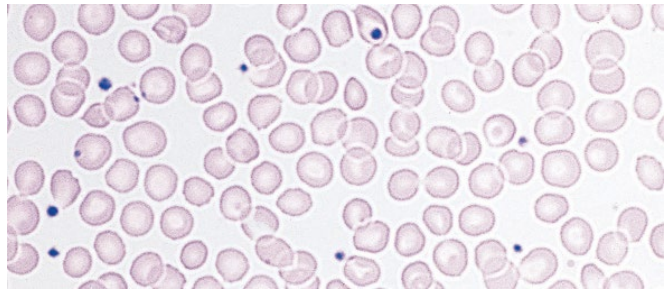

Fig. 9.41. β-Thalassemia trait: Peripheral blood film from a 20-year-old Cypriot woman shows microcytic hypochromic red cells with occasional target cells and poikilocytes. The red cell indices show a much reduced MCV (60.3 fL) and MCH (18.6 pg), despite the levels of the hemoglobin (10.8 g/dL) and packed cell volume (PCV, 35%) being only slightly below normal. The red cell count was raised to 5.81×10^{12}/L, and hemoglobin electrophoresis showed a raised HbA_2 (4.5%) with a normal HbF (0.9%).

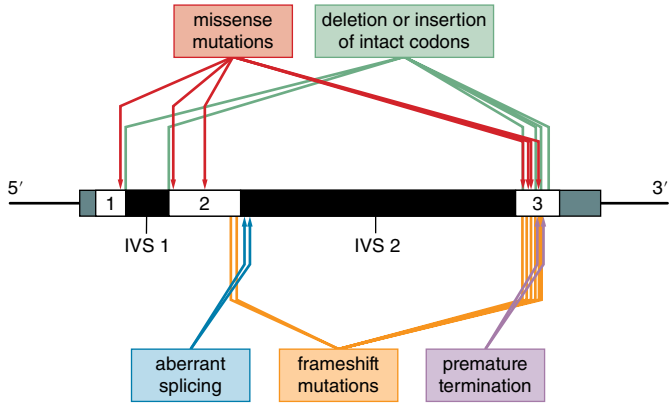

Fig. 9.42. β-Thalassemia with a dominant phenotype. (Courtesy of Professor SL Thein.)

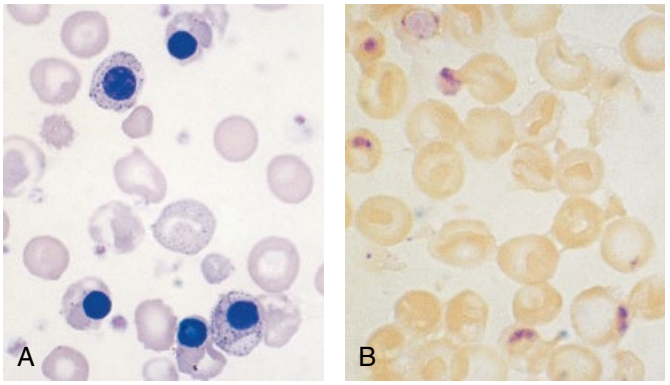

Fig. 9.43. β-Thalassemia with a dominant phenotype: Peripheral blood post-splenectomy. **A,** May-Grünwald–Giemsa stain showing target cells, irregular contracted cells, punctate basophilia, and numerous erythroblasts. **B,** Methyl violet stain showing inclusion bodies (pink) caused by precipitated α-globin chains. (Courtesy of Professor SL Thein.)

A spectrum of different mutations underlying these dominantly inherited forms of β-thalassemia have been identified, and it is now clear that the phenotype of these disorders overlaps both the β-thalassemias and the unstable hemoglobin variants.

ANTENATAL DIAGNOSIS

If both parents are carriers of β-thalassemia or other genetic defects likely to lead to a severe hemoglobin defect in the child, fetal diagnosis is carried out. Initially it was performed using fetoscopy to obtain fetal blood and measuring the α/β-chain synthesis ratio. It is now carried out by amniocentesis or trophoblast biopsy to obtain DNA for analysis by one of the polymerase chain reaction (PCR) techniques (Figs. 9.44–9.46).

α-THALASSEMIA

α-Thalassemia results from deletion or inactivation of one or more of the four α-globin genes (Fig. 9.47). The α-thalassemias are classified according to the number of genes affected.

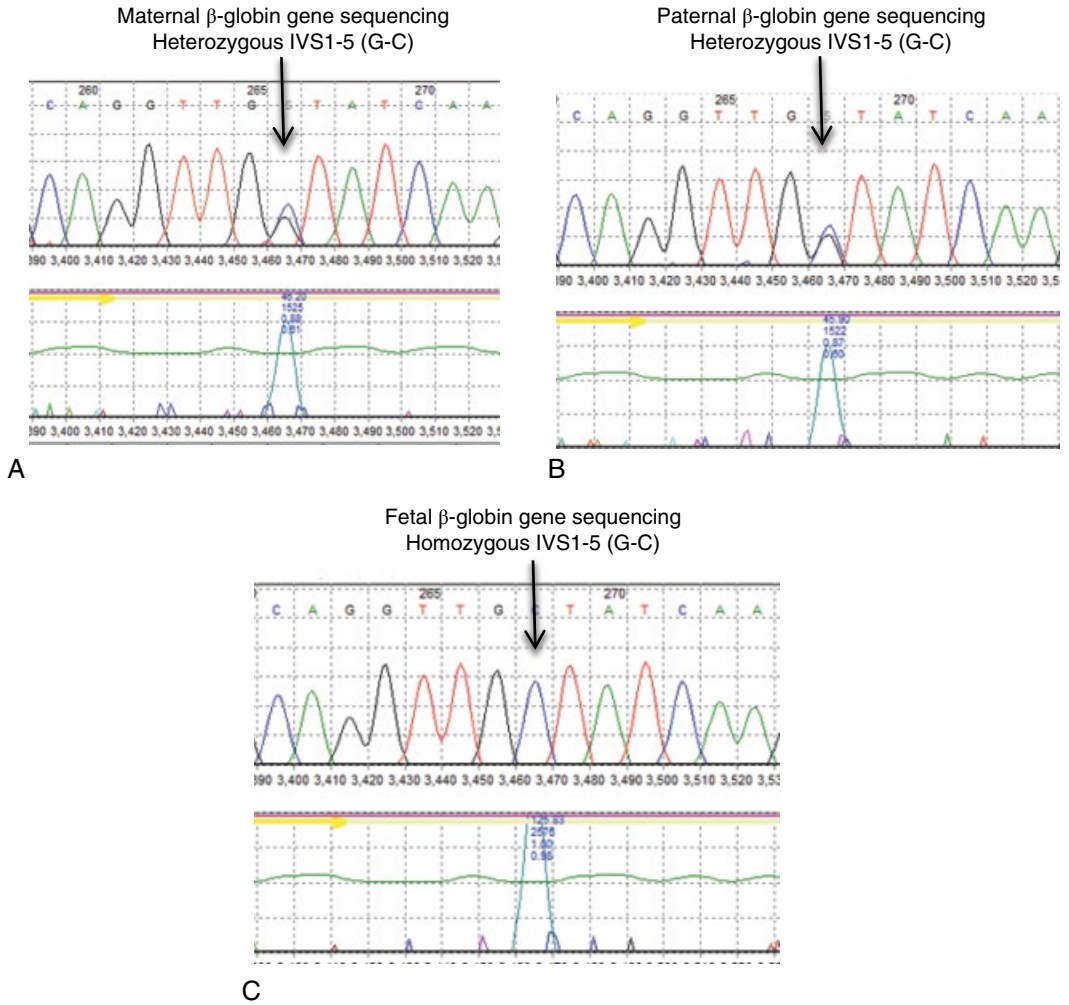

Fig. 9.44. β-Thalassemia: Prenatal diagnosis by Sanger (dideoxy) DNA sequencing. **A, B,** Sanger sequencing of the maternal and paternal β-globin genes shows that both parents are carriers of the severe β^+-thalassemia mutation IVS1–5 (G–C) (HBB:c.92+5G>C). This mutation greatly reduces the efficiency of splicing of the normal 5′ splice site for intron 1 in the β-globin gene. **C,** The fetus has inherited the mutation from both its parents and is therefore homozygous for IVS1–5 (G–C). The fetus is therefore predicted to be affected with β-thalassemia major. (Courtesy Dr. Shirley Henderson and Dr. Deborah Hay, National Reference Hemoglobinopathy Laboratory, Oxford.)

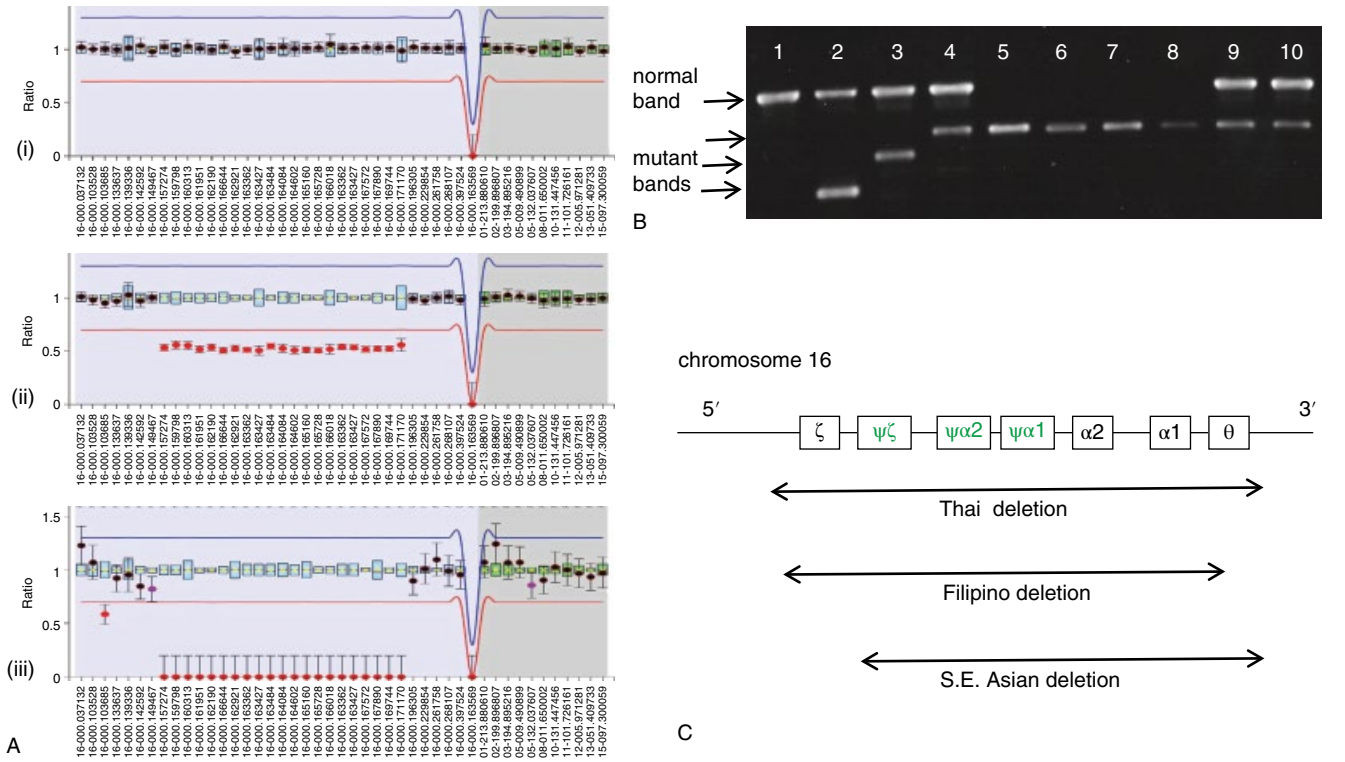

Fig. 9.45. α-Thalassemia: Prenatal diagnosis by multiplex ligation-dependent probe amplification (MLPA) and gap-PCR. **A,** MLPA analysis of the α-globin gene cluster in (i) a normal individual, (ii) an individual heterozygous for the Southeast Asian α^0-thalassemia deletion mutation, and (iii) a fetus with Bart's hydrops fetalis. MLPA is a multiplex PCR method for detecting chromosomal DNA copy number changes in multiple targets. The method depends on the hybridisation of multiple probes against the target DNA which are subsequently ligated and amplified. Amplification only occurs if the target DNA is present in the sample. The quantity of PCR product produced is proportional to the amount of target DNA present in the sample. The results are analyzed using PCR peak height analysis software. In analysis (i) each black ellipse represents a probe with a different target over the gene cluster, whereas in analysis (ii) red ellipses specify probes from which the PCR amplification has been reduced by 50% indicating the presence of a heterozygous deletion. Finally the red ellipses in analysis (iii) designate probes from which PCR amplification is absent, indicating the presence of a homozygous deletion mutation. **B,** Analysis of fetal and parental DNA for α-thalassemia deletion mutations by gap-PCR. Lane 1: normal control, lane 2: heterozygous Thai deletion control, lane 3: heterozygous Filipino deletion control, lane 4: heterozygous Southeast Asian deletion control. Lanes 5–8: serial dilutions of fetal DNA showing homozygosity for the Southeast Asian deletion, indicating the fetus is affected with Bart's hydrops fetalis. Lanes 9 and 10: Maternal and paternal DNA showing heterozygosity for the Southeast Asian deletion mutation. PCR primers are designed which flank the deletion being tested for. If the deletion is present then a PCR product will be obtained. If it is absent then the primers will be too far apart for successful amplification and no PCR product will be produced. A primer pair with target sequence located within the boundaries of the deletion is also included to confirm the presence or absence of normal sequence. **C,** α-Globin gene cluster on chromosome 16, showing the positions of the three common α^0 deletion mutations (Thai, Filipino, and Southeast Asian), all of which completely remove the α1- and α2-globin genes. (Courtesy Dr. Shirley Henderson and Dr. Deborah Hay, National Reference Hemoglobinopathy Laboratory, Oxford.)

There is duplication of the α-globin genes. In the α^0 lesion, both α genes on one chromosome are deleted or ineffective; in the milder α^+ lesion, only one of the two genes is deleted or defective (Fig. 9.47).

The gene deletions that produce α-thalassemia are shown in Fig. 9.48. In its most severe form, in which all four genes are deleted, α-thalassemia is incompatible with life and the fetus is stillborn or critically ill with hydrops fetalis (Fig. 9.49). The blood shows gross hypochromasia and erythroblastosis (Fig. 9.50).

Deletion of three α-globin genes (hemoglobin H disease) manifests as a moderately severe anemia (Hb, 7.0–11.0 g/dL) with splenomegaly and a hypochromic, microcytic blood film appearance (Fig. 9.51). Hemoglobin H (β4) is demonstrable by special staining (Fig. 9.52) or hemoglobin electrophoresis.

α-Thalassemia trait may be caused by deletion of two genes (α^0 trait). The α^+ trait may result from deletion of one of the pair of linked α-globin genes. In others both α genes are present, but one has a mutation or other genetic effect that partly or completely inactivates it. α-Thalassemia trait shows a hypochromic, microcytic blood appearance of varying severity in adults. At birth, as much as 5–15% of Hb Bart's (γ4) may be detected in α^0 trait and up to 2% in α^+ trait. In α^0 trait, an occasional cell in the adult blood film may show HbH bodies after incubation with a dye such as brilliant cresyl blue.

X-LINKED α-THALASSEMIA AND MENTAL RETARDATION SYNDROME

The X-linked α-thalassemia and mental retardation (ATR-X) syndrome is characterized by a severe form of mental retardation associated with characteristic dysmorphic facies (Fig. 9.53A), genital abnormalities, and an unusual, mild form of HbH disease. In comparison with α-thalassemia caused by deletions or point mutations in the α-globin cluster on chromosome 16p13.3, hypochromia and microcytosis are less prominent and, in some affected individuals, the red cell indices may fall in the normal range. Red cells with HbH inclusions can be demonstrated after incubation at room temperature in 1% brilliant cresyl blue solution. The frequency of such cells varies widely (0.001–40% red cells).

Carrier females are of normal appearance and intelligence. About 25% may exhibit very rare HbH inclusions, and this

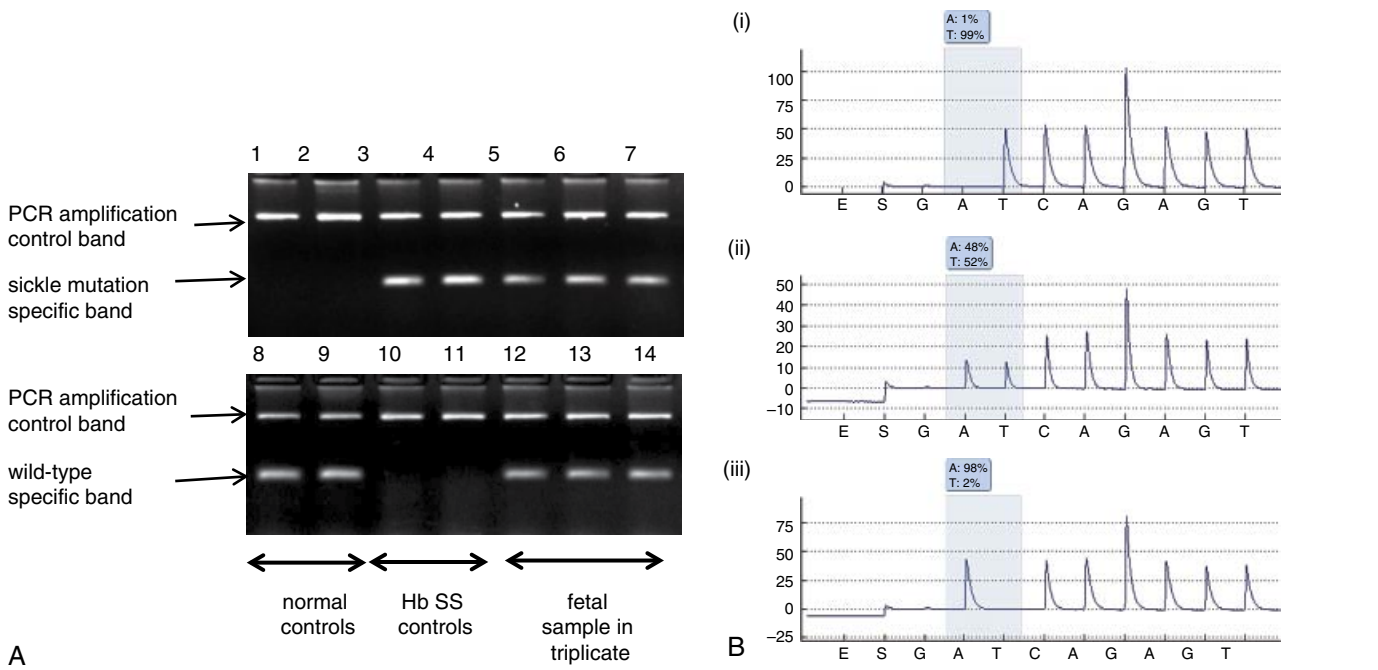

Fig. 9.46. Sickle cell disease: Prenatal diagnosis by amplification refractory mutation system (ARMS) PCR and pyrosequencing. **A,** ARMS PCR. The fetal DNA is tested using two template-specific PCR primers, one of which is complementary to the sickle mutation (Glu>Val at codon 6 of the β-globin gene HBB:c.20A>T) and the other is complementary to the wild-type allele. DNA amplification will only occur from the sickle primer when the sickle mutation is present and from the wild-type primer when the wild-type allele is present. All reactions include a primer pair designed to control for PCR amplification. Lanes 1–7: results using the sickle mutation-specific primer; lanes 8–14: results using the wild-type specific primer. Normal control lanes show the wild-type amplification band only. Hb SS control lanes show the sickle amplification band only. Fetal DNA sample in triplicate showing sickle and wild-type amplification bands which indicate the fetus is a sickle cell carrier. **B,** Pyrosequencing. Three pyrograms showing sequencing (reverse primer) of the sickle mutation site and nearby nucleotides. (i) Normal sequence at the sickle mutation site. (ii) Heterozygous substitution of an A for a T nucleotide, indicating sickle carrier status. (iii) Homozygous substitution of an A for a T nucleotide, indicating sickle disease status. (Courtesy Dr. Shirley Henderson and Dr. Deborah Hay, National Reference Hemoglobinopathy Laboratory, Oxford.)

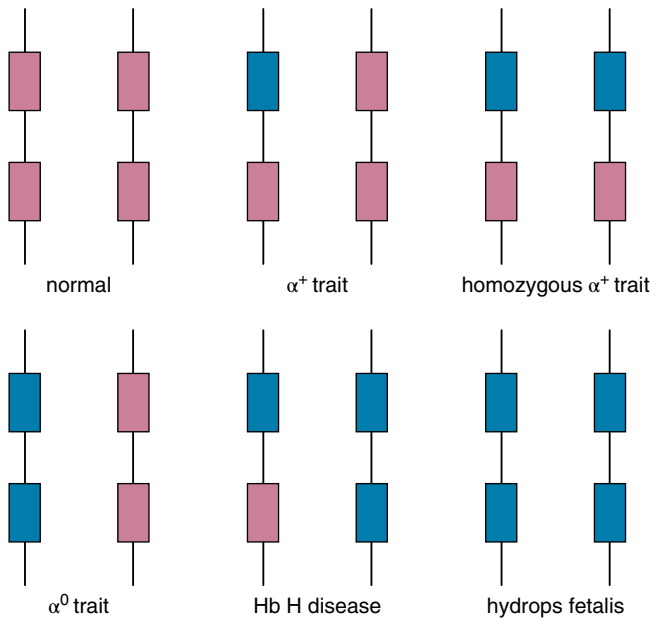

Fig. 9.47. The different types of α-thalassemia. The purple boxes represent normal genes, and the gray boxes represent gene deletions or partially or completely inactivated genes.

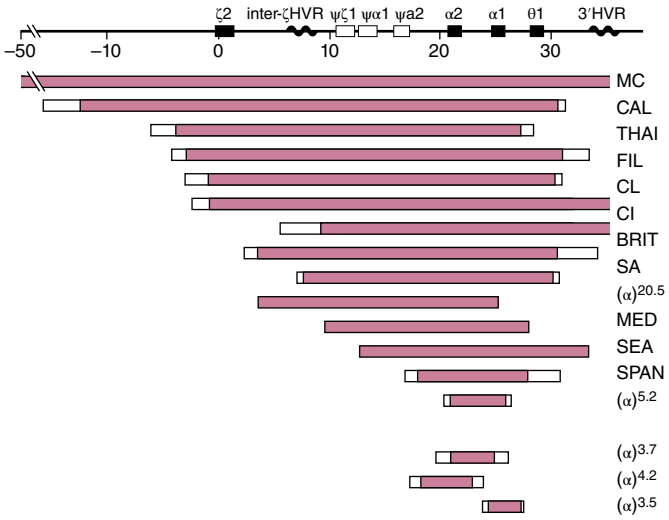

Fig. 9.48. The deletions that produce α-thalassemia. The missing DNA is indicated by black lines. α^0-Thalassemia results from deletion of both linked α-globin genes or mutations that completely inactivate both (not shown). α^+-Thalassemia results from either deletion of one of the pair of linked α-globin genes or from a mutation that inactivates one of them partly or completely. One mutation affects the chain termination codon TAA and results in an elongated α chain (hemoglobin constant spring), which is synthesized at a slower rate than normal. (Courtesy of Professor DJ Weatherall.)

reflects the very skewed pattern of X inactivation present, with the disease-bearing X chromosome being preferentially inactive.

The disease gene usually responsible for the syndrome has been identified and maps to Xq13.3. It is called the *ATRX* gene

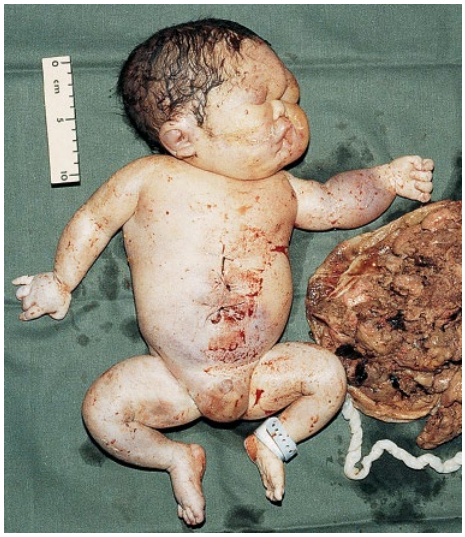

Fig. 9.49. α-Thalassemia: Hydrops fetalis, the result of deletion of all four α-globin genes (homozygous α^0-thalassemia). The main hemoglobin present is Hb Bart's (γ4). The condition is incompatible with life beyond the fetal stage. (Courtesy of Professor D Todd.)

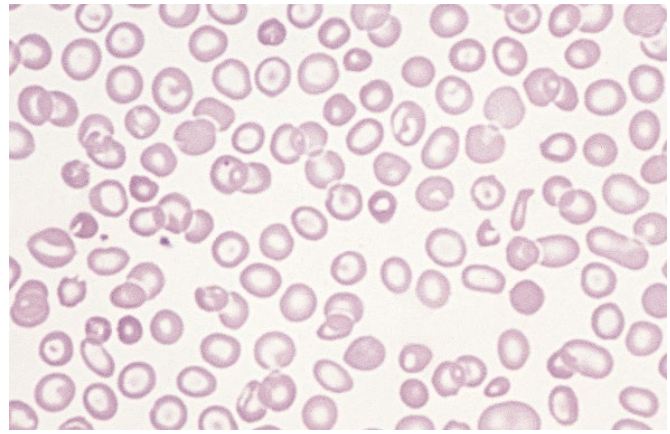

Fig. 9.51. α-Thalassemia: Peripheral blood film in hemoglobin H disease (three α-globin gene deletion or α^0/α^+-thalassemia) shows marked hypochromic and microcytic cells with target cells and poikilocytes. The patient was a normally developed 23-year-old man with a spleen enlarged to 6 cm below the costal margin, moderate anemia (Hb, 9.9 g/dL), and grossly reduced red cell indices. (MCV, 59 fL; MCH, 19 pg.) Electrophoresis showed HbA, 76.6%; HbA_2, 2.5%; HbF, 0.9%; HbH (β4), 20%.

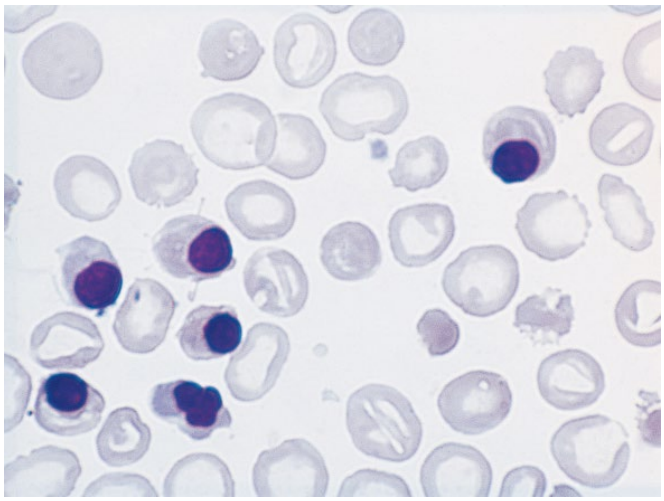

Fig. 9.50. α-Thalassemia: Peripheral blood film in homozygous α^0-thalassemia (hydrops fetalis) at birth shows marked hypochromasia, polychromasia, and many circulating erythroblasts.

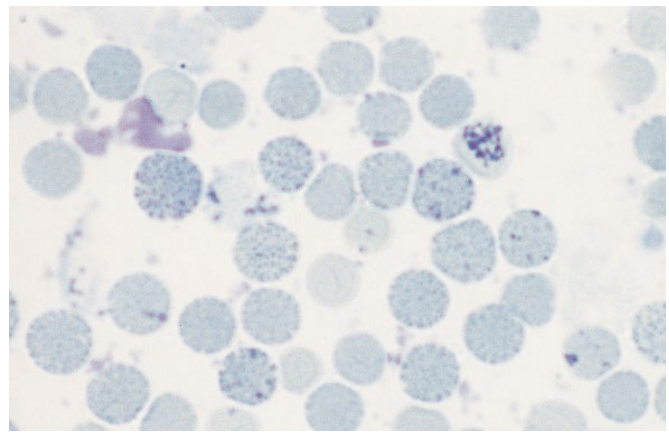

Fig. 9.52. α-Thalassemia: Peripheral blood film in hemoglobin H disease stained supravitally with brilliant cresyl blue. Some of the cells show multiple, fine, deeply staining deposits, which are precipitated aggregates of β-globin chains (Hb β4) ("golf ball" cells). Reticulocytes are also stained.

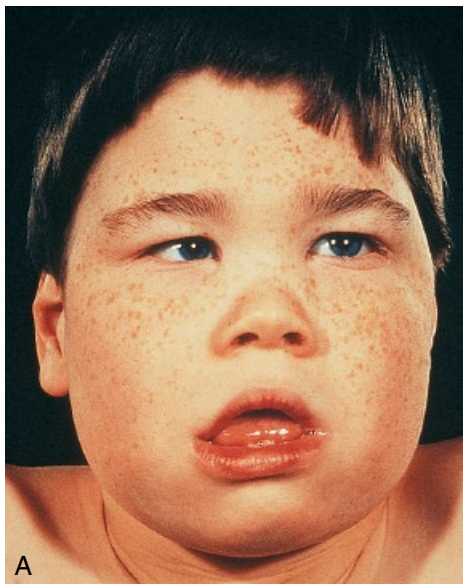

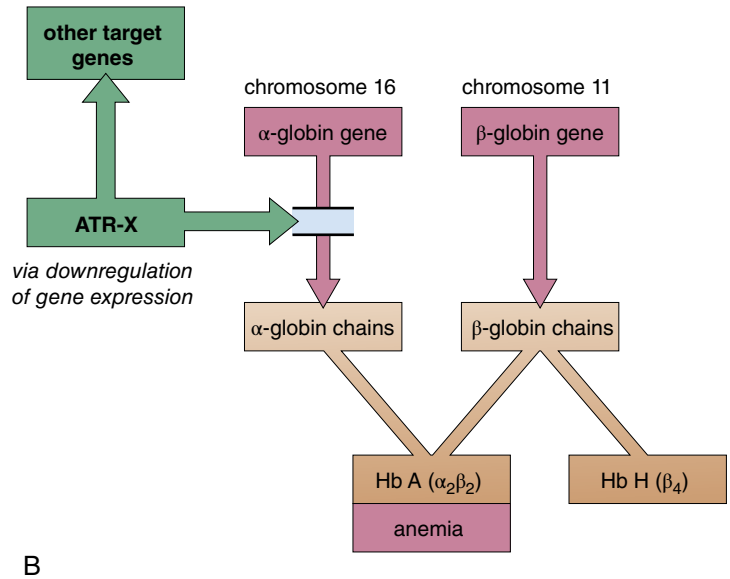

Fig. 9.53. A, α-Thalassemia/mental retardation syndrome: Boy with characteristic dysmorphic facies. **B,** Action of ATR-X (see text) on expression of α-globin and other genes. (Courtesy of Professor DR Higgs.)

and is a member of a family of proteins (SWI/SNF) with ATPase and putative helicase activity. Members of this group have a wide range of functions, but it is thought that they all act by interaction with chromatin. It seems likely that ATR-X acts on its target genes (including α-globin) as a transcriptional regulator (Fig. 9.53B).

STRUCTURAL HEMOGLOBIN VARIANTS

SICKLE CELL ANEMIA

Sickle cell anemia is the most common of the severe structural hemoglobin variants (Table 9.3). It is the result of substitution of valine for glutamic acid in the sixth position of the β chain, caused by a single base change (adenine to thymine) in the corresponding portion of DNA. Sickle hemoglobin (HbS) is insoluble at low oxygen partial pressures and tends to crystallize (Fig. 9.54), which causes the red cells to assume a sickle-like appearance. The oxygen is given up to tissues relatively easily because the oxygen dissociation curve is shifted to the right (Fig. 9.55).

The patient has few symptoms of anemia, despite a hemoglobin level in the steady state of 6–8 g/dL, and has a chronic hemolytic anemia punctuated by sickle crises. Typically, the patient is of asthenic build (Fig. 9.56) and is mildly jaundiced. Ulcers around the ankle are common (Fig. 9.57).

Bone deformities may be present (Figs. 9.58–9.60). If the small bones of the hands and feet are affected, there may be unequal growth of the digits ("hand-foot" syndrome; Figs. 9.61 and 9.62) due to infarcts to the epiphyses in infancy (Fig 9.63).

As a result of infections together with infarcts, pneumonia (Fig. 9.64) may occur. It may be difficult to distinguish from the chest syndrome caused by blockage of small vessels and fat embolism from infarcted bones, especially the ribs (Fig. 9.65). A ventilation–perfusion scan may help (Fig. 9.66). The central nervous system may be damaged by infarction. Transcranial Doppler studies may help determine the risk of a stroke by

TABLE 9.3. STRUCTURAL HEMOGLOBIN VARIANTS

Sickle syndromes
Sickle cell (SS) anemia
Sickle cell/hemoglobin C (SC)
Sickle cell/hemoglobin D (SD)
Sickle cell/β-thalassemia
Hemolytic anemia
Unstable hemoglobin
Polycythemia
High oxygen affinity hemoglobin
Congenital cyanosis
Hemoglobin M
Low oxygen affinity hemoglobin variants
Thalassemia syndromes
Hemoglobin Lepore
Chain-termination hemoglobins, variants (e.g. Hb constant spring)
Some unstable hemoglobins
Variants with inefficient synthesis due to alternative splicing (e.g. HbE)
Drug-induced hemolysis (e.g. Hb Zurich)

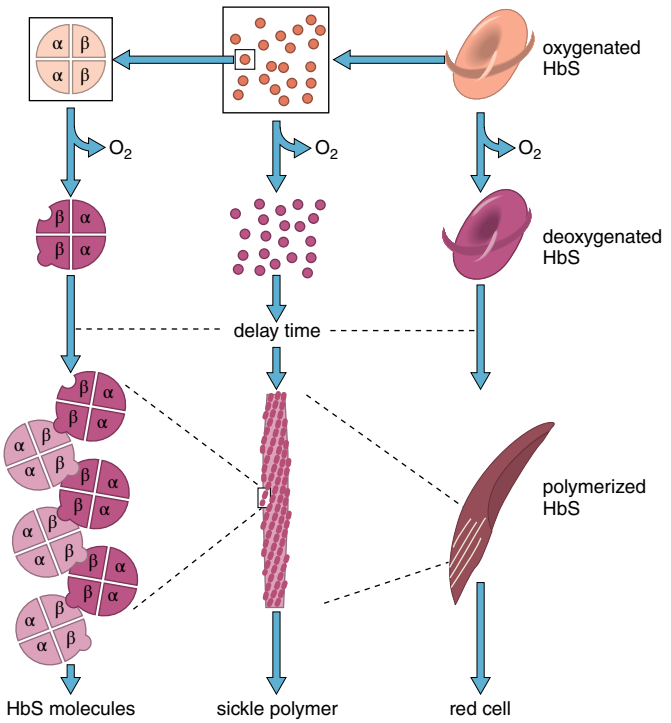

Fig. 9.54. Sickle cell anemia: Pathophysiology. Source: Bunn HF. *N Engl J Med* 1997;337:762. Reproduced with permission of Massachusetts Medical Society: *The New England Journal of Medicine*.

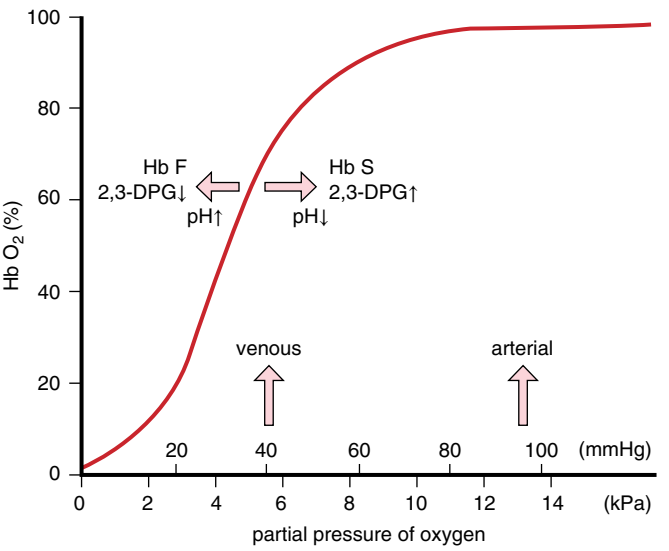

Fig. 9.55. Hemoglobin–oxygen dissociation. Normal sigmoid curve relating hemoglobin saturation to the partial pressure of oxygen (PaO_2) to which it is exposed. The curve is shifted to the left (less oxygen is released at any given PaO_2) by a fall in 2,3-DPG, by a rise in pH (Bohr effect), or if HbA is replaced by HbF or by a high-affinity Hb. The curve is shifted to the right by a rise in 2,3-DPG attached to the Hb, by a fall in pH, if HbA is replaced by HbS or an HbM (in which the heme iron is stabilized in the ferric form), or if the Hb is oxidized to methemoglobin.

showing increased blood flow due to arterial stenosis (Fig. 9.67). Silent cerebral infarcts are frequent in young children. These may be detected by MRI (Fig. 9.68). Ischemic damage in the brain occurs as a result of stenosis or occlusions of vessels in the circle of Willis and internal carotid arteries (Fig. 9.69). Sometimes moyamoya deformation with multiple small vessels in a damaged

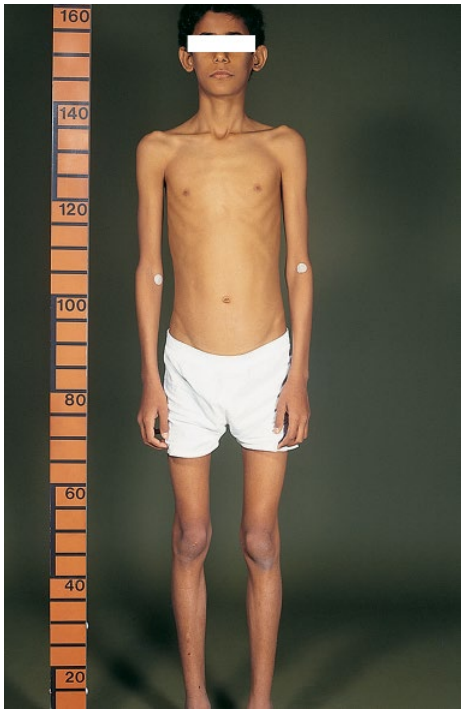

Fig. 9.56. Sickle cell anemia: This patient of Middle Eastern origin is tall with long thin limbs, a large arm span, and narrow pectoral and pelvic girdles. Sexual development is normal.

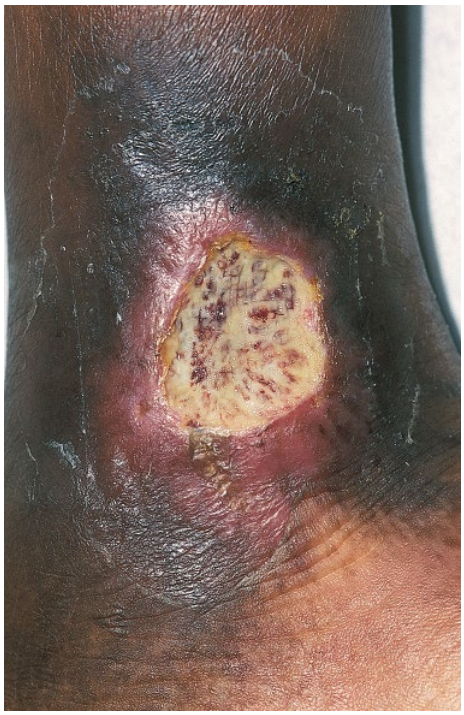

Fig. 9.57. Sickle cell anemia: Ulcer above ankle.

area of brain develops (Fig. 9.70). Osteomyelitis may also occur, usually from infection with *Salmonella* spp. (Fig. 9.71A), but sometimes from other organisms (Fig. 9.71B). Parvovirus infection may cause an "aplastic" crisis. Infarcts may also occur in the kidney, and papillary necrosis is particularly common (Fig. 9.72). Priapism is a common problem in males.

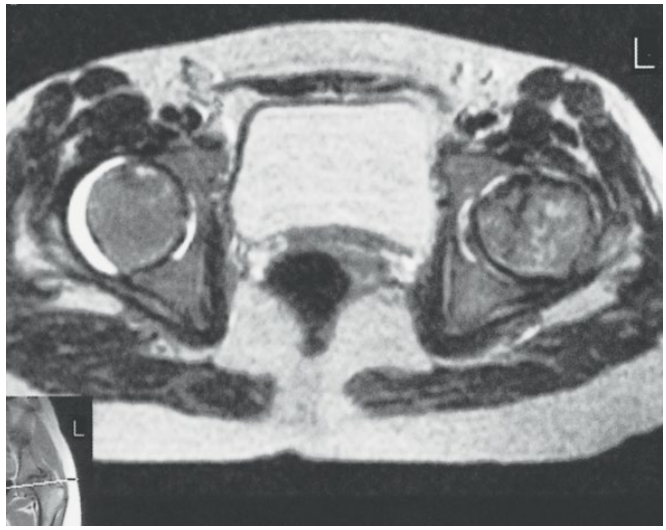

Fig. 9.58. Sickle cell/β-thalassemia: Axial T_2-weighted MRI scan of the hips of a 17-year-old female showing a small area of high signal in the anterior portion of the right hip with a low-intensity rim. This is typical of early avascular necrosis. The irregular outline and signal in the left hip results from more advanced avascular necrosis.

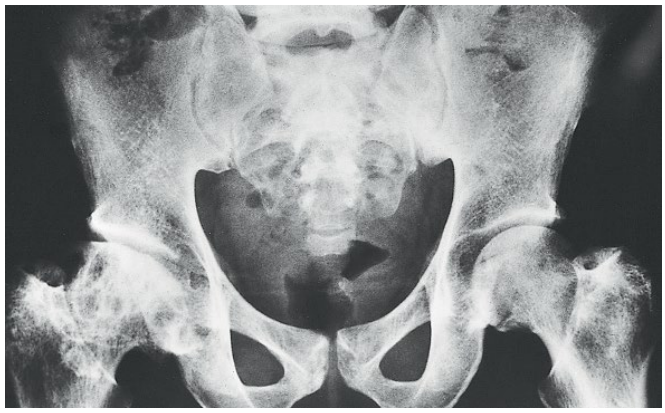

Fig. 9.59. Sickle cell anemia: Radiograph of the pelvis shows avascular necrosis with flattening of the femoral heads, more marked on the right; coarsening of the bone architecture; and cystic areas in the right femoral neck caused by previous infarcts.

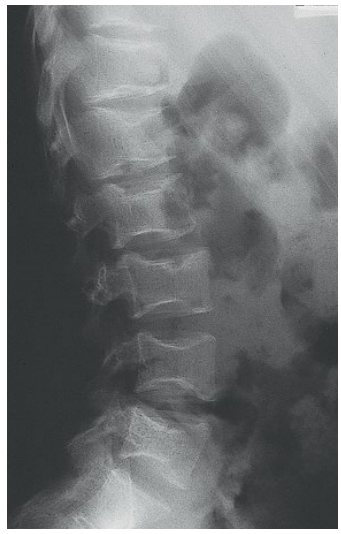

Fig. 9.60. Sickle cell anemia: Radiograph of spine showing "fish bone" deformity as a result of indentation of vertebral bodies by intervertebral discs.

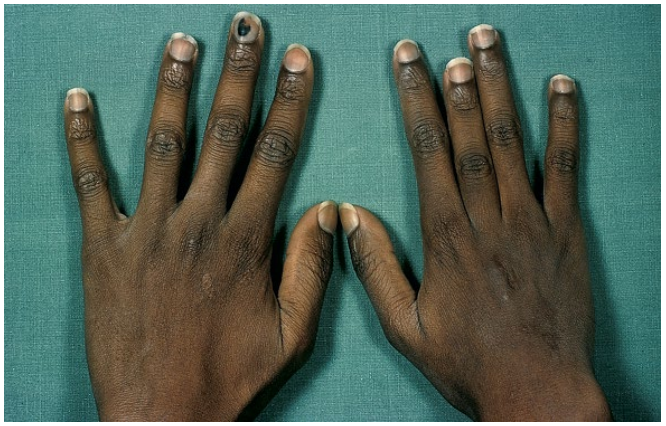

Fig. 9.61. Sickle cell anemia: Hands of an 18-year-old Nigerian male with the "hand-foot" syndrome. There is marked shortening of the right middle finger because the dactylitis in childhood affected the growth of the epiphysis.

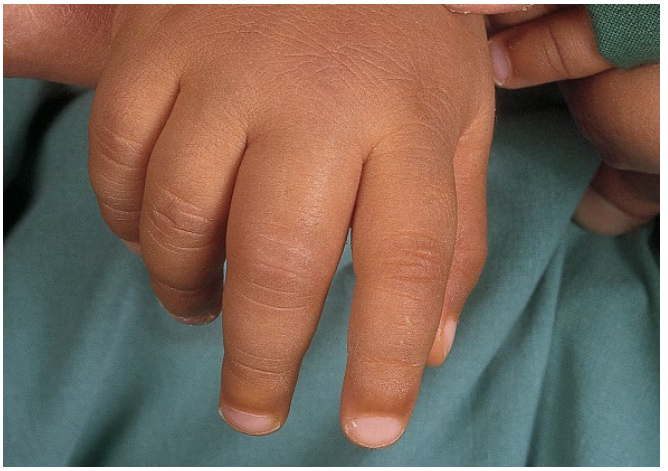

Fig. 9.63. Sickle cell anemia: Hand of an 18-month-old child with painful, swollen fingers (dactylitis) caused by infarction of the metacarpal bones of the index and ring fingers. This acute syndrome rarely occurs after 2 years of age.

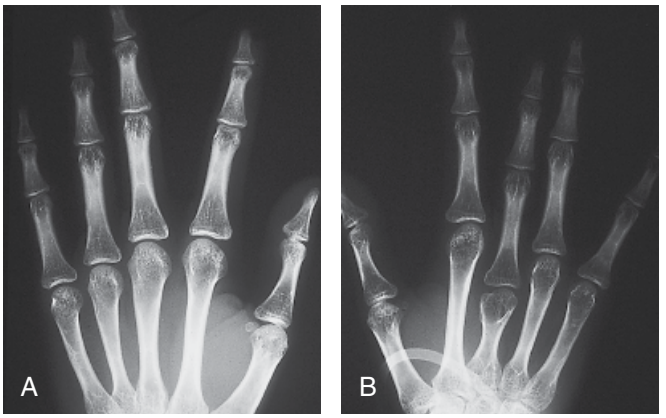

Fig. 9.62. Sickle cell anemia. **A, B,** Radiographs of the hands shown in Fig. 9.61. The right middle metacarpal bone is shortened because of infarction of the growing epiphysis during childhood. The patient was receiving intravenous rehydration during a painful crisis.

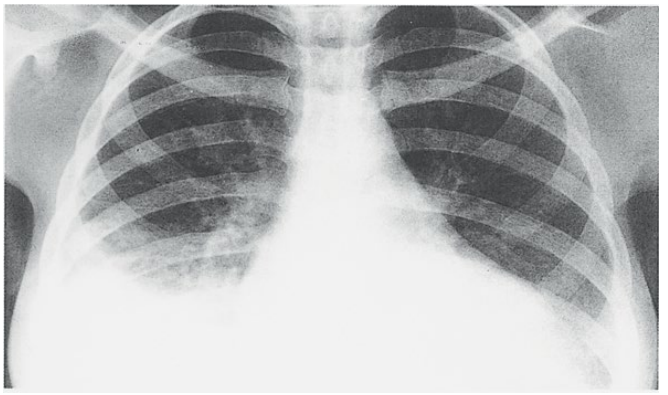

Fig. 9.64. Sickle cell anemia: Chest radiograph of an 18-year old female admitted in crisis with a pulmonary syndrome. There is generalized cardiomegaly and increased vascularity of the lungs, typical of a chronic hemolytic anemia. In addition, there is shadowing, particularly in the right lower and middle lobes, which resolved slowly on antibiotic therapy and was considered to result from infection and small vessel obstruction.

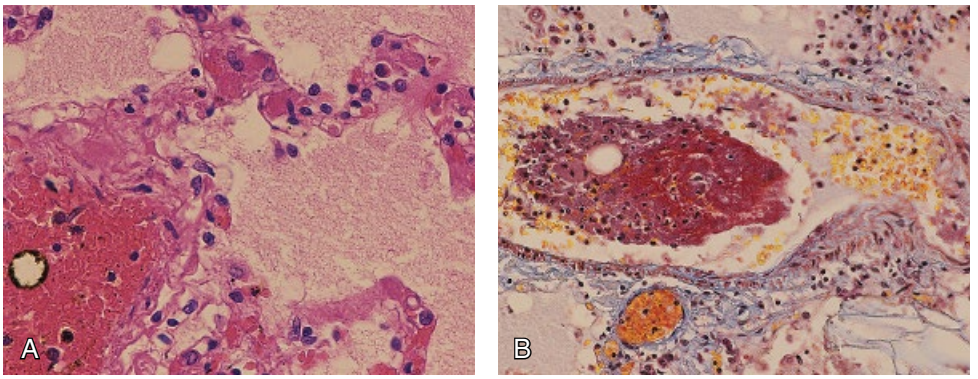

Fig. 9.65. Sickle cell anemia: Chest syndrome. High-power view of lung showing alveolar edema, fat embolism within an arteriole surrounded by sickle cells, and microthrombi in the alveolar capillaries. Fat embolism is the white nonstaining hole (from which fat has dissolved out in processing). (Courtesy of Professor S Lucas.)

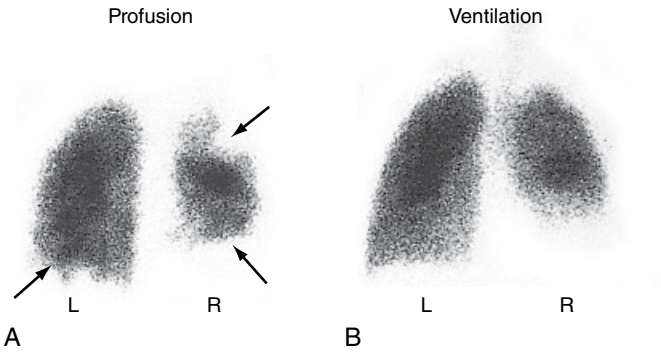

Fig. 9.66. Sickle cell anemia: Ventilation–perfusion lung scan of the patient in Fig. 9.64. **A,** Perfusion measured with technetium 99m-aggregated albumin (50 mm particles). **B,** Ventilation using krypton 81m. The ventilation defect at the base of the right lung (R) suggests infection only, but the multiple perfusion defects apparent in other areas of both lungs (arrows) suggest blockage of segmental and subsegmental arteries. (Courtesy of Dr. A Hilson.)

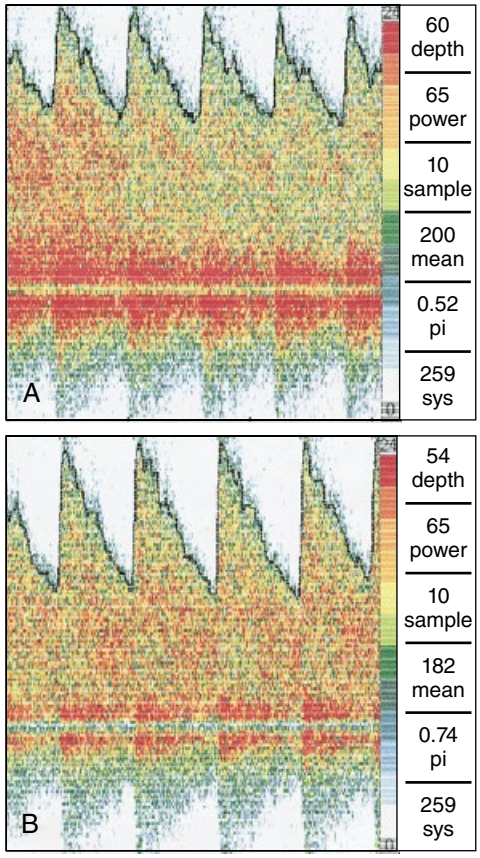

Fig. 9.67. Sickle cell anemia: sonograms obtained using a pulsed transcranial Doppler instrument from right **(A)** and left **(B)** middle cerebral arteries (MCAs) in an 11-year-old boy with sickle cell disease who had severe headaches but no neurologic signs. Maximum mean velocities in the right and left MCAs are 200 and 182 cm/s at depths of 6.0 and 5.4 cm, respectively. Although MRI was normal, magnetic resonance angiography showed bilateral turbulence, suggestive of stenosis in both MCAs. For patients with an MCA velocity >200 cm/s, the risk of stroke within 40 months is 40%; this child was therefore commenced on regular transfusions with resolution of his headaches. (Courtesy of Dr. JPM Evans and Dr. F Kirkham.)

Following occlusion of small vessels in the retina during sickle cell crises, there may be characteristic regrowth of blood vessels at the affected sites (Fig. 9.73). Infarction and atrophy of the spleen are usual after childhood. The blood film shows the presence of

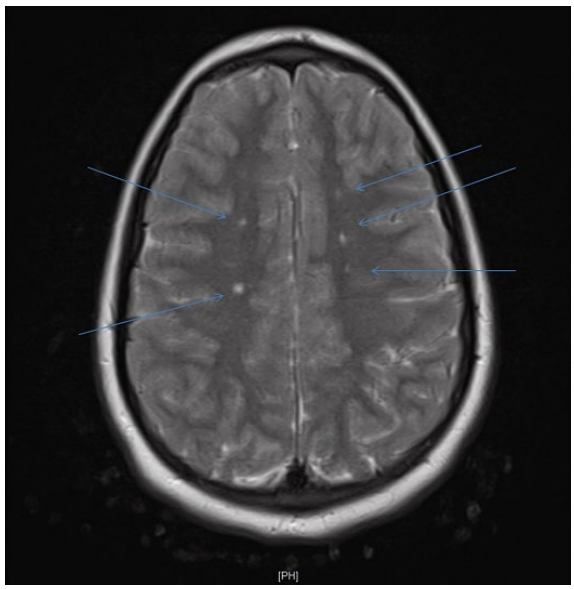

Fig. 9.68. Sickle cell anemia: T_2-weighted MRI of a 9-year-old girl with sickle cell anemia, showing five hyperintensities in the deep white matter (arrows), which are silent cerebral infarcts. (Courtesy Dr. David Rees, Kings College Hospital.)

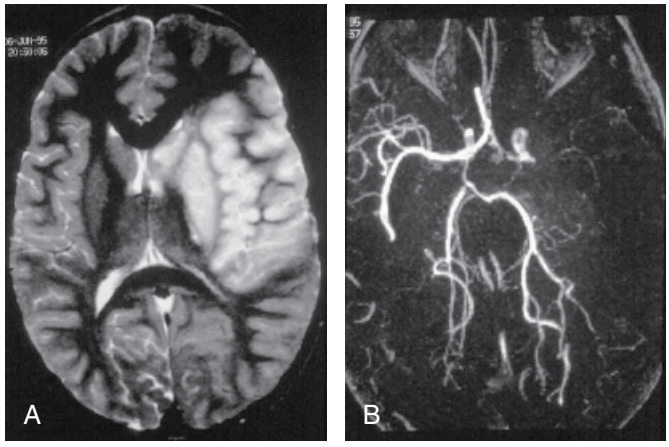

Fig. 9.69. Sickle cell anemia: Right-sided frontal and temporal lobe infarction due to blocked middle cerebral artery. **A,** T_2-weighted MRI; **B,** MR angiogram.

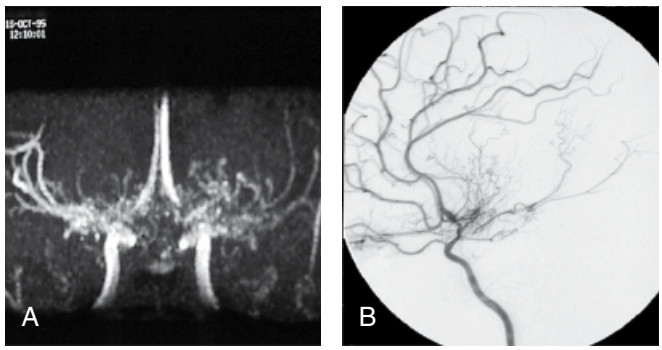

Fig. 9.70. Sickle cell anemia: Moyamoya arterial deformation. There is revascularization with small vessels after a major arterial occlusion. **A,** MR angiogram; **B,** carotid angiogram.

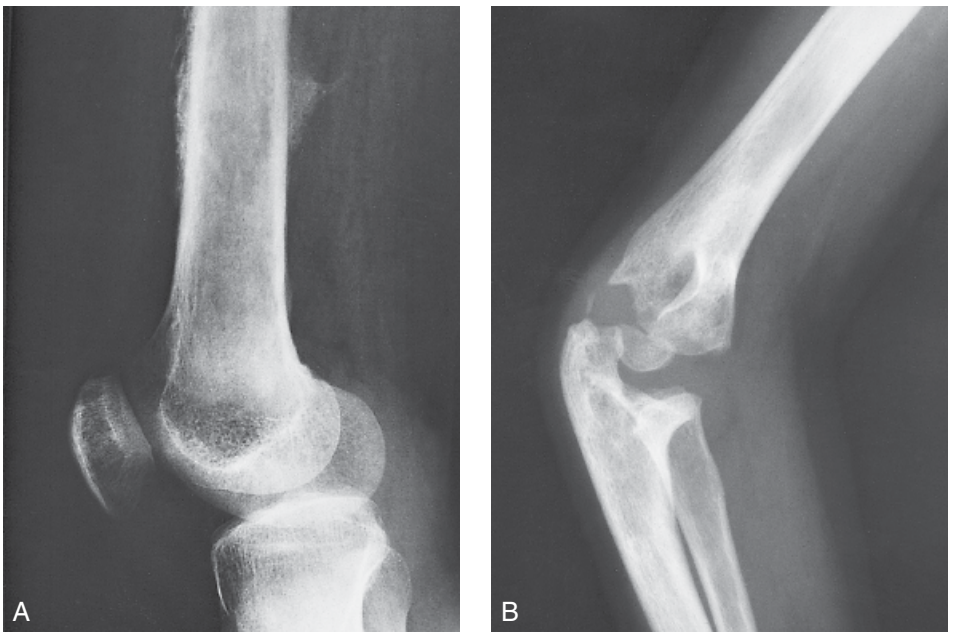

Fig. 9.71. A, Sickle cell anemia: Lateral radiograph of the lower limb and knee in *Salmonella* osteomyelitis. The periosteum is irregularly raised in the lower third of the femur. **B,** Lateral radiograph of the elbow joint in staphylococcal osteomyelitis shows destructive changes in the humerus and ulna.

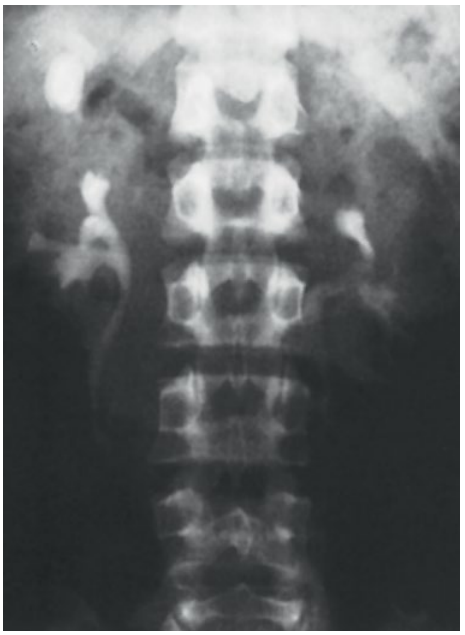

Fig. 9.72. Sickle cell anemia: Intravenous pyelogram. There is clubbing of the calyceal outline in the left kidney. The patient, a 24-year-old man, also shows two large opaque pigment gallstones. The bone trabeculae in the ribs and vertebrae are fine because of expanded erythropoiesis.

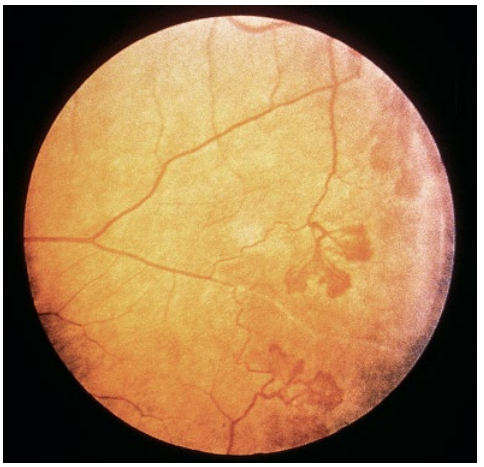

Fig. 9.73. Sickle cell anemia: Retina showing peripheral vascular fronds resulting from formation of arteriovenous anastomoses.

sickle cells and target cells (Fig. 9.74), as well as, in most adult cases, features of splenic atrophy (Fig. 9.75).

Laboratory diagnosis is made by measuring the HbS percentage in blood. The different types of hemoglobin may be separated and quantitated by electrophoresis in cellulose acetate (Fig. 9.76) or agar gel or by high-performance liquid chromatography (HPLC) (Fig. 9.77).

Sickle cell trait gives a normal blood appearance, possibly with an occasional sickle cell present, unless a crisis is induced, for example, by anoxia or severe infection. Recurrent hematuria because of renal papillary necrosis and exertional rhabdomyolysis are occasional problems. Usually combinations of sickle trait with other hemoglobin defects, such as β-thalassemia trait (Fig. 9.78) or C trait (Fig. 9.79), give rise clinically to mild forms of sickle cell disease. Antenatal diagnosis of sickle cell anemia is illustrated in Fig. 9.46.

The main clinical problem in sickle cell anemia – recurring crises – is managed by rehydration, pain relief, antibiotic therapy as appropriate, and, in severe cases, exchange transfusion. Blood transfusions may also be needed in aplastic crises, during pregnancy, and preoperatively to reduce the HbS content of the blood and are sometimes used long term to "switch off" recurring crises. Patients with sickle cell disease, especially those with SC disease, tend to suffer thromboembolic problems and may require antiplatelet or anticoagulant therapy. Hydroxyurea therapy results in fewer and milder painful crises in sickle cell disease. Upregulation of the adhesion molecule P-selectin contributes to the cell–cell interactions between sickle cells,

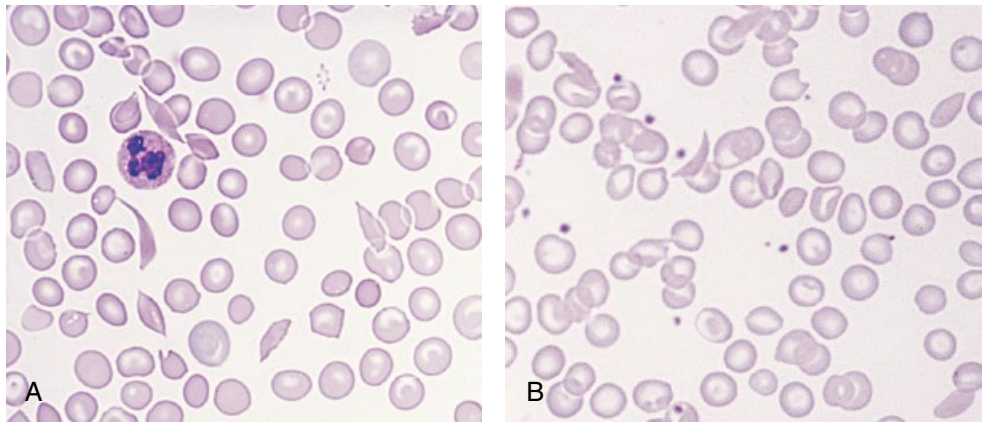

Fig. 9.74. Sickle cell anemia: Peripheral blood films showing deeply staining sickle cells with target cells and polychromasia **(A)** and sickle, hypochromic, and target cells **(B)**.

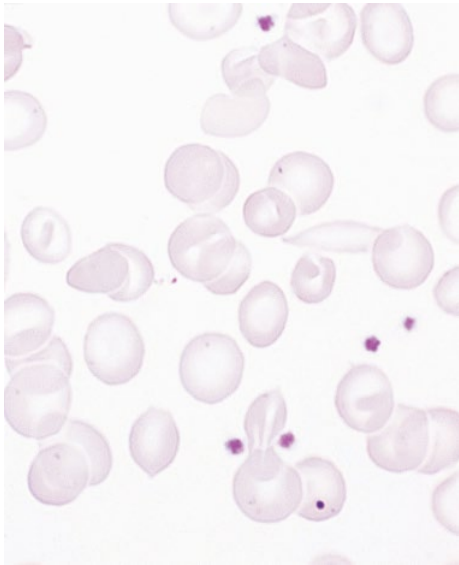

Fig. 9.75. Sickle cell anemia: Peripheral blood film in a patient with splenic atrophy. Howell–Jolly and Pappenheimer bodies are seen in addition to the sickle and target cells.

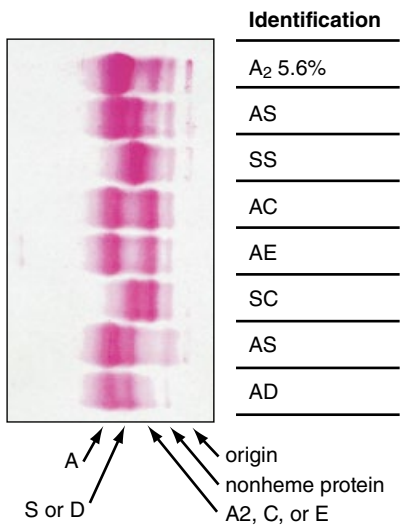

Fig. 9.76. Sickle cell anemia: Hemoglobin electrophoresis in cellulose acetate. (Ponceau S stain.) S and D and A2, C, and E run together. Agar gel separation is usually used to distinguish these. The uppermost lane shows the raised HbA_2 level of β-thalassemia trait. (Courtesy of Gareth Ellis.)

peak name	calibrated area (%)	area %	retention time (min)	peak area
F	13.1*	–	1.14	202892
P3	–	0.1	1.70	1088
Unknown	–	0.4	2.16	6567
Unknown	–	1.3	2.33	22689
Ao	–	3.8	2.52	64845
A2	5.8*	–	3.66	95946
S-window	–	77.1	4.50	1329203

Total area: 1723229

F concentration = 13.1%*
A2 concentration = 5.8%*
*Values outside of expected ranges

analysis comments

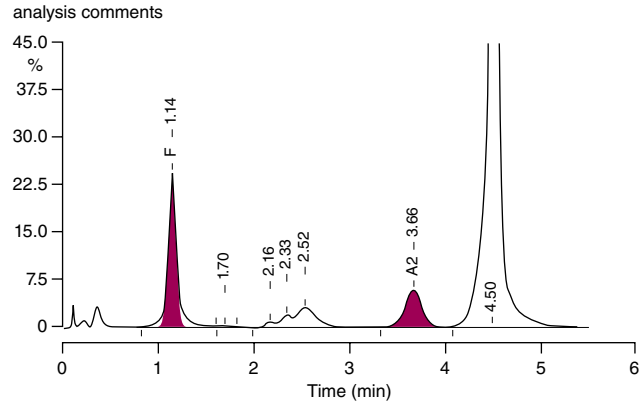

Fig. 9.77. Sickle cell/β-thalassemia: Hemoglobin analysis by high-performance liquid chromatography (HPLC). HbS, 77%; HbF, 13.1%; HbA_2, 5.8%. (Courtesy of Gareth Ellis.)

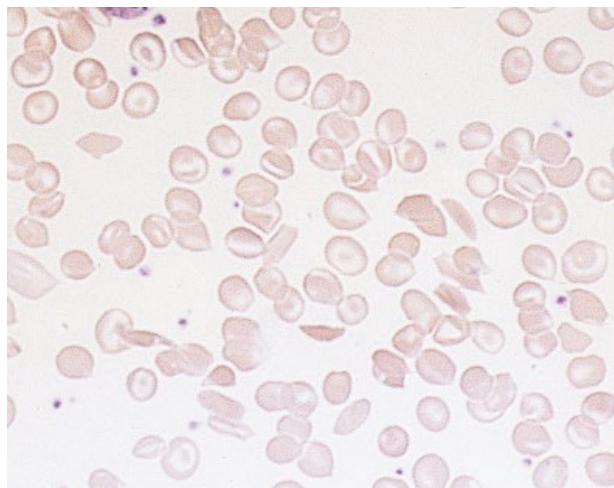

Fig. 9.78. Sickle cell/β-thalassemia: Peripheral blood film showing sickle cells, target cells, and microcytic hypochromic cells.

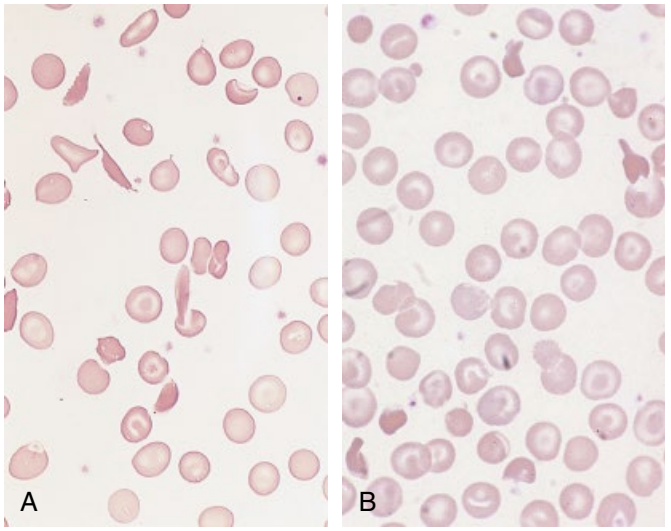

Fig. 9.79. Sickle cell/hemoglobin C disease. **A, B,** Peripheral blood films in which sickle cells and target cells are prominent. **B,** Shows typical irregularly contracted cells. (B, Courtesy of Professor BA Bain.)

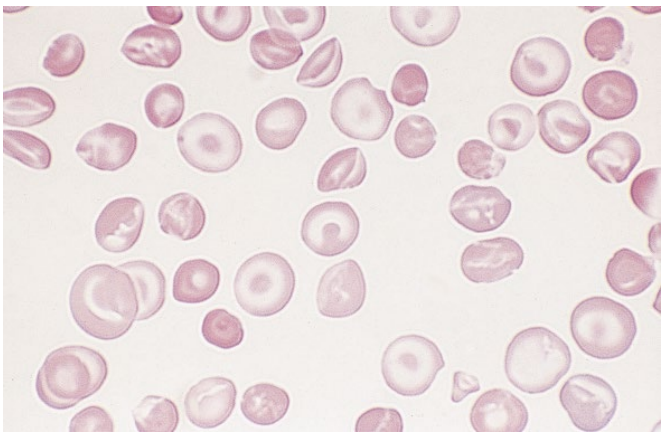

Fig. 9.80. Homozygous hemoglobin C disease: Peripheral blood film showing many target cells and irregularly contracted cells. The patient showed a mild hemolytic anemia with low MCV and MCH, splenomegaly, and gallstones.

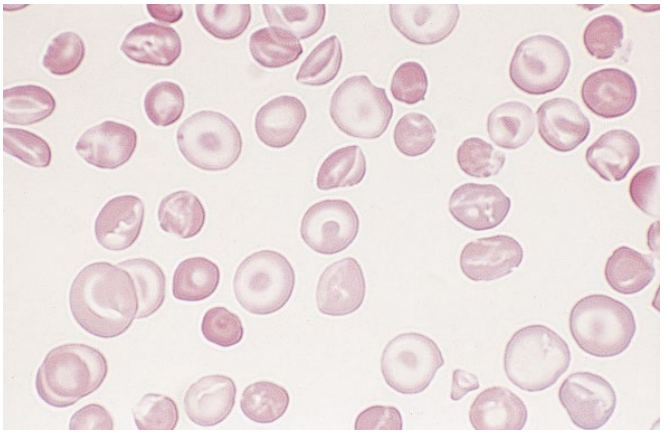

Fig. 9.81. Hemoglobin C/β^0-thalassemia: Peripheral blood film showing crystals of hemoglobin C in cells otherwise empty of hemoglobin. (Courtesy of Professor BA Bain.)

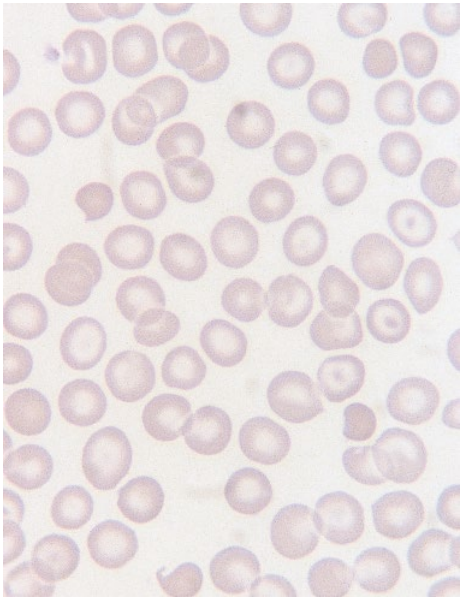

Fig. 9.82. Homozygous hemoglobin E: Blood film showing hypochromia, microcytosis, target cells, and irregularly contracted cells. (Hb, 11.9 g/dL; RBC, 6.84 × 10^9/L; MCV, 54 fL; MCH, 17.4 pg.) (Courtesy of Professor BA Bain.)

leukocytes, and vascular endothelium which result in vaso-occlusion and painful crises. The monoclonal antibody to P-selectin, crizanlizumab, reduces the frequency of painful sickle cell crises, even in patients taking hydroxyurea, with few adverse effects.

OTHER STRUCTURAL HEMOGLOBIN DEFECTS

Other common hemoglobin abnormalities include hemoglobin C (Fig. 9.80), which may be combined with β^0-thalassemia (Fig. 9.81), hemoglobin D, and hemoglobin E diseases (Fig. 9.82). Rare syndromes produced by hemoglobin abnormalities include hemolytic anemia because of an unstable hemoglobin (Fig. 9.83), hereditary polycythemia, hereditary methemoglobinemia (Fig. 9.84), and thalassemia syndromes caused by structural variants.

F-CELLS

In normal adults, the synthesis of fetal hemoglobin (HbF) is reduced to very low levels (<0.6%) and the HbF is restricted to a subpopulation of erythrocytes termed F-cells, which contain, in addition, adult hemoglobin (HbA). Increased levels of HbF in adult life are characteristic of a heterogeneous group of genetic disorders in which deletions result in disorders termed hereditary persistence of fetal Hb (*HPFH*) and δβ-thalassemias (see Fig. 9.8). There is considerable overlap between these two groups of disorders. The level of compensatory increase of HbF is usually higher in HPFH. The distribution of HbF is heterocellular in the δβ-thalassemias and pancellular in HPFH (Fig. 9.85), and this has been a criterion for differentiating the δβ-thalassemias from the HPFHs.

There is a slight increase of fetal hemoglobin in adult blood in a variety of acquired disorders, such as megaloblastic anemia, acute myeloid leukemia, and paroxysmal nocturnal hemoglobinuria.

Circulating fetal red cells may be found in mothers in the immediate postpartum period, following mixing of fetal and maternal blood at delivery. Such cells may be detected by the Kleihauer technique (Fig. 9.86).

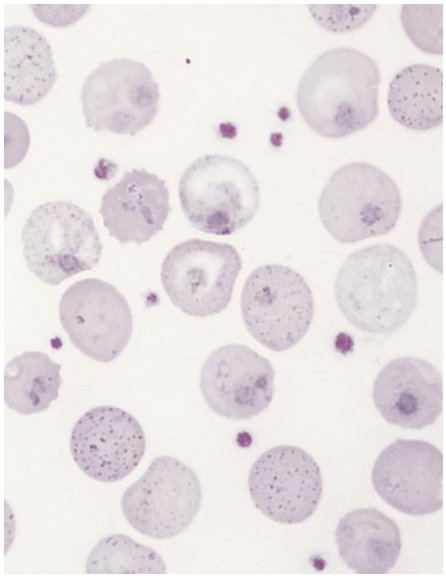

Fig. 9.83. Unstable hemoglobin (Hb-Hammersmith): Postsplenectomy peripheral blood film shows many cells with punctate basophilia or containing single or multiple inclusion bodies composed of precipitated, denatured hemoglobin (seen as Heinz bodies on special staining). The underlying lesion is substitution of the amino acid phenylalanine by serine at position 42 in the β chain.

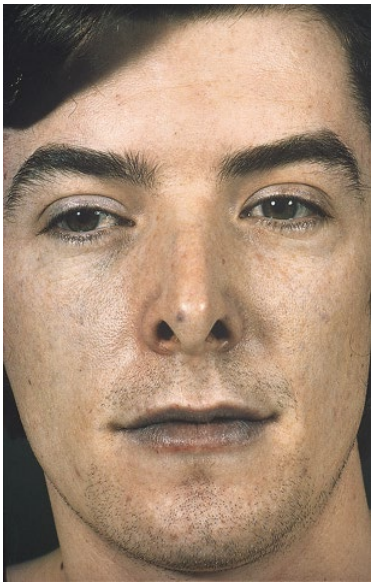

Fig. 9.84. Hereditary methemoglobinemia: cyanosis caused by NADH-methemoglobin reductase deficiency shows a typical slate-gray appearance in this 22-year-old man whose blood count was normal.

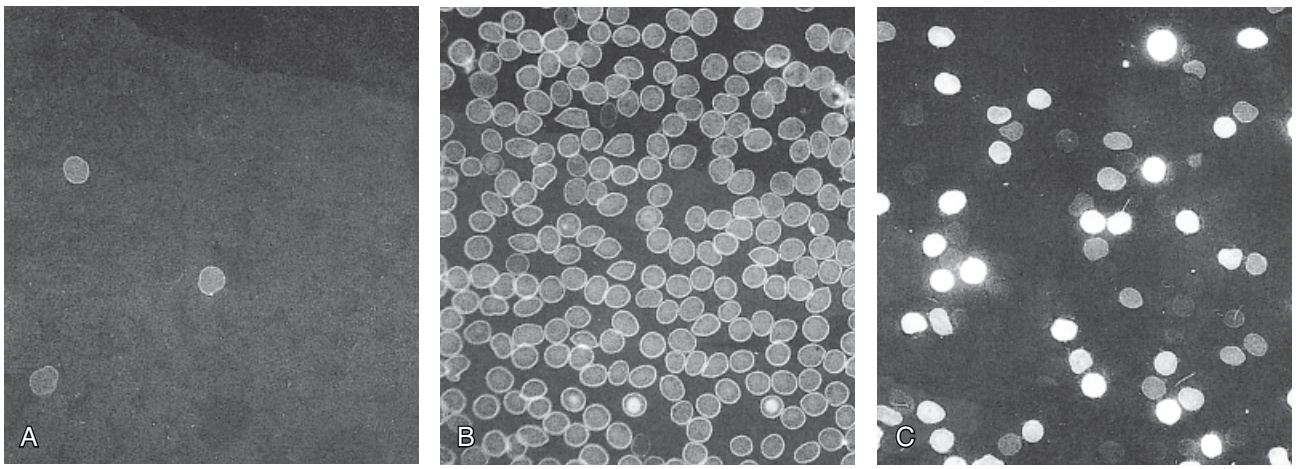

Fig. 9.85. Fetal hemoglobin in peripheral blood anti γ chain immunofluorescence stain. **A,** Normal blood heterocellular distribution (HbF, 0.4%; F-cells, 2.5%). **B,** Indian hereditary persistence of fetal hemoglobin (HPFH) (HbF, 22%; F-cells, 100%). **C,** Heterocellular HPFH (HbF, 2.5%; F-cells, 30%). (Courtesy of Professor SL Thein.)

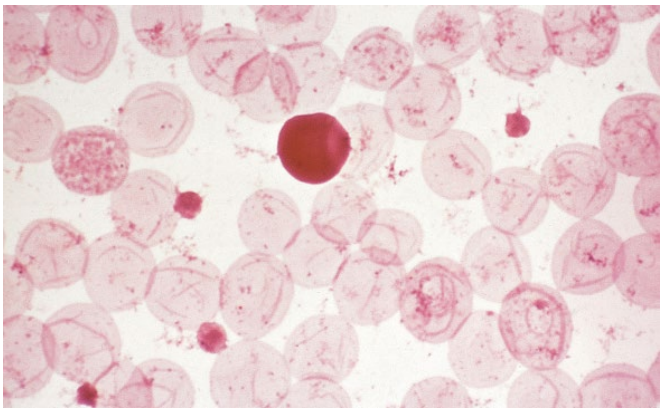

Fig. 9.86. Fetal hemoglobin: Acid elution (Kleihauer) technique showing a fetal red cell in maternal blood. The darkly staining fetal cell contains fetal hemoglobin that has resisted elution at low pH. The adult cells appear as "ghosts" because the adult hemoglobin has been leached out of the cells.

METHEMOGLOBINEMIA

The iron atoms in normal hemoglobin are in the ferrous state. Methemoglobin reductase enzymes use NADH or NADPH to reduce methemoglobin, which contains ferric iron, which is formed normally during the life span of the red cell. Methemoglobinemia may arise from an inherited defect in either the α- or β-globin chain of hemoglobin or from deficiency of the enzyme NADH-methemoglobin reductase (Fig. 9.84). In either case, there is an excess of hemoglobin containing ferric iron. Methemoglobin may also be acquired as a result of exposure to drugs or chemicals.

CHAPTER

10 BENIGN DISORDERS OF PHAGOCYTES

Normal white cell appearances and production are discussed first in this chapter, then benign conditions that may be associated with abnormal phagocyte (granulocyte and monocyte) cell morphology or numbers are covered. Only some of these are associated with clinical problems.

GRANULOPOIESIS AND MONOCYTE PRODUCTION

Granulocytes and monocytes derive from a common stem cell after multiple steps of differentiation and multiplication (see Chapter 2). The transcription and growth factors involved in phagocyte production are shown in Figs. 2.11 and 3.3, respectively. In granulopoiesis (Fig. 10.1), the first recognizable cell of the granulocytic series is the myeloblast. Following division and differentiation, the following sequence of cells may be seen (Figs. 10.2–10.4):

1. Promyelocyte (which contains primary granules)
2. Myelocyte
3. Metamyelocyte
4. Band cell
5. Segmented or mature granulocyte.

The distinction between immature myeloid precursors is dependent on the morphology of the nucleus and the cytoplasm. The most immature – the myeloblast – has immature nuclear chromatin with one or more nucleoli. The nuclear cytoplasmic ratio is high. Promyelocytes also have immature nuclear chromatin with nucleoli but they have more voluminous granulated cytoplasm with specific (secondary) granules (neutrophilic, eosinophilic, or basophilic) that remain from the promyelocyte stage onwards. Promyelocytes have a prominent paranuclear Golgi apparatus. Finally, myelocytes have more mature chromatin with granulated cytoplasm. All of these cells play a critical role in combating infection by generating an inflammatory response.

Osteoblasts and osteoclasts are occasionally seen during bone marrow examination (Figs. 10.5 and 10.6). They are derived from monocytic lineage cells and are important in laying down bone (osteoblast) and resorbing bone (osteoclast). When they are present in significant numbers, it is important not to confuse them with metastatic malignant cells.

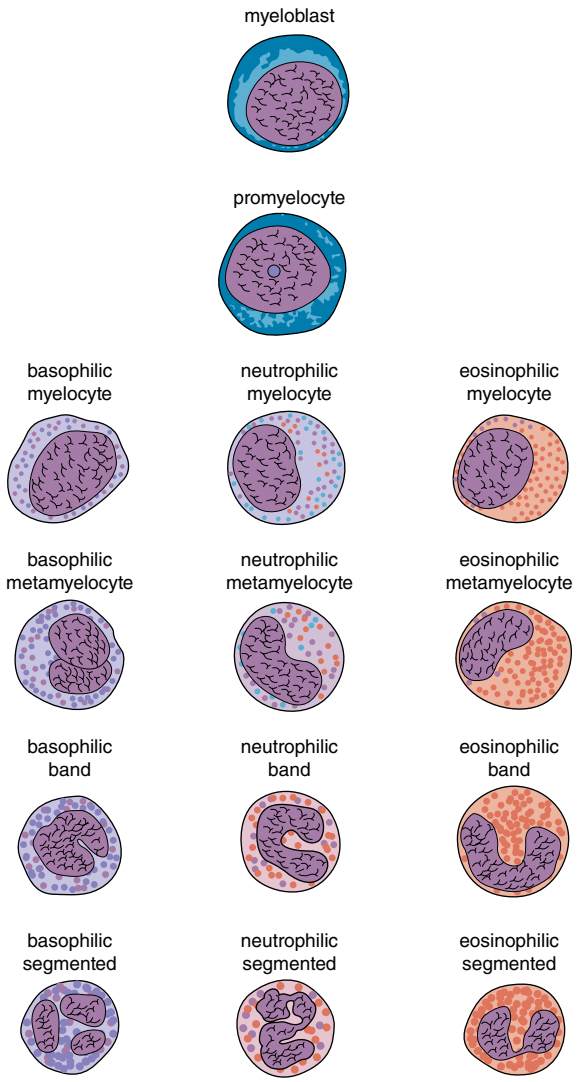

Fig. 10.1. Granulocyte differentiation and maturation: The myeloblast and promyelocyte give rise to three different cell lines, according to the type of secondary granules and nuclear morphology.

Color Atlas of Clinical Hematology: Molecular and Cellular Basis of Disease, Fifth Edition. A. Victor Hoffbrand, Paresh Vyas, Elías Campo, Torsten Haferlach, and Keith Gomez

NEUTROPHILS (POLYMORPHS)

The dominant granulocytic cells are neutrophils (Figs. 10.7 and 10.8), and neutrophil precursors account for the majority of granulocyte precursors in the marrow (see Table 4.2). Rare appearances in blood films include neutrophil–platelet rosetting (Fig. 10.9A) and neutrophil aggregation (Fig. 10.9B), neither of which are usually of clinical significance.

Neutrophil production and differentiation takes 6–10 days (Fig. 10.10). In the bone marrow there are 10–15 times the

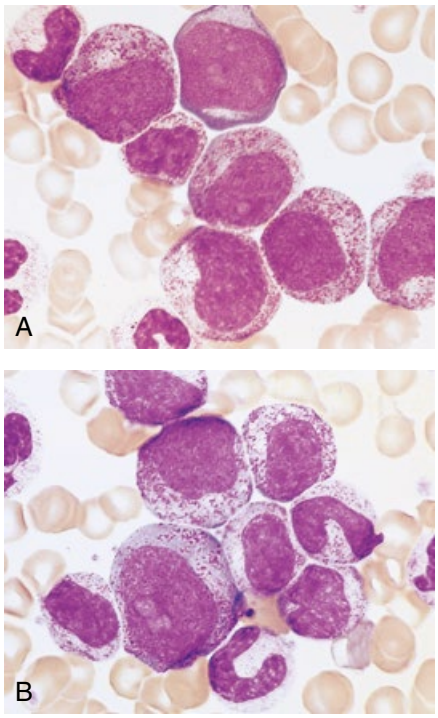

Fig. 10.2. Granulopoiesis. **A,** A myeloblast, late promyelocytes, and myelocytes. **B,** A promyelocyte, myelocytes, and metamyelocytes.

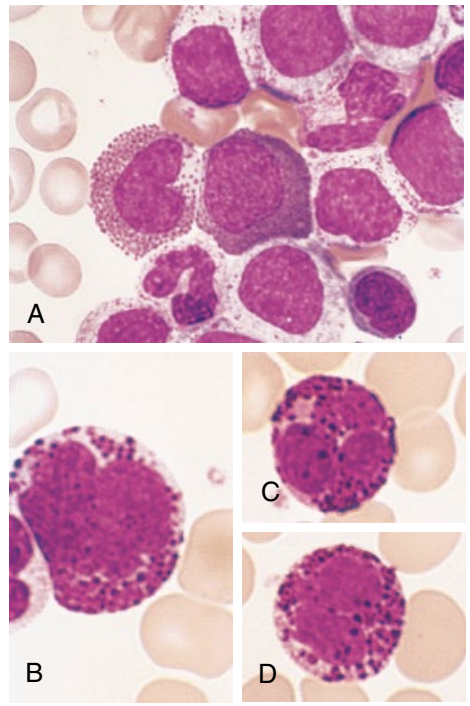

Fig. 10.4. Granulopoiesis: **(A)** eosinophilic myelocyte and metamyelocyte; **(B)** basophilic myelocyte; **(C, D)** more mature basophils.

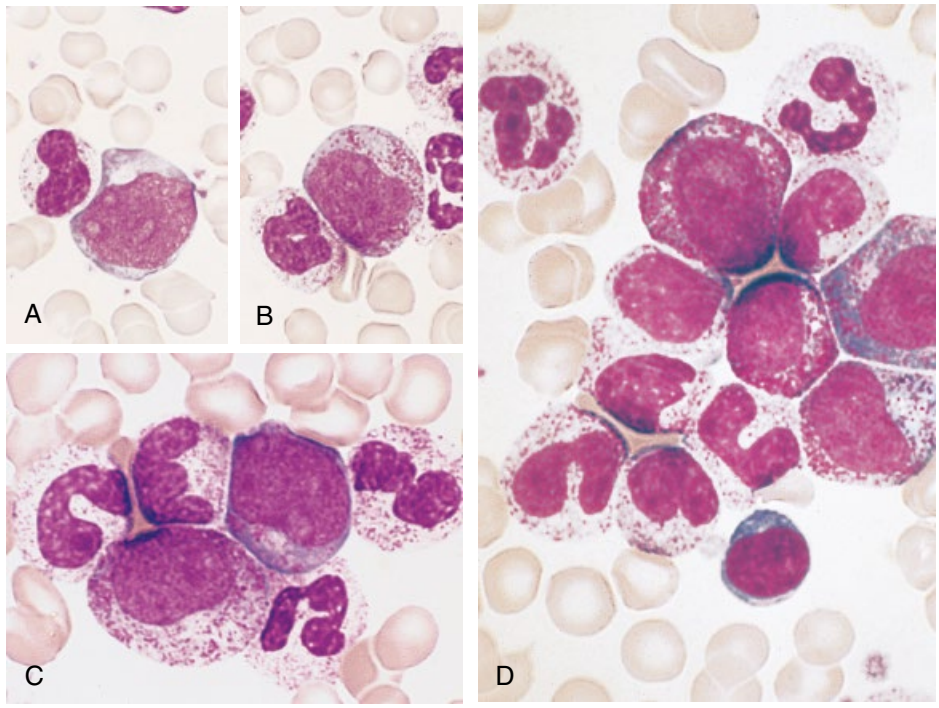

Fig. 10.3. Granulopoiesis. **A,** Myeloblast. **B,** Promyelocyte. **C,** Early promyelocyte, myelocyte, metamyelocyte, and band neutrophils. **D,** Sequence of cells from myelocytes through metamyelocytes and band forms, and a single segmented neutrophil.

number of band and segmented neutrophils compared with in peripheral blood, where they serve as a "reserve pool." The growth factors involved in neutrophil and other granulocytes are shown in Fig. 10.10 and Figs. 3.2 and 3.3. Once they enter the circulation, neutrophils have a half-life of only 6–12 hours before they migrate into tissues, usually via chemotaxis. In tissues they survive for only 2–4 days before they are destroyed or undergo senescence. Neutrophils destroy bacteria and fungi (Fig. 10.11). Organisms are ingested into phagosomes into which neutrophil granules (Table 10.1) are released and kill bacteria and fungi by a number of mechanisms. Primary azurophilic neutrophil granules contain lysozyme, myeloperoxidase, and serine proteases such as cathepsin G, proteinase 3, and azurocidin. Microbes are also killed by oxidant damage by superoxides generated by glucose metabolism. Finally, they are also killed by non-enzymatic proteins, defensins which form ion channels in the lipid layer, by bacterial permability-inducing factor (BPI) which increases Gram-negative bacterial permeability to extracellular solutes, and by lactoferrin which chelates iron that bacteria require.

There are far fewer eosinophil precursors. Eosinophils are derived from eosinophil myelocytes (see Fig. 10.4). Typically, mature cells have a bilobed nucleus and distinct eosinophilic granules (Fig. 10.12, Table 10.2). The granules are often membrane bound and have a crystalloid core. Eosinophil production is stimulated by interleukin 5 (IL-5) but also by IL-2, IL-3, and granulocyte–macrophage colony-stimulating factor (GM-CSF; Fig. 3.2). It may occur in extramedullary locations in allergic inflammation driven largely by IL-5 produced by local resident lymphoid cells. Most (>90%) eosinophils are found in the tissues, the gastrointestinal tract, reticuloendothelial system, and the mammary glands and uterus. In eosinophilic disorders, migration of the cells to these and other organs occurs due to local production of various chemokine (eotaxins) and nonchemokine mediators, including IL-5 leukotrienes, complement, and platelet factors.

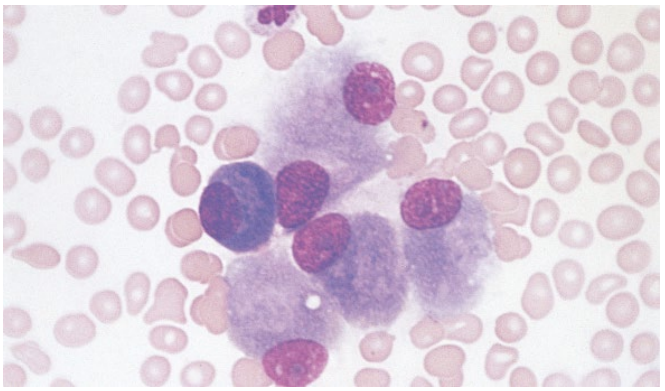

Fig. 10.5. Osteoblasts: A group of five osteoblasts and a plasma cell *(on the left)*. The osteoblasts are large cells that resemble plasma cells, but their chromatin pattern is more open, their cytoplasm is less basophilic, and they tend to occur in clumps.

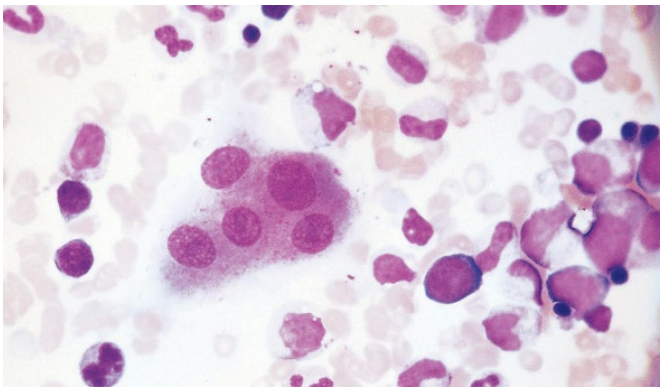

Fig. 10.6. Osteoclasts: These multinucleate cells are occasionally seen in normal marrow aspirates. In contrast to megakaryocytes, the nuclei of osteoclasts are usually discrete, round or oval, and often contain nucleoli.

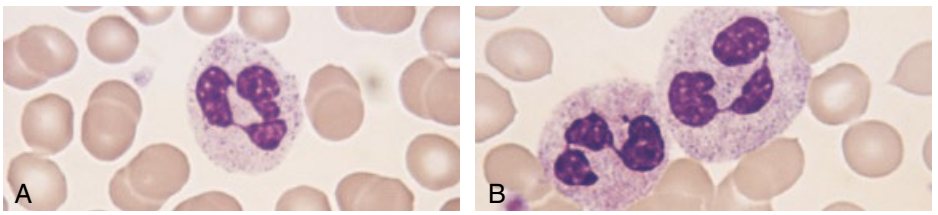

Fig. 10.7. Normal neutrophils. **A, B,** Mature forms showing typical nuclear lobe separation by fine filaments. Normal segmented neutrophils may show up to five lobes.

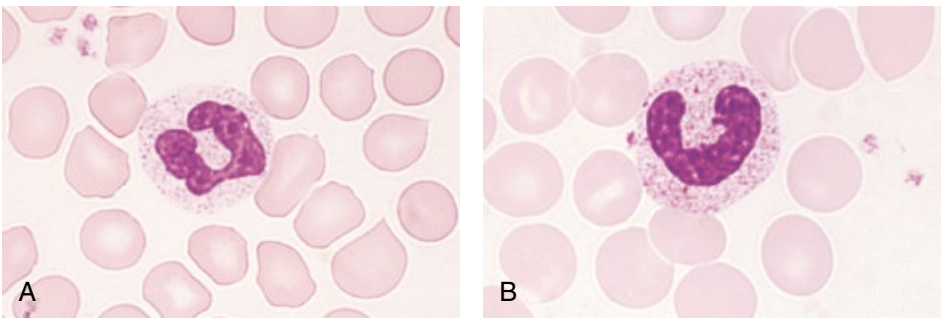

Fig. 10.8. Normal neutrophils. **A, B,** Stab or band forms. The nuclear segmentation of these less mature cells is incomplete.

Basophils (Fig. 10.13) and tissue mast cells (Fig. 10.14) are normally even rarer. Basophils are distinctive with large basophilic granules occupying most of the volume of the cell. Mast cells have deep purple granules. All three of these specialized granulocytic cells have specific granules (Tables 10.1–10.3) that are especially important in providing protective immunity against parasites (Fig. 10.15) and are important in allergic responses. They combine with T and B lymphocytes and the antibody response (especially specific immunoglobulin E [IgE] antibodies) to release toxic granules that destroy parasites such as helminths. Mast cells and basophils also release pharmacologic mediators such as histamine, SRS-A (slow reactive substance of anaphylaxis, a mixture of leukotrienes) and heparin that in part cause the adverse symptoms in allergic response. Eosinophils, by contrast, release histaminase and aryl sulfatase, which inactivate histamine and SRS-A, respectively.

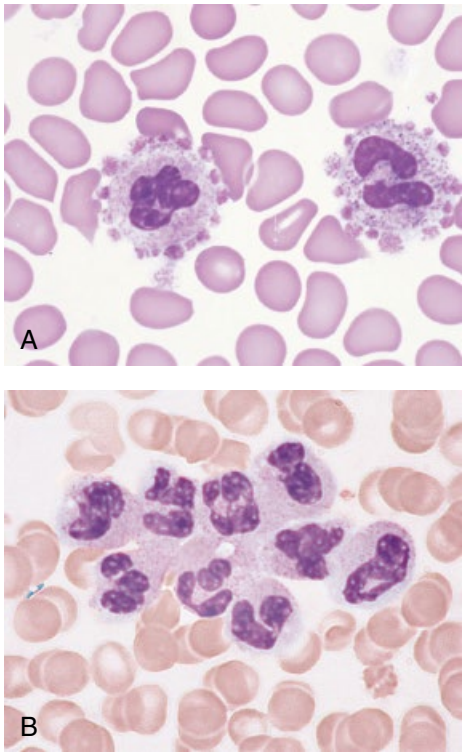

Fig. 10.9. A, Neutrophil–platelet adhesion: Rosetting of platelets around neutrophils is an occasional interesting, but unexplained, finding in blood films. It only occurs in the presence of the anticoagulant ethylenediamine tetra-acetic acid. **B,** Neutrophil agglutination: Clusters of aggregated neutrophils are also an occasional and unexplained finding during blood film examination. The phenomenon is sometimes seen in patients with viral infections.

MONONUCLEAR PHAGOCYTIC SYSTEM

Monocytes spend only a short time in the bone marrow, and normally few monocytes and their precursors, the monoblasts and promonocytes, are seen in normal marrow and peripheral blood (Fig. 10.16). Monoblasts and promonocytes can be difficult to distinguish from monocytes and occasionally from early myeloblasts. After circulating for 20–40 hours, monocytes migrate into tissues of the reticuloendothelial system where they are known as macrophages (Fig. 10.17). The life span of macrophages can be months to years. Functionally, they phagocytose and remove particulate antigen and present antigen to lymphocytes. In the various tissues of the reticuloendothelial system, macrophages may be produced locally after they have been colonized by monocytes from the blood.

Monocytes are phagocytes that will adhere to immunoglobulin G (IgG) and complement (e.g. C3b)-coated microorganisms via the Fc portion of the IgG molecule. This process also facilitates ingestion of the microbes. Monocyte lysosomes contain hydrolases and peroxidase, which are important for microbial killing. Monocytes are also "factories" that release a number of mediators that help propagate the immune and inflammatory response.

RETICULOENDOTHELIAL SYSTEM

The reticuloendothelial system consists of phagocytic monocytes and tissue macrophages (including macrophages in bone marrow, spleen, lymph nodes, liver Kupffer cells, alveolar macrophages, macrophages of serosal surfaces, and mesangial cells of the kidney) (see Fig. 10.17). Tissue macrophages are partly derived from circulating monocytes but also may self-replicate at local tissue sites independently.

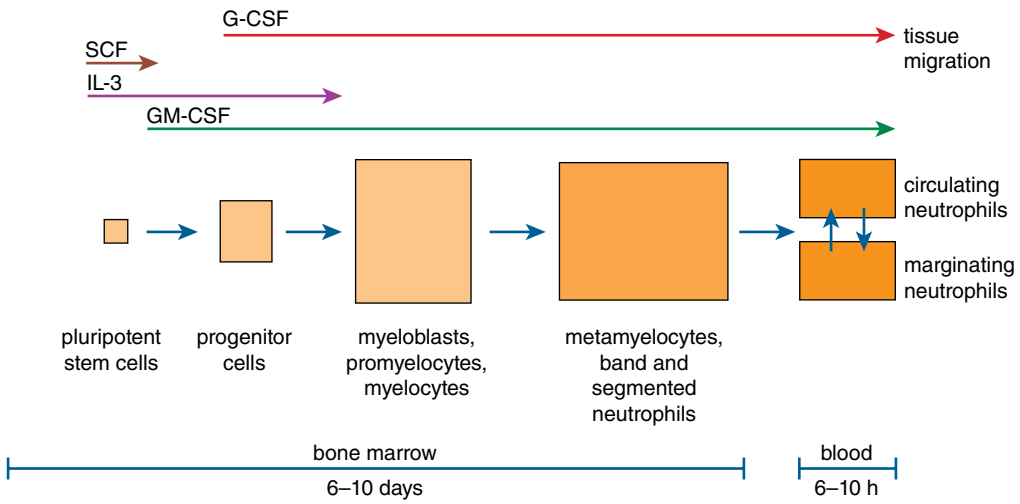

Fig. 10.10. Neutrophil kinetics. G-CSF, granulocyte colony-stimulating factor (GM-CSF); SCF, stem cell factor; IL-3, interleukin 3; GM-CSF, granulocyte–monocyte colony-stimulating factor. Source: Hoffbrand AV, Moss PAH. *Hoffbrand's Essential Haematology*, 7th edn. Wiley-Blackwell, 2015.

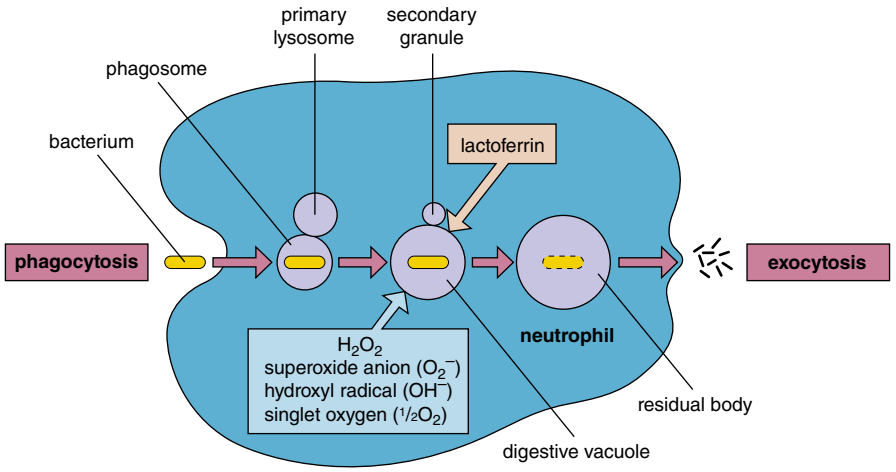

Fig. 10.11. Phagocytosis and bacterial destruction: The neutrophil surrounds the bacterium with an invaginated surface membrane to form a phagosome by fusion with a primary lysosome. The lysosomal enzymes attack the bacterium. Secondary granules also fuse with the phagosomes, and new enzymes and lactoferrin attack the organism. Various types of activated oxygen generated by glucose metabolism also help to kill bacteria. Undigested residual bacterial products are excreted by exocytosis.

TABLE 10.1. GRANULE CONTENTS OF HUMAN NEUTROPHILS

Primary (azurophil) granules	Specific granules	Other organelles
Microbicidal proteins		
Myeloperoxidase		
Lysozyme	Lysozyme	Lysozyme
Bactericidal permeability-inducing factor/CAP57		
Defensins		
Serprocidins (serine proteases):		
Cathepsin G		
Proteinase 3		
Azurocidin/CAP37		
Elastase	Collagenase	Alkaline phosphatase
	Gelatinase	Gelatinase
		Tetranectin
Acid hydrolases		
β-Glucuronidase		
β-Glycerophosphatase		
N-Acetyl-β-glucosaminidase		
α-Mannosidase		
Cathepsin B		
Cathepsin D	Neutrophil gelatinase-associated lipocalin	
Aryl sulfatase	Lactoferrin	
	Transcobalamin I and III	
	Plasminogen activator	
	Histaminase	
	β_2-Microglobulin	
	Cytochrome *b559*	
	Receptors	**Receptors**
	$\alpha_{2M}\beta_2$-Integrin = complement receptor 3 (C3bi)	$\alpha_M\beta_2$-Integrin
	Bacterial tripeptide receptor (formyl-methionyl-leucyl-phenylalanine)	Complement receptor 1 = CD35
	Laminin receptor	FcγRIIIB
	$\alpha_2\beta_2$-Integrin = victronectin receptor	

Source: Roberts PJ, et al. Phagocytes. In: Hoffbrand AV, et al., eds. *Postgraduate Haematology*, 4th edn. Butterworth-Heinemann, 1999, pp 235–266. Reproduced with permission of Elsevier.

Dendritic cells (DCs) are specialized antigen-presenting cells (APCs) found in the skin, lymph nodes, spleen, and thymus (Fig. 10.18). They have an irregular shape, numerous cell membrane processes, spiny dendrites, and bulbous pseudopods (Fig. 10.19). They have a paucity of intracellular organelles, lysosomes, endosomes, and prominent mitochondria (Fig. 10.20). They include myeloid- and lymphoid-derived DCs and Langerhans cells. They process antigen and interact with and stimulate T cells. Myeloid-derived DCs originate from bone marrow and make up 1–2% of the blood mononuclear cells. They are negative for lineage markers, but are HLA-DR positive. A separate set of DCs is derived

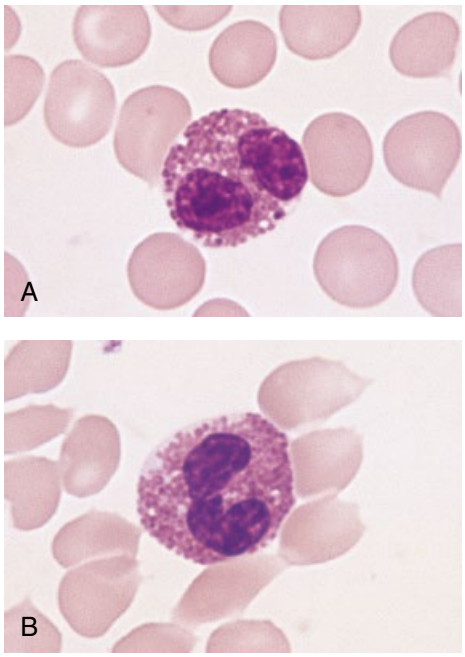

Fig. 10.12. Normal eosinophils.

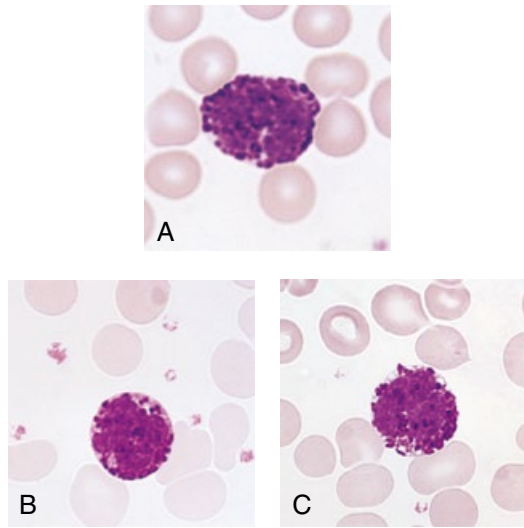

Fig. 10.13. Basophils: The coarse basophilic granules of these cells often overlie the nucleus, thus obscuring the detail of its segmented structure. Only small numbers of basophils are found in the normal blood film.

TABLE 10.2. GRANULE CONTENTS OF EOSINOPHILS

Granule type/protein	Function	Downstream physiological role
Primary granule		
Charcot–Leyden crystal protein	Cleaves fatty acids from lysophospholipids (lysophospholipase)	Phospholipid mechanism Neutralizes pulmonary surfactants
Eosinophil peroxidase	Generates hypothiocyanous acid from H_2O_2 Allosteric inhibitor of muscarinic receptors	Kills microorganisms (*Escherichia coli*, schistosomes, microfilariae, trypanosomes, *Toxoplasma* spp., and mycobacteria) Toxic to mammalian cells – mast cells and tumors Bronchoconstriction
Specific/secondary granule		
Eosinophil peroxidase	As above	As above
Major basic protein (forms crystalline core of the granule)	Binds to acidic lipids, disrupts membranes (nonenzymatic activity)	Widespread toxicity to parasites Toxic to mammalian cells – desquamation and hypertrophy of lung epithelium (bronchospasm)
Eosinophil cationic protein	Forms transmembrane pores	Bactericidal – *E. coli* and *Staphylococcus aureus* Toxic to parasites Damage to lung epithelium (as above) Stimulates mast cell degranulation
	Ribonuclease Neurotoxin (in vitro)	
	Neutralizes heparin	Effects on coagulation and fibrinolysis
Eosinophil-derived neurotoxin (eosinophil protein X)	Ribonuclease Neurotoxin	Toxic to parasites
Gelatinase	Metalloproteinase	Damage to extracellular matrix

Source: Roberts PJ, et al. Phagocytes. In: Hoffbrand AV, et al., eds. *Postgraduate Haematology*, 4th edn. Butterworth-Heinemann, 1999, pp 235–266. Reproduced with permission of Elsevier.

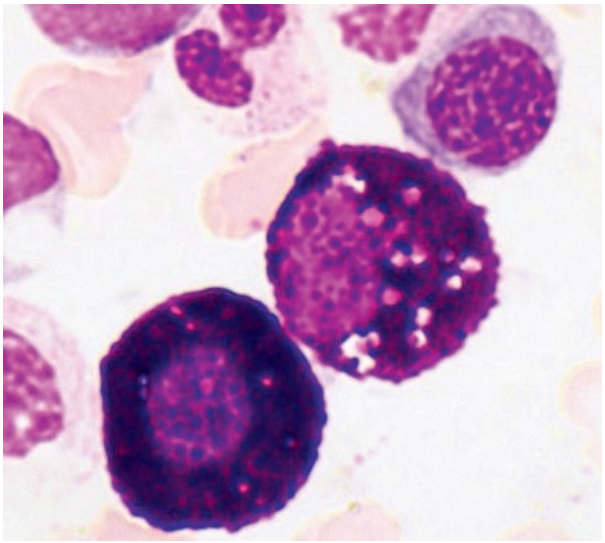

Fig. 10.14. Two mast cells.

from CD34-positive cells and populates the skin epidermis (where they are called Langerhans cells), but also are found in the liver, lymph nodes, and the interstitial spaces in organs such as the kidney and the heart. Following stimulation, Langerhans cells migrate to afferent lymphatics, into the paracortical areas of draining lymph nodes where they "interdigitate" with and present antigen to T cells (see Fig. 10.18). Lymphoid dendritic cells have a separate origin and within the thymus may be involved in tolerance induction to autoantigens.

Follicular dendritic cells (FDCs), also called germinal centrodendritic cells, form a dense network in germinal centers (GCs) of lymph nodes (B-cell areas). They are bone marrow derived and present retained antigen for prolonged periods (for several months), presumably to maintain B-cell activation and, indirectly, T-cell activation.

TABLE 10.3. GRANULE CONTENTS OF BASOPHILS AND MAST CELLS

Component	Function	Downstream physiological role	Other properties	Cell specificity
Protein				
Histamine	Binds to H1, H2, and H3 receptors	Major inducer of hypersensitivity reactions and inflammation		Basophils, mast cells
Proteoglycan				
Heparin	Packages basic proteins into granules		Binds and stabilizes proteases	Predominant in MC_{CT}
Chondroitin sulfates	Same function		Same function	Predominant in basophils
Enzymes: neutral proteases				
Chymase	Inactivates bradykinin	Affects microcirculation		MC_{CT}
	Injures lamina lucida of basement membrane at dermal–epidermal junction			
	Activates angiotensin I	Modulates microcirculation		
	Activates precursor IL-1b	Modulates skin inflammation		
Tryptase	Cleaves C3 into C3a + C3b	Proinflammatory; stimulates neutrophil chemotaxis and adherence	Tetrameric when bound to heparin; monomer active	Mast cells
	Cleaves C3a into inactive peptides		Restricted substrate specificity	
	Activates metalloproteinase 3	Regulates collagenase	Raised levels in mast cell disorders; anaphylaxis, mastocytosis	
	Inactivates fibrinogen	Attenuates fibrin deposition		
	Degrades calcitonin gene-related peptide			
Cathepsin G-like protease				MC_{CT}
Carboxypeptidase B				MC_{CT}
Other				
Charcot–Leyden crystal protein	Cleaves fatty acid from lysophospholipid (lysophospholipase)	Phospholipid mechanism		Basophils
		Neutralizes pulmonary surfactants		
Major basic protein		Disrupts membranes		
Sulfatase, exoglycosidase				

Mast cells = both connective tissue and mucosal mast cells; MC_{CT}, connective tissue mast cell.

Source: Roberts PJ, et al. Phagocytes. In: Hoffbrand AV, et al., eds. *Postgraduate Haematology*, 4th edn. Butterworth-Heinemann, 1999, pp 235–266. Reproduced with permission of Elsevier.

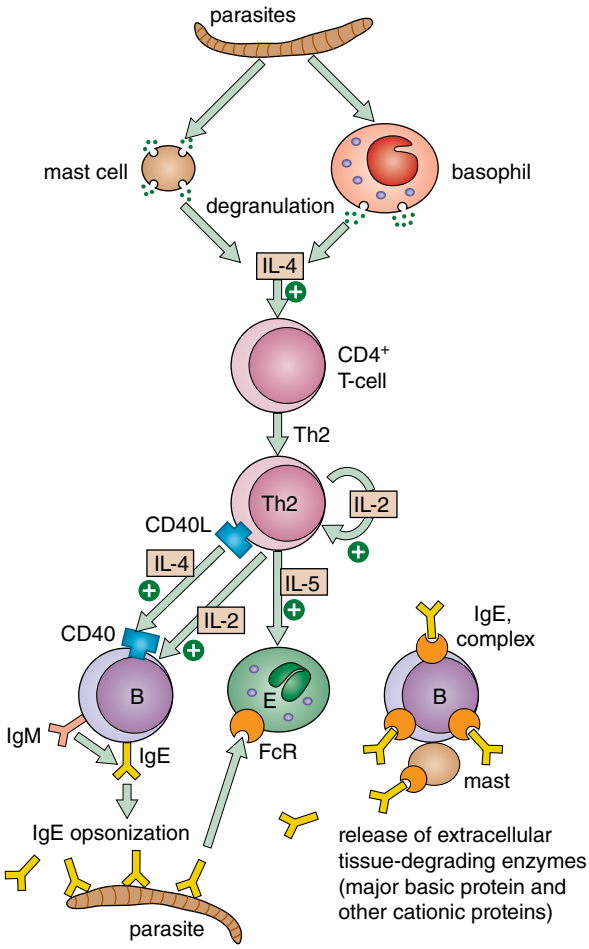

Fig. 10.15. T cells work with mast cells, basophils, and, most importantly, eosinophils to generate a protective immune response to parasites. Parasites trigger basophil and mast cell degranulation, release of IL-4, and activation of CD4+ and Th2 cells. Activated T cells promote protective antibody response (mainly IgE but also IgG and IgM) from B cells. IgE-opsonized parasites attract eosinophils that degranulate and release toxic granule components as shown.

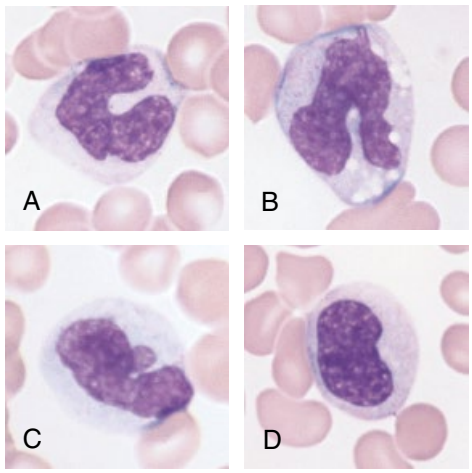

Fig. 10.16. Monocytes: These cells are usually the largest white cells found in normal blood. The nucleus is usually folded or convoluted, with a moderately fine chromatin pattern. The cytoplasm typically has a gray "ground-glass" appearance with fine azurophilic granules. Some **(B)** have rather prominent cytoplasmic vacuoles.

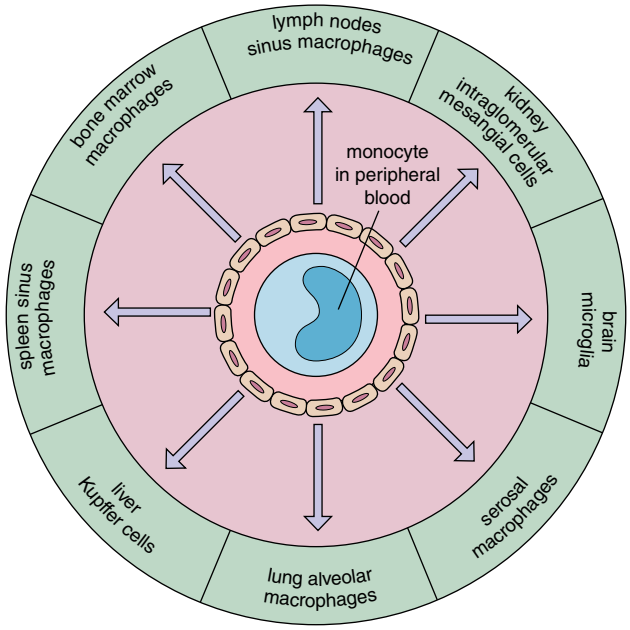

Fig. 10.17. Distribution of macrophages in the reticuloendothelial system.

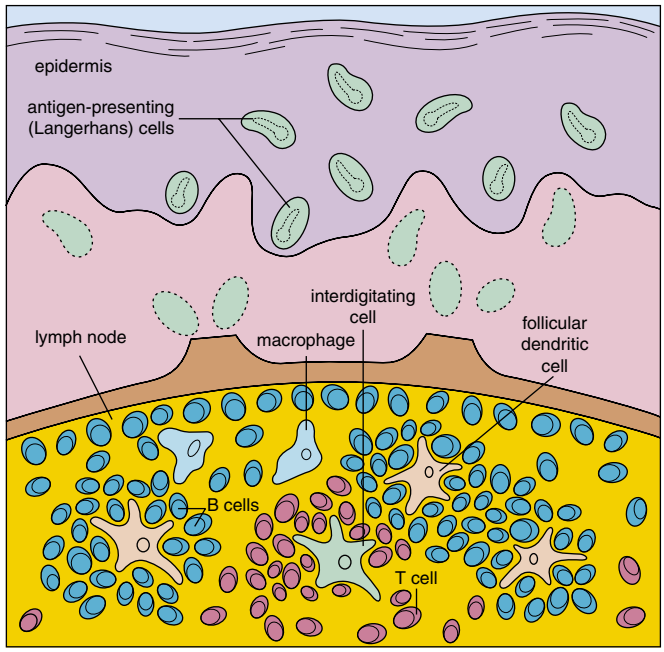

Fig. 10.18. Dendritic (antigen-presenting) cells (DCs) in the skin and lymph nodes: Langerhans cells in the epidermis are characterized by the presence of Birbeck bodies (tennis racquet-shaped collections of granules). These antigen-carrying cells migrate via afferent lymphatics to the neighboring lymph nodes and become interdigitating cells in the T-cell paracortical zone. Follicular DCs are found in the B-cell germinal centers (GCs).

HEREDITARY VARIATION IN WHITE CELL MORPHOLOGY

PELGER–HUËT ANOMALY

In the Pelger–Huët anomaly, characteristic bilobed neutrophils are found in the peripheral blood. Occasional unsegmented neutrophils with round nuclei are also seen, particularly during

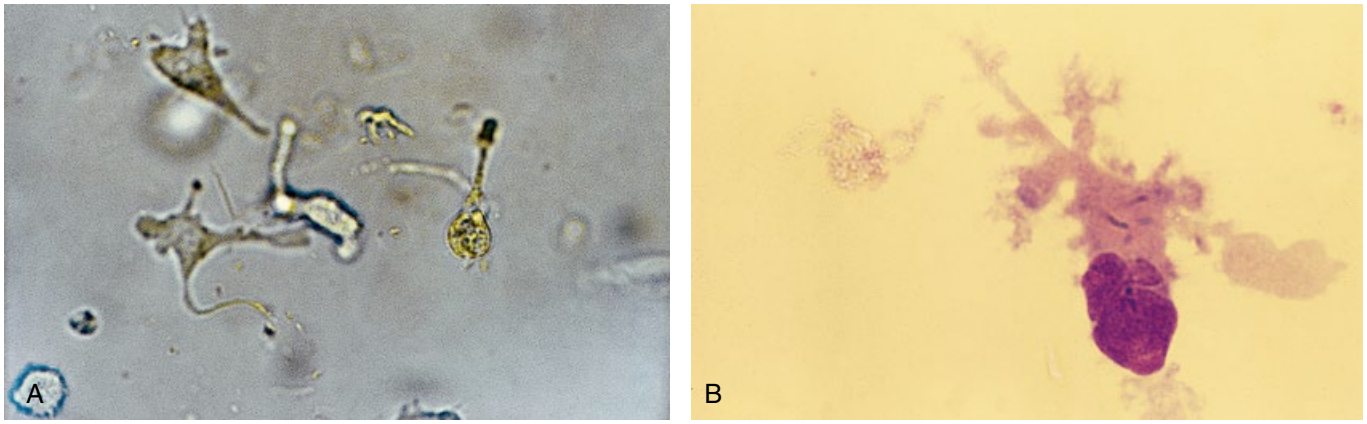

Fig. 10.19. A, Dendritic cells (DCs) developing in methylcellulose culture from CD34+ bone marrow progenitors after 14 days in TNFα and GM-CSF. Note the fine, long dendritic processes characteristic of DCs under these conditions. These cells generally have the appearance and phenotype of skin Langerhans cells, are CD1a+, CD14−, and HLA-DR+, but lack Birbeck granules. **B,** Giemsa-stained dendritic cell from 14-day cultures of CD34+ as shown in **(A)**. Note the fine, long dendritic processes and eccentric lobed nucleus characteristic of DCs under these conditions. (Courtesy of Dr. CDL Reid.)

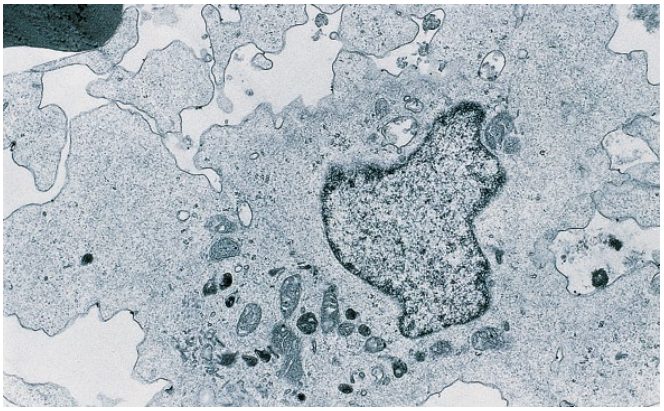

Fig. 10.20. Electron microscopic appearance of dendritic cells from 14-day cultures of CD34+ cells (as shown in Fig. 10.19A). Note the many blunt pseudopodia and dendritic processes, the pale and rather featureless cytoplasm with little endoplasmic reticulum, and many free ribosomes and polyribosomes. (Courtesy of Dr. CDL Reid.)

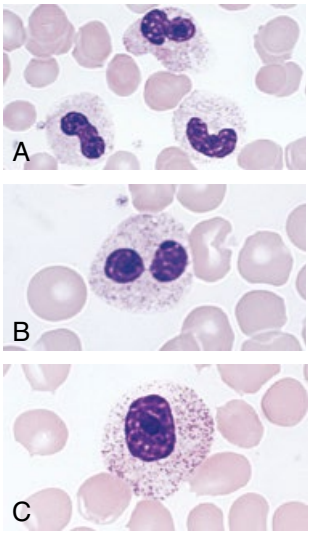

Fig. 10.21. Pelger–Huët anomaly: **A,** Coarse clumping of the chromatin in neutrophils. **B,** "Pince-nez" configurations. **C,** A single rounded nucleus seen mostly in rare homozygous patients. "Pseudo-Pelger" neutrophils can be seen in myeloid leukemias and the myelodysplastic syndromes.

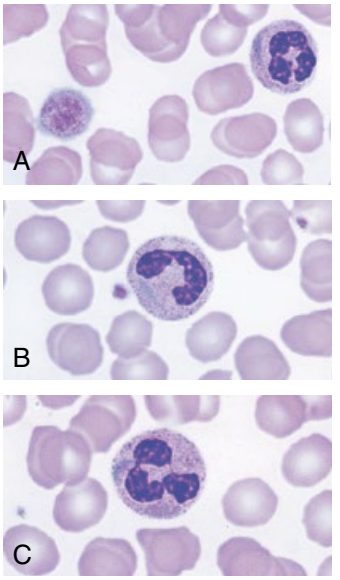

Fig. 10.22. May–Hegglin anomaly. **A–C**, The neutrophils contain basophilic inclusions 2–5 mm in diameter. These inclusions are similar to Döhle bodies (see Fig. 10.36), but are not related to infection. There is an associated mild thrombocytopenia with giant platelets.

infection (Fig. 10.21). The inheritance is dominant. The condition appears to be of no clinical significance, and the affected cells have not been shown to be functionally abnormal. "Pseudo-Pelger" cells occur in acute myeloid leukemia and the myelodysplastic syndromes.

MAY–HEGGLIN ANOMALY

In the May–Hegglin anomaly, a rare condition that has a dominant inheritance pattern, abnormal condensations of RNA appear as mildly basophilic inclusions in the neutrophil cytoplasm (Fig. 10.22). The majority of patients also have thrombocytopenia and giant platelets (Table 27.2). Although most affected individuals have no clinical abnormality, in some there are hemorrhagic manifestations. Similar cytoplasmic inclusions, which are termed Döhle bodies, may be seen in neutrophils during severe infections (see Fig. 10.36) and occasionally in normal pregnancy.

The gene *MYH9* encodes myosin-11A, a protein that enables morphogenesis in various cell types. Defective myosin-11A complexes are due to *MYH9* mutations that underlie various macrothrombocytopenias, including the May–Hegglin anomaly.

CHÉDIAK–HIGASHI SYNDROME

Chédiak–Higashi syndrome is a severe anomaly associated with giant neutrophil granules. A similar granular abnormality is seen in granulopoietic cells in the marrow and in eosinophils, monocytes, and lymphocytes (Fig. 10.23). The inheritance is autosomal recessive. Affected children usually have neutropenia and thrombocytopenia, and suffer from recurrent severe infections. Clinical examination frequently reveals partial albinism and marked hepatosplenomegaly. The majority die in childhood from infection or hemorrhage.

ALDER (ALDER–REILLY) ANOMALY

Alder (Alder–Reilly) anomaly gives rise to deep purple granules in neutrophils (Fig. 10.24). Similar abnormal granules are found in other granulocytes, monocytes, and lymphocytes. The inheritance is autosomal recessive, and the majority of affected individuals have no clinical problems. Similar leukocyte abnormalities are seen in patients with mucopolysaccharide storage disorders, such as Hurler and Maroteaux–Lamy syndromes, and occasionally in amaurotic family idiocy (e.g. Spielmeyer–Vogt syndrome; Figs. 10.25 and 10.26).

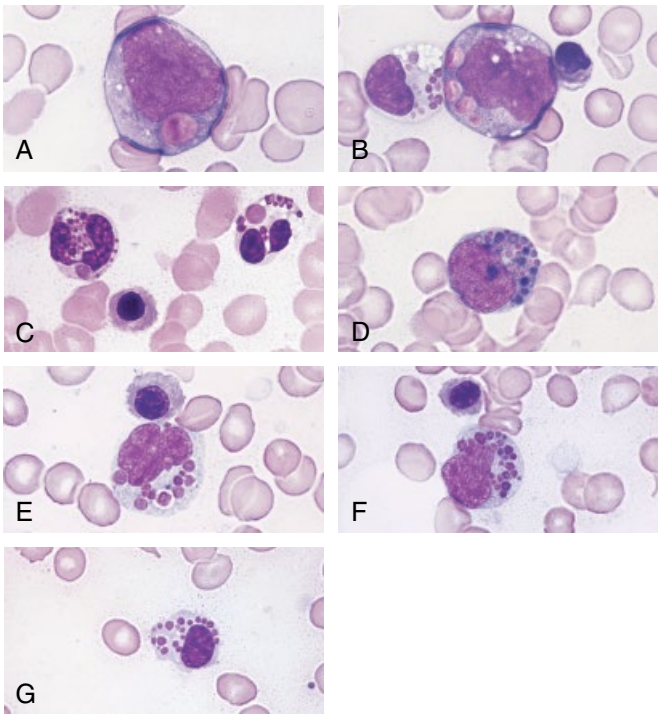

Fig. 10.23. Chédiak–Higashi syndrome: Bizarre giant granules are found in the cytoplasm of all types of leukocytes and their precursors. **A,** Promyelocyte. **B,** Promonocyte and lymphocyte. **C,** Neutrophils. **D,** Early eosinophil. **E, F,** Monocytes. **G,** Lymphocyte.

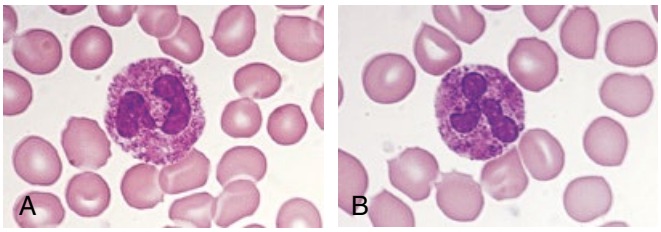

Fig. 10.24. Alder anomaly: Coarse red-violet granules in neutrophils. In this case there was no associated clinical abnormality.

MYELOPEROXIDASE DEFICIENCY

This is the most frequent of the inherited disorders of phagocytes. The gene is at 17q21.3-23. Inheritance is autosomal recessive. The deficiency usually causes no clinical problems except a higher incidence of fungal infections.

NEUTROPHIL-SPECIFIC GRANULE DEFICIENCY

This is a rare autosomal recessive disorder characterized clinically by recurring infections of the skin and lungs. The neutrophils are bilobed and lack specific (secondary) granules. The gene involved may be for a myeloid transcription factor, CCAAT/enhancer-binding protein.

MUCOPOLYSACCHARIDOSES VI AND VII

Abnormal granulation of blood granulocytes and monocytes, together with lymphocyte vacuolation, is found in the Maroteaux–Lamy syndrome, which is also known as mucopolysaccharidosis VI (Fig. 10.25). The striking white cell abnormality may also be seen in patients with mucopolysaccharidosis VII. These lysosomal storage disorders are caused by an inherited deficiency of enzymes concerned in the breakdown of acid mucopolysaccharides. Storage-related abnormalities of connective tissue, the

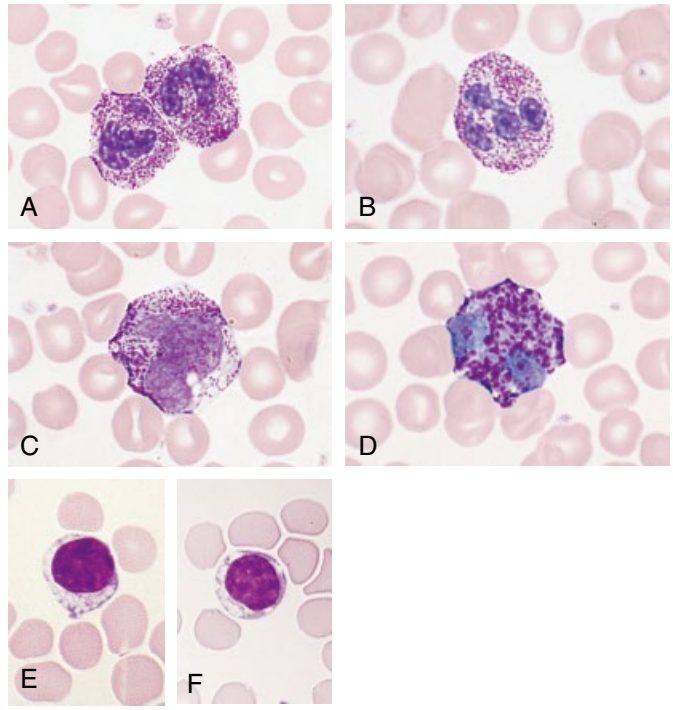

Fig. 10.25. Maroteaux–Lamy syndrome. **A, B,** Coarse red-violet granules in neutrophils. **C,** Monocyte. **D,** Basophil. **E, F,** Prominent vacuolation of lymphocytes. In this variant of Hurler syndrome, there are severe skeletal abnormalities and clouding of the cornea.

heart, the bony skeleton, and the central nervous system produce clinical disabilities similar to, but milder than, those found in classic Hurler syndrome (mucopolysaccharidosis I).

Similar lymphocyte vacuoles may be found (rarely) in patients with inherited defects of enzymes that are involved in the catabolism of oligosaccharide components of glycoproteins (e.g. mannosidosis), and in the rare Spielmeyer–Vogt syndrome (Fig. 10.26).

DORFMAN–CHANARIN SYNDROME

Lipid vacuoles in granulocytes occur in this rare autosomal recessive syndrome in which there is also ichthyosiform erythroderma with variable involvement of the liver, muscles, and central nervous system (Fig. 10.27). There are genetic faults in triacylglycerol metabolism.

LYSINURIC PROTEIN INTOLERANCE

Lysinuric protein intolerance is a rare, autosomal recessive, multisystem disorder characterized by failure to thrive, protein intolerance, pulmonary alveolar proteinosis, osteoporosis, and hemophagocytic-lymphohistiocytosis (Fig. 10.28). There are inherited mutations of the LP1 gene (*SLC7A7*) on chromosome 14, causing transport defects for lysine, cystine, or ornithine and arginine.

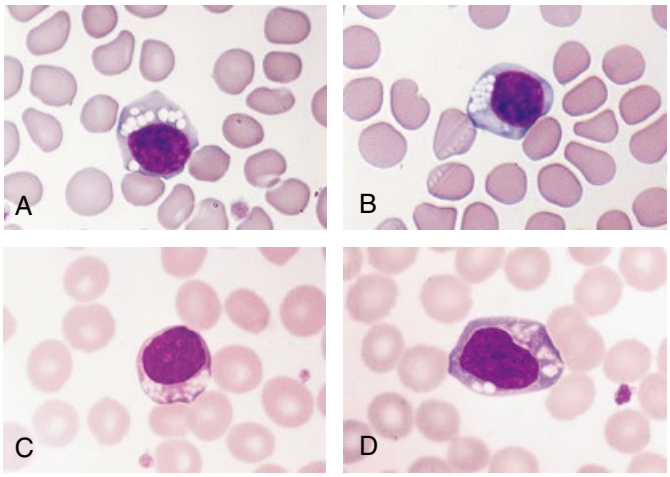

Fig. 10.26. Lymphocyte vacuolation: Further examples of prominent cytoplasmic vacuolation in lymphocytes. **A, B,** Mannosidosis. **C, D,** The Spielmeyer–Vogt syndrome (juvenile-onset amaurotic idiocy).

DISORDERS OF PHAGOCYTIC FUNCTION

Disorders of phagocytic function may be inherited or acquired (e.g. diabetes, renal failure). Inherited disorders involve adherence, mobility and migration (e.g. leukocyte adhesion deficiency), or phagocytosis and killing. The inherited diseases Chédiak–Higashi syndrome, myeloperoxidase deficiency, and deficiency of specific granules discussed earlier all cause reduced neutrophil function.

CHRONIC GRANULOMATOUS DISEASE

Chronic granulomatous disease (CGD) is a rare disease of killing; 60% of cases are X-linked caused by mutations of the gp91^{phox} subunit of cytochrome *b* (*CYBB*) located at Xp21.1. The rest are autosomal recessive due to mutations in p47^{phox}, p21^{phox}, p67^{phox}, and p40^{phox} (Fig. 10.29). Neutrophils, eosinophils, and monocytes are affected. The patient has recurrent infections, usually with catalase-positive organisms (Fig. 10.30), Gram-negative bacilli, or *Aspergillus* species, often in the first year of life.

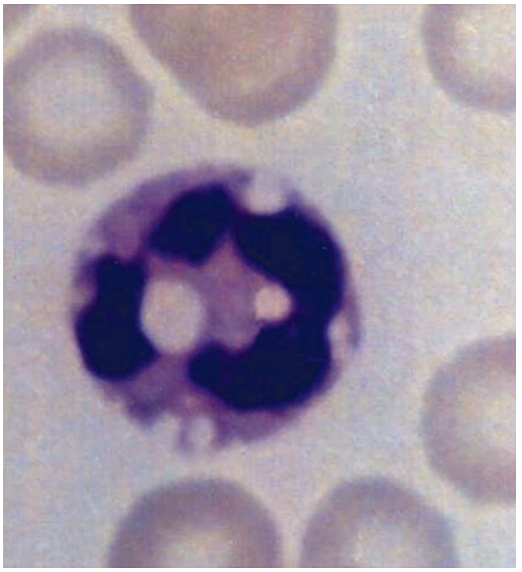

Fig. 10.27. Dorfman–Chanarin syndrome: Lipid-filled clear vacuoles are in neutrophils, eosinophils, and monocytes. Source: Taskin E, et al. *Acta Haematol* 2007;117:16–19. Reproduced with permission of *Acta Haematologica*: Karger Publishers.

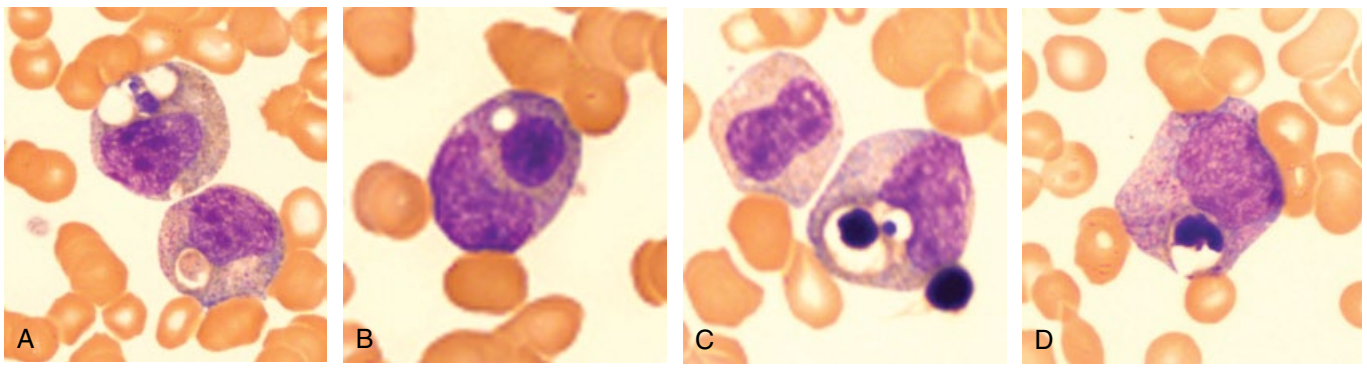

Fig. 10.28. Lysinuric protein intolerance. Hemophagocytosis by myeloid precursors. Source: Gordon WC, et al. *Br J Haematol* 2007;138:1. Reproduced with permission of John Wiley & Sons.

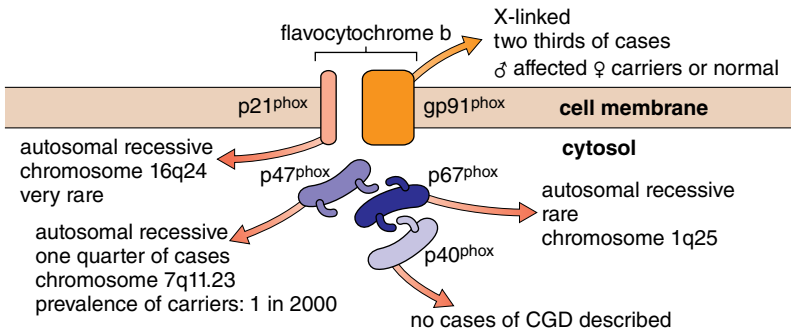

Fig. 10.29. Chronic granulomatous disease: The phagocyte NADPH oxidase (PHOX) flavoprotein *b558* is a membrane-bound heterodimer composed of a glycosylated subunit, gp91^{phox} and a nonglycosylated subunit p21^{phox}. The enzyme is present in the membrane of the phagocytic vacuole. These subunits have been shown to be defective in CGD. Gp91^{phox}, which which is the flavocytochrome itself, has the binding sites for NADPH flavin adenine dinucleotide (FAD) and for heme. Its gene, located on the X chromosome, is abnormal in about two-thirds of cases of CGD. The gene of the other subunit (p21^{phox}) is located on chromosome 16; very occasional defects of this can cause CGD. The genes of the cytosolic proteins p47^{phox} and p67^{phox} are located on chromosome 7 and 1, respectively. Activation of the oxidase is associated with translocation of these two proteins from the cytosol to the membrane, where they bind to the flavocytochrome *b*. Autosomal recessive CGD is normally associated with the lesion p47^{phox} in about a quarter of cases, and occasionally with p67^{phox}. (Courtesy of Professor AW Segal.)

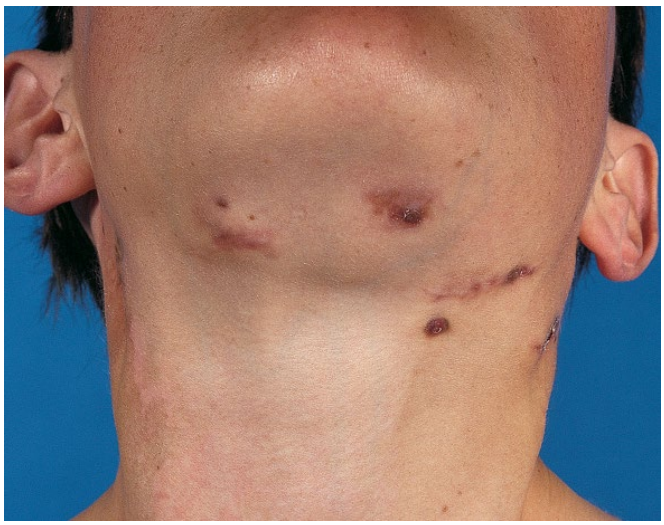

Fig. 10.30. Chronic granulomatous disease: Young man with large submental and cervical nodes with poorly healed sinuses as a result of staphylococcal infection. Cervical lymphadenitis, poor healing, and sinus formation are characteristic and can be confused with tuberculosis because of the granulomatous tissue reaction. (Courtesy of Professor AW Segal.)

Inability of the neutrophils to reduce nitroblue tetrazolium dye suggests the diagnosis.

PAPILLON–LEFEVRE SYNDROME

Papillon–Lefevre syndrome is characterized by early-onset palmoplantar keratoderma and peridontitis with later skin and liver infections. There is reduced neutrophil function due to recessive gene mutations in the gene *CTSC*, 11q14.2, which codes for cathepsin C.

LAZY LEUKOCYTE SYNDROME

Lazy leukocyte syndrome is an autosomal recessive disorder characterized by mild neutropenia with recurring infections in children, and often severe stomatitis with oral stenosis (Fig. 10.31), otitis media, and impaired wound healing. The neutrophils show nuclear herniation of nuclear lobes and agranular regions

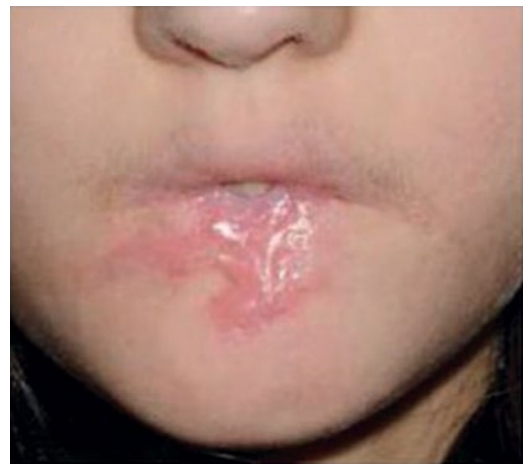

Fig. 10.31. Lazy leukocyte syndrome: Stomatitis with severe oral stenosis. Source: Kuhns DB, et al. *Blood* 2016;128(17):2135–2143. Reproduced with permission of Blood: journal of the American Society of Hematology.

in the cytoplasm (Fig. 10.32). Chemotaxis and chemokinesis is impaired. Mutation of the gene *WDR1* encoding the actin-interacting protein 1 (AIP1) underlies the disease.

LEUKOCYTE ADHESION DEFICIENCY

Leukocyte adhesion deficiency (LAD) disorders are due to a fault in the cell surface integrin or selectin glycoproteins required for adhesion of leukocytes to endothelium, tissue matrix, and microbes (Fig. 10.33). LAD-I, caused by a mutation of *ITGB2* gene coding for the CD18 subunit of β2-integrins, is the most common. LAD-II is due to failure of fucosylation of selectin ligands because of mutation in the gene *SLC365C1* for the fucose transporter. LAD-III is caused by mutation of the gene *FERMT3* involved in activation of β-integrins. All three are autosomal recessive disorders characterized clinically by skin and other more severe infections without pus formation. Delayed separation of the umbilical cord followed by omphalitis is a common presenting feature. LAD-II is the least severe of the three. Severe periodontitis is typical of LAD-I deficiency. Neutrophilia occurs in LAD deficiencies even in the absence of infection.

CARD9 DEFICIENCY

People with this disorder have a selective susceptibility to fungal infections. CARD9 is in the intracellular signaling pathway from the C-type lectin and toll-like cell surface receptors which recognize fungal cell wall components. It forms a trimeric complex with BCL10 and MALT1.

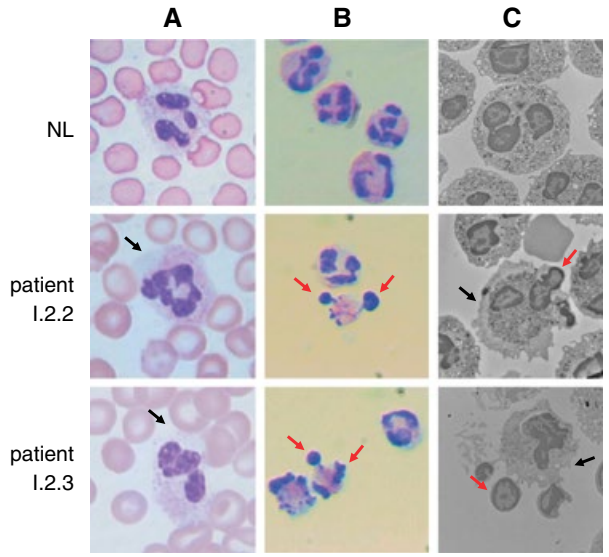

Fig. 10.32. Lazy leukocyte syndrome: Morphology of neutrophils. **A,** Neutrophils from whole blood smears of a normal subject (NL) *(top row)* and patients I.2.2 *(middle row)*, and I.2.3 *(bottom row)* stained with Diff-Quik. The black arrows indicate regions of abnormally agranular cytoplasm. **B,** Neutrophils prepared by Ficoll centrifugation, 3% dextran sedimentation, and sequential erythrocyte hypotonic lysis. Neutrophils were centrifuged onto slides at 100 g for 10 min and then stained. Red arrows indicate herniated nuclear lobes. **C,** Transmission electron micrographs of isolated neutrophils. Black arrows indicate areas of abnormally agranular cytoplasm; red arrows indicate herniated nuclear lobes. Overall, 40–60% of patient cells had abnormal morphology. Source: Kuhns DB, et al. *Blood* 2016;128(17):2135–2143. Reproduced with permission of Blood: journal of the American Society.

LEUKOCYTOSIS

The term leukocytosis refers to an increase in white blood cells (usually to above 12×10^9/L). The most frequent cause is an increase in blood neutrophils. Other leukocytoses involve a predominance of one of the other white cell types found in the blood.

NEUTROPHIL LEUKOCYTOSIS (NEUTROPHILIA)

An increase in neutrophils in the blood of more than 7.5×10^9/L is one of the most frequent abnormalities found in blood counts and blood films (Fig. 10.34). Clinically, fever often results from the release of leukocyte pyrogens. In most neutrophilias the number of band forms increases; occasionally, more primitive cells such as metamyelocytes and myelocytes appear in the peripheral blood (the so-called left shift). In most causes of reactive neutrophil leukocytosis (Table 10.4), toxic changes appear in the neutrophil cytoplasm and on occasion Döhle

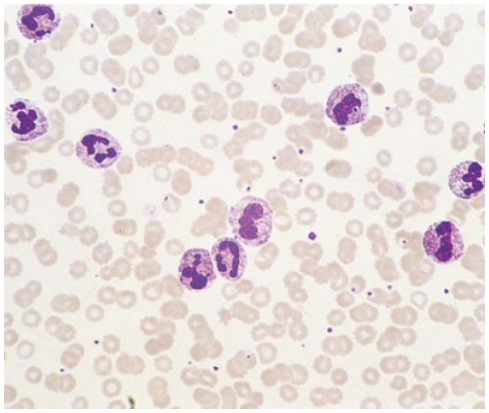

Fig. 10.34. Neutrophil leukocytosis: Large numbers of band-form and segmented neutrophils in the peripheral blood. The patient had abdominal sepsis. (WBC, 45×10^9/L; neutrophils, 41×10^9/L.)

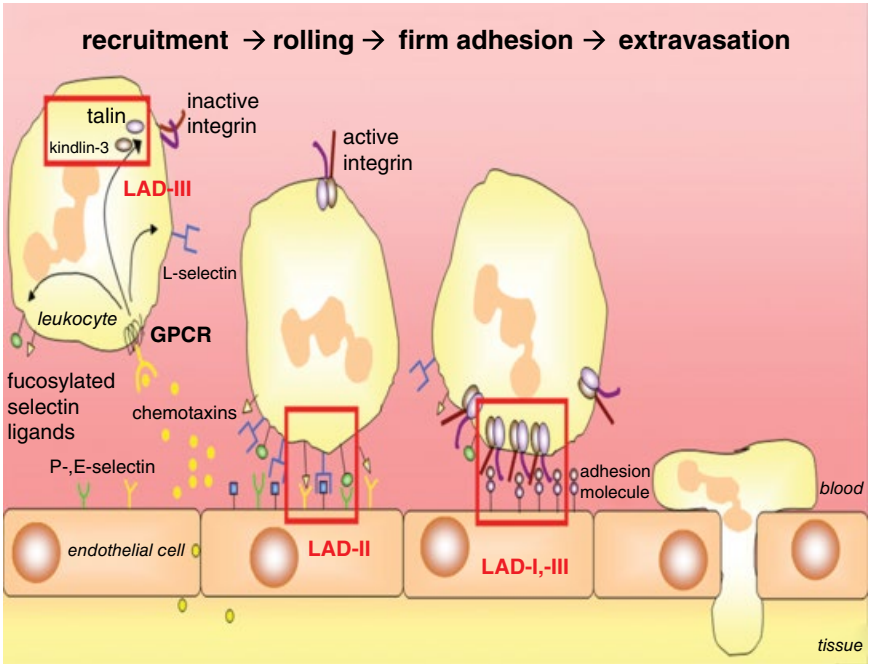

Fig. 10.33. Leukocyte recruitment and extravasation. Leukocytes migrate to the site of inflammation following a gradient of chemotaxins. The cells slow down because of transient interactions between selectins and their glycosylated ligands, which are defective in LAD-II. Next, stable adhesion by leukocyte integrins, absent in LAD-I, to ligands on the endothelium results in leukocyte arrest. Activation of blood cell integrins is decreased in LAD-III. Healthy neutrophils extravasate after firm adhesion. Source: van de Vijver E, et al. *Hematol/Oncol Clin* 2013;27(1):101–116. Reproduced with permission of Elsevier.

TABLE 10.4. CAUSES OF NEUTROPHIL LEUKOCYTOSIS

Bacterial infections
Pyogenic–localized or generalized

Inflammation, necrosis
Cardiac infarct, ischemia, trauma, vasculitis

Metabolic disorders
Uremia, acidosis, gout, poisoning, eclampsia

Corticosteroid therapy

Acute hemorrhage and hemolysis

Myeloproliferative disorders
Polycythemia vera, myelofibrosis, chronic myeloid leukemia
Chronic myelomonocytic leukemia
Malignant neoplasms

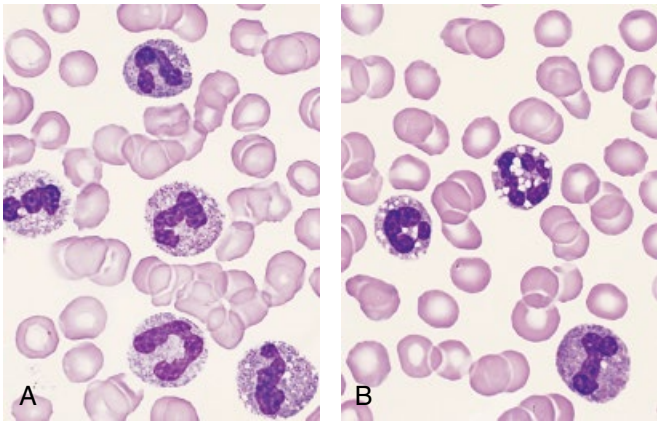

Fig. 10.35. Neutrophil leukocytosis: Toxic changes in neutrophils. **A,** The presence of red-purple granules in the band-form neutrophils. **B,** Cytoplasmic vacuolation.

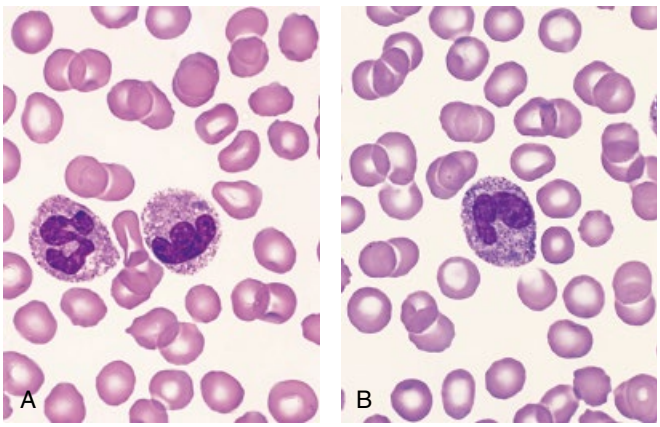

Fig. 10.36. Neutrophil leukocytosis: Döhle bodies, basophilic inclusions of denatured RNA, can be seen in the cytoplasm of these neutrophils.

bodies are present (Figs. 10.35 and 10.36). In some cases of bacterial septicemia, the bacteria ingested by neutrophils may be seen (Fig. 10.37).

HYPERTHERMIA

Body temperatures above 41.1°C (106°F)–most commonly due to heat stroke–are associated with a change in neutrophil (and

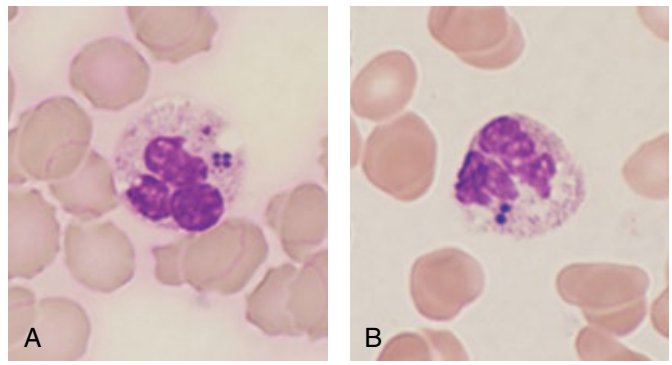

Fig. 10.37. Neutrophil leukocytosis: Neutrophils ingesting bacteria. **A,** Meningococci. **B,** Staphylococci.

lymphocyte and monocyte) morphology. The neutrophil change has been termed botryoid (Fig. 10.38).

EOSINOPHIL LEUKOCYTOSIS (EOSINOPHILIA)

Eosinophilia is the term applied to an increase in blood eosinophils above 0.4×10^9/L (Fig. 10.39). The causes of eosinophilia are listed in Table 10.5. The clonal eosinophilic disorders (myeloid neoplasms with eosinophilia) are discussed in Chapter 17.

Eosinophils may cause tissue fibrosis, vasculitis, thrombosis and allergic inflammation. Tissue damage may occur without a peripheral blood rise in eosinophils. On the other hand, a profound increase in blood eosinophils may occur without tissue damage. The hyper-eosinophilic syndrome (HES) is defined as:

- a peripheral eosinophilic count on at least two occasions of $>1.5 \times 10^9$/L or a marked tissue eosinophilia and
- clinical manifestations directly attributable to the eosinophilia. The most common organs involved are the skin, lung, gastrointestinal tract, heart, and neurological system.

Six categories have been proposed to cause this syndrome (Table 10.6). The same clinical manifestations may occur with any of the six; for example, endomyocardial fibrosis may be due to a clonal myeloproliferative eosinophilia, a parasitic infection, or idiopathic HES. Pulmonary eosinophilic syndromes of varying severity occur. Some are associated with transient pulmonary infiltrates (Fig. 10.40), cough, fever, as well as peripheral eosinophilia.. Similar clinical and X-ray manifestations may occur in some parasitic infestations when migrating parasites lodge in the lungs.

The presence of myelodysplastic or myeloproliferative features in the bone marrow morphology suggests clonal hematopoiesis and is associated with a shorter survival.

MONOCYTOSIS AND BASOPHIL LEUKOCYTOSIS

Conditions associated with monocytosis (Fig. 10.41) are listed in Table 10.7. A basophil leukocytosis is seen most frequently in patients with chronic myeloid leukemia (Fig. 10.42) or polycythemia vera. Moderate increases in blood basophils also occur in myxedema, chickenpox, smallpox, and ulcerative colitis.

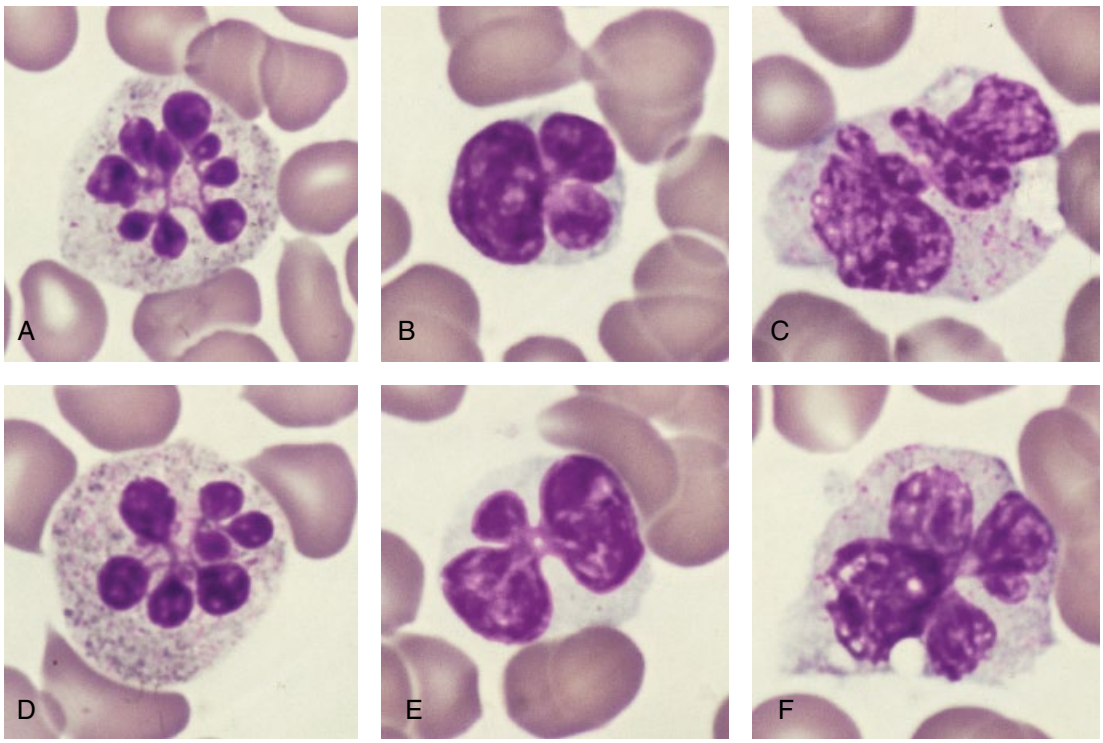

Fig. 10.38. Hyperthermia: Neutrophils with "botryoid" or grape-like nuclei each into six or more lobes *(left panels)*; lymphocytes show nuclear lobation or budding *(center panels)*; monocytes appear binucleate or hyperlobed *(right panels)*. Source: Ward PCJ. *Br J Haematol* 2007;138:130. Reproduced with permission of John Wiley & Sons.

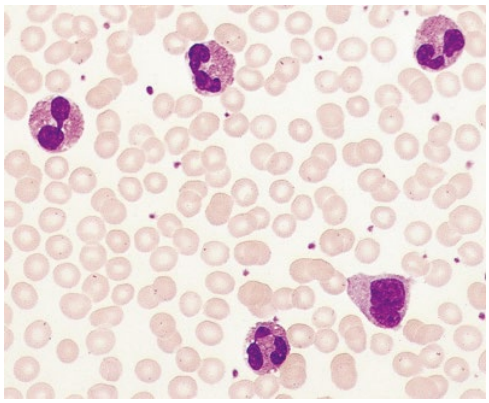

Fig. 10.39. Eosinophilia: Four eosinophils and a monocyte in dermatitis herpetiformis. (Total WBC, 20 × 10⁹/L.)

LEUKEMOID REACTION

The leukemoid reaction is a benign but excessive leukocytosis that is characterized by the presence of immature cells (myeloblasts, promyelocytes, and myelocytes) in the peripheral blood. Whereas most leukemoid reactions involve blood granulocytes (Fig. 10.43), lymphocytic reactions also occur in some. The majority of these reactions are found in association with severe or chronic infections, and sometimes they are also a feature of widespread metastatic cancer or severe hemolysis. Leukemoid reactions occur more frequently in children.

From the diagnostic point of view, the main problem is to distinguish these reactions from chronic myeloid leukemia. Changes such as toxic granulation and Döhle bodies are characteristically found in leukemoid reactions, whereas large numbers

TABLE 10.5. CAUSES OF EOSINOPHILIA

Hereditary (familial)—no evidence of reactive cause or of clonity

Secondary

Infections (mostly helminthic)
Drugs (anticonvulsants, antibiotics, sulfa drugs, antirheumatics, allopurinol, food allergy)
Pulmonary eosinophilia
Miscellaneous other causes of autoimmune/inflammatory/toxic origin:
- Eosinophilia–myalgia syndrome, toxic oil syndrome
- Eosinophilic fasciitis (Schulman syndrome), Kimura disease, Wells syndrome, Omenn syndrome
- Connective tissue diseases (scleroderma, polyarteritis nodosa, etc.)
- Sarcoidosis, inflammatory bowel disease, chronic pancreatitis

Malignancy (metastatic cancer, Hodgkin lymphoma, chronic lymphocytic leukemia)
Endocrinopathies (Addison disease, growth factor deficiency, etc.)

Clonal

Acute leukemia (both myeloid and lymphoblastic)
Chronic myeloid disorder
- Molecularly defined
  - BCR/ABL1+ chronic myeloid leukemia
  - PDGFRA-rearranged eosinophilic disorder (SM-CEL)
  - PDGFRB-rearranged eosinophilic disorder
  - KIT-mutated systemic mastocytosis
  - 8p11 syndrome
- Clinicopathologically assigned
  - Myelodysplastic syndrome
  - Myeloproliferative disorder
    - Classic myeloproliferative disorder (polycythemia vera, etc.)
    - Atypical myeloproliferative disorder
      - Chronic eosinophilic leukemia
      - Systemic mastocytosis
      - Chronic myelomonocytic leukemia
      - Unclassified myeloproliferative disorder

Idiopathic including hypereosinophilic syndrome

TABLE 10.6. CLASSIFICATION OF HYPEREOSINOPHILIC SYNDROMES (HES)

Clinical subtype	Definition	Examples
M-HES	HES with documented or presumed clonal eosinophilic involvement	PDGFR-associated myeloproliferative neoplasms
		Chronic eosinophilic leukemia – not otherwise specified
		Idiopathic HES with myeloproliferative features[a]
L-HES	HES with a demonstrable clonal or phenotypically aberrant lymphocyte population producing cytokines that drive eosinophilia	CD3–CD4+ L-HES
		Episodic eosinophilia and angioedema† (Gleich syndrome)
Overlap HES	Eosinophilic disease restricted to a single organ system accompanied by peripheral eosinophilia >1.5 × 10^9/L	Eosinophilic gastrointestinal disease
		Chronic eosinophilic pneumonia
		Eosinophilic granulomatosis with polyangiitis
Associated HES	Eosinophilia >1.5 × 10^9/L in the setting of a distinct diagnosis, in which eosinophilia has been described in a subset of affected patients	Primary immunodeficiency syndromes, such as autoimmune lymphoproliferative disease and hyper-IgE syndrome
		Sarcoidosis
		Inflammatory bowel disease
Familial HES	HES occurring in multiple members of a single family	Autosomal dominant familial HES
Idiopathic HES	HES of unknown cause that does not meet criteria for any of the other categories	

[a] Such as dysplastic eosinophils, circulating myeloid precursors, anemia, thrombocytopenia, splenomegaly, elevated serum B_{12} and/or tryptase levels, atypical mast cells, hypercellular marrow, and myelofibrosis.

Source: Klion AD. (2015) Hematology: American Society of Hematology. Education Program, pp. 92–97. Reproduced with permission of American Society of Hematology.

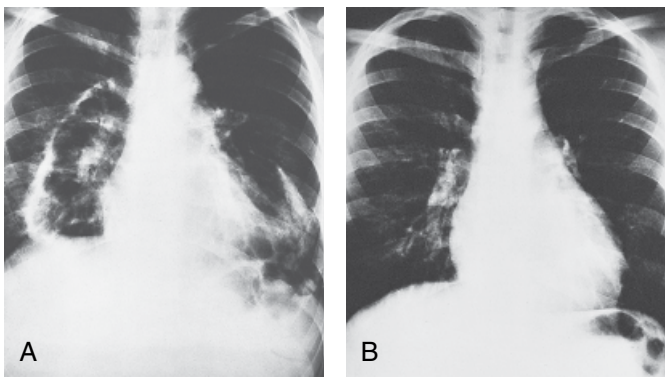

Fig. 10.40. Pulmonary eosinophilia: Chest radiographs. **A,** Diffuse infiltrates in the right middle and lower, and left lower zones. Prominent band shadows suggest areas of collapse. The patient had been taking sulfasalazine for ulcerative colitis. This drug was stopped and prednisolone commenced. **B,** The same patient three weeks later. There is almost complete resolution of the pulmonary changes.

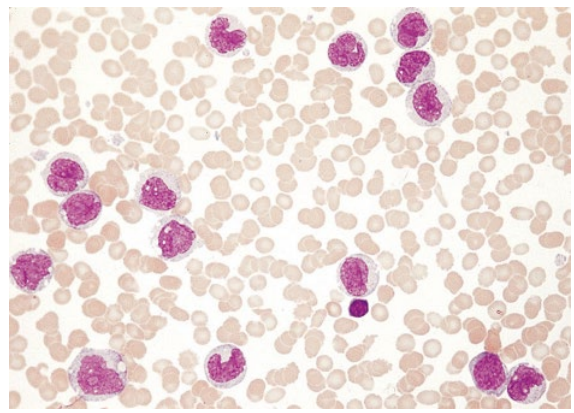

Fig. 10.41. Monocytosis: In this peripheral blood film of chronic myelomonocytic leukemia, with the exception of a single lymphocyte (center), all the nucleated cells shown are monocytes. (Total WBC, 36 × 10^9/L; monocytes, 30 × 10^9/L.)

of myelocytes and the presence of the *BCR-ABL1* fusion gene indicate chronic myeloid leukemia.

LEUKOERYTHROBLASTIC REACTION

Another blood cell variation is leukoerythroblastic reaction, in which erythroblasts as well as primitive white cells are found in the peripheral blood (Figs. 10.44 and 10.45). This reaction is most frequently found when a distortion of marrow architecture is present, because of either proliferative disorders of the marrow or marrow infiltrations, or extramedullary erythropoiesis. The principal causes of the leukoerythroblastic reaction are listed in Table 10.8.

TABLE 10.7. CAUSES OF MONOCYTOSIS

Infections
Tuberculosis, brucellosis, bacterial endocarditis, malaria, kala-azar, trypanosomiasis, typhus
Other inflammatory diseases
Sarcoidosis, ulcerative colitis, Crohn disease, rheumatoid arthritis, systemic lupus erythematosus
Hodgkin disease and other malignant neoplasms
Acute myelomonocytic and monocytic leukemias
Chronic myelomonocytic leukemia

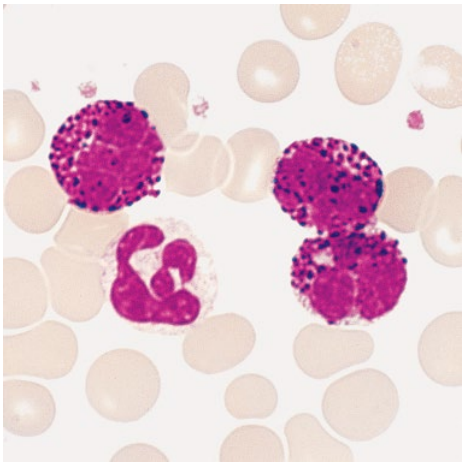

Fig. 10.42. Basophilia: High-power view of three basophils and a neutrophil in a peripheral blood film of chronic myeloid leukemia. (Total WBC, 73×10^9/L; basophils, 7.3×10^9/L.)

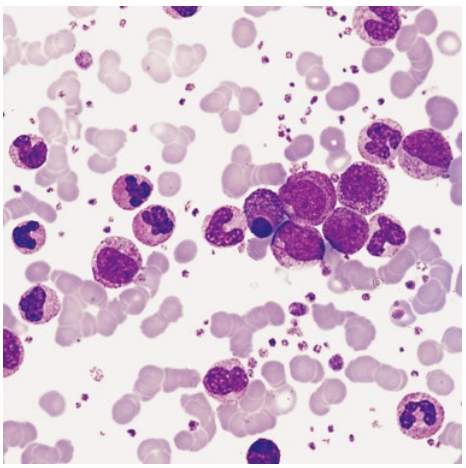

Fig. 10.43. Leukemoid reaction: Neutrophils, stab forms, metamyelocytes, myelocytes, and a single necrobiotic neutrophil (center) in staphylococcal pneumonia. (WBC, 94×10^9/L.)

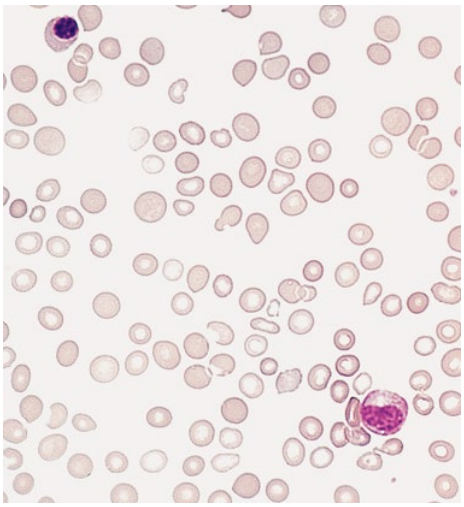

Fig. 10.44. Leukoerythroblastic change: An erythroblast, a myelocyte, red cell polychromasia, anisocytosis, and poikilocytosis, including "teardrop" forms, in primary cell myelofibrosis. (Hb, 9.5 g/dL; WBC, 5×10^9/L; 6 erythroblasts per 100 WBCs; platelets, 45×10^9/L.)

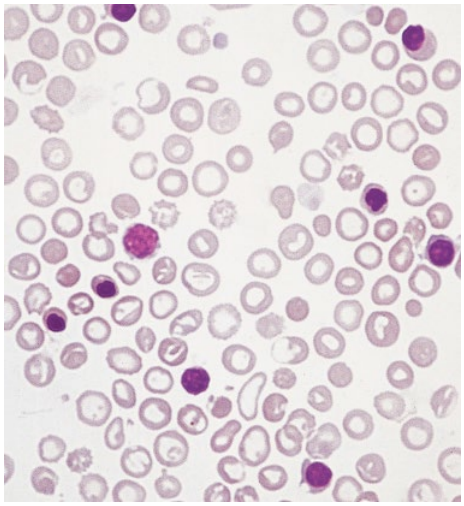

Fig. 10.45. Leukoerythroblastic change: Erythroblasts, two lymphocytes, red cell polychromasia, hypochromia, poikilocytosis, acanthocytosis, and spherocytosis. The differential white cell count included metamyelocytes and myelocytes. This is a case of homozygous α-thalassemia (Hb Bart disease).

TABLE 10.8. CAUSES OF LEUKOERYTHROBLASTIC CHANGE

Metastatic carcinoma in the marrow
Myelofibrosis
Myeloid leukemia
Multiple myeloma
Hodgkin lymphoma
Non-Hodgkin lymphoma and histiocytic tumors
Miliary tuberculosis
Severe megaloblastic anemia
Severe hemolysis, particularly in the young
Osteopetrosis (Albers–Schönberg disease)

NEUTROPENIA

Neutropenia is defined by a blood neutrophil count of less than 2.5×10^9/L. Note, however, that many African and Middle Eastern populations have normal ranges with significantly lower limits than this. Clinical problems related to recurrent infections are associated with absolute levels below 0.5×10^9/L, and neutrophil counts of less than 0.2×10^9/L carry serious risks. Neutropenia may be selective or part of a general pancytopenia (Table 10.9). The majority of neutropenias are caused by reduced granulopoiesis; however, in some patients, the reduced neutrophil counts are caused by increased removal of neutrophils by the reticuloendothelial system or by other tissues. Significant shifts of neutrophils from the circulating population to the marginal pool attached to the vascular endothelium may also be responsible.

SEVERE CONGENITAL NEUTROPENIA

Severe congenital neutropenia (SCN), also called Kostmann syndrome, is caused by a variety of genetic lesions, some of which are yet to be identified (Table 10.10). The inheritance

may be autosomal dominant, autosomal recessive, or X-linked (Table 10.10). It manifests as bacterial infections early in life. The neutrophil count is $<0.5 \times 10^9$/L and usually $<0.2 \times 10^9$/L. Bone marrow shows reduced or absent myeloid precursors. There is usually a block at the promyelocyte stage due to apoptosis of later cells. Apoptosis of cells such as neurons, urinary tract cells, lymphocytes, and natural killer cells accounts for the different syndromes that may be associated with SCN.

Mutations (more than 120 reported) of *ELANE*, encoding the neutrophil granule protease neutrophil elastase (Fig. 10.46), underlie 50–60% of SCN. Rarely, mutations of the transcriptional repressor *GFI1* (which regulates *ELANE* among other genes) or of enzymes *HAX1* (predominantly mitochondrial) and *CLBP* (mitochondrial), *G6PC3* (glucose metabolism), *WAS* (cytoskeleton), *VPS45*, *JAGN1*, or *CSF3R*, underlie such cases (Table 10.10). Some mutations (which may cause SCN) of *ELANE* also underlie cases of congenital cyclical neutropenia.

SCN may also occur with other conditions, such as Shwachman–Diamond syndrome (see Chapter 12), WHIM (warts, hypogammaglobulinemia, immunodeficiency, and myelokathexis) syndrome with *CXCR4* mutation, other immune deficiencies due to mutations in *CD40L*, Bruton kinase deficiency, Barth syndrome (X-linked with skeletal muscle and cardiovascular abnormalities; mutated gene tafazzin, *TAZ*), Cohen syndrome (with hypotonia, obesity, visual problems, and mental retardation; mutated gene *COH1* on chromosome 8), and myelokathexis.

The gene *AP3B1*, encoding a subunit of a complex involved in subcellular trafficking of vesicular cargo proteins (including neutrophil elastase), is mutated in the Hermansky–Pudlak syndrome type 2 (see Chapter 27), which is also associated with neutropenia. Noncyclic neutropenia rarely occurs with poikilodermia (paronychia, palmo-plantar hyperkeratosis, and skeletal defects). The inheritance is autosomal recessive and the gene involved is *USB1* (also known as *C160rf57* and *MPN7*). Mutation of this gene, which encodes a protein involved in RNA splicing, may also underlie a syndrome resembling dyskeratosis congenita (see Chapter 12). There is a risk of transformation to myelodysplastic syndrome or acute myeloid leukemia. This is more with some forms of SCN (e.g. that associated with the Shwachman–Diamond syndrome and some specific mutations of *ELANE2*). Also with the acquisition of truncating mutations of the *GSF3* receptor gene and subsequent mutations of genes such as *RUNX1* or *RAS*.

TABLE 10.9. CAUSES OF NEUTROPENIA

Selective
Drug-induced
Anti-inflammatory – aminopyrine, phenylbutazone
Antibacterial – chloramphenicol, co-trimoxazole
Anticonvulsants – phenytoin, phenobarbital
Antithyroids – carbimazole
Phenothiazines – chlorpromazine, promethazine
Miscellaneous – tolbutamide, phenindione, deferiprone, rituximab
Racial or familial
Congenital (Kostmann syndrome)
Shwachman–Diamond syndrome
Cyclical
Infections
Viral – particularly parvovirus, human immunodeficiency virus, hepatitis
Bacterial – typhoid, miliary tuberculosis
Protozoal – malaria, kala-azar
Autoimmune
Idiopathic, Felty syndrome, systemic lupus erythematosus
Alloimmune
Neonatal, allogeneic stem cell transplantation, Trali (see Chapter 32)
Bone marrow failure
Aplastic anemia, leukemia, myelodysplasia, myelofibrosis, marrow infiltrations, megaloblastic anemia, drugs, chemotherapy (e.g. alkylating agents, antimetabolites) and radiotherapy
Splenomegaly

TABLE 10.10. GENETIC AND HEMATOLOGIC FEATURES OF SEVERE CONGENITAL NEUTROPENIA (SCN)

SCN subtype	Affected gene	Inheritance	Hematopoietic manifestations additional to severe neutropenia	Proposed disease mechanisms
Mutated neutrophil elastase	*ELANE*	AD or sporadic	Leukemia predisposition	Unfolded protein response, excessive apoptosis of myeloid cells
Growth factor independent transcriptional repressor 1 deficiency	*GFI1*	AD	Lymphopenia	Defective transcription, myeloid differentiation block
HAX1-deficiency	*HAX1*	AR	Leukemia predisposition	Mitochondrial leakage, excessive apoptosis
Glucose-6-phosphatase deficiency	*G6PC3*	AR	Thrombocytopenia	Impaired intracellular glucose homeostasis; excessive apoptosis
X-linked neutropenia (XLN)	*WAS*	X-chromosome linked	Lymphopenia, leukemia predisposition	Defective cytoskeleton organization, vesicle trafficking
Vacuolar protein sorting-associated 45 deficiency	*VPS45*	AR	Myelofibrosis	Defective lysosomal trafficking
Jagunal homolog 1 deficiency	*JAGN1*	AR	Neutrophil dysfunction; CSF3 hyporesponsiveness	Aberrant *N*-glycosylation in biosynthetic pathway, reduced CSF3R signaling
Biallelic CSF3R deficiency	*CSF3R*	AR	CSF3 unresponsiveness	Defective CSF3R signaling

AD, Autosomal dominant; AR, Autosomal recessive.

Source: Touw IP (2015) Hematology: American Society of Hematology. Education Program, pp. 1–7. Reproduced with permission of American Society of Hematology.

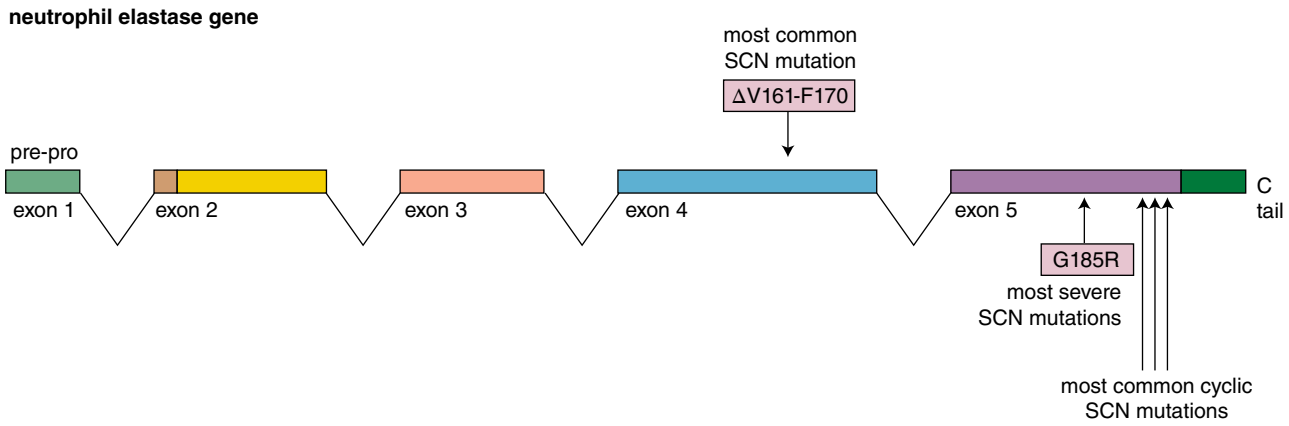

Fig. 10.46. Severe congenital neutropenia (SCN; Kostmann syndrome). Adapted from Horwitz MS, et al. *Blood* 2007;109:1817–1824.

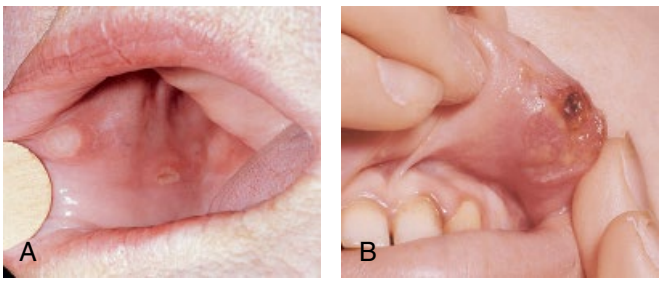

Fig. 10.47. Neutropenia: Ulceration of the buccal mucosa and upper lip in two patients with severe neutropenia.

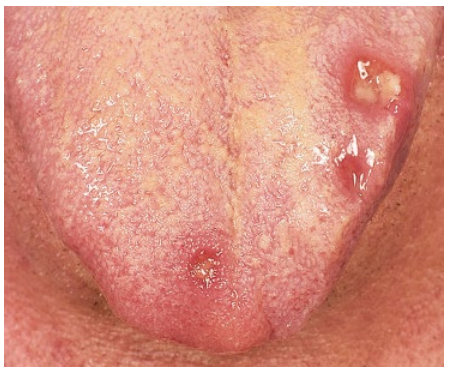

Fig. 10.48. Neutropenia: Ulceration of the tongue in severe neutropenia.

Clinical and bone marrow findings

In severe neutropenia, painful and intractable infections of the buccal mucosa (Figs. 10.47 and 10.48), throat, skin (Fig. 10.49), and the anal region often occur (see also Chapter 13). Pus is not formed.

Bone marrow examination is essential in all patients with severe neutropenia. Evidence of a myeloid neoplasm or an infiltration is found in many. In patients with selective depression of granulopoiesis, a reduction in all granulocyte precursors occurs (Fig. 10.50). In some cases, granulopoietic cells are absent (Fig. 10.51), but in others promyelocytes and myelocytes are present with no evidence of mature neutrophils.

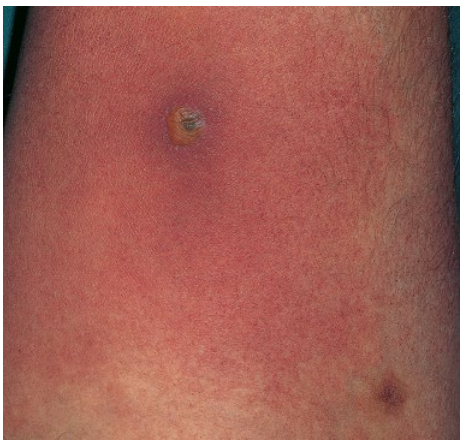

Fig. 10.49. Neutropenia: Infected skin lesion with extensive surrounding subcutaneous cellulitis in severe neutropenia. Cultures grew *Staphylococcus aureus* and *Pseudomonas pyocyanea*.

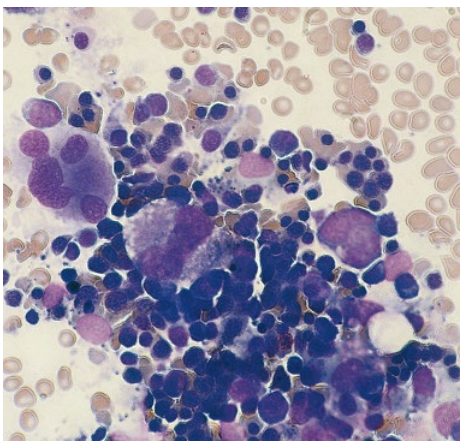

Fig. 10.50. Neutropenia: Bone marrow aspirate showing an absence of granulopoietic cells. The small fragment and cell trail contain mainly erythroblasts and megakaryocytes.

IDIOPATHIC CYTOPENIAS OF UNDETERMINED SIGNIFICANCE

The term idiopathic cytopenia of uncertain significance (ICUS) has been used to describe neutropenia, anemia, or thrombocytopenia

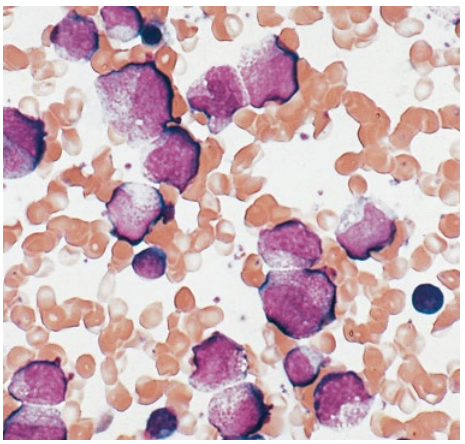

Fig. 10.51. Agranulocytosis: Bone marrow aspirate showing numerous promyelocytes and myelocytes with mature neutrophils absent. (Courtesy of Professor RD Brunning and the Armed Forces Institute of Pathology.)

with <10% dysplastic cells per lineage, without a clonal mutation detected by cytogenetics or fluorescence in situ hybridization (FISH), and with no obvious diagnosis (see Table 15.4). In patients with unexplained cytopenias, somatic mutations of genes frequently mutated in myeloid neoplasm, including myelodysplasia may be found by mutation profiling, implying clonal hematopoiesis. Mutation of spliceosome genes (*SF3B1*, *SRSF2*, *SF3B1*), of *JAK2* and *RUNX1* and comutation patterns involving *DNMT3A*, *TET2*, *ASXL1* have a strong predictive value for subsequent occurrence of a myeloid neoplasm. They are more frequent in males and older age. These gene mutations are most frequent in those showing some evidence of dysplasia in the bone marrow but may also be present in those with no dysplasia. These subjects could in the future be added to the World Health Organization classification of myelodysplastic syndrome. Unpaired mutations of *DNMT3A*, *TET2*, and *ASXL1* have a low predictive value on their own, being frequent in "CHIP" patients (see Table 15.4).

When a clonal mutation is present typical of myeloid neoplasia but criteria for myelodysplasia or other hematologic neoplasms are absent, the condition has been termed clonal cytopenia of uncertain significance (CCUS). If a clonal mutation is present with or without a cytopenia and with minimal dysplasia (<10% of cells per lineage), the term clonal hematopoiesis of indeterminate potential (CHIP) has been used (see Chapter 15 and Table 15.4).

MYELOKATHEXIS

A rare syndrome, myelokathexis may be related to myelodysplasia, but it occurs in young patients and is associated with chronic neutropenia and repeated infections. Marrow aspirates show many cells of the neutrophil series with hypersegmentation and longer than normal chromatin strands separating nuclear lobes (Fig. 10.52). Binucleate myelocytes, metamyelocytes, and band forms are a feature. The mature neutrophils are functionally defective.

WHIM SYNDROME

WHIM syndrome consists of warts, hypogammaglobulinemia, infections, and myelokathexis (Fig. 10.53). It is caused by inheritance of a mutation in the gene encoding the receptor CXCR4

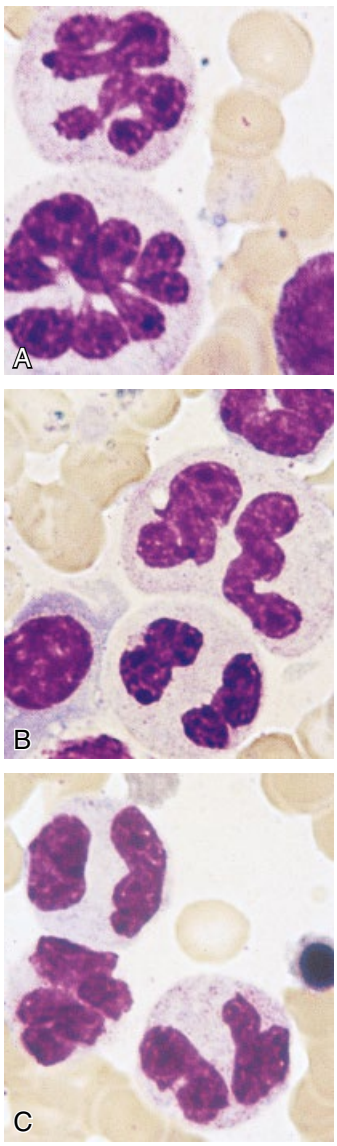

Fig. 10.52. Myelokathexis: Bone marrow aspirate showing large band and segmented neutrophils including hyperdiploid forms, with hypersegmentation and abnormal separation of nuclear lobes. Binucleate band forms are apparent.

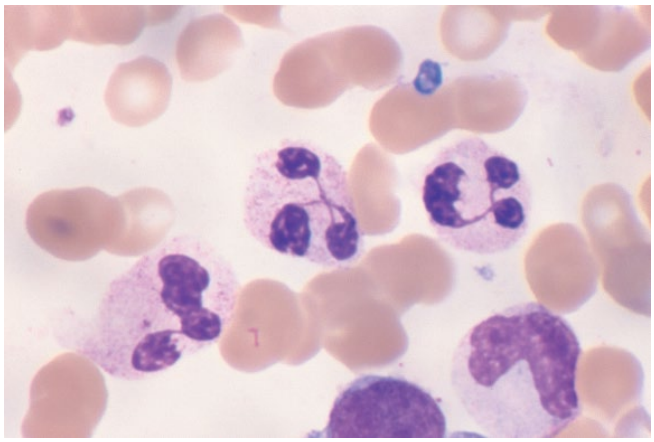

Fig. 10.53. Myelokathexis: WHIM syndrome. Neutrophils with abnormal separation of nuclear lobes. The neutrophils may also show cytoplasmic vacuoles and pyknotic nuclei. (Courtesy of Dr. S Imashuku.)

for the stromal factor 1 (SDF-1). CXCR4 plays a key role in cell adhesion to bone marrow stroma. The complex SDF-1–CXCR4 is important in regulating trafficking of leukocytes from marrow to blood and to stromal cells. Acquired CXCR4 mutations are present in the tumor cells in about 30% of cases of Waldenström macroglobulinemia.

LYSOSOMAL STORAGE DISEASES

The lysosomal storage diseases of the reticuloendothelial system (Table 10.11) may result in pancytopenia, vacuolation, or abnormal granulation of blood cells, and the accumulation of degenerate foam cells in the bone marrow, liver, and spleen. These lysosomal storage conditions result from defects in lysozomal hydrolytic enzymes (Fig. 10.54). The products of metabolism normally degraded by the specific enzyme that is defective disrupt the lysosomes and damage cell structure. Inheritance is autosomal recessive.

GAUCHER DISEASE

Gaucher disease is a relatively common familial disorder characterized by the accumulation of glucocerebrosides (especially glucosylceramide) in reticuloendothelial cells. It occurs because the enzyme glucocerebrosidase is deficient. There are three types (Table 10.12):

- Type 1: Chronic adult
- Type 2: Acute infantile neuropathic
- Type 3: Subacute neuropathic with onset in childhood or adolescence.

The gene is located on chromosome 1 band q21. There is a pseudogene 16 kbp downstream from the glucocerebrosidase gene, which is 95% homologous. The disease is caused by one of

TABLE 10.11. LYSOSOMAL STORAGE DISEASES

Sphingolipidoses
Gaucher disease
Niemann–Pick disease
Farber disease
GM gangliosidoses
Mucopolysaccharidoses
Hurler, Scheie, and Hurler–Scheie disease
Hunter disease
Sanfilippo disease
Marquio syndrome
Maroteaux–Lamy syndrome
Diseases of complex carbohydrate metabolism
Sialidoses
Mucolipidoses
Fucosidosis
Mannosidosis
Aspartylglucosaminuria
Sialic acid storage disease
Acid lipase deficiency
Wolman disease
Cholesterol ester storage disease
Neuronal ceroid lipofuscinoses

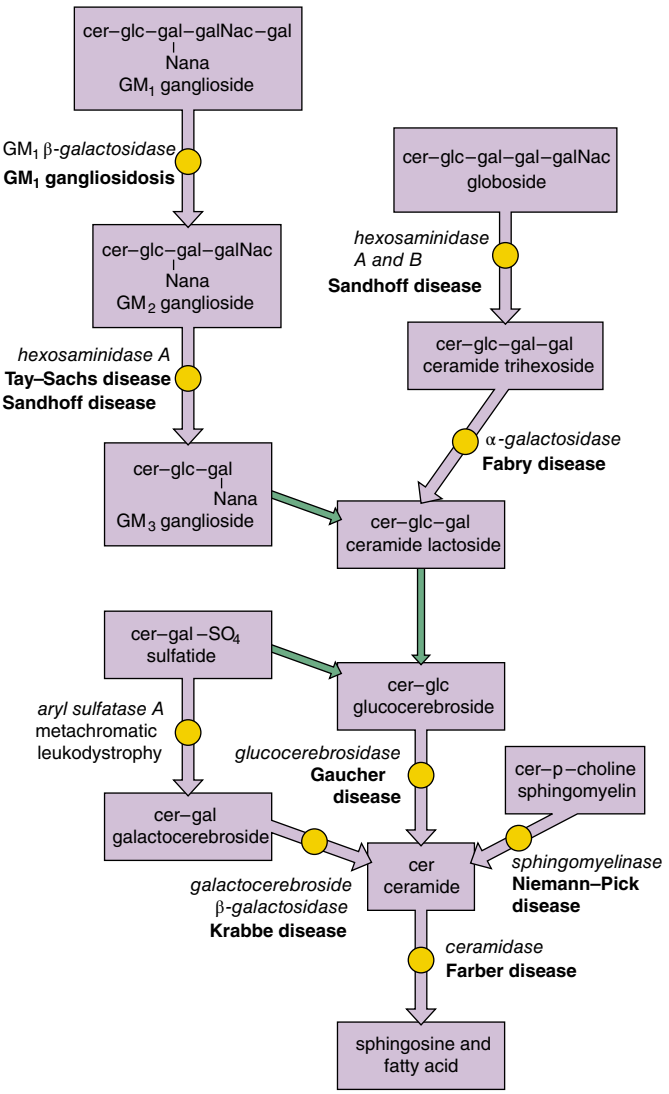

Fig. 10.54. Sphingolipid mechanism: Pathways and diseases. The enzymes involved are given in italics, and below each is the disease (in bold) that results from deficiency of that particular enzyme. cer, Ceramide; glc, glucose; gal, galactose; galNac, acetylgalactosamine; Nana, *N*-acetylneuraminic acid. Source: Kolodny EH, Tenembaum AL. In: Nathan DG, Oski FA, eds. *Hematology of Infancy and Childhood*, 4th edn. Saunders, 1992, p. 1452. Reproduced with permission of Elsevier.

TABLE 10.12. CLINICAL MANIFESTATIONS OF GAUCHER DISEASE

Manifestation	Type 1	Type 2	Type 3
Onset	1 year	<1 year	2–20 years
Hepatosplenomegaly	++	+/–	+
Bone disease	++	–	+/–
Cardiac valve disease	–	–	+
CNS disease	–	+++	+/–
Oculomotor apraxia	–	+	+/–
Corneal opacities	–	+/–	+/–
Age at death	60–90 years	<5 years	<30 years

Source: Hoffbrand AV, et al., eds. *Postgraduate Haematology*, 6th edn. Blackwell Scientific, 2005. Reproduced with permission of John Wiley & Sons.

more than 300 mutations or deletions or the formation of fusion genes between the functional gene and the pseudogene. The high prevalence in Ashkenazi Jews largely arises from a mutation at cDNA nucleotide 226 (amino acid 370). The chronic adult non-neuropathic form of the disease is accompanied by hepatosplenomegaly and bone lesions (Fig. 10.55), and sometimes by lymphadenopathy, skin pigmentation, and pingueculae (Fig. 10.56). The most acute neuropathic forms manifest in infancy, and survival beyond the first 3 years of life is rare. A juvenile form may manifest in childhood with features of the chronic adult form, as well as progressive neurologic dysfunction.

A presumptive diagnosis of Gaucher disease may be made when Gaucher cells are detected in marrow aspirates (Fig. 10.57A and C) and trephine biopsies (Fig. 10.57B). Diagnosis can be confirmed by the absence or severe deficiency of glucosylceramide β-glucosidase in fibroblast cultures and by DNA analysis. Gaucher cells are also found in the liver and spleen (Fig. 10.57D). Most patients with this condition have elevated plasma acid phosphatase, serum angiotensin-converting enzyme (SACE), ferritin, and transcobalamin II levels. Serum chitotriosidase is markedly raised and can be used to monitor efficacy of enzyme therapy. Over 50% of adult patients usually have asymptomatic radiographic changes, such as cortical expansion of the lower end of the femur, which produces a characteristic radiolucent area (Fig. 10.58).

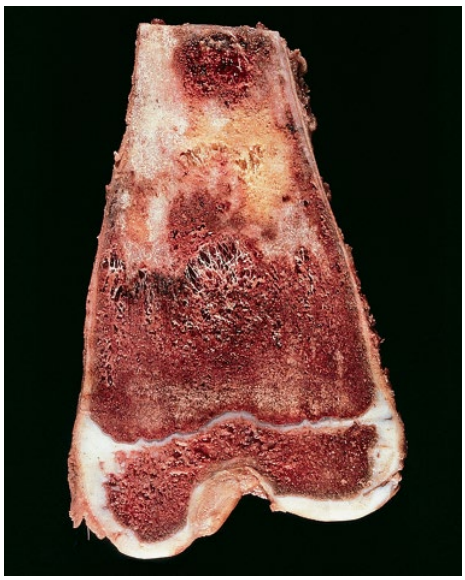

Fig. 10.55. Gaucher disease: Lower end of femur showing expansion of marrow cavity with thinning of cortical bone and multiple infarcted areas (white) giving typical Erlenmeyer flask deformity. There is subchondral bony collapse with osteonecrosis. (Courtesy of Professor R Brady.)

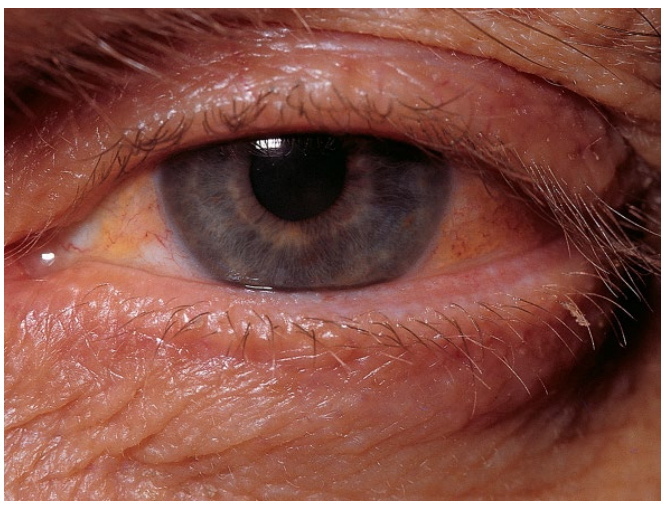

Fig. 10.56. Gaucher disease: Pingueculae – the brownish-yellow wedge-shaped thickenings of the bulbar conjunctiva.

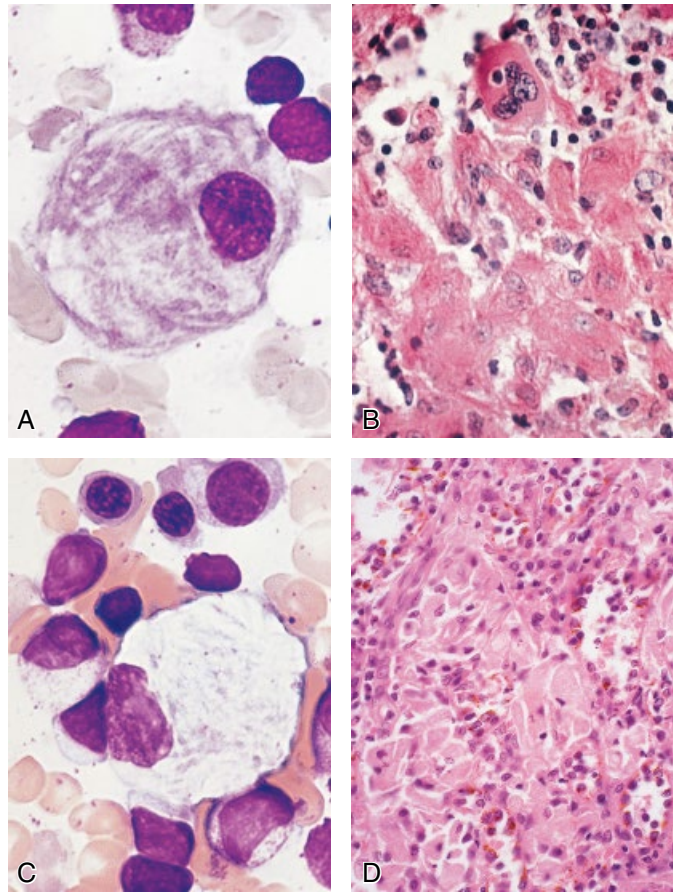

Fig. 10.57. Gaucher disease: **A, C,** Characteristic histiocytic cells with a fibrillar or "onion-skin" pattern of unstained inclusion material. **B,** In biopsy, these cells are histiocytes with a finely granular cytoplasmic PAS reaction. **D,** In the spleen, the histiocytic cells appear as pale clusters in the reticuloendothelial cords between the venous sinuses.

It is now possible to replace the missing enzyme using recombinant DNA techniques with enzymes such as imiglucerase, velaglucerase, and taliglucerase (Fig. 10.59). Following therapy there is improvement in blood counts, reduction in liver and spleen size, and remodeling of the bones with reduction of osteoporosis (Fig. 10.60), which can be demonstrated by magnetic resonance imaging (MRI) scan (Fig. 10.61). Substrate reduction therapy with oral agents (e.g. miglustat and eliglustat) are also used clinically.

NIEMANN–PICK DISEASE

Niemann–Pick disease is a sphingomyelin lipidosis that is rarer than Gaucher disease, and is characterized by extensive tissue storage of sphingomyelin, hepatic and splenic enlargement, and large lipid-filled macrophages in the bone marrow. In its best-defined forms there is an inherited deficiency of the enzyme

sphingomyelinase, and sphingomyelin concentration in the tissues is up to 100 times higher than normal. As in Gaucher disease, acute neuropathic and chronic non-neuropathic forms occur.

The disease is suspected in young children with hepatosplenomegaly when bone marrow aspirates show the presence of foam cells (Fig. 10.62). Confirmation is by showing low levels of sphingomyelinase in fibroblasts cultured from skin or bone marrow. In less severe adult forms of the disease, large numbers of sea-blue histiocytes may be found in bone marrow aspirates, in addition to the classic foam cells (Fig. 10.63).

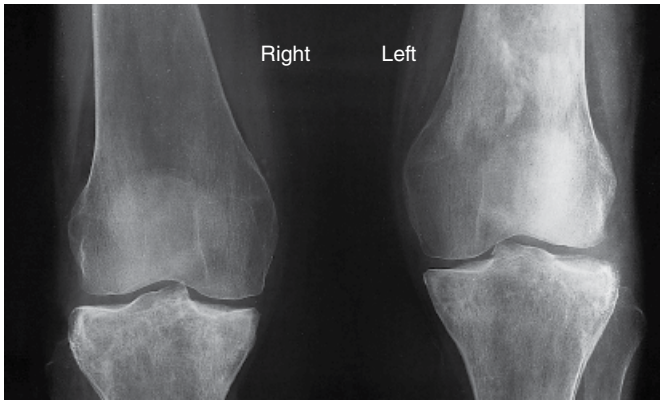

Fig. 10.58. Gaucher disease: Radiograph of the knee joints in a 45-year-old woman shows failure of correct modeling with expansion of the lower ends of the femurs. Bone thinning and loss of trabecular pattern are particularly apparent in the right femur. The sclerosis in the left femur and right tibia is caused by bone infarcts.

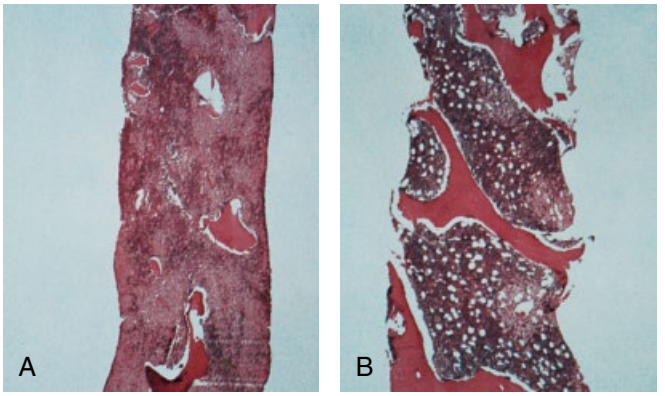

Fig. 10.60. Gaucher disease: Appearances of bone biopsy. **A,** Before aglucerase therapy. **B,** After 12 months of aglucerase therapy. (Courtesy of Professor R Brady.)

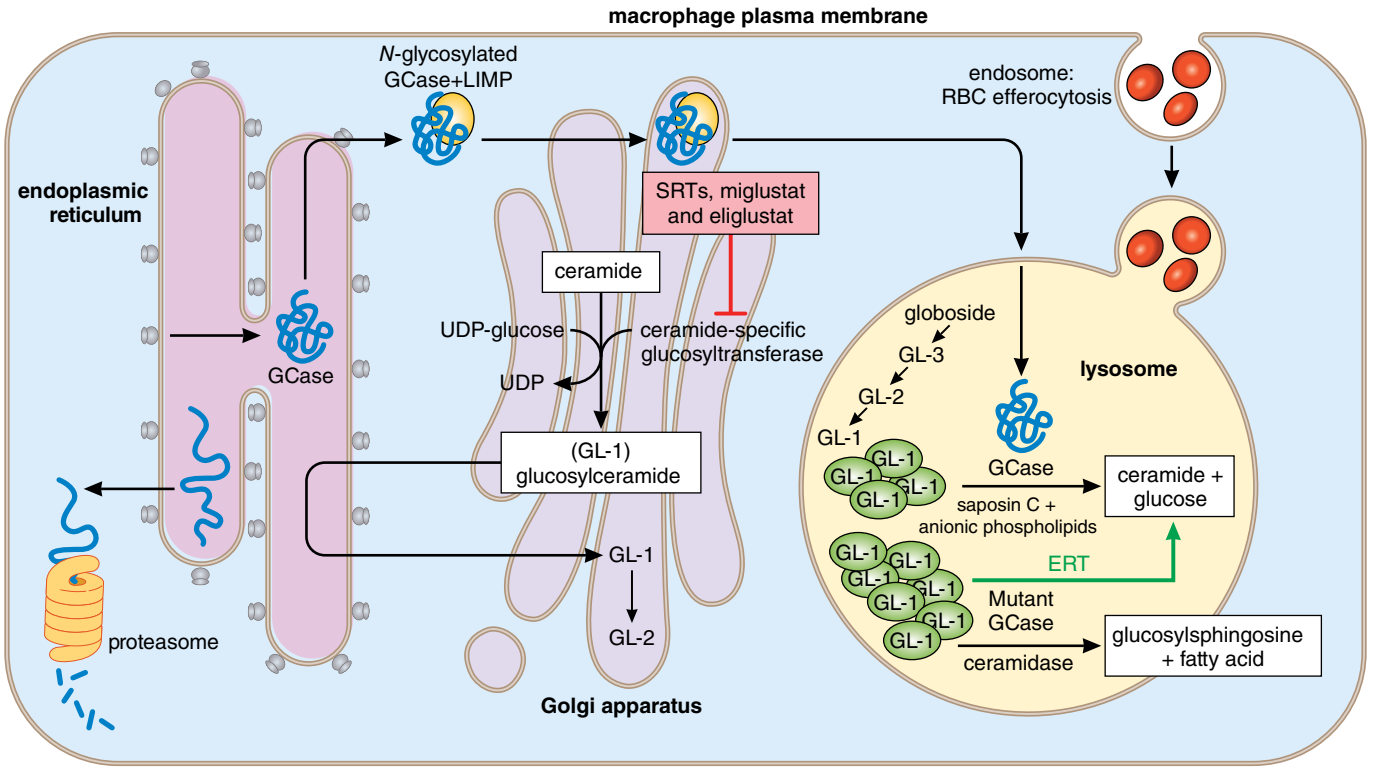

Fig. 10.59. The role of lysosomal acid–glucocerebrosidase in glycolipid metabolism. The site of action of substrate reduction drugs is indicated. Glucocerebrosidase (GCase) is manufactured and *N*-glycosylated in the rough endoplasmic reticulum (ER) and folded by intracellular chaperones (ER Hsp70 family member BiP/Grp78) into a functional conformation. After association with lysosomal integral membrane protein (LIMP), GCase undergoes further processing and packaging in the Golgi apparatus and is delivered to the lysosome where, in association with an essential cofactor, saposin C, and anionic phospholipids, it catalyzes the hydrolysis of glucocerebroside (GL-1) to ceramide and glucose. Mutant GCases fail to properly fold in the ER and trigger the unfolded protein response, ubiquitination, and disassembly in the proteasome. However, some mutant GCase with variably residual hydrolytic activity does traffic to the lysosome. Enzyme replacement therapy (ERT) is delivered directly to the lysosome where it augments the qualitatively and quantitatively deficient mutant GCase activity. GL-1 is synthesized de novo on the cytosolic surfaces of the Golgi and, via a detour to the smooth ER, is returned to the Golgi lumen where it is processed into more complex glycosphingolipids. Substrate reduction therapies (SRTs) slow the synthesis of GL-1 by the inhibition of ceramide glucsyltransferase. However, much of the GL-1 that is stored in Gaucher macrophages is derived exogenously, secondary to lysosomal degradation of senescent blood cells. Source: Weinreb NJ. *Blood* 2017;129(17):2337–2338. Reproduced with permission of *Blood: Journal of the American Society of Hematology*.

SEA-BLUE HISTIOCYTE SYNDROME

Patients with the rare sea-blue histiocyte syndrome usually have splenomegaly and thrombocytopenic purpura, in some cases with associated hepatic cirrhosis. The inheritance pattern is autosomal recessive. A Leu149 deletion in the gene apolipoprotein Ep (*APOE*) has been detected in some cases. Bone marrow aspirates contain large numbers of "sea-blue" histiocytes (Fig. 10.64). Phospholipids and sphingomyelin accumulate in tissue, and reduced levels of cellular sphingomyelinase activity have been reported. The syndrome is a variant of Niemann–Pick disease.

Other causes of sea-blue histiocytosis, all associated with lipid loading of histiocytes in the bone marrow and spleen are listed in Table 10.13.

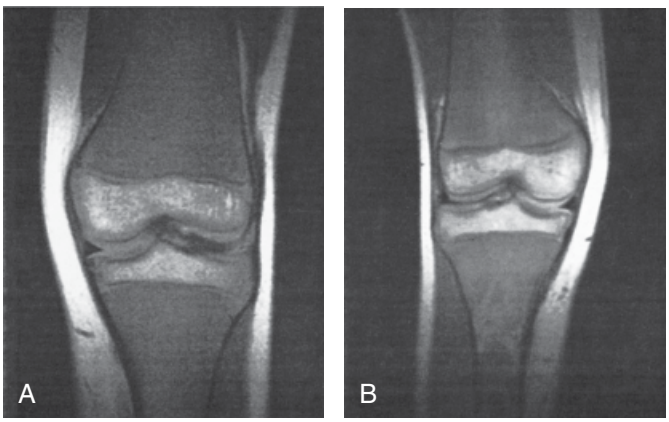

Fig. 10.61. Gaucher disease: MRI scan of the left knee of an 11-year-old girl. **A,** Before treatment showing Erlenmeyer flask deformity with expansion of the marrow and thinning of the cortical bone – the bone marrow images have uniformly low intensity. **B,** Following 1 year of aglucerase therapy the bone marrow intensity is brighter, and remodeling of the bone is occurring (accompanying a growth spurt). (Courtesy of Dr. L Berger.)

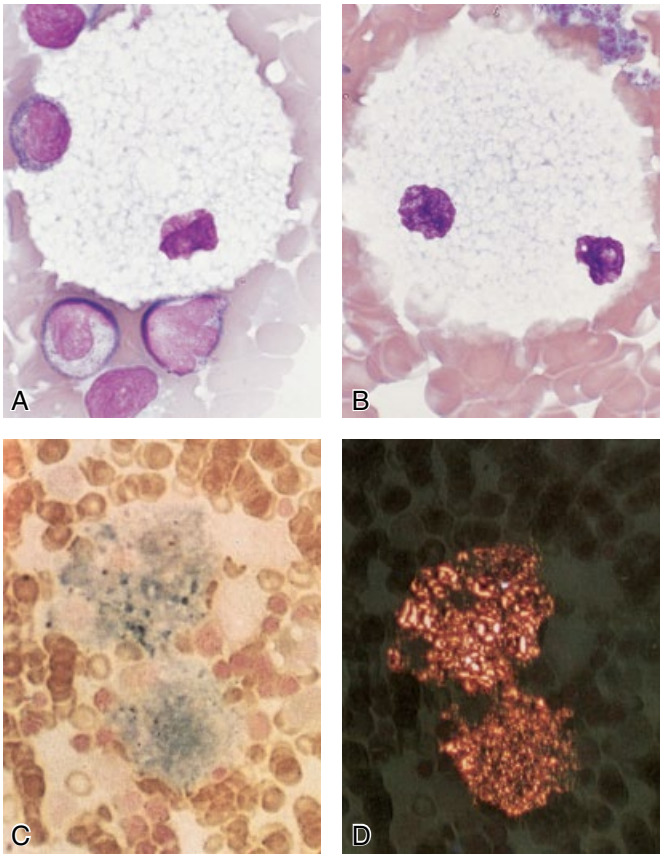

Fig. 10.62. Niemann–Pick disease (infantile): **A, C,** Bone marrow showing typical histiocytic cells with foamy deposits in the cytoplasm. **B,** The histiocytic cells stain weakly with Sudan black stain for lipid. **D,** In polarized light, strong red birefringence is present in the Sudan stain. Source: C, D, Hann IM, et al. *Color Atlas of Paediatric Hematology*, 2nd edn. Oxford University Press, 1990. Reproduced with permission from Oxford University Press.

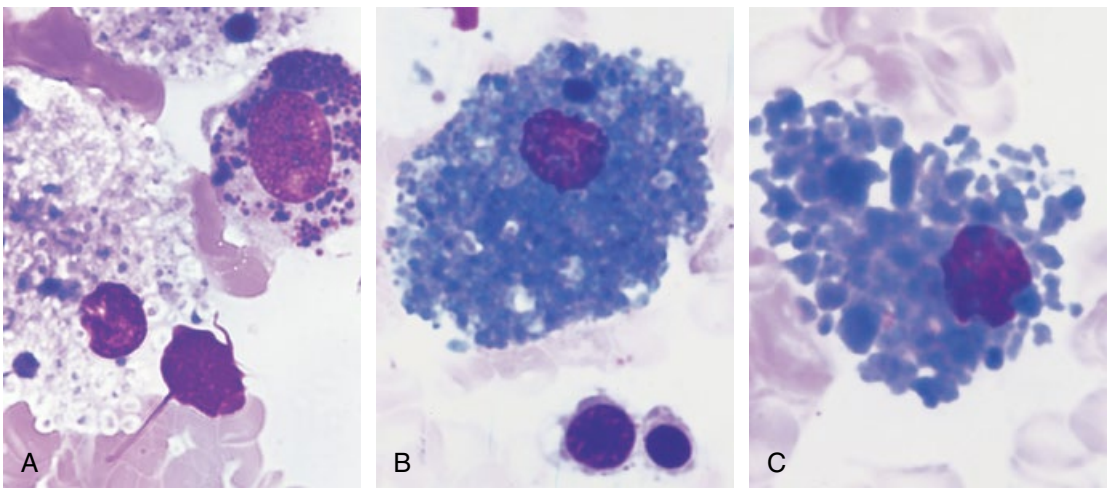

Fig. 10.63. Niemann–Pick disease (adult): **A,** Bone marrow showing typical foam cells. **B, C,** Prominent histiocytes with sea-blue cytoplasm.

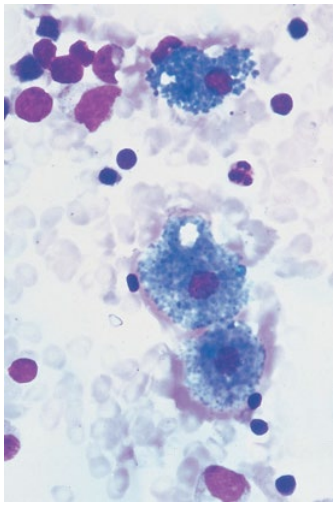

Fig. 10.64. Sea-blue histiocyte syndrome: Bone marrow showing typical cells in the cell trails.

TABLE 10.13. CAUSES OF SEA-BLUE HISTIOCYTES IN THE BONE MARROW OR SPLEEN

Frequent, in marrow
Sea-blue histiocyte syndrome
Niemann–Pick disease
Occasional, in marrow
Hyperlipoproteinemia
Hereditary acetyltransferase deficiency
Wolman disease
Other lipid storage disorders
Chronic myeloid leukemia
Polycythemia vera
Myelodysplasia
Chronic immune thrombocytopenia
Thalassemia
Sickle cell disease
Sarcoidosis
Chronic granulomatous disease
Parenteral nutrition

CHAPTER

BENIGN DISORDERS OF LYMPHOCYTES AND PLASMA CELLS

11

Lymphocytes provide acquired immunity (Fig. 11.1). They have cell surface receptors that bind specific antigens. They assist phagocytes in defense against infection and provide specificity. They are derived from hematopoietic stem cells (see Chapter 2). There are two types, B cells and T cells. B cells are so-called because in avians they differentiate in an organ called the bursa of Fabricius. T cells are initially processed in the thymus. The majority of circulating lymphoid cells (mature T and B cells) are produced in peripheral lymphoid tissue–lymph nodes, spleen, thymus, and lymphoid tissues of the gastrointestinal and respiratory tracts. Lymphocytes usually make up less than 10% of the normal bone marrow myelogram, and the progenitor lymphoblasts are difficult to differentiate from other blast cells. The growth factors involved in lymphocyte formation are shown in Fig. 3.5.

T CELLS

Mature T cells make up 65–80% of the circulating lymphocyte population. Early in T-cell development there is expression of nuclear terminal deoxynucleotidyl transferase (TdT) and the surface antigen CD7 followed by CD2 (Fig. 11.2). The CD2, CD5, and CD3 antigens are expressed on the surface later, although intracytoplasmic CD3 is one of the earliest markers. Finally, CD4 and CD8 antigens are expressed in medullary thymocytes after T-cell receptor (TCR) gene rearrangement is complete (see Fig. 11.2).

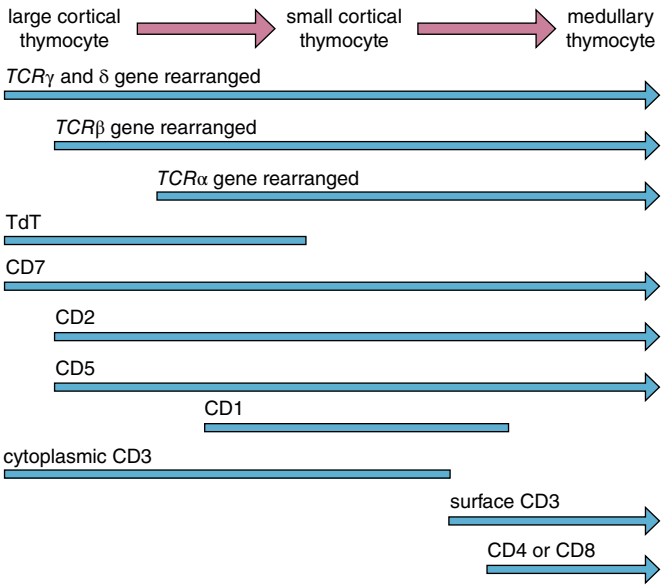

Fig. 11.2. Early T-cell development: Sequence of T-cell receptor (*TCR*) gene rearrangements and antigen expression.

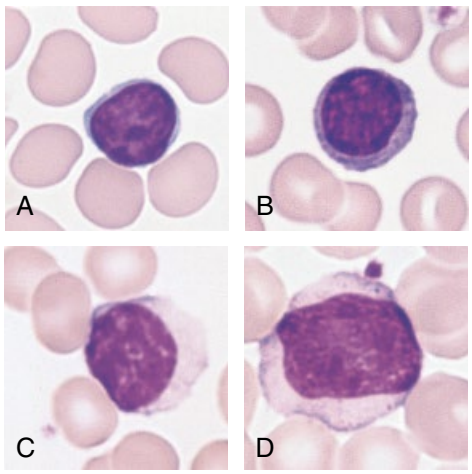

Fig. 11.1. T lymphocytes. **A, B,** Normal small lymphocytes are 7–12 μm in diameter with light blue scanty cytoplasm and a central round nucleus with a condensed amorphous chromatin pattern. **C, D,** Some lymphocytes have diameters up to 20 μm, and even larger forms are found during viral and other infections.

CD8+ cells, the major subpopulation of T cells in the marrow, include the suppressor and/or cytotoxic cells. CD8+ T cells can be seen after viral infection and may have large granules (Fig. 11.3). CD4+ (helper) cells predominate in the peripheral blood. CD4+ cells are in turn subdivided into Th1 and Th2 cells, which secrete different cytokines in response to stimulation by interleukin 2 (IL-2) and interferon γ (IFNγ) or IL-4, respectively (Fig. 11.4).

The T-cell surface contains an antigen receptor that consists of α and β chains, each with variable and constant portions (Fig. 11.5). A receptor coded for by γ and δ genes exists in a minority of T cells. The genes for these polypeptide chains, on chromosomes 14 and 7 (Table 11.1; see Fig. 11.9), are rearranged in T cells in a manner similar to the rearrangement of immunoglobulin (Ig) genes in B cells (see Figs. 11.9–11.11), which results in

Color Atlas of Clinical Hematology: Molecular and Cellular Basis of Disease, Fifth Edition. A. Victor Hoffbrand, Paresh Vyas, Elías Campo, Torsten Haferlach, and Keith Gomez

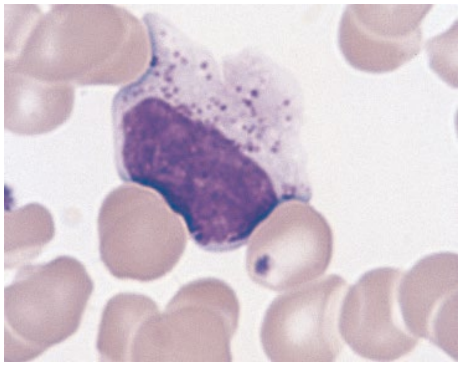

Fig. 11.3. Large granular lymphocyte: Cells of lymphoid appearance with multiple azurophilic granules probably include cells of both lymphocyte (CD8+) and myeloid origin and have NK activity.

a wide diversity among T lymphocytes. Rearrangement occurs in the sequence δ,γ, β, and, finally, α. Close by the T-cell receptor on the cell surface membrane is a complex of proteins termed the CD3 complex, which consists of γ, δ, and ε chains (Fig. 11.5). This complex is responsible for transducing signals derived from interaction of antigen with the T-cell receptor to the cell interior.

T cells recognize antigens only when they are presented by antigen-presenting cells (APCs) in the form of peptides held on HLA molecules. These are HLA class II for CD4 cells and HLA class I for CD8 cells (see Chapter 25).

PD-1–PD-L1

Cytotoxic T cells are limited from killing normal or neoplastic tissues by the presence of programmed cell death protein 1 (PD-1)

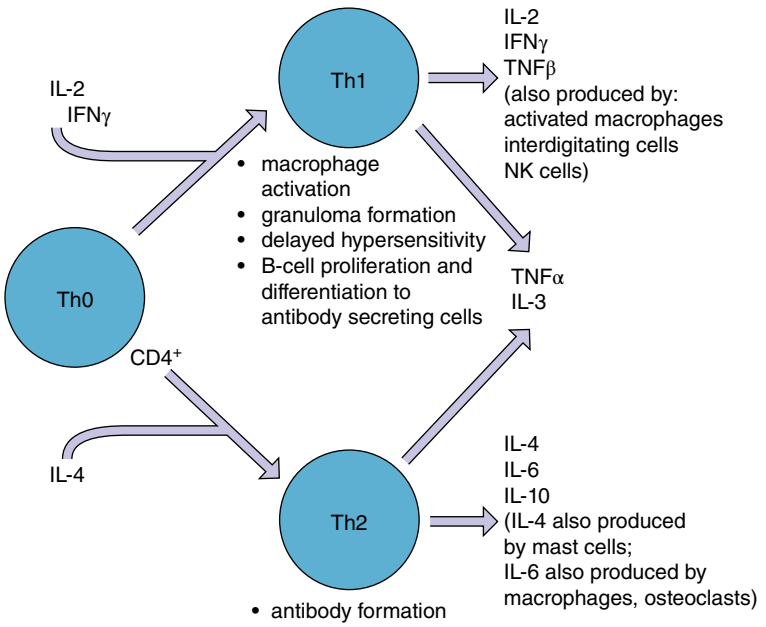

Fig. 11.4. Maturation pathways of CD4+ T helper cells. CD4+ T cells that have been activated by antigen acquire the capacity to produce cytokines. The cytokines produced depend on the environment in which activation occurs. Two main types of cytokine-producing Th cell are recognized: Th1 and Th2 cells. The cytokines produced by Th1 cells tend to promote further Th1 cell formation and inhibit Th2 cell formation, and IL-4 produced by Th2 cells promotes further differentiation toward Th2 cells. Th1-promoting cytokines are also produced by activated macrophages, interdigitating cells, and NK cells, whereas mast cells also produce IL-4.

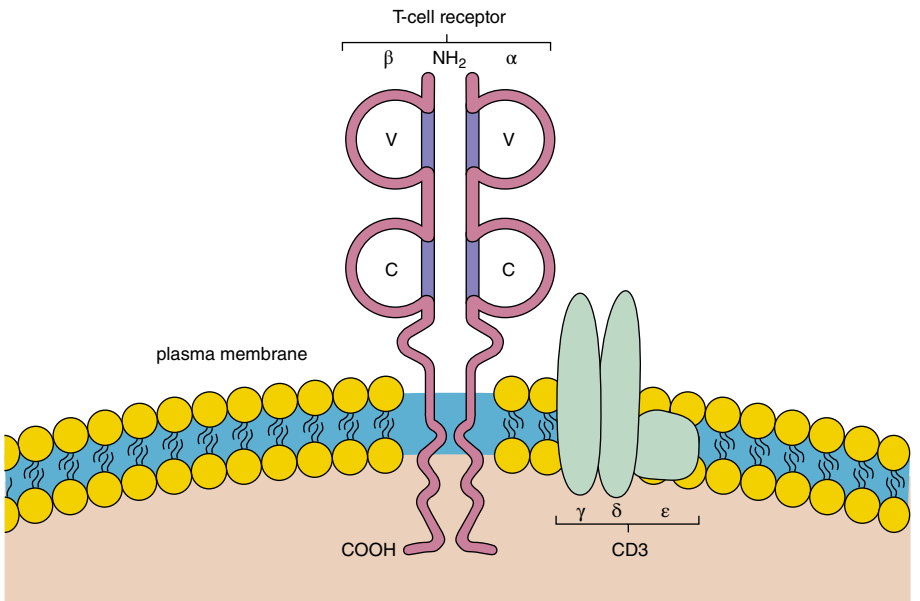

Fig. 11.5. The T-cell antigen receptor consists of α and β chains, each of which has a variable (V) and a constant (C) segment. The chains have transmembranous portions, but very short intracytoplasmic domains. The associated CD3 complex is involved in signal transduction to the cell interior.

TABLE 11.1. ORGANIZATION OF ANTIGEN RECEPTOR GENES

Gene	Chromosome localization	V	D	J	C	Additional diversity	Complementarity-determining region 3 diversity	Clonal rearrangement in (%) acute lymphoblastic leukemia	
								B lineage	T lineage
IgH	14q32	~50	30	6	10	N regions	V-N1-D1-N2-J V-N1-D1-N2-D2-N3-J	100	15–20
IgLκ	2p12	~40	–	5	1	N regions	V-N-J/V-J	20	0
IgLγ	22q11	~29	–	6	6	None	V-J	5	0
TCRα	14q11	~70	–	~90	1	N regions	V-N-J	NT	70
TCRδ	14q11	~4	3	3	1	N regions	V-N1-D1-N2-D2-N3-J	40–50	95[a]
TCRγ	7p15	12	–	5	2	N regions	V-N-J	40–50	95
TCRβ	7q32	~50	2	13	2	N regions	V-N1-D-N2-J	0	80

[a] At least 30% of these cases show deletion of TCRδ.

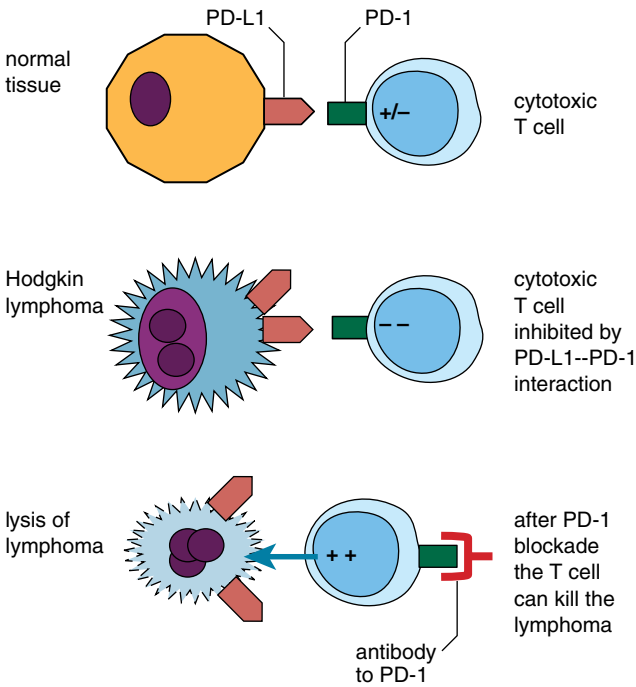

Fig. 11.6. Potential mechanism whereby Hodgkin lymphoma is controlled after treatment with antibodies to block PD-1. PD-1 and PD-L1 are natural molecules that limit the attack of normal tissues by cytotoxic T cells. Hodgkin lymphoma overexpresses PD-L1 due to gene amplification or effects of Epstein–Barr virus (EBV) infection. This delivers a strong negative signal to the T cells around the tumor. If antibody-mediated blockade of PD-1 is used, the T cells can then recognize and kill the tumor.

on the T cell and of its ligand PD-L1 on tissues (Fig. 11.6). Monoclonal antibodies which bind to PD-1 and so overcome this block are in trials to treat various neoplastic diseases, including Hodgkin lymphoma.

CHIMERIC ANTIGEN RECEPTOR CELLS

Chimeric antigen receptor (CAR) cells are T cells that have been modified so that they are cytotoxic without HLA restriction (Fig. 11.7). Target specificity is bestowed by a single-chain variable fragment usually derived from monoclonal antibodies raised against cell surface antigens. If the antigen is expressed on normal as well as tumor cells, toxicity can become unacceptable. B-cell malignancies are attractive targets for CAR cells as they express antigens (e.g. CD19, CD20, CD22), for which there are many existing monoclonal antibodies. Normal B cells will also be destroyed.

B CELLS

The bone marrow remains the principal site of "virgin" B-lymphocyte formation. A schema of the B-cell maturation in the marrow and the periphery is set out in Figs. 11.8 and 11.9 and this shows that the surface antigen profile allows identification of discrete stages of B-cell lymphopoiesis. As B cells mature in ontogeny there is a carefully coordinated program that leads to the production of nuclear (nuclear enzyme TdT), cytoplasmic, and surface markers (such as membrane-bound immunoglobulin molecules [Igs] that are antigen specific). Some surface antigens may be detected before surface Ig and others after Ig expression. The majority of B cells carry HLA-DR antigens, which are important in the regulation of the immune response. Complement receptors for C3b and C3d are also found on more mature B cells.

The key hallmark of B cells is production of surface Ig (and eventually the ability to secrete Ig when they mature to plasma cells – see later). Surface Igs are individual to each B-cell clone and are identical to those secreted as antibodies by the B lymphocyte or plasma cell. The Ig can be one of five classes – IgM, IgD, IgG (divided into four subtypes), IgE, and IgA (divided into two subtypes). Each Ig molecule consists of two light chains (κ or λ) and heavy chains (μ, δ, γ, ε, or α), which determine the class of Ig (Fig. 11.10). Both heavy and light chains contain constant and variable regions.

The heavy chain genes are on chromosome 14 and the light chain genes on chromosomes 2 (κ) and 22 (λ) (Fig. 11.11; see Table 11.1). The production of Igs requires a complex rearrangement of the immunoglobulin gene loci (Fig. 11.10). Diversity is produced by differences in the rearrangement of the genes for the variable (V), diversity (D), joining (J), and constant (C) regions of the Ig molecules they secrete (see Figs. 11.11 and 11.12), and also by insertions of a variable number of random bases in "N" regions of TdT.

Gene rearrangement processes are mediated by a recombinase enzyme system, the RAG enzymes, that recognizes specific joining sequences, which consist of a palindromic heptamer and nonamer sequences separated by spacer regions of 12 or 23 base pairs.

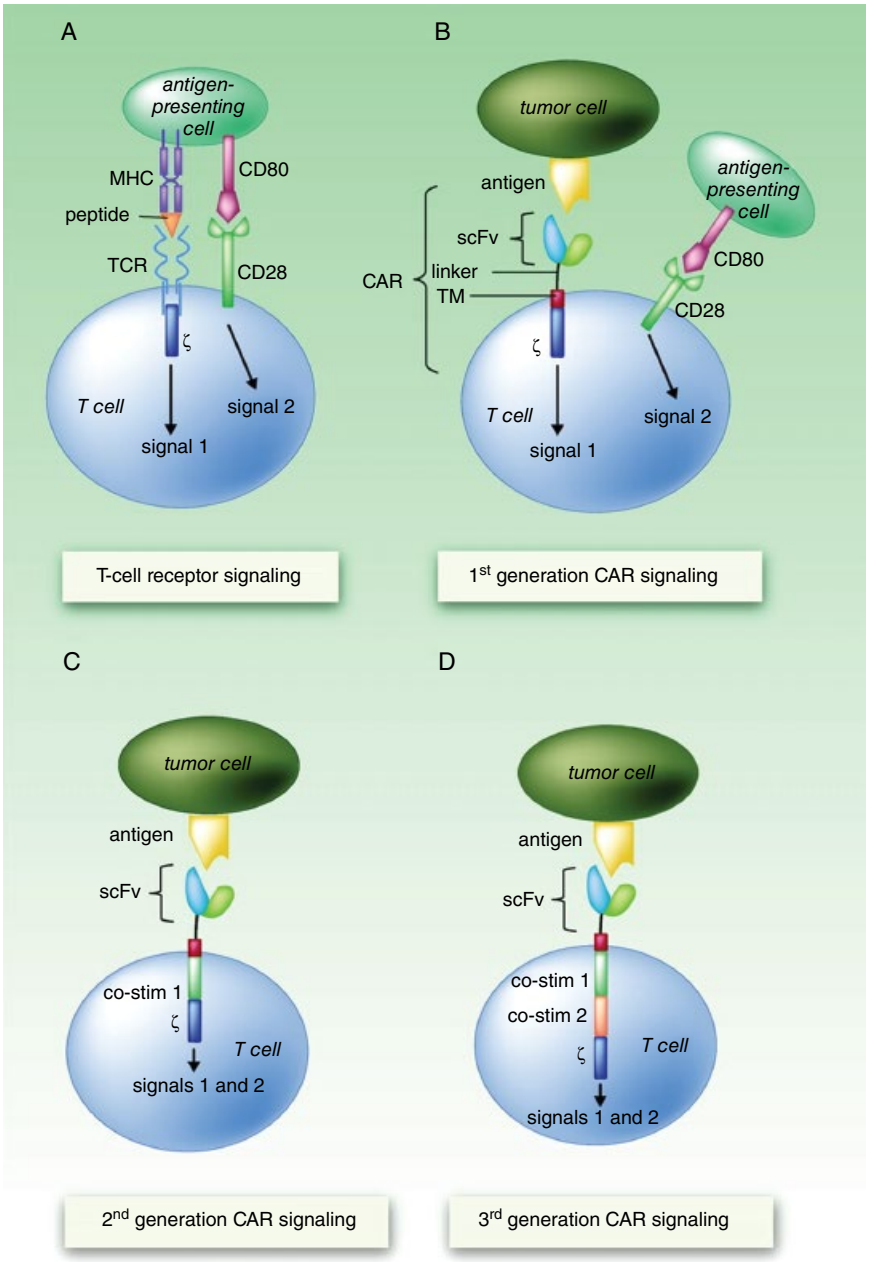

Fig. 11.7. Current chimeric antigen receptor (CAR) design allows for major histocompatibility complex (MHC)-independent antigen recognition and incorporates costimulatory signal(s) endowing the transduced T cell with potent cytotoxic activity. In contrast to the TCR, which recognizes peptide in the context of MHC and provides signal 1, CARs interact in an MHC-independent manner. All CARs must provide signal 1 in the form of the TCRζ-activating subunit (first generation), but the addition of one (second generation) or two (third generation) costimulatory signals (CD28, 4-1BB, or OX40) provides the CAR-transduced T cell with both signals 1 and 2, leading to full activation, proliferation, and cytotoxicity. Source: Lee DW, et al. *Clin Cancer Res* 2012;18:2780–2790. Reproduced with permission of *Clinical Cancer Research*: American Association for Cancer Research.

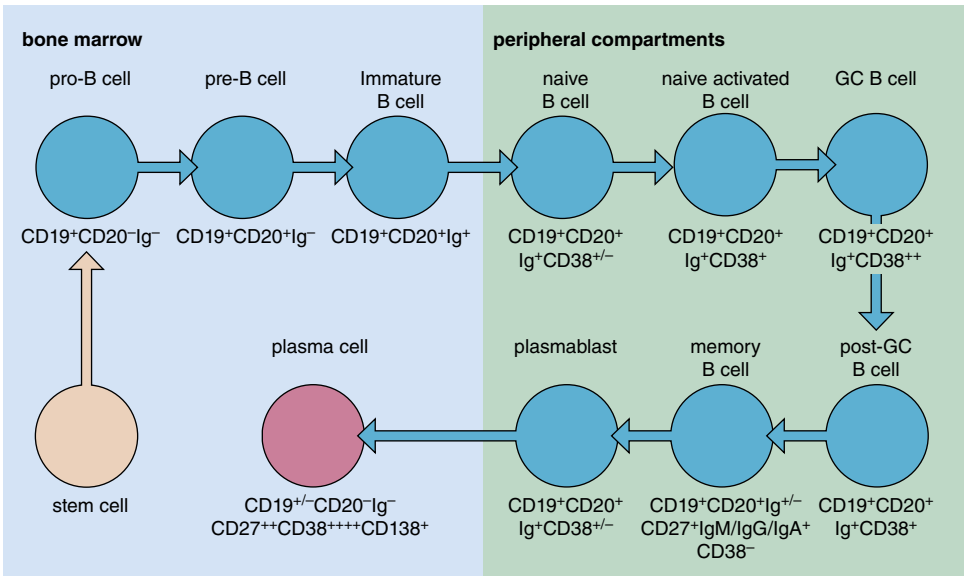

Fig. 11.8. Schematic pathway of cellular intermediates from a stem cell and the earliest recognized B cell (a pro-B cell) to more mature B cells. The location of the cell types is shown, as is the surface immunophenotype (below the cell).

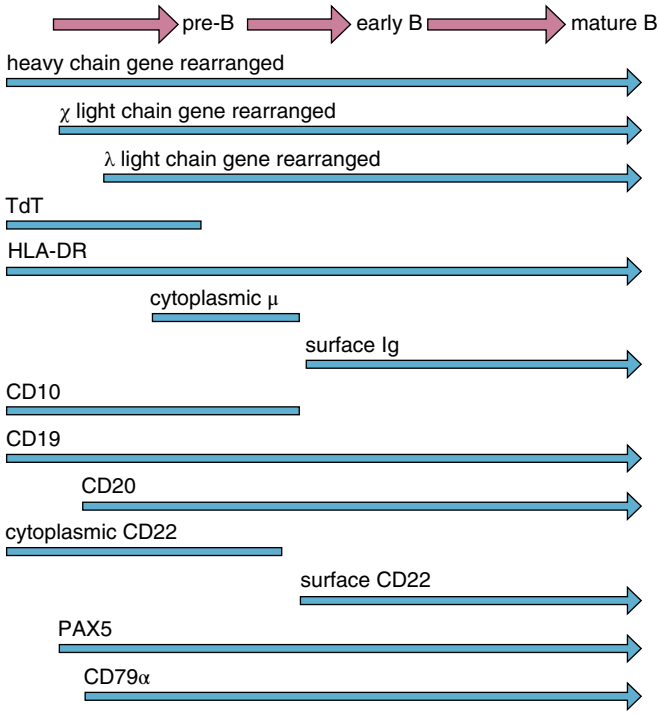

Fig. 11.9. Immunoglobulin gene: Sequence of rearrangement, and antigen and Ig expression during early B-cell development. Intracytoplasmic CD22 is also a feature of very early B cells.

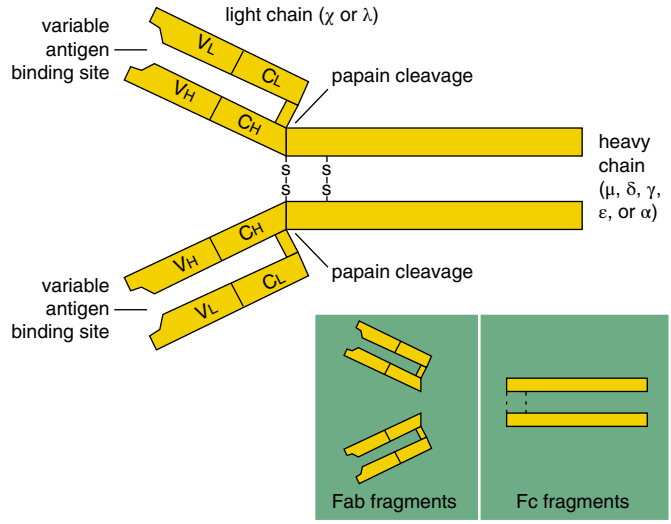

Fig. 11.10. Basic structure of an immunoglobulin molecule: Each molecule is made up of two light (κ or λ) and two heavy chains, and each chain is made up of variable (V) and constant (C) portions. The V portions include the antigen-binding site. The heavy chain (μ, δ, γ, ε, or α) varies according to the Ig class. IgA molecules form dimers, whereas IgM forms a ring of five molecules. Papain cleaves the molecules into an Fc fragment and two Fab fragments.

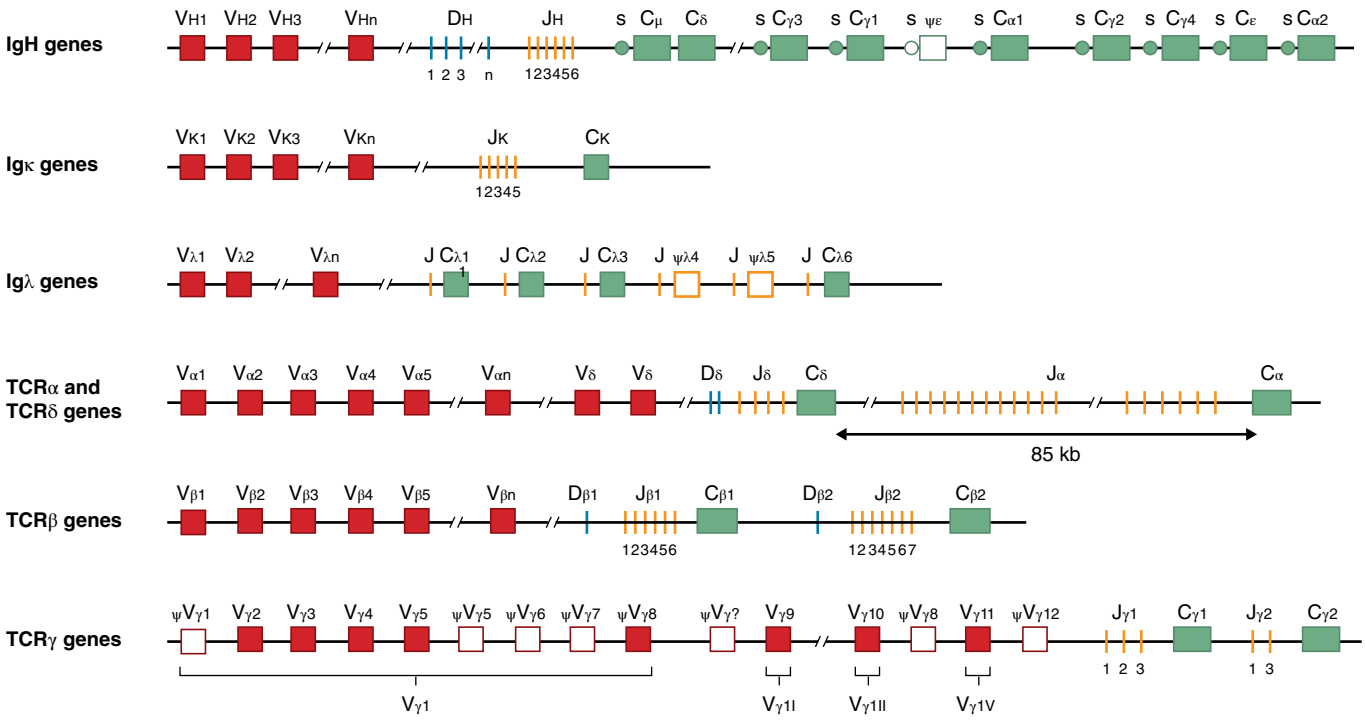

Fig. 11.11. Human Ig genes: The IgH genes consist of many V genes, at least 30 D genes, approximately 6 J genes, and 10 C genes for the various IgH classes and subclasses. Most C genes are preceded by a switch (s) gene, which plays a role in IgH (sub)class switch. The Igκ gene complex consists of a series of V genes, approximately 5 J genes, and 1 C gene, while the Igγ gene complex consists of many V genes and 6 C genes, all of which are preceded by a J gene. Pseudo genes (c) are indicated with open symbols. The TCRα genes consist of many V genes, a remarkably long stretch of J genes, and 1 C gene. The TCRβ gene complex consists of a series of V genes and 2 C genes, both of which are preceded by 1 D gene and 6 or 7 J genes. The TCRγ genes consist of a restricted number of V genes (12 functional Vγ genes and 7 pseudo genes) and 2 C genes, each preceded by 2 or 3 J genes. Interestingly, the TCRδ genes are located between the Vα and Jα genes and probably consist of a few V genes, 3 D genes, 3 J genes, and 1 C gene. Source: Van Dongen JJM, Wolvers-Tettero ILM. *Clin Chim Acta* 1991;198:1–92. Reproduced with permission of Elsevier.

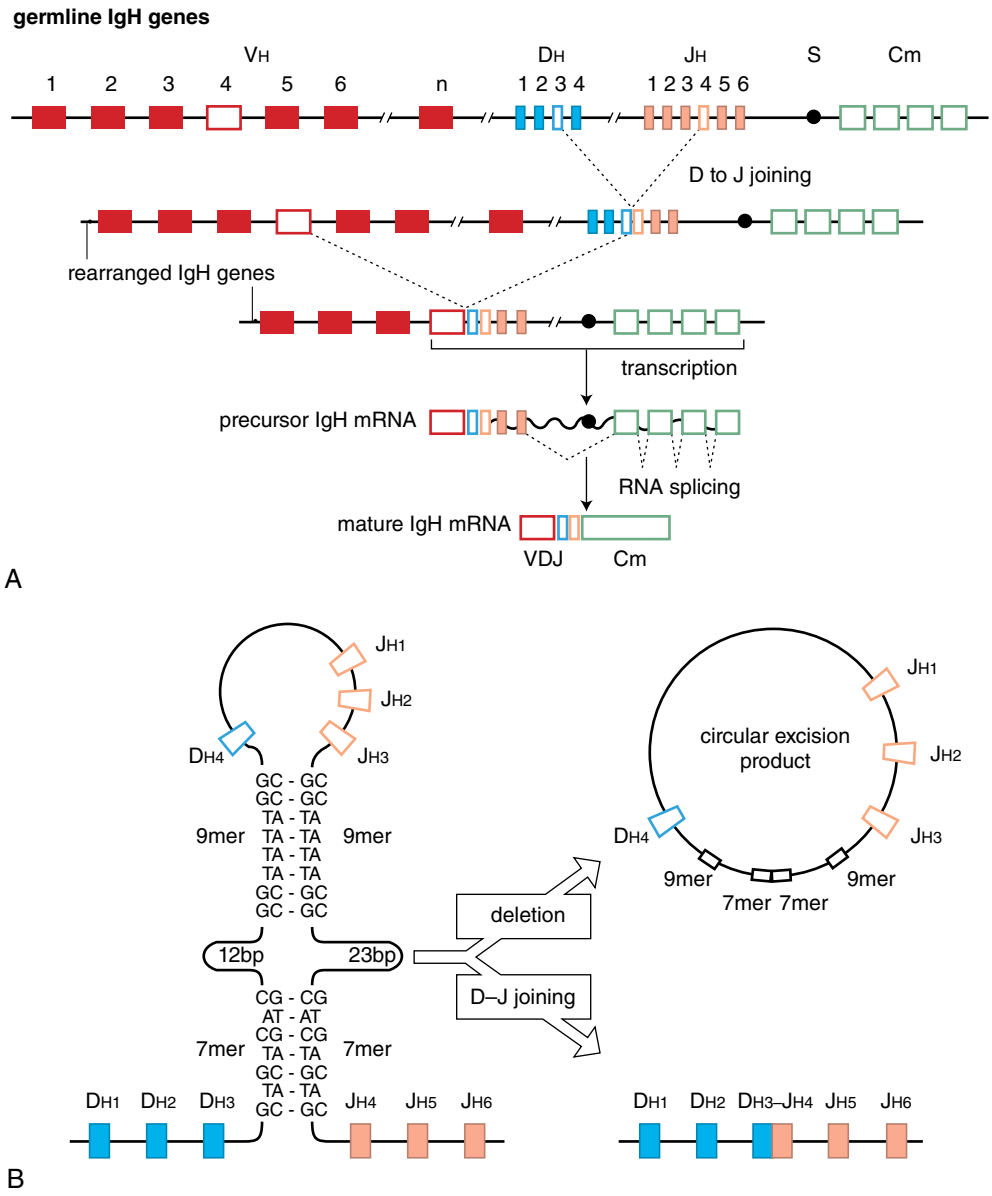

Fig. 11.12. Gene rearrangement. **A,** Rearrangement and transcription of IgH genes. First D to J joining occurs, followed by V to D–J joining. The rearranged genes can be transcribed into a precursor IgH mRNA, which becomes a mature IgH mRNA after splicing all noncoding intervening sequences. **B,** Function of the joining sequences during gene rearrangement. In this typical rearrangement the 3′ DH3 and 5′ JH4 heptamer–nonamer sequences fuse back to back. This is followed by a DH3–JH4 joining and the deletion of a circular excision product. The heptamer–nonamer sequences shown are not those exactly associated with DH3 and JH4, but represent consensus sequences well conserved in Ig as well as TCR genes. Source: Van Dongen JJM, Wolvers-Tettero ILM. *Clin Chim Acta* 1991;198:1–92. Reproduced with permission of Elsevier.

The sequence starts with the heptamers that border the 3′ side of each V and D segment and the 5′ side of each D and J segment. The gene rearrangement first requires back-to-back fusion of the heptamer–nonamer sequences. These sequences and a circular intervening sequence, including the sequences to be deleted, are excised and the ends of two gene segments joined up (Fig. 11.12). Class switching is achieved by deletion of the constant region genes upstream from the gene to be expressed. The process is similar to that of Ig variable gene rearrangement. The order of the heavy chain constant region genes downstream from the variable region genes is μ, δ, γ3, γ1, α1, γ2, γ4, ε, α2. Class switching is triggered by interactions between T and B cells in the T-cell zone of secondary lymphoid organs (see later). The Igs are initially expressed in the cytoplasm before they can be detected on the surface. Eventually mature B cells enter the peripheral circulation where they make up 5–15% of circulating lymphocytes.

B cells transmit a signal from the B-cell receptor (BCR) to the nucleus by a complex series of biochemical reactions (Fig. 11.13). Clinically highly effective inhibitors of these reactions include ibrutinib and idelalisib, which inhibit the Bruton tyrosine kinase (Fig. 11.14) and phosphatidylinositol 3-kinase, respectively.

NATURAL KILLER CELLS

Cytotoxic lymphocytic cells that do not express a TCR and do not carry markers of either T or B cells but do express CD56 (neural cell adhesion molecule, NCAM) are known as natural

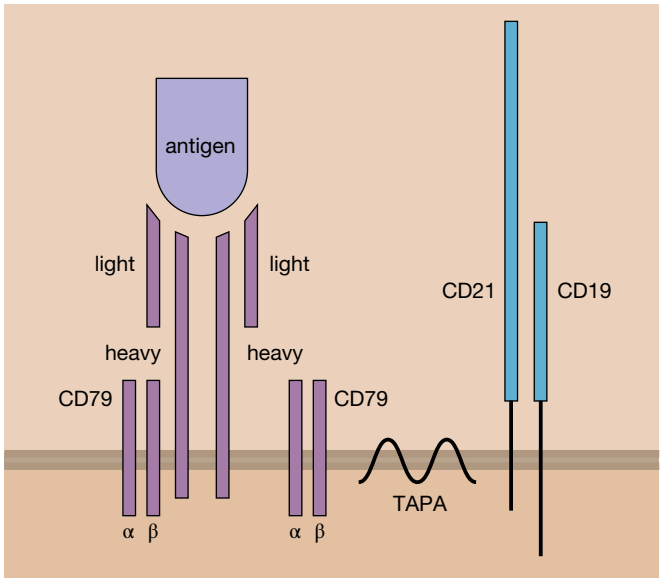

Fig. 11.13. The B-cell antigen receptor. Antibody molecules on the cell surface bind antigen which is then internalized. The B cell then proliferates and produces specific antibody to the antigen or becomes a memory cell. CD79 α β and the CD19, CD21, TAPA complex when activated by antigen, transmit the message to the cell nucleus. TAPA, Tyr-D-Arg-Phe-β-Ala.

killer (NK) cells. They are part of the innate immune system. They express a range of activating and inhibitor receptors which vary according to whether the cells have bright or dim CD56 expression. The majority of NK cells appear as large granular lymphocytes (see Fig. 11.3) in the peripheral blood. This population of cells contains the majority of NK cells, which can kill target cells that fail to express HLA class I, such as cells after a viral infection or some cancer cells. Recognition of HLA class I by killer inhibitory receptors prevents this action (Fig. 11.15).

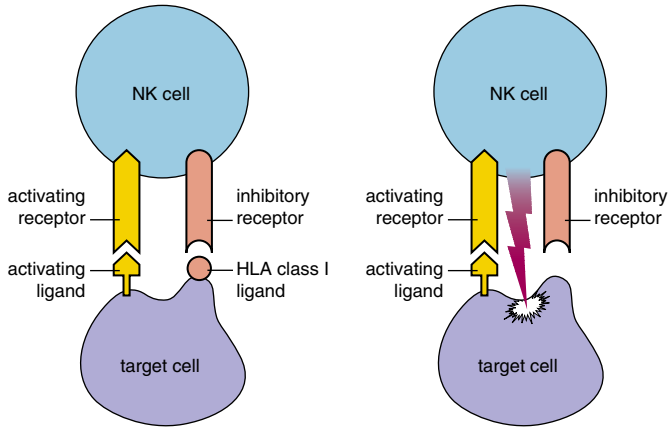

Fig. 11.15. Natural killer cell cytotoxicity. Source: Hoffmann R, et al., eds. *Hematology Basic Principles and Practice*. Churchill Livingstone, Elsevier, 2008. Reproduced with permission of Elsevier.

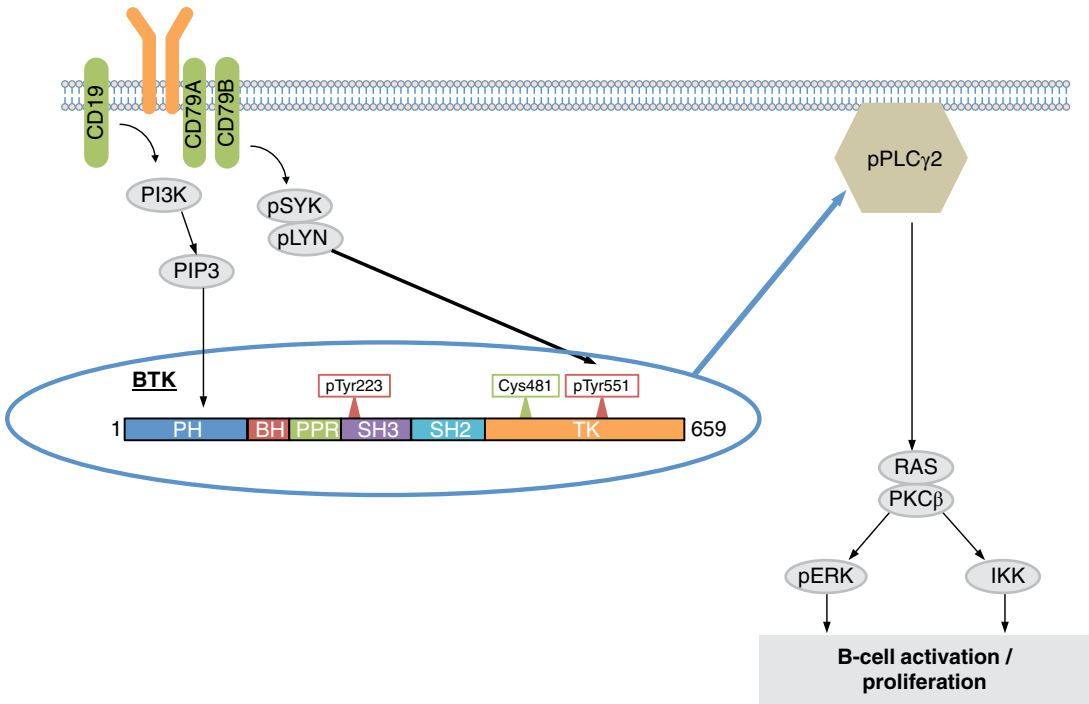

Fig. 11.14. Bruton tyrosine kinase and its involvement in B-cell receptor signaling. Bruton tyrosine kinase (BTK) comprises several domains including the: (i) pleckstrin homology (PH) domain, which targets BTK to the plasma membrane, (ii) BTK homology (BH) domain, (iii) polyproline (PPR) domain, (iv) Src homology (SH3 and SH2) domains (SH2 domain of BTK binds to the B-cell adapter protein BLNK, which is required for full BTK activation), and (v) tyrosine kinase (TK) domain. Activation of BTK requires phosphorylation and binding of phosphatidylinositol (3,4,5)-trisphosphate (PIP3). Following BCR engagement and activation, and following PIP3 binding, BTK translocates to the plasma membrane, where it is phosphorylated at Tyr551 by LYN and SYK, leading to autophosphorylation of Tyr223. Once bound to BLNK, BTK phosphorylates PLCG2 at several sites, leading to calcium mobilization and activation of the protein kinase C (PKC) family members and other effectors, including RAS, and to NFκB activation and phosphorylation of ERK. Most BTK inhibitors bind irreversibly to Cys481 within the ATP-binding site of the BTK kinase domain, thus preventing BTK activation. Apart from its role in BCR signaling, BTK is also implicated in cytokine and toll receptor signaling pathways. Source: Hutchinson CV, Dyer MJS. *Br J Haematol* 2014;166:12–22. Reproduced with permission of John Wiley & Sons.

They therefore complement cytotoxic CD8+ T cells, which require HLA class I molecules to bind to the target cell. NK cells are also involved in graft rejection. Their proliferation is stimulated by IL-2 and IFNγ. A minor population of NK cells express an invariant TCR but also cell surface receptors characteristic of NK cells.

LYMPHOCYTE PROLIFERATION AND DIFFERENTIATION

T and B cells proliferate and develop in reactive lymphoid tissue (e.g. lymph nodes, and lymphoid tissues of the alimentary and respiratory tracts and spleen). Both T and B cells acquire receptors for antigens, which commit them to a single antigenic specificity, and are activated when they bind their specific antigen in the presence of accessory cells.

Provided there is major histocompatibility complex (MHC) (see start of Chapter 25) recognition (Class I for CD8+ and Class II for CD4+ cells), APCs interact with T cells bearing the appropriate receptor for that particular antigen. B cells with the appropriate surface receptor (Ig) for the antigen are also stimulated (Fig. 11.16). Adhesion molecules are involved in the cell-to-cell binding (Fig. 11.17). Subsequently, these stimulated T and B cells proliferate and differentiate under the stimulus of factors released from APCs (IL-1, IL-6, and IL-7) and activated T helper cells (IL-2, IL-4, IL-6, IL-10, IFNγ, and tumor necrosis factor [TNF]; see Fig. 11.4). The B cells are also stimulated to secrete antibody. Clones of both effector and memory T and B cells are produced (Figs. 11.18 and 11.19). When the memory cells are stimulated at a later date by their specific antigen, they are able to proliferate again in an accelerated fashion (secondary response).

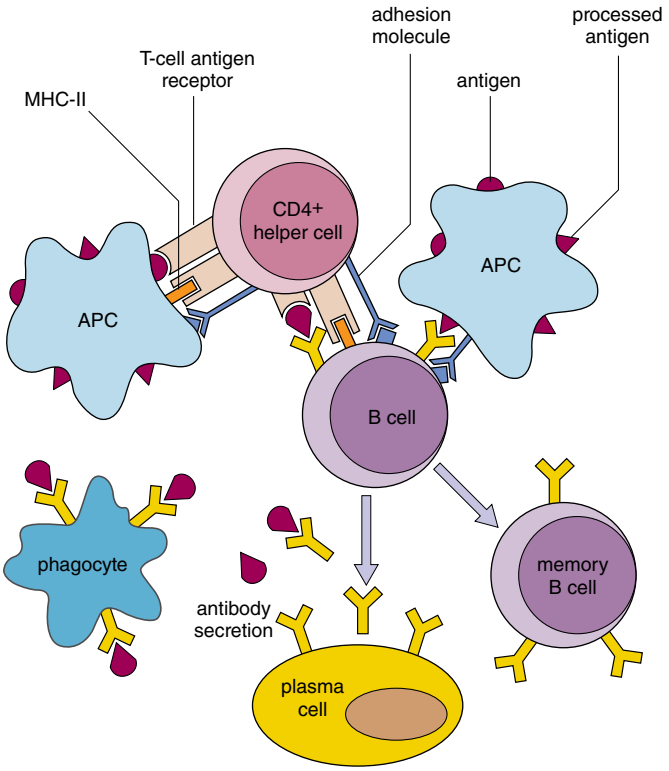

Fig. 11.16. The immune response. There is interaction between an antigen-presenting cell (APC) and a CD4+ (helper) T cell, with MHC Class II and antigen T-cell receptor recognition, and both cells interact with a B cell, with recognition between its surface Ig and the antigen. T cells and B cells interact with different epitopes of the antigen. As a result, clones of T cells and B cells are stimulated to proliferate, the B cells becoming either plasma cells (secreting antibody to the antigen) or memory B cells. A phagocyte takes up the antigen–antibody complex.

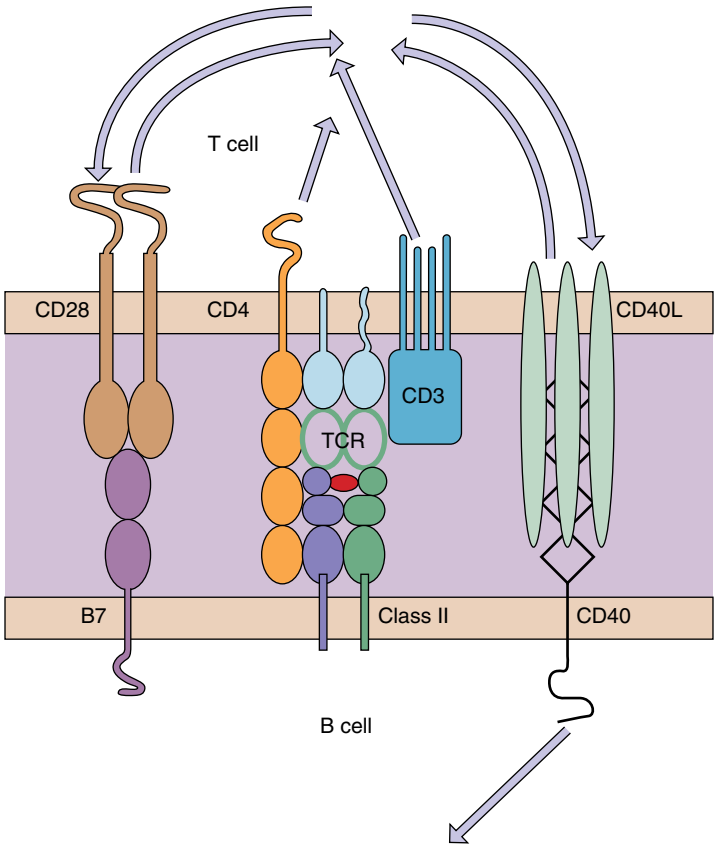

Fig. 11.17. Surface molecule involvement in T-dependent B-cell activation in T zones. B cells take up antigen, which they bind specifically through their surface Ig. This is internalized and broken down into peptides, which are presented on the B-cell surface, held in the peptide-binding grooves of MHC Class II molecules. Cross-linking of surface Ig by antigen induces endocytosis of the antigen–antibody complex and signals upregulation of CD40 expression and de novo B7.1 and B7.2 expression. If this B cell interacts with a primed T cell that recognizes the peptide complex with MHC Class II molecules, this can induce the T cell to express CD40 ligand (CD40L), CTLA4, or both transiently, and to start to secrete cytokines. Cytokine receptor expression by the B and T cells is initiated or upregulated. The arrows indicate that T-cell receptor (TCR) engagement induces CD40L and CTLA4 expression, and that engagement of these molecules by their counterstructures on the B cell delivers further signals to the T cell. CD40 ligation induces Ig class switching in the B cell and migration. Source: MacLennan ICM, Drayson MT. Normal lymphocytes and non-neoplastic lymphocyte disorders. In: Hoffbrand AV, et al., eds. *Postgraduate Haematology*, 5th edn. Butterworth-Heinemann, 1999, pp. 267–308. Reproduced with permission of Elsevier.

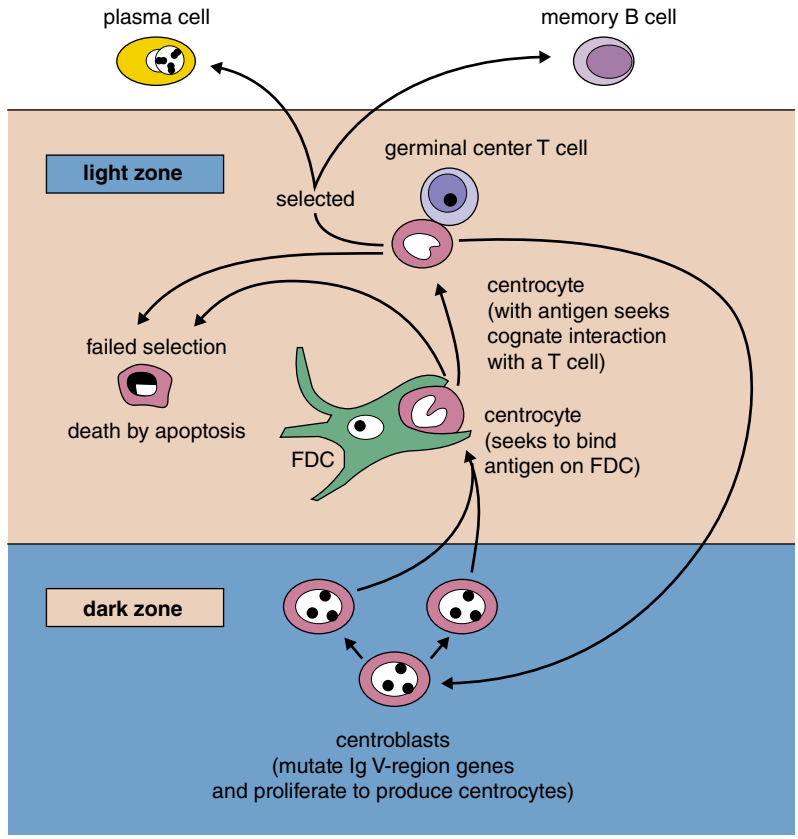

Fig. 11.18. Selection of cells that have undergone Ig V-region hypermutation in germinal centers (GCs). The hypermutation mechanism is active in centroblasts, which are the rapidly dividing cells of the dark zone that give rise to centrocytes. Centrocytes die by apoptosis unless they pick up and process antigen held on follicular dendritic cells (FDCs), and find a T cell in the GC that recognizes the peptides from this antigen presented on centrocytes in association with self-MHC Class II. The T-cell-dependent selection mechanism makes it unlikely that centrocytes with mutated Ig V-region genes that encode self-reactive antibody will be selected. Most B cells that are selected leave the GC either to migrate to distant sites of antibody production (the gut or bone marrow) where they differentiate to become plasma cells, or to differentiate into memory B cells. Some selected cells remain within the GC and return to the dark zone as centroblasts. Source: MacLennan ICM, Drayson MT. Normal lymphocytes and non-neoplastic lymphocyte disorders. In: Hoffbrand AV, et al., eds. *Postgraduate Haematology*, 5th edn. Butterworth-Heinemann, 1999, pp. 267–308. Reproduced with permission of Elsevier. 4.68

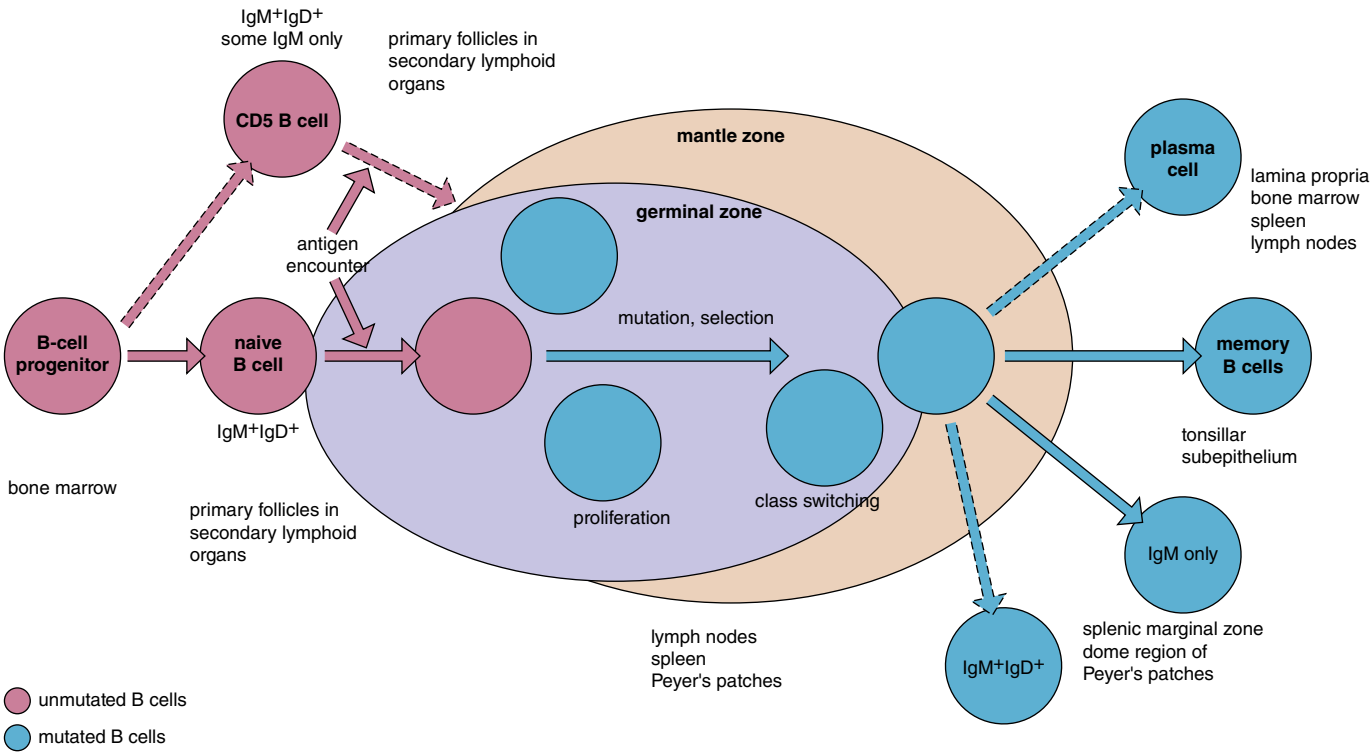

Fig. 11.19. Molecularly defined human B-lineage subsets: These have been characterized by V-gene sequence analysis, and their location in the human body is shown. Hypothetical differentiation pathways are indicated by dashed arrows. PB, peripheral blood. Source: Klein U, et al. *Immunol Rev* 1998;162:261–280. Reproduced with permission of John Wiley & Sons.

Activated Th1 cells become responsible for cell-mediated immunity (see Fig. 11.4). Other lymphokines activate killer T cells, enabling them to attack an invading organism or cell, and induce macrophages to stay at the site of infection and help to digest the cells they have phagocytosed. They may also have a direct action on organisms by inhibiting proliferation or activating apoptosis.

Thus, T helper cells are important in the initiation of a B-cell response to antigens; T suppressor cells reduce the B lymphocytic response; and T cytotoxic cells are capable of directly damaging cells recognized as foreign or virus infected (Fig. 11.20).

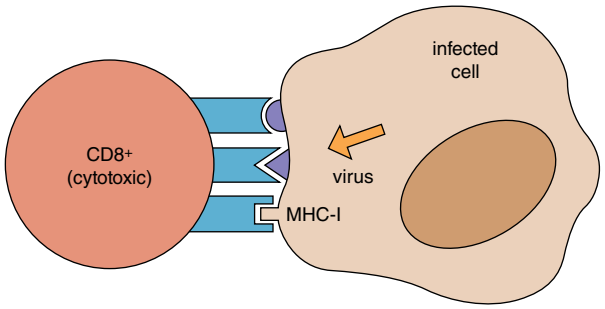

Fig. 11.20. Interaction between a CD8+ (cytotoxic) T cell and a virus-infected cell. In contrast to NK cells, when there is MHC Class I recognition between the two cells, as well as correspondence between the antigens of the virus expressed on the cell surface and the T-cell antigen receptor on the surface of the CD8+ cell, the cytotoxic CD8+ cell kills the virus-infected cell.

Activated B cells are responsible for humoral immunity. Many B cells mature into plasma cells, which produce and secrete antibodies of one specificity and Ig class (Figs. 11.21–11.23). B lymphocytes at different stages of differentiation and activation are shown in Fig. 11.24.

SOMATIC HYPERMUTATION IN NORMAL B CELLS

B cells released from the bone marrow into the peripheral blood have generated a functional non-autoreactive antigen receptor. They remain "naïve' until they encounter antigen, whereupon the antibody expressed by the B cell may be modified, both by class-switch recombination and somatic hypermutation (see Figs. 11.18 and 11.19). Somatic hypermutation is restricted to B cells that proliferate in the germinal center (GC) microenvironment. Somatically mutated V-region genes therefore characterize GC B cells or post-GC B cells. B-lineage-derived lymphoma can thus be characterized as arising from GC or post-GC somatically hypermutated cells.

LYMPHOCYTE CIRCULATION

Lymphocytes from the primary lymphoid organs of the marrow and thymus migrate via the blood through post-capillary venules into the substance of lymph nodes, into unencapsulated lymphoid collections of the body, and into the spleen. T cells

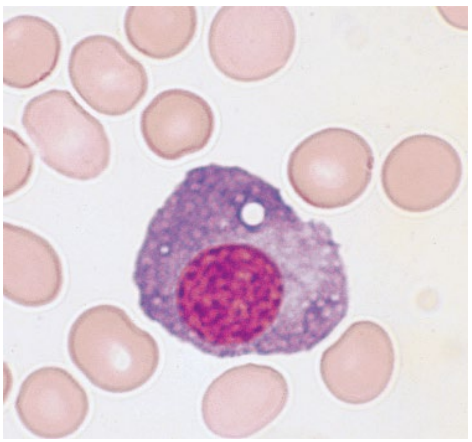

Fig. 11.21. Plasma cell, showing typical eccentric nucleus with basophilic cytoplasm, prominent perinuclear clearing, and a single vacuole.

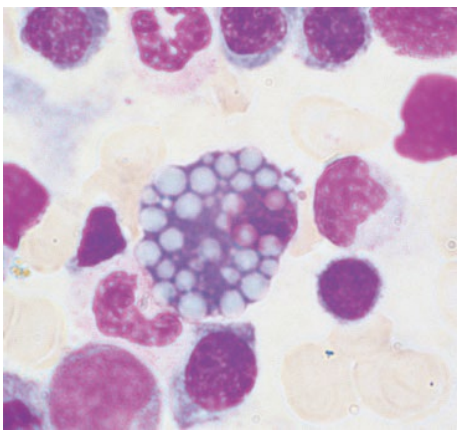

Fig. 11.22. This type of plasma cell contains many spherical cytoplasmic inclusions and is sometimes referred to as a "Mott" cell.

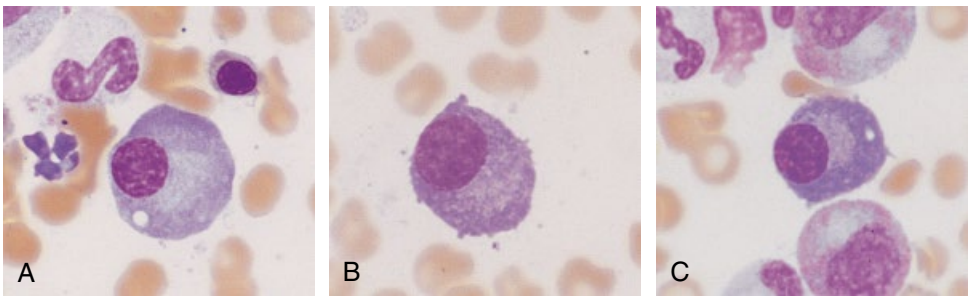

Fig. 11.23. Plasma cells. These occur in bone marrow and in other tissues of the reticuloendothelial system, including the intestine. They are not found in normal peripheral blood. The cells are usually oval. They show a deeply basophilic cytoplasm with a perinuclear halo, and an eccentric nucleus with coarse chromatin condensation ("clock-face" pattern).

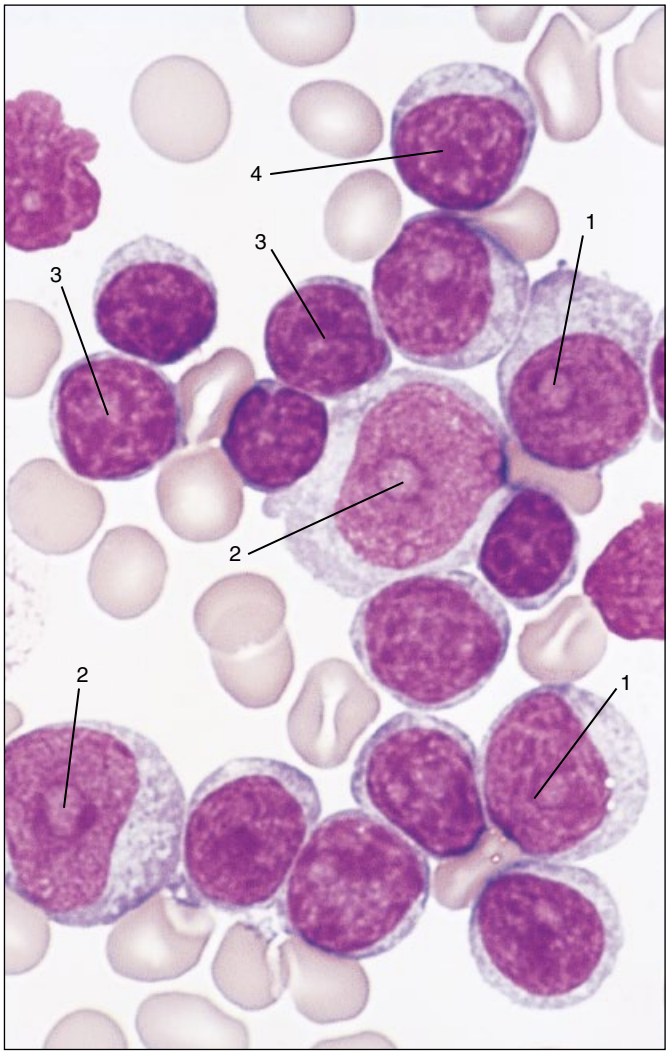

Fig. 11.24. B lymphocytes: Peripheral blood film of a patient with chronic lymphocytic leukemia with prolymphocytoid transformation shows B cells at various stages of development. 1, Prolymphocytes; 2, immunoblasts; 3, small lymphocytes; 4, large lymphocytes. Prolymphocytes probably represent a stage of activated B cell. (Courtesy of Professor JV Melo.)

home to the paracortical areas of the nodes and to the periarteriolar sheaths of the spleen. B cells accumulate selectively in germinal follicles of lymphoid tissue, in the subcapsular periphery of the cortex, and in the medullary cords of the lymph nodes (Figs. 11.25 and 11.26). Lymphocytes return to the peripheral blood by the efferent lymphatic system and the thoracic duct. The median duration of a complete circulation is about 10 hours. The majority of recirculating cells are T cells. B cells are mainly sessile and spend long periods in lymphoid tissue and the spleen. Many lymphocytes have long life spans and may survive as memory cells for several years

COMPLEMENT

Complement consists of a series of proteins which, as in the coagulation cascade, are activated in turn as one protein or group of proteins gains enzyme activity and activates the next (Fig. 11.27). There is also amplification since a molecule of cell-bound C3 convertases (see later) can activate many thousands of molecules of C3. There are two stages: (i) Generation of C3b which coats (opsonizes) bacteria, red cells, or other cells. This makes them liable to phagocytosis by macrophages in the reticuloendothelial system that have receptors to C3b. C3b is rapidly degraded to C3d, which can be detected in the anticomplement agent in the direct antiglobulin test. (ii) Generation of a lytic phospholipase membrane attack complex, consisting of activated C5b, C6, C7, C8, and C9.

The opsonic phase which generates C3b may be via a classical pathway activated by IgG or IgM antibodies or antigen–antibody complexes, or other factors or by an alternative pathway which is activated by IgA, endotoxin or in vitro by lowering the pH, as in the acid lysis test for paroxysmal nocturnal hemoglobin (PNH) (see Chapter 8). A third pathway activated by lectin (not shown in Fig. 11.27) is, like the alternative pathway, part of the innate immune system. In the classical pathway small molecular weight fragments C4a, C3a, C5a are released which have chemotactic and anaphylactic activities. The alternative pathway is a feedback loop in which C3b is both a product and an activator. Other complement components termed factor B, factor D, and properdin are involved. C3 is activated to C3b by a complex of C3bBb rather than by the C4b2b in the classical pathway, both complexes being C3 convertases.

Complement is present in fresh plasma, the most abundant being C3 at about 1.2 g/L. It is C3b that initiates the lytic phase by activating C5 to membrane-bound C5b, which associates with C6, C7, C8, and C9 and forms a complex that punches cylindrical pores in the membrane. Water and ions can enter the cell through these pores.

LYMPHOCYTOSIS

The main causes of an increase in the absolute lymphocyte count are listed in Table 11.2. The count is usually $5–50 \times 10^9$/L. Greatly raised levels ($>100 \times 10^9$/L) may be seen in adults with chronic lymphocytic leukemia. Infants with pertussis and children with acute infectious lymphocytosis, an unusual viral disease, may also have very high lymphocyte counts (Fig. 11.28A). Lymphocytoses with large numbers of atypical or "reactive" cells (Fig. 11.29) are most often seen in infectious mononucleosis, in other viral illnesses (including infectious hepatitis), and in toxoplasmosis. Unusually heavy smoking is associated with a benign polyclonal lymphocytosis, the mechanism for this is unclear (Fig. 11.28B).

INFECTIOUS MONONUCLEOSIS

Infectious mononucleosis is a disorder characterized by sore throat, fever, lymphadenopathy, and atypical lymphocytes in the blood. The disease appears to be the result of infection with the Epstein–Barr virus (EBV). In affected patients, heterophile antibodies against sheep red cells are found in the serum at high titers (Paul–Bunnell or monospot test).

Most patients have lethargy, malaise, and fever. On examination, the majority show lymphadenopathy. Generalized inflammation of the oral and pharyngeal surfaces with follicular tonsillitis is usual, and some patients show palatal petechiae). Periorbital and facial edema or a morbilliform rash may be present. Palpable splenomegaly occurs in over half the patients. Occasionally, subcapsular hematomas of the spleen are present and have a tendency to rupture.

The diagnosis is suspected by finding a moderate lymphocytosis ($10–20 \times 10^9$/L) and large numbers of atypical lymphocytes in the peripheral blood film (see Fig. 11.29). Lymph node biopsy

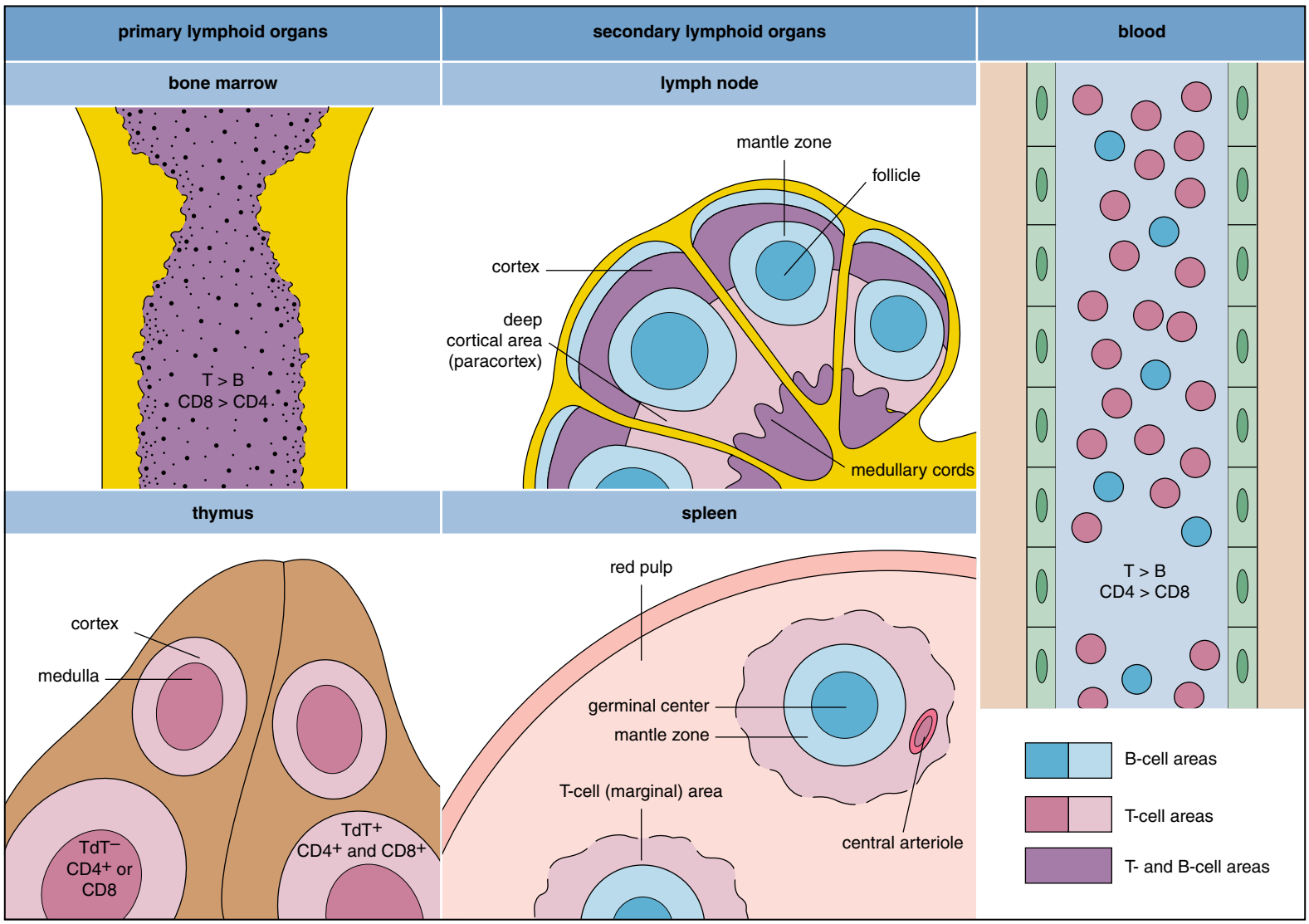

Fig. 11.25. Lymphocyte distribution: Primary and secondary lymphoid organs and blood. Aggregates of secondary lymphoid tissue are found elsewhere in the body (e.g. Peyer's patches of the small intestine). The mantle zones of the lymph nodes and spleen also contain macrophages and antigen-presenting cells, and the paracortex also contains many interdigitating reticulum cells.

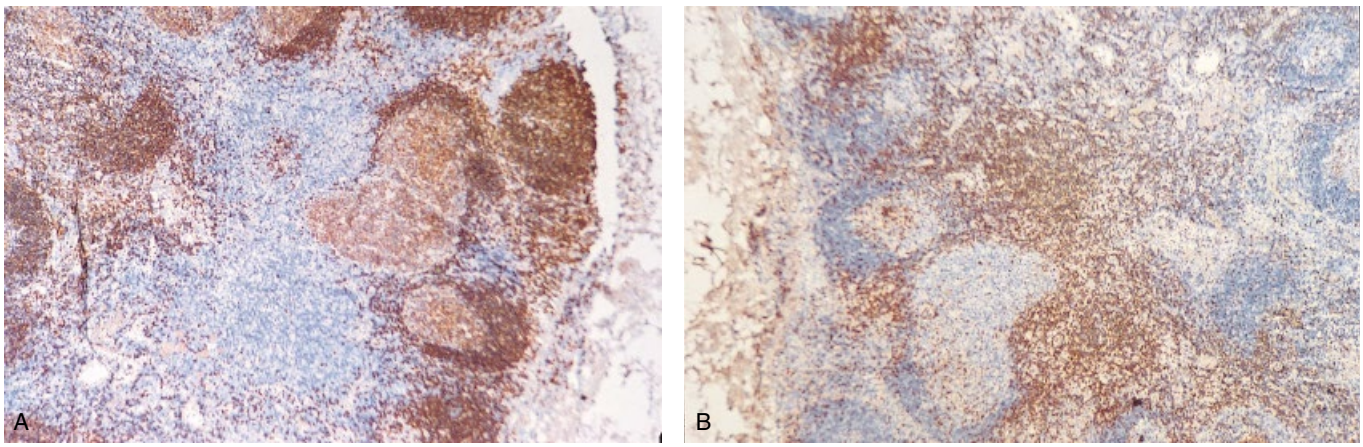

Fig. 11.26. B- and T-lymphocyte distribution. **A,** Lymph node section showing B cells in the germinal centers, their coronas (heavy staining) in the subcapsular cortex and medullary cords. **B,** Lymph node section showing T cells, most numerous in perifollicular areas of the deeper cortical region. Immunoperoxidase technique using **(A)** pan-B monoclonal antibody (anti-CD19) and **(B)** pan-T (anti-CD3) monoclonal antibody.

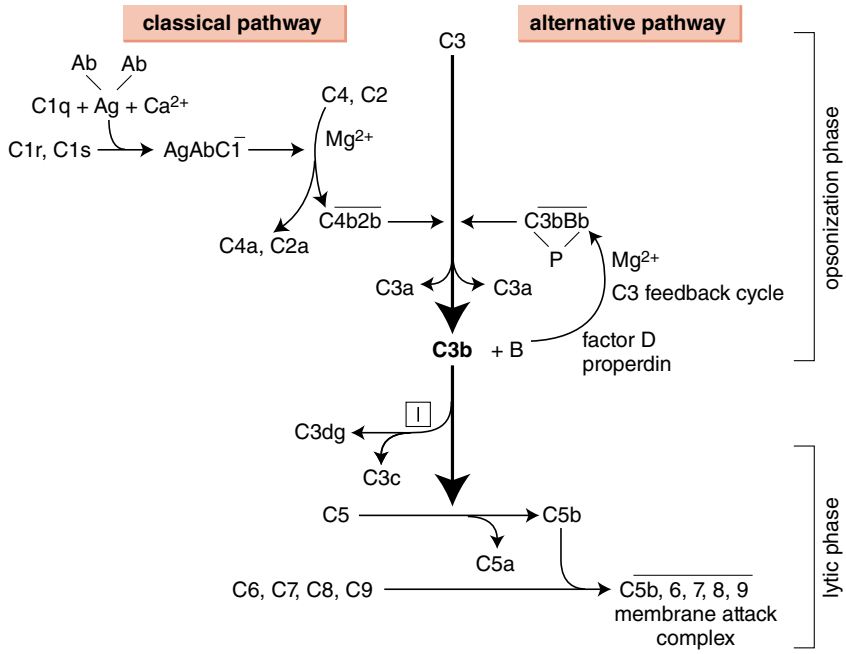

Fig. 11.27. The complement cascade: Component C3b plays a central role in the classical and alternative pathways. Source: Hoffbrand AV, et al., eds. *Postgraduate Haematology*, 7th edn. John Wiley & Sons, 2016. Reproduced with permission of John Wiley & Sons.

is not usually performed. The histologic appearances are those of a reactive node with proliferating germinal follicles, increased numbers of T cells, especially CD8+, and positive staining for the EBV antigens (Fig. 11.30). Jaundice and abnormal liver function occurs in a minority of patients. Liver histology shows mixed inflammatory cells in the portal tracts and sinusoids with a predominance of CD8+ T cells (Fig. 11.31).

LYMPHADENOPATHY

Infectious mononucleosis is one cause of generalized lymphadenopathy (Table 11.3). A number of conditions, including acute lymphoblastic leukemia, toxoplasmosis, infectious hepatitis, human immunodeficiency virus (HIV) infection, and follicular tonsillitis are likely to create initial problems in diagnosis. Lymph node biopsy (either tru-cut or whole node) of the affected nodes may be helpful in differential diagnosis.

Fine-needle aspiration cytology was used for diagnosis of hematologic disorders but with the advent of tru-cut biopsy it is no longer used in hematologic practice. Reactive lymph nodes are characterized by an overall retention of normal node structure with expansion of follicle cells, which show the presence of mixed inflammatory cells, tingible body macrophages, and polyclonal T cells, and expansion of B cells (centroblasts) at the edge of the germinal centers (Fig. 11.32). T cells may infiltrate the germinal center and are a mixture of CD4+ and CD8+ cells (Fig. 11.33). Fine-needle aspirates showed the node to contain a pleomorphic lymphoid population (Fig. 11.34) which by flow cytometry can be shown to be polyclonal, expressing κ and λ light chains. In toxoplasmosis, characteristic small groups of histiocytes may be found (Fig. 11.35). Lymph node biopsy may be needed to distinguish benign conditions (e.g. infections, immune reactions, vasculitides) from malignant conditions (Figs. 11.36–11.41).

KIKUCHI DISEASE

Kikuchi disease (also called Kikuchi–Fujimoto and histiocytic necrotizing lymphadenitis) was first recognized in Japan, but is now known to have worldwide distribution. It is more common in young women, manifesting with persistent tender or non-tender lymphadenopathy. Fever and a viral-like prodromal syndrome are frequent, and mild leukopenia may be present. Cervical nodes are involved most often, but any group of nodes may be affected. No associated virus has been found, and although systemic lupus erythematosus (SLE) is suggested by the histopathology, Kikuchi patients rarely develop SLE (Figs. 11.42–11.44).

TABLE 11.2. CAUSES OF LYMPHOCYTOSIS

Reactive lymphocytosis	**Stress**
Acute infections	Trauma
Bacterial	Major surgery
Bordetella	Myocardial infarction
Pertussis	Status epilepticus
Viral	Septic shock
Mononucleosis syndrome	Sickle cell crisis
Epstein–Barr	**Hypersensitivity reactions**
Cytomegalovirus	Insect bites
HIV	Drugs
Rubella	**Chronic polyclonal**
Herpes simplex	Cigarette smoking
Adenovirus	Cancer
Viral hepatitis	Hyposplenism
Dengue fever	Thymoma
Human herpesvirus type 6 (HHV-6)	**NK Lymphocytosis**
HHV-8	**Primary**
Varicella zoster	Acute lymphoblastic leukemia
Toxoplasma gondii	Chronic lymphocytic, prolymphocytic, hairy cell, adult T-cell leukemia-lymphoma
Acute infectious lymphocytosis (unexplained)	Non-Hodgkin lymphoma
Chronic infections	Monoclonal B-cell lymphocytosis
Tuberculosis, brucellosis, syphilis, leprosy, leishmaniasis, stronygloidiasis	Persistent polyclonal B-cell lymphocytosis
	Large granular lymphocytic leukemia, $CD8^+$, $CD4^+$, α/β or γ/δ T cell types

SINUS HISTIOCYTOSIS WITH MASSIVE LYMPHADENOPATHY (ROSAI–DORFMAN DISEASE) (SEE ALSO CHAPTER 24)

Sinus histiocytosis with massive lymphadenopathy is a rare condition seen most frequently in young black people and is characterized by lymphadenopathy, fever, leukocytosis, and hypergammaglobulinemia (see Chapter 24).

PRIMARY IMMUNODEFICIENCY DISORDERS

The main types of primary immunodeficiency disease are listed in Table 11.4. A detailed map of the sites of the defects in the congenital immune deficiencies is given in Fig. 11.45. In severe combined immunodeficiency disease (SCID), the T- and B-lymphocyte systems fail to develop. There is severe lymphopenia and hypogammaglobulinemia. Affected infants fail to thrive and die early in life from recurrent infections, such as by *Pneumocystis carinii*, cytomegalovirus, other viruses, fungi, and bacteria. Atrophy of the thymus occurs (Fig. 11.46) and the lymph nodes and spleen are small and devoid of lymphoid cells. The most common cause is deficiency of the enzyme adenosine deaminase (ADA) (Fig. 11.47). Deficiency of another enzyme, purine nucleoside phosphorylase, causes a more selective lack of T cells. Deficiency of ADA has been treated successfully by stem cell transplantation and by "gene therapy" in which the ADA gene is introduced into the patient's lymphocytes in vitro, and the lymphocytes are then reinfused.

In the very rare syndrome of lymphoreticular dysgenesis, development of both the reticuloendothelial and lymphoid systems fails. Affected infants die soon after birth from overwhelming infection. Lymphopenia is marked, and stigmata of splenic atrophy may be found in the peripheral blood (Fig. 11.48). There are mutations of *AK2*, a gene important for mitochondrial function and apoptosis. Neutropenia is usual.

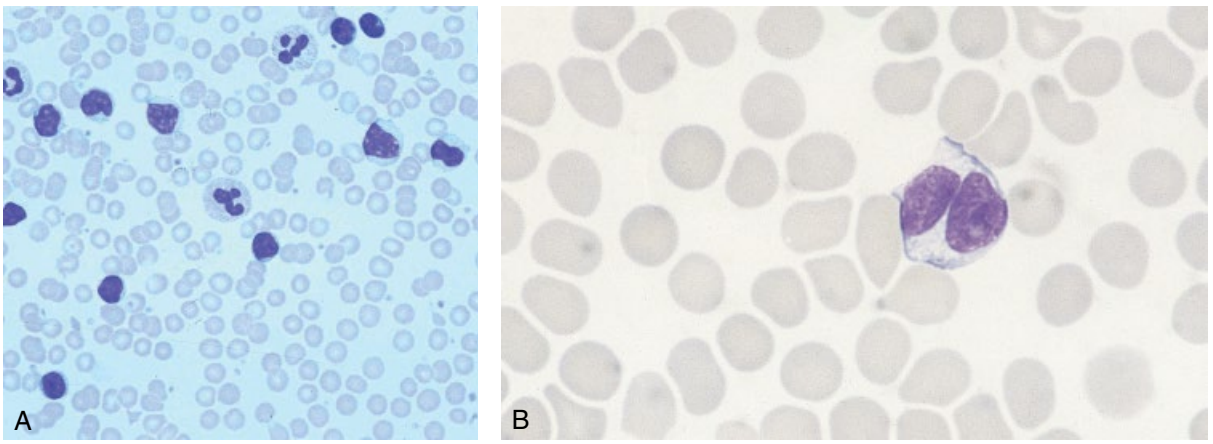

Fig. 11.28. Benign lymphocytosis: **A,** *Bordetella pertussis* infection. Girl aged 4 presenting with a limp. (White cell count 130×10^9/L; normal hemoglobin and platelet count.) Immunophenotyping showed the lymphocytes to be T cells, CD4+ or CD8+. Serology was positive for *B. pertussis*. (Courtesy of Dr. W Erber). **B,** Representative binucleate lymphocyte in the peripheral blood of a heavy smoker with polyclonal lymphocytosis. (Courtesy of Professor BA Bain.)

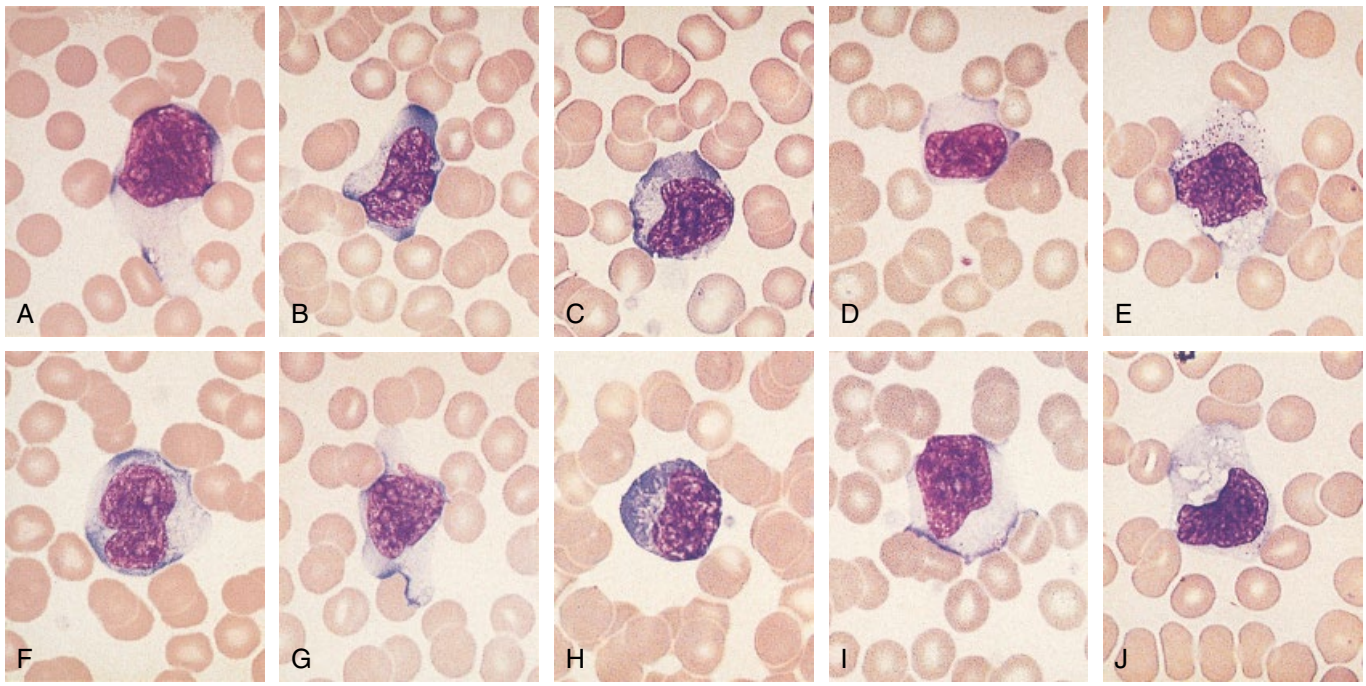

Fig. 11.29. Infectious mononucleosis: **A–J,** Representative "reactive" lymphocytes in the peripheral blood film of a 21-year-old man. These are T lymphocytes reacting to B cells infected by the Epstein–Barr virus. The cells are large with abundant vacuolated cytoplasm. The nuclei often show a fine blast-like chromatin pattern. The edges of the lymphocytes are often indented by adjacent red cells.

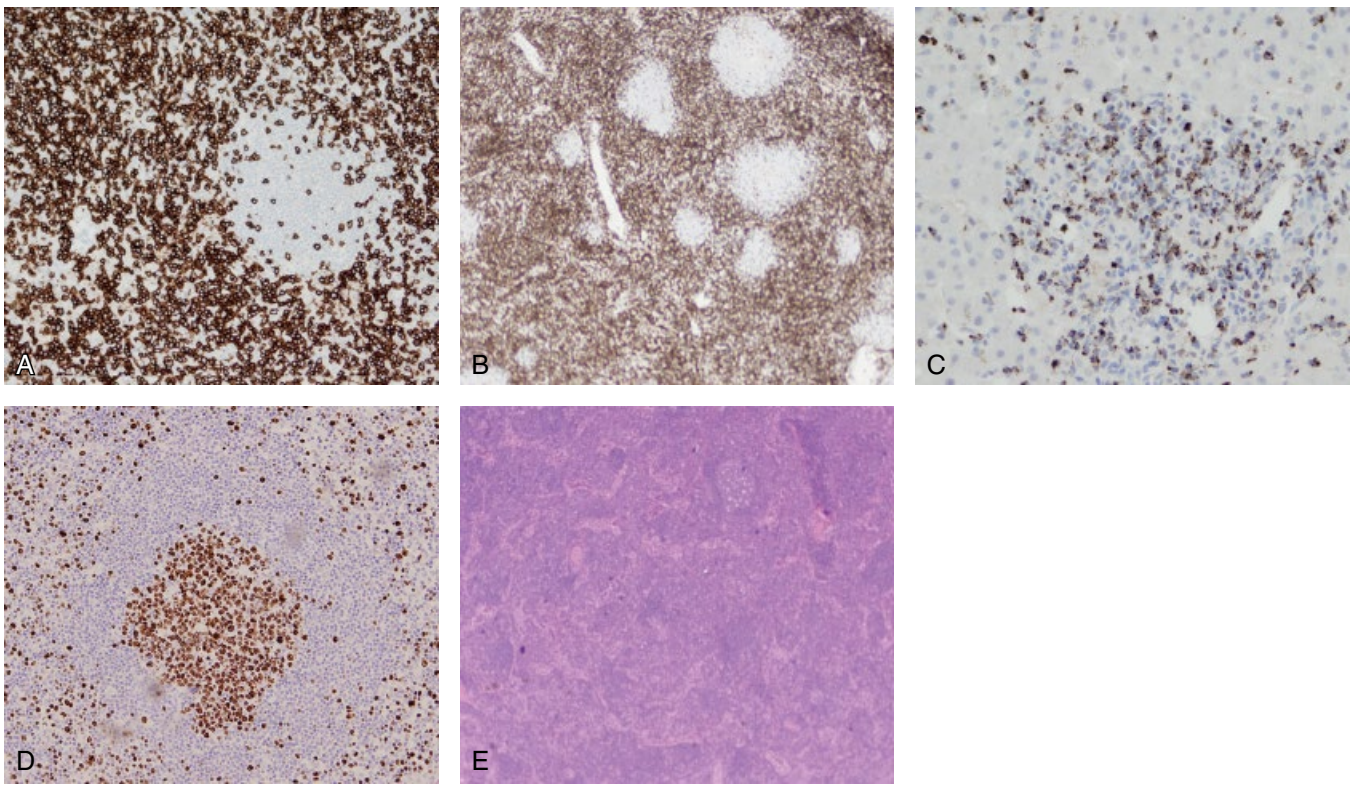

Fig. 11.30. Infectious mononucleosis: Lymph node sections. **A**, Epstein–Barr virus-encoded RNAs (EBER) immunostain is positive. **B,** CD8 immunostain to show CD8 T cells in the paracortex and scattered in germinal follicles. **C,** T cell intracytoplasmic antigen (TIA) immunostain showing T cells in germinal center and scattered in mantle zone. **D**, MIB-1 immunostain showing proliferative (Ki67+) cells in germinal follicles. **E**, Reactive germinal follicles. (Courtesy of Professor P Isaacson.)

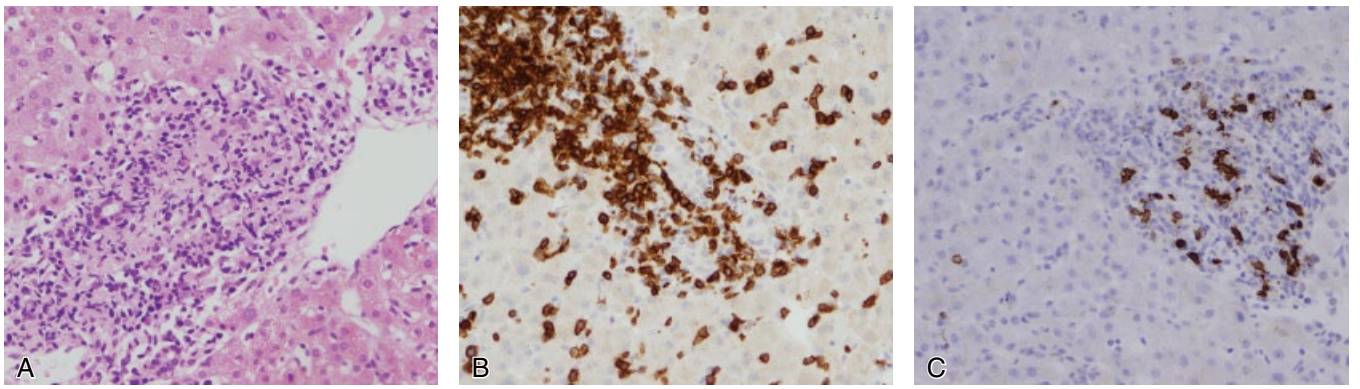

Fig. 11.31. Infectious mononucleosis. **A,** Liver biopsy showing mixed inflammatory cells in portal tract and scattered in sinusoids. **B**, CD8 immunostain showing CD8 T cells in portal tracts and sinusoids. **C**, CD20 immunostain showing B cells in portal tracts and sinusoids. (Courtesy of Professor P Isaacson.)

TABLE 11.3. CAUSES OF LYMPHADENOPATHY

Localized	Generalized
Local infection	Infections
Pyogenic infection (e.g. pharyngitis, dental abscess, otitis media), actinomyces	Viral (e.g. infectious mononucleosis, measles, rubella, viral hepatitis), human immunodeficiency virus
Viral infection (e.g. cat scratch fever, lymphogranuloma venereum)	Bacterial (e.g. brucellosis, syphilis, tuberculosis, salmonella, bacterial endocarditis)
Tuberculosis	
Lymphoma	Fungal (e.g. histoplasmosis)
Hodgkin lymphoma	Protozoal (e.g. toxoplasmosis)
Non-Hodgkin lymphoma	Noninfectious inflammatory diseases
Metastatic tumors	For example, sarcoidosis, rheumatoid arthritis, systemic lupus erythematosus, other connective tissue diseases, Kikuchi disease, serum sickness
Carcinoma	Leukemia, especially CLL, ALL
Malignant melanoma	Lymphoma
	Non-Hodgkin
	Hodgkin
	Rarely, metastatic tumors
	Angioimmunoblastic lymphadenopathy
	Sinus histiocytosis with massive lymphadenopathy (Rosai–Dorfman)
	Autoimmune lymphoproliferative disease
	Reaction to drugs and chemicals (e.g. hydantoins and related chemicals, beryllium)
	Hyperthyroidism

ACQUIRED IMMUNODEFICIENCY SYNDROME

Acquired immunodeficiency syndrome (AIDS) is caused by infection with HIV, a retrovirus of the lentivirus subgroup. The predominant effects of HIV are produced through infection of T helper (CD4+) cells (Fig. 11.49). Some CD4+ cells are lysed directly by replicating HIV, but the virus remains latent in most host cells, unrecognized by the patient's immune system. When such latently infected T cells are activated, the virus replicates and cell death follows. The CD4 antigen appears to be the main receptor for HIV, and CD4+ APCs are also an important site for viral replication. A chemokine receptor, CCR5 or CCR4, is also required for cell entry.

Transmission of the virus is usually by sexual contact, or by blood or blood products, or by breast milk. Particularly common in homosexual men, AIDS is also seen frequently in intravenous drug abusers as well as in heterosexual contacts of AIDS cases. but much less frequently now with improved blood products in hemophiliacs, and other patients who require multiple blood transfusions,

The viral load may be as high as 10^7 RNA copies/mL during acute infection. A prodromal period of about six weeks follows the initial infection, after which symptoms that resemble infectious mononucleosis may occur. A proportion of patients pass through the asymptomatic and persistent lymphadenopathy stages to the AIDS-related complex (ARC) and fully developed AIDS.

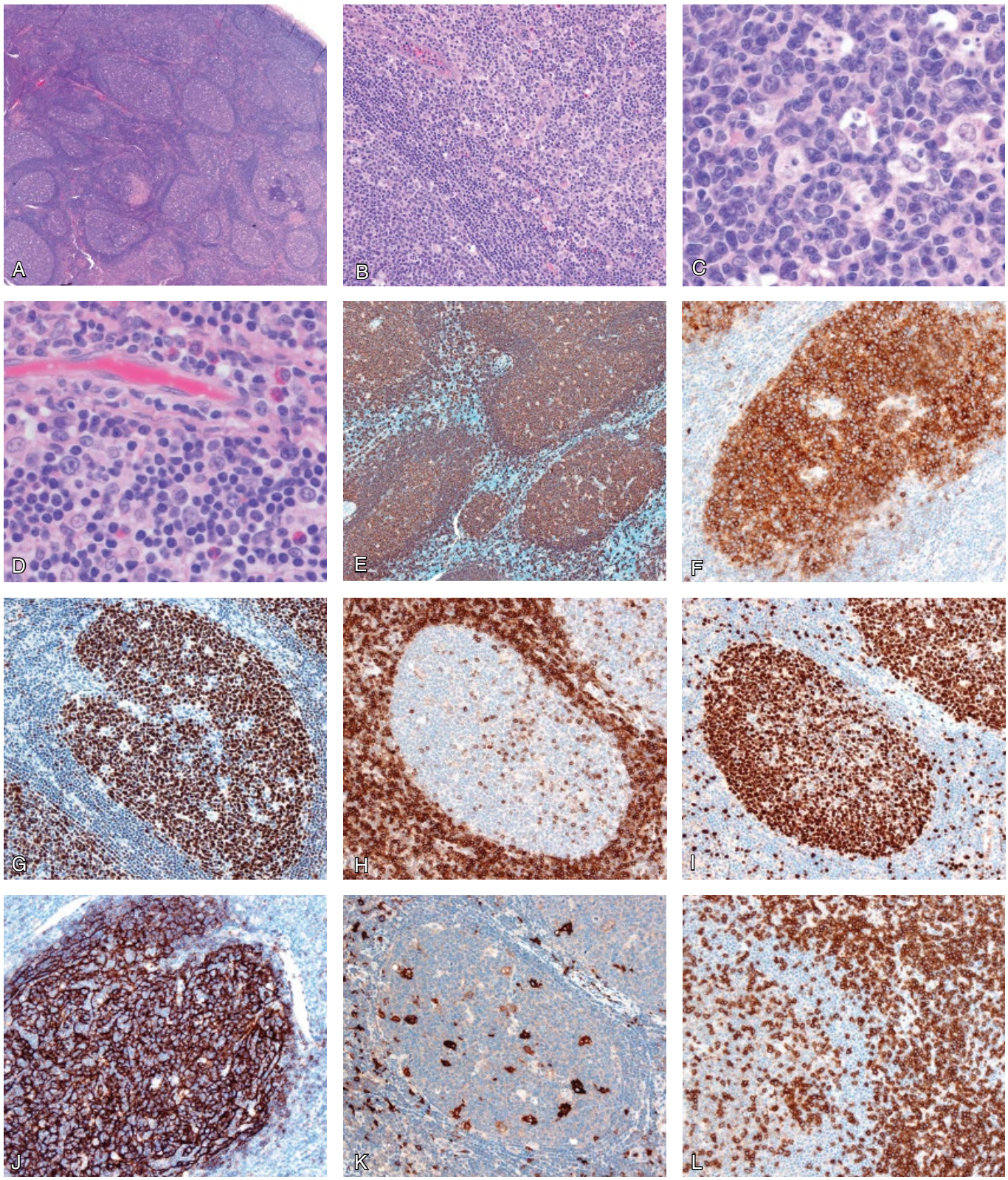

Fig. 11.32. Reactive lymphadenopathy: Lymph node histologic findings. **A,** Low-power view showing expanded follicles with mixture of lymphocytes, macrophages, infiltrating cells with surrounding mantle zone intact. **B**, Higher power showing germinal center with tingible body macrophages, centrocytes, and centroblasts. High endothelial blood vessel and lymphocyte trafficking. **C**, High-power view showing centrocytes and centroblasts. **D**, Paracortex showing mixed inflammatory cells and blood vessels. **E**, CD20 immunostain showing germinal center and mantle zone B cells. **F**, CD10 immunostain showing germinal center B cells. **G**, BCL-6 immunostain showing nuclear staining of germinal B cells. **H**, BCL-2 immunostain. Mantle zone B cells and scattered T cells are positive. **I**, MIB-1 immunostain. This is a proliferation marker detecting the Ki67 antigen. The cells in the germinal follicle are positive with a darker zone at the edge. **J**, CD21 immunostain. Follicular dendritic cells are positive and show a network of cell processes. **K**, CD163 immunostain. Tingible body macrophages are positive in the germinal center. **L,** CD3 immunostain. T cells in the paracortex and a few scattered T cells in the germinal center are positive. (Courtesy of Dr. A Ramsay.)

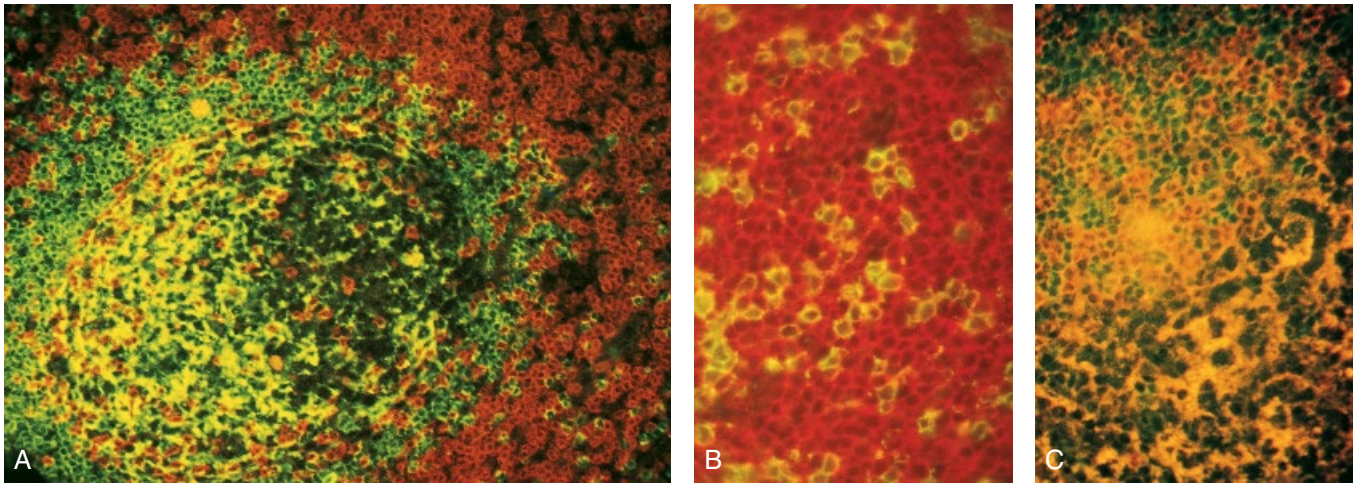

Fig. 11.33. Reactive lymphadenopathy. **A,** T cells (red rhodamine labeling) occupy the paracortical area surrounding the mainly B-lymphocyte corona that expresses IgM (green fluorescein labeling). A number of T cells are scattered within the germinal center, where immune complexes are also stained strongly by the IgM antisera. **B,** The T cells within the paracortical area are a mixture of CD4+ helper (red) and CD8+ suppressor/cytotoxic (green) cells. **C,** At the edge of a germinal center is a mixture of B lymphocytes expressing κ (red) or λ (green) light chains. (Courtesy of Professor M Chilosi, Professor G Janossy, and Professor G Pizzolo.)

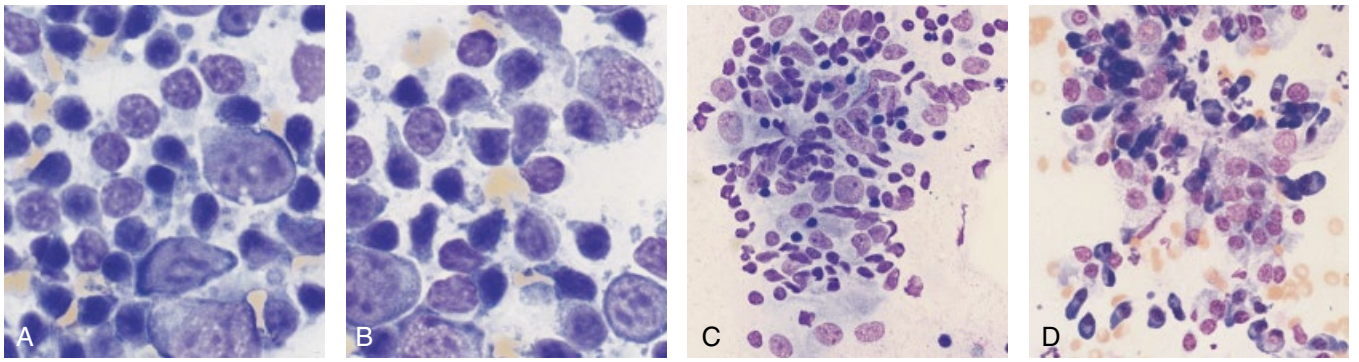

Fig. 11.34. Reactive lymphadenopathy: Fine-needle aspirate of cervical lymph node. **A, B,** Pleomorphic lymphoid population with large immunoblasts, centroblasts, paler centrocytes, and small lymphocytes. **C,** Small and medium-sized lymphoid cells and histiocytes. **D,** Plasma cells, histiocytes, and lymphocytes.

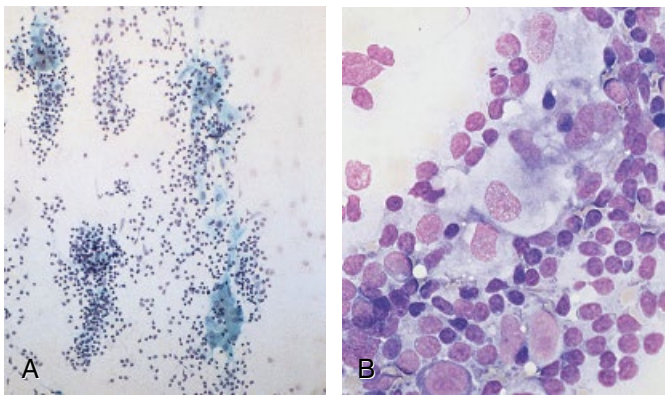

Fig. 11.35. Toxoplasmosis: Fine-needle aspirate of cervical lymph node. **A,** Groups of histiocytic cells in the cell trails. **B,** At higher magnification predominantly small lymphocytes that surround these histiocytes are seen. (A, Papanicolaou's stain; B, May-Grünwald–Giemsa stain.)

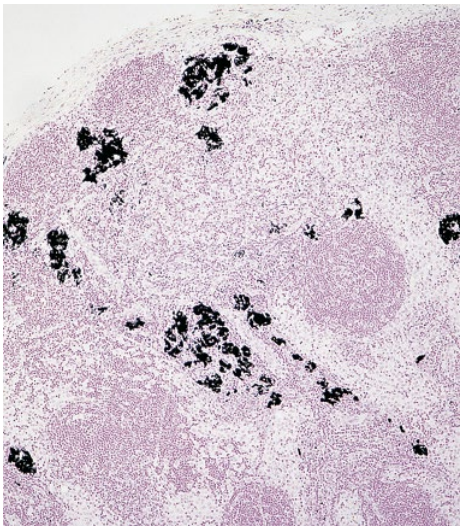

Fig. 11.36. Tattoo pigment in the sinus areas of a lymph node. (Courtesy of Dr. JE McLaughlin.)

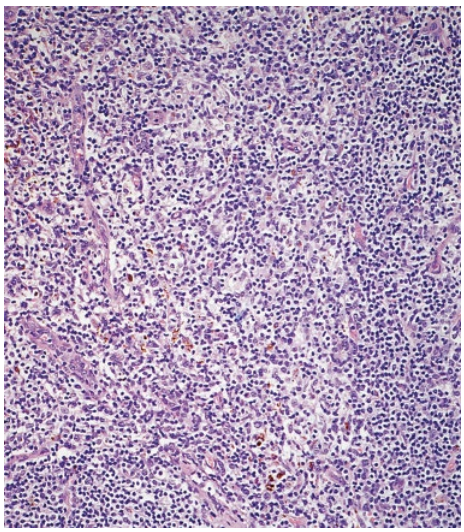

Fig. 11.37. Dermatopathic lymphadenopathy: Clear cytoplasm of interdigitating reticulum cells gives an area of pallor above a follicle. Occasional phagocytic cells that contain melanin are visible. (Courtesy of Dr. JE McLaughlin.)

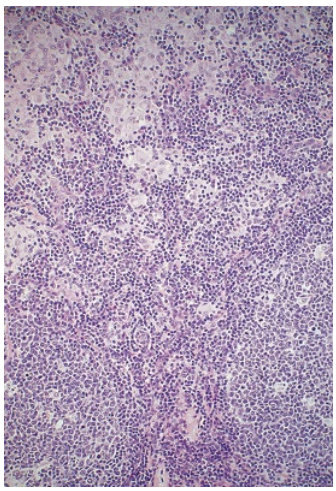

Fig. 11.38. Toxoplasmosis: Small clusters of epithelial histiocytes above two hyperplastic follicles. (Courtesy of Dr. JE McLaughlin.)

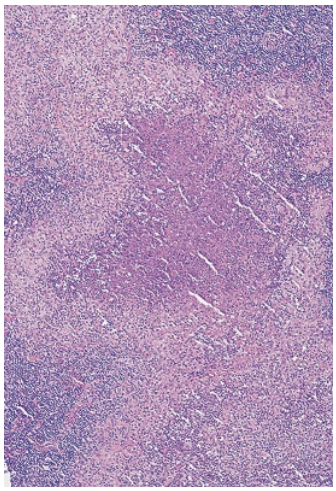

Fig. 11.39. Cat scratch disease: A geographic area of necrosis within a granuloma is visible. (Courtesy of Dr. JE McLaughlin.)

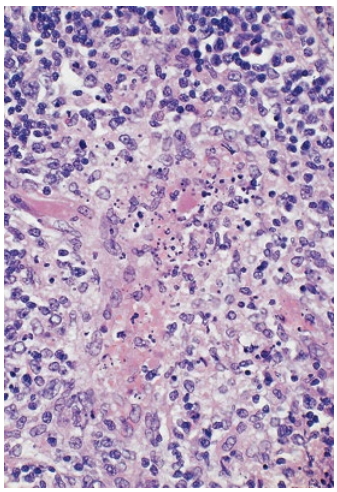

Fig. 11.40. Kawasaki disease: Casculitic reaction in a lymph node. (Courtesy of Dr. JE McLaughlin.)

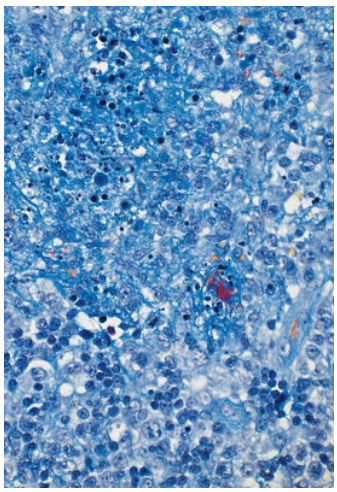

Fig. 11.41. Kawasaki disease: Fibrin (red) deposition in the wall of a small blood vessel. (Courtesy of Dr. JE McLaughlin.)

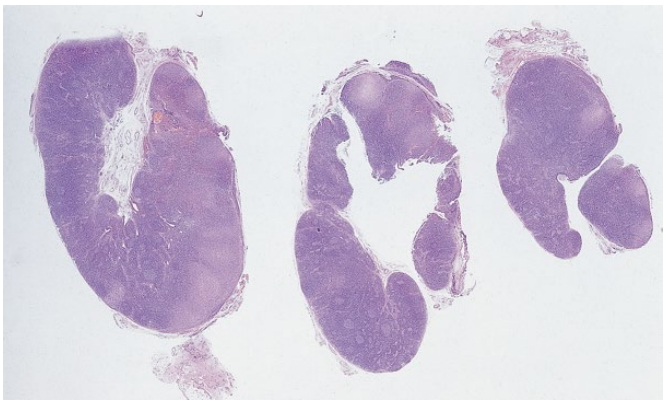

Fig. 11.42. Kikuchi disease: Whole mount of lymph node "bread-sliced" into three parts showing pale circumscribed areas of necrosis. (Courtesy of Dr. T Levine.)

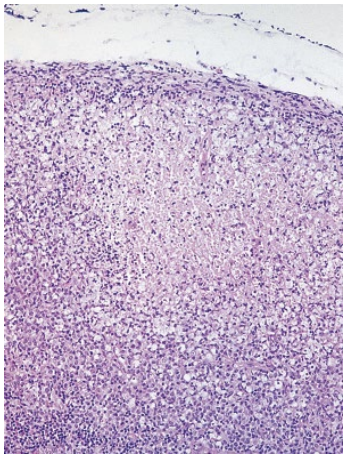

Fig. 11.43. Kikuchi disease: Low-power view of cortical area of necrosis. (Courtesy of Dr. T Levine)

Examination of involved lymph nodes reveals characteristic abnormalities (Figs. 11.50 and 11.51). Depletion of CD4 cells is progressive, and the peripheral blood shows lymphopenia and an alteration in the T-lymphocyte subsets, with a fall in the CD4+:CD8+ (helper:suppressor) ratio from the normal value of 1.5 to 2.5:1 to less than 1:1. A polyclonal rise in serum immunoglobulins is often found, in some cases with a paraprotein present. The diagnosis is confirmed by detection of antibodies to one or more HIV surface antigens, or by detection of the antigens themselves (Fig. 11.52). Hematologic abnormalities may include anemia, neutropenia, or thrombocytopenia (Table 11.5). These are often autoimmune in origin, but sometimes result from direct infection of hematopoietic stem and progenitor cells in the bone marrow. The cytopenias may also be caused by dysplastic changes (Figs. 11.53–11.56), fibrosis (Fig. 11.57), or lymphoma in the marrow.

A wide spectrum of opportunistic organisms cause infections in people with AIDS, including atypical mycobacteria

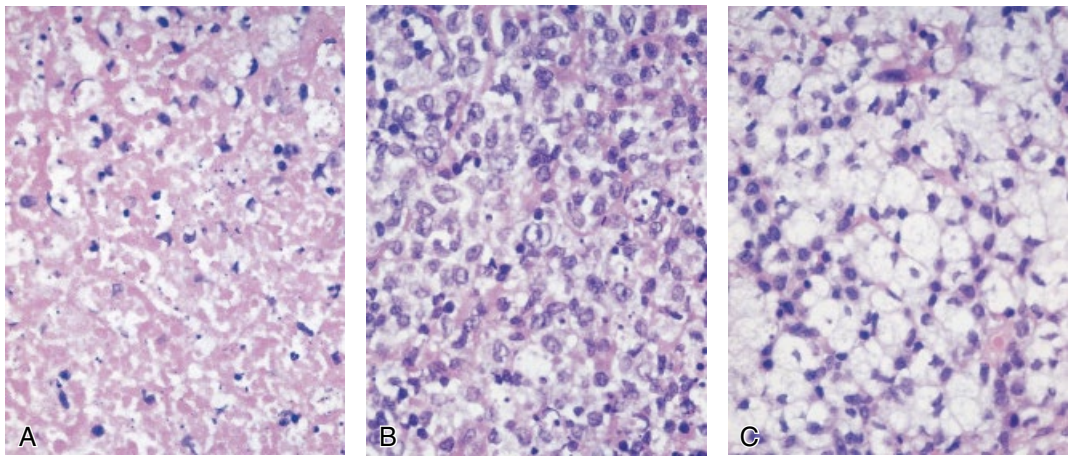

Fig. 11.44. Kikuchi disease. **A,** High-power view of necrosis with karyorrhectic debris (note the absence of neutrophils). **B,** Adjacent "cuff" of lymphoblasts, including T-cell blasts and macrophages. **C,** Characteristic "crescentic" or "signet cell" macrophages adjacent to areas of necrosis. (Courtesy of Dr. T Levine.)

TABLE 11.4. PRIMARY IMMUNODEFICIENCY DISORDERS

B-cell disorders

X-linked agammaglobulinemia (defect of Bruton tyrosine kinase, BTK)
Autosomal agammaglobulinemia
- Recessive λ5, Igα, BLNK
- Human inducible costimulator (ICOS)

Selective IgA or IgM deficiency
IgG subclass deficiencies
Hyper IgM
- Activation-induced cytidine deaminase (AICD) deficiency
- Uracil DNA glycosylase (UNG) deficiency
- CD40 ligand deficiency
- CD40 deficiency

B-cell activation factor from tumor necrosis factor (Baff-R) deficiency
TAC1 deficiency
Common variable immune deficiency

Severe combined immune deficiency

X-Linked Interleukin (IL) receptor γ chain defects in receptors for IL-2, IL-4, IL-7, IL15; α chain defect for IL-7
JAK-3 deficiency
ZAP-70 deficiency
Adenosine deaminase (ADA), purine nucleoside phosphorylase deficiencies
Recombination activating gene (RAG-1 or RAG-2) deficiencies
Reticular dysgenesis

Primary T-cell deficiency

Congenital thymic aplasia (DiGeorge Syndrome)
MHC class II deficiency
Transporter associated with antigen presentation (TAP-1 or TAP-2) MHC class 1 deficiency
Th1 deficiency (affect T cell/macrophage interaction)
- IFNγ and IFNγ receptor deficiency
- IL-12 and IL-12 receptor deficiency

Disorders of cytotoxic T-cell/NK-cell function with acute organ damage after viral infection

X-linked lymphoproliferative (Duncan syndrome)
Chédiak–Higashi (see Chapter 10)
Griscelli syndrome
Familial hemophagocytic syndrome (perforin gene defect) (see Chapter 24)

Multisystem disorders

Wiskott–Aldrich syndrome (X-linked)
Immune dysregulation polyendocrinopathy enteropathy, X-linked (IPEX)
WHIM (warts, hypogammaglobulinemia, infections, and myelokathexis)
Autoimmune polyendocrinopathy and ectodermal dysplasia
Hyper IgE – eczema, hypermobility of joints, lung abnormalities

Defects of DNA repair with chromosome instability and sensitivity to X-radiation

Ataxia telangiectasia (immunodeficiency)
Nijmegen breakage syndrome

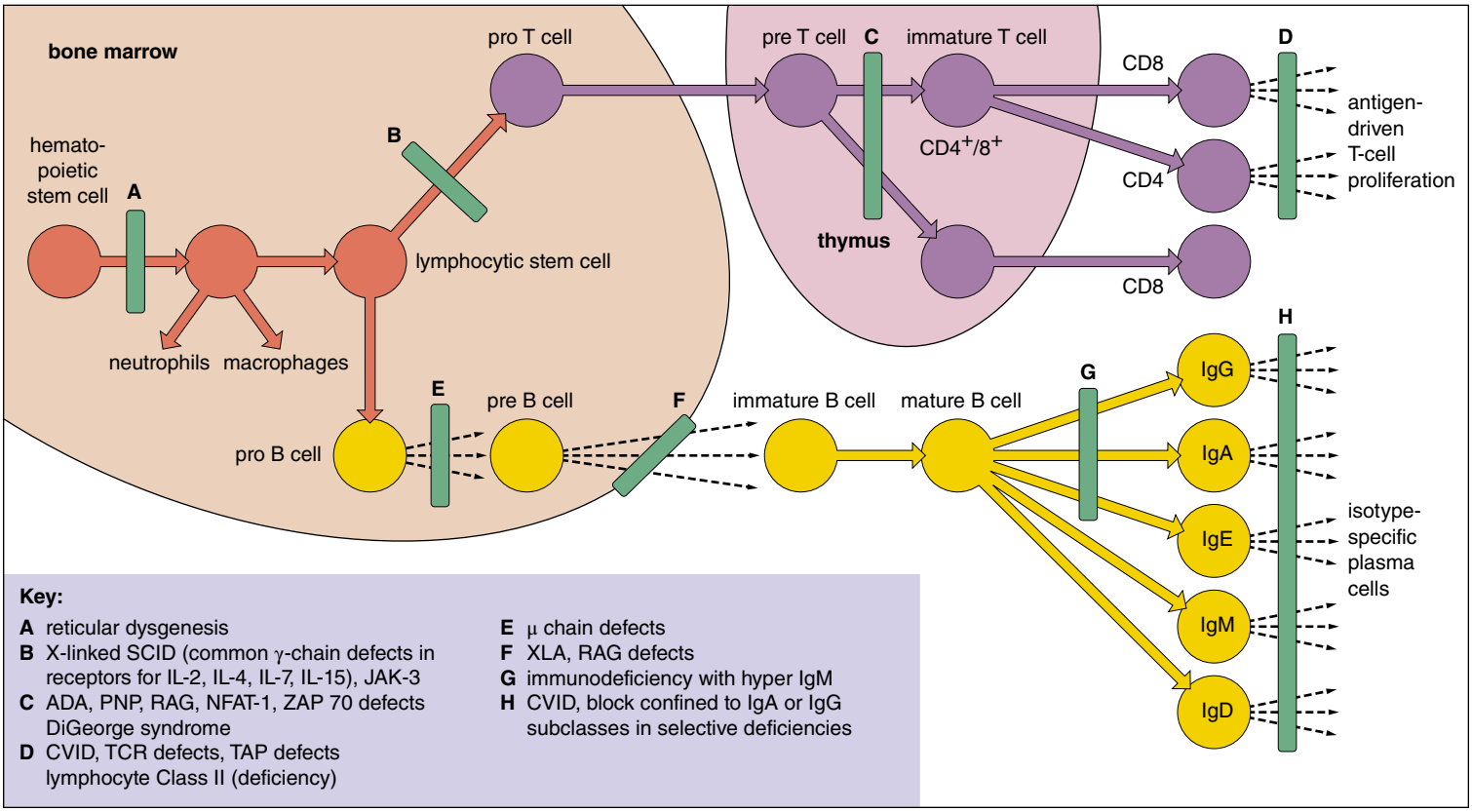

Fig. 11.45. Immunodeficiency disorders: Sites of the defects in B- and T-cell development in different types of congenital immune deficiency. ADA, adenosine deaminase; CVID, common variable immunodeficiency; JAK-3, Janus-associated kinase; NFAT-1, nuclear factor of activated T cells; PNP, purine nucleoside phosphorylase; RAG, V-D-J recombination activation genes: these include RAG1 and 2, DNAPKcs, Artemis (DCLRE1C), DNA ligase 4 (LIG4) and Cermunnos (NHEJ1 XLF); SCID, severe combined immunodeficiency; TAP, transporter associated with antigen presentation; XLA, X-linked agammaglobulinemia; ZAP-70, zeta-associated protein. (Courtesy of Dr. ADB Webster.)

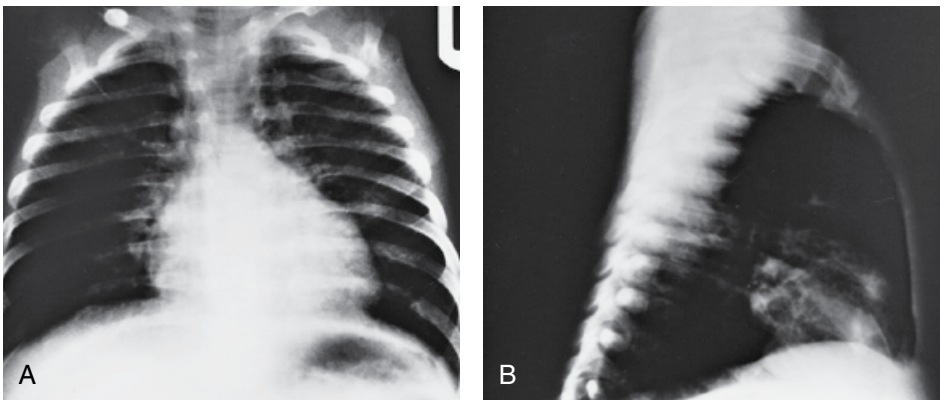

Fig. 11.46. Severe combined immunodeficiency disease: Chest radiographs. **A,** The posteroanterior view shows absence of thymic shadow in the superior mediastinum. **B,** The lateral view confirms the lack of thymus tissue deep in the sternum. (Courtesy of Professor RI Levinsky.)

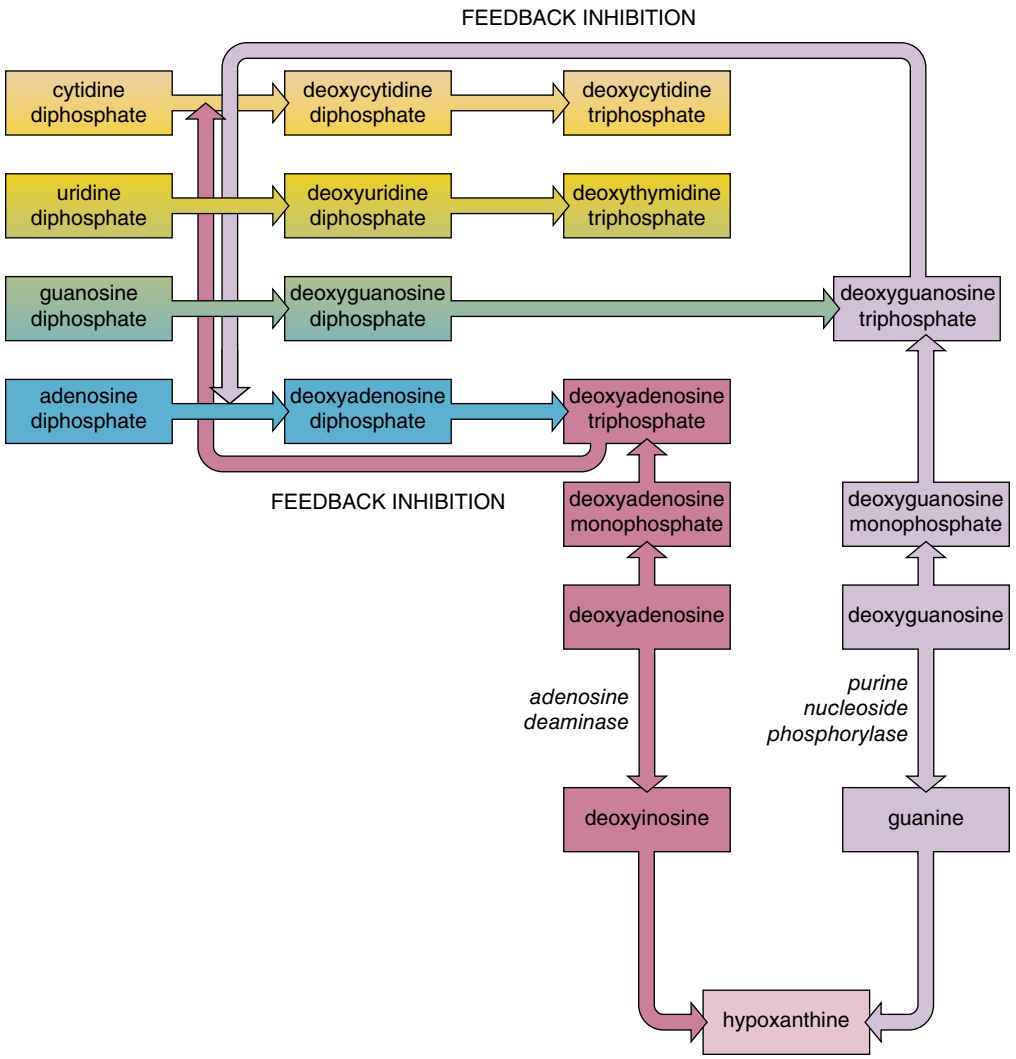

Fig. 11.47. Role of adenosine deaminase (ADA) and purine nucleoside phosphorylase (PNP) in purine degradation. ADA deficiency causes death of cortical thymocytes by accumulation of deoxyadenosine triphosphate (which inhibits DNA synthesis). PNP deficiency produces toxicity to T cells by accumulation of deoxyguanosine triphosphate. ADA and PNP are also involved in adenosine and guanosine degradation, respectively. In both types of deficiency, other biochemical mechanisms of toxicity to proliferating and nonproliferating lymphoid cells may occur.

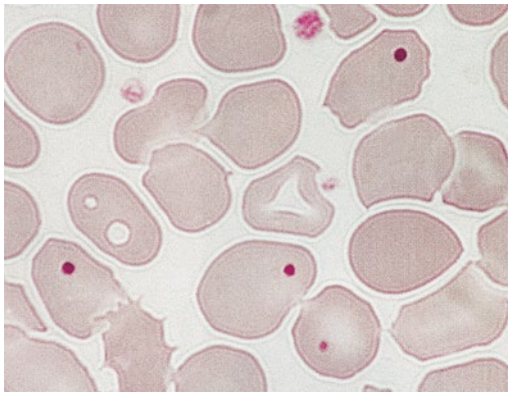

Fig. 11.48. Lymphoreticular dysgenesis: Peripheral blood film of a one-week-old infant. The large numbers of Howell–Jolly bodies (small granular remnants of DNA) are the result of splenic agenesis. There was severe lymphopenia. (Absolute lymphocyte count, 0.1×10^9/L.)

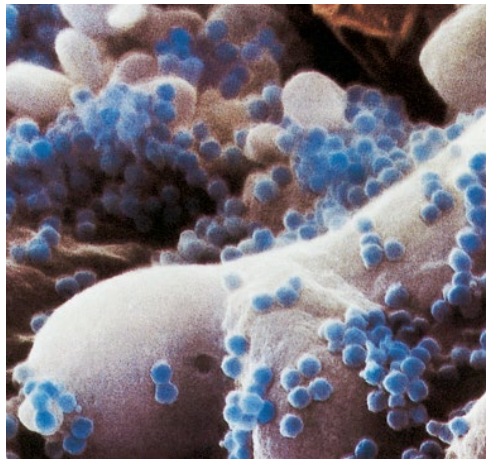

Fig. 11.49. AIDS: Scanning electron micrograph of a T lymphocyte infected by HIV. This close-up view shows the hexagonal outline of the virus particles. The virus subgroups (clades) differ in viral sequence. (Courtesy of Lennart Nilsson; © Boehringer Ingelheim International GmbH.)

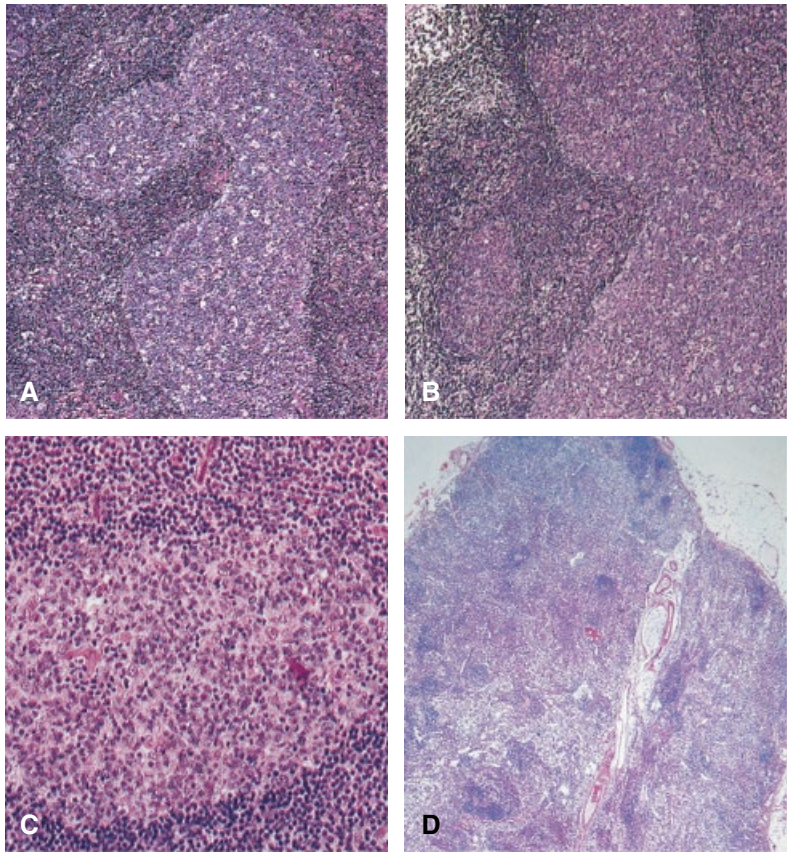

Fig. 11.50. AIDS: Sections of lymph nodes infected by HIV show a spectrum of histologic changes. **A, B,** Type I includes follicular and paracortical hyperplasia. Mitotically active germinal centers are numerous in the medulla, as well as the cortex, and present a "geographic outline." Mitotic figures are abundant, and there is extensive cytolyis and phagocytosis of cell remnants by tingible body histiocytes. The mantle zones are attenuated and (in places) absent, and the follicles appear confluent. The interfollicular tissue shows an increase in small vessels. (A, B, Courtesy of Dr. JE McLaughlin.) **C,** In the Type II pattern, there is loss of germinal centers but diffuse lymphoid hyperplasia. Source: C, Ioachim HL. *Pathology of AIDS*. Gower Medical Publishing, 1989. Reproduced with permission of Elsevier. **D,** In Type III, an end-stage in fatal cases, lymphocyte depletion predominates.

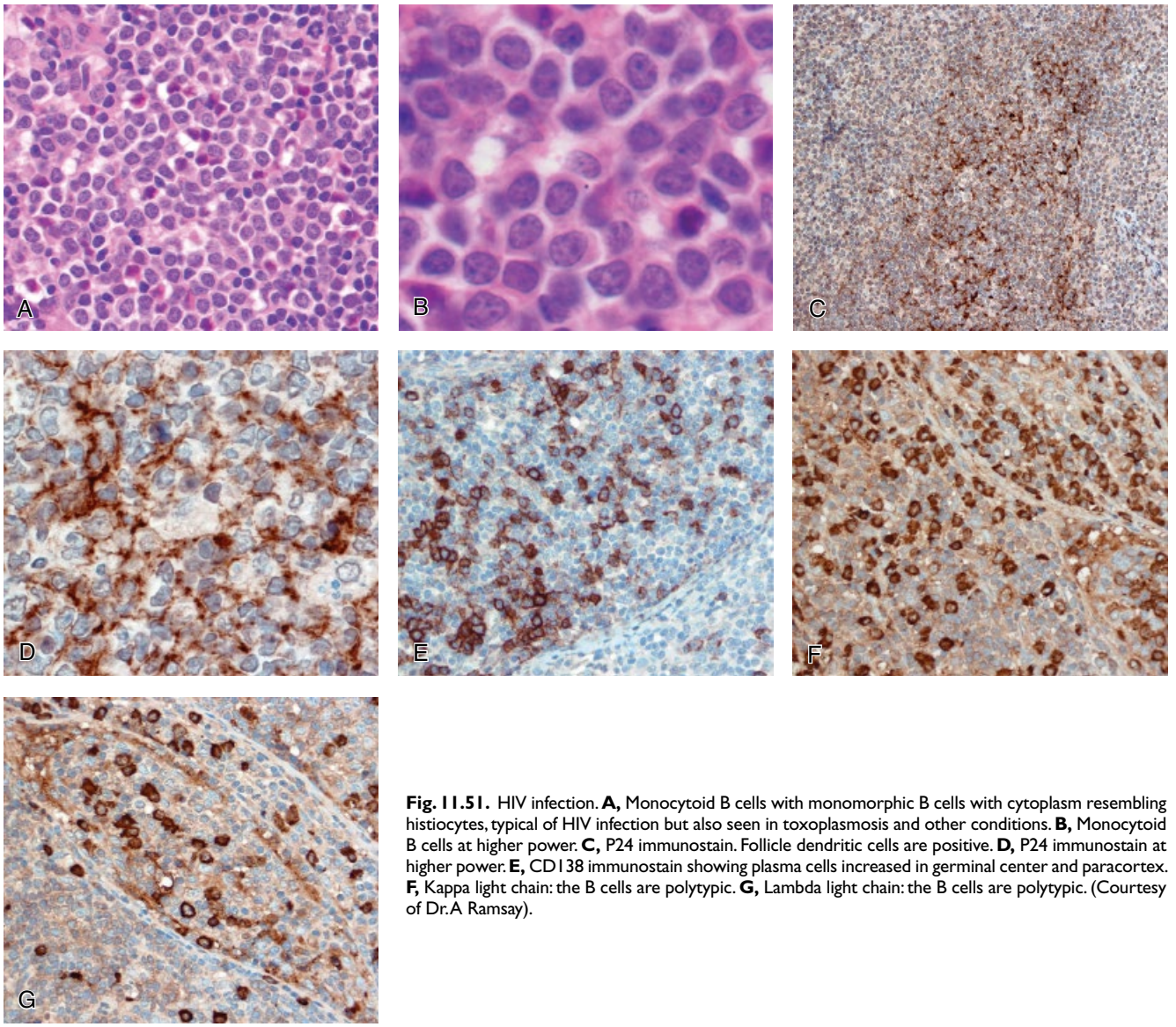

Fig. 11.51. HIV infection. **A,** Monocytoid B cells with monomorphic B cells with cytoplasm resembling histiocytes, typical of HIV infection but also seen in toxoplasmosis and other conditions. **B,** Monocytoid B cells at higher power. **C,** P24 immunostain. Follicle dendritic cells are positive. **D,** P24 immunostain at higher power. **E,** CD138 immunostain showing plasma cells increased in germinal center and paracortex. **F,** Kappa light chain: the B cells are polytypic. **G,** Lambda light chain: the B cells are polytypic. (Courtesy of Dr.A Ramsay).

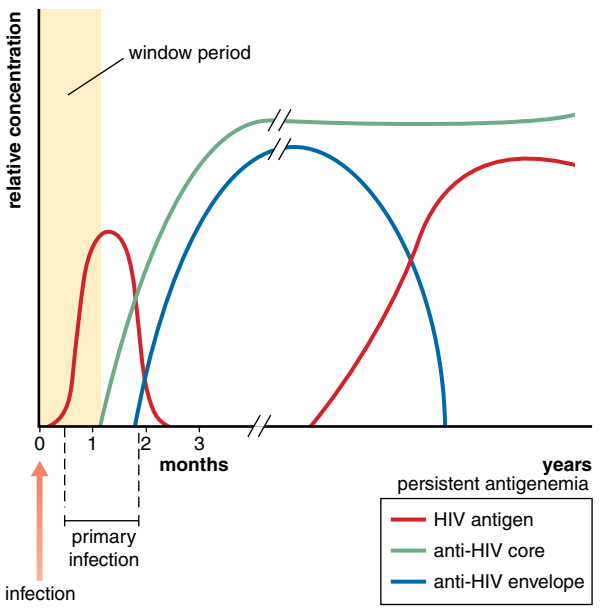

Fig. 11.52. HIV infection: The sequence of expression of HIV antigens and different antibodies following primary infection. (Courtesy of Professor MC Contreras and the North London Blood Transfusion Center.)

TABLE 11.5. HEMATOLOGIC MANIFESTATIONS OF HUMAN IMMUNODEFICIENCY VIRUS INFECTION

Fall in CD4 lymphocyte count and lymphopenia
Anemia, neutropenia, thrombocytopenia–either singly or combined
Bone marrow changes
Hypercellular (increased plasma cells, lymphocytes)
Normocellular
Hypocellular
Dysplastic changes:
Normoblasts
Granulocytic (giant metamyelocytes, Pelger forms, detached nuclear fragments)
Megakaryocytes
Increased fibrosis
Granulomas (AFB, cryptococcal, uncertain etiology)
Other infections (e.g. histoplasma, leishmania, pneumocystis (may need culture to demonstrate))
Benign nodules
Gelatinous degeneration
Infiltration by lymphoma
Low serum vitamin B_{12} and folate levels
Toxic change as a result of drugs (e.g. megaloblastosis caused by azidothymidine, pentamidine)
Plasma protein changes
Polyclonal rise in IgG
Paraprotein

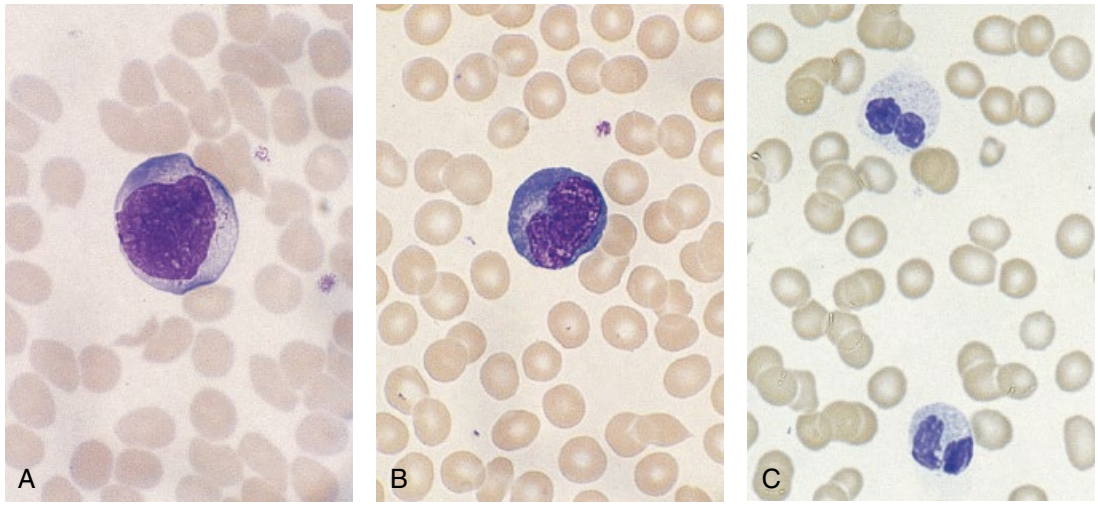

Fig. 11.53. HIV infection: Peripheral blood film. **A, B,** Immunoblasts. **C**, Pseudo-Pelger cells. (C, Courtesy of Dr. D Swirsky.)

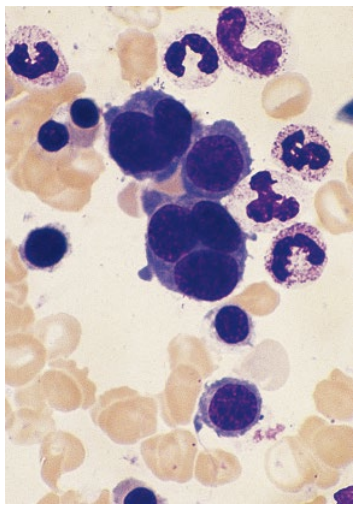

Fig. 11.54. HIV infection: Bone marrow aspirate showing dyserythropoietic changes.

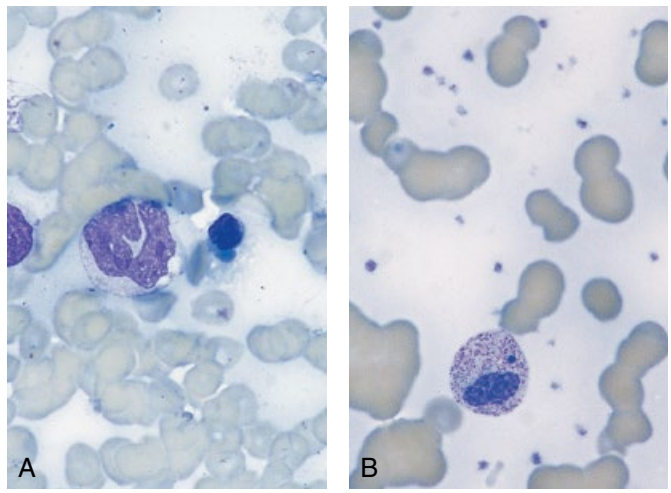

Fig. 11.55. HIV infection: Dysmyelopoiesis. **A**, Giant metamyelocyte. **B,** Detached nuclear fragment. (B, Courtesy of Professor. BA Bain.)

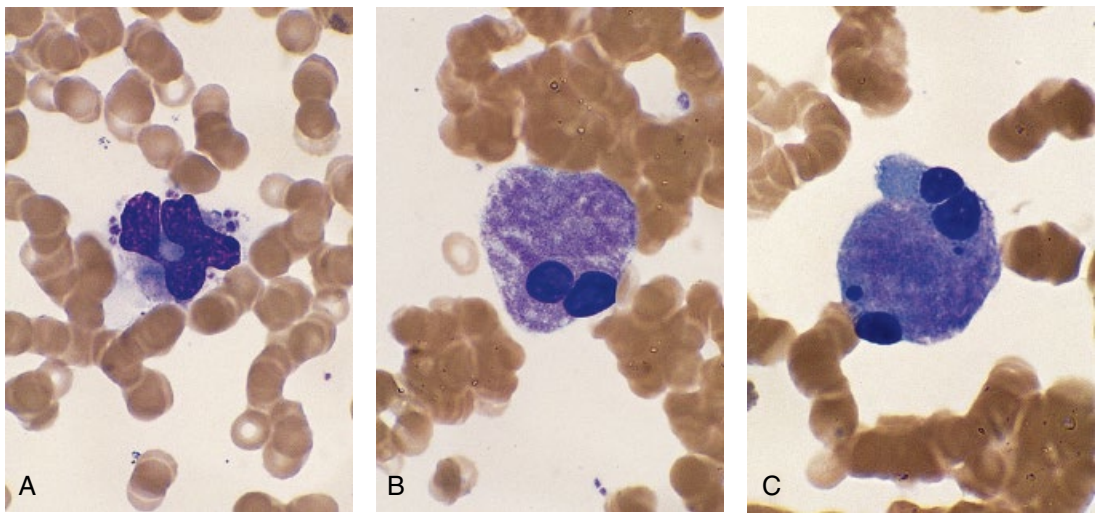

Fig. 11.56. HIV infection: Bone marrow aspirate showing dysplastic megakaryoctes.

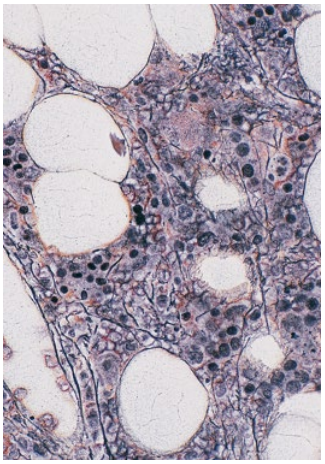

Fig. 11.57. HIV infection: Bone marrow trephine biopsy showing dense reticulin network. (Silver stain.) (Courtesy of Dr. C Costello.)

(Fig. 11.58), *Pneumocystis carinii* (Fig. 11.59), cytomegalovirus (Fig. 11.60) and *Cryptococcus*, *Histoplasma* (Fig. 11.61), and *Leishmania* (Fig. 11.62). Often nonspecific granulomas are found (Fig. 11.63). A proportion of the patients develop Kaposi sarcoma, a vascular skin tumor of endothelial cell origin associated with Kaposi sarcoma herpesvirus (KSHV) or human herpesvirus 8 (HHV8) (Figs. 11.64 and 11.65). Other patients may develop non-Hodgkin lymphoma, which is likely to be high grade, and they have a 20% incidence of lymphoma in the central nervous system (Figs. 11.66–11.69). Primary effusion lymphoma is an unusual B-cell lymphoma associated with HHV8 viral infection (see Chapter 20).

AUTOIMMUNE LYMPHOPROLIFERATIVE SYNDROME

Autoimmune lymphoproliferative syndrome is characterized by lymphadenopathy, hepatosplenomegaly, autoimmune hemolytic anemia, neutropenia, thrombocytopenia, and hypergammaglobulinemia with a high proportion of circulating CD3+, CD4–,

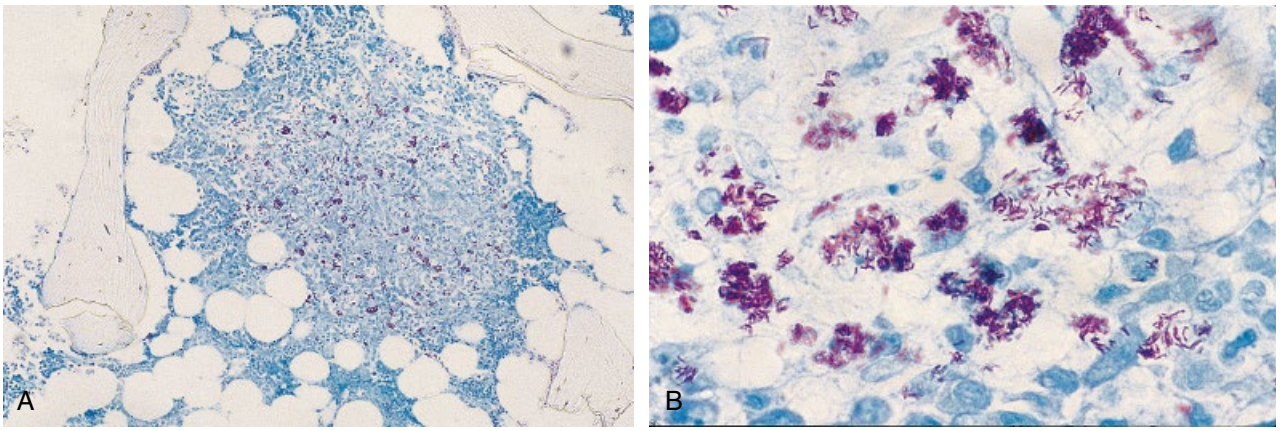

Fig. 11.58. AIDS: Bone marrow trephine biopsy. **A,** Granuloma showing strong positivity with Ziehl–Nielsen stain. **B,** Higher power shows large numbers of acid-fast bacilli. (Courtesy of Dr. BW Baker and Dr. EB Knottenbelt.)

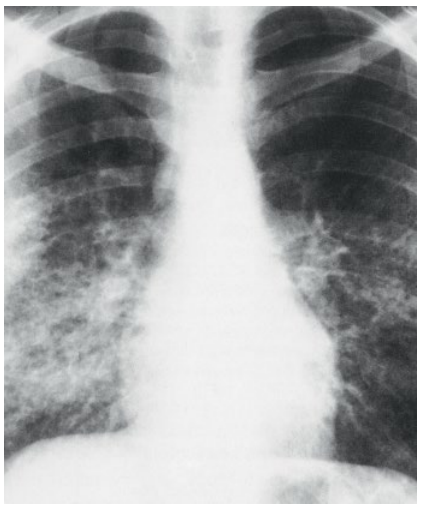

Fig. 11.59. AIDS: Chest radiograph in *Pneumocystis jiroveci* infection, showing extensive, predominantly central interstitial opacities.

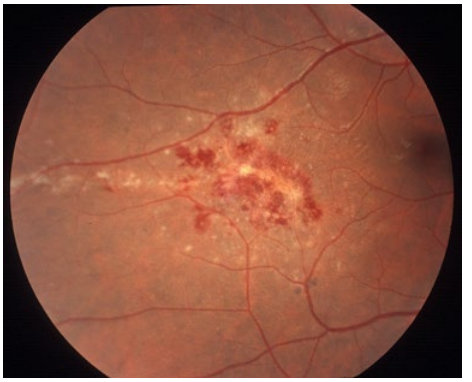

Fig. 11.60. AIDS: Cytomegalovirus retinitis. (Courtesy of Dr. S Imashuku.)

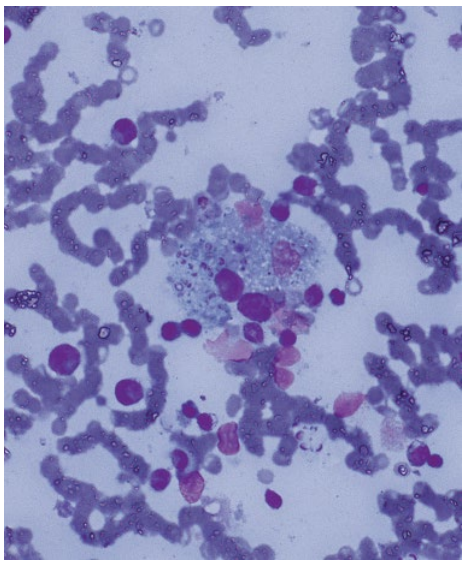

Fig. 11.61. AIDS: Bone marrow aspirate showing histoplasmosis, visible as faintly staining fine fungal organisms in macrophages. (Courtesy of Dr. C Costello.)

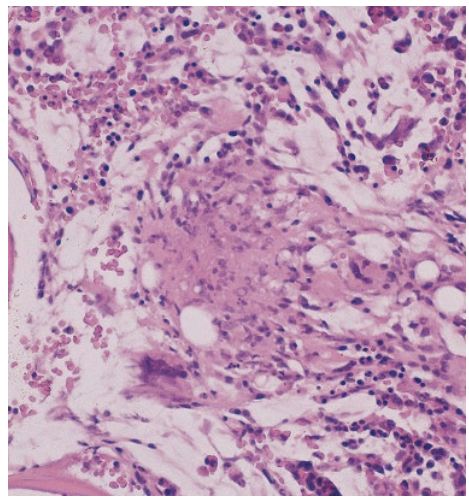

Fig. 11.63. AIDS: Bone marrow trephine biopsy showing granuloma of uncertain etiology. (Courtesy of Dr. C Costello.)

Fig. 11.62. AIDS: Bone marrow aspirate showing Leishman–Donovan bodies.

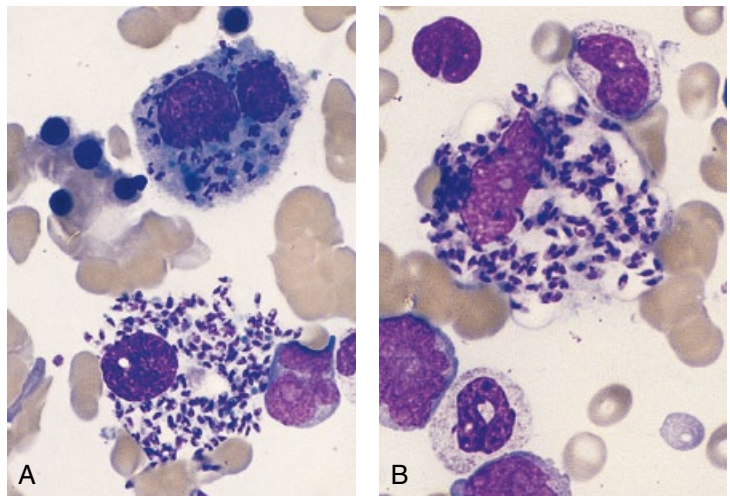

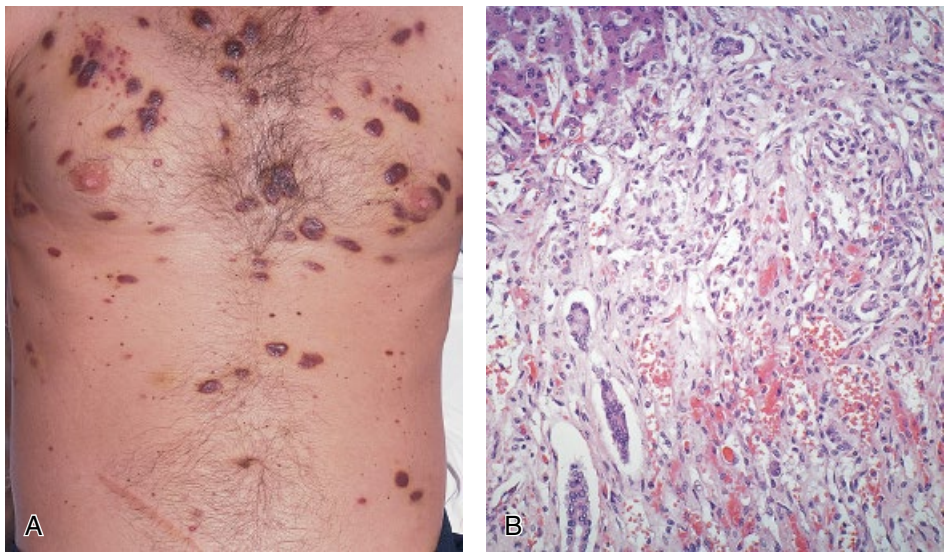

Fig. 11.64. AIDS: Kaposi sarcoma. **A,** Multiple vascular tumors of endothelial origin on the chest of an HIV antigen-positive homosexual male. **B,** Infiltration of the portal areas of the liver. (A, Courtesy of Dr. IVD Weller.)

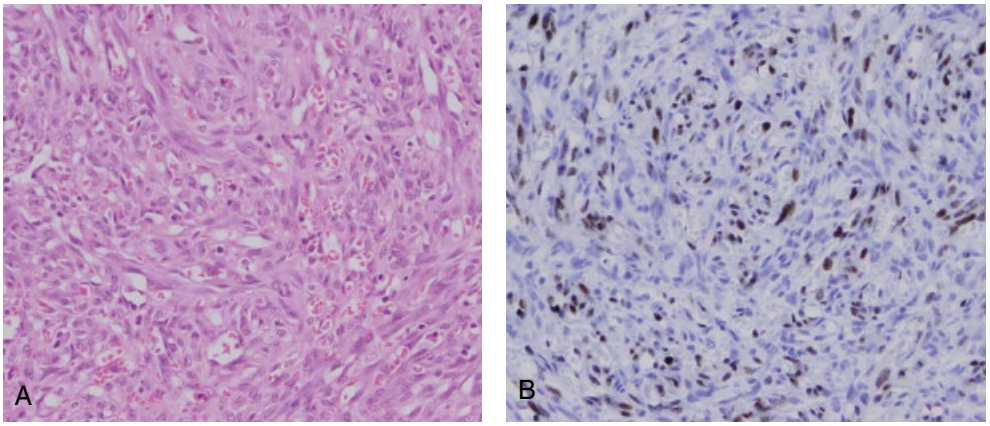

Fig. 11.65. AIDS: Kaposi sarcoma. **A,** Vascular endothelial cells with blood lakes. **B,** p24 immunostain is positive.

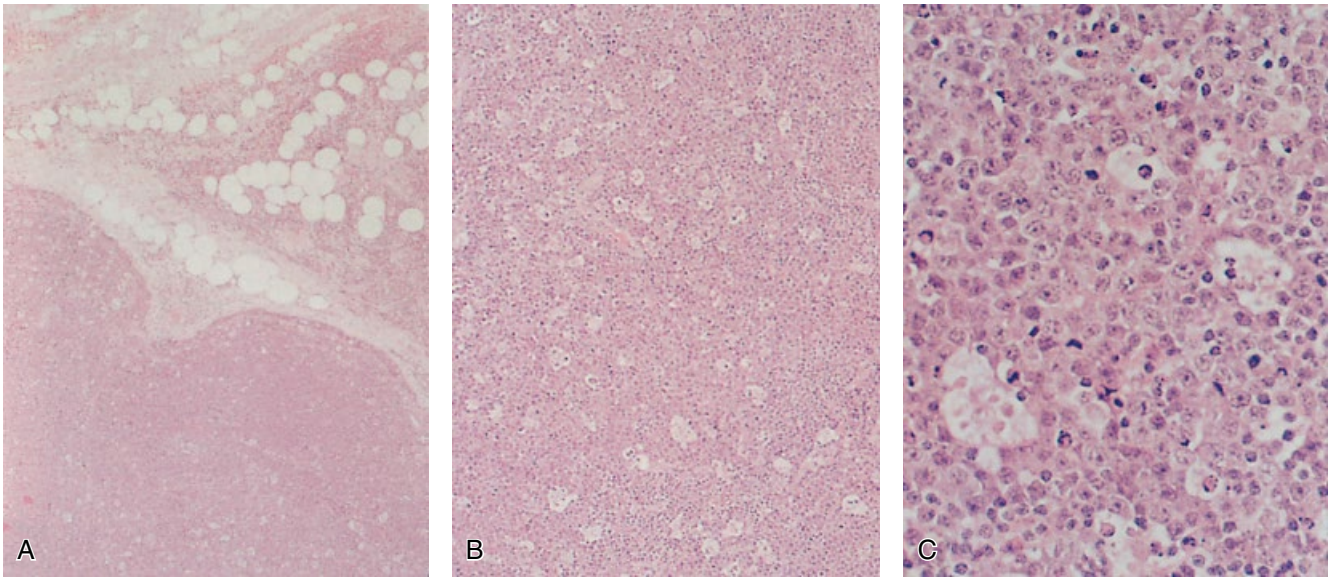

Fig. 11.66. AIDS, non-Hodgkin lymphoma. **A,** Lymph node showing replacement of normal architecture by tumor, which is extending into surrounding fat. **B, C,** Higher magnifications show the tumor to comprise lymphoblasts and "starry sky" tingible body macrophages.

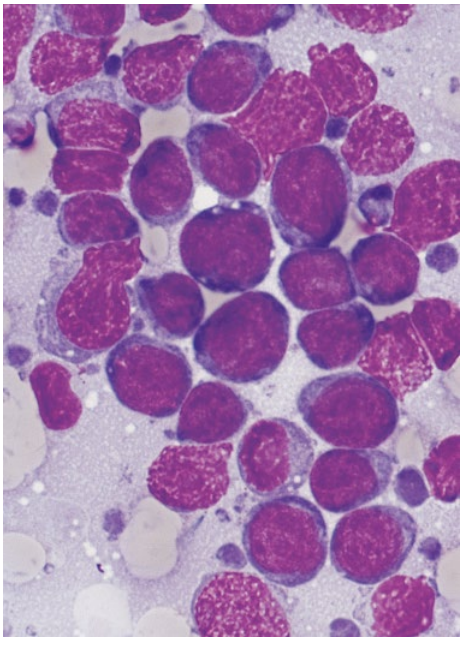

Fig. 11.67. AIDS, non-Hodgkin lymphoma: Fine-needle aspirate of cervical lymph node showing lymphoblasts with cytoplasm that is strongly basophilic. Some of the cells show prominent cytoplasmic vacuoles (same case as shown in Fig. 11.66).

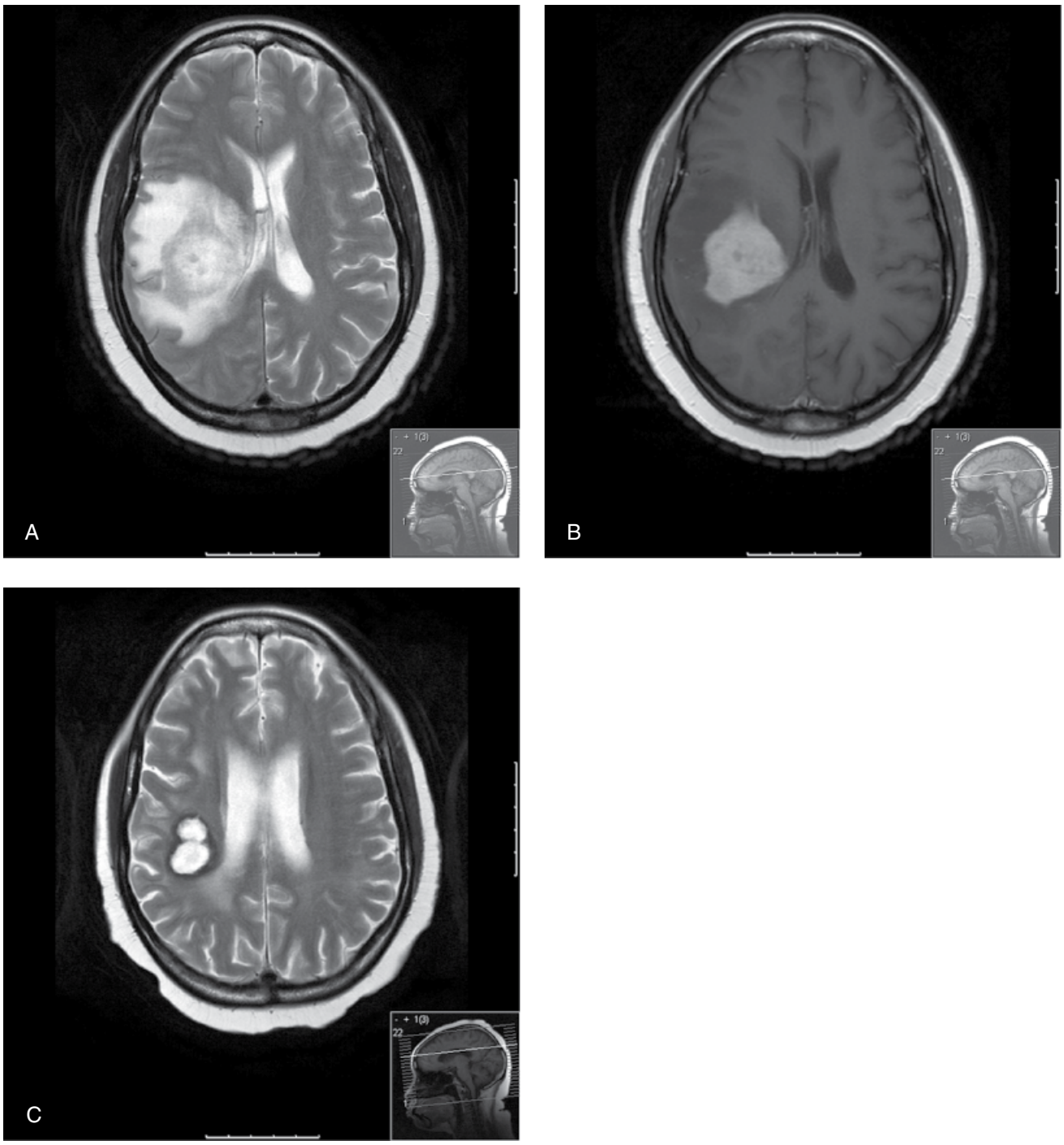

Fig. 11.68. AIDS: Cerebral lymphoma magnetic resonance imaging (MRI). **A,** T_2-weighted MR brain scan showing heterogeneous mass and adjacent edema in right inferior frontoparietal region. There is compression of the right lateral ventricle and displacement of midline structures. Biopsy showed diffuse large B-cell lymphoma. **B,** The mass enhances after intravenous gadolinium injection. **C,** Enhanced image after chemotherapy showing regression of the mass. (Courtesy of the Department of Radiology, the Royal Free Hospital.)

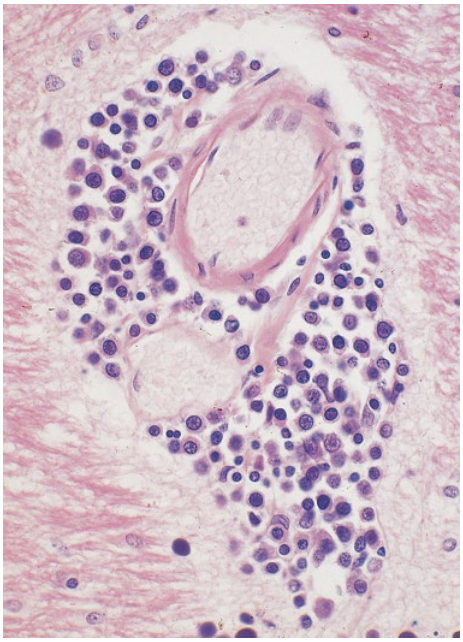

Fig. 11.69. AIDS, non-Hodgkin lymphoma: Invasion of perivascular space of the brain by a high-grade systemic lymphoma. (Courtesy of Dr. JE McLaughlin.)

and CD8+ T cells. Kidney, liver, skin, and connective tissues are other targets of the autoimmune attack on body cells. The lymph nodes show loss of normal architecture with reduction of B cells

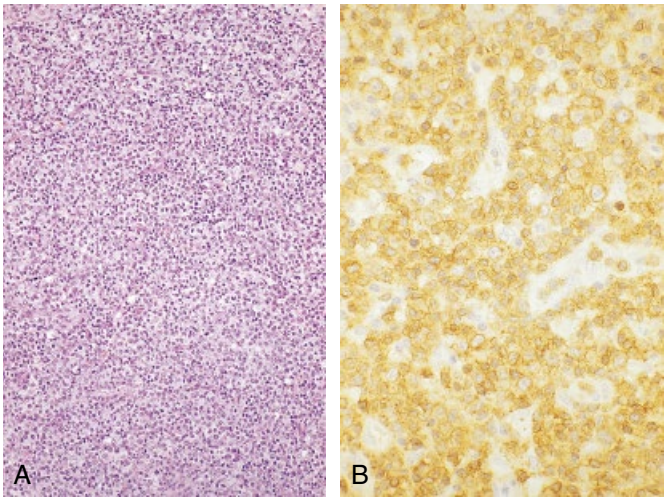

Fig. 11.70. Autoimmune lymphoproliferative syndrome. **A,** Lymph node biopsy at low power showing replacement of normal architecture by a uniform population of T lymphocytes with effacement of cortical structures. **B,** Immunoperoxidase stain at higher power showing that the majority of lymphocytes express CD3 antigens. (Courtesy of Dr. JE McLaughlin and Professor HG Prentice.)

(Fig. 11.70). The disease is associated in 75% of cases with mutations in the *FAS* gene with defective apoptosis in response to anti-FAS antibody and presumably failure of normal apoptosis by lymphoid cells in vivo.

CHAPTER

APLASTIC AND DYSERYTHROPOIETIC ANEMIAS

12

APLASTIC ANEMIA

Aplastic (hypoplastic) anemia is characterized by pancytopenia caused by hypoplasia of the marrow in the absence of an abnormal marrow infiltrate or increase in reticulin. It may be transient, as following cytotoxic therapy, but the term is usually used to denote the chronic forms of the condition. The condition may be inherited (Table 12.1) or acquired (Table 12.2). The acquired form may be difficult to distinguish from clonal disorders of the marrow, including myelodysplasia, paroxysmal nocturnal hemoglobinuria, and large granular lymphocytosis.

ACQUIRED APLASTIC ANEMIA

In about half of the acquired cases, no cause can be found. The response to antilymphocyte globulin (ALG) or cyclosporin in a substantial proportion of these idiopathic cases, however, suggests that an immune mechanism may be involved. The success of bone marrow transplantation implies that the hematopoietic microenvironment of the marrow is intact, at least in the majority of cases.

TABLE 12.1. THE INHERITED BONE MARROW FAILURE SYNDROMES

Pancytopenia (usually associated with a global hematopoietic defect)
Fanconi anemia
Dyskeratosis congenita
Shwachman–Diamond syndrome
Reticular dysgenesis
Pearson syndrome
Familial aplastic anemia (autosomal and X-linked forms)
Myelodysplasia
Nonhematologic syndromes (Down, Dubowitz syndromes)
Single cytopenia (usually)
Anemia
Diamond–Blackfan anemia
Congenital dyserythropoietic anemia
Neutropenia
Severe congenital neutropenia including Kostmann syndrome
Thrombocytopenia
Congenital amegakaryocytic thrombocytopenia
Amegakaryocytic thrombocytopenia with absent radii

Source: Hoffbrand AV, et al., eds. *Postgraduate Haematology*, 7th edn. John Wiley & Sons, 2016. Reproduced with permission of John Wiley & Sons.

TABLE 12.2. CAUSES OF ACQUIRED APLASTIC ANEMIA

Idiopathic
Secondary
Drugs–hypersensitivity (e.g. chloramphenicol, gold, sulfonamides)
Drugs–cytotoxics (e.g. busulfan, cyclophosphamide)
Irradiation
Infection: postviral hepatitis
Toxins (e.g. insecticides, benzene)

The cause of the anemia in about a third of patients appears to be damage to the hematopoietic stem cells by a drug or toxin. The cells are then reduced in number as they lose their ability to self-renew and proliferate. The drugs most frequently associated with aplastic anemia are the sulfonamides, chloramphenicol, and gold; however, a wide range of drugs has been implicated. In some patients these drugs give rise to only a selective neutropenia or thrombocytopenia. Aplastic anemia may also be caused by radiation or infection, particularly viral hepatitis (non-A, non-B, non-C). In the idiopathic form, an autoimmune assault on bone marrow stem cells by oligoclonal CD8+ cytotoxic T cells appears to be the underlying mechanism.

Clonal hematopoiesis with somatic mutations of such genes as *PIGA* and copy-neutral loss-of-heterozygosity or uniparental disomy (UPD) in 6p and mutations of the genes commonly mutated in the myeloid malignancies–*ASXL1*, *DNMT3A*, and *BCOR/BCORL1*–occur in about 50% of cases (Fig. 12.1). These are more likely to arise in a failed marrow rather than being a cause of the disease. The presence of *PIGA* and *BCOR/BCORL1* mutations predicts a response to antilymphocyte therapy and a better outcome than for *ASXL1* and *DNMT3A* mutations. When a clone with *ASXL1* and *DNMT3A* or other "myeloid" mutations is found in the bone marrow of otherwise healthy but usually elderly subjects, the condition has been given the acronym CHIP (clonal hematopoiesis of indeterminate prognosis) (see Chapter 15).

The anemia is mildly macrocytic or normocytic. The clinical features are those of anemia, hemorrhage caused by thrombocytopenia, or infections because of neutropenia. Bleeding is usually

Color Atlas of Clinical Hematology: Molecular and Cellular Basis of Disease, Fifth Edition. A. Victor Hoffbrand, Paresh Vyas, Elías Campo, Torsten Haferlach, and Keith Gomez

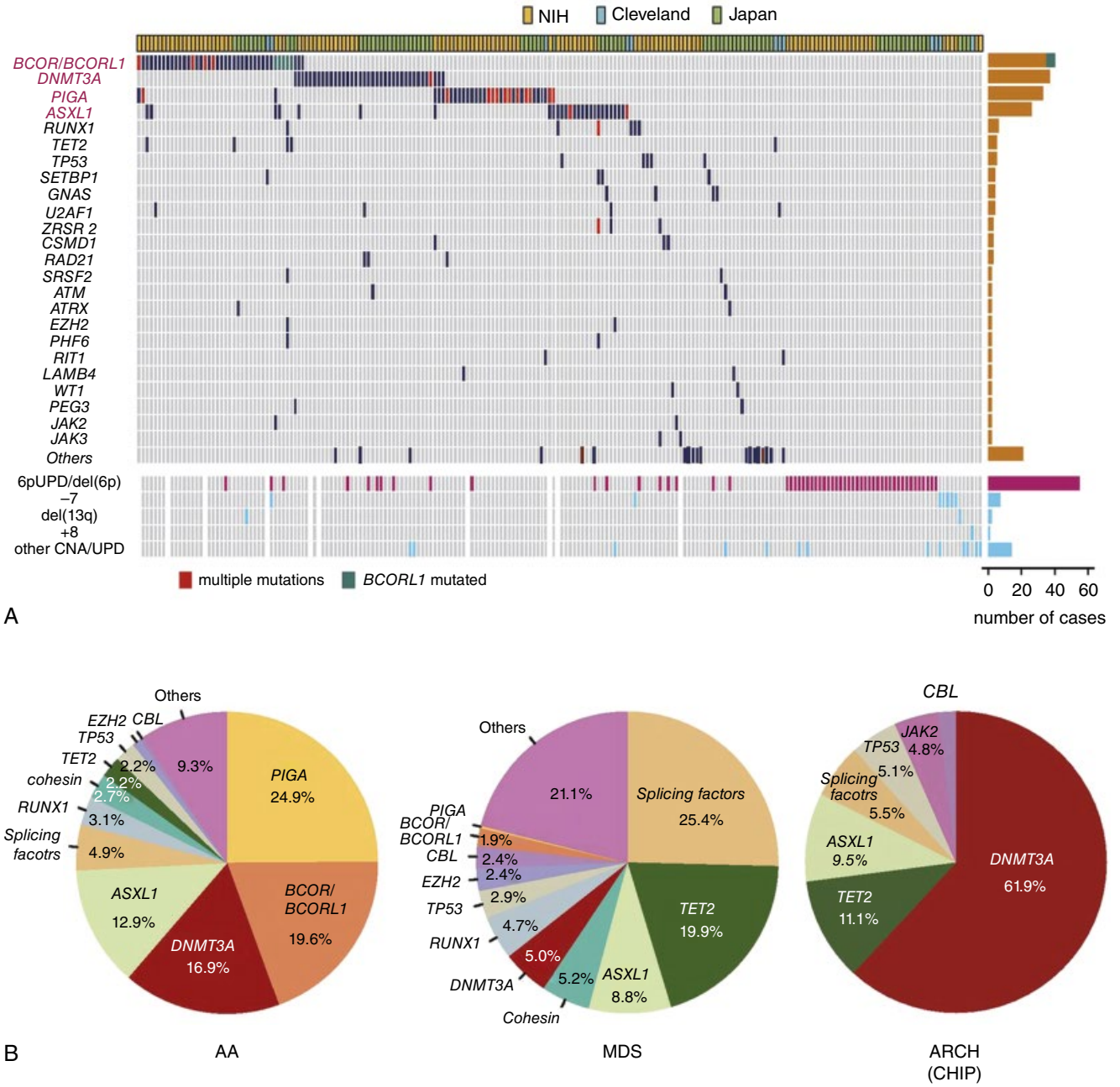

Fig. 12.1. Genetic alterations in aplastic anemia. **A**, Somatic mutations and other genetic lesions in aplastic anemia. Mutations and copy number abnormalities indicated on the left are shown for individual patients (shown horizontally). Frequency of each genetic lesion is presented on the right. **B**, Frequency of mutations in aplastic anemia, myelodysplastic syndrome, and age-related clonal hematopoiesis, according to the reports from Yoshizato et al. (*N Engl J Med* 2015;373(1):35–47), Haferlach et al. (*Leukemia* 2014;28(2):241–247), and Jaiswal et al. (*N Engl J Med* 2014;371(26):2488–2498), respectively, for which the denominators are the total numbers of mutations in each report. ARCH, age-related clonal hematopoiesis; CHIP, clonal hematopoiesis with indeterminate potential; NIH, National Institutes of Health. Source: Ogawa S. *Blood* 2016;128(3):337–347. Reproduced with permission of *Blood: Journal of the American Society of Hematology*.

into the skin, as petechiae or ecchymoses, or into or from interior mucosal surfaces (Fig. 12.2) but may also occur into internal organs (Fig. 12.3), with cerebral hemorrhage being the major risk. Infections are usually bacterial (Fig. 12.4), but viral (Fig. 12.5), fungal (Fig. 12.6), and protozoal infections may also occur, particularly later in the disease.

INHERITED APLASTIC ANEMIA

Fanconi Anemia

The inherited forms of aplastic anemia may be associated with other somatic congenital defects, as in the Fanconi syndrome, an autosomal recessive inherited disease that is genetically and phenotypically heterogeneous. It is defined by cellular hypersensitivity to DNA cross-linking agents (e.g. diepoxybutane and mitomycin C). There are random chromosomal breaks with endo-reduplication, and chromatid exchange can be demonstrated in peripheral lymphocytes. Patients may be mildly or severely affected with many congenital anomalies. The disease often progresses to myelodysplasia and acute myeloid leukemia (AML). The somatic abnormalities in order of frequency are: skeletal, skin pigmentation, small stature, eyes (microphthalmia), renal and urinary tract, male genital, mental retardation (Figs. 12.7–12.11).

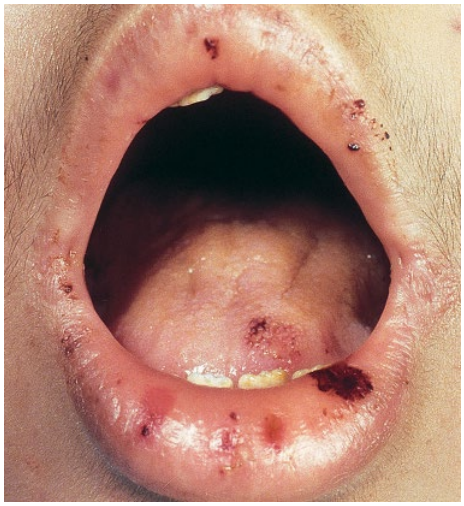

Fig. 12.2. Aplastic anemia: Spontaneous mucosal hemorrhages in a 10-year-old boy with severe congenital (Fanconi) anemia. (Hb, 7.3 g/dL; white blood cell count [WBC], 1.1×10^9/L [neutrophils, 21%; lymphocytes, 77%]; platelets $<5.0 \times 10^9$/L.)

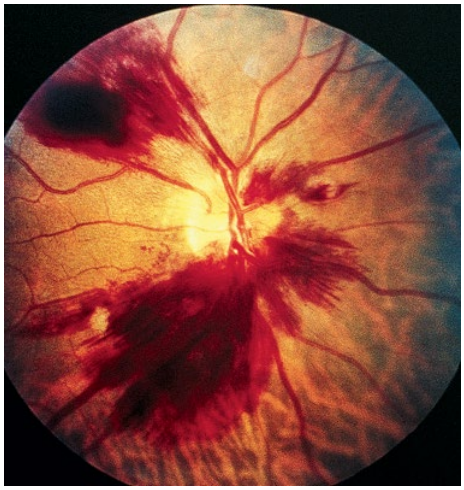

Fig. 12.3. Aplastic anemia: Retinal hemorrhages in a patient with acquired disease and profound thrombocytopenia.

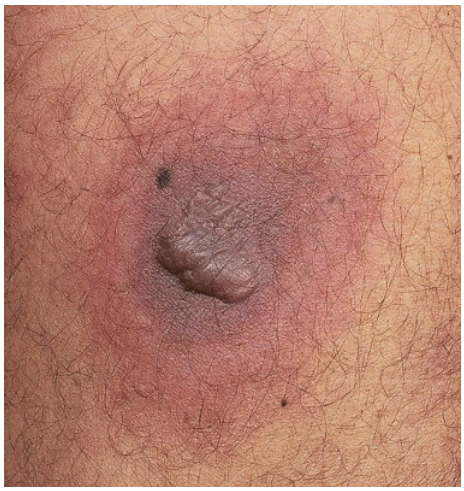

Fig. 12.4. Aplastic anemia: Purple discoloration and blistering of the skin caused by infection with *Pseudomonas aeruginosa*.

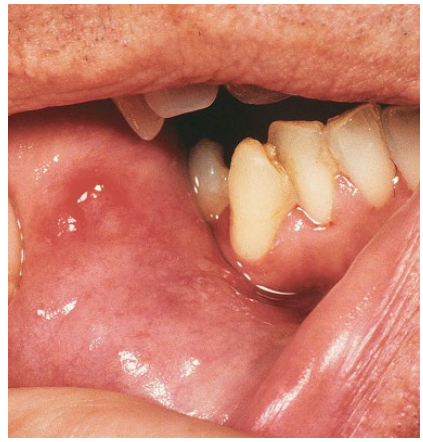

Fig. 12.5. Aplastic anemia: Ulceration of the buccal mucosa associated with severe neutropenia. Herpes simplex virus was grown from the ulcers. (Total leukocyte count, 0.8×10^9/L; neutrophils, 20%.)

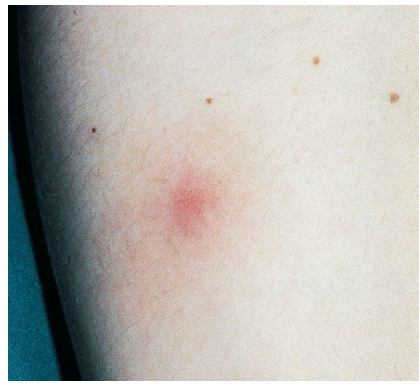

Fig. 12.6. Aplastic anemia: Raised erythematous skin nodule from infection with *Candida albicans*, which was also present in the bloodstream. The patient, a 27-year-old woman, had previously been treated with antibacterial agents for prolonged periods of fever caused by bacterial infections.

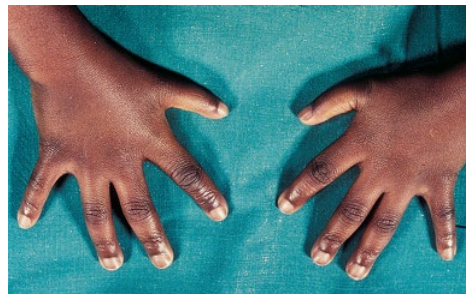

Fig. 12.7. Fanconi anemia. The hands of a child show symmetric abnormalities of the thumbs, resulting in their resemblance to fingers. (Courtesy of Dr. B Wonke.)

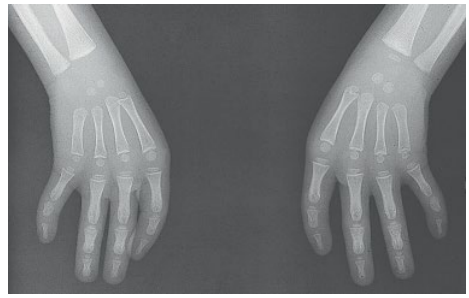

Fig. 12.8. Fanconi anemia: Radiograph showing absent thumbs.

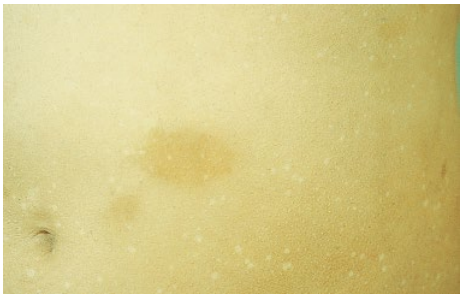

Fig. 12.9. Fanconi anemia: Café-au-lait spot, pigmentation, and punctate areas of depigmentation over the abdominal wall. (Courtesy of Professor EC Gordon-Smith.)

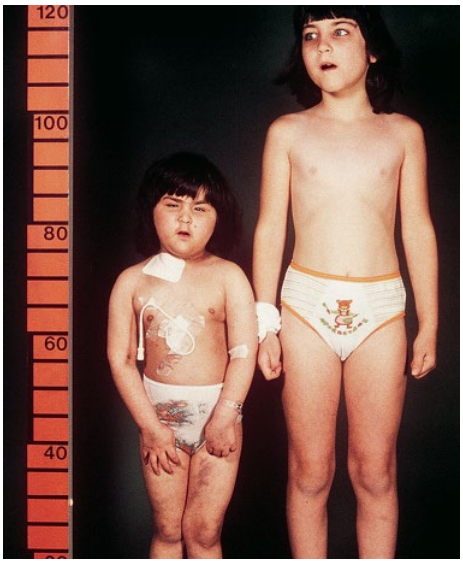

Fig. 12.10. Fanconi anemia. The 6-year-old patient shows short stature and a minor degree of microcephaly compared with her normal older sister, who was human leukocyte antigen (HLA) identical and the donor for bone marrow transplantation.

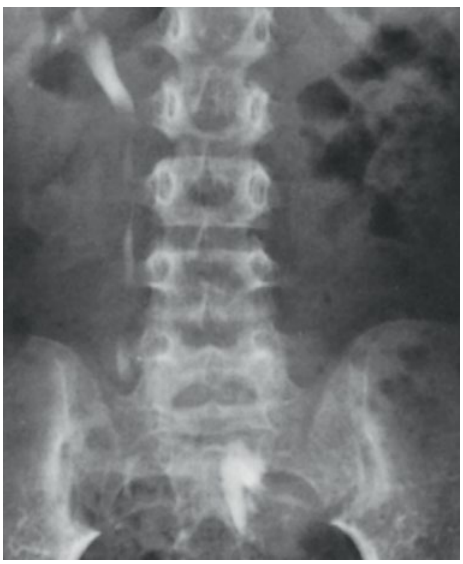

Fig. 12.11. Fanconi anemia. Intravenous pyelogram shows a normal right kidney but a left kidney that is abnormally placed in the pelvis. Source: Hoffbrand AV, et al., eds. *Postgraduate Haematology*, 7th edn. John Wiley & Sons, 2016. Reproduced with permission of John Wiley & Sons.

TABLE 12.3. COMPLEMENTATION GROUP AND CHROMOSOME LOCATION OF 16 PROTEINS, MUTATION OF WHICH MAY RESULT IN FANCONI ANEMIA

Complementation group/gene	Approximate percentage of FA patients	Chromosome location	Protein (amino acids)	Exons
A (*FANCA*)	65	16q24.3	1455	43
B (*FANCB*)	<1	Xp22.2	859	10
C (*FANCC*)	12	9q22.3	558	14
D1 (*FANCD1*)	<1	13q12.3	3418	27
D2 (*FANCD2*)	<1	3p25.3	1451	44
E (*FANCE*)	4	6p21.3	536	10
F (*FANCF*)	4	11p15	374	1
G (*FANCG*)	12	9p13	622	14
I (*FANCI*)	<1	15q26.1	1328	35
J (*FANCJ/BRIP1*)	<5	17q23.2	1249	20
L (*FANCL*)	<1	2p16.1	375	14
M (*FANCM*)	<1	14q21.3	2048	23
N (*FANCN/PALB2*)	<1	16p12.1	1186	13
O (*FANCO/RAD51C*)	<1	17q25.1	376	9
P (*FANCP/SLX4*)	2	16p13.3	1834	15
Q (*FANCQ/ERCC4*)	<1	16p13.12	916	11

Source: Hoffbrand AV, et al., eds. *Postgraduate Haematology*, 7th edn. John Wiley & Sons, 2016. Reproduced with permission of John Wiley & Sons.

The Fanconi anemia (FA) proteins exist in various complexes in the cytoplasm and nucleus. They fall into 16 subtypes/complementation groups currently characterized (Table 12.3), and at least 21 proteins have been implicated in the disease. All mutations are recessive except those of *FANCB*, which is X-linked, and *FANCR/RAD51*, which are dominant. The complex in the nucleus acts to facilitate the mono-ubiquitination of *FANC1-FANCD2*, which then interacts with the DNA repair proteins including BRCA2 (*FANCD1*), BRAC1, and RAD51 to repair DNA damage following DNA damage caused by exposure to cross-linking agents (e.g. ionizing radiation or sunlight, smoking, infections, or alcohol) (Fig. 12.12). The ataxia telangiectasia mutated (ATM) protein, together with RAD3-related protein (the complex abbreviated to ATR) is essential by phosphorylation of *FANCD2 (D2)* at serine 222 in response to double-stranded DNA breaks. This phosphorylation activates ubiqutinization by the FA core complex. *FANCD1* is the breast cancer susceptibility gene *BRAC2*; *FANCN* is *PALB2* (partner of *BRAC2*) and *FANCJ* is *BRIP1* (partner of *BRAC1*). Cells lacking functioning *BRAC1* or *BRAC2* inaccurately repair damaged DNA.

In addition to ATM, the FA proteins interact with other proteins, mutations of which are responsible for the rare genetic chromosome instability syndromes, including the ataxia telangiectasia (AT)-like disorder, Bloom syndrome, Nijmegen breakage syndrome, and Seckel syndrome. The Seckel syndrome results from mutation of the *RAD3*-related gene affecting ATR function (Fig. 12.12). It manifests with growth failure, microcephaly, abnormal facies, and occasional pancytopenia. The cartilage–hair hypoplasia syndrome with macrocytic anemia with or without neutropenia is also recessive (gene *RMRP* is at 9p-21-p12). It is involved in mitochondrial and nuclear function.

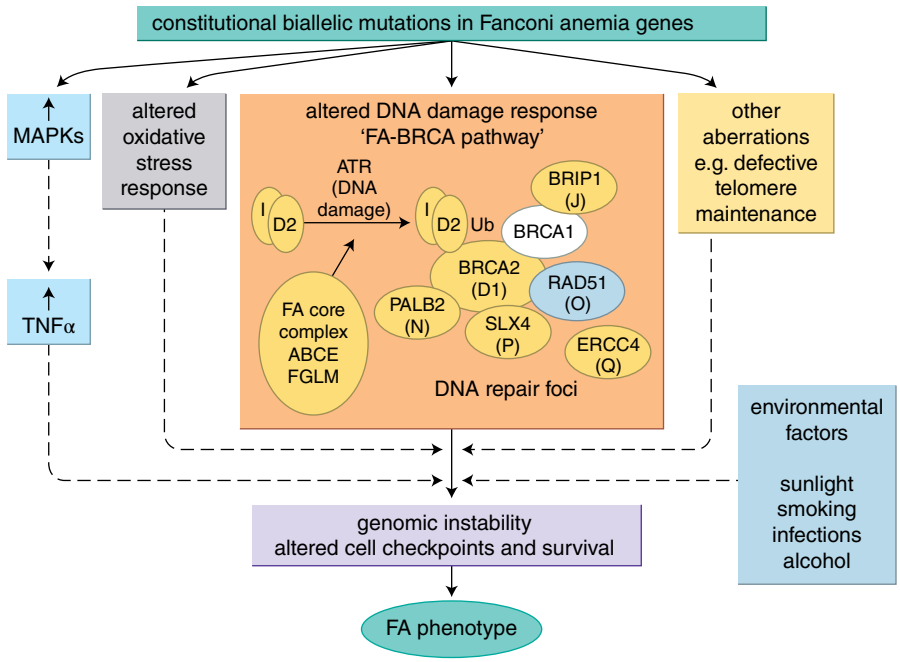

Fig. 12.12. The FA-BRCA pathway. The FA core complex together with ATR (ataxia telangiectasia and RAD3-related protein) mono-ubiquitinates the *FANC1-FANCD2* complex, which then activates *BRAC2* and the other DNA repair complex of proteins. I, *FANC1-FANCD1* is the breast cancer susceptibility gene *BRAC2*; N, *FANCN* is *PALB2* (partner of *BRAC2*); J, *FANCJ* is *BRIP1* (partner of *BRAC1*); O, *FANCO* is *RAD51C*; P, FANCP is *SLX4*; Q, FANCQ is *ERCC4*. Source: Hoffbrand AV, et al., eds. *Postgraduate Haematology*, 7th edn. John Wiley & Sons, 2016. Reproduced with permission of John Wiley & Sons.

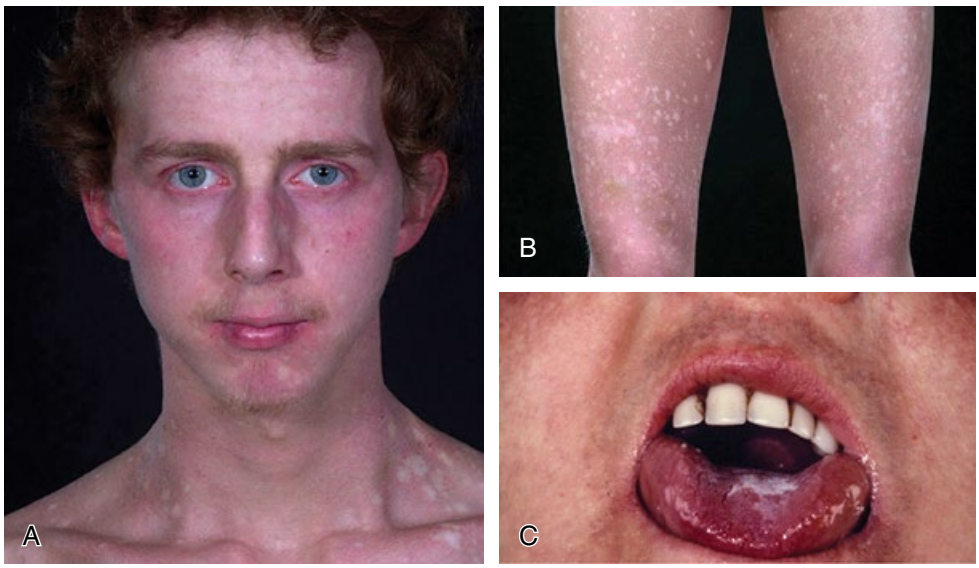

Fig. 12.13. Dyskeratosis congenita: face **(A),** skin pigmentation **(B),** mouth **(C).**

Defects of the FA genes have also been found in a variety of human cancers in people without FA.

At least 20% of patients with FA develop malignant disease, most frequently AML or myelodysplasia but also head and neck or gynecologic squamous cell tumors and, less frequently, esophageal, liver, brain, skin, and renal tumors.

Dyskeratosis Congenita

A less common association of the congenital form of aplastic anemia is dyskeratosis congenita, in which there is abnormal skin pigmentation, nail dystrophy (Figs. 12.13 and 12.14), and mucosal leukoplakia (Figs. 12.13 and 12.15). There may also be epiphora, mental retardation, growth failure, pulmonary fibrosis, hypogonadism, dental caries and/or loss, esophageal stricture, alopecia or premature hair graying, hyperhidrosis, malignancy, skeletal and other somatic abnormalities. In contrast to FA, the chromosomal pattern is normal.

The mutations in 11 different genes, the most frequent being *DKC1, TERC*, *TERT*, and *TIN2*, are now known to underlie most cases of dyskeratosis congenita. *DKC1* codes for dyskerin; *TERC* for the telomerase RNA component; *TERT* for telomerase reverse transcriptase; and *TIN2* for a component of the "shelterin" complex (Fig. 12.16). Telomerase adds telomeric repeats (TTAGGG) to the 3′ lagging strand during semi-conservative

DNA replication. It is essential in rapidly dividing cells, as in the bone marrow, to maintain telomere length, otherwise telomeres shorten with each round of cell replication until the cell dies prematurely by apoptosis. Telomerase is mainly present in germ cells, stem cells, and their immediate progeny, activated T cells and monocytes. Dyskerin is involved in the ribonucleoprotein complexes involved in RNA modification (Fig. 12.16). The other genes that may be mutated in dyskeratosis congenita include *NOP10*, *NHP2*, *WRAP53*, *CTC1*, *RTEL1*, *ACD*, *TINF2*, and *PARN*. They all encode proteins involved in telomere elongation or maintenance (Fig. 12.16).

All patients with dyskeratosis congenita have very short telomeres, below the first percentile for a healthy control group of the same age range measured in total lymphocytes or T or B cells.

Dyskeratosis congenita usually may be inherited as an X-linked recessive (mutated *DKC1*, dyskerin), autosomal dominant (mutated *TERC* or *TERT*) or much more rarely, as autosomal recessive (mutated *NOP10*, *TERT*, *NHP2*, *TCAB1*, *USB1*, *CTC1*, *RTEL1*). In about 30% of patients the genetic basis is uncharacterized. The disease is heterogeneous in its clinical manifestations and is often milder and of later onset with *TERC* or *TERT* mutations than with *DKC1* mutations. Female carriers of *DKC1* mutations are normal or only mildly affected. Some carriers of mutations of these genes do not express the disease

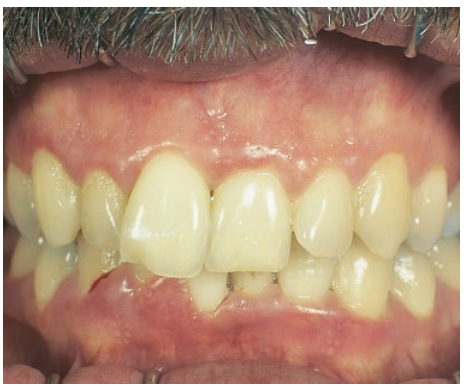

Fig. 12.14. Dyskeratosis congenita. This 24-year-old man with long-standing aplastic anemia has irregularities of tooth size and shape and of the gum margins.

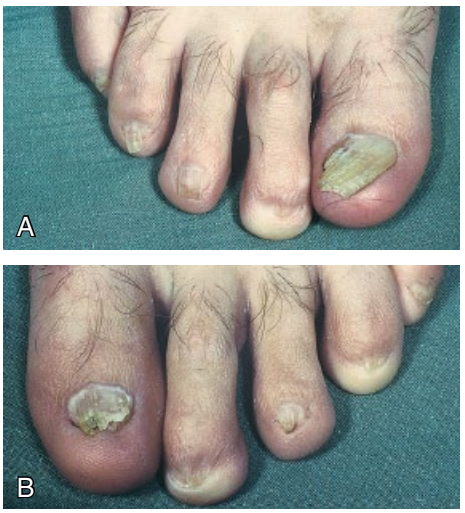

Fig. 12.15. Dyskeratosis congenita. **A** and **B,** The feet of the patient shown in Fig. 12.14 show grossly abnormal nails and excessive hair in an abnormal distribution.

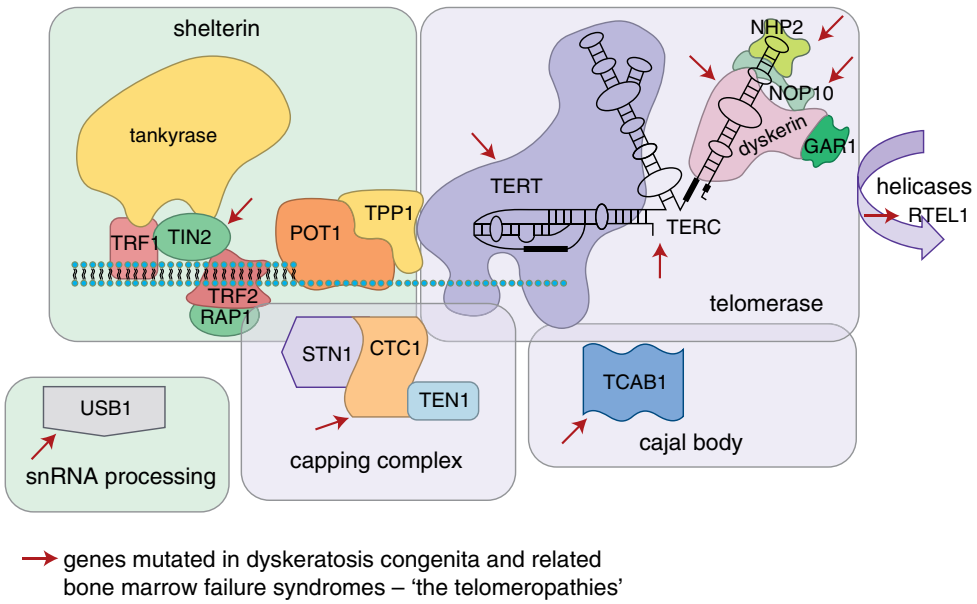

Fig. 12.16. Schematic representation of complexes involved in telomere maintenance. The telomerase complex includes TERC, TERT, dyskerin, NOP10, NHP2, and GAR1. The shelterin complex includes the six proteins TRF1, TRF2, TPP1, POT1, RAP1, and TIN2. The telomere capping (CST) complex is composed of CTC1, STN1, and TEN1. Protein/RNA names indicated by red arrows are mutated in dyskeratosis congenita and related disorders. Hemizygous *DKC1* (dyskerin) mutations are observed in X-linked dyskeratosis congenita and Hoyeraal–Hreidarsson syndrome (HHS). Heterozygous *TERC* mutations are associated with dyskeratosis congenita, aplastic anemia, myelodysplastic syndrome (MDS), acute myeloid leukemia (AML), and pulmonary fibrosis. Heterozygous *TERT* mutations are responsible for some cases of aplastic anemia, dyskeratosis congenita, MDS, AML, and pulmonary/liver fibrosis. Biallelic mutations in *TERT* can cause classic dyskeratosis congenita and HHS. Heterozygous *TIN2* mutations have been observed in dyskeratosis congenita, aplastic anemia, HHS, and Revesz syndrome. Biallelic *NOP10*, *NHP2*, *TCAB1*, *USB1*, and *CTC1* mutations have been seen in autosomal recessive dyskeratosis congenita. Biallelic *RTEL1* mutations are observed in autosomal recessive HHS. Source: Hoffbrand AV, et al., eds. *Postgraduate Haematology*, 7th edn. John Wiley & Sons, 2016. Reproduced with permission of John Wiley & Sons.

and the inheritance pattern may then falsely seem autosomal recessive or sporadic. The disease with *TERC* or *TERT* mutations often shows genetic anticipation, the disease manifesting at an earlier age in a more severe form in successive generations.

Homozygous mutations of other genes – *USB1*, *LIG4*, and *GRHL2* – lead to clinical syndromes including aplastic anemia resembling dyskeratosis congenita but without telomere shortening. These genes may also be mutated in poikilodermia with neutropenia (see Chapter 10) and other clinical syndromes that overlap with dyskeratosis congenita.

Hoyeraal–Hreidarsson syndrome (HHS) is a rare severe variant of dyskeratosis congenita, manifesting in early childhood and characterized by fetal growth retardation, mental retardation, combined immunodeficiency, and aplastic anemia. Mutations in the *DKC1* gene have been identified in some cases. Biallelic mutations of *RTEL1* have also been described. RTEL1 is a DNA helicase required for telomere replication and stability.

GATA2 Disorders

Heterozygous mutations of *GATA2*, encoding a zinc finger transcription factor, result in an autosomal dominant disorder associated with bone marrow failure, myelodysplastic syndrome (MDS), and AML. Warts, atypical mycobacterial infections, lymphedema, deafness and pulmonary alveolar proteinosis have been described. The marrow is hypocellular with usually considerable dysplasia.

Shwachman–Diamond Syndrome

This autosomal recessive disease results in >90% of cases from a mutation in the *SBDS* gene on 7q11.22 involved in RNA processing (Fig. 12.17). Mutation of gene *DNAJC21*, which codes for a protein involved in 60S ribosomal subunit maturation, accounts for some of the other cases, usually familial. The syndrome is characterized by exocrine pancreatic insufficiency with fat malabsorption, osteopenia, metaphyseal dysplasia, and bone marrow failure. Neutropenia occurs in 60% of cases. Some cases also show thrombocytopenia, and about 20% of patients have pancytopenia with a hypocellular marrow. It may be accompanied by skeletal abnormalities, short stature, metaphyseal dysostosis (Fig. 12.18), mental retardation, and skin changes such as icthyosis or pigmentation abnormalities. It progresses to myelodysplasia (Fig. 12.18) or AML in a significant proportion of patients.

Reticular Dysgenesis

This rare X-linked recessive disease is characterized by severe combined immune deficiency, deafness, lymphopenia, thrombocytopenia, granulocytopenia, and often anemia (Fig. 11.48). One gene involved is adenylate kinase 2 (*AK2*) involved in mitochondrial energy metabolism and in apoptosis.

BONE MARROW APPEARANCES

Bone marrow fragments in aplastic anemia, whatever the cause, show reduced cellularity (Fig. 12.19), with fat spaces occupying >75% of the marrow. The trails are also reduced in cellularity, with particularly low numbers of megakaryocytes and often a predominance of lymphocytes and plasma cells. The hypoplasia is best shown by trephine biopsy (Fig. 12.20). There may be areas of normal cellularity despite the overall hypocellularity (Fig. 12.21), and lymphoid follicles may be prominent (Fig. 12.22). Marrow hypoplasia can also be detected by magnetic resonance imaging (MRI) scanning (Fig. 12.23).

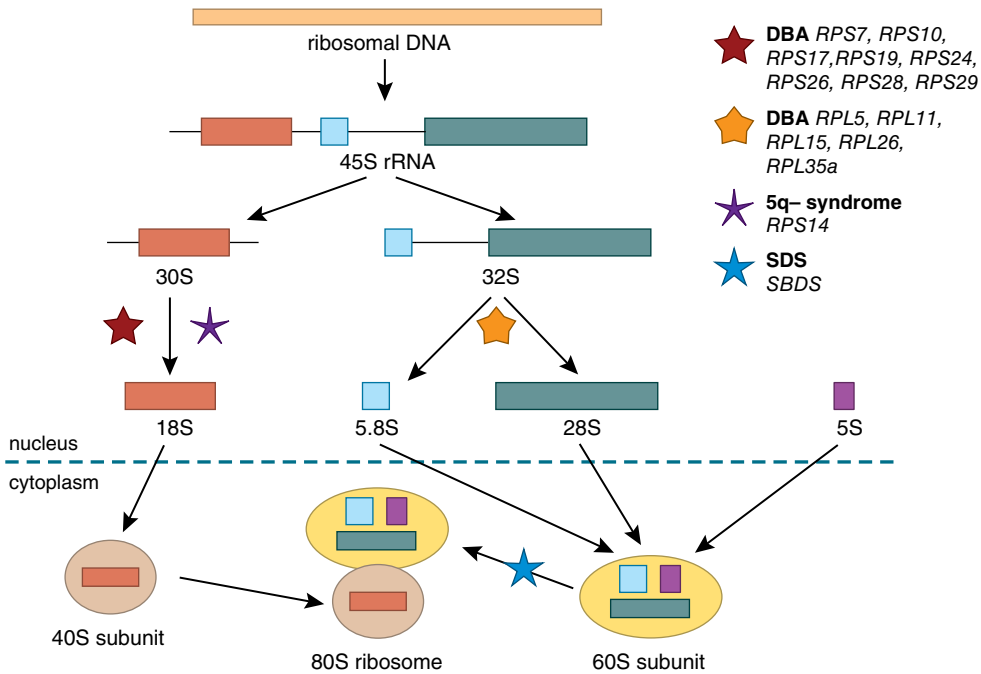

Fig. 12.17. Schematic diagram showing scheme of ribosomal (r)RNA processing in human cells and the points at which this is possibly disrupted in the different bone marrow failure syndromes. The rRNAs are transcribed by RNA polymerase I as a single precursor transcript (45S rRNA). The 45S rRNA is then processed to 18S, 5.8S, and 28S rRNAs. The 18S is a component of the 40S ribosomal subunit. The 5.8S and 28S together with 5S (synthesized independently) are components of the 60S ribosomal subunit. The 40S and 60S subunits are assembled to form the 80S ribosome. The processing steps affected in Diamond–Blackfan anemia (heterozygous mutations in *RPS7*, *RPS10*, *RPS17*, *RPS24*, *RPS26*, *RPS28*, *RPS29*, *RPL5*, *RPL11*, *RPL26*, and *RPL35a*), 5q– syndrome (haplo-insufficiency of *RPS14*), and Shwachman–Diamond syndrome (biallelic mutations in *SBDS*) are indicated by the different colored stars. Source: Hoffbrand AV, et al., eds. *Postgraduate Haematology*, 7th edn. John Wiley & Sons, 2016. Reproduced with permission of John Wiley & Sons.

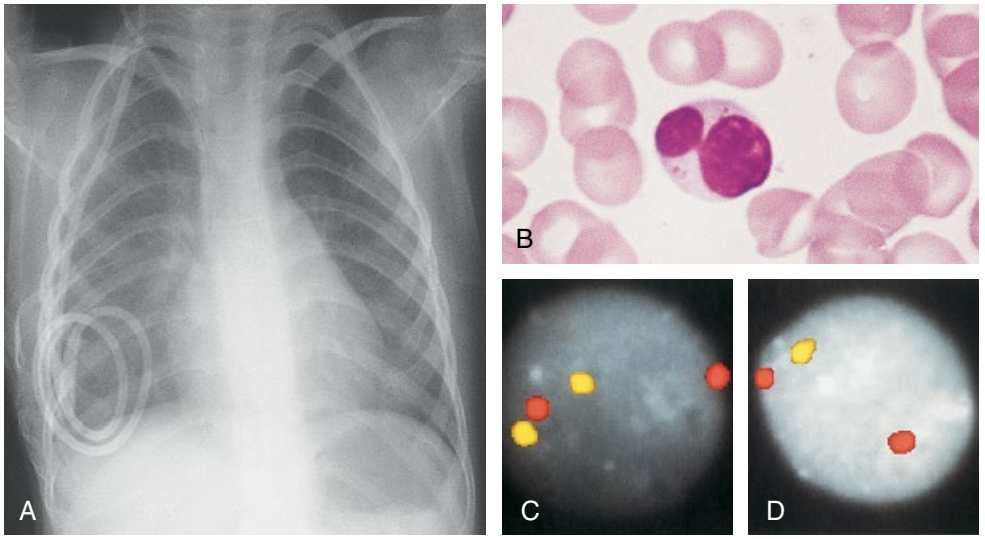

Fig. 12.18. A, Chest radiograph showing characteristic "cupping" deformity in the ribs. **B,** Peripheral blood showing Pelger neutrophil. **C, D,** Fluorescence in situ hybridization technique showing control **(C)** and patient with monosomy 7 **(D)** (red, internal control; yellow, chromosome 7 centromeric probe). (Courtesy of Professor OP Smith.)

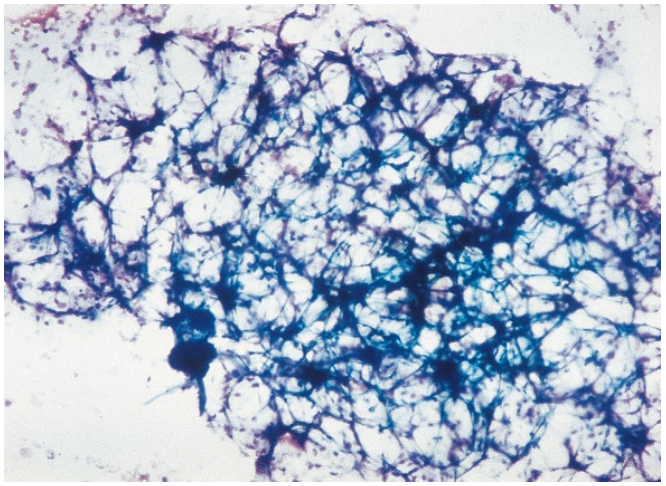

Fig. 12.19. Aplastic anemia: Low-power view of bone marrow fragment showing severe reduction of hematopoietic cells and an increase in fat spaces.

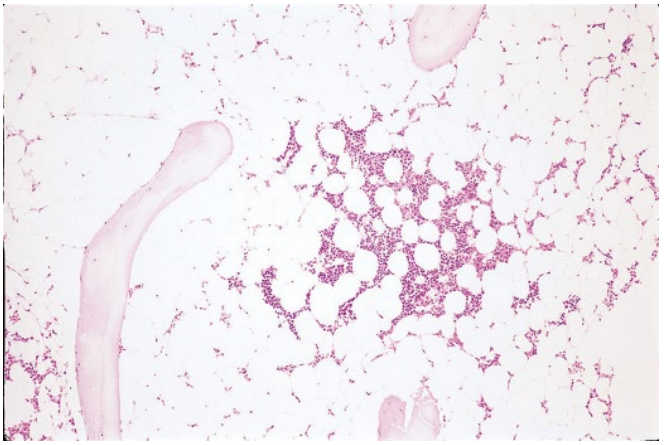

Fig. 12.21. Aplastic anemia: Trephine biopsy showing some hematopoietic cellular foci in an otherwise grossly hypocellular marrow.

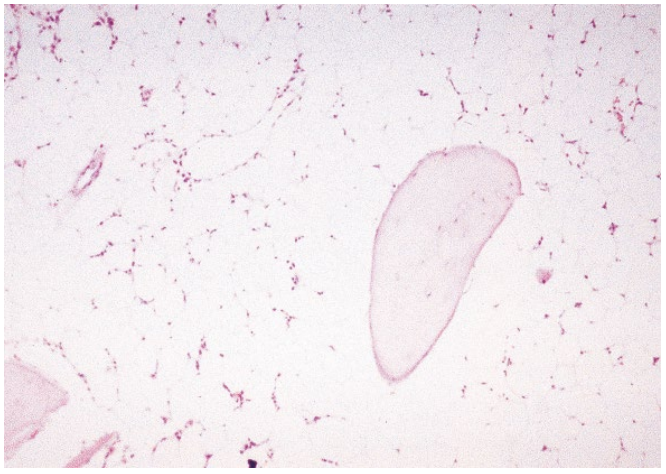

Fig. 12.20. Aplastic anemia: Trephine biopsy of posterior iliac crest showing gross hypocellularity with replacement by fat.

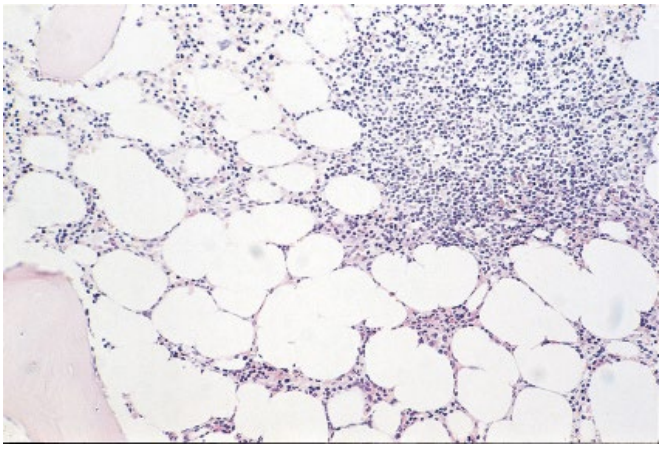

Fig. 12.22. Aplastic anemia: Higher power view of the biopsy shown in Fig. 12.20, showing grossly hypocellular marrow with a remaining lymphoid follicle in the upper right field.

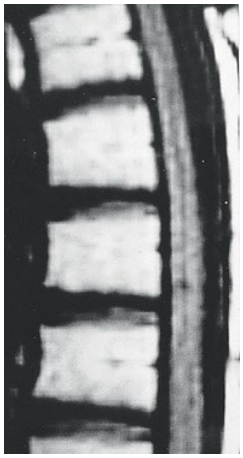

Fig. 12.23. Aplastic anemia: Magnetic resonance imaging. Dorsal vertebrae in T_1 sequence. A marked increase in signal intensity can be observed in comparison with that of the spinal cord.

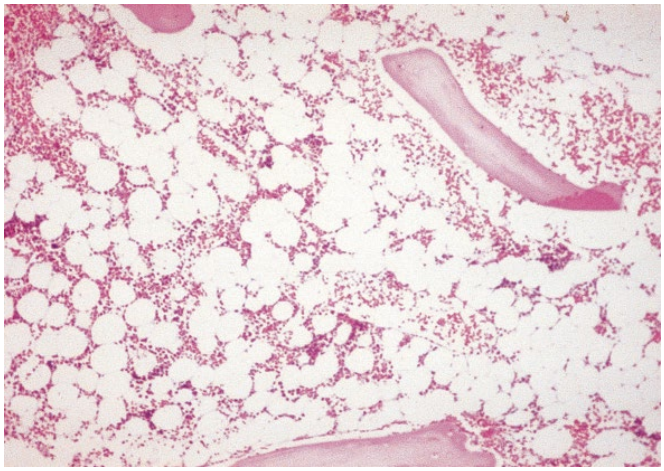

Fig. 12.24. Aplastic anemia: Trephine biopsy (same case as shown in Fig. 12.20), showing partial recovery of cellularity four weeks after treatment with antilymphocyte globulin. Peripheral blood cell counts also rose moderately.

As therapy differs according to the degree of aplasia, a standard classification of severity has been adopted. Criteria for severe disease are marrow cellularity <25% or <30% residual hematopoietic cells and any two of:

- $<20 \times 10^9$/L reticulocytes
- $<20 \times 10^9$/ L platelets
- $<0.5 \times 10^9$/L neutrophils in peripheral blood.

The anemia is classified very severe if the severe criteria are fulfilled but the neutrophil count is $<0.2 \times 10^9$/L.

During the recovery phase, cellularity increases to normal (Fig. 12.24). The platelet count is usually the last of the blood cell counts to recover completely. Overt paroxysmal nocturnal hemoglobinuria (PNH) or a subclinical PNH defect may develop transiently or chronically, and some patients diagnosed with PNH have aplasia of the marrow.

Androgens are used rarely in treatment. They may be associated with liver and splenic damage (Fig. 12.25).

RED CELL APLASIA

The causes of pure red cell aplasia are listed in Table 12.4. Like aplastic anemia, it may be congenital (familial) or acquired.

DIAMOND–BLACKFAN ANEMIA

Diamond–Blackfan anemia (DBA) presents with anemia in infancy and shows marrow erythroid hypoplasia, often with somatic abnormalities affecting the skeleton (Fig. 12.26), urogenital tract, or heart but without chromosomal abnormalities.

The patient may be transfusion-dependent and then needs iron chelation therapy (Fig. 12.27). Alterations of ribosomal subunit proteins underlie the disease (see Fig. 12.17). One gene, *RPS19*, mutation of which is responsible for 25% of cases, is located on chromosome 19q13 and codes for the ribosomal protein S19. Heterozygous mutations of other genes coding for ribosomal proteins include *RPS7*, *RPS10*, *RPS15*, *RPS17*, *RPS19*, *RPS24*, *RPS26*, *RPS27*, *RPS28*, *RPS29*, which are genes for small ribosomal proteins, and *RPL5*, *RPL11*, *RPL15*, *RPL23*, *RPL26*, *RPL27*, *RPL28*, *RPL29*, and *RPL35a*, which are for large ribosomal proteins. A heterozygous mutation may also be present in clinically unaffected family members. There is a

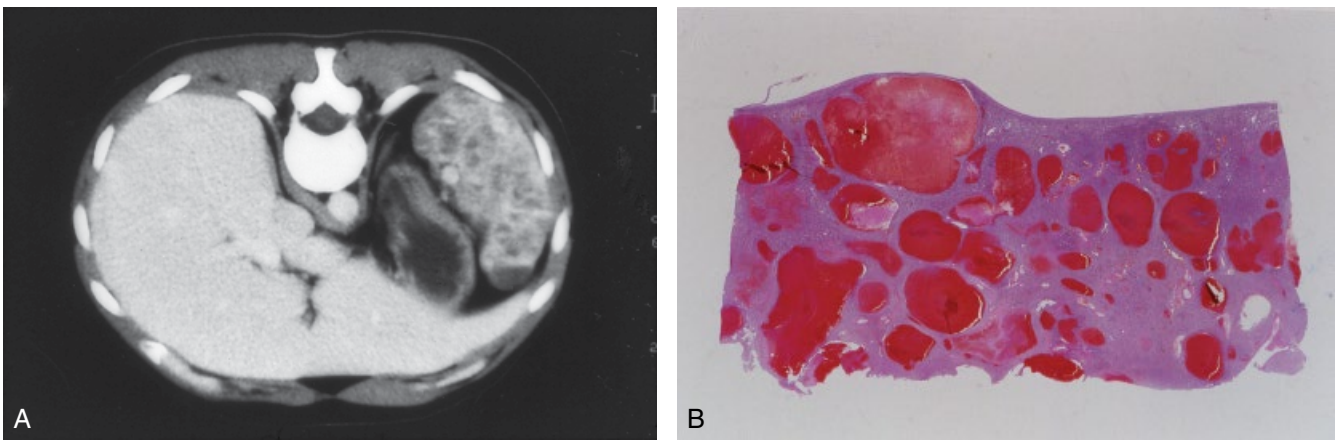

Fig. 12.25. Splenic peliosis in acquired aplastic anemia treated with oxymetholone and prednisolone. These are large blood-filled cavities that may or may not be lined by sinusoidal cells. They are randomly distributed and range from 1 mm to several centimeters in diameter. **A,** Computed tomography scan showing multiple filling defects in spleen. **B,** Low-power view of section of spleen showing multiple vascular lobes. (Courtesy of Dr. S Imashuku.)

TABLE 12.4. CAUSES OF RED CELL APLASIA

Congenital
Diamond–Blackfan syndrome
Acquired
Primary
Autoimmune
Immunoglobulin inhibitors of erythroid precursors or of erythropoietin
T-cell inhibition of erythroid precursors
Transient erythroblastopenia of childhood
Secondary
Thymoma
Other tumors
Cancer of stomach, breast, lung, thyroid, biliary tract, kidney
Lymphoma
Hodgkin
Non-Hodgkin
Chronic lymphocytic leukemia
Large granular lymphocytic leukemia
Acute lymphoblastic leukemia
Viral infections
T-cell leukemia/lymphoma virus
Cytomegalovirus
Parvovirus (transient)
Human immunodeficiency virus
Viral hepatitis
Infectious mononucleosis
Bacterial infections
Bacterial sepsis
Streptococcal
Tuberculosis
Immune disorders
Systemic lupus erythematosus
Rheumatoid arthritis
Drugs and chemicals (e.g. benzene, diphenylhydantoin, isoniazid, allopurinol, azathioprine, carbamezapine, dapsone, fludarabine, lamivudine, trimethoprim/sulfamethoxazole and many others)
Nutritional deficiencies
Riboflavin
Vitamin B_{12} or folate deficiency
Pregnancy
Erythropoietin antibody induced by rh-EPO
ABO-incompatible stem cell transplantation

functional defect in ribosomal assembly, faulty cleavage of ribosomal RNA, with arrested maturation of the 18S RNA species, resulting in a decreased number of mature ribosomes (see Fig. 12.17). Rarely, an X-linked *GATA-1* mutation may underlie the disease.

The acquired form of red cell aplasia may be idiopathic or may appear in conjunction with another disease, such as a thymoma (Figs. 12.28 and 12.29) or other lymphoproliferative disease (see Table 12.4). A transient form of red cell aplasia occurs in the course of chronic and other hemolytic anemias but is best recognized in sickle cell anemia. This form is the result of parvovirus B19 infection, with selective damage by the virus to bone

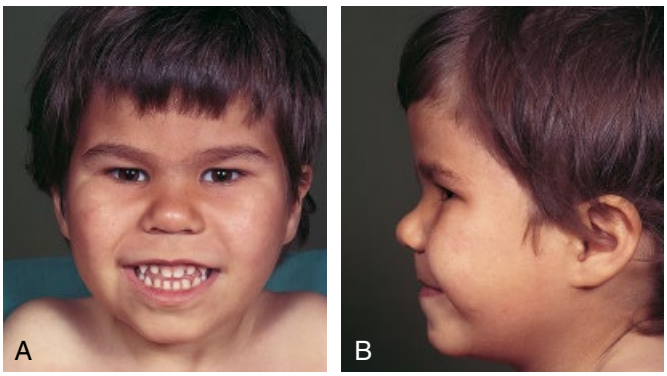

Fig. 12.26. Diamond–Blackfan syndrome. **A**, **B,** Three-year-old boy with congenital red cell aplasia shows the typical facies, with a sunken bridge of the nose. He was treated with blood transfusions and subsequently corticosteroids to which he made a partial response and became transfusion-independent. His mental development is normal, but his growth has been partly retarded because of the corticosteroid therapy. (Hb, 6.1 g/dL; WBC, 7.2×10^9/L [neutrophils, 55%; lymphocytes, 41%]; monocytes, 4%; platelets, 289×10^9/L.)

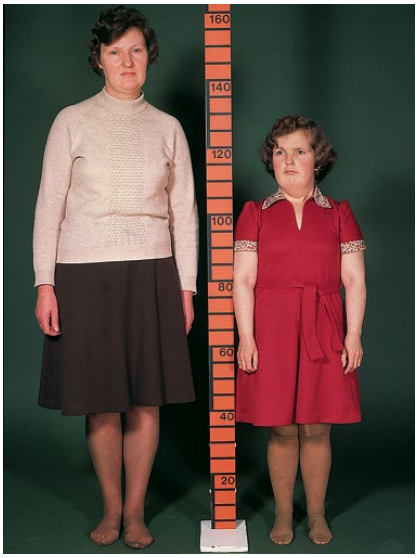

Fig. 12.27. Diamond–Blackfan syndrome. The 24-year-old woman on the right had received corticosteroid therapy as an infant and child to reduce the need for blood transfusions. This led to stunted growth (compare her normal mother). The patient had received over 100 units of blood and developed transfusional hemosiderosis with enlargement of the liver and spleen.

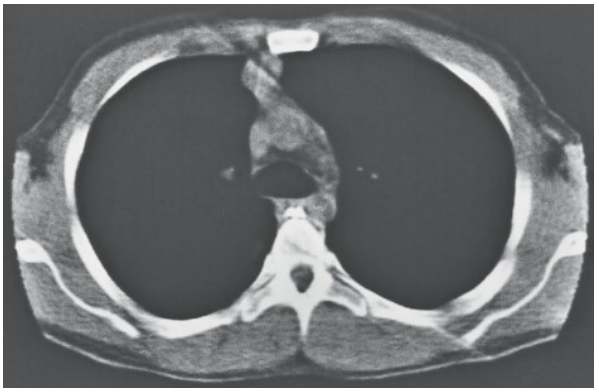

Fig. 12.28. Acquired red cell aplasia: Upper mediastinal computed tomography scan showing a thymoma as a retrosternal mass of irregular outline. The patient, a 62-year-old man, had developed myasthenia gravis and pure red cell aplasia, which required regular blood transfusions. (Courtesy of Dr. R Dick.)

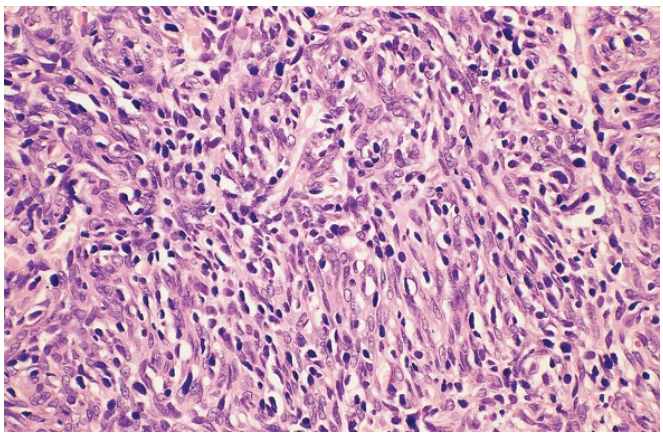

Fig. 12.29. Red cell aplasia: Section of thymoma showing spindle cells and epithelial cells. The thymoma was removed surgically from a patient with severe red cell aplasia (Hb, 6.1 g/dL) and neutropenia (WBC, 3.2×10^9/L; neutrophils, 0.4×10^9/L; platelets, 168×10^9/L). (H&E.) (Courtesy of Dr. JE McLaughlin.)

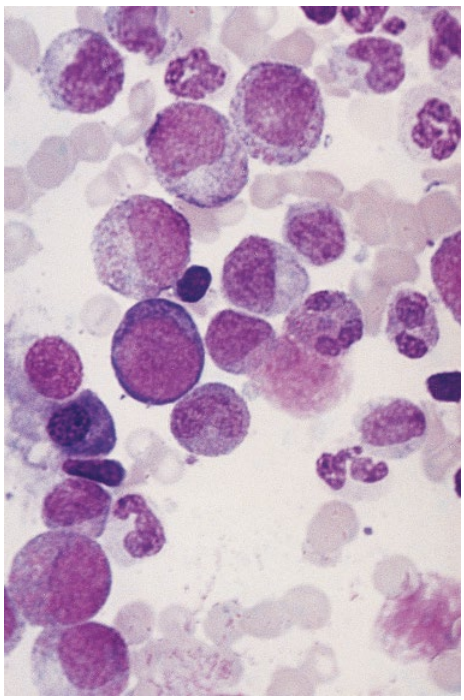

Fig. 12.30. Acquired red cell aplasia: Bone marrow aspirate cell trail shows normal numbers of granulocytes and their precursors, but an absence of erythroblasts.

marrow red cell progenitors. It is likely that a similar red cell aplasia occurs in normal subjects with this infection but is not clinically apparent because of the longer red cell life span. In all forms the bone marrow is of normal cellularity, but there is a relative absence of erythroid precursors (Fig. 12.30). In parvovirus B19 infection, giant proerythroblasts may be a feature (Fig. 12.31).

Pure red cell aplasia occasionally responds to thymectomy or other immunosuppressive therapy, corticosteroids, rituximab, or ciclosporin. If severe, it usually needs regular blood transfusions and iron chelation therapy.

CONGENITAL DYSERYTHROPOIETIC ANEMIAS

The congenital dyserythropoietic anemias (CDAs) are rare autosomal recessive diseases characterized clinically by anemia, often with jaundice as a result of ineffective erythropoiesis and shortened red cell survival, and morphologically by abnormal red cell precursors in the bone marrow. The anemia is usually macrocytic, and the reticulocyte count may be raised, but is low relative to the degree of anemia.

The diseases are divided into three main groups according to the appearance of the bone marrow. In CDA I (Figs. 12.32

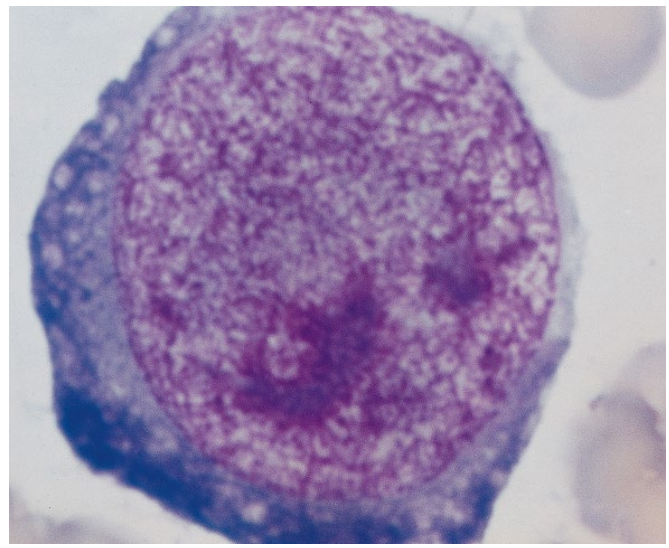

Fig. 12.31. Acquired red cell aplasia: Bone marrow aspirate in parvovirus B19 infection showing a giant proerythroblast with cytoplasmic vacuolation and poorly defined intranuclear viral inclusions. (Courtesy of Professor EC Larkin.)

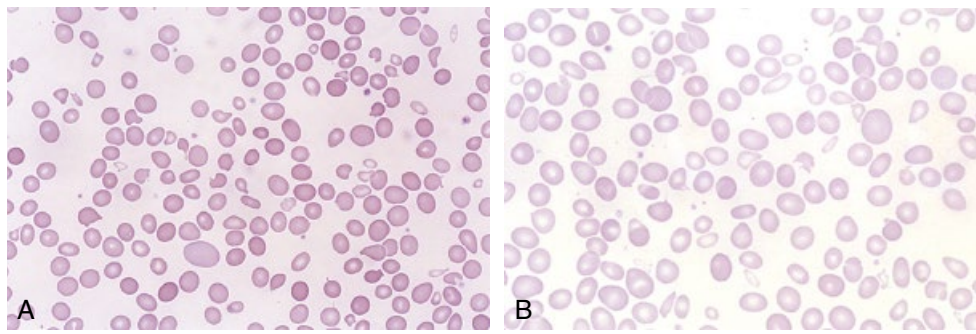

Fig. 12.32. Congenital dyserythropoietic anemia (type I): **A, B,** Peripheral blood films showing oval macrocytes, poikilocytes, and small fragmented cells. The platelets and granulocytes are normal.

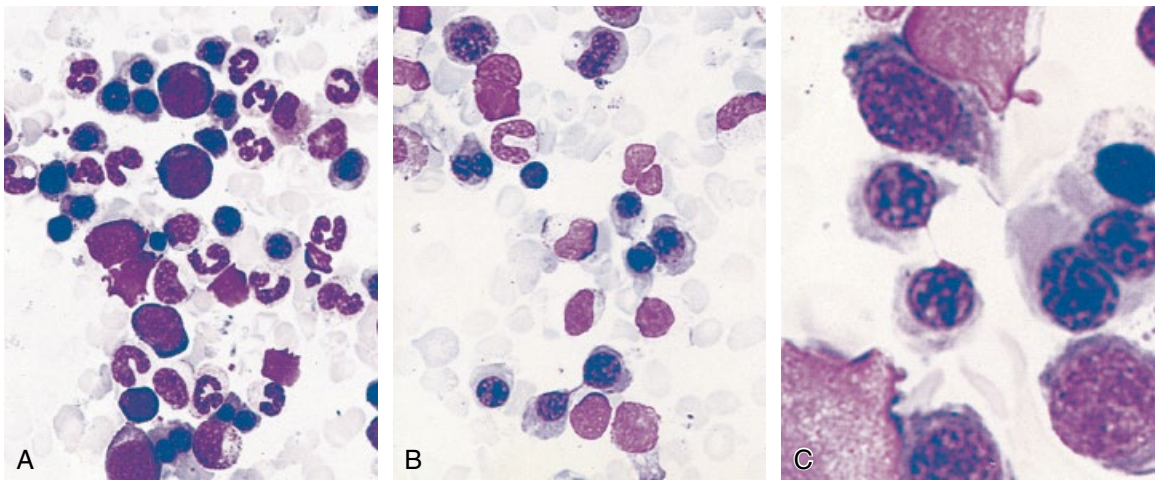

Fig. 12.33. Congenital dyserythropoietic anemia (type I): Bone marrow aspirates. A, Erythroid hyperplasia, megaloblastic erythropoiesis, and binucleate erythroblasts. B, C, Examples of cells with internuclear bridges.

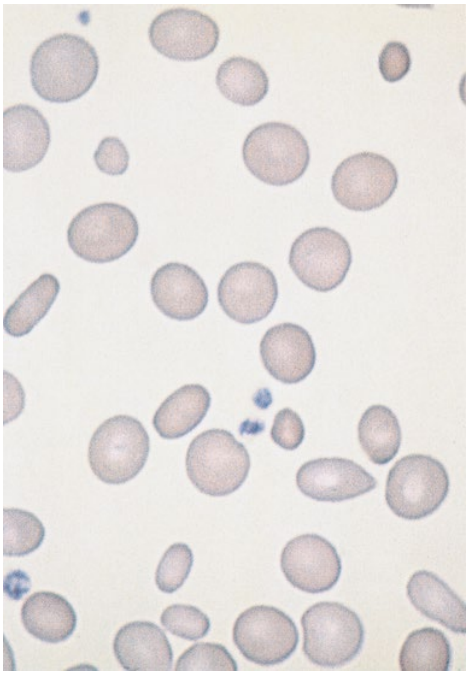

Fig. 12.34. Congenital dyserythropoietic anemia (type II): Peripheral blood film showing marked red cell anisocytosis and poikilocytosis.

and 12.33), megaloblastic changes and internuclear chromatin bridges are prominent. Mutation of gene *CDAN1* (codamin) or of a second gene *C150RF41* are present in some cases. In the most frequent type, CDA II– also known as hereditary erythroblast multinuclearity with positive acidified serum test (HEMPAS)–there are binucleate and multinucleate erythroblasts (Figs. 12.34 and 12.35). The cells lyse in acidified serum from about 30% of normal subjects, but not in the patient's own serum (Fig. 12.36). This is because a naturally occurring immunoglobulin M (IgM) complement-binding antibody is present, but the antigen on HEMPAS red cells recognized by this antibody is not known. The pathogenesis is a defect of the gene *COP11*, the secretory component of *SEC23B*,which results in defective glycosylation of membrane glycoproteins. Defects in α-mannosidase II and *N*-acetylglucosaminyl transferase II have been detected. CDA III (Figs. 12.37 and 12.38) is characterized by multinuclearity and gigantoblasts. It is caused by mutations of *KIF23* which encodes mitotic kinesin-like protein 1 involved in cytokinesis during cell division. The existence of a type IV CDA, similar to a type II CDA but with a negative acid lysis test, has been postulated.

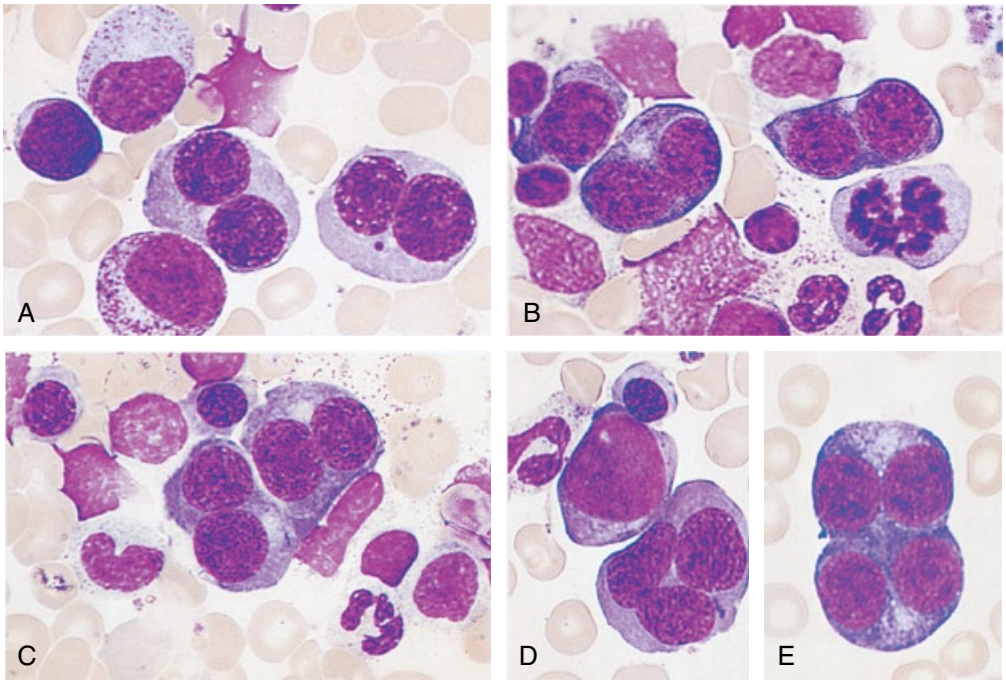

Fig. 12.35. Congenital dyserythropoietic anemia (type II). **A–E,** Selected high-power views of bone marrow aspirate showing multinucleate erythroblasts.

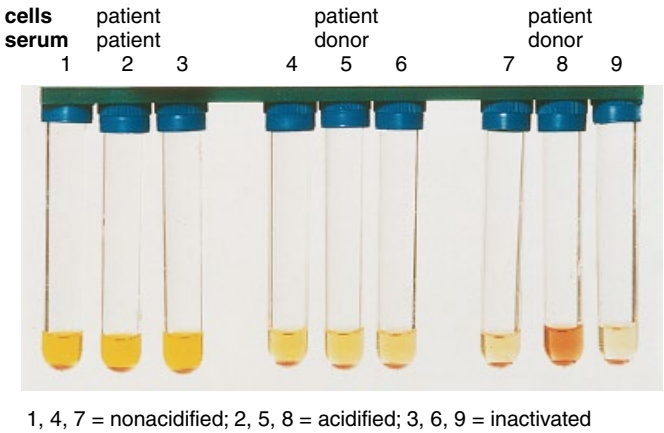

Fig. 12.36. Congenital dyserythropoietic anemia (HEMPAS, type II). In the samples from some normal donors, the affected red cells show complement-dependent lysis in fresh acidified serum at 37°C, but not in the patient's own serum.

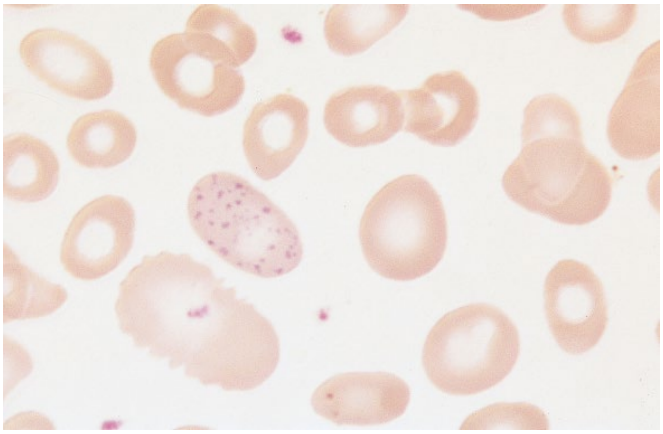

Fig. 12.37. Congenital dyserythropoietic anemia (type III). Peripheral blood film shows gross macrocytosis, anisocytosis, poikilocytosis, and punctate basophilia. (Courtesy of Dr. IM Hann.)

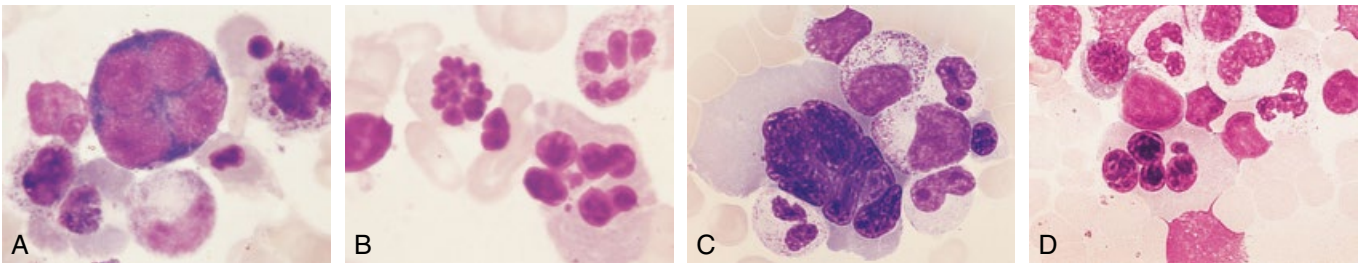

Fig. 12.38. Congenital dyserythropoietic anemia (type III). **A–D,** Selected high-power views of bone marrow aspirate showing multinucleate erythroblasts and karyorrhexis. (Courtesy of Dr. IM Hann.)

CHAPTER

13 THE HEMATOLOGIC NEOPLASMS: LABORATORY TECHNIQUES AND ACUTE MYELOID LEUKEMIA

DIAGNOSTIC TECHNIQUES

Diagnosis of the hematologic neoplasms depends on a combination of several techniques based on phenotype and genotype (Fig. 13.1). Basic tests are examination of peripheral blood and bone marrow smears and trephine biopsies as well as of biopsies of lymph nodes or of other masses or infiltrations of disease. Staining of blood and bone marrow is by May-Grünwald–Giemsa or Wright's stain and by Perls' reaction for iron. Differential counts should include 100–200 cells in peripheral blood and 200–500 cells in bone marrow smears. For histology, hematoxylin and eosin and silver impregnation stains are used routinely. For anticoagulants, EDTA, heparin, or citrate are used, depending on the tests to be performed (Tables 13.1 and 13.2). Cytochemistry (e.g. myeloperoxidase, nonspecific esterase) may be diagnostically useful in the diagnosis of hematologic neoplasms but is now much less used since diagnosis by immunophenotyping and molecular genetic analysis has been established (Fig. 13.2).

IMMUNOHISTOCHEMISTRY

Immunohistochemistry for hematologic diagnosis is carried out on tissue sections, particularly from lymph nodes or bone marrow trephine biopsy specimens. It is an essential part of the diagnostic procedure in hematologic neoplasms, especially for

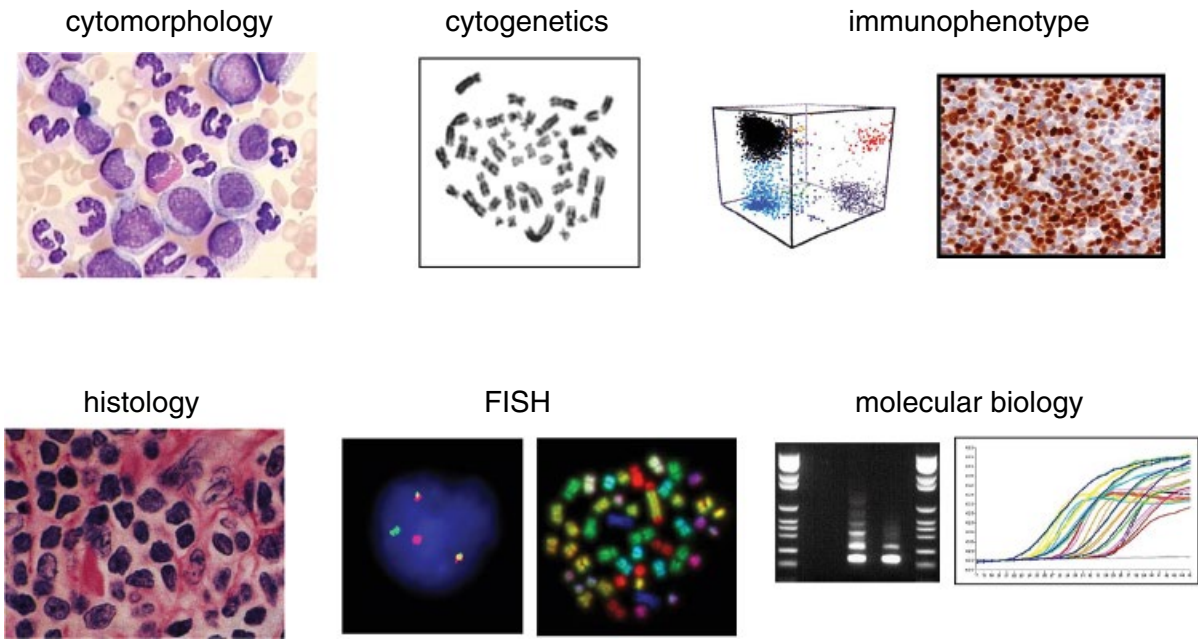

Fig. 13.1. Diagnostic methods used in hematology (i.e. phenotype based on cytomorphology, immunophenotyping, and histology), and genetic methods (i.e. cytogenetics, accompanied by FISH and molecular genetics). Source: Hoffbrand AV, et al. *Postgraduate Haematology*, 7th edn. John Wiley & Sons, 2016. Reproduced with permission of John Wiley & Sons.

Color Atlas of Clinical Hematology: Molecular and Cellular Basis of Disease, Fifth Edition. A. Victor Hoffbrand, Paresh Vyas, Elías Campo, Torsten Haferlach, and Keith Gomez

TABLE 13.1. TECHNIQUES AND RESPECTIVE ANTICOAGULANTS THAT ARE USED IN LEUKEMIA DIAGNOSTICS

	EDTA	Heparin	Citrate
Morphology	+	–	+
FACS/MFC	+	+	+
Cytogenetics	–	+	–
FISH	+	+	+
PCR	+	+	+

FACS/MFC, fluorescence-activated cell sorting/multicolor flow cytometry; FISH, fluorescence in situ hybridization; PCR, polymerase chain reaction.

lymphomas and myeloma but also for myeloid and histiocytic neoplasms (see Chapters 16–24). Depending on the diagnosis suspected, a panel of specific antibodies can be applied to the formalin-fixed paraffin-embedded (FFPE) materials.

FLOW CYTOMETRIC IMMUNOPHENOTYPING

Flow cytometric immunophenotyping is carried out using multichannel instruments that permit the simultaneous assessment of forward light scatter (indicative of cell size), sideways light scatter (indicative of granularity and cell complexity), and the expression of up to 10 surface membrane antigens, all simultaneously in one vial (Figs. 13.3 and 13.4). With the addition of techniques to "permeabilize" the cells, cytoplasmic and

TABLE 13.2. SELECTED ANTIBODIES USED IN IMMUNOHISTOCHEMISTRY IN LYMPHOID NEOPLASMS

Neoplasm	CD5	CD10	BCL-2	IgD	BCL-6	MUM-1	CD43	Cyclin D1	CD23	Annexin-A1
MCL	+	–	+	+	–	–	+	+	–/+	–
CLL/SLL	+	–	+	+	–	+/–[a]	+	–/+[b]	+	–
FL	–	+	+	–/+	+	–[c]	–[c]	–	–/+	–
MALT	–	–	+	–	–	+/–	+/–	–	–	NT
MZL, nodal	–	–	+	+/–[d]	–/+	+	+/–	–	–	–
MZL, splenic	–	–	+	+	–	+/–	–	–	–	–
LPL/WM	–	–/+	+	–	–	+[e]	–/+	–	–/+	–
HCL	–	–/+	+	–	–	NT	NT	+	–/+	+

IgD, immunoglobulin D; MCL, mantle cell lymphoma; +, more than 50%; –, less than 5%; –/+, 5–25%; CLL/SLL, chronic lymphocytic leukemia/small lymphocytic lymphoma; +/–, more than 25–50%; FL, follicular lymphoma; MALT, mucosa-associated lymphoid tissue; NT, not tested in a large number of cases; MZL, marginal zone lymphoma; LPL/WM, lymphoplasmacytic lymphoma/Waldenström macroglobulinemia; HCL, hairy cell leukemia.

[a] Positive in proliferation centers and variable in the small lymphocytes.

[b] Positive primarily in proliferation centers.

[c] May be positive in FL, grade 3.

[d] Positive in nodal MZL of "splenic type."

[e] More positivity in the plasma cells rather than in the small lymphocytic component.

Source: Higgins RA, et al. *Arch Pathol Lab Med* 2008;132:441–461. Reproduced with permission from Archives of Pathology & Laboratory Medicine. Copyright 2008 College of American Pathologists.

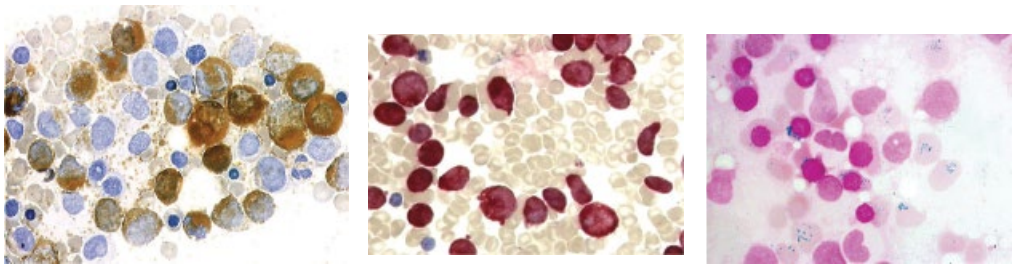

MPO	NSE	Fe
myeloid cells dysplasia	monocytic cells	iron storage and ring sideroblasts (MDS)

Fig. 13.2. Myeloperoxidase (MPO) is used in cytomorphology to detect cells of myeloid origin as well as dysgranulopoiesis. Nonspecific esterase (NSE) detects cells of the monocytic lineage. Iron staining (Fe) provides information on iron storage and detects ring sideroblasts. This is especially of importance in cases of suspected myelodysplastic syndrome (MDS).

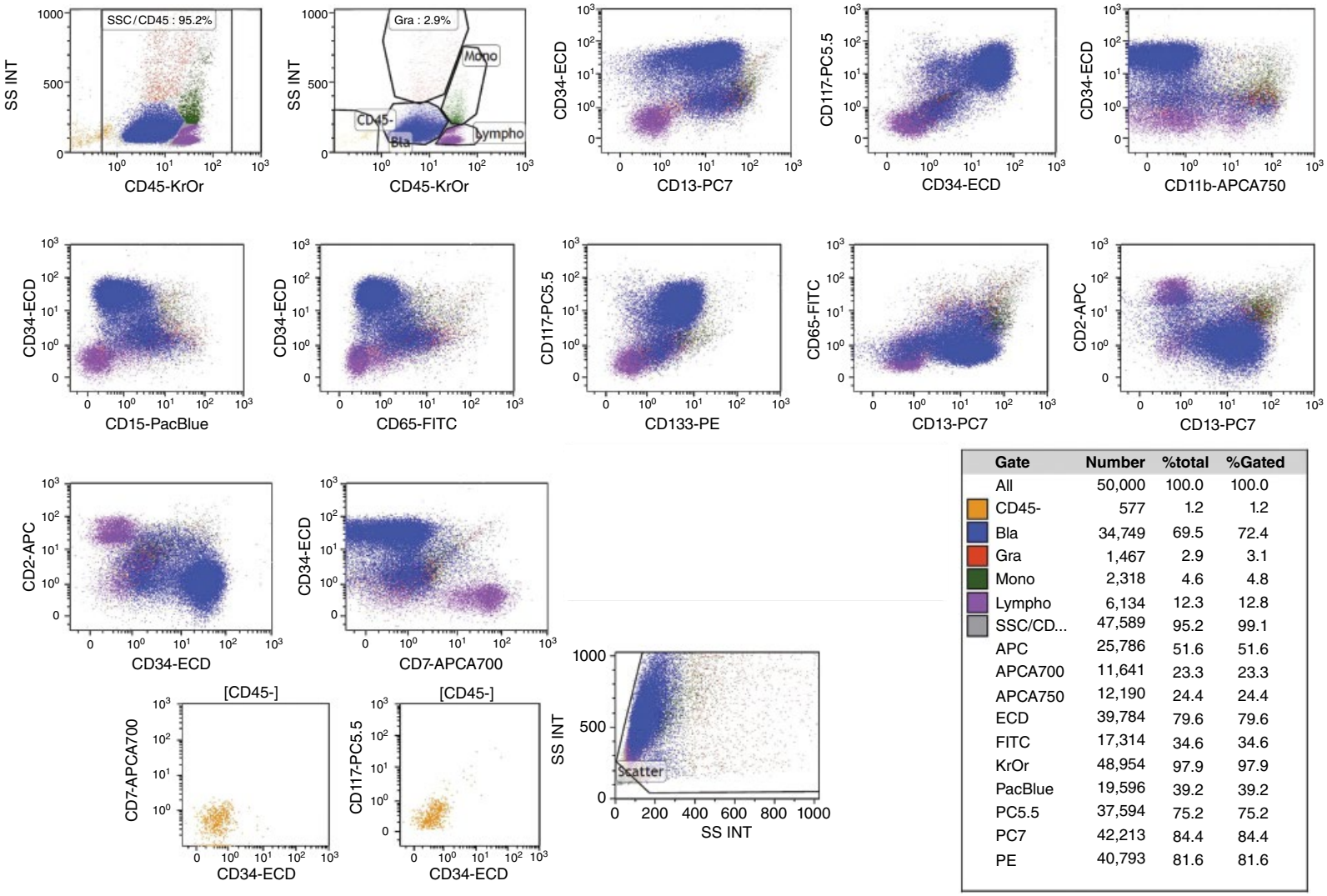

Gate	Number	%total	%Gated
All	50,000	100.0	100.0
CD45-	577	1.2	1.2
Bla	34,749	69.5	72.4
Gra	1,467	2.9	3.1
Mono	2,318	4.6	4.8
Lympho	6,134	12.3	12.8
SSC/CD...	47,589	95.2	99.1
APC	25,786	51.6	51.6
APCA700	11,641	23.3	23.3
APCA750	12,190	24.4	24.4
ECD	39,784	79.6	79.6
FITC	17,314	34.6	34.6
KrOr	48,954	97.9	97.9
PacBlue	19,596	39.2	39.2
PC5.5	37,594	75.2	75.2
PC7	42,213	84.4	84.4
PE	40,793	81.6	81.6

Fig. 13.3. The use of 10-color flow for the diagnosis of acute myeloid leukemia. First, populations are identified based on their SSC/CD45 pattern: blasts (SSClow/CD45dim), lymphocytes (SSC−/CD45+), monocytes (SSClow/CD45+) and granulocytes (SSC+/CD45dim). These populations are displayed in various plots of a further nine antigens. AML population in blue is characterized by expression of the myeloid antigens CD13 and CD117 (partial) and of progenitor cell markers CD34 and CD133 and negativity for the lymphoid antigens CD7 and CD2.

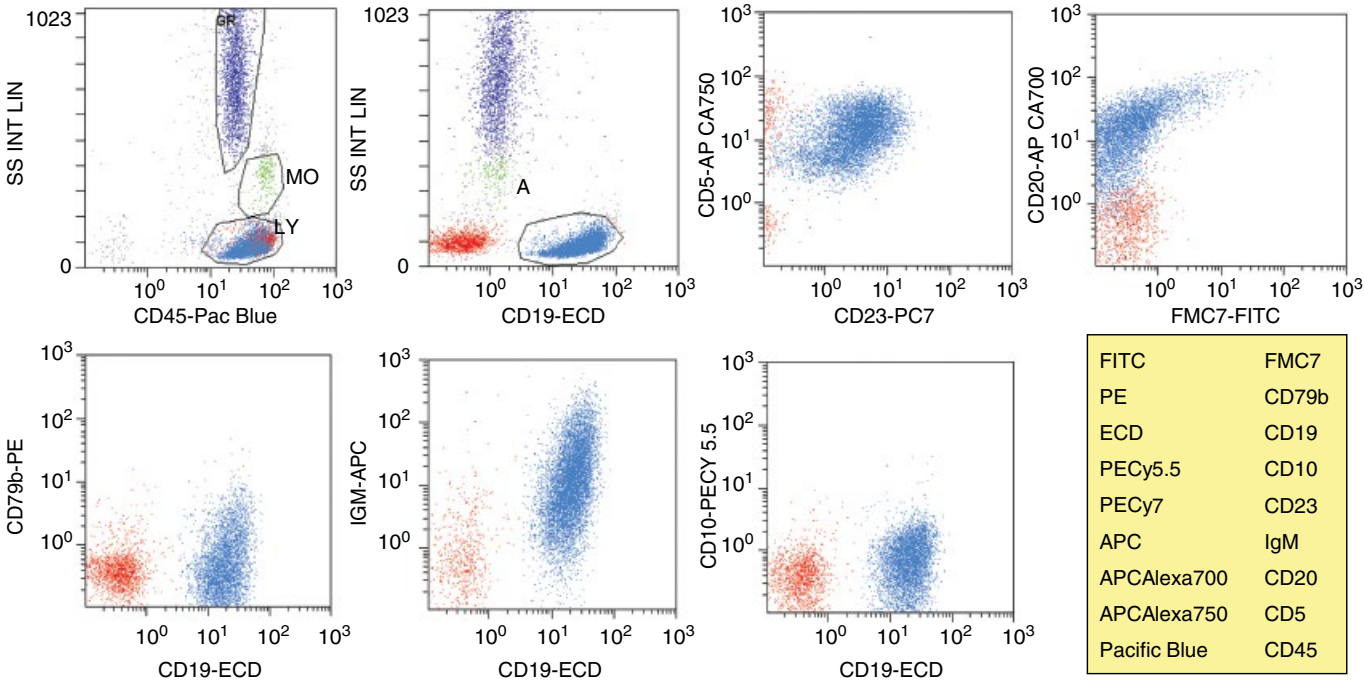

Fig. 13.4. Flow cytometric immunophenotypic diagnostics of chronic lymphocytic leukemia. First, populations are identified based on their SSC/CD45 pattern: lymphocytes (SSC−/CD45+), monocytes (SSClow/CD45+), and granulocytes (SSC+/CD45dim). These populations are displayed in various plots of further nine antigens. CLL population in blue is characterized by expression of the B-lymphoid antigens CD19, CD23, CD20, and dim CD79b, coexpressed with the T-lymphoid antigen CD5. Typically, FMC7 is negative in CLL.

nuclear antigens can also be studied. When there are numerous circulating neoplastic cells, immunophenotyping is conveniently done on a peripheral blood sample. Otherwise it can be performed on a bone marrow aspirate or on a cell suspension from any infiltrated tissue. The main indications for immunophenotyping are as follows: diagnosis and subtyping acute and chronic leukemias and lymphomas (Fig. 13.4), detection of paroxysmal nocturnal hemoglobinuria (see Chapter 12) and measurement of minimal residual disease (Fig. 13.5).

CYTOGENETIC ANALYSIS

Cytogenetic analysis is the study of chromosomes by light microscopy of their morphology and their characteristic banding pattern, demonstrated by staining with a Giemsa stain (Figs. 13.6 and 13.7) or a quinacrine stain (for viewing as fluorescent bands under UV illumination). Classical cytogenetic analysis (chromosome banding analysis) requires cells in metaphase, so that for diseases with a low mitotic rate such as multiple myeloma, fluorescence in situ hybridization (FISH) or molecular analysis may be preferred. Cytogenetic analysis can provide evidence of clonality and thus confirm that a condition is neoplastic when other evidence is absent or equivocal. It further allows in many cases the classification of the respective disease and provides information on prognosis.

FLUORESCENCE IN SITU HYBRIDIZATION

FISH uses labeled oligonucleotide probes that bind to specific DNA sequences. These may be locus-specific probes (including those detecting oncogenes and tumor-suppressor genes), centromeric probes, telomeric probes, and whole chromosome paints. FISH can be used on interphase nuclei as well as on metaphases. It can be used to detect gains and losses, translocations, and also for painting of parts or all chromosomes in a cell (Figs. 13.8 and 13.9).

MOLECULAR GENETIC ANALYSIS

Molecular genetic analysis includes Southern blotting (now rarely used in routine diagnostics), the polymerase chain reaction (PCR) to study genomic DNA, and reverse transcriptase polymerase chain reaction (RT-PCR) to study RNA after its reverse transcription (Fig. 13.10). Table 13.3 provides a glossary of the terms used. A PCR reaction can also be made quantitative, as in real-time quantitative PCR, an important technique for monitoring minimal residual disease (MRD) (Fig. 13.11). Molecular analyses permit the detection of prognostically and therapeutically relevant information, including cryptic rearrangements, such as the *ETV6-RUNX1* rearrangement associated with a cryptic t(12;21)(p13;q22) in acute lymphoblastic leukemia (ALL). Genomic PCR can be applied to stored cells and on FFPE samples.

Gene Expression Profiling

High-density gene expression profiling (GEP) is a well-established molecular method and has been demonstrated to yield information of both diagnostic and prognostic value (Figs. 13.12 and 13.13). GEP involves the hybridization of the labeled RNA to the cDNA of interest with probes positioned in high density on a microarray surface. The use of GEP is limited in routine diagnostics in hematology today.

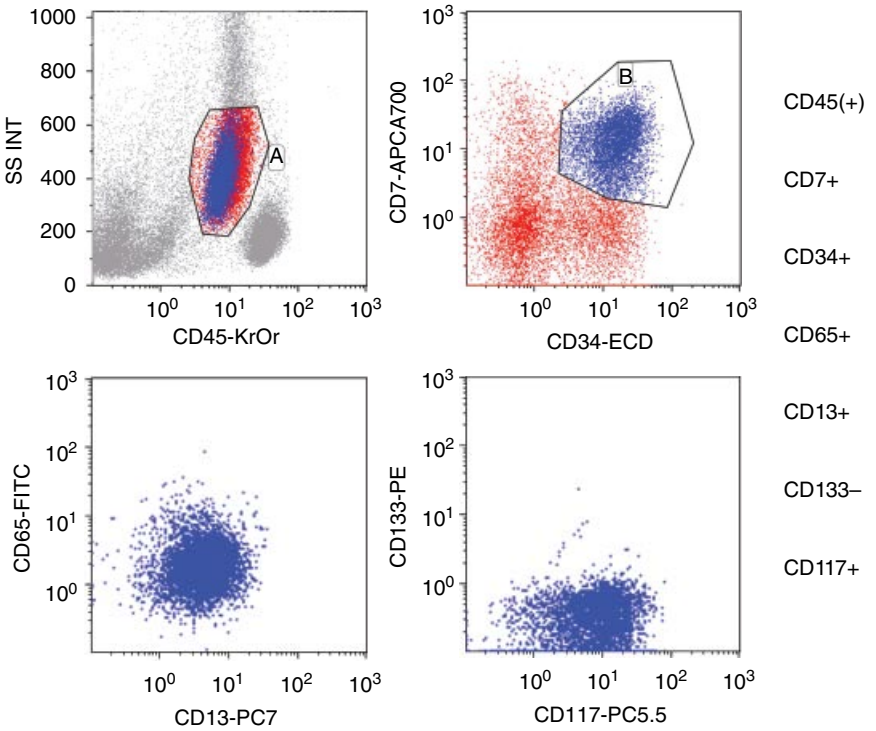

Fig. 13.5. The definition of leukemia-associated immunophenotype (LAIP) by flow cytometry. As a first step, leukemic cells are identified based on their SSC/CD45 expression pattern (A). Out of this population those with expression of CD34 and aberrant expression of the T-lymphatic antigen CD7 are gated (B). These CD34+CD7+ cells are displayed in the two remaining plots, proving myeloid lineage (positivity for CD13 and CD117) as well as aberrant lack of expression of the progenitor cell marker CD133.

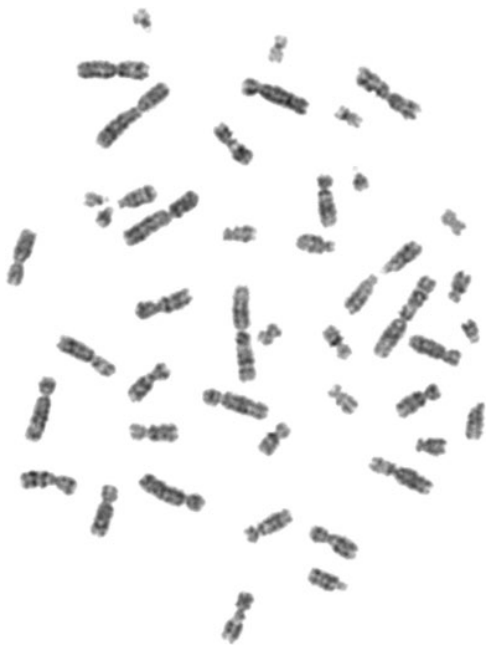

Fig. 13.6. Giemsa-banded metaphase after culture of AML blasts and capture by an automized microscope.

Array Comparative Genomic Hybridization

Array comparative genomic hybridization (CGH) is performed using fluorochrome-labeled patient DNA that is hybridized to normal control DNA. CGH arrays are frequently used for the detection of genome-wide single-nucleotide polymorphisms (SNPs). CGH microarray analysis is also used for the detection of underrepresentation or overrepresentation of specific genomic regions in the test DNA. Deletions and amplifications can thus be detected, for example deletion of 13q14 and 11q22 in chronic lymphocytic leukemia (CLL) or iAMP21 in ALL.

In SNP array analysis, genomic DNA of a sample of interest is digested by restriction enzymes, amplified, labeled, and hybridized to oligonucleotide probes. Probes are either bound to microbeads or are synthesized in situ in high density on a microarray surface (Fig. 13.14). SNP analysis can be applied to genotyping and is able to distinguish heterozygosity from homozygosity. It can thus be used to detect both loss of heterozygosity and alterations of copy numbers of a genomic region (i.e. gains and losses). Acquired somatic uniparental disomy can be detected by comparison of tumor DNA with constitutional DNA. Sensitivity for the detection of a clonal population is similar to that of metaphase cytogenetics. With SNP array technology it is possible to identify uniparental disomy for chromosomal regions that include mutated genes such as *JAK2*, *CEBPA*, *FLT3*, or *RUNX1*.

Next-Generation Sequencing

The constantly increasing spectrum of molecular mutations is a tremendous challenge for hematologic laboratories. The introduction of high-throughput sequencing technologies, which allow the parallel analysis of hundreds of thousands of alleles in a short time, provides new options for molecular mutation analyses and for follow-up diagnostics (Fig. 13.15). In contrast to whole-genome or exome analyses, which might today still not be feasible in a routine setting, amplicon (i.e. piece of DNA or RNA that is produced by amplification) deep sequencing focuses on distinct genomic loci and their mutation patterns and enables

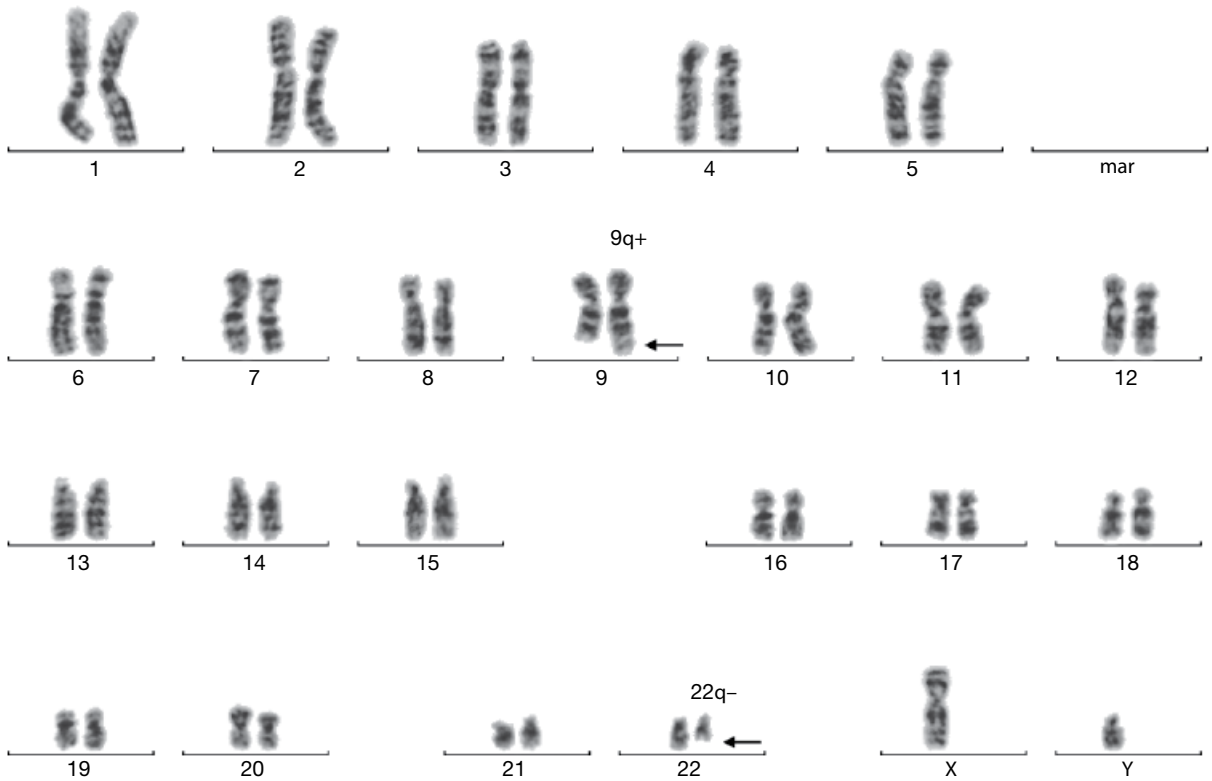

Fig. 13.7. Karyogram of a patient with chronic myeloid leukemia after Giemsa banding showing a reciprocal translocation between the long arm of chromosome 9 and the long arm of chromosome 22 described as 46,XY,t(9;22)(q34;q11) according to the International System for Human Cytogenetic Nomenclature (ISCN).

a comprehensive biomarker analysis in a multitude of patients per analysis. In panel testing it is feasible to investigate up to several hundreds genes or hotspot regions of genes in one test. The coverage is above 500× in most loci of interest, and turnaround time is less than a week.

Figure 13.16 shows the complete workflow and Table 13.4 lists the key features of different sequencing strategies. Several international guidelines have been published in recent years to discuss and describe best laboratory practice for the different analytical steps, such as (i) design study, (ii) wet lab needs, (iii) bioinformatics, and (iv) interpretation and reporting of results. Defined algorithms for molecular investigations are on the way to foster diagnosis in hematology by including next-generation sequencing (NGS) as a routine method in the near future. Several issues need further discussion, such as the best approaches to data curation (including web-based tools), the role and interpretation of "variants of uncertain significance" (VUS), ethical aspects of data to be delivered and stored, use of NGS for MRD detection, and reimbursement. It is anticipated that whole-exome sequencing (WES) or even whole-genome sequencing (WGS) combined with total RNA sequencing will be technically applicable in the diagnosis in hematology in few years with acceptable costs and turnaround times.

Single Genes

For targeted sequencing of single genes or gene regions an amplicon-based method is mostly used for amplification of the regions of interest. After PCR amplification a patient-specific index is attached by ligation or an additional single amplification cycle to guarantee the patient-specific assignment of the sequencing read by a unique barcode. A high coverage of >1000× allows variant calling with variant allele frequencies of 2%.

Panel Testing

A number of diagnostic and/or prognostically relevant single or multiple gene mutations can be detected using commercial or customized panels. Two different methodologies are commonly used for targeted library preparation: the amplicon-based method and an enrichment-based strategy. Whereas the DNA input in the former method is low, the latter requires a higher DNA input, because no PCR amplification is used to enrich the regions of interest. After enrichment of the regions of interest by either PCR or pull-down and ligation of the patient-specific index, a large number (up to several hundred genes) can be sequenced in parallel for every patient. With a predefined gene panel approximately 100 kb of DNA are sequenced with a high coverage of >500×, allowing variant calling with variant allele frequencies of 2%. Targeted panel sequencing allows detection of single-nucleotide variants (SNVs) but not of structural variants.

Whole-Exome and Whole-Genome Sequencing

In contrast to targeted panel sequencing, large-scale approaches such as whole-exome or whole-genome sequencing allow the sequencing of complete coding regions or even the complete genome of a patient. Although the human exome covers only 1–2% of the human genome, both approaches need large sequencing capacities, with 60 Mbp and 3.3 Gbp needing to be sequenced (Table 13.4). For whole-exome sequencing the exonic regions (exons) of the genomic DNA are enriched by capture probes (small single-stranded DNA oligos for isolation

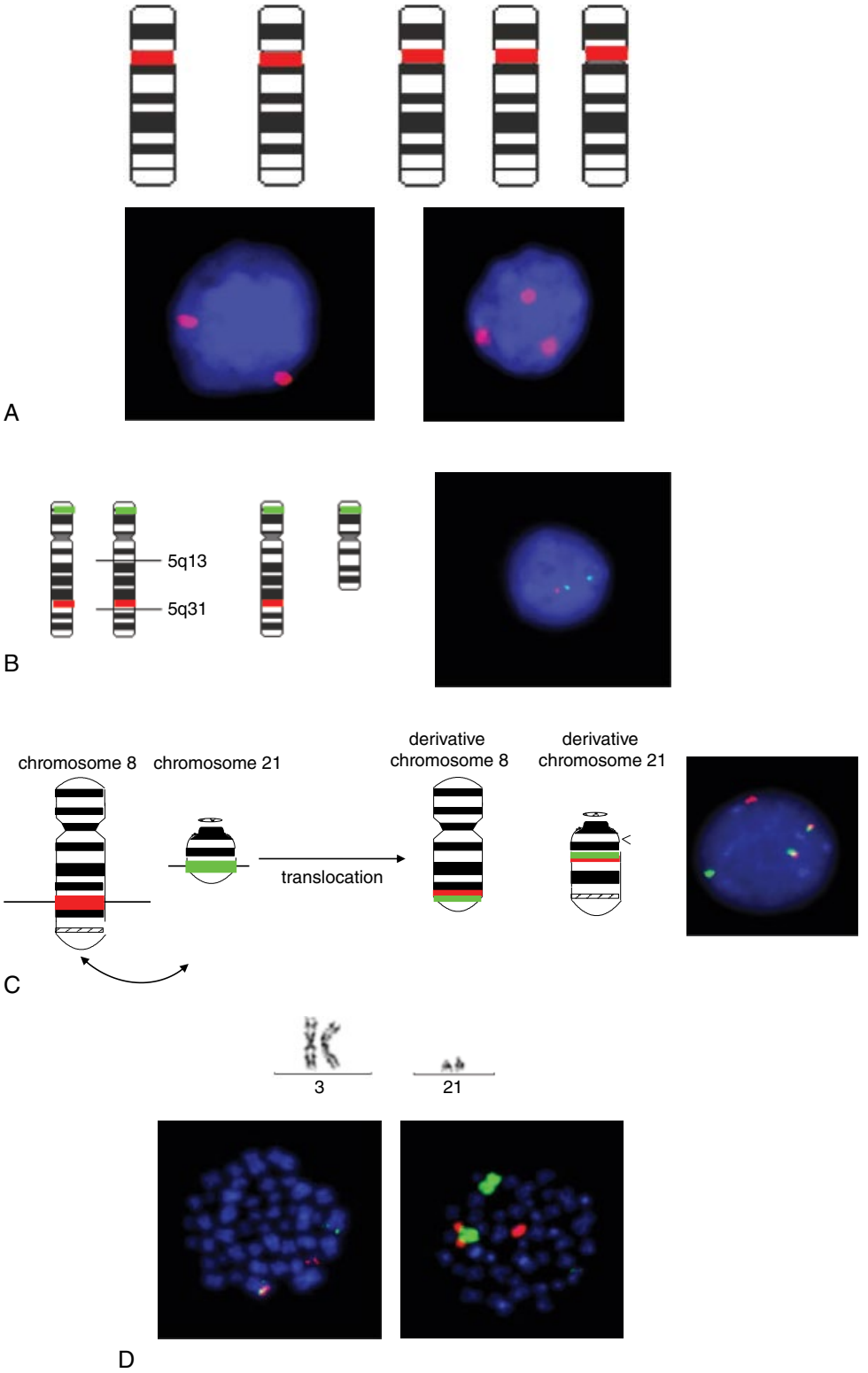

Fig. 13.8. Fluorescence in situ hybridization (FISH) is a targeted diagnostic techniques that allows the detection of copy number changes (gains and losses) and fusion genes. **A,** Centromeric probes can be used for the detection of monosomies and trisomies. An example is depicted of a cell with two copies of the centromeric region of chromosome 12 *(left)* and three copies indicating trisomy 12 *(right)*. **B,** Otherwise, locus-specific probes are most widely used, illustrating gains or losses when the number of signals differs from 2 which is the expected number in a normal cell. As an example, a 5q deletion is depicted. A probe located on the short arm of chromosome 5 (green) was hybridized as a control probe together with a probe located in the commonly deleted region (red, 5q31). Thus two green signals and only 1 red signal are present, indicating a 5q31 deletion in the depicted cell. **C,** By labeling two probes with different fluorochromes it is possible to study two genes that are involved in a specific translocation or other rearrangement. If the probes span the breakpoint, both will be disrupted by the translocation and signals will be adjacent or optically fused on the derivative chromosomes. This is a double-color double-fusion technique. Often one probe gives a green signal and the other a red signal, so that the fusion signal appears yellow. As an example, the translocation t(8;21)(q22;q22), leading to a *RUNX1-RUNX1T1* fusion, is shown. **D,** FISH is also applicable on metaphase chromosomes. For example, a partial karyotype of a translocation t(3;21)(q26;q11) is shown, which is cryptic on chromosome banding analysis as the exchanged chromosome pieces are of a comparable size and banding pattern. This translocation can be detected by FISH with so-called "whole chromosome painting probes." In this example the whole chromosomes 3 are green and whole chromosomes 21 red *(left)*. The involvement of the MECOM locus can also be confirmed by FISH on metaphase by a double-color break apart probe labeling a centromeric (green) and a telomeric part (red) of the MECOM locus. The telomeric probe (red) is translocated to the derivative chromosome 21 while the centromeric probe (green) resides on the derivative chromosome 3, indicating an involvement of the MECOM locus in the translocation.

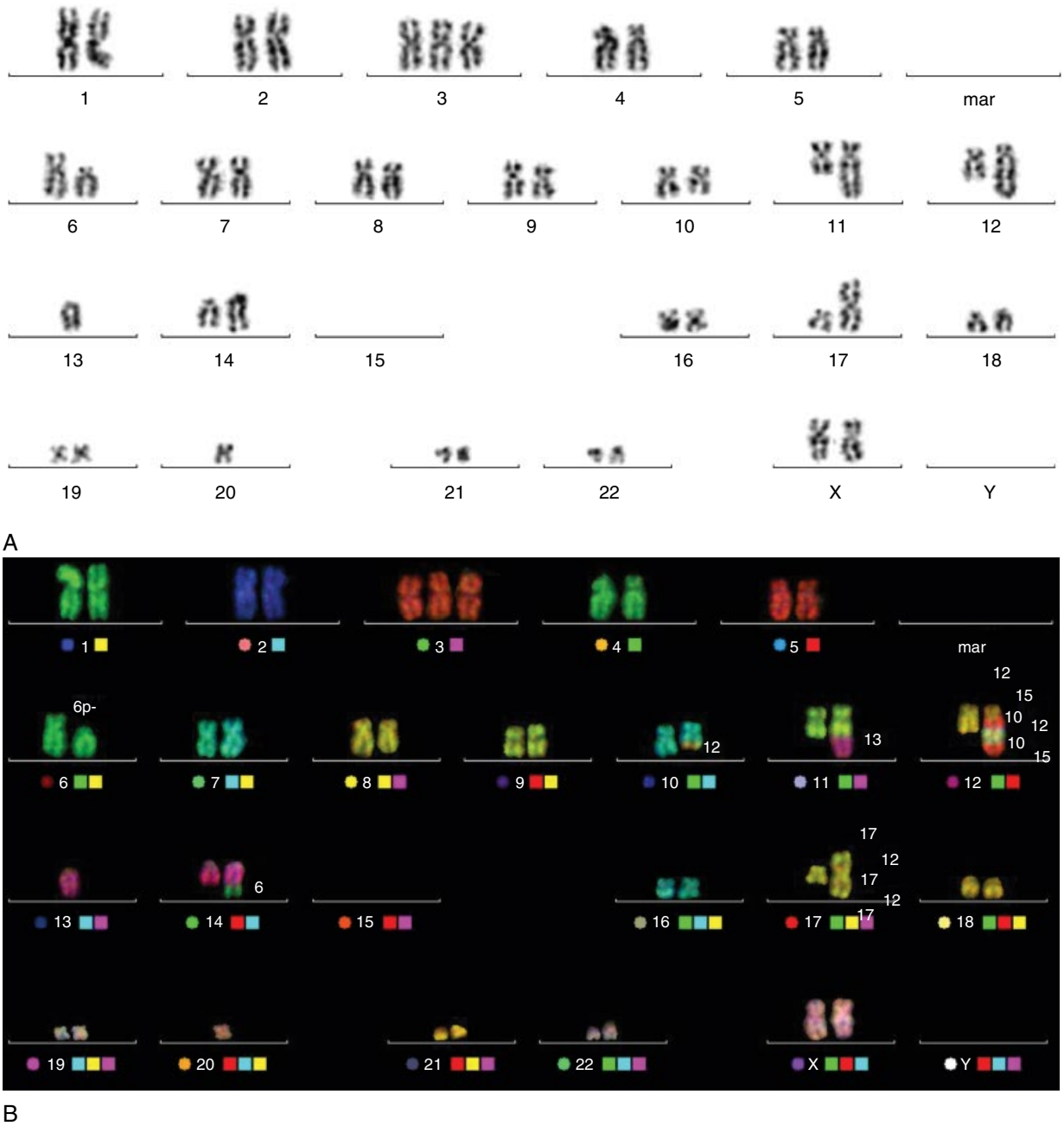

Fig. 13.9. A, A complex aberrant karyotype in AML depicted after Giemsa banding. **B,** Twenty-four-color FISH of the same metaphase is used to decipher complex karyotypes in combination with G-banding to resolve complex rearrangements.

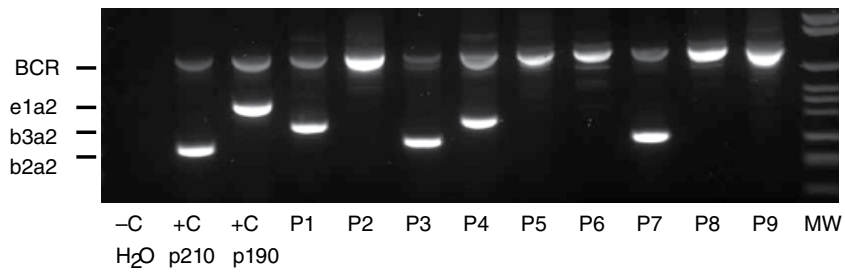

Fig. 13.10. Polymerase chain reaction (PCR) is a simple method for detection of specific gene regions, either showing up in every cell or, for example, specifically after rearrangement of gene regions in tumor cells (e.g. *BCR-ABL1* in chronic myelogenous leukemia). Multiplexing of several primers allows the parallel detection of control genes (*BCR*) as well as the target gene regions (*BCR-ABL1*). After gel electrophoresis PCR product are visualized by staining of the DNA. Both the detection of an expected target gene as well as size can be proven. The figure shows the two different PCR products of nine patients (P1–P9), p190 (e1a2), and p210 (b2a2 or b3a2) of the rearranged fusion gene *BCR-ABL1*. Positive controls (C+) as well as mock controls (H_2O) and the molecular weight marker (MW) should always be considered.

TABLE 13.3 GLOSSARY

Acquired mutation: see 'somatic mutation'

Allele burden: The fraction of alleles with a specific sequence in relation to the total number of alleles for the same region of the genome. For example a heterozygous mutation in a pure population of leukaemia cells has an allele burden of 0.5. If 70% of cells are leukaemic and 30% of cells are normal, the mutant allele burden of the heterozygous mutation would be 0.7 × 0.5 = 0.35.

Amplification: A genetic modification producing an increased number of copies of a genomic region

Branching evolution (of cancer): A form of clonal evolution of cancer which leads to the generation of more than one clone of cells characterized by distinct somatic mutations, but which share at least one mutation traceable back to a single ancestral cell.

Cancer genome: The genome of a cancer cell, which differs from the germline genome as a result of somatic mutations.

Chromosomal translocation: see 'genomic rearrangements'.

Chromothripsis: a single catastrophic event by which hundreds to thousands of chromosomal rearrangements occur in confined genomic regions of one or a few chromosomes (from Greek θρύΨις = shattering into small pieces).

Clonal evolution (of cancer): The stepwise acquisition of mutations in a founder cell and its progeny leading towards the development of a cancer.

Clonal mutation: A mutation present in a population of related cells derived from a single cell.

Constraint hypothesis: A hypothesis about clonal evolution proposing that the observed order of acquisition of somatic mutations during cancer evolution reflects a requirement for a specific mutation to occur before another for a growth advantage to be gained by the host cell(s).

Co-occurrence (of cancer mutations): The occurrence of two or more mutations in the same type cancer more often than would be expected by chance.

Convergent evolution (of cancer): A pattern of cancer evolution during which independent clones expand after acquiring the same or very similar mutation. This is likely to reflect the fact that such a mutation is particularly advantageous to the specific cancer cell, giving a marked growth advantage when acquired by chance.

Deletion: A genetic modification leading to the loss of a genomic region.

Dominant negative mutation: A heterozygous mutation that leads to marked or complete loss of function of the coded protein and of the normal protein coded by the other (wild-type) copy of the gene.

Driver gene or driver mutation: A mutated gene that confers a selective growth advantage to a cancer cell

Epigenetics: The study of changes to DNA and chromatin, other than those that alter the DNA nucleotide sequence, that alter the transcriptional potential of a cell and are usually heritable

Exome: The collection of all exons in a genome.

Exome sequencing: Sequencing of all exons in a genome. This has referred to exons of protein-coding genes, but increasingly non-protein-coding genes are included (e.g. long non-coding RNAs).

Gain-of-function mutation: A mutation that gives the coded protein a novel or markedly enhanced function

Genome-wide association studies (GWAS): studies of many common and uncommon genetic variants in different individuals to determine if any variant is associated with a disease or trait. The primary outcome of these studies is the identification of variants such as SNPs which are *associated* with, but do not necessarily cause the disease in question.

Genomic rearrangement: A mutation that juxtaposes nucleotides that are normally distant from each other, such as a chromosomal translocation, inversion or deletion.

Germline genome: An individual's genome as formed at the time of conception (fertilized oocyte). This genome is shared by all cells in the body.

Germline mutation: Mutations present in the germline genome. Sporadic mutations acquired in the germ cells of parents are also included in this category.

Germline variants: Variations in sequences or copy number of DNA segments observed between different individuals that are responsible of the phenotypic variation between people. Two unrelated individuals differ by approximately 3 million such variants.

Haplotype: A haplotype is a contiguous region of the genome containing a set of tightly linked genes that are likely to be inherited together.

Indel: A mutation that results in insertion or deletion of one or a few nucleotides to DNA.

Kataegis: Localized hypermutation of a region of the genome, thought to be mediated by APOBEC enzymes (from Greek καταιγίς = storm).

Linear evolution (of cancer): A form of clonal evolution of cancer that generates a single final clone of cancer cells which harbours all mutations that ever arose during its evolution.

Loss-of-function mutation: A mutation that leads to marked or complete loss of function of the coded protein.

Loss-of-heterozygosity (LOH): A genetic modification leading to the loss of the maternally- or paternally-derived copy of a genomic region. This can happen as a result of deletion or uniparental disomy (uPD).

Methylation: Covalent addition of a methyl group to a DNA, RNA, protein or other molecule.

Missense mutation: A nucleotide substitution (e.g. G to T) that results in an amino acid change (e.g. valine to phenylalanine).

Mutational signature: A recurrent pattern of DNA mutations attributable to a particular type of mutagen or mutational process, characterized by certain nucleotide mutations in a specific 5′ and 3′ nucleotidic context.

Mutual exclusivity: The occurrence of two or more mutations in the same cancer type less often than would be expected by chance.

Next-generation sequencing (NGS): DNA sequencing using one of the methodologies developed since 2005 and which allow massively parallel sequencing of thousands or millions of fragments of DNA simultaneously.

Nonsense mutation: A nucleotide substitution that results in the generation of a stop codon (i.e. TAA, TGA or TAG).

Non-synonymous mutation: A mutation that alters the encoded amino acid sequence of a protein. These include missense, nonsense, splice site, gain of translation start, loss of translation stop and indel mutations.

Proto-oncogene: A gene that when activated by mutations, becomes an **oncogene** and imparts a growth advantage of its host cell.

Opportunity hypothesis: A hypothesis proposing that the observed order of acquisition of somatic mutations during cancer evolution reflects the statistical likelihood that mutations are acquired in this order. This likelihood is determined by the earlier mutation influencing the opportunity for acquiring the next. Implicit in this hypothesis is that the reverse order can also be observed, albeit less often.

Passenger mutation: A mutation that does not give a selective growth advantage to its host cell.

Single nucleotide polymorphism (SNP): A DNA sequence variation occurring commonly within a population (e.g. 1%) in which a single nucleotide in the genome differs between individuals.

Somatic mutation: A mutation that occurs in any cell of the body after conception. Sometimes called *acquired mutation*.

Substitution (or nucleotide substitution): A DNA mutation leading to the replacement of a native nucleotide with another.

Splice sites: DNA sequences flanking exons which are important for mRNA splicing.

Subclonal mutation: A mutation that exists in only a subset of the neoplastic cells within a tumour.

Transition (mutation): Change of a nucleotide to another of the same group such as C>T (both pyrimidines) or G>A (both purines).

Transversion (mutation): Change of a nucleotide to another of the opposite group such as A>C (purine to pyrimidine).

Uniparental disomy (uPD): A genetic modification leading to the loss of the maternally or paternally derived copy of a genomic region as a result of replacement of this sequence with the equivalent sequence derived from the other parent.

Untranslated region (UTR): Exonic region located before the start (5′ UTR) or after the stop (3′UTR) codon of a gene and which do not encode amino acids.

Whole genome sequencing: Sequencing of the entire sequence of an individual genome using germline DNA, tumour-derived DNA or DNA from another cellular source such as cell lines, single cells etc.

Whole exome sequencing: Sequencing of all the exons of all the genes in an individual genome (there are approximately 30,000 coding genes in a mammalian genome). As with whole genome sequencing this could be done using germline DNA, tumour-derived DNA or DNA from another cellular source.

Source: Hoffbrand AV, et al. *Postgraduate Haematology*, 7th edn. John Wiley & Sons, 2016. Reproduced with permission of John Wiley & Sons.

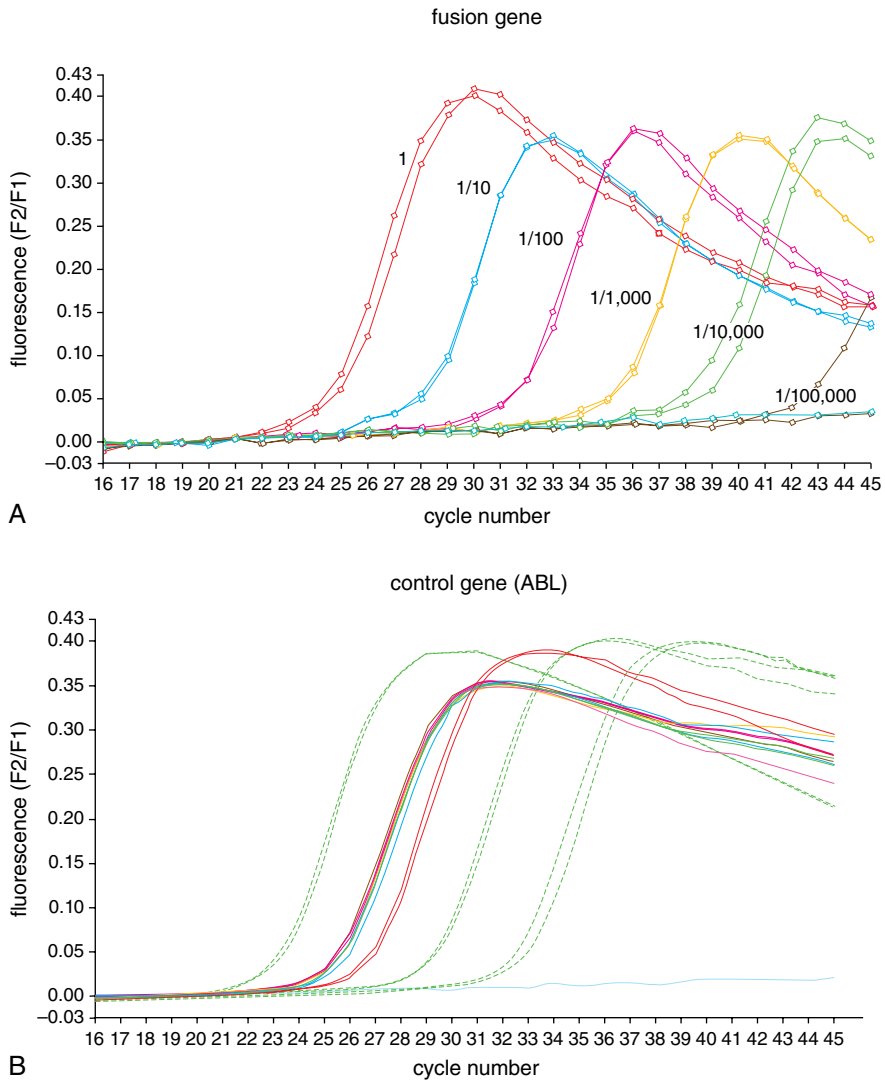

Fig. 13.11. Quantitative polymerase chain reaction (PCR) is a highly sensitive method to detect even low level of tumor burden by quantification of the tumor marker (e.g. *BCR-ABL1*). The fusion gene **(A)** is quantified in respect to a reference gene **(B)** and given as ratio target/reference gene * 100. Absolute quantification is performed by using standard curves. The earlier the labeled PCR product rises above the detection limit, the higher the input amount of target gene, indicated by low Cp values (CP, crossing point; the cycle in which fluorescence increases significantly over background fluorescence for the first time; the further to the left the curve rises, the lower the Cp value). The dilution series **(A)** illustrates different input amounts of the target gene.

of specific regions). Therefore whole-exome sequencing represents a targeted enrichment-based assay covering all exonic regions by sequencing. For exome sequencing a coverage of 100× is often reached, while the commonly sequenced genome is covered by 30×. Although exome sequencing results in higher data quality, the advantages of the whole-genome approach are that it also covers the detection of SNVs and structural variants, including loss of heterozygosity (LOH) and copy number variations (CNVs). Detection of structural variants is limited in exome sequencing.

RNA Sequencing

The importance of RNA sequencing is increasing for diagnostics as well as for predictive assessment of patients. For RNA sequencing, targeted and complete-transcriptome approaches are available. The transcriptome approach covers all types of RNA, whereas the targeted approach enriches a set of genes of interest that are then sequenced. RNA sequencing is based on the reverse transcription of RNA to cDNA, which allows DNA sequencing methodologies in a routine workflow. RNA sequencing enables the detection of fusion transcripts by sequencing the junction reads spanning two fused gene fragments.

Digital Polymerase Chain Reaction

Digital PCR (also sometimes called droplet PCR) is emerging as a useful technique in the detection of MRD in hematology. The key to digital PCR lies in the dilution and division of the sample into small compartments. These aliquots form hundreds or even millions of separate reaction chambers. Ideally, each chamber contains one or no copies of the target of interest, leading to a positive or negative signal. This is why the term "digital" is used. Digital PCR allows the exact copy number in the original sample to be determined. Two different commercial platforms are currently available. The reaction chambers may be either created on specially designed chips (e.g. Fluidigm, Life Technologies) or as individual droplets (e.g. Bio-Rad [Fig. 13.17], RainDance).

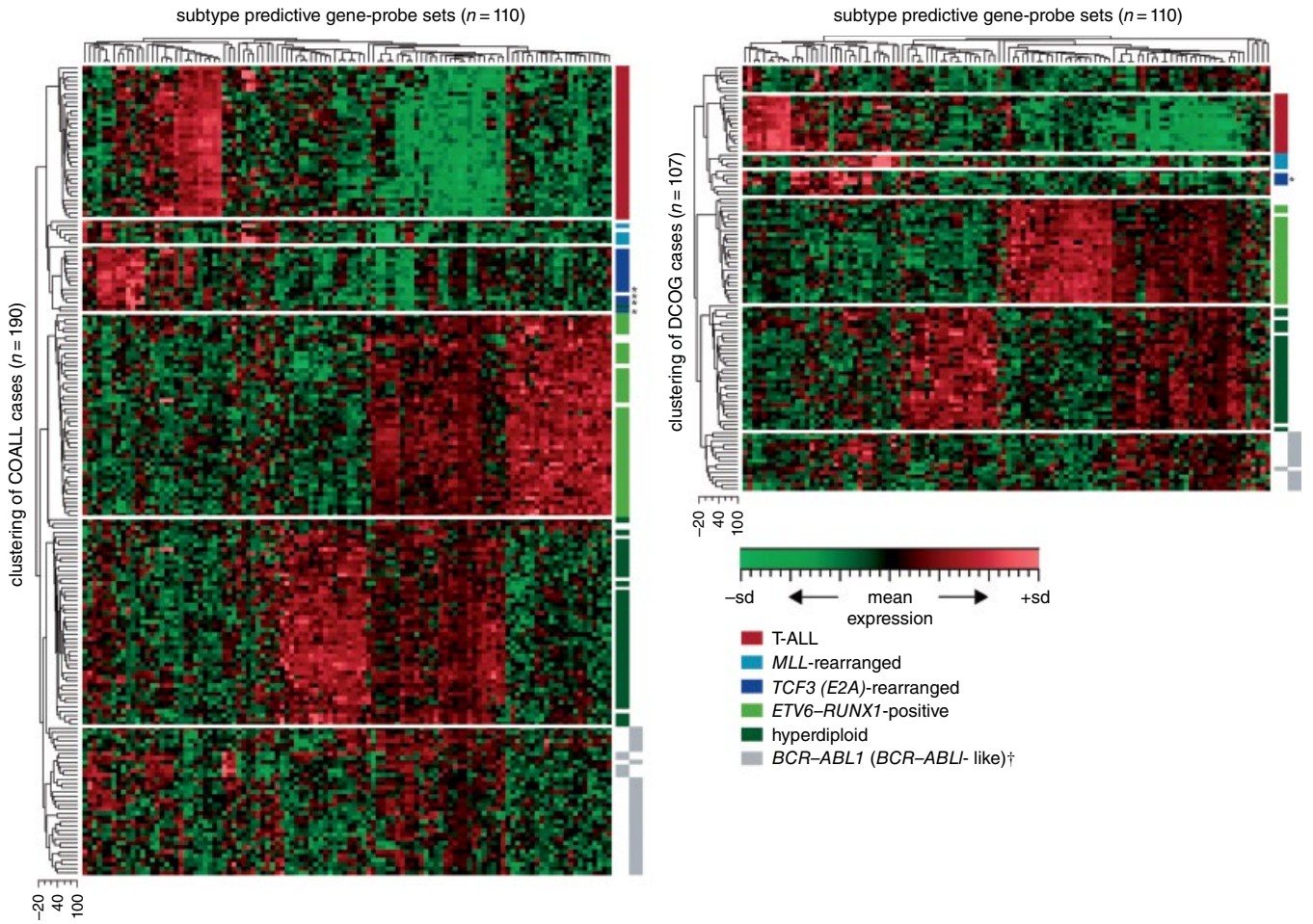

Fig. 13.12. Gene expression profiling (GEP) led to the discovery of a Ph-like acute lymphoblastic leukemia (ALL) entity (new provisional entity in WHO 2016 classification: B-lymphoblastic leukemia/lymphoma, *BCR-ABL1*-like). These cases intercalated with *BCR-ABL1*-mutated ALL in their respective GEP pattern, but are *BCR-ABL1* negative. Prognosis is bad, and worst as *BCR-ABL1* mutated ALL. As GEP cannot be applied in all cases of ALL routinely, an alternative would be a combination of FISH and PCR. Results may lead to targeted treatment strategies. Source: Den Boer ML, et al. *Lancet Oncol* 2009;10(2):125–134. Reproduced with permission of Elsevier.

Digital PCR is primarily applied for quantifying rare variants, targets in a complex background, and subtle changes in gene expression. It may reach higher sensitivity and precision compared to real-time quantitative PCR and does not require calibration as it gives absolute counts. Digital PCR will enable us to follow each individual mutation in a given gene with a patient-specific approach and a sensitivity comparable to that of quantitative PCR.

Free Circulating DNA

Free circulating DNA is present in normal plasma, free fetal DNA is present in maternal blood, and free tumor DNA may be detected in plasma in patients with lymphoma and plasma cell neoplasms. The free tumor DNA is highly degraded and fragmented and must be distinguished from normal white cell contaminating DNA. Nevertheless studies suggest, for example, that sequencing of this free DNA may help to detect transformation of follicular lymphoma and determine the tumor burden in diffuse large B-cell lymphoma. It may also determine the genotype of classical Hodgkin lymphoma and plasma cell neoplasms. Free circulating DNA can also be used to monitor response to therapy and change in genotype during the course of these diseases.

ACUTE MYELOID LEUKEMIA

The acute myeloid leukemias (AMLs) are the result of accumulation of early myeloid precursors in the bone marrow, blood, and other tissues, and are thought to arise by somatic mutation(s) of a single cell within a minor population of stem or early progenitor cells in the bone marrow. The World Health Organization (WHO) (2016) definition includes ≥20% of all marrow cells or ≥20% of peripheral blood cells are blasts but allow the diagnosis with fewer blasts if certain clonal cytogenetic abnormalities are present. AML may arise de novo (90% of cases) both in children and adults, most frequently after the age of 70 years, or be induced by prior chemo- and/or radiotherapy (therapy-related AML [t-AML]) (see Appendix 1). The AML-like phenotype can also appear as the terminal event (blast phase) in a number of preexisting blood disorders, for example

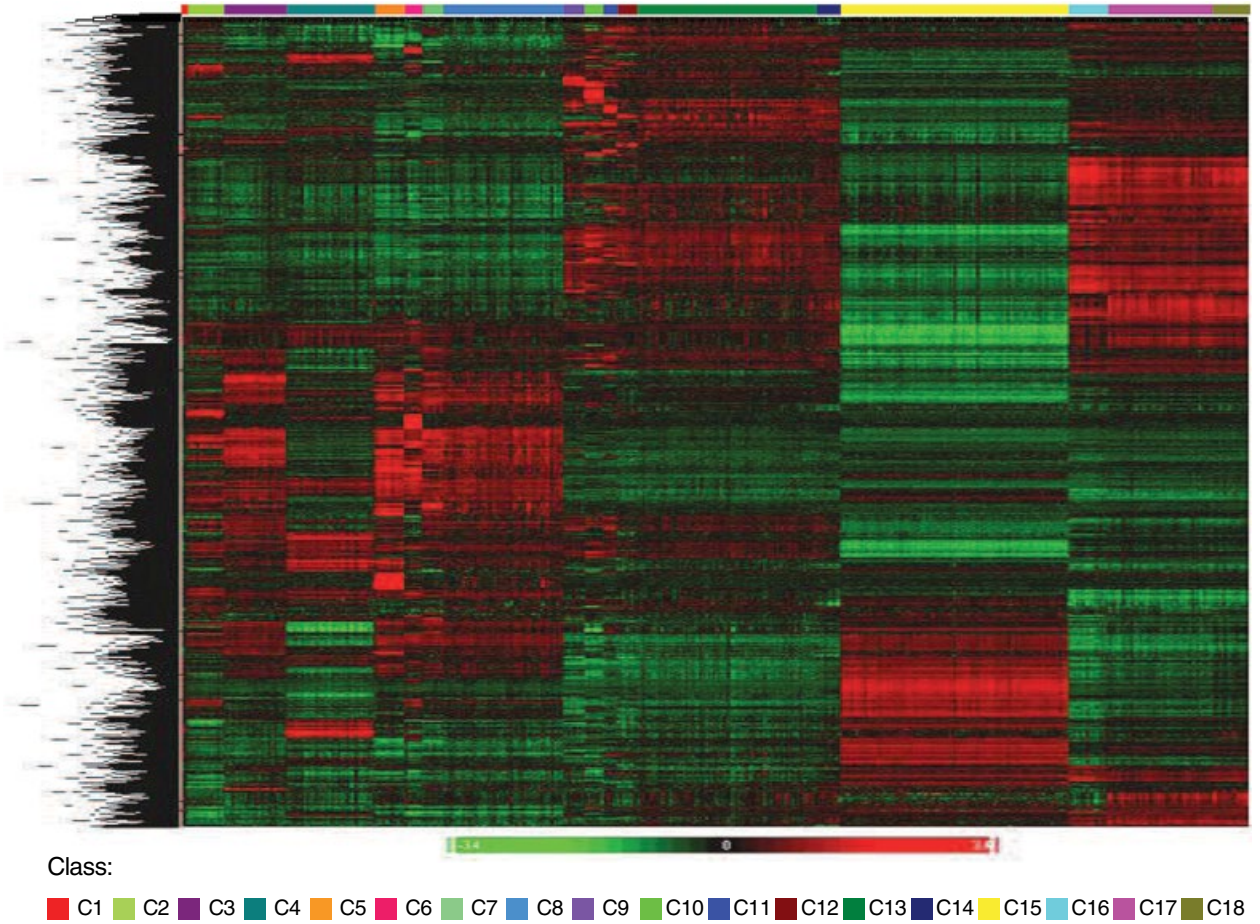

Fig. 13.13. Supervised hierarchical clustering. The exploratory whole-genome clustering analysis was performed for all classes (C1–C18 in ascending order) including 2096 samples from stage I. For every class pair, the top 100 differentially expressed probes sets with the largest absolute values of *t* statistic were selected. The union of these sets contained 3556 probe sets used in the clustering. Source: Haferlach T, et al. *J Clin Oncol* 2010. Published online ahead of print at www.jco.org on April 20, 2010. doi: 10.1200/JCO.2009.23.4732. Reproduced with permission of *Journal of Clinical Oncology*: American Society of Clinical Oncology.

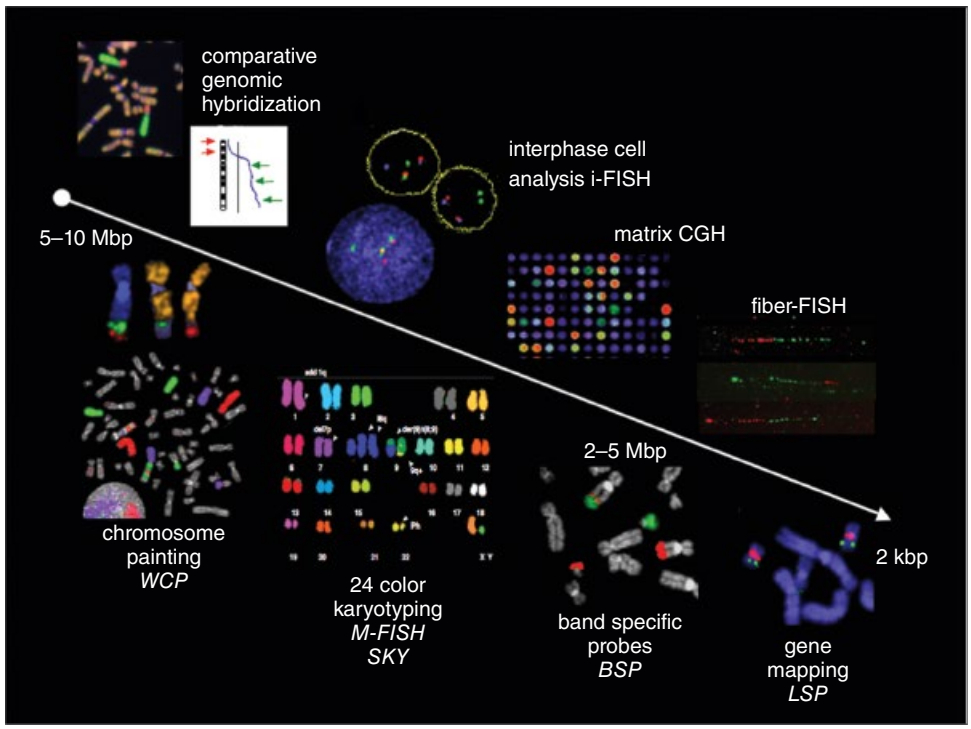

Fig. 13.14. Summary of fluorescence in situ hybridization (FISH) techniques. Below the diagonal line methods for analysis of dividing cells are illustrated: whole chromosome painting (WCP), color karyotyping (SKY and multicolor FISH [M-FISH]), band-specific probes (BSP), and locus-specific probes (LSP). Above the diagonal line methods for analysis of interphase cells are illustrated: comparative genomic hybridization (CGH), interphase FISH (i-FISH), matrix CGH, and fiber-FISH. (Courtesy of Dr. E Nacheva.)

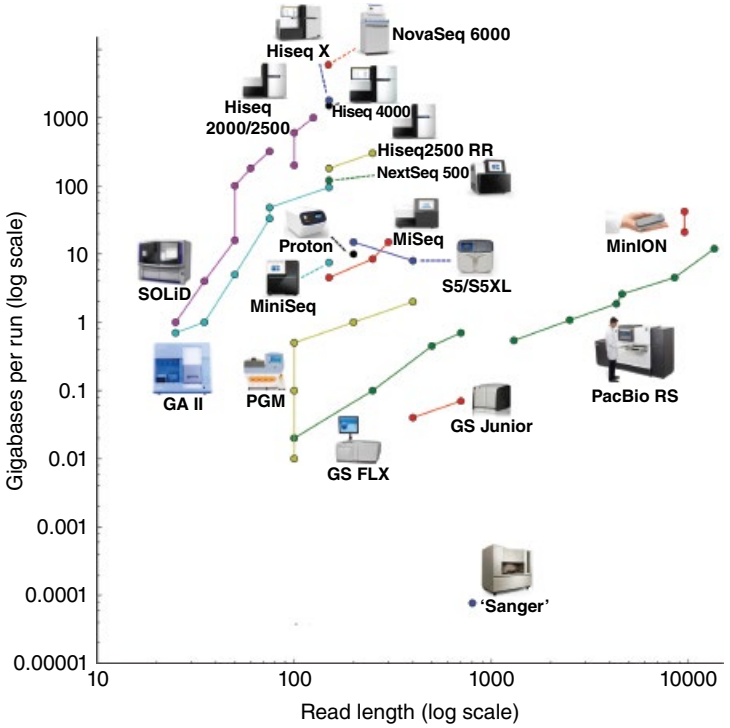

Fig. 13.15. Overview of recently developed next-generation sequencing (NGS) instruments with increasing sequencing capacities.

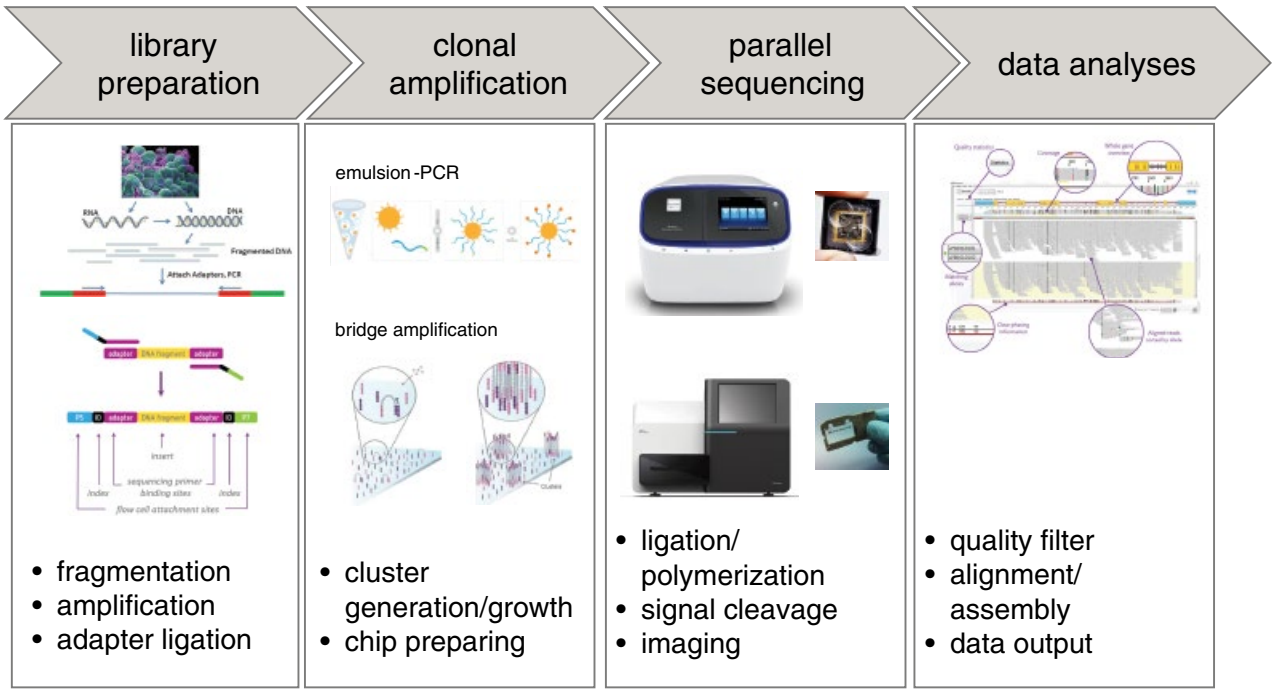

Fig. 13.16. Main components of the next-generation sequencing workflow: library preparation, clonal amplification, sequencing, and data analyses.

TABLE 13.4. OVERVIEW ON DIFFERENT SEQUENCING STRATEGIES, THE DNA AMOUNT SEQUENCED, MAIN COVERAGE REACHED, TURNAROUND TIME (TAT) IN DAYS, AND THE APPLICATION INDICATIONS FOR THE RESPECTIVE SEQUENCING STRATEGY

	Description	Gbp	Coverage	TAT	Application
Gene	Coding region of single gene	0.00001	500×	3	SNV, InDels
Panel	Collection of relevant genes	0.001	500×	3	SNV, InDels
Exome	Targeted view of the protein coding region of the genome	0.3	120×	4	SNV, InDels, (SV)
WGS	Whole genome	3.3	30×	4	SNV, InDels, SV, CNV, Fusions
Transcriptome (RNA seq)	Whole cellular RNA or protein coding mRNA	0.3		3	SNV, Fusions

WGS, whole-genome sequencing; SNV, single-nucleotide variant; SV, structural variants; InDels, insertions and deletions; CNV, copy number variant.

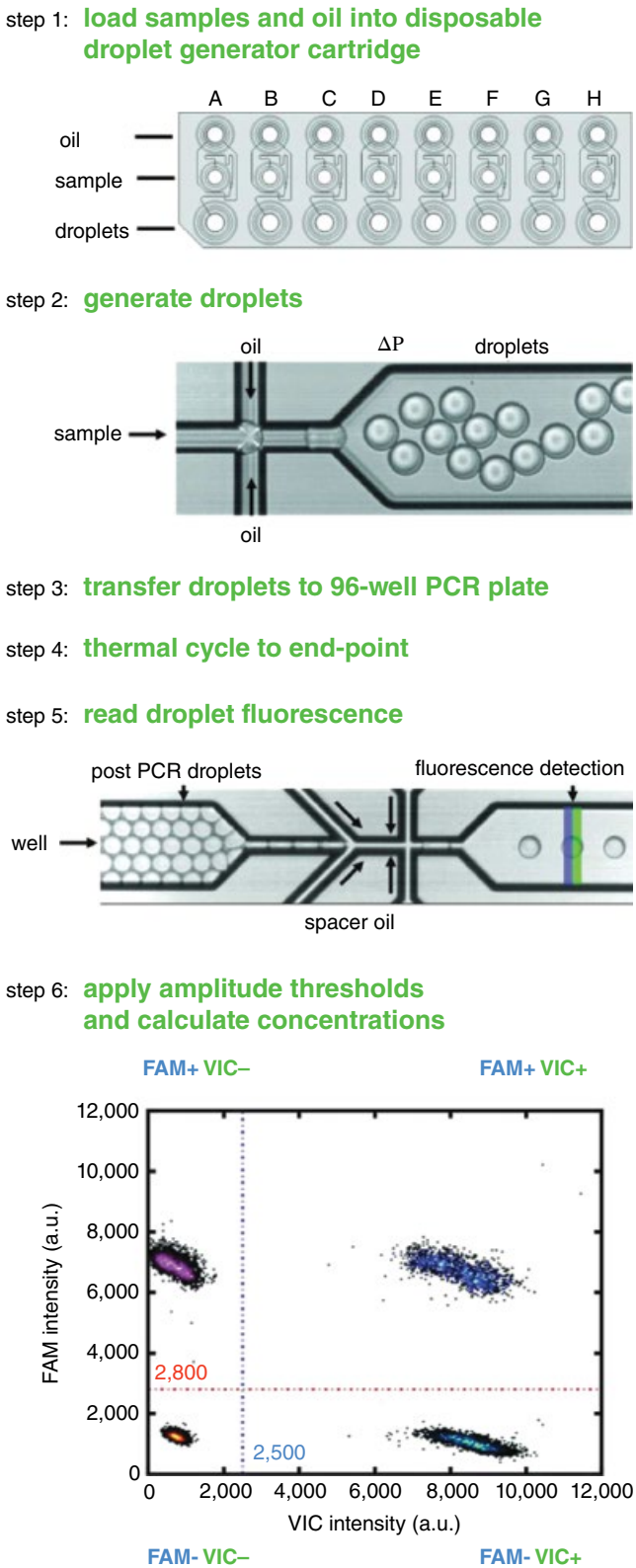

Fig. 13.17. Droplet digital PCR workflow. Step 1: Samples and droplet generation oil are loaded into an eight-channel droplet generator cartridge. Step 2: A vacuum is applied to the droplet well, which draws sample and oil through a flow-focusing nozzle where monodisperse 1 nL droplets are formed. In <2 minutes, eight samples are converted into eight sets of 20 000 droplets. Step 3: The surfactant-stabilized droplets are pipet transferred to a 96-well PCR plate. Step 4: Droplet PCR amplification to end-point (35–45 cycles) is performed in a conventional thermal cycler. Step 5: The plate is loaded onto a reader which sips droplets from each well and streams them in single file past a two-color detector at the rate of ~ 1000 per second. Step 6: Droplets are assigned as positive or negative based on their fluorescence amplitude. The number of positive and negative droplets in each channel is used to calculate the concentration of the target and reference DNA sequences and their Poisson-based 95% confidence intervals. Source: Hindson BJ, et al. *Anal Chem* 2011;83:8604–8610. Adapted with permission from ACS Publication.

TABLE 13.5. WHO (2016): CLASSIFICATION OF MYELOID NEOPLASMS WITH GERMLINE PREDISPOSITION

Myeloid neoplasms with germ line predisposition without a preexisting disorder or organ dysfunction
AML with germline *CEBPA* mutation
Myeloid neoplasms with germline *DDX41* mutation[a]
Myeloid neoplasms with germline predisposition and preexisting platelet disorders
Myeloid neoplasms with germline *RUNX1* mutation[a]
Myeloid neoplasms with germline *ANKRD26* mutation[a]
Myeloid neoplasms with germline *ETV6* mutation[a]
Myeloid neoplasms with germline predisposition and other organ dysfunction
Myeloid neoplasms with germline *GATA2* mutation
Myeloid neoplasms associated with BM failure syndromes
Myeloid neoplasms associated with telomere biology disorders
JMML associated with neurofibromatosis, Noonan syndrome or Noonan syndrome-like disorders
Myeloid neoplasms associated with Down syndrome[a]

[a] Lymphoid neoplasms also reported.

Source: Arber DA, et al. *Blood* 2016;127:2391–2405. Reproduced with permission of *Blood: Journal of the American Society of Hematology*.

polycythemia vera, chronic myeloid leukemia, or following myelodysplastic syndromes (secondary AML [s-AML]).

CLASSIFICATION

The full WHO (2016) classification of the tumors of the hematopoietic and lymphoid tissues is given in Appendix 1. The WHO classification of AML is primarily based on cytogenetics and molecular genetic aberrations (see Appendix 1). The WHO recognizes at the first level of hierarchy seven cytogenetic subgroups of AML, two more diagnosed only by molecular genetics (mutated *NPM1* and bialleleic mutations of *CEBPA*), and two "provisional entities" (with *BCR-ABL1* or with mutated *RUNX1*). The *PML-RARA* fusion usually occurs because of the t(15;17)(q24.1q21.2) rearrangement but may be cryptic or result from other complex cytogenetic rearrangements, so all these cases are classed together as acute promyelocytic leukemia (APL) with *PML-RARA* for treatment purposes. Similarly the provisional rare group with *BCR-ABL1* fusion is added as these cases may respond to tyrosine kinase inhibitor therapy.

Morphological appearances are important in classification and can correlate with specific cytogenetic types. Certain germline mutations may predispose to AML as well as to other myeloid neoplasms (Table 13.5).

CLINICAL FEATURES

AML manifests with features of bone marrow failure (anemia, infections, easy bruising, or hemorrhage) and may or may not include features of organ infiltration by leukemic cells. The organs usually involved are the spleen, liver, skin, and other tissues (Figs. 13.18 and 13.19). Infiltration of the skin that manifests as a widespread, raised, non-itchy hemorrhagic rash and swelling of the gums are characteristic of the monoblastic/monocytic subtypes of AML; nodular and localized skin infiltrates may also occur (Figs. 13.20 and 13.21). Occasionally, patients show Sweet syndrome (acute febrile neutrophilic dermatitis), which occurs in other malignant diseases (Fig. 13.22).

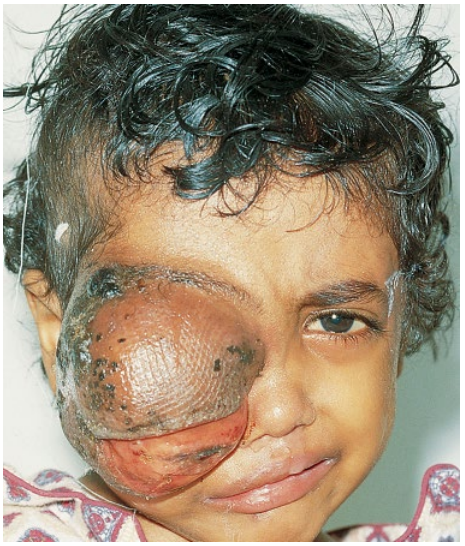

Fig. 13.18. Acute myeloid leukemia: Chloroma of the eye in a 12-year-old girl with AML.

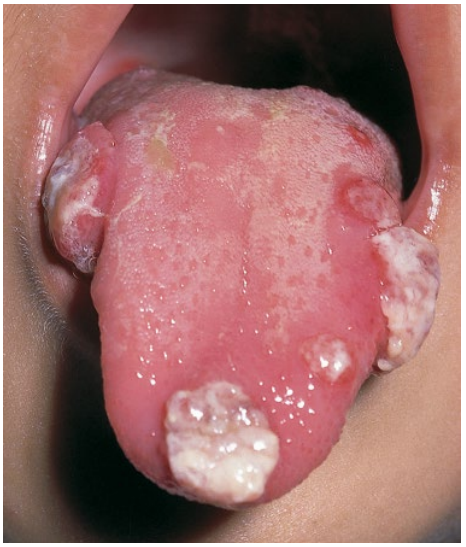

Fig. 13.19. Acute myeloid leukemia: Raised lesions on the tongue caused by deposits of leukemic blasts in a 41-year-old man with AML.

Infections are often bacterial in the early stages and particularly affect the skin (Figs. 13.23 and 13.24), pharynx, and perianal (Fig. 13.25) and perineal (Fig. 13.26) regions. Bacterial infections may lead to the adult respiratory distress syndrome (Fig. 13.27). Fungal infections are particularly common in patients with prolonged periods of neutropenia, who have undergone multiple courses of chemotherapy and antibiotic therapy (Figs. 13.28–13.32).

Viral (especially herpetic) and protozoal infections are frequent, particularly in the mouth, and may become generalized and life threatening (Figs. 13.32–13.34). Hemorrhage of the skin or mucous membranes is usually petechial (Figs. 13.35 and 13.36).

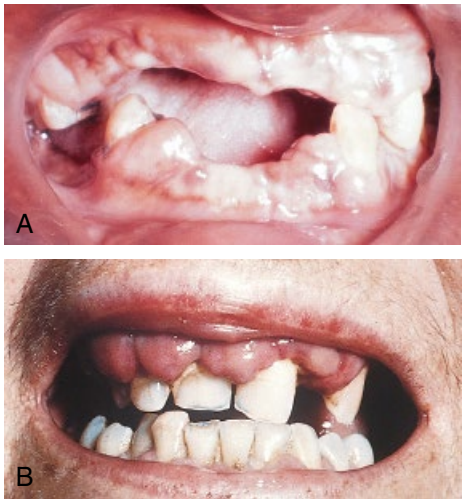

Fig. 13.20. Acute myeloid leukemia, monoblastic subtype. **A, B,** Leukemic infiltration of the gums results in their expansion and thickening, and partial covering of the teeth. (Courtesy of Dr. AR Valentine.)

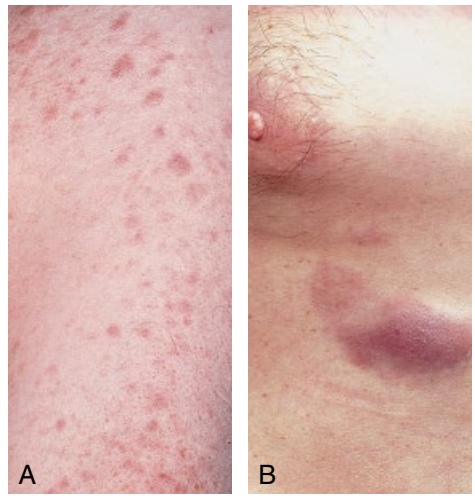

Fig. 13.21. Acute myeloid leukemia, monoblastic subtype. **A,** Multiple, raised, erythematous skin lesions caused by leukemic infiltration. **B,** Close-up view of nodular skin lesion. (Courtesy of Professor HG Prentice.)

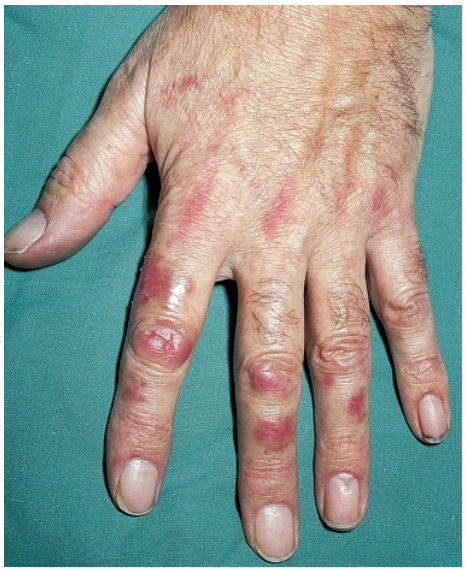

Fig. 13.22. Acute myeloid leukemia: Sweet syndrome (acute febrile neutrophilic dermatosis) in a 62-year-old man with AML myelo-monocytic: bullous pyoderma.

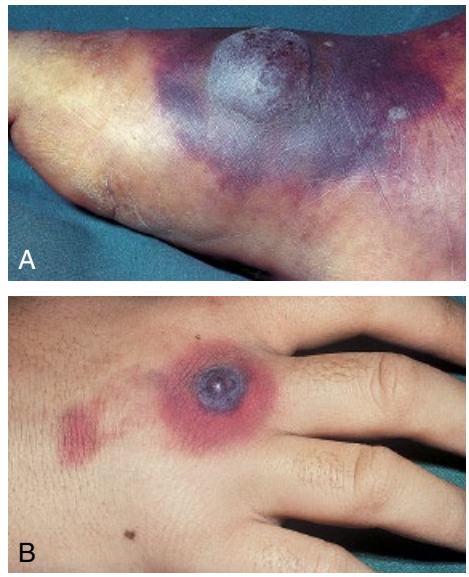

Fig. 13.23. Acute myeloid leukemia. **A,** A purplish black bullous lesion with surrounding erythema caused by infection from *Pseudomonas pyocyanea* on the foot. **B,** Similar but less marked infection on the back of the hand.

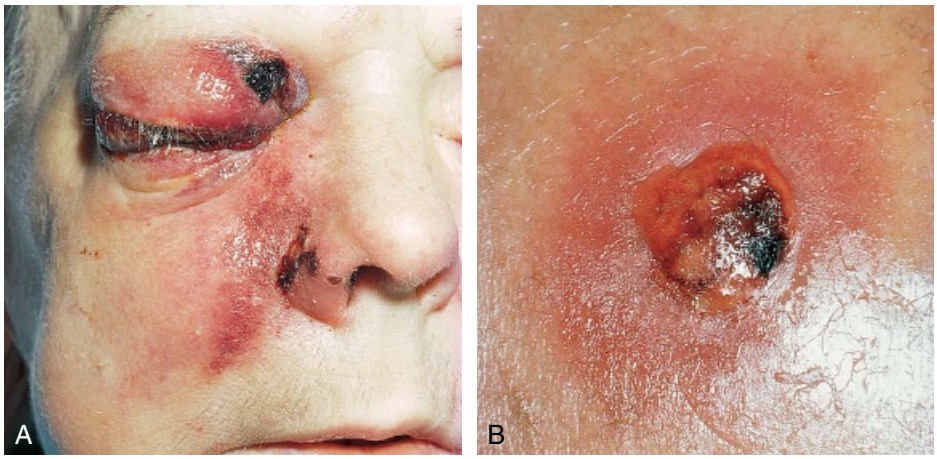

Fig. 13.24. Acute myeloid leukemia: *Staphylococcus aureus* was isolated from **(A)** infection of the right orbit and surrounding tissue and **(B)** a necrotic erythematous skin ulcer.

MICROSCOPIC APPEARANCES

The microscope provides the initial suspicion that AML is present and may be sufficient to make a diagnosis. Immunophenotyping, cytogenetic, and molecular genetic tests then confirm the diagnosis of AML, ascribe the patient to one or other subtype and provide prognostic information. This is also indicated by the history of the patient which might reveal: (i) therapy-related AML following chemotherapy and/or radiotherapy, (ii) pre-phase of myelodysplastic syndrome (MDS) or a myeloproliferative neoplasm, or (iii) myeloid neoplasms with germline predisposition, which lead to individual subgroups of AML.

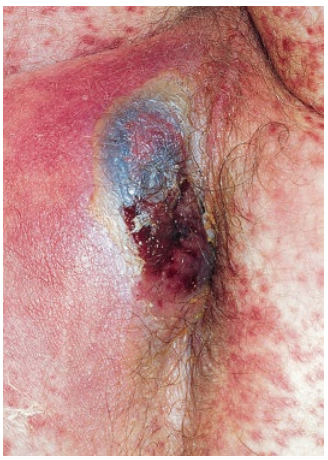

Fig. 13.25. Acute myeloid leukemia: This perianal lesion was found to be the result of a mixed infection by *Escherichia coli* and *Streptococcus faecalis*.

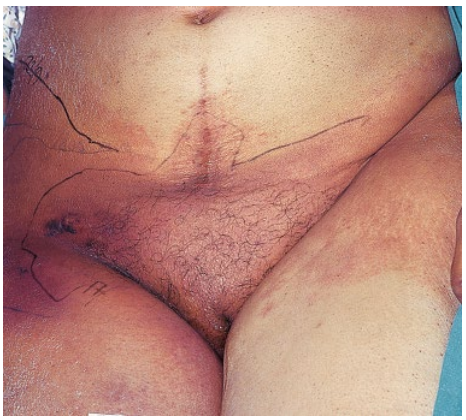

Fig. 13.26. Acute myeloid leukemia: Cellulitis of the perineum, lower abdomen, and upper thighs caused by *Pseudomonas pyocyanea*.

WHO 2016 SUBGROUPS

AML with Recurrent Genetic Abnormalities

Figures 13.37–13.42 show the morphological features that correlate with the first three cytogenetic subtypes. In AML with t(8;21); *RUNX1-RUNX1T1*, the morphology is in nearly all cases without (10%) or with maturation (90%). In many cases dysgranulopoiesis is detected, with some normal eosinophils and single, needle-like Auer rods in the blasts. The differential is difficult and blasts may also be below 20% of all cells (Fig. 13.37). Inv(16) or t(16;16); *CBFB-MYH11* AML is a type of myelomonocytic leukemia with abnormal eosinophils containing basophilic granules (Fig. 13.38). For *PML-RARA*-positive acute promyelocytic leukemia (APL), detection of the molecular

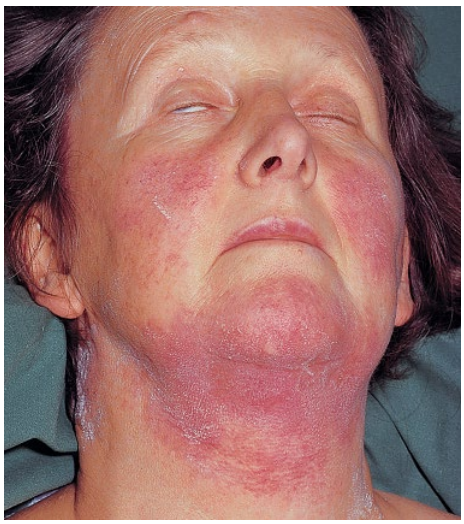

Fig. 13.28. Acute myeloid leukemia: Spreading cellulitis of the neck and chin resulting from mixed streptococcal and candidal infection, previous chemotherapy, and prolonged periods of neutropenia.

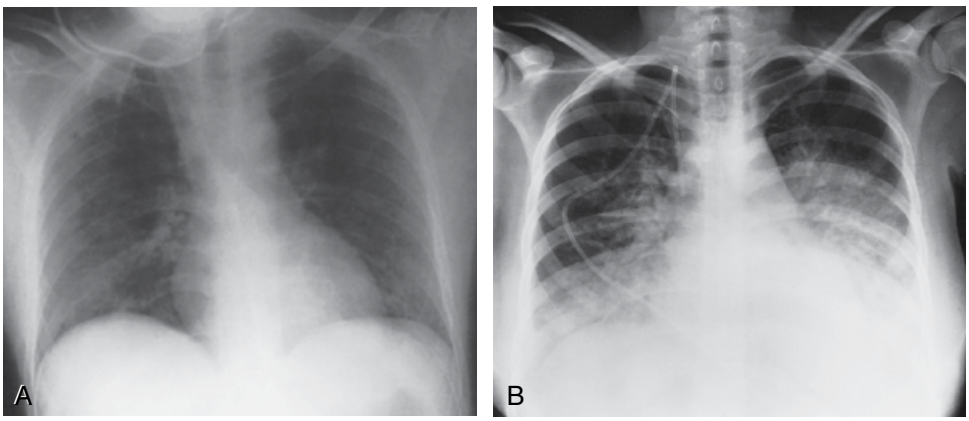

Fig. 13.27. Acute myeloid leukemia. **A,** Chest radiograph of 22-year-old man showing widespread interstitial shadowing resulting from adult acute respiratory distress syndrome associated with *Streptococcus mitis* infection during induction therapy. **B,** Interstitial shadowing in lower and middle zones bilaterally in a 23-year-old woman with septicemia from *Pseudomonas pyocyanea* following chemotherapy. She developed a fatal adult respiratory distress syndrome.

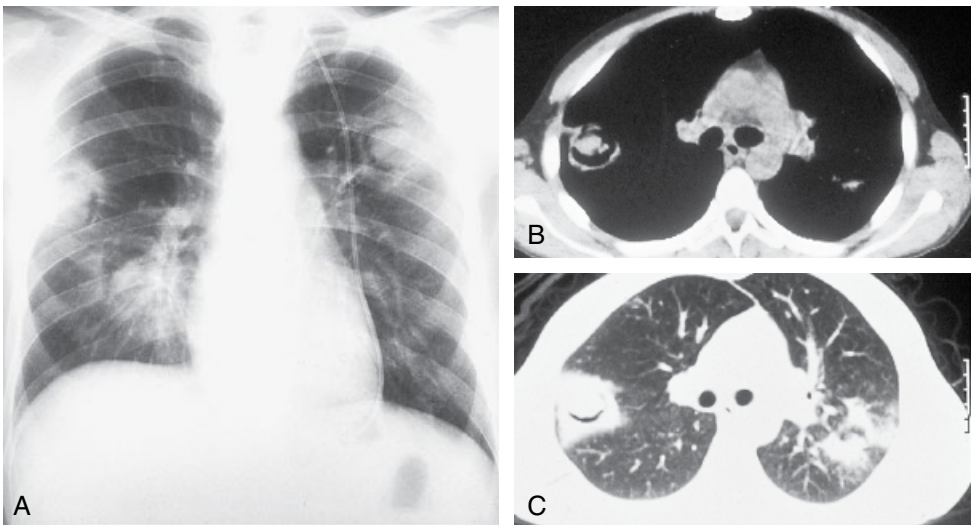

Fig. 13.29. Acute myeloid leukemia: This 32-year-old-man had received repeated chemotherapy for refractory disease. Three pulmonary mycotic cavities are visible. **A,** Radiograph. **B, C,** Computed tomography (CT) scans. (B, C, Courtesy of Dr. AR Valentine.)

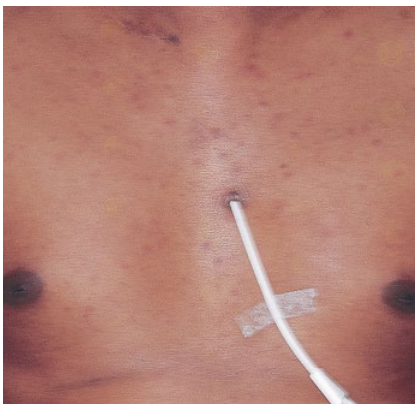

Fig. 13.30. Acute myeloid leukemia: Candidal septicemia. Typical skin rash in a 22-year-old Sri Lankan man with severe neutropenia caused by intensive chemotherapy.

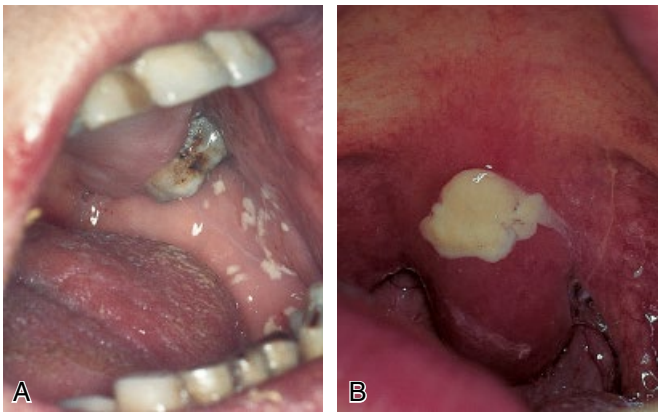

Fig. 13.32. Acute myeloid leukemia. **A,** Plaques of *Candida albicans* in the mouth, with a lesion of herpes simplex on the upper lip. **B,** Candidal plaque on the soft palate.

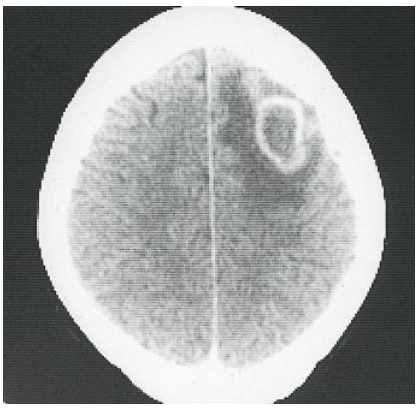

Fig. 13.31. Acute myeloid leukemia: CT scan showing encapsulated brain lesion in right frontal zone caused by aspergillosis infection with surrounding hypodense area caused by inflammation.

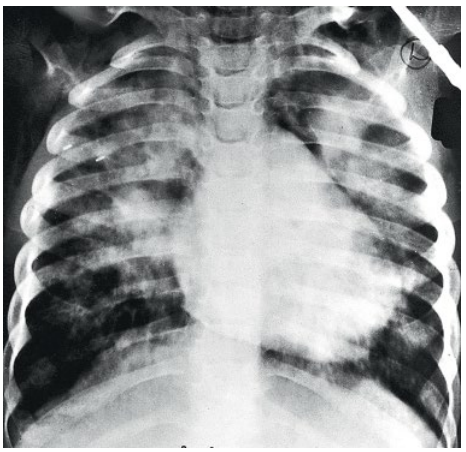

Fig. 13.33. Acute myeloid leukemia: Chest radiograph showing patchy consolidation bilaterally caused by measles infection in a child. (Courtesy of Professor JM Chessells.)

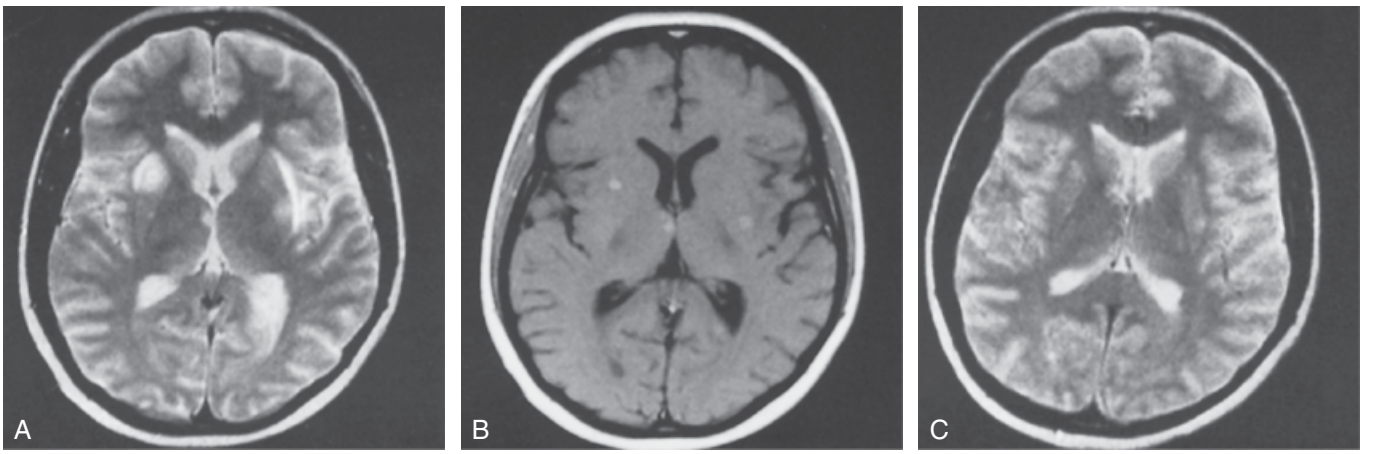

Fig. 13.34. Acute myeloid leukemia. **A, B,** Magnetic resonance imaging scans showing multiple small opacities. The patient, a 23-year-old woman, complained of headaches and diplopia. **C,** The diagnosis of toxoplasmosis was made, and she responded rapidly to antitoxoplasmosis therapy.

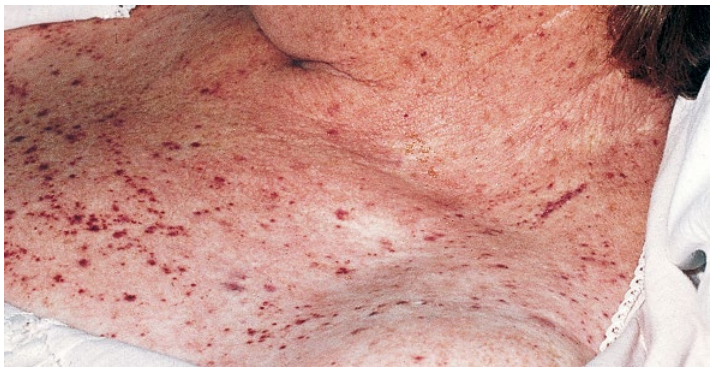

Fig. 13.35. Acute myeloid leukemia: petechial hemorrhages covering the upper chest and face in severe thrombocytopenia.

Fig. 13.36. Acute myeloid leukemia. **A,** Marked ecchymoses, petechial hemorrhages, and bruises over the groin and thigh. **B,** Close-up view of petechial hemorrhages over the leg.

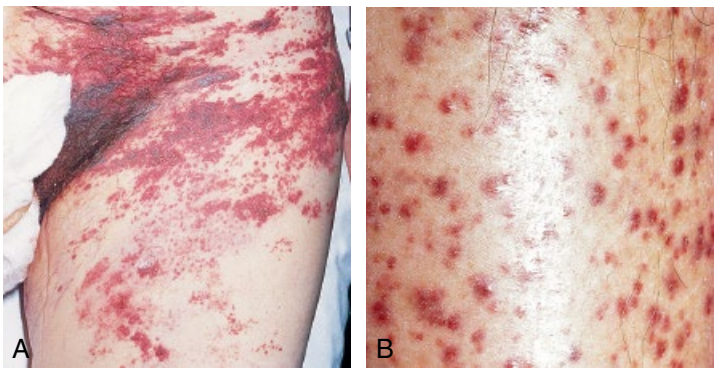

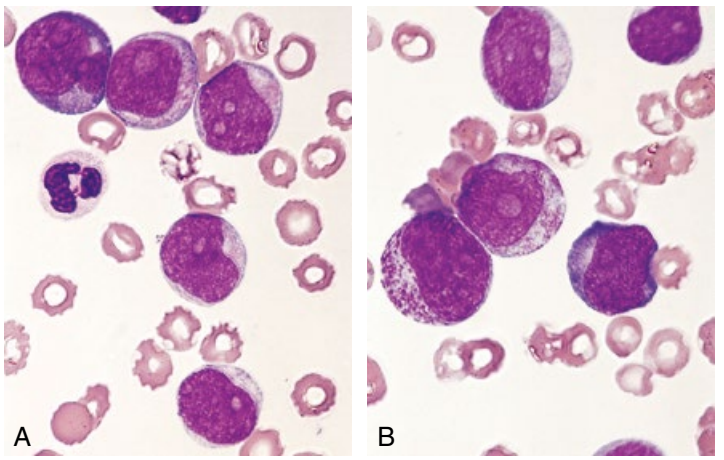

Fig. 13.37. Acute myeloid leukemia, t(8;21) subtype: **A,** Bone marrow aspirates showing myeloblasts with promyelocytes with azurophilic granules also present. **B,** Blast cells with folded nuclei, one or two nucleoli, and occasional Auer rods.

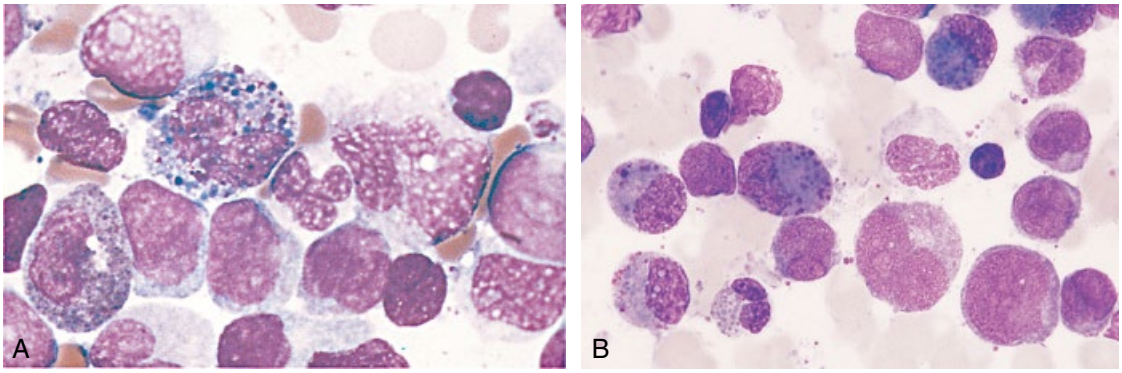

Fig. 13.38. Acute myeloid leukemia, inv(16) subtype. **A, B,** Blast cells, abnormal myelomonocytic cells, and eosinophils with basophilic granules.

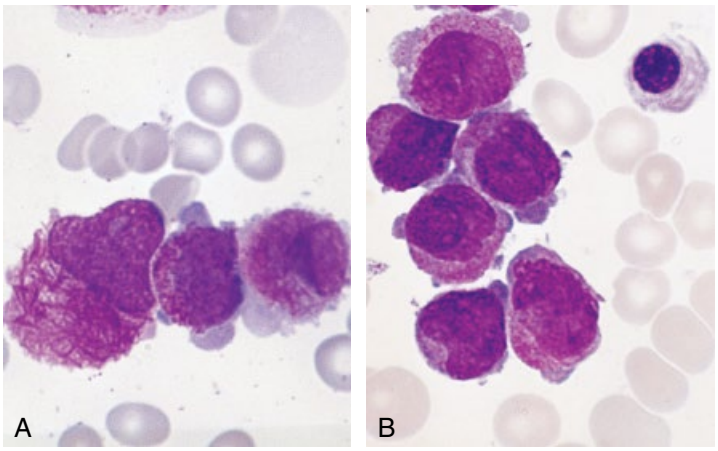

Fig. 13.39. Acute promyelocytic leukemia, t(15;17) subtype. **A, B,** Promyelocytes containing coarse azurophilic granules, and bundles of Auer rods ("faggots") in **(A)**. The nuclei contain one or two nucleoli.

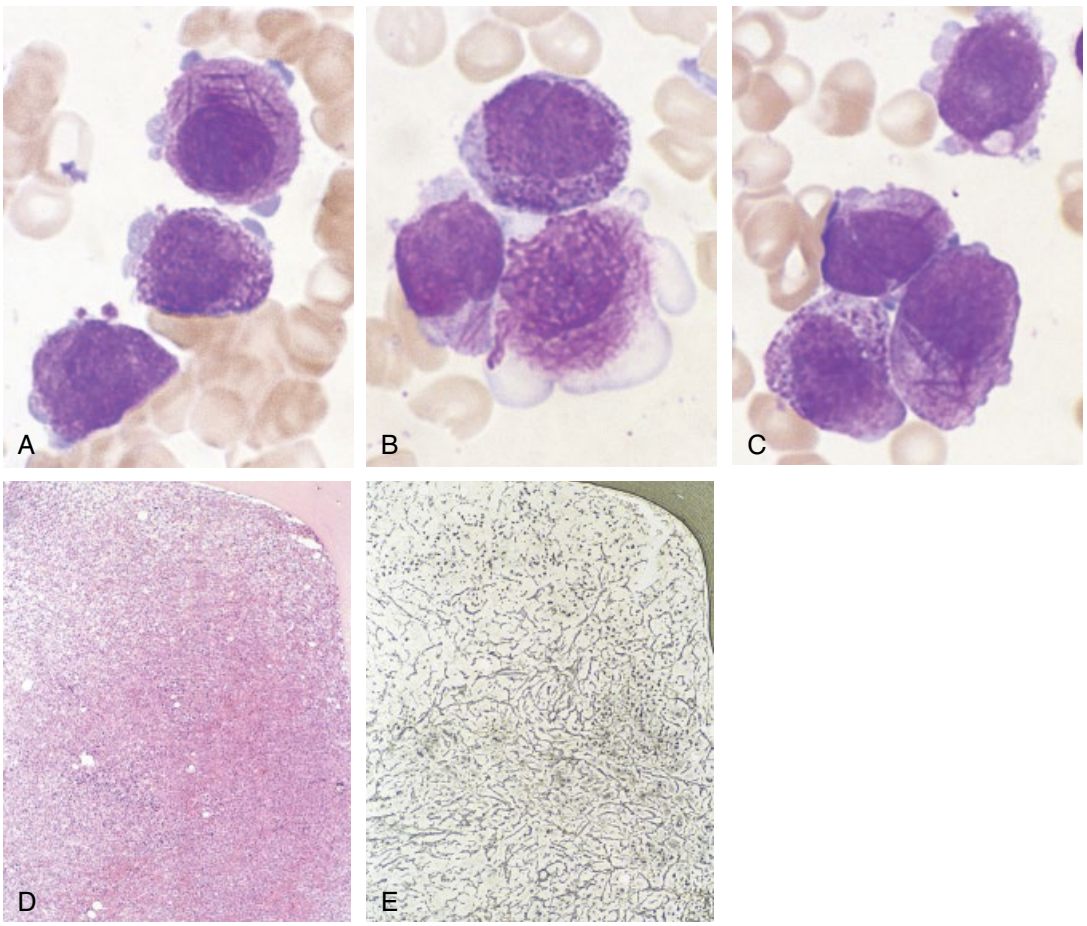

Fig. 13.40. Acute promyelocytic leukemia, t(15;17) subtype. **A–E,** A further case showing promyelocytes with multiple Auer rods. The intertrabecular space is replaced by primitive myeloid cells. Reticulin increased (grade I fibrosis).

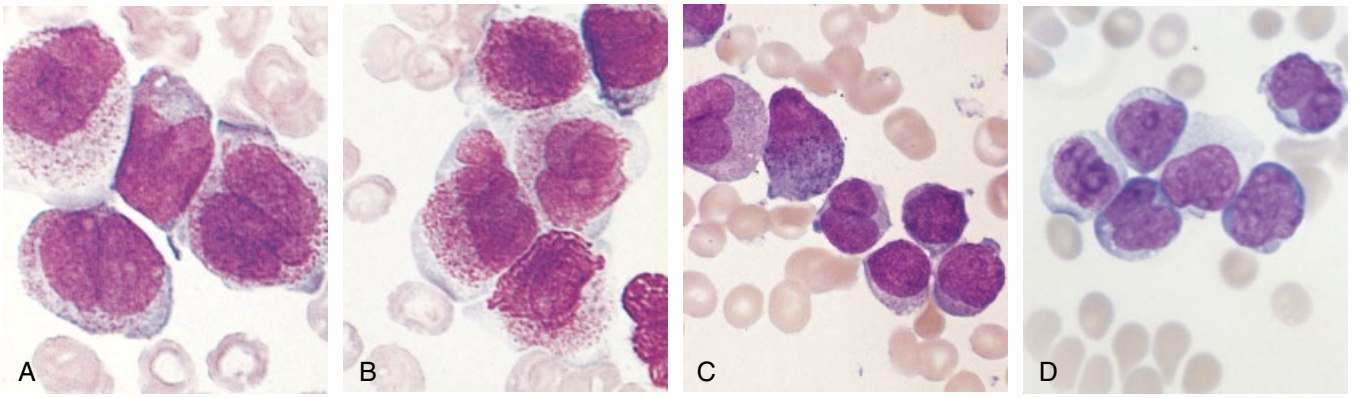

Fig. 13.41. Acute promyelocytic leukemia, t(15;17) subtype. **A–D,** Microgranular variant. The usually bilobed cells contain numerous small azurophilic granules. (C, D, Courtesy of Professor JM Bennett.)

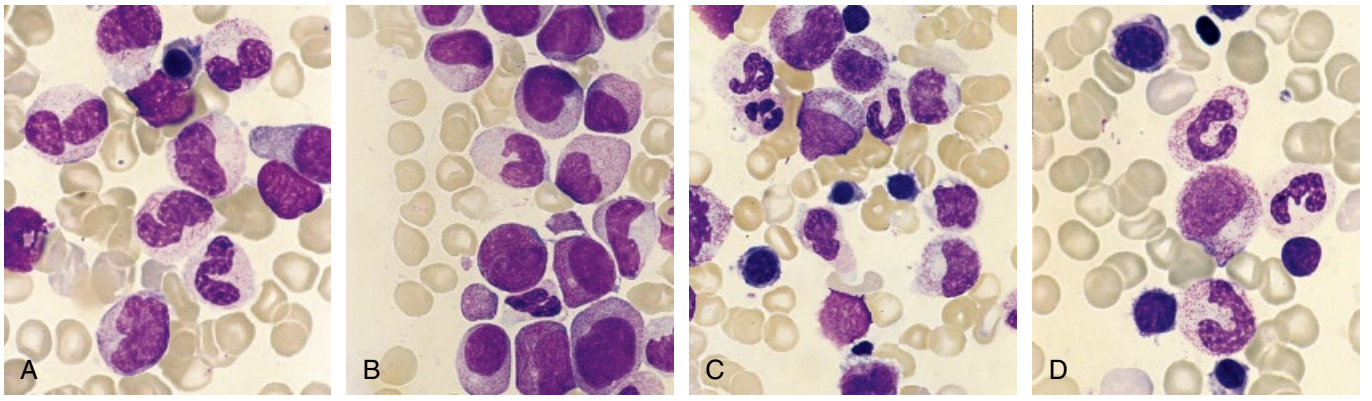

Fig. 13.42. Acute promyelocytic leukemia, t(15;17) subtype. **A–D,** Differentiation of myeloblasts into myelocytes and neutrophils during treatment with all-*trans* retinoic acid (ATRA). Abnormal myelocytes and neutrophils containing Auer rods are seen. (Courtesy of Professor MT Daniel.)

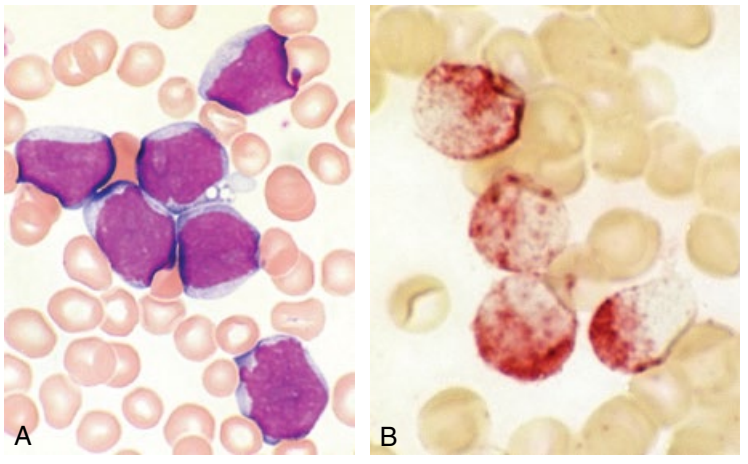

Fig. 13.43. Acute myeloid leukemia, t(9;11) (p22;q23) (*KMT2A* rearranged). **A,** Monoblastic with over 80% blasts in the marrow. **B,** Nonspecific esterase-positive confirming monocytic lineage. FISH showed disruption of *KMT2A* gene in 96% of interphase nuclei analyzed. The patient was a 24-year-old man with no previous chemotherapy or radiotherapy.

abnormality is sufficient for diagnosis. The t(15;17); *PML-RARA* APL has two quite different morphologic appearances: (i) promyelocytic subtype (Figs. 13.39–13.40). This typical form shows bundles of Auer rods ("faggot" cells), which are aggregates of granules and can be seen in May-Grünwald–Giemsa (MGG) staining and in myeloperoxidase staining. The variant form of APL is also named microgranular variant (Fig. 13.41). These blasts at a first view appear from the monocytic lineage with bilobed nucleus, but are strongly myeloperoxidase positive (as APL) and nonspecific esterase negative (monocytes are positive). All blasts in APL contain procoagulant material, which, when released into the circulation, causes disseminated intravascular coagulation. APL treatment with all-*trans* retinoic acid (ATRA) and/or AS203 produces differentiation of the blasts (Fig. 13.42), often with full remission and cure being obtained. All cases with the cytogenetic or molecular findings t(8;21), inv(16), or t(15;17) are automatically called AML. The blast counts do not need to exceed 20%.

AML with t(9;11) (p22;q23); *MLL3-KMT2A* in many cases show myelomonocytic or monoblastic appearance (Fig. 13.43).

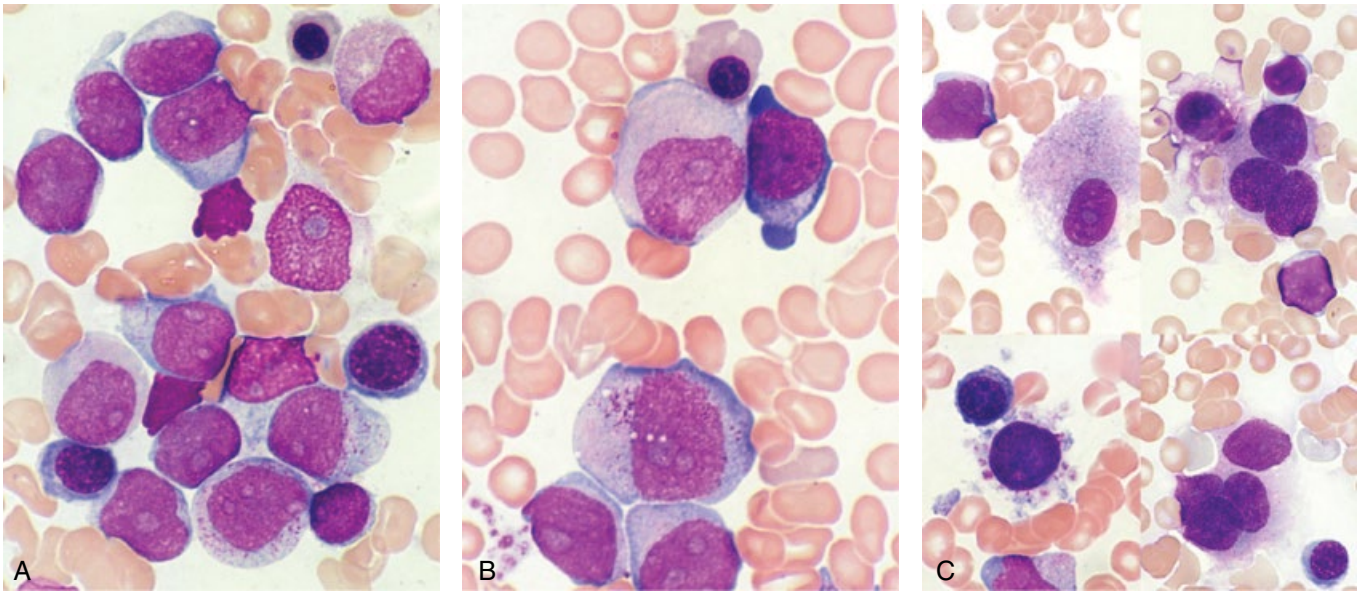

Fig. 13.44. A–C, Acute myeloid leukemia with multilineage dysplasia. **A,** Myeloblasts, many with Auer rods. Dysplastic changes in granulopoiesis erythropoiesis and megakaryocytes. The patient was a 68-year-old woman with no previous history of myelodysplasia.

TABLE 13.6. CYTOGENETIC ABNORMALITIES SUFFICIENT TO DIAGNOSE AML WITH MYELODYSPLASIA-RELATED CHANGES WHEN ≥20% PB OR BM BLASTS ARE PRESENT AND PRIOR THERAPY HAS BEEN EXCLUDED

Complex karyotype (3 or more abnormalities)
Unbalanced abnormalities
–7/del(7q)
del(5q)/t(5q)
i(17q)/t(17p)
–13/del(13q)
del(11q)
del(12p)/t(12p)
idic(X)(q13)
Balanced abnormalities
t(11;16)(q23.3;p13.3)
t(3;21)(q26.2;q22.1)
t(1;3)(p36.3;q21.2)
t(2;11)(p21;q23.3)
t(5;12)(q32;p13.2)
t(5;7)(q32;q11.2)
t(5;17)(q32;p13.2)
t(5;10)(q32;q21.2)
t(3;5)(q25.3;q35.1)

Source: Arber DA, et al. *Blood* 2016;127:2391–2405. Reproduced with permission of *Blood: Journal of the American Society of Hematology*.

AML with Myelodysplasia-Related Changes

This category of poor-prognosis AML is based on specific cytogenetic findings and/or dysplasia in two or three lineages (Fig. 13.44). This presentation is more common in the elderly. Patients present without a history of previous myelodysplasia.

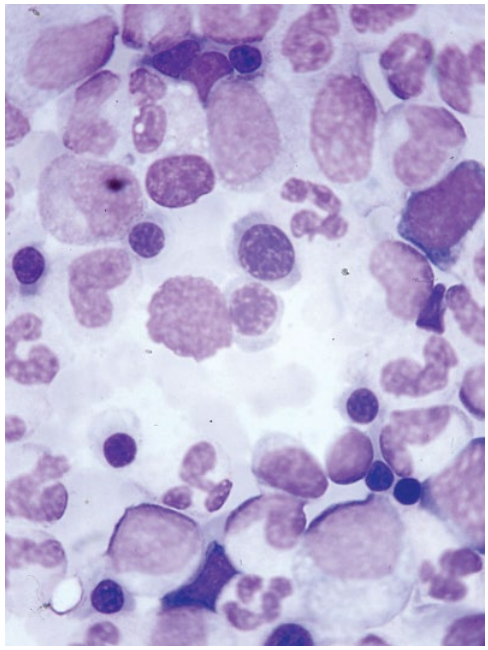

Fig. 13.45. Acute myeloid leukemia, t(8;13) after topoisomerase inhibitor therapy. Myeloblasts and abnormal monocytes and neutrophils are present. (Courtesy of Professor BA Bain.)

The cytogenetic findings for this category of AML are listed in Table 13.6. Dysplasia has to be detectable in ≥50% cells in at least two cell lineages. If *NPM1* or *CEBPA* double mutations are present, the classification is as AML with these mutations, irrespective of dysplasia, for which the prognosis is more favorable.

Therapy-Related Myeloid Neoplasms

These cases may be divided into t-MDS or t-AML. The genetics are similar. *KMT2A* (previously called *MLL*) rearrangements are frequent after topoisomerase therapy with etoposide (Fig. 13.45).

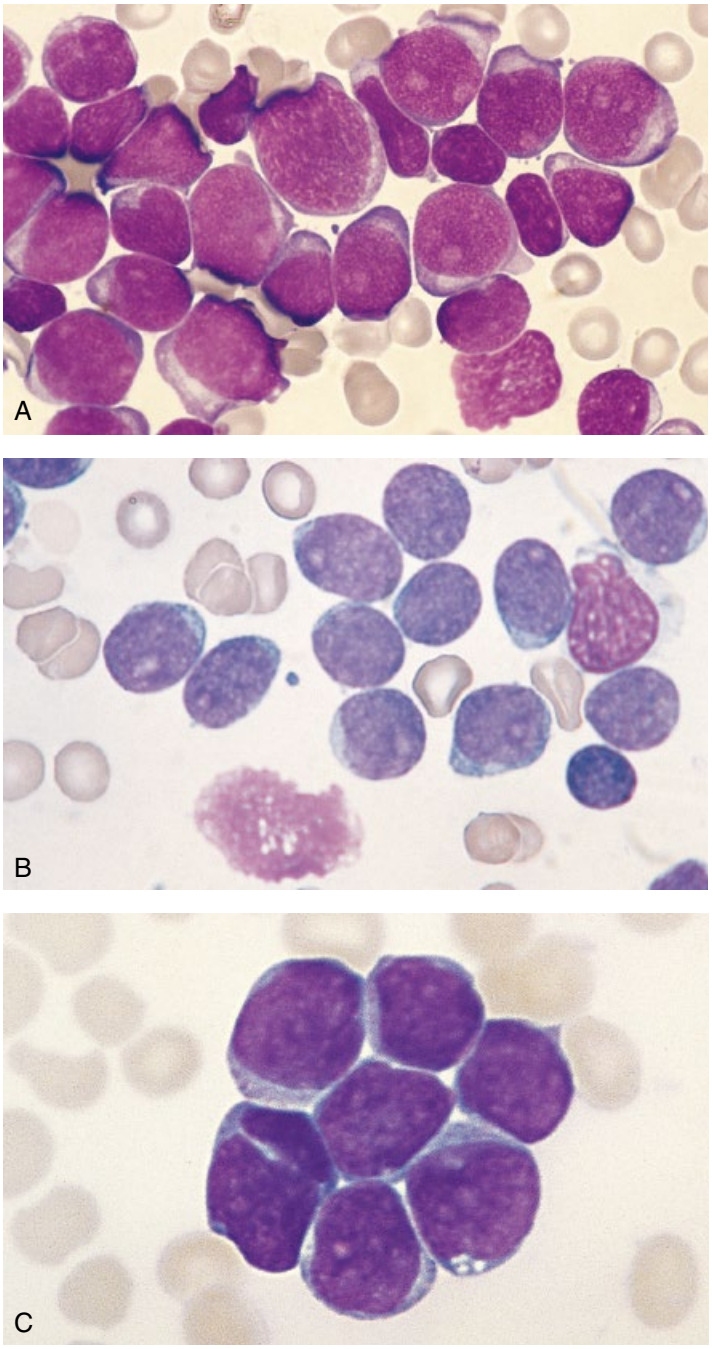

Fig. 13.46. Acute myeloid leukemia minimally differentiated subtype. **A–C,** Bone marrow aspirates showing large blasts resembling ALL. Granules are absent, myeloperoxidase and Sudan black staining negative, CD13 and/or CD33 positive; myeloperoxidase is positive by electron microscopy or immunocytochemistry. TdT may be positive. (Courtesy of Dr. MT Daniel, Professor JM Bennett, and Dr. AB Mehta.)

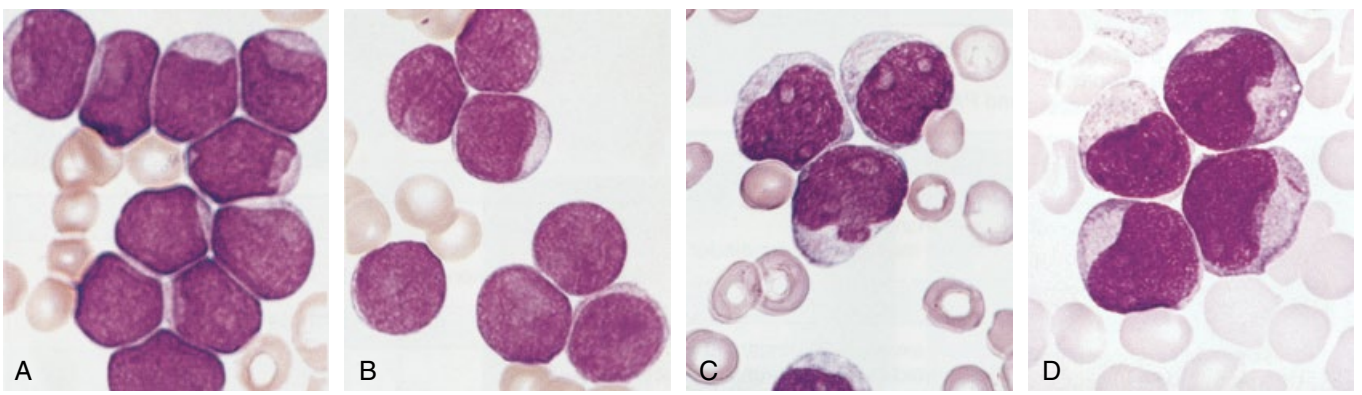

Fig. 13.47. Acute myeloid leukemia without differentiation subtype. **A,** Bone marrow aspirates showing blasts with large, often irregular nuclei with one or more nucleoli, and with varying amounts of eccentrically placed cytoplasm. Either no definite granulation is present or a few azurophilic granules and occasional Auer rods can be seen. **B–D,** At least 3% of cells stain with Sudan black or myeloperoxidase.

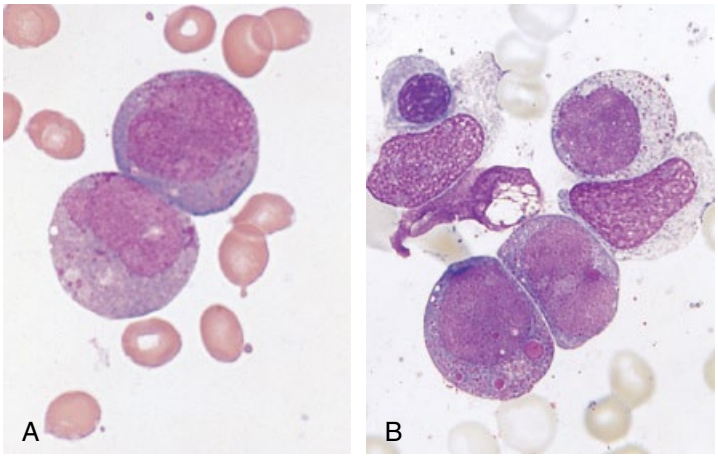

Fig. 13.48. Acute myeloid leukemia with differentiation subtype. **A, B,** Unusual large, vacuolated inclusions (pseudo-Chédiak–Higashi) are present in blast cells. (Courtesy of Dr. D Swirsky.)

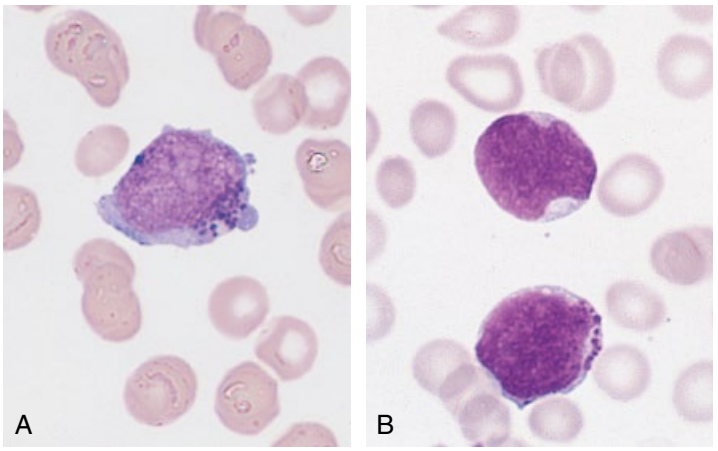

Fig. 13.49 Acute myeloid leukemia with differentiation subtype: Rare basophilic differentiation (peripheral blood). (Courtesy of Professor D Catovsky.)

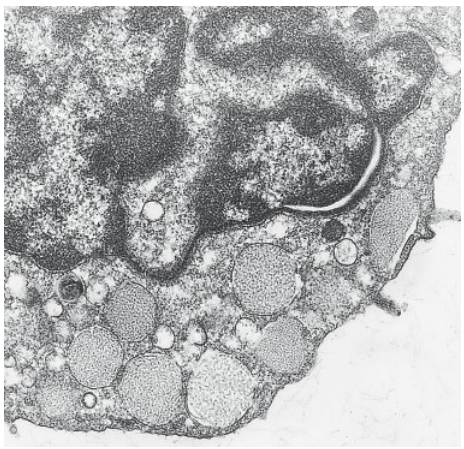

Fig. 13.50. Acute myeloid leukemia: Ultrastructure of the blasts shown in Fig. 13.49. Cytoplasmic granules show stippled pattern. (Courtesy of Professor D Catovsky.)

Some of these cases also show germline mutations in cancer-susceptibility genes (Table 13.5).

AML Not Otherwise Specified

All other cases (not being with recurrent genetic abnormalities, AML with myelodysplasia-related changes, or t-AML) are classified according to phenotypic appearance. On MGG staining the minimally differentiated subclass is the least differentiated (Fig. 13.46) and can only be diagnosed with certainty after immunophenotyping or immunocyto-/histochemistry. Cases without maturation show agranular and granular blasts (Fig. 13.47). The subclass with maturation shows definite differentiation to promyelocytes in ≥10% of all cells (Fig. 13.48). Rare subtypes show abnormal metachromatic granules (Fig. 13.49) with or without basophilic granules (Figs. 13.50 and 13.51).

Acute myelomonocytic leukemia shows a mixture of blasts with promyelocytic or with monocytic differentiation, the monocytic cells consisting of less than 80% of the total (Figs. 13.52 and 13.53).

Acute monoblastic leukemia (Fig. 13.54) shows over 80% monoblasts. The monocytic type shows more differentiated promonocytes or monocytic cells. An unusual subtype with myelomonocytic features often shows erythrophagocytosis and a strong myeloperoxidase as well as nonspecific esterase concomitantly in the same cells (Figs. 13.55 and 13.56). These cases often are t-AML and bear the t(8;16); *MYST3-CBP* translocation.

The cytomorphologic subclass of acute erythroid leukemia has been newly defined in the WHO 2016 classification. In this subclass ≥50% of bone marrow cells are erythroid precursors, in some cases with bizarre dyserythropoietic forms. Furthermore, ≥20% of myeloid blasts are detectable among all nucleated cells (same as for all other AML definitions). Features of myelodysplasia may also be present in other cell lineages. In the pure erythroid form over 80% of the cells are erythroid and myeloid blasts are rare (Figs. 13.57 and 13.58).

Acute megakaryoblastic leukemia is rare, more common in children than in adults. It is often associated with fibrosis of the marrow (Figs. 13.59 and 13.60) and is recognized by the

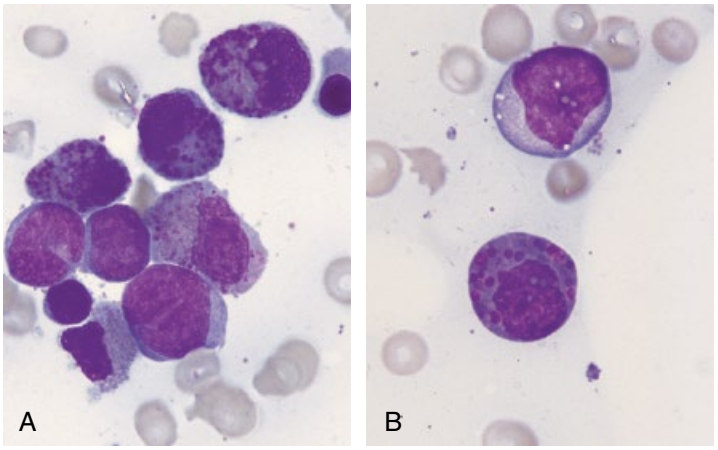

Fig. 13.51. Acute myeloid leukemia with differentiation, rare subtype. **A,** With abnormal eosinophils, three myeloblasts, and four abnormal eosinophils with metachromatic granules. **B,** Neoplastic myelocyte with coarse basophilic and eosinophilic granulation but with no inv(16) detectable. (Courtesy of Dr. K van Poucke and Professor M Peetermans.)

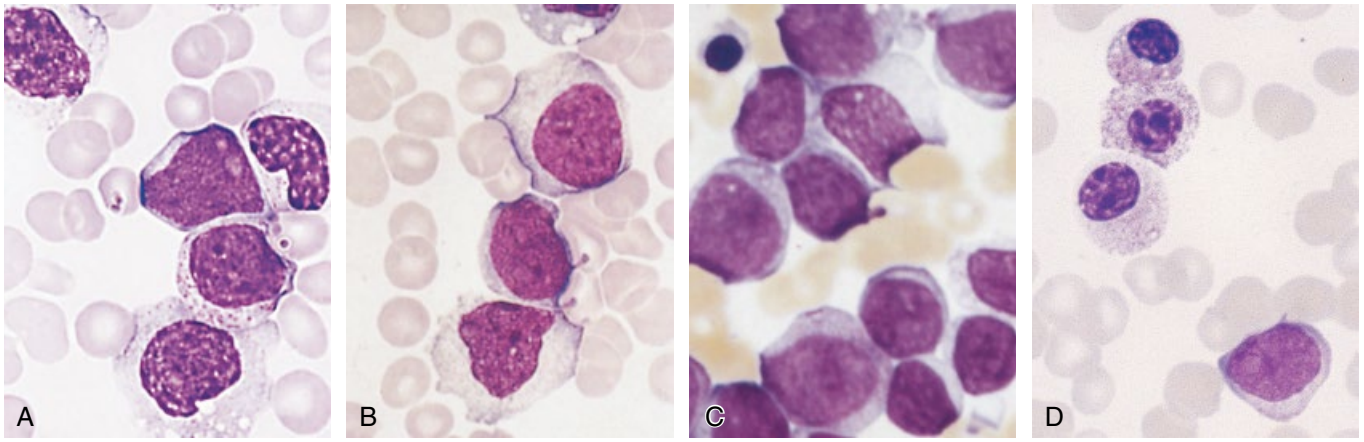

Fig. 13.52. Acute myeloid leukemia, myelomonocytic subtype but with no inv(16) detectable. **A–C,** Blast cells contain cytoplasmic granules (myeloblasts and promyelocytes) or pale cytoplasm with occasional vacuoles and granules, and folded or rounded nuclei (monoblasts). **D,** Abnormal pseudo-Pelger forms may occur.

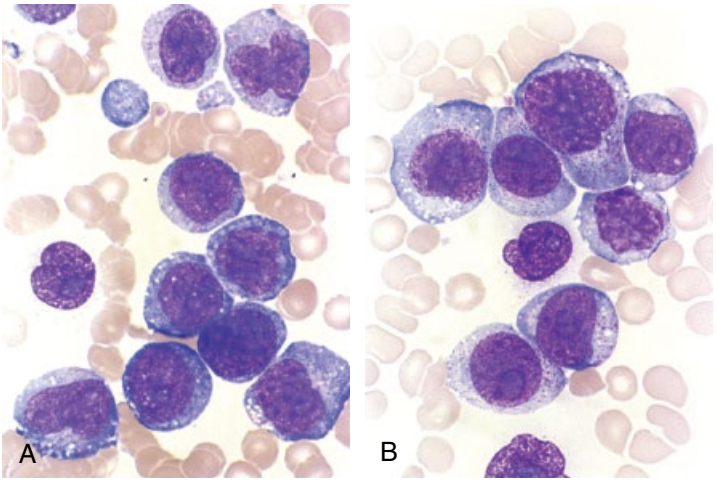

Fig. 13.53. Acute myeloid leukemia, myelomonocytic subtype: Mixture of blast cells with features of primitive myeloid and monocytic cells; CD13 and CD33 were positive.

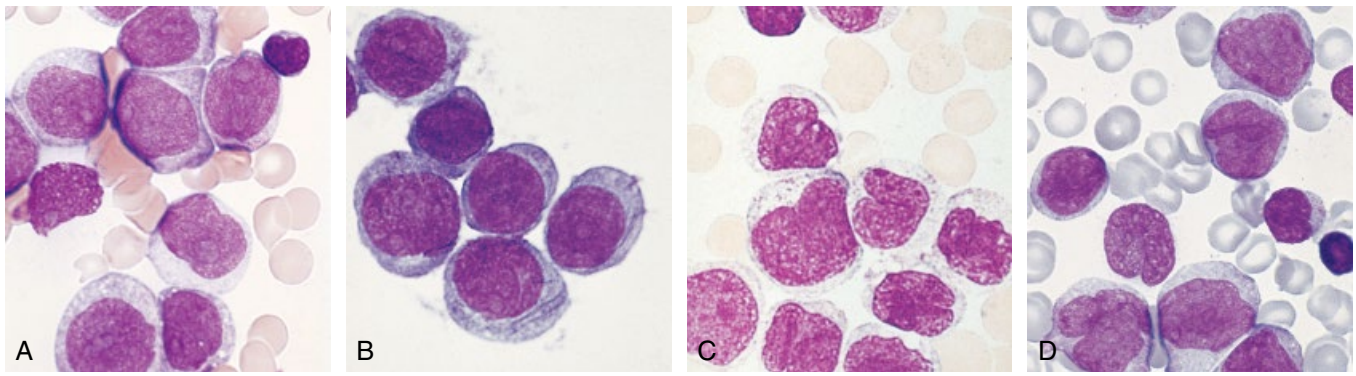

Fig. 13.54. Acute leukemia, monoblastic and monocytic subtype: Blast cells with pale cytoplasm or perinuclear "haloes" and cytoplasmic vacuoles but only occasional granules. Their usually centrally placed nuclei are folded, rounded, or kidney shaped. **A, B,** Monoblastic subtype: 80% of the cells are monoblasts. **C, D,** Monocytic subtype: less than 80% of the cells are monoblasts. The remaining cells are promonocytes and monocytes. The cells in **(B)** show ribosome lamellar complexes. (B, D, Courtesy of Professor D. Catovsky.)

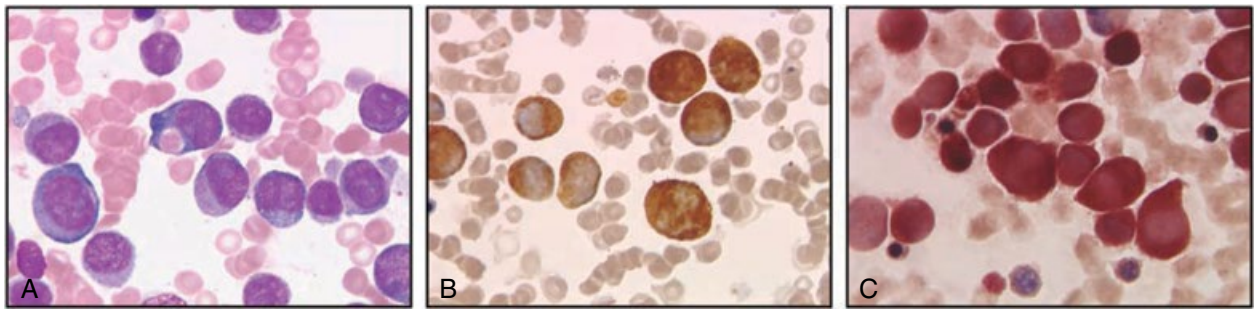

Fig. 13.55. Cytomorphology of a typical case of acute myeloid leukemia (AML) with t(8;16). Bone marrow smears are displayed according to **A,** May–Gruenwald–Giemsa (MGG) staining. **B,** Myeloperoxidase (MPO) staining. **C,** Non-specific esterase (NSE) staining.

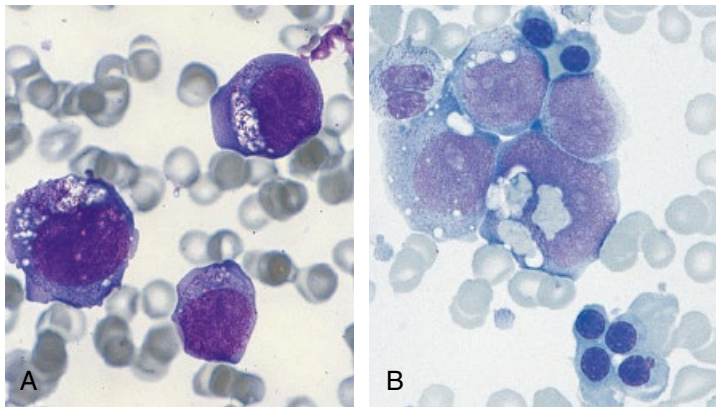

Fig. 13.56. Acute myelomonocytic/monoblastic leukemia subtype with erythrophagocytosis and t(8;16). **A,** In this case the blasts were of the myelomonocytic subtype. A bleeding diathesis with features of fibrinolysis (not disseminated intravascular coagulation as in APL) is often present. (Courtesy of Professor D. Catovsky.) **B,** Child with AML and t(8;16) showing erythrophagocytosis. (Courtesy of Dr. D Swirsky.)

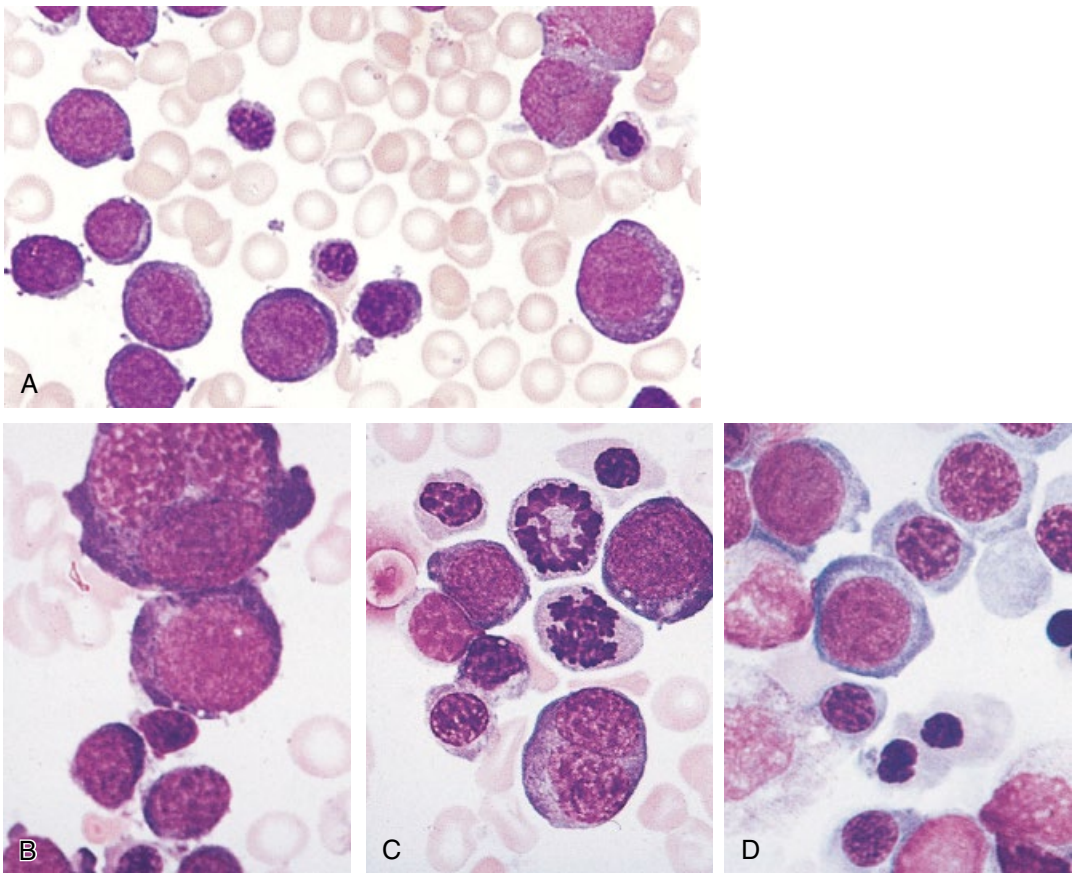

Fig. 13.57. Acute erythroid leukemia subtype. **A,** There is a preponderance of erythroid cells at all stages of development. **B–D,** High-power views of bone marrow aspirate showing erythroid predominance with many dyserythropoietic features, such as multinucleate cells (gigantoblasts), vacuolated cytoplasm, abnormal mitoses, and megaloblastic nuclei.

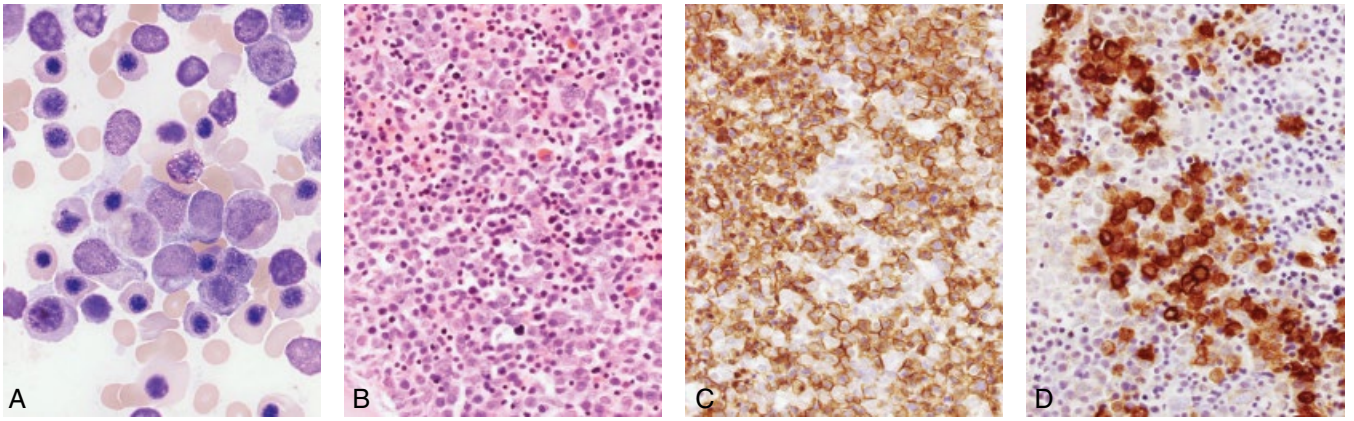

Fig. 13.58. Acute erythroid leukemia, erythroid/myeloid. **A,** Bone marrow aspirate, predominance of erythroid cells, many with dyserythropoietic features: large, paler myeloblasts, one with an Auer rod also present. **B–D,** Bone marrow trephine biopsy: **B,** Hypercellularity with a mixture of smaller, densely straining erythroblasts and pale, larger myeloblasts. **C,** Anti-glycophorin immunostain shows erythroid cells positive, myeloblasts negative. **D,** Myeloperoxidase stain shows myeloblasts positive, erythroid cells negative. (Courtesy of Dr.W Erber.)

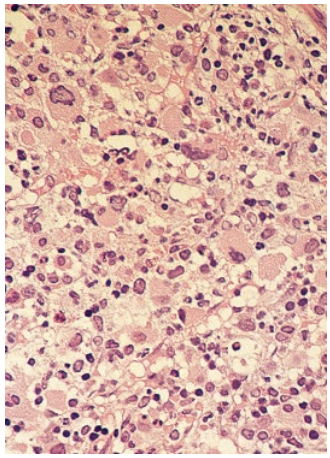

Fig. 13.59. Acute megakaryoblastic leukemia, megakaryoblastic subtype: Bone marrow trephine biopsy showing large blasts with amorphous pink cytoplasm interspersed with residual small hematopoietic cells.

appearance of the blasts but needs confirmation by flow cytometry or immunohistochemistry. Other rare types of AML included in the WHO 2016 classification are acute basophilic leukemia (Fig. 13.61), acute panmyelosis with myelofibrosis (Fig. 13.62), and myeloid sarcoma (Fig. 13.63). Not included is acute eosinophilic leukemia (Fig. 13.64). Hemophagocytosis by myeloid blasts is an infrequent finding in several subgroups (Fig. 13.65).

CLASSIFICATION OF MYELOID NEOPLASMS WITH GERMLINE PREDISPOSITION

The WHO classification is given in Table 13.5. These neoplasms may occur alone or with preexisting platelet disorders or with dysfunction of other organs as well as of the bone marrow. Figure 13.66 illustrates a rare type of acute leukemia, congenital acute leukemia. This is usually myeloid and characterized by extensive extramedullary infiltration, including in the skin. The underlying genetic defect in this case was unknown.

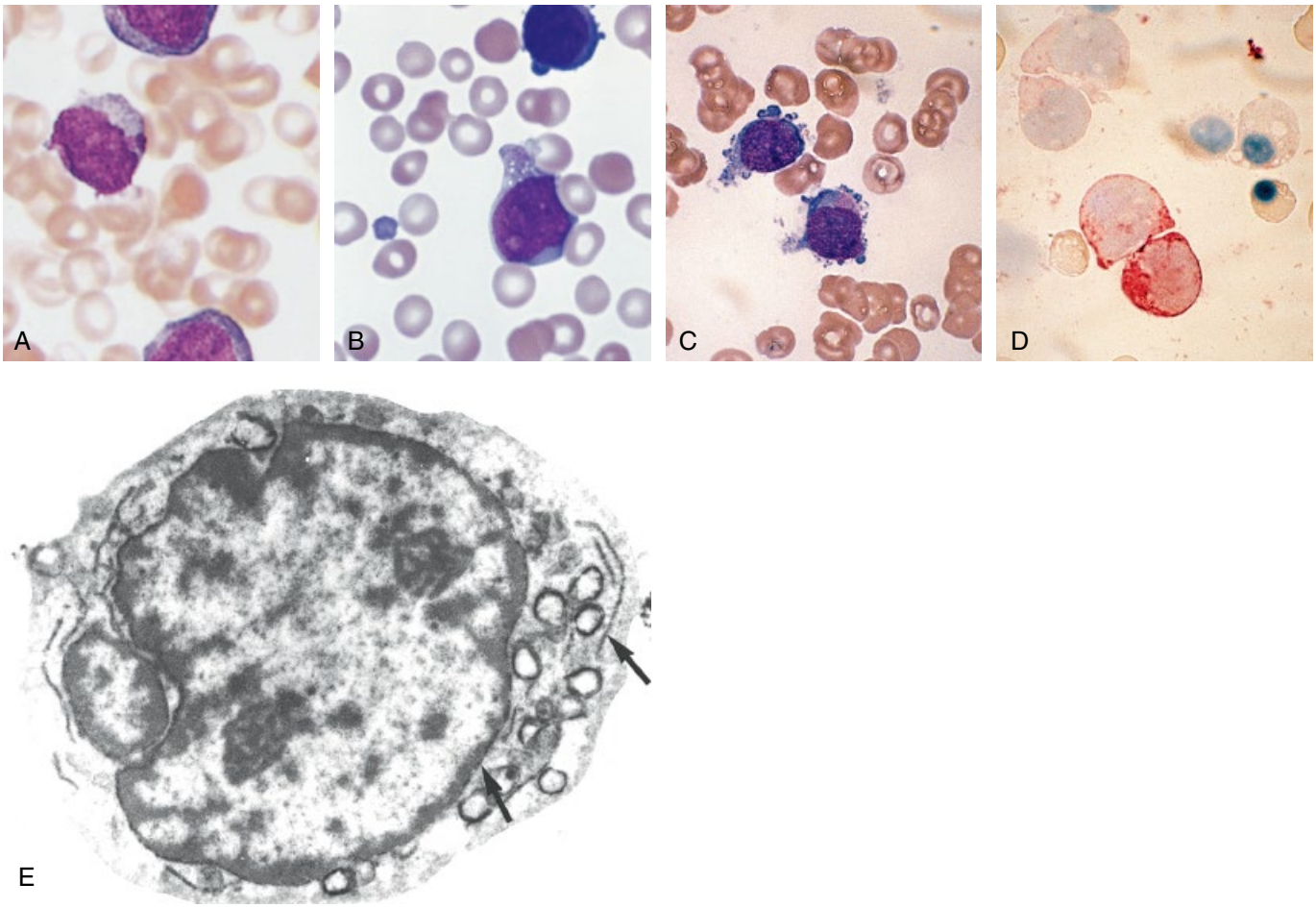

Fig. 13.60. Acute megakaryoblastic leukemia. **A–D,** The megakaryoblasts are large, primitive cells with basophilic cytoplasm. Some show abortive platelet budding. **D,** The cells are positive for platelet peroxidase; immunoperoxidase stain. **E,** Megakaryoblast: Morphologically, this cell resembles a lymphoblast but is identified by the reactivity with the platelet peroxidase reaction (linear black areas) in the endoplasmic reticulum and nuclear membrane (arrows). Mitochondria are nonspecifically positive. (Courtesy of Dr. E Matutes and Professor D Catovsky.)

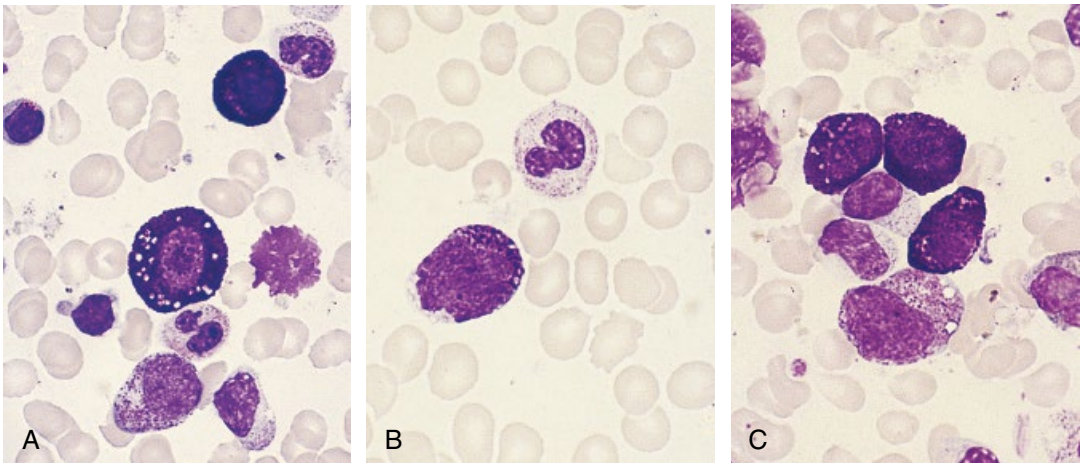

Fig. 13.61. Acute mast cell leukemia. **A–C,** Bone marrow showing typical blasts with basophilic and vacuolated cytoplasm. In this case the leukemia arose de novo; other cases follow systemic mastocytosis (although usually other forms of AML complicate this disease) or occur as transformation of chronic myeloid leukemia.

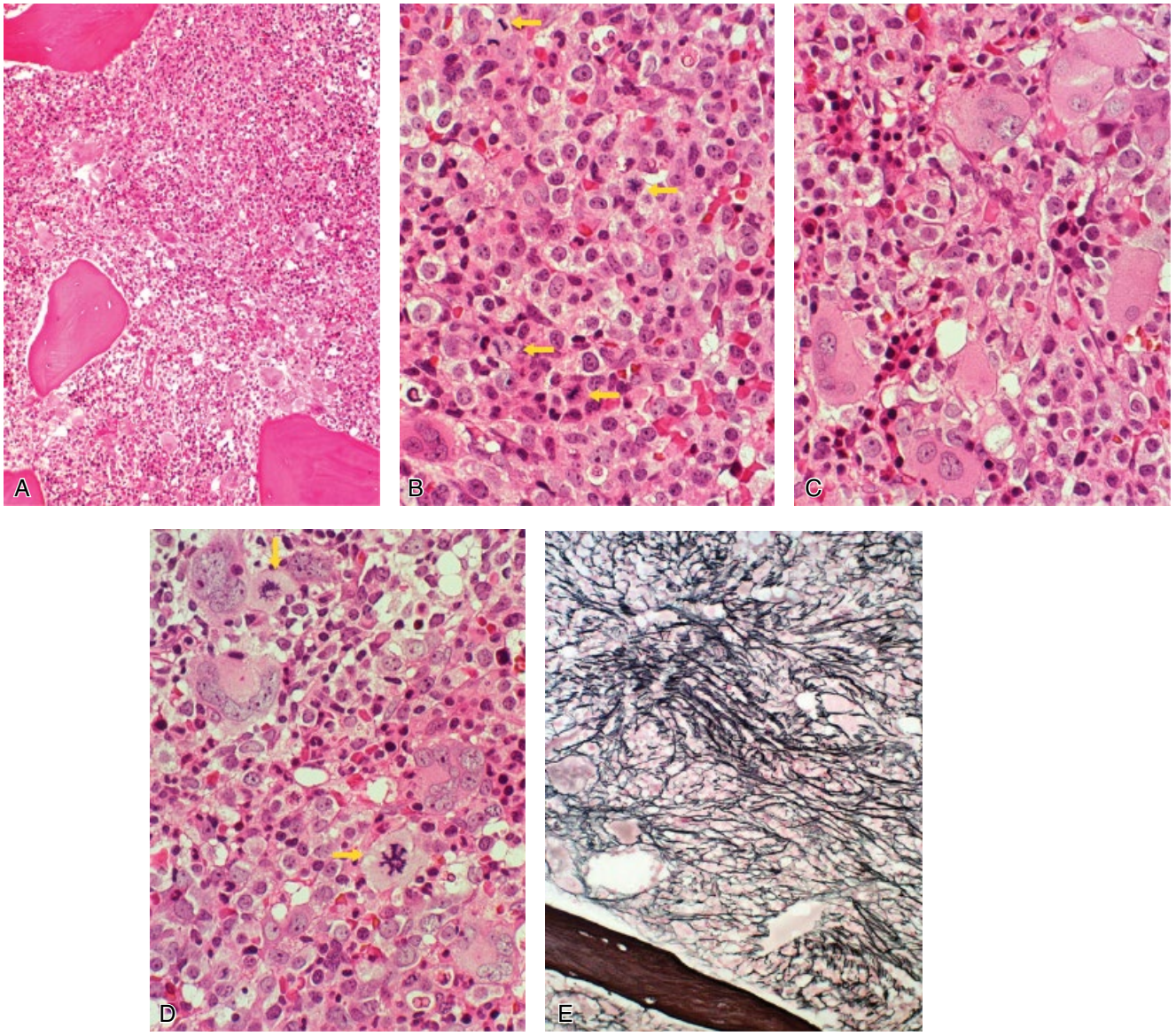

Fig. 13.62. Acute panmyelosis with myelofibrosis: The patient had pancytopenia. (Hb, 9.0 g/dL; WBC, 2.3 × 10^9/L; neutrophils, 0.16 × 10^9/L; blasts, 0.9 × 10^9/L; platelets, 37 × 10^9/L.) The blood film showed only mild anisocytosis and poikilocytosis with no teardrop cells. A very occasional erythroblast was present; there was no splenomegaly. Attempts at marrow aspiration failed. **A,** The trephine biopsy shows a hypercellular marrow with replacement of normally developing cells with primitive myeloid and erythroid cells and megakaryocytes. **B,** Myeloid and erythroid blasts at higher magnification. Arrows point to cells in mitosis. **C, D,** Abnormal small and large megakaryoblasts and megakaryocytes showing nonlobated and hypolobated nuclei with a dispersed vesicular chromatin pattern. There are two megakaryoblasts in mitosis. **E,** Reticulin staining shows a marked increase in reticulin fiber density and thickness with extensive fiber intersections (grade 2 fibrosis).

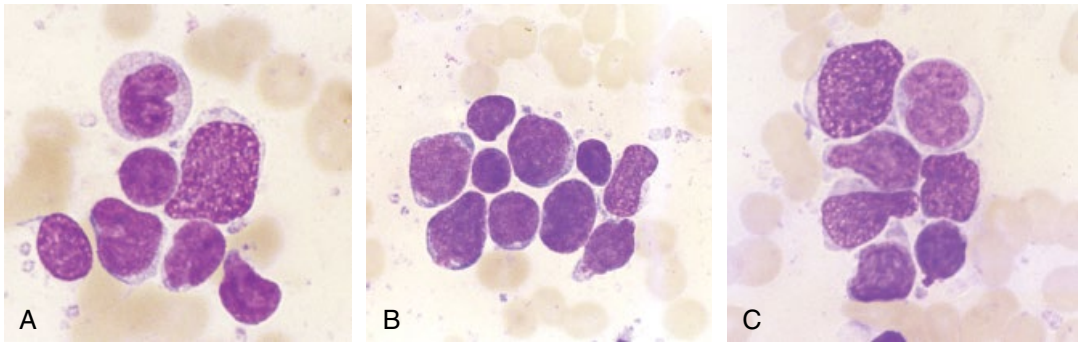

Fig. 13.63. A–C, Myeloid sarcoma: The patient was an 85-year-old man with a 6.5 cm mass in the left axilla. Normal blood count. Smears from a fine-needle aspirate show replacement of normal nodal lymphocytes with primitive myeloid hematopoietic cells. Marker studies showed positivity for CD33, CD34, CD15, CD117, aberrant CD56, and CD7. Bone marrow at presentation was normal. Seven months later he developed typical and fatal AML myelomonocytic subtype.

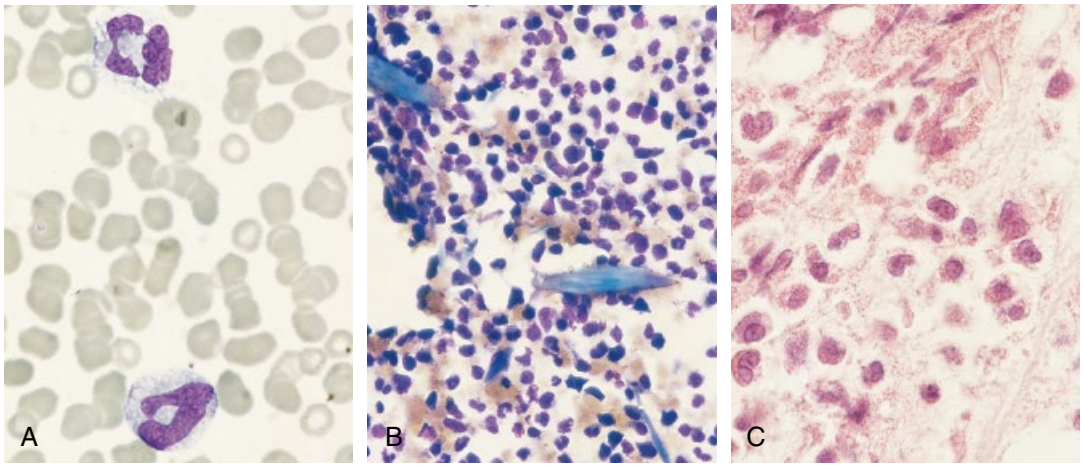

Fig. 13.64. Acute myeloid leukemia, rare eosinophilic subtype: A 55-year-old man treated with chemotherapy for carcinoma of the bladder 10 years previously. **A,** Peripheral blood showing abnormal eosinophils. **B,** Bone marrow aspirate showing eosinophilic blasts, necrotic cells, and Charcot–Leyden crystals. **C,** Bone marrow trephine showing necrotic cells and Charcot–Leyden crystals. (Hb, 11.0 g/dL; WBC, 23.2 × 10^9/L; platelets, 24 × 10^9/L.) (Courtesy of Dr. AG Smith.)

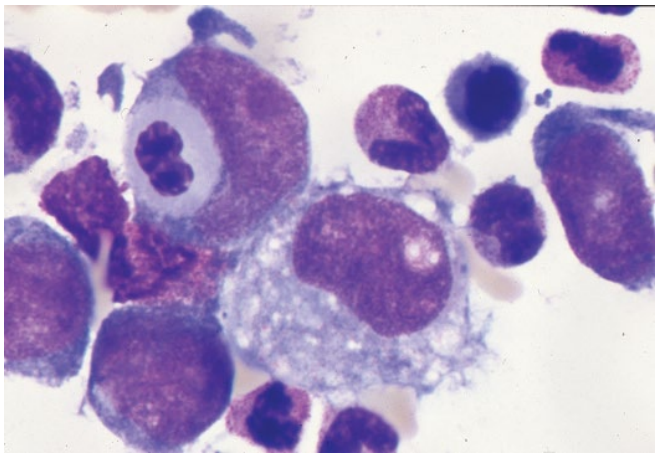

Fig. 13.65. Acute myeloid leukemia, t(16; 21) subtype. Marked hemophagocytosis by leukemic blasts cells. (Courtesy Dr. S Imashuku.)

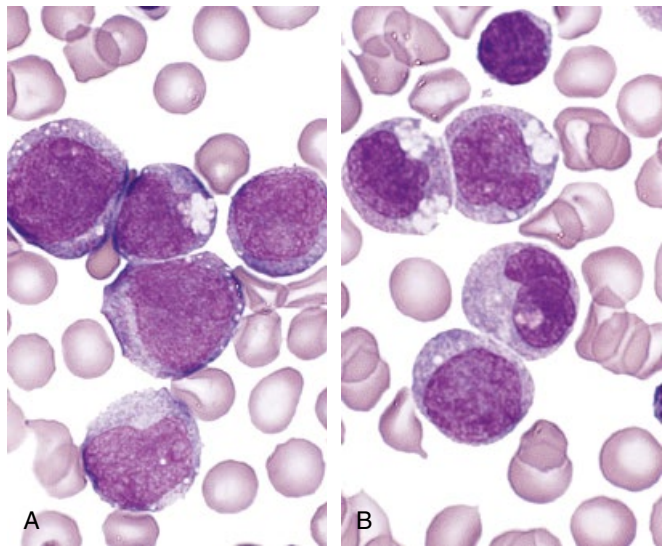

Fig. 13.66. Congenital acute myeloid leukemia. **A, B,** Peripheral blood films of a male infant born with anemia, hepatosplenomegaly, and skin lesions. There are large numbers of myeloblasts with prominent cytoplasmic vacuolation. (Hb, 10.1 g/dL; WBC, 92 × 10^9/L; blasts, 85%; platelets, 15 × 10^9/L.) (Courtesy of Professor JM Chessels.)

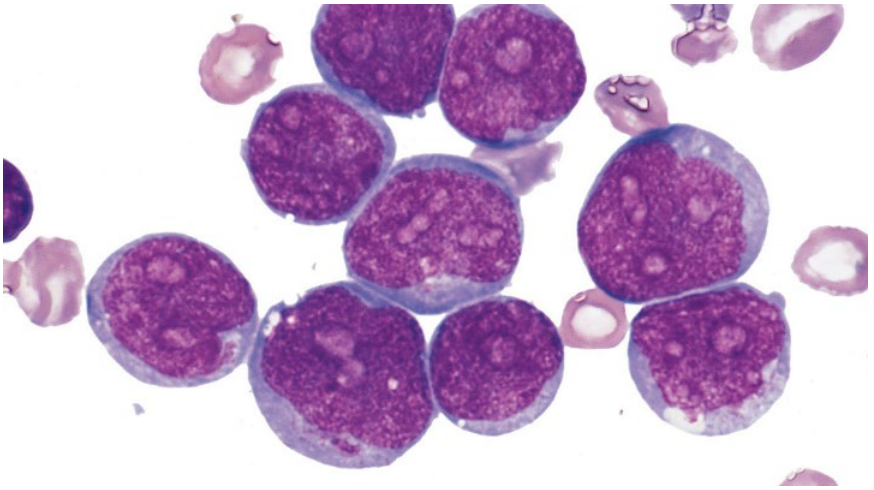

Fig. 13.67. Acute myeloid leukemia: Down syndrome. Peripheral blood showing numerous myeloblasts in a child younger than 1 year old. (Courtesy of Professor RD Brunning and the US Armed Forces Institute of Pathology.)

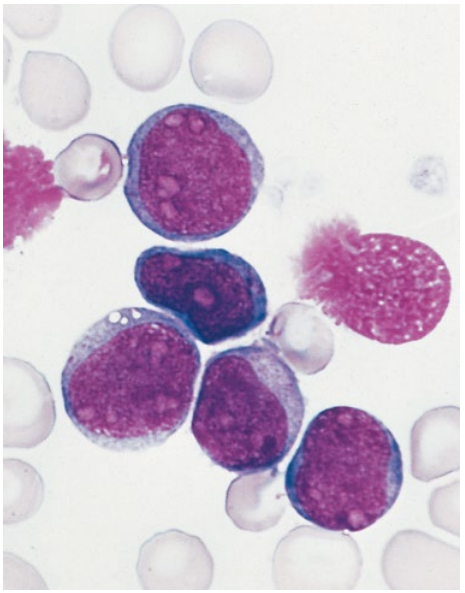

Fig. 13.68. Transient myeloproliferative disorder: Down syndrome. Peripheral blood film from a 3-day-old girl with Down syndrome. (Hb, 16.2 g/dL; WBC, 62×10^9/L [blasts 50–55%]; platelets, 28×10^9/L.) The blasts have basophilic cytoplasm, dispersed nuclear chromatin, and several nucleoli. Azurophilic granules are present in one of the blasts. The WBC increased to 77×10^9/L on day 5, but then resolved spontaneously by 8 weeks, when the blood film was normal. There was no recurrence within a 5-year follow-up. (Courtesy of Professor RD Brunning and the US Armed Forces Institute of Pathology.)

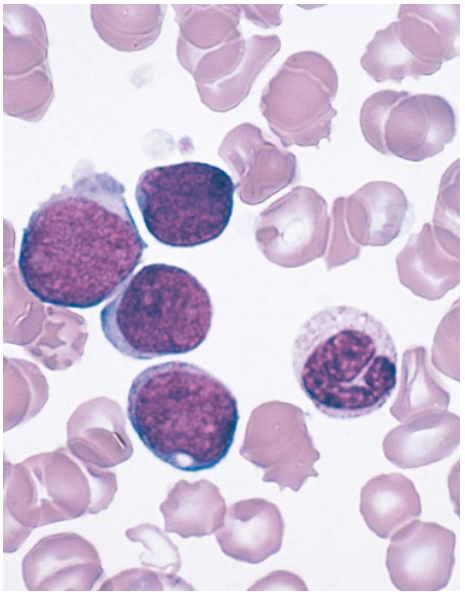

Fig. 13.69. Transient myeloproliferative disorder: Down syndrome. Peripheral blood film from a 20-day-old girl. (Hb, 16.4 g/dL; WBC, 54×10^9/L; platelet count normal.) Approximately 50% of the white blood cells are blasts. The platelets are large; occasional platelets are poorly granulated. The white cell count returned to normal after three weeks, but increased three months later following a bacterial infection when blast cells were again numerous. This resolved but relapsed two months later, at which time the child was treated for acute leukemia. (Courtesy of Professor RD Brunning and the US Armed Forces Institute of Pathology.)

Juvenile myelomonocytic leukemia and neurofibromatosis or Noonan syndrome are discussed in Chapter 17.

Germline *GATA2* mutations may be familial or sporadic and cause increased susceptibility to infections, pulmonary dysfunction, autoimmune syndromes, lymphedema, and malignancy, especially myelodysplasia/AML. The heterozygous mutations include frameshifts, insertions, deletions, or amino acid substitutions spread throughout the gene and cause progressive loss of immune function (dendritic cells, monocytes, B cells, and NK lymphocytes).

Myeloid proliferations of Down syndrome include transient abnormal myelopoiesis (TAM) and myeloid leukemia associated with Down syndrome (Fig. 13.67). A TAM occurs more frequently in Down syndrome than in normal infants. The blood and bone marrow appearances are morphologically similar to those in AML, usually with over 20% of blasts in the blood (Figs. 13.68–13.70). Both show *GATA1* mutations and mutations in the JAK-STAT pathway.

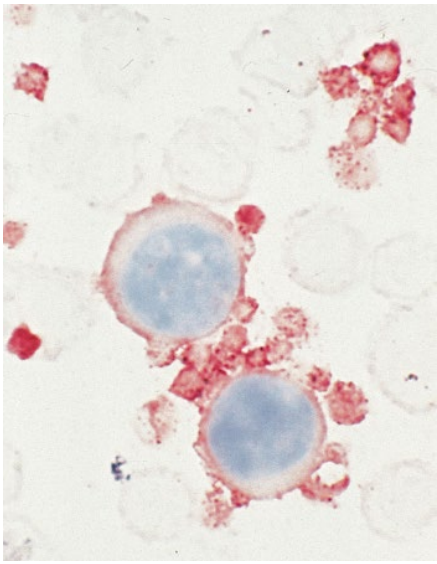

Fig. 13.70. Transient myeloproliferative disorder: Down syndrome. Peripheral blood from the child described in Fig. 13.68 reacted with monoclonal antibody to CD61 (platelet glycoprotein IIIa; AP-AAP technique). The megakaryocytes, promegakaryocytes, and platelets are positive; the blasts (not shown) were nonreactive. (Courtesy of Professor RD Brunning and the US Armed Forces Institute of Pathology.)

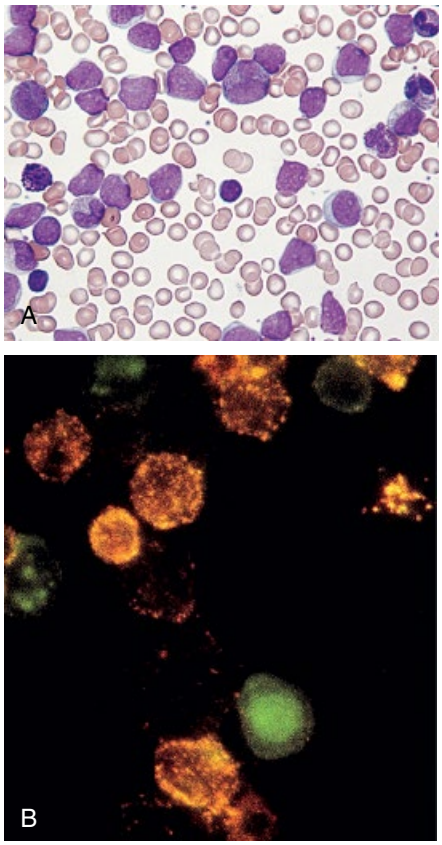

Fig. 13.71. Acute mixed phenotype leukemia, myeloid/lymphoblastic type. **A,** Bone marrow aspirate showing blasts of varying size and morphology. Some have scanty cytoplasm without granules, whereas others, usually larger, have eccentric nuclei, substantial cytoplasm, and granules. **B,** Bone marrow aspirate seen by indirect immunofluorescence shows one population of cells (lymphoblastic) to have nuclear TdT (green) whereas another population (myeloid) has myeloid (CD33) surface antigen (yellow/orange). (Courtesy of Professor G Janossy.)

TABLE 13.7. CRITERIA FOR LINEAGE ASSIGNMENT FOR A DIAGNOSIS OF MIXED PHENOTYPE ACUTE LEUKEMIAS

Myeloid lineage
MPO[a] (flow cytometry, immunohistochemistry, or cytochemistry)
or
Monocytic differentiation (at least 2 of the following: nonspecific esterase cytochemistry, CD11c, CD14, CD64, lysozyme)
T-lineage
Strong[b] cytoplasmic CD3 (with antibodies to CD3 ε chain)
or
Surface CD3
B-lineage
Strong[b] CD19 with at least 1 of the following strongly expressed: CD79a, cytoplasmic CD22, or CD10
or
Weak CD19 with at least 2 of the following strongly expressed: CD79a, cytoplasmic CD22, or CD10

[a] See "Acute Leukemias of Ambiguous Lineage" in reference below for caveats related to weaker antigen expression, or to expression by immunohistochemistry only.
[b] Strong defined as equal or brighter than the normal B or T cells in the sample.
Source: Arber DA, et al. *Blood* 2016;127:2391–2405. Reproduced with permission of *Blood: Journal of the American Society of Hematology*.

ACUTE LEUKEMIAS OF AMBIGUOUS LINEAGE

Blast cells may show features of both myeloid and lymphoid cells. These may be due to aberrant expression of markers on the same blasts or to the presence of two populations (Fig. 13.71). The criteria for diagnosis of mixed phenotype acute leukemias (MPALs) are given in Table 13.7.

SPECIFIC DIAGNOSTIC ASPECTS IN AML

Cytochemistry

In AML, in addition to MGG staining as the gold standard for peripheral blood and bone marrow smears, cytochemistry may help to identify phenotypic subtypes of AML and to discriminate from ALL, acute leukemias of ambiguous lineage, and MPALs. It is still also mandatory to classify morphologic phenotypes according to WHO 2016 cases in the subcategory AML, not otherwise specified (NOS) (see Appendix 1). This is true especially when immunophenotyping is not available. Myeloperoxidase or Sudan black shows the presence of cytoplasmic granules and can identify the leukemia as myeloid if ≥3% blasts are positive (Fig. 13.72). Positivity for nonspecific esterase detects monocytic differentiation (Fig. 13.73). Cytochemistry has been largely replaced for diagnosis by flow cytometry, and where this is available, cytochemistry may only be useful in the diagnosis of MPALs.

Immunophenotype

The markers recommended by European LeukemiaNet (ELN) for the diagnosis of AML are shown in Table 13.8 and the use of these (and cytochemistry) for lineage assignment in MPAL. The pattern of antigen expression varies according to the subtype of AML, determined by cytogenetics, molecular genetics and morphology. Figure 13.3 shows typical flow cytometry findings

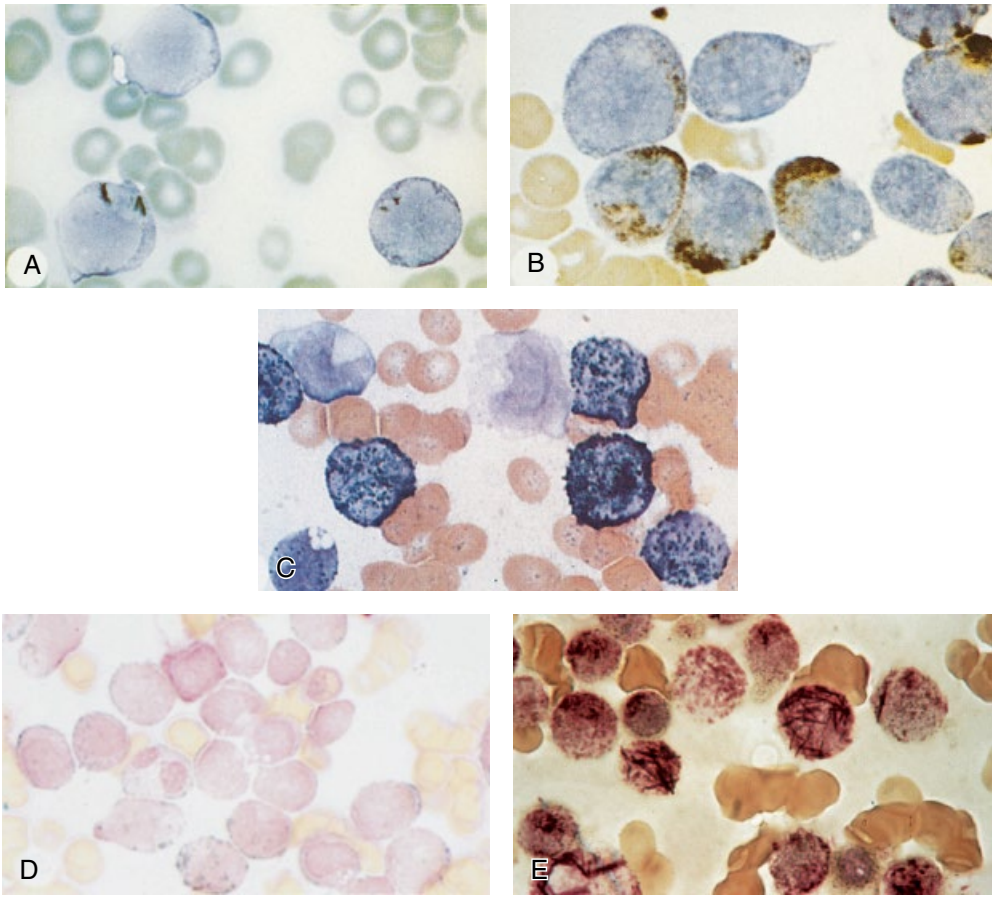

Fig. 13.72. Acute myeloid leukemia: Bone marrow aspirates. **A, B,** These subtypes show black-staining cytoplasmic granules and Auer rods. **C,** Myelomonocytic subtype myeloblasts with black cytoplasmic granules (the monoblasts show only background staining). **D,** t(8;21) subtype shows multiple, blue-staining cytoplasmic granules. **E,** t(15;17) subtype shows multiple Auer rods ("faggots"). A–C, Sudan black; D, myeloperoxidase; E, dual esterase stains. (E, Courtesy of Professor JM Bennett.)

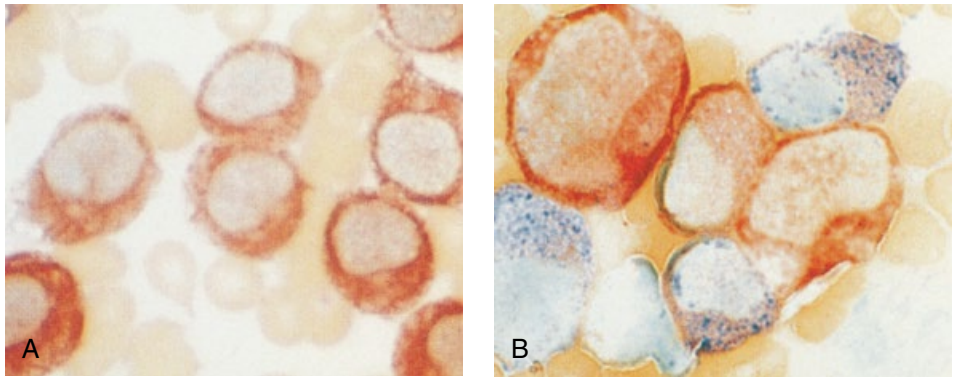

Fig. 13.73. Acute myeloid leukemia: Bone marrow aspirates. **A,** Monoblastic subtype shows deep orange staining by nonspecific esterase. **B,** Myelomonocytic subtype shows deep orange staining of the monoblast cytoplasm by nonspecific esterase and blue staining of myeloblast cytoplasm by chloracetate.

TABLE 13.8. EXPRESSION OF CELL SURFACE AND CYTOPLASMIC MARKERS FOR THE DIAGNOSIS OF ACUTE MYELOID LEUKEMIAS AND MIXED PHENOTYPE ACUTE LEUKEMIAS

Diagnosis of AML[a]	
Precursors[b]	CD34, CD117, CD33, CD13, HLA-DR
Granulocytic markers[c]	CD65, cytoplasmic MPO
Monocytic markers[d]	CD14, CD36, CD64
Megakaryocytic markers[e]	CD41 (glycoprotein IIb/IIIa), CD61 (glycoprotein IIIa)
Erythroid markers	CD235a (glycophorin A), CD36
Diagnosis of MPAL[f]	
Myeloid lineage	MPO (flow cytometry, immunohistochemistry, or cytochemistry) or monocytic differentiation (at least 2 of the following: nonspecific esterase cytochemistry, CD11c, CD14, CD64, lysozyme)
T-lineage	Strong[g] cytoplasmic CD3 (with antibodies to CD3 ε chain) or surface CD3
B-lineage[h]	Strong[g] CD19 with at least 1 of the following strongly expressed: cytoplasmic CD79a, cCD22, or CD10 or weak CD19 with at least 2 of the following strongly expressed: CD79a, cCD22, or CD10

MPO, myeloperoxidase.

[a] The markers proposed in this table are according to European LeukemiaNet Work Package 10 recommendations.

[b] CD38 and other markers such as CD123 or CD133 can be added to identify leukemic stem cells, but do not contribute to diagnosis.

[c] Of note, cells engaged in granulocytic maturation will retain the expression of CD13 and CD33 at various fluorescence levels. Seeking for the expression of CD15 and CD11b can provide further information. CD16 is only present on normal mature granulocytes. The absence of MPO together with myeloid markers defines AML with minimal differentiation which is different from acute undifferentiated leukemia.

[d] Of note, cells engaged in monocytic differentiation will retain the expression of CD13 and CD33. Seeking the expression of CD64 and CD11b can provide additional information, notably for promonocytes.

[e] CD42 (glycoprotein 1b) can also be used.

[f] The category MPAL includes leukemias with expression of antigens of >1 lineage. They can either contain distinct blast populations of different lineages, or 1 blast population with expression of antigens of different lineages on the same cells, or a combination. The proposal in this table includes the modifications brought in the current update of the WHO classification of hematopoietic tumors.

[g] Strong defined as equal or brighter than the normal B or T cells in the sample.

[h] Other markers can be used to confirm B-lineage involvement.

See also Table 14.4.

Source: Döhner H, et al. *Blood* 2017;129(4):424–447. Reproduced with permission of *Blood: Journal of the American Society of Hematology*.

TABLE 13.9. LEUKEMIA-ASSOCIATED IMMUNOPHENOTYPES THAT CAN BE IDENTIFIED AT DIAGNOSIS OF ACUTE LEUKEMIA AND SUBSEQUENTLY BE USED TO MONITOR MINIMAL RESIDUAL DISEASE

Type of abnormality	Example
Adherent expression of an antigen more appropriate to another lineage	Lymphoid-associated antigens, such as CD2, CD4, CD5, CD7, CD19, or CD20, on myeloid cells Myeloid-associated antigens, such as CD13, CD15, CD33, CD65, or CD66c, on lymphoid cells Natural killer or T-lineage-associated antigens, such as CD56, expressed on B lymphoblasts
Asynchronous expression of antigens or failure to express expected antigens synchronously	Coexpression of terminal deoxynucleotidyl transferase, CD10 and strong CD34 with cytoplasmic μ chain or strong CD19, CD20, CD21, or CD22 Coexpression of CD34 or terminal deoxynucleotidyl transferase with CD11b, CD14, CD15, strong CD33, or CD65 Failure to express CD13 and CD33 synchronously
Abnormally weak or abnormally strong antigen expression	Increased expression of CD10 Increased expression of CD33
Expression of antigens that are not usually expressed in cells being examined	Presence in the bone marrow of cells (i) expressing CD1a or (ii) expressing both cytoplasmic CD3 and either terminal deoxynucleotidyl transferase or CD34 or (iii) coexpressing CD4 and CD8

in a case of AML and Fig. 13.5, the findings in a case with aberrant phenotype. This may be subsequently useful in detection of MRD (Table 13.9).

Cytogenetics

Figure 13.74 shows the cytogenetic and molecular genetic abnormalities that are found in adult AML. WHO 2016 uses these abnormalities to classify AML although some cases, AML, NOS are still classified on morphological criteria (see Appendix 1). Conventional cytogenetics using karyotyping is illustrated in Figs. 13.75–13.77, showing the abnormalities in three favorable groups, t(8;21), t(15;17), and inv(16) and also t(6:9) as an example of a translocations found in AML. The translocation t(8;21) and inv(16) both involve the transcription factor corticotropin-releasing factor (CBF) (Fig. 13.78).

Molecular Genetics

In comparison to solid tumors, the number of mutated genes in patients with AML is quite low (Fig. 13.79). Cytogenetics and molecular genetics are used for risk stratification of AML (Table 13.10). Mutational analysis of 1540 cases found 5234 driver mutations in 96% of cases across 76 genes or genomic regions with two or more driver mutations in 86% of cases (Fig. 13.80). On the basis of co-mutation compartmentalization, this study identified 11 classes with distinct diagnostic features and clinical outcomes (Figs. 13.81 and 13.82). These subgroups included inv(16), t(15;17), t(8;21) *KMT2A (MLL)* fusions, inv(3), t(6;9), NPM1, *CEBPA* biallelic, *TP53* aneuploidy, chromatin spliceosome, and *IDH2* mutations (Fig. 13.81). Internal tandem duplication (ITD) of FLT3 is a frequent molecular mutation in AML (Fig. 13.83). It is more common in cases

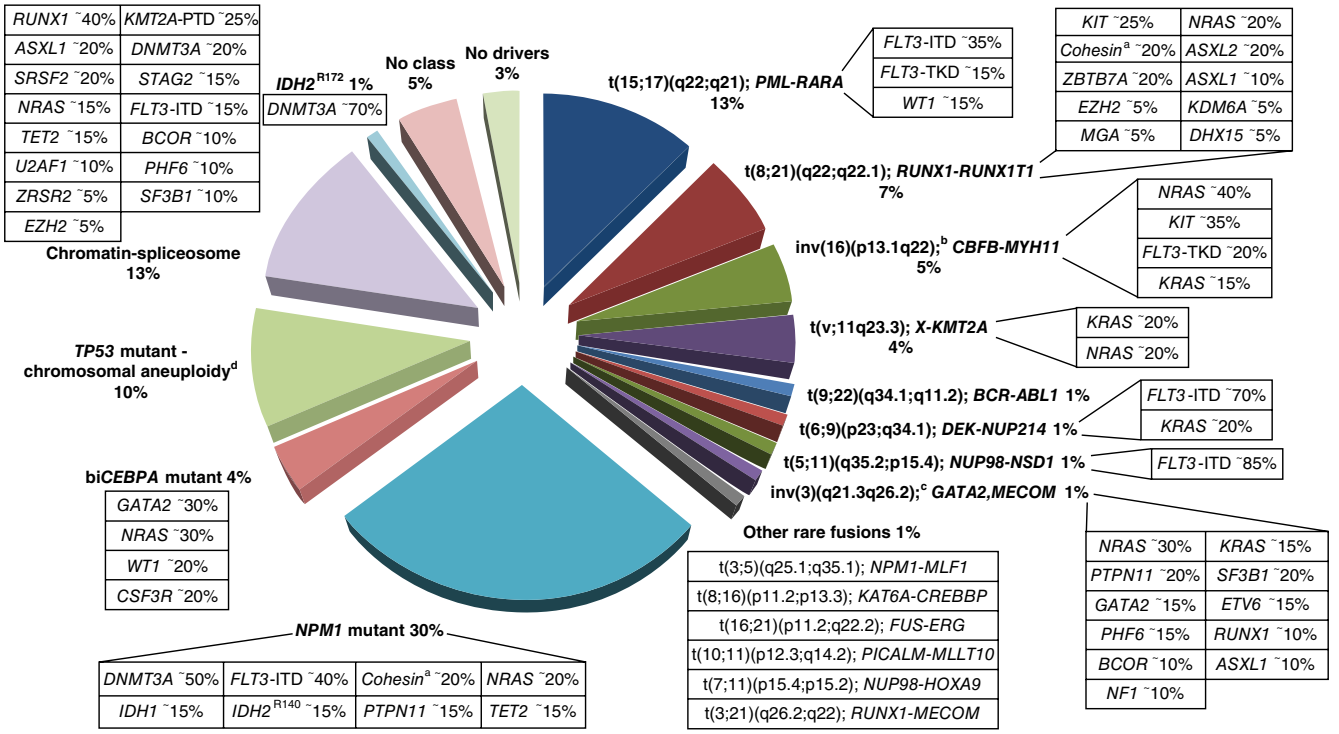

Fig. 13.74. Molecular classes of acute myeloid leukemia and concurrent gene mutations in adult patients up to the age of ~65 years. For each AML class denoted in the pie chart, frequent co-occurring mutations are shown in the respective boxes. Data on the frequency of genetic lesions are compiled from the databases of the British Medical Research Council (MRC), the German-Austrian AML Study Group (AMLSG), and from selected studies. [a]Indicates cohesin genes including *RAD21* (~10%), *SMC1A* (~5%), and *SMC3* (~5%); [b]inv(16)(p13.1q22) or t(16;16)(p13.1;q22); *CBFB-MYH11*; [c]inv(3)(q21.3q26.2) or t(3;3)(q21.3;q26.2); *GATA2,MECOM*(*EVI1*); and [d]*TP53* mutations are found in ~45%, and complex karyotypes in ~70% of this class. Source: Döhner H, et al. *Blood* 2017;129:424–447. Reproduced with permission of *Blood: Journal of the American Society of Hematology*.

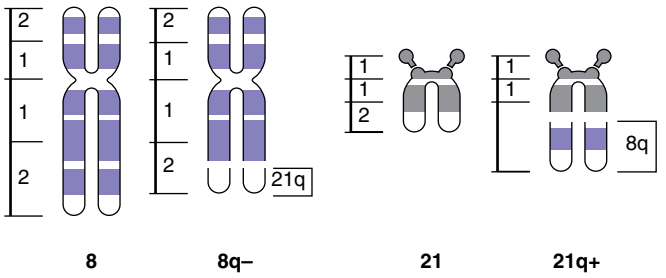

Fig. 13.75. Acute myeloid leukemia, t(8;21) subtype: Diagrammatic systematized description of the structural aberration t(8;21). (Courtesy of Professor LM Secker-Walker.)

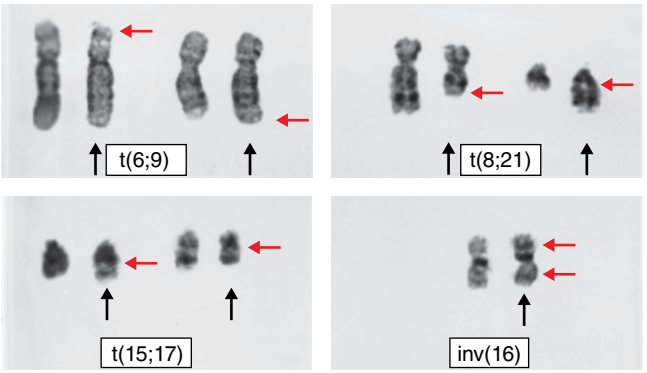

Fig. 13.76. Acute myeloid leukemia: Partial karyograms showing common rearrangements in AML. In each karyogram, the translocated chromosome is on the right (arrowed) in each pair; red arrows mark the regions of chromosome breakage and rejoining: t(6;9) (p22;q34); t(8;21) (q22;q22); t(15;17) (q22;q12); inv(16) (p13;q22). (Courtesy of Professor LM Secker-Walker.)

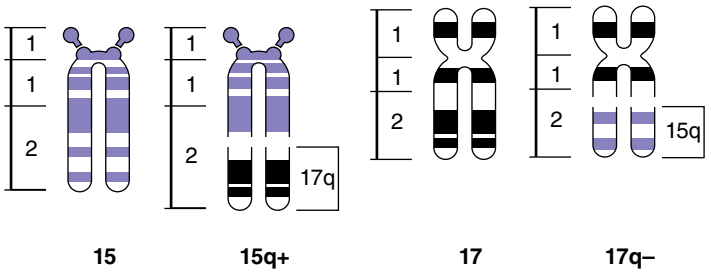

Fig. 13.77. Acute myeloid leukemia, t(15;17) subtype (acute promyelocytic leukemia [APL]): Systematized description of the structural aberration t(15;17). (Courtesy of Professor LM Secker-Walker.)

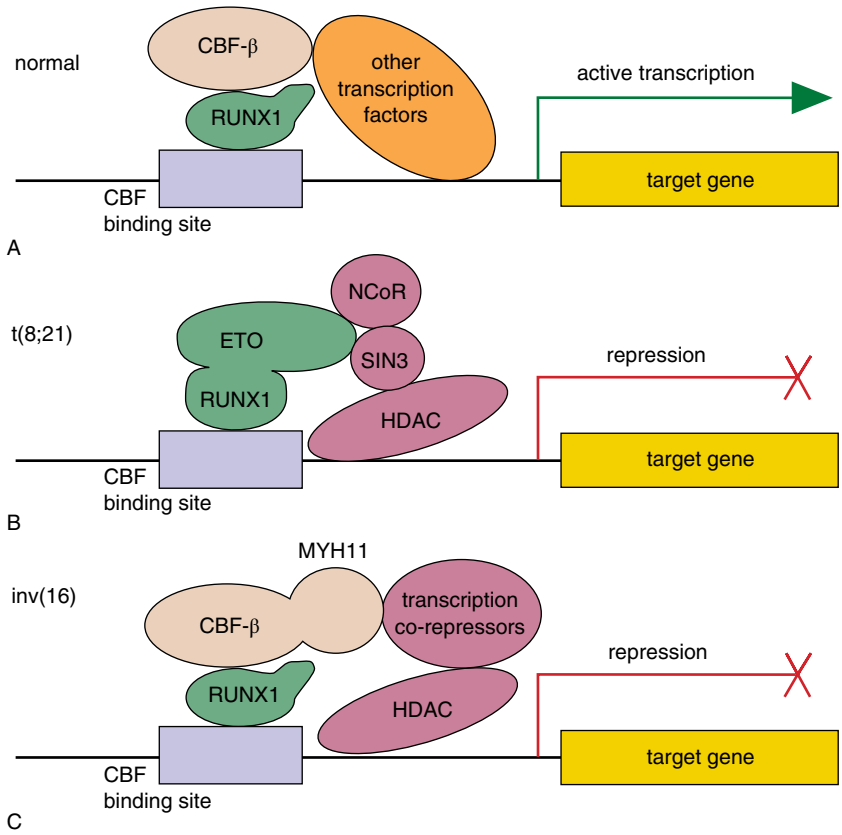

Fig. 13.78. The genes encoding components of the corticotropin-releasing factor (CBF) transcription factor complex are frequent targets in acute myeloid leukemia. **A,** RUNX1 binds a specific DNA sequence motif, and recruits CBF-β to form a heterodimeric complex. This then acts as a transcriptional organizer, attracting other specific transcription factors and promoting target gene transcription. **B,** The t(8;21) translocation results in fusion of RUNX1 to the *RUNX1T1* protein, which recruits a series of transcriptional repressors, including histone deacetylases, leading to target gene inactivation. **C,** In cells carrying the inv(16) rearrangement, the CBF-β–MYH11 fusion protein binds to RUNX1 and then recruits transcriptional repressors.

without cytogenetic abnormalities and those with t(15;17). It is unfavorable whereas the less frequent point mutation of FLT3-TKD has no prognostic significance.

*N*6-Methyladenosine (m6A) is an abundant internal RNA modification in both coding and noncoding RNAs that is catalyzed by the METTL3-METTL14 methyltransferase complex. The specific role of these enzymes in cancer is still largely unknown. METTL3 has been identified, however, as an essential gene for growth of AML cells in genetic screens. Downregulation of METTL3 results in cell cycle arrest, differentiation of leukemic cells, and failure to establish leukemia in immunodeficient mice. METTL3, independently of METTL14, associates with chromatin and localizes to the transcriptional start sites of active genes through the CAATT-box binding protein CEBPZ, which is present at the transcriptional start site. Promoter-bound METTL3 induces m6A modification within the coding region of the associated mRNA transcript, and enhances its translation by relieving ribosome stalling. In this way METTL3 ensures the translation of proteins necessary for AML.

Mutations in the nucleophosmin member1 (*NPM1*) gene are found in 46–62% of normal karyotype AML patients. The protein has several functions, including prevention of nucleolar aggregation and regulation of ribosomal protein assembly and transport. The protein is normally localized to the nucleus but if mutated is usually aberrantly expressed in the cell cytoplasm (Figs. 13.84–13.86). Both *FLT3* and *NPM1* mutations may be detected using molecular techniques.

Acquired mutations of *TET2*, a tumor-suppressor gene at 4q24, occur in 10–20% of patients with myeloid neoplasms, including AML, MDS, myeloproliferative diseases, BCR-ABL1+ chronic myelogenous leukemia (CML), chronic myelomonocytic leukemia (CMML), and systemic mastocytosis. *TET2* mutations may precede other clonal genetic lesions (e.g. *JAK2* or chromosome translocations).

Minimal Residual Disease

MRD in AML is investigated by immunologic or molecular genetic tests.

Immunophenotyping for Minimal Residual Disease

Immunophenotyping can (i) detect leukemia-associated immune phenotypes (LAIPs) or (ii) identify different-from-normal patterns. LAIPs are usually cross-lineage expression of antigens, antigen overexpression, lack of antigen expression, or asynchronous expression of antigens. There are about 100 different LAIPs that can be used for MRD detection in AML (Table 13.9). The panel includes the panleukocyte antigen CD45, markers for primitive cells (CD34, CD117, CD133), and a myeloid antigen (CD33, CD13), which are expressed on a normal regenerating population and, for example, for lymphoid cells markers aberrantly expressed. Different-from-normal patterns are recognized using a standard fixed antibody panel to recognize leukemic cells based on their difference from normal hematopoietic cells (Fig. 13.87). In contrast to LAIP testing, this also allows for immunophenotype shifts.

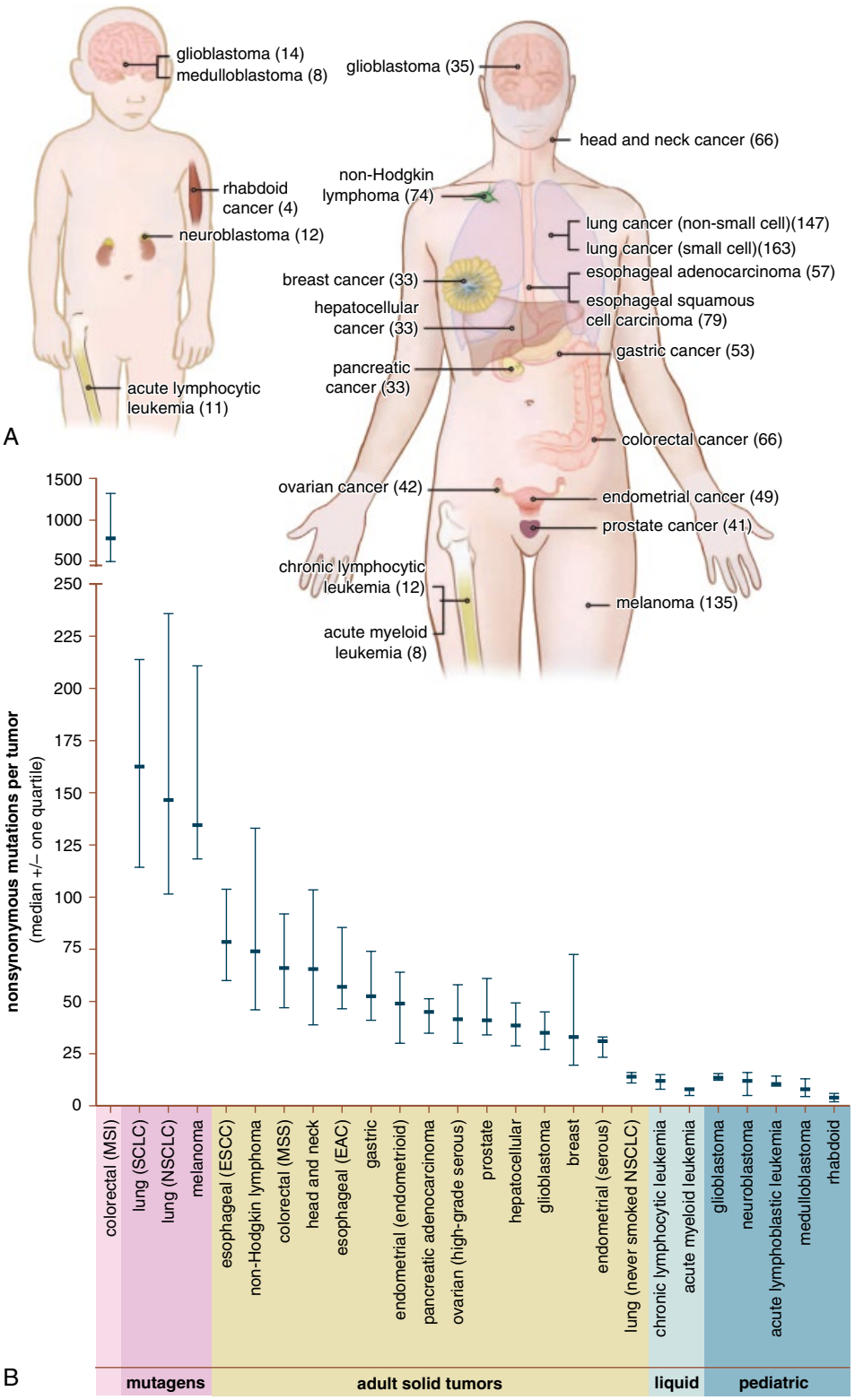

Fig. 13.79. Number of somatic mutations in representative human cancers, detected by genome-wide sequencing studies. **A,** The genomes of a diverse group of adult (*right*) and pediatric (*left*) cancers have been analyzed. Numbers in parentheses indicate the median number of nonsynonymous mutations per tumor. Reproduced with permission of Elizabeth Cook. **B,** The median number of nonsynonymous mutations per tumor in a variety of tumor types. Horizontal bars indicate the 25% and 75% quartiles. MSI, microsatellite instability; SCLC, small cell lung cancers; NSCLC, non-small cell lung cancers; ESCC, esophageal squamous cell carcinomas; MSS, microsatellite stable; EAC, esophageal adenocarcinomas. Source: Vogelstein B, et al. *Science* 2013;339:1546–1558.

PCR Techniques for Minimal Residual Disease

Samples can be tested from peripheral blood or bone marrow sample quantitatively for disease-related molecular aberrations, most frequently using reverse transcriptase polymerase chain reaction (RT-PCR). In patients who have a chromosomal translocation (Table 13.11) or a mutation, this can also be used as a marker for MRD (Fig. 13.88), using either DNA analysis or RT-PCR (Figs. 13.89 and 13.90). PCR techniques can achieve a

TABLE 13.10. 2017 EUROPEAN LEUKEMIANET (ELN) RISK STRATIFICATION BY GENETICS

Risk category[a]	Genetic abnormality
Favorable	t(8;21)(q22;q22.1); *RUNX1-RUNX1T1* inv(16)(p13.1q22) or t(16;16)(p13.1;q22); *CBFB-MYH11* Mutated *NPM1* without *FLT3*-ITD or with *FLT3*-ITD[low b] Biallelic mutated *CEBPA*
Intermediate	Mutated *NPM1* and *FLT3*-ITD[high b] Wild-type *NPM1* without *FLT3*-ITD or with *FLT3*-ITD[low b] (without adverse-risk genetic lesions) t(9;11)(p21.3;q23.3); *MLLT3-KMT2A*[c] Cytogenetic abnormalities not classified as favorable or adverse
Adverse	t(6;9)(p23;q34.1); *DEK-NUP214* t(v;11q23.3); *KMT2A* rearranged t(9;22)(q34.1;q11.2); *BCR-ABL1* inv(3)(q21.3q26.2) or t(3;3)(q21.3;q26.2); *GATA2,MECOM(EVI1)* –5 or del(5q); –7; –17/abn(17p) Complex karyotype,[d] monosomal karyotype[e] Wild-type *NPM1* and *FLT3*-ITD[high b] Mutated *RUNX1*[f] Mutated *ASXL1*[f] Mutated *TP53*[g]

Frequencies, response rates, and outcome measures should be reported by risk category, and, if sufficient numbers are available, by specific genetic lesions indicated.

[a] Prognostic impact of a marker is treatment dependent and may change with new therapies.

[b] Low, low allelic ratio (<0.5); high, high allelic ratio (≥0.5); semiquantitative assessment of *FLT3*-ITD allelic ratio (using DNA fragment analysis) is determined as ratio of the area under the curve "*FLT3*-ITD" divided by area under the curve "*FLT3*-wild-type." Recent studies indicate that AML with *NPM1* mutation and *FLT3*-ITD low allelic ratio may also have a more favorable prognosis and patients should not routinely be assigned to allogeneic hematologic stem cell transplantation.

[c] The presence of t(9;11)(p21.3;q23.3) takes precedence over rare, concurrent adverse-risk gene mutations.

[d] Three or more unrelated chromosome abnormalities in the absence of one of the WHO-designated recurring translocations or inversions, that is, t(8;21), inv(16), or t(16;16), t(9;11), t(v;11)(v;q23.3), t(6;9), inv(3), or t(3;3); AML with *BCR-ABL1*.

[e] Defined by the presence of one single monosomy (excluding loss of X or Y) in association with at least one additional monosomy or structural chromosome abnormality (excluding core-binding factor AML).

[f] These markers should not be used as an adverse prognostic marker if they co-occur with favorable-risk AML subtypes.

[g] *TP53* mutations are significantly associated with AML with complex and monosomal karyotype.

Source: Döhner H, et al. *Blood* 2017;129(4):424–447. Reproduced with permission of *Blood: Journal of the American Society of Hematology*.

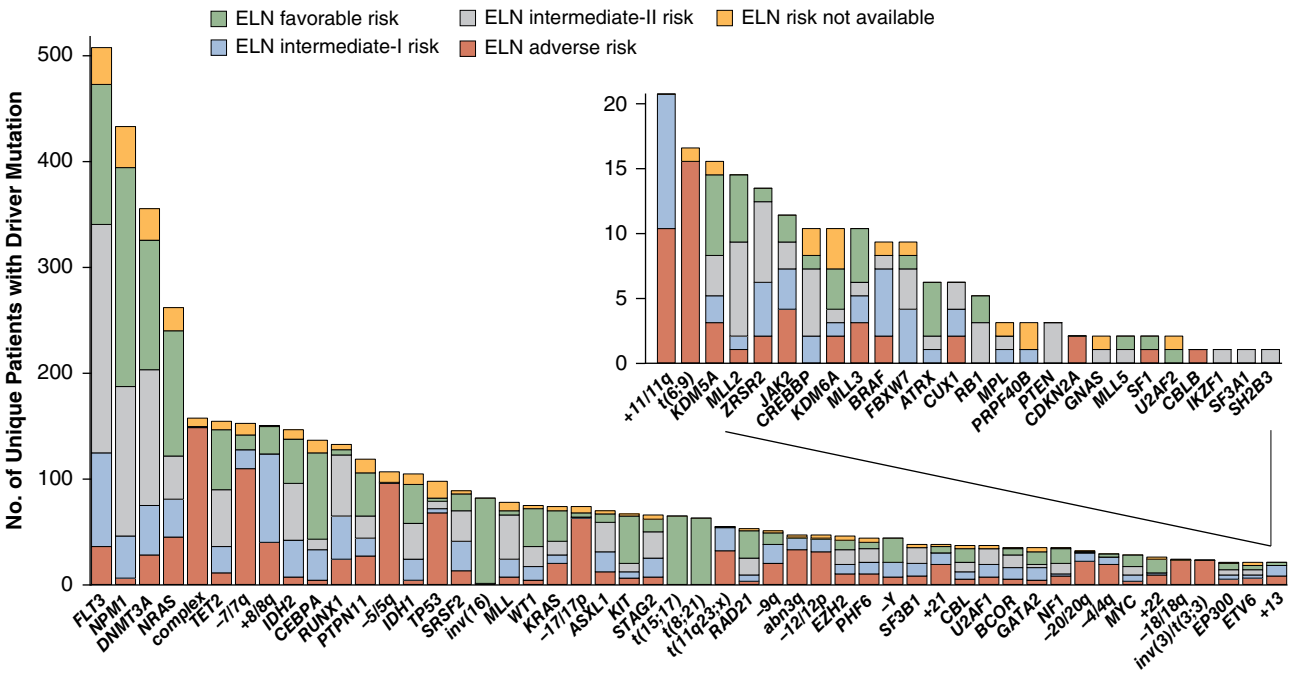

Fig. 13.80. Landscape of driver mutations in AML. Driver events in 1540 patients with AML. Each bar represents a distinct driver lesion; the lesions include gene mutations, chromosomal aneuploidies, fusion genes, and complex karyotypes. The colors in each bar indicate the molecular risk according to the European LeukemiaNet (ELN) classification (see Table 13.10). Source: Papaemmanuil E, et al. *N Engl J Med* 2016; 374: 2209–2221. Reproduced with permission from Massachusetts Medical Society; *The New England Journal of Medicine*.

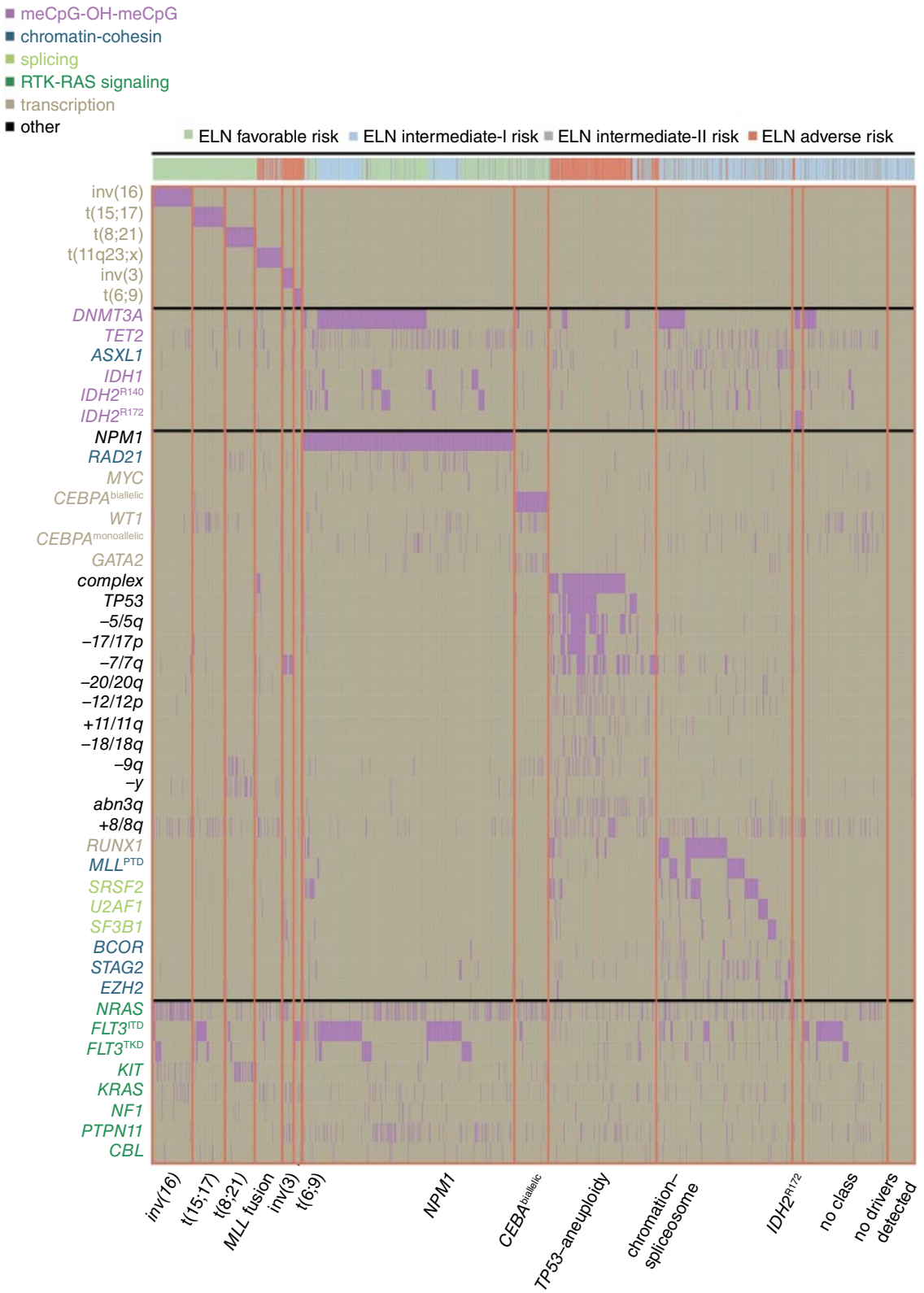

Fig. 13.81. Identification of molecular subgroups in acute myeloid leukemia. The rows in the graph represent individual genomic lesions, and the columns represent patients in the study. Vertical purple lines (some of which appear as blocks because of clustering) indicate the presence of a specified driver mutation in a patient. The patients have been ordered by group membership; orange lines demarcate boundaries between classes. OH-meCpG, hydroxymethyl CpG. MLL is now termed *KMT2A*. Source: Papaemmanuil E, et al. *N Engl J Med* 2016;374:2209–2221. Reproduced with permission of Massachusetts Medical Society: *The New England Journal of Medicine*.

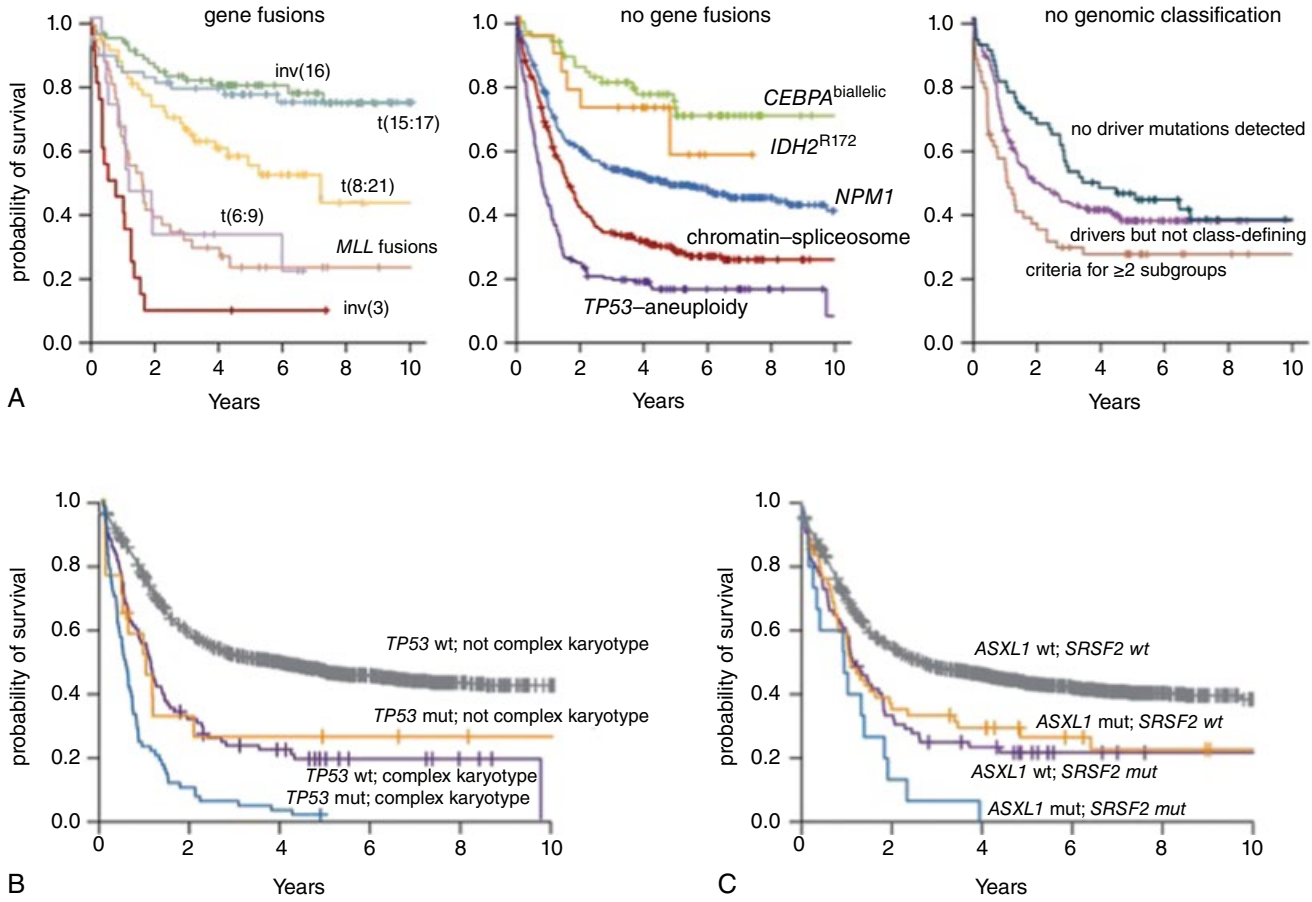

Fig. 13.82. Molecular subclassification and overall survival. **A,** Kaplan–Meier curves for overall survival among patients in the 11 genomically defined subgroups and patients who did not have a straightforward classification. **B,** Kaplan–Meier curves for overall survival with the additive and independent prognostic effects of *TP53* mutation and complex karyotype (*TP53* mutation, 17 patients; complex karyotype, 89; and *TP53* mutation with complex karyotype, 70). **C,** Kaplan–Meier curves for overall survival with the additive and independent prognostic effects of *ASXL1* and *SRSF2* mutations (*ASXL1* mutation, 55 patients; *SRSF2* mutation, 74; and *ASXL1* and *SRSF2* mutations, 15). wt, wild type; mut, mutation. Source: Papaemmanuil E, et al. *N Engl J Med* 2016;374:2209–2221. Reproduced with permission of Massachusetts Medical Society: *The New England Journal of Medicine*.

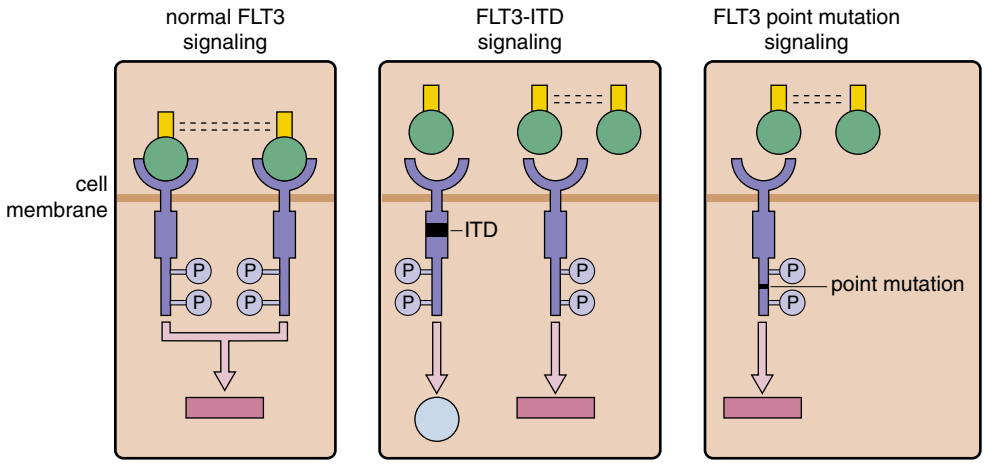

Fig. 13.83. Normal FLT3 signaling and disruption that may occur because of two major classes of mutations: internal tandem duplications (ITD) of 3–400 base pairs in exons 14 or 15 (15–35% of cases of AML) or missense point mutations in exon 20 in the intracellular domain (5–10% of cases of AML). Source: Modified from Emanuel P (2007) *The Hematologist ASH News and Reports*, p. 10.

sensitivity of 1 in 10/6. RT-qPCR is used in cases with chimeric fusion genes (e.g. t(15;17), t(8;21), inv16, t(16;16), t(6;9), t(5;11)). It can also be used for insertions/duplications (e.g. *NPM1*, *FLT3-ITD*, *MLL-PTD*); point mutations (e.g. *CEBPA*, *IDH1/2*, *KIT*, *RAS*, *RUNX1*, *TP53*), and gene overexpression (e.g. of *WT1*, *EV11*, *ERG*).

As an increasing number of molecular aberrations are detected using NGS-based approaches in AML, the spectrum of MRD targets increases. The respective follow-up can be set up with increased coverage by NGS or patient-specific PCR, focusing only on the respective mutated region. Digital PCR is a new platform that will allow investigation for MRD

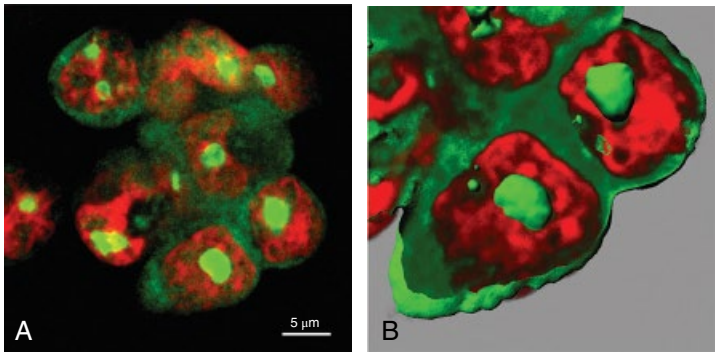

Fig. 13.84. Subcellular distribution of nucleophosmin (NPM) in the human acute myeloid leukemia cell line OCI-AML3, which carries a mutation of the *NPM1* gene. **A,** Cells show the expected nucleolar positivity and the aberrant cytoplasmic expression of NPM (immunofluorescence and confocal microscope analysis; nuclei are stained red with propidium iodide). **B,** Three-dimensional reconstruction of two OC1-AML3 cells. An electronic cut of the image-sparing nucleoli was performed to better visualize nuclear and aberrant cytoplasmic distribution of NPM. (Courtesy of Professor I Nicoletti and Professor B Falini.)

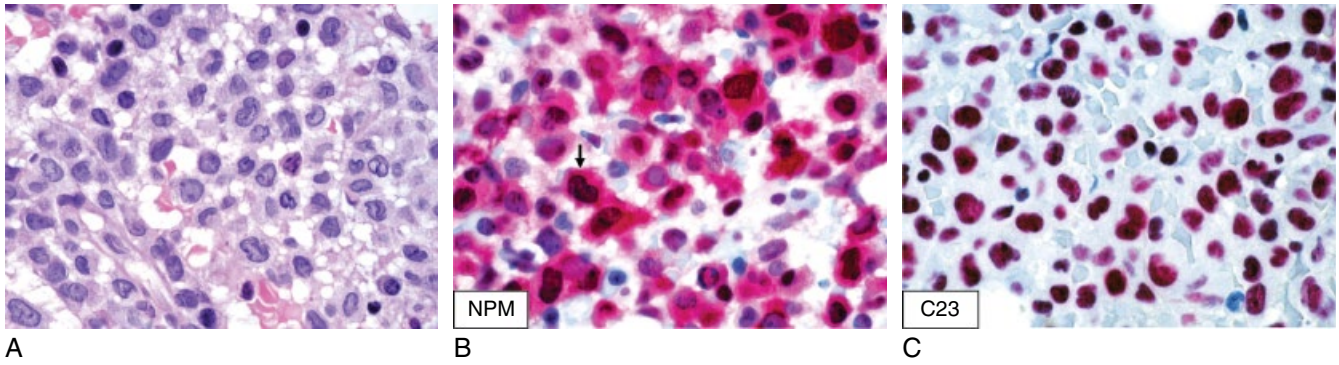

Fig. 13.85. Bone marrow biopsy from acute myeloid leukemia with mutated *NPM1*. **A,** Diffuse infiltration by leukemic cells with monoblastic appearance. **B,** Most leukemic cells show the expected nuclear positivity and the aberrant cytoplasmic expression of NPM (arrow). **C,** The leukemic cells from the same case show nucleus-restricted expression of C23/nucleolin. Immunostaining of paraffin sections with monoclonal antibodies recognizing both wild-type and mutated *NPM* **(B)** or C23/nucleolin **(C)**. Immuno-alkaline phosphatase anti-alkaline phosphatase (AP-AAP) technique with hematoxylin counterstaining. (Courtesy of Professor B Falini.)

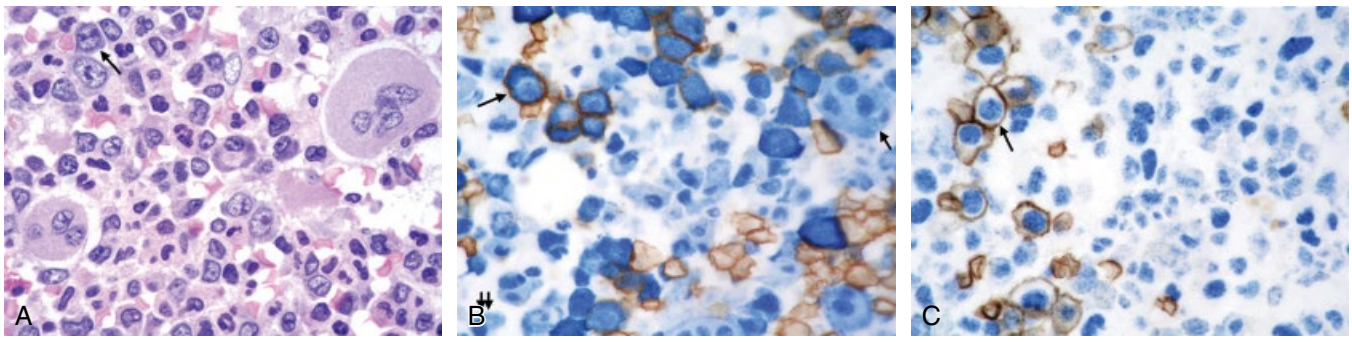

Fig. 13.86. Multilineage involvement in AML with mutated *NPM1* (bone marrow biopsy, paraffin sections). **A,** The marrow is infiltrated by myeloid blasts, abnormal immature erythroid cells (long arrow), and dysplastic megakaryocytes. **B,** Double AP-AAP/immunoperoxidase staining for NPM (blue) and glycophorin (brown). All leukemic cells of the erythroid lineage (long arrow), and dysplastic megakaryocytes (short arrow). **C,** Double AP-AAP/immunoperoxidase staining for all C23/nucleolin (blue) and glycophorin (brown). All leukemic cells of different lineages (the long arrow indicates an immature erythroid cell) show nucleus-restricted expression of C23/nucleolin. (Courtesy of Professor B Falini.)

by detecting individual mutations. It can detect, for example, different types of *NPM1*. Sensitivities for MRD options differ with respect to techniques applied and markers to be tested. The best marker and most sensitive technique should be defined for the respective patient at diagnosis to enable subsequent MRD testing of clinical relevance. Targeted next-generation genome-wide sequencing enables detection of many different mutations among cases of AML in complete remission that were present at diagnosis. In the report of Jongen-Lavrencic et al. (2018) (Fig. 13.91), their presence in remission predicted relapse within 4 years and reduced overall survival except for persistent mutations of *DNMT3A*, *TET2*, and *ASXL1*(DTA). Persistent mutations of these three genes, which are mutated in age-related clonal hematopoiesis, did not predict relapse.

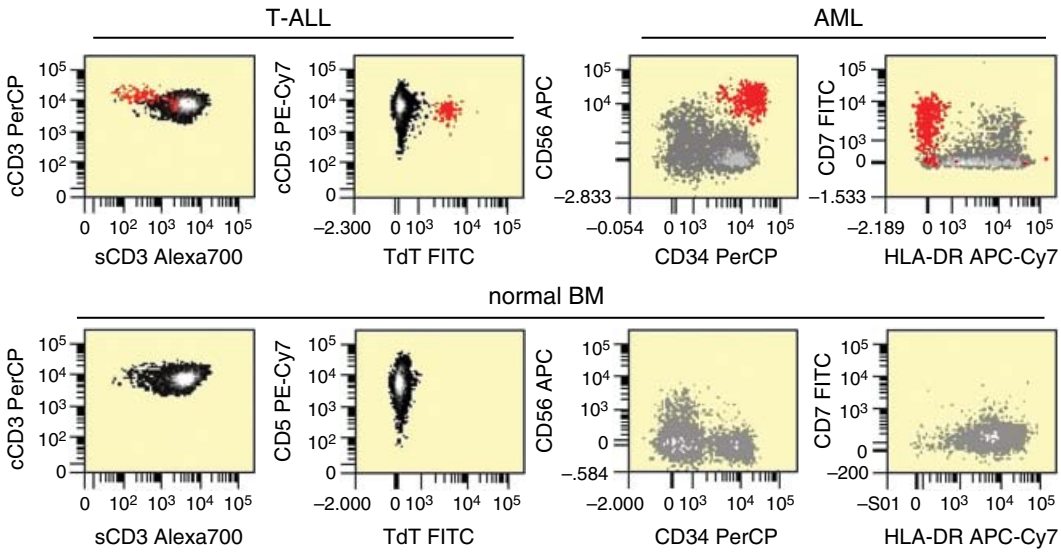

Fig. 13.87. Immunophenotypes: Detection of minimal residual disease (MRD) in acute leukemia by flow cytometry. *Top,* Bone marrow (BM) samples from a patient with T-lineage acute lymphoblastic leukemia (T-ALL) and from one with acute myeloid leukemia (AML), both in morphologic remission, were labeled with combinations of 8–10 monoclonal antibodies simultaneously. Red dots in the density plots are the result of the combined immunophenotypic profile of the cell population and indicate MRD. They correspond to 0.02% of mononuclear cells in the T-ALL sample and 0.3% in the AML sample. *Bottom,* Results of a BM sample obtained from a healthy individual and stained with the same antibodies is shown. (Courtesy of Professor D Campana.)

TABLE 13.11. TRANSLOCATIONS IN ACUTE MYELOID LEUKEMIA SUITABLE FOR PCR ANALYSES (MRD)

Preferred morphologic phenotype	Chromosomal translocation	Molecular target
AML without or with maturation	t(8;21)(q22;q22.1)	*RUNX1-RUNX1T1*
Acute myelomonocytic leukemia with abnormal eosinophils	inv(16)(p13.1q22) or t(16;16)(p13.1;q22)	*CBFB-MYH11*
Acute promyelocytic leukemia or its variant	t(15;17)(q22;q12)	*PML-RARA*
Acute monoblastic/monocytic leukemia	t(9;11)(p22;q23)	*KMT2A-MLLT3*
AML with maturation	t(6;9)(p23;q34)	*DEK-NUP214*
AML with maturation or acute myelomonocytic leukemia	inv(3)(q21q26.2) or t(3;3)(q21;q26.2)	*MECOM*
Acute megakaryoblastic leukemia	t(1;22)(p13;q13)	*RBM15-MKL1*
AML without or with maturation	t(9;22)(q34;q11)	*BCR-ABL1*

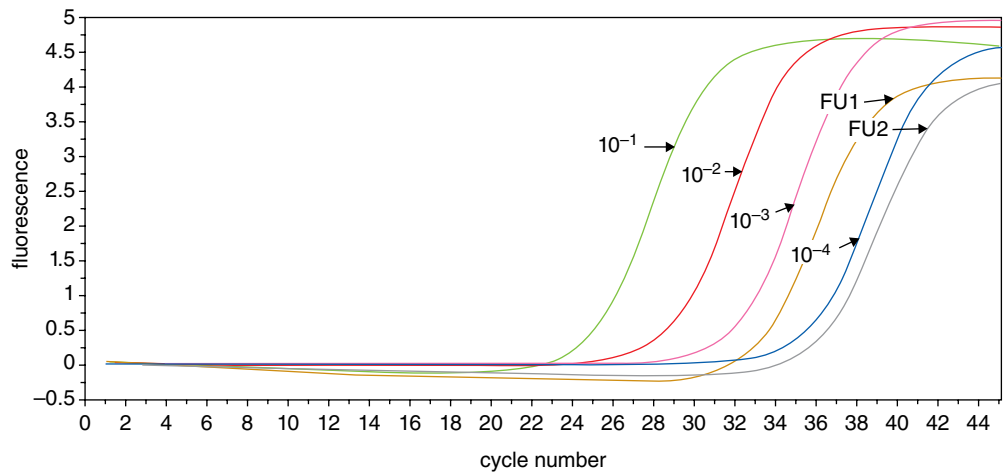

Fig. 13.88. RT-PCR quantification of minimal residual disease using immunoglobulin gene analysis of peripheral blood. This image illustrates RT-PCR for antigen-receptor gene analysis. Dilution of presentation material from 10^1 to 10^4 of DNA from the leukemic sample into normal mononuclear cells (obtained from six normal donor buffy-coats) is shown, and each dilution is marked by an arrow and the individual dilution amount. Two follow-up samples (FU1 and FU2) measurements are given. FU1 is quantified between 10^4 and 10^3 whereas FU2, though positive, is outside the quantitative range (POQR) of the presentation standard curve. (Courtesy of Dr. L Foroni.)

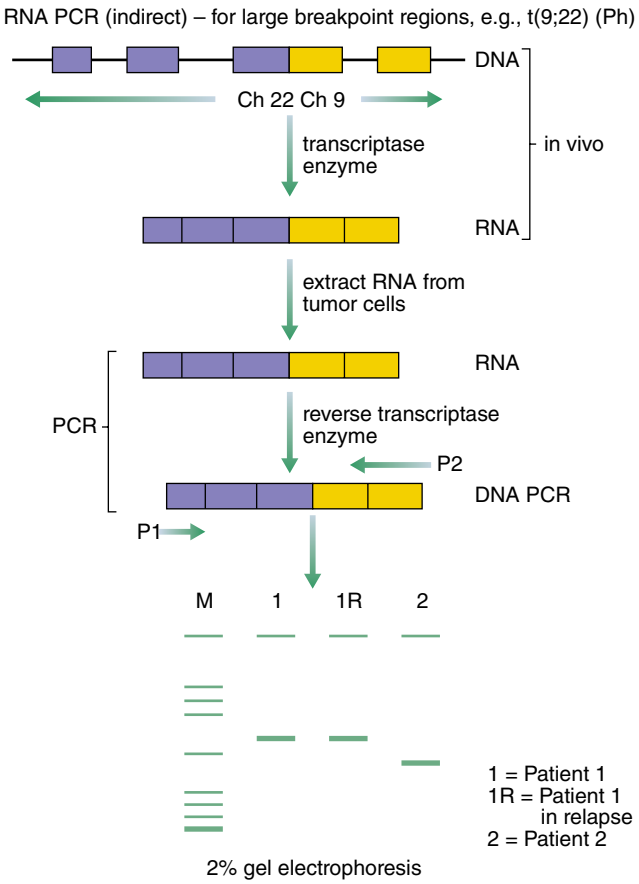

Fig. 13.89 Molecular cytogenetics: RNA PCR [indirect–for large breakpoint regions, e.g., t(9;22) (Ph)].

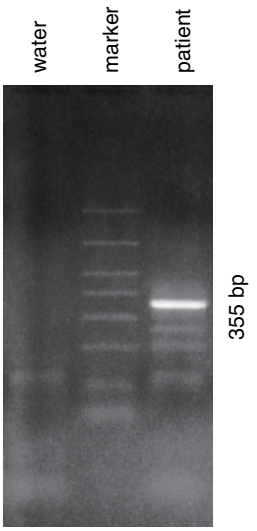

Fig. 13.90. Reverse transcriptase PCR analysis of an APL patient at diagnosis. The *PML-RARA* fusion product (cDNA) has been amplified using nested oligonucleotides from the *PML* and *RARA* genes. Lane 1, water control; Lane 2, low-molecular-weight (Cambio) DNA marker; Lane 3, patient sample. All APL patients with a t(15;17) translocation express either the 5′ (a single 355 bp fusion message) or the 3′ (a series of various fusion messages caused by alternate splicing) PML breakpoint. (Courtesy of Dr. P Devaraj.)

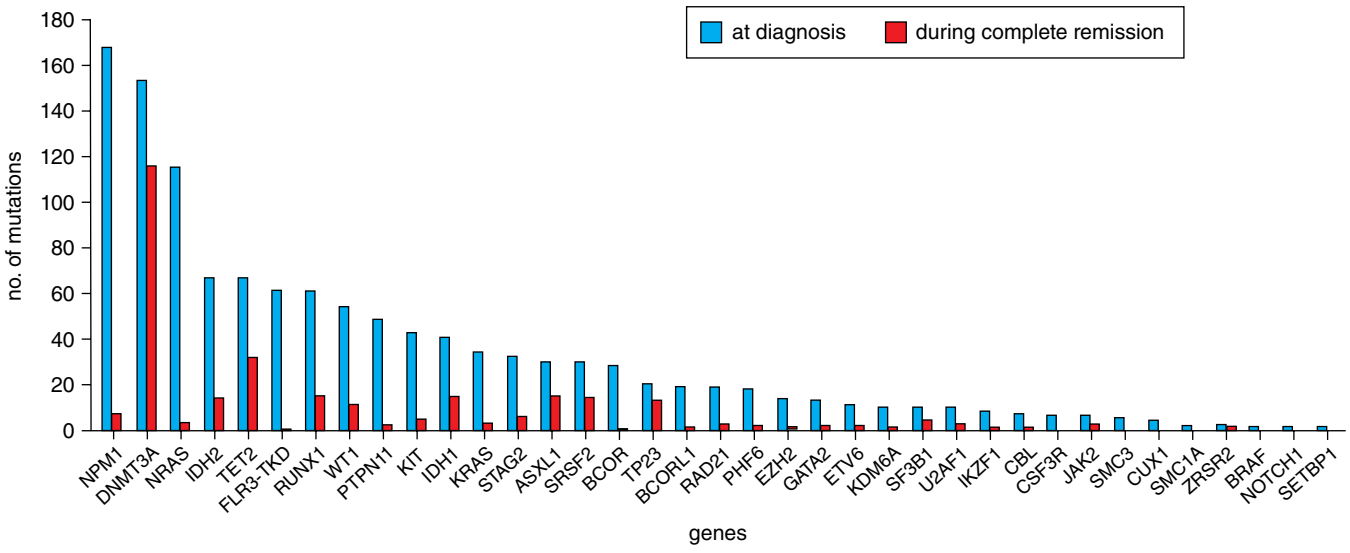

Fig. 13.91. Acute myeloid leukemia. Detection of mutations at diagnosis and in complete remission by next-generation sequencing among 430 patients aged 18–65 years. Source: Jongen-Lavrencic M, et al. *N Engl J Med* 2018;378:1193.

CHAPTER

ACUTE LYMPHOBLASTIC LEUKEMIA

14

Acute lymphoblastic leukemia (ALL) is the result of accumulation of early lymphoid precursors in the bone marrow, blood, thymus, and other tissues. It is thought to arise by somatic mutation(s) of a single cell within a minor population of stem or early progenitor cells in the bone marrow or thymus. In childhood ALL, certain genetic polymorphisms in genes associated with the development and function of the immune system predispose to the disease as do certain genetic syndromes, particularly Down syndrome (Table 14.1). Common gene mutations in ALL associated with Down syndrome are of *CRLF2* and *JAK2* and of *IZKF1*. In some instances ALL arises before birth, for example with the t(4;11)/*MLL* (now termed *KMT2A*)-*AF4* translocation and hyperdiploidy, whereas with others, such as t(1;19)/*TCF3-PBX1*, the disease is usually postnatal in origin. A second event, particularly infection, is probably necessary with an abnormal immune response due to genetic predisposition and little or no previous exposure to the infection.

CLASSIFICATION

B-lymphoblastic leukemia (B-ALL)/lymphoblastic lymphoma (B-LBL) is a neoplasm of precursor lymphoid cells committed to the B-cell lineage, typically composed of small to medium-sized blast cells with scant cytoplasm, moderately condensed to dispersed chromatin and inconspicuous nucleoli, involving bone marrow and blood (B-ALL) and occasionally presenting with primary involvement of nodal or extranodal sites (B-LBL).

TABLE 14.1. GENETIC PREDISPOSITION TO CHILDHOOD ACUTE LYMPHOBLASTIC LEUKEMIA

Germline polymorphisms (detected by GWAS)
ARID5B, *KZF1*, *CEBPE*, *CDKN2A*, *BMI1-PIP4K2A*, *GATA3*
Genetic diseases
Down syndrome (10–30 fold)
Ataxia telangiectasia
Shwachman–Diamond syndrome
Bloom syndrome
Germline *TP53* mutations (Li–Fraumeni syndrome)

GWAS, genome-wide association studies.

By convention, the term lymphoma is used when the process is confined to a mass lesion with no or minimal evidence of blood and marrow involvement. With extensive marrow and blood involvement, lymphoblastic leukemia is the appropriate term. If the patient presents with a mass lesion and lymphoblasts in the marrow, the distinction between leukemia and lymphoma is arbitrary. The genetic abnormalities, prognosis and treatment are identical. For many treatment protocols, a threshold of 25% marrow blasts is used to define leukemia. In contrast to myeloid leukemias, there is no agreed-upon lower limit for the percentage of blasts required to establish a diagnosis of ALL. In general, the diagnosis should be avoided when there are <20% blasts.

T-lymphoblastic leukemia/lymphoblastic lymphoma is a neoplasm of lymphoblasts committed to the T-cell lineage, typically composed of small to medium-sized blast cells with scant cytoplasm, moderately condensed to dispersed chromatin and inconspicuous nucleoli, involving bone marrow (BM) and blood (T-acute lymphoblastic leukemia, T-ALL) or presenting with primary involvement of thymus, nodal or extranodal sites (T-acute lymphoblastic lymphoma). By convention, the term lymphoma is used when the process is confined to a mass lesion with no or minimal evidence of peripheral blood and BM involvement. With extensive BM and peripheral blood involvement, lymphoblastic leukemia is the appropriate term. As for the B-cell lineage, if the patient presents with a mass lesion and lymphoblasts in the BM, the distinction between leukemia and lymphoma is arbitrary and the underlying mutations, prognosis, and treatment are identical for T-ALL and T-lymphoblastic lymphoma.

The World Health Organization (WHO) (2016) subclassification of B-ALL is based on cytogenetics (Table 14.2). Provisional entities in WHO 2016 are *BCR-ABL1*-like, B-ALL with iAMP21, early T-cell lymphoblastic leukemia and a natural killer (NK) cell lymphoblastic leukemia/lymphoma.

B-LYMPHOBLASTIC LEUKEMIA/LYMPHOMA, *BCR-ABL1*-LIKE

This is a high-risk subtype of B-ALL which occurs in 15% of children and about 20% of adults between the ages of 40 and 79 years (see Fig. 14.22). It is more frequent in males. There are a wide range of underlying genetic abnormalities that activate kinase signaling pathways and cytokine receptors. Gene expression profiling reveals a characteristic pattern (Fig. 13.12). The genetic abnormalities have been divided into five subgroups:

Color Atlas of Clinical Hematology: Molecular and Cellular Basis of Disease, Fifth Edition. A. Victor Hoffbrand, Paresh Vyas, Elías Campo, Torsten Haferlach, and Keith Gomez

TABLE 14.2. WHO (2016): CLASSIFICATION OF PRECURSOR LYMPHOID NEOPLASMS (ACUTE LYMPHOBLASTIC LEUKEMIA/ LYMPHOMA)

B-lymphoblastic leukemia/lymphoma, NOS
B-lymphoblastic leukemia/lymphoma with recurrent genetic abnormalities
B-lymphoblastic leukemia/lymphoma with t(9;22)(q34.1;q11.2); *BCR-ABL1*
B-lymphoblastic leukemia/lymphoma with t(v;11q23.3); *KMT2A* rearranged
B-lymphoblastic leukemia/lymphoma with t(12;21)(p13.2;q22.1); *ETV6-RUNX1*
B-lymphoblastic leukemia/lymphoma with hyperdiploidy
B-lymphoblastic leukemia/lymphoma with hypodiploidy
B-lymphoblastic leukemia/lymphoma with t(5;14)(q31.1;q32.3); *IL3-IGH*
B-lymphoblastic leukemia/lymphoma with t(1;19)(q23;p13.3); *TCF3-PBX1*
Provisional entity: B-lymphoblastic leukemia/lymphoma, *BCR-ABL1*-like
Provisional entity: B-lymphoblastic leukemia/lymphoma with iAMP21
T-lymphoblastic leukemia/lymphoma
Early T-cell precursor lymphoblastic leukemia
NK-lymphoblastic leukemia/lymphoma

Source: Adapted from Swerdlow SH, et al., eds. *WHO Classification of Tumours of the Haematopoietic and Lymphoid Tissues*, revised 4th edn. International Agency for Research on Cancer, Lyon, 2017.

1. Rearrangement of *CRLF2* (cytokine receptor-like factor 2) in 50% of cases. The translocation causes upregulation of the thymic stromal lymphopoietin receptor (detectable by flow cytometry). There may be associated transcription factor *IKZF1* deletion. About half the *CRLF2*-mutated cases also have a *JAK2* point mutation, usually R683G in the pseudokinase region (see Fig. 16.32). The *CRLF2* translocations are frequent in Down syndrome ALL cases.
2. *ABL*-class gene rearrangements. These include fusions to *ABL1*, *ABL2*, *CSF1R*, and other genes.
3. *JAK2* and *EPOR* rearrangements. *JAK2* may have at least 14 different partners.
4. Sequence mutations or deletions activating JAK-STAT or RAS/MAPK signaling pathways.
5. Rearrangements of *ABL*-class tyrosine kinase genes.

B-ALL WITH INTRACHROMOSOMAL AMPLIFICATION OF CHROMOSOME 21

B-ALL with intrachromosomal amplification of chromosome 21 (iAMP21) is a rare form of ALL, most often in older children with low white cell counts. There is amplification of a part of chromosome 21 usually detected by fluorescence in situ hybridization (FISH) for the gene *RUNX1*. There are five or more copies (or three or more extra copies) on a single abnormal chromosome 21 in metaphase FISH. The prognosis is unfavorable.

T-LYMPHOBLASTIC LEUKEMIA/LYMPHOMA

The majority of cases of T-ALL show different genetic mutations but these are not yet clearly related to stage of differentiation shown by antigen expression (Table 14.3) or prognosis, so T-ALL is not separated into different subgroups based on immunological or cytogenetic findings.

TABLE 14.3. T-CELL CD ANTIGEN EXPRESSION IN PRO-, PRE-, CORTICAL (THYMIC), AND MATURE T-CELL ALL

	cyCD3	CD7	CD5	CD2	CD1a	sCD3	CD34
Pro-T	+	+	−	−	−	−	±
Pre-T	+	+	+	+	−	−	±
Cortical (thymic)	+	+	±	±	+	±	−
Mature	+	+	±	+	−	+	−

cyCD3, cytoplasmic CD3; sCD3, surface CD3.
Source: Marks DI, Rowntree C. *Blood* 2017;129:1134–1142. Reproduced with permission of *Blood: Journal of the American Society of Hematology*.

EARLY T-CELL PRECURSOR ALL

The WHO (2016) classification recognizes only one small subtype of T-ALL, early T-cell precursor (ETP) ALL. As in other cases of T-ALL the blasts express CD7 but lack CD1a and CD8 and are positive for one or more early myeloid/stem cell markers, CD34, CD117, HLA-DR, CD13, CD11b, or CD65. They typically express cytoplasmic CD3 and may express CD4. Typical T-ALL mutations such as in *NOTCH1* are infrequent, whereas typical myeloid mutations are often present, including those of *FLT3*, *NRAS/KRAS*, *DNMT3A*, *IDH1*, and *IDH2*. The gene expression profile of ETP-ALL resembles that of hematopoietic stem cells. With effective chemotherapy the prognosis is similar to that for other forms of T-ALL.

ACUTE NATURAL KILLER CELL LEUKEMIA

A provisional entry in WHO (2016) is natural killer (NK) cell lymphoblastic leukemia/lymphoma (see Fig. 14.11c).

CLINICAL FEATURES

Acute lymphoblastic leukemia may present with features of bone marrow failure (anemia, infections, easy bruising, or hemorrhage) and may or may not include features of organ infiltration by leukemic cells. The organs usually involved are the lymph nodes (Fig. 14.1), spleen and liver, meninges (Figs. 14.2

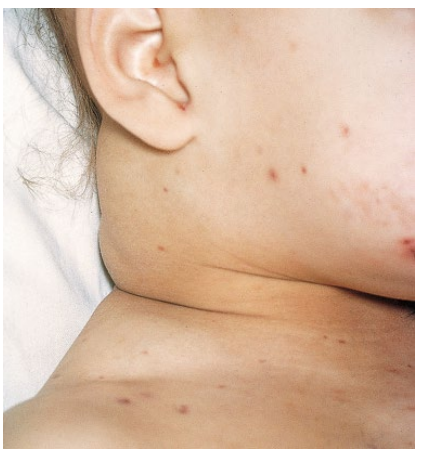

Fig. 14.1. Acute lymphoblastic leukemia: Marked cervical lymphadenopathy in a 4-year-old boy. (Courtesy of Professor JM Chessells.)

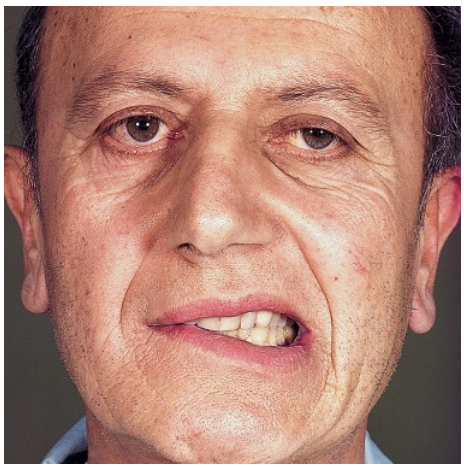

Fig. 14.2. Acute lymphoblastic leukemia: This 59-year-old man has facial asymmetry because of a right lower motor neuron seventh nerve palsy resulting from meningeal leukemic infiltration. (Courtesy of Professor HG Prentice.)

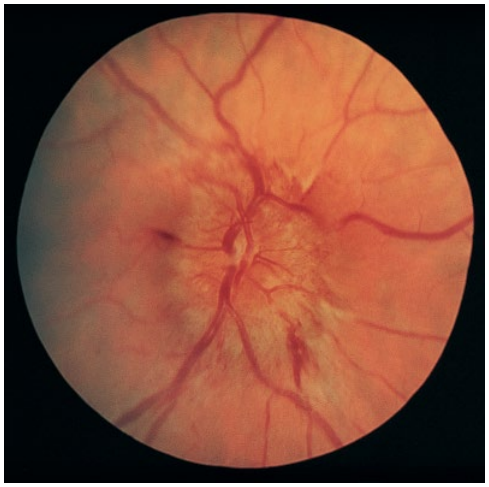

Fig. 14.3. Acute lymphoblastic leukemia: Papilledema caused by meningeal disease. There is blurring of the disk margin with venous enlargement and retinal hemorrhages.

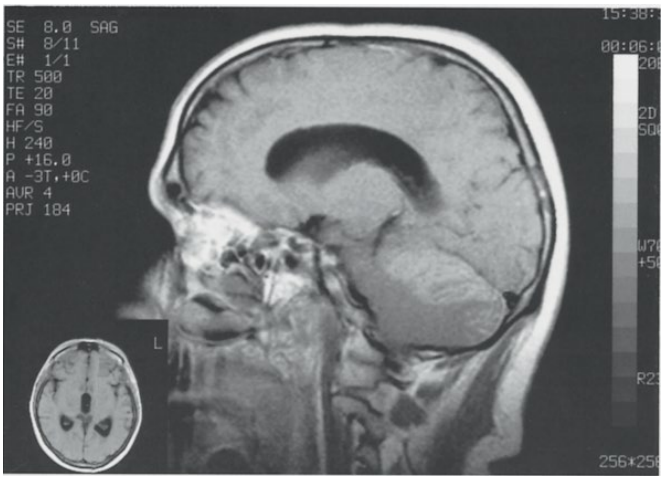

Fig. 14.4. Acute lymphoblastic leukemia: Magnetic resonance imaging (MRI) scan showing dilated cerebral ventricles with expansion of the cerebellum and blockage of the viaduct between the third and fourth ventricles. The patient, a 33-year-old man, had headache, diplopia, and blast cells in the cerebrospinal fluid. (Courtesy of Dr. AR Valentine.)

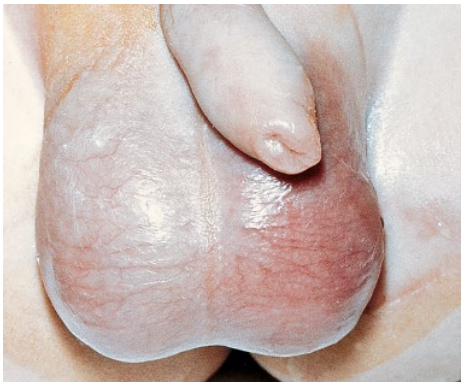

Fig. 14.5. Acute lymphoblastic leukemia: Testicular swelling and erythema of the left side of the scrotum caused by testicular infiltration. (Courtesy of Professor JM Chessells.)

and 14.3) and central nervous system (Fig. 14.4), testes (most often at relapse) (Fig. 14.5). Rarely, a visible deposit of leukemic blasts is seen in the eye (Fig. 14.6). Infections are often bacterial in the early stages and particularly affect the skin, pharynx, and perineal regions. They are not usually as severe as in acute myeloid leukemia (AML).

Other viral (especially herpetic), protozoal, or fungal infections, especially *Pneumocystis jiroveci* (see Chapter 11) are frequent, and may become life threatening. Hemorrhage of the skin or mucous membranes is usually petechial.

In the T-cell variant (T-ALL), there is often upper mediastinal enlargement, caused by a thymic mass, which responds rapidly to therapy (Fig. 14.7). Although meningeal involvement is more frequent in children and younger subjects with ALL, it may occur at all ages, manifesting with nausea, vomiting, headaches, visual disturbances, photophobia, and features of the cranial nerve palsies (see Fig. 14.2). Papilledema may be found on examination (see Fig. 14.3). Bone involvement may produce characteristic radiographic findings (Fig. 14.8).

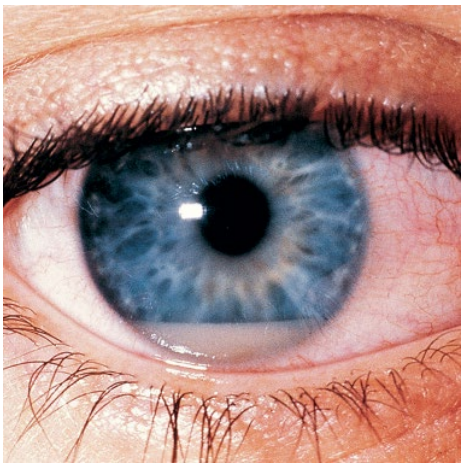

Fig. 14.6. Acute lymphoblastic leukemia: Leukemic infiltration in the anterior chamber of the eye obscures the lower rim of the iris. (Courtesy of Professor JM Chessells.)

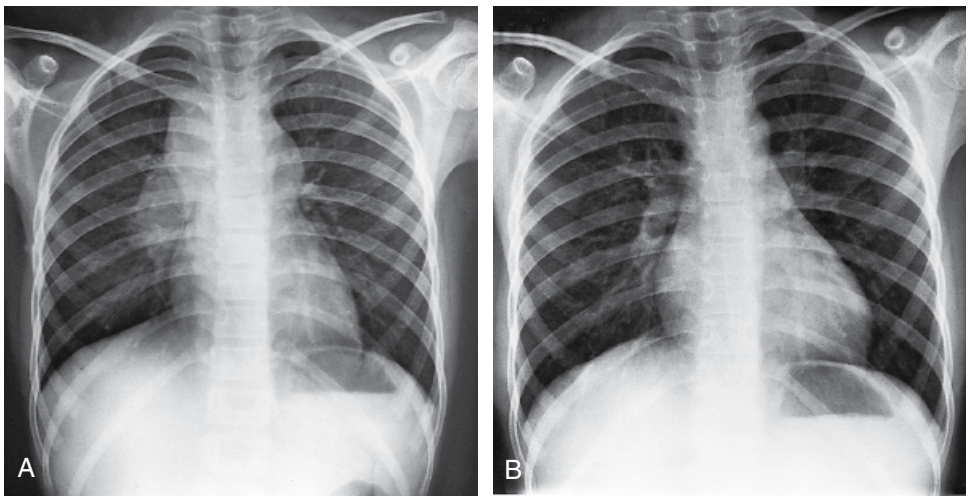

Fig. 14.7. Acute lymphoblastic leukemia, T-cell subtype. **A**, Chest radiograph of a 4-year-old boy showing upper mediastinal widening caused by thymic enlargement; **B,** Chest radiograph shows disappearance of thymic mass following one week of therapy with vincristine and prednisolone.

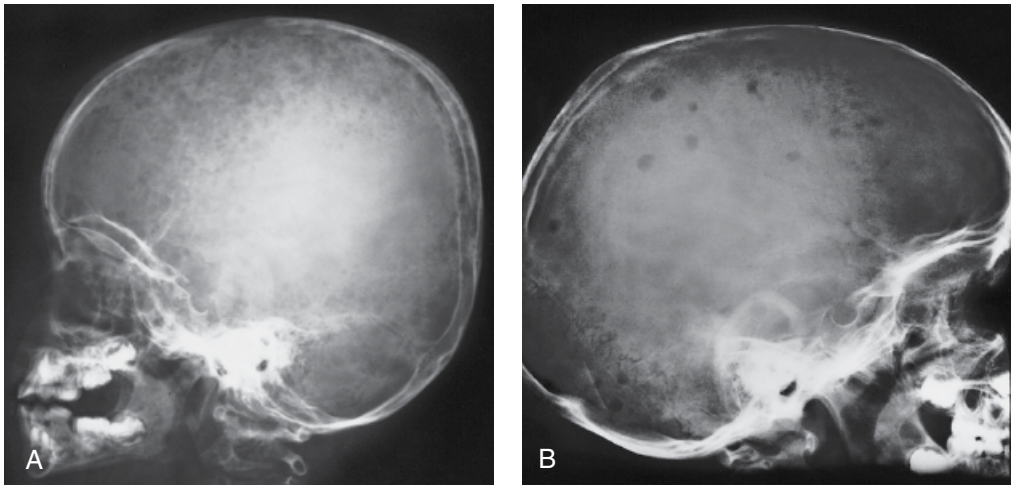

Fig. 14.8. Acute lymphoblastic leukemia: Radiographs of childrens' skulls. **A,** Mottled appearance caused by widespread leukemic infiltration of bone. **B,** Multiple punched-out lesions caused by leukemic deposits. (Courtesy of Professor JM Chessells.)

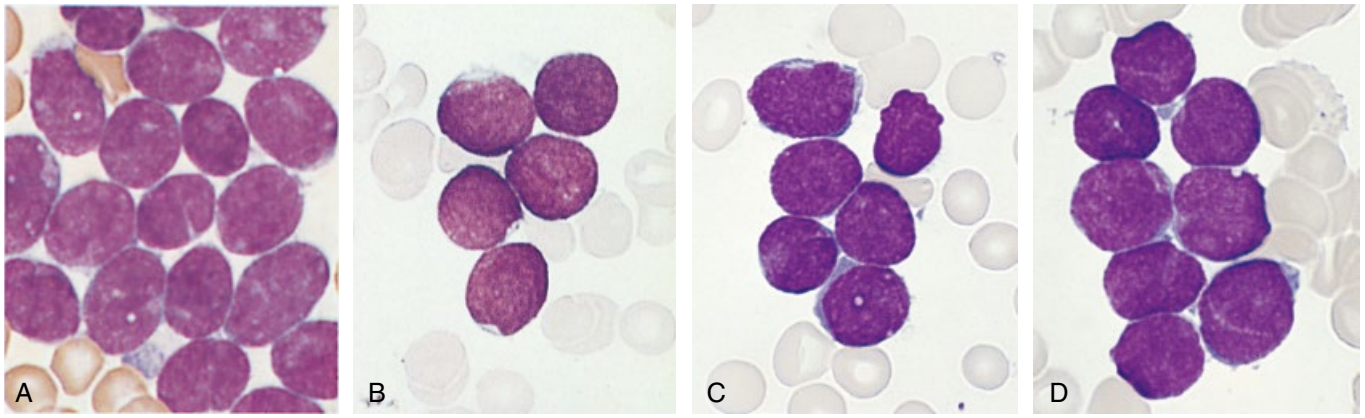

Fig. 14.9. Acute lymphoblastic leukemia, small cell subtype. **A,** Rather small, uniform blast cells with scanty cytoplasm, **B,** and rounded or cleft nuclei with usually a single nucleolus (**C, D**).

MICROSCOPIC APPEARANCES

Lymphoblasts show little evidence of differentiation and the appearances of the cells are similar whether the case is classified as leukemia or lymphoma and whether B-ALL or T-ALL. Cases with smaller, more uniform cells with scanty cytoplasm (Fig. 14.9) and those with blasts differing widely in size, with prominent nucleoli and greater amounts of cytoplasm (Fig. 14.10) were previously given prognostic significance but this distinction is now obsolete. Rare subtypes show coarse granules (Fig. 14.11A) or a reactive eosinophilia (Fig. 14.11B). Figure 14.11C illustrates a rare NK type of acute leukemia with an aberrant phenotype of both ALL and AML and Fig. 14.11D shows a probable NK leukemia.

T-ALL blasts are indistinguishable from B-lineage blasts morphologically (Fig. 14.12). Special stains, flow cytometry, cytogenetics, and gene rearrangement studies are needed to distinguish them.

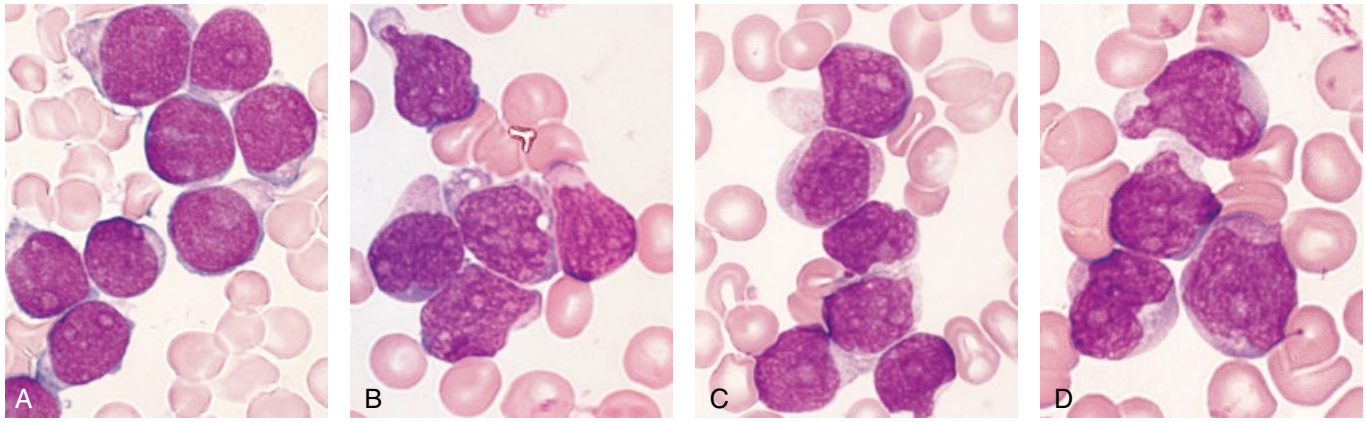

Fig. 14.10. A–D, Acute lymphoblastic leukemia. Blast cells that vary considerably in size and amount of cytoplasm; the nuclear-to-cytoplasmic ratio is rarely as high as in L1. The nuclei are variable in shape and often contain many nucleoli.

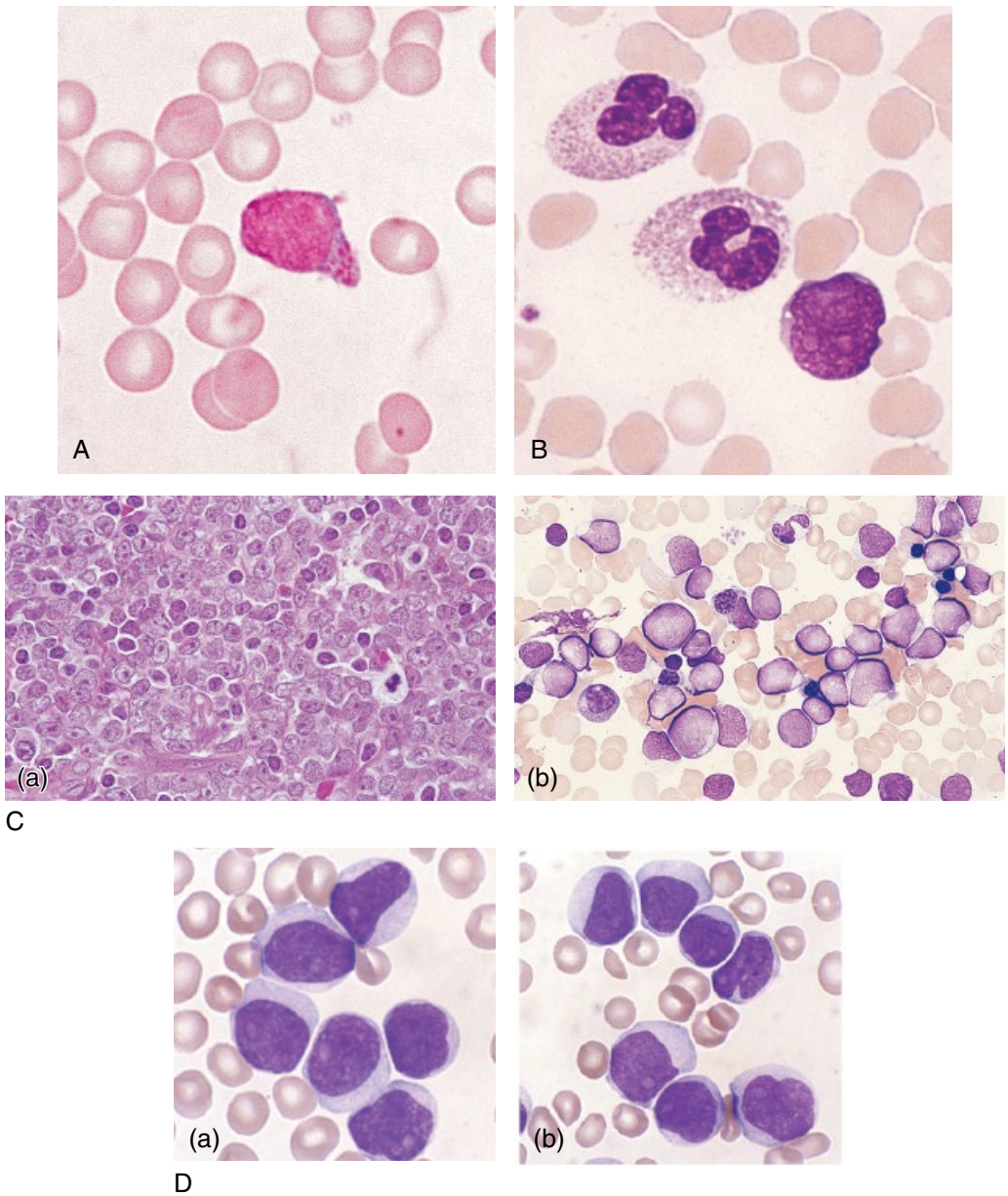

Fig. 14.11. Acute lymphoblastic leukemia. **A,** Rare subtype with granules. **B,** Rare subtype with eosinophilia. Peripheral blood film shows a lymphoblast and two eosinophils. (WBC, 36×10^9/L; lymphoblasts, 14×10^9/L; eosinophils, 20×10^9/L.) **C**, Natural killer cell leukemia: 54-year old man with cervical lymphadenopathy. (a) Biopsy showed diffuse infiltration of cells with round and irregular nucleoli and scanty cytoplasm. (b) The bone marrow shows an infiltrate of immature blast of varied morphology. The cells were myeloperoxidase negative but CD2+, CD7+, CD56+, and DR+. (Courtesy of Dr R Suzuki). **D,** Acute NK leukemia. The cells were CD56+ and CD4+. The large blast cells have a vesicular chromatin pattern, prominent nucleoli, and pale, relatively agranular cytoplasm. Source: **A, B,** Cantu-Reynoldi A, et al. *Br J Haematol* 1989;73:309–314. Reproduced with permission of John Wiley & Sons.

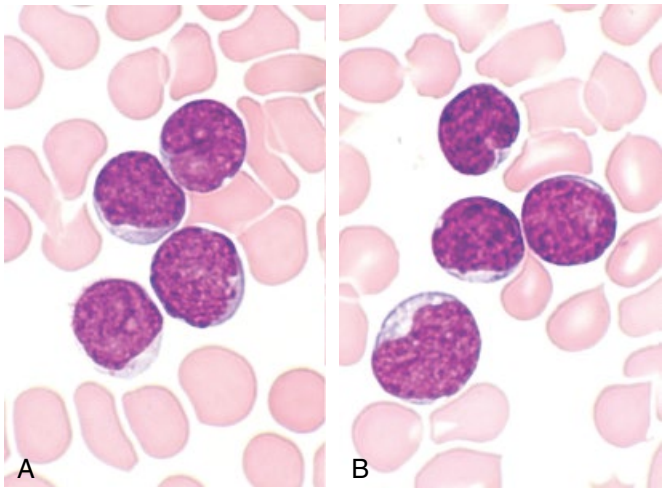

Fig. 14.12. A, B, Acute T-lymphoblastic leukemia. The majority of the blasts cells in the peripheral blood are small with sparse cytoplasm, condensed chromatin, and inconspicuous nucleoli. Some of the cells have a nuclear cleft. The patient was a 24-year-old man. (Hb, 12.0 g/dL, WBC, 115×10^9/L; platelets, 15×10^9/L.) The cells were CD1a+, CD2+, cCD3+, CD5+, CD4/CD8+, CD7+, and TdT+.

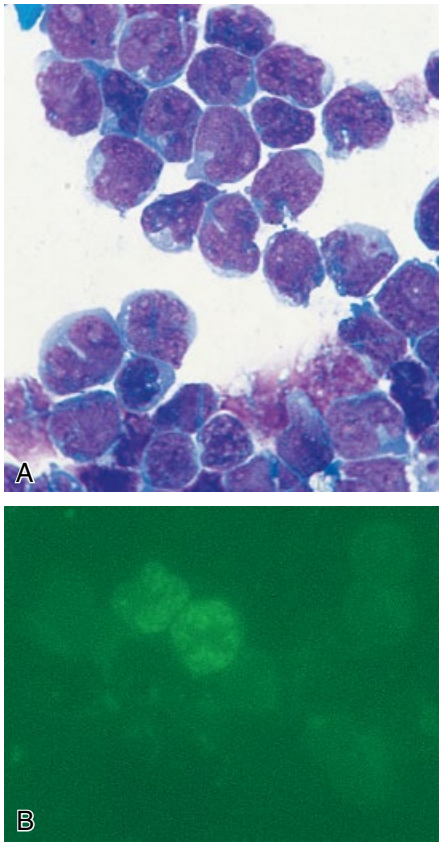

Fig. 14.13. Acute lymphoblastic leukemia. **A,** High-power view of cytospin of cerebrospinal fluid, showing a deposit of blast cells of varying morphology. The patient had the features of meningeal leukemia. **B,** Indirect immunofluorescent staining of cerebrospinal fluid for terminal deoxynucleotidyl transferase (TdT). These few cells, difficult to recognize morphologically, show nuclear TdT staining typical of lymphoblasts. (Courtesy of Professor KF Bradstock.)

The bone marrow in all variants is hypercellular, with leukemic blasts usually making up >80% of the marrow cell total. Blasts may be seen in the cerebrospinal fluid (Fig. 14.13) or testes (Fig. 14.14).

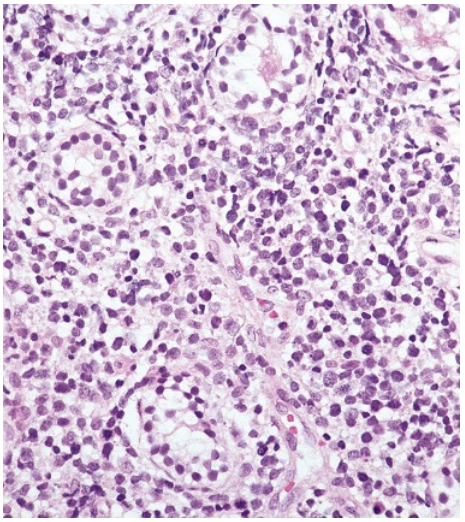

Fig. 14.14. Acute lymphoblastic leukemia: Low-power view of testicular infiltrate, showing leukemic blast cells in the interstitial tissues and in the seminiferous tubular epithelium.

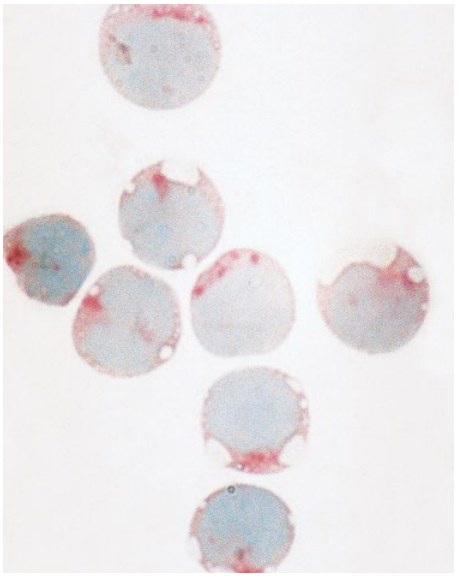

Fig. 14.15. Acute lymphoblastic leukemia, T-cell subtype: Bone marrow aspirate shows red cytoplasmic staining with marked coloration of the Golgi zone adjacent to or indented into the nucleus. (Acid phosphatase stain.)

T-ALL stained by acid phosphatase shows eccentric Golgi body staining (Fig. 14.15). Cytochemical stains may be helpful in acute leukemia of ambiguous lineage (see Chapter 13).

With the availability of flow cytometry and cytogenetics, cytochemistry is now rarely needed but it may still have value when dealing with acute leukemias of ambiguous lineage.

IMMUNOLOGY

Immunologic characterization of ALL cells is essential to the diagnosis. Fluorescence-labeled antibodies to surface, cytoplasmic, and nuclear B- or T-cell antigens are used with multiparameter-flow cytometry (FACS) analysis (see Chapter 13). Panels of

antibodies have been established for initial screening and for subsequent more detailed analysis (Table 14.4). Typical findings in B-lineage ALL and T-cell ALL are shown in Figs. 14.16 and 14.17. Cytoplasmic (c) immunoglobulin (cIg) and cCD3 are relatively specific markers for B-lineage and T-lineage ALL, respectively. Nuclear terminal deoxynucleotide transferase-like surface antigens (TdT-like surface antigens) can be detected by FACS but also by immunoperoxidase staining of blood or bone marrow (Fig. 14.18). The value of TdT detection in identifying extramedullary ALL cells is shown in Fig. 14.13.

The criteria for diagnosis of leukemias of ambiguous lineage are given in Chapter 13.

CYTOGENETICS

Cytogenetic analysis is now essential for the exact characterization of ALL and for decisions on management, and prognosis. The WHO classification of B-ALL is based on the cytogenetic findings (see Table 14.2).

The frequencies of the various genotypes in childhood, adolescent, and adult ALL are shown in Fig. 14.19 and the prognostic significance of these primary cytogenetic findings listed in Table 14.5.

KMT2A (*MLL*) rearrangements, especially t(4;11), are most frequent before the age of 1 year. B-ALL high hyperdiploidy with

TABLE 14.4. ACUTE LEUKEMIA: PANELS OF MONOCLONAL (OR POLYCLONAL) ANTIBODIES RECOMMENDED BY THE BRITISH COMMITTEE FOR STANDARDS IN HEMATOLOGY AND BY THE US CANADIAN CONSENSUS GROUP FOR THE DIAGNOSIS AND CLASSIFICATION OF ACUTE LEUKEMIA

		BCSH	Consensus group
Primary panel	B lymphoid	CD19, cCD22, cCD79a, CD10	CD10, CD19, anti-κ, anti-λ
	T lymphoid	cCD3, CD2	CD2, CD5, CD7
	Myeloid	CD13, CD117, anti-cMPO	CD13, CD14, CD33
	Not lineage specific	Nuclear TdT	CD34, HLA-DR
Secondary panel	B lymphoid	μ, SmIg (anti-κ and anti-λ),	CD20, Sm/cCD22
	T lymphoid	CD138	CD1a, Sm/cCD3, CD4, CD8
	Myeloid	CD7	CD15, CD16, CD41, CD42b, CD61,
	Not lineage specific	CD33, CD41, CD42, CD61,	CD64, CD71, CD117, anti-cMPO,
	Nonhematopoietic	anti-glycophorin A	anti-glycophorin A
		CD45	CD38, nuclear TdT
		MAb for the detection of small round cell tumors of childhood	
Optional	B lymphoid	CD15 (a myeloid marker often expressed on *KMT2A*-rearranged B lymphoblasts) and 7.1/NG2 (also for *KMT2A*-rearranged ALL)	
	T lymphoid	Anti-TCRαβ, anti-TCRγδ	
	Myeloid	Anti-lysozyme, CD14, CD36, anti-PML (MAb PL1-M3, HLA-DR for negativity in M3 AML)	

c, cytoplasmic; CD, cluster of differentiation; MAb, monoclonal antibody; MPO, myeloperoxidase; Sm, surface membrane; TCR, T-cell receptor; TdT, terminal deoxynucleotidyl transferase. See also Table 13.8.

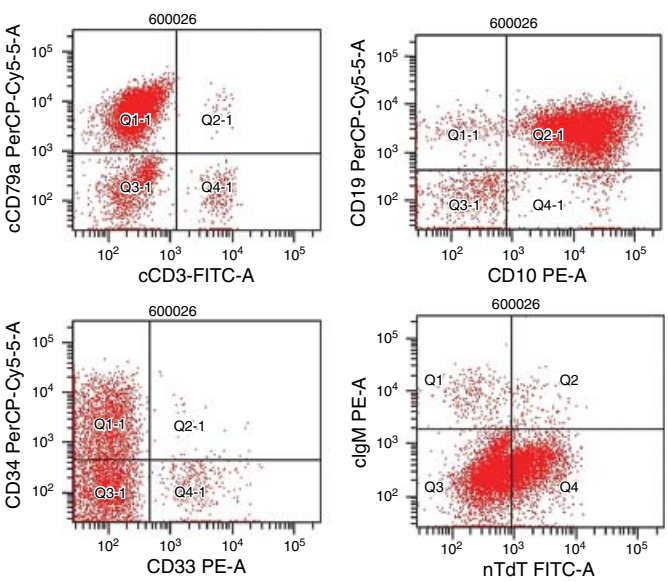

Fig. 14.16. Acute lymphoblastic leukemia, B-lineage: Flow cytometry. The blast cells are CD10, CD19, CD34, CD79a, and TdT positive; cCD3 and IgM negative. (Courtesy of Immunophenotyping Laboratory, Royal Free Hospital.)

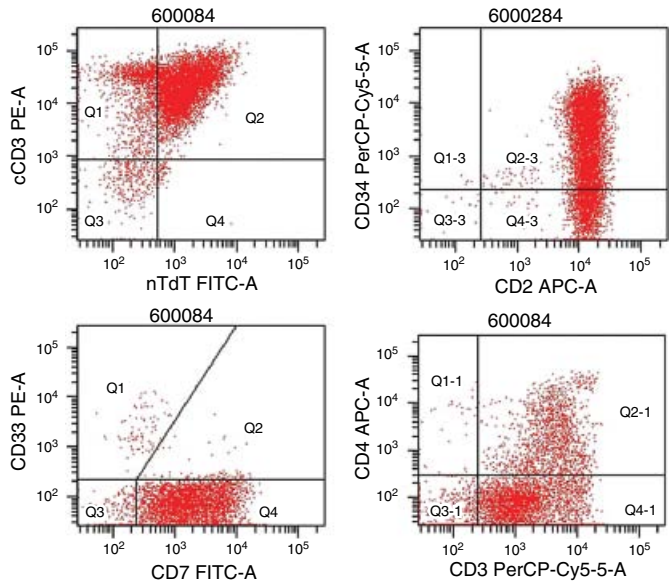

Fig. 14.17. Acute lymphoblastic leukemia, T-lineage: The blast cells are CD4, CD7, cCD3, CD34, and TdT positive. (Courtesy of Immunophenotyping Laboratory, Royal Free Hospital.)

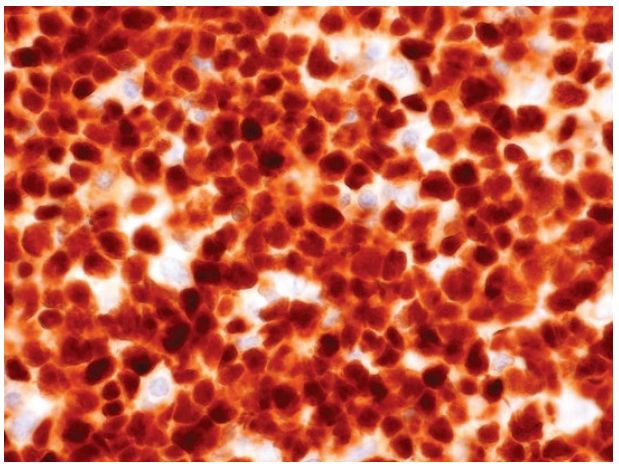

Fig. 14.18. Acute lymphoblastic leukemia: Bone marrow cells staining positive for TdT by immunoperoxidase. (Courtesy of Dr. A Ramsay.)

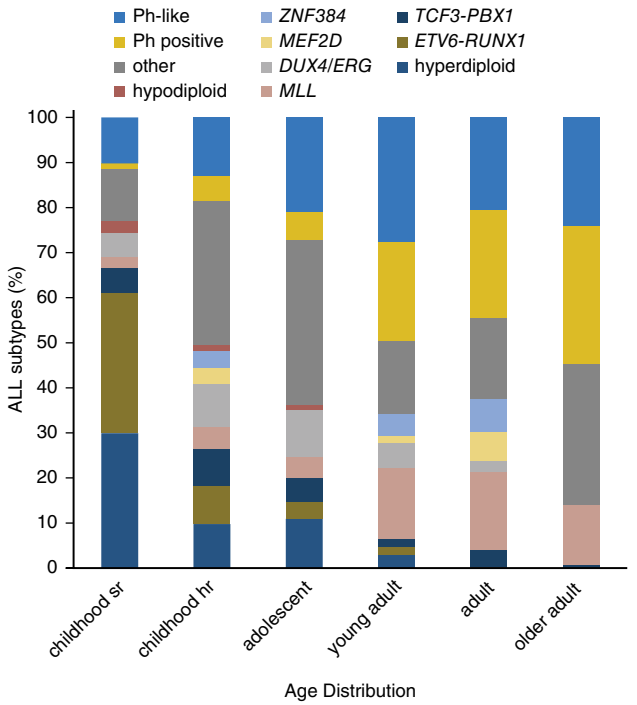

Fig. 14.19. Age distribution of acute lymphoblastic leukemia subtypes. The prevalence of ALL subtypes varies in children with standard-risk (SR) ALL (age 1–9 years and WBC count 50×10^9/L), children with high-risk (HR) ALL (age 10–15 years and/or WBC count 50×10^9/L), and adolescents (age 16–20 years), young adults (age 21–39 years), adults (age 40–59 years), and older adults (age 60–86 years) with ALL. Other, B-cell ALL lacking recurrent abnormalities; Ph, Philadelphia chromosome. Source: Iacobucci I, Mullighan CG. *J Clin Oncol* 2017;35:1–11. Reproduced with permission of *Journal of Clinical Oncology*: American Society of Clinical Oncology.

gain of at least five chromosomes (Fig. 14.20) and the presence of *ETV6-RUNX1* is more frequent in children and carries a favorable prognosis (Fig. 14.20). The translocation t(1;19)(q23;p13) is also favorable. More frequent in adults, Ph+ (*BCR-ABL1*+) ALL is unfavorable, although with addition of tyrosine kinase inhibitors to therapy the prognosis for *BCR-ABL1*+ ALL and *BCR-ABL1*-like ALL is improving. *RAS*-activating mutations and *IKZF3* alterations and those with 32–39 chromosomes with *KZF2* and *TP53* mutations, which are frequently inherited, are unfavorable. Secondary DNA deletions, gains and mutations occur commonly in B-ALL.

Hypodiploid ALL (<44 chromosomes) carries an unfavorable prognosis. It is divided into those near haploid (24–31 chromosomes) who usually have *RAS*-activating and *IKZF3* alterations and low hypodiploidy 32–39 chromosomes with *IKZF2* alterations and *TP53* mutations.

Approximately 50% of cases of T-ALL have chromosomal translocations which most commonly involve 14q11, where the TCRα and δ genes are located, or 7q34 where the TCRβ gene is located. The translocations result in the association of the TCR genes with various transcription factors. There also may be cryptic translocations of *ABL1*. The genetic abnormalities in B-ALL and T-ALL detected only by molecular methods are described below.

FLUORESCENCE IN SITU HYBRIDIZATION

FISH can be used to examine interphase as well as dividing cells. It is able to detect gain or loss of all or part of a chromosome or a translocation, in some cases where the translocated or lost material is not visible by light microscopy. A cryptic translocation t(12;21) (p13;q22) occurs in 30% of B-lineage ALL (see Fig. 14.21A). Using the *KMT2A* probe, FISH can show rearrangements within the gene (Fig. 14.21B).

MOLECULAR FINDINGS

B-ALL

The molecular lesions in Ph-like ALL subtypes are shown in Fig. 14.22. Up to 7% of B-ALL show deregulation of the double homeobox 4 gene (*DUX4*) and the ETS transcription factor gene (*ERG*). This subtype of B-ALL is detectable by gene expression or sequencing analysis but not by cytogenetics or FISH. It is associated with a favorable prognosis. Rearrangements of myocyte enhancer factor 2D (*MEF2D*) and of zinc finger 384 (*ZNF384*) account for a few per cent of pediatric and adult cases. There are many different fusion partners. Other rearrangements include those of *PAX5*, translocations of *IGH*, *CEBP* gene family members and *IDH4*. In relapsed cases, common genetic lesions acquired or selected for include those of *CREBBP* (CREB-binding protein), the 5′-nucleotidase catalytic enzyme NT5C2, *RAS* pathway mutations, and mutations of other genes involved in DNA repair or epigenetic modification.

T-ALL

Oncogenic activating mutations in the NOTCH signaling pathway occur in 65% of cases of T-ALL, involving the genes *NOTCH1* and *FBXW7* (Figs. 14.23 and 14.24). There also may be sequence mutations and DNA copy number alterations in genes in the JAK-STAT (*JAK1*, *JAK3*, *IL7R*) and RAS/PIK/AKT (*NRAS*, *KRAS*, *PTEN*) pathways. Similar lesions are found in genes involved in epigenetic modification, transcription regulation, and mRNA maturation.

TABLE 14.5. KEY GENETIC SUBTYPES OF ALL AND RECURRENT GENOMIC FEATURES

Category	Age	Description
B-cell precursor ALL		
Hyperdiploidy with >50 chromosomes	Children >> adults	Excellent prognosis; mutations in Ras signaling pathway and histone modifiers
Near-haploid	Children and adults	24–31 chromosomes; poor prognosis; Ras-activating mutations and inactivation of *IKZF3*
Low hypodiploid	Children and adults	32–39 chromosomes; poor prognosis; *TP53* mutations, deletions of *CDKN2A/B* and *RB1,* and inactivation of *IKZF2*
High hypodiploid	Children and adults	40–43 chromosomes; rare; poor prognosis
Near-diploid	Children and adults	44–45 chromosomes; distinct entity frequently with *ETV6-RUNX1* fusion or rearrangements forming dicentric chromosomes
t(12;21)(p13;q22) translocation encoding *ETV6-RUNX1*	Children >> adults	Excellent prognosis; cryptic rearrangement that is detectable by FISH or PCR
t(1;19)(q23;p13) translocation encoding *TCF3-PBX1*	Children and adults	Increased incidence in African Americans; generally excellent prognosis; association with CNS relapse
t(9;22)(q34;q11.2) translocation encoding *BCR-ABL1*	Children << adults	Historically poor outcome, improved with tyrosine kinase inhibitors; common deletions of *IKZF1, CDKN2A/B,* and *PAX5*
Ph-like ALL	Children < adults	Multiple kinase-activating lesions; poor outcome; amenable to tyrosine kinase inhibitor therapy
CRLF2 rearrangement (*IGH-CRLF2, P2RY8-CRLF2)*	Children and adults	Common in Down syndrome-associated and Ph-like ALL (approximately 50%); associated with *IKZF1* deletion and/or mutation and *JAK1/2* mutation and poor prognosis in non-Down syndrome-associated ALL
KMT2A (*MLL*) rearrangements	Infants >>> children and adults	Common in infant ALL; poor prognosis; low number of additional somatic mutations, commonly in kinase-PI3K-RAS signaling pathway
DUX4- and *ERG*-deregulated ALL	Children and adults	Distinct gene expression profile; majority have focal *ERG* deletions and favorable outcome despite *IKZF1* alterations
MEF2D-rearranged ALL	Children and adults	Distinct gene expression profile and aberrant immunophenotype (CD10 negative, CD38 positive); sensitivity to HDAC inhibitors
ZNF384-rearranged ALL	Children < AYA and adults	Fusions are associated with early pro-B-ALL, expression of myeloid markers, and activation of the JAK-STAT pathway
PAX5 rearrangements	Children and adults	Multiple partners, commonly from dic(7;9), dic(9;12), and dic(9; 20)
iAMP21	Older children	Complex structural alterations of chromosome 21; rarely associated with a constitutional Robertsonian translocation rob(15;21)(q10;q10)c; poor prognosis
T-ALL		
TAL1 deregulation	Children < adults	t(1;7)(p32;q35) and t(1;14)(p32;q11) translocations and interstitial 1p32 deletion; generally favorable outcome
LMO2 deregulation	Children	(11;14)(p15;q11) translocation and 5′ *LMO2* deletion; generally favorable outcome
TLX1 (*HOX11*) deregulation	Children < adults	t(10;14)(q24;q11) and t(7;10)(q35;q24) translocations; good prognosis
TLX3 (*HOX11L2*) deregulation	Children and adults	t(5;14)(q35;q32) translocation; commonly fused to *BCL11B,* also a target of deletion and/or mutation; poor prognosis
KMT2A rearrangements	Children	Multiple partners; disruption of *HOX* gene expression and of self-renewing; poor outcome
9q34 amplification encoding *NUP214-ABL1*	Children	Amenable to tyrosine kinase inhibitors, also identified in high-risk B-ALL; other kinase fusions identified in T-ALL include *EML1-ABL1, ETV6-JAK2,* and *ETV6-ABL1*
t(7;9)(q34;q34.3)	Children	Rearrangement of *NOTCH1*
NOTCH1 mutations	Children and adults	Impairment of differentiation and proliferation; overall favorable outcome
FBXW7 mutations	Children and adults	Impairment of differentiation and proliferation; usually evaluated in combination with *NOTCH1*
Early T-cell precursor ALL	Children and adults	Immature immunophenotype; expression of myeloid and/or stem cell markers; poor outcome; genetically heterogeneous with mutations in hematopoietic regulators, cytokine and Ras signaling, and epigenetic modifiers

NOTE. The frequency of some alterations in the adult cohort may be underestimated as a result of lack of studies.
ALL, Acute lymphoblastic leukemia; AYA, adolescents and young adults; B-ALL, B-cell acute lymphoblastic leukemia; FISH, fluorescence in situ hybridization; HDAC, histone deacetylase; PCR, polymerase chain reaction; Ph-like, Philadelphia chromosome-like; T-ALL, T-cell acute lymphoblastic leukemia; >, high; >>, very high; >>>, considerably high; <, low; <<, very low.
Source: Iacobucci I, Mullighan CG. *J Clin Oncol* 2017;35(9):975–983. Reproduced with permission of *Journal of Clinical Oncology*: American Society of Clinical Oncology.

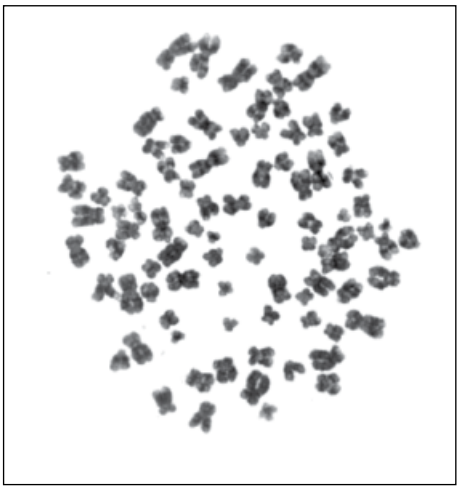

Fig. 14.20. Acute lymphoblastic leukemia: Representative hyperdiploid bone marrow cell pre–B-ALL with 73 chromosomes. (Courtesy of Dr. E Nacheva.)

MINIMAL RESIDUAL DISEASE

FLOW CYTOMETRY

Detection of residual ALL cells in the peripheral blood or bone marrow of patients in complete remission clinically, by blood count and by examination of blood or bone marrow by light microscopy using normal staining, can be performed immunologically by flow cytometry, in which residual cells of an aberrant leukemic phenotype are sought (Fig. 14.25), or by molecular methods. One example could be a standardized flow cytometry using an eight-color antibody panel (CD19, CD10, CD20, CD34, CD45, CD38, and two from CD66c, CD123, CD73, and CD304 in the EuroFlow Consortium, Thenunissen P, et al. *Blood* 2017;129:347–357) can detect, if sufficient cells are analyzed (>4 million), with a sensitivity of 1 in 10^5 cells. Flow cytometry for minimal residual disease (MRD) detection can be carried out on virtually all ALL cases

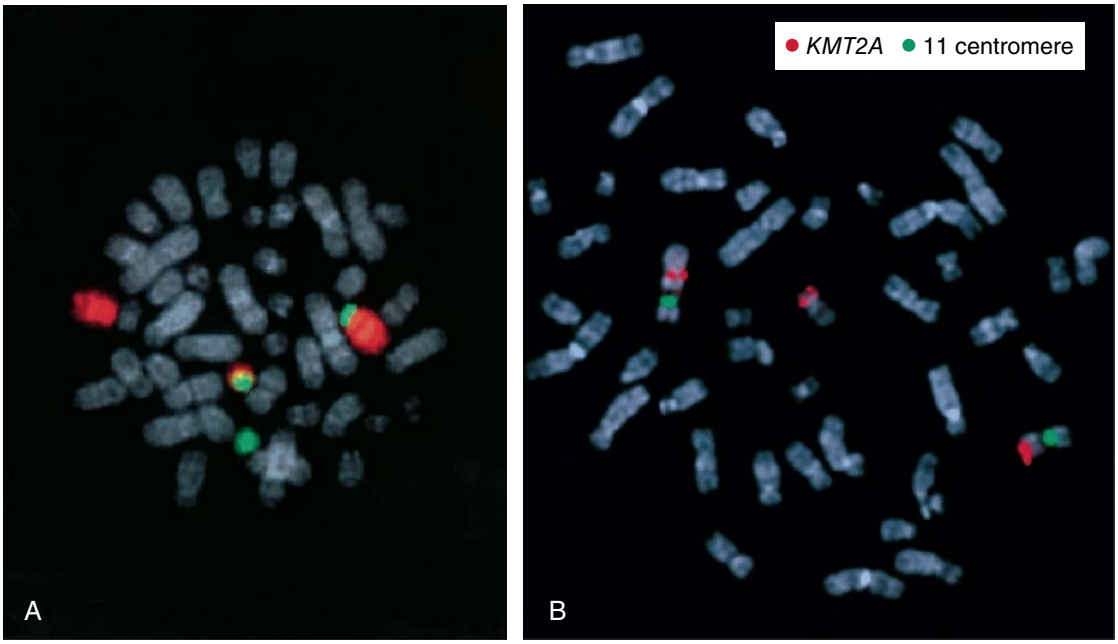

Fig. 14.21. Acute lymphoblastic leukemia: FISH analysis. **A,** Metaphase from a childhood patient with ALL showing the translocation t(12;21) by chromosome "painting." Chromosomes 12 are painted red and chromosomes 21 green. This chromosome abnormality is not visible by conventional cytogenetic analysis. FISH elegantly reveals the exchange of material on the derived chromosomes 12 and 21. **B,** FISH using probes for the centromere of chromosome 11 (green) and the *KMT2A* gene (red), normally on chromosome 11, reveals a reciprocal translocation between chromosomes 6 and 11 that results in the rearrangement of *MLL*, which is detected as a splitting of the *KMT2A* signal between the derived chromosomes 6 and 11. (Courtesy of Dr. CJ Harrison.)

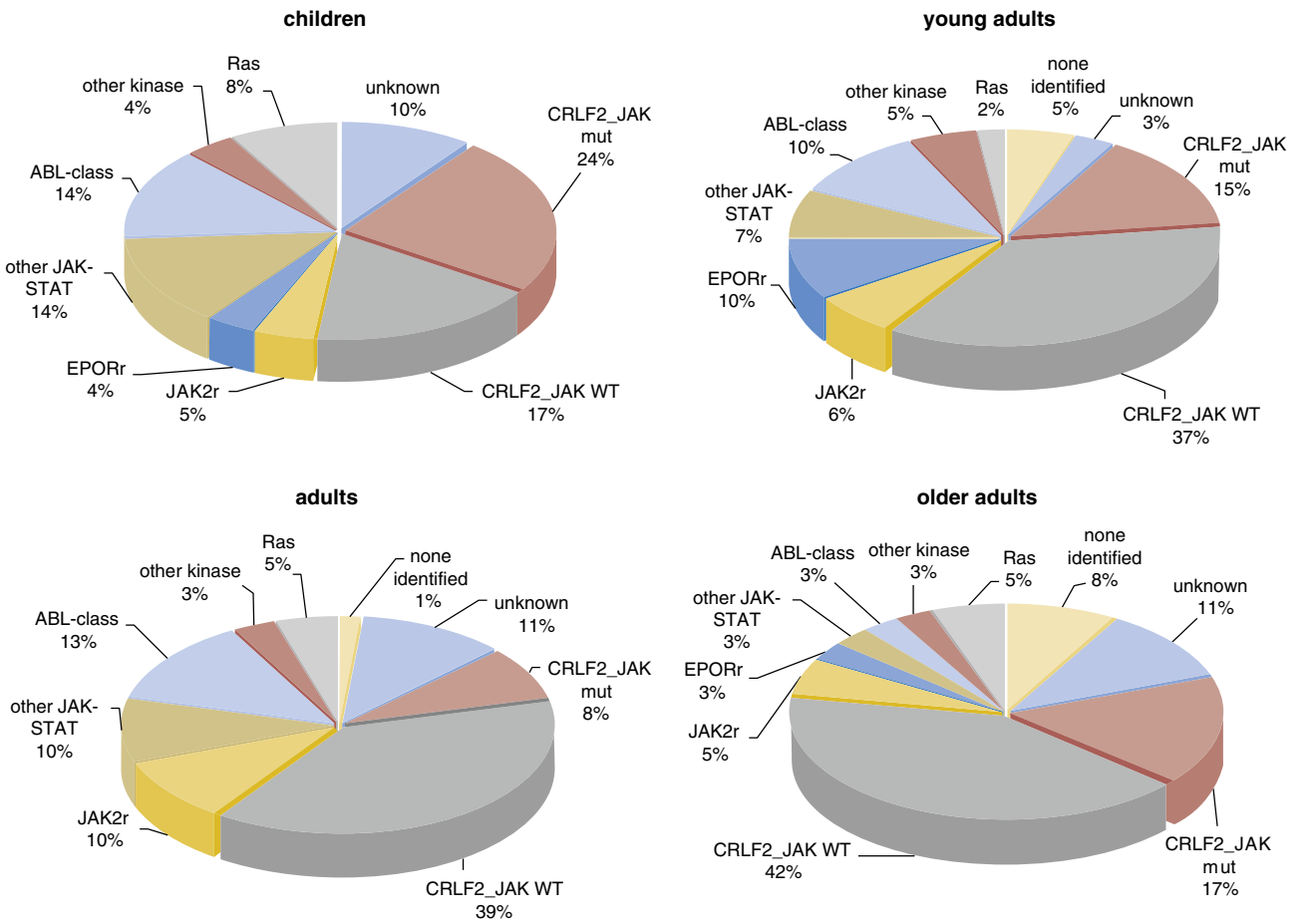

Fig. 14.22. Frequency of Philadelphia chromosome (Ph)-like acute lymphoblastic leukemia subtypes across age. Prevalence of *CRFL2*-rearranged JAK mutant (mut), *CRFL2*-rearranged JAK wild-type (WT), *JAK2* rearrangements (JAK2r), *EPOR* rearrangements (EPORr), other *JAK-STAT* alterations, *ABL1*-class fusions, all other kinase lesions, and unknown subtype in children, young adults, adults, and older adults. Source: Iacobucci I, Mullighan CG. *J Clin Oncol* 2017;35(9):975–983. Reproduced with permission of *Journal of Clinical Oncology*: American Society of Clinical Oncology.

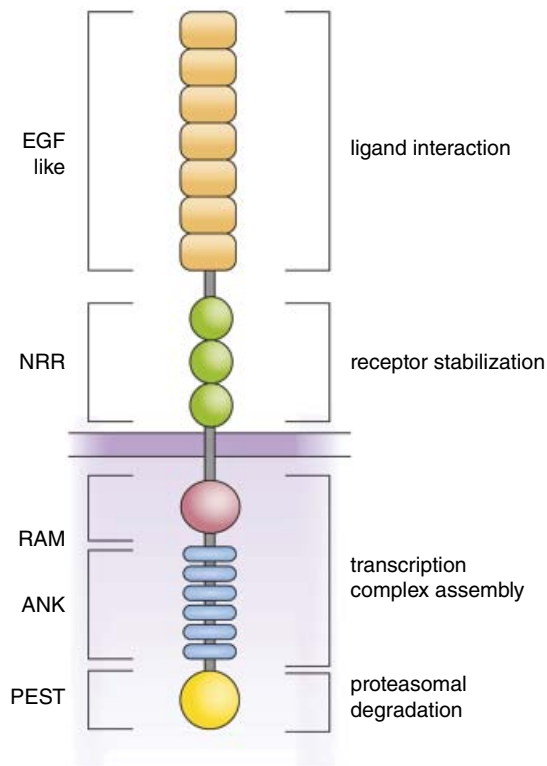

Fig. 14.23. Schematic representation of the NOTCH1 receptor. NOTCH1 is a class I transmembrane protein with a modular structure. The N-terminal EGF repeats are involved in interaction with Jagged and Δ-like ligands. The NRR holds the receptor inactive in the absence of ligand by limiting the access of the ADAM10 protease. Intracellular domains include the RAM (RBP-Jκ-associated module) and ANK (ankyrin repeat) domains involved in the interaction with the RBPJ DNA-binding protein and the recruitment of transcriptional coactivators and the C-terminal PEST domain responsible for termination of NOTCH1 signaling by *FBXW7*-mediated proteasomal degradation. Source: Sanchez-Martin M, Ferrando A. *Blood* 2017;129(9):1124–1133. Reproduced with permission of *Blood: Journal of the American Society of Hematology*.

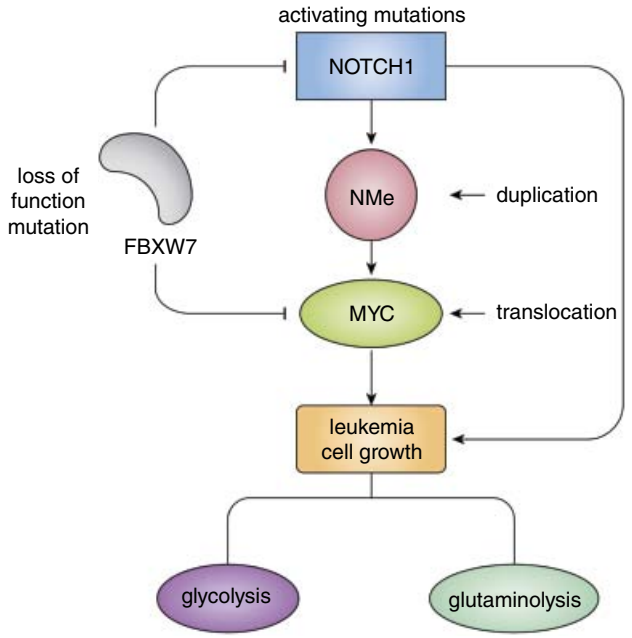

Fig. 14.24. NOTCH1 and MYC regulate leukemia cell growth. Activation of NOTCH1 signaling in T-ALL is typically triggered by activating mutations in the *NOTCH1* gene and loss-of-function mutations in *FBXW7*. NOTCH1 directly activates MYC expression via NMe, a long-range NOTCH-dependent T-cell-specific enhancer duplicated in about 5% of T-ALLs. Chromosomal translocations involving MYC can also be found in 1% of T-ALLs, and *FBXW7* mutations contribute to activating MYC expression by stabilizing the MYC protein. NOTCH1 and MYC regulate common transcriptional targets in a feed-forward loop circuitry that promotes leukemia cell growth, proliferation, and self-renewal. Source: Sanchez-Martin M, Ferrando A. *Blood* 2017;129(9):1124–1133. Reproduced with permission of *Blood: Journal of the American Society of Hematology*.

MOLECULAR METHODS

Molecular methods using real-time quantitative polymerase chain reaction (RQ-PCR) (Fig. 14.26) reach a sensitivity up to 1 : 10^6. The molecular techniques are applicable to B-lineage or T-lineage ALL in which the exact clonal rearrangement of immunoglobulin or T-cell receptor genes is first analyzed (Figs. 14.27–14.30). The remission blood or bone marrow sample is then tested quantitatively for this clone, most frequently using patient-specific PCR primers and RQ-PCR. Deep-sequencing analysis of PCR-amplified fragments can improve the sensitivity to 1 in 10^6. Digital PCR (see Chapter 13) may also increase sensitivity. Alternatively, if the patient has a chromosomal translocation, this can also be used as a marker for MRD, using either DNA analysis or, more frequently, when the breakpoint is large, reverse transcriptase PCR. The detection of MRD is now an important prognostic determinant in acute leukemia, as illustrated for childhood ALL (Table 14.6). Randomized trials are designed based on the level of persisting detectable MRD at specific time points.

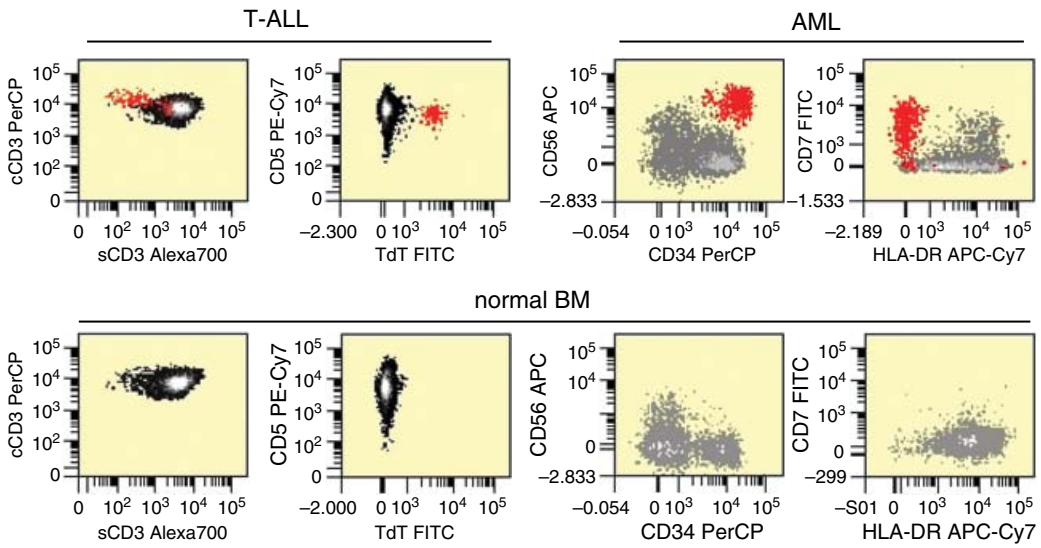

Fig. 14.25. Detection of minimal residual disease (MRD) in acute leukemia by flow cytometry. *Top*, Bone marrow (BM) samples from a patient with T-lineage acute lymphoblastic leukemia (T-ALL) and for comparison from one with acute myeloid leukemia (AML). Both in morphologic remission, were labeled with combinations of 8–10 monoclonal antibodies simultaneously. Red dots in the density plots are the result of the combined immunophenotypic profile of the cell population and indicate MRD; they correspond to 0.02% of mononuclear cells in the T-ALL sample and 0.3% in the AML sample. *Bottom*, Results of a BM sample obtained from a healthy individual and stained with the same antibodies is shown. (Courtesy of Professor D Campana.)

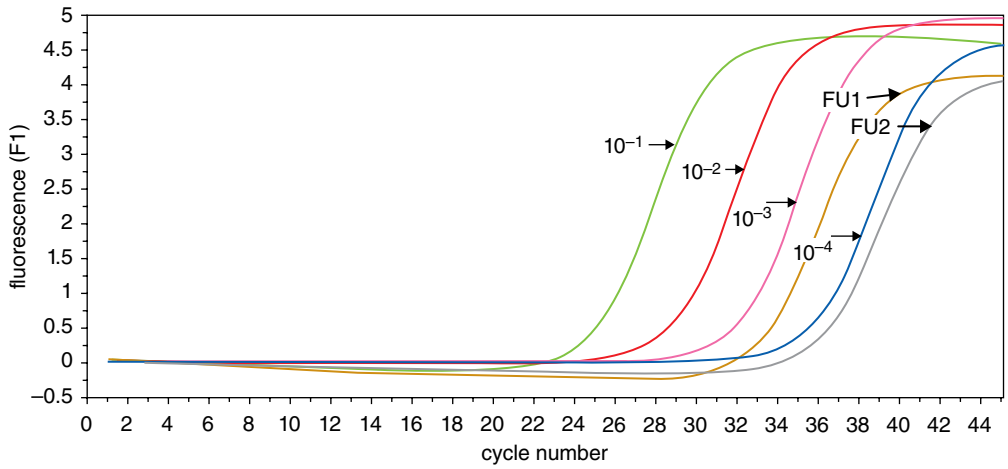

Fig. 14.26. Real-time quantitative polymerase chain reaction (RQ-PCR) of minimal residual disease (MRD) using immunoglobulin gene analysis of peripheral blood. This image illustrates RQ-PCR for antigen-receptor gene analysis. Dilution of presentation material from 10^1 to 10^4 of DNA from the leukemic sample into normal mononuclear cells (obtained from six normal donor buffy coats) is shown, and each dilution is marked by an arrow and the individual dilution amount. Two follow-up samples (FU1 and FU2) measurements are given. FU1 is quantified between 10^4 and 10^3, whereas FU2, though positive, is outside the quantitative range (POQR) of the presentation standard curve. (Courtesy of Dr. L Foroni.)

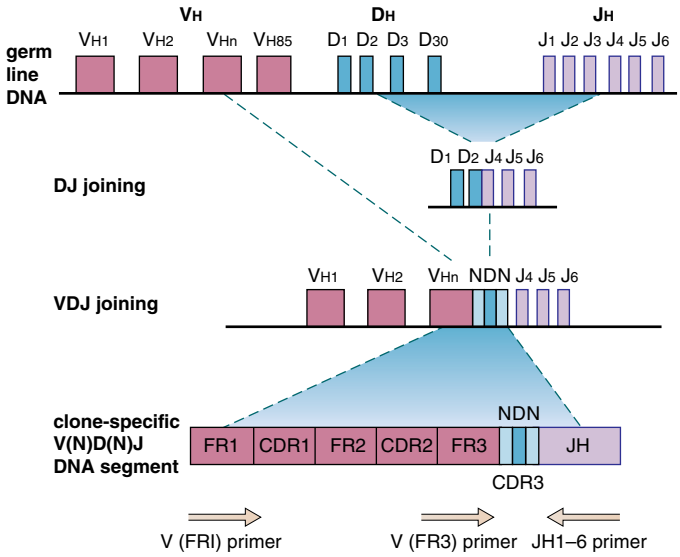

Fig. 14.27. IgH locus: The partial germline locus is shown on top, followed by a hypothetical rearrangement event. Positions of primers that can be used for PCR gene amplification of the resulting rearrangement are shown by orange arrows. V, variable regions; D, diversity regions; J, joining regions; N, random regions inserted by TdT during gene rearrangement. (Courtesy of Dr. L Foroni.)

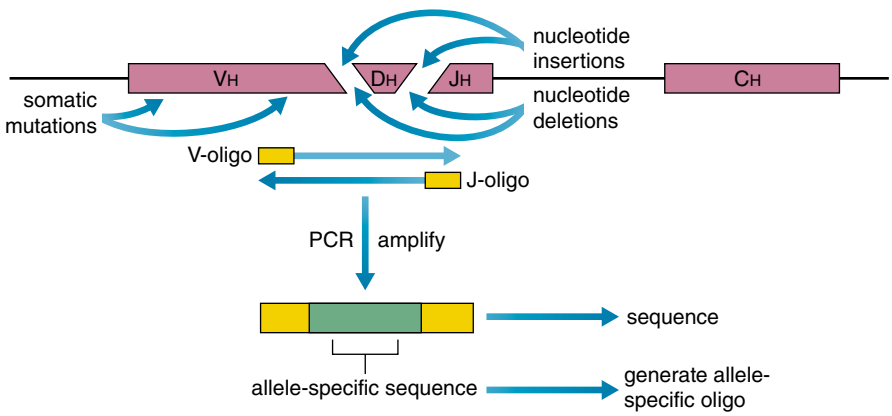

Fig. 14.28. Minimal residual disease: Detection in precursor B-ALL using PCR amplification with clone-specific primers or probe.

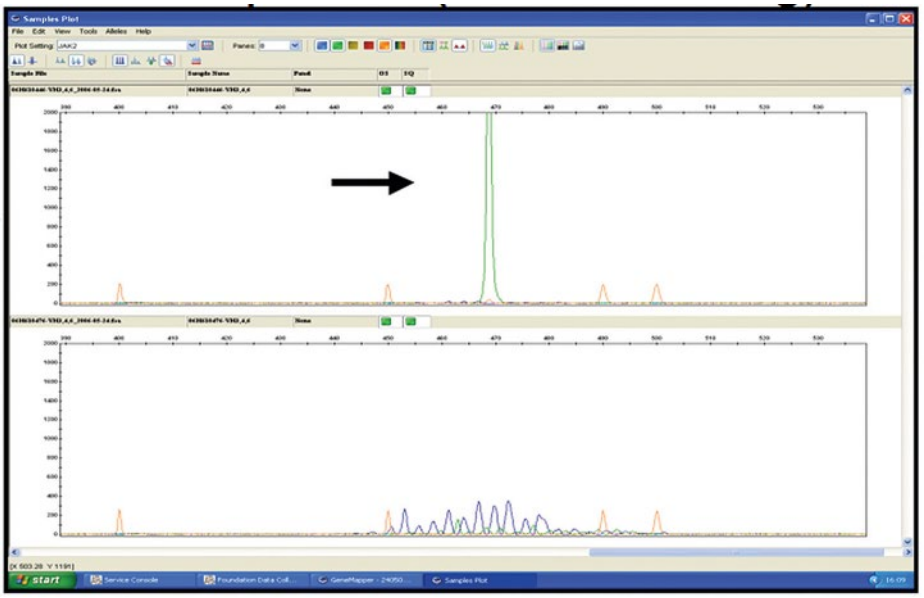

Fig. 14.29. Gene scan fragment analysis. Detection of IgV_H clone in patients with B-precursor acute lymphoblastic leukemia. PCR is performed using one fluorescently labeled primer and one nonlabeled primer. PCR products are then run together with formamide on the ABI 3130. Each V_H gene primer is labeled with a different fluorescent label, allowing for the PCR reactions to be pooled before running on the fragment collector. Size standard appears orange. *Top,* Clone identified as a single peak on fragment analysis. *Bottom,* Polyclonal IgV_H trace seen when there is no individual clone present. (Courtesy of V Duke and Dr. L Foroni.)

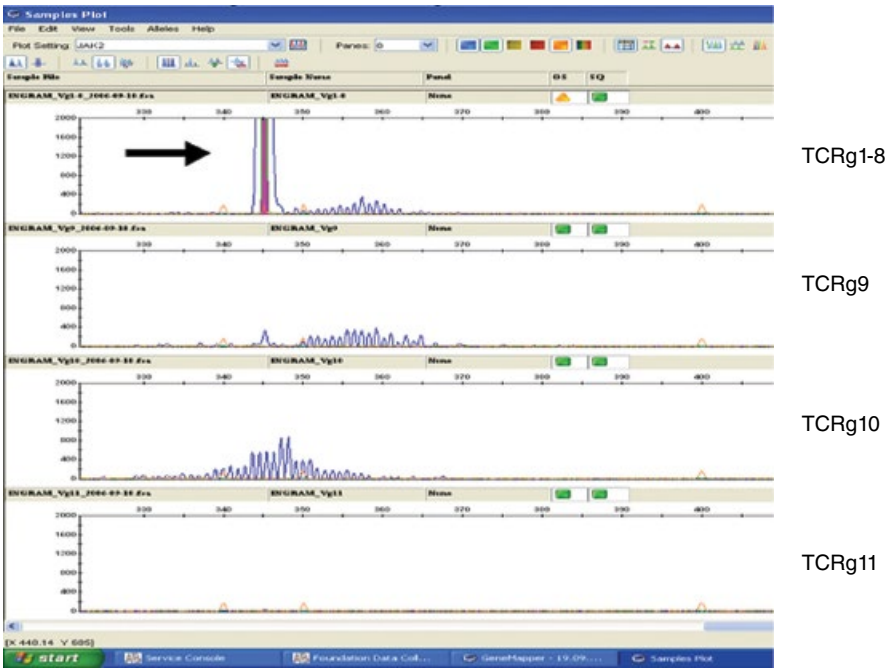

Fig. 14.30. Gene scan fragment analysis. T-cell receptor gamma clone identification. PCR performed using fluorescently labeled forward primers for TCRγ 1 to 8, 9, 10, and 11 together with nonlabeled Jγ reverse primer. PCR products are then run on the ABI 3130 fragment analyzer. This patient has a TCRγ 1–8 clone, which will need to be sequenced to identify the clone and the CDR3 region. (Courtesy of V Duke and Dr. L Foroni.)

TABLE 14.6. IMPORTANT PROGNOSTIC FACTORS IN ACUTE LYMPHOBLASTIC LEUKEMIA IN CHILDREN

Variable	Favorable factor	Adverse factor
Demographic and clinical features		
Age	1 to <10 yr	<1 yr or ≥10 yr
Sex	Female	Male
Race or ethnic group	White, Asian	Black, Native American, Hispanic
Initial white cell count	Lower (<50 000/mm^3)	Higher (≥50 000/mm^3)
Biologic or genetic features of leukemia cells		
Immunophenotype	B-cell lineage	T-cell lineage
Cytogenetic features	*ETV6-RUNX1*, hyperdiploidy, favorable chromosome trisomies	*BCR-ABL1*, *KMT2A* rearrangements, hypodiploidy
Genomic features	*ERG* deletions	*IKZF1* deletions or mutations; Philadelphia chromosome-like ALL with kinase gene alterations
Early response to treatment		
Response to 1 wk of glucocorticoid therapy	Good response to prednisone (<1000 blasts/mm^3)	Poor response to prednisone (≥1000 blasts/mm^3)
Marrow blasts after 1–2 wk of multiagent therapy	M1 marrow (<5% blasts) by day 8 or 15	No M1 marrow (≥5% blasts) by day 8 or 15
MRD quantitation during or at end of induction	Reaching low (<0.01%) or undetectable MRD by specific time points	Persistence of MRD ≥0.01% at specific time points; the higher it is, the worse the prognosis Most important single prognostic factor for contemporary therapy; critical for modern risk stratification
MRD at 3–4 mo	Low (<0.01%), preferably undetectable	Persistence of MRD ≥0.01% May help select patients for HSCT or new therapies in first remission

HSCT, hematopoietic stem cell transplantation; MRD, minimal residual disease; NCI, National Cancer Institute.
Source: Hunger SP, Mullighan CG. *N Engl J Med* 2015;373:1541–1552. Reproduced with permission of Massachusetts Medical Society: *The New England Journal of Medicine*.

CHAPTER

15 MYELODYSPLASTIC SYNDROMES

The myelodysplastic syndromes (MDS) are a group of clonal hematopoietic stem cell diseases with cytopenia(s) and dysplastic features in one or more myeloid lineage. The World Health Organization (WHO) defines cytopenia as hemoglobin <10 g/dL, platelets $<100 \times 10^9$/L, absolute neutrophil count $<1.8 \times 10^9$/L. The threshold for dysplasia is a minimum of 10% in any hematopoietic lineage. These may be difficult to ascribe to MDS rather than a reactive cause of cytopenia and dysplasia, especially if only one lineage is involved. There is ineffective hematopoiesis. The proportion of blasts in the marrow may be normal or increased but below 20%; otherwise the disease is classified as acute myeloid leukemia (AML). MDS usually occurs in elderly subjects who have anemia, persistent neutropenia and thrombocytopenia, or various combinations of these. Typically, the anemia is macrocytic and there is no enlargement of the liver, spleen, and lymph nodes.

The MDS are classified by the WHO 2016 into seven main subgroups (Table 15.1). Three of these, MDS with ring sideroblasts, MDS with excess blasts, and MDS unclassifiable are further subdivided.

CLINICAL FEATURES

Clinically, patients with MDS have symptoms related to bone marrow failure with frequent infective episodes (Figs. 15.1 and 15.2) and bleeding abnormalities (Fig. 15.3). As a consequence of these complications, many patients die of severe neutropenia or thrombocytopenia, but in others the disease progresses to frank AML.

MICROSCOPIC FEATURES

The blood film abnormalities in each subgroup are highly variable. General features include macrocytic red cells, qualitative granulocytic and monocytic changes (see later), and giant platelets. In patients with single lineage dysplasia (SLD), gross morphologic changes may not occur (Fig. 15.4). In MDS with single lineage dysplasia and ring sideroblasts (MDS-SLD-RS), a dimorphic red cell population frequently occurs (Fig. 15.5). Agranular neutrophils, pseudo-Pelger cells, and cells difficult to diagnose as monocytic or granulocytic are seen in peripheral blood (Fig. 15.6). Patients with excess blasts often show leukoerythroblastic changes. Thrombocytosis occurs, typically associated with MDS and 5q – aberrations (an interstitial deletion, usually 5q11 or 5q13 to 5q33) (Fig. 15.7). In this syndrome, bone marrow megakaryocytes have a characteristic hypolobulated appearance (Fig. 15.8). In WHO 2016, these morphologic and cytogenetic features lead to an MDS entity called MDS with isolated del(5q).

The bone marrow in MDS is typically hypercellular and shows morphologic abnormalities, often in all three series of hematopoietic cells. As mentioned above, dysplasia in MDS is defined as ≥10% or more cells with dysplastic features of the respective cell lineage. There is usually evidence of dyserythropoiesis, with nuclear atypia (budding, bridging, karyorrhexis, multinuclearity, hyperlobation), some megaloblastosis, and ring sideroblasts (Figs. 15.9–15.14). The presence of ring sideroblasts closely correlates with the presence of the *SF3B1* mutation. For the first time the detection of a gene mutation has to be taken into account for WHO classification of MDS: in cases with ring sideroblasts between 5% and 14% in the bone marrow, the detection of an *SF3B1* mutation leads also to the diagnosis of MDS-SLD-RS or MDS with multilineage dysplasia and ring sideroblasts (MDS-MLD-RS). In about 20% of cases in all MDS subgroups, an increase in reticulin occurs (Fig. 15.15), and in occasional cases, the marrow is hypocellular.

Granulocytic abnormalities include hypogranular or agranular myelocytes, metamyelocytes and neutrophils, pseudo-Pelger cells (Figs. 15.16 and 15.17), pseudo-Chédiak–Higashi granules, and hypersegmented or polyploid neutrophils. Megakaryocytic abnormalities include small mononuclear or binucleate forms (see Figs. 15.8 and 15.18) or large megakaryocytes with multiple round nuclei and large granules in the cytoplasm.

In the more advanced MDS, there is also an increase in the blast cell population, but by definition, these cells remain <20% of the marrow cell total. When the level of blast cells exceeds this figure, evolution to AML has occurred (Fig. 15.19). Cases with excess blasts in histology may show localization of the blasts to the intertrabecular area (Fig. 15.20). Copper deficiency has been reported to mimic myelodysplasia in the blood and bone marrow (Fig. 15.21). In patients with comorbidities likely to result in nutritional deficiency (e.g. intestinal malabsorption), copper deficiency should be excluded. Further, chemotherapy such as hydroxyurea and methotrexate lead to dysplasia. Morphologic features of MDS should also suggest diseases such as paroxysmal nocturnal hemoglobinuria or congenital dyserythropoietic anemia, when typical cytogenetic or molecular genetic aberrations of MDS are missing.

Color Atlas of Clinical Hematology: Molecular and Cellular Basis of Disease, Fifth Edition. A. Victor Hoffbrand, Paresh Vyas, Elías Campo, Torsten Haferlach, and Keith Gomez

TABLE 15.1 WHO (2016): CLASSIFICATION OF MYELODYSPLASTIC SYNDROMES

Entity name	Number of dysplastic lineages	Number of cytopenias[a]	Ring sideroblasts as percentage of marrow erythroid elements	Bone marrow (BM) and peripheral blood (PB) blasts	Cytogenetics by conventional karyotype analysis
MDS-SLD	1	1–2	<15%/<5%[b]	BM <5%, PB <1%, no Auer rods	Any, unless fulfills all criteria for MDS with isolated del(5q)
MDS-MLD	2–3	1–3	<15%/<5%[b]	BM <5%, PB <1%, no Auer rods	Any, unless fulfills all criteria for MDS with isolated del(5q)
MDS-RS					
MDS-SLD-RS	1	1–2	≥15%/≥5%[b]	BM <5%, PB <1%, no Auer rods	Any, unless fulfills all criteria for MDS with isolated del(5q)
MDS-MLD-RS	2–3	1–3	≥15%/≥5%[b]	BM <5%, PB <1%, no Auer rods	Any, unless fulfills all criteria for MDS with isolated del(5q)
MDS with isolated del(5q)	1–3	1–2	None or any	BM <5%, PB <1%, no Auer rods	del(5q) alone or with 1 additional abnormality, except loss of chromosome 7 or del(7q)
MDS-EB					
MDS-EB-1	1–3	1–3	None or any	BM 5–9% or PB 2–4%, BM <10% and PB <5%, no Auer rods	Any
MDS-EB-2	1–3	1–3	None or any	BM 10–19% or PB 5–19% or no Auer rods, BM and PB <20%	Any
MDS-U					
with 1% blood blasts	1–3	1–3	None or any	BM <5%, PB = 1%[c], no Auer rods	Any
with SLD and pancytopenia	1	3	None or any	BM <5%, PB <1%, no Auer rods	Any
based on defining cytogenetic abnormality	0	1–3	<15%[d]	BM <5%, PB <1%, no Auer rods	MDS-defining abnormality

[a] Cytopenias defined as hemoglobin concentration <10 g/dL, platelet count $<100 \times 10^9$/L, and absolute neutrophil count $<1.8 \times 10^9$/L, although MDS can present with mild anemia or thrombocytopenia above these levels; PB monocytes must be $<1 \times 10^9$/L.

[b] If *SF3B1* mutation is present.

[c] 1% PB blasts must be recorded on ≥2 separate occasions.

[d] Cases with ≥15% ring sideroblasts by definition have significant erythroid dysplasia and are classified as MDS-SLD-RS.

MDS-EB, MDS with excess blasts; MDS-MLD, MDS with multilineage dysplasia; MDS-RS, MDS with ring sideroblasts; MDS-RS-MLD, MDS with ring sideroblasts and multilineage dysplasia; MDS-RS-SLD, MDS with ring sideroblasts and single lineage dysplasia; MDS-SLD, MDS with single lineage dysplasia; MDS-U, MDS, unclassifiable; SLD, single lineage dysplasia.

Source: Adapted with permission from Swerdlow SH, et al., eds. *WHO Classification of Tumours of Haematopoietic and Lymphoid Tissues*, revised 4th edn. International Agency for Research on Cancer, Lyon, 2017.

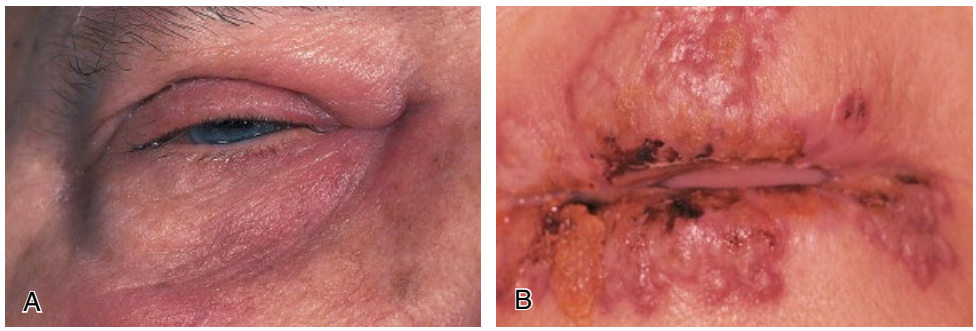

Fig. 15.1. Myelodysplastic syndrome. **A,** Skin infection spreading from the eyelids. **B,** Extensive herpes simplex eruptions spreading from the lip margins to adjacent skin. Both patients had MDS with excess blasts (MDS-EB).

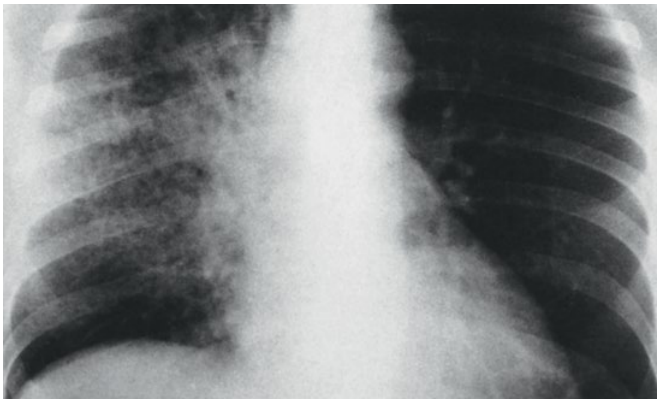

Fig. 15.2. Myelodysplastic syndrome: Chest radiograph (portable film) of a 62-year-old man with Legionnaires' disease. There is widespread patchy consolidation throughout the right lung.

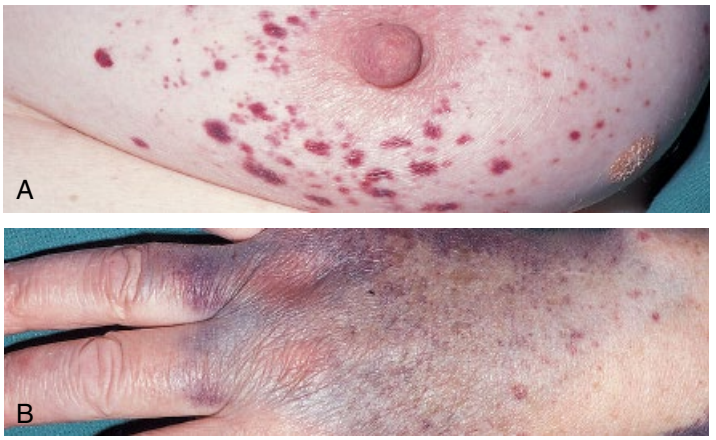

Fig. 15.3. Myelodysplastic syndrome with single lineage dysplasia (MDS-SLD): **A,** Extensive purpura of the skin of the breast in a 35-year-old woman with MDS-SLD. **B,** Extensive ecchymoses and purpura of the skin over the back of the hand (same patient). (Hb, 8 g/dL; white blood cell count [WBC], 4×10^9/L; platelets, 20×10^9/L.)

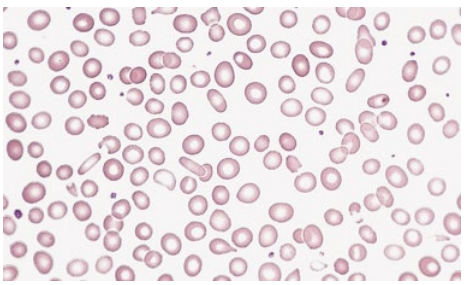

Fig. 15.4. Myelodysplastic syndrome: Peripheral blood film in MDS-SLD shows marked anisocytosis and poikilocytosis. (Hb, 7.9 g/dL; WBC, 5.4×10^9/L [neutrophils, 1.8×10^9/L]; platelets, 120×10^9/L.)

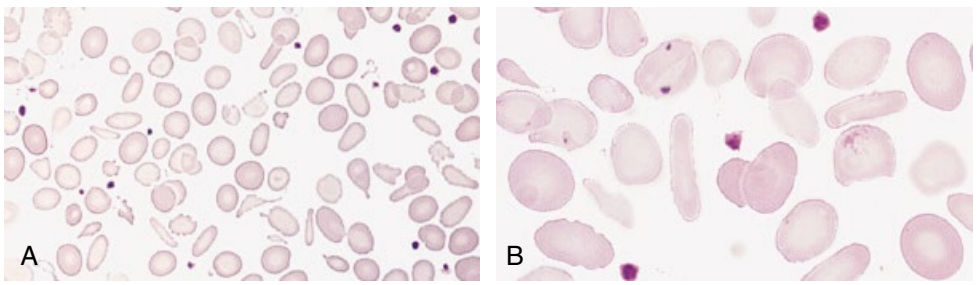

Fig. 15.5. Myelodysplastic syndrome with ring sideroblasts (MDS-RS): **A,** Peripheral blood films showing marked red cell anisocytosis and poikilocytosis. Although the majority of cells are markedly hypochromic, there is a second population of normochromic cells. **B,** At higher magnification a red cell shows two small basophilic inclusions (Pappenheimer bodies). Perls' staining demonstrated that similar inclusions were Prussian blue positive (siderotic granules). These granules were far more numerous after splenectomy.

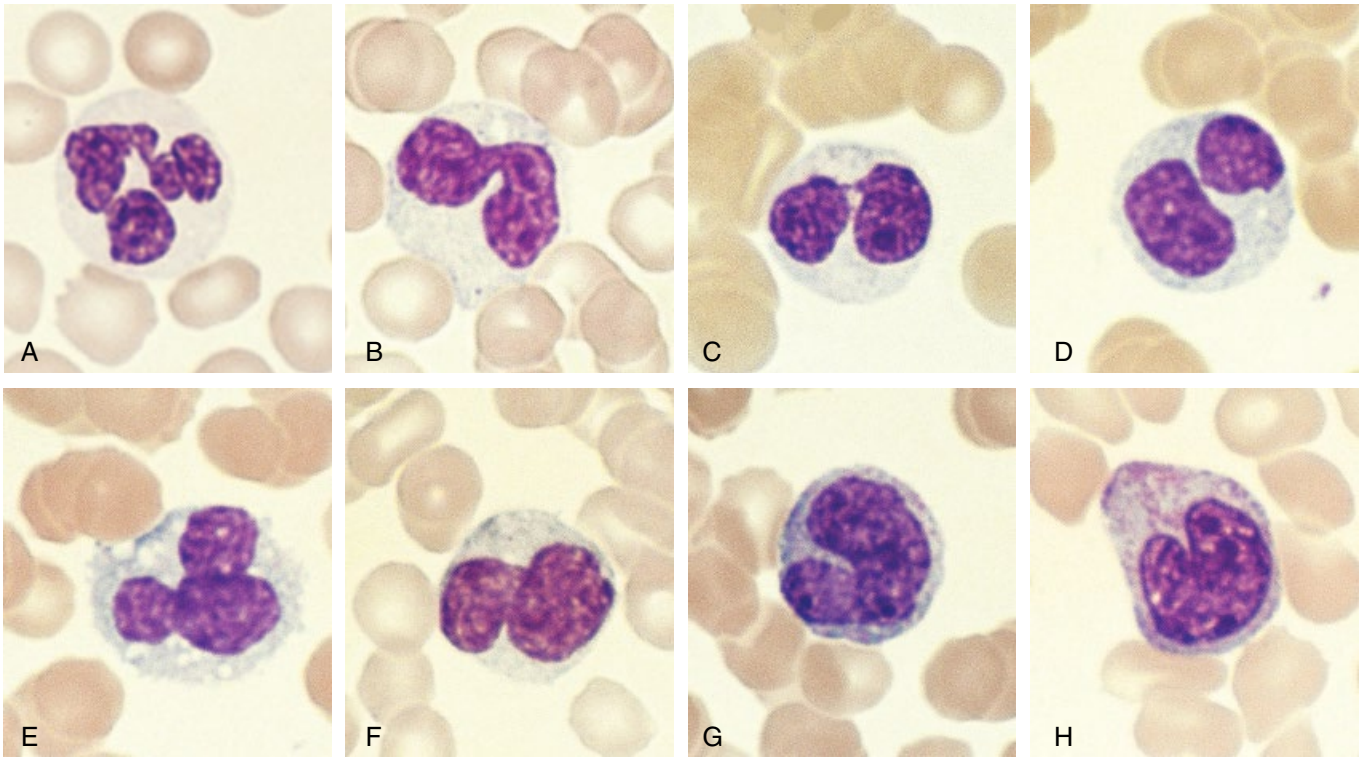

Fig. 15.6. Myelodysplastic syndrome with multilineage dysplasia (MDS-MLD): Peripheral blood films showing white cells. Agranular neutrophils, atypical myelomonocytic cells, and pseudo-Pelger neutrophils, some also agranular, are shown.

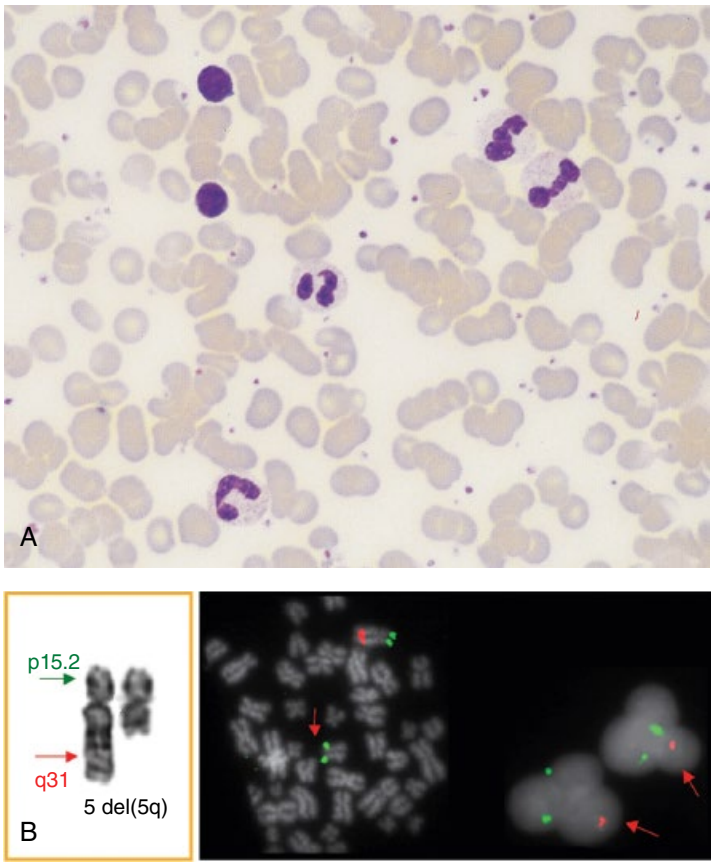

Fig. 15.7. Myelodysplastic syndrome with isolated del(5q). **A,** Peripheral blood film from a 75-year-old woman showing macrocytes, hyposegmented neutrophils, and thrombocytosis. **B,** Fluorescence in situ hybridization (FISH) analysis showing loss of long (q) arm of chromosome 5. G-banded partial karyotype with arrows pointing to the location of the FISH probes. (Courtesy of Dr. E Nacheva.)

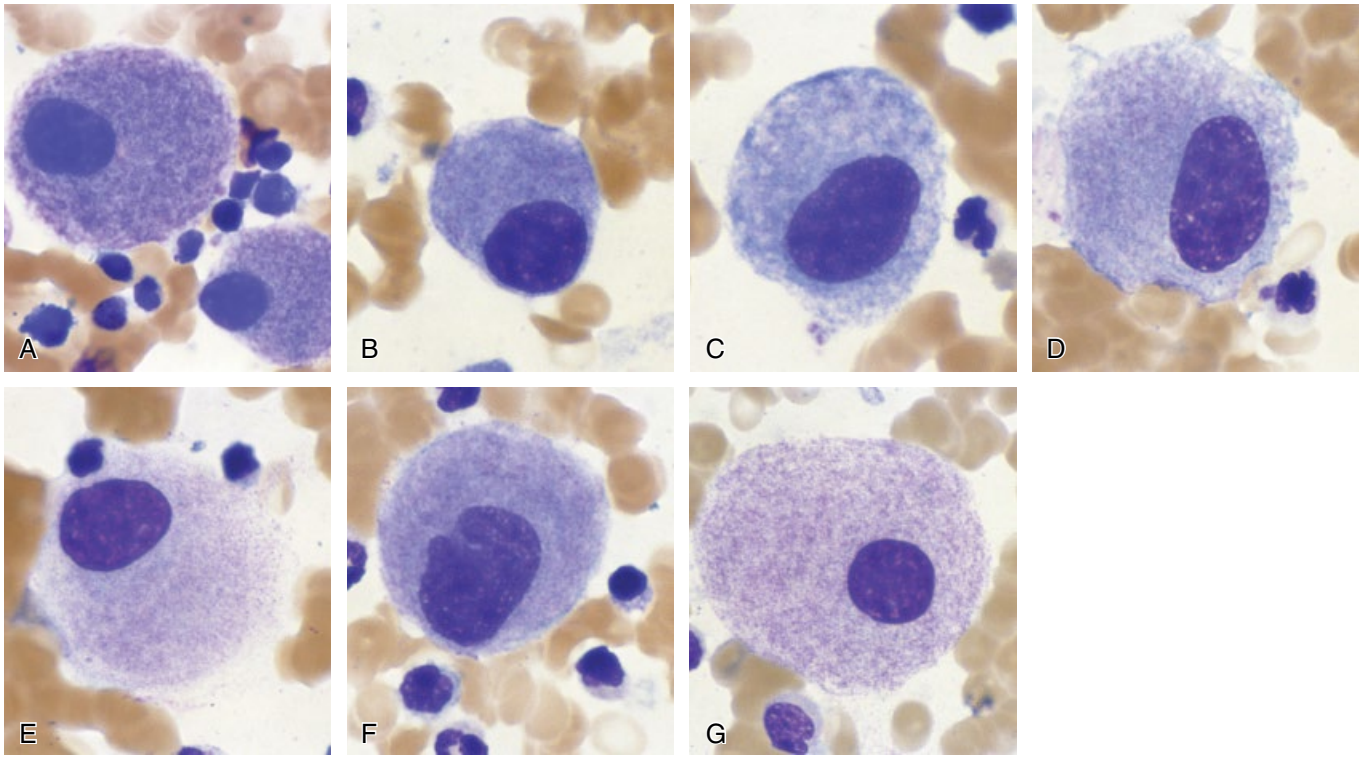

Fig. 15.8. Myelodysplastic syndrome with isolated del(5q): Bone marrow aspirates show abnormal hypolobulated megakaryocytes.

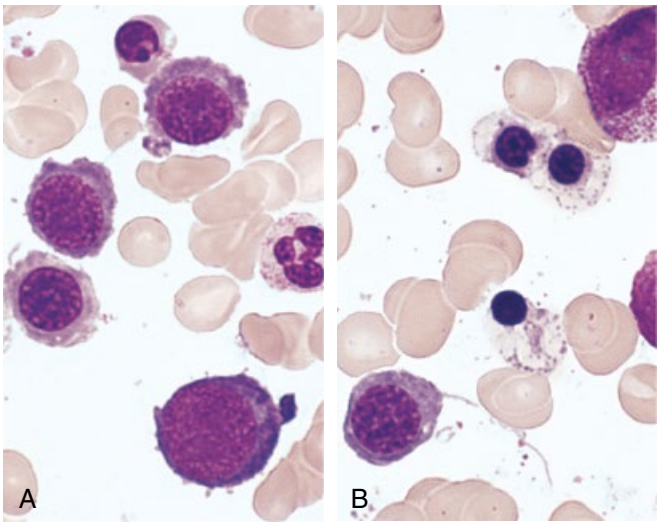

Fig. 15.9. Myelodysplastic syndrome with single lineage dysplasia and ring sideroblasts (MDS-SLD-RS). **A, B,** Bone marrow cell trails in MDS-SLD-RS showing marked defective hemoglobinization and vacuolation in later stage polychromatic and pyknotic erythroblasts.

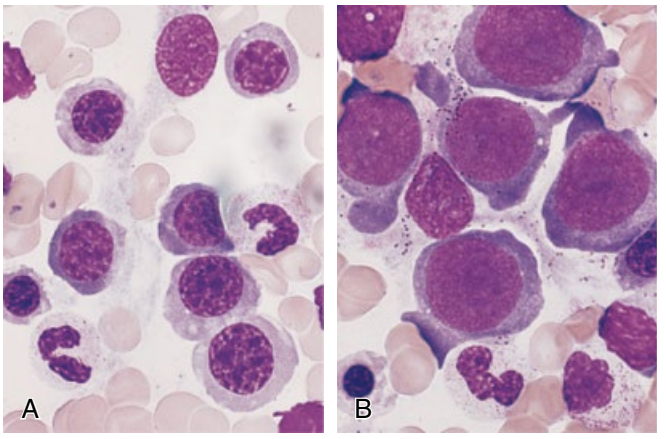

Fig. 15.10. Myelodysplastic syndrome with single lineage dysplasia and ring sideroblasts (MDS-SLD-RS): Bone marrow cell trails in MDS-SLD-RS showing erythroblasts with vacuolation of cytoplasm in later cells and mild megaloblastic features **(A)** and a prominent group of proerythroblasts **(B)**.

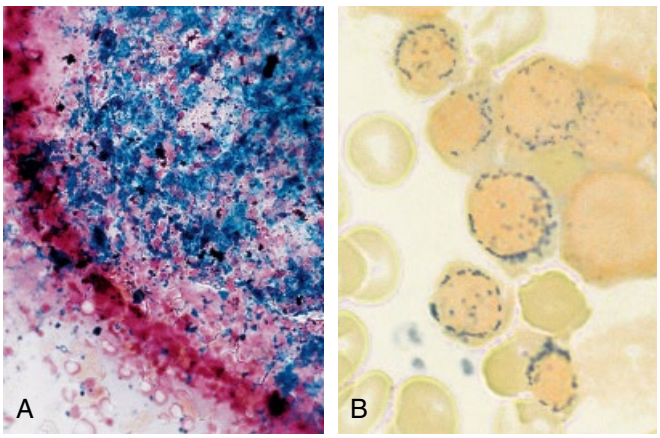

Fig. 15.11. Myelodysplastic syndrome with single lineage dysplasia and ring sideroblasts (MDS-SLD-RS): Bone marrow fragment in MDS-SLD-RS showing increased iron stores **(A)** and pathologic ring sideroblasts at higher magnification **(B)**. (Perls' stain.)

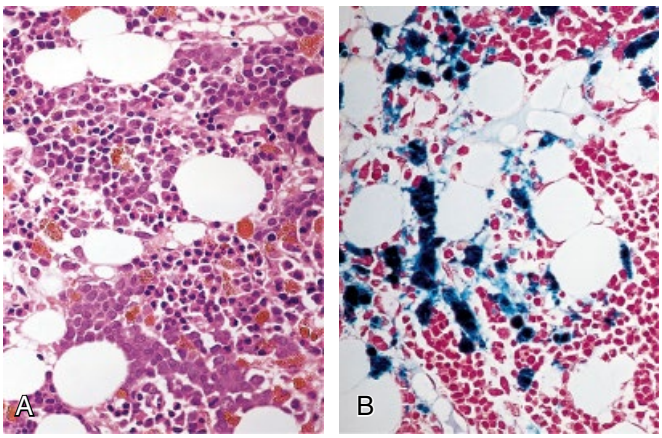

Fig. 15.14. Myelodysplastic syndrome with excess blasts 1 (MDS-EB-1): Trephine biopsies in MDS-EB-1. **A,** Clusters of blast forms and prominent hemosiderin-laden macrophages. **B,** Gross increase in reticuloendothelial iron stores is confirmed by Perls' staining.

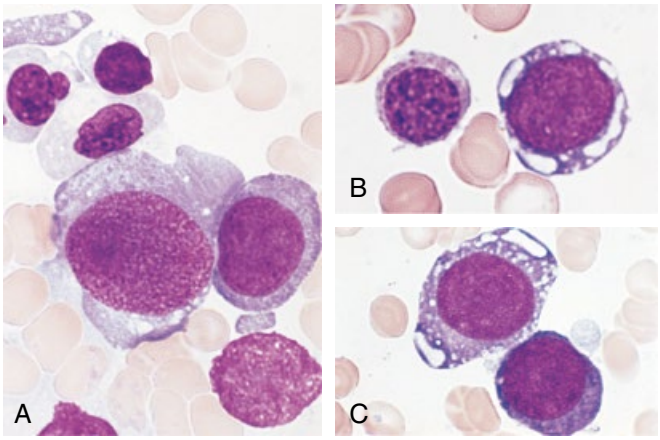

Fig. 15.12. Myelodysplastic syndrome with excess blasts 1 (MDS-EB-1): Bone marrow aspirates. **A,** Abnormal proerythroblasts and megaloblast-like changes. **B,** Prominent cytoplasmic vacuolation in the basophilic erythroblasts. **C,** Evidence of dyserythropoiesis.

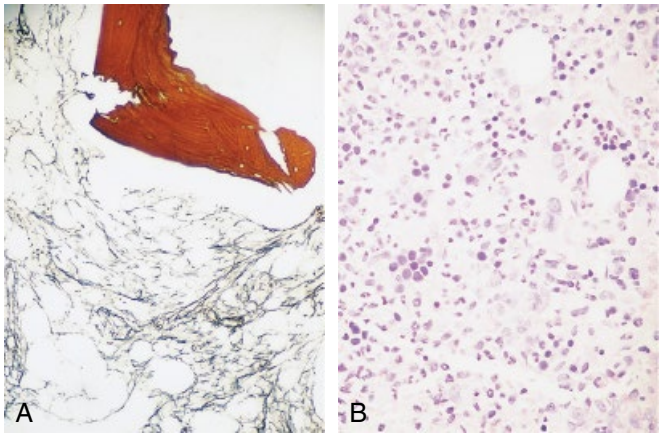

Fig. 15.15. Myelodysplastic syndrome with multilineage dysplasia (MDS-MLD). **A,** Trephine biopsy showing increased reticulin fiber density. (Silver impregnation stain.) **B,** Foci of immature myeloid cells in intertrabecular area (ALIP).

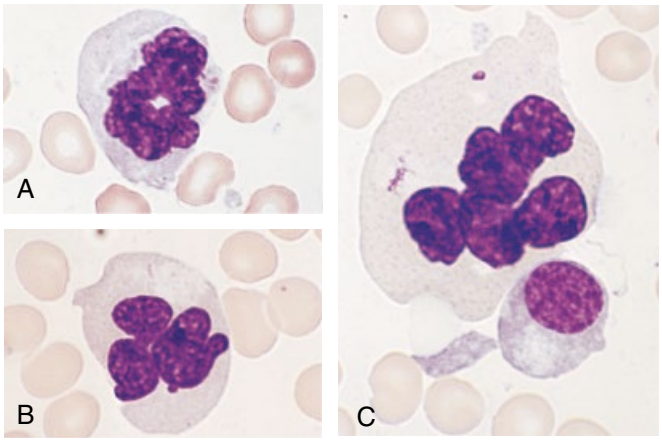

Fig. 15.13. Myelodysplastic syndrome with excess blasts 1 (MDS-EB-1). **A–C,** Bone marrow aspirates in MDS-EB-1 showing three examples of polyploid multinucleate polychromatic erythroblasts, further evidence of gross dyserythropoiesis.

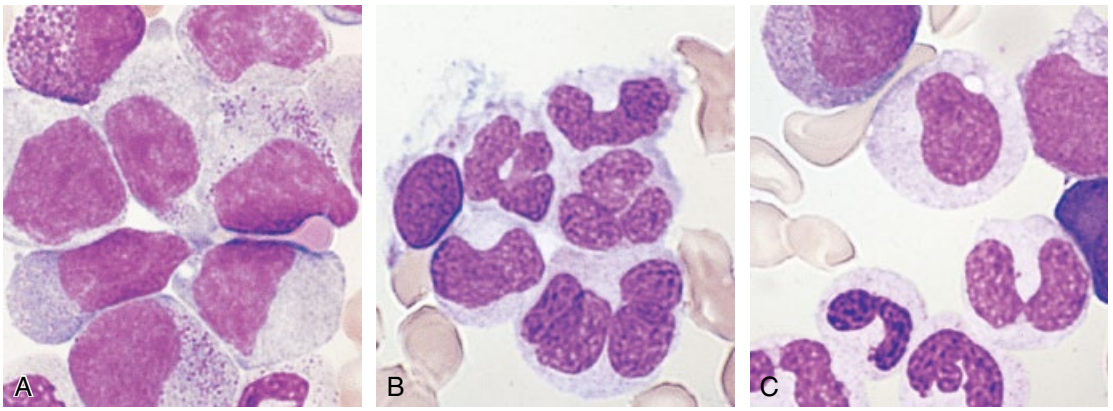

Fig. 15.16. Myelodysplastic syndrome with excess blasts 1 (MDS-EB-1): Bone marrow aspirates. **A,** Disturbed granulopoiesis with agranular promyelocytes. **B, C,** Agranular neutrophils and abnormal myelomonocytic cells. Some cells ("paramyeloid" cells) are difficult to classify as monocytic or granulocytic.

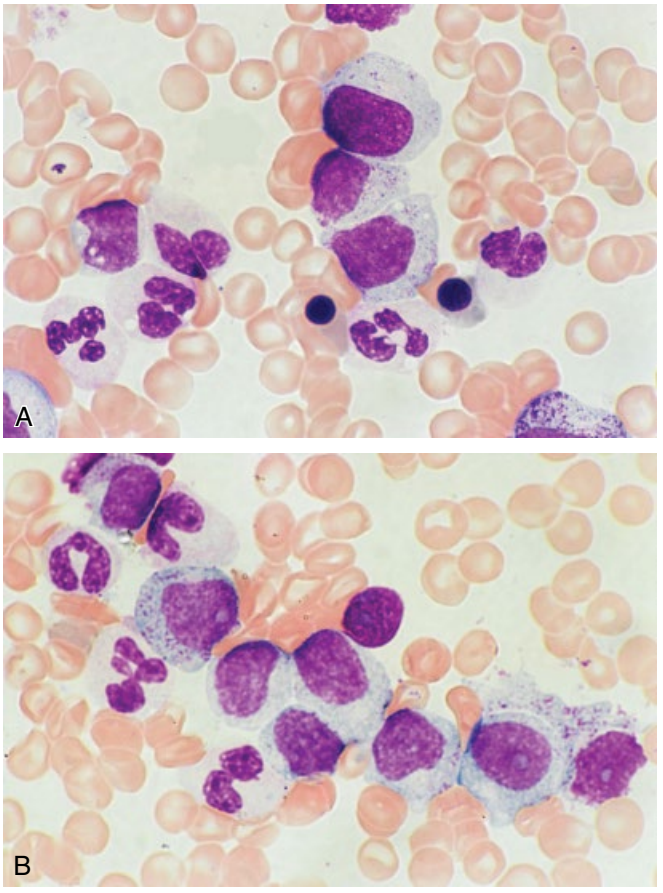

Fig. 15.17. Myelodysplastic syndrome with multilineage dysplasia (MDS-MLD). Bone marrow aspirate showing abnormal agranular neutrophils, myelocytes, promyelocytes, and abnormal myelomonocytic cells.

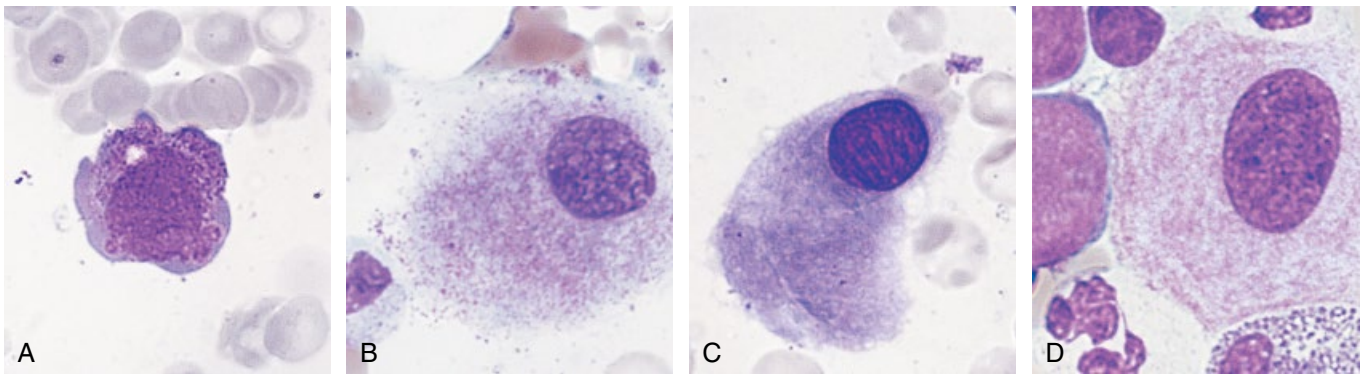

Fig. 15.18. Myelodysplastic syndrome: Bone marrow aspirates showing an atypical megakaryoblast and three atypical mononuclear megakaryocytes, all of which show evidence of cytoplasmic maturation and granulation.

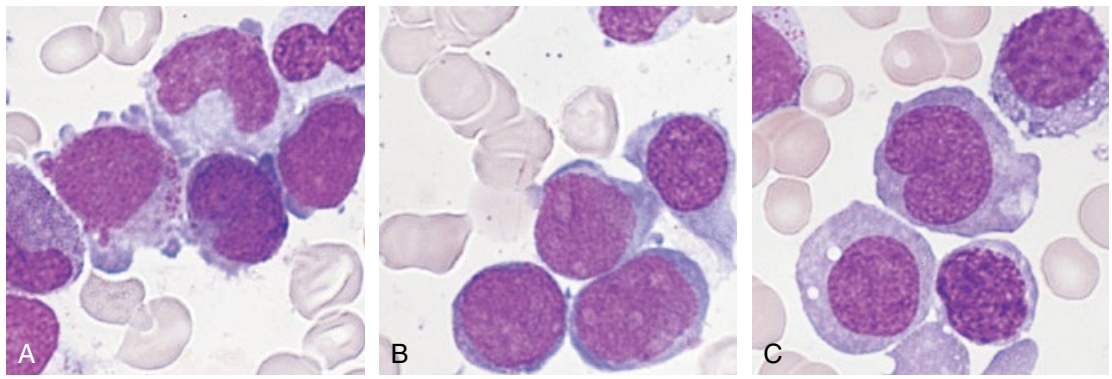

Fig. 15.19. Myelodysplastic syndrome transformed to acute myeloid leukemia. Bone marrow aspirates in MDS-EB-2, which has progressed to acute myeloid leukemia after a period of observation, showing increased numbers of blast cells, some of which have atypical features. The blast cells make up 23% of the marrow cell total. Agranular neutrophils and myelomonocytic cells are also evident.

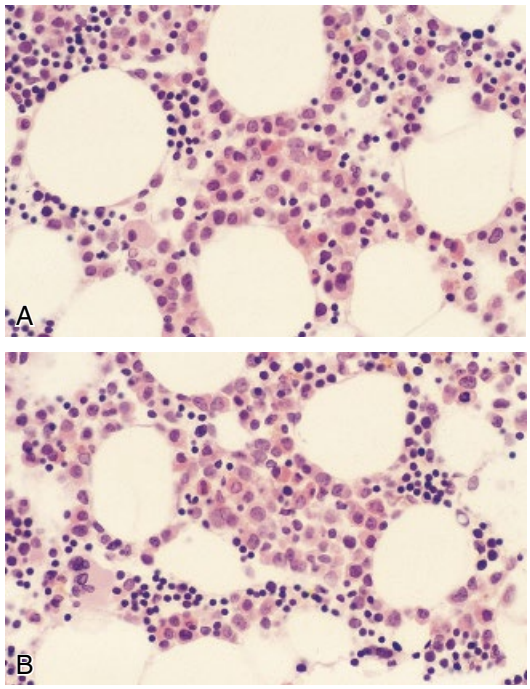

Fig. 15.20. Myelodysplastic syndrome. Trephine biopsy. Both views show abnormal intertrabecular localization of nests of immature myeloid cells (ALIPs).

CYTOGENETIC ABNORMALITIES

Cytogenetic abnormalities are common, occurring in about 40–50% of primary and 90% of treatment-related MDS (Fig. 15.22). If detected by karyotyping, some of these define MDS even in the absence of morphological dysplasia. They are more common in MDS with excess blasts (MDS-EB) than in MDS with single lineage dysplasia (MDS-SLD). Table 15.2 lists the abnormalities according to their prognostic significance. Abnormalities include the following:

- Chromosome deletion or loss (e.g. del5q/monosomy 5 [see Fig. 15.5], del7q/monosomy 7, del11q, del12p, del13q, del17p, del20q, loss of Y)
- Chromosome gain (e.g. trisomy 8, trisomy 11)
- Chromosome rearrangement (e.g. inv3/t3q, t1;7, t11q23)
- Three abnormalities
- Complex > 3 abnormalities

The hematologic findings combined with cytogenetic findings can be used to obtain a prognostic score according to the Revised International Prognostic Scoring System (IPSS-R) (Table 15.3).

MOLECULAR GENETICS

Somatic mutations of genes involved in RNA splicing, DNA modification, chromatin regulation (see Fig. 1.23) and cell signaling occur frequently. In one large study oncogenic mutations were detected in 47 different genes (Fig. 15.23). *TET2*, *SF3B1*, *ASXLI*, *SRSF2*, *DNMT3A*, and *RUNX1* were the only six genes mutated in more than 10% of patients.

The mutations relate to some extent to the WHO type of MDS (Fig. 15.24). They can be organized into groups according to their function in the cell (Fig. 15.25).

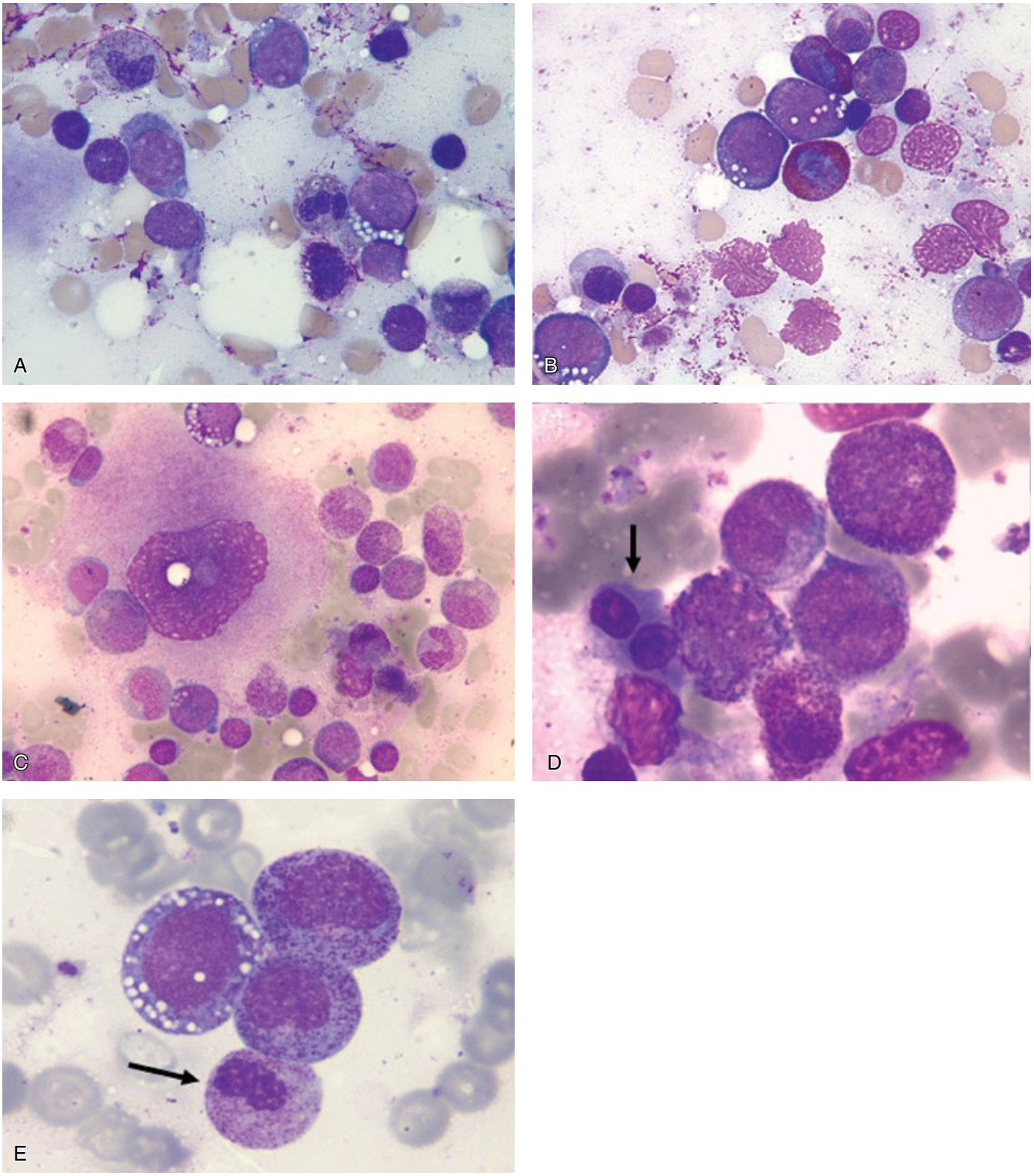

Fig. 15.21. Copper deficiency mimicking MDS with excess blasts (MDS-EB-1). Male age 19 with familial Mediterranean fever, nephrotic syndrome, and secondary amyloidosis with anemia and thrombocytopenia. **A–E,** The marrow aspirate showed vacuolated erythroid and myeloid precursors and increased immature cells with displastic features in three lineages with hypergranular myeloid cells, mononuclear megakaryocytes, binucleate erythroblasts (arrow, **D**) and pseudo-Pelger cells (arrow, **E**). Copper deficiency was detected, and oral copper replacement resulted in correction of peripheral blood counts and normal bone marrow appearance. (Courtesy of Dr. E Koca and *Leukaemia Research* 2007.)

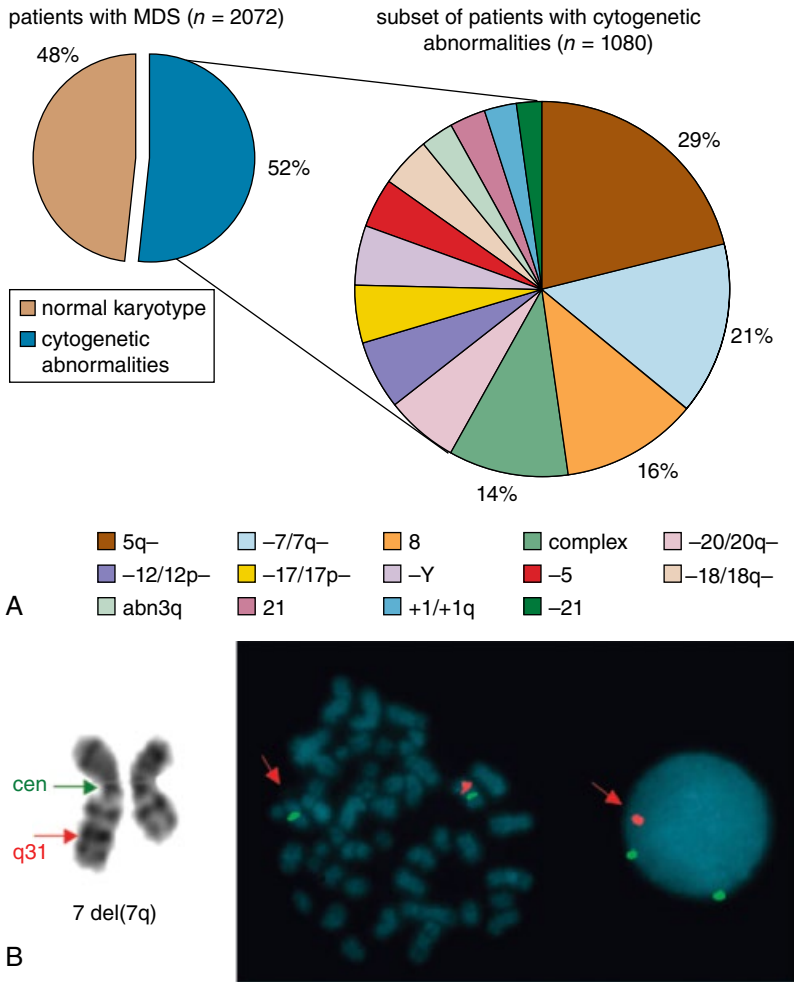

Fig. 15.22. Myelodysplastic syndromes. **A,** Frequency of cytogenetic abnormalities. **B,** Deletion or loss of the long arm of chromosome 7 by FISH. G-banded partial karyotype with arrows pointing to the location of the FISH probes. Metaphase and nondividing cells display typical loss of the signal from the long arm of chromosome 7. Source: A, Adapted with permission from Giagounidis A: *Haematological Reports* 2(14):5–10, 2006. B, Courtesy of Dr. E. Nacheva.

TABLE 15.2. CYTOGENETIC SCORING SYSTEM FOR MYELODYSPLASTIC SYNDROME ($n = 2754$)[a]

			Abnormality		Overall survival					AML transformation			
Prognostic subgroup	**No. of patients**	**%**	**Single**	**Double**	**Complex**	**Median (mo)[b]**	**95% CI**	**HR**	**95% CI**	**Median (mo)[b]**	**95% CI**	**HR**	**95% CI**
Very good	81	2.9	del(11q) -Y	–	–	60.8	50.3 to NR	0.5[b]	0.3 to 0.7	NR	121.2 to NR	0.5	0.2 to 1.2
Good (reference)	1809	65.7	Normal del(5q) del(12p) del(20q)	Including del(5q)	–	48.6	44.6 to 54.3	1.0	0.9 to 1.1	NR	189.0 to NR	1.0	0.9 to 1.2
Intermediate	529	19.2	del(7q) +8 i(17q) +19 Any other Independent clones	Any other	–	26.0	22.1 to 31.0	1.61[b]	1.4 to 1.8	78.0	42.6 to NR	2.21[b]	1.8 to 2.7
Poor	148	5.4	inv(3)/t(3q)/del(3q) –nv(3)/t(3q)/del(3q)t c		3	15.8	12.0 to 18.0	2.61[b]	2.1 to 3.2	21.0	13.4 to 42.2	3.41[b]	2.5 to 4.6
Very poor	187	6.8	–	–	>3	5.9	4.9 to 6.9	4.21[b]	3.4 to 5.2	8.2	6.4 to 15.4	4.91[b]	3.6 to 6.7

AML, acute myeloid leukemia; HR, hazard ratio; NR, not reached.

[a] Patients with complete data.

[b] $P < 0.01$.

Source: Schanz J, et al. *J Clin Oncol* 2012;30(8):820–829. Reproduced with permission of *Journal of Clinical Oncology*: American Society of Clinical Oncology.

TABLE 15.3. REVISED INTERNATIONAL PROGNOSTIC SCORING SYSTEM (IPSS-R) FOR MYELODYSPLASTIC SYNDROMES

Prognostic variable	0	0.5	1	1.5	2	3	4
Cytogenetics	Very good	–	Good	–	Intermediate	Poor	Very poor
BM blast, %	≤2	–	>2–<5%	–	5–10%	>10%	–
Hemoglobin	≥10	–	8–<10	<8	–	–	–
Platelets	≥100	50–<100	50	–	–	–	–
ANC	≥0.8	<0.8	–	–	–	–	–

–, not applicab le; ANC, absolute neutrophil count.
Source: Greenberg PL, et al. *Blood* 2012;120(12):2454–2465. Reproduced with permission of *Blood: Journal of the American Society of Hematology*.

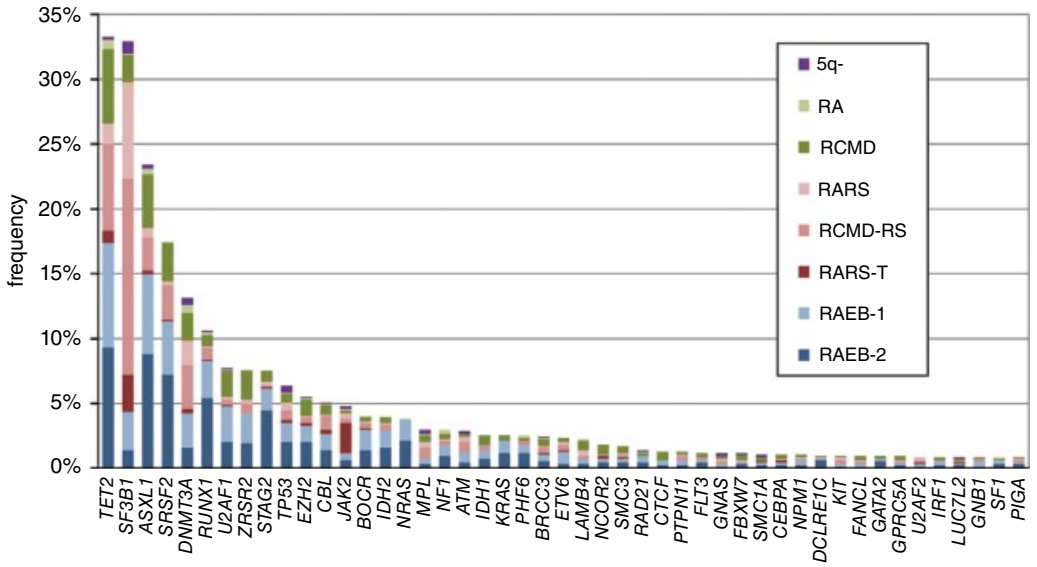

Fig. 15.23. Myelodysplastic syndrome. Significantly mutated genes in MDS. Frequency of mutations in 47 significantly mutated genes in 944 cases with different WHO subtypes, which are shown in indicated colors. The mutations are related to the MDS subtypes used in the WHO 2008 classification. RA, refractory anemia; RCMD, refractory cytopenia with multilineage dysplasia; RARS, refractory anemia with ring sideroblasts; RARS-T, refractory sideroblastic anemia with thrombocytosis; RAEB1, refractory anemia with 5–9% marrow blasts; RAEB2, refractory anemia with 10–19% marrow blasts. Source: Haferlach T, et al. *Leukemia* 2014;28:241–247. Reproduced with permission of Springer Nature.

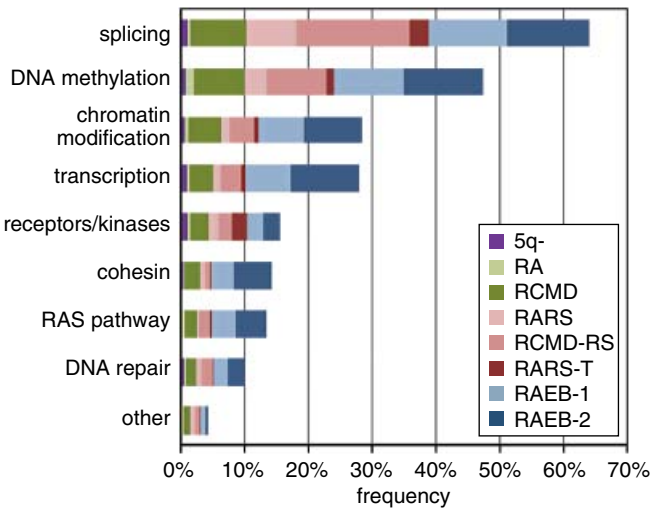

Fig. 15.24. Significantly mutated genes in MDS. Frequency of gene mutations involved in common functional pathways, which are defined in Fig. 15.23. Source: Haferlach T, et al. *Leukemia* 2014;28:241–247. Reproduced with permission of Springer Nature.

SPLICING FACTORS

Genes involved in the spliceosome (Fig. 15.26) are mutated in 60% of patients with MDS. Usually these are heterozygous, involve single amino acid substitutions at "hot spots." *SF3B1* is mutated in 80% of patients with MDS-RS.

EPIGENETIC REGULATORS

Genes involved in DNA methylation (Fig. 15.27) and in histone modification (e.g. *ASXL1* and *EZH2*; Figs. 1.23 and 1.24) are the next most frequently mutated (Fig. 15.25). Those of *TET2*, *ASXL1*, and *DNMT3A* are among the most frequent.

COHESINS

Cohesin is a closed loop multiprotein. It normally functions to align sister chromatids during mitosis. Mutations of some of the component genes (e.g. *STAG2*) occur in 11% of patients with low-risk MDS and 17% of patients with high-risk MDS. They are thought to cause aberrant transcription programs.

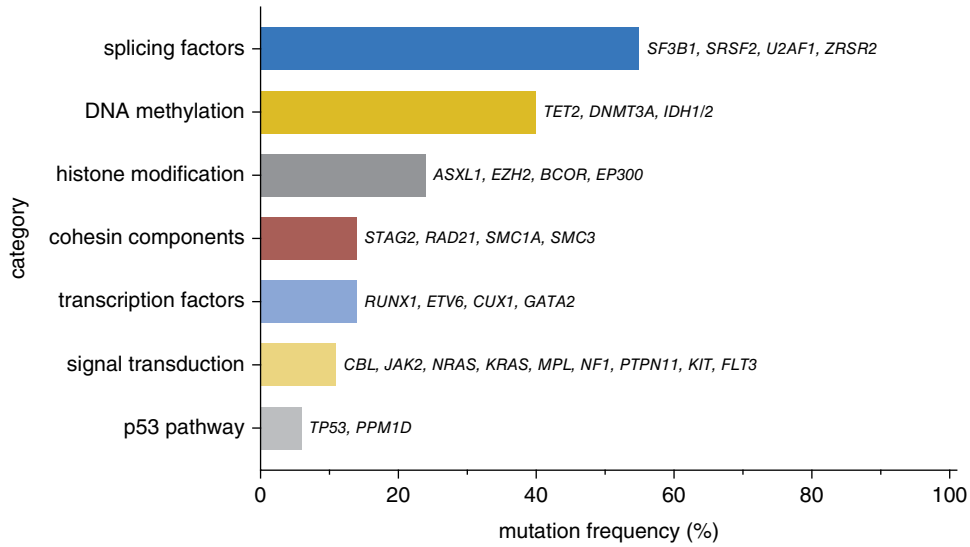

Fig. 15.25. The recurrently mutated genes in MDS can be organized into a limited number of biologic categories. Estimated mutation frequencies within an unselected population of patients with MDS are displayed, with examples of the most commonly implicated genes in each category listed to the right of each bar. Source: Kennedy JA, Ebert BL. *J Clin Oncol* 2017;35(9):968–974 . Reproduced with permission of *Journal of Clinical Oncology*: American Society of Clinical Oncology. Data also from Papaemmanuil E, et al. *Blood* 2013;122: 3616–3627 and Haferlach T, et al. *Leukemia* 2014;28:241–247.

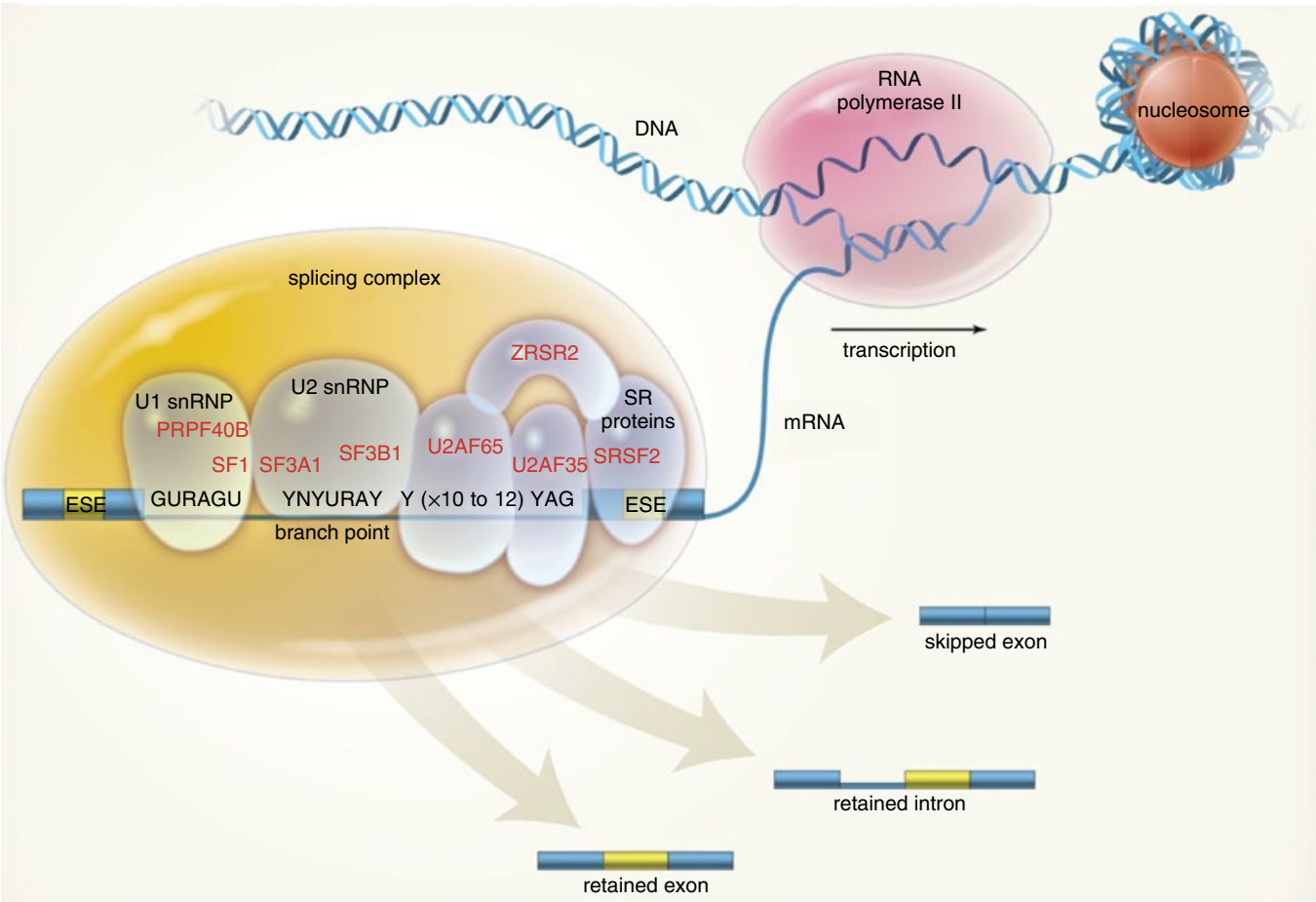

Fig. 15.26. Schematic representation of RNA splicing. Source: Ebert B, Bernard OA. *N Engl J Med* 2011;365:2534. Reproduced with permission of Massachusetts Medical Society: *The New England Journal of Medicine*.

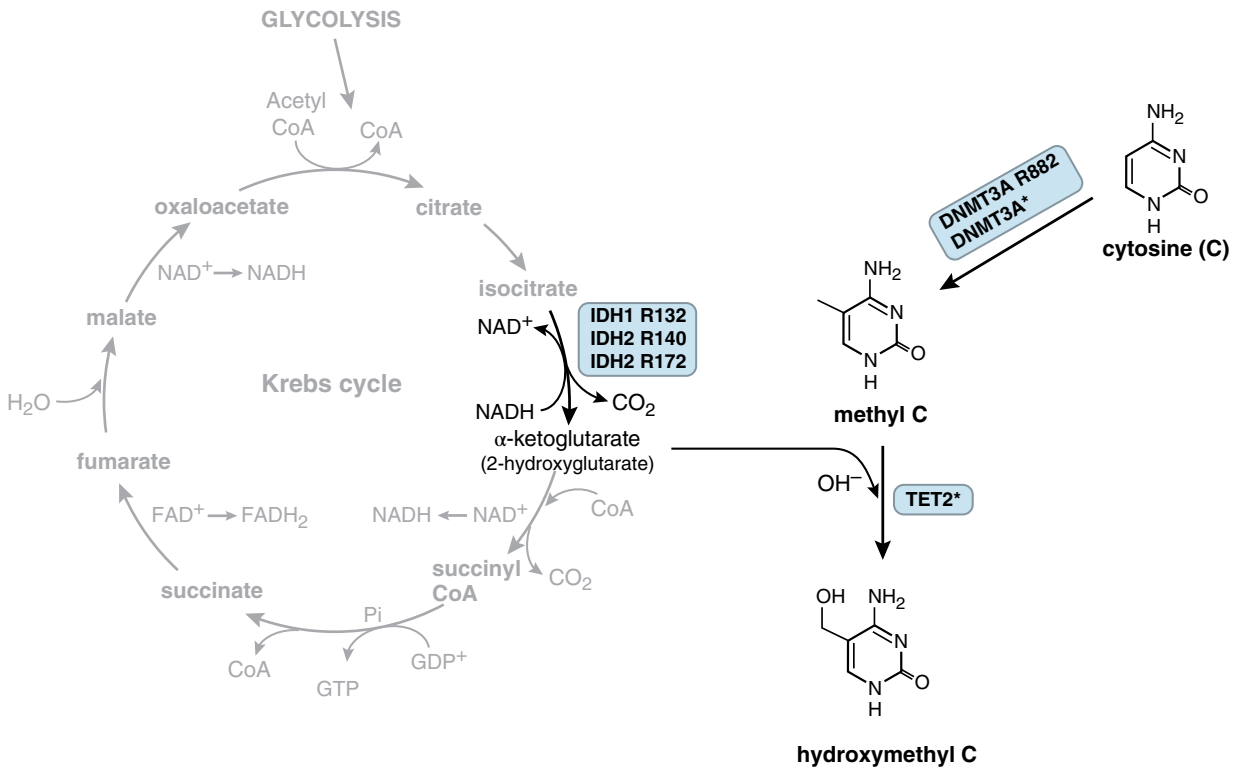

Fig. 15.27. Enzymes involved in DNA methylation whose mutations are implicated in myeloid disorders. The metabolic reaction catalyzed by each enzyme is indicated along with the most frequent leukemogenic mutations (blue boxes + see text). The oncometabolite 2-hydroxyglutarate is produced, instead of α-ketoglutarate, by the action of mutant IDH1 or IDH2. 2-Hydroxyglutarate inhibits TET dioxygenases (including TET2) and other epigenetic enzymes. Source: Hoffbrand AV, et al., eds. *Postgraduate Haematology*, 7th edn. John Wiley & Sons, 2016. Reproduced with permission of John Wiley & Sons.

TRANSCRIPTION FACTORS

Mutation in genes such as *RUNX1* and *GATA2* may be acquired or occur in the germline and predispose to familial marrow failure syndrome, which may progress to MDS or other myeloid malignancies.

SIGNAL TRANSDUCTION

Some of these genes are more commonly mutated in AML (e.g. *FLT3*) and the myeloproliferative neoplasms (e.g. *JAK2*), but rarely are associated with MDS.

TP53

Missense mutations are associated with a poor prognosis, especially after chemotherapy and if associated with loss of the second *TP53* allele because of deletion of 17p.

The prognosis is increasingly unfavorable with an increasing number of driver mutations present. The presence of mutations in one or more genes such as *TP53*, *EZH2*, *RUNX1*, *ASXL1*, or *ETV6* is unfavorable. On the other hand, a single mutation of *SF3B1* carries a favorable prognosis, with the subjects usually showing isolated erythroid dysplasia and a high proportion of ring sideroblasts. Those with this mutation and multilineage dysplasia show only mild dysplastic features in the granulocytic and megakaryocytic lineages. Those multilineage cases with ring sideroblasts and *SF3B1* mutation segregate with mutations of genes involved in DNA methylation (*TET2* and *DNMT3A*), whereas those with wild-type *SF3B1* segregate with *TP53* mutations and have a worse prognosis. Of these wild-type cases some have mutations of other RNA-splicing genes (e.g. of *SRSF2*).

The *SF3B1* mutation has been associated with a high degree of ineffective hematopoiesis, low serum hepcidin levels, increased iron absorption, and increased liver iron, even without transfusions. The *JAK2* mutation, if present, is associated with a raised platelet count.

MOLECULAR GENETICS DURING FOLLOW-UP

Figure 15.28 illustrates various sequences of molecular events that may occur during follow-up of patients with MDS, in this example for 11 patients presenting with del(5q). There may be expansion of a subclone present at diagnosis and/or gain of new mutations (Fig. 15.28A). There may be associated transformation to secondary AML. Transformation to secondary AML may also occur with cytogenetic evolution as in Fig. 15.28C or with no change in cytogenetics or molecular genetics as in Fig. 15.28D. There may also be loss of a subclone present at diagnosis as in Fig. 15.28B.

MIRAGE SYNDROME

Adrenal hypoplasia is a rare, life-threatening congenital disorder. A congenital form of adrenal hypoplasia with associated defects, has been termed MIRAGE (myelodysplasia, infection, restriction of growth, adrenal hypoplasia, genital phenotypes, and enteropathy) syndrome. The syndrome is caused by mutations in *SAMD9*, which codes for a protein facilitating endosome fusion. Of interest patients may develop MDS accompanied by loss of the chromosome 7. Considering the potent growth-restricting activity of the *SAMD9* mutation, the loss of chromosome 7 presumably occurs as an adaptation to the growth restriction.

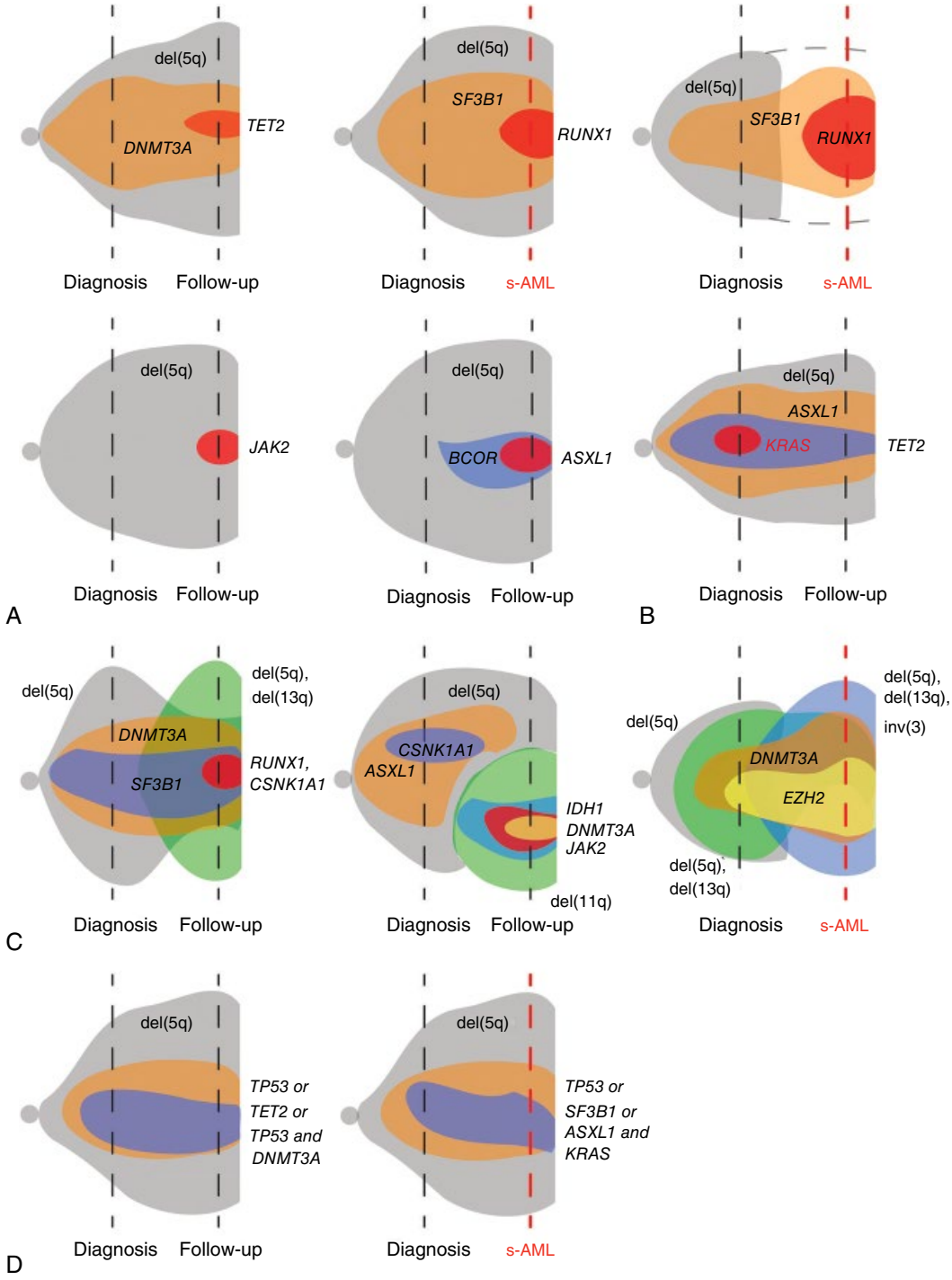

Fig. 15.28. The dynamic of variant allele frequency (VAF) and acquisition and loss of mutated genes as well as cytogenetic lesions at diagnosis and follow-up. VAF and clone size are indicated by the height of the shapes. Cases evolving to s-AML are indicated by the red dashed time line, while follow-up without progression to s-AML is indicated by a black dashed time line. Disease course showing **(A)** gain of gene mutations, **(B)** loss of a gene mutation, **(C)** cytogenetic evolution, and **(D)** no significant change in del(5q) clone size as well as gene mutation (VAF). D, both illustrations represent three patients. For the third patient in the first row no cytogenetics was available at s-AML stage. s-AML, secondary acute myeloid leukemia; del(5q), deletion of the long arm of chromosome 5. Source: Meggendorfer M. et al. *Haematologica* 2017;102:1502–1510.

CLONAL HEMATOPOIESIS OF INDETERMINATE POTENTIAL

Clonal hematopoiesis occurs with increasing age. Clonal mutations are rare in the peripheral blood cells of persons younger than 40 years but increase in frequency with age, reaching nearly 20% in those over 90 years old. This finding has been termed ARCH (age-related clonal hematopoiesis) and recently also CHIP (clonal hematopoiesis of indeterminate potential) (Table 15.4). CHIP has been defined as the presence in the blood white cell DNA of clonal mutations at an allele frequency of at least 2%, without definite morphological evidence

TABLE 15.4. CYTOPENIAS AND CLONAL HEMATOPOIESIS: DEFINITIONS

Acronym	Condition	Description/definition
ARCH	Aging-related clonal hematopoiesis	Describes the presence of detectable, benign clonal hematopoiesis (defined by the presence of somatic mutations in the blood or bone marrow) whose incidence increases with age. No formal definition involving clonal abundance or types of mutations. No clinical significance is implied
CHIP	Clonal hematopoiesis of indeterminate potential	Defined by somatic mutations of myeloid malignancy-associated genes in the blood or bone marrow present at ≥2% variant allele frequency in individuals without a diagnosed hematologic disorder
CHOP	Clonal hematopoiesis of oncogenic potential	Describes clonal hematopoiesis in a clinical context where it is associated with a significant likelihood of progressing to a frank malignancy
IDUS	Idiopathic dysplasia of undetermined significance	Individuals with unexplained morphologic dysplasia of blood cells who are not cytopenic. Can occur with or without clonal hematopoiesis
ICUS	Idiopathic cytopenia of undetermined significance	Patients with one or more unexplained cytopenias who do not meet diagnostic criteria for myelodysplastic syndrome or another hematologic disorder. Can occur with or without clonal hematopoiesis although often used to refer to cytopenias without evidence of clonal hematopoiesis
CCUS	Clonal cytopenia of undetermined significance	Patients with one or more unexplained cytopenias who do not meet diagnostic criteria for myelodysplastic syndrome or another hematologic disorder, but who have somatic mutations of myeloid malignancy-associated genes in the blood or bone marrow present at ≥2% variant allele frequency. Can be considered as the intersection between CHIP and ICUS

Source: Bejar R. *Leukemia* 2017;31:1869–1871. Reproduced with permission of Springer Nature.

of a hematologic neoplasm (Table 15.4). The genes most frequently involved have been listed as: *DMT3A*, *TET2*, *ASXL1*, *JAK2*, *SF3B1*, *TP53*, *CBL*, *GNB1*, *BCOR*, *U2AF1*, *CREBBP*, *CUX1*, *SRSF2*, *MLL2*, *SETD2*, *GNAS*, *PPM1D*, *BCORL1* in one study but include also *PPMID*, *MYD88*, *STAT3*, *IDH2*, and *ATM* in another report. The subjects with CHIP show no diagnostic criteria for paroxysmal nocturnal hemoglobinuria, monoclonal gammopathy of undetermined significance, or monoclonal B lymphocytosis. Dysplasia may be present but is minimal (<10% of cells per lineage). The risk of progression to MDS or AML appears to be of the order of 0.5–1.0% per year. A doubling of the risk for atherosclerotic cardiovascular disease has been found in patients with CHIP. Idiopathic cytopenias of uncertain significance (ICUS), some of which also show somatic gene mutations and are then designated as clonal cytopenias of uncertain significance (CCUS), are discussed in Chapter 10.

CHAPTER

MYELOPROLIFERATIVE NEOPLASMS

16

In the World Health Organization (WHO) 2016 classification, chronic myeloid leukemia (CML), *BCR-ABL1+*, chronic neutrophilic leukemia, chronic eosinophilic leukemia, polycythemia vera (PV), essential thrombocythemia (ET), and primary myelofibrosis (PMF) (divided into prefibrotic/early stage and overt fibrotic stage), and myeloproliferative disease unclassifiable, are included as myeloproliferative neoplasms (MPNs) (Table 16.1). These leukemic MPNs and the nonleukemic MPNs, PV, ET, and PMF are discussed in this chapter. Mastocytosis is not considered in WHO 2016 as a subgroup of the MPNs because of its separate clinical and pathological features, ranging from a cutaneous disease to systemic disease. Mastocytosis, eosinophilia associated with four specific cytogenetic mutations, and the myelodysplastic/myeloproliferative neoplasms are described in Chapter 17.

CHRONIC MYELOID LEUKEMIA, *BCR-ABL1+*

CML, *BCR-ABL1+* is most frequently seen in middle-aged people but occurs at all ages. In most patients there is replacement of normal marrow by cells with an abnormal G-group chromosome, the Ph chromosome (Fig. 16.1). This abnormality is a result of reciprocal translocation involving chromosome 9 band q34 and chromosome 22 band q11. The cellular oncogene *ABL1*, which codes for a tyrosine protein kinase (TPK), is translocated to a specific breakpoint cluster region (BCR) of chromosome 22. Part of the BCR (the 5′ end) remains on chromosome 22, and the 3′ end moves to chromosome 9 together with the oncogene *SIS* (which codes for a protein with close homology to one of the two subunits of platelet-derived growth factor). As a result of the translocation onto chromosome 22, a chimeric BCR/ABL1 messenger ribonucleic acid (mRNA) is produced (Fig. 16.2), which results in the synthesis of a 210 kDa protein with considerably enhanced TPK activity compared with the normal 145 kDa *ABL1* oncogene product (Table 16.2). The fusion gene may be detected by the fluorescence in situ hybridization (FISH) technique (Fig. 16.3).

Cases of Ph-positive acute lymphoblastic leukemia (ALL) may show a similar molecular abnormality to that in typical Ph-positive CML, but some show a breakpoint on chromosome 22

TABLE 16.1 WHO (2016): CLASSIFICATION OF THE MYELOPROLIFERATIVE DISEASES

Myeloproliferative neoplasms (MPNs)
Chronic myeloid leukemia, *BCR-ABL1+*
Chronic neutrophilic leukemia
Polycythemia vera
Primary myelofibrosis (PMF)
Primary myelofibrosis, prefibrotic/early stage
Primary myelofibrosis, overt fibrotic stage
Essential thrombocythemia
Chronic eosinophilic leukemia, not otherwise specified (NOS)
Myeloproliferative neoplasm, unclassifiable

Adapted from Swerdlow SH, et al., eds. *WHO Classification of Tumours of Haematopoietic and Lymphoid Tissues*, revised 4th edn. International Agency for Research on Cancer, Lyon, 2017.

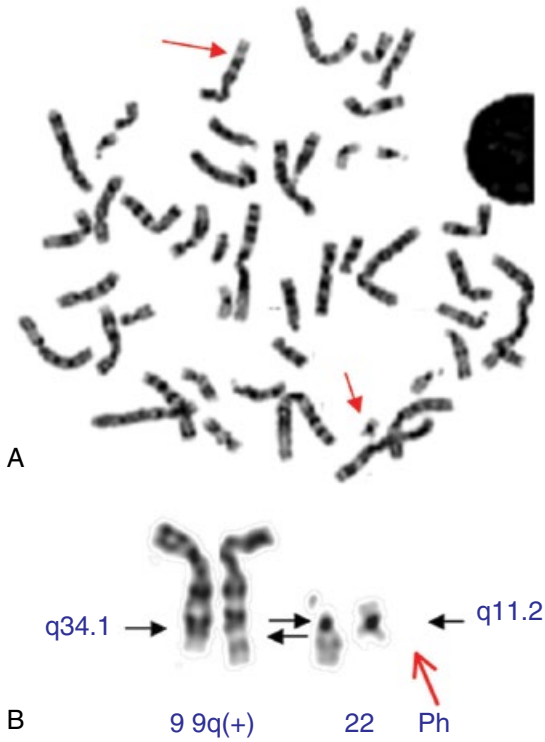

Fig. 16.1. Chronic myeloid leukemia. **A,** G-banded metaphase cell with arrows pointing to the Ph and der(9) chromosomes. **B,** Partial karyotype showing the reciprocal translocation t(9;22)(q34;q11). The arrows indicate the breakpoints. (Courtesy of Dr. E Nacheva.)

Color Atlas of Clinical Hematology: Molecular and Cellular Basis of Disease, Fifth Edition. A. Victor Hoffbrand, Paresh Vyas, Elías Campo, Torsten Haferlach, and Keith Gomez

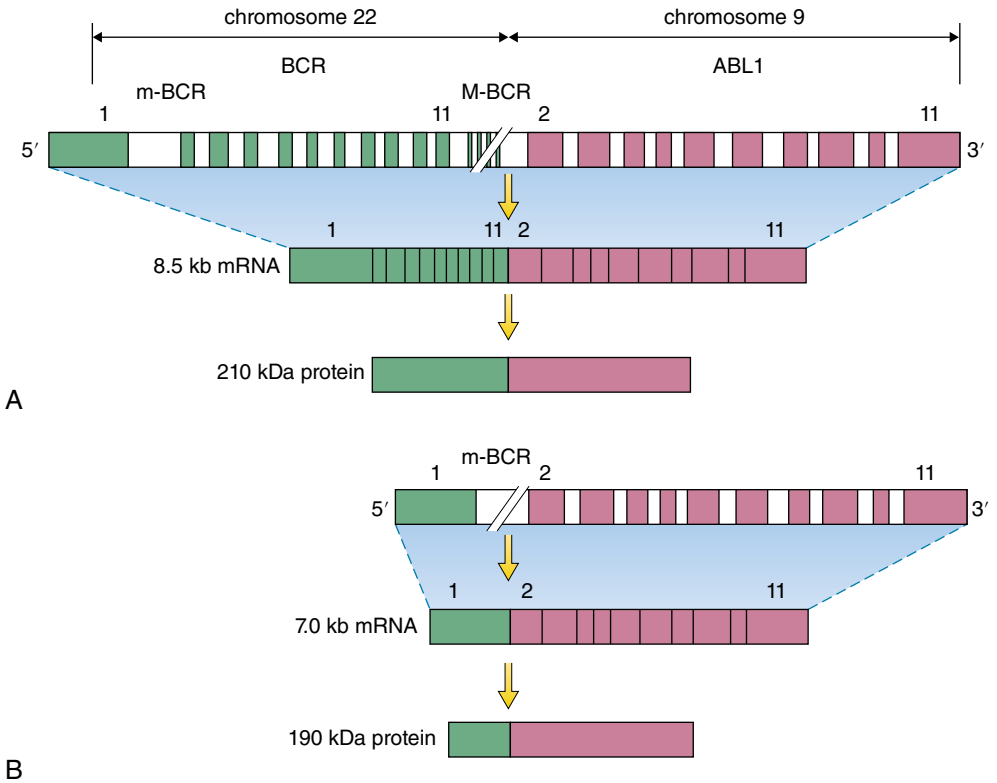

Fig. 16.2. Chronic myeloid leukemia. **A,** Chimeric *BCR-ABL1* mRNA encoded for partly by the breakpoint cluster region (BCR) of chromosome 22 and partly by the *ABL1* oncogene translocated from chromosome 9 to 22. The breakpoint is almost always in the major BCR (M-BCR), a 5–6 kb region 3′ to exon 11. Small exons numbered b1, b2, b3, and so on occur in the M-BCR, and the breakpoint is usually between b3 and b4 or b2 and b3, giving rise to fusion genes *b3a2* or *b2a2*, respectively. The resultant 85 kb mRNA is expressed as a 210 kDa protein (p210). **B,** In Ph-positive acute lymphoblastic leukemia (ALL) the breakpoint may be in the M-BCR, but may also occur in the first intron, the minor BCR (m-BCR). The fusion gene is termed *e1a2*. A 7.0 kb mRNA is formed that codes for a 190 kDa protein (p190).

TABLE 16.2. CHRONIC MYELOID LEUKEMIA, *BCR-ABL1*+: PATTERNS OF INVOLVEMENT OF THE Ph CHROMOSOME, THE BCR (5.8 kb) REGION, AND THE *ABL1* IN CHRONIC MYELOID LEUKEMIA AND ACUTE LYMPHOBLASTIC LEUKEMIA

Condition	Pattern
Normal	Ph–, BCR– → 145 kDa TPK
CML	Ph+, BCR+ → 210 kDa TPK Ph–, BCR+ → 210 kDa TPK Ph–, BCR– → 145 kDa TPK (atypical cases; ?myelodysplasia)
ALL	Ph+, BCR+ → 210 kDa TPK (?blast transformation of CML) Ph+, BCR– → 190 kDa TPK (?de novo ALL) Ph–, BCR– → 145 kDa TPK (de novo ALL)

ALL, Acute lymphoblastic leukemia; BCR1, rearrangement within the 5.8 kb BCR region; CML, chronic myeloid leukemia; TPK, tyrosine protein kinase.

outside the major BCR region but in the first intron of the gene (minor BCR, or m-BCR breakpoint). In these, the product of the translocated *ABL1* gene is a 190 kDa protein also of enhanced TPK activity (see Table 16.2).

CLINICAL FEATURES

The symptoms of CML are related to hypermetabolism and include anorexia, lassitude, weight loss, and night sweats. Splenomegaly is usual and can be massive (Fig. 16.4). Features of anemia, a bleeding disorder, visual disturbance because of retinal disease (Figs. 16.5 and 16.6), neurologic symptoms, and occasionally gout (Fig. 16.7) may occur. As in chronic lymphocytic leukemia (CLL), CML may only be discovered in some patients during routine blood counting. The white cell count is usually between 50×10^9/L and 500×10^9/L (but may be over 500×10^9/L; Fig. 16.8), and a complete spectrum of granulocytic cells is seen in the blood film (Figs. 16.9–16.11). Basophils are often prominent, and the levels of myelocytes, metamyelocytes, and neutrophils exceed those of the more primitive blast cells and promyelocytes. Bone marrow aspiration is essential to get sufficient material for a complete karyotype and to determine the phase of the disease. The marrow is hypercellular with a granulocytic predominance (Figs. 16.12–16.15).

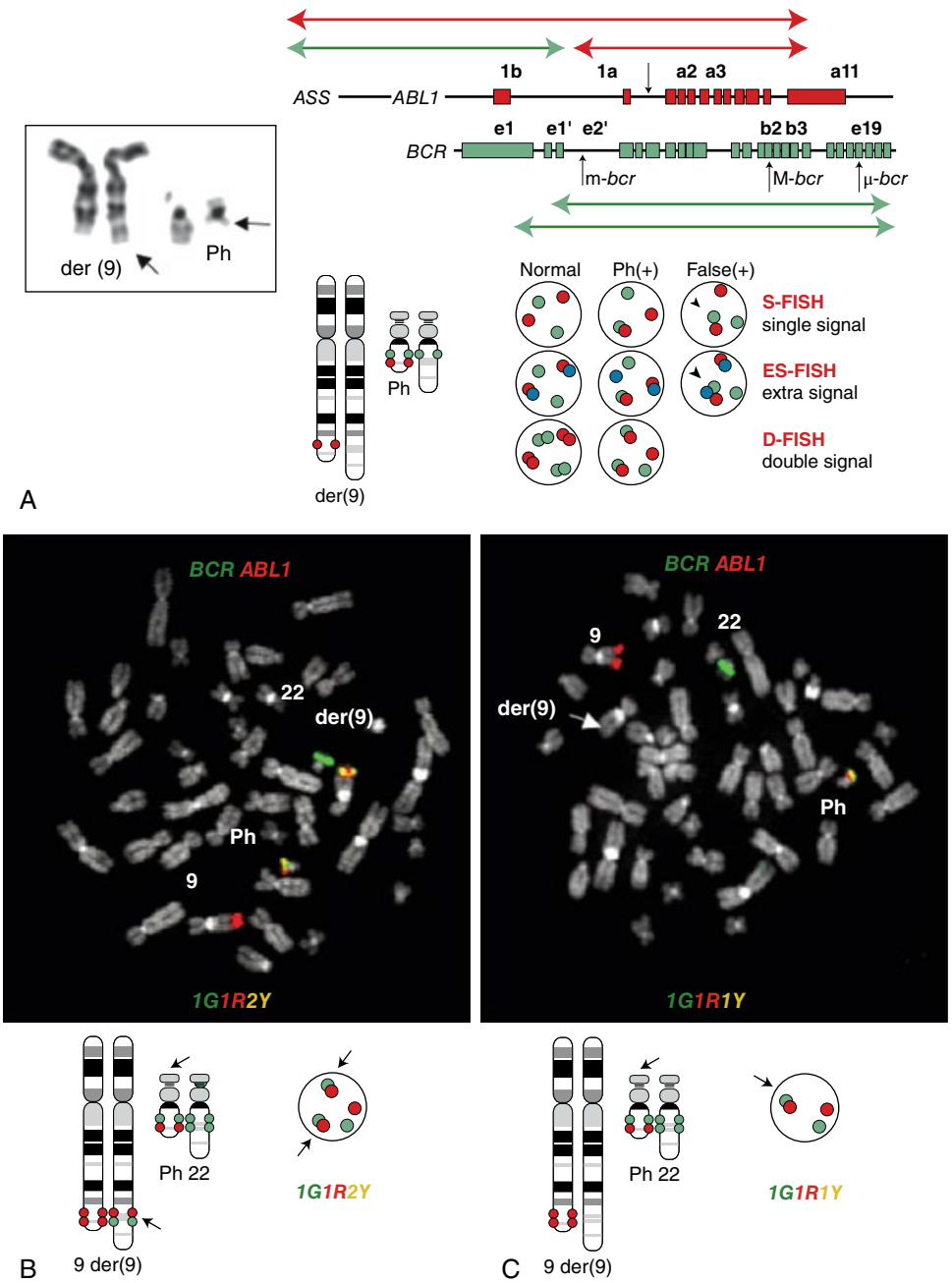

Fig. 16.3. Chronic myeloid leukemia. **A,** Different types of fluorescence in situ hybridization (FISH) probes to detect the *BCR-ABL1* fusion. The top part shows the sequence of the *BCR* (green) and *ABL1* (red) covered by the FISH probes. S-FISH detects the fusion signal only on the Ph chromosome. Extra signal FISH (ES-FISH, blue) detects the der(9) chromosome, and a blue–red–green cluster identifies the *BCR-ABL1* fusion. Double FISH (D-FISH) uses probes to specify *BCR* and *ABL1* breakpoints, and both products, Ph and der(9), give a fusion signal. **B,** D-FISH *BCR-ABL1* probe image showing a typical Ph-positive cell with FISH signals *(top)* and diagram *(bottom)* showing a one G (green), one R (red), and two Y (yellow) signal pattern. **C,** A cell with typical deletions of der(9) chromosome with only one fusion signal on the Ph chromosome as seen in 10–15% of patients with CML. (Courtesy of Dr. E Nacheva.)

ACCELERATED PHASE

The accelerated phase of CML is characterized by anemia, white cell count $>10 \times 10^9$/L, and/or spleen size not responding to therapy, peripheral blood basophils to >20% of circulating white cells (Fig. 16.16), persistent thrombocytopenia ($<100 \times 10^9$/L), or thrombocytosis ($>1000 \times 10^9$/L) not responding to therapy, with increased blasts in the blood or marrow to 10–19% (Table 16.3; Figs. 16.16–16.18). There may be proliferation of dysplastic cells in the granulocytic lineage (Figs. 16.19 and 16.20) with small dysplastic megakaryocytes in sheets (Fig. 16.21A) in the marrow with increased fibrosis (Fig. 16.21B). Cytogenetic analysis often shows clonal evolution (e.g. a second Ph chromosome, trisomy 8, isochromosome 17q, trisomy 19), complex karyotype, or abnormalities of 3q26.2.

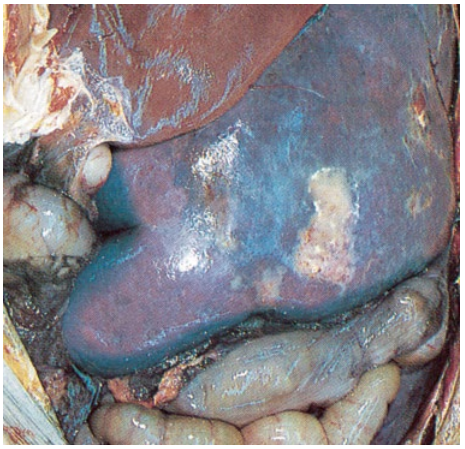

Fig. 16.4. Chronic myeloid leukemia: Abdominal contents at autopsy of a 54-year-old man. The grossly enlarged spleen extends toward the right iliac fossa. The central pale area covered by fibrinous exudate overlays an extensive splenic infarct. The liver is moderately enlarged.

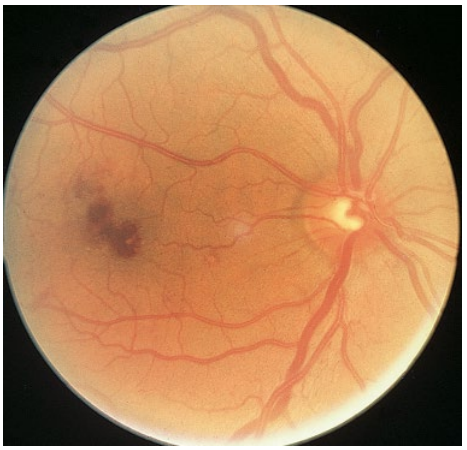

Fig. 16.5. Chronic myeloid leukemia: Ocular fundus in the hyperviscosity syndrome showing distended retinal veins and deep retinal hemorrhages at the macula. (Hb, 14 g/dL; white blood cell count [WBC], 590 × 10^9/L; platelets, 1050 × 10^9/L.)

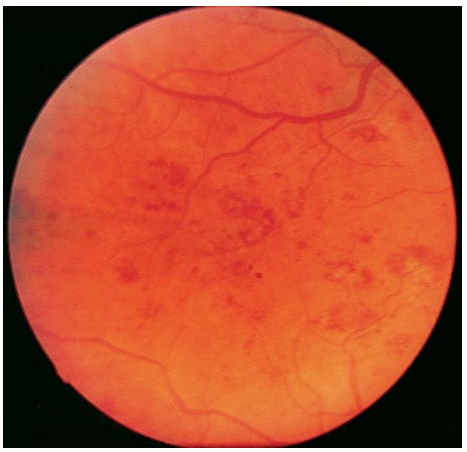

Fig. 16.6. Chronic myeloid leukemia: Ocular fundus (same case as shown in Fig. 16.5) showing prominent leukemic infiltrates fringed by areas of retinal hemorrhage.

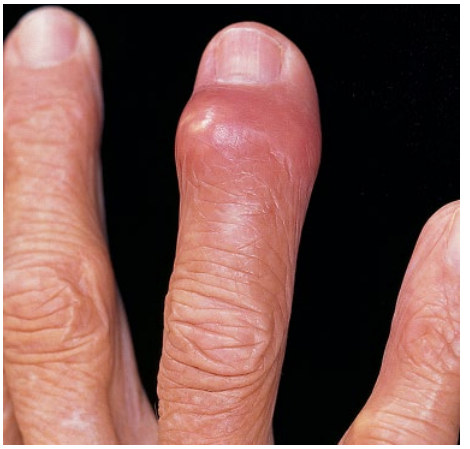

Fig. 16.7. Chronic myeloid leukemia: Acute inflammation and swelling of the fourth finger because of uric acid deposition. (Hb, 8.6 g/dL; WBC, 540 × 10^9/L; platelets, 850 × 10^9/L; serum uric acid, 0.85 mmol/L.)

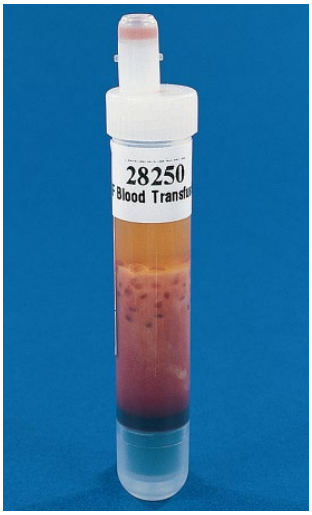

Fig. 16.8. Chronic myeloid leukemia: Peripheral blood from a 22-year-old woman showing vast increase in buffy coat. (Hb, 6.1 g/dL; WBC, 532 × 10^9/L; platelets, 676 × 10^9/L.)

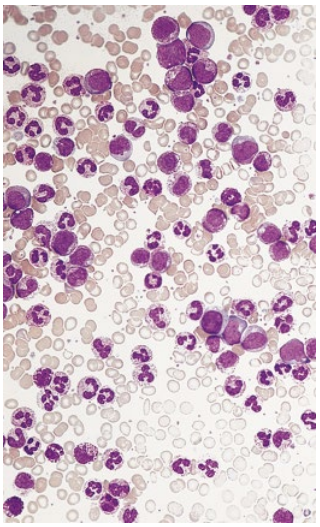

Fig. 16.9. Chronic myeloid leukemia: Peripheral blood film showing cells in all stages of granulocytic development. (Hb, 16.8 g/dL; WBC, 260 × 10^9/L; platelets, 140 × 10^9/L.)

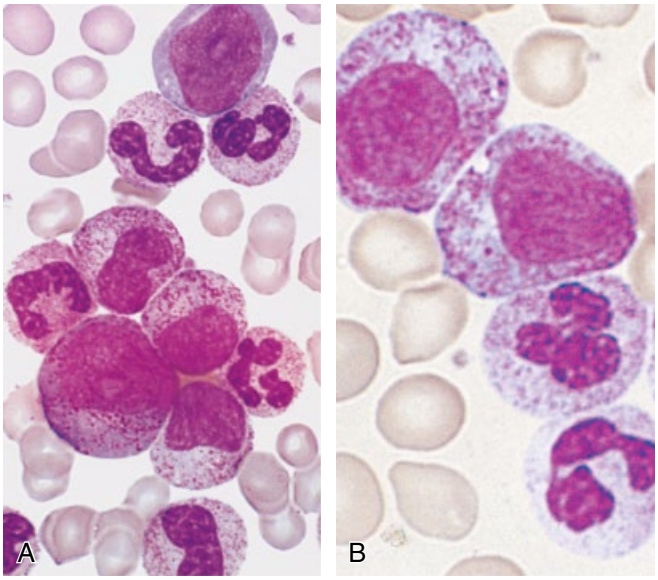

Fig. 16.10. Chronic myeloid leukemia. **A, B,** Peripheral blood films showing a myeloblast, promyelocytes, myelocytes, metamyelocytes, and band and segmented neutrophils.

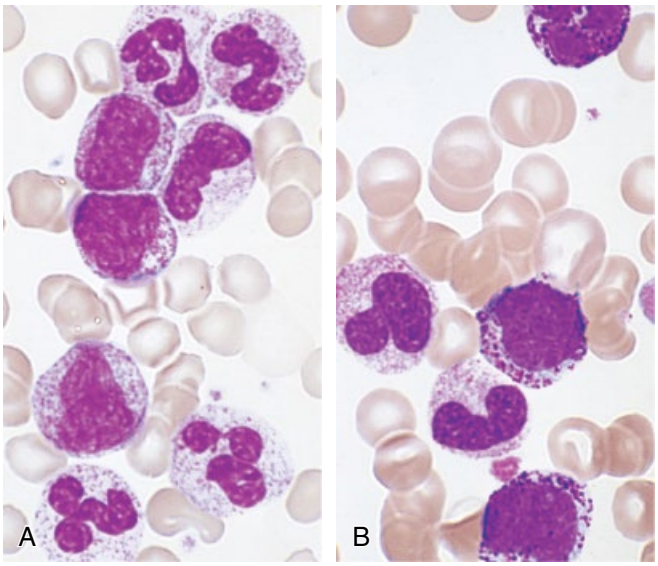

Fig. 16.11. Chronic myeloid leukemia: Peripheral blood films. **A,** Myelocytes, a metamyelocyte, and band and segmented neutrophils. **B,** Basophils and metamyelocytes.

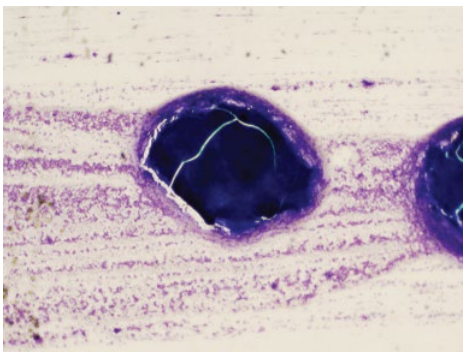

Fig. 16.12. Chronic myeloid leukemia: Bone marrow aspirate showing hypercellular fragment and trails.

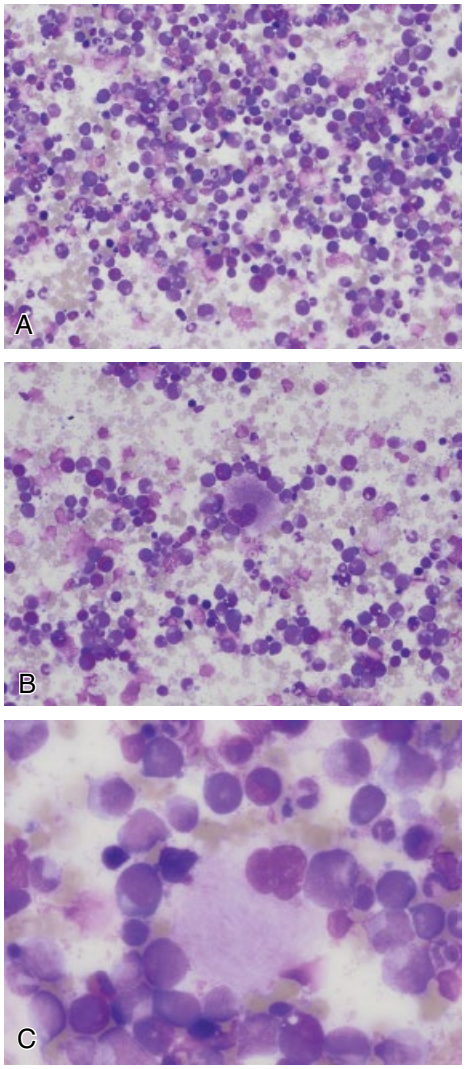

Fig. 16.13. Chronic myeloid leukemia: Bone marrow aspirates. **A,** Increased granulocytes and precursors with blasts <5%. **B,** Small megakaryocyte. **C,** Pseudo-Gaucher cell.

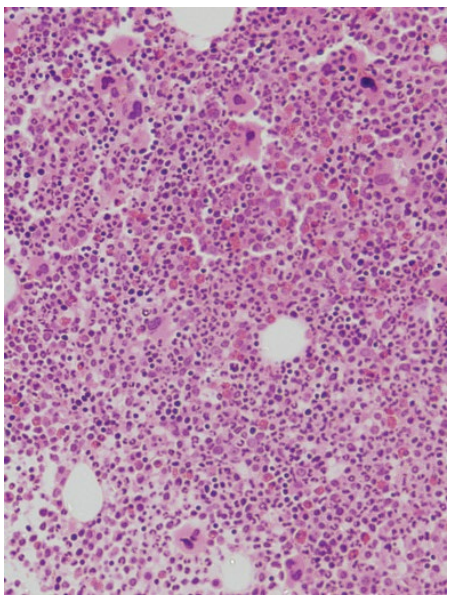

Fig. 16.14. Chronic myeloid leukemia: Trephine biopsy showing hypercellular hematopoiesis with increased granulopoiesis and small megakaryocytes.

BLAST TRANSFORMATION

Before the introduction of imatinib, in about 70% of patients there was a terminal metamorphosis to an acute malignant form of leukemia (Figs. 16.22–16.25) within a few years of diagnosis. This is associated with rapid clinical deterioration and progressive bone marrow failure. Splenic enlargement and infiltration of the skin (Figs. 16.26 and 16.27), CNS, and other nonhematopoietic tissues may occur. The transformation may be myeloblastic, lymphoblastic (see Fig. 16.25), mixed, or (rarely) megakaryoblastic (Figs. 16.28 and 16.29). At least 20% of the marrow cells are blasts.

Blast transformation of CML is much less frequent since the introduction of imatinib and second-generation tyrosine kinase inhibitors for initial treatment (Fig. 16.30).

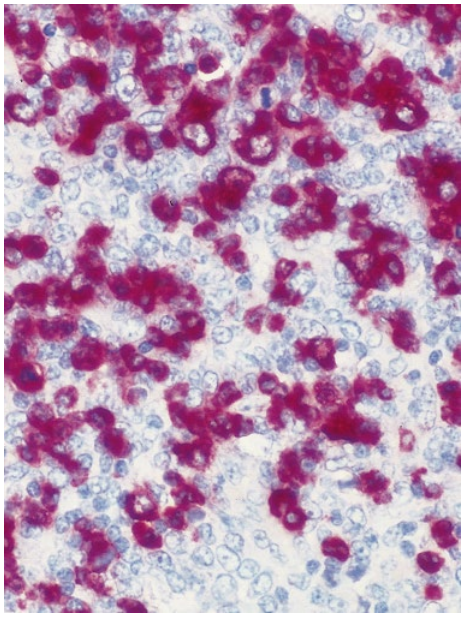

Fig. 16.15. Chronic myeloid leukemia: Trephine bone marrow biopsy stained for neutrophil elastase (a myeloid-specific marker) with immunophosphatase. (Courtesy of Professor DY Mason.)

TABLE 16.3. WHO (2016): CRITERIA FOR CHRONIC MYELOID LEUKEMIA, ACCELERATED PHASE (CML-AP)

CML-AP is defined by the presence of ≥1 of the following hematologic/cytogenetic criteria or provisional criteria concerning response to tyrosine kinase inhibitor (TKI) therapy:
Hematologic/cytogenetic criteria[a]
Persistent or increasing high white blood cell count (>10 × 10^9/L), unresponsive to therapy
Persistent or increasing splenomegaly, unresponsive to therapy
Persistent thrombocytosis (>1000 × 10^9/L), unresponsive to therapy
Persistent thrombocytopenia (<100 × 10^9/L), unrelated to therapy
≥20% basophils in the peripheral blood
10–19% blasts in the peripheral blood and/or bone marrow[b,c]
Additional clonal chromosomal abnormalities in Philadelphia (Ph) chromosome-positive (Ph+) cells at diagnosis, including so-called major route abnormalities (a second Ph chromosome, trisomy 8, isochromosome 17q, trisomy 19), complex karyotype, and abnormalities of 3q26.2
Any new clonal chromosomal abnormality in Ph+ cells that occurs during therapy
Provisional response-to-TKI criteria
Hematologic resistance (or failure to achieve a complete hematologic response)[d] to the first TKI
Any hematologic, cytogenetic, or molecular indications of resistance to two sequential TKIs
Occurrence of two or more mutations in the *BCR-ABL1* fusion gene during TKI therapy

[a] Large clusters or sheets of small, abnormal megakaryocytes associated with marked reticulin or collagen fibrosis in biopsy specimens may be considered presumptive evidence of accelerated phase, although these findings are usually associated with one or more of the criteria listed above.

[b] The finding of bona fide lymphoblasts in the peripheral blood or bone marrow (even if <10%) should prompt concern that lymphoblastic transformation may be imminent, and warrants further clinical and genetic investigation.

[c] ≥ 20% blasts in the peripheral blood or bone marrow, or an infiltrative proliferation of blasts in an extramedullary site, is diagnostic of the blast phase of CML.

[d] Complete hematologic response is defined as white blood cell count <10 × 10^9/L, platelet count <450 × 10^9/L, no immature granulocytes in the differential, and spleen not palpable.

Source: Adapted with permission from Swerdlow SH, et al., eds. *WHO Classification of Tumours of Haematopoietic and Lymphoid Tissues*, revised 4th edn. International Agency for Research on Cancer, Lyon, 2017.

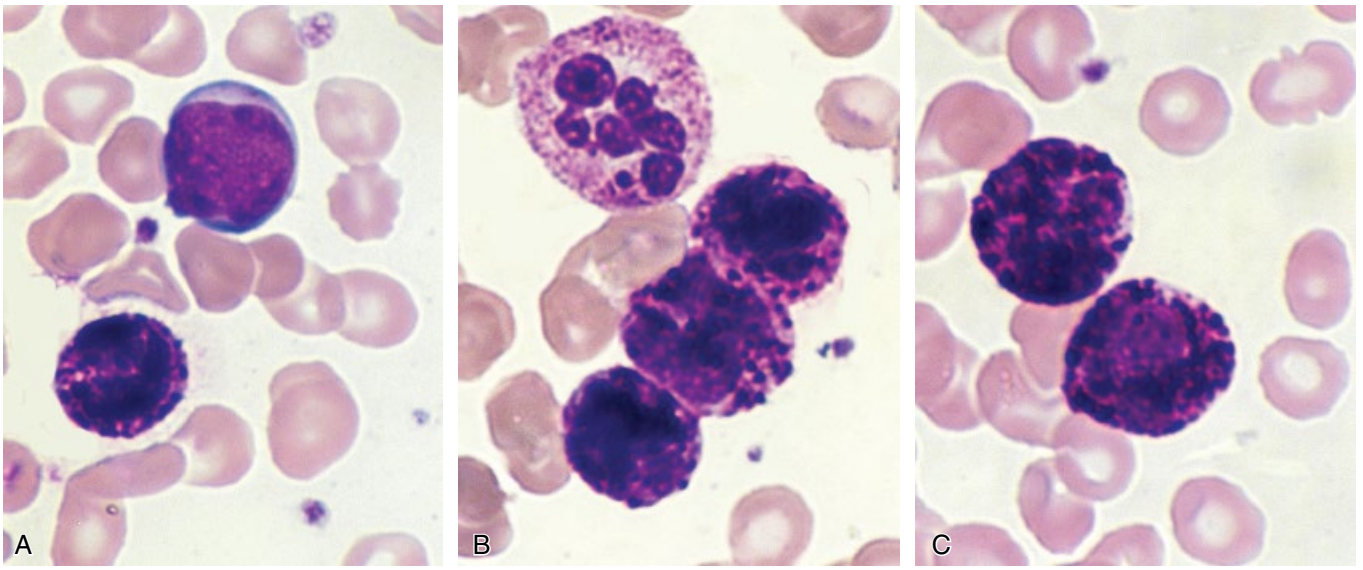

Fig. 16.16. Accelerated phase of chronic myeloid leukemia: Peripheral blood films showing marked basophilia and presence of a myeloblast.

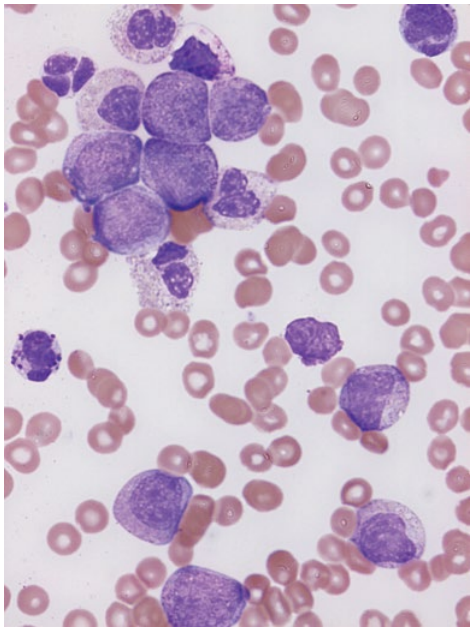

Fig. 16.17. Accelerated phase of chronic myeloid leukemia: Peripheral blood film showing basophils, myeloblasts, and thrombocytopenia. (Courtesy of Dr.W Erber.)

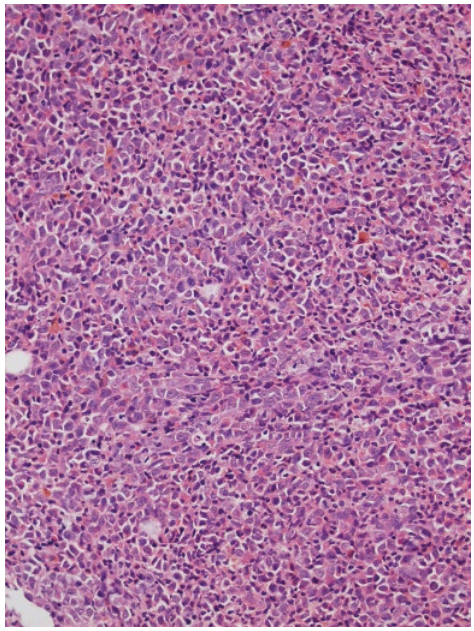

Fig. 16.19. Accelerated phase of chronic myeloid leukemia: Trephine biopsy showing myeloid hyperplasia with increased population of early cells. (Courtesy of Dr.W Erber.)

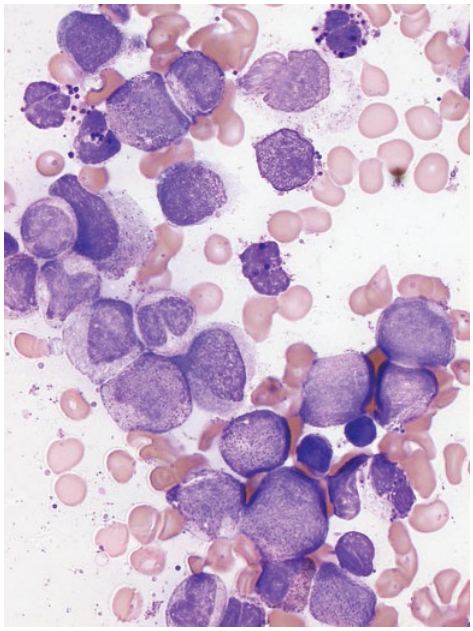

Fig. 16.18. Accelerated phase of chronic myeloid leukemia: Bone marrow aspirate showing basophilia, myeloblasts 10%, and increased promyelocytes. (Courtesy of Dr.W Erber.)

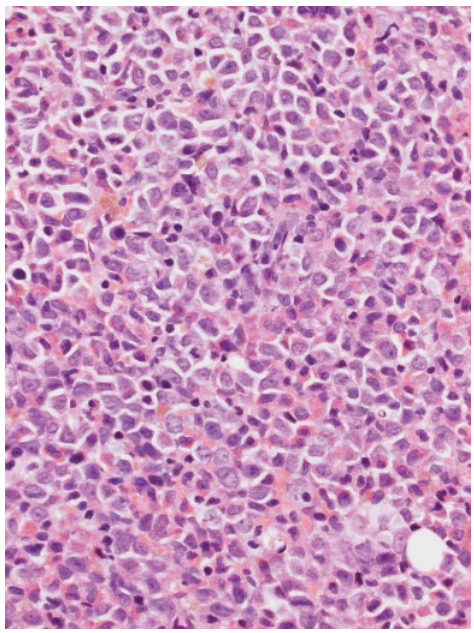

Fig. 16.20. Accelerated phase of chronic myeloid leukemia: Higher power to show myeloid hyperplasia with increased early granulocyte precursors. (Courtesy of Dr.W Erber.)

CHRONIC NEUTROPHILIC LEUKEMIA

Chronic neutrophilic leukemia (CNL) is a rare myeloproliferative disease characterized by sustained peripheral blood neutrophilia to $>25 \times 10^9$/L, bone marrow hypercellularity caused by neutrophil proliferation, and hepatosplenomegaly (Table 16.4; Fig. 16.31). The Ph chromosome and *BCR-ABL1* fusion gene are absent. In contrast to CML, *BCR-ABL1*+, neutrophil precursors are not present in the blood. In contrast to atypical CML, dysgranulopoiesis is absent. The mutation *CSFR3* T618I is present in about 80% of cases and other mutations of the *CSFR3* gene or of *SETBP1*, *U2AF1*, and *SRSF2* genes mutated in other myeloid neoplasms have been reported.

THE NONLEUKEMIC MYELOPROLIFERATIVE DISEASES

In PV, ET, and primary myelofibrosis (PMF), a clonal proliferation is responsible for the overlapping expansion of erythropoietic, granulopoietic, and megakaryocytic components in the

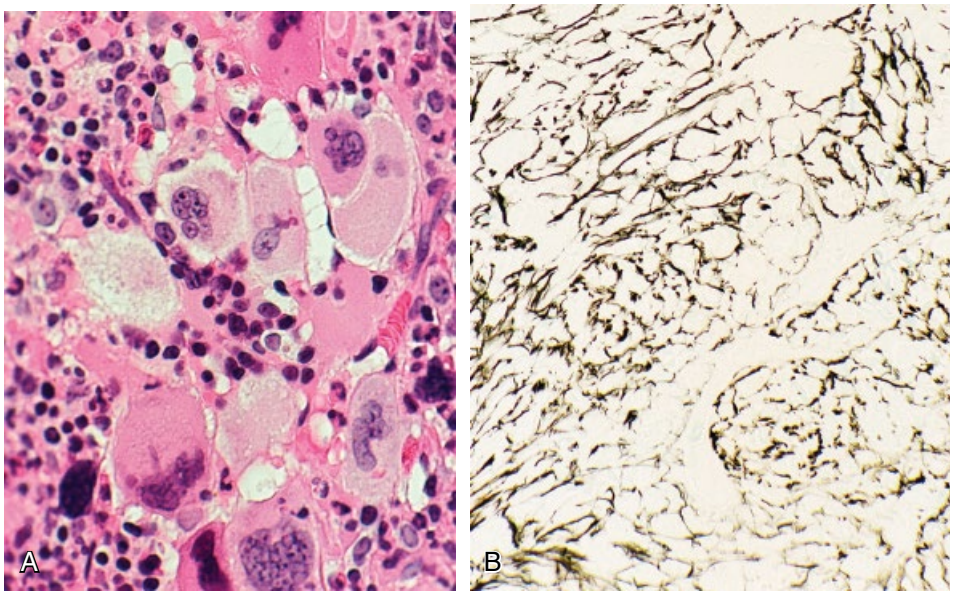

Fig. 16.21. Accelerated phase of chronic myeloid leukemia: Trephine biopsies. **A,** Clustering of abnormal small megakaryocytes. **B,** Increase in reticulum fiber density and thickness with some cross-linking of fibers—Thiele scale grade 2 fibrosis. (Silver stain.)

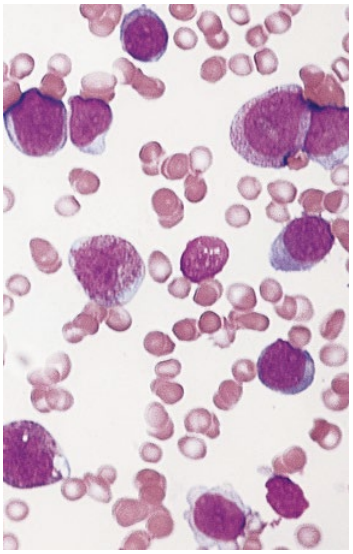

Fig. 16.22. Chronic myeloid leukemia: Peripheral blood film showing blast cell transformation. Over half the white cells seen are primitive blast forms. (Hb, 8.5 g/dL; WBC, 110×10^9/L [blasts, 65×10^9/L]; platelets, 45×10^9/L.)

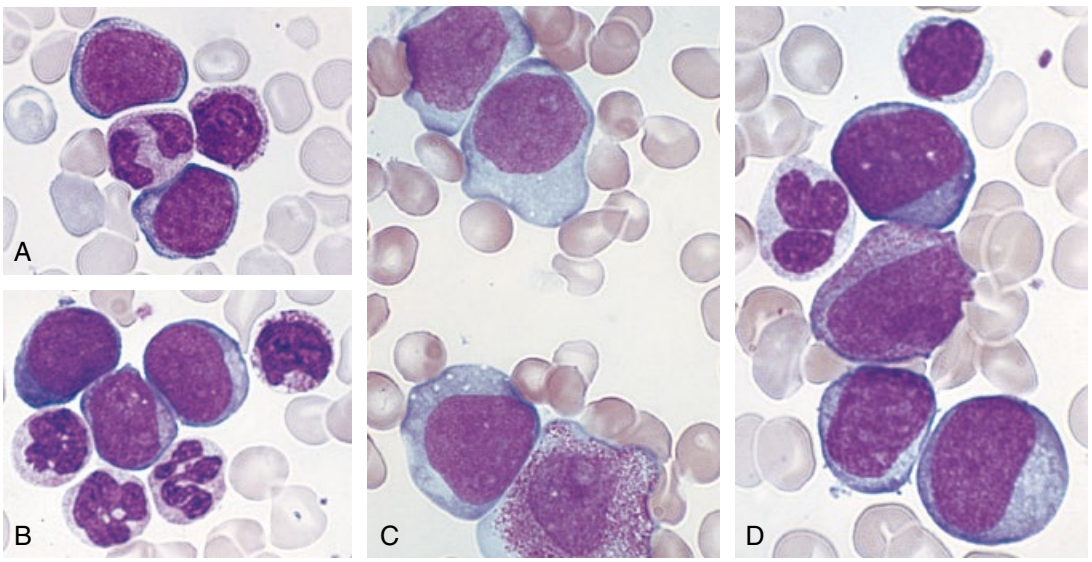

Fig. 16.23. Chronic myeloid leukemia. Peripheral blood films at high magnification showing myeloblastic transformation. Numerous myeloblasts, atypical neutrophils, and abnormal promyelocytes are seen.

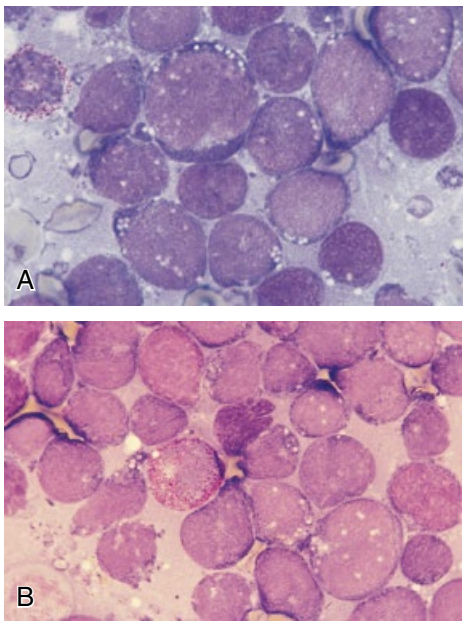

Fig. 16.24. Chronic myeloid leukemia. **A**, **B,** Bone marrow aspirates showing lymphoblastic transformation. There are vacuolated lymphoblasts and residual basophil granulocytes or precursors. (A, Courtesy of Dr. K van Pouche and Professor Z Berneman.)

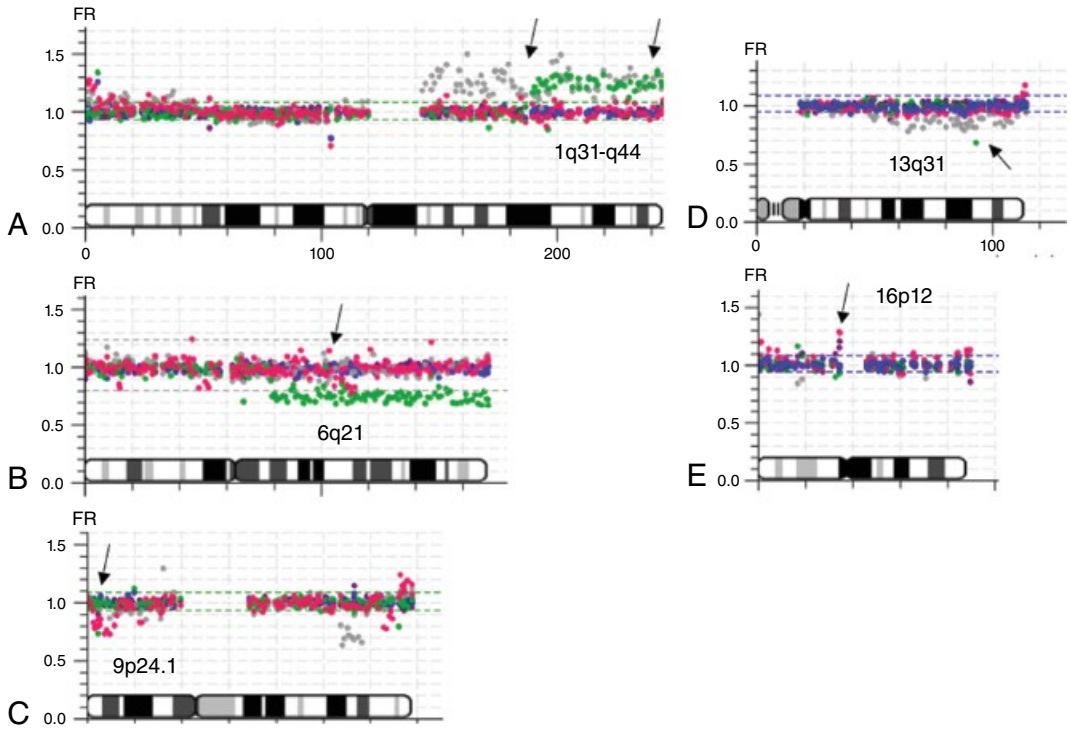

Fig. 16.25. Chronic myeloid leukemia: Common features in the genome profile of CML samples at lymphoid blast transformation revealed by 1 Mb bacterial artificial chromosome (BAC) array comparative genomic hybridization (CGH) analysis (SGI2600 chip) as seen in four cases, including **(A)** gain of the 1q31–q44 region, **(B)** loss of about 300 kbp at 6q21, **(C)** loss of the BAC clones at 9p, **(D)** loss of 13q31, and **(E)** gain at 16p12. Colored dots represent the fluorescent ratio (FR) of the BAC clones along a chromosome, and each color represents a different sample. (Courtesy of Dr. E Necheva.)

marrow and, in advanced disease, of the liver and spleen. The clone includes virtually all myeloid cells as well as B and NK cells and, in late stages, T cells.

ETIOLOGY

A single acquired point driving mutation of the cytoplasmic Janus-associated tyrosine kinase *JAK2* (V617F) (heterozygous or homozygous) in the marrow and blood underlies almost all patients with PV and approximately half of those with ET and PMF (Figs. 16.32 and 16.33). The mutation occurs in a highly conserved region exon 14 of the pseudokinase domain that is believed to negatively regulate *JAK2* signaling. *JAK2* is involved in transducing signals from cytokines and growth factors, including erythropoietin, granulocyte–macrophage colony-stimulating factor, and thrombopoietin. The mutation is responsible for uncontrolled myeloproliferation associated with these disorders. The variable allele frequency (VAF) in granulocytes ranges from

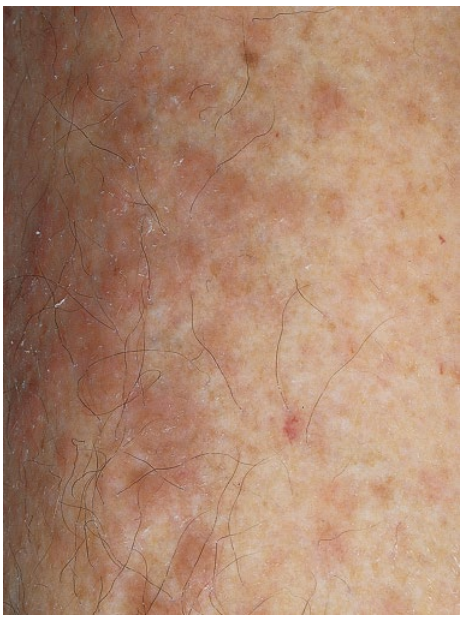

Fig. 16.26. Chronic myeloid leukemia: Nodular leukemic infiltrates in the skin over the anterior surface of the tibia in a 48-year-old woman with blast cell transformation.

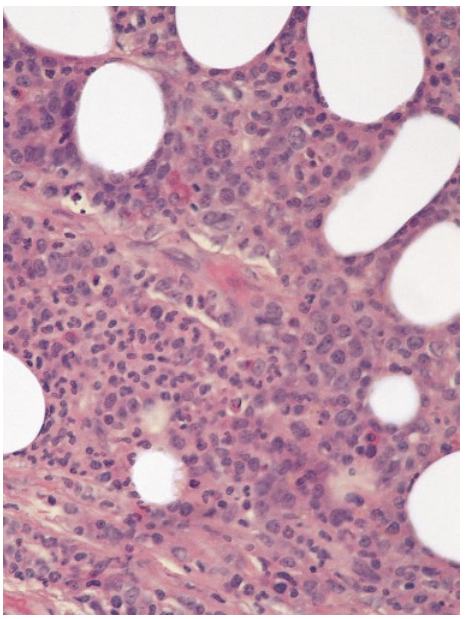

Fig. 16.27. Chronic myeloid leukemia: Histologic section of the skin lesion shown in Fig. 16.26, illustrating extensive perivascular infiltration with mononuclear cells and polymorphs in the deeper layers of the dermis.

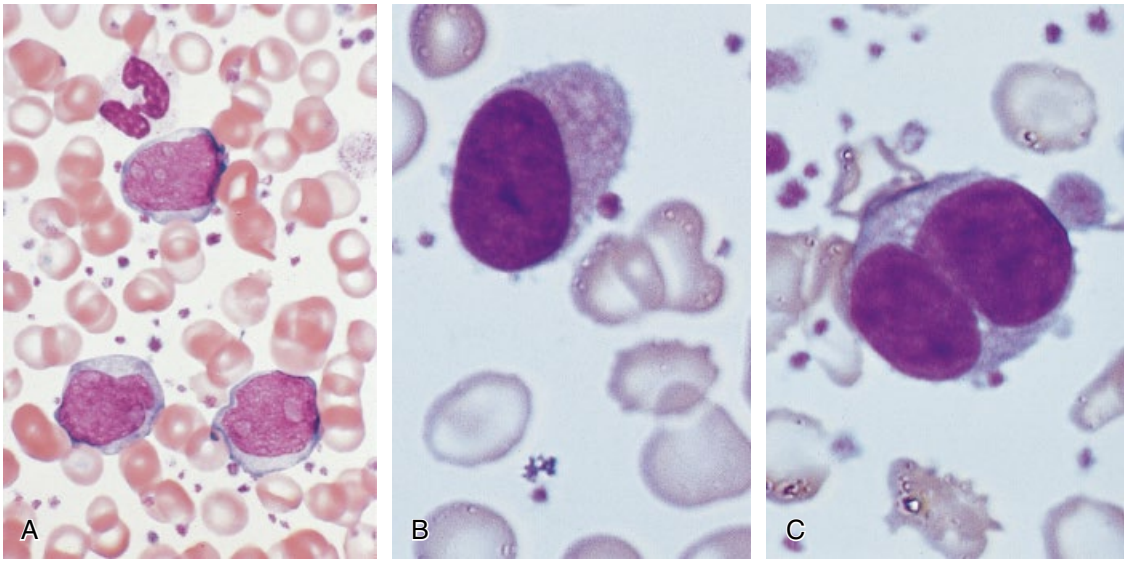

Fig. 16.28. Chronic myeloid leukemia: Megakaryoblastic transformation. **A–C,** Peripheral blood films showing blast cells that stained positive for CD41. (A, Courtesy of Dr. RD Brunning and the US Armed Forces Institute of Pathology.)

about 1% (the level of detection) to 100%, being on average low in ET (around 25%) but higher in PV, often >50%, and up to 100% in myelofibrosis post-PV or -ET. In PV the presence of homozygosity increases with time. In 1–2% of patients with PV the mutation is in exon 12 of *JAK2*.

Mutation of the calreticulin (*CALR*) gene occurs in 25–35% of cases of ET and so in the majority of cases negative for the *JAK2* mutation (Fig. 16.33). Over 50 different mutations have been described, all located in exon 9, those resulting in a +1 frameshift being pathogenic. *CALR* is involved in calcium uptake and release in the endoplasmic reticulum. The mutations appear to promote thrombopoietin (TPO) independence by direct binding of mutated *CALR* to *MPL*, leading to autocrine activation of *MPL* and so to downstream signaling.

The least common of the mutations underlying ET and PMF are those of the *MPL* gene, which codes for the cell surface receptor for TPO (Fig. 16.33). Several different mutations have been described in exon 10. Mutations of other genes coding for proteins involved in the downstream pathways as well as of negative regulators of the receptor tyrosine kinases are also rarely described. As in other myeloid neoplasms mutations of epigenetic regulators such as *TET2*, *ASXL1*, *DNMT3A*, and *EZH2* also may occur. Those of *TET2* have been associated with a worse prognosis.

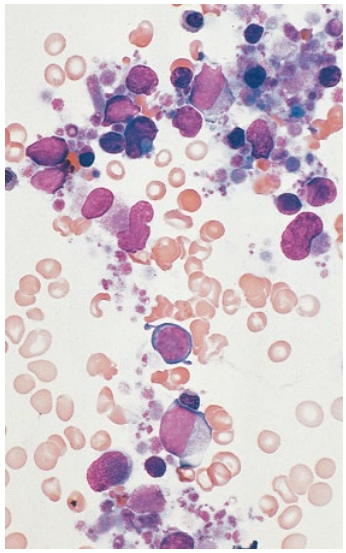

Fig. 16.29. Chronic myeloid leukemia: Megakaryoblastic transformation. Bone marrow showing atypical megakaryocytes and megakaryoblasts. (Courtesy of Dr. RD Brunning and the US Armed Forces Institute of Pathology.)

Germline mutations of the genes *RBBP6* (involved in the p53 pathway) and high penetrance duplication at 14q32.2 leading to overexpression of *ATG2B* and *GSKIP*, which increase TPO sensitivity have been found in families with clustering of MPNs (see Fig. 16.82). Other germline variants, including of different single-nucleotide polymorphisms (SNPs) have also been found in affected families. Genetic polymorphisms associated with an increased risk of *JAK2* V617F-positive MPNs include those of *TERT* and *MYB* close to *JAK2*. Also genes in JAK-STAT signaling (*SH2B3*), DNA cytosine methylation (*TET2*), transcriptional regulation (*GF11B*, *PINT*), and cell cycle control (*CHEK2*, *ATM*). These germline mutations may determine which patients with minor clones of the *JAK2*, *CALR*, or *MPL* acquired mutation progress to develop overt disease. Germline mutations of *TERT* and *JAK2* may also give rise to *JAK2* V671F-negative MPN, indicating that other unknown genes interact with the germline genome. Many patients with PV and ET have features of both, and as with CML, *BCR-ABL1*+, there is a natural evolution or acceleration of the proliferation, which may be associated with further genetic lesions. In PV and ET, an increase in fibrosis results in findings indistinguishable from PMF. The accelerated phase may be associated not only with

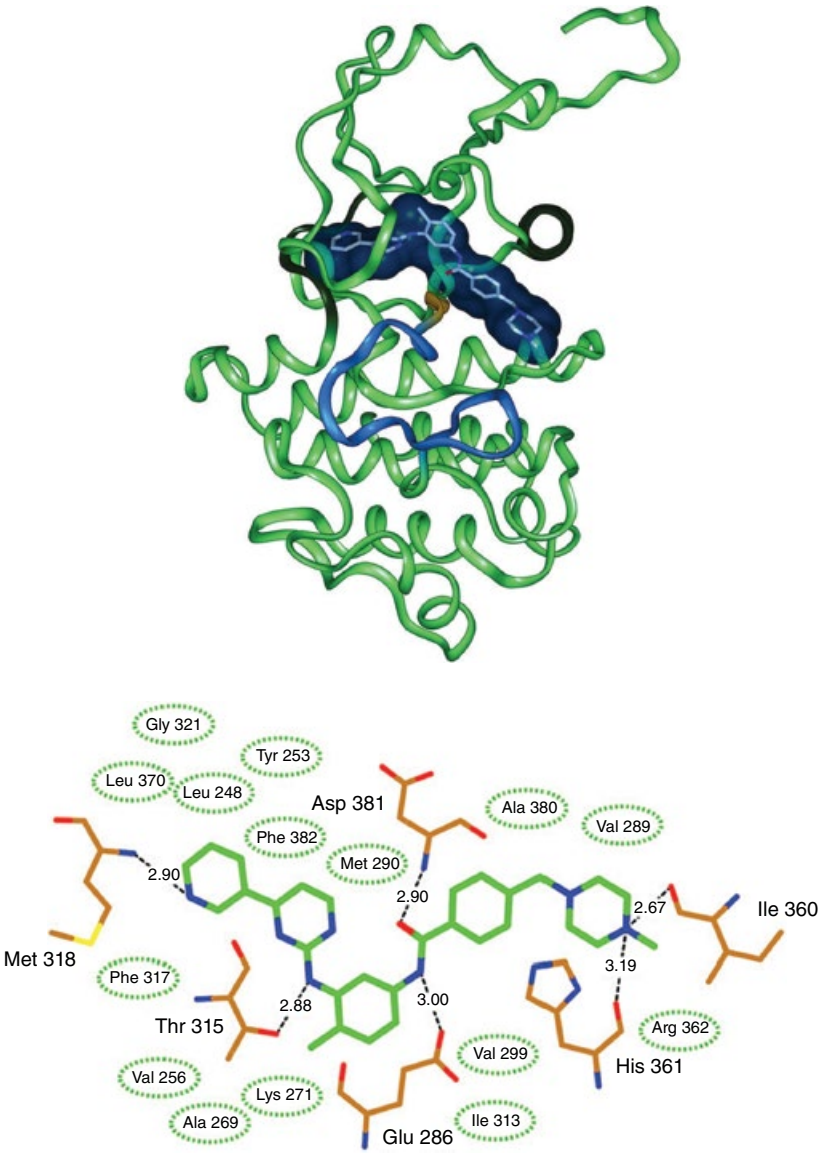

Fig. 16.30. Chronic myeloid leukemia: Crystal structure of the kinase domain of *ABL1* in complex with imatinib. Source: Kuriyan J, Seeliger M. *Cancer Res* 2002;62:4236–4243. Reproduced with permission of *Clinical Cancer Research*: American Association for Cancer Research.

TABLE 16.4. WHO (2016): DIAGNOSTIC CRITERIA FOR CHRONIC NEUTROPHILIC LEUKEMIA

1. Peripheral blood white blood cell count ≥25 × 10^9/L
Segmented neutrophils plus banded neutrophils constitute ≥80% of the white blood cells
Neutrophil precursors (promyelocytes, myelocytes, and metamyelocytes) constitute <10% of the white blood cells
Myeloblasts rarely observed
Monocyte count < 1 × 10^9/L
No dysgranulopoiesis
2. Hypercellular bone marrow
Neutrophil granulocytes increased in percentage and number
Neutrophil maturation appears normal
Myeloblasts constitute <5% of the nucleated cells
3. Not meeting WHO criteria for CML, *BCR-ABL1*+, polycythemia vera, essential thrombocythemia, or primary myelofibrosis
4. No rearrangement of *PDGFRA*, *PDGFRB*, or *FGFR1*, and no *PCM1-JAK2* fusion
5. *CSF3R* T618I or another activating *CSF3R* mutation or
Persistent neutrophilia (≥3 mo), splenomegaly, and no identifiable cause of reactive neutrophilia including absence of a plasma cell neoplasm or, if a plasma cell neoplasm is present, demonstration of clonality of myeloid cells by cytogenetic or molecular studies

Source: Adapted with permission Swerdlow SH, et al., eds. *WHO Classification of Tumours of Haematopoietic and Lymphoid Tissues*, revised 4th edn. International Agency for Research on Cancer, Lyon, 2017.

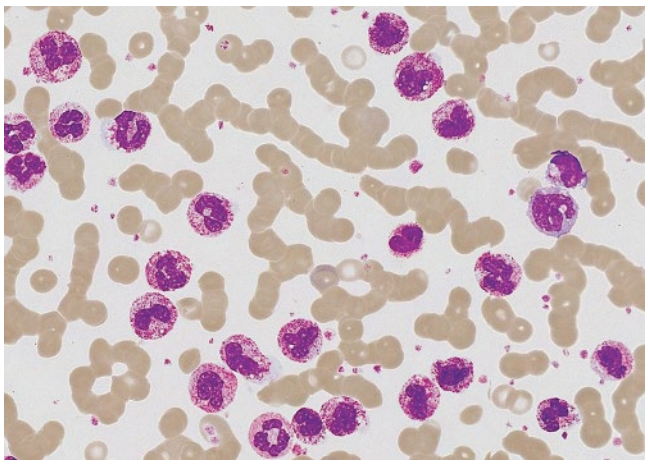

Fig. 16.31. Chronic neutrophilic leukemia: Peripheral blood film from a 64-year-old man with increased neutrophils of 86%, 5 bands and no blasts, *BCR-ABL1* and *JAK2* negative, *CSF3R* mutated; WBC 128 × 10^9/L, hemoglobin 9.7 g/dL, platelets 440 × 10^9/L.

myelofibrosis, but also with either increasing white cell counts or neutropenia or thrombocytopenia. The transformation to acute leukemia in a minority of patients reflects the acquisition of further mutations (see Fig. 16.82).

POLYCYTHEMIA VERA

PV is predominantly a disease of middle-aged and elderly people. Clinical problems are related to the increase in blood volume and viscosity and to the hypermetabolism associated with the myeloproliferation. Table 16.5 lists the 2016 WHO criteria for diagnosing PV. The clinical features include plethora (Figs. 16.34 and 16.35), headaches, lethargy, dyspnea, fluid retention, bleeding symptoms, weight loss, night sweats, and general pruritus made worse by hot baths, acne rosacea (Fig. 16.36), and other forms of dermatitis. There is often suffusion of the conjunctivae (see Fig. 16.34) and marked engorgement of retinal vessels (Figs. 16.37 and 16.38).

Mild to moderate splenomegaly (Fig. 16.39) is found in 70% of patients, and the liver is palpable in 50%. High blood uric acid levels are accompanied by gout (Fig. 16.40) in about 15% of cases. Major thrombosis and hemorrhage dominate the course of untreated PV. Portal or hepatic venous thrombosis is a serious complication and the Budd–Chiari syndrome may be the presenting clinical feature both of PV and *JAK2* mutated ET.

The blood count reveals erythrocytosis and often a neutrophil leukocytosis and thrombocytosis; no primitive cells are seen in the peripheral blood film. There may be an increase in basophils.

The *JAK2* mutation (see Fig. 16.32) is present in blood granulocytes and marrow in over 95% of patients.

Bone marrow aspirates typically show hyperplastic, normoblastic erythropoiesis, and granulopoiesis with increased numbers of megakaryocytes (Figs. 16.41 and 16.42). Trephine biopsies confirm the hyperplastic hematopoiesis, and clusters of megakaryocytes are often prominent (Figs. 16.43 and 16.44). In most patients, hematopoietic tissue makes up 90% or more of the intertrabecular space. Silver impregnation techniques often show some increase in reticulin fiber density, maximum WHO grade 1 (Fig. 16.45). The patients with gain-in-function mutations involving the exon 12 region of the *JAK2* gene tend to have isolated erythrocytosis, low serum erythropoietin levels, and bone marrows showing erythroid hyperplasia without abnormalities of granulopoiesis or megakaryocytes (Figs. 16.46 and 16.47). In the presence of the *JAK2* mutation, the traditional measurement of red cell mass is now only performed occasionally. *JAK2*-negative PV, which is extremely rare, must be differentiated from other causes of polycythemia (Table 16.6), for example, by identifying a low serum erythropoietin and abormal arterial oxygen saturation. In PV, circulating erythroid progenitors BFU-E and CFU-E are increased and grow in vitro independently of added erythropoietin. Relative polycythemia is excluded by blood volume studies.

Typically there is a median survival of 10–15 years. Transition to the accelerated phase with myelofibrosis occurs in about 30% of cases, and death from acute myeloid leukemia occurs in less than 10% of patients. The cytogenetics in the polycythemic phase are normal or show sole del20q, +8, +9, or other single abnormalities. Double and increasingly complex abnormalities are found more frequently in the myelofibrotic, accelerated, or blast phases (Fig. 16.82).

Primary Congenital Polycythemia

In this rare condition mutations in the genes coding for factors involved in the hypoxia-sensing pathway have been found to be associated with increased erythropoietin production (see Fig. 4.4). A homozygous mutation in the von Hippel–Lindau (*VHL*) gene is present in familial erythrocytosis found in the Chuvash population. In other isolated cases there have been mutations in the gene for the propyl hydroxlase domain-containing proteins (*PHD2*) or the hypoxia-inducible factor (*HIF2A*). Gene mutations in the erythropoietin receptor gene (*EPOR*) have been found in a few patients.

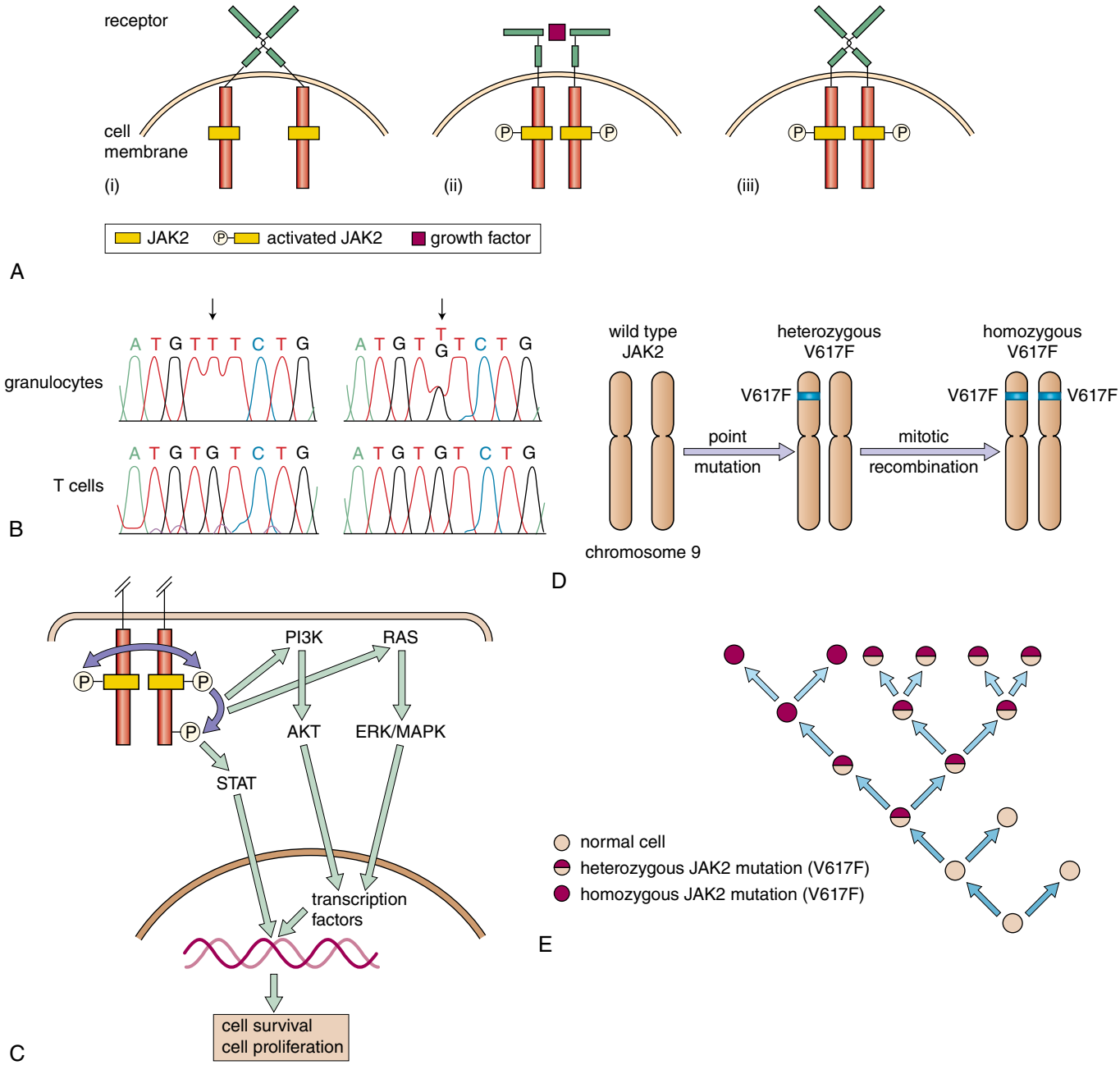

Fig. 16.32. The role of *JAK2* mutation in the myeloproliferative diseases. **A,** (i) Most hematopoietic growth factor receptors do not have intrinsic kinase activity but associate with a protein kinase such as *JAK2* in the cytoplasm. (ii) When the receptor binds a growth factor the cytoplasmic domains move closer together and the *JAK2* molecules can activate each other by phosphorylation. (iii) The V617F *JAK2* mutation allows the JAK protein to become activated even when no growth factor is bound. **B,** DNA sequencing shows homozygous G to T mutation in *JAK2* in granulocytes but not in T lymphocytes *(left)* and heterozygous mutation *(right)*. **C,** *JAK2* activation leads to cell survival and proliferation through activation of three major pathways: the STAT transcription factors, the PI3K pathway acting through *Akt*, and *Ras* activation, which subsequently activates ERK and MAPK. **D,** The development of homozygosity for the V617F mutation is a two-step process, with the initial point mutation followed by mitotic recombination of chromosome 9p between the *JAK2* locus and the centromere. (This results in loss of heterozygosity but a diploid DNA copy.) **E,** A model for the development of myeloproliferative disease following *JAK2* (V617F). This leads to a survival advantage of the neoplastic cells. Source: Kralovic R et al. *N Engl J Med* 2005;352:1779–1790. Reproduced with permission of Massachusetts Medical Society: *The New England Journal of Medicine*.

ESSENTIAL THROMBOCYTHEMIA

A diagnosis of ET is considered when a sustained rise in platelet count occurs, in some cases in excess of 1000×10^9/L, with no other underlying cause. WHO 2016 diagnostic criteria for ET are shown in Table 16.7, and the condition must be differentiated from other causes of a high platelet count (Table 16.8). There are usually abnormalities of platelet function, and in severe cases the clinical course may be dominated by recurrent hemorrhage and thrombosis. In many patients the raised platelet count is found on routine testing and there are no symptoms for many years, particularly in younger patients. In some patients this disorder is not easily distinguished from primary myelofibrosis and particularly PV.

The *JAK2* V617F mutation is found in 60–65% of patients, *CALR* exon 9 mutation in 20–25%, and *MPL* exon

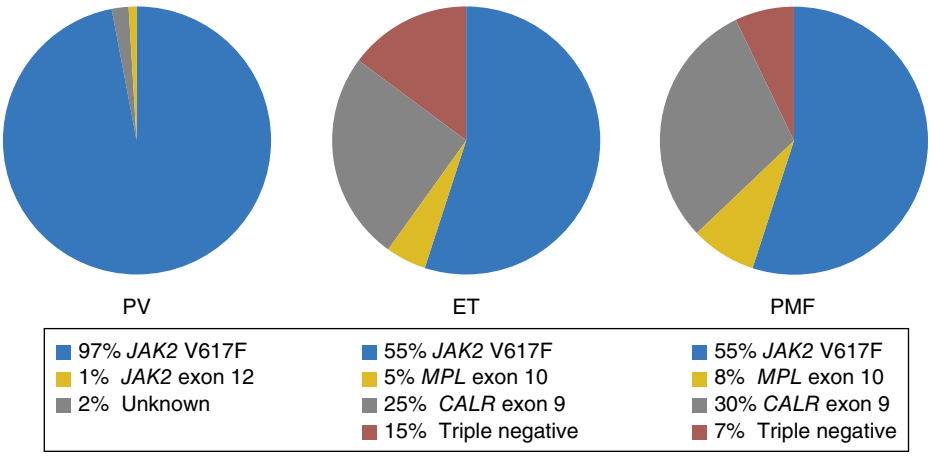

Fig. 16.33. Phenotype driver mutations in classic *BCR-ABL1*-negative myeloproliferative neoplasms. ET, essential thrombocythemia; PMF, primary myelofibrosis; PV, polycythemia vera. Source: Zoi K, Cross NCP. *J Clin Oncol* 2017;35(9):947–954. Reproduced with permission of *Journal of Clinical Oncology*: American Society of Clinical Oncology.

TABLE 16.5. WHO (2016): DIAGNOSTIC CRITERIA FOR POLYCYTHEMIA VERA

The diagnosis of polycythemia vera requires either all 3 major criteria or the first 2 major criteria plus the minor criterion[a]

Major criteria

1. Elevated hemoglobin concentration (>16.5 g/dL in men; >16.0 g/dL in women) or Elevated hematocrit (>49% in men; >48% in women) or Increased red blood cell mass (>25% above mean normal predicted value)
2. Bone marrow biopsy showing age-adjusted hypercellularity with trilineage growth (panmyelosis), including prominent erythroid, granulocytic, and megakaryocytic proliferation with pleomorphic, mature megakaryocytes (differences in size)
3. Presence of *JAK2* V617F or *JAK2* exon 12 mutation

Minor criterion

Subnormal serum erythropoietin level

[a] Major criterion 2 (bone marrow biopsy) may not be required in patients with sustained absolute erythrocytosis (hemoglobin concentrations of >18.5 g/dL in men or >16.5 g/dL in women and hematocrit values of >55.5% in men or >49.5% in women), if major criterion 3 and the minor criterion are present. However, initial myelofibrosis (present in as many as 20% of patients) can only be detected by bone marrow biopsy, and this finding may predict a more rapid progression to overt myelofibrosis (post-PV myelofibrosis).
Source: Adapted with permission Swerdlow SH, et al., eds. *WHO Classification of Tumours of Haematopoietic and Lymphoid Tissues*, revised 4th edn. International Agency for Research on Cancer, Lyon, 2017.

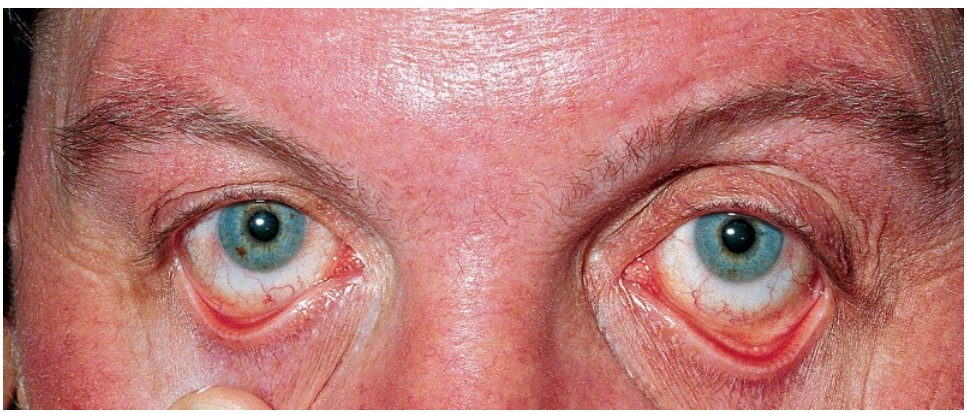

Fig. 16.34. Polycythemia vera: Facial plethora and conjunctival suffusion in a 40-year-old woman. (Hb, 19.5 g/dL.)

10 mutation in 5%. The clinical features and prognosis of the disease differ according to whether the underlying mutation is of *JAK2* or *CALR* (Table 16.9), the prognosis being more favorable for *CALR* mutation than *JAK2* mutation. About 5–10% of cases are triple negative and have a worse prognosis. Unlike PV, homozygosity for the mutation is not a feature. In some patients, the disease appears to have a polyclonal origin.

The dominant clinical problem is bleeding from the gastrointestinal tract and, less frequently, epistaxis, menorrhagia, hematuria, or hemoptysis. Spontaneous bruising often appears (Fig. 16.48), and cerebrovascular accidents may occur in elderly

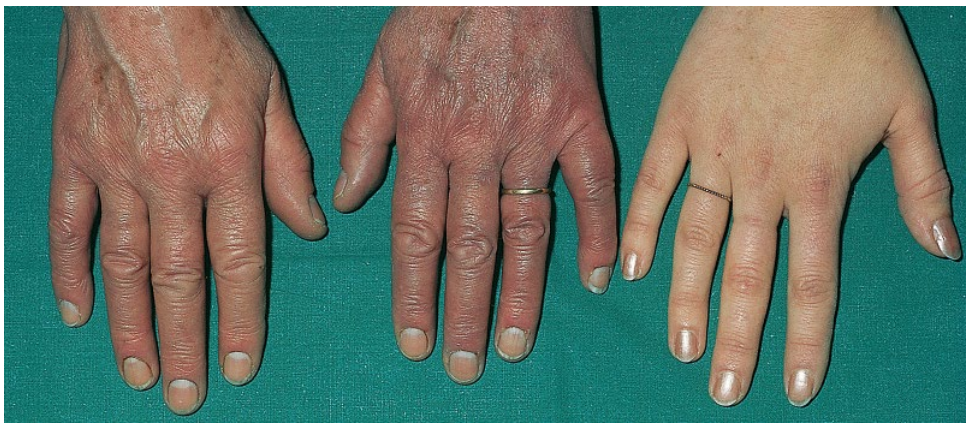

Fig. 16.35. Polycythemia vera: The hands of a 50-year-old woman *(on the left)* appear congested and plethoric. (Hb, 20 g/dL; WBC, 15 × 10^9/L; platelets, 490 × 10^9/L.) The hand on the *right* is of a healthy 35-year-old woman. (Hb, 14.5 g/dL.)

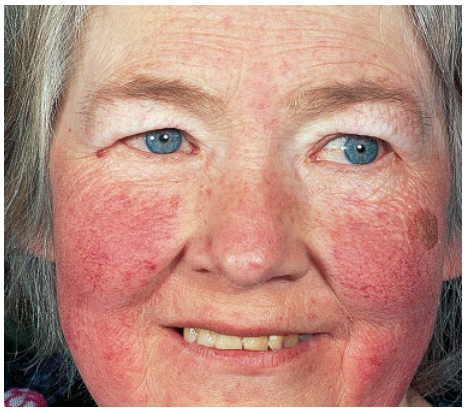

Fig. 16.36. Polycythemia vera: Acne rosacea in a middle-aged woman after treatment by venesection.

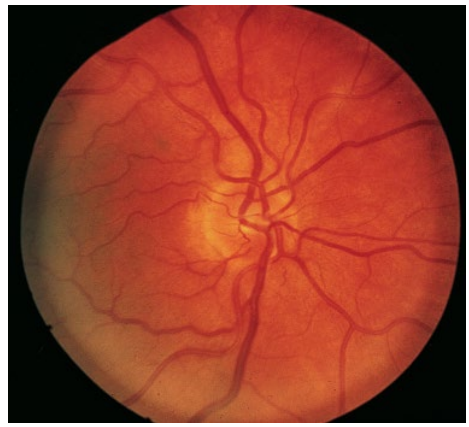

Fig. 16.38. Polycythemia vera: Same retina as shown in Fig. 16.37 following venesection. The vessels and disc have returned to normal, and the areas of hemorrhage have resolved. (Courtesy of Professor JC Parr.)

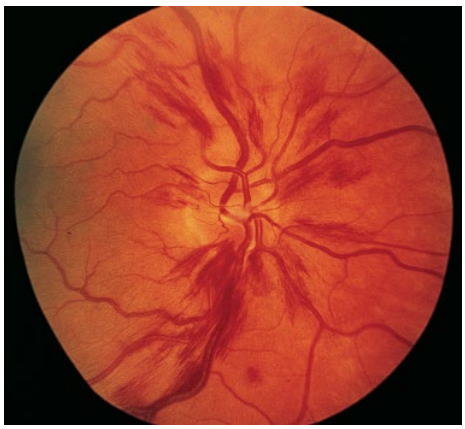

Fig. 16.37. Polycythemia vera: Gross distention of retinal vessels with conspicuous hemorrhage and mild swelling of the optic disc in hyperviscosity syndrome. The patient had headaches, lassitude, confusion, and blurred vision. (Hb, 23.5 g/dL; WBC, 35 × 10^9/L; platelets, 950 × 10^9/L.) (Courtesy of Professor JC Parr.)

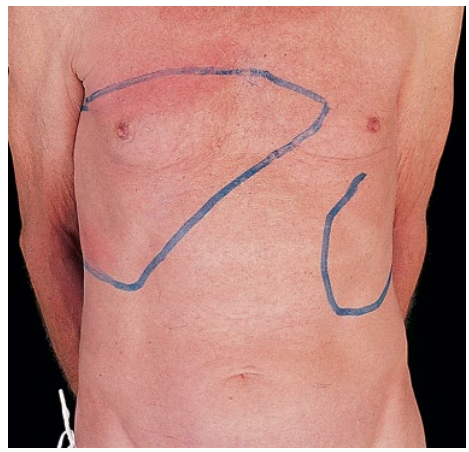

Fig. 16.39. Enlarged liver and spleen may be seen in polycythemia vera.

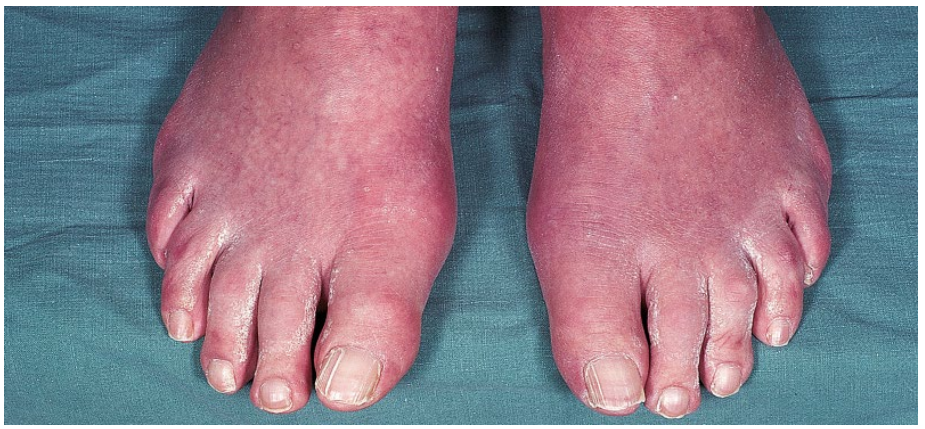

Fig. 16.40. Polycythemia vera: Acute gout with inflammation and swelling of the metatarsal and interphalangeal joints of the right great toe. The skin also shows a dusky plethora. (Hb, 21.5 g/dL; total RCV, 53 mL/kg; serum uric acid, 0.9 mmol/L.)

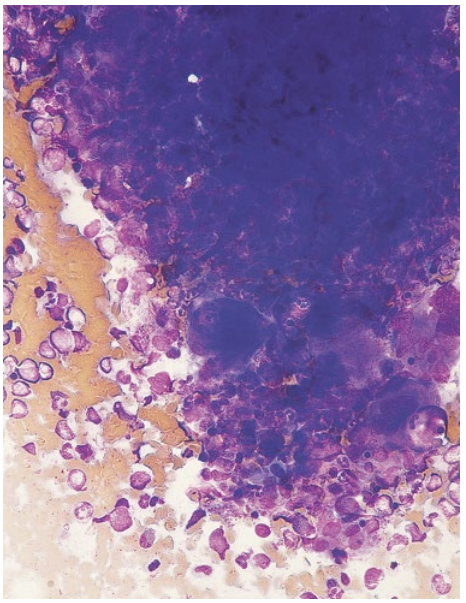

Fig. 16.41. Polycythemia vera: Bone marrow aspirate showing the edge of a hypercellular fragment. Marrow fat cells are absent.

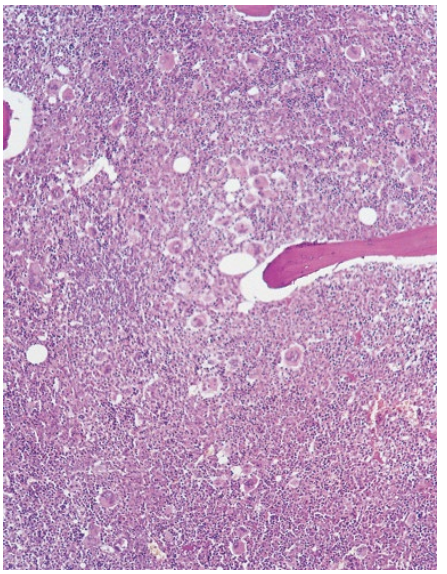

Fig. 16.43. Polycythemia vera: Trephine biopsy showing almost complete filling of the intertrabecular space with hyperplastic hematopoietic tissue.

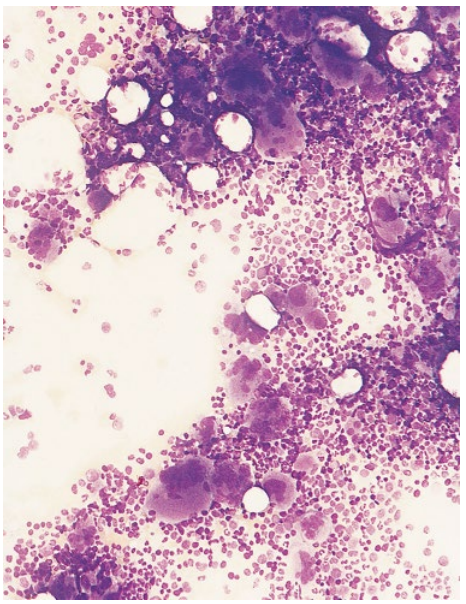

Fig. 16.42. Polycythemia vera: Bone marrow aspirate with hypercellular cell trails and bone marrow fragments but incomplete replacement of marrow fat spaces. Megakaryocytes are especially prominent in the cell trails.

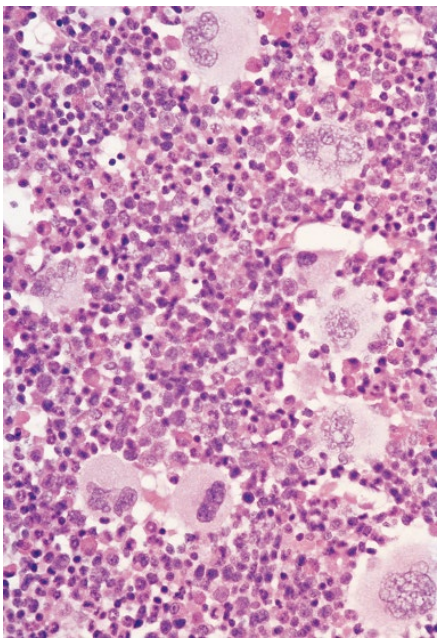

Fig. 16.44. Polycythemia vera: Higher power view of Fig. 16.43 showing hyperplasia of erythropoiesis, granulopoiesis, and megakaryocytes.

patients. Blockage of peripheral blood vessels may result in erythromelalgia (Fig. 16.49), ischemia, and gangrene (Fig. 16.50).

The peripheral blood film shows a distinctive increase in platelet count, and the platelets are often of abnormal morphology with many giant forms (Fig. 16.51). Howell–Jolly bodies and other stigmata of splenic atrophy are found in a third of severe cases, and careful search may reveal the presence of megakaryocyte fragments (Figs. 16.52–16.54).

Splenic atrophy (Fig. 16.55) often increases the severity of platelet elevation in the peripheral blood as obliteration of the splenic red pulp areas, in which platelet pooling normally occurs, results in the entire marrow platelet production being accommodated in the general circulation.

Aspiration of bone marrow may be difficult. There is usually a general hyperplasia of hematopoietic cells with a striking increase in the number of megakaryocytes (Fig. 16.56), which

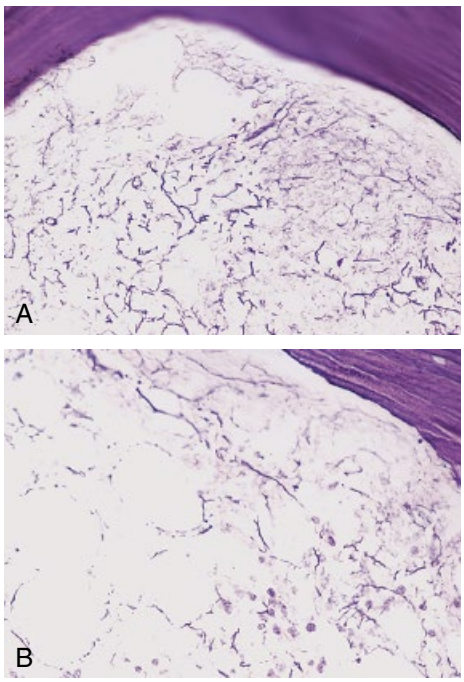

Fig. 16.45. Polycythemia vera: **A,** Silver impregnation staining shows a moderate increase in the density of reticulin fibers (WHO 2016 grade 1) compared with normal. **B,** Normal bone marrow.

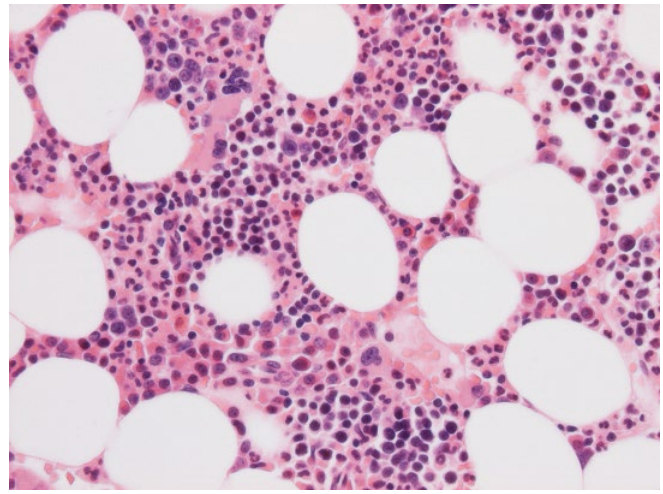

Fig. 16.46. Polycythemia (idiopathic erythrocytosis) with *JAK2* exon 12 mutation. Trephine biopsy in a patient with K539L *JAK2* mutation. There is only mild hypercellularity and isolated erythroid hyperplasia. Megakaryocytes show normal morphology and no clustering. (Courtesy of Dr. Wendy Erber.)

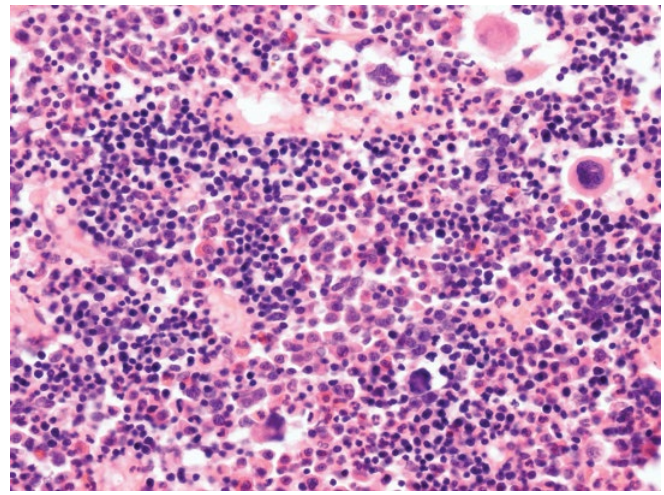

Fig. 16.47. Polycythemia (idiopathic erythropoiesis) with *JAK2* exon 12 mutation. Trephine biopsy in a patient with 12del 542,543 *JAK2* mutation. There is marked hypercellularity with dominant erythropoiesis and normal megakaryocytes. (Courtesy of Dr. Wendy Erber.)

TABLE 16.6. CAUSES OF POLYCYTHEMIA

Primary (increased RCV)	Secondary (increased RCV)	Relative (normal RCV)
Polycythemia vera Familial (congenital)	As a result of compensatory erythropoietin increase in: high altitudes heavy smoking cardiovascular disease pulmonary disease and alveolar hypoventilation increased affinity hemoglobins (familial polycythemia) methemoglobinemia (rarely)	"Stress" or "spurious" polycythemia Dehydration: water deprivation vomiting diuretic therapy
	As a result of inappropriate erythropoietin increase in: renal disease–hydronephrosis, vascular impairment, cysts, carcinoma massive uterine fibromyomata hepatocellular carcinoma cerebellar hemangioblastoma	Plasma loss: burns enteropathy

RCV, Red cell volume.

TABLE 16.7. WHO (2016): DIAGNOSTIC CRITERIA FOR ESSENTIAL THROMBOCYTHEMIA

The diagnosis of essential thrombocythemia requires that either all major criteria or the first 3 major criteria plus the minor criterion are met

Major criteria

1. Platelet count ≥450 × 10^9/L
2. Bone marrow biopsy showing proliferation mainly of the megakaryocytic lineage, with increased numbers of enlarged, mature megakaryocytes with hyperlobulated nuclei; no significant increase or left shift in neutrophil granulopoiesis or erythropoiesis; very rarely a minor (grade 1a) increase in reticulin fibers
3. WHO criteria for *BCR-ABL1*+ chronic myeloid leukemia, polycythemia vera, primary myelofibrosis, or other myeloid neoplasms are not met
4. *JAK2*, *CALR*, or *MPL* mutation

Minor criterion

Presence of a clonal marker or

Absence of evidence or reactive thrombocytosis

Source: Adapted with permission from Swerdlow SH, et al., eds. *WHO Classification of Tumours of Haematopoietic and Lymphoid Tissues*, revised 4th edn. International Agency for Research on Cancer, Lyon, 2017.

TABLE 16.8. CAUSES OF A HIGH PLATELET COUNT

Reactive	Endogenous
Hemorrhage	Essential thrombocythemia
Trauma	Some cases of polycythemia vera, myelofibrosis, and chronic myeloid leukemia
Postoperative	
Chronic iron deficiency	
Malignancy	
Chronic infections	
Connective tissue diseases	
Postsplenectomy with continuing anemia and active marrow	

TABLE 16.9. COMPARISON OF THE CLINICAL AND LABORATORY FEATURES OF *JAK2* AND *CALR* MUTATED ESSENTIAL THROMBOCYTHEMIA

	***JAK2* mutated**	***CALR* mutated**
Age	Older	Younger
Hemoglobin	Higher	Lower
White cell count	Higher	Lower
Platelet count	Lower	Higher
Serum erythropoietin	Lower	Higher
Thrombosis risk	Higher	Lower
Transformation to polycythemia (rubra) vera	Yes	No
Risk of transformation to myelofibrosis	Equal	Equal
Approximate survival	9 years	17 years

Source: Hoffbrand AV, Moss PAH. *Hoffbrand's Essential Haematology*, 7th edn. John Wiley & Sons, 2016. Reproduced with permission of John Wiley & Sons.

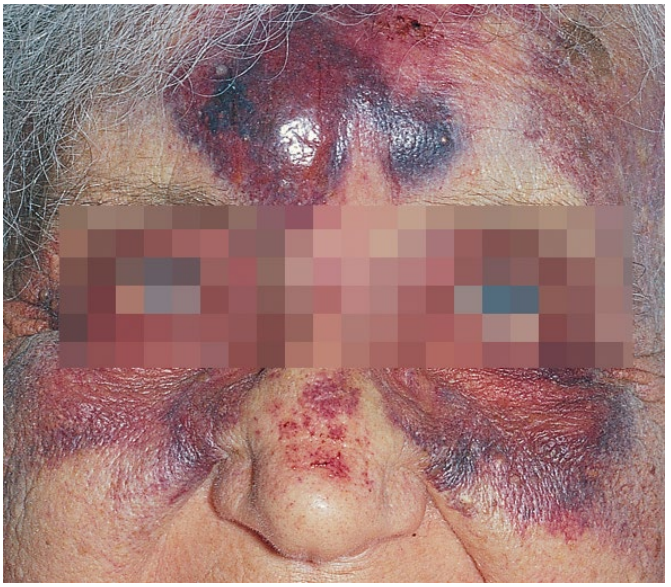

Fig. 16.48. Essential thrombocythemia: Hemorrhage into subcutaneous tissues following minor trauma. Gross defects of platelet aggregation with adenosine diphosphate, adrenaline, and thrombin were found. (Platelets, 2300 × 10^9/L.)

are often found in cohesive clusters (Fig. 16.57). The megakaryocytes tend to show many nuclear lobes and their average cell volume is above normal (Figs. 16.58 and 16.59). In many patients the dominant feature is masses of adherent platelets that may be confused with marrow fragments (Fig. 16.60). Trephine biopsy preparations reflect the dramatic increase in the megakaryocyte population; large numbers of abnormal megakaryocytes are seen at all stages of development (Figs. 16.61–16.63). Silver impregnation techniques demonstrate an increase in reticulin patterns intermediate between those of PV and myelofibrosis.

PRIMARY MYELOFIBROSIS

In primary myelofibrosis (PMF)—a myeloproliferative disease that was also known as myelosclerosis, agnogenic myeloid metaplasia, or idiopathic myelofibrosis—the hematopoietic cell proliferation is more generalized, with splenic and hepatic involvement. There is often extension of hematopoietic marrow from central skeletal sites into the long bones of the leg and arm. WHO 2016 divides PMF into an early, prefibrotic stage (pre-PMF) (Table 16.10A) and overt PMF (Table 16.10B). Pre-PMF occurs on average in younger patients than overt PMF, has a shorter overall survival than ET (but still with a median similar to that of PV of >10 years), and has a greater female proportion than overt PMF (Table 16.11). The severity of anemia, neutropenia, or thrombocytopenia is less and spleen size smaller than in overt PMF. The blast count is higher in overt PMF. PMF must be differentiated from causes of reactive marrow fibrosis (Table 16.12).

PMF is related closely to PV, and over 30% of patients have a previous history of that disease. In overt PMF, the associated increase in marrow fiber production is marked and the effectiveness of hematopoiesis is decreased.

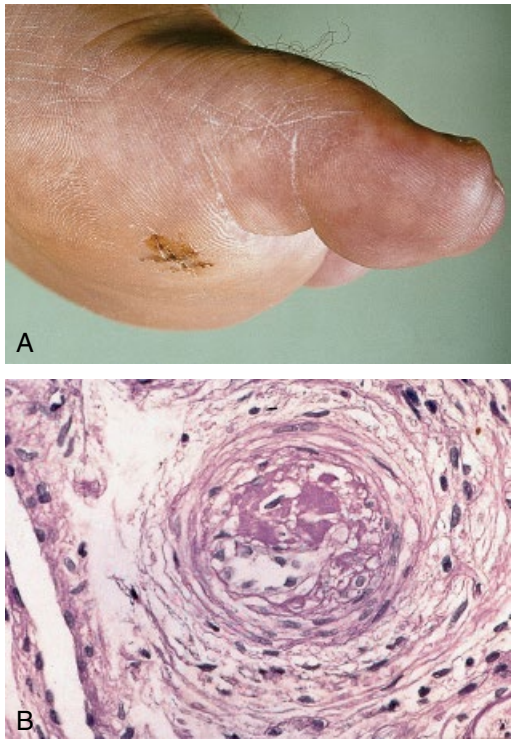

Fig. 16.49. Essential thrombocythemia: Erythromelalgia. **A,** Severe burning pain and hot, red congestion of the forefoot and toes in a 39-year-old man. (Platelet count, 875×10^9/L.) **B,** Section of a skin biopsy showing thrombotic occlusion of an arteriole with proliferative changes in the peripheral wall. (Courtesy of Professor JJ Michiels.)

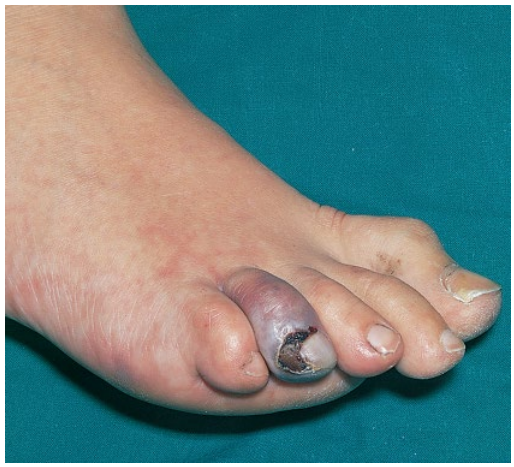

Fig. 16.50. Essential thrombocythemia: Gangrene of the right fourth toe. (Platelets, 1900×10^9/L.)

The V617F *JAK2* mutation is present in over 50% of patients. In *JAK2*-negative patients other mutations may be responsible for the myeloproliferation. Mutation of *CALR* exon 9 occurs in 20–25%; an activating mutation in exon 10 of the thrombopoietic receptor *(MPL)* gene is found in 5% (see Fig. 16.33). Triple negative PMF has a worse prognosis than PMF with one or other of these three driver mutations. The different types of driver mutations (of *JAK2*, *CALR*, and *MPL*) are similar in the two groups of pre- and overt PMF. In contrast, the incidence of high molecular risk nondriver gene mutations (e.g. of *ASXL1*, *SRSF2 IDH1/2*, *EZH2*) is higher in the overt PMF group

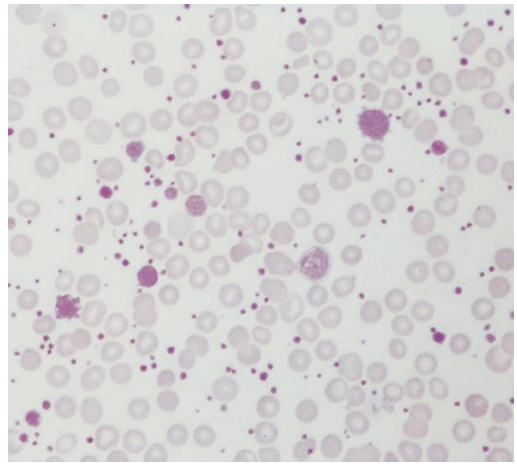

Fig. 16.51. Essential thrombocythemia: Peripheral blood film showing a gross increase in platelet numbers.

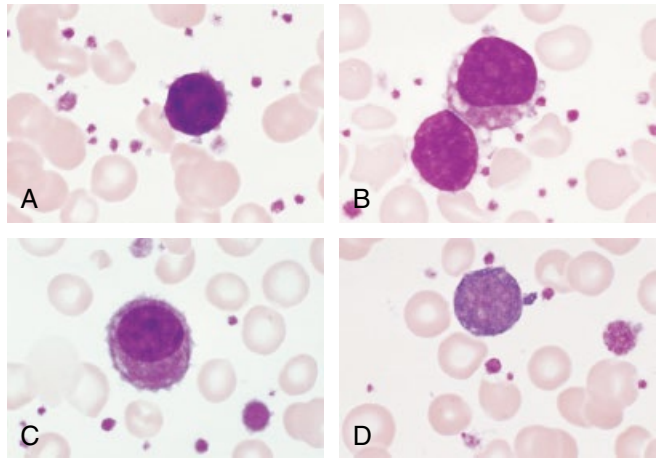

Fig. 16.52. Essential thrombocythemia. **A–D,** Peripheral blood films showing circulating megakaryocyte fragments.

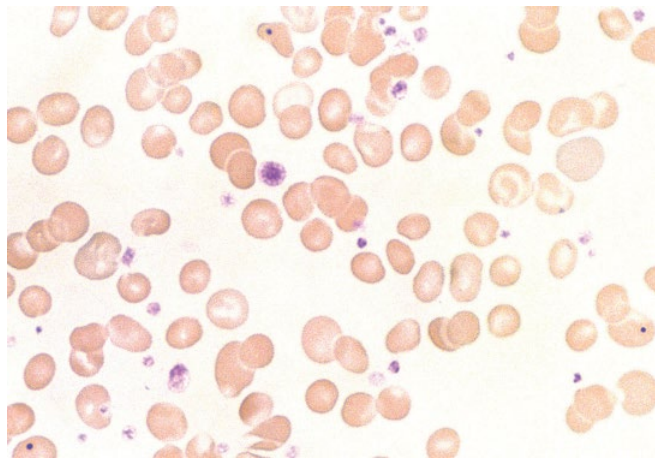

Fig. 16.53. Essential thrombocythemia: Blood film showing features of splenic atrophy. The red cells show anisocytosis and mild polychromasia and three contain Howell–Jolly bodies. There is an increase in both platelet number and size.

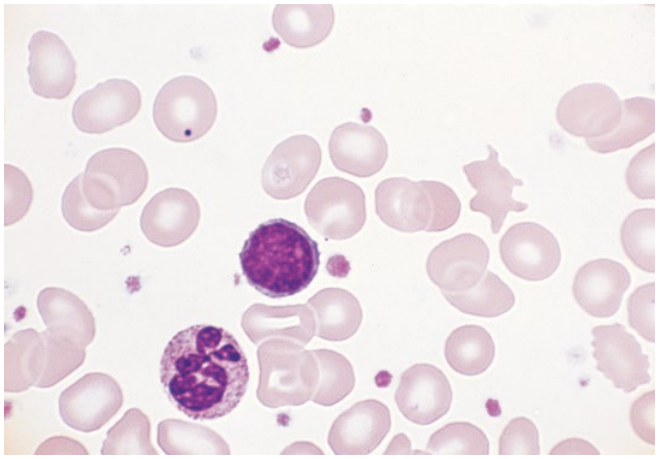

Fig. 16.54. Essential thrombocythemia: Peripheral blood film at high magnification showing features of splenic atrophy, including a Howell–Jolly body, red cell targeting, crenation, and acanthocytosis.

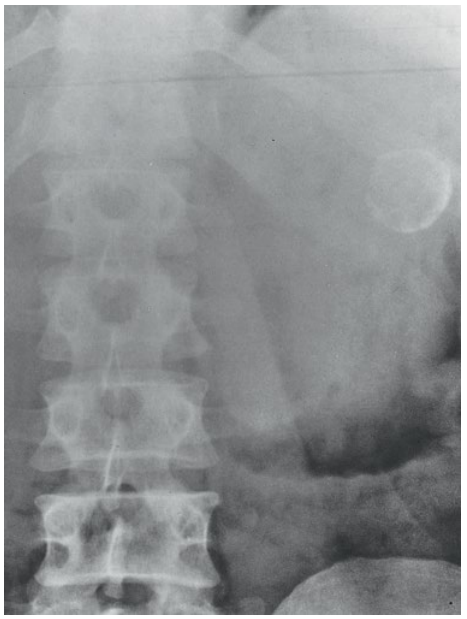

Fig. 16.55. Essential thrombocythemia: Abdominal radiograph showing a small spherical calcified mass (at *upper right*). The blood film showed features of splenic atrophy. At autopsy the fibrotic remnant of spleen weighed only 30 g and had extensive areas of dystrophic calcification.

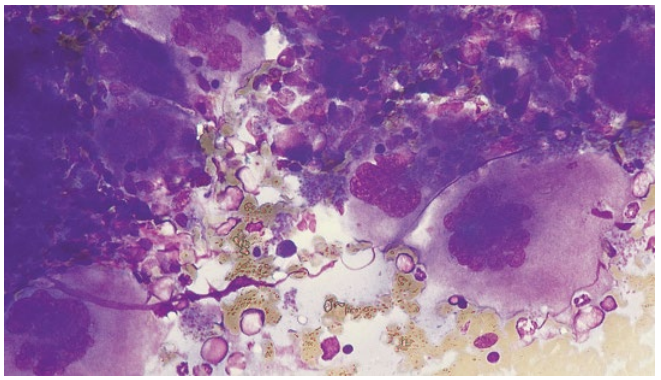

Fig. 16.56. Essential thrombocythemia: Bone marrow aspirate fragment showing a marked increase in the number of megakaryocytes.

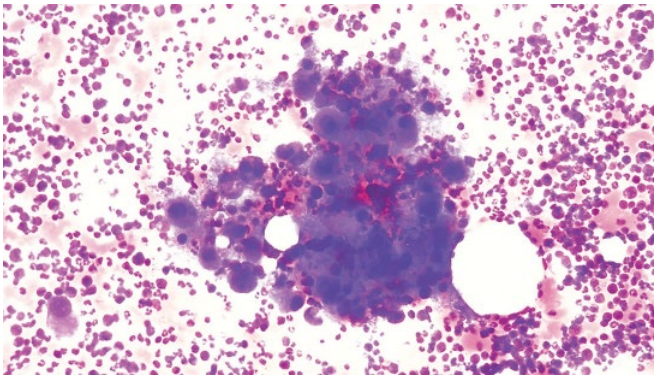

Fig. 16.57. Essential thrombocythemia: Bone marrow aspirate cell trail showing a prominent cluster of megakaryocytes.

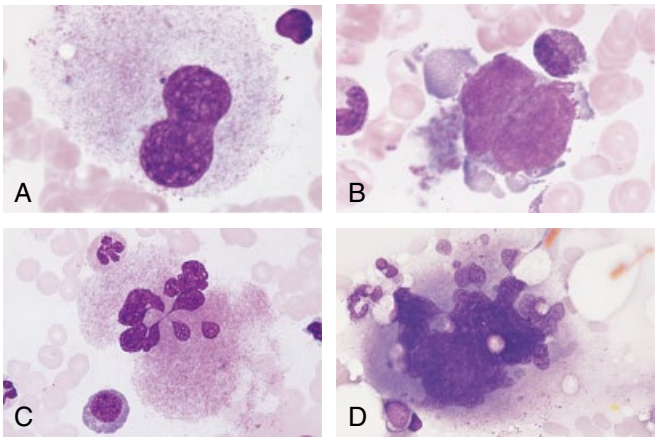

Fig. 16.58. Essential thrombocythemia: Bone marrow aspirates. **A,** Binucleate megakaryocyte. **B,** Binucleate megakaryoblast with cytoplasmic differentiation. **C,** Relatively low nuclear ploidy in hypersegmented megakaryocytes. **D,** Relatively high nuclear ploidy in hypersegmented megakaryocytes.

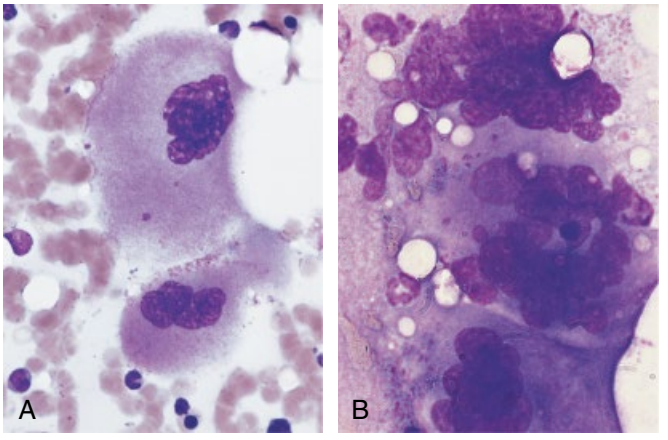

Fig. 16.59. Essential thrombocythemia: Bone marrow aspirates. **A,** Clumping of megakaryocytes with definite cell borders. **B,** Lack of cytoplasmic separation.

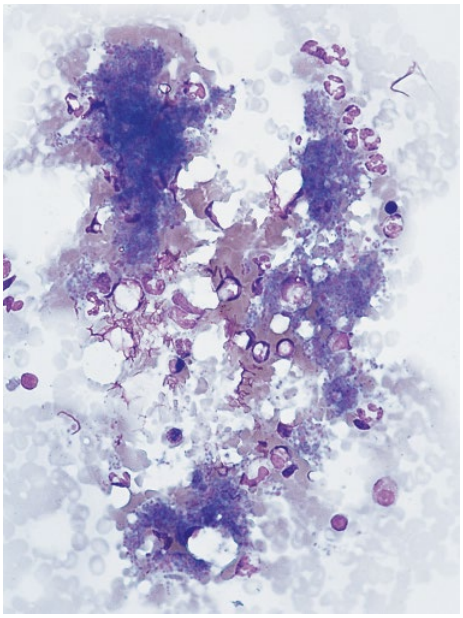

Fig. 16.60. Essential thrombocythemia: Bone marrow aspirate cell trail showing large masses of aggregated platelets.

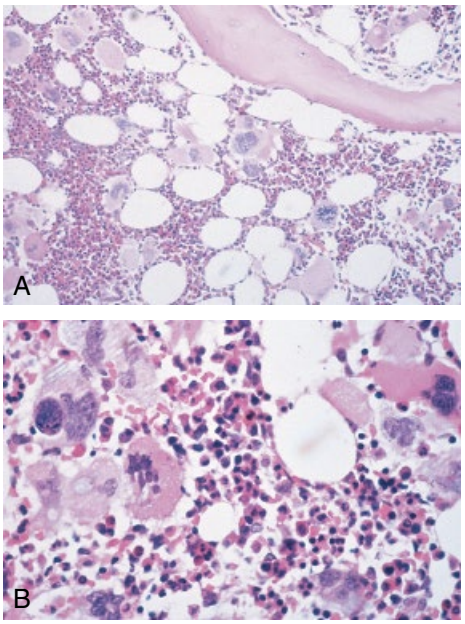

Fig. 16.61. Essential thrombocythemia. **A,** Trephine biopsy shows that the overall cellularity of hematopoietic tissue is not greatly increased. **B,** Also shows large numbers of megakaryocytes, seen particularly well at higher magnification.

(see Table 16.11). The prognosis in both pre-PMF and overt PMF is related to the patterns of driver and nondriver mutations.

PMF is indistinguishable from myelofibrosis secondary to PV or ET and the diagnostic criteria for these conditions are the same. Some patients diagnosed with PMF are probably in the accelerated phase of previously undiagnosed PV or ET. The fibrosis, angiogenesis, and new bone formation in PMF are the result of a polyclonal response to cytokines and growth factors (e.g. transforming growth factor β [TGF-β], basic fibroblast growth factor [bFGF], and vascular endothelial growth factor [VEGF]) produced by megakaryocytes and monocytes from the myeloproliferative clone.

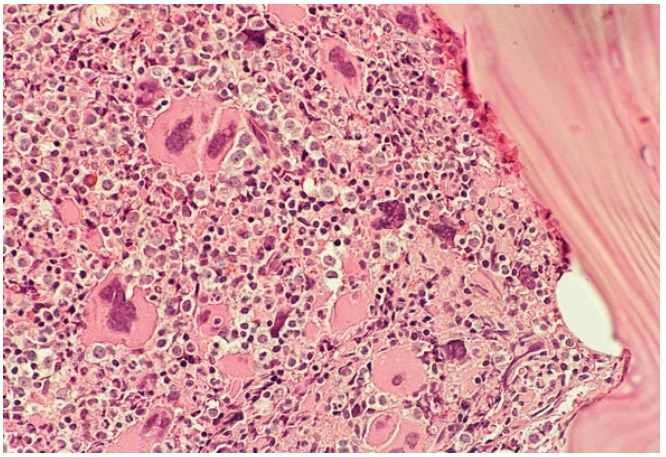

Fig. 16.62. Essential thrombocythemia: Trephine biopsy showing a marked increase in cellularity, with prominent megakaryocytes.

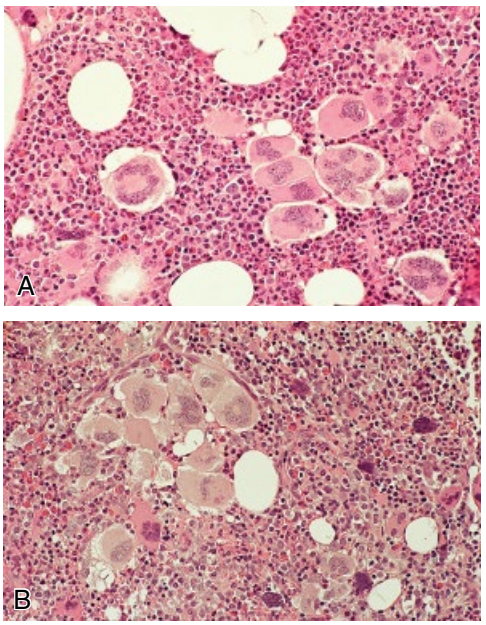

Fig. 16.63. Essential thrombocythemia: Trephine biopsy. In two different patients **(A** and **B)** there is clustering of large megakaryocytes of high nuclear ploidy.

PMF usually occurs in middle-aged and elderly patients. Most patients initially have symptoms caused by anemia, splenic enlargement (Fig. 16.64), or hypermetabolism, such as night sweats, anorexia, and weight loss. Some may complain of bone pain and gout (Fig. 16.65).

MRI imaging (Fig. 16.66) is able to provide evidence of the expansion of skeletal myeloproliferative activity. A minority of cases show generalized osteosclerosis (Fig. 16.67).

As a result of a hyperkinetic portal circulation, in some long-standing cases, the patient develops portal hypertension and may have bleeding esophageal varices or ascites (Figs. 16.68).

Most patients with PMF have a normochromic anemia of moderate or marked severity. It may be macrocytic in those who are folate deficient or microcytic with associated iron deficiency. The peripheral blood usually shows florid leukoerythroblastic change, and the number of nucleated red cells often exceeds the number of leukocytes. Marked polychromasia, anisocytosis, and poikilocytosis with "teardrop" red cells are typical changes

TABLE 16.10A. WHO (2016): DIAGNOSTIC CRITERIA FOR PREFIBROTIC/EARLY PRIMARY MYELOFIBROSIS (Pre-PMF)

The diagnosis of prefibrotic/early primary myelofibrosis requires that all 3 major criteria and at least 1 minor criterion are met

Major criteria

1. Megakaryocytic proliferation and atypia, without reticulin fibrosis grade >1, accompanied by increased age-adjusted bone marrow cellularity, granulocytic proliferation, and (often) decreased erythropoiesis
2. WHO criteria for *BCR-ABL1*+ chronic myeloid leukemia, polycythemia vera, essential thrombocythemia, myelodysplastic syndromes, or other myeloid neoplasms are not met
3. *JAK2*, *CALR*, or *MPL* mutation or
   Presence of another clonal marker[a] or
   Absence of minor reactive bone marrow reticulin fibrosis[b]

Minor criteria

Presence of at least 1 of the following, confirmed in two consecutive determinations:
Anemia not attributed to a comorbid condition
Leukocytosis ≥11 × 10^9/L
Palpable splenomegaly
Lactate dehydrogenase level above the upper limit of the institutional reference range

[a] In the absence of any of the three major clonal mutations, a search for other mutations associated with myeloid neoplasms (e.g. *ASXL1*, *EZH2*, *TET2*, *IDH1*, *IDH2*, *SRSF2*, and *SF3B1* mutations) may be of help in determining the clonal nature of the disease.
[b] Minor (grade 1) reticulin fibrosis secondary to infection, autoimmune disorder or other chronic inflammatory conditions, hairy cell leukemia or another lymphoid neoplasm, metastatic malignancy, or toxic (chronic) myelopathies.
Source: Adapted with permission Swerdlow SH, et al., eds. *WHO Classification of Tumours of Haematopoietic and Lymphoid Tissues*, revised 4th edn. International Agency for Research on Cancer, Lyon, 2017.

TABLE 16.10B. WHO (2016): DIAGNOSTIC CRITERIA FOR OVERT PRIMARY MYELOFIBROSIS

The diagnosis of overt primary myelofibrosis requires that all 3 major criteria and at least 1 minor criterion are met

Major criteria

1. Megakaryocytic proliferation and atypia, accompanied by reticulin and/or collagen fibrosis grades 2 or 3
2. WHO criteria for essential thrombocythemia, polycythemia vera, *BCR1-ABL1*–positive chronic myeloid leukemia, myelodysplastic syndrome, or other myeloid neoplasms[a] are not met
3. *JAK2*, *CALR*, or *MPL* mutation or
   Presence of another clonal marker[b] or
   Absence of reactive myelofibrosis[c]

Minor criteria

Presence of at least 1 of the following, confirmed in two consecutive determinations:
Anemia not attributed to a comorbid condition
Leukocytosis ≥11 × 109/L
Palpable splenomegaly
Lactate dehydrogenase level above the upper limit of the institutional reference range
Leukoerythroblastosis

[a] Myeloproliferative neoplasms can be associated with monocytosis or they can develop it during the course of the disease; these cases may mimic chronic myelomonocytic leukemia (CMML); in these rare instances, a history of MPN excludes CMML, whereas the presence of MPN features in the bone marrow and/or MPN-associated mutations (in *JAK2*, *CALR*, or *MPL*) tend to support the diagnosis of MPN with monocytosis rather than CMML.
[b] In the absence of any of the three major clonal mutations, a search for other mutations associated with myeloid neoplasms (e.g. *ASXL1*, *EZH2*, *TET2*, *IDH1*, *IDH2*, *SRSF2*, and *SF3B1* mutations) may be of help in determining the clonal nature of the disease.
[c] Bone marrow fibrosis secondary to infection, autoimmune disorder or another chronic inflammatory condition, hairy cell leukemia or another lymphoid neoplasm, metastatic malignancy, or toxic (chronic) myelopathy.
Source: Adapted with permission from Swerdlow SH, et al., eds. *WHO Classification of Tumours of Haematopoietic and Lymphoid Tissues*, revised 4th edn. International Agency for Research on Cancer, Lyon, 2017.

TABLE 16.11. COMPARISON OF CLINICAL FEATURES OF PRE(EARLY)-PMF AND OVERT PMF

	Early PMF	Overt PMF
Age	Younger	Older
Sex	Females > males	Females = males
Spleen	Smaller	Larger
Cytopenias	Absent or mild	Mild or severe
Circulating blasts	Fewer	More
Driver mutations	Similar incidence of *JAK2*, *CALR*, *MPL* mutations	
Additional mutations	Greater incidence of mutations of *ASXL1*, *SRSF2*, *IDH1/2*, *EZH2* in overt PMF	
Median survival	>10 years	<10 years

TABLE 16.12. CAUSES OF MARROW FIBROSIS

Primary myelofibrosis

Infections: tuberculosis (see Chapter 30); osteomyelitis (focal fibrosis)

Malignant lymphoma, including Hodgkin lymphoma (see Chapters 19, 20, 22, 23)

Occasionally, chronic myeloid leukemia and other leukemias, especially AML M7 (see Chapter 13)

Metastatic carcinoma, especially breast and prostate (see Chapter 30)

Excess irradiation

Benzene poisoning

Excess fluorine

Paget disease (focal fibrosis; see Chapter 30)

Osteopetrosis (see Chapter 30)

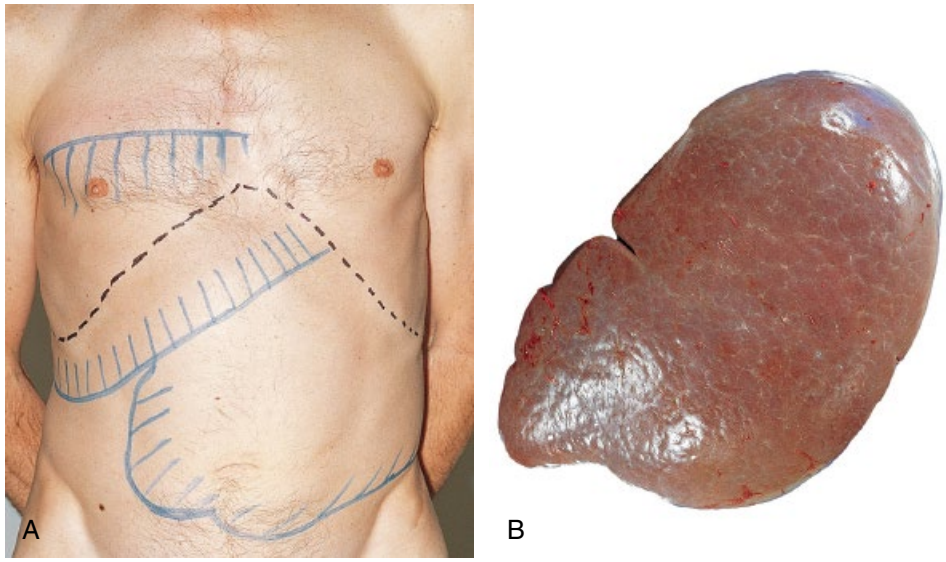

Fig. 16.64. Primary myelofibrosis. **A,** Splenohepatomegaly. **B,** The patient's spleen shows a well-defined notch in the superior border. The prominent indent in the inferior border was palpable during clinical examination.

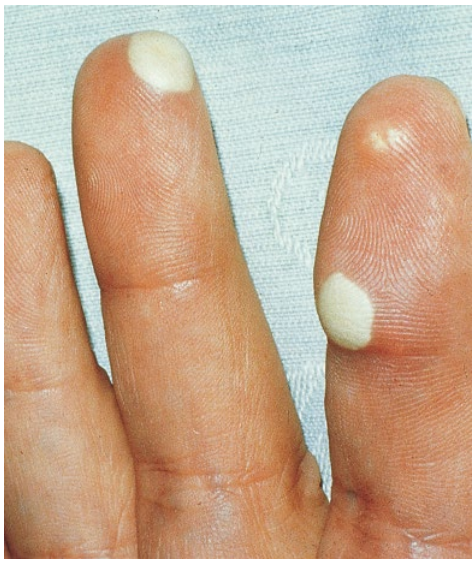

Fig. 16.65. Primary myelofibrosis: Gouty tophi on the index and middle fingers of a 55-year-old man.

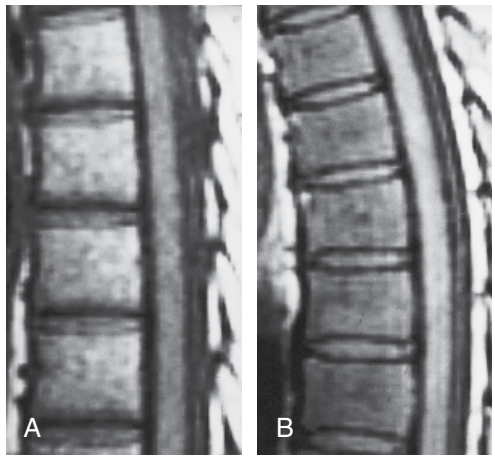

Fig. 16.66. Magnetic resonance imaging: T_1 sequence. Dorsal vertebrae in essential thrombocythemia **(A)** and primary myelofibrosis **(B)**. By comparison with the spinal cord, it can be seen that in **A** the vertebral signal is not decreased, whereas in **B** there is a marked decrease. (Courtesy of Professor C Rozman.)

(Fig. 16.69). In occasional patients with extensive osteosclerosis, the blood film shows marked leukoerythroblastic change with circulating megakaryocyte fragments (Fig. 16.70). Occasionally these fragments dominate the blood film (Fig. 16.71).

Attempts at bone marrow aspiration are usually unsuccessful, but trephine biopsy reveals a variable degree of hematopoietic cell activity and marrow fibrosis (Figs. 16.72–16.75). Silver impregnation techniques show an increase in reticulin fiber density and thickness (Fig. 16.76). Only in advanced disease is there collagen deposition and, in 10% of cases, osteosclerosis (Figs. 16.77 and 16.78). The severity of marrow fibrosis is graded on a scale of 0 to 3 by WHO, 2016 (Fig. 16.79). Extramedullary hematopoiesis may be confirmed from a liver biopsy or after splenectomy (Figs. 16.80 and 16.81).

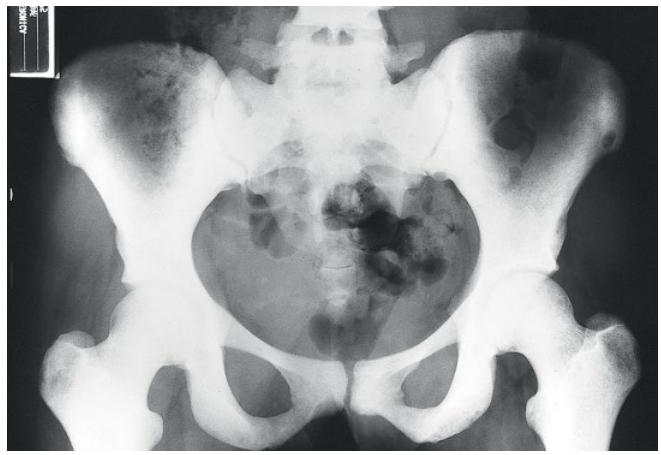

Fig. 16.67. Primary myelofibrosis: Pelvic radiograph showing a generalized increase in bone density from osteosclerosis.

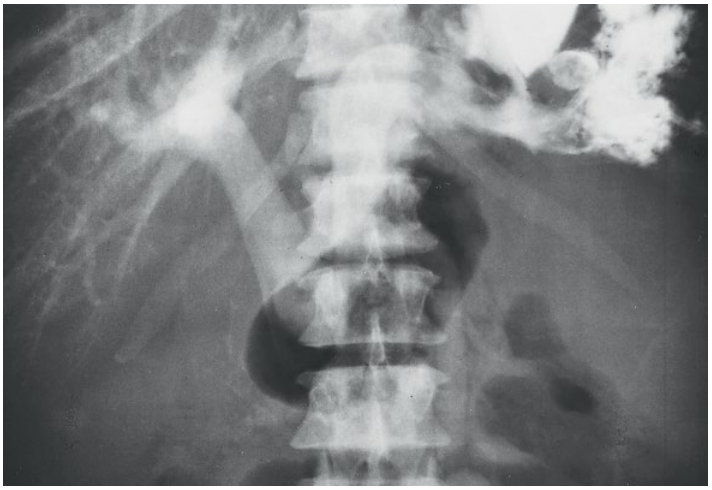

Fig. 16.68. Primary myelofibrosis: Transsplenic portal venogram showing gross dilation of the splenic, inferior mesenteric, and portal veins and increased bone density in the vertebral bodies. A great increase in splenic blood flow results in a hyperkinetic portal circulation, which, together with the obstructive effects of extramedullary hematopoiesis, may be important in the pathogenesis of portal hypertension.

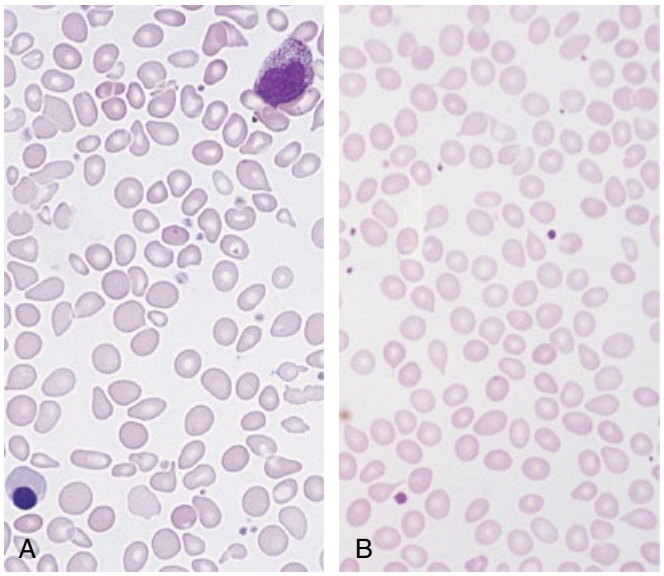

Fig. 16.69. Primary myelofibrosis: Peripheral blood films. **A,** Leukoerythroblastic changes with red cell polychromasia, anisocytosis, and poikilocytosis, including "teardrop" forms (the nucleated cells are an erythroblast and a late myelocyte). **B,** Red cell anisocytosis and poikilocytosis with "teardrop" forms in early disease.

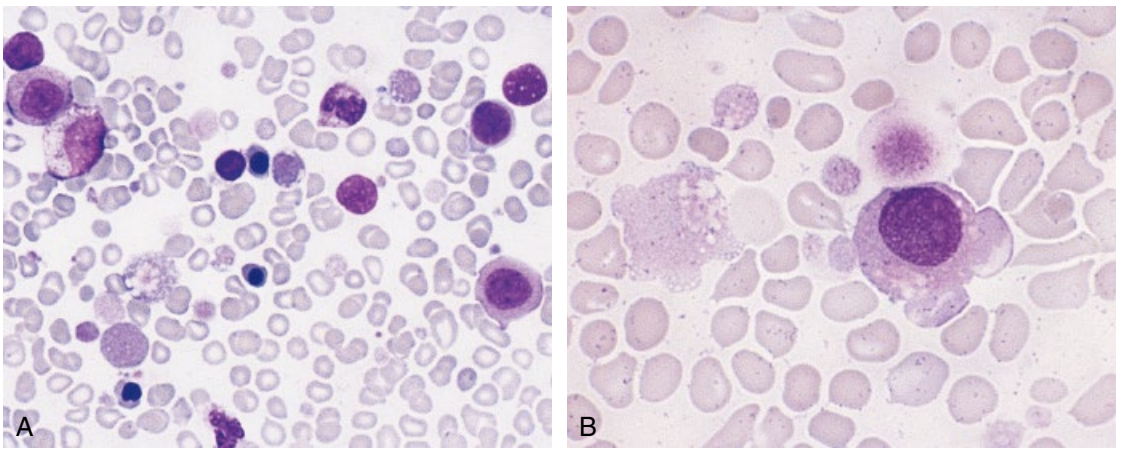

Fig. 16.70. Primary myelofibrosis/osteomyelofibrosis: Peripheral blood films. **A,** Myelocytes, erythroblasts, and megakaryocyte fragments. **B,** Megakaryocyte fragments at higher magnification.

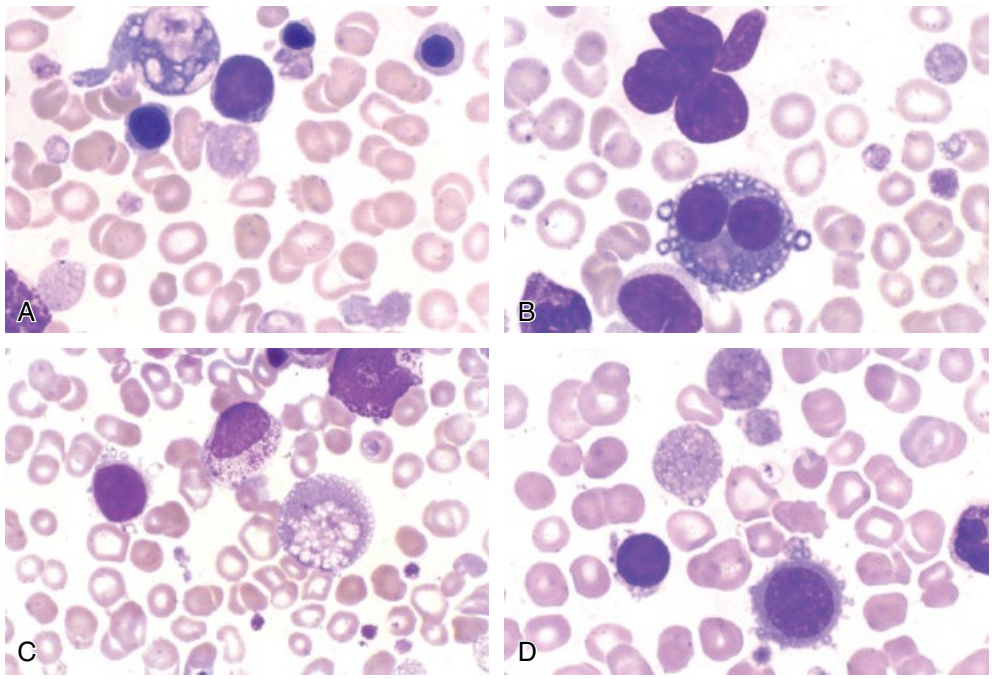

Fig. 16.71. Primary myelofibrosis: Blood film showing bizarre giant platelets and megakaryocyte fragments.

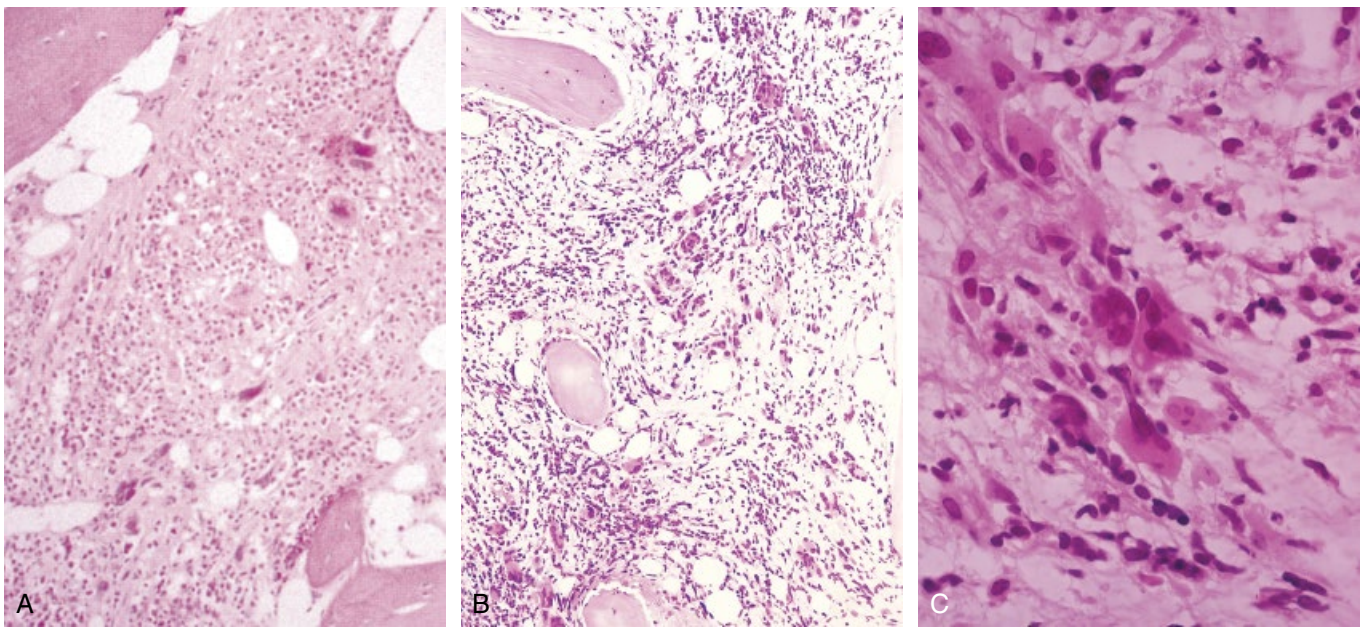

Fig. 16.72. Primary myelofibrosis: **A, B,** Trephine biopsies showing most of the intertrabecular space occupied by cellular loose connective tissue contains scattered hematopoietic cells, including prominent megakaryocytes, fat cells making up less than 15% of the intertrabecular space, and extensive deposition of loose connective tissue around hematopoietic cells. **C,** The prominence of megakaryocytes in the myelofibrotic tissue at higher magnification.

LEUKEMIC TRANSFORMATION OF POLYCYTHEMIA VERA AND MYELOFIBROSIS

It is generally accepted that transformation is part of the natural history of the myeloproliferative syndromes and probably reflects the acquisition of further mutations (Fig. 16.82). Transition to myelofibrosis from PV occurs in approximately 30% of cases and to acute leukemia in less than 10%. The latter is usually acute myeloid leukemia (AML), but the occurrence of ALL has been described.

The incidence of leukemia was similar in those treated with either radioactive phosphorus or alkylating agents. Hydroxyurea is now used in preference to either because it is considered not to predispose to leukemic transformation. Of patients with primary myelofibrosis, 10% develop a terminal leukemia (Figs. 16.82–16.85). New mutations underlie the transitions from PV and ET to myelofibrosis and from myelofibrosis to

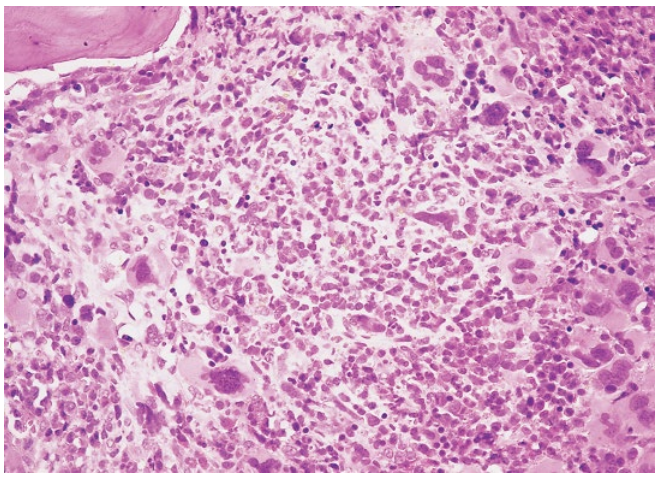

Fig. 16.73. Transitional or accelerated phase myeloproliferative disease: Trephine biopsy showing complete filling of intertrabecular space by hyperplastic hematopoietic tissue with large numbers of megakaryocytes and increased stromal connective tissue between hematopoietic cells. This patient has clinical features of both polycythemia vera and myelofibrosis. The blood film showed leukoerythroblastic features and splenic enlargement extending 20 cm below the left costal margin. (Hb, 18.5 g/dL; WBC, 120 × 10^9/L; platelets, 450 × 10^9/L; total RCV, 49 mL/kg.)

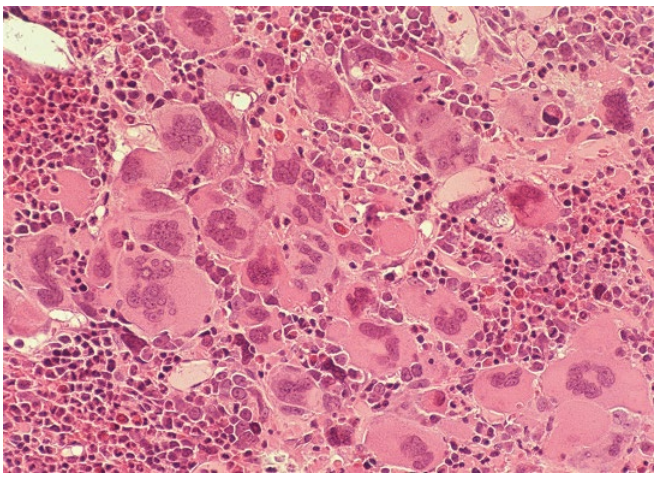

Fig. 16.74. Primary myelofibrosis: Trephine biopsy showing a large cluster of adherent and aggregated megakaryocytes with high nuclear ploidy.

Fig. 16.75. Transitional or accelerated phase myeloproliferative disease: Trephine biopsy showing prominent dilated venous sinuses surrounded by hyperplastic and fibrotic hematopoietic tissue. The blood film showed leukoerythroblastic change. (Hb, 19.5 g/dL; WBC, 38 × 10^9/L; platelets, 850 × 10^9/L; total RCV, 44 mL/kg.)

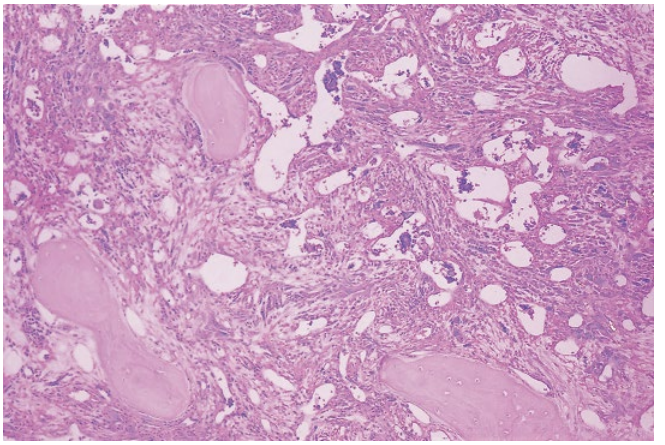

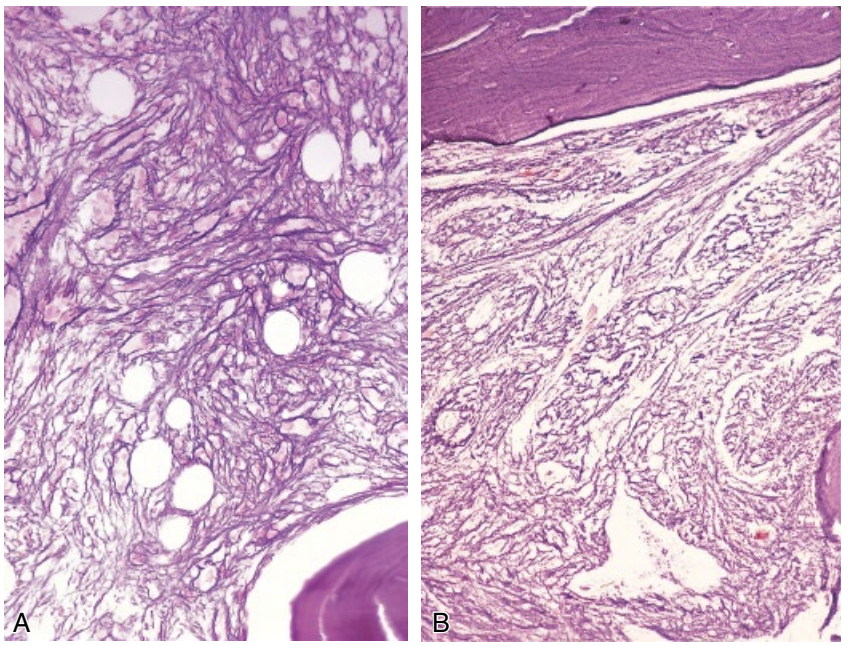

Fig. 16.76. Primary myelofibrosis: Silver impregnation stains of the cases shown in Fig. 16.75 **(A)** and Fig. 16.72B **(B)**. In both biopsies there is a marked diffuse increase in reticulin fiber density and thickness with many intersections (WHO scale grade 2).

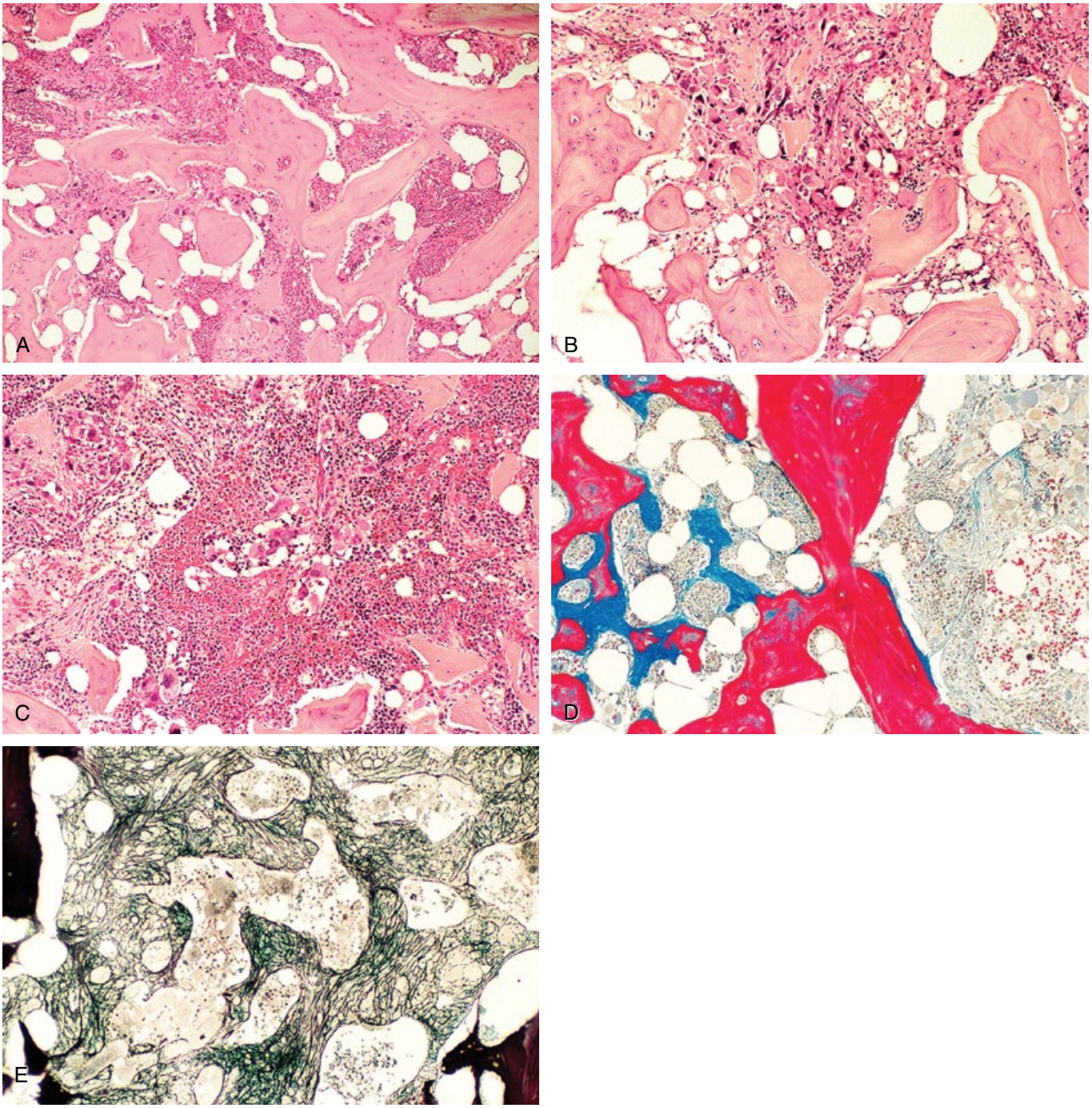

Fig. 16.77. Osteomyelofibrosis: Trephine biopsy. **A,** There is a marked expansion of new trabecular and intertrabecular bone, which is restricting the area available for the hyperplastic hematopoietic tissue. **B,** A higher power view of the irregularly thickened trabeculae and new woven bone formation in the central area dominated by dysplastic megakaryocytes and a dilated vascular sinus. **C,** New bone formation and prominent dilated vascular spaces containing hematopoietic cells and aggregated megakaryocytes. **D,** Trichrome staining highlights new bone (blue) and collagen deposition above the large vascular space on the right. **E,** Reticulin staining shows a marked increase in fiber density and thickness and outlines numerous vascular sinuses.

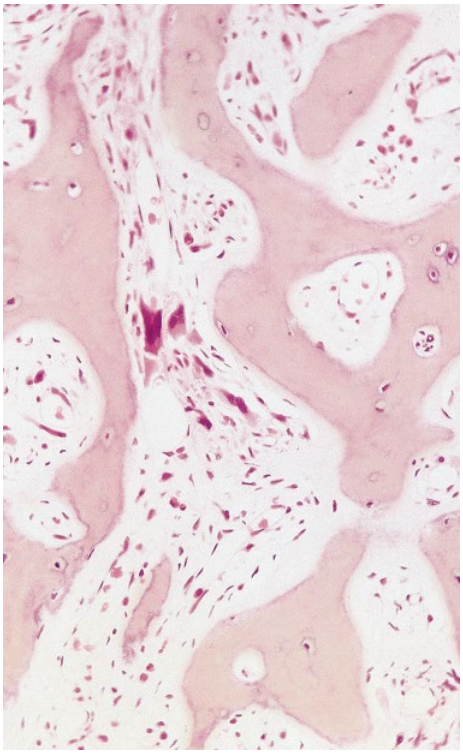

Fig. 16.78. Osteomyelofibrosis: Trephine biopsy showing replacement of normal intertrabecular tissue by a fibrous connective tissue containing only isolated hematopoietic cells (the larger central cells are megakaryocytes). There is an increased amount of trabecular bone with an irregular lamellar pattern.

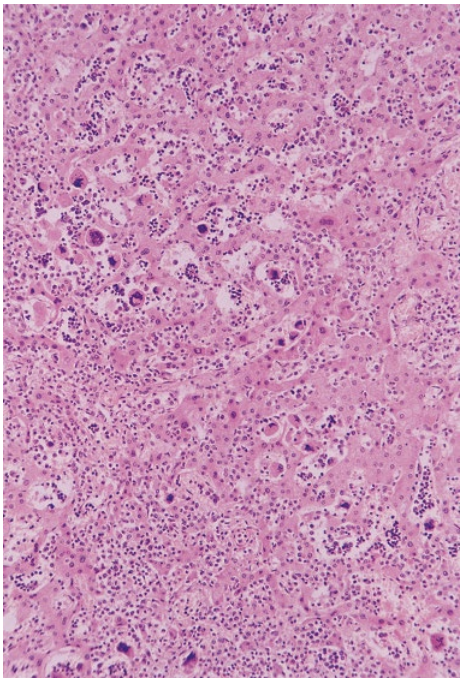

Fig. 16.80. Extramedullary hematopoiesis. Liver biopsy shows groups of erythroblasts, granulopoietic cells, and multinucleate megakaryocytes in the sinuses.

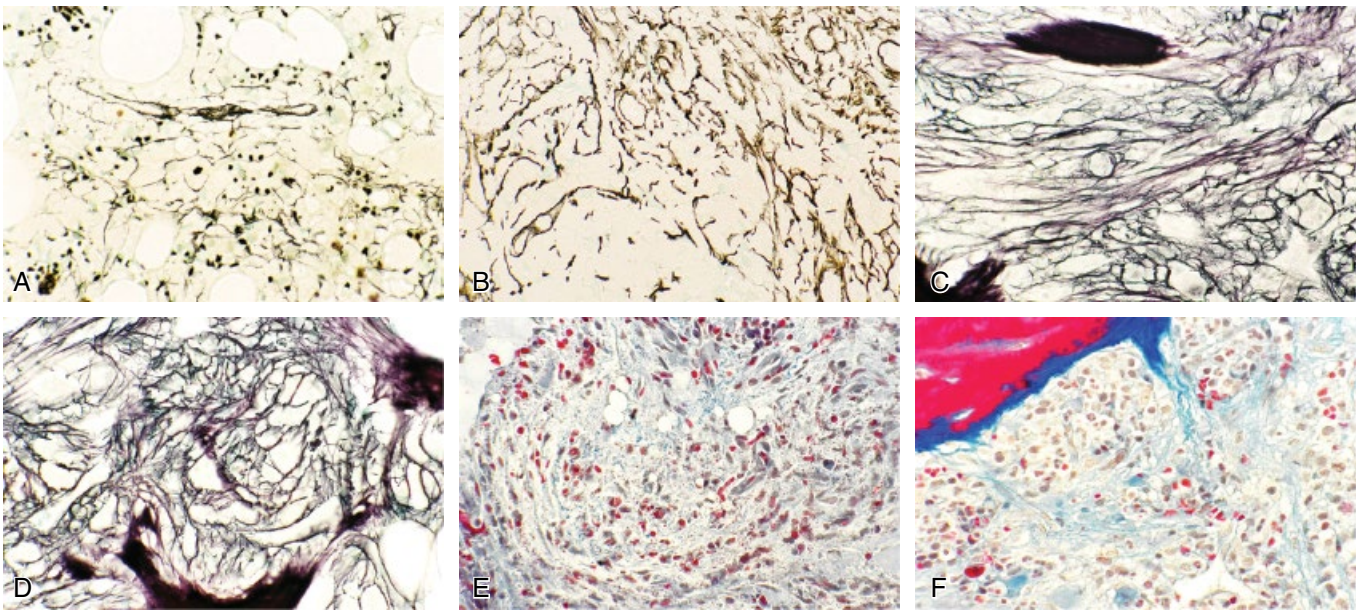

Fig. 16.79. WHO grading of myelofibrosis. **A,** MF-0: scattered linear reticulin with no crossovers corresponding to normal marrow. The reticulin aggregation in the center is a small blood vessel. **B,** MF-1: loose network of reticulin with many intersections. **C,** MF-2: diffuse and dense increase in reticulin with extensive intersections, occasionally with focal thick fibers mostly consistent with collagen and/or focal osteosclerosis. **D,** MF-3: diffuse and dense increase in reticulin with extensive intersections with coarse bundles of collagen usually with extensive osteosclerosis. **E,** MF-2: same case as **C** showing a few focal collagen fibers staining blue. (Masson trichrome stain.) **F,** MF-3: same case as **D** showing coarse bundles of collagen and associated osteosclerosis. (Masson trichrome stain.)

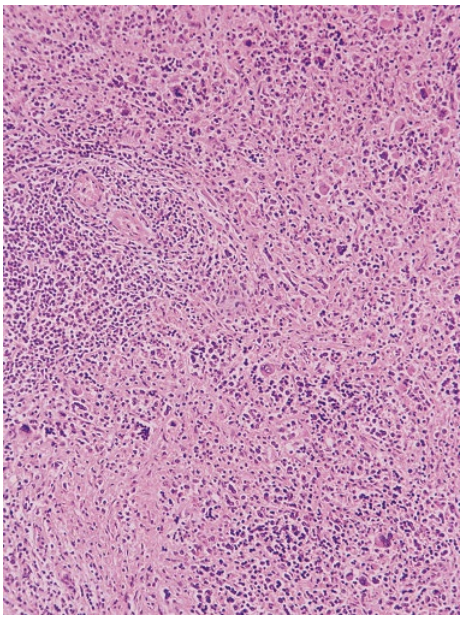

Fig. 16.81. Extramedullary hematopoiesis. Section of spleen following splenectomy shows similar groups of hematopoietic cells in the reticuloendothelial cords and sinuses.

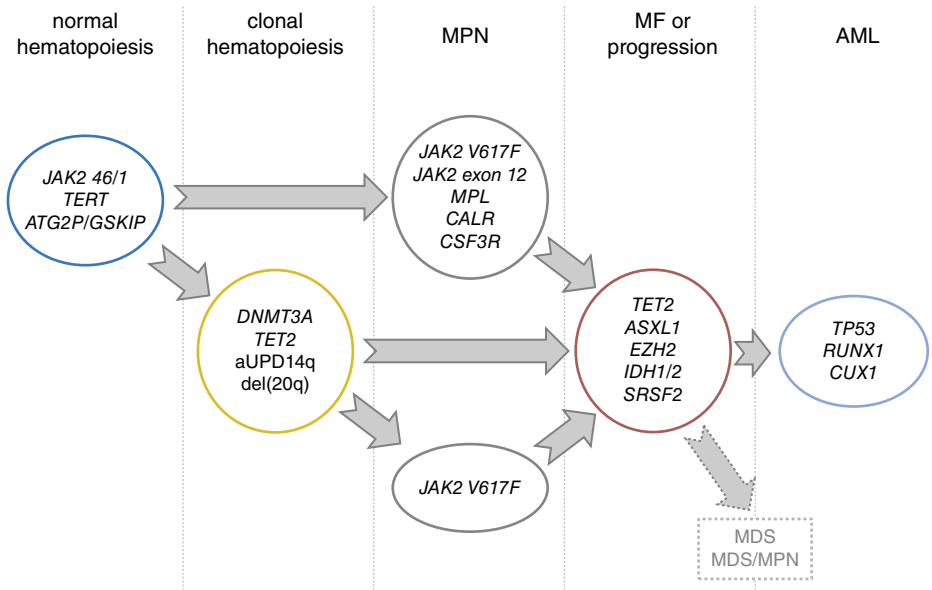

Fig. 16.82. Pathways and principal genetic abnormalities in the evolution of *BCR-ABL1*-negative myeloproliferative neoplasms (MPNs). AML, acute myeloplastic syndrome; MDS/MPN, myelodysplastic/myeloproliferative neoplasm; MF, myelofibrosis. Source: Zoi K, Cross NCP. *J Clin Oncol* 2017;35(9):947–954. Reproduced with permission of *Journal of Clinical Oncology*: American Society of Clinical Oncology.

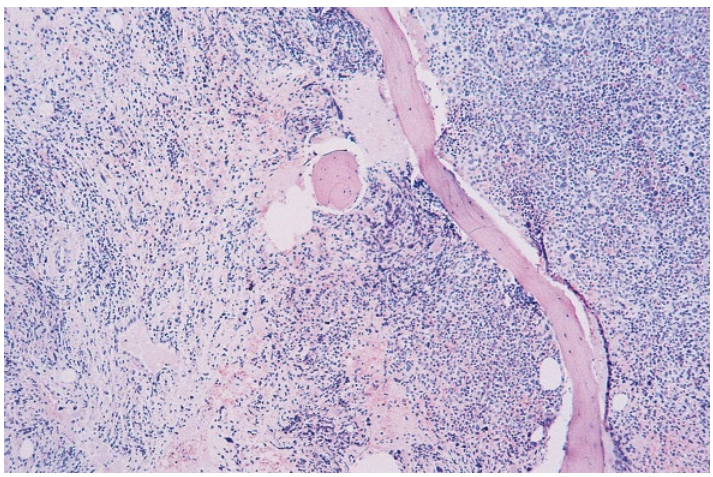

Fig. 16.83. Primary myelofibrosis transformed into acute leukemia. Trephine biopsy shows areas *(left field)* that are consistent with myelofibrosis, but the intertrabecular space *(right field)* contains sheets of closely packed mononuclear cells with no obvious stromal connective tissue.

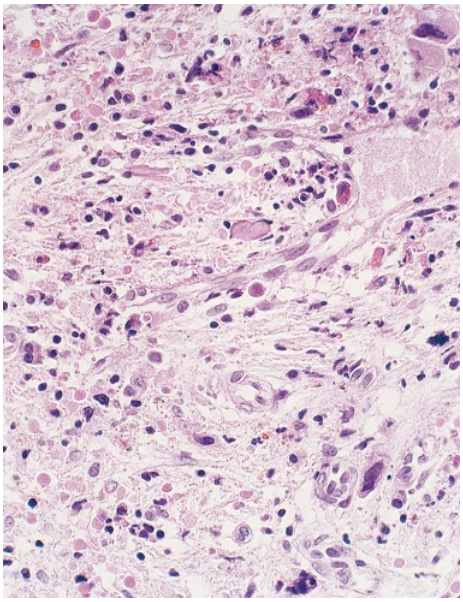

Fig. 16.84. Primary myelofibrosis transformed into acute leukemia. Higher power view of the left field in Fig. 16.82 shows isolated hematopoietic cells surrounded by a loose fibrous connective tissue.

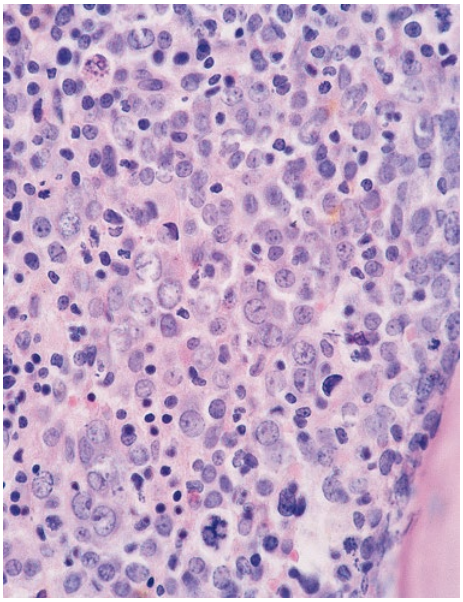

Fig. 16.85. Primary myelofibrosis transformed into acute myeloid leukemia. Higher power view of the right field in Fig. 16.82 shows predominantly primitive myeloid blast cells and promyelocytes. Following a 9-year history of myelofibrosis, the patient sought treatment for a fever and bronchopneumonia. (Hb, 7.1 g/dL; WBC, 6×10^9/L; blasts, 4.5×10^9/L; neutrophils, 0.6×10^9/L; platelets, 40×10^9/L.)

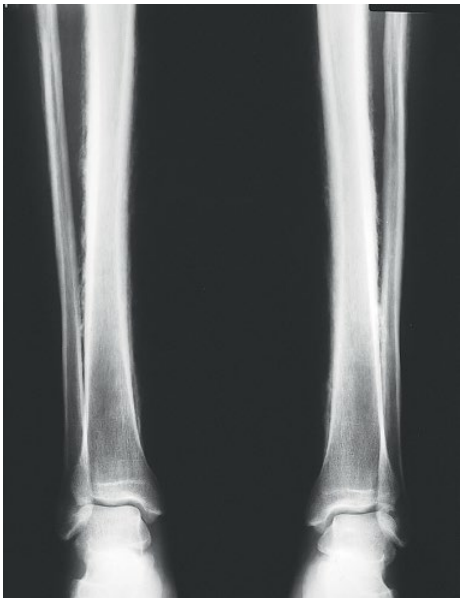

Fig. 16.86. Primary myelofibrosis transformed into acute myeloid leukemia: Radiograph of the lower legs of a middle-aged man showing extensive periosteal elevation caused by infiltration of myeloid blast cells from underlying medullary bone. Although the medullary cavities of these bones in adults usually contain only fat, hematopoietic tissue may extend to distal skeletal tissue in long-standing myeloproliferative disease.

AML (Fig. 16.86). Survival beyond leukemic transformation in either condition is brief.

CHRONIC EOSINOPHILIC LEUKEMIA, NOT OTHERWISE SPECIFIED

These cases have the same clinical and hematologic features as those with the specific chromosome rearrangements listed in Table 17.6. They may show other rearrangements (e.g. of *JAK2*).

MYELOPROLIFERATIVE DISORDER UNCLASSIFIABLE

This designation is applied to cases with clinical and laboratory features of a myeloproliferative disease but who fail to satisfy the diagnostic criteria for any specific entity or features that overlap two or more categories (Fig. 16.87). Some cases represent an early stage of development, and others may be at an advanced accelerated phase of myeloproliferation that obscures the earlier disorder.

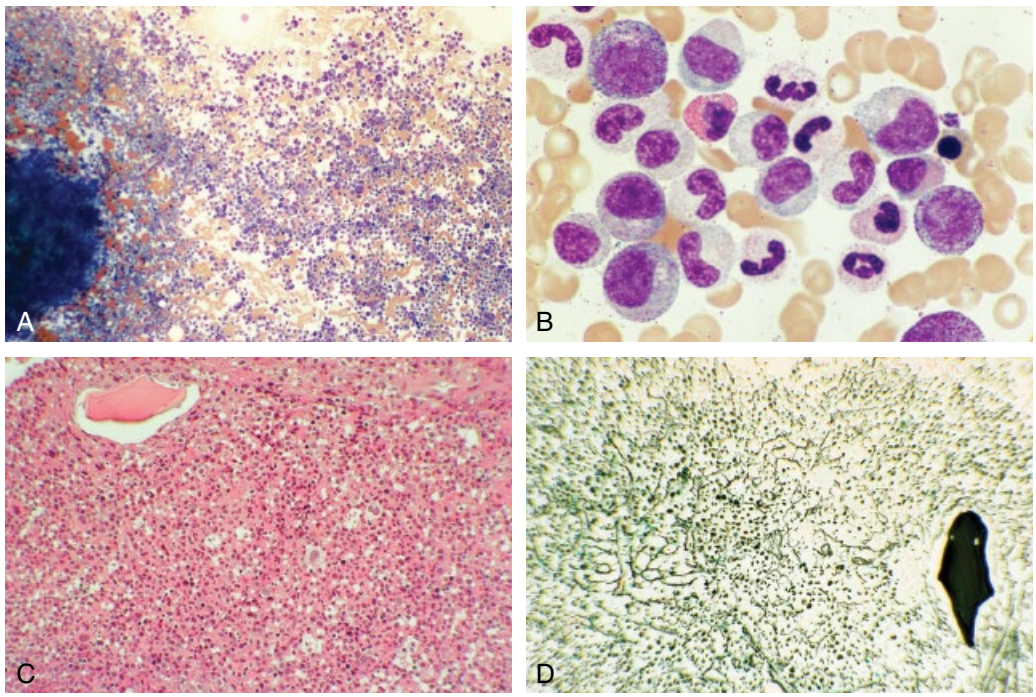

Fig. 16.87. Myeloproliferative disease unclassifiable. Bone marrow images from a 78-year-old man with mild splenomegaly. (Hb, 15.1 g/dL; neutrophils, 32×10^9/L; myelocytes, 4.0×10^9/L; promyelocytes, 1.2×10^9/L; platelets, 530×10^9/L; mild red cell anisocytosis.) **A,** Marrow aspirate showing hypercellular fragment and cell trail. **B,** At higher power the aspirate shows a dominance of granulopoiesis. **C,** Trephine biopsy showing complete replacement of fat by predominantly myelopoietic cells. Megakaryocytes are of low nuclear ploidy and are not seen in clusters. **D,** The reticulin stain shows a minimal increase in fiber density and thickness.

CHAPTER

17

MASTOCYTOSIS, MYELOID/ LYMPHOID NEOPLASMS WITH EOSINOPHILIA AND SPECIFIC CYTOGENETIC REARRANGEMENTS, MYELODYSPLASTIC/ MYELOPROLIFERATIVE NEOPLASMS

MASTOCYTOSIS

Mast cells are derived from hematopoietic stem cells. The World Health Organization (WHO) classification of mastocytosis is shown in Table 17.1 and the criteria for diagnosis of the different subtypes in Table 17.2. In mast cell disease (mastocytosis) there is a proliferation of neoplastic mast cells in the skin, bone marrow, gastrointestinal tract, spleen, or other organs. In many variants of mastocytosis, particularly those with systemic involvement, there is a somatic mutation of c-*KIT*, the proto-oncogene that encodes a receptor tyrosine kinase for stem cell factor (SCF). The most

TABLE 17.1. WHO (2016): CLASSIFICATION OF MASTOCYTOSIS VARIANTS

Cutaneous mastocytosis
Urticaria pigmentosa/maculopapular cutaneous mastocytosis
Diffuse cutaneous mastocytosis
Mastocytoma of skin
Systemic mastocytosis
Indolent systemic mastocytosis[a] (including the bone marrow mastocytosis subtype)
Smouldering systemic mastocytosis[a]
Systemic mastocytosis with an associated hematologic neoplasm[b]
Aggressive systemic mastocytosis[a]
Mast cell leukemia
Mast cell sarcoma

[a] The complete diagnosis of these variants requires information regarding B and C findings (Table 17.4), all of which may not be available at the time of initial tissue diagnosis.

[b] This variant is equivalent to the previously described entity "systemic mastocytosis with an associated clonal hematologic non-mast cell lineage disease," and the terms can be used synonymously.

Source: Swerdlow SH, et al., eds. *WHO Classification of Tumours of Haematopoietic and Lymphoid Tissues*, revised 4th edn. International Agency for Research on Cancer, Lyon, 2017.

TABLE 17.2. WHO (2016): DIAGNOSTIC CRITERIA FOR CUTANEOUS AND SYSTEMIC MASTOCYTOSIS

Cutaneous mastocytosis

Skin lesions demonstrating the typical findings of urticaria pigmentosa/maculopapular cutaneous mastocytosis, diffuse cutaneous mastocytosis, or solitary mastocytoma, and typical histologic infiltrates of mast cells in a multifocal or diffuse pattern in an adequate skin biopsy.[a] In addition, features/criteria sufficient to establish the diagnosis of systemic mastocytosis must be absent. There are three variants of cutaneous mastocytosis (see Table 17.1).

Systemic mastocytosis

The diagnosis of systemic mastocytosis can be made when the major criterion and at least one minor criterion are present, or when ≥3 minor criteria are present

Major criterion

Multifocal dense infiltrates of mast cells (≥15 mast cells in aggregates) detected in sections of bone marrow and/or other extracutaneous organ(s)

Minor criteria

1. In biopsy sections of bone marrow or other extracutaneous organs, >25% of the mast cells in the infiltrate are spindle-shaped or have atypical morphology or >25% of all mast cells in bone marrow aspirate smears are immature or atypical
2. Detection of an activating point mutation at codon 816 of *KIT* in the bone marrow, blood or another extracutaneous organ
3. Mast cells in bone marrow, blood, or another extracutaneous organ express CD25, with or without CD2, in addition to normal mast cell markers[b]
4. Serum total tryptase is persistently >20 ng/mL, unless there is an associated myeloid neoplasm, in which case this parameter is not valid

[a] This criterion applies to both the dense focal and the diffuse mast cell infiltrates in the biopsy.

[b] CD25 is the more sensitive marker, by both flow cytometry and immunohistochemistry.

Source: Swerdlow SH, et al., eds. *WHO Classification of Tumours of Haematopoietic and Lymphoid Tissues*, revised 4th edn. International Agency for Research on Cancer, Lyon, 2017.

Color Atlas of Clinical Hematology: Molecular and Cellular Basis of Disease, Fifth Edition. A. Victor Hoffbrand, Paresh Vyas, Elías Campo, Torsten Haferlach, and Keith Gomez

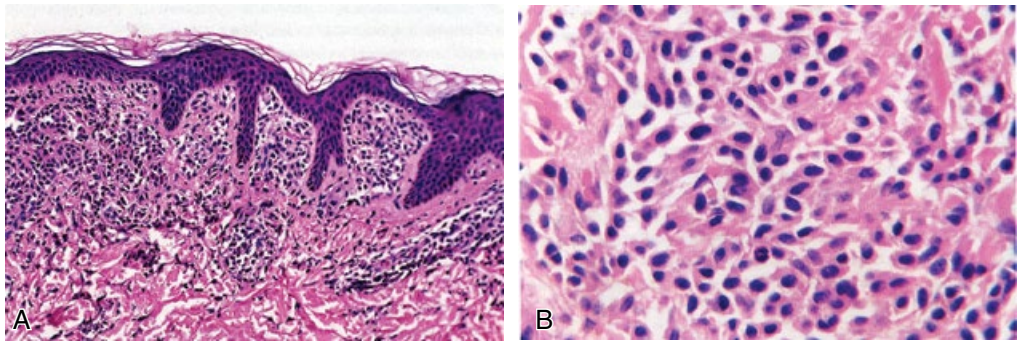

Fig. 17.1. Urticaria pigmentosa. **A,** Mast cells fill the papillary dermis. **B,** A higher power view of the mast cells. (H&E.) Source: Weedon D. *Skin Pathology*, 2nd edn. Churchill Livingstone, 2002. Reproduced with permission of Elsevier.

common mutation (>80% of cases) is the point mutation D816V, which results in spontaneous activation of the KIT protein and a consequent clonal expansion of mast cells.

Other activating mutations affecting the same or other codons of KIT have been identified in a minority of adult cases of mastocytosis. In advanced systemic mastocytosis (SM) additional molecular defects are often present and these contribute to the progression and drug resistance of the disease. These include somatic mutations of *TET2*, *SRSF2*, *ASXL1*, *CBL*, *RUNX1*, and *RAS* among others. If there is an associated non-mast cell-lineage hematologic neoplasm (AHNMD), there may be mutations due to that component. Other activating mutations affecting the same or other codons of KIT have been identified in a minority of adult cases of mastocytosis.

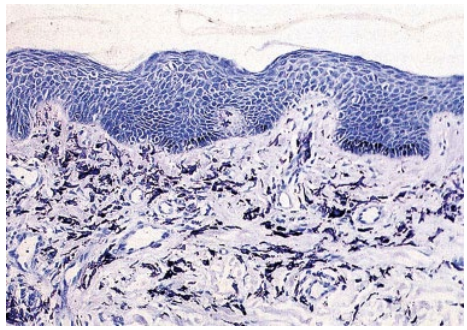

Fig. 17.2. Urticaria pigmentosa. Numerous mast cells are present in the upper dermis. There is also mild hyperpigmentation of the basal layer. (Toluidine blue.) Source: Weedon D. *Skin Pathology*, 2nd edn. Churchill Livingstone, 2002. Reproduced with permission of Elsevier.

TYPES OF MASTOCYTOSIS

Cutaneous Mastocytosis

Cutaneous mastocytosis is the most frequently found form, accounting for 80% of all cases of mastocytosis. The mastocytosis is confined to the skin. The lesions show urticaria when stroked and are pigmented. Urticaria pigmentosa, or macular papular mastocytosis (Figs. 17.1 and 17.2), is the most common form and occurs in both children and adults. Diffuse cutaneous mastocytosis, another variant, is less common and is seen only in children. Cutaneous mastocytoma (Fig. 17.3) occurs as a solitary, benign-appearing tumor usually in infants. In all of these conditions there is no systemic involvement and no elevation of the serum tryptase.

Systemic Mastocytosis

The major criteria for diagnosis are the multifocal clustering of mast cells in one or more visceral organ (Table 17.3). Minor criteria are also listed in Table 17.3. SM is subdivided into indolent SM (ISM), smoldering SM (SSM), SM with associated hematological neoplasm (SM-AHN), aggressive SM (ASM), and mast cell leukemia (MCL). The criteria for each are given in Table 17.3.

In SM, patients may have weight loss, fatigue, or fever. Persistent and progressive eruptive cutaneous lesions (Fig. 17.4) may be associated with pruritus and urticaria. Symptoms such as abdominal pain, diarrhea, flushing, syncope, headaches, tachycardia, or dyspnea result from release of mediators (e.g. histamine, proteases, eicosanoids, or heparin). Occasionally bone pain, fractures, or arthralgia may occur. There may be splenomegaly and, less frequently, hepatomegaly or lymphadenopathy. Radiography may reveal osteosclerosis or multiple irregular lytic skeletal lesions.

In many patients there is anemia, leukocytosis, eosinophilia, or leukopenia. In patients with aggressive forms of the disease, bone marrow failure may occur. In approximately 30% of patients, there is an associated hematological neoplasm (AHN), and the blood count and film may show abnormality related to these conditions. Significant numbers of mast cells are seen in blood films and only in very rare cases classified as mast cell leukemia (see the following section). Serum tryptase levels are elevated in most patients.

Although bone marrow involvement by SM is usually established in trephine biopsies, the diagnosis may also be evident in marrow aspirates (Fig. 17.5). Because most mast cells tend to adhere to the marrow fragments, squash preparations often produce the greatest number of mast cells (Fig. 17.6). The aspirate may show findings consistent with a coexisting hematopoietic clonal disorder (e.g. myelodysplastic syndrome [Figs. 17.7 and 17.8], acute myeloid leukemia, or myeloproliferative or lymphoproliferative disease [Fig. 17.9]).

In trephine biopsies the distribution of the neoplastic mast cells may be focal, peritrabecular, perivascular, or random. Multifocal aggregates of 15 or more cells are found in the bone marrow or other extracutaneous organs. There may be associated lymphocytes, eosinophils, or fibroblasts. In patients with aggressive disease, the involvement is more extensive, with widespread

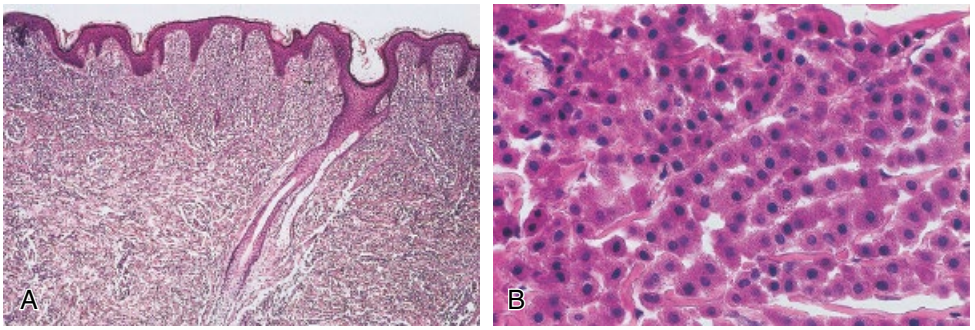

Fig. 17.3. Cutaneous mastocytoma. **A,** Low-power view. **B,** High-power view. The tumor cells have abundant eosinophilic cytoplasm and uniform darkly staining nuclei. Source: McKee PH, et al. *Pathology of the Skin*, 3rd edn. Elsevier Mosby, 2005. Reproduced with permission of Elsevier.

TABLE 17.3. WHO (2016): DIAGNOSTIC CRITERIA FOR THE VARIANTS OF SYSTEMIC MASTOCYTOSIS

Indolent systemic mastocytosis
Meets the general criteria for systemic mastocytosis
No C findings[a]
No evidence of an associated hematologic neoplasm
Low mast cell burden
Skin lesions are almost invariably present
Bone marrow mastocytosis
As above (indolent systemic mastocytosis) but with bone marrow involvement and no skin lesions
Smouldering systemic mastocytosis
Meets the general criteria for systemic mastocytosis
≥2 B findings; no C findings[a]
No evidence of an associated hematologic neoplasm
High mast cell burden
Does not meet the criteria for mast cell leukemia
Systemic mastocytosis with an associated hematologic neoplasm
Meets the general criteria for systemic mastocytosis
Meets the criteria for an associated hematologic neoplasm (i.e. a myelodysplastic syndrome, myeloproliferative neoplasm, acute myeloid leukemia, lymphoma, or another hematologic neoplasm classified as a distinct entity in the WHO classification)
Aggressive systemic mastocytosis
Meets the general criteria for systemic mastocytosis
≥1 C finding[a]
Does not meet the criteria for mast cell leukemia
Skin lesions are usually absent
Mast cell leukemia
Meets the general criteria for systemic mastocytosis
Bone marrow biopsy shows diffuse infiltration (usually dense) by atypical, immature mast cells
Bone marrow aspirate smears show ≥20% mast cells
In classic cases, mast cells account for ≥10% of the peripheral blood white blood cells, but the aleukemic variant (in which mast cells account for <10%) is more common
Skin lesions are usually absent

[a] B and C findings indicate organ involvement without and with organ dysfunction, respectively; these findings are listed in Table 17.4.

Source: Swerdlow SH, et al., eds. *WHO Classification of Tumours of Haematopoietic and Lymphoid Tissues*, revised 4th edn. International Agency for Research on Cancer, Lyon, 2017.

TABLE 17.4. B ("BURDEN OF DISEASE") AND C ("CYTOREDUCTION-REQUIRING") FINDINGS IN SYSTEMIC MASTOCYTOSIS, WHICH INDICATE ORGAN INVOLVEMENT WITHOUT AND WITH ORGAN DYSFUNCTION, RESPECTIVELY

B findings
1. High mast cell burden (shown on bone marrow biopsy): >30% infiltration of cellularity by mast cells (focal, dense aggregates) and serum total tryptase >200 ng/mL
2. Signs of dysplasia or myeloproliferation in non-mast cell lineage(s), but criteria are not met for definite diagnosis of an associated hematologic neoplasm, with normal or only slightly abnormal blood counts
3. Hepatomegaly without impairment of liver function, palpable splenomegaly with hypersplenism and/or lymphadenopathy on palpation or imaging
C findings
1. Bone marrow dysfunction caused by neoplastic mast cell infiltration, manifested by ≥1 cytopenia; absolute neutrophil count $<1.0 \times 10^9$/L, hemoglobin level <10 g/dL, and/or platelet count $<100 \times 10^9$/L
2. Palpable hepatomegaly with impairment of liver function, ascites, and/or portal hypertension
3. Skeletal; involvement, with large osteolytic lesions with or without pathologic fractures (pathologic fractures caused by osteoporosis do not qualify as a C finding)
4. Palpable splenomegaly with hypersplenism
5. Malabsorption with weight loss due to gastrointestinal mast cell infiltrates

Source: Swerdlow SH, et al., eds. *WHO Classification of Tumours of Haematopoietic and Lymphoid Tissues*, revised 4th edn. International Agency for Research on Cancer, Lyon, 2017.

replacement of normal hematopoietic cells (Figs. 17.10 and 17.11). Thickening of bony trabeculae and osteosclerosis may be evident. Osteolytic lesions are less common. Although mast cell metachromatic granules may be seen with Giemsa or toluidine blue stains (Fig. 17.11), immunostaining for mast cell tryptase is the most reliable method of identification (Fig. 17.12A). Neoplastic mast cells, unlike normal mast cells, express both CD25 (Fig. 17.12C) and CD2 on their surface. CD117 is also a positive marker for mast cells (Fig. 17.12B) but is not specific. Splenectomy may reveal extensive splenic disease (Fig. 17.13), and liver biopsy may identify periportal and sinus mast cell infiltration with associated fibrosis (Figs. 17.14 and 17.15) or even cirrhosis.

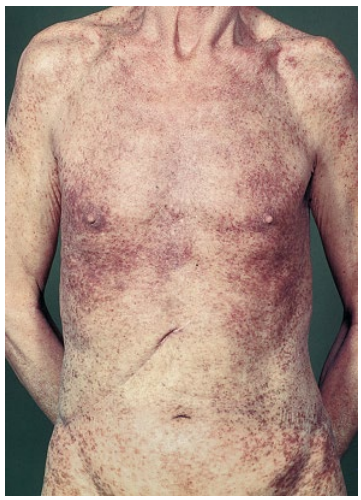

Fig. 17.4. Systemic mastocytosis: Generalized pigmented and nodular cutaneous eruption seen after splenectomy and psoralen and ultraviolet A (PUVA) therapy.

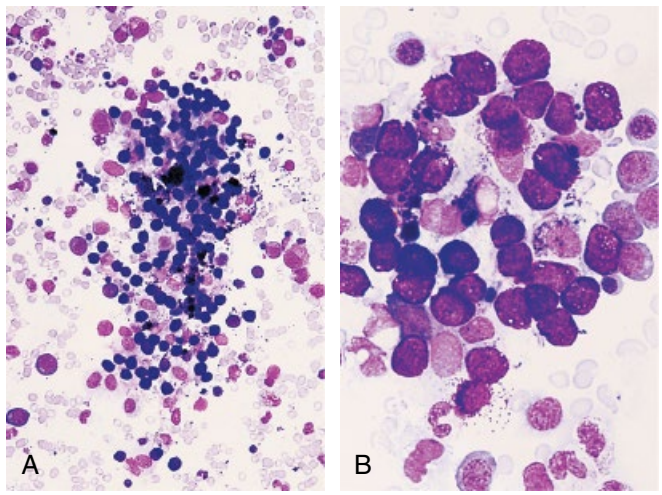

Fig. 17.5. Systemic mastocytosis: **A,** Bone marrow aspirate showing an extensive accumulation of mast cells at low power. **B,** Higher power view.

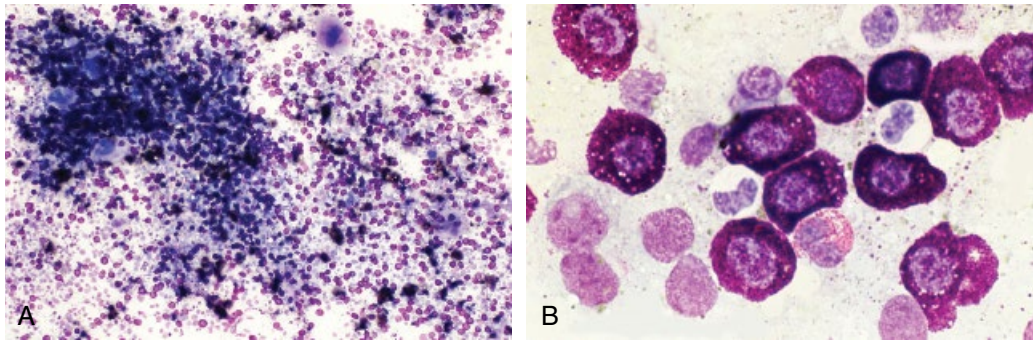

Fig. 17.6. Systemic mastocytosis: Bone marrow aspirate. **A,** Large numbers of mast cells are seen in the squashed fragment and cell trails. **B,** Typical mast cells at higher magnification.

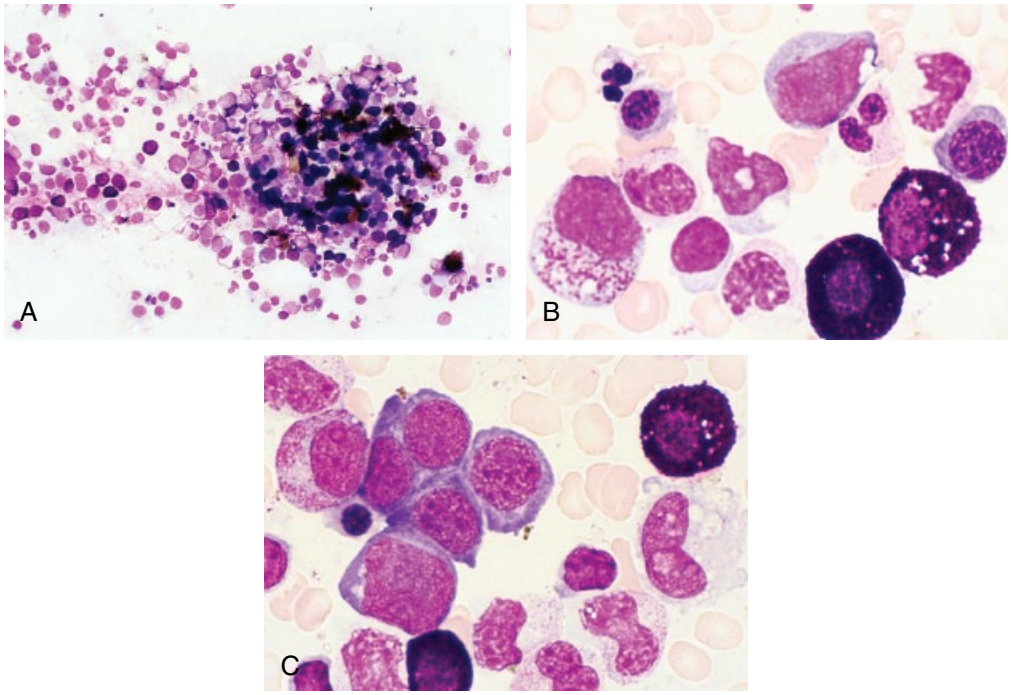

Fig. 17.7. Systemic mastocytosis and myelodysplastic syndrome (refractory anemia with ring sideroblasts): Bone marrow aspirate. **A,** The fragment and cell trail are hypercellular with hematopoietic cells and large numbers of mast cells. **B,** At higher magnification, two mast cells and a dysplastic late erythroblast are shown. **C,** Macronormoblastic basophilic erythroblasts and mast cells.

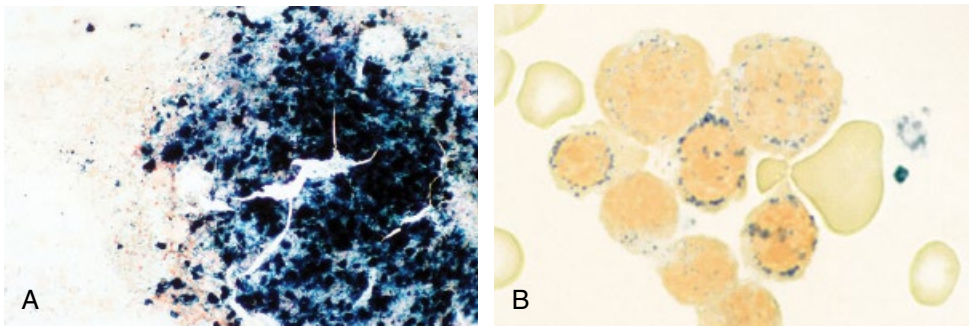

Fig. 17.8. Systemic mastocytosis and myelodysplastic syndrome (refractory anemia with ring sideroblasts): Bone marrow aspirate in patient shown in Fig. 17.7. **A,** Fragmental iron stores are markedly increased. **B,** "Ring" sideroblasts.

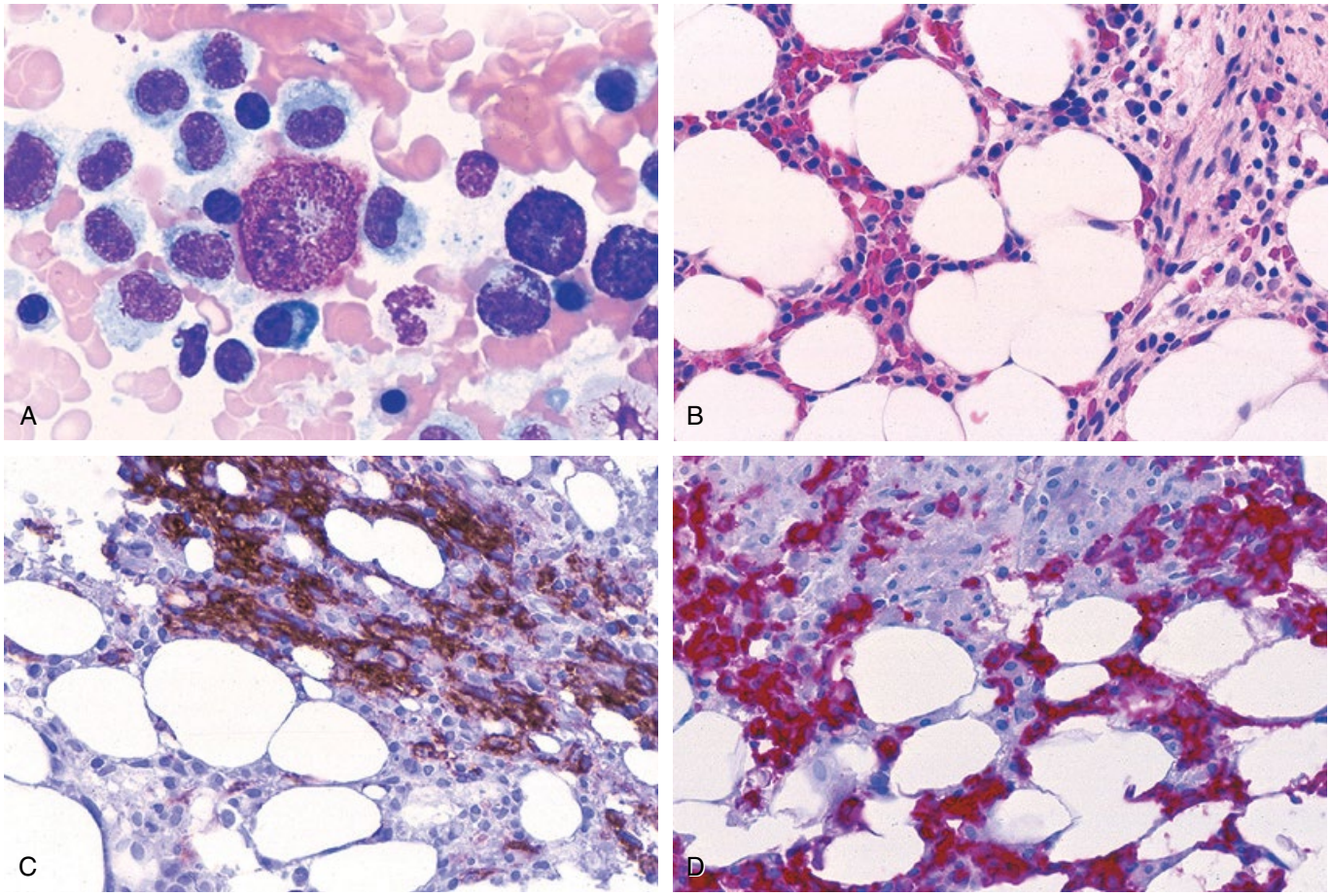

Fig. 17.9. Systemic mastocytosis and hairy cell leukemia. **A,** Bone marrow aspirate showing typical hairy cells and atypical mast cells. **B,** Bone marrow trephine biopsy shows spindle-shaped mast cells adjacent to marrow containing many hairy cells. **C,** Immunohistologic staining for mast cell tryptase shows strong positivity in the spindle-shaped mast cells. **D,** Immunohistologic staining for CD20 identifies the hairy cell population. (Courtesy of Dr. James W Vardiman.)

Mast Cell Leukemia

Mast cell leukemia is the rarest form of aggressive SM. Abnormal mast cells make up more than 20% of cells in marrow and usually over 10% of white cells in the blood (Fig. 17.16A). Trephine biopsies show extensive involvement similar to aggressive SM (Fig. 17.16B–D). The initial manifestation of the disease is similar to other forms of aggressive SM, with flushing, hypotension, and diarrhea. Later there is multiple organ involvement with weight loss, bone pain, hepatomegaly, and splenomegaly. Plasma tryptase levels are extremely high.

Mast Cell Sarcoma

Mast cell sarcoma is an exceedingly rare tumor with only a few well-documented cases. At presentation it may be a localized tumor with an invasive growth pattern and pleomorphic immature cytology. All reported cases have evolved in an aggressive

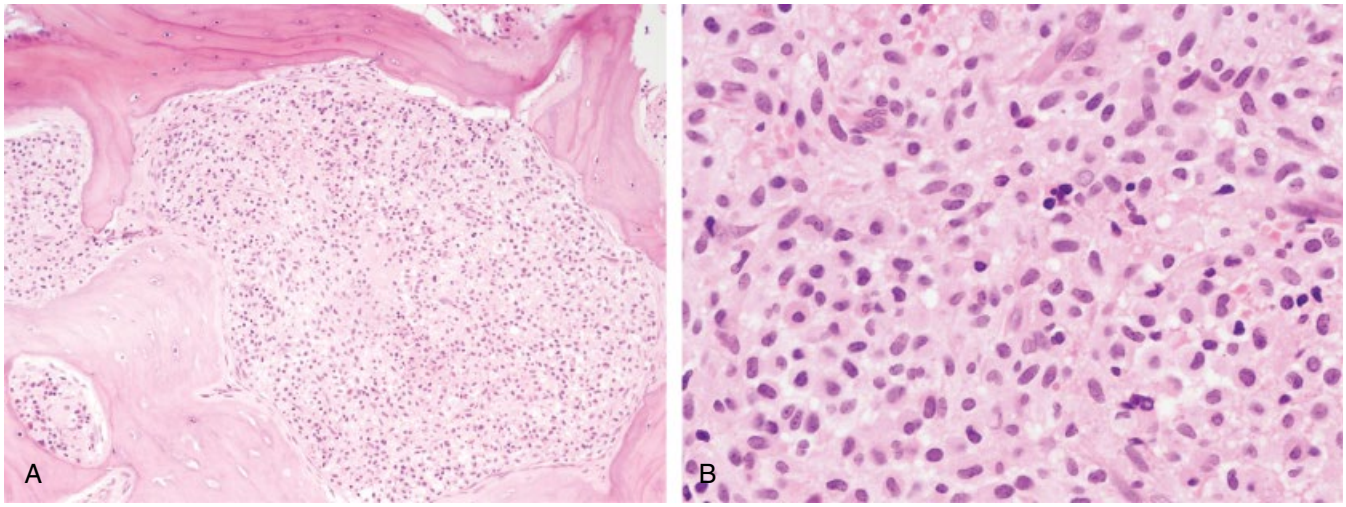

Fig. 17.10. Systemic mastocytosis: Trephine biopsy. **A,** In the intertrabecular spaces there is almost complete replacement of normal hematopoietic cells by sheets of neoplastic mast cells. The bony trabeculae are thickened and show changes of early osteosclerosis. **B,** At higher magnification the densely packed mast cells include spindled forms with oval nuclei. (Courtesy of Dr. Christopher McNamara.)

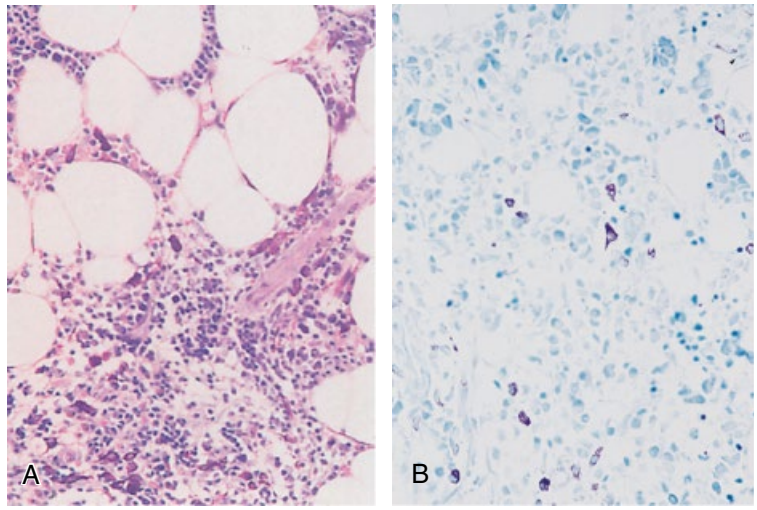

Fig. 17.11. Systemic mastocytosis: Trephine biopsy. **A,** Low-power view showing perivascular accumulation of mast cells. Mast cells are also present around the edge of a lymphoid follicle. **B,** Characteristic metachromatic staining reaction in the cytoplasm of mast cells with toluidine blue.

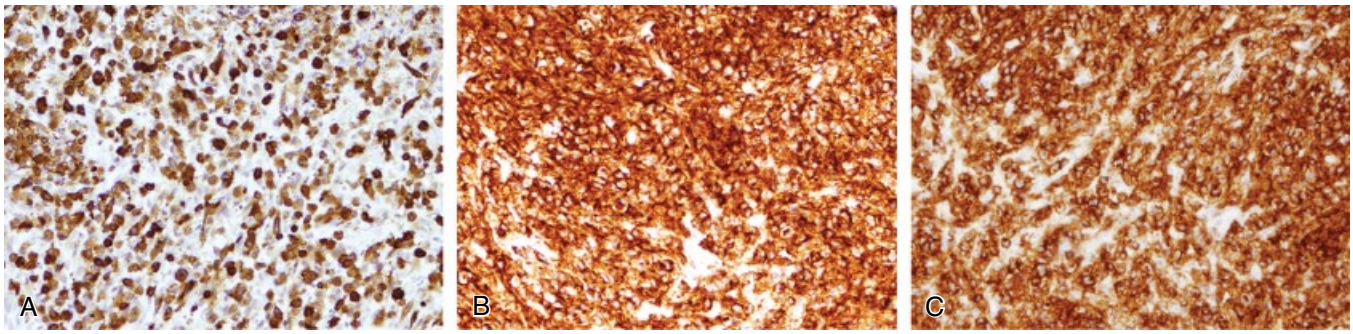

Fig. 17.12. Systemic mastocytosis: Trephine biopsy. Immunohistologic staining reveals strong positivity for mast cell tryptase **(A)**, CD117 **(B)**, and CD25 **(C)**. (Courtesy of Dr. Christopher McNamara.)

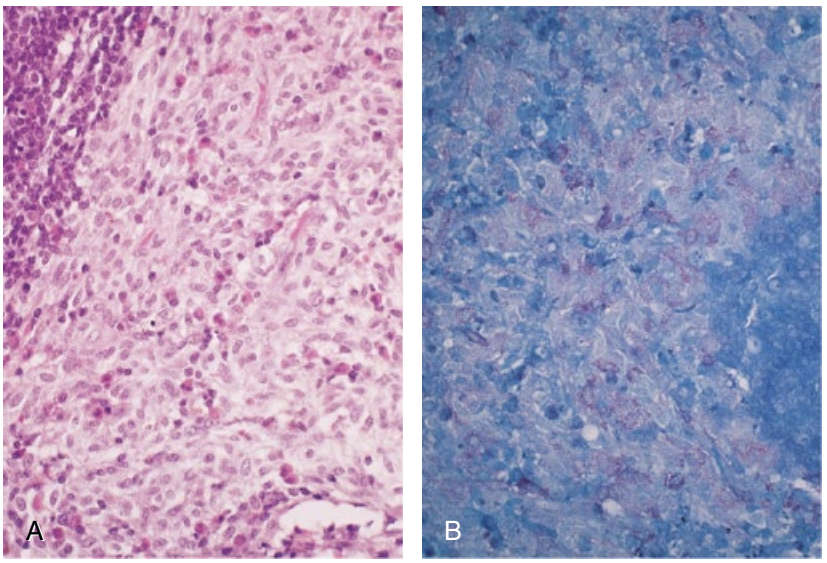

Fig. 17.13. Systemic mastocytosis: Sections of spleen showing mononuclear histocyte-like cells on staining with hematoxylin and eosin **(A)** and toluidine blue **(B)** to demonstrate the cytoplasmic metachromasia. (Courtesy of Dr. JE McLaughlin.)

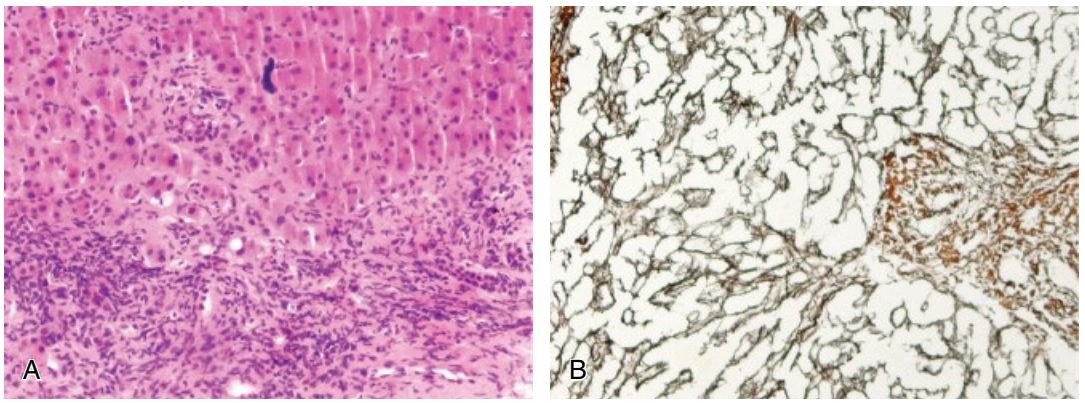

Fig. 17.14. Systemic mastocytosis: Liver biopsy. **A,** There is a dense infiltrate of spindle-shaped mast cells in the periportal zone with extension of these neoplastic mast cells into the sinusoids. **B,** Reticulin staining shows periportal fibrosis and widespread thickening around the sinusoids. (Courtesy of Dr. Christopher McNamara.)

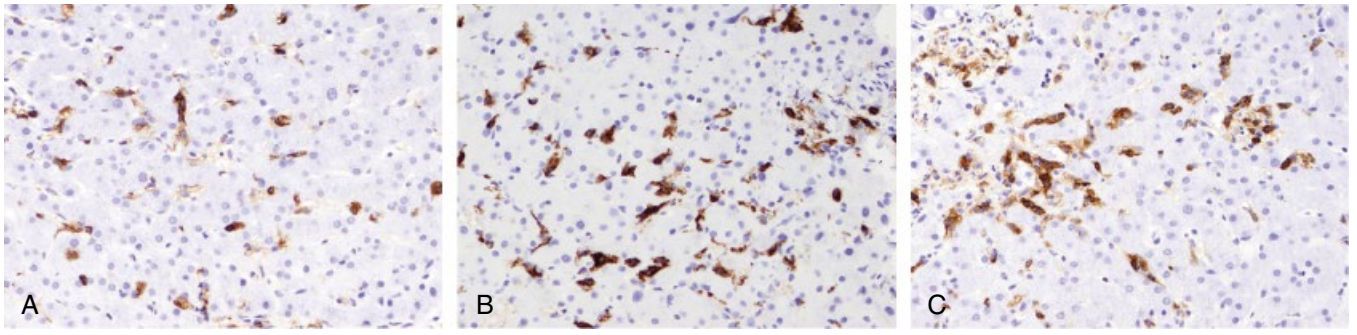

Fig. 17.15. Systemic mastocytosis: Liver biopsy. Immunohistologic staining shows strong positivity in mast cells with mast cell tryptase **(A)**, CD117 **(B)**, and CD25 **(C)**. (Courtesy of Dr. Christopher McNamara.)

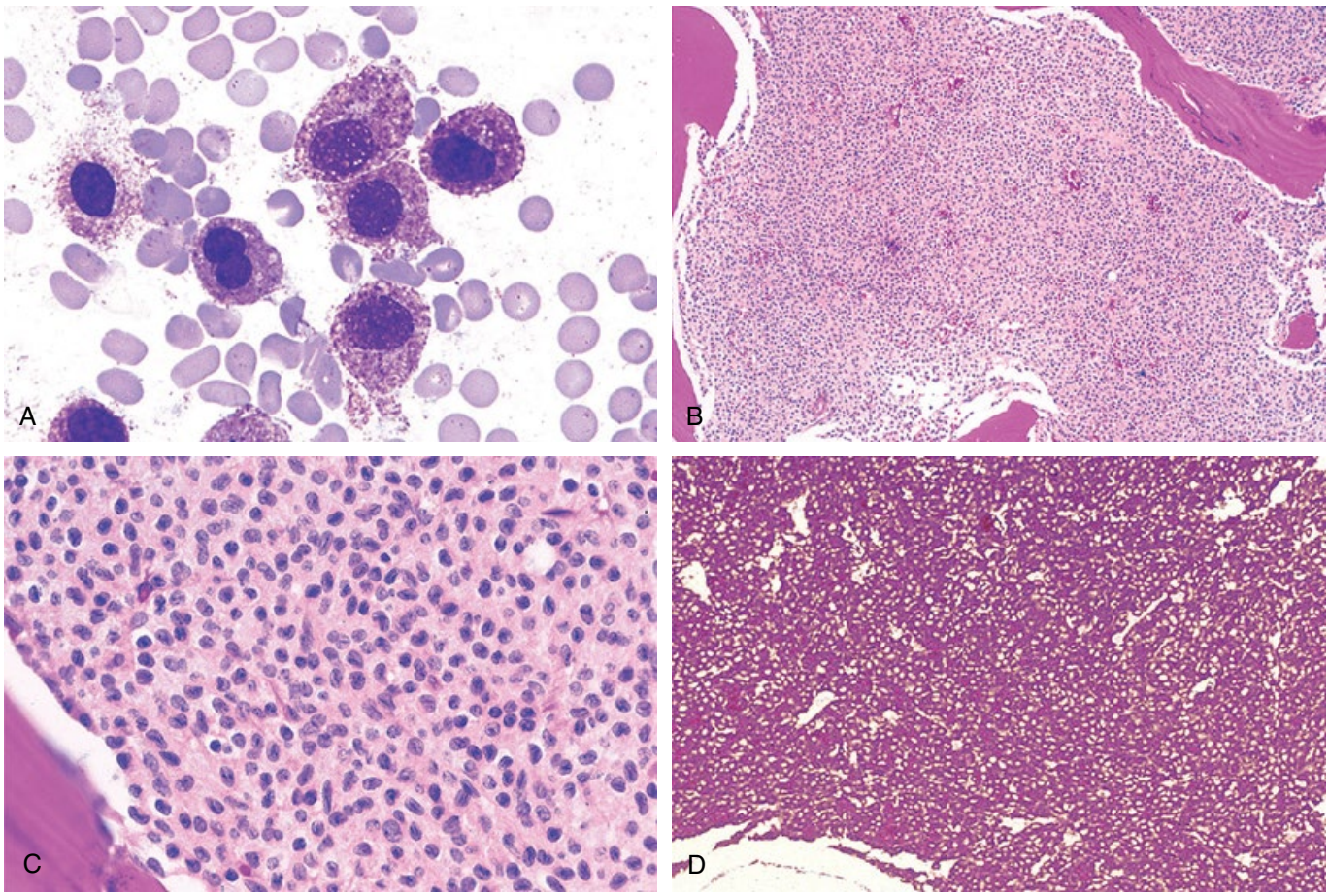

Fig. 17.16. Mast cell leukemia. **A,** Peripheral blood film shows numerous mast cells, some with defective granulation and one with a bilobed nucleus. **B,** Bone marrow trephine biopsy shows a diffuse sheet-like proliferation of neoplastic mast cells. **C,** At higher magnification, the cells have a clear cell appearance resulting from poor granulation of the immature leukemic mast cell population. **D,** Immunohistologic staining shows strong positivity for mast cell tryptase. (Courtesy of Dr. James W Vardiman.)

form of SM. Images from a primary skin mast cell sarcoma are shown in Fig. 17.17.

Extracutaneous Mastocytoma

Extracutaneous mastocytoma, also rare and mostly reported in the lung, is a tumor of typical mature mast cells similar to those seen in cutaneous mastocytoma.

PROGNOSIS

The prognosis in mastocytosis is variable. Cutaneous mastocytosis in children usually resolves before or during puberty, but in adults regression is rare and skin involvement is often associated with systemic disease. Table 17.5 gives the prognostic scoring system for SM. Although patients with indolent forms and skin involvement may have a normal life expectancy, those with aggressive disease have a life expectancy of weeks or, at best, less than a year.

PARANEOPLASTIC PEMPHIGUS

This is a rare autoimmune skin and mucosal disease, most commonly associated with non-Hodgkin lymphoma (80%), Castleman disease, and, rarely, solid tumors. There is blistering of the skin and ulceration and scarring of mucosal membranes, for example, of the mouth (Fig. 17.18). The conjunctivae may ulcerate and scar. The prognosis is poor. Antibodies to proteins expressed at epithelial cell junctions, desmoglein I and III, and members of the plakin family are found in serum. Antibodies to bullus pemphigoid antigen 2 and to an unknown 170 kDa antigen are unique to the condition. The patient illustrated in Fig. 17.18 had all of the clinical and laboratory features of paraneoplastic pemphigus, with underlying SM.

MYELOID/LYMPHOID NEOPLASMS WITH EOSINOPHILIA AND ABNORMALITIES OF *PDGFRA*, *PDGFRB* OR *FGFR1*, OR WITH *PCM1-JAK2*

These neoplasms (Table 17.6) are characterized by a clonal proliferation of eosinophil precursors in the marrow with a persistent peripheral blood eosinophilia of $>1.5 \times 10^9$/L often with eosinophil precursors (Fig. 17.19). There may be organ damage caused by eosinophil infiltration. There is activation of a protein kinase caused by formation of fusion genes in four distinct recurrent breakpoint clusters that code for the following: (i) platelet-derived growth factor α (*PDGFRA*) at 4q12; (ii) platelet-derived

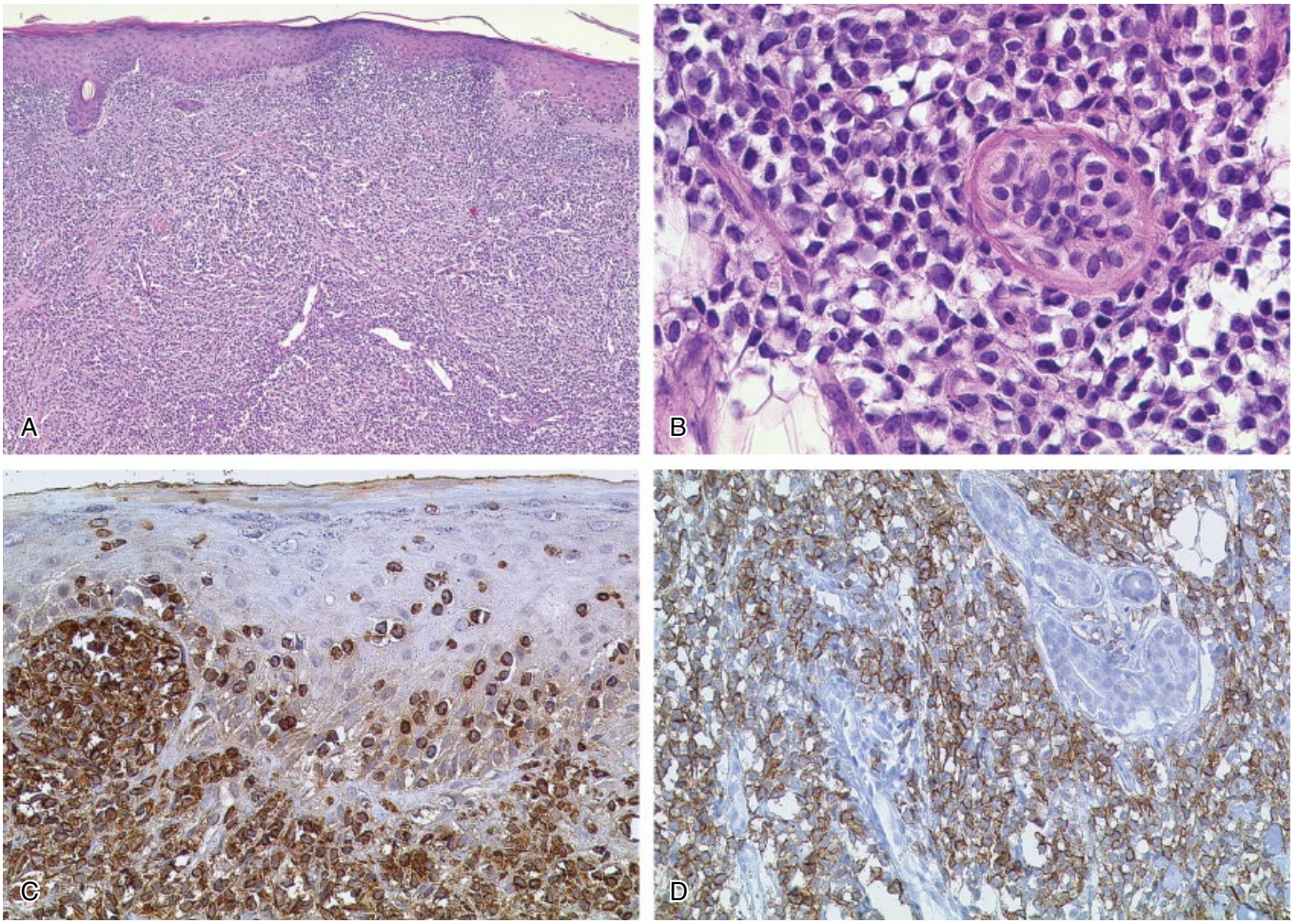

Fig. 17.17. Mast cell sarcoma. **A,** Sheets of malignant mast cells occupy the dermis with extension into the subcutaneous tissue. **B,** At higher magnification the tumor consists of pleomorphic, oval, and polygonal neoplastic cells that show no evidence of mast cell differentiation in the H&E-stained section. There is invasion of subcutaneous fat, and the malignant cells are seen within a lymphatic or venous vascular space. **C,** Immunohistologic staining for mast cell tryptase identifies the mast cell origin of the malignant cells. The tumor cells are seen migrating through the epidermis (epidermotrophism). **D,** Immunohistologic staining for CD117 is also positive in the malignant mast cells, which in this image are adjacent to sweat glands in the superficial subcutaneous fat. (Courtesy of Professor H-P Horny.)

TABLE 17.5. PROGNOSTIC SCORING OF SYSTEMIC MASTOCYTOSIS WITH THE INCLUSION OF NEXT-GENERATION SEQUENCING

Variable	Score allotment
Platelet count $<150\times10^9$/L	2 points
Serum albumin <35 g/L	1.5 points
Hemoglobin <10 g/dL or red blood cell transfusion dependence	1 point
Age >60 years	1.5 points
ASXL1 mutation	1.5 points
Risk score (cumulative points)	Median survival
Low risk (0–1.5)	86 months
Intermediate risk (2–4.5)	21 months
High risk (5–7.5)	5 months

Source: Scherber RM, Borate U. *Br J Haematol* 2018;180:11–23. Reproduced with permission of John Wiley & Sons.

growth factor receptor β (*PDGFRB*) at 5q31–33; (iii) fibroblastic growth factor receptor 1 (*FGFR1*) at 8p11; and (iv) Janus kinase 2 (*JAK2*) at 9p24. More than 35 different fusion genes have been associated with chronic eosinophilic leukemia (CEL) or an eosinophil myeloproliferative disease. The most common is *FIP1L1-PDGFRA*, generated by an 800 kb interstitial deletion on chromosome 4q12 that is not visible cytogenetically.

CEL has a male preponderance. The disease may be associated with marrow fibrosis and terminate as acute myeloid leukemia. The *FIP1L1-PDGFRA*-positive and *PDGFRB*-positive patients respond to tyrosine kinase inhibitors.

Eosinophilia–myeloproliferative disease "8p11" is associated with rearrangement of *FGFR1* caused by 8p11 translocations. The patients show a myeloproliferative/myelodysplastic disease with usually marked eosinophilia in the blood. There is a high incidence of associated T-cell acute lymphoblastic leukemia (T-ALL) or acute myeloid leukemia (AML) or non-Hodgkin lymphoma. The disease often rapidly transforms into AML.

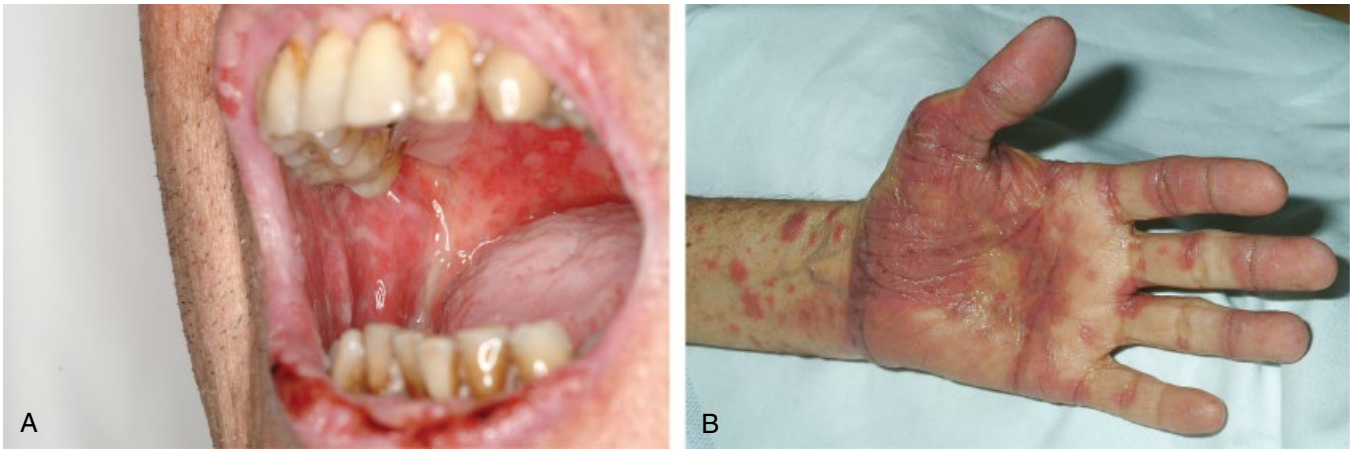

Fig. 17.18. Paraneoplastic pemphigus. **A,** Oral mucosal lesion showing bright red, bleeding, and denuded mucosa. **B,** Skin showing thin-walled blisters and widespread violaceous plaques. The patient had underlying systemic mastocytosis.

TABLE 17.6. WHO (2016): MOLECULAR AND GENETIC ABNORMALITIES IN MYELOID/LYMPHOID NEOPLASMS ASSOCIATED WITH EOSINOPHILIA

Disease	Presentation	Genetics	Treatment
PDGFRA	Eosinophilia ↑Serum tryptase ↑Marrow mast cells	Cryptic deletion at 4q12 *FIP1L1-PDGFRA*, at least 66 other partners	Respond to TKI
PDGFRB	Eosinophilia Monocytosis mimicking CMML	t(5;12)(q32;p13.2) *ETV6-PDGFRB*, at least 25 other partners	Respond to TKI
FGFR1	Eosinophilia Often presents with T-ALL or AML	Translocations of 8p11.2 *FGFR1*—various partners	Poor prognosis; do not respond to TKI
PCM1-JAK2	Eosinophilia Rarely presents with T-LBL or B-ALL Bone marrow shows left-shifted erythroid predominance and lymphoid aggregates	t(8;9)(p22;p24.1) *PCM1-JAK2*	May respond to JAK2 inhibitors

↑, Increased.
TKI, tyrosine kinase inhibitor; T-ALL, T-cell acute lymphoblastic leukemia; AML, acute myeloid leukemia; T-LBL, T-cell lymphoblastic lymphoma; B-ALL, B-cell acute lymphoblastic leukemia.
Source: Arber DA, et al. *Blood* 2016;128:462–463. Reproduced with permission of *Blood: Journal of the American Society of Hematology*.

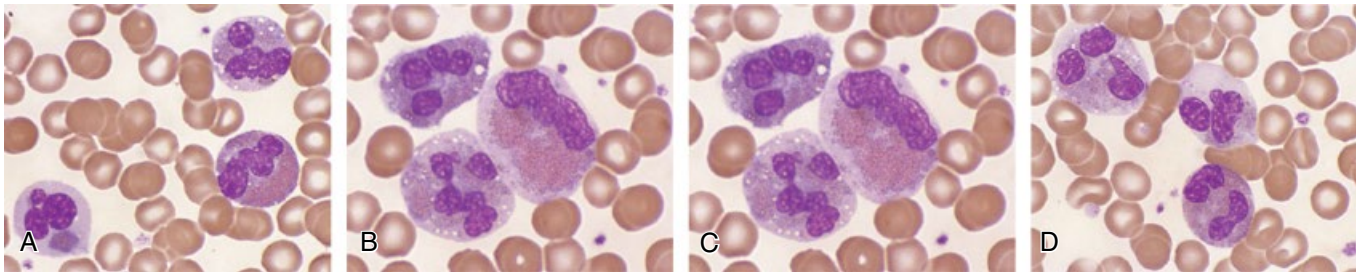

Fig. 17.19. Chronic eosinophilic leukemia: Peripheral blood film. *FIPL1-PDGFRA* positive, *BCR-ABL1* negative, cytogenetics normal. (Hb, 11.0 g/dL, WBC, 45.0×10^9/L; eosinophils, 37.4×10^9/L; eosinophil myelocytes and promyelocytes, 2.7×10^9/L; platelets, 190×10^9/L). Compleet remission was achieved by treatment with imatinib.

CHRONIC MYELOMONOCYTIC LEUKEMIA

Chronic myelomonocytic leukemia (CMML) (Table 17.7) is a myeloproliferative/myelodysplastic syndrome characterized by a persistent monocytosis of $\geq 1.0 \times 10^9$/L and monocytes accounting for more than 10% of the white blood cells (WBC) in the peripheral blood, the absence of the *BCR-ABL1* fusion gene, <20% blasts in the marrow, and dysplasia in one or more myeloid lineage (Fig. 17.20). The blood monocytes may appear normal or show abnormal granulation, unusual nuclear lobe formation, or finely dispersed chromatin (Figs. 17.21 and 17.22). Dysgranulopoiesis is usually present. There may be anemia and thrombocytopenia, both mild at presentation. The bone marrow is usually hypercellular with granulocytic hyperplasia with increased monocytes, dyserythropoiesis that may also show ringed sideroblasts, and micromegakaryocytes. CMML on molecular and clinical grounds has been separated into a proliferative type with WBC $\geq 13 \times 10^9$/L and dysplastic type with WBC $< 13 \times 10^9$/L. CMML is divided by WHO 2016 into three prognostic groups: CMML-0 with <2% blasts in the blood and <5% in the marrow, CMML-1 with 2–4% blasts in the blood and 5–9% in the marrow and CMML-2 with 5–19% blasts in the blood and 10–19% in the marrow and/or if Auer rods are present. Cytogenetic changes are rare and not specific and may include +8, −7/del (7q), and abnormalities of 12. Frequent gene mutations include *TET2*, *SRSF2*, *ASXL1*, and mutations of the RAS pathway. Mutations of *JAK2*, *CALR*, or *MPL* suggest a myeloproliferative disease with monocytosis.

ATYPICAL CHRONIC MYELOID LEUKEMIA, *BCR-ABL1* −

Atypical chronic myeloid leukemia (Table 17.8), *BCR-ABL1* negative (aCML) is defined by a WBC $\geq 13 \times 10^9$/L with $< 1 \times 10^9$/L monocytes and shows in most cases dysgranulopoiesis and in a third of patients mutations in *SETBP1* and/or *ETNK1*. In two-thirds of aCML *ASXL1* and *SRSF2* mutations can be found, comutated in some cases with *SETBP1*. Neutrophil precursors occur in the peripheral blood, but blasts have to be <20% in the blood or bone marrow (Fig. 17.23). A detection of *CSF3R* mutation should lead to a morphologic review to exclude borderline cases from chronic neutrophilic leukemia (CNL).

TABLE 17.7. WHO (2016): DIAGNOSTIC CRITERIA FOR CHRONIC MYELOMONOCYTIC LEUKEMIA

1. Peripheral blood monocytosis of $>1 \times 10^9$/L
2. Absence of the Philadelphia Chromosome or the *BCR-ABL1* fusion oncogene
3. Absence of *PDGFRA*[a] or *PDGFRB*[a] rearrangements
4. Less than 20% blasts[b] in the peripheral blood and/or the bone marrow
5. Dysplasia present in one or more myeloid lineages.
   If myelodysplasia is minimal or absent, CMML can still be diagnosed if: an acquired, clonal cytogenetic or molecular abnormality is demonstrated in the hematopoietic stem cell OR

If peripheral blood monocytosis has persisted for greater than 3 mo, and all other causes of monocytosis have been excluded

[a] Platelet-derived growth factor A and platelet-derived growth factor B.

[b] Blasts include myeloblasts, monoblasts, and promonocytes.

Source: Patnaik MM, Tefferi A. *Am J Hematol* 2016;91:631–642. Reproduced with permission of John Wiley & Sons.

MYELODYSPLASTIC/ MYELOPROLIFERATIVE NEOPLASMS WITH RING SIDEROBLASTS AND THROMBOCYTOSIS

This disorder shows anemia, 15% or more ringed sideroblasts in the marrow, erythroid and megakaryocytic dysplasia, and platelet counts $\geq 450 \times 10^9$/L (Fig. 17.24). It is now a full entity in WHO 2016 classification (Table 17.9). The *SF3B1* mutation is present in 80–90%, often being comutated with *JAK2* V617F in about 60% the patients. *MPL* W515 mutations are present in a minority of the *JAK2* V617F-negative patients.

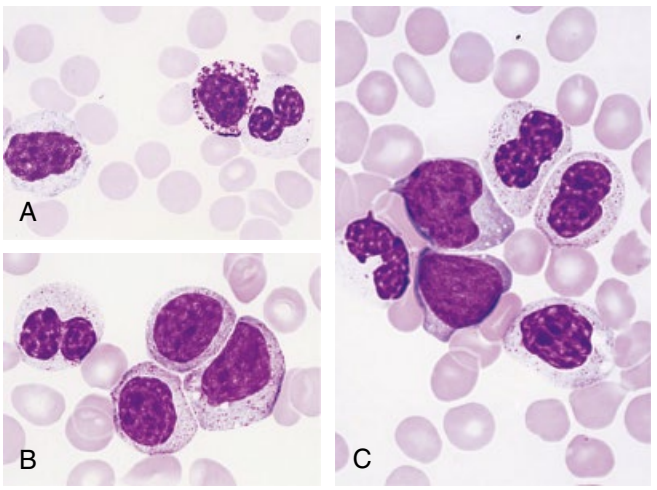

Fig. 17.20. Chronic myelomonocytic leukemia (CMML). **A–C,** Peripheral blood films showing white cells in CMML. Many atypical myelomonocytic cells and pseudo-Pelger neutrophils, some agranular, are shown.

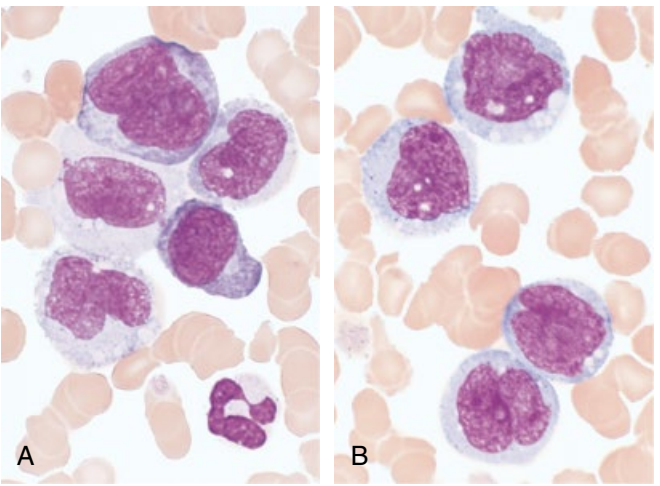

Fig. 17.21. Chronic myelomonocytic leukemia (CMML): Myelodysplastic syndrome. **A, B,** Peripheral blood films showing white cells in CMML. Most cells are more monocytoid than those in Fig. 17.22, and the neutrophil shown is agranular.

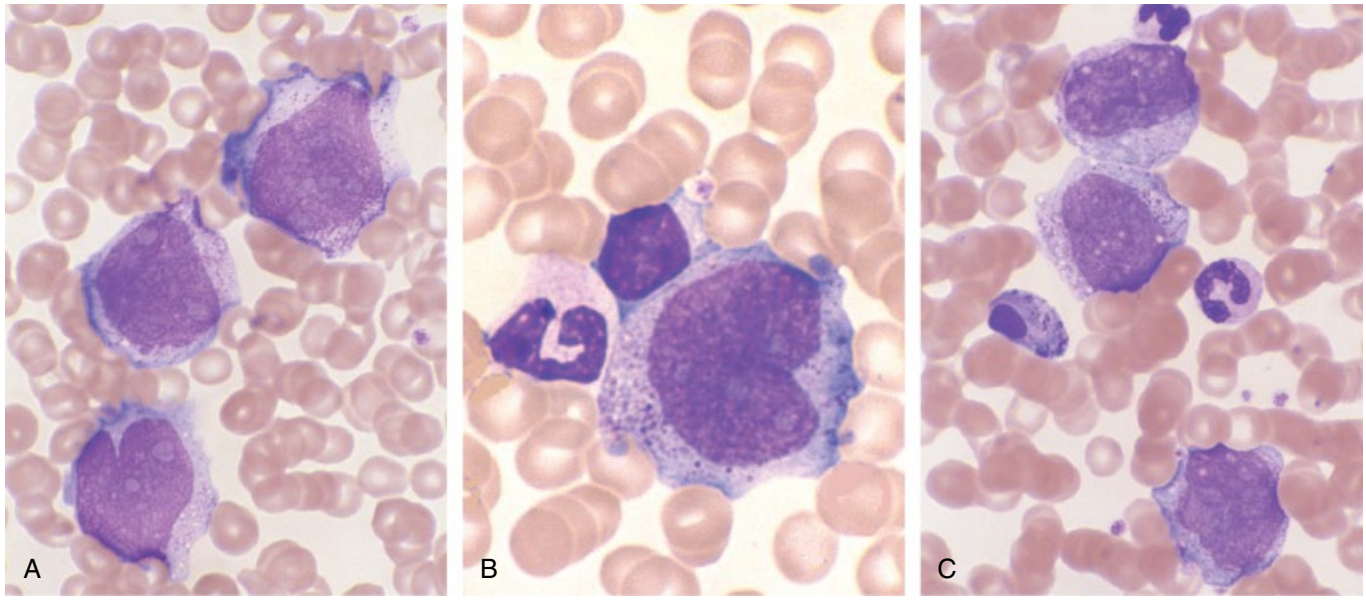

Fig. 17.22. Chronic myelomonocytic leukemia (CMML): **A–C,** Peripheral blood films showing promonocytyes and a monoblast.

TABLE 17.8. WHO (2016): DIAGNOSTIC CRITERIA FOR ATYPICAL CHRONIC MYELOID LEUKEMIA, *BCR-ABL1*-NEGATIVE

PB leukocytosis due to increased numbers of neutrophils and their precursors (promyelocytes, myelocytes, metamyelocytes) comprising ≥10% of leukocytes)
Dysgranulopoiesis, which may include abnormal chromatin clumping
No or minimal absolute basophilia; basophils usually <2% of leukocytes
No or minimal absolute monocytosis; monocytes <10% of leukocytes
Hypercellular BM with granulocytic proliferation and granulocytic dysplasia, with or without dysplasia in the erythroid and megakaryocytic lineages
<20% blasts in the blood and BM
No evidence of *PDGFRA*, *PDGFRB*, or *FGFR1* rearrangement, or *PCM1-JAK2*
Not meeting WHO criteria for *BCR-ABL1*+ CML, PMF, PV, or ET

Source: Arber DA, et al. *Blood* 2016;127:2391–2405. Reproduced with permission of *Blood: Journal of the American Society of Hematology*.

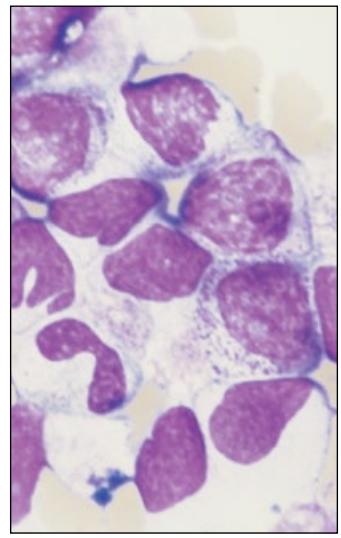

Fig. 17.23. Atypical chronic myeloid leukemia: Ph chromosome negative, *BCR-ABL1* rearrangement negative. Bone marrow aspirate showing myelocytes, metamyelocytes, and features of myelodysplasia.

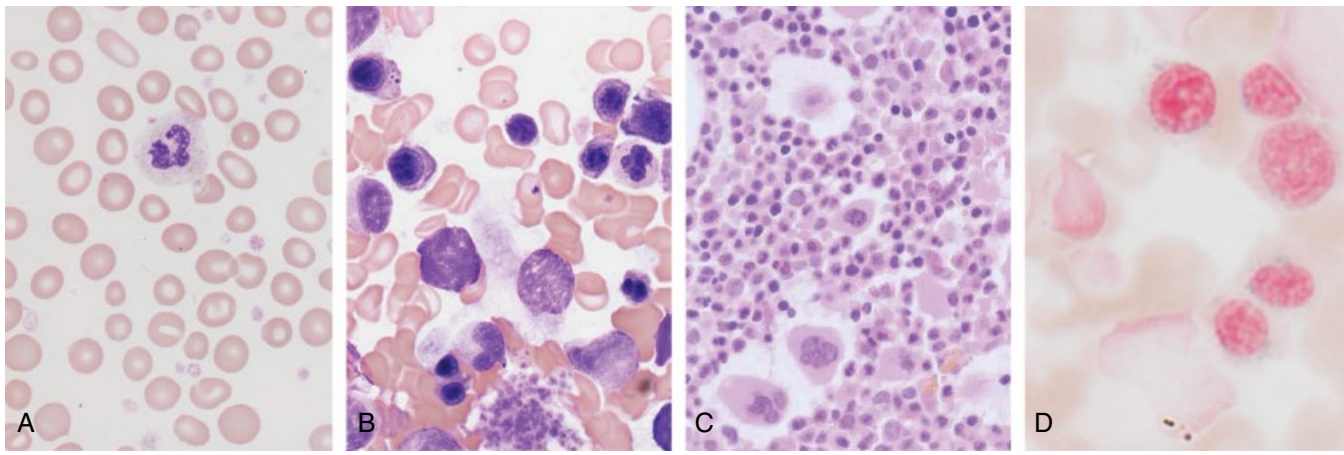

Fig. 17.24. Refractory anemia with ring sideroblasts associated with marked thrombocytosis (MDS/MPN-RS-T). **A,** Peripheral blood film shows marked red cell anisocytosis with increased platelets. **B,** Bone marrow aspirate shows dyserythropoesis with bi- and tri-nucleated erythroblasts. **C,** Trephine biopsy shows increased megakaryocytes with mononuclear forms. **D,** Perls' stain shows ring sideroblasts. (Courtesy of Dr.W Erber.).

JUVENILE MYELOMONOCYTIC LEUKEMIA

Juvenile myelomonocytic leukemia (JMML) is a disease of children characterized by overproduction of myeloid cells that infiltrate the bone marrow and systemic tissues (Table 17.10). There is often marked lymphadenopathy and eczematoid rash (Fig. 17.25). The blood film shows myelomonocytoid cells usually with anemia and thrombocytopenia (Figs. 17.26 and 17.27). Up to 30% of patients progress to AML. A characteristic in vitro feature of the disease is that the cells are exquisitely sensitive to the growth factor granulocyte–macrophage colony-stimulating factor (GM-CSF) and form abnormal numbers of colonies in culture. Children with two genetic disorders, Noonan syndrome (NS) and neurofibromatosis 1 (NF1), are at increased risk of developing JMML, as well as, more rarely, monocytosis or transient myelomonocytic disorders. About 90% have somatic or germline mutations of *NF1*, *PTPN11*, *KRAS*, or *NRAS*. Acquired mutations in the bone marrow in the genes *NF1* or *PTPN11* are present in cases of JMML not associated with NS or NF1. The protein products of both genes are involved in the RAS signaling pathway (Fig. 17.28). RAS activation to the guanosine triphosphate (GTP) state is necessary for its intracellular signaling in the RAS/MAPK pathway from external stimuli such as growth factors, including GM-CSF. In addition to mutations of *PTPN11* and *NF1*, mutations of *NRAS* and *KRAS2* have been found in about 25% of cases of JMML. These mutations introduce amino acid substitutions that result in proteins that remain in the GTP-bound active conformation because of resistance to GTPase-activating protein, as well as lack of intrinsic GTPase activity.

NOONAN SYNDROME

This dominant developmental disorder is characterized by short stature; facial abnormalities, including hypertelorism, low-set ears, and ptosis (Figs. 17.29 and 17.30); cardiac defects; skeletal

TABLE 17.10. WHO (2016): DIAGNOSTIC CRITERIA FOR JUVENILE MYELOMONOCYTIC LEUKEMIA

I. Clinical and hematologic features (all four features mandatory)
PB monocyte count ≥1 × 10^9/L
Blast percentage in PB and BM <20%
Splenomegaly
Absence of Philadelphia chromosome (*BCR/ABL1* rearrangement)
II. Genetic studies (one finding sufficient)
Somatic mutation in *PTPN11*[a] or *KRAS*[a] or *NRAS*[a]
Clinical diagnosis of NF1 or *NF1* mutation
Germline CBL mutation and loss of heterozygosity of CBL[b]
III. For patients without genetic features, besides the clinical and hematologic features listed under I, the following criteria must be fulfilled:
Monosomy 7 or any other chromosomal abnormality or at least two of the following criteria:
Hemoglobin F increased for age
Myeloid or erythroid precursors on PB smear
GM-CSF hypersensitivity in colony assay
Hyperphosphorylation of STAT5

[a] Germline mutations (indicating Noonan syndrome) need to be excluded.
[b] Occasional cases with heterozygous splice site mutations.
Source: Arber DA, et al. *Blood* 2016;127:2391–2405. Reproduced with permission of *Blood: Journal of the American Society of Hematology*.

TABLE 17.9. WHO (2016): DIAGNOSTIC CRITERIA FOR MYELODYSPLASTIC/MYELOPROLIFERATIVE NEOPLASMS WITH RING SIDEROBLASTS AND THROMBOCYTOSIS

Anemia associated with erythroid lineage dysplasia with or without multilineage dysplasia, ≥15% ring sideroblasts,[a] <1% blasts in PB and <5% blasts in the BM
Persistent thrombocytosis with platelet count ≥450 × 10^9/L
Presence of a *SF3B1* mutation or, in the absence of *SF3B1* mutation, no history of recent cytotoxic or growth factor therapy that could explain the myelodysplastic/myeloproliferative features[b]
No *BCR-ABL1* fusion gene, no rearrangement of *PDGFRA*, *PDGFRB*, or *FGFR1*; or *PCM1-JAK2*; no (3;3)(q21;q26), inv(3)(q21q26) or del(5q)[c]
No preceding history of MPN, MDS (except MDS-RS), or other type of MDS/MPN

[a] At least 15% ring sideroblasts required even if *SF3B1* mutation is detected.
[b] A diagnosis of MDS/MPN-RS-T is strongly supported by the presence of *SF3B1* mutation together with a mutation in *JAK2* V617F, *CALR*, or *MPL* genes.
[c] In a case which otherwise fulfills the diagnostic criteria for MDS with isolated del(5q)-no or minimal absolute basophilia; basophils usually <2% of leukocytes.
MPN, myeloproliferative neoplasms; MDS, myelodysplastic syndrome; MDS-RS, MDS with ring sideroblasts.
Source: Arber DA, et al. *Blood* 2016;127:2391–2405. Reproduced with permission of *Blood: Journal of the American Society of Hematology*.

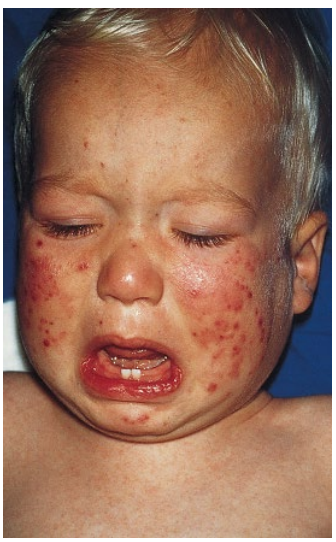

Fig. 17.25. Juvenile chronic myeloid leukemia: Eczematoid facial rash and lip bleeding in an eight-month-old infant. There was moderate splenomegaly. Cytogenetic studies failed to demonstrate the presence of the Ph chromosome. (Hb, 10.5 g/dL; WBC, 120 × 10^9/L; platelets, 85 × 10^9/L.) (Courtesy of Professor JM Chessells.)

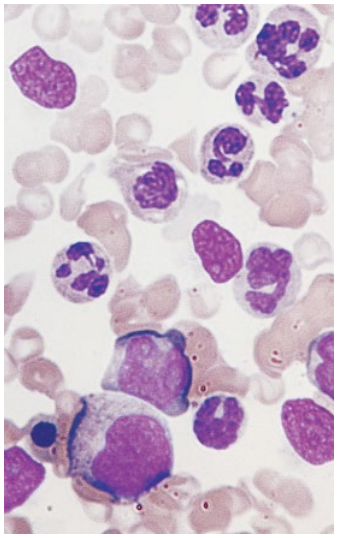

Fig. 17.26. Juvenile chronic myeloid leukemia: Peripheral blood film from the infant in Fig. 17.25 shows a predominance of myelomonocytoid cells.

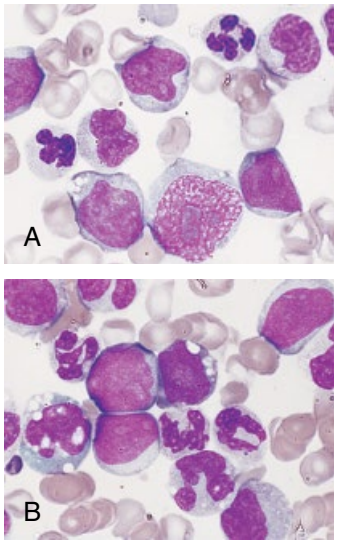

Fig. 17.27. Juvenile chronic myeloid leukemia. **A, B,** Peripheral blood films showing occasional blast forms, myelomonocytic cells, and atypical agranular band and segmented neutrophils.

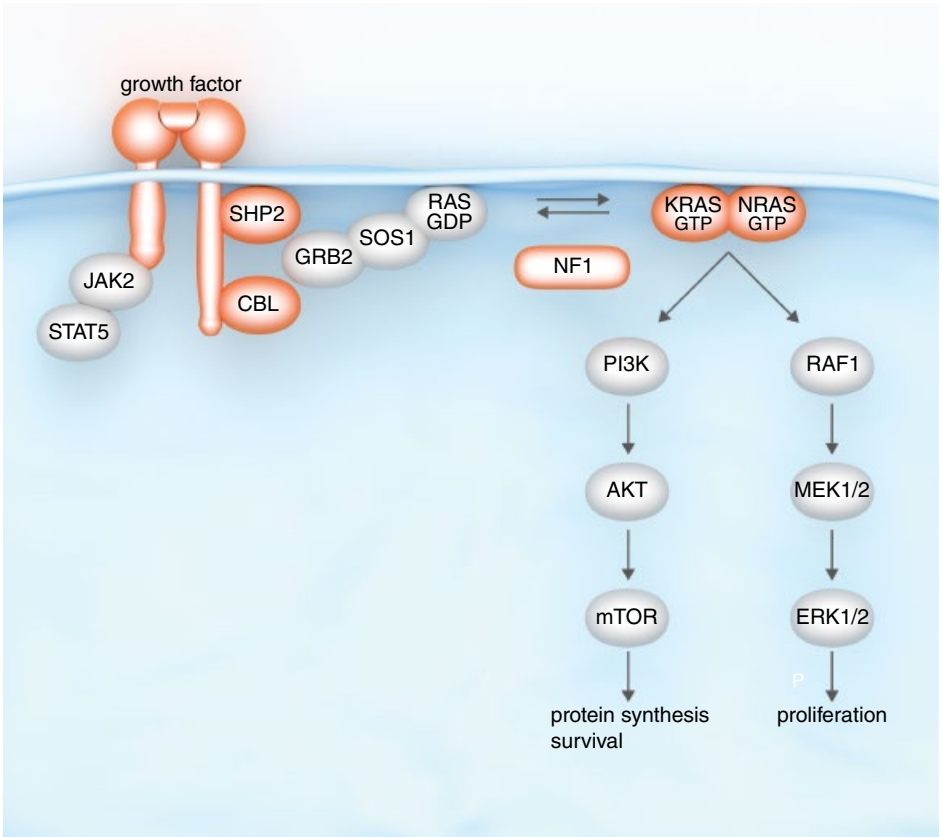

Fig. 17.28. The RAS signaling pathway and genes mutated in juvenile myelomonocytic leukemia (in black). Source: Niemeyer C. Haematologica 2014; 99(11): 1653–1662.

abnormalities; mental retardation; genitourinary defects; and factor XI deficiency. About half of these patients have germline missense mutations of the gene *PTPN11*, encoding a tyrosine phosphatase SHP-2 involved in the RAS signaling pathway (Fig. 17.28). Mutations in *SOS1, KRAS*, and *RAF1* have also been described in NS. Approximately a third of patients with NS develop JMML.

NEUROFIBROMATOSIS 1

Individuals with NF1 mutations are at increased risk of benign and malignant diseases that arise in the embryonic neural crest. Children (but not adults) with NF1 are also predisposed to JMML and, less frequently, other myeloid malignancies. The *NF1* gene codes for neurofibromin, which acts as a GTPase-activating protein. This appears to act as a tumor suppressor gene for JMML.

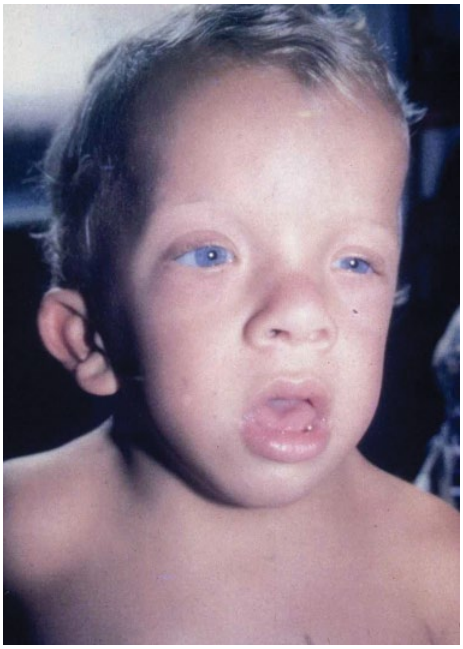

Fig. 17.29. Noonan syndrome. Young child showing facial features of Noonan syndrome, including hypertelorism, ptosis, and low-set ears. (Courtesy of Professor MA Patton.)

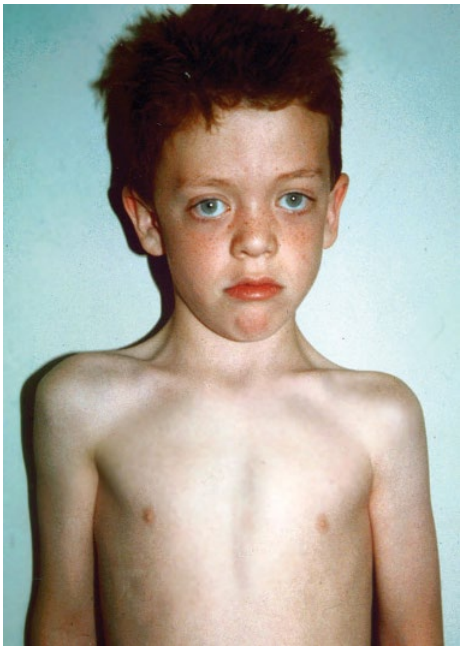

Fig. 17.30. Noonan syndrome. Older child showing neck webbing and pectus excavatum. (Courtesy of Professor MA Patton.)

CHAPTER

18

CHRONIC LYMPHOCYTIC LEUKEMIA AND OTHER MATURE B- AND T-CELL LEUKEMIAS

The mature lymphoid neoplasms presenting with leukemic expression are a heterogeneous group of B- and T/NK-cell tumors that in most instances have an indolent clinical course. However, some entities, particularly of T/NK-cell phenotype, have a very aggressive evolution (Table 18.1). The use of the term leukemia refers to the common involvement of the peripheral blood and bone marrow in these diseases but in all of them the tumor cells can infiltrate tissues, particularly lymph nodes and spleen but also extranodal sites. Other lymphoid neoplasms classified as lymphomas mainly occur with involvement of tissues, particularly lymph nodes. However, in most of these diseases the tumor cells may also "spill over" into the peripheral blood in a leukemic phase. This occurs particularly in mantle cell lymphoma and splenic marginal zone lymphoma, but can be also seen in follicular lymphoma, lymphoplasmacytic lymphoma, diffuse large cell lymphoma, and plasma cell myeloma (plasma cell leukemia). This chapter reviews the diseases developing primarily as leukemias and Chapters 19–23 deal with the lymphomas and plasma cell neoplasms.

MATURE B-CELL LEUKEMIAS

CHRONIC LYMPHOCYTIC LEUKEMIA

Chronic lymphocytic leukemia (CLL) is a neoplasm composed of monoclonal small mature B-cells that usually coexpress CD5 and CD23 with low-density surface immunoglobulin. There must be $\geq 5 \times 10^9$/L of these cells in the peripheral blood that persist for at least 3 months. The cells accumulate predominantly in the blood, bone marrow, spleen, liver, and lymph nodes. Individuals with $<5 \times 10^9$/L clonal cells with the CLL phenotype and without lymphadenopathy, organomegaly, or other extramedullary disease are considered to have monoclonal B-cell lymphocytosis (MBL). Small lymphocytic lymphoma (SLL) and CLL are the same disease. The term SLL is used for cases with $<5 \times 10^9$/L circulating CLL cells and documented nodal, splenic, or other extramedullary involvement by CLL cells.

TABLE 18.1. MATURE LYMPHOID LEUKEMIAS

Mature B-cell neoplasms
Chronic lymphocytic leukemia/small lymphocytic lymphoma
B-cell prolymphocytic leukemia
Hairy cell leukemia
Hairy cell leukemia variant
Mature T-cell neoplasms
T-cell prolymphocytic leukemia
T-cell large granular lymphocytic leukemia
Adult T-cell leukemia/lymphoma
Aggressive NK-cell leukemia

Clinical Features

CLL is predominantly a disease of the elderly. Clinical manifestations are very variable. Most patients diagnosed with CLL are asymptomatic and the diagnosis is made only when a routine blood test is performed. Symmetric enlargement of the superficial lymph nodes is found except in patients with early stage disease (Figs. 18.1 and 18.2) and, rarely, there is also tonsillar involvement (Fig. 18.3). In advanced disease, there is both splenomegaly and hepatomegaly, and patients with thrombocytopenia can show bruising and extensive skin purpura (Fig. 18.4). Infections frequently result from immunoglobulin deficiency, neutropenia, lymphoid dysfunction, and immunosuppressive therapy. In some patients, herpes zoster (Figs. 18.5 and 18.6) or herpes simplex (Fig. 18.7) infections occur, and oral candidiasis and other infections are also a frequent complication (Fig. 18.8). In advanced disease, normochromic anemia and thrombocytopenia often occur. About 10% of patients develop a

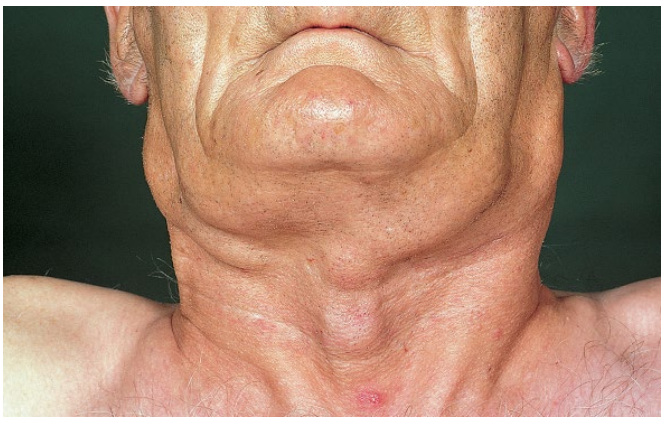

Fig. 18.1. Chronic lymphocytic leukemia: Bilateral cervical lymphadenopathy in a 65-year-old man. (Hb, 12.5 g/dL; WBC, 150×10^9/L [lymphocytes, 140×10^9/L]; platelets, 120×10^9/L.)

Color Atlas of Clinical Hematology: Molecular and Cellular Basis of Disease, Fifth Edition. A. Victor Hoffbrand, Paresh Vyas, Elías Campo, Torsten Haferlach, and Keith Gomez

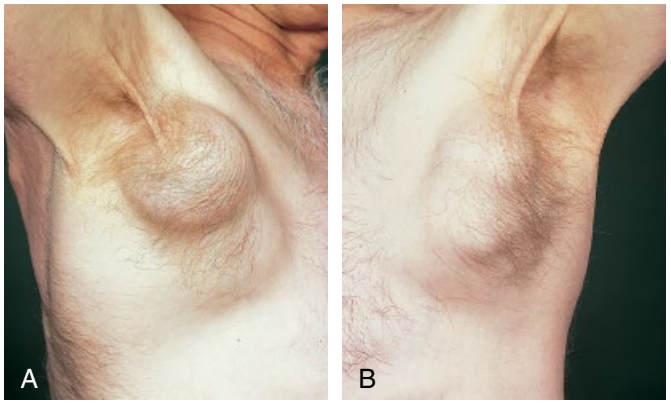

Fig. 18.2. Chronic lymphocytic leukemia. **A,B,** Bilateral axillary lymphadenopathy (same patient as shown in Fig. 18.1).

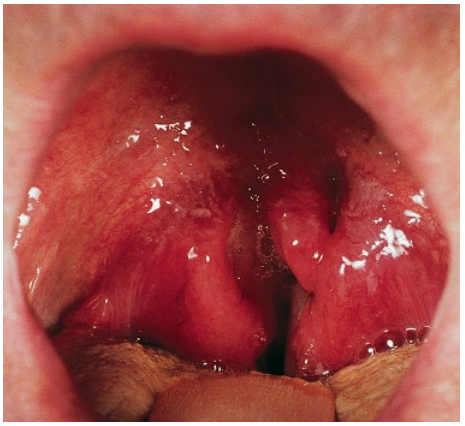

Fig. 18.3. Chronic lymphocytic leukemia: Massive enlargement of the pharyngeal tonsils (same patient as shown in Fig. 18.1).

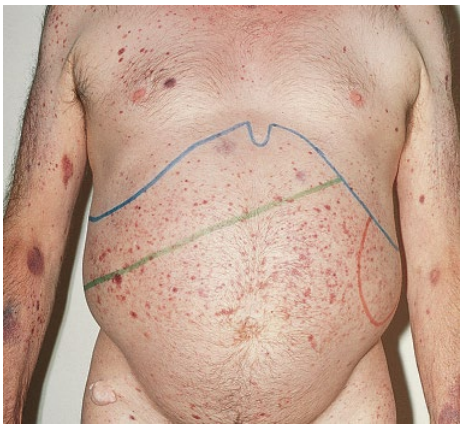

Fig. 18.4. Chronic lymphocytic leukemia: Purpuric hemorrhage and abdominal swelling in a 54-year-old man. The extent of liver and splenic enlargement is indicated. (Hb, 10.9 g/dL; WBC, 250×10^9/L [lymphocytes, 245×10^9/L]; platelets, 35×10^9/L.)

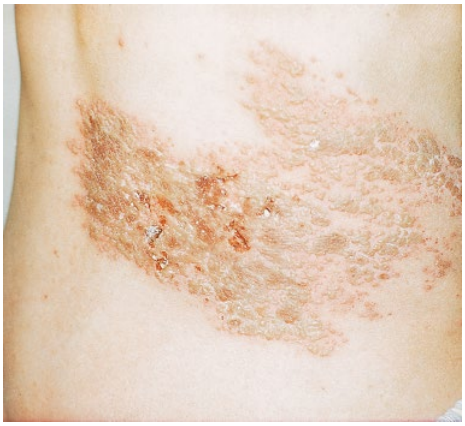

Fig. 18.5. Chronic lymphocytic leukemia: Herpes zoster infection in a 68-year-old woman.

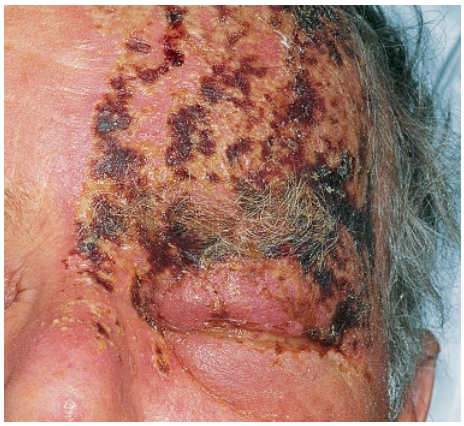

Fig. 18.6. Chronic lymphocytic leukemia: Herpes zoster infection in the territory of the ophthalmic division of the fifth cranial nerve.

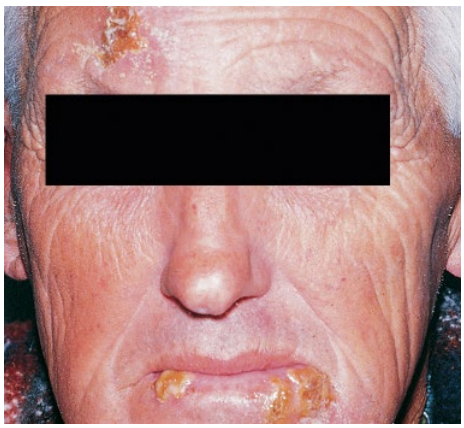

Fig. 18.7. Chronic lymphocytic leukemia: Herpes simplex eruptions of the lower lip and of the skin of the forehead.

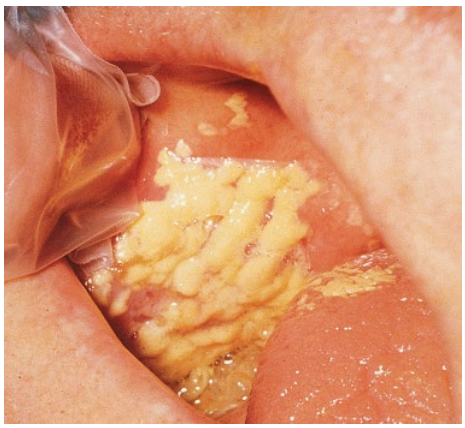

Fig. 18.8. Chronic lymphocytic leukemia: Extensive *Candida albicans* infection of the buccal mucosa of a 73-year-old woman.

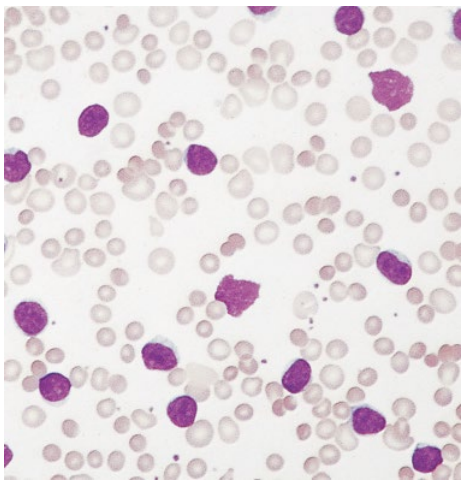

Fig. 18.9. Chronic lymphocytic leukemia with autoimmune hemolytic anemia: peripheral blood film shows increased numbers of lymphocytes, red cell spherocytosis, and polychromasia. The direct antiglobulin test was strongly positive with IgG on the surface of the cells. (Hb, 8.3 g/dL; reticulocytes, 150 × 10^9/L; WBC, 110 × 10^9/L [lymphocytes, 107 × 10^9/L]; platelets, 90 × 10^9/L.)

secondary warm-type autoimmune hemolytic anemia (Fig. 18.9), and in a smaller number of cases an autoimmune thrombocytopenia occurs.

Morphology

The tumor cells in bone marrow and peripheral blood are small lymphocytes with clumped chromatin and scanty cytoplasms (Figs. 18.10 and 18.11). In some cases, prolymphocytes, atypical lymphocytes with irregular nuclei, and occasional larger cells can also be seen in variable proportions but usually less than 15% of the tumor cells. These atypical cells increase in some patients with more advanced and aggressive disease. In some patients, the prolymphocytes increase to more than 55% in prolymphocytc transformation of CLL (Figs. 18.12 and 18.13). Rarely, the lymphocytes show crystalline deposits of immunoglobulin (Fig. 18.14).

Bone marrow examination shows extensive replacement of normal marrow elements by lymphocytes, reaching 30–95% of the marrow cell total. Trephine biopsies (Fig. 18.15) show nodular, interstitial, or diffuse collections of abnormal cells.

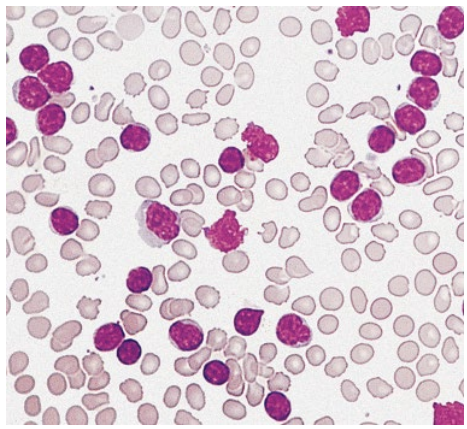

Fig. 18.11. Chronic lymphocytic leukemia: Peripheral blood film showing the increased numbers of lymphocytes and occasional characteristic "smudge" cells. (Hb, 9.0 g/dL; WBC, 190 × 10^9/L; platelets, 70 × 10^9/L.)

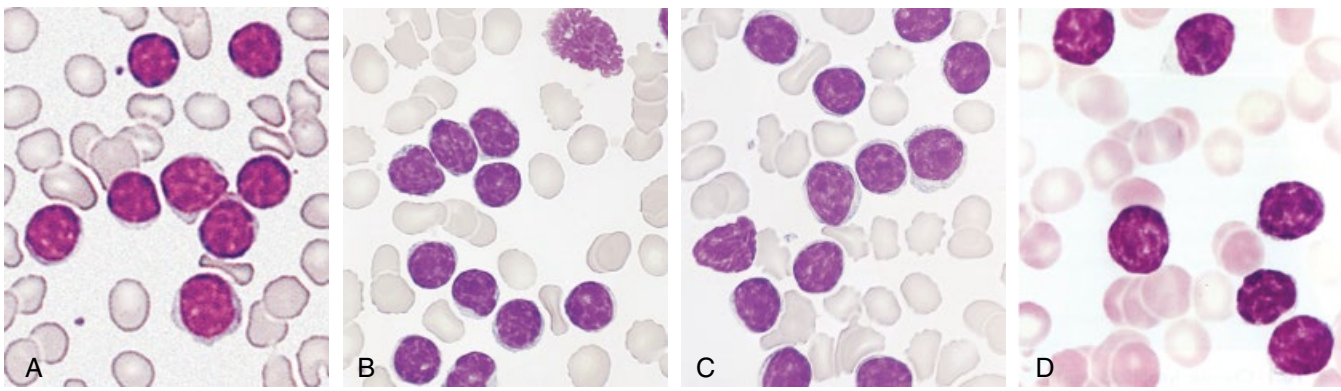

Fig. 18.10. Chronic lymphocytic leukemia. **A–D,** Lymphocytes from the peripheral blood of four different patients show thin rims of cytoplasm, condensed coarse chromatin, and only rare nucleoli.

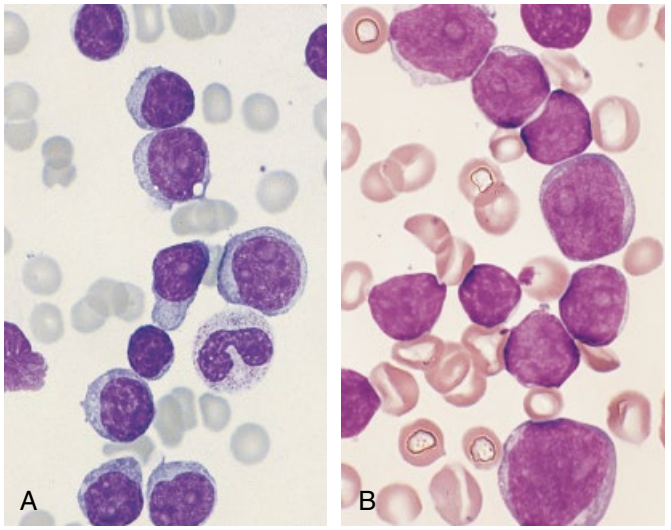

Fig. 18.12. Chronic lymphocytic leukemia with atypical cytological features. **A,B** The circulating lymphoid cells include greater than 10% but less than 55% prolymphocytes.

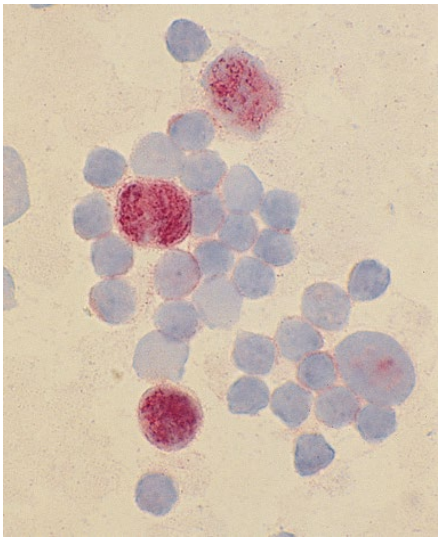

Fig. 18.13. Chronic lymphocytic leukemia: Mixed cell (CLL/PLL) type. Immunoperoxidase reaction using anti-Ki-67 monoclonal antibody to detect proliferating cells. A positive reaction is seen in these cells. (Courtesy of Professor D Catovsky.)

Patients with nodular or interstitial histology have a better prognosis. Immunohistology typically shows the cells to be B cells, C19+, CD20+, CD23+, and CD79+, also expressing CD5 (Fig. 18.16). In patients with autoimmune hemolytic anemia or thrombocytopenia, the spleen is sometimes removed and shows a characteristic histology (Fig. 18.17). Lymph nodes involved by CLL show a characteristic pattern that is also seen in patients with SLL. The lymph node architecture is replaced by a diffuse and monotonous infiltration of small cells with round nuclei and densely clumped heterochromatin (Figs. 18.18A and 18.19). Virtually all patients have regularly distributed pale areas in a background of small darker cells composed of clusters of larger cells with round nucleus and prominent nucleolus (prolymphocytes and paraimmunoblasts). These areas have been called pseudofollicles or proliferation centers because it is in these areas that the tumor cells proliferate (Fig. 18.18B). Occasionally, the neoplastic cells differentiate to a plasma cell stage, but this should not prompt a diagnosis of lymphoplasmacytic lymphoma. SLL can have diffuse or focal involvement of the bone marrow in spite of the low tumor cells counts in the peripheral blood (Figs. 18.20 and 18.21).

Membrane Markers

The results of different membrane markers in chronic B-cell leukemias are shown in Table 18.2. Figure 18.22 illustrates the different phenotypes of the main diseases, and typical findings on fluorescent activated cell sorting (FACS) analysis in CLL are shown in Fig. 18.23. A scoring system using a selection of five

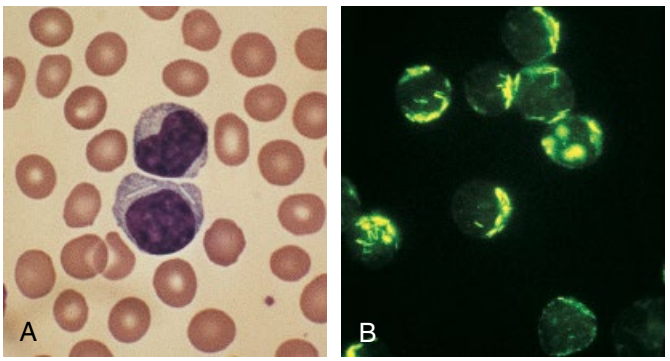

Fig. 18.14. Chronic lymphocytic leukemia: The clonal B cells show crystalline deposits of immunoglobulin. **A,** Jenner–Giemsa stain. **B,** Immunofluorescence. (A, B, Courtesy of Professor TJ Hamblin.)

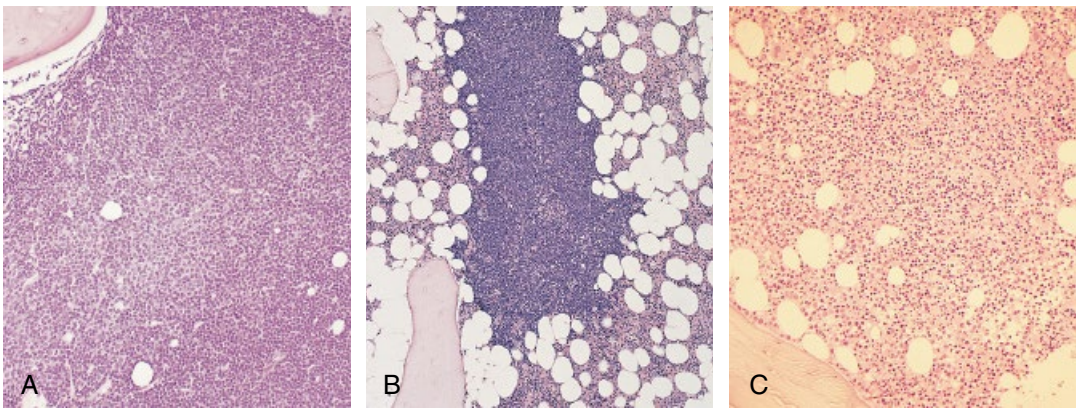

Fig. 18.15. Chronic lymphocytic leukemia. Trephine biopsies showing: **A,** a marked diffuse increase in marrow lymphocytes (closely packed cells with small dense nuclei); **B,** a nodular pattern of lymphocyte accumulation (in a different patient); and **C,** interstitial infiltration.

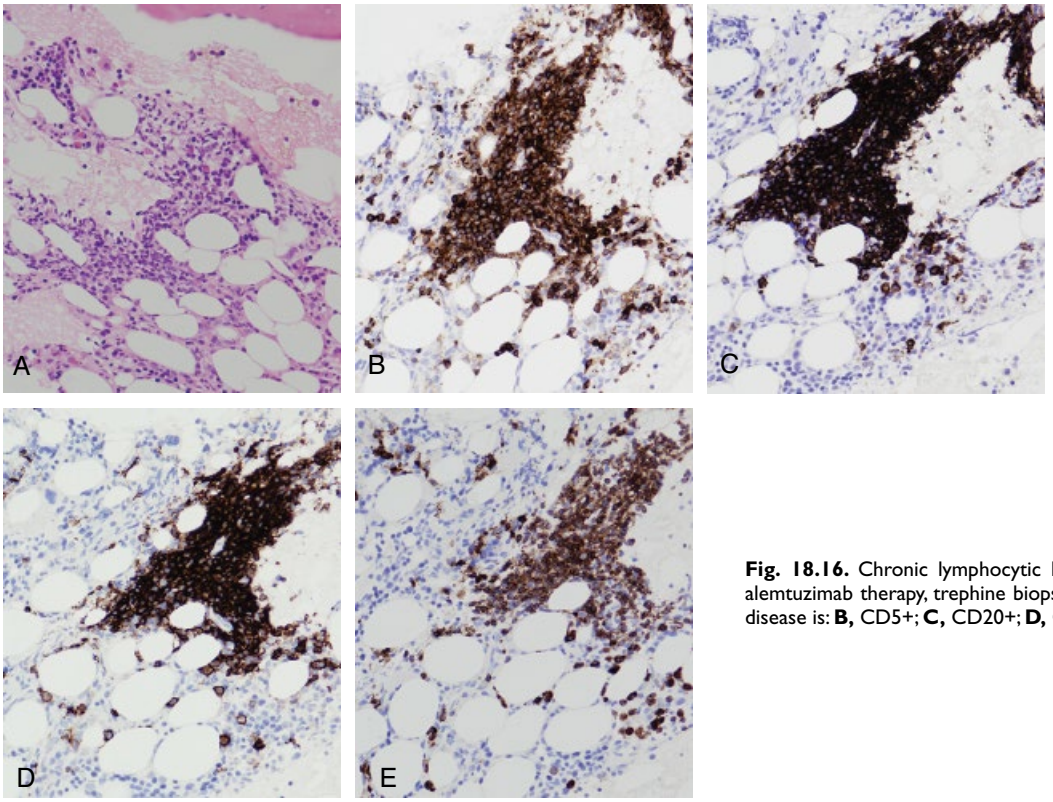

Fig. 18.16. Chronic lymphocytic leukemia: **A,** Residual disease after alemtuzimab therapy, trephine biopsy. Immunohistology shows that the disease is: **B,** CD5+; **C,** CD20+; **D,** CD23+; and **E,** CD79+.

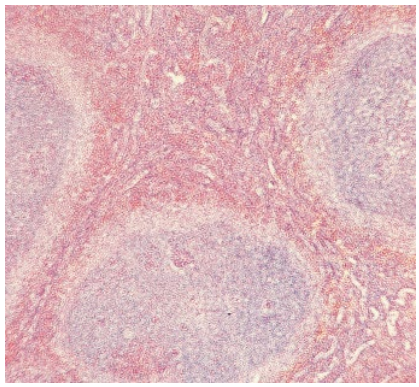

Fig. 18.17. Chronic lymphocytic leukemia: Histologic section of spleen in a patient with secondary autoimmune hemolytic anemia. There is expansion of lymphoid tissue in the periarterial sheaths of the white pulp and obvious red cell entrapment in the reticuloendothelial cords and splenic sinuses.

of these markers has been used to distinguish CLL from other chronic B-lymphoid diseases. Characteristically, in CLL a score of 4 or 5 is obtained: weak expression of SmIg (score 1), negative staining for FMC7 (score 1) and CD79b (score 1), and positive staining for CD5 (score 1) and CD23 (score 1). B-cell disorders other than CLL usually score 0–2.

Cytogenetics

Frequent chromosomal changes detected by fluorescence in situ hybridization (FISH) on interphase cells in CLL are deletions or translocations of the long arm of chromosome 13 at band q14 (55%) (Fig. 18.24), trisomy 12 (+12) (15%), 11q22-23 deletions of (18%), or deletions of 17p13 (5–15%). Other alterations occur, including deletions or translocations of 6q21 (10%), especially in patients in blastic transformation. Deletion 13q14 usually targets two micro-RNAs, mir-15a, mir-16-1, which can be relevant to the disease process. *ATM* and *TP53* are

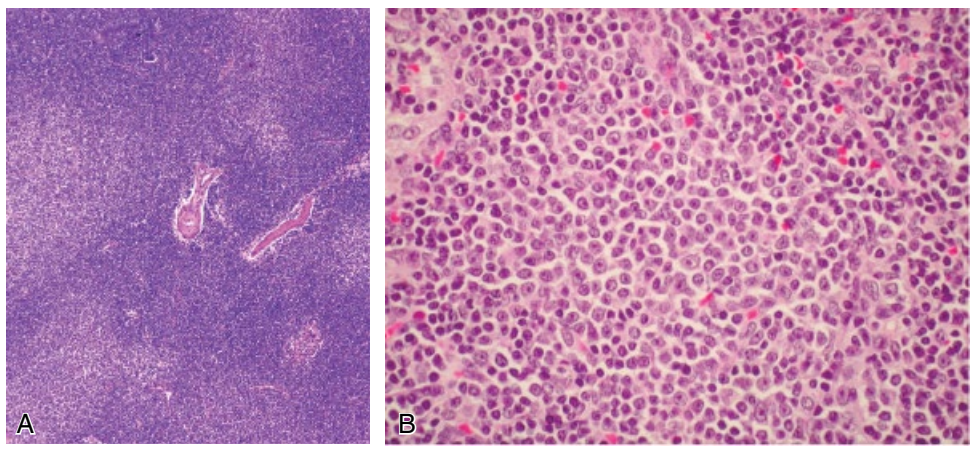

Fig. 18.18. Lymph node infiltration by CLL. **A,** Lymph node shows a diffuse pattern of involvement, with total replacement of the normal architecture by a uniform population of neoplastic lymphocytes. Pale nodular areas correspond to proliferation centers. **B,** High power of a proliferation center in which larger cells with round nucleolus and prominent central nucleolus can be seen.

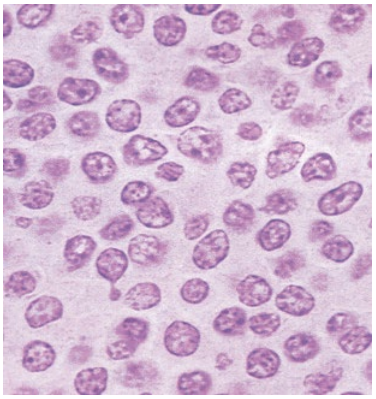

Fig. 18.19. High power of tumor CLL cells in the lymph node. The lymphocytes are small with round nuclei that contain densely clumped heterochromatin.

the main targets of 11q22-23 and 17p13 deletions and are frequently associated with mutations of the genes.

Molecular Features

Immunoglobulin heavy chain variable (IGHV) genes in CLL can be either mutated (<98% identity with the germline) or unmutated (≥98% identity) in 50–70% and 30–50% of cases, respectively. Patients with CLL with mutated IGHV tend to have a more indolent clinical course than patients with unmutated IGHV. The VH family used by CLL cells is highly selected and around 30% of patients have similar if not identical immunoglobulin sequences, a phenomenon designated as "BCR stereotypy." These findings suggest that CLL cells are antigen driven.

DNA methylation studies have identified three epigenetic subgroups of CLL related to different stages of B-cell differentiation: naive B-cells (naive-like); memory B-cells (memory-like); and a subgroup with a signature intermediate between these two (intermediate) that have different biologic characteristics and prognosis. They only partially overlap with the IGHV mutational status.

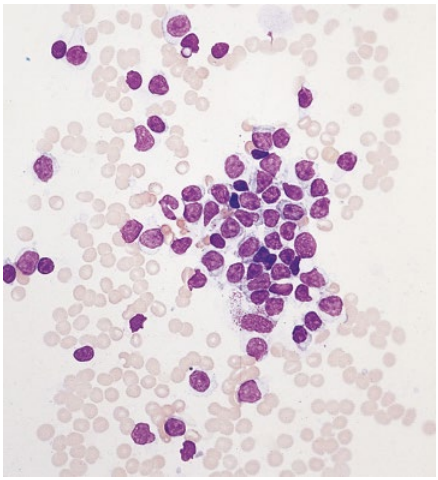

Fig. 18.20. Small lymphocytic lymphoma: Bone marrow aspirate showing dominance of neoplastic lymphocytes in the cell trail.

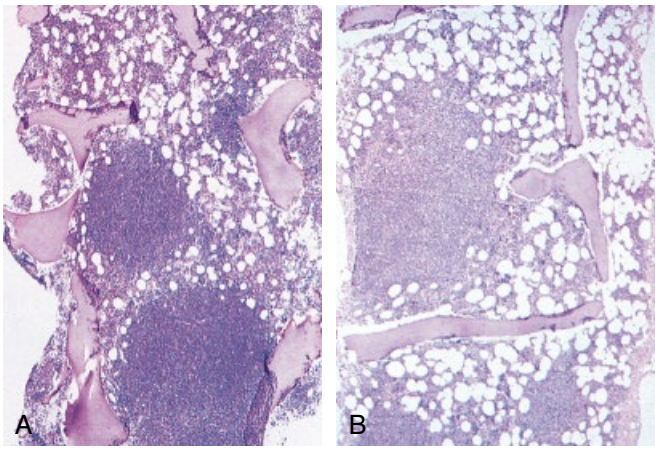

Fig. 18.21. Small lymphocytic lymphoma. **A,B,** Bone marrow trephine biopsies from two patients, showing extensive focal deposits of lymphoma cells.

TABLE 18.2. MEMBRANE IMMUNOPHENOTYPE OF MATURE B-CELL LEUKEMIAS

	CLL	PLL	HCL	HCL-v	SMLZ	FL	MCL	PCL
SIg	+/–	++	++	++	++	+	+	– (cyt Ig⁺)
CD5	+	–	–	–	–	–	+	–
CD19/CD20/37	+	+	+	+	+	+	+	–
FMC7/CD22	–/+	+	+	+	+	+	++	–
CD23	+	–/+	–	–	–	–/+	–	–
CD25	–	–	++	–	–	–	–	–
CD38	–/+	–	–/+	–/+	–	–/+	–	++
CD103/CD123	–	–	+	–	–	–	–	–
HLA-DR	+	+	+	+	+	+	+	–
CD79b	–/+	++	–/+	?	++	++	++	?
CD200	+	–/+	+		+	–/+	–	+/–

CLL, B-cell chronic lymphocytic leukemia; FL, follicular lymphoma; HCL, hairy cell leukemia; HCL-v, hairy cell leukemia variant; MCL, mantle cell lymphoma; PCL, plasma cell leukemia; PLL, prolymphocytic leukemia; SIg, surface immunoglobulin; SMLZ, splenic lymphoma marginal zone (± villous lymphocytes).

Source: Dighiero G, Hamblin TJ. *Lancet* 2008;371:1017. Reproduced with permission of Elsevier.

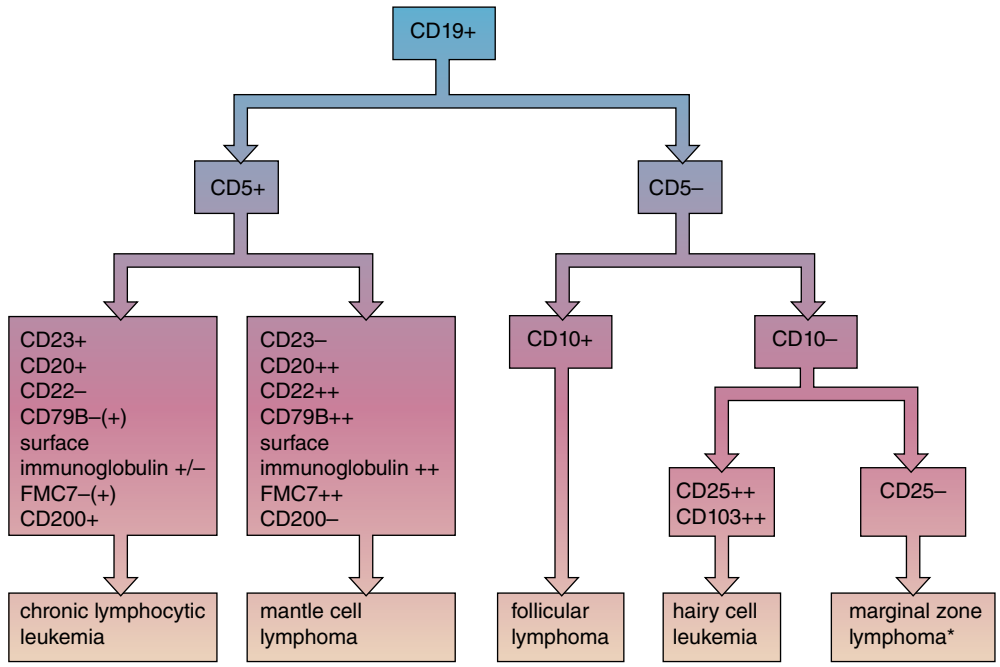

Fig. 18.22. Mature B-cell leukemic lymphoid neoplasms: Differential diagnosis of CLL from other frequent causes of mature B-cell leukemic lymphoid neoplasms. * Suggestive of this lymphoma because there are no specific markers. (Source: Dighiero G, Hamblin TJ. *Lancet* 2008;371:1017. Reproduced with permission of Elsevier.)

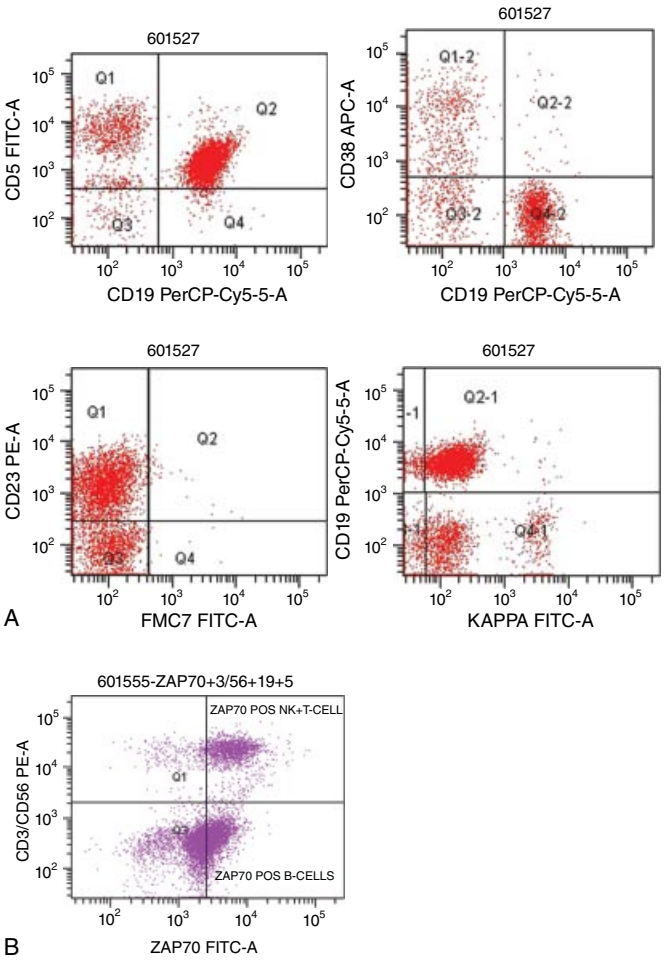

Fig. 18.23. Chronic lymphocytic leukemia: Immunophenotype analysis by fluorescence activated cell sorting (FACS). **A,** In this case the cells are CD19+, CD5+, CD23+, CD38−, FMC7−, κlight chain +. **B,** In this case the cells are ZAP 70+, CD3+, CD56+. (Courtesy of Immunophenotyping Laboratory, Royal Free Hospital.)

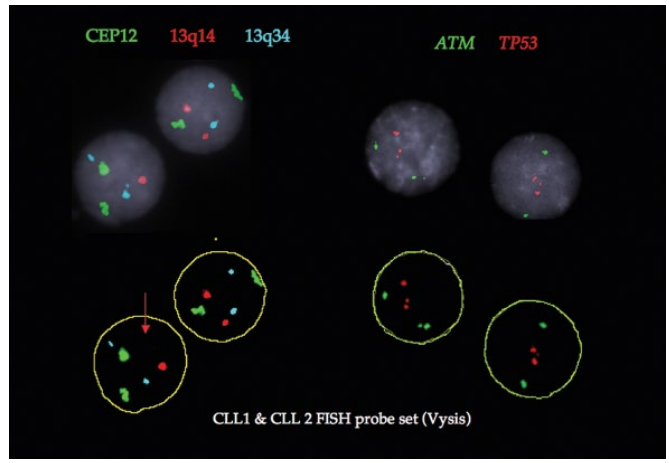

Fig. 18.24. Chronic lymphocytic leukemia: FISH panel (Vysis) screening for the most frequent genetic changes. CLL panel 1 consists of probe CEP 12 (green) for the centromere of chromosome 12 and two probes for chromosome 13 (red and blue). CLL panel 2 consists of probes for the ATM gene (green) and P53 gene (red). In this case the patient showed heterozygous deletion of 13q14 (arrowed) but no other abnormality. The second set of images circled in yellow are the nuclei stained with DAPI to enhance visualization of the FISH signals. (Courtesy of Dr. E Necheva.)

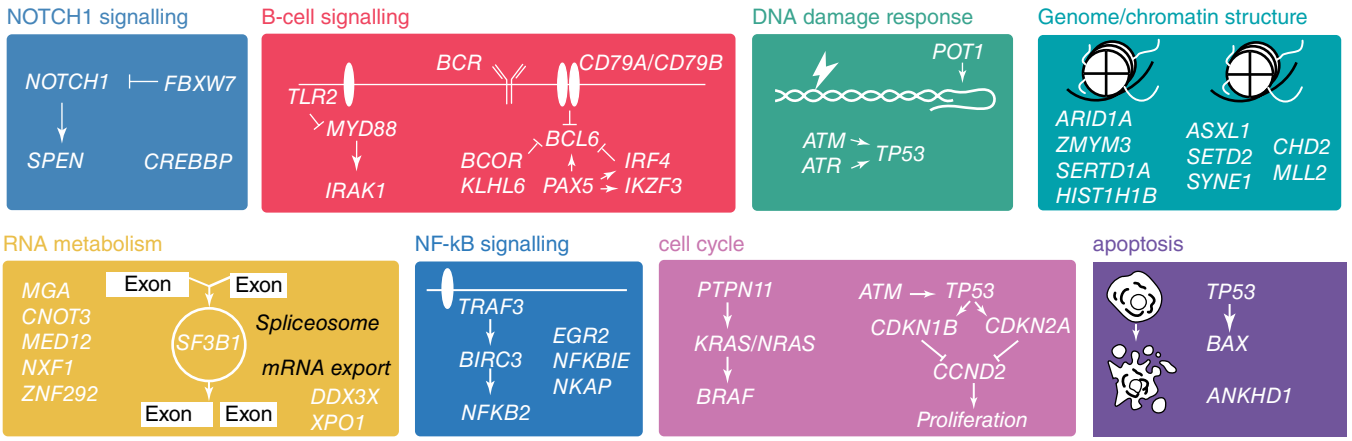

Fig. 18.25. Whole genome/exome sequences of CLL have revealed mutations in many genes that cluster in several biologic pathways (Source: Puente XS, et al. *Nature* 2015;526:519–524. Reproduced with permission of Springer Nature.)

TABLE 18.3. CLASSIFICATION OF CLINICAL STAGES OF CHRONIC LYMPHOCYTIC LEUKEMIA

Rai classification of chronic lymphocytic leukemia	
Stage 0	Lymphocytes >5 × 10^9/L and >40% of bone marrow cells
Stage I	As Stage 0, with enlarged lymph nodes
Stage II	As Stages 0 or I, with enlarged liver and/or spleen
Stage III	As Stages 0, I, or II, with Hb <10 g/dL
Stage IV	As Stages 0, I, II, or III, with platelets <100 × 10^9/L
Revised international (Binet) classification of chronic lymphocytic leukemia	
Group A (good prognosis)	Hb >10 g/dL Platelets >100 × 10^9/L < three sites of palpable organ enlargement
Group B (intermediate prognosis)	Hb >10 g/dL platelets >100 × 10^9/L ≥ three sites of palpable organ enlargement (one site = spleen or liver, or lymph nodes in the neck, axillae, or groin)
Group C (poor prognosis)	Hb <10 g/dL platelets <100 × 10^9/L

Source: Kai KR, et al. *Blood* 1975;46:219–234. Reproduced with permission of *Blood: Journal of the American Society of Hematology.*

TABLE 18.4. CLINICAL AND LABORATORY PROGNOSTIC MARKERS OF CHRONIC LYMPHOCYTIC LEUKEMIA

Prognostic factor	Good	Bad
Stage	Binet A (Rai 0–1)	Binet B,C (Rai 2–4)
Sex	Female	Male
Chromosomes	Deletion 13q14	Trisomy 12,[a] del 17p13, p53 mutations, del 11q22-23 (ATM)
Gene mutations		*TP53, ATM, NOTCH1, SF3B1, BIRC3, POT1, NFKBIE*
Lymphocyte doubling time	>1 year	<6 months
VH immunoglobulin genes	Hypermutated	Unmutated
VH family	Not VH 1-6, VH 3-21	VH 1-69, VH 3-21
ZAP expression	Low	High
CD38 expression	Low	High
Telomeres	Long (negative)	Short (positive)
CLLU.I expression	Low	High
CD49d expression	Low	High
Lipoprotein lipase	High	Low
Serum thymidine kinase	Low	High
Serum β_2-microglobulin	Low	High
Serum CD23	Low	High

[a] Trisomy 12 is not a bad prognostic indicator in some trials using fludarabine-containing regimens.

Recent whole genome/exome sequencing studies have revealed the landscape of somatic mutations in CLL characterized by a few genes mutated in 3–15% of cases (*NOTCH1*, *SF3B1*, *TP53*, *ATM*, *BIRC3*, *POT1*, and *MYD88*) and many other genes mutated at a lower frequency. These mutated genes tend to involve a limited number of pathogenic pathways including NOTCH and BCR signaling, DNA damage response, RNA metabolism, NFκB signaling among others (Fig. 18.25).

Clinical Staging

According to the extent of involvement of different lymphoid organs and the presence or absence of anemia and thrombocytopenia from bone marrow failure, CLL can be divided into a number of clinical stages (Table 18.3). The stage, sex of patient, presence or absence of autoimmune hemolytic anemia or positive direct antiglobulin test, and peripheral blood lymphocytic doubling time have prognostic significance (Table 18.4).

Prognostic Markers

Abnormalities detected by molecular or biochemical tests also give prognostic information. The IGHV mutational status and the epigenetic subgroups are powerful predictors of outcome (Table 18.4). Phenotypic prognostic markers include CD38, ZAP-70, and

TABLE 18.5. IPI-PROGNOSTIC GROUPS OF CHRONIC LYMPHOCYTIC LEUKEMIA

	Favorable	Unfavorable
Age	Under 65 years	Over 65 years
Clinical stage	Binet A or Rai O	Binet B–C or Rai I–IV
Ig VH status	Mutated	Unmutated
TP53 status	No abnormalities	del(17p) and/or TP53 mutated
Serum β_2-microglobulin	Under 3.5 mg/L	Over 3.5 mg/L

Source: International CLL-IPI working group. *Lancet Oncol* 2016;17:779–790. Reproduced with permission of Elsevier.

CD49b expression, as well as serum levels of biologic markers of disease burden (Table 18.4). Individual cytogenetic alterations as well as complex karyotypes (three or more alterations) give important prognostic information. *TP53* mutations and 17p deletions predict for shorter overall survival. Detection is mandatory to orient therapy when the patient requires treatment. Mutations in *NOTCH1*, *SF3B1*, *ATM*, *BIRC3*, and *POT1* among other genes have also been associated with worse outcome.

The International Prognostic Index, introduced in 2016, uses weighted grading of five parameters: age, clinical stage, *TP53* status, IGVH mutation status, and serum β_2-microglobulin to define four groups of low, intermediate, high, and very high risk (Table 18.5).

Richter Syndrome (Diffuse Large B-Cell Lymphoma Transformation)

Some cases of CLL transform into a more aggressive neoplasm, with the local formation (often retroperitoneal) of a mass of a diffuse large B-cell lymphoma. This can be clonally related or unrelated to the original disease. In some cases, circulating large immunoblastic cells can be seen, usually when transformation is present in the marrow (Figs. 18.26–18.29). There is usually loss of CD5 and CD23 expression, and the cells often express ZAP-70 and CD38. Richter transformation occurs more frequently in CLL with unmutated IGVH genes, and *TP53* or *NOTCH1* mutations. Positron emission tomography (PET) scanning can reveal the site of disease transformation (Fig. 18.30). Some patients with CLL develop a transformation into Hodgkin lymphoma, frequently positive for EBV, which can also be clonally related or unrelated to the original disease.

B-CELL PROLYMPHOCYTIC LEUKEMIA

B-cell prolymphocytic leukemia (B-PLL) is a neoplasm characterized by more than 55% of prolymphocytes in the peripheral blood. The blood film shows larger lymphocytes than are found in classic CLL, with round nucleus, condensed chromatin, and prominent nucleolus (Fig. 18.31). Electron microscopy highlights the differences between CLL and B-PLL lymphocytes (Figs. 18.32 and 18.33). The surface marker studies indicate a mature B-cell phenotype with strong expression of surface immunoglobulin, FMC7, CD20, CD79, and CD22, and weaker or negative expression of CD5, CD23, and CD200. This disease usually occurs in the elderly and is associated with marked splenomegaly, absolute lymphocytosis (usually over 100×10^9/L), and minimal lymph node enlargement. The prognosis is worse than for CLL.

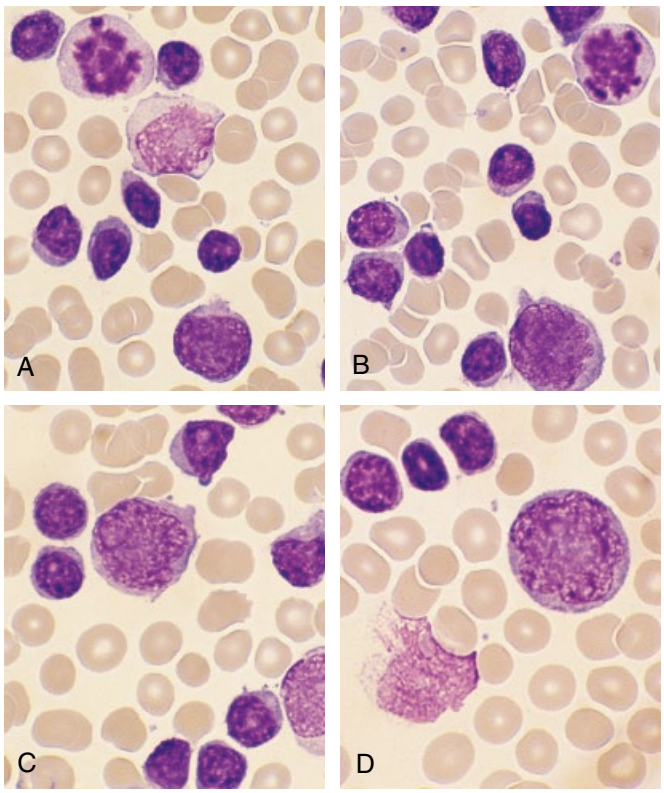

Fig. 18.26. Chronic lymphocytic leukemia. **A–D,** Richter syndrome (large cell transformation). Peripheral blood films showing typical small lymphocytes, large blast cells, and mitotic cells.

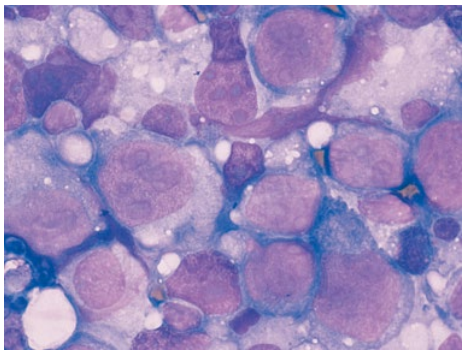

Fig. 18.27. Chronic lymphocyte leukemia: Richter syndrome. Imprint from enlarged lymph node showing large "immunoblastic" cells with multiple prominent nucleoli and a few residual small lymphocytes. (Courtesy of Professor D Catovsky.)

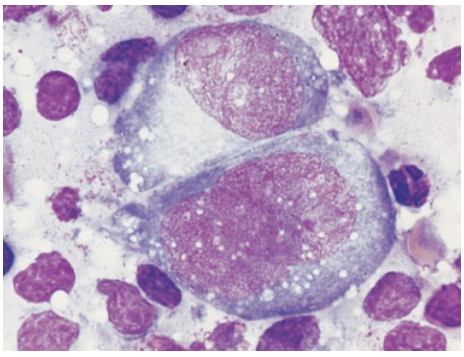

Fig. 18.28. Chronic lymphocytic leukemia: Richter syndrome. Imprint from lymph node showing two large immunoblasts surrounded by small lymphocytes.

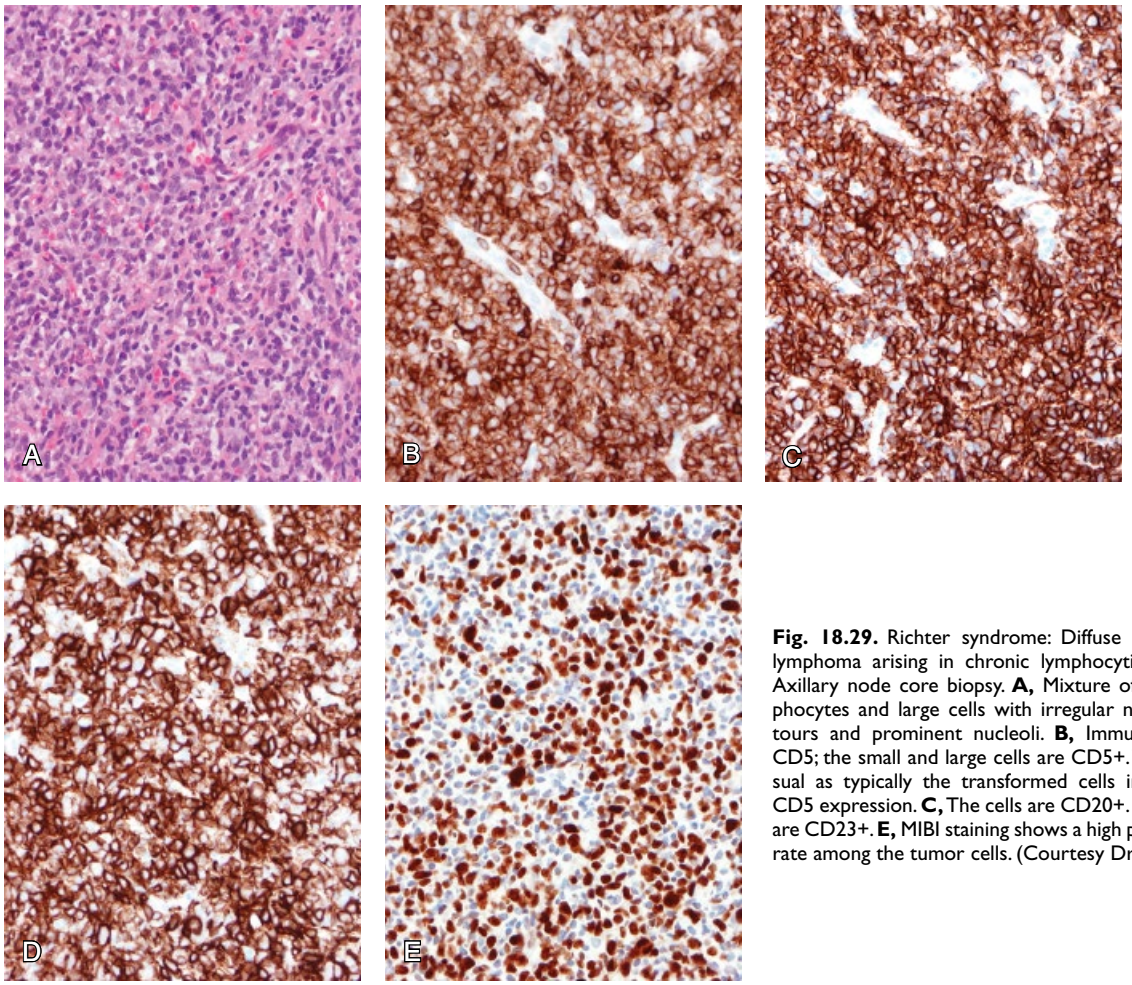

Fig. 18.29. Richter syndrome: Diffuse large B-cell lymphoma arising in chronic lymphocytic leukemia. Axillary node core biopsy. **A,** Mixture of small lymphocytes and large cells with irregular nuclear contours and prominent nucleoli. **B,** Immunostain for CD5; the small and large cells are CD5+. This is unusual as typically the transformed cells in CLL lose CD5 expression. **C,** The cells are CD20+. **D,** The cells are CD23+. **E,** MIBI staining shows a high proliferation rate among the tumor cells. (Courtesy Dr. A Ramsay.)

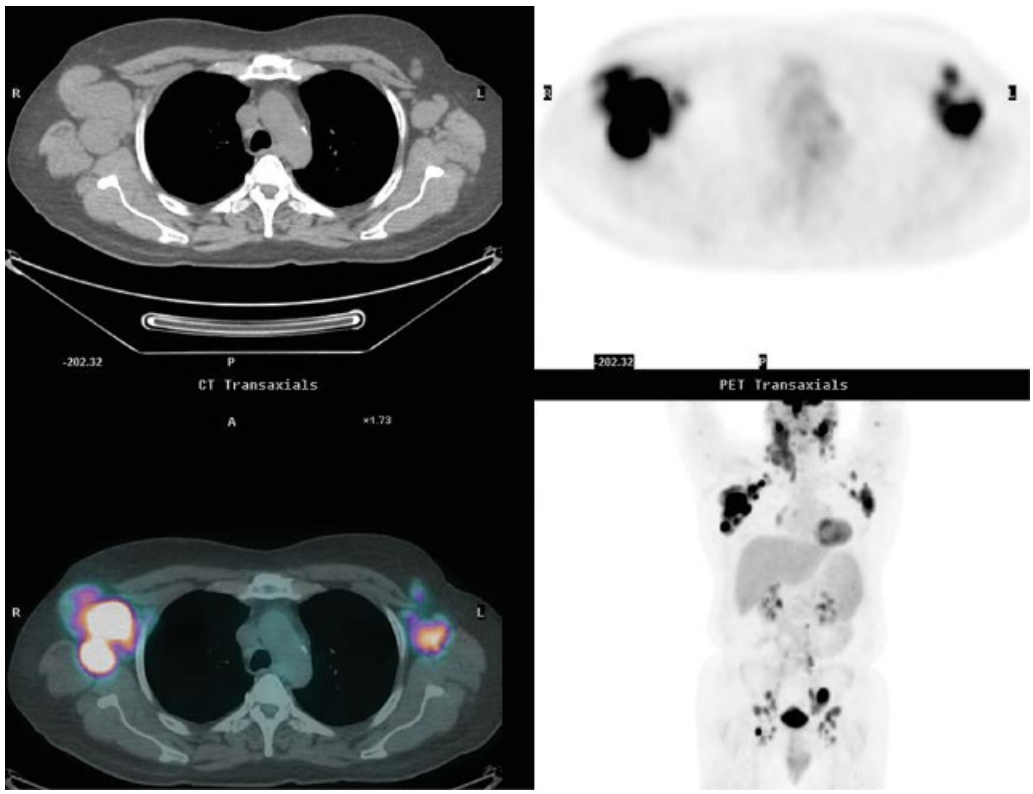

Fig. 18.30. Chronic lymphocytic leukemia: Richter syndrome. Axial CT, FDG PET, fused PET/CT, and maximum intensity projection (MIP) images showing massive, active axillary lymphadenopathy, right greater than left. Biopsy of the right axillary mass showed diffuse large B-cell lymphoma, CD5+, in a patient with long-standing multitreated CLL. There is also active disease in the cervical, pharyngeal, and pelvic lymph nodes, implying Richter transformation at multiple sites.

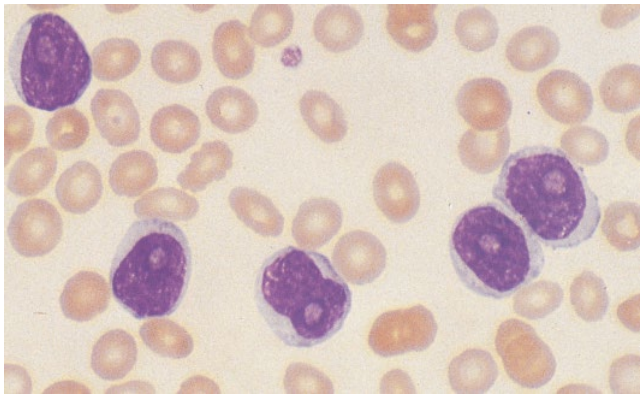

Fig. 18.31. B-cell prolymphocytic leukemia: Blood film showing prolymphocytes that have prominent central nucleoli and an abundance of pale cytoplasm. A high density of surface immunoglobulin confirmed their B-cell nature.

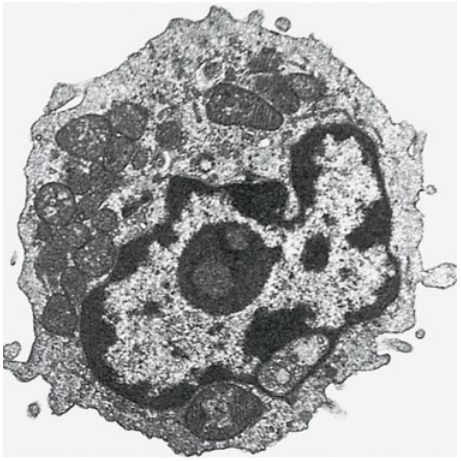

Fig. 18.32. B-cell prolymphocytic leukemia: The B prolymphocyte is characterized by its relatively large size, moderately abundant cytoplasm, chromatin condensed in the periphery of the nucleus, and a prominent nucleolus. (Courtesy of D Robinson and Profesor D Catovsky.)

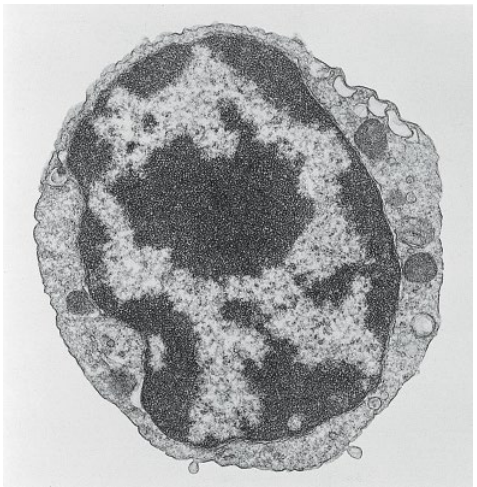

Fig. 18.33. B-cell chronic lymphocytic leukemia: Compared with Fig 18.32, this cell is smaller and has less cytoplasm (high nuclear:cytoplasmic [N:C] ratio) and more marked nuclear chromatin with no visible nucleolus. (Courtesy of D Robinson and Professor D Catovsky.)

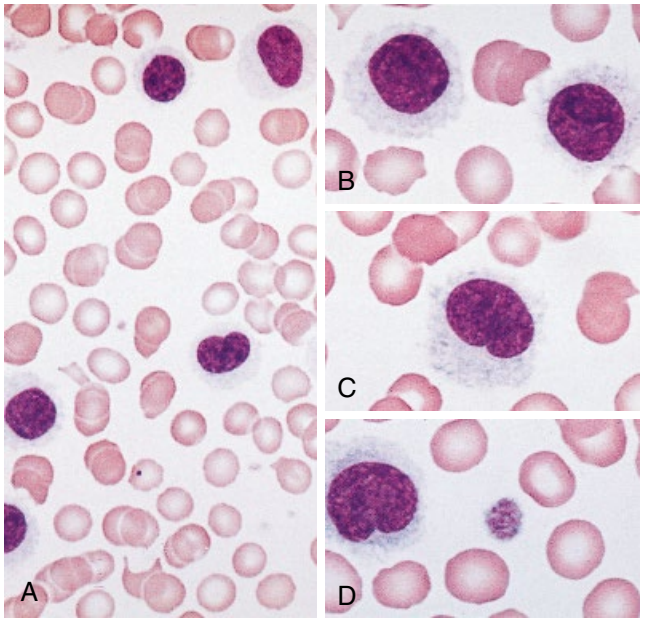

Fig. 18.34. Hairy cell leukemia: Peripheral blood films showing: **A,** typical "hairy" cells, which have round or oval nuclei and a moderate amount of finely mottled, pale gray cytoplasm with irregular serrated ("hairy") edges; the chromatin is less dense than in typical small lymphocytes; **B–D,** at higher magnification the nucleoli are clearly visible. (Hb, 9.4 g/dL: WBC, 25×10^9/L [hairy cells, 23.5×10^9/L]; platelets, 90×10^9/L.)

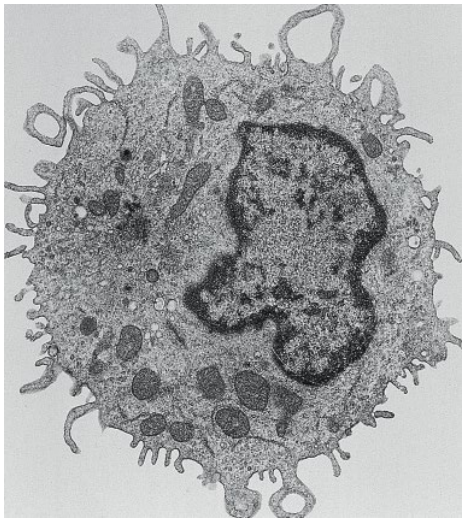

Fig. 18.35. Hairy cell leukemia: Hairy cell from the peripheral blood. Typical features are the abundant cytoplasm, low N:C ratio, and cytoplasmic projections or villi that give the cell a "hairy" appearance (×9200). (Courtesy of D Robinson and Professor D Catovsky.)

HAIRY CELL LEUKEMIA

Hairy cell leukemia (HCL) is a mature B-cell neoplasm whose cells have oval nuclei and abundant cytoplasm with "hairy" prolongations that involve the peripheral blood, bone marrow, and spleen (Figs. 18.34–18.36). Patients with HCL usually have pancytopenia and splenomegaly without lymphadenopathy. In many patients, the marrow is difficult to aspirate and trephine biopsy is necessary for diagnosis. In these patients, interstitial or diffuse infiltration by hairy cells and a dense reticulin fiber pattern are usually seen (Fig. 18.37). The nuclei of the

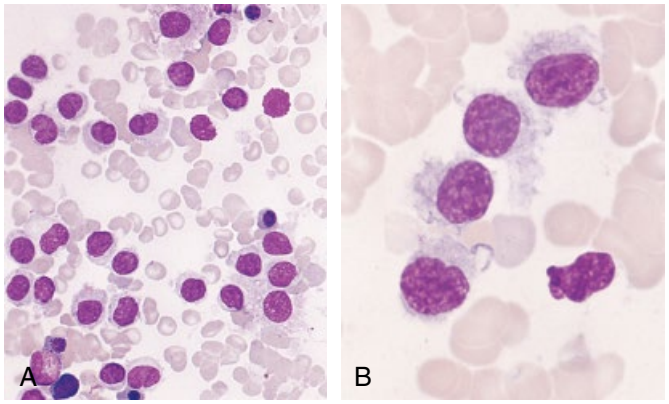

Fig. 18.36. Hairy cell leukemia. **A,** Bone marrow aspirate showing a predominance of hairy cells in the cell trail. **B,** Splenic imprints showing typical nuclear and cytoplasmic features of the abnormal hairy cells.

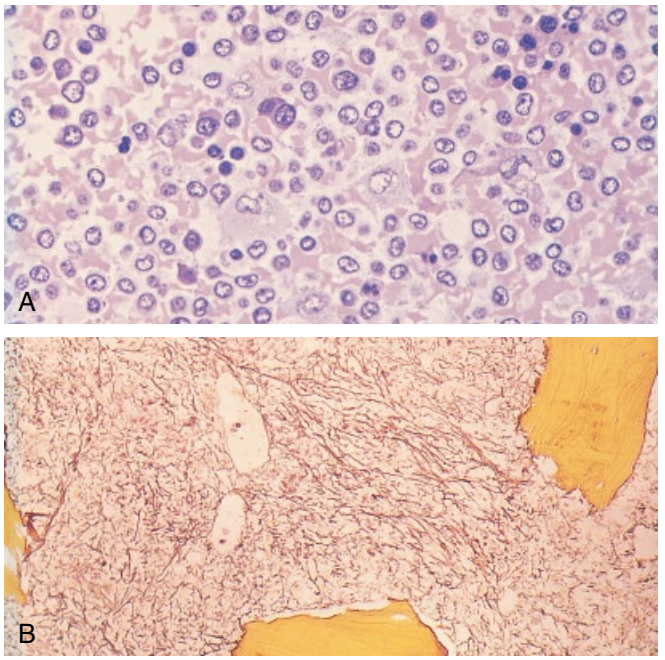

Fig. 18.37. Hairy cell leukemia. **A,** Bone marrow trephine biopsy showing extensive replacement of normal hematopoietic tissue by discrete mononuclear hairy cells. The nuclei are typically surrounded by a clear zone of cytoplasm, which is accentuated by a contraction artifact in vitro. (Methacrylate section.) **B,** Showing increased fiber density and thickness in the reticulin fiber pattern. (Silver impregnation technique.)

cells are widely spaced, giving a "frog spawn"-like appearance. Hairy cells show characteristic cytochemical reaction tartrate-resistant acid phosphtase (TRAP) but this technique has been substituted by immunophenotypic studies (Figs. 18.38 and 18.39). The cells show a characteristic phenotype with expression of CD11c, CD19, CD20, CD22, CD25, CD103, CD123, DBA44, and annexin A1 and negativity for CD10, CD23, and FMC7 (Fig. 18.40). Virtually all cases have the *BRAF* V600E mutation. Histologic sections of the spleen (Figs. 18.41 and 18.42) and liver (Figs. 18.43 and 18.44) can demonstrate unusual vascular "lakes" caused by hairy cell infiltration of these organs.

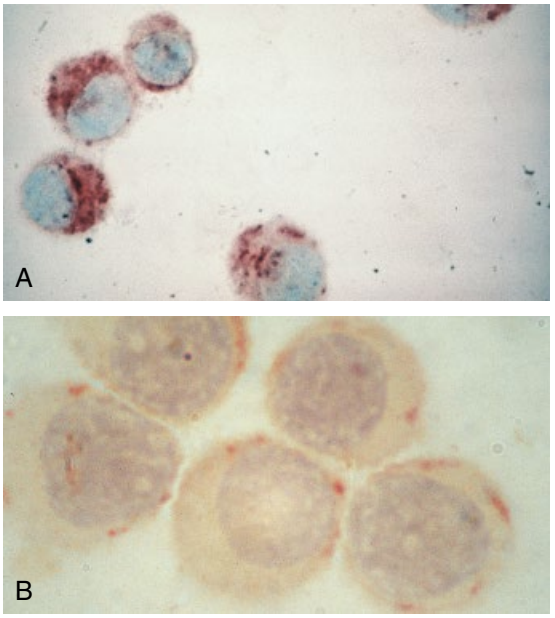

Fig. 18.38. Hairy cell leukemia: Typical cytochemical findings of hairy cells include: **A,** a strongly positive reaction to tartaric acid–resistant acid phosphatase (TRAP); and **B,** a fine granular positivity with crescentic accumulation at one side of the nucleus following alpha-naphthyl butyrate esterase staining.

Hairy Cell Leukemia Variant

HCL variant (HCL-v) is an uncommon disease that resembles HCL morphologically but corresponds to a different biologic and clinical entity. The WHO classification includes HCL-v together with the "Splenic diffuse red pulp small B-cell lymphoma" in the provisional category of "Splenic B-cell lymphoma/leukemia, unclassifiable." Patients with HCL-v usually manifest with a white cell count greater than 40×10^9/L and splenomegaly. Monocytes are within the normal range. HCL-v cells have a prominent nucleoli, blastic or convoluted nuclei, and irregular cytoplasmic borders but lack the characteristic "villi" of HCL (Fig. 18.45). The cells express mature B-cell markers similar to HCL but lack CD25, CD123, annexin-A1, and TRAP. *BRAF* is not mutated but some cases have mutations in *MAP2K1* and *TP53* is frequently mutated. HCL-v is resistant to conventional HCL therapy (i.e., lack of response to cladribine).

MATURE T-CELL LEUKEMIAS

The T-cell diseases that manifest primarily as leukemia described here are listed in Table 18.1, and their membrane immunophenotypes are shown in Table 18.6. The peripheral T-cell lymphomas, including Sézary syndrome, are discussed in Chapter 22.

T-CELL PROLYMPHOCYTIC LEUKEMIA

T-cell prolymphocytic leukemia (T-PLL) is characterized by the proliferation of small mature T cells involving the peripheral blood, usually with a high white cell count (greater than 100×10^9/L), and is often associated with widespread lymphadenopathy, splenomegaly, serous effusions, and skin lesions, and runs an aggressive course. The cells resemble those of B-PLL but may have a more irregular outline, a higher N : C ratio, and an inconspicuous nucleolus (Figs. 18.46 and 18.47). The

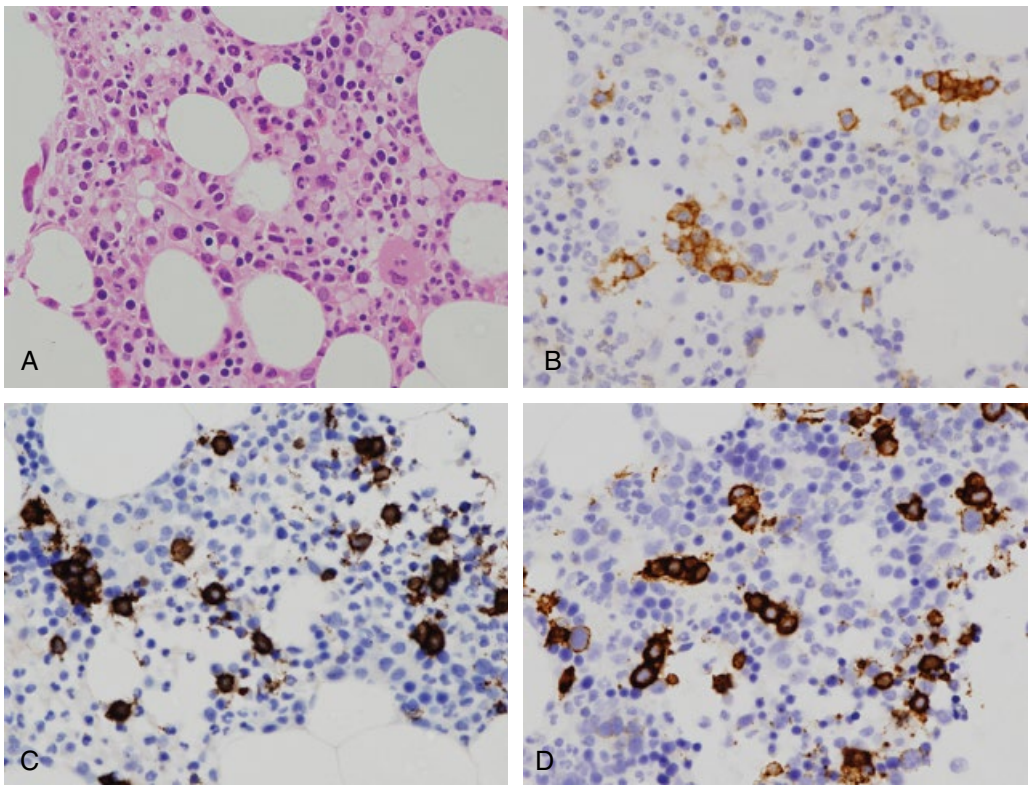

Fig. 18.39. Hairy cell leukemia: Bone marrow trephine biopsy. **A,** Many discrete cells with clear cytoplasm present. Immunohistology shows the cells are **B** CDHc+; **C** CD20+; and **D** CD103+. The cells are also DBA44+ (not shown).

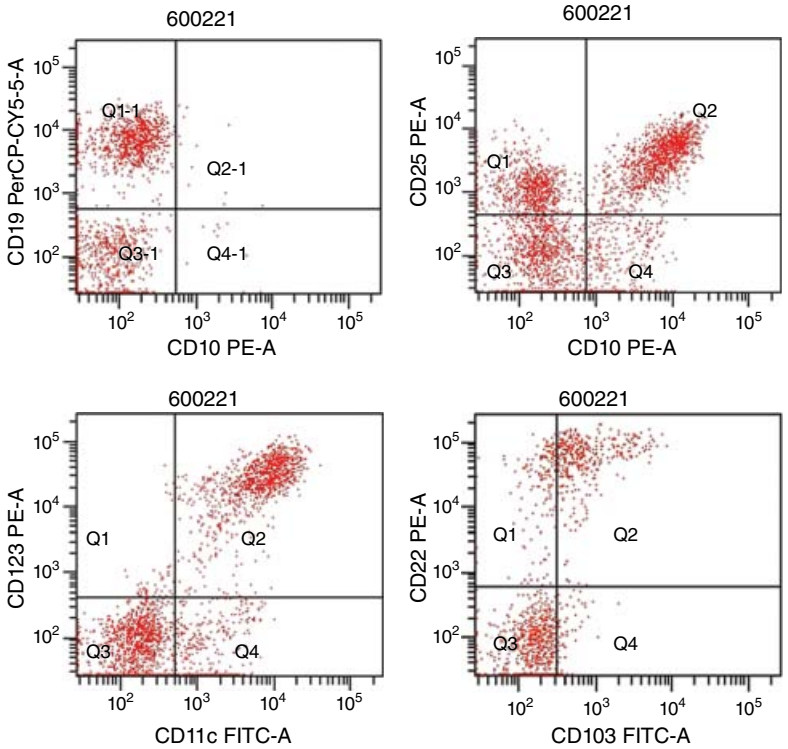

Fig. 18.40. Hairy cell leukemia. FACS scan of peripheral blood cells. The hairy cells are typically CD11c+, CD19+, CD20+, CD22+, CD25+, CD103+, CD123+, CD10–, CD23–, and FMC7–. (Courtesy of Immunophenotyping Laboratory, Royal Free Hospital, London.)

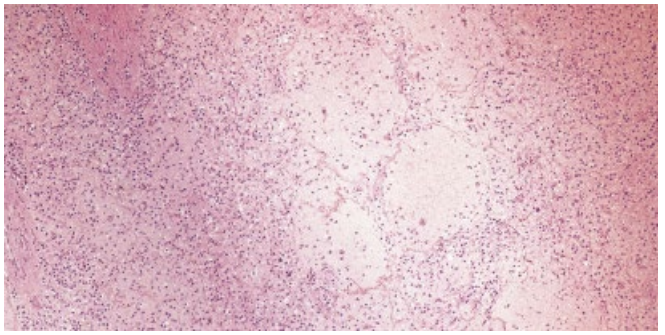

Fig. 18.41. Hairy cell leukemia: Histologic section of spleen showing hairy cell infiltration of reticuloendothelial cords and sinuses. Numerous blood "lakes" are seen in the center of the field.

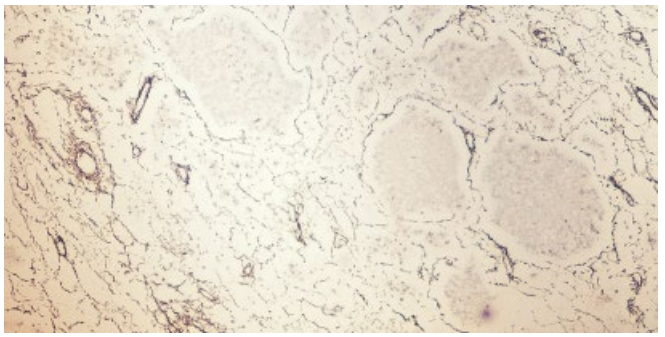

Fig. 18.42. Hairy cell leukemia: Histologic section of spleen (same case as shown in Fig. 18.41) showing more clearly the reticulin fiber pattern outlining the abnormal venous "lakes." The presence of these structures may explain the extensive splenic red cell pooling that occurs in this disease. (Silver impregnation technique.)

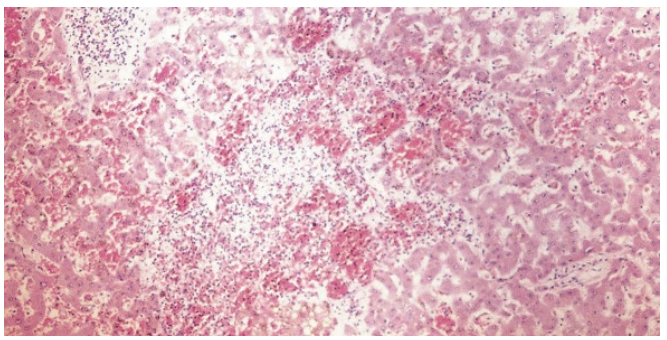

Fig. 18.43. Hairy cell leukemia: Histologic section of liver shows hairy cell infiltration of sinusoids and portal tracts. There is sinusoidal ectasia and pseudoangiomatous transformation of hepatic blood vessels.

cells express mature T-cell markers and most (60%) are CD4+, CD8–, 25% of the cases coexpress CD4 and CD8, and 15% are CD8+ CD4– (Table 18.5). Two-thirds of the cases show inv(14) (Fig. 18.48), with similar breakpoints in 14q11 and 14q32. Around 10% of cases have t(14;14)(q11;q32). These translocations activated the TCL1 locus *ATM* and *TP53* mutations are frequent.

T-CELL LARGE GRANULAR LYMPHOCYTIC LEUKEMIA

T-cell large granular lymphocytic leukemia is characterized by a persistent (>6 months) increase in the number of peripheral blood large granular lymphocytes, usually in the range of $2–20 \times 10^9$/L, without a clearly identified cause. The disease often runs a benign course. Patients usually have chronic neutropenia, anemia, and some show seropositive rheumatoid arthritis

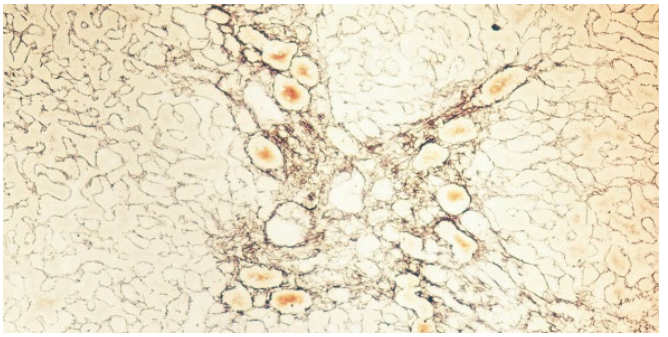

Fig. 18.44. Hairy cell leukemia: Histologic section of liver (same case as shown in Fig. 18.43) showing the reticulin fiber pattern clearly, confirming the gross distortion of hepatic vascular architecture. It is thought that attachment of large numbers of hairy cells to the sinusoidal lining cells causes cell damage that results in these characteristic vascular abnormalities in the liver and spleen. (Silver impregnation technique.)

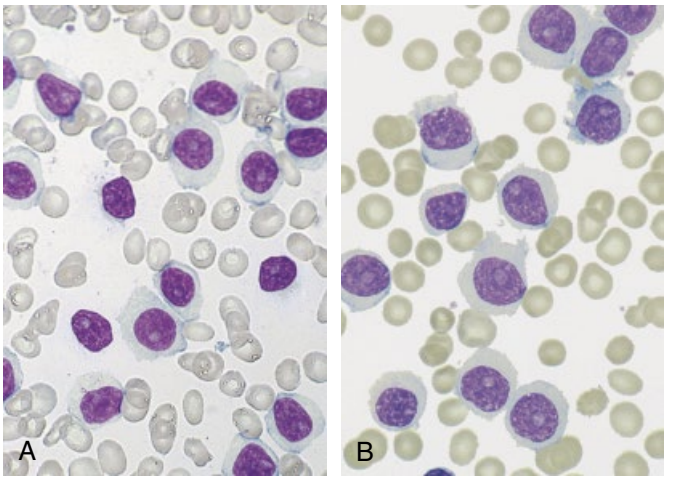

Fig. 18.45. Hairy cell leukemia variant. **A,B,** Peripheral blood films showing cells with a prominent nucleolus, abundant pale cytoplasm, and an irregular cytoplasmic border. (Courtesy of Professor D Catovsky.)

TABLE 18.6. MEMBRANE IMMUNOPHENOTYPE OF MATURE T-CELL LEUKEMIAS

	LGLL[a]	T-PLL	ATLL	Sézary syndrome	ANKL
CD2	+	+	+	+	+
CD3	+	+/–	+	+	–(CD3ε+)
CD5	–	+	+	+	–
CD7	–/+	++	–	–	+
CD4	–	+	+	+	–
CD8	+	+/–	–	–	–/+
CD25	–	–/+	++	–	–
CD56/57	+	–	–	–	+/–

Note: These marker patterns are usual, but variant patterns also occur.
ANKL, aggressive NK-cell leukemia; ATLL, adult T-cell leukemia/lymphoma; LGLL, large granular lymphocytic leukemia; T-PLL, T-cell prolymphocytic leukemia.
[a] Approximately 15% of LGLL have an NK phenotype ($CD3^-$, $CD56^+$).

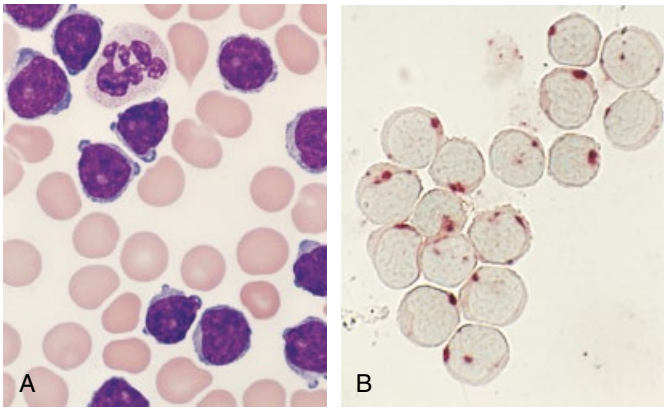

Fig. 18.46. Prolymphocytic leukemia (T-cell type): Blood films. **A,** Prolymphocytes, each with a prominent central nucleolus and a single neutrophil. Cell marker studies showed positive reactions with anti-T-cell antibodies (CD2+, CD3+, CD4+, CD5+, CD7+, CD8−, CD25+) and an absence of surface immunoglobulin. **B,** "Clump" positivity of these cells using acid phosphatase staining. (Hb, 10.5 g/dL; WBC, 240 × 10^9/L; platelets, 60 × 10^9/L.) (Courtesy of Professor D Catovsky.)

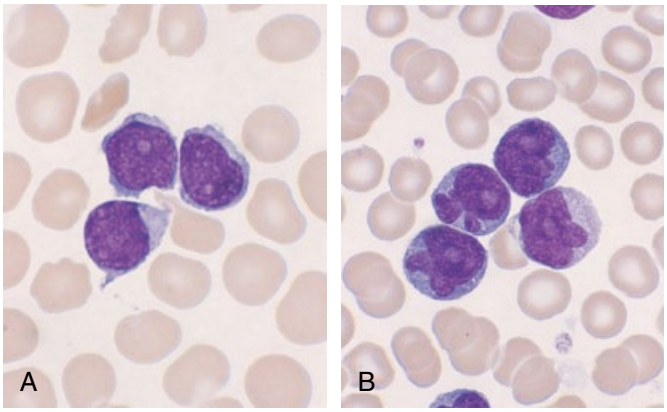

Fig. 18.47. T-cell prolymphocytic leukemia. **A,B,** Small cell type with scant cytoplasm and irregular nuclear outline.

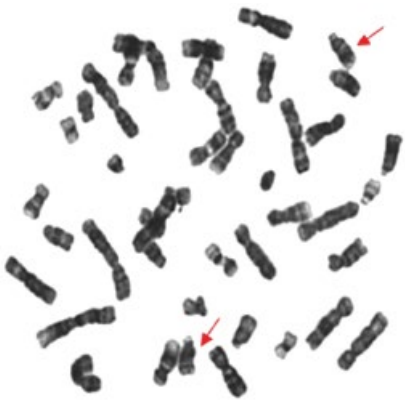

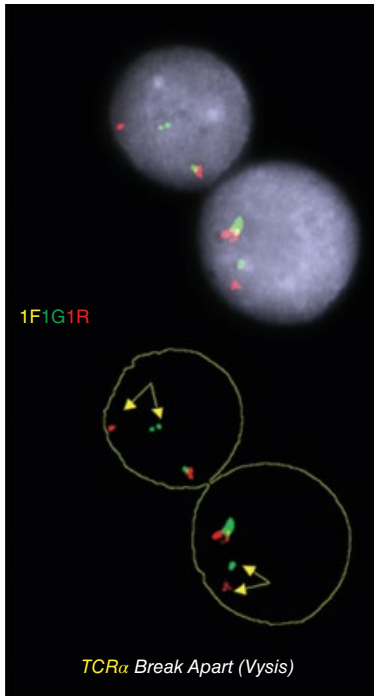

Fig. 18.48. T-cell prolymphocytic leukemia: inv (14). The left-hand panel shows a G-banded metaphase with arrows pointing to a normal chromosome 14 (at 6 o'clock) and an inverted chromosome 14 (1 o'clock), both shown enlarged below with arrows indicating the breakpoint positions. The right-hand panel shows interphase nuclei with FISH signals from TCRα dual color breakpoint (Vysis) probes. The signal pattern 1 fusion, 1 green, 1 red shows that one of the TCRα genes at 14q11 loci is rearranged (split signal indicated by arrows). Top panel, unprocessed images; bottom panel, processed images. (Courtesy of Dr. E Nacheva.)

and splenomegaly. The cells can be large, have abundant cytoplasm, and show multiple fine or coarse azurophil granules (Figs. 18.49 and 18.50). In the majority of cases, the cells are positive for T-cell markers CD3 and CD2 but CD5 and CD7 tend to be weak. CD57 and CD16 are also commonly expressed. Most cases are CD8+. Some uncommon cases express CD4 or CD4 and CD8 (Fig. 18.51). T-cell receptor gene rearrangement analysis shows that the cells are usually clonal, but most cases show T-cell receptor α/β rearrangement but rare cases have rearrangement of the T-cell γ/δ receptor. Approximately 15% of cases have an immunophenotype of natural killer cells (CD3−, CD56+, CD57+). *STAT3* and *STAT5B* activating mutations have been detected in around one-third of cases.

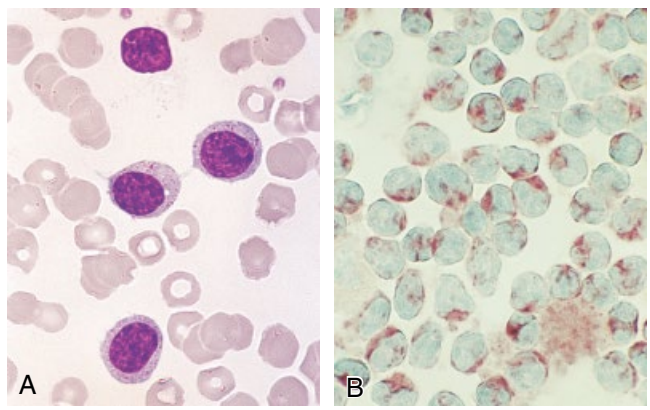

Fig. 18.49. Large granular lymphocytic leukemia: Peripheral blood films showing: **A,** abnormal lymphocytes; and **B,** characteristic "clump" positivity in the Golgi zone using acid phosphatase staining.

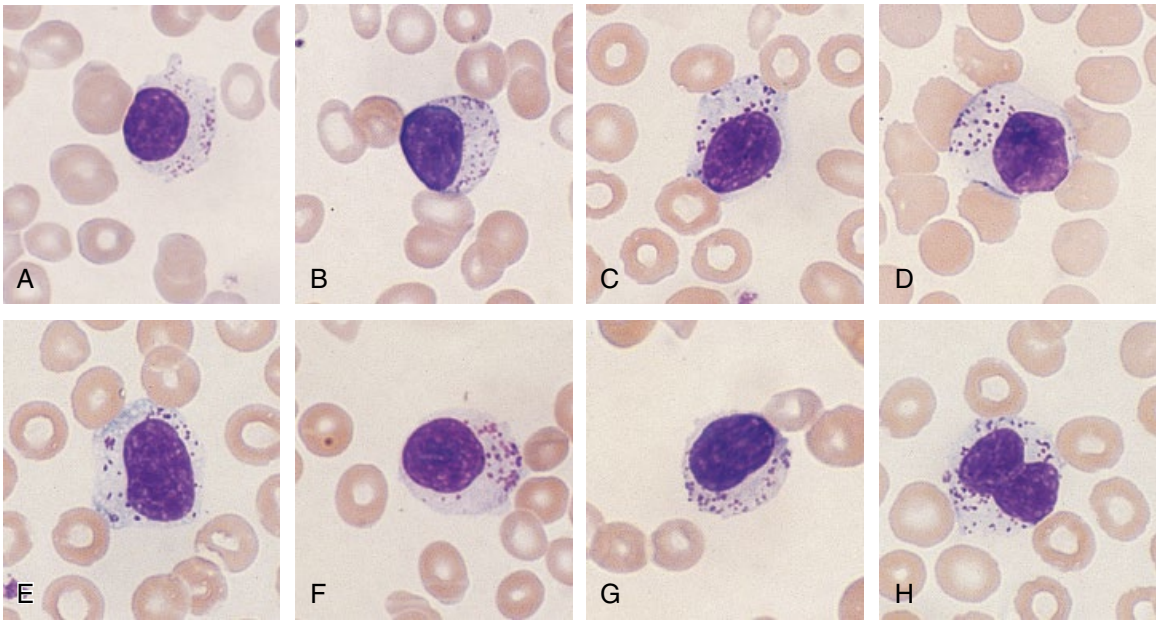

Fig. 18.50. Large granular lymphocytic leukemia. **A–H,** Peripheral blood films showing representative large lymphocytes with multiple coarse, azurophilic, cytoplasmic granules. Immunologic marker studies showed the cells to be CD8+, CD4−, CD3+, CD16+, and CD57+. The patient had splenomegaly, chronic neutropenia, and lymphocytosis. (Absolute lymphocyte count, 9.4×10^9/L.)

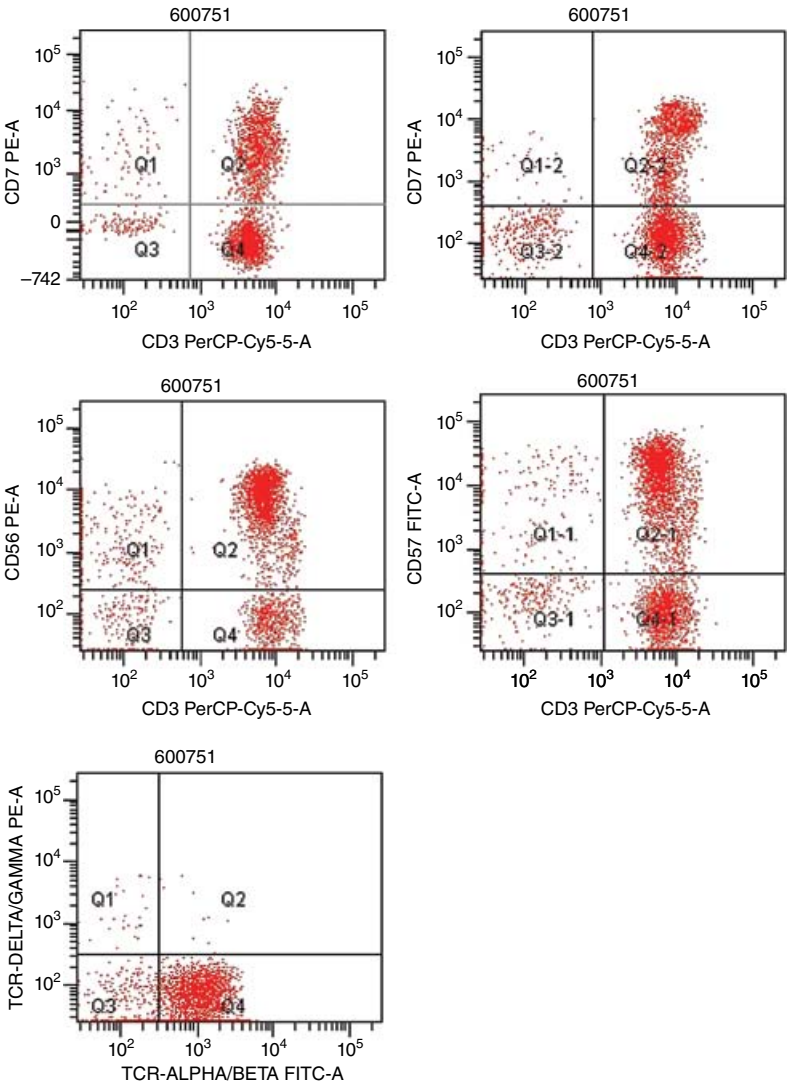

Fig. 18.51. Large granular lymphocytic leukemia: FACS analysis. In this rare type, the cells are CD3+, CD4+, CD8+, CD56+, CD57+, and TCR α/β receptor positive. More usually (as in Fig. 18.50), the cells are CD8+, CD4−. (Courtesy of the Immunophenotyping Laboratory, Royal Free Hospital.)

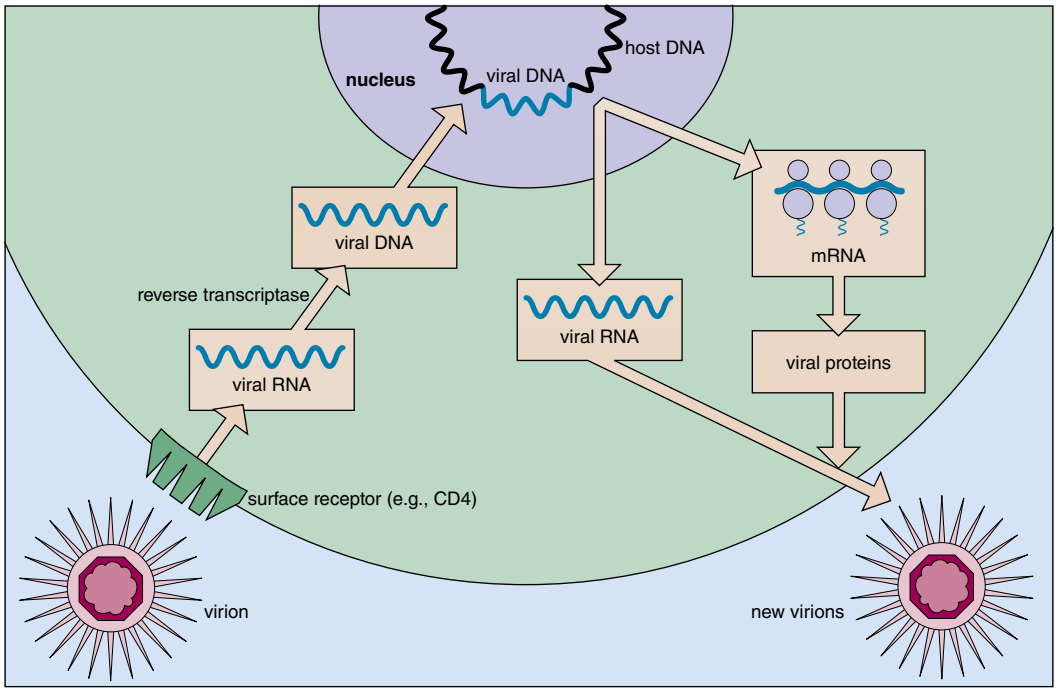

Fig. 18.52. Replication of a retrovirus within a host cell.

ADULT T-CELL LEUKEMIA/LYMPHOMA

Adult T-cell leukemia/lymphoma is an unusual lymphoproliferative malignancy composed of highly pleomorphic lymphoid cells caused by the human T-cell leukemia virus type I (HTLVI). The life cycle of a typical retrovirus is illustrated in Fig. 18.52. Invasion of the host cell causes cell proliferation, but there is no consistent integration site and no identified oncogene activation. The disease occurs predominantly in southwestern Japan and in black populations of the West Indies and other Caribbean countries and parts of Central Africa (Figs. 18.53 and 18.54). Typically, the lymphoma evolves rapidly with early involvement of the lymph nodes (Fig. 18.55), skin (Fig. 18.53), blood (Fig. 18.56), and bone marrow. The cells are CD4+, CD3+, CD25+ (Fig. 18.57). The white cell count varies widely with between 10% and 80% of tumor cells. The neoplastic lymphoid cells vary in size and have an irregular nucleus, often with marked convolutions (Figs. 18.55 and 18.56). Associated hypercalcemia can lead to death in coma.

AGGRESSIVE NK-CELL LEUKEMIA

Aggressive NK-cell leukemia is a neoplasm of NK cells virtually always infected by the Epstein–Barr virus (EBV) that involves the bone marrow and peripheral blood. In some patients, the cells infiltrate tissues particularly liver, spleen, and, less frequently, lymph nodes. The disease has a very aggressive clinical course with fever, constitutional symptoms, and cytopenias. Some patients develop hemophagocytic syndrome, coagulopathy, and multiorgan failure. The tumor cells have NK phenotype (Table 18.5) and are EBV-positive. Frequent recurrent mutations occur in *STAT3* (21%), *RAS-MAPK* pathway genes (21%), *DDX3X* (29%), and epigenetic modifiers (50%).

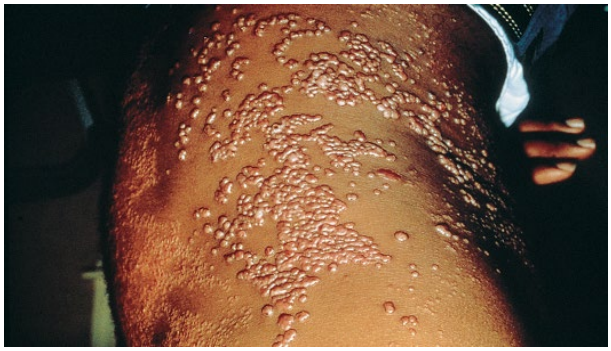

Fig. 18.53. Adult T-cell leukemia/lymphoma syndrome: Extensive involvement of the skin. (Courtesy of Dr. JW Clark.)

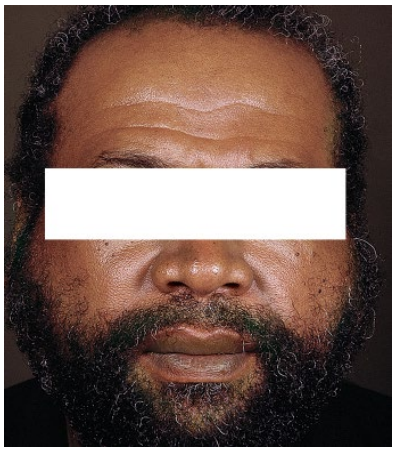

Fig. 18.54. Adult T-cell leukemia/lymphoma in a 42-year-old male patient. He was diagnosed in Jamaica 5 years earlier to have paraplegia because of spinal disease. He had firm swelling of the salivary glands, but no superficial lymphadenopathy. (Hb, 12.3 g/dL; WBC, 28×10^9/L; platelets, 134×10^9/L; serum positive for anti-HTLVI; serum calcium normal; no skin rash.)

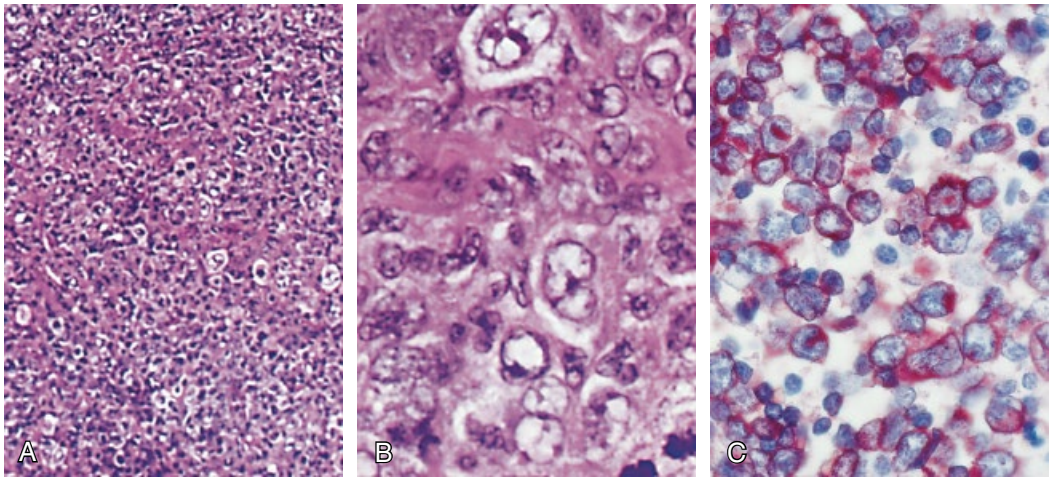

Fig. 18.55. Adult T-cell lymphoma/leukemia syndrome. Histologic sections of lymph node showing: **A,** replacement of normal architecture by pleomorphic lymphoid cells; **B,** occasional bizarre polylobulated giant cells and prominent mitotic figures at high magnification; and **C,** paraffin-stained (immunophosphatase) section for CD3. (Courtesy of Professor DY Mason.)

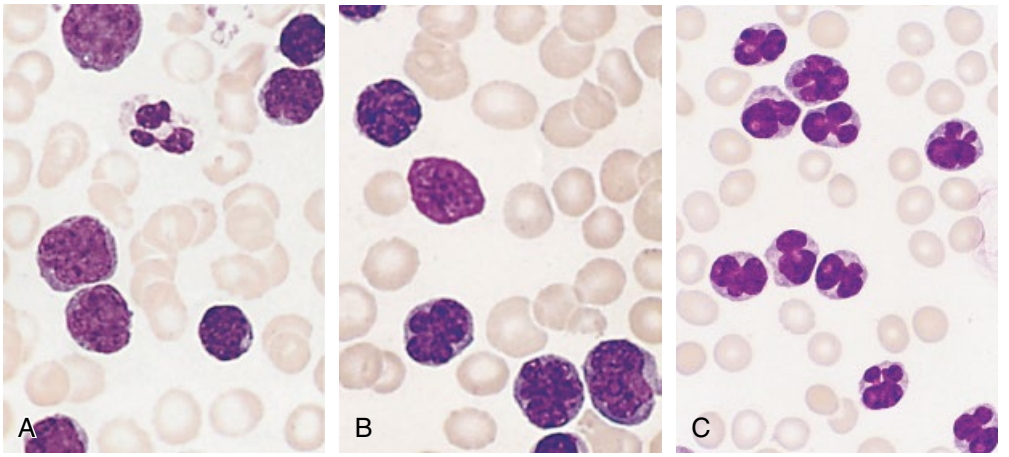

Fig. 18.56. Adult T-cell leukemia/lymphoma syndrome. **A–C,** Peripheral blood films showing the characteristic abnormal lymphocytes with convoluted nuclei.

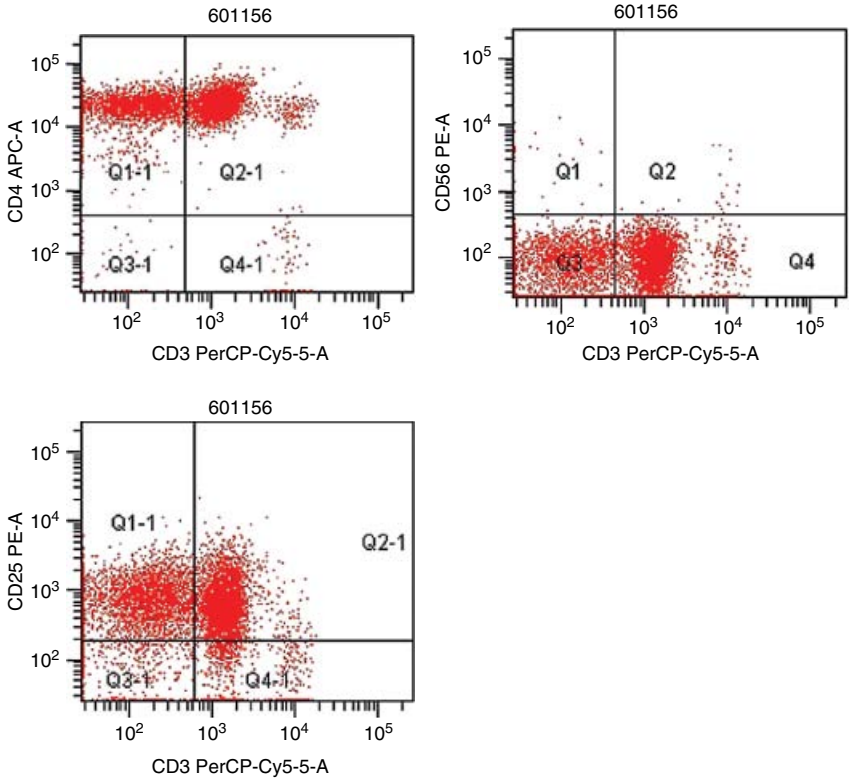

Fig. 18.57. Adult T-cell leukemia/lymphoma syndrome: FACS analysis. The cells are CD3+, CD4+, CD25+, and CD56−. (Courtesy of the Immunophenotyping Laboratory, Royal Free Hospital.)

CHAPTER

19

SMALL B-CELL LYMPHOMAS

The term malignant lymphoma embraces all lymphoid neoplasms usually originated in the lymph nodes or extranodal lymphatic tissue. Classically, these neoplasms have been classified in two major categories: Hodgkin lymphoma (discussed in Chapter 23) and the large heterogeneous category known as the non-Hodgkin lymphomas, which vary from highly proliferating and rapidly fatal disorders to indolent, although often incurable, malignancies that may be well tolerated for very long periods of time. Lymphoid neoplasms are monoclonal expansions of B, T, or natural killer (NK) cells. Evidence of this comes from studies of IG or T-cell receptor gene rearrangements and the expression of a single type of immunoglobulin (Ig) on the cell surface and/or within the cytoplasm. Most lymphomas can be related to different stages of the normal lymphoid cell differentiation process and therefore it is possible to attribute a putative normal cell counterpart for these tumors (Fig.19.1). However, there are some particular lymphomas (e.g. anaplastic large cell lymphoma or hairy cell leukemia) that do not correspond to a

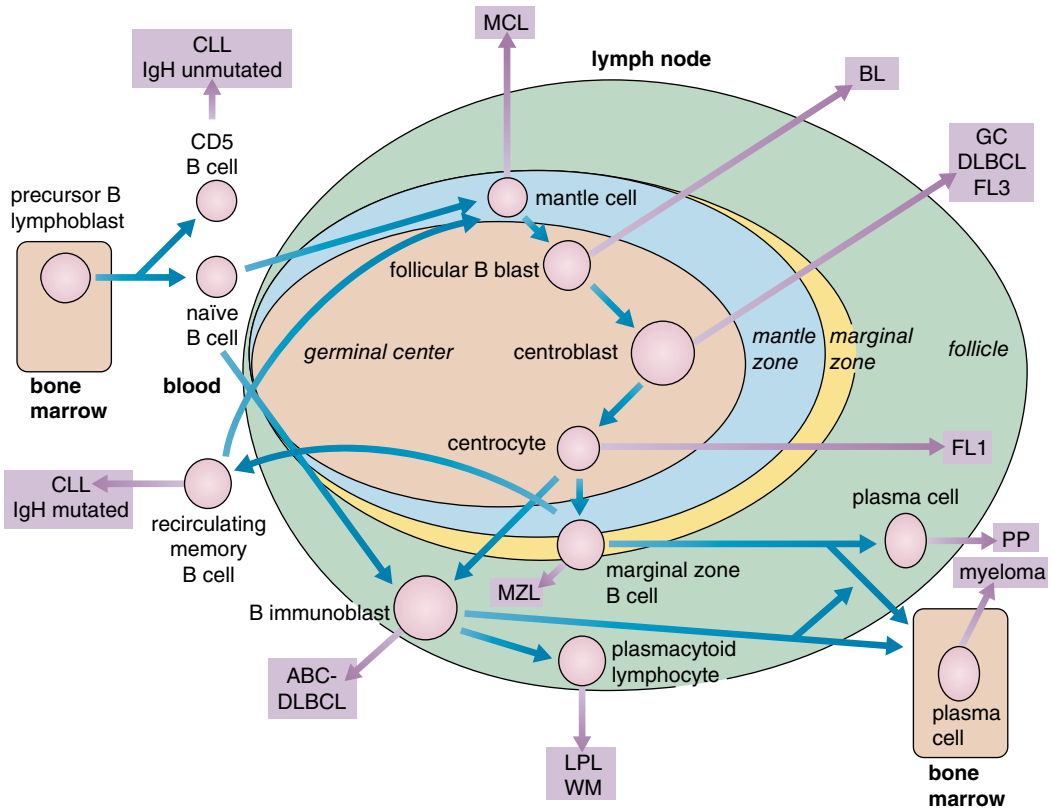

Fig. 19.1. Suggested lymphoid cell of origin of the mature B-cell neoplasms. For diffuse large B-cell lymphoma (DLBCL) two types, one arising from the germinal center (GC), the other from an activated B cell (ABC), have been identified by gene expression profile and immunohistologic markers. Chronic lymphocytic leukemia (CLL) may originate from a cell with mutated IGH genes or from an antigen experienced cell with unmutated IGH genes. FLI-2, FL3, follicular lymphoma grades I-2 and 3; LPL, lymphoplasmacytic lymphoma; MCL, mantle cell lymphoma, can also originated from a cell with unmutated IGH, and then is usually SOX11-positive and from a cell with mutated IGH and usually SOX11-negative; MZL, marginal zone lymphoma; PP, peripheral plasmacytoma; WM, Waldenström macroglobulinemia.

Color Atlas of Clinical Hematology: Molecular and Cellular Basis of Disease, Fifth Edition. A. Victor Hoffbrand, Paresh Vyas, Elías Campo, Torsten Haferlach, and Keith Gomez

known normal lymphoid cell counterpart. The large number of these diseases reflects the rich diversity of much of the maturation stages and subpopulations of normal human lymphoid cells. In this chapter we review the group of mature small B-cell neoplasms (Table 19.1). The aggressive B-cell neoplasms are presented in Chapter 20 and the peripheral T-cell lymphomas in Chapter 22.

EPIDEMIOLOGY

The frequencies of some types of non-Hodgkin lymphoma vary markedly between the different parts of the world. For example, two lymphoma categories that are common in Western countries, Hodgkin lymphoma and follicular lymphoma, are much rarer in Eastern and less developed countries. Burkitt lymphoma is endemic in equatorial Africa but it is less frequent in Western countries. Enteropathy-associated T-cell lymphoma is most common in northern Europe and in individuals of Welsh and Irish descent. Some subtypes of non-Hodgkin lymphoma that are only rarely seen in Western countries are found at much higher frequency elsewhere, and this may be partly accounted for by the genetic background of the different populations or local patterns of exposure to viruses and other pathogens (Table 19.2). NK- and T-cell lymphomas related to Epstein–Barr virus (EBV) are more common in Far East Asians and American natives. Human T-lymphotropic virus type 1 (HTLV-1) related adult T-cell leukemia lymphoma is common in the endemic areas for the virus in southwestern Japan, the Caribbean basin, central Africa, western South America, and Iran.

ETIOLOGIC FACTORS

The etiologic factors underlying the development of most subtypes of lymphoid neoplasms are mainly unknown. The presence of certain lymphoid neoplasms in familial context and the recognition of specific genetic loci linked to an increased risk of developing certain lymphomas highlight the relevance of the genetic background in the pathogenesis of some tumors.

TABLE 19.1. THE 2016 UPDATED WORLD HEALTH ORGANIZATION CLASSIFICATION OF THE MATURE SMALL B-CELL NEOPLASMS

Mature small B-cell neoplasms
Chronic lymphocytic leukemia/small lymphocytic lymphoma
Monoclonal B-cell lymphocytosis
B-cell prolymphocytic leukemia
Splenic marginal zone lymphoma
Hairy cell leukemia
Splenic B-cell lymphoma/leukemia, unclassifiable • *Splenic diffuse red pulp small B-cell lymphoma* • *Hairy cell leukemia variant*
Lymphoplasmacytic lymphoma • Waldenström macroglobulinemia
Monoclonal gammopathy of undetermined significance (MGUS), IgM
μ heavy chain disease
γ heavy chain disease
α heavy chain disease
Monoclonal gammopathy of undetermined significance (MGUS), IgG/A
Plasma cell myeloma
Solitary plasmacytoma of bone
Extraosseous plasmacytoma
Monoclonal immunoglobulin deposition diseases
Extranodal marginal zone lymphoma of mucosa associated lymphoid tissue (MALT lymphoma)
Nodal marginal zone lymphoma • *Pediatric nodal marginal zone lymphoma*
Follicular lymphoma • In situ follicular neoplasia • Duodenal-type follicular lymphoma
Pediatric-type follicular lymphoma
Large B-cell lymphoma with IRF4 rearrangement
Primary cutaneous follicle center lymphoma
Mantle cell lymphoma • In situ mantle cell neoplasia

Provisional entities are listed in italics.
Source:Swerdlow SH, et al. *Blood* 2016;127:2375–2390. Reproduced with permission of American Society of Hematology.

TABLE 19.2. LYMPHOMA AND INFECTIOUS AGENTS: GEOGRAPHIC DISTRIBUTION

Lymphoma type	Infectious agent	Geographic distribution
Viruses		
Burkitt	Epstein–Barr virus and malaria	Endemic form – areas with malaria in Africa and New Guinea
Extranodal NK/T-cell lymphoma, nasal type	Epstein–Barr virus	Asia, Mexico, Central and South America
Lymphoplasmacytic; cryoglobulinemia; rarely, lymphomas of liver, salivary glands	Hepatitis C	Mediterranean area
Primary effusion lymphoma; HHV8 + DLBCL, NOS	Human herpes virus 8 (HHV8) usually in conjunction with HIV	Non-HIV associated in Mediterranean area (high prevalence of HHV8 infection)
Adult T-cell leukemia/lymphoma	Human T-cell leukemia virus type 1 (HTLV1)	Japan, Caribbean, central Africa
Bacteria		
Extranodal marginal zone B-cell lymphoma of mucosa associated lymphoid tissue (MALT)	*Helicobacter pylori*	High incidence in northeast Italy
α Heavy chain disease Immunoproliferative small intestinal disease (IPSID)	*Campylobacter jejuni*	Middle East, South Africa
Primary cutaneous marginal zone lymphoma	*Borrelia burgdorferi*	
Occular adnexal marginal zone	*Chlamydia psittaci*	

Infectious agents are also important etiologic factors of some lymphomas (Table 19.2). EBV underlies 100% of endemic, 10–25% of sporadic, and 40% of HIV-associated Burkitt lymphoma. EBV is also associated with many cases of Hodgkin lymphoma, NK/T-cell lymphomas and lymphomas emerging in immunodeficient conditions. Human herpes virus 8 (HHV8) (previously called Kaposi sarcoma herpes virus) is associated with primary effusion lymphoma, HHV8+ DLBCL, NOS, and non-neoplastic disorders such as multicentric Castleman disease and germinotropotic lymphoproliferative disorder. HHV8 causes lymphomas mainly in HIV-infected patients but also in elderly individuals in endemic areas as the Mediterranean. Hepatitis C virus (HCV) has been epidemiologically related to marginal zone lymphomas and lymphoplasmacytic lymphomas, particularly with cryoglobulinemia. Bacteria have been associated with marginal zone lymphomas of different extranodal sites (Table 19.2). *Helicobacter pylori,* by stimulating an immune response to its bacterial antigens, is thought to be responsible for gastric mucosa associated lymphoid tissue (MALT) lymphomas, and *Borrelia burgdorferi, Chlamydia psittaci,* and *Campylobacter jejuni* have been implicated in cutaneous, ocular, and intestinal MALT lymphoma, respectively.

Major risk factors for mature B-cell neoplasms are abnormalities of the immune system, particularly primary or secondary immune deficiencies and autoimmune diseases. Secondary immune deficiency can be caused by human immunodeficiency virus (HIV) infection or secondary to immunosuppressive therapy; MALT lymphomas of the salivary glands or thyroid are examples of lymphomas associated with autoimmune disease.

GENETIC AND MOLECULAR ABNORMALITIES

The identification of recurrent chromosomal alterations, translocations, deletions, and amplifications in several lymphoid neoplasms has been the first step towards the identification of relevant target genes in the pathogenesis of these tumors (Table 19.3). The identification of these chromosomal or molecular alterations is an important element in the differential diagnosis of some entities. The most common alterations are translocations of the IG genes, mainly the heavy chain gene, with different oncogenes that are constitutively activated by the enhancer of the IG gene (Fig. 19.2). The most common translocations are summarized in Table 19.3. Chromosomal alterations and DNA copy number alterations are also frequent with deletions and amplifications of regions containing tumor suppressor and oncogenes, respectively. Recent studies using next generation sequencing techniques of DNA have revealed a large number of recurrent somatic mutations in lymphoid neoplasms which are starting to be used in clinical practice as tools for the differential diagnosis of some of these tumors (Table 19.4). Some of these mutations are also useful in helping to improve the prognosis of patients and can assist in management decisions.

CLINICAL FEATURES AND DIAGNOSIS

The clinical presentation of non-Hodgkin lymphoma is more variable than that of Hodgkin lymphoma and the pattern of tumor spread is not as regular. Staging is with the Ann Arbor system (Table 19.5) but is less useful than in Hodgkin lymphoma.

TABLE 19.3. CHROMOSOME TRANSLOCATIONS AND THEIR GENETIC CONSEQUENCES IN MATURE LYMPHOMAS

Neoplasm	Translocation	Genes involved	Consequences
B-cell neoplasms			
Burkitt	t(8;14)(q24;q32)	IGH and *MYC*	Activation of MYC (DNA-binding protein)
	t(2;8)(p12;q24)	IGK and *MYC*	Activation of MYC (DNA-binding protein)
	t(8;22)(q24;q11)	IGL and *MYC*	Activation of MYC (DNA-binding protein)
MALT	t(11;18)(q21;q21)	*BIRC3-MALT1*	Reduced apoptosis
	t(1;14)(p24;q32)	IGH and *BCL10*	More aggressive disease
	t(14;18)(q32;q21)	IGH and *MALT1*	
	t(3;14)(p14;q32)	IGH and *FOXP1*	
Follicular	t(14;18)(q32;q21)	IGH and *BCL2*	Activation of BCL2 (apoptosis inhibitor)
Mantle cell	t(11;14)(q13;q32)	IGH and *CCND1*[a]	Activation of cyclin D1, cyclin D2, and cyclin D3 (Cell cycle regulators)
	t(12,14)(p13;q32)	IGH and *CCND2*[a]	
	t(6;14)(p21;q32)	IGH and *CCND3*[a]	
Diffuse large B cell	t(3;14)(q27;q32)	IGH and *BCL6*	Extranodal disease; better prognosis
	t(14;18)(q32;q21)	IGH and *BCL2*	Activation of BCL2 (apoptosis inhibitor)
	t(8;14)(q24;q32)	IGH and *MYC*[b]	Activation of MYC (DNA-binding protein)
ALK-positive large B-cell lymphoma	t(2;17)(p23;q23)	*CLTC-ALK*	Chimeric ALK that activates STAT pathway
T-cell neoplasms (see Chapter 22)			
Peripheral T-cell lymphoma	Complex rearrangements	TCR[c]	
Anaplastic large cell	t(2;5)(p23;q35)	*NPM-ALK*[d]	Creation of hybrid NPM–ALK tyrosine kinase

[a] *CCND1, CCND2* and *CCND3* can also be translocated to IGK or IGL.
[b] *MYC* in DLBCL can also be translocated to IGK/L or non-IG genes.
[c] T-cell receptor genes are also usually clonally rearranged in enteropathy-type T-cell lymphoma, subcutaneous panniculitis-like T-cell lymphoma, mycosis fungoides, Sézary syndrome cells, and other T-cell neoplasms.
[d] *ALK* can also be translocated to other partners (e.g. *TPM3*, *TFG*, *CLTC*).

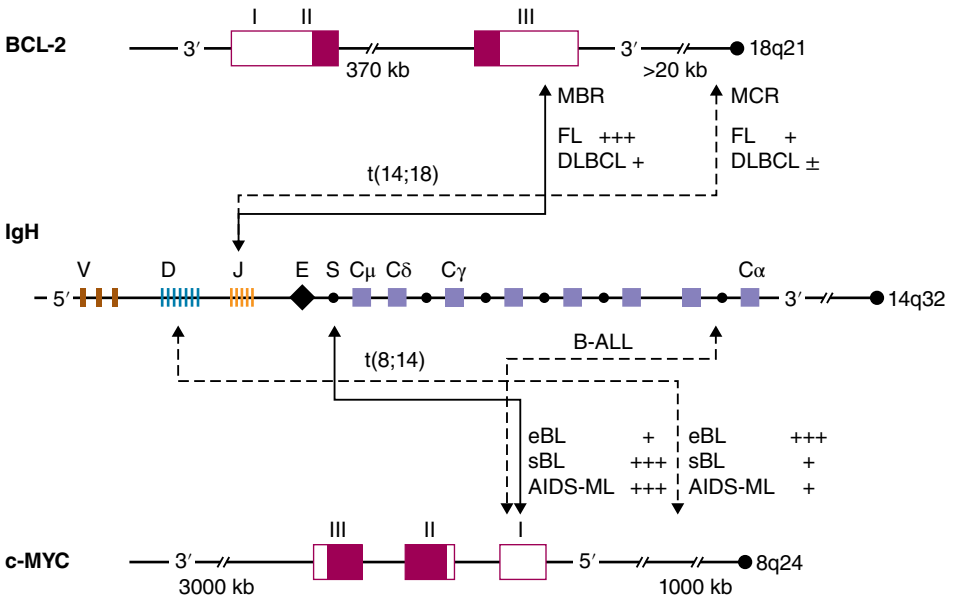

Fig. 19.2. Non-Hodgkin lymphoma: Molecular analysis of common breakpoints found in reciprocal translocations involving IGH and *BCL2* (follicular lymphoma) or IGH and *MYC* (in Burkitt lymphoma). Exons of *BCL2* and *MYC* are represented by rectangles with roman numeral designation above. Coding regions of *BCL2* and *MYC* are solid red rectangles. (MBR, major breakpoint cluster region; MCR, minor breakpoint cluster region; V, variable region; D, diversity region; J, joining region; E, enhancer; S, switch region; C, constant regions of IGH genes; FL, follicular lymphoma; DLBCL, diffuse large B-cell lymphoma type; ALL, acute lymphoblastic leukemia; eBL, endemic Burkitt lymphoma; sBL, sporadic Burkitt lymphoma; AIDS-ML, AIDS-related malignant lymphoma; +++, majority of cases; +, minority of cases; ±, some cases.)

TABLE 19.4. FREQUENT MUTATED GENES IN B-CELL LYMPHOID NEOPLASMS

Neoplasm	Mutated genes
Chronic lymphocytic leukemia	*ATM, NOTCH1, TP53, SF3B1, BIRC3, POT1 MYD88, RPS15, CHD2*
Lymphoplasmacytic lymphoma	*MYD88, CXCR4*
Hairy cell leukemia	*BRAF, CDKN1B*
Hairy cell leukemia variant	*MAP2K1*
Splenic marginal zone lymphoma	*KLF2, NOTCH2, TP53, TNFAIP3*
Follicular lymphoma	*EZH2, KMT2D (MLL2) , EPHA7, CREBBP, RRAGC, TNRSF14*
Mantle cell lymphoma	*ATM, TP53, KMT2D (MLL2), NSD2, NOTCH1/2*
MALT lymphoma	*MYD88*
Diffuse large B-cell lymphoma GCB subtype	*KMTD2 (MLL2), EZH2, CREBBP, GNA13, RRAGC*
Diffuse large B-cell lymphoma ABC subtype	*BLIMP1, MYD88, TNFAIP3, CD79B, CARD11*
Burkitt lymphoma	*ID3, TCF3, CCND3*
Plasma cell myeloma	*TP53, NRAS, KRAS, FAM46C*

TABLE 19.5. REVISED STAGING SYSTEM FOR PRIMARY NODAL LYMPHOMAS

Stage	Involvement	Extranodal (E) Status
Limited		
I	One node or group of adjacent nodes	Single extranodal lesions without nodal involvement
II	Two or more nodal groups on the same side of the diaphragm	Stage I or II by nodal extent with limited contiguous extranodal involvement
II bulky[a]	II as above with "bulky" disease	Not applicable
Advanced		
III	Nodes on both sides of the diaphragm; nodes above the diaphragm with spleen involvement	Not applicable
IV	Additional noncontiguous extralymphatic involvement	Not applicable

Extent of disease is determined by positron emission tomography–computed tomography for avid lymphomas and computed tomography for nonavid histologies. Tonsils, Waldeyer ring, and spleen are considered nodal tissue.

[a] Whether stage II bulky disease is treated as limited or advanced disease can be determined by histology and a number of prognostic factors.

Source: Cheson BD, et al. *J Clin Oncol* 2014;32:3059–3067, table 2, p.3062. Reproduced with permission of Journal of Clinical Oncology: American Society of Clinical Oncology.

Furthermore, a greater proportion of patients have disease in organs other than lymph nodes or have leukemic manifestations. The median age of presentation of low grade and large B-cell lymphomas is 55–60 years. Patients with indolent histology do not usually have B symptoms (fever 38°C or more, night sweats, or loss of more than 10% of body weight in 6 months), but these features are common in those with aggressive histology.

Patients can have asymmetric painless enlargement of lymph nodes in one or more peripheral node regions (Fig. 19.3). This presentation is often associated with widespread involvement of lymph nodes (e.g. mesenteric or retroperitoneal) which is not detectable on routine clinical examination (Fig. 19.4). The liver and spleen can also be enlarged (Fig. 19.5).

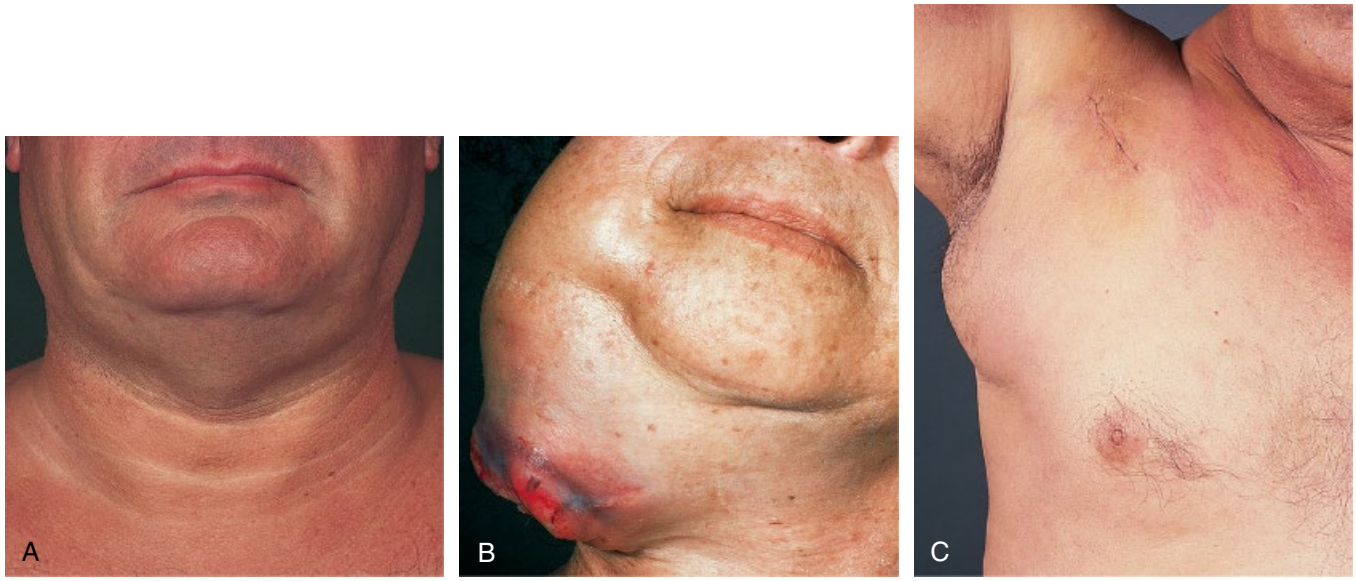

Fig. 19.3. Non-Hodgkin lymphoma. **A,** Bilateral cervical lymphadenopathy. **B,** Massive enlargement of axillary nodes with mass extending subcutaneously and also intramuscularly in the right infraclavicular and supraclavicular regions in a patient with diffuse large B-cell lymphoma.

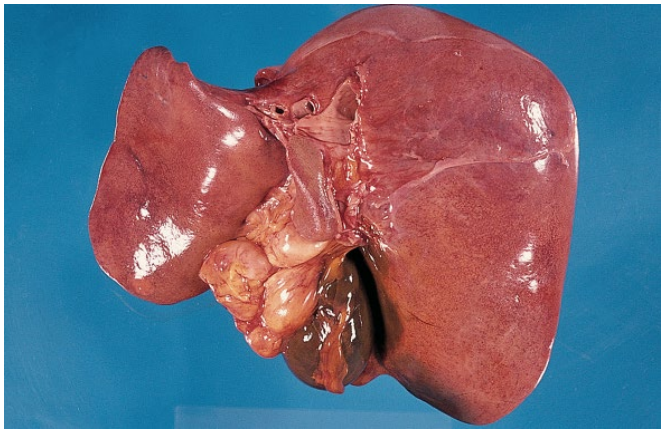

Fig. 19.4. Diffuse large B-cell lymphoma: Enlarged porta hepatis lymph nodes seen at autopsy.

At least 10% of patients with B-cell non-Hodgkin lymphoma have extranodal disease that includes skin (Fig. 19.6) and soft tissues, sometimes as an extension from lymph nodes (Fig. 19.7). When the gastrointestinal tract is involved, patients may present with acute abdominal symptoms. Gastrointestinal tract, lung, and salivary glands are extranodal sites frequently involved by marginal zone lymphomas (Fig. 19.8). Some B-cell (and T-cell) lymphomas show a predilection for certain tissues, such as mucosas and glandular tissues in marginal zone lymphomas or jaw, ovary, and breast in Burkitt lymphoma (see Fig. 20.29), which sometimes reflects the distribution of the normal counterpart from which they derive (Table 19.6).

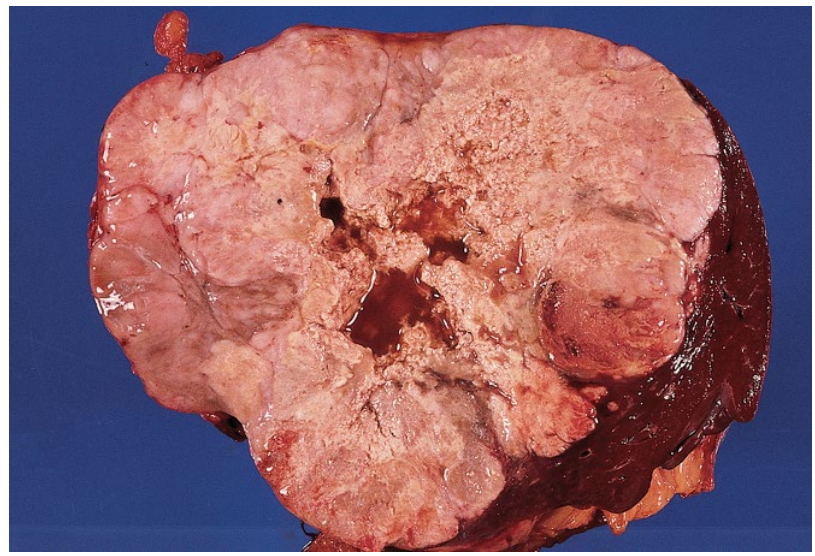

Fig. 19.5. Diffuse large B-cell lymphoma: Macroscopic appearance of spleen removed at laparotomy, showing widespread replacement of splenic tissue by pale tumor and extensive areas of necrosis.

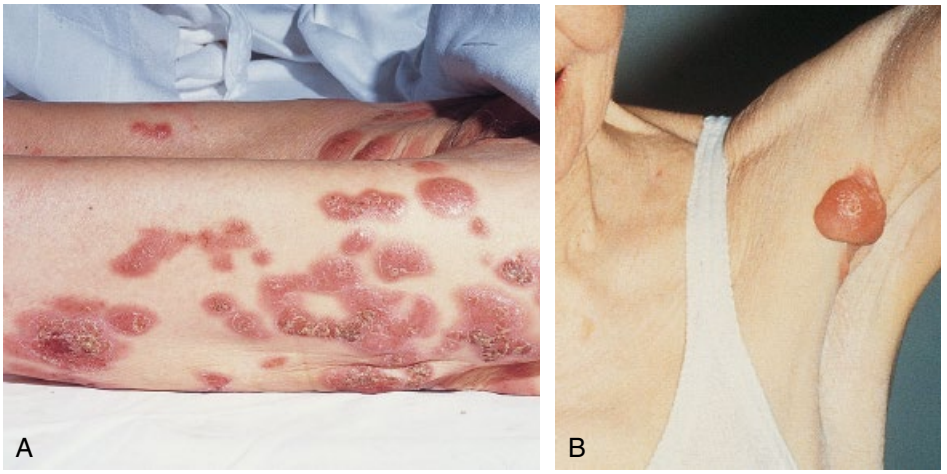

Fig. 19.6. Cutaneous deposits in advance diffuse large B-cell lymphoma.

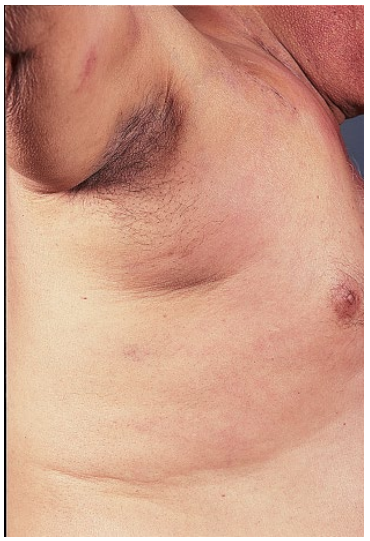

Fig. 19.7. Diffuse large B-cell lymphoma invading the anterior and lateral chest wall by direct spread into muscle from the axillary lymph nodes.

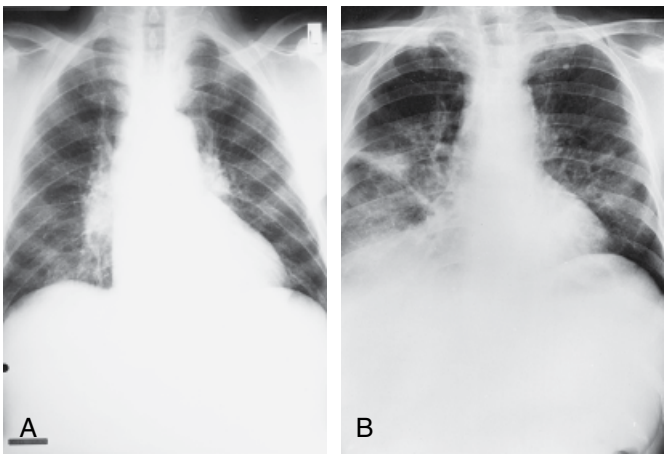

Fig. 19.8. Non-Hodgkin lymphoma: Chest radiographs showing: **A,** Bilateral hilar lymph node enlargement; and **B,** interstitial and confluent shadowing particularly in the lower and middle zones caused by lymphomatous infiltration (as shown by biopsy) in a patient with MALT lymphoma.

TABLE 19.6. NORMAL CELL COUNTERPARTS OF MATURE B-CELL LYMPHOID NEOPLASMS

Neoplasm	Postulated normal counterpart
B-cell neoplasms	
Chronic lymphocytic leukemia	Antigen-experienced B cell: Pregerminal (CLL with unmutated IGHV) or postgerminal center (CLL with mutated IGHV) cells
Lymphoplasmacytic lymphoma	Postfollicular B cell that differentiates to plasma cell?
Hairy cell leukemia	Memory B cell?
Splenic marginal zone lymphoma	Marginal zone cells
Follicular lymphoma	Germinal center cell
Mantle cell lymphoma	Mantle zone cell
	Antigen-experienced cell: Pregerminal (conventional MCL) or postgerminal center (leukemic non-nodal MCL) cells
MALT lymphoma	Marginal zone cell of extranodal follicles and/or intraepithelial associated B cells
Diffuse large B-cell lymphoma GCB subtype	Germinal center cell
Diffuse large B-cell lymphoma ABC subtype	Activated B cell
Burkitt lymphoma	Germinal center cell
Plasmablastic lymphoma	Plasmablast
Plasma cell myeloma	Bone marrow plasma cell

IMAGING

Imaging plays an important part in diagnosing and assessing the distribution (staging) of non-Hodgkin lymphoma. Involvement of intrathoracic and intra-abdominal sites can be evaluated by computed tomography (CT) scanning (Figs. 19.9 and 19.10). Magnetic resonance imaging (MRI) is particularly useful for detecting central nervous system (CNS) disease.

Positrons are positively charged electrons produced by decay of certain radionuclides. They travel a few millimeters before colliding with an electron where the two particles annihilate each other. Two equal protons are produced, which can be detected by a positron emission tomography (PET) camera. 18-Fluorodeoxyglucose (FDG) is used as radionuclide in oncology and detects increased glucose metabolism by the tumor compared with normal tissues. Compared with CT or MRI, PET scanning has the advantage of differentiating active tumor from residual scar tissue.

PET scanning combined with CT is valuable for initial staging (Fig. 19.11) and in detecting residual disease, confirming remission or restaging after chemotherapy or radiotherapy (Fig. 19.12), or

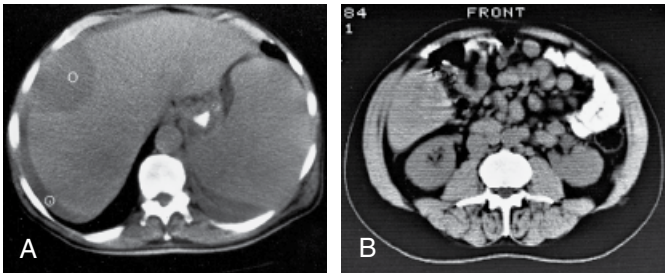

Fig. 19-9. Non-Hodgkin lymphoma: CT scans through the abdomen show: **A,** hepatic and splenic enlargement and a prominent radiolucent focus in the right lobe of the liver (ascitic fluid is present and contrast medium is present in the gut); and **B,** mesenteric and some para-aortic lymph node enlargement.

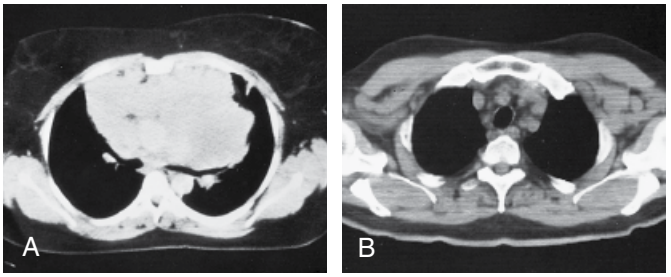

Fig. 19.10. Non-Hodgkin lymphoma: CT scans through the midthorax show **A,** gross enlargement of anterior mediastinal, paratracheal, and hilar nodes in T-lymphoblastic lymphoma; and **B,** anterior mediastinal and paratracheal lymph node enlargement in follicular lymphoma.

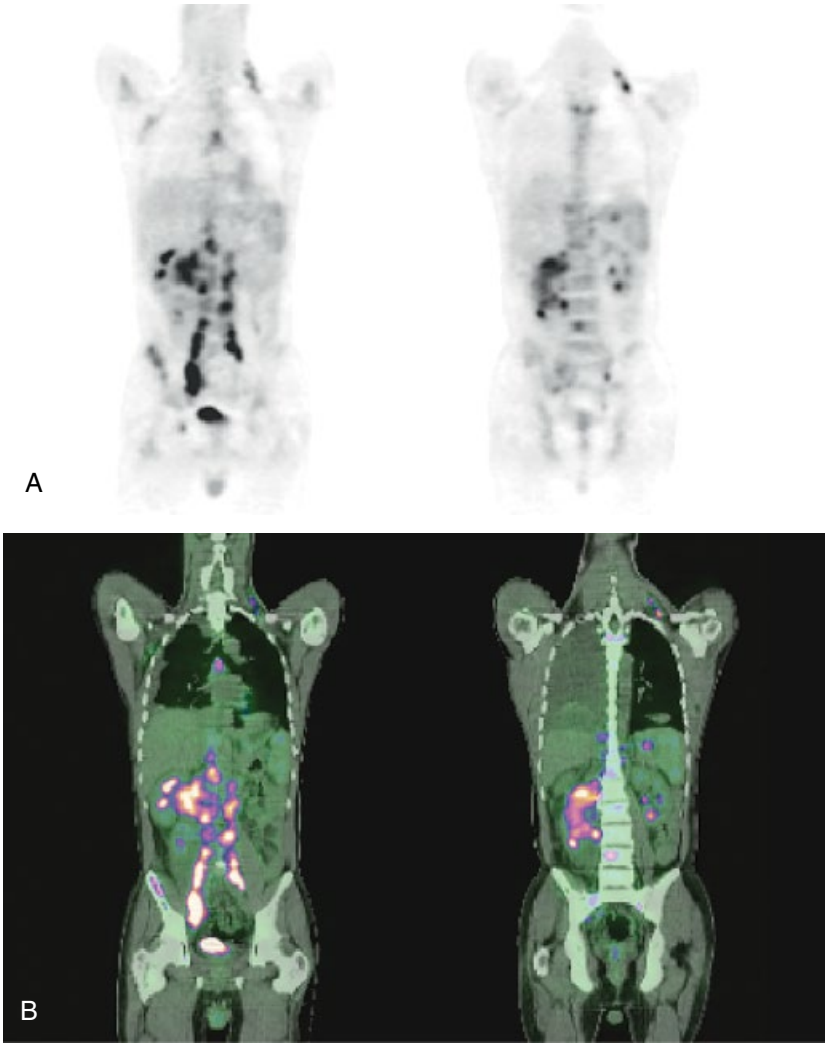

Fig. 19.11. Non-Hodgkin lymphoma. **A,** Coronal FDG PET. Diffuse large B-cell lymphoma showing abnormal FDG uptake in lymph nodes above and below the diaphragm, as well as a focus within the spleen and the bone marrow involvement (lumbar spine and right pelvis). **B,** Fused FDG PET/CT images. A right pleural effusion is also noted on the CT component. (*A, B,* Courtesy of Professor G Cook.)

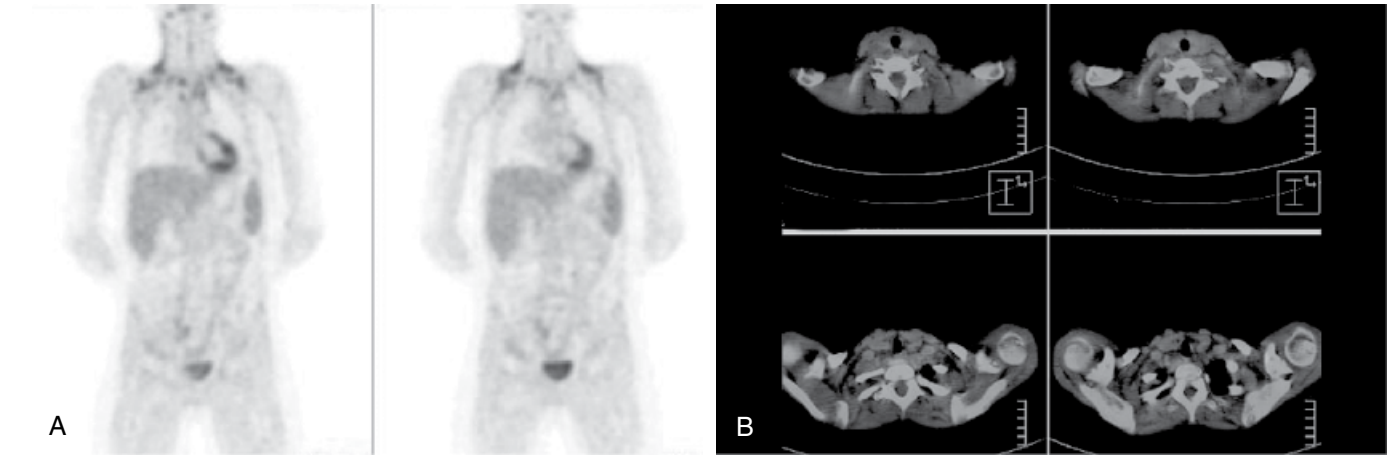

Fig. 19.12. Non-Hodgkin lymphoma. **A,** Coronal FDG PET slices of a patient with diffuse large B-cell lymphoma following chemotherapy showing symmetric activity in the supraclavicular fossae. **B,** Fused FDG PET/CT transaxial slices showing that the FDG activity is confined to fat and therefore represents physiologic brown fat activity rather than active lymphoma. (Courtesy of Professor G Cook.)

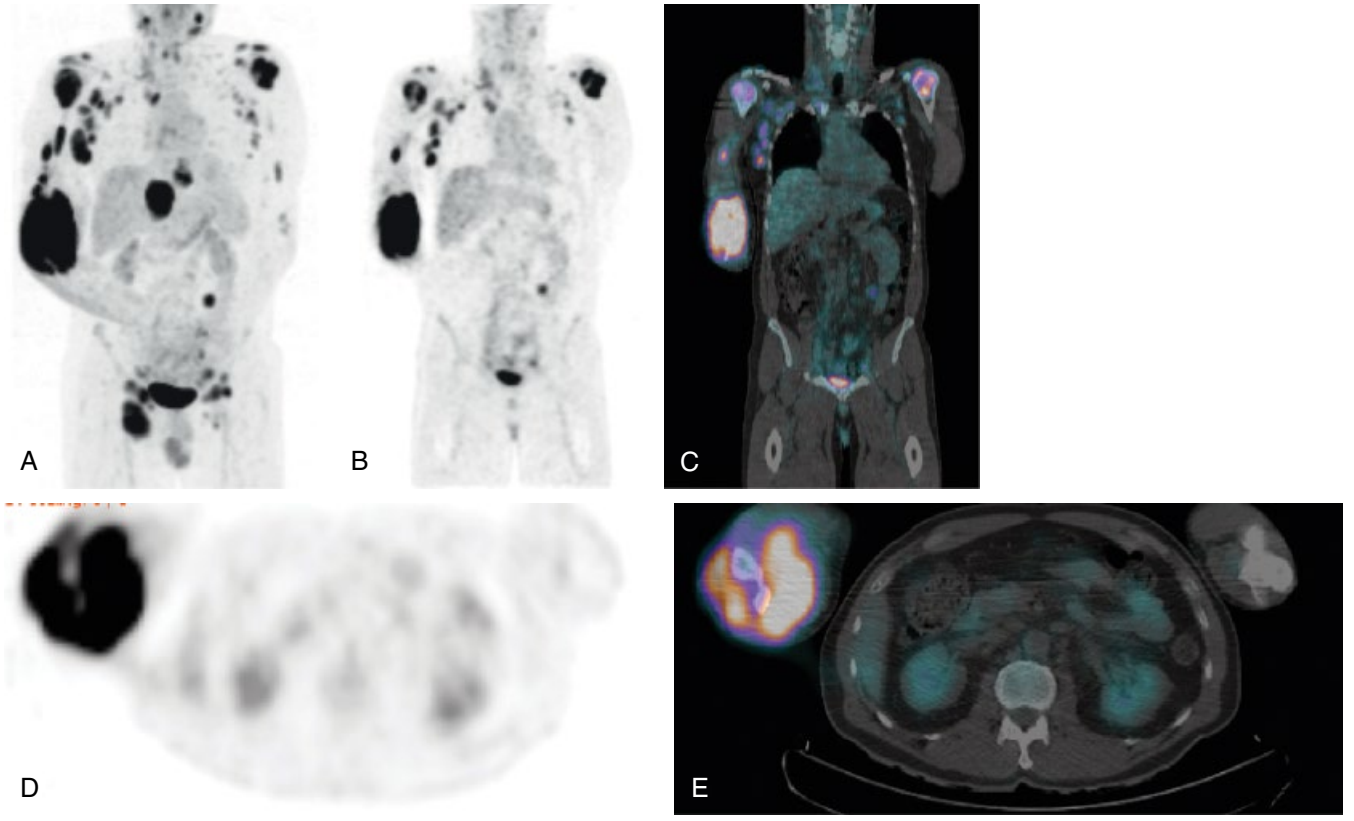

Fig. 19.13. Non-Hodgkin lymphoma. **A,** FDG PET MIP; **B,** coronal; **C,** fused coronal PET/CT; **D,** axial PET; and **E,** axial fused PET/CT through elbow. The patient had a previous diagnosis of follicular lymphoma with lymph nodes above and below the diaphragm and bone marrow involvement **(A)** with a sudden increase in size of nodal tissue at the right elbow, which on biopsy proved to be caused by transformed high-grade diffuse B-cell lymphoma. (Courtesy of Professor G Cook.)

detecting relapse or transformation to low- or high-grade disease (Fig. 19.13).

DIAGNOSIS

Diagnosis of lymphoid neoplasms requires a multidisciplinary approach integrating clinical features, the histologic pattern and cytology, the immunologic phenotype (Table 19.7), and the genetic abnormality detected by conventional cytogenetics, fluorescence in situ hybridization (FISH) analysis, or molecular genetic techniques (Table 19.3). In each particular entity the relevance of these different features varies.

Histologic diagnosis of lymph node, bone marrow, or extranodal mass tissue is essential. The recommended procedure to obtain the histologic diagnosis is the excisional biopsy of a whole lymph node or from the involved extranodal site. In some inaccessible sites or patients in poor general condition, an ultrasound or CT-guided

TABLE 19.7A. IMMUNOPHENOTYPE OF MATURE B-CELL NEOPLASMS

Neoplasm	sIg; cIg	CD20	PAX5	CD5	CD10	CD23	CD43	CD103	Cyclin D1	SOX11	LEF1	CD38/ CD138	Additional markers
Chronic lymphocytic leukemia	+; –/+	+ (weak)	+	+	–	+	+	–	–	–	+	–	FMC7–, CD79b–/+ CD200+
Lymphoplasmacytic lymphoma	+; +	+	+	–	–	–	+/–	–	–	–	–	+	
Hairy cell leukemia	+; –	+	+	–	–	–	+	++	+/–	–/+	–	–	CD25+, CD123+, CD11c+, DBA44+ Annexin A1
Splenic marginal zone lymphoma	+; –/+	+	+	–	–	–	–	–	–	–	–	–	
Follicular lymphoma	+; –	+	+	–	+/–	–/+	–	–	–	–	–	–/+	BCL6+, LMO2+, HGAL+
Mantle cell lymphoma	+; –	+	+	+	–	–	+	–	+	+*	–	–	
MALT lymphoma	+; +/–	+	+	–	–	–/+	–/+	–	–	–	–	–	
Diffuse large B-cell lymphoma GCB subtype	+/–;	+	+	–	+	NA	–	NA	–	–	–	–	BCL6+, IRF4–
Diffuse large B-cell lymphoma ABC subtype	+/–; –/+	+	+	–	–	NA	–	NA	–	–	–/+	–	IRF4+, FOXP1+
Primary mediastinal large B-cell lymphoma	–; –/+	+	+	–	–/+	+	–	NA	–	–	–	–	CD30+, MAL+
Burkitt lymphoma	+; –	+	+	–	+	–	–	NA	–	–/+	–	–	BCL2–, LMO2–
Plasmablastic lymphoma	–; +	–	–	–	–/+	–	–	–	–	–	–	+	IRF4+, BLIMP1+
Plasma cell myeloma	–; +	–/+	–	–	+/–	–	–/+	–	–/+	–	–	+	IRF4+, BLIMP1+

TABLE 19.7B. IMMUNOLOGIC MARKERS OF VALUE IN MATURE B-CELL NEOPLASMS

Reagent	Normal distribution of staining	Clinical utility in mature B-cell neoplasms	Comments
CD5	T cells and minor B-cell subset	Expression on some B cells and CLL, MCL	Expression in some DLBCL
CD10	Immature T and B cells, subset of mature T cells (TFH) and B cells (germinal center), and neutrophils	Germinal center phenotype derived lymphomas: FL, DLBCL, BL; frequently present in ALL	Also expressed in some T-cell lymphomas derived from TFH
CD11c	Some B cells, some T cells	HCL CD11c (+ br)	Frequent weaker expression on CLL, MCL, and others
CD15	Myeloid and monocytic cells	Can be aberrantly expressed in B-cell neoplasia Hodgkin lymphoma	More frequently seen in ALL than in mature neoplasm
CD19	All B cells, including lymphoblasts, mature B-lymphoid cells, and most plasma cells	Indicates B-cell lineage; may demonstrate abnormal intensity in B-cell neoplasms; usually absent in PCN	Aberrant expression on myeloid cells in AML or MDS
CD20	Acquired during maturation of precursor B cells (hematogones); mature B-lymphoid cells positive; absent on most BM plasma cells; minor T-cell subset	Supports B-cell lineage; intensity often differs between subtypes: CLL/SLL dim, FL brighter	Present on occasional T-cell lymphoid neoplasms
CD22	Cytoplasmic expression in early B cells; surface expression acquired during maturation of precursor B cells, basophils	Indicates B-cell lineage in ALL and mature lymphoid neoplasms; intensity often differs between subtypes of mature B-cell neoplasm: CLL/SLL dim	Unspecific staining of some clones with monocytes
CD23	Weak intensity expression on resting B cells and increased with activation. Positive in mantle zone cells Expressed in FDC	Distinguish CD5+ B-cell lymphoid neoplasms; CLL/SLL+	Expressed in some FL, particularly in the diffuse variant, and primary mediastinal large B-cell lymphoma
CD25	Activated B cells and T cells	HCL in combination with CD11c and CD103	–

(*Continued*)

TABLE 19.7B. (CONTINUED)

Reagent	Normal distribution of staining	Clinical utility in mature B-cell neoplasms	Comments
CD38	Precursor B cells (hematogones), normal follicle center B cells, immature and activated T cells, NK cells, plasma cells (bright intensity), myeloid and monocytic cells, and erythroid precursors	Bright intensity staining can indicate plasmacytic differentiation; prognostic marker in CLL/SLL	–
CD43	T cells, myeloid, monocytes, small B-cell subset, plasma cells	Aberrant expression in CLL, MCL, some MZL	–
CD21	Complement C3d receptor, Epstein–Barr virus receptor. Expressed in B cells and FDC	Useful to recognize follicular structures. Distinction of follicular and diffuse components in FL	
CD22	Cytoplasmic expression in early B cells; surface expression acquired during maturation of precursor B cells, basophils	Indicates B-cell lineage in ALL and mature lymphoid neoplasms; intensity often differs between subtypes of mature B-cell neoplasm: CLL/SLL dim	Unspecific staining of some clones with monocytes
CD45	Pan leukocytes. Negative erythrocytes and nonhematologic neoplasm	Useful in distinguishing mature lymphoid neoplasms (bright intensity) from ALL and PCN (weak intensity to negative)	Negative in Hodgkin lymphoma, PCN and some ALL
CD49d	Integrin α subunit Expressed in many hematologic cells	Adverse prognostic factor in CLL	
CD79a and b	Cytoplasmic staining in precursor B cells, plasma cells positive, variable expression mature B cells	Indicates B-cell lineage in ALL and mature lymphoid neoplasms; intensity often differs between subtypes of mature B-cell neoplasm; CLL/SLL dim CD79b	CD79a staining has been reported in some T-ALL and rare mature T-cell lymphoid neoplasms
CD103	B-cell subset, intramucosal T cells	HCL and some MZL	Also EATCL
CD123	Interleukin 3 receptor Expressed in hematopoietic precursors	Expressed in HCL but not in CLL, FL. HCL-variant or SMZL	Also expressed in AML, plasmacytoid dendritic cells and derived neoplasms
CD200	Membrane glycoprotein of the immunoglobulin superfamily. Expressed in B cells, a subset of T cells, thymocytes, endothelial cells, and neurons	Expressed in CLL, HCL, and B-ALL. Negative in FL, SMZL, and conventional MCL. Positive in some leukemic non-nodal MCL	
BCL2	T cells, some B cells; negative normal germinal center cells	Distinguish CD10+ lymphoid neoplasms: FL+, DLBCL-GCB+ but BL–	Variable staining in DLBCL
BCL6	Transcription factor essential for germinal center formation	Expressed in germinal center-derived lymphomas	Also expressed in some T-cell lymphomas derived from TFH
FMC-7	B cells	Distinguish CD5+ lymphoid neoplasms: CLL–, MCL often positive. Also HCL+	
κ and λ	Mature B cells	Monotypic expression supports clonal proliferation Different surface and cytoplasmic expression in several entities	Monotypic λ expression in Castleman disease is polyclonal
IgM	First Ig component in precursor B cells; expressed by subset of plasma cells and mature B cells	IgM-producing neoplasms that might be associated with Waldenström macroglobulinemia	–
MUM1/IRF4	Transcription factor essential for plasma cell differentiation	Expressed in plasma cell-derived neoplasms and DLBCL activated B-cell type	Also expressed in some T-cell lymphomas
PAX5	Transcriptional factor determining B-cell differentiation. Negative in plasma cells	Expressed in all B-cell neoplasms but negative in PCN	Weak expression in classic Hodgkin lymphoma
TdT	B- and T-cell precursors	ALL	Also some AML
ZAP-70	T cells, NK cells, precursor B cells	Prognostic marker in CLL/SLL	–

+ indicates usually positive; – usually negative; ALL, acute lymphoblastic lymphoma; AML, acute myeloid leukemia; b, bright or strong intensity; BL, Burkitt lymphoma; cIg, cytoplasmic immunoglobulin; CLL, chronic lymphocytic leukemia; DLBCL, diffuse large B-cell lymphoma; EATCL, enteropathy associated T-cell lymphoma; FDC, follicular dendritic cells; FL, follicular lymphoma; HCL, hairy cell leukemia; Ig, immunoglobulin; MCL, mantle cell lymphoma; MZL, marginal zone lymphoma; PCN, plasma cell neoplasm; SLL, small lymphocytic lymphoma; SMZL, splenic marginal zone lymphoma; TdT, terminal deoxynucleotidyl transferase; TFH, T follicular helper cells.
Table compiled with contributions from Dr. Estella Matutes and Neus Villamor.

core biopsy can provide appropriate tissue material for the diagnosis. Surgical resections are performed in some patients with extranodal masses or splenomegaly. Bone marrow trephine is performed for staging in some lymphomas. Fine-needle aspirates do not provide sufficient material for diagnosis although can be useful to demonstrate infection in patients with unexplained lymphadenopathy.

The topographic site of the tumor can be essential for the diagnosis of some entities such as primary mediastinal large B-cell lymphoma. Some lymphomas predominate in different age groups or gender. The performance status of the patient, sites of involvement, and lactate dehydrogenase (LDH) levels define prognostic subgroups that can assist in therapeutic decisions. Other laboratory findings include cytopenias due to marrow involvement, hypersplenism, or the anemia of chronic disorders, but anemia can also be autoimmune, especially in those with low-grade disease. There may be circulating lymphoma cells. This is more common in late-stage disease. Paraproteins are found in serum in the indolent B-cell lymphomas; for example, small lymphocytic, lymphoplasmacytic, and splenic marginal zone lymphomas, and more rarely in large cell lymphomas.

LYMPHOPLASMACYTIC LYMPHOMA/ WALDENSTRÖM MACROGLOBULINEMIA

Lymphoplasmacytic lymphoma (LPL) is a neoplasm of small B lymphocytes, plasmacytoid lymphocytes, and plasma cells, usually involving bone marrow and sometimes lymph nodes and spleen (Figs. 19.14 and 19.15). As other small B-cell neoplasms can have these morphologic features, the diagnosis of LPL requires the exclusion of other tumors with plasmacytic differentiation. In plasmacytic cells, IgM is detectable in the cytoplasm or intranuclear inclusions called "Dutcher bodies," which also stain positive for periodic acid–Schiff (PAS) (Figs. 19.14 and 19.16).

The lymphocyte infiltration can replace the normal architecture of the lymph node, although usually spares the sinuses and frequently is interfollicular. Pseudofollicles, neoplastic follicles, or monocytoid B cells are absent and their presence should suggest other lymphoid neoplasms. The tumor cells, small lymphocytes, plasmacytoid lymphocytes, and plasma cells circulate in the peripheral blood (Fig. 19.17) and can be

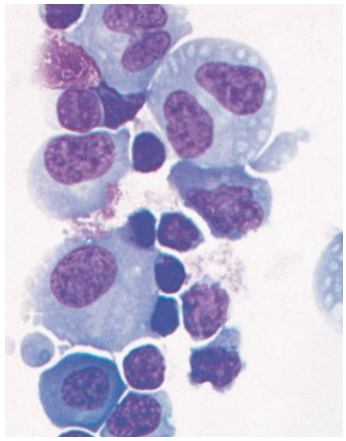

Fig. 19.15. Lymph node fine-needle aspirate showing lymphoplasmacytic lymphoma (May-Grünwald–Giemsa stain). Some of the cells show plasma cell differentiation with blue cytoplasm with pale staining perinuclear zone ("hof") and eccentric nucleus.

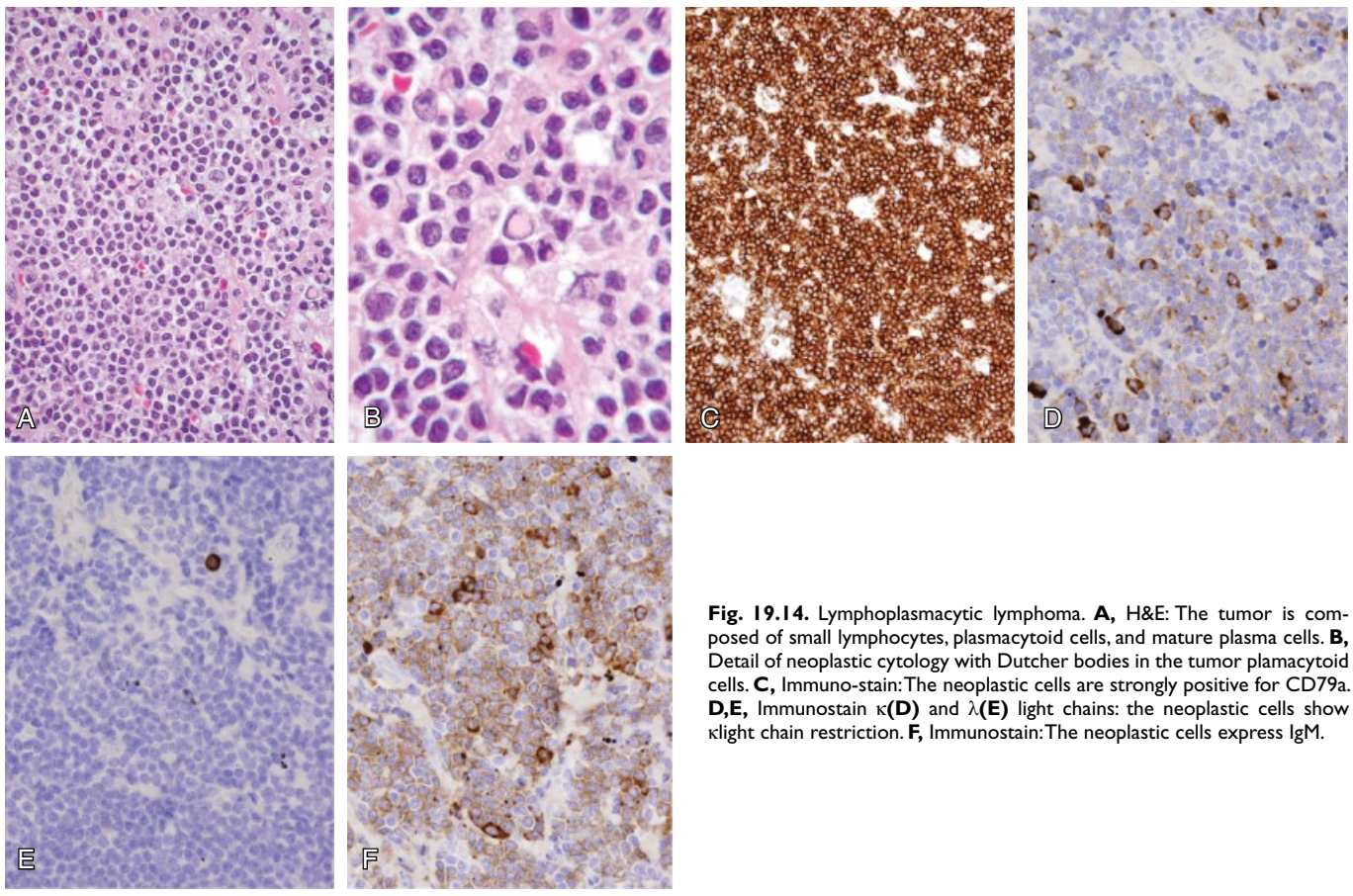

Fig. 19.14. Lymphoplasmacytic lymphoma. **A,** H&E: The tumor is composed of small lymphocytes, plasmacytoid cells, and mature plasma cells. **B,** Detail of neoplastic cytology with Dutcher bodies in the tumor plamacytoid cells. **C,** Immuno-stain: The neoplastic cells are strongly positive for CD79a. **D,E,** Immunostain κ**(D)** and λ**(E)** light chains: the neoplastic cells show κlight chain restriction. **F,** Immunostain: The neoplastic cells express IgM.

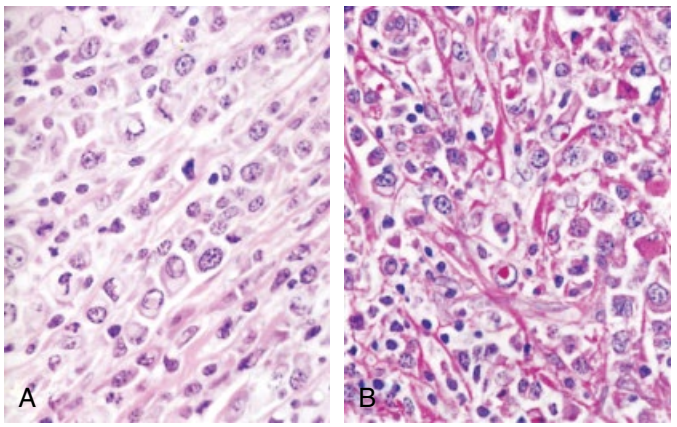

Fig. 19.16. Lymphoplasmacytic lymphoma. **A,** Diffuse sheet of small lymphoid cells, some with plasmacytoid differentiation and pink intranuclear hyaline inclusions (Dutcher bodies) commonly encountered in lymphoplasmacytic lymphoma. **B,** A periodic acid–Schiff (PAS) stain shows more marked plasma cell differentiation (center) with the positive Dutcher body. Small scattered lymphocytes and lymphoplasmacytoid cells are also present.

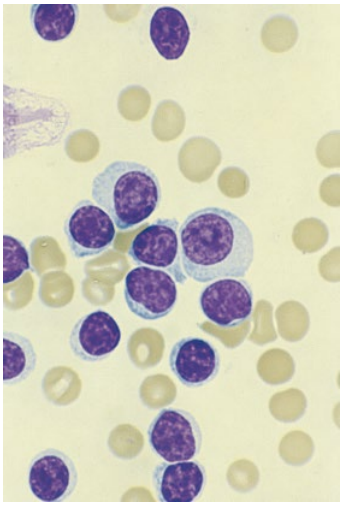

Fig. 19.17. Lymphoplasmacytic lymphoma in leukemic phase: Peripheral blood film.

detected as an interstitial, diffuse, or nodular infiltration in the bone marrow (Figs. 19.18 and 19.19).

The cells are CD20, CD79a positive with strong cytoplasmic IgM and light chain restriction (Fig. 19.14). CD5, CD10, CD23, and BCL6 are negative but the cells express BCL2 and IRF4/MUM1. The L265P *MYD88* mutation can be found in more than 90% of cases and mutations in *CXCR4* in around 40%, usually associated with disease more resistant to therapy. The disease can transform into a large cell lymphoma.

A paraprotein is usually present in the serum; when this is IgM and there is bone marrow involvement the disease can be termed Waldenström macroglobulinemia. This is often associated with hyperviscosity syndrome (Fig. 19.20) or cryoglobulinemia. Hyperviscosity syndrome is characterized by loss of vision, CNS symptoms, a hemorrhagic diathesis, and heart failure; the most severely affected patient may be in coma. The retina shows a variety of changes, including engorged veins, hemorrhages, exudates, and blurred optic discs (Fig. 19.20).

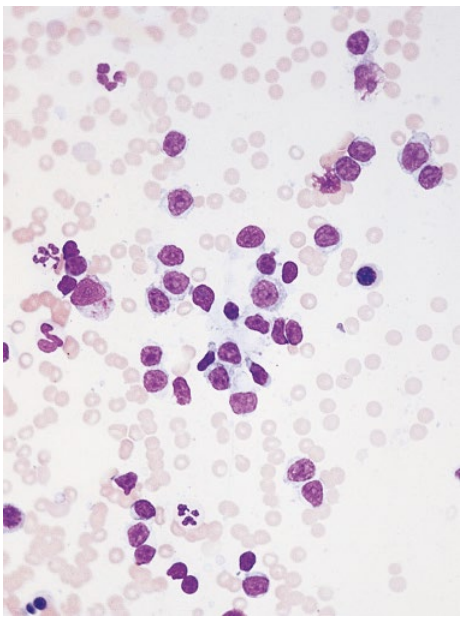

Fig. 19.18. Lymphoplasmatic lymphoma/Waldenström macroglobulinemia: Bone marrow cell trail shows a predominance of lymphocytes and lymphoplasmacytoid cells.

MONOCLONAL GAMMOPATHY OF UNDETERMINED SIGNIFICANCE IgM+

The 2016 update of the World Health Organization (WHO) classification considers the IgM monoclonal gammopathy of undetermined significance (MGUS) a precursor lesion of LPL or other B-cell lymphoid neoplasms rather than plasma cell myeloma. It is defined by a serum IgM protein <30 g/L, bone marrow lymphoplasmacytic infiltration <10%, and no evidence of anemia, constitutional symptoms, hyperviscosity syndrome, lymphadenopathy, hepatosplenomegaly, or other end-organ damage that can be attributed to the underlying lymphoproliferative disorder. Patients with IgM MGUS can also develop primary amyloidosis. Approximately 50% of these patients may have the L265P *MYD88* mutation.

HEAVY CHAIN DISEASES

Heavy chain diseases (HCDs) are a rare group of disorders in which the neoplastic cells secrete immunoglobulin heavy chains (γ, α, or μ) without light chains attached to them. The secreted heavy chains in all types of HCD are usually incomplete.

γ-HCD is a small B-cell neoplasm with plasmacytic differentiation. The disease is slightly more frequent in males, with a peak incidence in the seventh decade of life, with lymphadenopathy, hepatosplenomegaly, fever, and anemia as usual clinical features. Autoimmune diseases (e.g. rheumatoid arthritis and hemolytic anemia) occur in 25% of cases. The histologic substrate is heterogeneous. The lymph nodes and marrow show a mixture of lymphocytes, immunoblasts, histiocytes, and plasma cells, often with eosinophilia. Some cases have a splenic marginal zone lymphoma or MALT lymphoma. The cells in the peripheral blood can resemble chronic lymphocytic leukemia or lymphoplasmacytic lymphoma. The serum shows a monoclonal

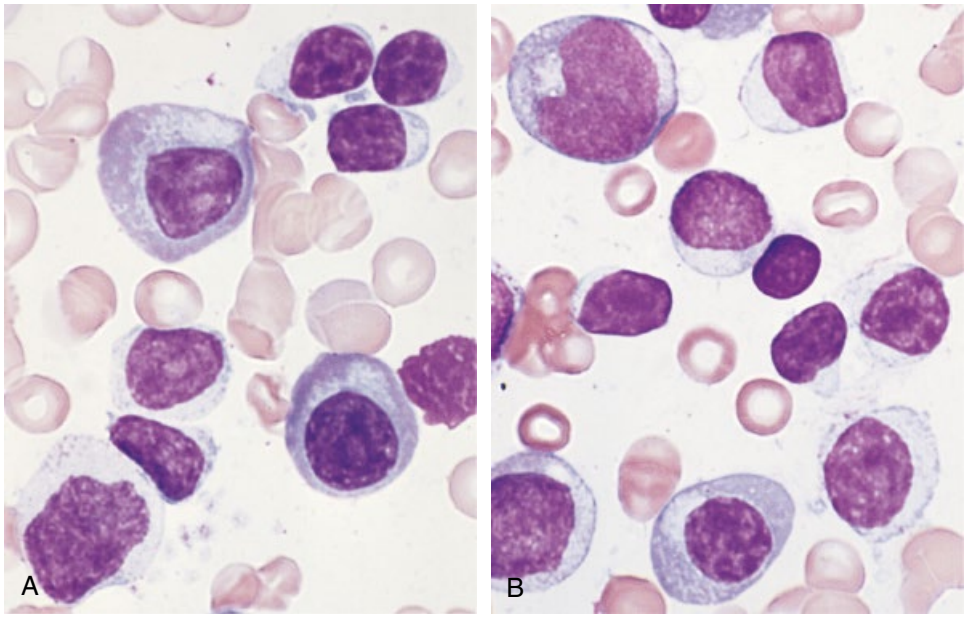

Fig. 19.19. Lymphoplasmacytic lymphoma/Waldenström macroglobulinemia bone marrow aspirate. **A,B,** The cells have features varying between those of lymphocytes and plasma cells. The chromatin patterns in the larger nuclei are more open and primitive.

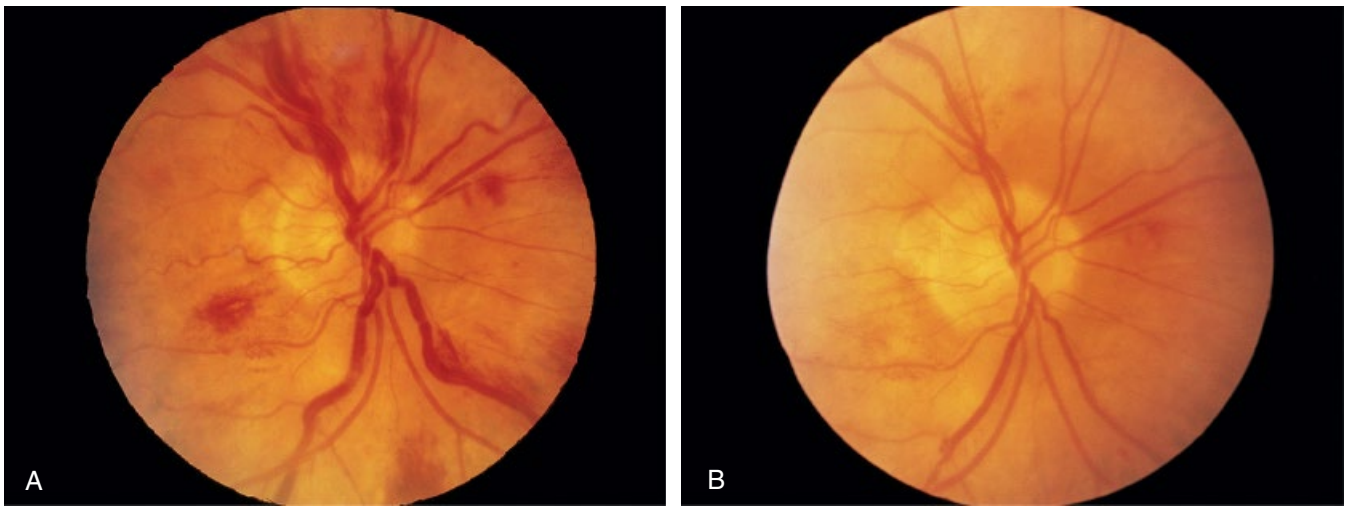

Fig. 19.20. Lymphoplasmacytic lymphoma/Waldenström macroglobulinemia: Hyperviscosity syndrome. The patient complained of blurred vision, headache, and dizziness. **A,** The retina before plasmapheresis shows gross distention of vessels, particularly the veins, which show bulging and constriction ("linked sausage effect") and areas of hemorrhage. **B,** Following plasmapheresis, the vascular diameters are normal and the hemorrhagic areas have cleared.

spike in the γ region. The protein usually consists of two γ heavy chains linked together. The variable region and part of the first domain of the constant region are sometimes deleted. *MYD88* is not mutated.

The most common form of HCD, **α-HCD**, also known as immunoproliferative small intestinal disease (IPSID), is now classified as a form of MALT lymphoma. It occurs largely in the Mediterranean area and Africa, often in young adult patients with an Arabic genetic background, and in areas where intestinal parasites (e.g. *Campylobacter jejuni*) are common. It commences as a relatively benign plasma cell proliferation in the gastrointestinal tract (Fig. 19.21); subsequently, a poorly differentiated lymphoma of the small bowel develops and can spread, although usually within the abdominal cavity (Fig. 19.22). The serum shows a monoclonal protein in the α2 or β region in 50% of cases, and the protein can also be found in the urine. It consists of a heavy chain with an internal deletion. A rare form of α-HCD occurs sporadically outside the areas in which intestinal infection is common and is characterized by a lymphoplasmacytoid infiltrate of the respiratory tract.

The rarest form is **μ-HCD**; patients are usually African, particularly from parasite-infected zones (as for α-HCD). However, μ-HCD manifests with a clinical picture that resembles chronic lymphocytic leukemia, with enlargement of the liver and spleen and infiltration of the marrow with vacuolated plasma cells admixed with small lymphocytes. Light chains of one type can also be found in urine, but these remain separate from the μ heavy chain.

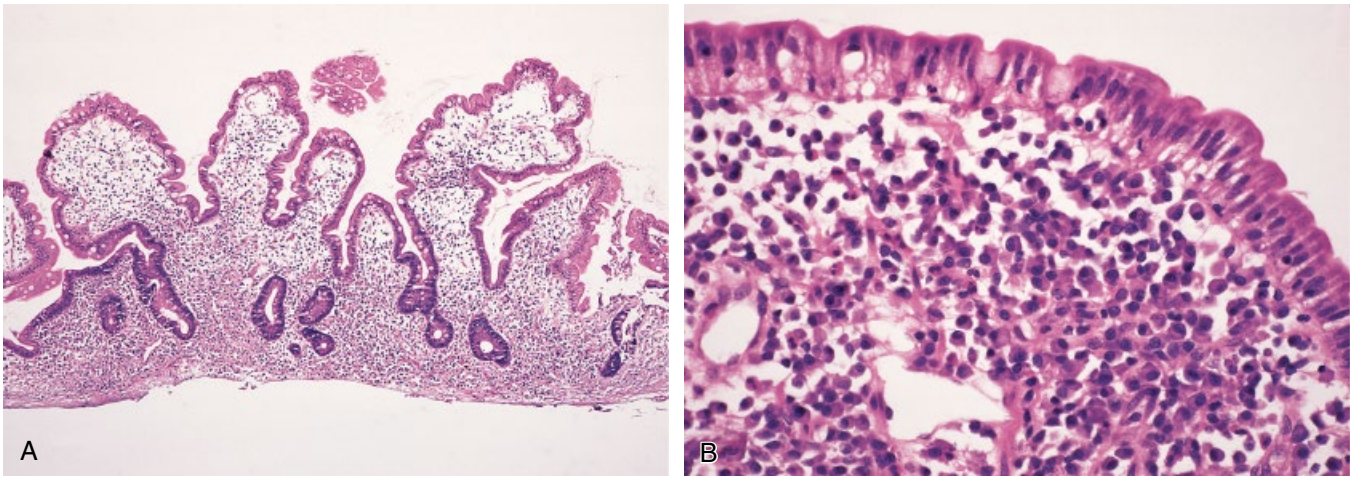

Fig. 19.21. α Heavy chain disease: this 25-year-old Algerian man was treated for a malabsorption syndrome, consisting of weight loss, chronic diarrhea, steatorrhea, and hypocalcemia, which responded to broad-spectrum antibiotics. **A,** At this stage, small intestinal biopsy showed a diffuse infiltration of the lamina propria. **B,** The cells were a mixture of lymphocytes, plasma cells, and plasmacytoid cells. Immunocytochemical staining showed that a vast majority of these cells contained α heavy chains without κ or γ light chains. Serum and urine samples revealed a broad band in the α2 globulin region, which precipitated with anti-IgA but showed no reactivity to anti-κ or anti-γ. (*A, B,* Courtesy of Dr. JE McLaughlin.)

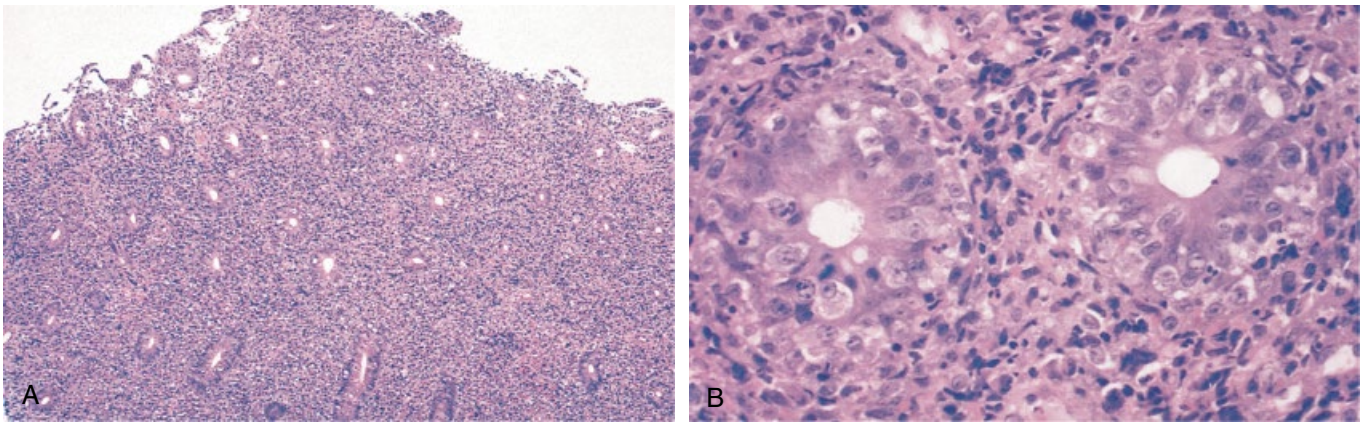

Fig. 19.22. α Heavy chain disease (same patient as shown in Fig. 19.22): 2 years after treatment the patient developed small intestinal obstruction; intestinal resection revealed the small bowel to be heavily infiltrated by a large cell lymphoma with an additional mixed infiltrate of neutrophils, plasma cells, and macrophages. Despite intensive chemotherapy, the tumor relapsed, involving the large and small bowel, and intraabdominal lymph nodes showed similar histologic findings. The appearances of the rectal mucosa at **(A)** low and **(B)** high power show complete loss of normal architecture, with remaining crypt cells surrounded by the diffuse infiltrate consisting of immunoblasts and mixed inflammatory cells. The α heavy chain could still be detected in serum, but not in urine at this relapse. (*A, B,* Courtesy of Dr. JE McLaughlin.)

SPLENIC MARGINAL ZONE LYMPHOMA

This is a primary splenic disease characterized by a proliferation of splenic marginal zone cells that infiltrate and overrun the white pulp nodules, usually with a follicular structure, and also infiltrate the red pulp. The spleen can be massively enlarged and peripheral blood and bone marrow involvement is usual, but lymphadenopathy is rare. A small monoclonal serum paraprotein occurs in about one-third of cases, and warm-type autoimmune hemolytic anemia or immune thrombocytopenia is frequent. The peripheral blood shows a moderate lymphocytosis (up to 25×10^9/L). The cells have an irregular plasma membrane with villi, often confined to one pole of the cell. Based on these lymphocytes the disease had been termed splenic lymphoma with villus lymphocytes (Fig. 19.23).

Histologically, the neoplastic lymphocytes surround and infiltrate the germinal centers in the white pulp (Fig. 19.24). There may be a population of larger tumor cells at the periphery of the germinal center. The red pulp is also infiltrated usually with tumor cells in the sinuses. The cells can also show some lymphoplasmacytic differentiation. The lymphocytes have the immunophenotype SIgM+, IgD+/-, cytoplasmic Ig-/+, CD19, CD20, CD22, CD79a+, CD5-, CD10-, CD23-, and CD43+/-. The bone marrow shows nodular or interstitial infiltration (Fig. 19.25). Cytogenetic abnormalities include trisomy 3 and structural abnormalities including allelic loss of chromosome 7q31-32. Sequencing studies have revealed frequent mutations in *NOTCH2* (10–25%), *KLF2* (10–40%), and genes of the NFκB pathway (Table 19.4).

The disease is quite different from the other two marginal zone lymphomas: MALT lymphoma and nodal marginal zone lymphoma.

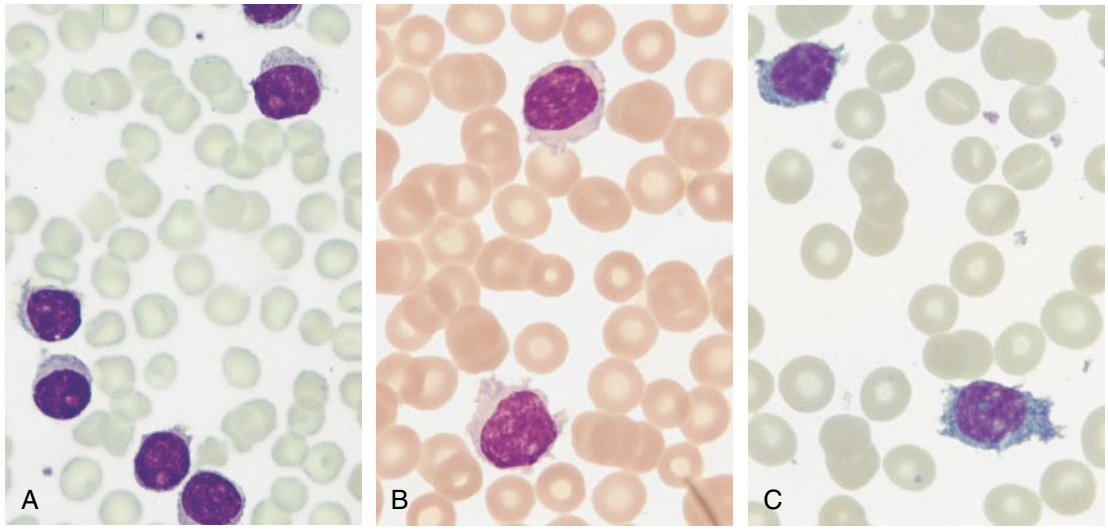

Fig. 19.23. Splenic marginal zone lymphoma. **A–C,** Peripheral blood films on a case with villus lymphocytes showing characteristic cells with irregular plasma membranes with short and thin villi often concentrated at one or two poles of the cells; the cells are larger than in typical CLL, the nucleus is round or ovoid, and sometimes eccentric with a clumped chromatin pattern. (*A,* Courtesy of Professor D Catovsky; *B, C,* Courtesy of Professor M Peetermans.)

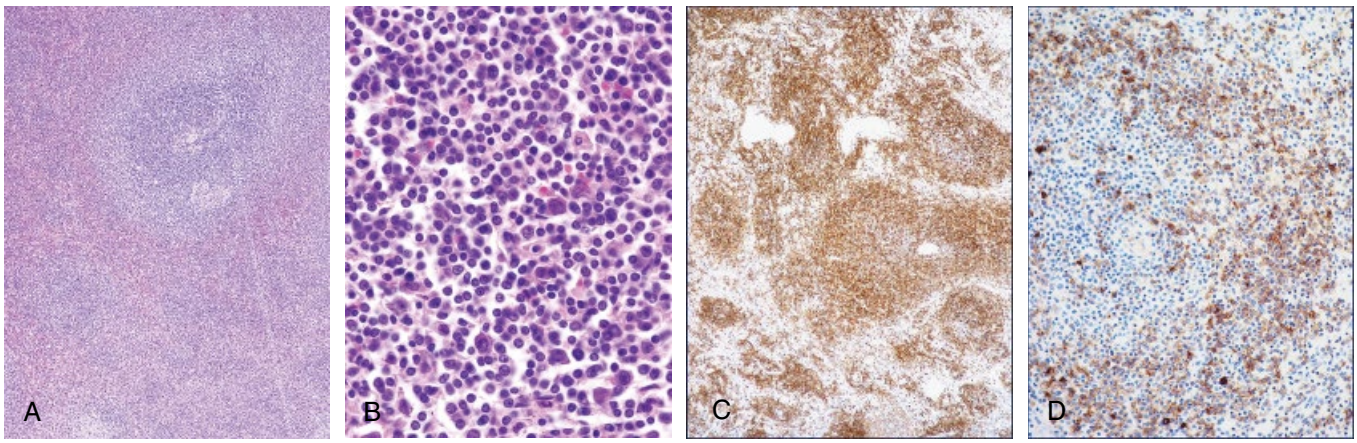

Fig. 19.24. Splenic marginal zone lymphoma. **A,** H&E: The white pulp is expanded with an increase of the marginal zone by neoplastic cells with paler cytoplasm surrounding a residual follicle. **B,** H&E: Detail of the characteristic biphasic pattern of small lymphocytes and scattered larger cells. **C,** Immunostain: The neoplastic cells are CD20 positive and infiltrate the white and red pulp. **D,** Immunostain: The neoplastic cells are IgD positive.

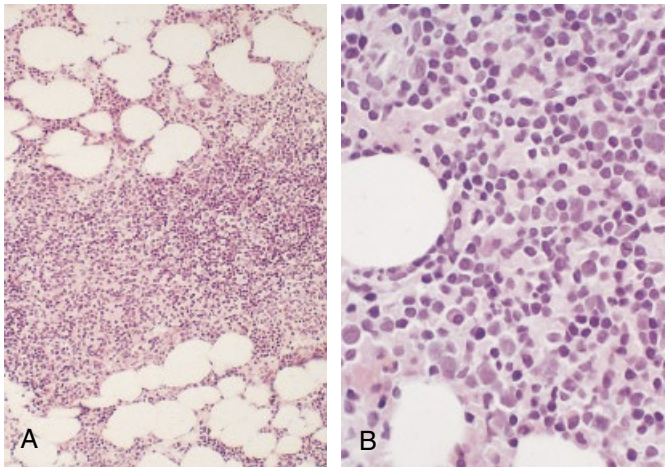

Fig. 19.25. Splenic marginal zone lymphoma: Bone marrow trephine biopsies showing: **A,** nodular infiltrate; **B,** diffuse interstitial infiltration by lymphocytes with lymphoplasmacytic forms. (Courtesy of Professor KA MacLellan.)

EXTRANODAL MARGINAL ZONE LYMPHOMA OF MUCOSA-ASSOCIATED LYMPHOID TISSUE (MALT LYMPHOMA)

This lymphoma is characterized by a heterogeneous proliferation of small B cells including marginal zone cells with clear cytoplasm (monocytoid cells), centrocyte-like cells, small lymphocytes, scattered large cells, and cells with plasmacytic differentiation. The proportion of these cells varies from case to case. These tumors originate in a background of chronic inflammation mainly caused by infection or autoimmune diseases (Table 19.2).

These tumors arise in extranodal tissues, frequently in the gastrointestinal tract in at least 50% of cases (Fig. 19.26), skin (Fig. 19.27), lung, thyroid, breast, and salivary glands (Figs. 19.28 and 19.29). Gastric MALT lymphoma recapitulates the histology of Peyer patches. Infection with *Helicobacter pylori* is thought to induce a T-cell reaction against bacterial antigens,

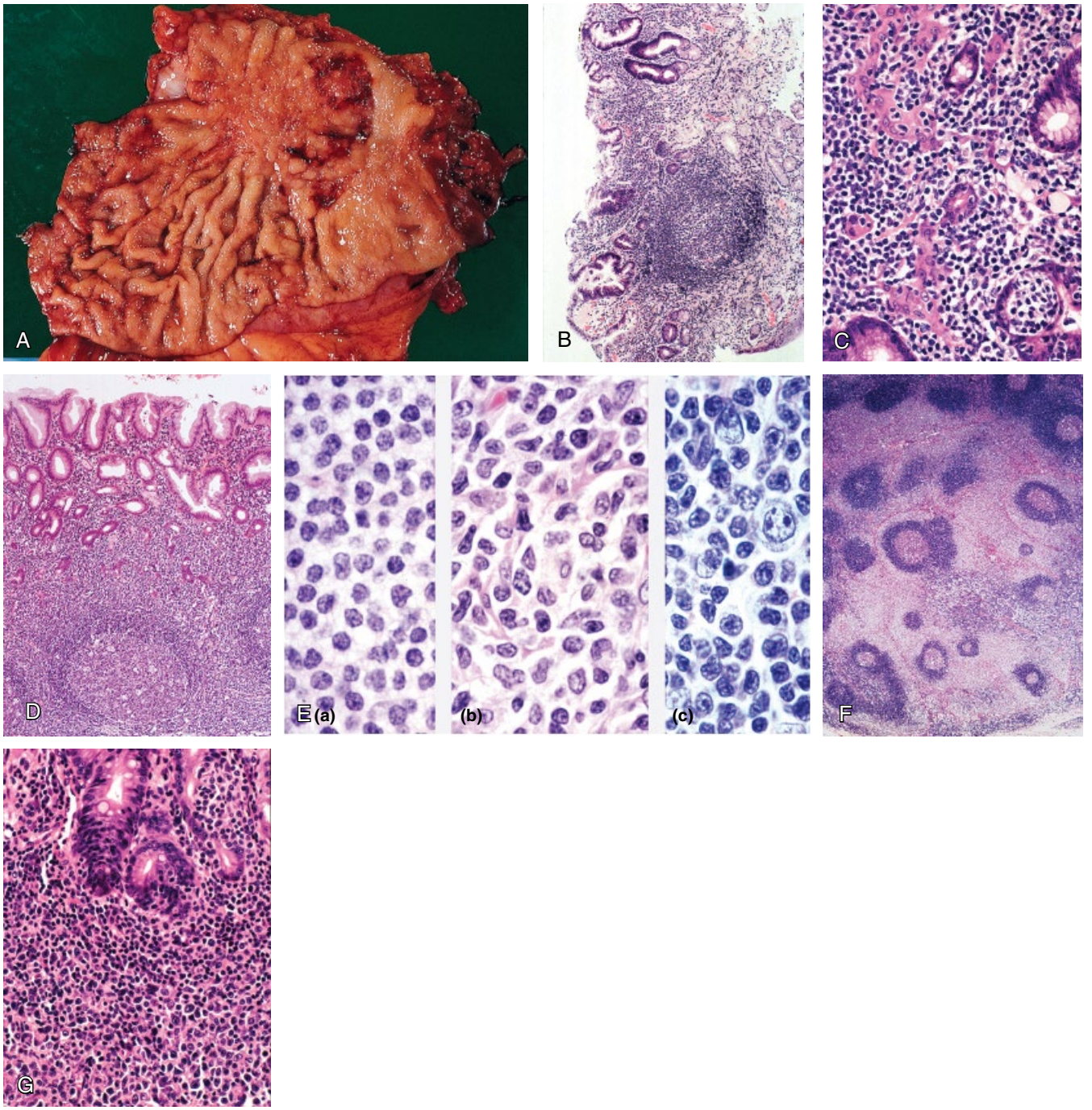

Fig. 19.26. Extranodal marginal zone lymphoma, MALT type. **A,** Partial gastrectomy specimen showing mucosal irregularity and lymphoma infiltration. **B,** *Helicobacter pylori* gastritis. Mixed inflammatory cells with prominent lymphocytes infiltrate around a reactive B-cell follicle. **C,** Gastric MALT lymphoma: Lymphoepithelial lesions with lymphocytes surrounding and infiltrating epithelial structures. **D,** Gastric MALT lymphoma: The tumor cells surround reactive follicles and infiltrate the mucosa. The follicle has a "starry sky" appearance. **E,** Gastric MALT lymphoma. Cytology: (a) Tumor cells resembling centrocytes with abundant cytoplasm; (b) characteristic small to medium-sized cells with irregular nuclei, inconspicuous nucleoli, and abundant pale cytoplasm; (c) cells resembling small lymphocytes with scattered larger cells. **F,** Gastric MALT lymphoma: Gastric lymph node. The tumor cells are largely in the marginal zone of the follicles and interfollicular areas. **G,** Gastric MALT lymphoma: Transformation to diffuse large B-cell lymphoma in the lower field with residual MALT lymphoma in the superficial areas. (*B–G,* Courtesy of Professor P Isaacson.)

which stimulates a B-lymphoid proliferation in the stomach. Elimination of the infection can cause regression of the lymphoma or of the preceding polyclonal lymphoid proliferation. The autoimmune disease Sjögren syndrome can underlie salivary gland MALT and Hashimoto disease MALT lymphoma of the thyroid.

The neoplastic cells reside and expand the marginal zones of reactive B-cell follicles and extend into the interfollicular region as well as into the follicular germinal center (follicular colonization). Tumor cells are heterogeneous including marginal centrocyte-like cells with irregular nuclei, monocytoid cells, small lymphocytes, and scattered large cells. Plasma cell

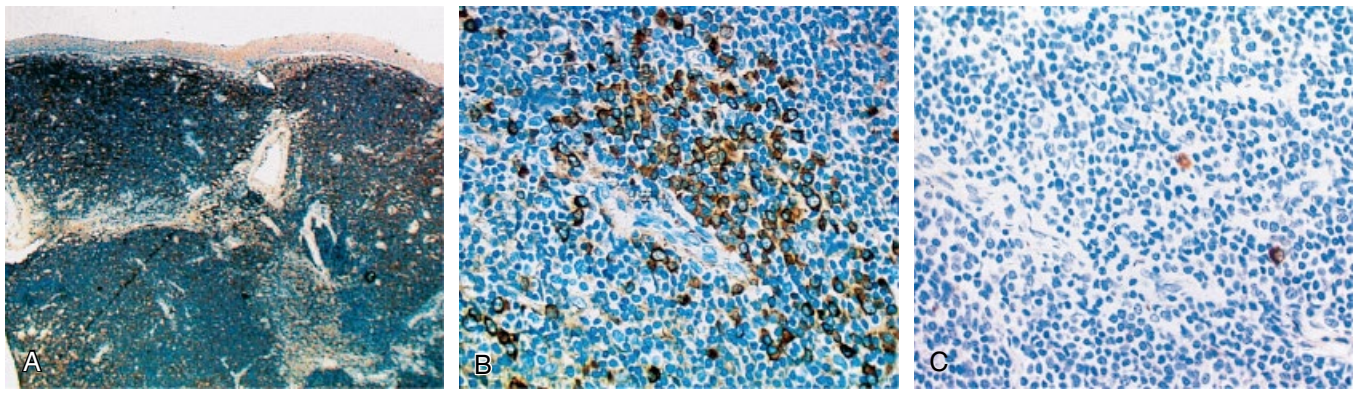

Fig. 19.27. Extranodal Marginal zone lymphoma of the skin. **A,** Low-power view of immunoperoxidase (CD20) stain showing extensive B-cell infiltrate. **B,C,** Clonality of tumor cells shown by **(B)** κ positivity in cells with plasmacytic differentiation) and **(C)** negativity for λ, only positive in occasional reactive cells.

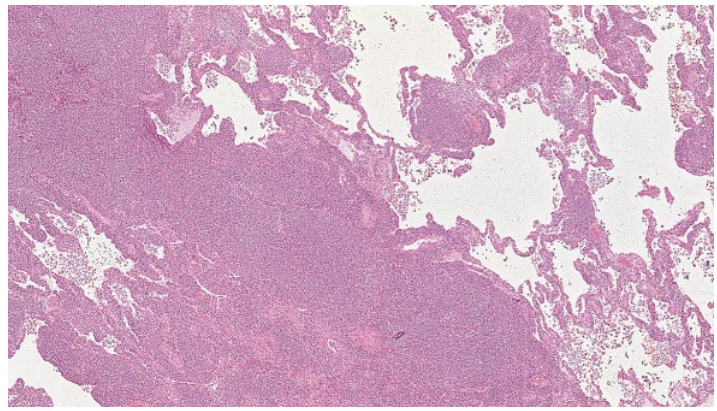

Fig. 19.28. Marginal zone (MALT) lymphoma in the lung: Low-power view of a histologic section shows sheets of neoplastic lymphocytes at the edge of the tumor infiltrating the surrounding lung along bronchovascular bundles and alveolar septae.

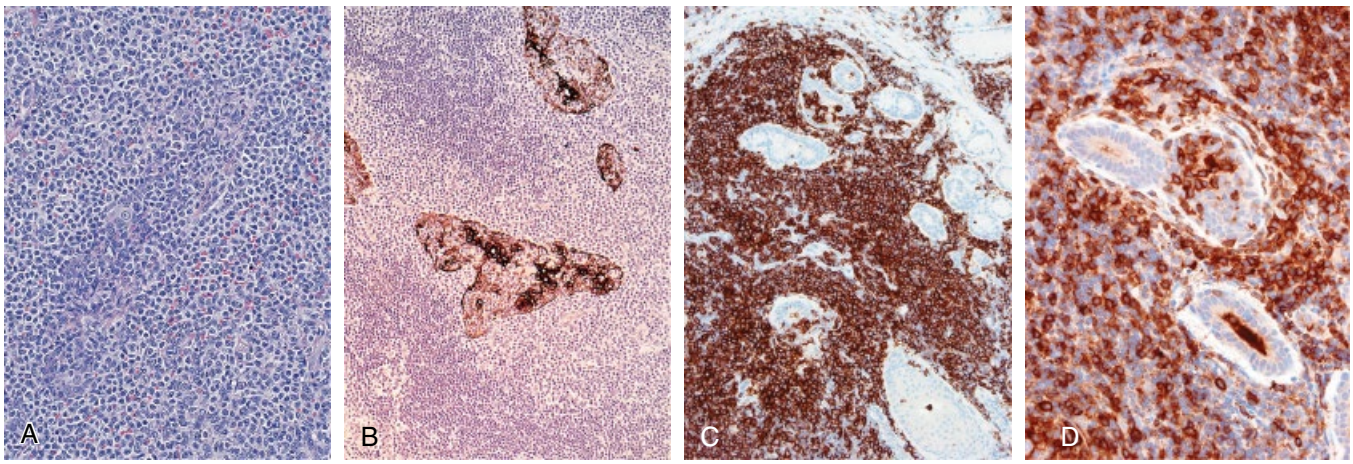

Fig. 19.29. Extranodal MALT lymphoma of salivary gland. **A,** Sheets of marginal zone B cells and formation of lymphoepithelial lesions. **B,** Immunoperoxidase stain for low-molecular-weight cytokeratin (MNF116) shows positive staining of normal epithelial cells infiltrated by lymphoma. **C,** Immunostain showing CD20+ tumor cells surrounding and invading epithelial structures. **D,** The tumor cells express IgM. (*C, D,* Courtesy of Dr. A Ramsay.)

differentiation may be present. Epithelial tissues can be invaded to form lymphoepithelial lesions (Fig. 19.29). The bone marrow is less frequently involved in MALT lymphomas than in splenic marginal zone lymphoma. The tumor cells are CD19+, CD20+, CD22+, and CD79a+ and CD10-, CD23-, and CD43+/-. Transformation to a diffuse large B-cell lymphoma can occur. The IPSID is now termed a subtype of MALT lymphoma. It was previously called α chain disease.

NODAL MARGINAL ZONE B-CELL LYMPHOMA

This is an uncommon lymphoma involving peripheral lymph nodes and only occasionally bone marrow or blood. The marginal zones and interfollicular areas are infiltrated by neoplastic marginal zone B cells (Figs. 19.30 and 19.31) which

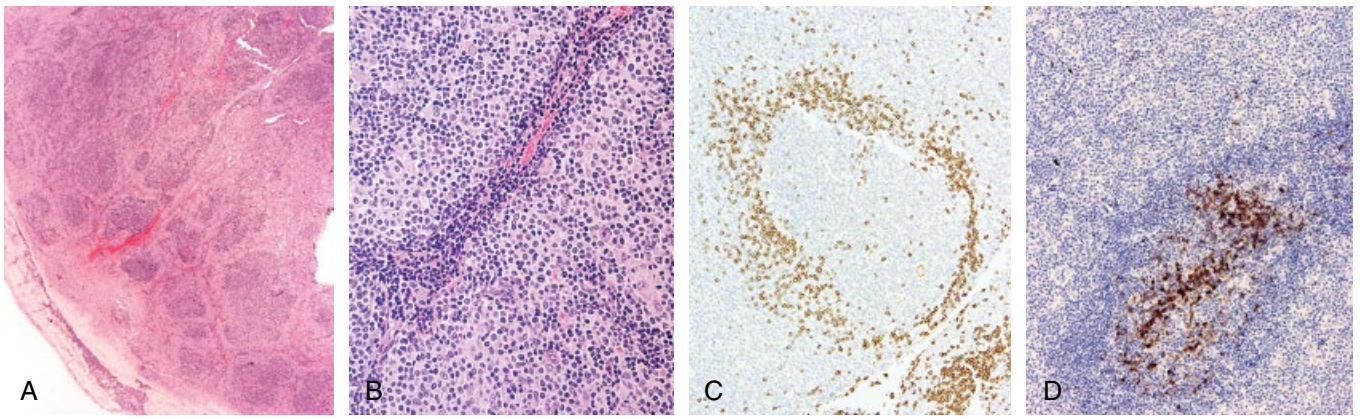

Fig. 19.30. Nodal marginal zone B-cell lymphoma. **A,** H&E: The neoplastic cells infiltrate the interfollicular area. **B,** H&E: Perivascular infiltrate of monocytoid cells with pale cytoplasm. **C,** Immunostain: The neoplastic cells are IgD negative whereas the residual mantle cuff is positive. The tumor cells grow in the perifollicular areas. **D,** Immunostain: CD10 staining highlights the residual germinal center of the follicle colonized by CD10-negative tumor cells.

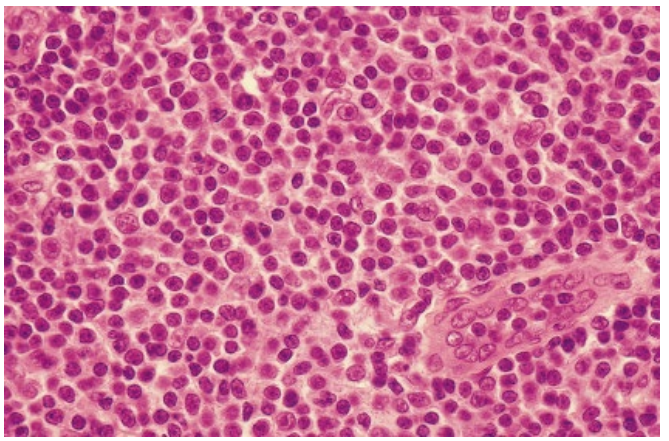

Fig. 19.31. Nodal marginal zone lymphoma: Lymph node shows an admixture of small to medium-sized B cells with abundant clear cytoplasm and scanty, admixed, large, transformed lymphoid cells. A venule with high endothelial cells is present, as typically encountered in this form of lymphoma.

include some centrocyte-like cells, monocytoid B cells, and small lymphocytes with scatted large blast cells. The cells can surround small blood vessels and colonize germinal centers of the follicles. The immunophenotype is similar to that of MALT lymphomas.

FOLLICULAR LYMPHOMA

Follicular lymphoma is a neoplasm of follicular germinal center B cells which usually grows at least with a partially follicular pattern. These tumors account for 35% of all adult non-Hodgkin lymphomas in Western countries and about 20% worldwide. Histologically, the neoplastic follicles can be poorly defined and the mantle zone absent or attenuated. The follicular pattern is highlighted by the staining of the meshwork of follicular dendritic cells (Fig. 19.32). There may be diffuse areas with sclerosis and involvement of interfollicular areas. The tumor is composed of variable proportion of centrocytes and centroblasts. Centrocytes are small- to medium-sized cells with angular or elongated nuclei, indistinct nucleoli, and scant pale cytoplasm (Fig 19.33). Centroblasts are larger with a rounded or oval nucleus and prominent nucleoli, many of which are adjacent to the nuclear membrane. Follicular lymphoma are graded on the proportion of centroblasts present: grade 1, 0–5 centroblasts per high-power

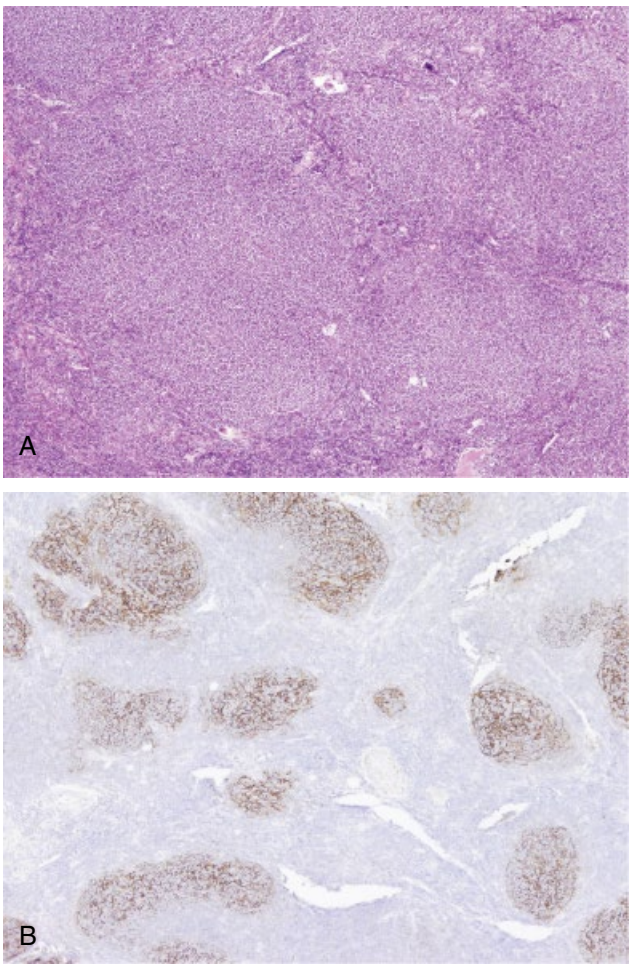

Fig. 19.32. Lymph node involved by follicular lymphoma. **A,** H&E: The nodal architecture is effaced by a lymphoid proliferation with a nodular pattern. The nodules are composed of monotonous population of cells, lack the starry sky pattern of the reactive germinal centers, and the mantel zone are attenuated. **B,** An immunohistochemical staining for CD21 reveals the underlying meshwork of follicular dendritic cells.

field; grade 2, 6–15 centroblasts per high-power field; and grade 3, greater than 15 centroblasts per high-power field (Fig. 19.33). The WHO classification recommends to group together grades 1 and 2. Grade 3 is further subdivided into A and B, which

is entirely composed of centroblasts. Grade 3B follicular lymphoma is considered biologically and clinically closer to diffuse large B-cell lymphoma and treated as these tumors. Cytologic variants include cases with marginal zone differentiation at the periphery of the follicle, cases with plasma cell differentiation, or with numerous signet ring cells (Fig. 19.34B). The follicular lymphoma phenotype of these cases is crucial to establish the correct diagnosis. Marrow involvement can be diffuse or show characteristic paratrabecular infiltration (Figs. 19.35 and 19.36).

Immunophenotypically, the tumor cells are CD20+, SIg+ (usually IgM), CD10+, BCL2+, BCL6+, CD3–, CD5-, and CD43- (Figs. 19.37 and 19.38). This is in contrast to the normal

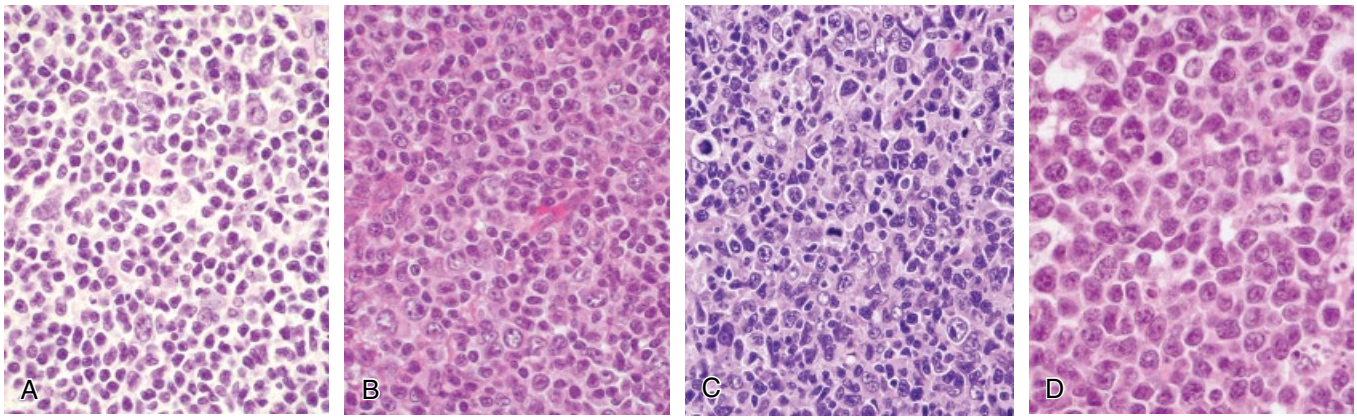

Fig. 19.33. Follicular lymphoma. **A,** Grade 1: The neoplastic population is monotonous, with scattered centroblasts, less than 5 per high-power field (HPF). **B,** Grade 2: There are more than 5 but less than 15 centroblasts per HPF with admixed centrocytes. **C,** Grade 3A: There are more than 15 centroblasts/HPF with admixed centrocytes. **D,** Grade 3B: Monotonous population of large cells ("centroblasts").

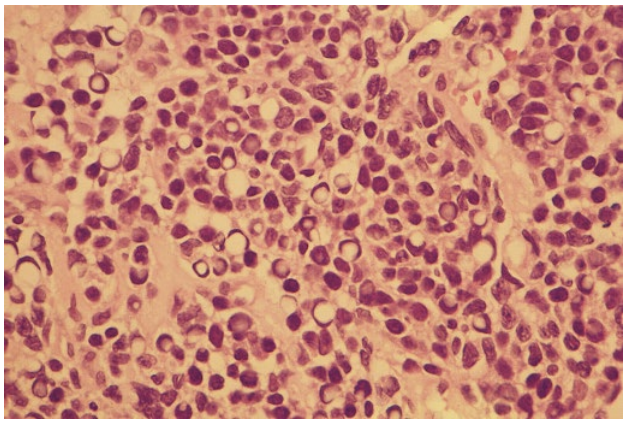

Fig. 19.34. Follicular lymphoma of a rare "signet ring" variety. The tumor cells have a vacuolar clear cytoplasm representing an accumulation of Ig. The cells are B lymphocytes with germinal center phenotype.

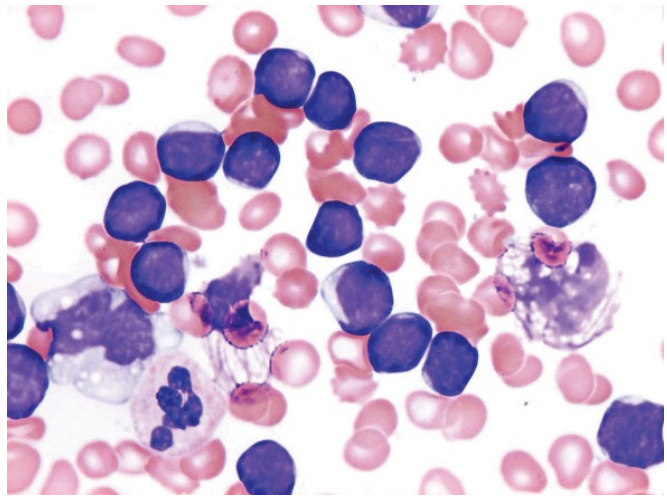

Fig. 19.35. Follicular lymphoma: Bone marrow aspirate shows infiltration by small lymphocytes with diffuse nuclear chromatin. (Courtesy of Dr. W Erber.)

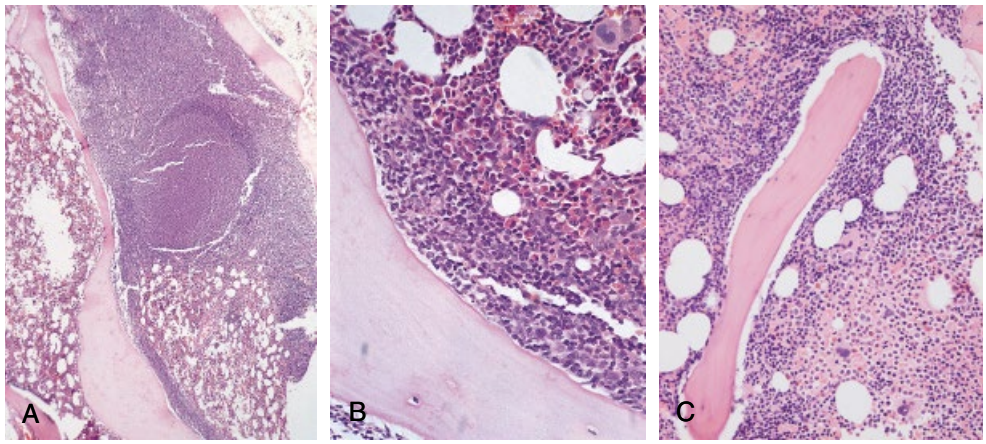

Fig. 19.36. Follicular lymphoma. **A,** Bone marrow trephine biopsy shows almost complete replacement of normal hematopoietic tissue in the upper field and a paratrabecular collection of neoplastic lymphoid cells below. **B,** Higher power shows the demarcation between the paratrabecular centrocytes and centroblasts and the normal hematopoietic cells and fat. **C,** Diffuse marrow infiltration with cells concentrated in paratrabecular zones. (*C,* Courtesy of Dr. W Erber.)

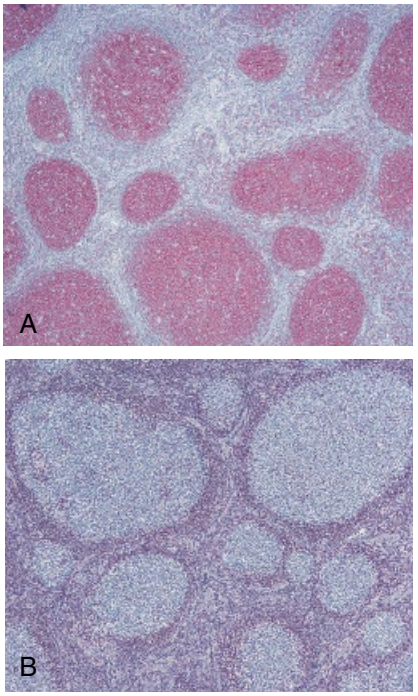

Fig. 19.37. Follicular lymphoma: Immunostain. **A,** CD20 expressed in tumor cells. **B,** CD3 is confined to reactive T cells.

germinal follicles in which the BCL2 is negative (Fig. 19.39). Genetically, the translocation t(14;18)(q32;q21) involving *BCL2* and IGH genes is present in more than 80% of cases, particularly grade 1–2, and it is easily detected by FISH in routine practice (Fig. 19.40). Two different breakpoint sites occur on chromosome 18. The major breakpoint region is in 80–90%

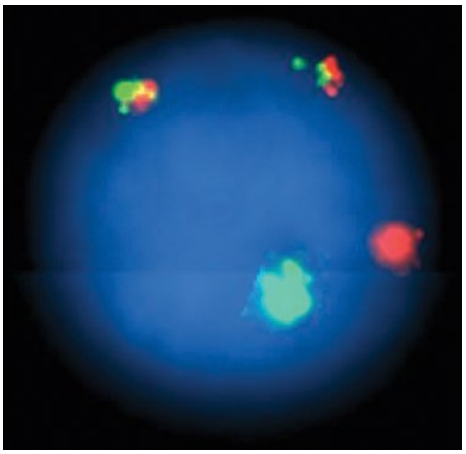

Fig. 19.40. Follicular lymphoma. FISH analysis using probes to chromosomes 14 (green) and 18 (red) demonstrating the translocation t(14;18)(q32;q21) by the two fusion product. (Courtesy of Dr. W Erber.)

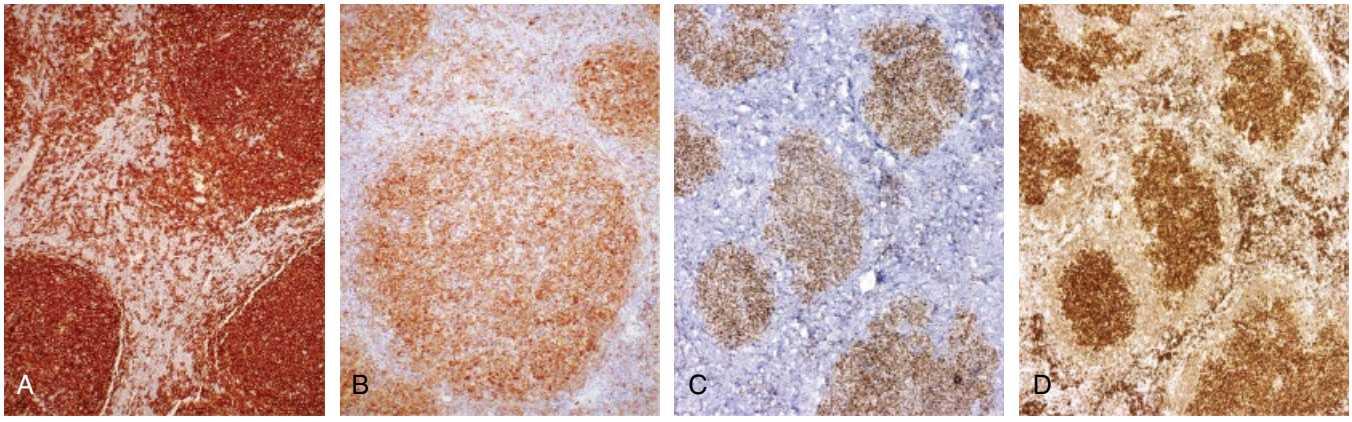

Fig. 19.38. Follicular lymphoma: CD20 immunostain. **A,** The neoplastic cells are positive for B-cell markers. **B,** Immunostain: The neoplastic cells are positive for CD10, a germinal center marker, and are located in the follicular and interfollicular areas. **C,** The neoplastic cells are positive for BCL-6, a germinal center marker. **D,** Immunostain: The neoplastic cells are positive for BCL2.

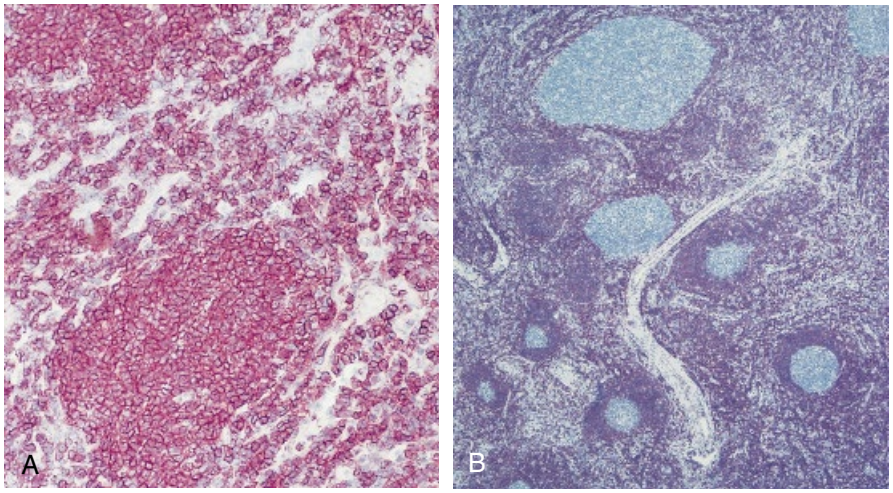

Fig. 19.39. Immunohistologic detection of BCL2 protein in reactive and neoplastic lymphoid cells. **A,** A follicular lymphoma is positive, reflecting activation of the *BCL2* gene by the (14;18) translocation. **B,** In reactive lymphoid tissue unstained germinal centers are surrounded by numerous positive mantle zone B and T cells.

of translocations and a minor cluster region in the remainder (Fig. 19.2). *BCL6*, at 3q27, rearrangements are found in 5–15% of follicular lymphoma negative for BCL2 rearrangements. Follicular lymphoma lacking these translocations exist and have similar pathologic and clinical characteristics. Next generation sequencing has identified recurrent mutations in *EZH2*, *KMT2D (MLL2)*, *CREBBP,* and *RRAGC*, among others (Table 19.4).

About 20% of patients initially have nonbulky localized disease but in the majority the disease is at a more advanced stage at presentation. There can also be involvement of soft tissues and gastrointestinal tract. Skin involvement can be seen in disseminated follicular lymphoma. The differential diagnosis with primary cutaneous follicular center lymphoma should be established (Fig. 19.41). Circulating lymphoma cells are seen in some cases (Fig. 19.42) with liver, spleen, and bone marrow involvement. A simple prognostic index (Follicular Lymphoma International Prognostic Index, FLIPI) has been proposed based on five adverse prognostic factors that define three risk groups (low, intermediate, and high), with a 5-year overall survival of 91%, 78%, and 53%, respectively (Table 19.8).

The disease can transform to a diffuse large B-cell lymphoma, often with B-cell symptoms, raised serum LDH, and a localized, rapidly expanding mass that can be detected by CT or PET scanning (Fig. 19.13) and shows the histology of a diffuse large cell lymphoma.

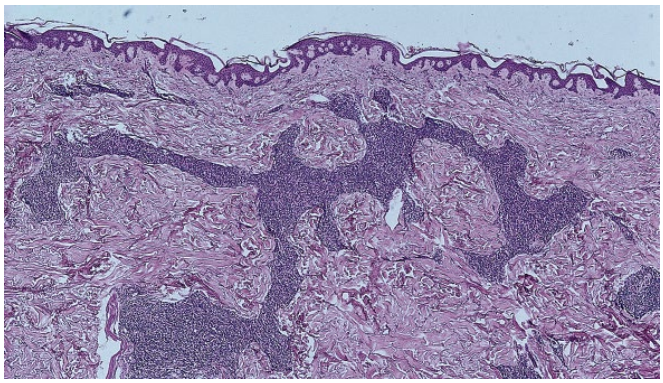

Fig. 19.41. Skin involvement by follicular lymphoma with sheets of tumor cells in the dermis.

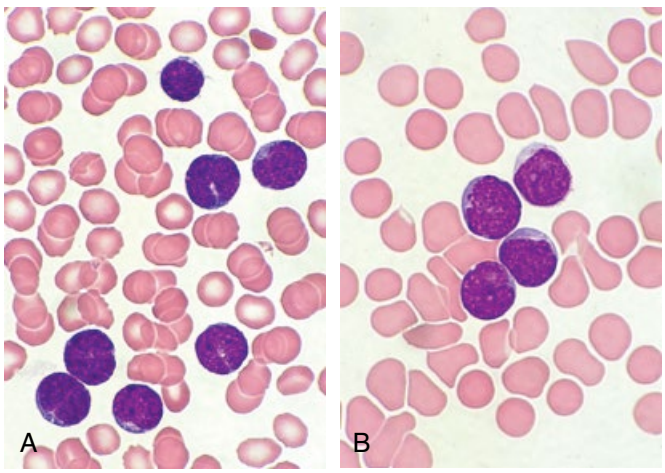

Fig. 19.42. Follicular lymphoma: Peripheral blood shows presence of small lymphoid cells with nuclear clefts, diffuse nuclear chromatin, and scant, darkly staining cytoplasm.

TABLE 19.8. FOLLICULAR LYMPHOMA PROGNOSTIC INDEX (FLIPI)

Factors adversely affecting survival
• Age >60 years • Ann Arbor stage III–IV • Hemoglobin level <12 g/dL • Serum LDH level > upper limit of normal • Number of nodal sites >4

Risk group	Number of factors
Low	0–1
Intermediate	2
High risk	≥3

Source:Solal-Celigny P, et al. *Blood* 2004;104:1258–1265. Reproduced with permission of *Blood: Journal of the American Society of Hematology.*

TABLE 19.9. CLINICOPATHOLOGIC SUBTYPES OF FOLLICULAR LYMPHOMA

Follicular lymphoma with predominant diffuse pattern
Primary cutaneous follicle center lymphoma
Duodenal-type follicular lymphoma
Pediatric-type follicular lymphoma
Large B-cell lymphoma with IRF4 rearrangement

OTHER SUBTYPES OF FOLLICULAR LYMPHOMAS

A subgroup of follicular lymphomas do not carry the t(14,18) translocation. Most of these cases have similar morphology, phenotype, and clinical features to conventional follicular lymphoma with the translocation. However, some subtypes of follicular lymphoma negative for the translocation have specific pathologic and clinical characteristics (Table 19.9). One of these subtypes is the **follicular lymphoma with predominant diffuse pattern**. These tumors usually present in the inguinal and/or pelvic region with large masses and limited stage. Histologically, the tumor is composed of small cells with germinal center phenotype growing in a predominant diffuse pattern. The tumors lack the t(14;18) translocation but have frequent losses of 1p36. **Primary cutaneous follicle center lymphoma** is also negative for the translocation. The tumor tends to occur in the upper half of the body, has a follicular or diffuse pattern, and is composed of centrocytes and centroblasts. The tumor cells are CD20, CD10, and BCL6 positive but BCL-2 negative and are associated with abundant reactive T cells (Fig. 19.43). **Duodenal-type follicular lymphoma** is usually an incidental finding. The tumor expresses CD10, BCL-6, and BCL-2 and carries the t(14,18) translocation but remains localized and very rarely disseminates. Follicular lymphoma in pediatric age has specific pathologic and biologic features**. Pediatric-type follicular lymphoma** is a localized nodal disease mainly involving the head and neck region with an excellent prognosis with local therapy. Paradoxically, the tumor cells are large and highly proliferative, do not carry the t(14,18) translocation, and are BCL-2 negative. **Large B-cell lymphoma with *IRF4* rearrangement** has been recently identified in children and young adults as a lymphoma derived from germinal center cells with high expression of IRF4/MUM1 because of rearrangements of the gene with the IGH. The lesion

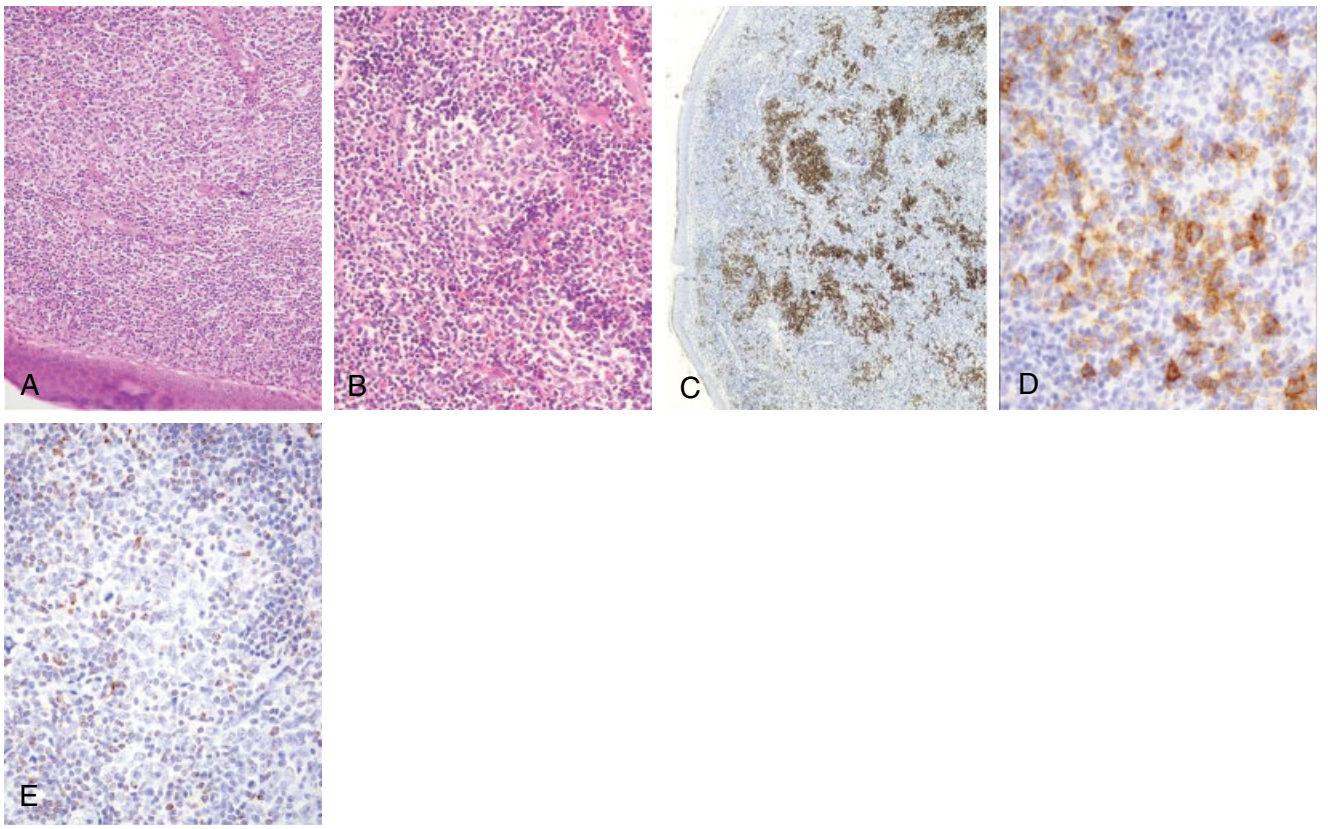

Fig. 19.43. Cutaneous follicle center lymphoma. **A,** H&E: Low power showing a follicular growth pattern and extensive infiltration of the dermis. **B,** More detail of the follicular growth pattern. **C,** Immunostain: The neoplastic cells are CD20 positive. **D,** Immunostain: The neoplastic cells are CD10 positive. **E,** Immunostain: The neoplastic cells are BCL2 negative.

is usually localized and patients have favorable evolutions after treatment. The entity is considered provisional in the updated WHO classification.

MANTLE CELL LYMPHOMA

This is a mature B-cell lymphoma of small irregular lymphocytes that overexpress CCND1 (cyclin D1) as a result of gene translocations, usually with the IGH in the t(11,14) translocation (Fig. 19.44). The neoplastic cells are usually monomorphic, of small to medium size, with an irregular nucleus without nucleoli (Fig. 19.45). In some cases, the tumor cells have a blastic appearance resembling lymphoblastic lymphoma (blastoid variant) or are larger, resembling large cell lymphoma (pleomorphic variant) (Fig. 19.46). The growth pattern is diffuse or nodular (Fig. 19.47). In some cases, the lymph node has a preserved architecture and the neoplastic cells tend to home to mantle zones of the reactive lymphoid follicles (mantle zone pattern). The tumor cells express B-cell markers with strong surface Ig (IgM/IgD) and FMC7, express CD5 and are negative for CD23, CD10, and BCL6. Most mantle cell lymphomas (MCL) express the nuclear transcription factor SOX11 that is negative in all other mature B-cell neoplasms with the exception of around 30% of Burkitt lymphomas (Table 19.7). A minority of MCL are negative for t(11;14) and cyclin D1 expression although express SOX11. These cases can express cyclin D2 or D3. Cyclin D2 and D3 translocations with Ig genes have been found in virtually all these cases. Somatic mutations in *ATM* are found in 50% of MCL. *TP53* and *NOTCH1/2* mutations are associated with more aggressive evolution. Other recurrent mutations occur in *KMT2D (MLL2)* and *NSD2* (Table 19.4).

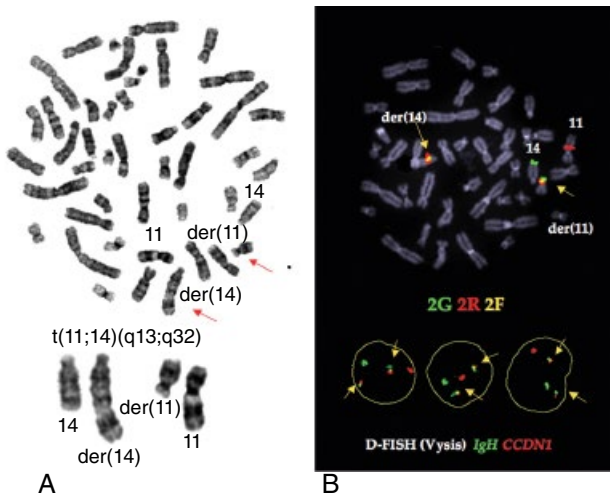

Fig. 19.44. Mantle cell lymphoma cytogenetics. **A,** G-banded metaphase cell with abnormal products of the t(11;14) indicated by red arrows. Partial karyotype below shows the normal and rearranged homologues of chromosomes 11 and 14. **B,** FISH analysis using D (double fusion) FISH probes to detect IgH (green) and CCDN1 (red) loci shows the fusion signals (arrowed) in the metaphase (above) and interphase (below). (Courtesy of Dr. E Nacheva.)

The disease usually manifests with lymphadenopathy and splenomegaly. Blood or bone marrow involvement is common. The cells are of medium size with nuclear indentations or clefts

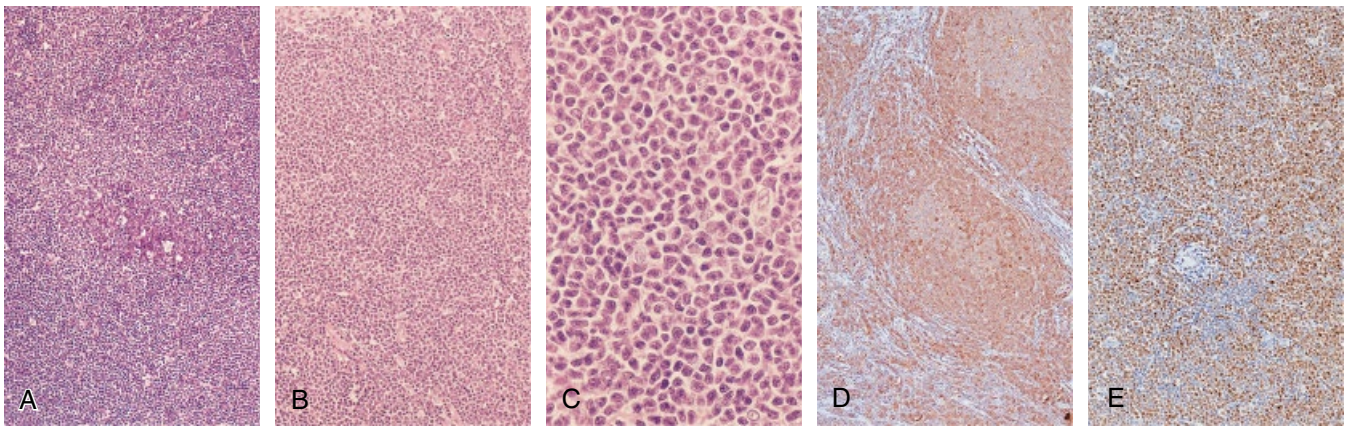

Fig. 19.45. Mantle cell lymphoma. **A,** At low power the neoplasm is seen surrounding a naked reactive germinal center. **B,** Medium-power view shows diffuse growth pattern with some hyaline fibrosis around small vessels. **C,** At high power irregular small lymphoid cells (small cleaved cells, centrocytes) typical of mantle cell lymphoma are seen. No large lymphoid cells are present (see also Fig. 19.48). **D,** Immunostain for CD5 shows strong positivity. **E,** Immunostain for cyclin D1 shows characteristic nuclear positivity.

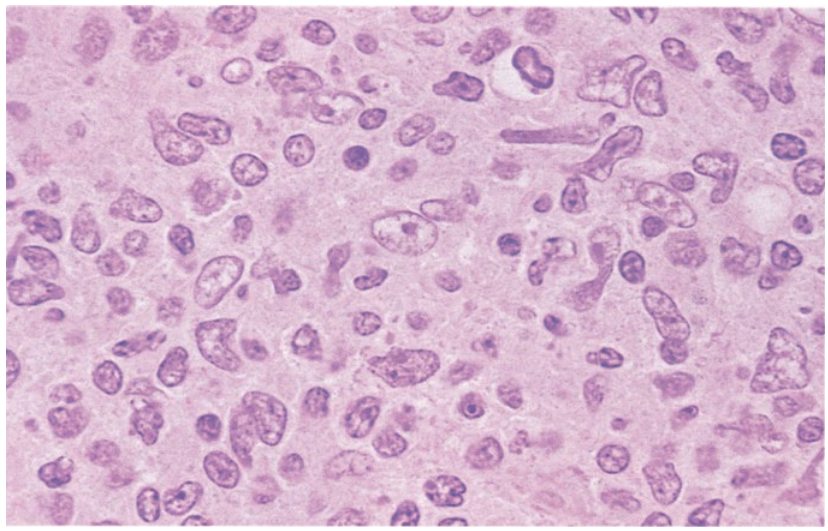

Fig. 19.46. Mantle cell lymphoma: Lymph node biopsy. Large cells are seen with considerable nuclear pleomorphism and pale indistinct cytoplasm; the deformed nuclei have a light chromatin pattern. Contrary to conventional large cell lymphomas, nucleoli are small or inconspicuous.

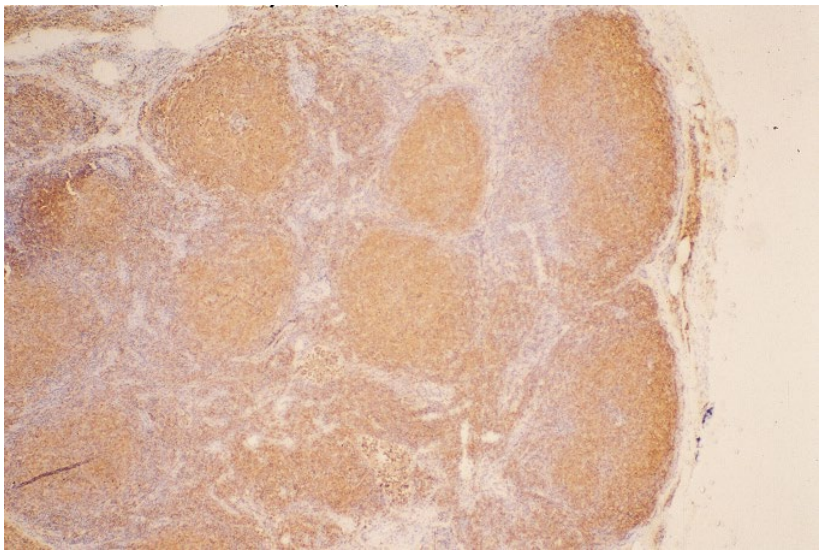

Fig. 19.47. Mantle cell lymphoma: Immunostaining for CD20 reveals a nodular growth pattern.

(Figs. 19.48–19.51). The disease can be found at extranodal sites, especially in the gastrointestinal tract (it is a cause of lymphomatous polyposis; Fig. 19.52). A simple prognostic index has been proposed to include the white cell count, the Eastern Cooperative Oncology Group (ECOG) performance status, age, and serum LDH (Table 19.10).

The clinical behavior of MCL is usually aggressive with frequent relapses. In recent years, a more indolent subtype has been recognized as leukemic non-nodal MCL. These tumors usually develop with leukemic involvement without other manifestations for long periods of time. Splenomegaly can be present but nodal dissemination only occurs late in the evolution associated with more aggressive behavior. These cases carry the t(11;14) translocation and cyclin D1 expression but are SOX11 negative. Conventional MCL seems to derive from mature B cells that have not passed through the germinal center whereas the leukemic non-nodal MCL subtype originates from cells that have transited through this microenvironment where they have acquired somatic mutations in the IGHV genes (Fig. 19.53).

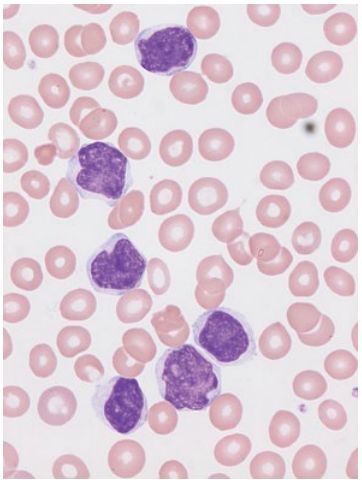

Fig. 19.49. Mantle cell lymphoma: Peripheral blood film showing medium-sized lymphocytes with irregular nuclear contours and scant pale cytoplasm. (Courtesy of Dr.W Erber.)

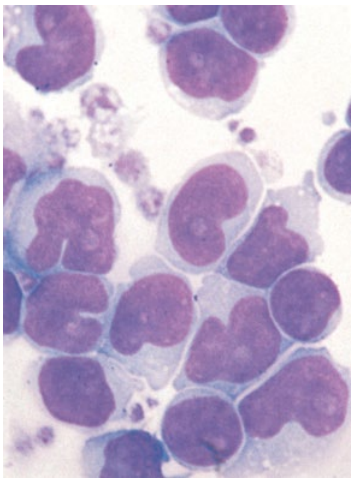

Fig. 19.48. Mantle cell lymphoma: Fine-needle aspirate showing small and medium-sized cells with convoluted and angular nuclei, indistinct nucleoli, and pale cytoplasm.

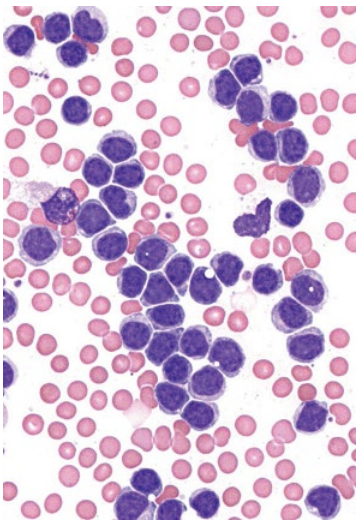

Fig. 19.50. Mantle cell lymphoma: Bone marrow aspirate showing diffuse infiltration with medium-sized lymphoid cells with scanty pale cytoplasm, nuclei, some clefted, with indistinct nucleoli. (Courtesy of Dr.W Erber.)

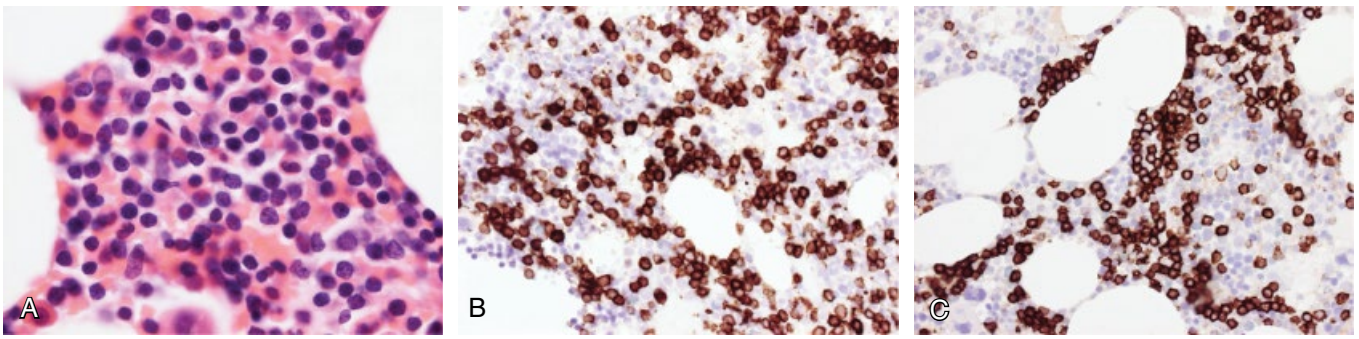

Fig. 19.51. Mantle cell lymphoma. Bone marrow trephine biopsy: **A,** Infiltration with lymphoid cells showing angulated nuclei that stain positively for **B,** CD5 and **C,** CD20. (Courtesy of Dr.W Erber.)

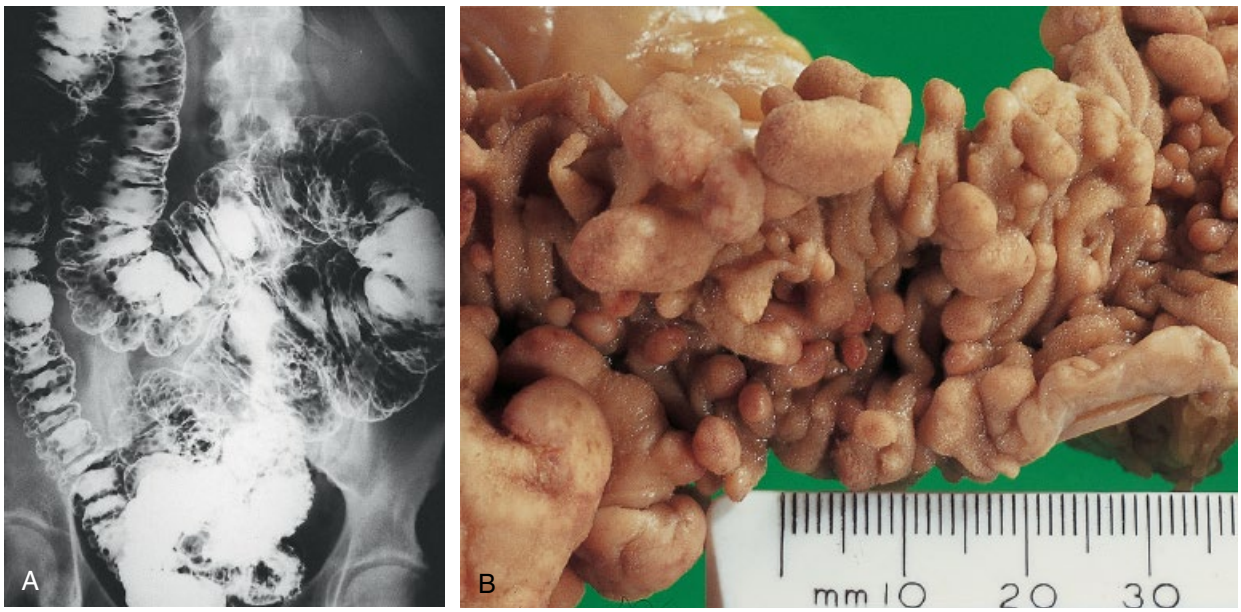

Fig. 19.52. Mantle cell lymphoma: Lymphomatous polyposis affecting the ileocecal region. **A,** Barium study shows mucosal and mural involvement. **B,** Macroscopic appearances showing the presence of multiple mucosal polyps that range in size from a few millimeters to a few centimeters.

TABLE 19.10. MANTLE CELL LYMPHOMA INTERNATIONAL PROGNOSTIC INDEX (MIPI)

Points	Age (years)	ECOG PS	LDH/ULN	WBC (10^{12}/L)
0	<50	0–1	<0.67	<6.7
1	50–59	–	0.67–0.99	6.7–9.9
2	60–69	2–4	1–1.49	10–14.9
3	≥70	–	≥1.50	≥15 000
Risk	Points	Median OS (months)	Low	**0–3**
61	Intermediate	**4–5**	**45**	High
6–11	**20**			

ECOG PS, Eastern Cooperative Oncology Group performance status; LDH, lactate dehydrogenase; ULN, upper level of normal; WBC, white blood cells.
Source:Hoster E, et al. *Blood* 2008;111:558–565. Reproduced with permission of *Blood: Journal of the American Society of Hematology*.

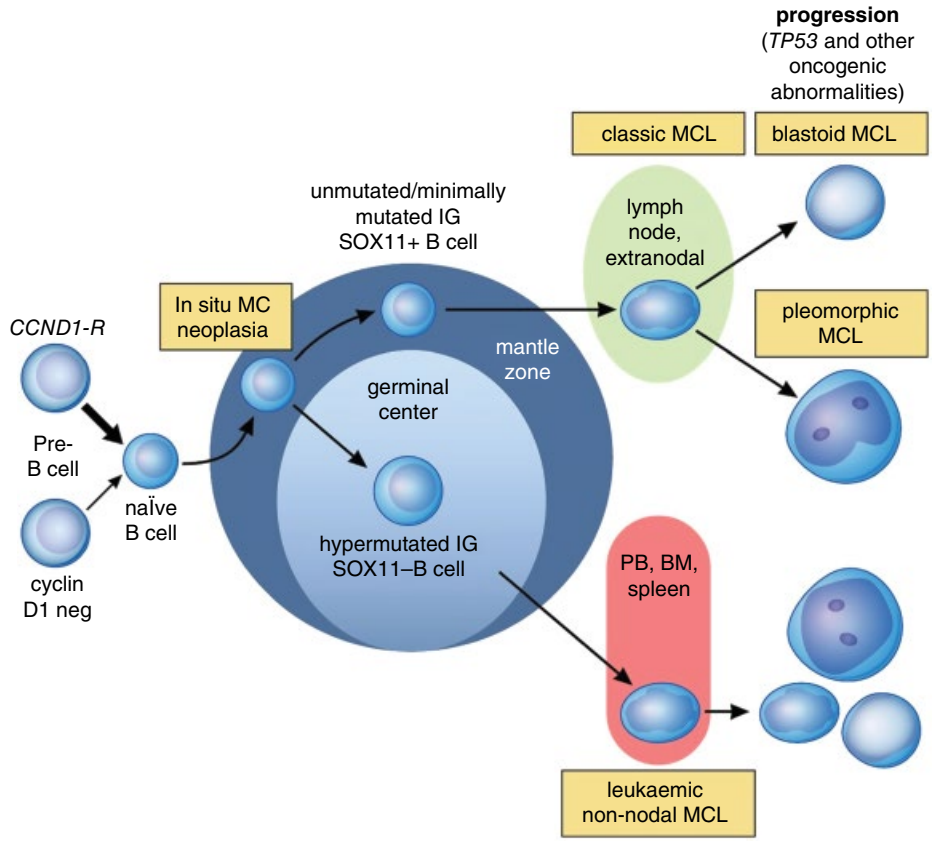

Fig. 19.53. Proposed model of molecular pathogenesis in the development and progression of major subtypes of MCL. Precursor B cells usually with, but sometimes without, a *CCND1* rearrangement mature to abnormal naïve B cells which may initially colonize, often the inner portion of the mantle zones, representing in situ mantle cell neoplasia. These cells already have additional molecular genetic abnormalities, such as inactivating *ATM* mutations. They may progress to classic MCL which most frequently is SOX11+, has no evidence of transit through the germinal center, and is genetically unstable acquiring additional abnormalities related to cell cycle dysregulation, the DNA damage response pathway, cell survival, and other pathways. Ultimately, progression to blastoid or pleomorphic MCL can occur. A smaller proportion of neoplastic mantle cells, usually SOX11-negative, undergo somatic hypermutation, presumably in germinal centers, leading to SOX11−MCL that are more genetically stable for long periods of time and which preferentially involve the peripheral blood, bone marrow, and sometimes the spleen. Even these MCL, however, can undergo additional molecular and/or cytogenetic abnormalities, particularly *TP53* abnormalities, leading to clinical and sometimes morphologic progression. Source: Adapted from Jares et al. and Swerdlow et al. Professional illustration by Patrick Lane, ScEYEnce Studios. Reproduced with permission of *Blood: Journal of the American Hematology Society*.

CHAPTER

AGGRESSIVE MATURE B-CELL NEOPLASMS

20

The aggressive mature B-cell lymphomas are a heterogeneous group of tumors with different biologic and pathologic characteristics that are associated with a broad spectrum of clinical manifestations. Some of the subtypes are relatively common whereas other are less frequent. The recent update of the World Health Organization (WHO) classification of lymphoid neoplasms includes different entities of aggressive mature B-cell lymphomas with well-defined diagnostic criteria (Table 20.1). The most common subtype accounting for approximately 80% of all these neoplasms is diffuse large B-cell lymphoma, not otherwise specified (DLBCL, NOS), a category that includes tumors that cannot be recognized in any of the other more specific entities. The other diseases are less common but have distinctive features. T-cell/histiocyte-rich large B-cell lymphoma is a subtype in which the tumor cells are overrun by an exuberant proliferation of reactive T cells and histiocytes. Some large B-cell lymphomas (LBCL) are originated in particular topographic sites suggesting their relationship to specific cell subsets present in these sites or the influence of the microenvironment in their pathogenesis. A group of LBCL is associated with Epstein–Barr virus (EBV) infection and occurs in patients who may have a certain immunologic impairment in controlling the infection. Most LBCL have a mature B-cell phenotype but some tumors acquire a terminal B-cell differentiation phenotype losing mature B-cell markers and expressing proteins related to plasma cell differentiation. Some of these tumors are associated with human herpes virus 8 (HHV8) and/or EBV infection. Burkitt lymphoma is a well-defined aggressive neoplasm that can be cured in most patients. Finally, the updated WHO classification has revised the concept of aggressive B-cell lymphomas with features intermediate between DLBCL and Burkitt lymphoma and tumors with *MYC* and *BCL2* and/or *BCL6* translocations. This chapter reviews these entities emphasizing the new aspects included in the updated WHO classification (Table 20.1).

TABLE 20.1. THE 2016 UPDATED WORLD HEALTH ORGANIZATION CLASSIFICATION OF THE AGGRESSIVE B-CELL NEOPLASMS

Diffuse large B-cell lymphoma (DLBCL), NOS
• Germinal center B-cell type
• Activated B-cell type
T-cell/histiocyte-rich large B-cell lymphoma
Primary DLBCL of the central nervous system (CNS)
Primary cutaneous DLBCL, leg type
EBV+ DLBCL, NOS
EBV+ mucocutaneous ulcer
DLBCL associated with chronic inflammation
Lymphomatoid granulomatosis
Primary mediastinal (thymic) large B-cell lymphoma
Intravascular large B-cell lymphoma
ALK$^+$ large B-cell lymphoma
Plasmablastic lymphoma
Primary effusion lymphoma
HHV8$^+$ DLBCL, NOS
Burkitt lymphoma
Burkitt-like lymphoma with 11q aberration
High-grade B-cell lymphoma, with *MYC* and *BCL2* and/or *BCL6* rearrangements
High-grade B-cell lymphoma, NOS
B-cell lymphoma, unclassifiable, with features intermediate between DLBCL and classic Hodgkin lymphoma

Provisional entities are listed in italics.
Source: Swerdlow SH, et al. *Blood* 2016;127:2375–2390. Reproduced with permission of *Blood: Journal of the American Hematology Society.*

DIFFUSE LARGE B-CELL LYMPHOMA, NOS

Diffuse large B-cell lymphoma, NOS accounts for 30% of all non-Hodgkin lymphomas. The tumors are composed of a diffuse proliferation of large cells, at least twice the size of a normal lymphocyte, with vesicular nuclei, prominent nucleoli, and usually basophilic cytoplasm. Three morphologic variants have been recognized: centroblastic, immunoblastic or anaplastic, according to the predominant cell. Centroblasts typically have two small nucleoli close to the nuclear membrane, immunoblast have a central large nucleoli, and anaplastic DLBCL has pleomorphic cells of different size and often multinucleated (Figs. 20.1–20.3). Some cases have morphologic features that are difficult to classify. No reproducible survival differences have been found between the groups.

Gene expression profiling studies (Fig. 20.4) have recognized two molecular subtypes related to a different cell of origin (COO)

Color Atlas of Clinical Hematology: Molecular and Cellular Basis of Disease, Fifth Edition. A. Victor Hoffbrand, Paresh Vyas, Elías Campo, Torsten Haferlach, and Keith Gomez

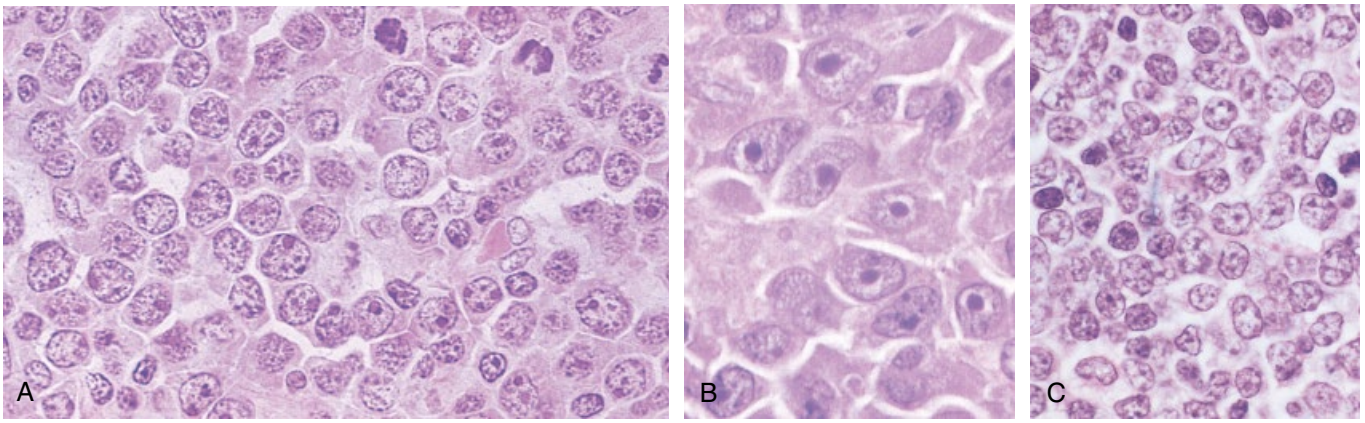

Fig. 20.1. Diffuse large B-cell lymphoma (DLBCL) at high magnification. **A,** The neoplastic cells are much larger than normal lymphocytes and have an oval nucleus with prominent nucleoli, many of which are adjacent to the nuclear membrane (centroblasts). A number of mitotic figures are seen. **B,** The large cells show prominent central nucleoli (immunoblasts). **C,** The round or oval nuclei have delicate, evenly distributed chromatin with one to three nucleoli, either central or near the nuclear membrane, and scant cytoplasm.

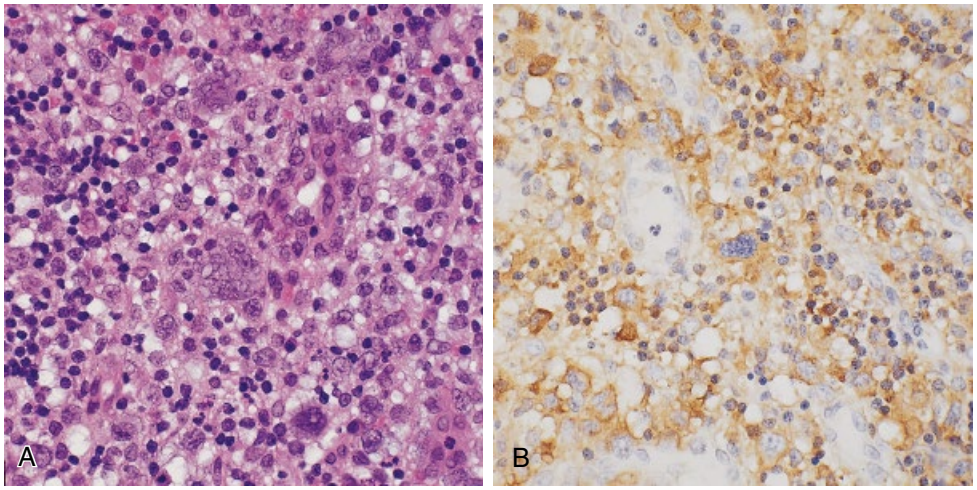

Fig. 20.2. **A**, H&E: DLBCL, anaplastic variant. The large cells have different sizes and some are multinucleated. **B,** The cells are CD30+ but ALK−.

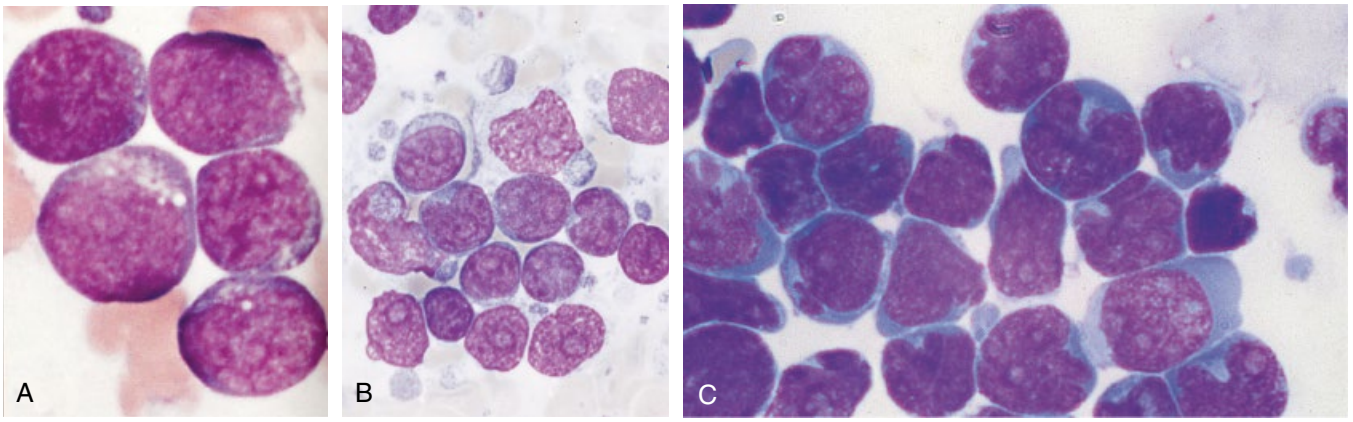

Fig. 20.3. Diffuse large B-cell lymphoma: Fine-needle lymph node aspirate: **A,** centroblasts; **B,** immunoblasts; and **C,** pleomorphic large cells with irregular nuclear outline, nuclear clefts, and prominent nucleoli.

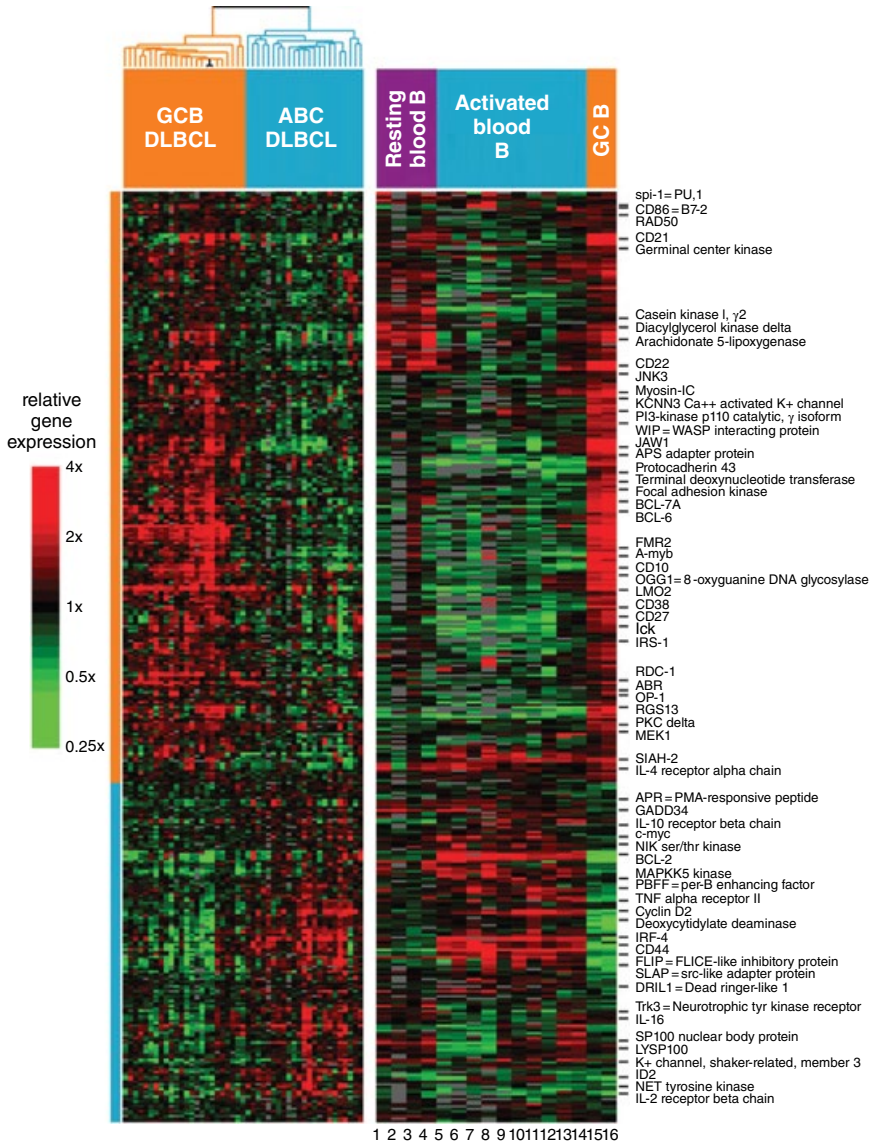

Fig. 20.4. Diffuse large B-cell lymphoma: Gene array studies. The left-hand panel shows gene expression data in the two subgroups (germinal center and activated B cell); the right-hand panel shows expression data in normal B-cell samples (for full details see Alizadeh AA, et al. *Nature* 2000;403:503–511. Reproduced with permission of Springer Nature). (Courtesy of Professor LM Staudt.)

either in normal germinal center B-cells (GCB) or activated B-cells (ABC). These tumors are biologically and clinically different, with most studies showing worse prognosis for ABC than GCB-DLBCL. GCB tumors rely preferentially on the activation of the PI3K pathway whereas ABC tumors have a constitutive activation of the NFκB pathway. Genetic alterations in GCB include *BCL2* and *BCL6* rearrangements and mutations in histone modifiers (*EZH2*, *KMT2D*, *CREBB*) and *GNA13,* whereas ABC tumors have frequent mutations in *MYD88* and *CD79a* (see Table 19.4). The distinctive molecular pathogenesis can orient to more precise therapeutic strategies. For all these reasons the updated WHO classification recommends the recognition of these two molecular subtypes by the pathologists (Table 20.1).

Given the current limitations for the use of gene expression profiling in clinics, pathologists have designed several immunohistochemical algorithms with a small panel of genes to identify GCB and non-GCB or ABC DLBCL. The most common is the Hans algorithm based on CD10, BCL6, and IRF4/MUM1 expression (Fig. 20.5). The germinal centerDLBCL (GC type) is CD10+, BCL6+ or –, and IRF4/MUM1–, whereas non-GCB DLBCL are CD10–, BCL6+ or –, and IRF4/MUM1+ (Fig. 20.6). Other germinal centermarkers are HGAL and LMO2, and FOXP1 is an ABC marker. Both types express pan B-cell markers CD19, CD20, PAX5, and CD79a to a varying degree. Some DLBCL express CD5 and are not related to CLL. BCL2 is positive in 30–50% of cases and MYC protein expression may be seen in 30% of cases independently of gene rearrangements. The proliferation fraction measured by Ki-67 (MIB1) staining is usually greater than 40%.

Genetic studies show rearrangement of the *BCL6* gene at 3q27 in one-third of cases and mutations within the gene in

additional cases. *BCL6* is a transcription factor of the zinc finger family that is involved in maintaining B cells in a germinal center-like state, inhibiting B-cell differentiation. The t(14;18)(q32;q21) translocation is also found in 20–30% of de novo DLBCL. The 8q24/MYC rearrangement also occurs in DLBCL in 10–15% as a secondary event.

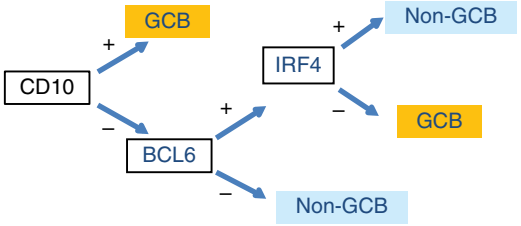

Fig. 20.5. Hans algorithm for the immunohistochemical classification of DLBCL, NOS in germinal center (GC) and non-GC. Note that contrary to gene expression profiling (GEP) studies, this algorithm classifies the tumors in GC and non-GCB. GEP usually leaves 10–15% of the DLBCL as unclassified whereas IHC algorithm forces all cases into one of the two groups.

Clinically, DLBCL, NOS can present localized or widespread with involvement of the bone marrow (Figs. 20.7–20.9) and rarely peripheral blood (Fig. 20.10). The disease is nodal or extranodal in up to 40% of cases including the gastrointestinal tract, skin, central nervous system (CNS), bone, testes, ovary, lung,

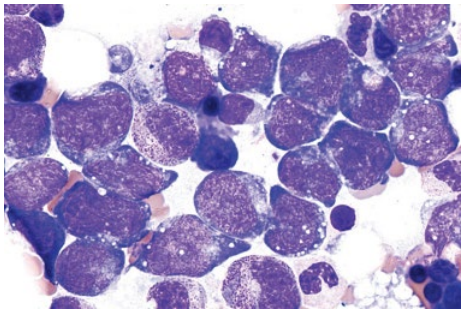

Fig. 20.7. Diffuse large B-cell lymphoma: Bone marrow aspirate showing large cells with abundant dark blue, cytoplasmic, and nuclear vacuoles and nuclei with open chromatin and prominent nucleoli. (Courtesy of Dr. W Erber.)

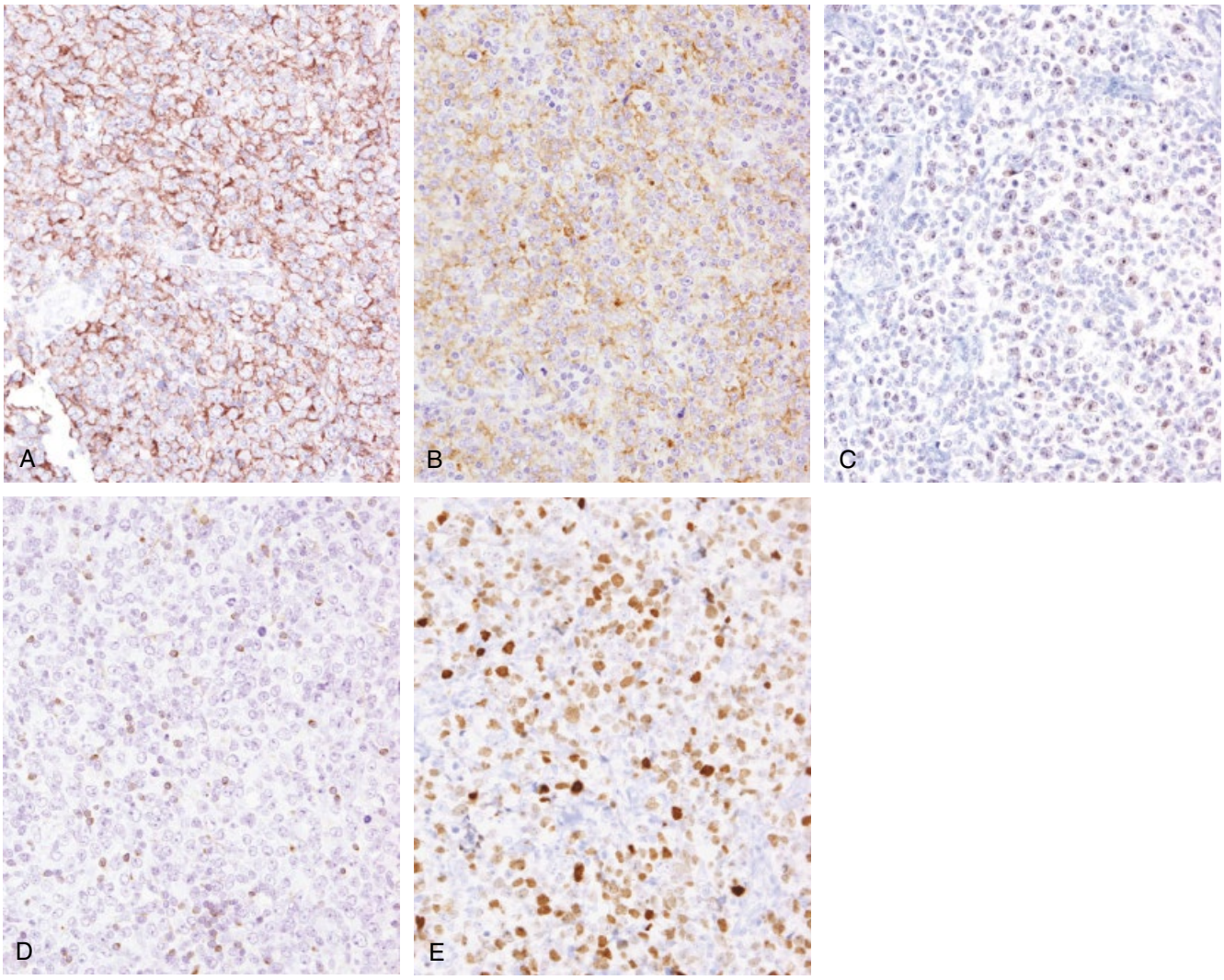

Fig. 20.6. Diffuse large B-cell lymphoma immunostains. **A,** The neoplastic cells are diffusely positive for B-cell markers as shown for CD20. **B,** The neoplastic cells are diffusely positive for CD10, a germinal center marker. **C,** The neoplastic cells are diffusely positive for BCL6, a germinal center marker. **D,** The neoplastic cells are negative for BCL2. **E,** The neoplastic cells are positive for IRF4/MUM1.

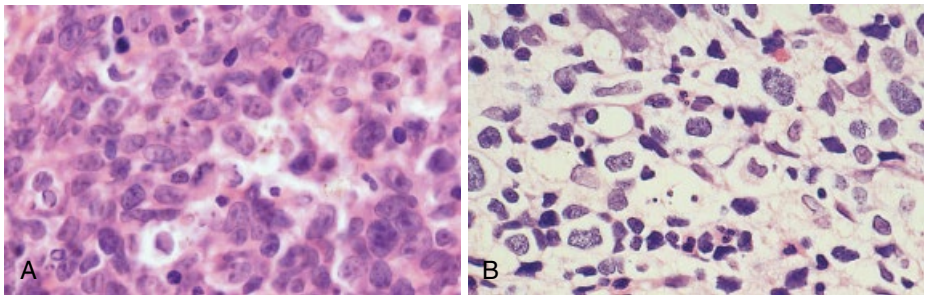

Fig. 20.8. Diffuse large B-cell lymphoma: Bone marrow trephine biopsy. **A,** Low power: Pleomorphic large cells with vesicular nuclei, prominent nucleoli, and apoptotic forms replacing hematopoietic marrow. **B,** High power: Mixture of "centroblasts" and "immunoblasts" infiltrating bone marrow. (Courtesy of Dr.W Erber.)

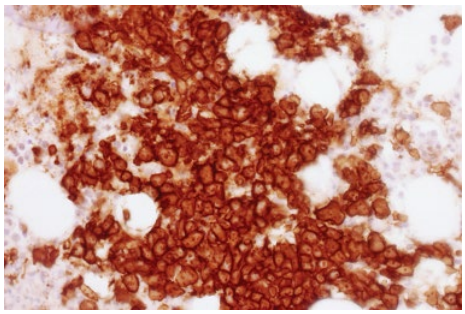

Fig. 20.9. Diffuse large B-cell lymphoma, bone marrow trephine biopsy: Immunostain showing infiltrate of large cells, CD20 positive. (Courtesy of Dr.W Erber.)

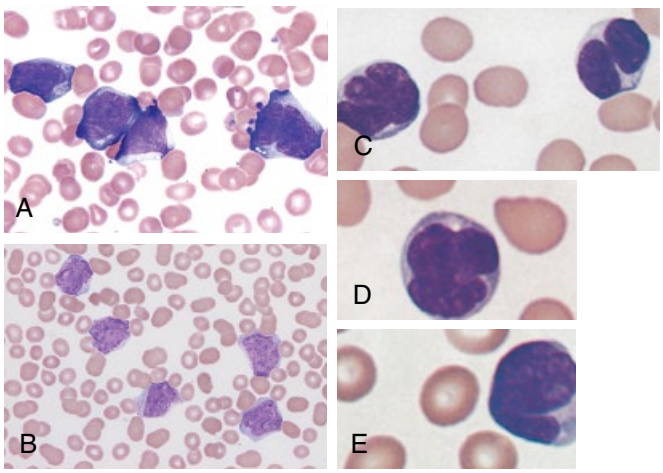

Fig. 20.10. Diffuse large B-cell lymphoma: Peripheral blood films showing large lymphoid cells: **A,** dark and **B,** paler blue with vacuolated cytoplasm and irregularly shaped nuclei occupying most of the cell, and prominent nucleoli. **C–E**, Bizarre cells in terminal, widely disseminated "centroblastic" lymphoma. (*A, B,* Courtesy of Dr.W Erber.)

liver, thyroid, and spleen (Figs. 20.11 and 20.12). The international prognostic index (IPI) is based on several clinical parameters including the Involvement of extranodal sites that stratifies aggressive lymphomas in different risk groups (Table 20.2).

T-CELL/HISTIOCYTIC-RICH LARGE B-CELL LYMPHOMA

T-cell/histiocytic-rich large B-cell lymphoma is an aggressive lymphoma usually presenting in advanced stage. Involved lymph nodes show a diffuse growth pattern in which the large neoplastic B cells (less than 10% of the total) are scarce and best

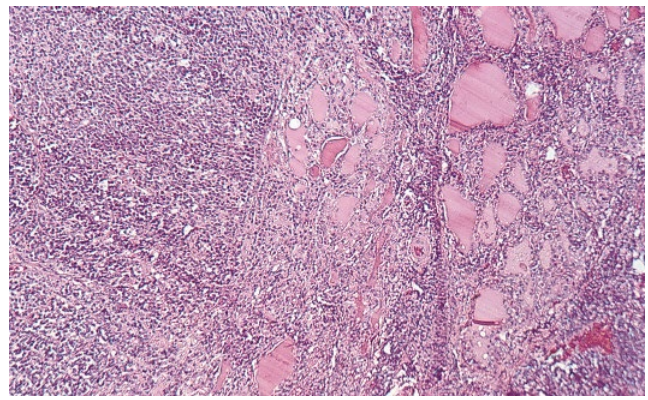

Fig. 20.11. Diffuse large B-cell lymphoma of the thyroid: Histologic section shows sheets of neoplastic cells (left) and remaining colloid-filled acini (right). Immunoperoxidase staining for light chains confirmed the monoclonality of the tumor cells.

detected by immunohistology with B-cell markers. The tumor cells are immersed in a dense background of reactive CD3+ T cells and histiocytes (Figs. 20.13 and 20.14).

PRIMARY CUTANEOUS DIFFUSE LARGE B-CELL LYMPHOMA, LEG TYPE

This tumor is composed of large monomorphic B cells that infiltrate the dermis with very few if any reactive T-cells (Fig. 20.15). The cells have a non-germinal center phenotype (IRF4 and FOXP1 positive, CD10-negative) and are strongly BCL2+. The behavior is aggressive with frequent systemic dissemination.

LYMPHOMATOID GRANULOMATOSIS

This is an angiocentric lymphoproliferative disease of extranodal sites composed of EBV+ B cells mixed with reactive and inflammatory cells and T cells (Fig. 20.16). Depending on the number of large EBV+ B cells the lesion may be graded from 1 (scarce) to 3 (abundant). The most common site involved is lung, but kidney, brain, and subcutaneous tissue can be affected. Blood vessel infiltration occurs often with vascular damage and necrosis.

PRIMARY MEDIASTINAL (THYMIC) LARGE B-CELL LYMPHOMA

This is a tumor manifesting as a large anterior mediastinal mass, sometimes with superior vena cava obstruction, mainly in young females. The tumor is composed of large B cells usually with dense fibrosis, which can compartmentalize the tumor (Fig. 20.17A).

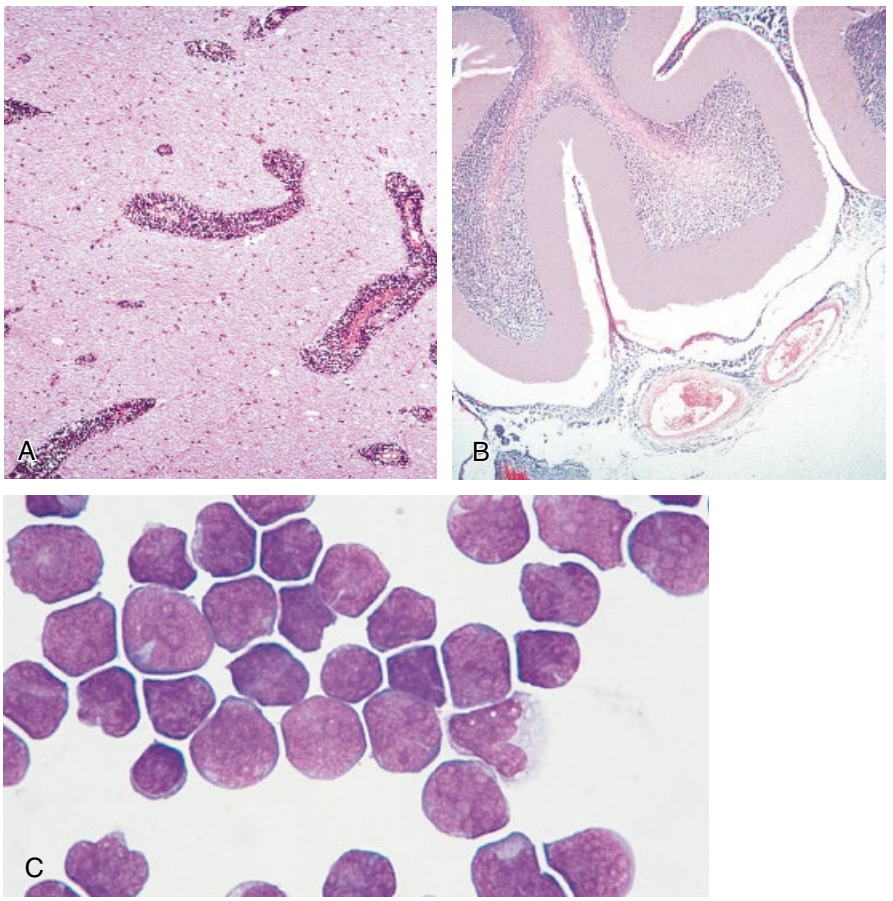

Fig. 20.12. Diffuse large B-cell lymphoma in the brain: sections of brain in CNS relapse showing: **A,** invasion along perivascular spaces and **B,** extensive involvement of the meninges. A similar pattern of involvement occurs in primary lymphoma of the brain. **C,** Cerebrospinal fluid: Cytospin preparation shows typical large lymphoid cells with prominent nucleoli. (*A, B,* Courtesy of Dr. BB Berkeley.)

TABLE 20.2. INTERNATIONAL PROGNOSTIC INDEX (IPI) FOR AGGRESSIVE LYMPHOMAS[a]

IPI Unfavorable factors	
Age >60 years Poor performance status (ECOG ≥2) Advance Ann Arbor stage (III–IV) Extranodal involvement ≥2 sites High serum LDH > normal	
Risk group	**Number of unfavorable factors**
Standard IPI	
Low	0,1
Low-intermediate	2
High-intermediate	3
High	4,5
Revised IPI[b]	
Very good	0
Good	1,2
Poor	3–5

[a] International Non-Hodgkin's Lymphoma Prognostic Factors Project. *N Engl J Med* 1993;329:987–994.
[b] Sehn LH, et al. *Blood* 2007;109:1857–1861.

Thymic remnants and scattered benign lymphocytes and eosinophils may be present. The tumor cells usually have abundant pale cytoplasm (Fig. 20.17B). The immunophenotype is of a B-cell tumor, CD10 negative, with weak or absent expression of surface immunoglobulin and frequent expression of CD23 and CD30 (see Table 19.7). The tumor can spread locally to neighboring viscera or more distally, especially to extranodal sites (e.g. kidney, lung, skin, and brain).

INTRAVASCULAR LARGE B-CELL LYMPHOMA

This is a rare type of extranodal B-cell lymphoma characterized by the presence of tumor cells only in the lumina of the small vessels (Fig. 20.18). It occurs particularly in the skin, CNS, lung, kidneys, or bone marrow (Figs. 20.19 and 20.20). Cells are large with vesicular nuclei, prominent nucleoli, and frequent mitosis. They express pan B-cell antigens and rarely CD5. The clinical behavior is very aggressive and not infrequently is diagnosed at autopsy.

ALK-POSITIVE DIFFUSE LARGE B-CELL LYMPHOMA

This is an aggressive lymphoma, predominantly nodal, occurring in immunocompetent young adults. The tumor is composed

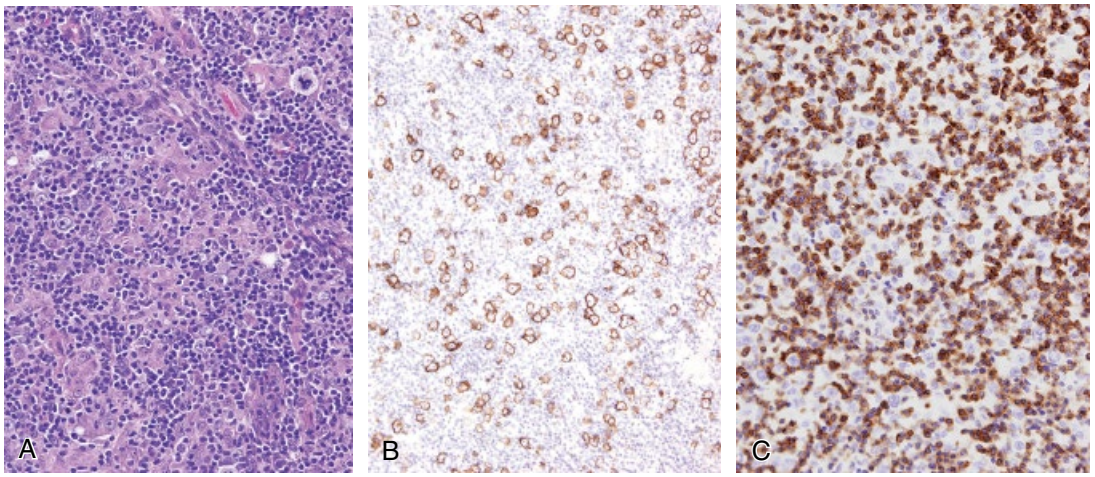

Fig. 20.13. Diffuse large B-cell lymphoma, T-cell rich variant. **A,** H&E: The neoplastic cells are scarce and are intermingled with an intense infiltrate of small lymphocytes and histiocytes. **B,** Immunostaining for CD20 shows scattered and isolated neoplastic cells. **C,** CD3 positive T cells clearly outnumber the neoplastic component.

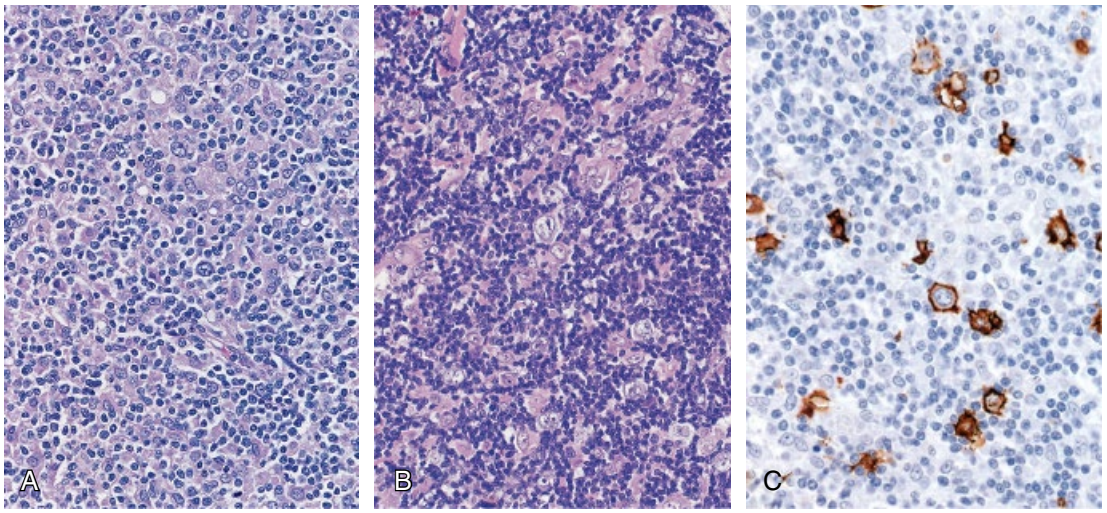

Fig. 20.14. Diffuse large B-cell lymphoma, T-cell rich. **A,** Low-power view showing diffuse architecture with scattered large cells admixed with numerous small lymphocytes. **B,** High-power view showing large blast cells with immunoblastic cytology. **C,** Immunostain for CD20 showing neoplastic large B cells.

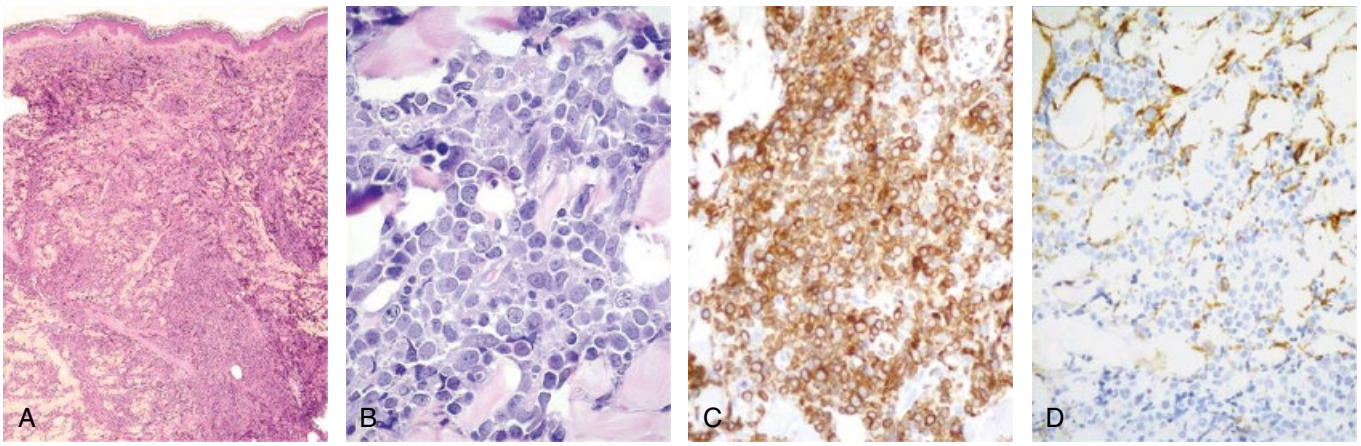

Fig. 20.15. Primary cutaneous diffuse large B-cell lymphoma: leg type. **A,** H&E: The neoplastic cells are infiltrating the dermis and extending to the subcutis. The epidermis is spared. **B,** H&E: The neoplastic cells are large and monomorphic. **C,** Immunostain: The neoplastic cells are strongly positive for BCL2. **D,** Immunostain: The neoplastic cells are negative for CD10.

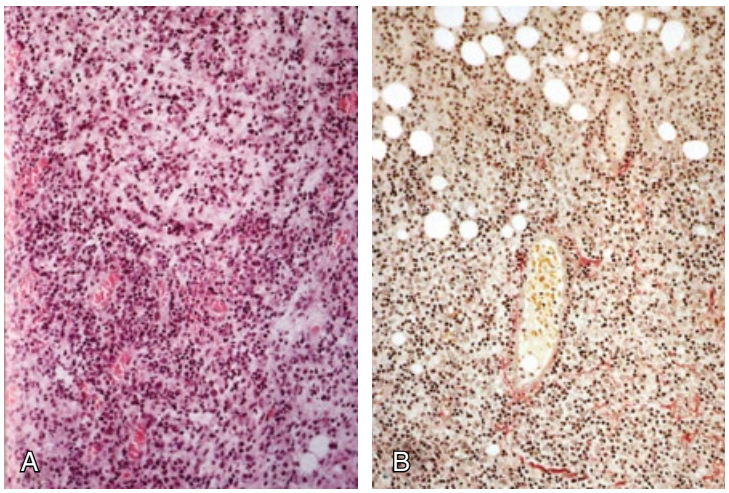

Fig. 20.16. Lymphomatoid granulomatosis: lung sections. **A,** Prominent blood vessels with **B,** thickened walls and areas of necrosis. (Elastic van Giesen stain.) (Courtesy of Dr. JE McLaughlin.)

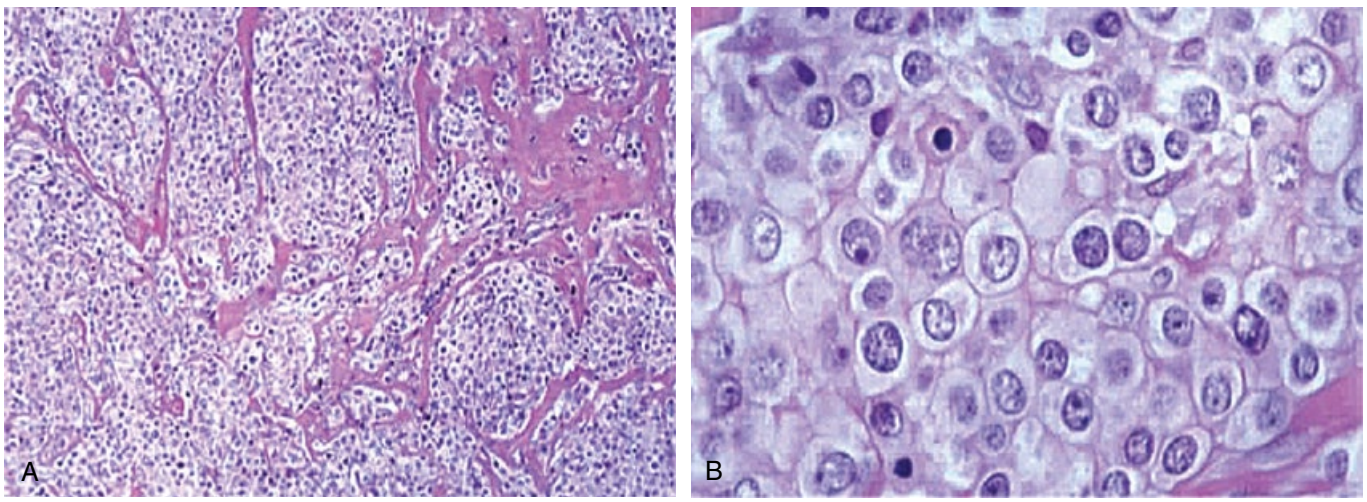

Fig. 20.17. Primary mediastinal (thymic) large B-cell lymphoma. **A,** Typical fibrosis between the sheets of tumor cells. **B,** The cells, abundant pale cytoplasm, and centroblast-type nuclei.

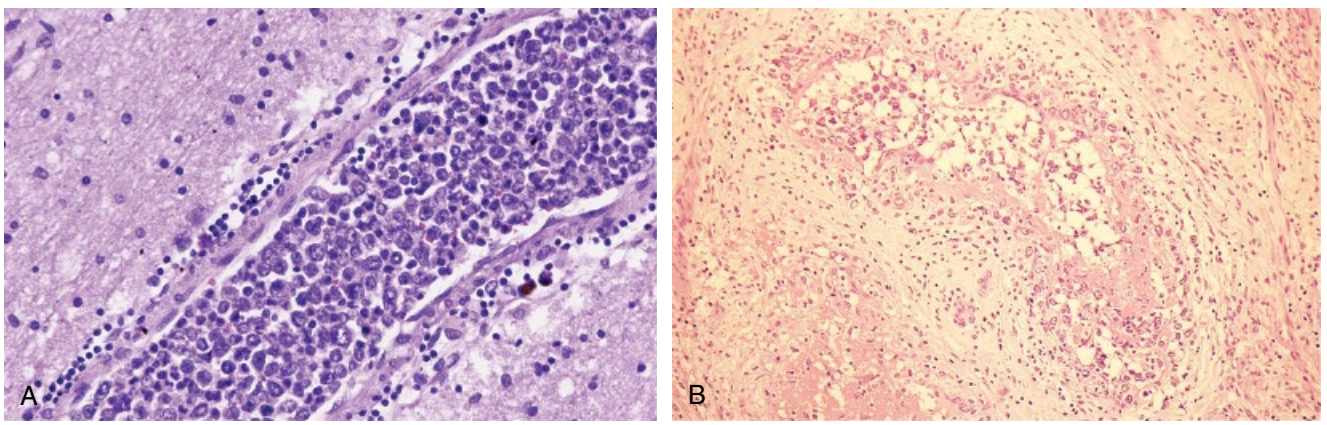

Fig. 20.18. A, Intravascular large B-cell lymphoma. The neoplastic cells fill the intraparenchymatous vessels of the brain. **B,** Section of cervix showing vascular distention by large lymphoid cells.

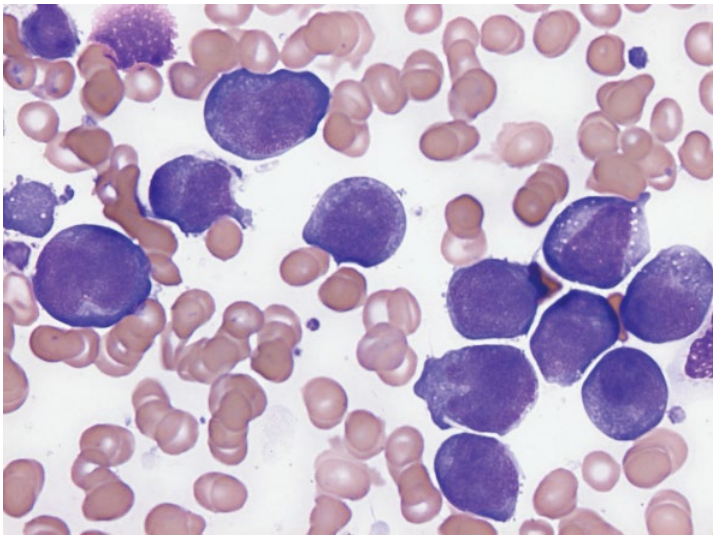

Fig. 20.19. Intravascular large B-cell lymphoma: Bone marrow aspirate showing infiltration of large cells with irregular nuclei, open chromatin, and vacuoles (mainly cytoplasmic). (Courtesy of Dr. W Erber.)

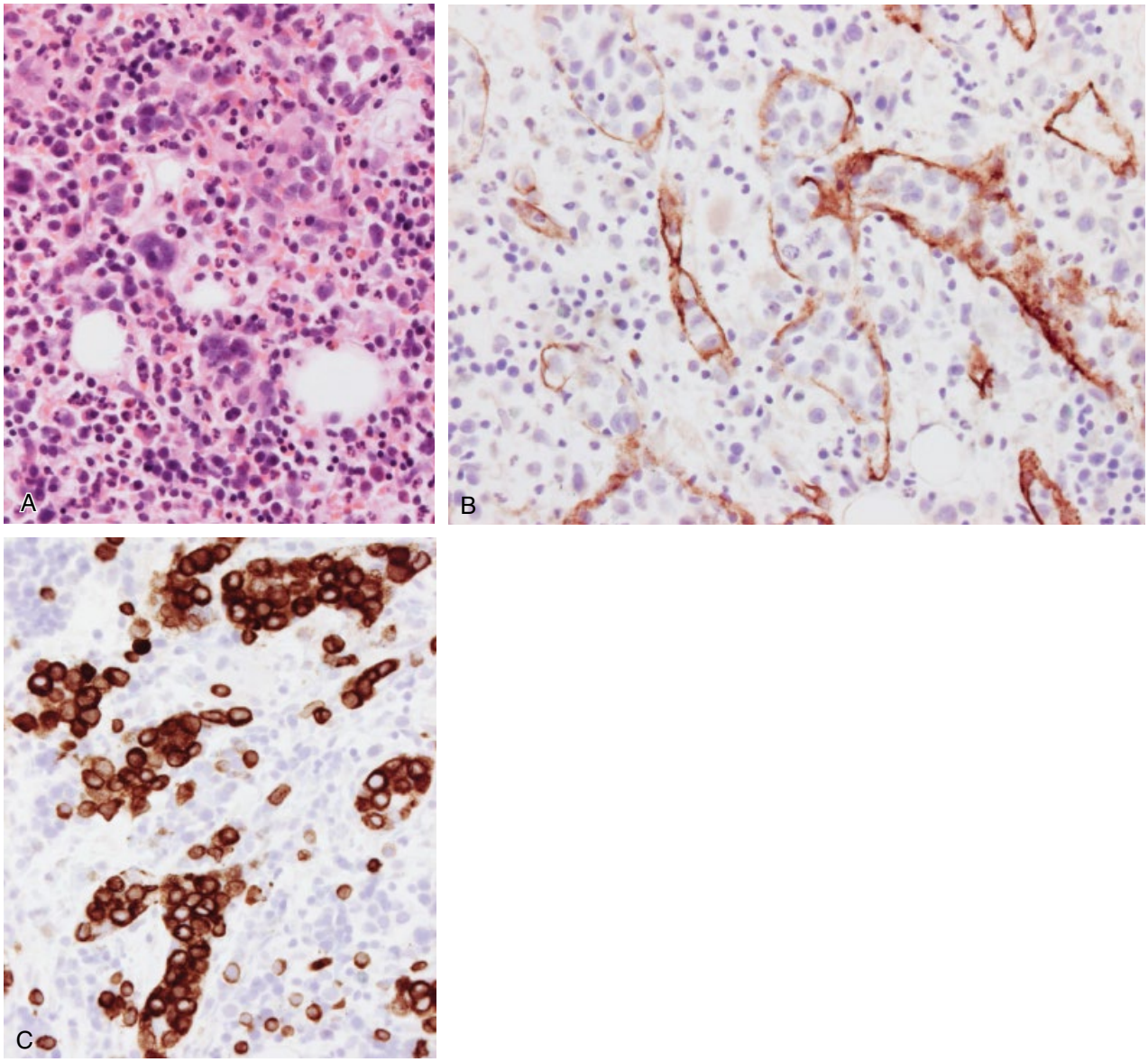

Fig. 20.20. Intravascular large B-cell lymphoma: Bone marrow trephine biopsy. **A,** H&E: The large tumor cells are present within a vascular sinus. **B,** Immunostain: CD34 shows the sinus lining and intrasinusoidal lymphoid cells. **C,** Immunostain: CD79a shows the tumor cells largely confined to the sinusoidal spaces. (Courtesy of Dr. W Erber.)

of large B cells with terminal B-cell differentiation phenotype that lack CD20 and PAX5 but express CD138 and cytoplasmic Ig, usually IgA. Characteristically, the cells express ALK due to t(2;17) or t(2;5) translocations, which induces formation of a chimeric protein of the anaplastic large-cell kinase (ALK) with clathrin (CLTC-ALK) or nucleophosmin (NPM-ALK), respectively. As a consequence ALK is expressed in these tumors (Fig. 20.21). This tumor should not be confused with the T/Null ALK-positive anaplastic large cell lymphoma which has a better prognosis.

PLASMABLASTIC LYMPHOMA

This is a very aggressive tumor, usually extranodal, mainly occurring in immunodeficient or elderly patients. The tumor cells have morphology of large B-cell lymphoma but phenotypic plasma cell differentiation (Figs. 20.22 and 20.23). Like myeloma, the cells express CD138, BLIMP1, and IRF4 but lack the mature B-cell markers CD20 and PAX5 (see Table 19.7).

PRIMARY EFFUSION LYMPHOMA AND OTHER HHV8-RELATED DISORDERS

Primary effusion lymphoma (PEL) is an aggressive tumor that causes serous effusions, especially pleural, pericardial, or peritoneal, usually without tumor masses. It is associated with infection with the human herpes virus 8 (HHV8), previously called Kaposi sarcoma herpes virus. Coinfection with EBV is common. Rarely, cases with similar morphology and clinical presentation that are HHV8 negative have been reported but they are not considered the same disease. In some cases, solid tumors, usually extranodal, with the same morphology and phenotype (extracavitary PEL),

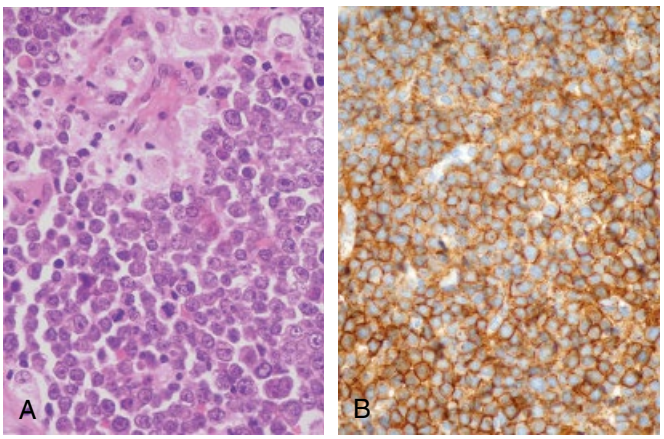

Fig. 20.22. Plasmablastic lymphoma. **A,** H&E: The neoplastic cells are large with prominent centrally located nucleoli. The cytoplasm is amphophilic with a paranuclear hof. **B,** Immunostain: The neoplastic cells are strongly positive for CD138.

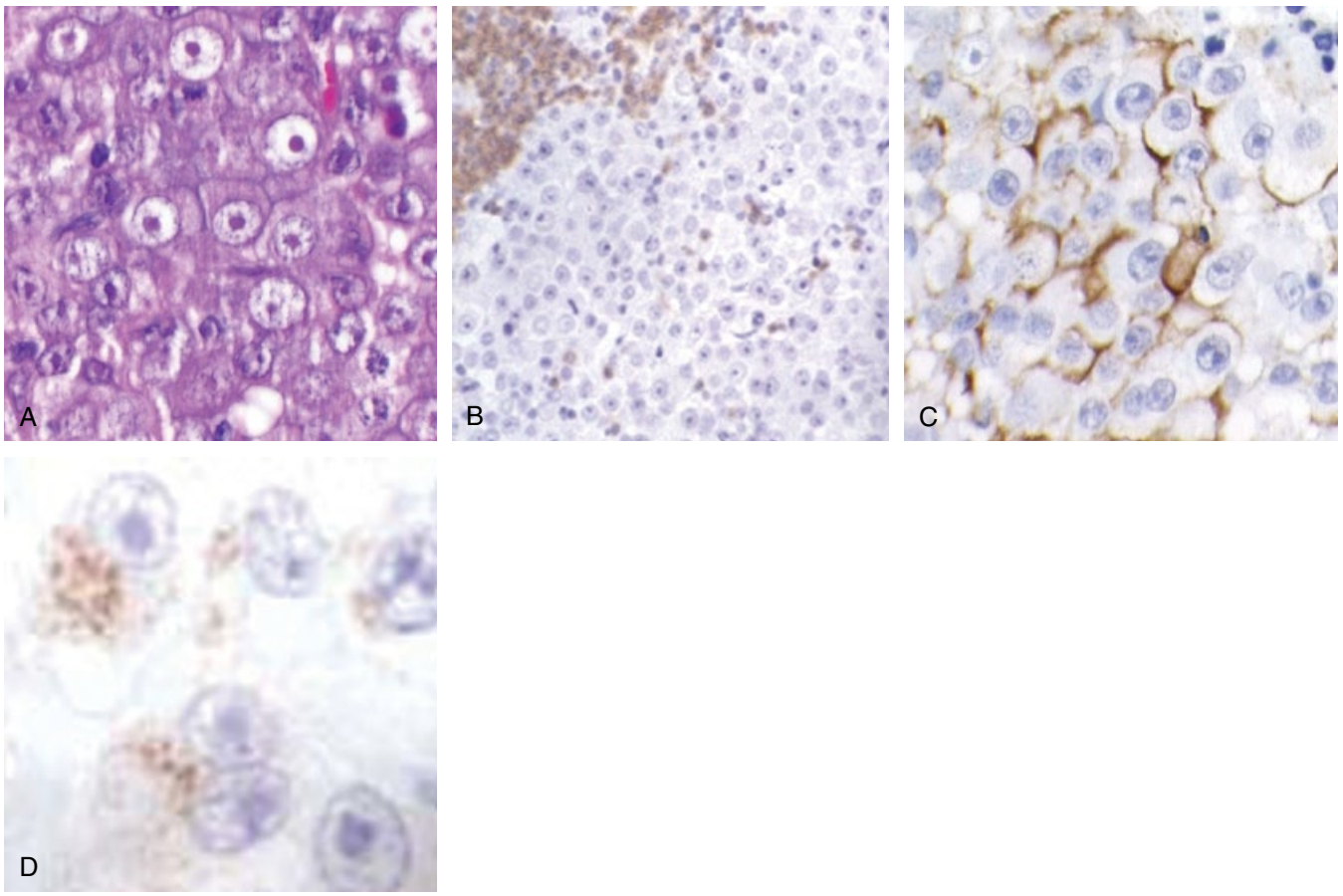

Fig. 20.21. ALK+. Diffuse large B-cell lymphoma **A,** H&E: The neoplastic cells are very large and grow in a cohesive pattern with an immunoblastic morphology. **B,** Immunostain with CD79a: The neoplastic cells are negative for B-cell markers. **C,** Immunostain: The neoplastic cells are positive for CD138, a plasma cell marker. **D,** Immunostain: ALK is positive with a cytoplasmic granular pattern, suggestive of the clathrin translocation (CTLC-ALK).

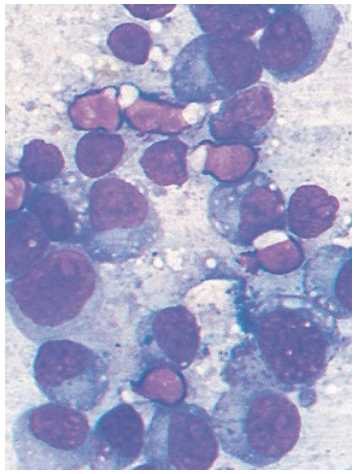

Fig. 20.23. Plasmablastic lymphoma: Fine-needle aspirate. The large lymphoid cells show plasmablastic and plasmacytic forms.

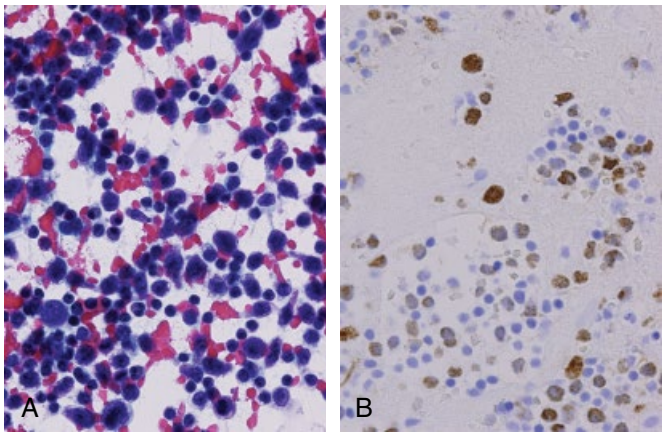

Fig. 20.24. Primary effusion lymphoma. **A,** Papanicolaou stain: Large neoplastic cells in a pleural effusion. **B,** The LANA-1 HHV8-associated antigen is strongly positive in the nuclei of the neoplastic cells.

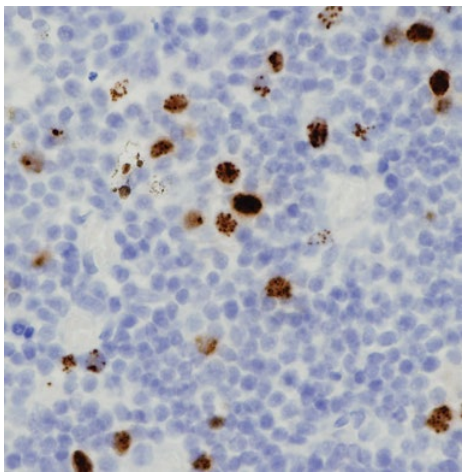

Fig. 20.25. Multicentric Castleman disease immunostain: Scattered HHV8-positive cells in an HIV-positive patient. (Courtesy of Dr. M Heller.)

also HHV8 positive, precede the development of PEL or occur after its resolution. Most patients with PEL are HIV positive, but negative cases occur especially in elderly males in the Mediterranean area or other areas where HHV8 is frequent.

The PEL cells have a morphology with immunoblastic, anaplastic, and plasmablastic cells and regardless of the morphologic type express a plasma cell-related phenotype and stain positive for HHV8 (Fig. 20.24). Vacuoles are common. Pan-B markers are negative but CD30, CD38, and CD138 are usually positive.

Other HHV8-positive lymphoproliferative lesions are the multicentric Castleman disease that also occurs frequently in HIV+ patients and the uncommon germinotropic lymphoproliferative disorder usually in immunocompetent patients. In the former, the HHV8+ cells are in the mantle zone of the follicle (Fig. 20.25) and in the second in the germinal center cells.

Multicentric Castleman disease must be distinguished from localized Castleman disease which mainly affects young adults without immunodeficiency as mediastinal or abdominal masses. Histologically, two variants can be distinguished, the hyaline vascular and plasma cellular. The hyaline vascular variant is composed of multiple follicles with depleted germinal centers, expanded mantle zones, and marked vascular proliferation in the interfollicular areas that penetrate the germinal centers. The germinal centers have a proliferation of follicular dendritic cells and frequent hyalinization (Fig. 20.26). The plasma cell variant has prominent follicular hyperplasia with intense interfollicular infiltration by mature plasma cells (Fig. 20.27). This variant is associated with general symptoms that regress after excision. Some cases show combined features of the hyaline vascular and plasma cell variants.

BURKITT LYMPHOMA

Burkitt lymphoma was first found in young African children and has an unusual predilection for massive jaw lesions (Fig. 20.28); extranodal abdominal involvement and ovarian, intestinal, kidney, or breast tumors also occur (Fig. 20.29). The disease is now known to be endemic in equatorial Africa, sporadic throughout the world, and associated with immunodeficiency. All three types are associated with a high incidence of CNS disease and to a variable degree with EBV infection.

The most frequent underlying cytogenetic change is t(8;14)(q24;q32) (Fig. 20.30). This involves the *MYC* oncogene and IGH. *MYC* is also rearranged in the less frequent t(2;8) and t(8;22) translocation with the immunoglobulin κ and λ light chains, respectively. *BCL2* and *BCL6* translocations are not present.

The cells are medium sized with basophilic cytoplasm and lipid-filled vacuoles. The nuclei are round with nucleoli. The tumor has a high proliferation rate with frequent mitoses and apoptotic cells. Macrophages dispersed throughout the tumor cells give a "starry sky" appearance (Fig. 20.31). Rare cases manifest purely with acute leukemia with bone marrow involvement and circulating blasts. Some cases of Burkitt lymphoma show plasmacytoid differentiation, especially in immunodeficiency states.

The immunophenotype is of a mature B-cell neoplasm with germinal center phenotype that is SIgM+, CD10+, BCL6+, BCL2–, CD5–, CD23–, and TDT–. MIB1 staining approaches 100% (Fig. 20.32). The serum lactate dehydrogenase (LDH) is high, reflecting the high cell turnover rate. In endemic African

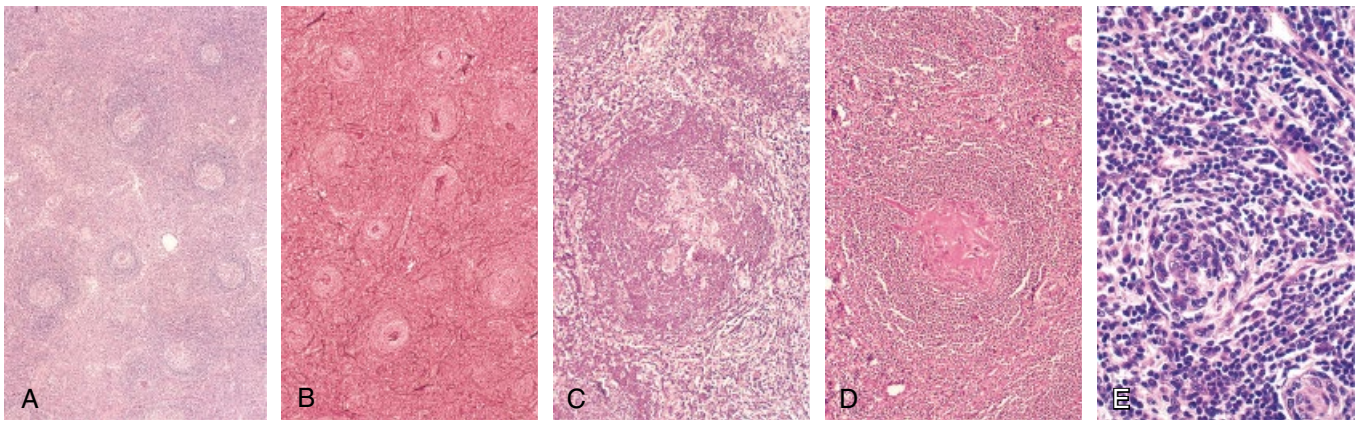

Fig. 20.26. Localized Castleman disease: Hyaline vascular variant. Low-power views of a lymph node biopsy show increased follicular centers with prominent central arterioles and whorls of mantle lymphocytes in sections stained using **(A)** H&E and **(B)** silver impregnation for reticulin. At higher power **(C)** prominent vascular proliferation in the center of a follicle, **(D)** extensive hyalinization of central vessels, and **(E)** whorling of mantle lymphocytes are seen. (*E,* Courtesy of Dr. JE McLaughlin.)

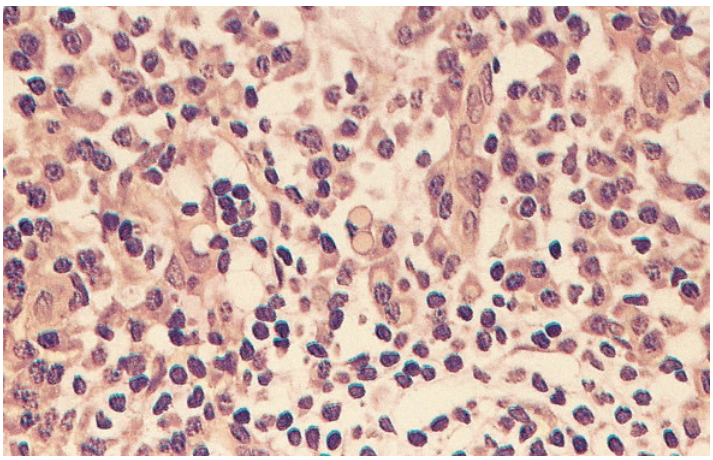

Fig. 20.27. Localized Castleman disease: plasma cell variant. High-power view showing plasma cells, many of which contain Russell bodies; other fields showed typical follicular hyalinization.

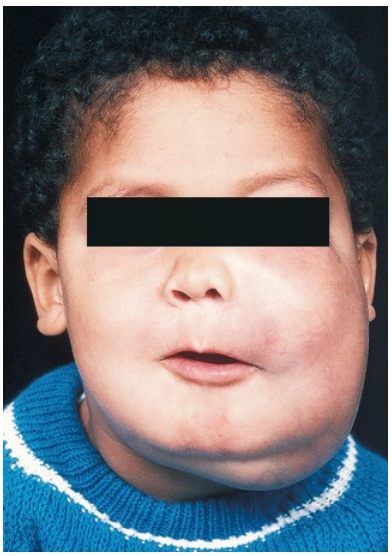

Fig. 20.28. Burkitt lymphoma. Characteristic facial swelling caused by extensive tumor involvement of the mandible and surrounding soft tissues. (Courtesy of Professor JM Chessells.)

patients, EBV is found in virtually all cases. Sporadic cases in Western countries that occur mainly in children and young adults are histologically and phenotypically identical. They arise in the absence of immune impairment, and EBV is only identifiable in 20–30% of cases.

HIGH GRADE B-CELL LYMPHOMA

The updated 2016 WHO classification has considered high grade B-cell lymphomas (HGBL) as a provisional category that substitutes the previous "B-cell lymphoma, unclassifiable with features intermediate between DLBCL and Burkitt lymphoma" (Table 20.1). This category includes highly aggressive lymphomas that cannot be considered in either of the two entities. A subset of these tumors with *MYC*, and *BCL2* and/or *BCL6* rearrangements are named **HGBL with *MYC* and *BCL2* and/or *BCL6* rearrangements** (Fig. 20.33). These cases have been also termed "double hit" HGBL (HGBL-DH). The relevant criteria for the diagnosis are the genetic alterations independently of the morphology of the tumor that may be DLBCL, blastoid, or with features intermediate between DLBCL and BL. The specific morphology should be noted because it may have prognostic impact.

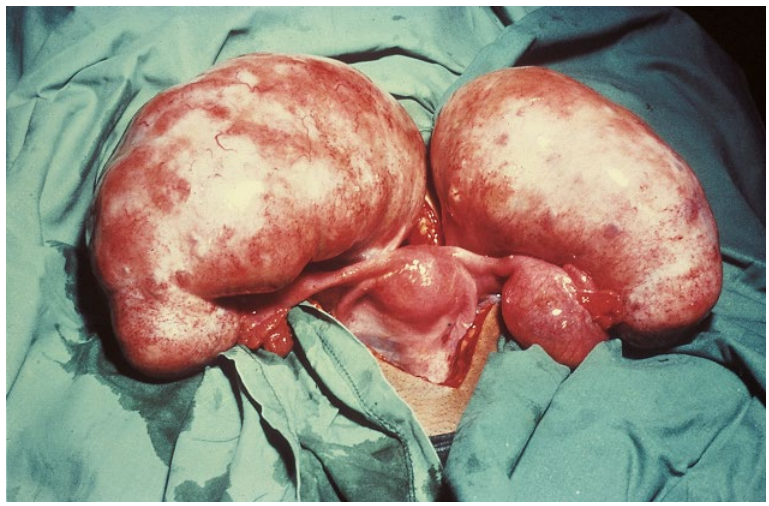

Fig. 20.29. Burkitt lymphoma. Gross bilateral involvement of the ovaries.

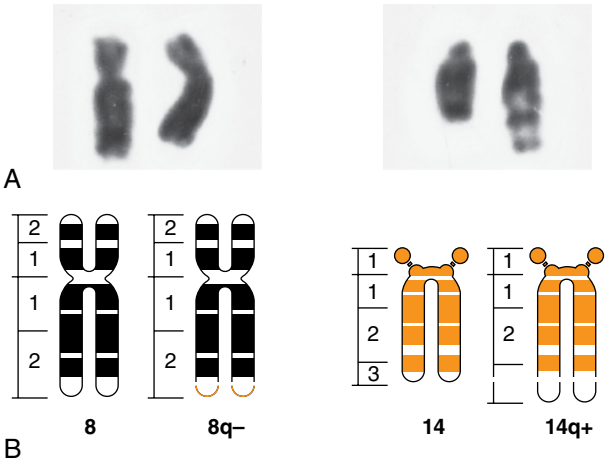

Fig. 20.30. Burkitt lymphoma. **A,** Partial karyotypes of G-banded chromosomes 8 and 14 from a child. The translocated chromosomes are on the right in each pair. The cellular oncogene *MYC* moves with the translocated portion of chromosome 8 and is juxtaposed to the Ig heavy-chain locus. **B,** A systematized description of the structural aberration. More rarely, cases of Burkitt lymphoma show (8;22) or (2;8) translocations, involving, respectively, the λ and κ light chain genes. (Courtesy of Professor LM Secker-Walker.)

The immunophenotype of these cases is of germinal center subtype (CD10+, BCL6+) with high expression of MYC and BCL2 proteins. The proliferation is usually high (Fig. 20.33). Cases with blastoid morphology or with features intermediate between DLBCL and BL without translocations are named **high grade B-cell lymphoma, NOS.** DLBCL with high expression of MYC and BCL2 proteins without genetic alterations have been called "dual-expressors" (DLBCL-DE). This double expression is considered an adverse prognostic factor but these tumors are not included in the HGBL category because the outcome does not seem so adverse, and the biologic consequences of having a genetic alteration may be different. The differential diagnosis of HGBL includes DLBCL and BL as well as other lymphomas with blastoid morphology such as B-lymphoblastic leukemia/lymphoma and blastoid mantle cell lymphoma. The diagnosis should be established based on the morphology, phenotype, and cytogenetic/FISH studies (Fig. 20.34).

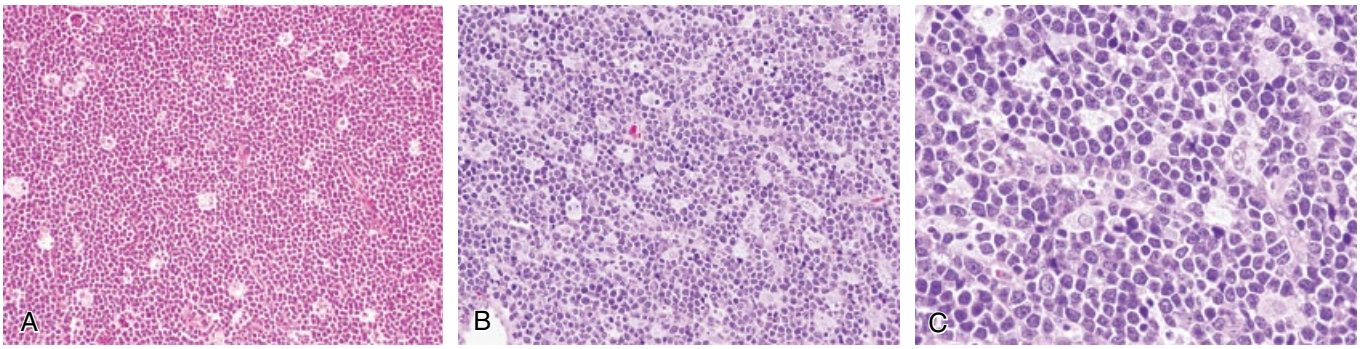

Fig. 20.31. Burkitt lymphoma. **A,** H&E: Diffuse infiltration of a lymph node with a "starry sky" appearance. **B,** diffuse infiltration with a prominent "starry sky" appearance and many mitotic figures and apoptotic cells. **C,** At high power the cells are uniform in size and contain multiple basophilic nucleoli.

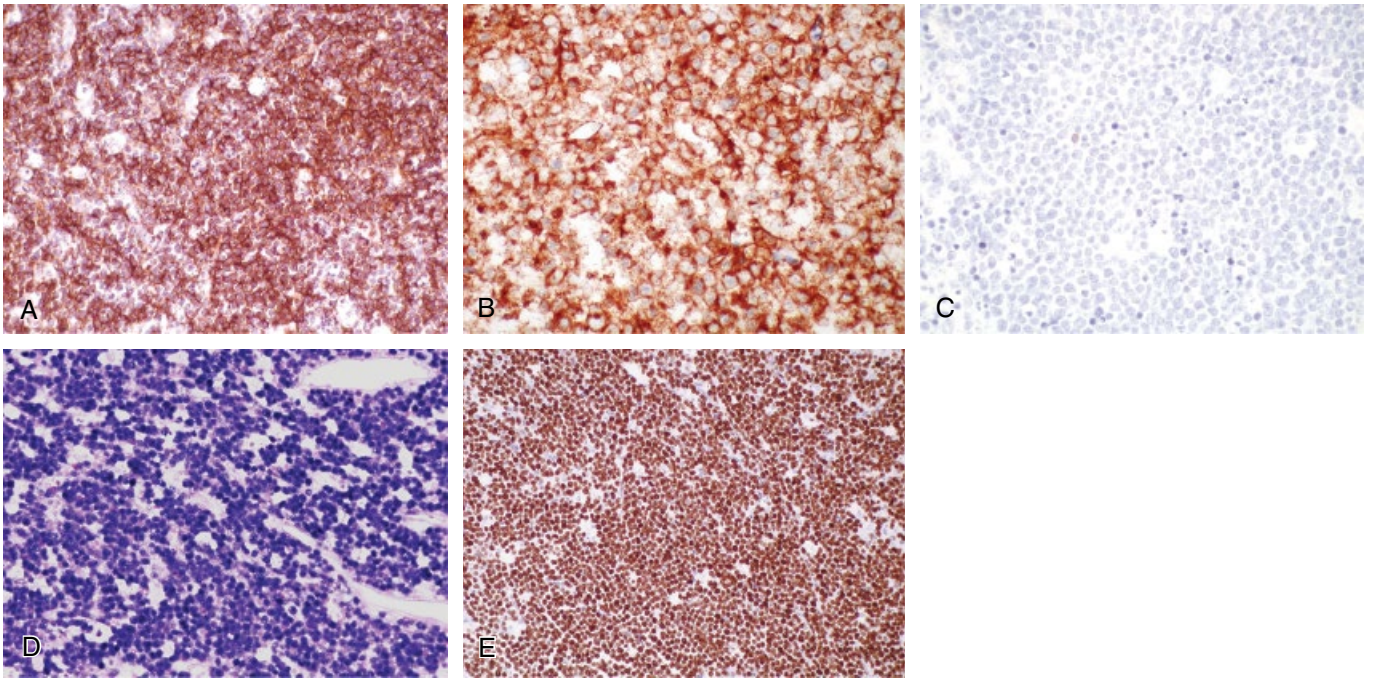

Fig. 20.32. Burkitt lymphoma: immunostains. **A,** All neoplastic cells express CD20. **B,** The tumor is positive for CD10. **C,** The neoplastic cells are BCL2 negative; occasional T lymphocytes are BCL2 positive. **D,** In situ hybridization (ISH) for Epstein–Barr virus RNA (EBERs) shows staining in the majority of the neoplastic cells. **E,** Nearly all neoplastic cells are positive for the proliferation-associated antigen Ki-67 (MIB1 staining).

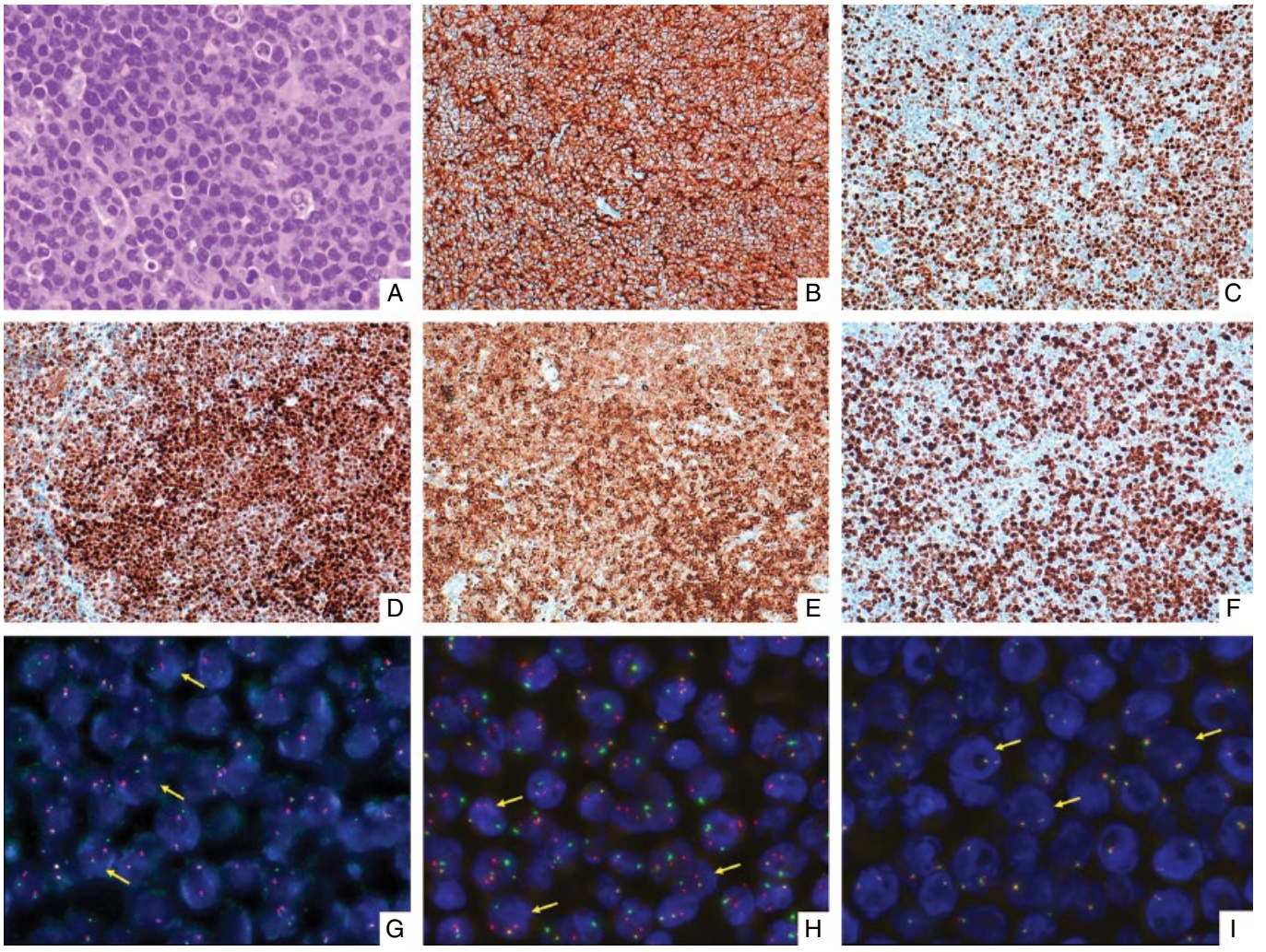

Fig. 20.33. High grade B-cell lymphomas (HGBLs) with *MYC* and *BCL2* rearrangements. **A,** H&E: The morphology of this case correspond to a DLBCL with tumor cells that contain irregular nuclei and evident nuclei in some of them. Mitotic figures are present. **B,** The tumor has a germinal center phenotype with expression of CD10 and **(C)** BCL6. **D,** The tumor cells are also strongly positive for MYC and **(E)** BCL2. **F,** The tumor cells are highly proliferative with expression of KI67 in most of them. **G,–I,** FISH analysis with break-apart probes show a rearrangement of *MYC* **(G)** and *BCL2* **(H)**, but not *BCL6* **(I)**.

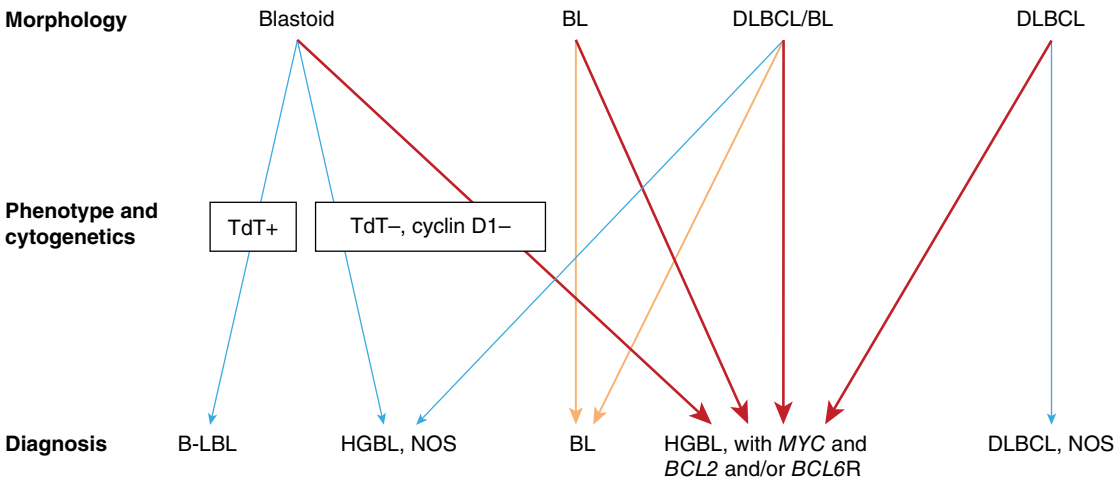

Fig. 20.34. Diagnostic approach to HGBLs. Lymphomas that potentially fall into the HGBL categories can morphologically resemble B-lymphoblastic leukemia/lymphoma (B-LBL), Burkitt lymphoma (BL), and DLBCL as well as lymphomas that are intermediate between DLBCL and BL (DLBCL/BL). These distinctions can be very subjective. The orange arrows indicate cases with a BL phenotype and a *MYC* rearrangement without *BCL2* or *BCL6* rearrangements ("single hit"). The red arrows indicate cases with *MYC* and *BCL2* and/or *BCL6* rearrangements ("double or triple hit"). Neither MCLs, subtypes of LBCLs, not Burkitt-like lymphoma with 11q aberration are indicated in the diagram. Source: Swerdlow SH, et al. Blood 2016;127:2375–2390. Reproduced with permission of *Blood: Journal of the American Society of Hematology*.

CHAPTER

21 MYELOMA AND RELATED NEOPLASMS

MULTIPLE (PLASMA CELL) MYELOMA

Table 21.1A classifies the plasma cell neoplasms according to the World Health Organization (WHO) 2016. Plasma cell (multiple) myeloma is characterized by proliferation in the bone marrow of a clonal population of malignant plasma cells. These cells produce cytokines that are responsible for bone loss and nearly always secrete monoclonal proteins that appear in plasma and often in urine. There are major interactions between the plasma cells and the marrow microenvironment (Fig. 21.1). Table 21.1B lists the criteria for diagnosis of multiple myeloma, dominantly the triad of 10% or greater plasma cell infiltration of the bone marrow on trephine biopsy, presence of a paraprotein in serum and/or Bence Jones protein in urine, and lytic bone lesions. Smoldering myeloma has similar features on bone marrow examination and paraprotein measurement but no end-organ damage (no hypercalcemia, renal damage, anemia, or bone lesions; CRAB) (Table 21.1B). The malignant neoplastic proliferation of plasma cells is usually estimated lower in aspirates, based on morphology and flow cytometry, than in trephines using immunohistochemistry and it is the higher result that is used in diagnosis. In advanced disease the abnormal cell population can exceed 60% of the total marrow cell level (Figs. 21.2 and 21.8). The morphology of these cells is often abnormal, with more primitive features and a greater variation in size than found in classic plasma cells (Figs. 21.3–21.5). Clonality can be shown by flow cytometry, the cells expressing CD138 and light chain restriction, or by immunohistochemistry. Multinucleate cells can be frequent. Flaming plasma cells are most frequent when the plasma cells secrete immunoglobulin A (IgA) (Fig. 21.5). As a result of abnormal immunoglobulin deposits, inclusion bodies can occur in the cytoplasm (Figs. 21.6 and 21.7). Trephine biopsy shows a uniform infiltration by plasma cells and plasmablasts (Figs. 21.8 and 21.9), which stain positive for CD38 or CD138 (Fig. 21.10) but negative for CD19 or CD20. The cells express either κ or λlight chains (Fig. 21.11).

In most patients a monoclonal protein (M-protein or paraprotein) can be demonstrated in the serum and/or urine. Typically, serum protein is increased and electrophoresis shows an abnormal paraprotein in the globulin region (Fig. 21.12). Immunodiffusion or immunoturbidometry reveals which immunoglobulin fraction is increased, and the serum levels of the uninvolved classes of immunoglobulin are usually depressed. Immunoelectrophoretic techniques confirm the presence of an abnormal immunoglobulin and are able to establish the monoclonal nature of this protein (Fig. 21.13). In most cases, whether or not a paraprotein is present, there is an excess in serum of κ or λ light chains (Fig. 21.14). In nonsecretory myeloma (3% of cases) there is absence of an M-protein but in up to two-thirds there is elevation of a free light chain or abnormal free light chain ratio. Cytoplasmic immunoglobulin is present in the plasma cells in 85% of cases. The urine contains Bence Jones protein in two-thirds of cases. This consists of free light chains, either κ or λ, of the same type as the serum M-protein and the serum light chain in excess. Occasionally, patients have two or more M-proteins, but in less than 1% of patients no M-proteins are found in the serum or urine.

TABLE 21.1A. PLASMA CELL NEOPLASMS (WHO, 2016)

Plasma cell neoplasms
Non-IgM (plasma cell) monoclonal gammopathy of undetermined significance (precursor lesion)
Plasma cell myeloma
Clinical variants:
Smouldering (asymptomatic) plasma cell myeloma
Nonsecretory myeloma
Plasma cell leukemia
Plasmacytoma
Solitary plasmacytoma of bone
Extraosseous (extramedullary) plasmacytoma
Monoclonal immunoglobulin deposition diseases
Primary amyloidosis
Systemic light and heavy chain deposition diseases
Plasma cell neoplasms with associated paraneoplastic syndrome
POEMS syndrome
TEMPI syndrome (provisional)

Source: Adapted with permission fromSwerdlow SH, et al., eds. *WHO Classification of Tumours of Haematopoietic and Lymphoid Tissues*, revised 4th edn. International Agency for Research on Cancer, 2017.

Color Atlas of Clinical Hematology: Molecular and Cellular Basis of Disease, Fifth Edition. A. Victor Hoffbrand, Paresh Vyas, Elías Campo, Torsten Haferlach, and Keith Gomez

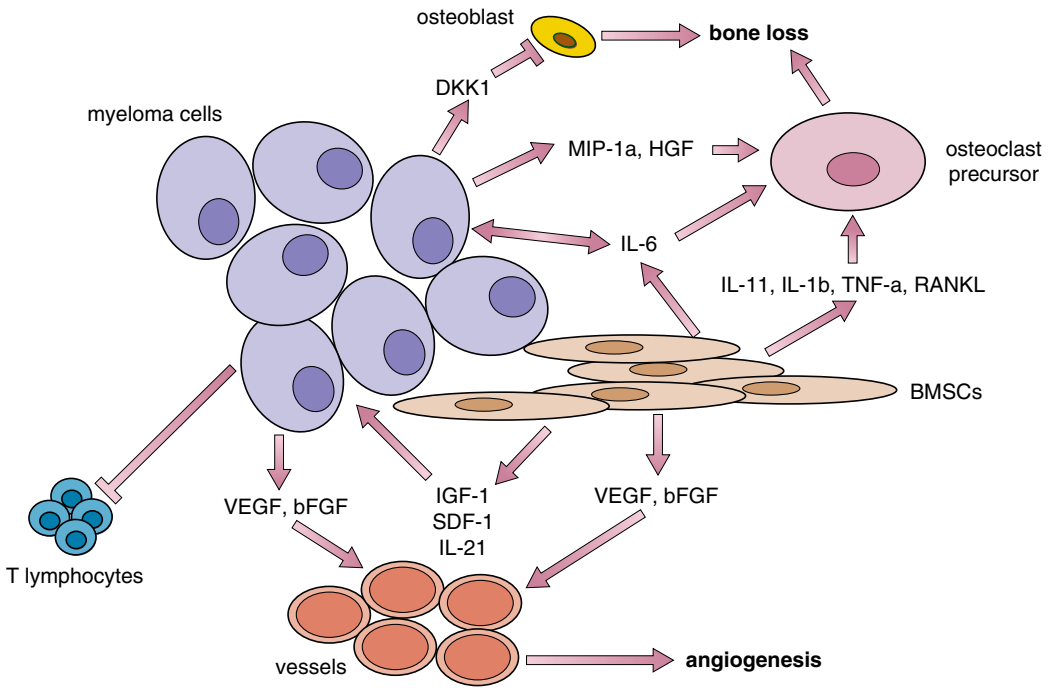

Fig. 21.1. Pathophysiology of plasma cell myeloma. bFGF, basic fibroblast growth factor; BMSC, bone marrow stromal cell; DKKI, dickkop-1 protein; HGF, hepatocyte growth factor; IGF-1, insulin-like growth factor; MIP.I, macrophage inhibitor factor; RANK, receptor activator of nuclear factor-κB ligand; SDF-1, stromal derived factor 1;VEGF, vascular endothelial growth factor.

TABLE 21.1B. REVISED INTERNATIONAL MYELOMA WORKING GROUP DIAGNOSTIC CRITERIA FOR MULTIPLE MYELOMA AND SMOLDERING MYELOMA

Definition of multiple myeloma

Clonal bone marrow plasma cells more than 10% or biopsy-proven bony or extramedullary plasmacytoma and any one or more of the following myeloma defining events:

Myeloma defining events:
Evidence of end organ damage that can be attributed to the underlying plasma cell proliferative disorder, specifically:
Hypercalcemia: Serum calcium >0.25 mmol/L (0.1 mg/dL) higher than the upper limit of normal or >2.75 mmol/L (>11 mg/dL)

- Renal insufficiency: Creatinine clearance, 40 mL/min or serum creatinine >177 μmol/L (>2 mg/dL)
- Anemia: Hemoglobin value of >2.0 g/dL below the lower limit of normal, or a hemoglobin value <10.0 g/dL
- Bone lesions: One or more osteolytic lesions on skeletal radiography, CT, or PET-CT

Any one or more of the following biomarkers of malignancy:

- Clonal bone marrow plasma cell percentage ≥60%
- Involved: Uninvoled serus free light chain ration ≥100
- >1 focal lesions on MRI studies

Definition of smoldering multiple myeloma

Both criteria must be met:

- Serum monoclonal protein (IgG or IgA) ≥30 g/L or urinary monoclonal protein ≥500 mg per 24 h and/or clonal bone marrow plasma cells 10–60%
- Absence of myeloma defining events or amyloidosis

Further details of the criteria are given in this article

Source: *Lancet Oncol* 2014;15:539–548. http://www.thelancet.com/journals/lanonc/article/PIIS1470-2045(14)70442-5/fulltext. Reproduced with permission of Elsevier.

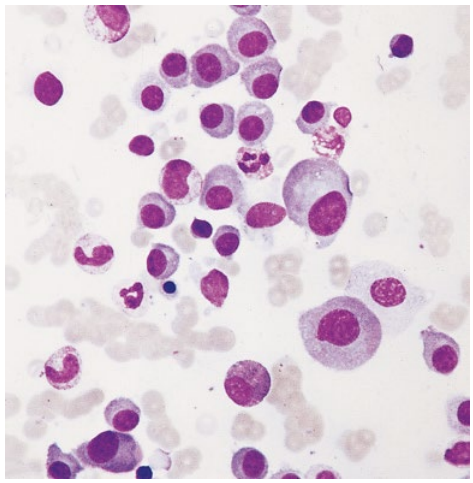

Fig. 21.2. Multiple myeloma: Marrow cell trail. Most cells seen are atypical plasma cells.

In the advanced stage of this disease a normochromic normocytic anemia is present, often with an associated neutropenia and thrombocytopenia, reflecting the development of bone marrow failure. The increased globulin in the serum is frequently associated with an increased erythrocyte sedimentation rate (ESR), and the blood can show marked red cell rouleaux formation and increased background staining (Fig. 21.15). In some cases a leukoerythroblastic blood picture is seen. Abnormal plasma cells appear in the blood film in about 15% of patients (Fig. 21.16).

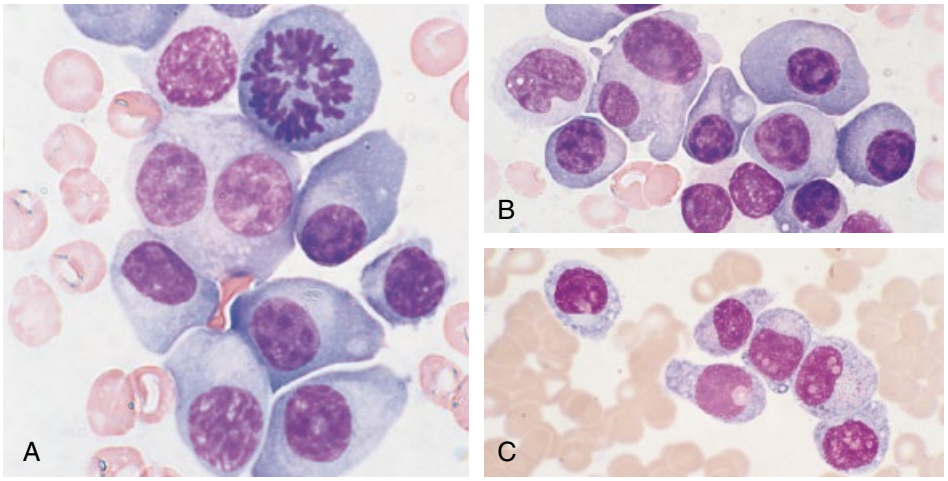

Fig. 21.3. Multiple myeloma: Abnormal plasma cells in marrow in two cases. **A,** Myeloma cells, one binucleate, with nucleoli, and one with a mitotic figure. **B,** The nuclei in a binucleate cell vary greatly in size. **C,** Abnormal cytoplasmic and nuclear vacuolation.

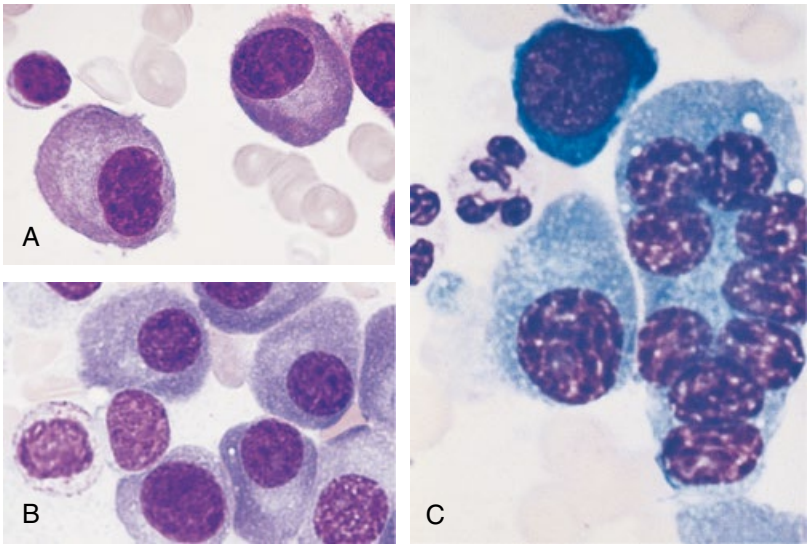

Fig. 21.4. Multiple myeloma. **A–C,** Abnormal plasma cells in bone marrow. Considerable variation occurs in nuclear size and cytoplasmic volume, and one of the myeloma cells is multinucleate **(C).**

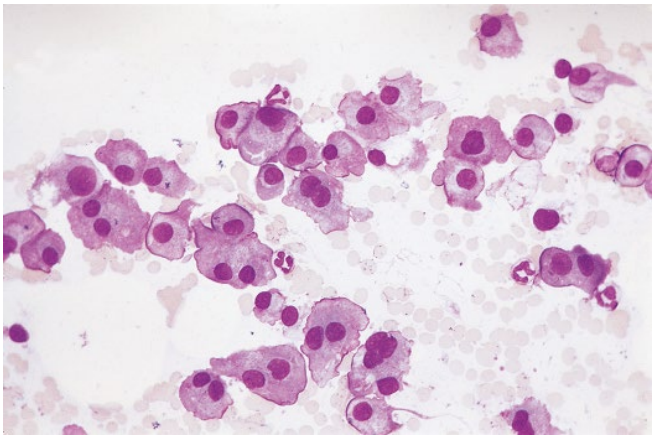

Fig. 21.5. Multiple myeloma: "Flaming" plasma cells in marrow with IgA M-protein in serum. There are numerous thesaurocytes, large plasma cells with small, sometimes pyknotic, nuclei, and expanded fibrillary cytoplasm, which also shows "flaming" of the cell rim (inset). Although "flaming" occurs most frequently with IgA production, it may also be seen with M-proteins of other classes.

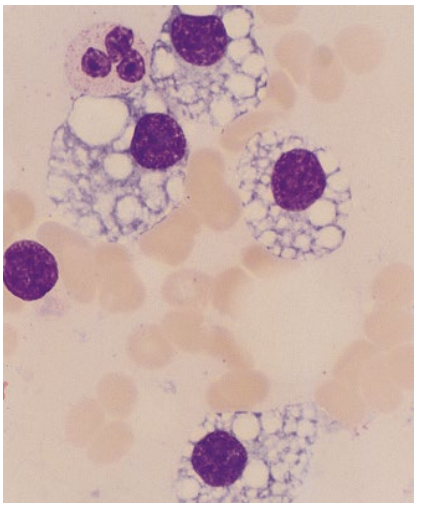

Fig. 21.6. Multiple myeloma: Bone marrow aspirate showing abnormal plasma cells with many large cytoplasmic vacuoles (Mott cells or morular cells). Each vacuole is an accumulation of immunoglobulin. (Courtesy of Dr. M Saary.)

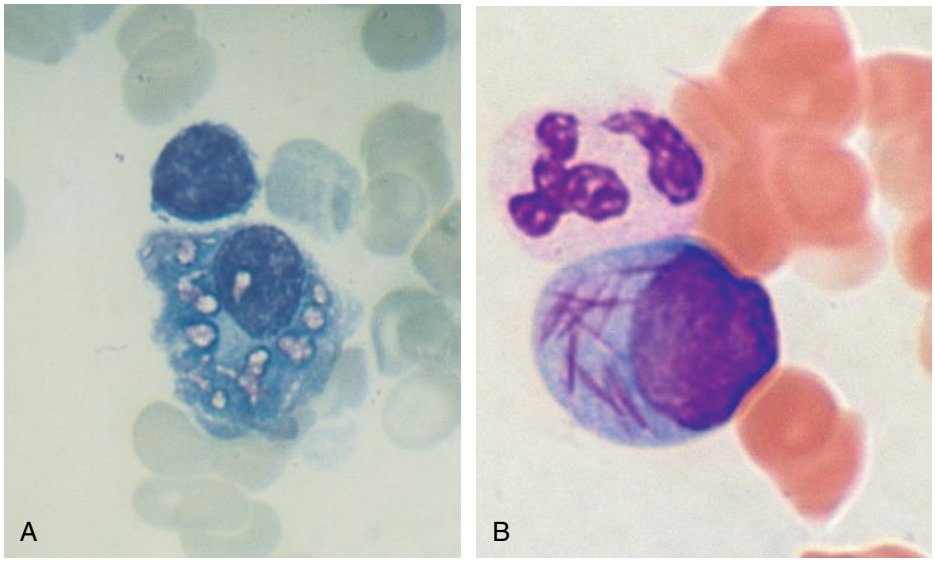

Fig. 21.7. Multiple myeloma. **A,** Plasma cell showing crystalline pink inclusions of abnormal immunoglobulin. **B,** Plasma cell showing slender rod-like cytoplasmic inclusions. (*A,* Courtesy of Dr. R Britt.)

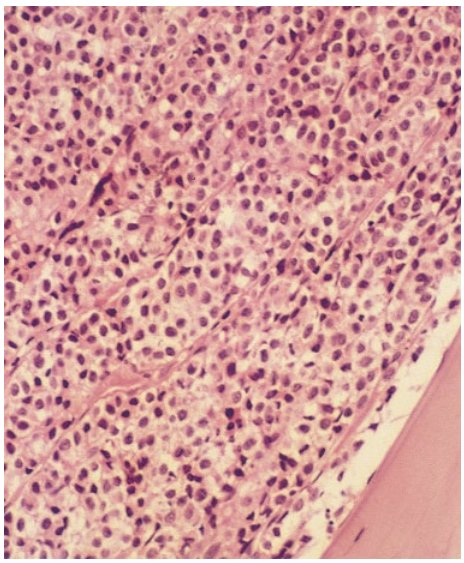

Fig. 21.8. Multiple myeloma. Trephine biopsy shows almost complete replacement of hematopoietic tissue by sheets of abnormal plasma cells.

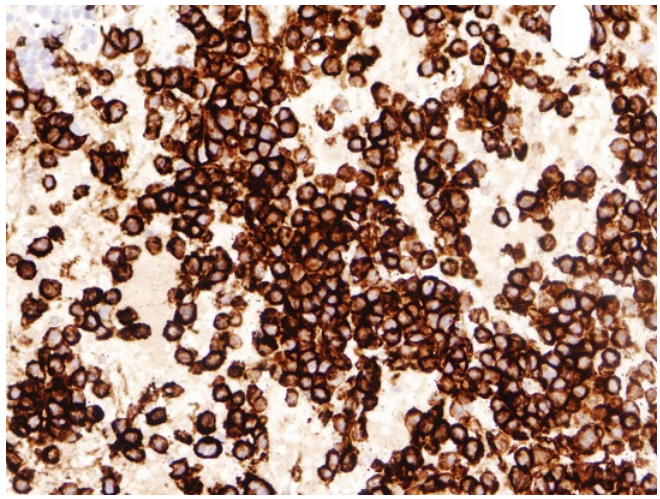

Fig. 21.10. Multiple myeloma. Immunostaining showing that the malignant plasma cells are CD138 positive.

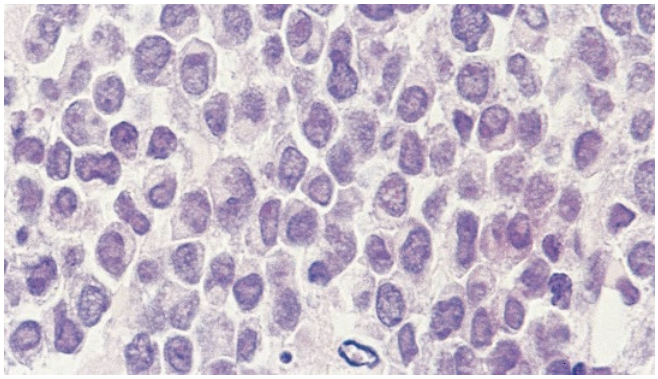

Fig. 21.9. Multiple myeloma/plasma cell leukemia. Trephine biopsy showing almost complete replacement of hematopoietic cells by plasma cells and plasmablasts. (Courtesy of Dr. DM Swirsky.)

However, sensitive gene rearrangement studies reveal typical cells of the malignant clone in the peripheral blood in a higher proportion of patients.

Cytogenetic abnormalities, detected by conventional cytogenetics or fluorescence in situ hybridization (FISH), are present in the marrow cells in 80–90% of cases (Table 21.2). These are most frequently trisomies involving the odd-numbered chromosomes 3, 5, 7, 9, 15, and 17. Monosomy 13/del(13q) detected by conventional karyotyping were thought to be driver mutations but it now appears on FISH studies that the abnormality is a surrogate marker for high risk IgH translocations. Later changes involve RAS mutations, MYC translocations, del17 and 1p deletion. The cytogenetic changes help to predict prognosis (Table 21.2). There is usually overexpression of cyclin D1, D2, or D3 (Fig. 21.17). Gene expression studies can also be used to assess prognosis (Fig. 21.18).

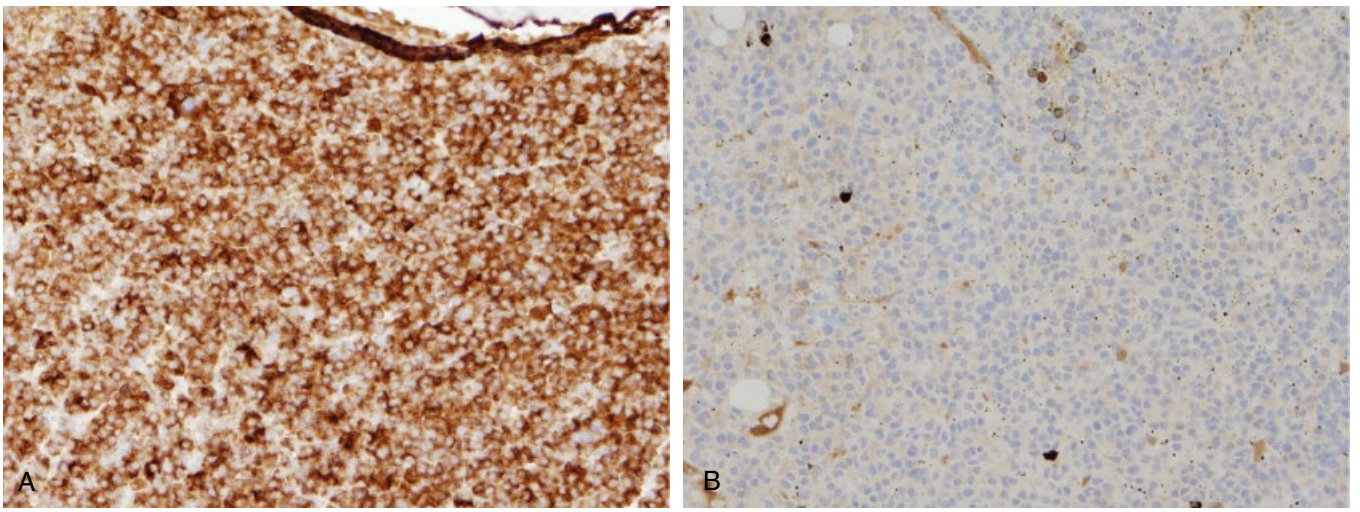

Fig. 21.11. Multiple myeloma. **A,** Immunostaining positive for κlight chains. **B,** Immunostaining negative for λlight chains.

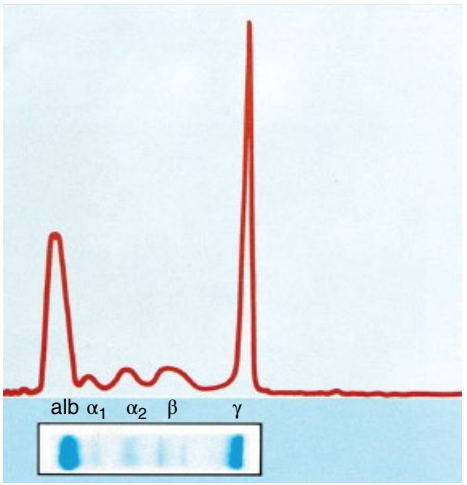

Fig. 21.12. Multiple myeloma: Serum protein electrophoresis showing an M-protein in the γ-globulin region and reduced levels of background β- and α-globulins. This "spike" and deficiency pattern is typical of patients with myeloma. (Total protein, 99 g/L; IgG M-protein component, 41 g/L.)

Skeletal radiology shows osteolytic lesions in 60% of patients, and associated pain is characteristic. The lesions include the classic "punched-out" lesions of the skull (Fig. 21.19), lytic lesions, and generalized bone rarefaction of the spine, ribs, pelvis, humerus and femur, and pathologic fractures (Figs. 21.20 and 21.21). CT has the highest sensitivity for detecting bone disease (Fig. 21.21 *B, C*). It can be combined with positron emission tomography (PET) scanning to show the activity of the tumor (Fig. 21.22). Extensive bone resorption (Fig. 21.23) is thought to be caused by excessive production of osteoclast activating factor (OAF), probably a combination of tumor necrosis factor and interleukin-1, which results in elevation of serum calcium in half of patients. In occasional patients, myeloma deposits extend beyond the skeleton into surrounding soft tissues (Figs. 21.24 and 21.25). Magnetic resonance imaging (MRI) is the best modality for assessing sites of soft tissue and bone marrow invasion. Rarely, osteosclerosis occurs (Fig. 21.26). Osteosclerotic myeloma shows fibrosis and sclerosis of bone trabeculae (Table 21.1A). POEMS syndrome consists of polyneuropathy, osteosclerotic myeloma, and systemic involvement

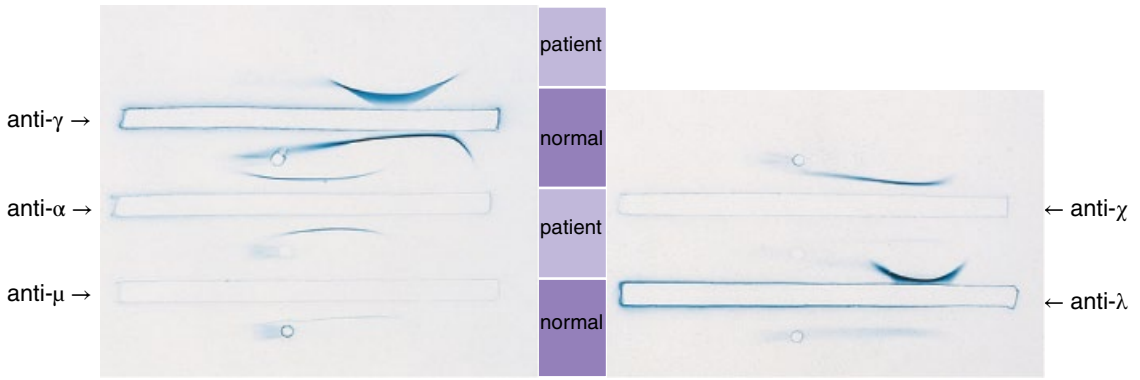

Fig. 21.13. Multiple myeloma: Immunoelectrophoresis. Normal protein is recognized by characteristic arc patterns. In the reactions against anti-γ and anti-l, the IgG-l M-protein maintains its electrophoretic position, but appears as a "bow" or thickened arc with a smaller than usual radius. Reduced levels of IgA and IgM are reflected in small or absent arcs in the reactions with anti-α and anti-μ.

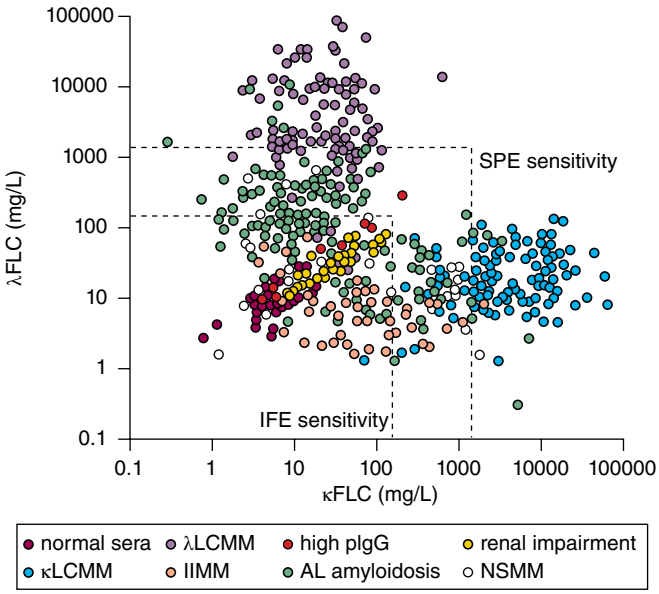

Fig. 21.14. Multiple myeloma. There is usually an excess of either κ or λ light chains in the serum. Dotted lines indicate sensitivity of these tests. IFE, immunofixation electrophoresis; II, intact immunoglobulin; LC, light chain; MM, multiple myeloma; NS, nonsecretory; P, polyclonal; SPE, serum protein electrophoresis. (Courtesy of Professor AR Bradwell.)

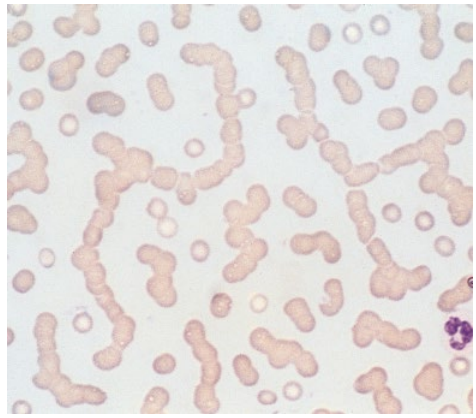

Fig. 21.15. Multiple myeloma: Peripheral blood film shows marked rouleaux formation of red cells and increased background staining.

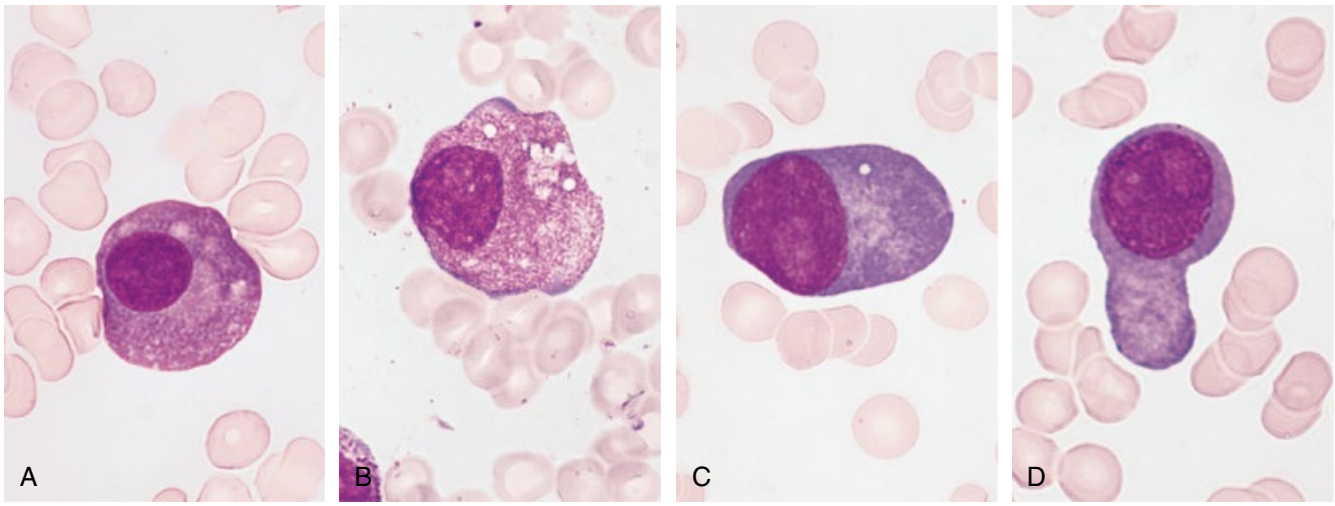

Fig. 21.16. Multiple myeloma. **A–D,** Isolated myeloma cells in peripheral blood films from two patients.

TABLE 21.2. PROGNOSTIC CYTOGENETIC ABNORMALITIES IN NEWLY DIAGNOSED MULTIPLE MYELOMA

Standard risk		High risk	
Cytogenetic abnormality	**Incidence (%)**	**Cytogenetic abnormality**	**Incidence (%)**
t(11;14)	15	t(4;14)	15
t(6;14)	5	t(14;16)	2–3
Hyperdiploidy	50	t(14;20)	1
		del(17p)	10
		del(1p)	10
		gain(1q)	35–40

Del(13q) occurs in 40% of cases but is usually associated with high risk features, e.g. t(4;14).
Source: Smith D, Yong K. *Br J Haematol* 2016;175:367–380. Reproduced with permission of John Wiley and Sons.

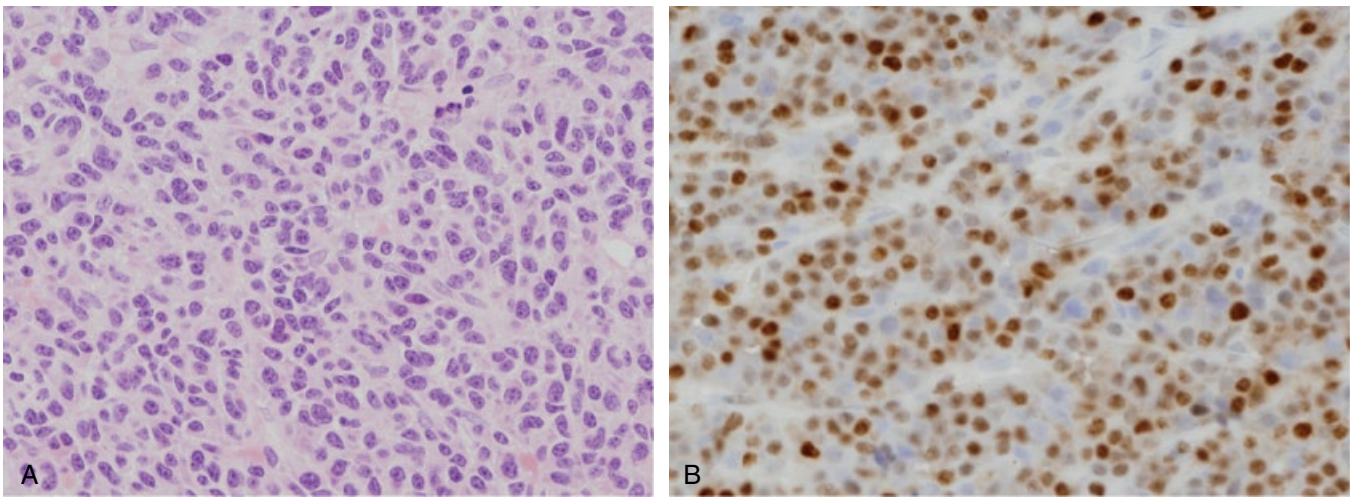

Fig. 21.17. Multiple myeloma. **A,** The cells usually expressing cyclin D1 show a characteristic morphologic appearance of immature myeloma cells with eccentrically located nuclei and prominent central nucleoli. **B,** Immunostaining positive for cyclin D1.

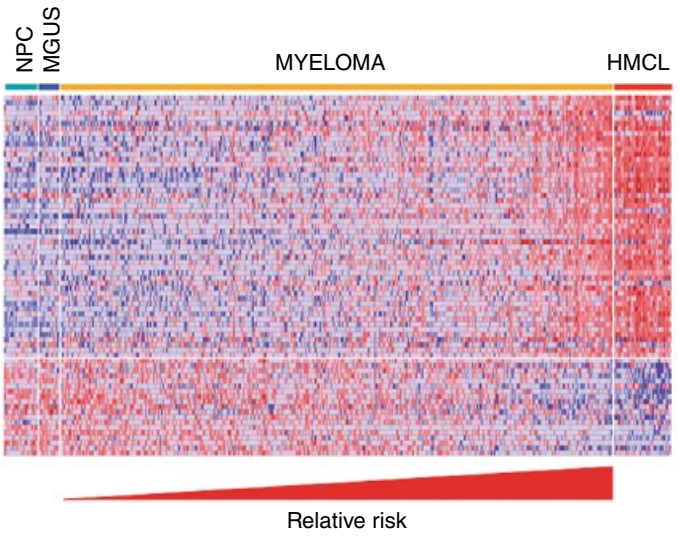

Fig. 21.18. Multiple myeloma: Gene expression clustergram of 70 high-risk genes in plasma cells, of 22 healthy subjects (NPC), 14 with MGUS, 351 patients with newly diagnosed myeloma, and 42 human myeloma cell lines. Red indicates above the median and blue below the median. Source: Adapted from-Shaughnessy JD, et al. *Blood* 2007;109:2276–2284, fig. 2, p. 2279. Reproduced with permission of *Blood: Journal of the American Hematology Society*.

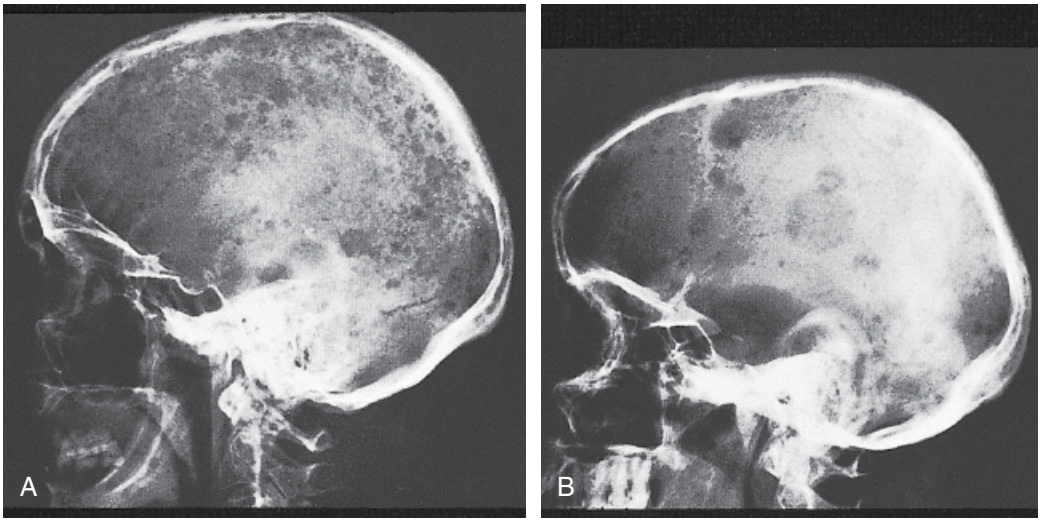

Fig. 21.19. Multiple myeloma: Radiographs of skulls showing: **A,** Typical multiple, small, "punched-out" osteolytic lesions; **B,** a case in which the lesions vary much more in size; **C,** inside of skull shows characteristic 'moth-eaten' lytic lesions.

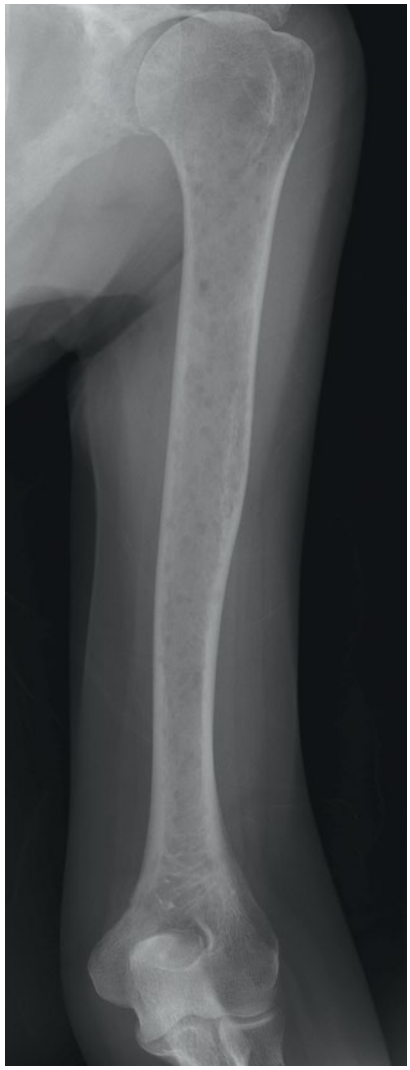

Fig. 21.20. Multiple myeloma: Humerus showing punched out lesions and expanded mid-shaft.

(e.g. endocrinopathy, skin pigmentation, clubbing and arthropathy, hepatosplenomegaly, and lymphadenopathy).

Renal complications have an important influence on the course of multiple myeloma. Patients with persistent renal failure and blood urea in excess of 14 mmol/L have a poor prognosis. Damage from heavy Bence Jones proteinuria (Fig. 21.27), amyloid disease (Fig. 21.28), nephrocalcinosis (Fig. 21.29), and pyelonephritis (Fig. 21.30) are important in the pathogenesis. A more generalized amyloid disease occurs in a small number of patients, and macroglossia with tongue ulceration (Figs. 21.31 and 21.32), carpal tunnel syndrome (Fig. 21.33), skin deposits (Figs. 21.34 and 21.35) and cardiac involvement (Fig. 21.36) can occur.

PLASMA CELL LEUKEMIA

At presentation, patients may have large numbers of circulating plasma cells, or this blood picture can arise during the course of the disease (Figs. 21.37 and 21.38). In plasma cell leukemia, there are $>2 \times 10^9$/L plasma cells in the peripheral blood and sometimes $>100 \times 10^9$/L. The circulating cells may have features of lymphoplasmacytic cells, typical plasma cells, or plasma blasts. The immunophenotyping is similar to myeloma. The prognosis is poor.

PROGNOSIS

The International Staging System (ISS) is widely used for assessing prognosis. This depends on the serum albumin and the serum β_2-microglobulin (Table 21.3). The Revised ISS incorporates cytogenetics as well as serum lactate dehydrogenase (Table 21.4).

SMOLDERING (ASYMPTOMATIC) MYELOMA

This condition is defined by the presence of M-protein ≥30 g/L and/or ≥10% plasma cells in the marrow without any of the clinical features of multiple myeloma (Table 21.1B): hypercalcemia, renal impairment, anemia (hemoglobin 2.0 g/dL < the lower limit of normal) and bone lesions (CRAB). Bone lesions include lytic lesions or osteoporosis with compression fractures, possibly confirmed by CT or MRI. Less frequent clinical features of symptomatic myeloma include hyperviscosity, amyloidosis, recurrent bacterial infections, and extramedullary plasmacytoma.

The disease resembles MGUS but with a much greater tumor burden and higher risk of transformation to symptomatic disease (10% a year for the first 5 years). Asymptomatic myeloma can be further divided into whether both criteria (plasma cells in marrow ≥10%, M-protein ≥30 g/L, or only one or other of these is present, when the prognosis is more favorable. Other criteria used include cytogenetics; for example, t(4;14), del(17p), gain (1q21) are high risk, whereas no cytogenetic abnormality detected low risk, and other abnormalities are standard risk except for trisomies which give an intermediate risk between high and standard. Percentage of plasma cells of aberrant phenotype in the marrow, free light chain ratio, degree of immunosuppression, and rising serum paraprotein level are also of prognostic significance.

OTHER PLASMA CELL TUMORS

Solitary and soft tissue plasmacytomas each make up half of the 6% of plasma cell tumors that are not multiple myeloma.

SOLITARY PLASMACYTOMA OF BONE

In solitary plasmacytoma of bone (Figs. 21.39–21.41), no plasma cell proliferation occurs in parts of the skeleton beyond the primary lesion; marrow aspirates and trephine biopsy distant from the primary tumor are normal. Associated M-proteins disappear following radiotherapy to the primary lesion.

EXTRAOSSEOUS (EXTRAMEDULLARY) PLASMACYTOMA

Soft tissue plasmacytomas are found most frequently in the submucosa of the upper respiratory and gastrointestinal tracts, in the cervical lymph nodes, and in the skin. They tend to remain localized and most are well controlled by excision or local irradiation.

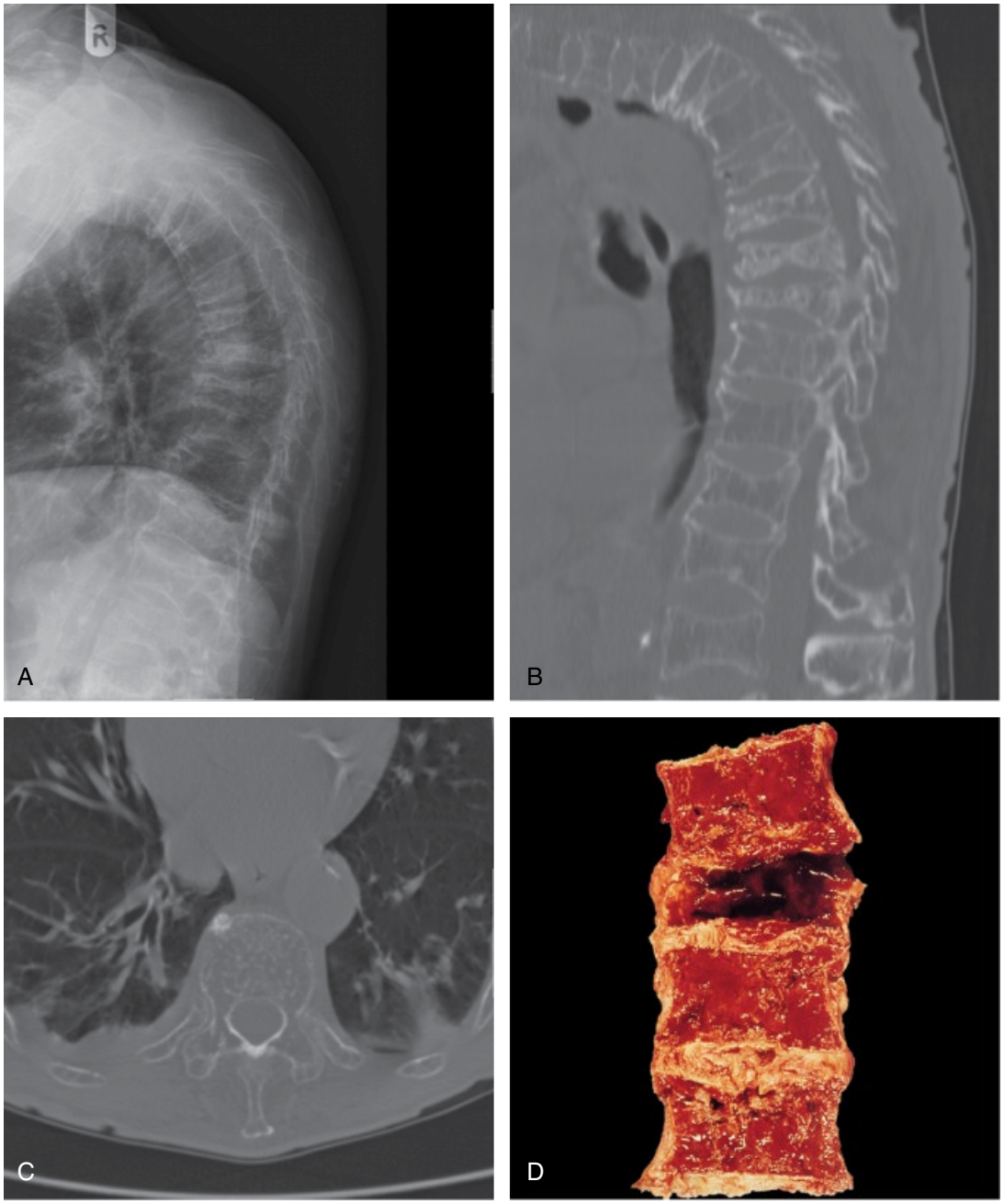

Fig. 21.21. Multiple myeloma. **A,** X-ray: Thoracic vertebrae showing collapse, diffuse demineralization, and mottled appearance. **B,** CT scan: Wedge-shaped collapsed vertebrae in upper and mid-thoracic regions leading to hyperkyphosis. **C,** CT scan: Cross-section of a thoracic vertebra showing demineralization of vertebra and ribs. **D,** Longitudinal section of lumbar spine shows a generalized replacement of normal medullary bone by vascular myeloma tissue.

HYPERVISCOSITY SYNDROME

The hyperviscosity syndrome is characterized by loss of vision, symptoms involving the central nervous system, hemorrhagic diathesis, and heart failure; the most severely affected patients may be in coma. The retina can show a variety of changes including engorged veins, hemorrhages, exudates, and a blurred optic disc (Fig. 21.42; see also Fig. 19.20).

The hyperviscosity syndrome occurs with M-proteins such as in multiple myeloma when there is polymerization of the abnormal immunoglobulin; a similar syndrome is occasionally caused by increased levels of blood components other than M-proteins (Table 21.5). IgM M-protein increases blood viscosity more than equivalent concentrations of IgG or IgA.

OTHER CAUSES OF SERUM M-PROTEINS

The appearance of an M-protein spike during serum electrophoresis is usually associated with more than 5 g/L of that protein. Uncontrolled proliferation of an M-protein producing clone, as in multiple myeloma or Waldenström disease,

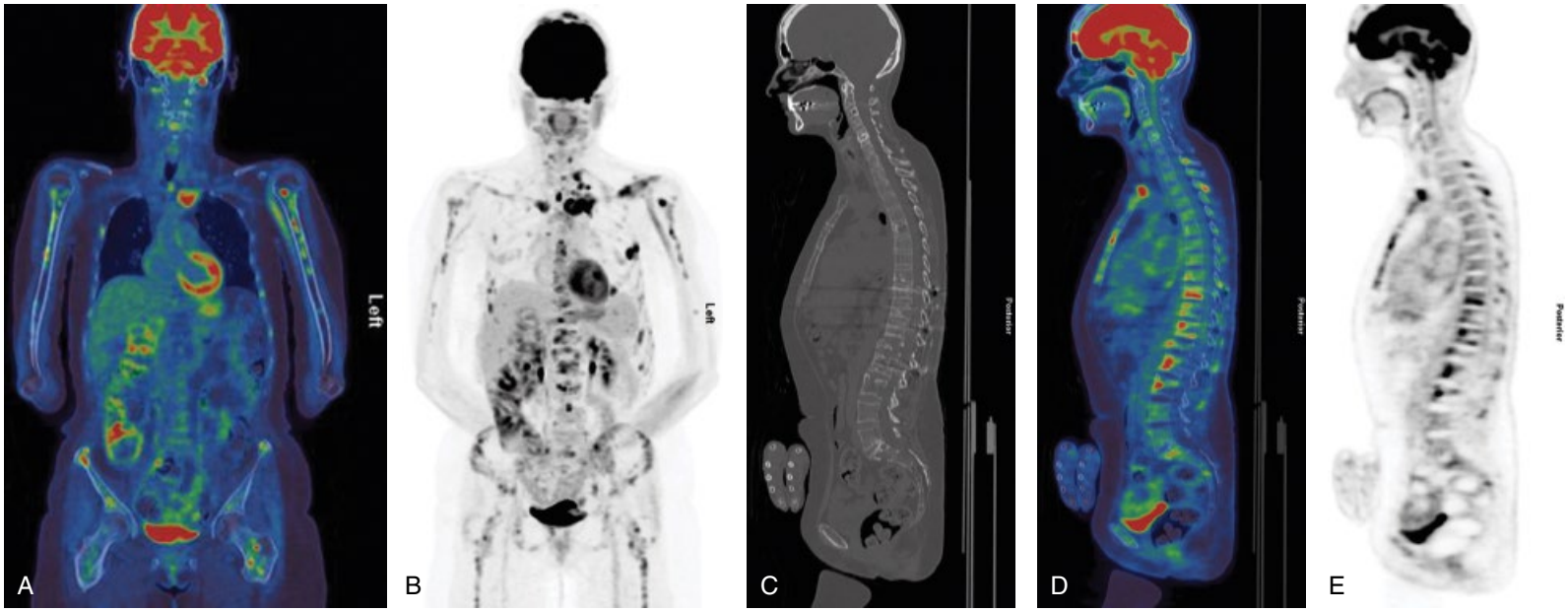

Fig. 21.22. Relapsed multiple myeloma in a 57-year-old patient. **A**, Coronal fused FDG PET-CT shows intense uptake in the humeri, pelvis and proximal left femur. **B**, Maximum intensity projection (MIP) shows multiple foci of disseminated uptake throughout the axial and appendicular skeleton. **C**, Sagittal CT shows multiple lytic lesions in the spine. **D**, Sagittal fused and **E**, sagittal PET show multiple foci of intense uptake in lytic lesions in the spine and sternum. (Courtesy of Dr. T Wagner, Department of Nuclear Medicine, Royal Free Hospital.)

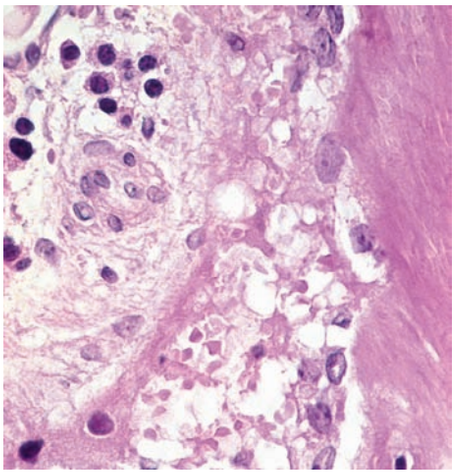

Fig. 21.23. Multiple myeloma: Bone biopsy. Although plasma cells are seen in the upper left, osteoclasts (the multinucleate cells at the bone intertrabecular tissue interface) are the cells responsible for the bone absorption around the osteolytic lesion.

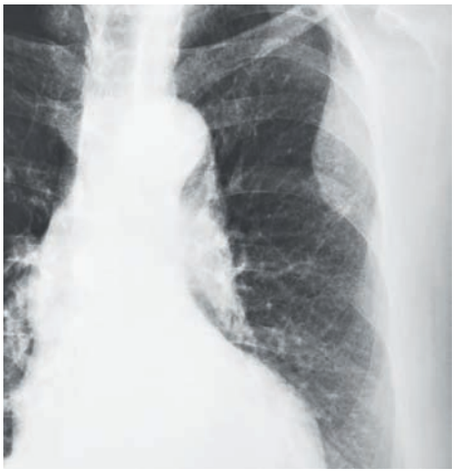

Fig. 21.24. Multiple myeloma: Chest radiograph showing a prominent extrapleural soft tissue mass adjacent to the third left rib.

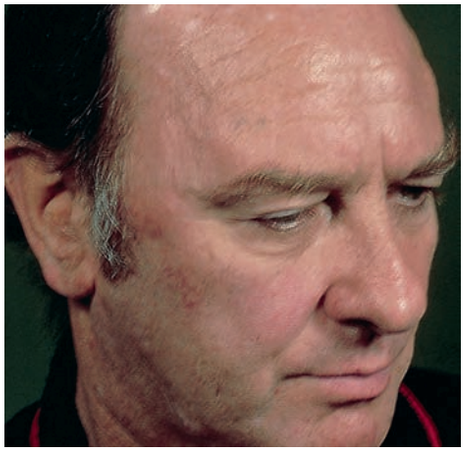

Fig. 21.25. Multiple myeloma: Skull deposits have invaded the soft tissues and appear as lumps on the forehead. In this case, a proportion of marrow cells were positive for the surface antigen CD10 but negative for TdT. Such cells have been associated with aggressive disease.

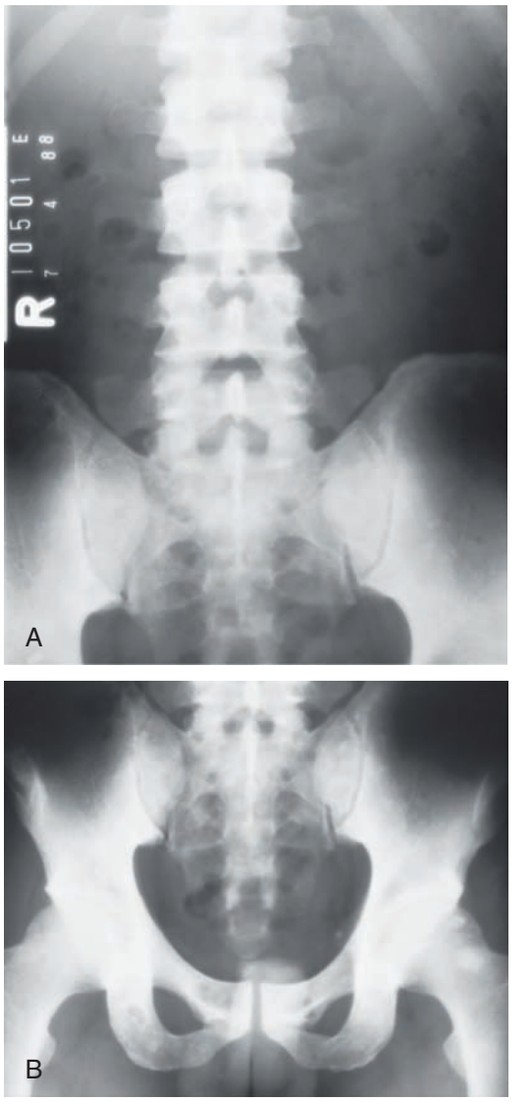

Fig. 21.26. Multiple myeloma: POEMS syndrome. **A,** Radiographs of lumbar spine, and **B,** pelvis showing sclerosis and lytic areas with sclerotic rims. (*A, B,* Courtesy of Dr. R Liang.)

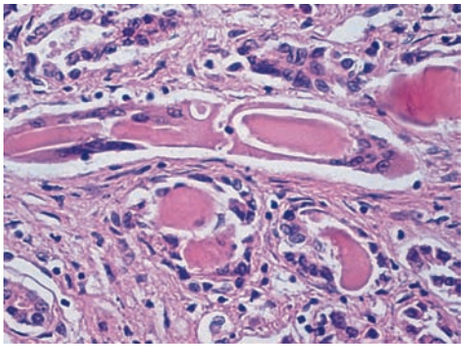

Fig. 21.27. Multiple myeloma: Section of kidney showing acidophilic casts of myeloma protein blocking the renal tubules. There is surrounding giant cell reaction and interstitial fibrosis.

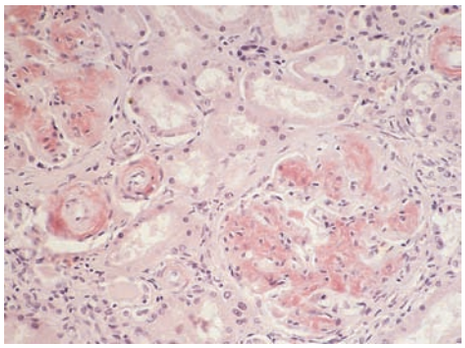

Fig. 21.28. Multiple myeloma: Renal amyloid disease. Amyloid deposition in the glomeruli and associated arterioles is extensive. Congo red stain.

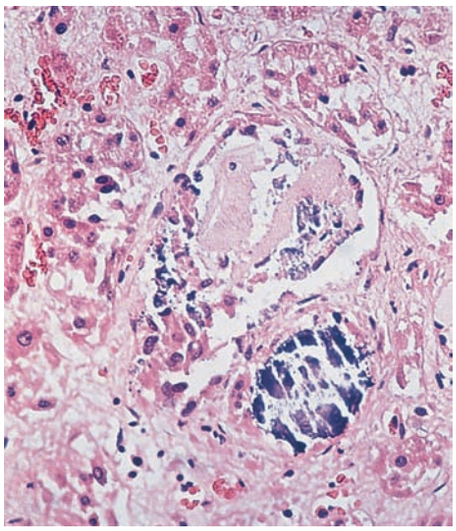

Fig. 21.29. Multiple myeloma: Nephrocalcinosis. Irregular fractured hematoxylinophilic deposits of calcium are seen in the fibrotic renal tissue.

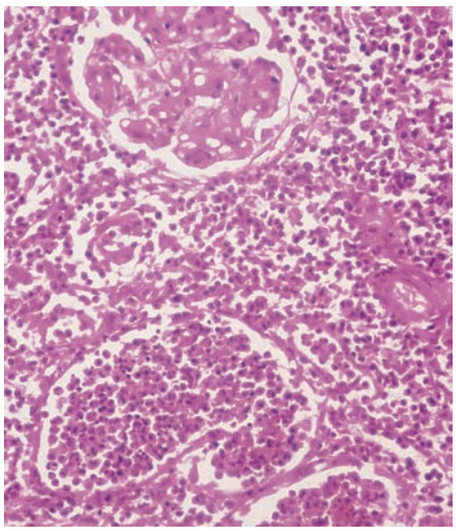

Fig. 21.30. Multiple myeloma: Destruction of the renal parenchyma and acute inflammatory cellular infiltration of the interstitial tissues and tubular spaces in pyelonephritis.

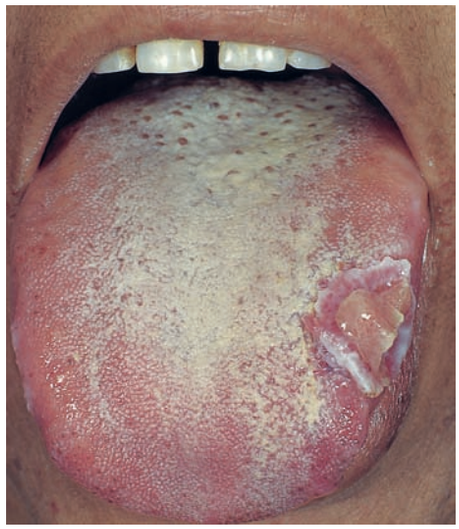

Fig. 21.31. Multiple myeloma. In amyloid disease, the tongue shows macroglossia and a deep ulcer on the upper and lateral anterior surfaces. The floor of the ulcer has the waxy appearance typical of amyloid deposition.

is distinguished by a progressive increase in the serum M-protein concentration. Production of M-protein is controlled or stable in benign monoclonal gammopathy (MGUS) and chronic cold agglutinin disease (see section on cold autoimmune hemolytic anemia, Chapter 8). Occasionally, production of M-protein is transient; for example, following recovery from infection or during a reaction to a drug.

MONOCLONAL GAMMOPATHY OF UNCERTAIN SIGNIFICANCE

Monoclonal gammopathy of uncertain significance (MGUS) is the most common cause of a serum M-protein. Its benign nature is shown by the level of M-protein in the serum remaining stable over many years. It is not associated with Bence Jones proteinuria, bone lesions, or soft tissue plasma cell tumors or immunoparesis. The bone marrow can have up to 10% of plasma cells, but patients are generally asymptomatic, with no evidence of bone marrow failure (Table 21.6). Cytogenetic changes similar to those in overt myeloma occur in most patients. When affected patients are followed, about 1% transform each year. IgG or IgA MGUS can develop into myeloma or malignant lymphoma, IgM MGUS into Waldenström macroglobulinemia. Transformation is more likely in those with IgA (IgA isotype relevant) or IgM rather than IgG paraproteins, those with >5% plasma or phenotypically aberrant plasma cells in the marrow, unbalanced serum light chains, and in those with few (<3%) polyclonal plasma cells (CD38+, CD56-, CD19+) compared with malignant plasma cells (CD38+, CD56+, CD19-) in the marrow. A rising M-protein in the early years after diagnosis is also associated with subsequent transformation.

Although benign paraproteinemia is usually symptomless, associated clinical features include peripheral neuropathy, acquired von Willebrand syndrome, papular mucinosis, cold hemagglutinin disease (see Chapter 8), amyloid, and cryoglobulinemia. These syndromes also occur when the disease that causes the paraprotein is primary amyloidosis or clearly malignant; for example, in lymphoma, myeloma, or macroglobulinemia

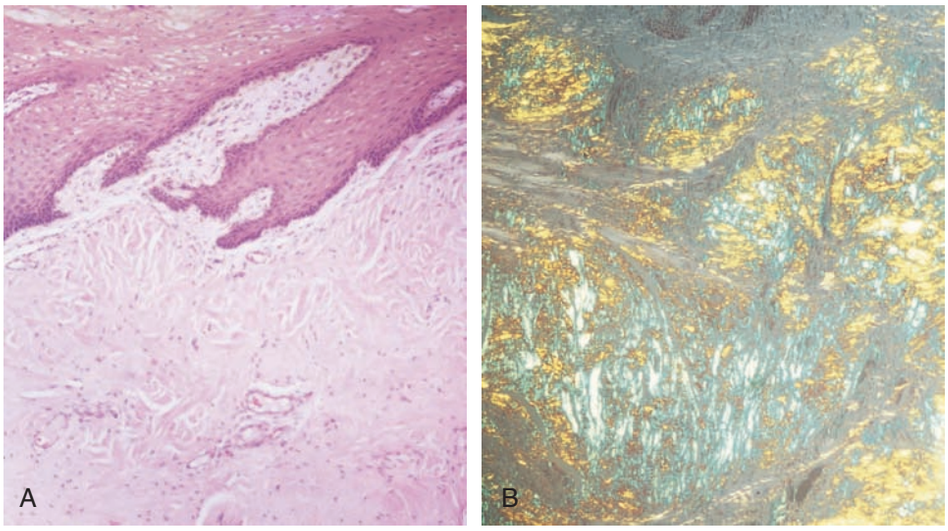

Fig. 21.32. Multiple myeloma. **A,** Biopsy of the ulcer seen in Fig. 21.31 shows extensive deposition of pale staining acidophilic material. **B,** Stained with Congo red, this material shows the characteristic green birefringence of amyloid when viewed with polarized light.

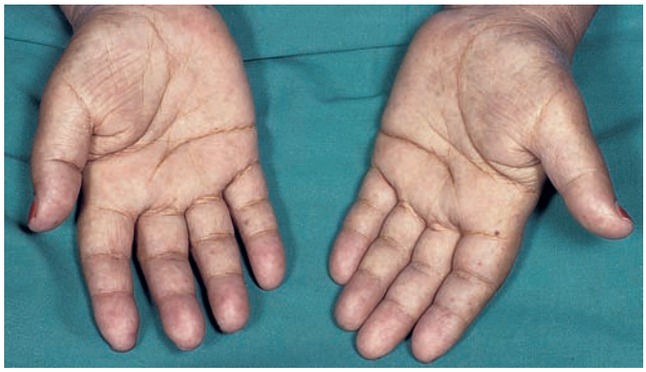

Fig. 21.33. Multiple myeloma: Carpal tunnel syndrome caused by deposition of amyloid in the flexor retinaculum and resulting in compression of the median nerve. The thenar muscles are wasting. The patient complained of paresthesias and weakness of both hands.

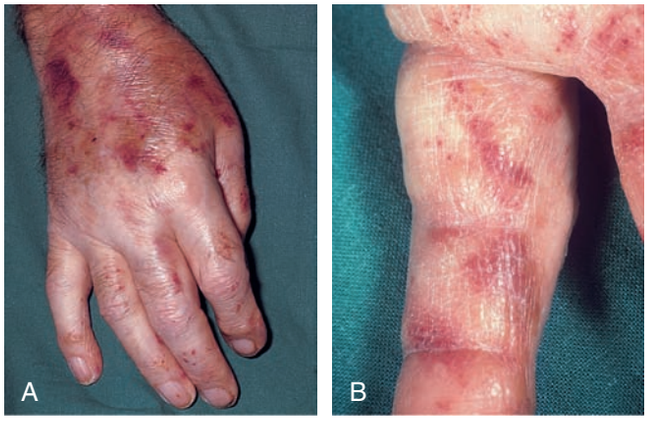

Fig. 21.35. Multiple myeloma. **A,** Amyloid disease on the back of the hand. Extensive diffuse and nodular deposits in the skin, subcutaneous tissues, and tendon sheaths have resulted in irregular swelling over the metacarpal heads; the skin surface appears hard, tense, and waxy. **B,** Extensive purpura, a characteristic feature, probably results from involvement of small cutaneous blood vessels.

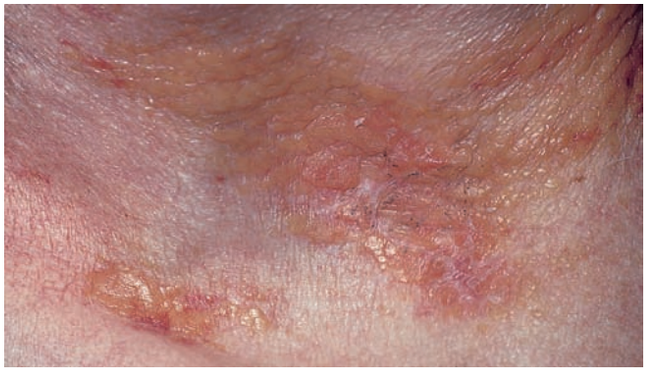

Fig. 21.34. Multiple myeloma: Amyloid disease of the skin. There are plaque-like hyaline infiltrations of the skin folds in the supraclavicular area.

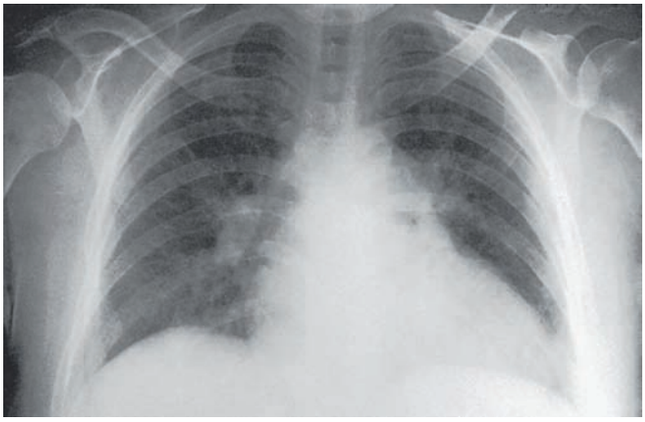

Fig. 21.36. Multiple myeloma: Amyloid disease of the heart. This radiograph shows cardiomegaly and pulmonary congestion. Evidence of myeloma includes osteolytic lesions in the right humerus and ribs, as well as pathologic fractures of the left clavicle and the eighth right rib.

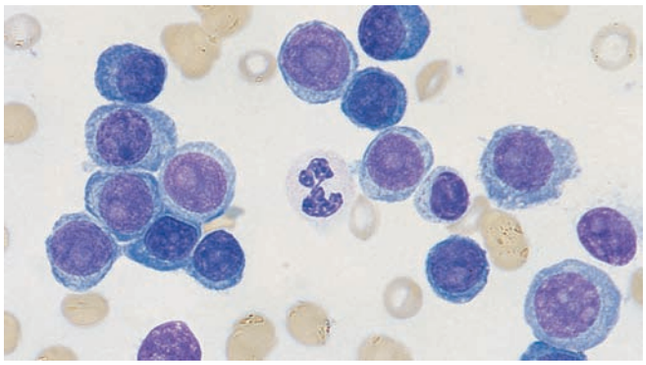

Fig. 21.37. Plasma cell leukemia: Peripheral blood fi lm showing large numbers of plasma cells and/or plasmablasts. (WBC, 100 × 10⁹/L.) (Courtesy of Dr. DM Swirsky.)

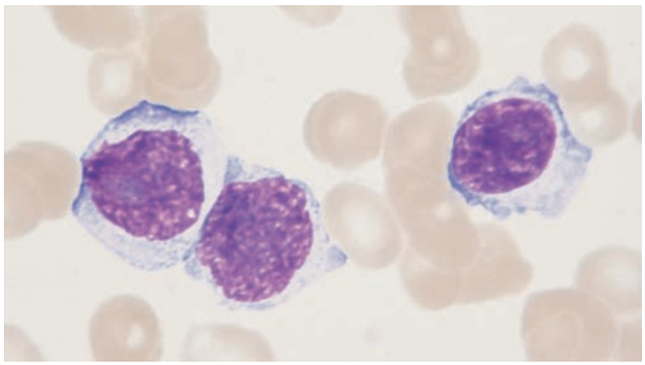

Fig. 21.38. Plasma cell leukemia: Peripheral blood film showing lymphocytoid plasma cells. The patient, a 44-year-old man, had been treated 1 year earlier for myeloma with six courses of intensive therapy (vincristine, doxorubicin [adriamycin], and methylprednisolone [VAMP]). He relapsed with widespread lytic lesions and many circulating plasma cells. (Hb, 6.3 g/dL;WBC, 22.1 × 10⁹/L; plasma cells, 18 × 3 10⁹/L; platelets, 64 × 10⁹/L.)

TABLE 21.3. INTERNATIONAL STAGING SYSTEM (ISS)

Stage I	Stage II	Stage III
β_2-microglobulin <3.5 mg/L *and* albumin ≥35 g/L	Not fitting criteria for stage I or III	β_2-microglobulin ≥5.5 mg/L

TABLE 21.4. REVISED INTERNATIONAL STAGING SYSTEM (R-ISS)

	Stage I	Stage II	Stage III
	ISS I and standard risk cytogenetics[a] by FISH *and* normal LDH	Not fitting criteria for stage I or III	ISS III and either high risk cytogenetics[b] by FISH or high LDH
Median PFS (months)	66	42	29
Median OS (months)	Not reached	83	43

FISH, fluorescence in situ hybridization; LDH, lactate dehydrogenase; OS, overall survival; PFS, progression-free survival.

[a] Standard risk cytogenetics by FISH = no high risk abnormality.

[b] High risk cytogenetics by FISH = del(17p) and/or t(4;14) and/or t(14;16).

Note: Host factors such as age and performance status also determine prognosis.

Source:Hoffbrand AV, et al. eds. *Postgraduate Haematology*, 7th edn. John Wiley & Sons, Ltd. 2016. Reproduced with permission of John Wiley and Sons.

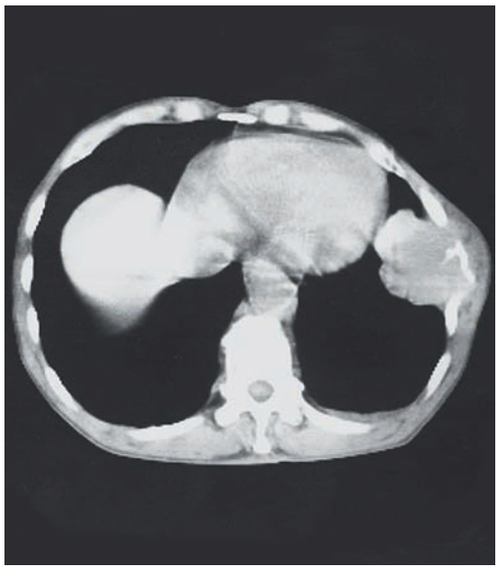

Fig. 21.39. Solitary plasmacytoma of bone: Computed tomography scan showing erosion of the rib, with soft tissue extension into both the pleural space and external soft tissues.

(Table 21.7). Schnitzler syndrome consists of monoclonal gammopathy and chronic urticaria combined with at least two of: fever, arthralgia (or arthritis), bone pain, hepato- and/or splenomegaly, lymphadenopathy, leukocyosis, and raised ESR.

CRYOGLOBULINEMIA

Globulins that precipitate in the cold can occur in a primary disease (monoclonal or oligoclonal). Ulcers and vascular abnormalities of the skin can be the main clinical problem (Figs. 21.43–21.45). Cryoglobulinemia also occurs in association with abnormal globulin production in myeloma, macroglobulinemia, or non-Hodgkin lymphoma.

AMYLOIDOSIS

Amyloidosis is caused by extravascular deposition of insoluble abnormal fibrils derived from aggregation of misfolded, normally soluble protein (Fig. 21.46). The fibrillary structure is visible on electron microscopy, and following Congo red staining amyloid

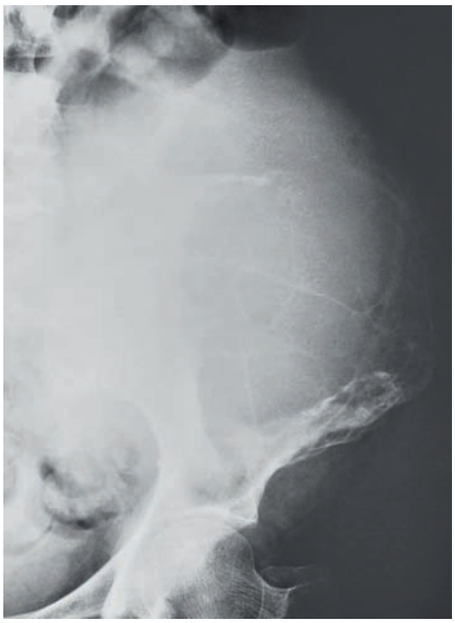

Fig. 21.40. Solitary plasmacytoma of bone: Radiograph of left pelvic area shows massive destruction of the iliac bone and the tumor extending into the pelvis and abdomen. Linear residual streaks of bone produce the "soap bubble" appearance seen in this type of tumor.

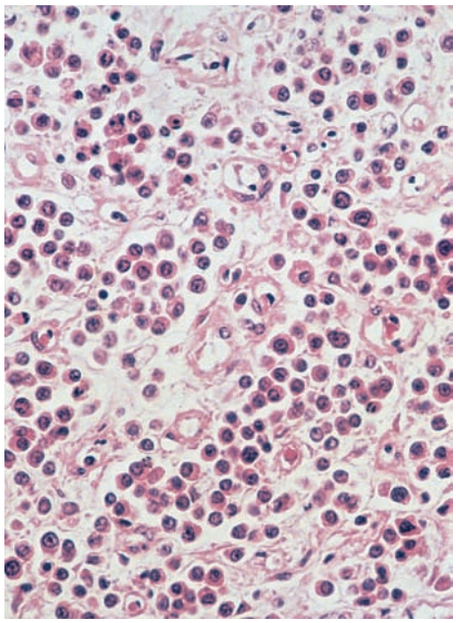

Fig. 21.41. Solitary plasmacytoma of bone: Biopsy shows dense collections of plasma cells supported by a vascular stroma.

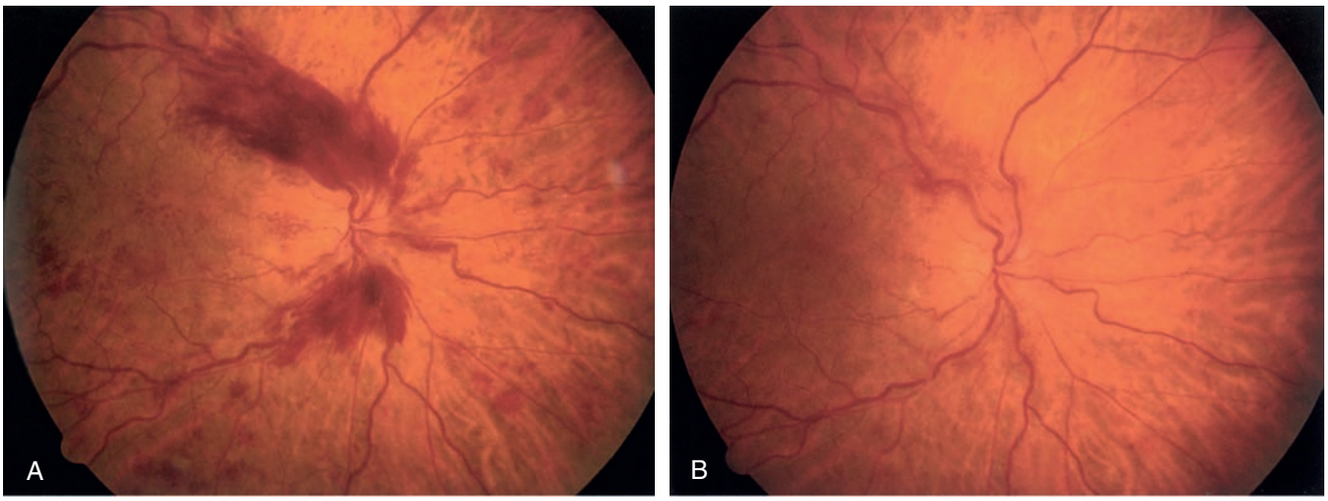

Fig. 21.42. Multiple myeloma. **A,** Distention of retinal veins and widespread hemorrhage in the hyperviscosity syndrome. **B,** Two months after plasmapheresis and chemotherapy the vessels are normal and almost all hemorrhage has cleared. The patient had some loss of vision and headache. (*A, B,* Courtesy of Professor JC Parr.)

TABLE 21.5. CAUSES OF THE HYPERVISCOSITY SYNDROME: M-PROTEINS ARE THE DOMINANT CAUSE, BUT OTHERS OF IMPORTANCE ARE POLYCYTHEMIA, LEUKOSTASIS, AND HYPERFIBRINOGENEMIA

Causes	Diseases
M-proteins	Waldenström macroglobulinemia Multiple myeloma
Polycythemia	Polycythemia vera Severe secondary polycythemia
Leukostasis	Chronic myeloid leukemia Other leukemias with very high white cell counts
Hyperfibrinogenemia	Following factor VIII replacement therapy with large amounts of cryoprecipitate

TABLE 21.6. DIAGNOSTIC CRITERIA FOR NON-IGM MONOCLONAL GAMMOPATHY OF UNDETERMINED SIGNIFICANCE (MGUS) AND LIGHT-CHAIN MGUS

Non-IgM MGUS
Serum M protein (non-IgM) concentration <30 g/L
Clonal bone marrow plasma cells <10%
Absence of end-organ damage; e.g. CRAB (Table 21.1B) and amyloidosis attributable to the plasma cell proliferative disorder
Light-chain MGUS
Abnormal free light chain ratio (<0.26 or >1.65)
Increased level of the involved free light chain
No immunoglobulin heavy chain expression on immunofixation electrophoresis
Urinary M protein <500 mg/24 hours
Clonal plasma cells <10%
Absence of end-organ damage (CRAB) and amyloidosis

CRAB, hypercalcemia, renal insufficiency, anemia, and bone lesions.
Source: Adapted fromSwerdlow SH, et al., eds. *WHO Classification of Tumours of Haematopoietic and Lymphoid Tissues*, revised 4th edn. International Agency for Research on Cancer, 2017/Rajkumar SV, et al. *Lancet Oncol* 2014;15e:538–565. Reproduced with permission of Elsevier.

TABLE 21.7. M-PROTEINS: UNCONTROLLED PRODUCTION OF M-PROTEIN OCCURS WITH PLASMA CELL DYSCRASIAS, LYMPHOPROLIFERATIVE DISORDERS, AND PRIMARY AMYLOID

Malignant or uncontrolled production
Multiple myeloma
Plasma cell leukemia
Lymphoplasmacytic lymphoma/Waldenström macroglobulinemia
Other non-Hodgkin lymphomas
Chronic lymphocytic leukemia
Primary amyloidosis
Heavy chain disease (λ, α, and μ)
Benign or stable production
Monoclonal gammopathy of uncertain significance
Chronic cold hemagglutinin disease
Transient M-proteins
Solitary plasmacytoma
Extramedullary plasmacytoma
Gaucher disease
Acquired immunodeficiency syndrome (AIDS)
Occasional association with carcinoma, connective tissue and skin disorders, and many other conditions

The most common cause is benign monoclonal gammopathy with no apparent disease association. Benign controlled M-protein production has a number of causes, including human immunodeficiency virus and other infections, carcinoma, and other tumors; "benign" refers to the limited clone of M-protein producing cells.

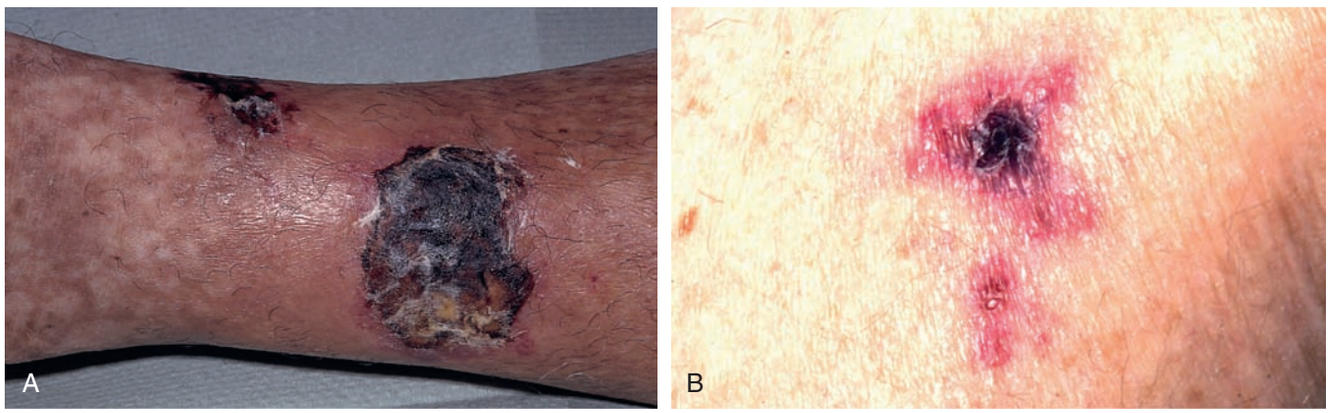

Fig. 21.43 Cryoglobulinemia. **A,** Discoloration of the leg with pigment deposition in a reticulated pattern because of vascular distention and hemorrhage. Areas of superficial necrosis and ulceration are seen. The patient showed a serum IgM paraprotein but no other evidence of myeloma or lymphoma. **B,** Ulceration and vascular distention in a 78-year-old man with chronic lymphocytic leukemia.

shows an amorphous pink material that gives a distinct apple-green birefringence under polarized microscopy (Figs. 21.32, 21.52, 21.53, 21.55, and 21.56). Many different proteins form amyloid fibrils, causing different and distinct clinical entities (Table 21.8). Some of these are hereditary and others acquired.

Amyloid fibrils associate with other nonfibrillar components, including serum amyloid P protein (SAP) and glycosaminoglycans, forming stable deposits that disrupt the structure and function of involved organs and tissues. In systemic amyloidosis, there are widespread deposits in viscera, blood vessel walls, and connective tissue. In local amyloidosis, the amyloid is restricted to an organ or tissue. In acquired amyloidosis, preexisting conditions produce an amyloidogenic protein or are associated with production of large amounts of potentially amyloidogenic normal protein. In hereditary amyloidosis, mutant genes encode variant amyloidogenic proteins.

PRIMARY (AL) AMYLOIDOSIS

Systemic primary amyloid monoclonal immunoglobin light chain (AL) amyloidosis is caused by an otherwise benign low-grade monoclonal gammopathy. There are <10 plasma cells in the bone marrow (Fig. 21.47). AL amyloidosis can also complicate multiple myeloma or other clonal B-cell proliferative disorders. The fibrils are formed from the N-terminal variable domain of immunoglobulin light chains.

Fig. 21.44. Cryoglobulinemia (same patient as shown in Fig. 21.43A). Serum from a patient with primary disorder, prepared from whole blood at 37°C, showing protein precipitation on cooling to room temperature. In this case the protein was monoclonal IgM.

Primary AL amyloidosis syndrome is dominated by clinical features caused by amyloid deposition. As with amyloid complicating myeloma, this can occur in the tongue (Figs. 21.31 and 21.48), heart (Fig. 21.36), tendon sheaths (Figs. 21.33 and 21.49), blood vessels (Fig. 21.50), and skin (Figs. 21.34, 21.35, and 21.55). There can also be associated purpura, nephrotic syndrome, peripheral neuropathy, orthostatic hypotension, and massive hepatomegaly. The disease can be assessed by serum amyloid P component scintigraphy (SAP scan) (Fig. 21.51). The serum paraprotein is <30 g/L and is present in 50–60% of patients.

Staging of AL amyloid by the Mayo system depends on markers of cardiac involvement. In Stage 1 both the serum troponin and NT-pro BNP are normal (median survival 26.4 months), in Stage 2 either of these cardiac markers is raised (median survival 10.5 months), and in Stage 3 both cardiac markers are raised (median survival of only 3.5 months).

Patients with hereditary amyloidosis can also show a monoclonal paraprotein. Serum light chains are useful for diagnosis and essential for follow-up (Figs. 21.14 and 21.51). Amyloid can be detected in the bone marrow by Congo red staining and polarized light microscopy (Fig. 21.52). Fine-needle abdominal fat aspiration can give sufficient material for Congo red staining (Fig. 21.53) and for histochemical studies to determine the exact type of amyloid. The prognosis depends largely on the degree of cardiac involvement (Fig. 21.36).

LOCALIZED AL AMYLOIDOSIS

Deposits of AL amyloid occur anywhere in the body with the skin, airways, conjunctiva (Fig. 21.54), and urogenital tracts the most frequent sites. Histology shows typical features of amyloid and stains with an anti-AL amyloid antibody (Figs. 21.55 and 21.56).

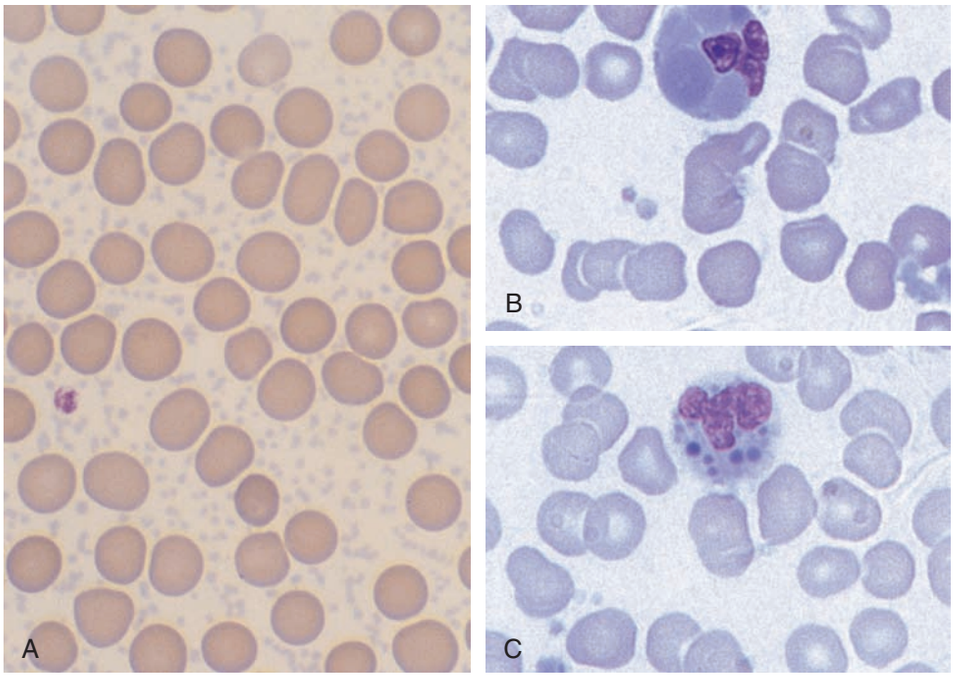

Fig. 21.45. Multiple myeloma. **A,** Cryoglobulin IgM protein: Peripheral blood film showing pink-staining aggregates of immunoglobulins between red cells. **B, C,** Neutrophils with multiple blue-staining inclusion bodies from ingested cryoglobulin. (*B, C,* Source: Bain BJ. *Blood Cells: A Practical Guide,* London, 1989, Gower. Reproduced with permission of Elsevier.)

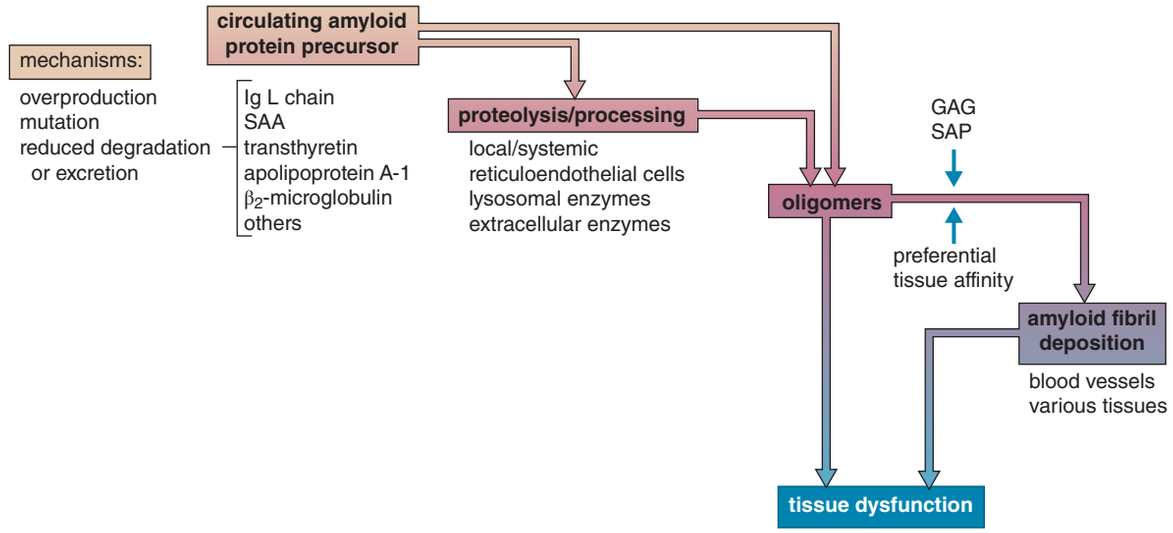

Fig. 21.46. Amyloidosis: The general mechanisms involved in amyloid formation. The amyloidogenic protein can be synthesized in excess and persist in serum in high concentration, as for the acute-phase protein serum amyloid A (SAA) or monoclonal light chains, or can reach high serum concentrations because of reduced clearance, such as β_2-microglobulin in chronic dialysis, or can be mutated as in hereditary amyloidosis. Certain proteins with intrinsic amyloidogenic properties, such as transthyretin, can cause amyloidosis late in life, as in senile systemic amyloidosis. Some of these proteins undergo a proteolytic remodeling that facilitates polymerization. The early protein aggregates can exert a direct cytotoxic effect. The concurrence of tissue components and common constituents, for example, glycoaminoglycans (GAGs) and serum amyloid P (SAP) component, favors deposition of amyloid fibrils. (Source: Merlini G, Stone MJ. *Blood* 2006;108:2520–2530. Reproduced with permission of *Blood: Journal of the American Hematology Society*.)

TABLE 21.8. CLASSIFICATION OF AMYLOIDOSIS[a]

Type	Fibril precursor protein	Clinical syndrome
AA	Serum amyloid A protein	Systemic amyloidosis associated with acquired or hereditary chronic inflammatory diseases. Formerly known as secondary or reactive amyloidosis
AL	Monoclonal immunoglobulin light chains	Systemic amyloidosis associated with myeloma, monoclonal gammopathy, occult B-cell dyscrasia. Formerly known as primary amyloidosis
ATTR	Normal plasma transthyretin	Senile systemic amyloidosis with predominant cardiac involvement
ATTR	Genetic variants of transthyretin (e.g., ATTR Met30, Ala60, Ile122)	Familial amyloid polyneuropathy (FAP), with systemic amyloidosis and often prominent amyloid cardiomyopathy
$A\beta_2M$	β_2-Microglobulin	Dialysis-related amyloidosis (DRA) associated with renal failure and long-term dialysis. Predominantly musculoskeletal symptoms
Aβ	β-Protein precursor (and rare genetic variants)	Cerebrovascular and intracerebral plaque amyloid in Alzheimer disease. Occasional familial cases
AApoAI	Genetic variants of apolipoprotein A-I (e.g., AApoAI Arg26, Arg60)	Autosomal dominant systemic amyloidosis. Predominantly non-neuropathic with prominent visceral involvement, especially nephropathy. Minor wild-type ApoAI amyloid deposits may occur in the aorta
AApoAII	Genetic variants of apolipoprotein A-II	Autosomal dominant systemic amyloidosis with predominant renal involvement
AFib	Genetic variants of fibrinogen α chain (e.g., AFib Val526)	Autosomal dominant systemic amyloidosis. Non-neuropathic usually with prominent nephropathy
ALys	Genetic variants of lysozyme (e.g., ALys His67)	Autosomal dominant systemic amyloidosis. Non-neuropathic with prominent renal and gastrointestinal involvement
ACys	Genetic variant of cystatin C (Gln68)	Hereditary cerebral haemorrhage with cerebral and systemic amyloidosis
AGel	Genetic variants of gelsolin (e.g., Asn187)	Autosomal dominant systemic amyloidosis. Predominant cranial nerve involvement with lattice corneal dystrophy
AIAPP	Islet amyloid polypeptide	Amyloid in islets of Langerhans in type 2 diabetes mellitus and insulinoma
ALECT2	Leukocyte chemotactic factor II	Systemic amyloidosis with predominant renal involvement

[a] Amyloid composed of peptide hormones, prion protein, and unknown proteins not included.
Source: Hoffbrand AV, et al. eds. *Postgraduate Haematology*, 7th edn. John Wiley & Sons, Ltd. 2016. Reproduced with permission of John Wiley and Sons.

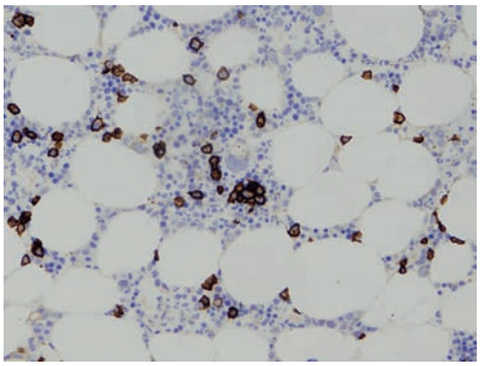

Fig. 21.47. Primary amyloid: Immunostaining for CD138 confirms less than 10% of plasma cells in the bone marrow.

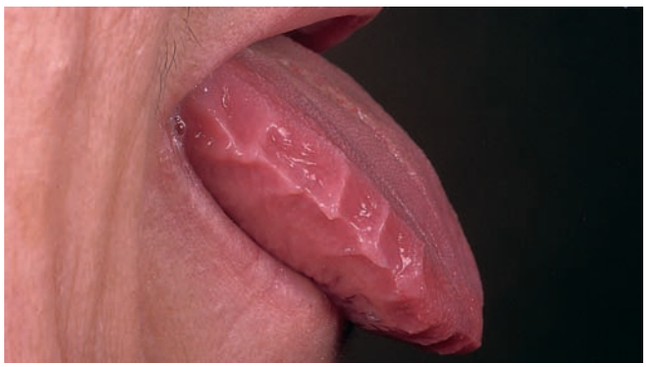

Fig. 21.48. Systemic primary AL amyloidosis: Tongue enlarged with a waxy, smooth appearance.

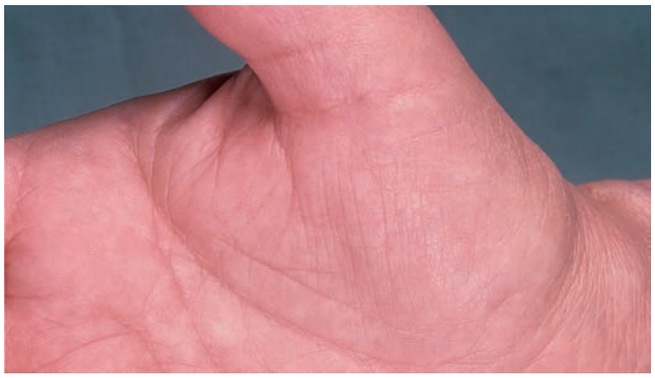

Fig. 21.49. Systemic AL amyloidosis: Flattening of the thenar eminence caused by carpal tunnel syndrome. Same patient as in Fig. 21.48.

There is an associated small collection of clonal B cells producing amyloidogenic light chains. Progression to systemic amyloidosis is rare.

REACTIVE SYSTEMIC (AA) AMYLOIDOSIS

Reactive systemic amyloid precursor amyloid A protein (AA) amyloidosis is a complication of chronic infectious or inflammatory disease; for example, rheumatoid arthritis, Still

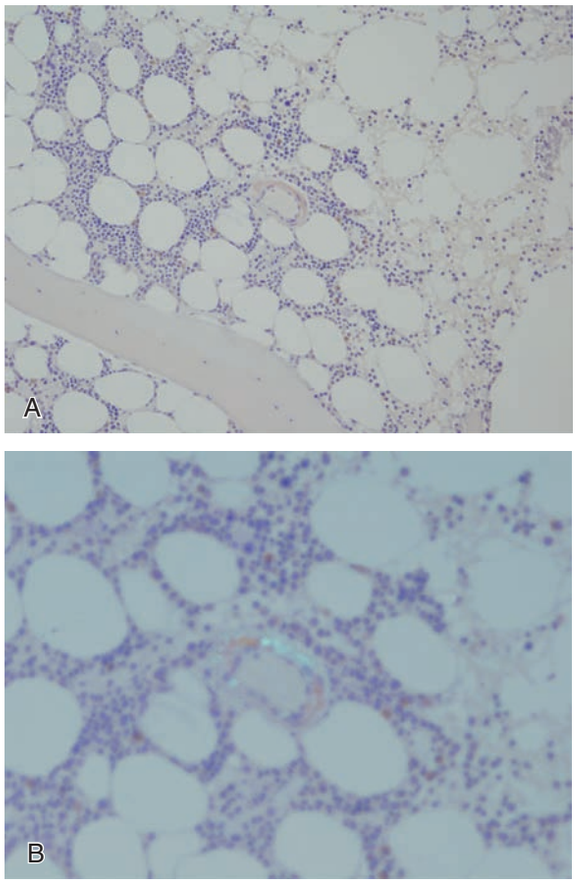

Fig. 21.50. Primary amyloid. **A**,**B,** Congo red staining and polarized light examination shows amyloid in the wall of a blood vessel.

disease, Crohn disease, familial Mediterranean fever, bronchiectasis, or Castleman disease in which there is a sustained acute-phase response with high levels of serum amyloid A protein. This protein is an apoprotein made in the liver and regulated by proinflammatory cytokines. The plasma concentration can rise 1000-fold during an acute-phase response. Patients can have nephropathy, especially proteinuria. Liver, gastrointestinal, and splenic involvement occur with advanced disease. Cardiac and neural involvement are rare. Bone marrow involvement can be shown by trephine biopsy (Fig. 21.52, *E–G*). When the disease is suspected, diagnosis can be confirmed by fine needle biopsy of abdominal fat (Fig. 21.53, *A* and *B*), renal biopsy (Fig. 21.53, *C–E*), or most commonly by rectal biopsy. Anti-SAA antibodies can be used for immunohistochemical diagnosis (Figs. 21.53 and Fig. 21.56). Apparently localized AA amyloid is always found on SAP scan to be systemic (Fig. 21.56).

LIGHT CHAIN DEPOSITION DISEASE

This rare syndrome is characterized by the deposition of monoclonal nonamyloid light chains in the kidneys and other organs. The deposits do not stain with Congo red (Fig. 21.57). About half of patients have underlying myeloma and about 20% have MGUS. There is a clone of plasma cells in the bone marrow that produces κ or λ light chains with an altered free light chain ratio in plasma. Clinically, patients present with renal failure, proteinuria, and nephrotic syndrome.

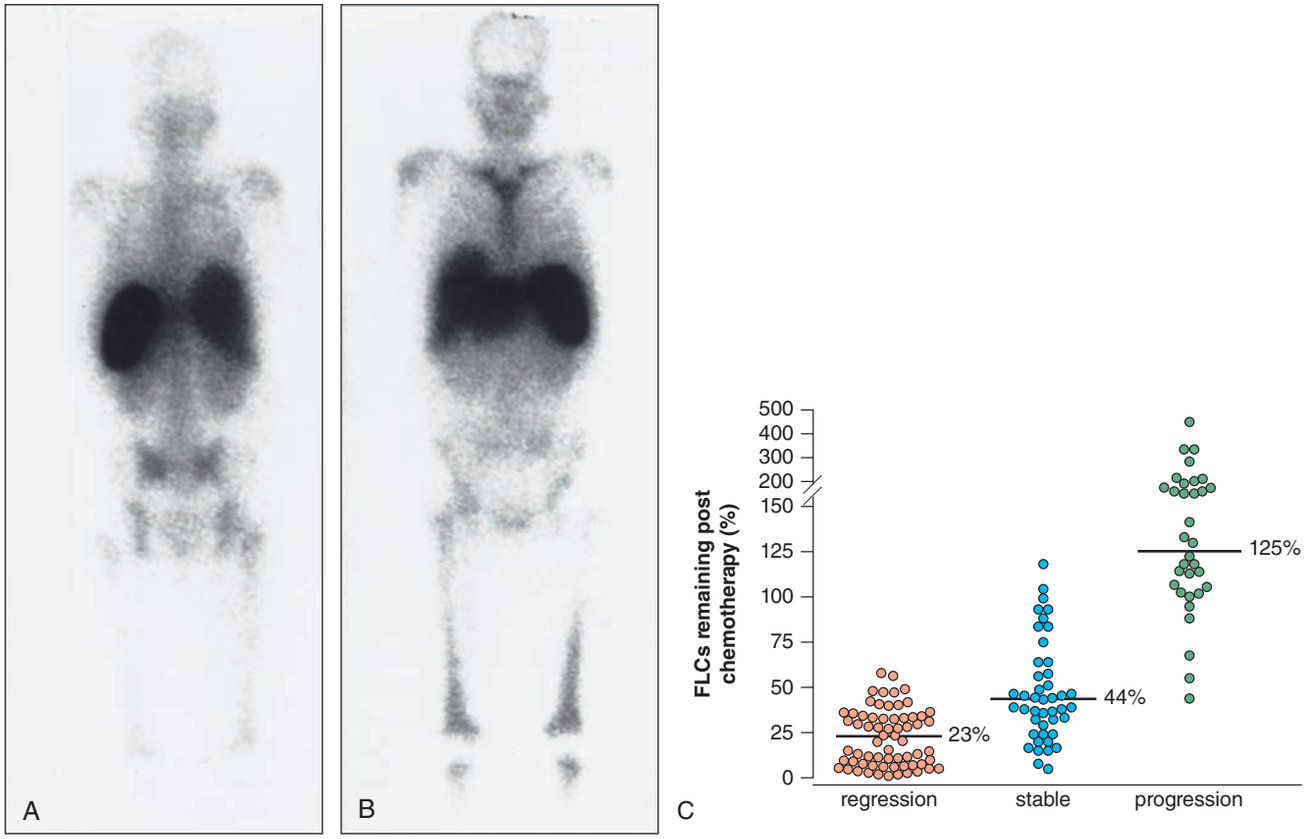

Fig. 21.51. Systemic AL amyloidosis: Serum amyloid P component scintigraphy. **A,** Posterior and **B,** anterior whole-body scans obtained 24 hours after injection of ^{123}I-labeled serum amyloid P (SAP) component in a 62-year-old woman with systemic AL amyloidosis. The tracer has localized to amyloid deposits in the liver, spleen, and kidneys and throughout the bone marrow. **C,** Free light chains (FLCs) in 127 patients with AL amyloidosis before and 12 months after commencing chemotherapy. The mean percentages of remaining serum FLCs in each group are indicated (Kruskal-Wallis test: $P < 0.0001$). (*A, B,* Courtesy of Professor PN Hawkins and Professor MB Pepys. *C,* Courtesy of Bradwell AG. *Serum Free Light Chain Analysis,* 4th edn. Birmingham, UK, 2005, Binding Site.)

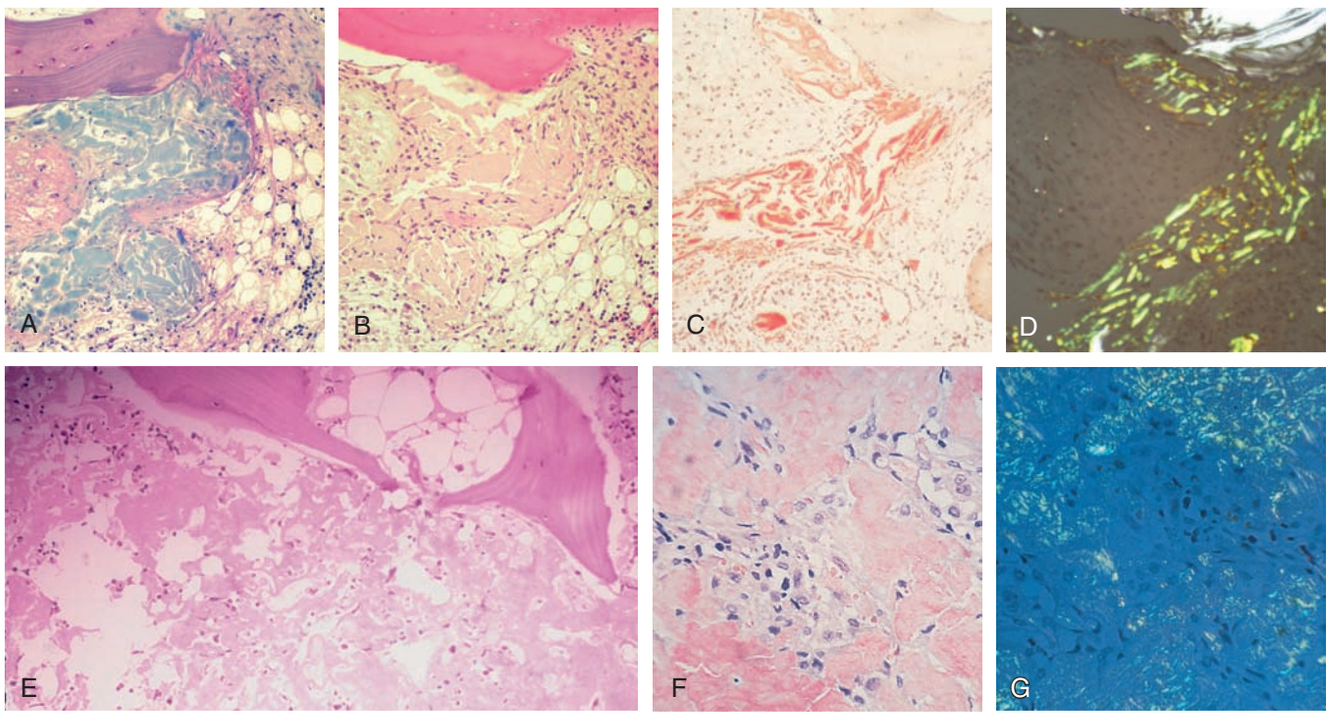

Fig. 21.52. Amyloidosis: Trephine biopsies. Systemic AL amyloid. **A,** Giemsa and **B,** H&E stains show replacement of hematopoietic tissue by loose collections of foamy histiocytes and an amorphous material that is salmon pink in the Congo red stain **(C)** with characteristic yellow green birefringence with polarized light **(D)**. Systemic reactive AA amyloid in a patient with bronchiectasis shows extensive replacement of hematopoietic tissue by pale acidophilic material in H&E **(E)** and salmon pink staining with Congo red **(F)** with characteristic yellow green birefringence with polarized light **(G)**.

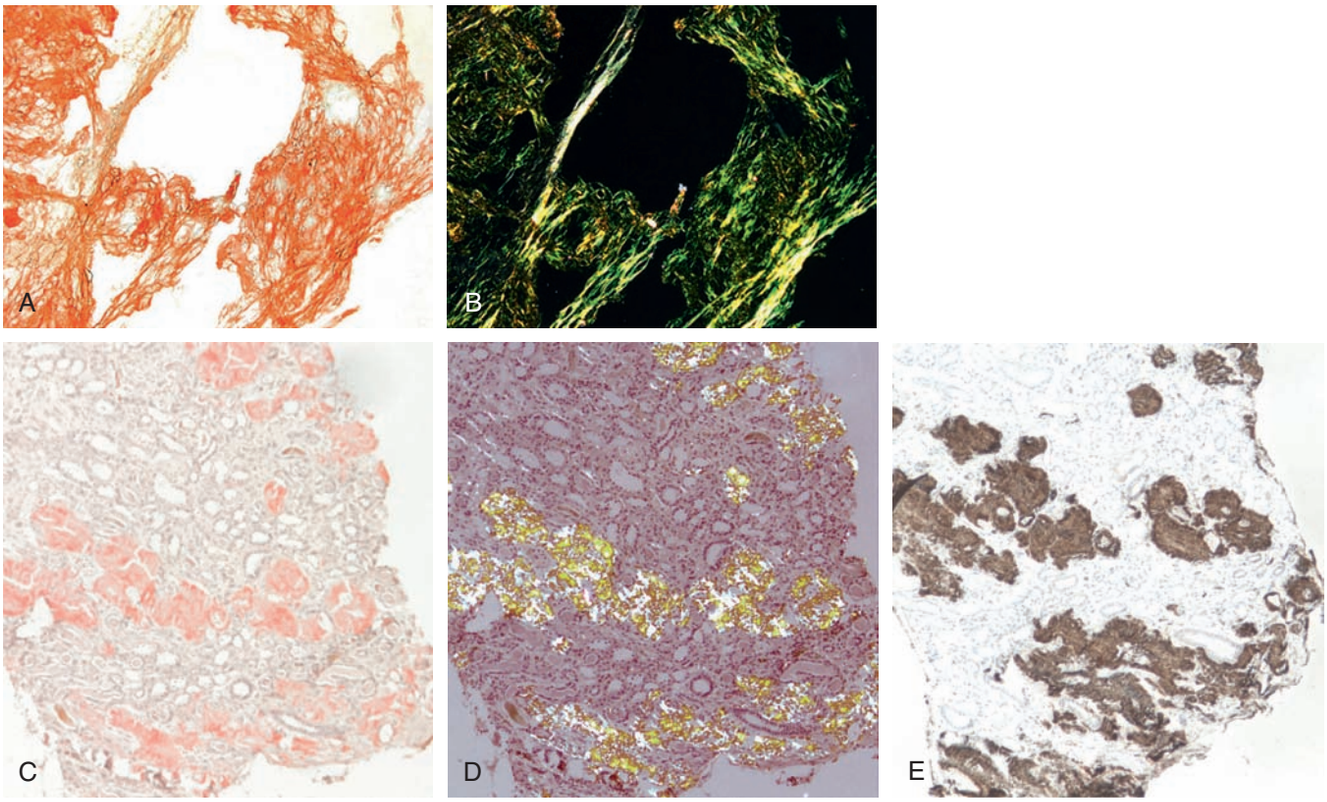

Fig. 21.53. Systemic AA amyloid. Fine needle aspirate of abdominal fat stained with Congo red. **A,** Strong positivity with light microscopy. **B,** Birefringence under polarized light. Renal biopsy in a patient with a 15-year history of adult-onset Still disease. **C,** Congo red staining shows pink amyloid deposits. **D,** Under polarized light the deposits show a characteristic apple-green birefringence. **E,** Immunohistologic staining using a monoclonal antiserum amyloid A protein antibody shows intense positivity confirming that the amyloid deposits are of AA type. (*A*, *B*, Courtesy of Professor G Merlini; *C–E,* Courtesy of Professor P Hawkins.)

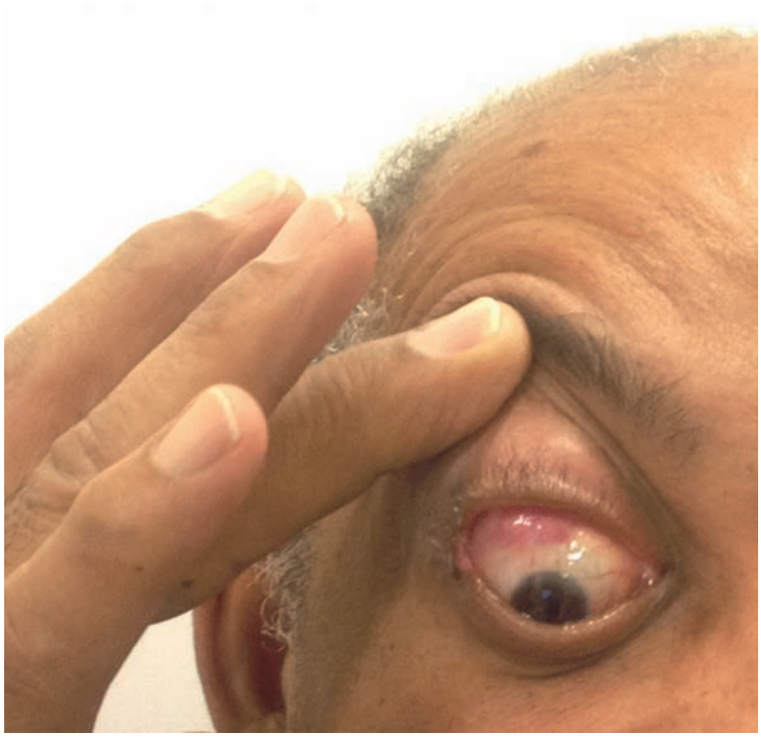

Fig. 21.54 Localized AL amyloid: Conjunctival amyloid. (Courtesy of Professor PN Hawkins.)

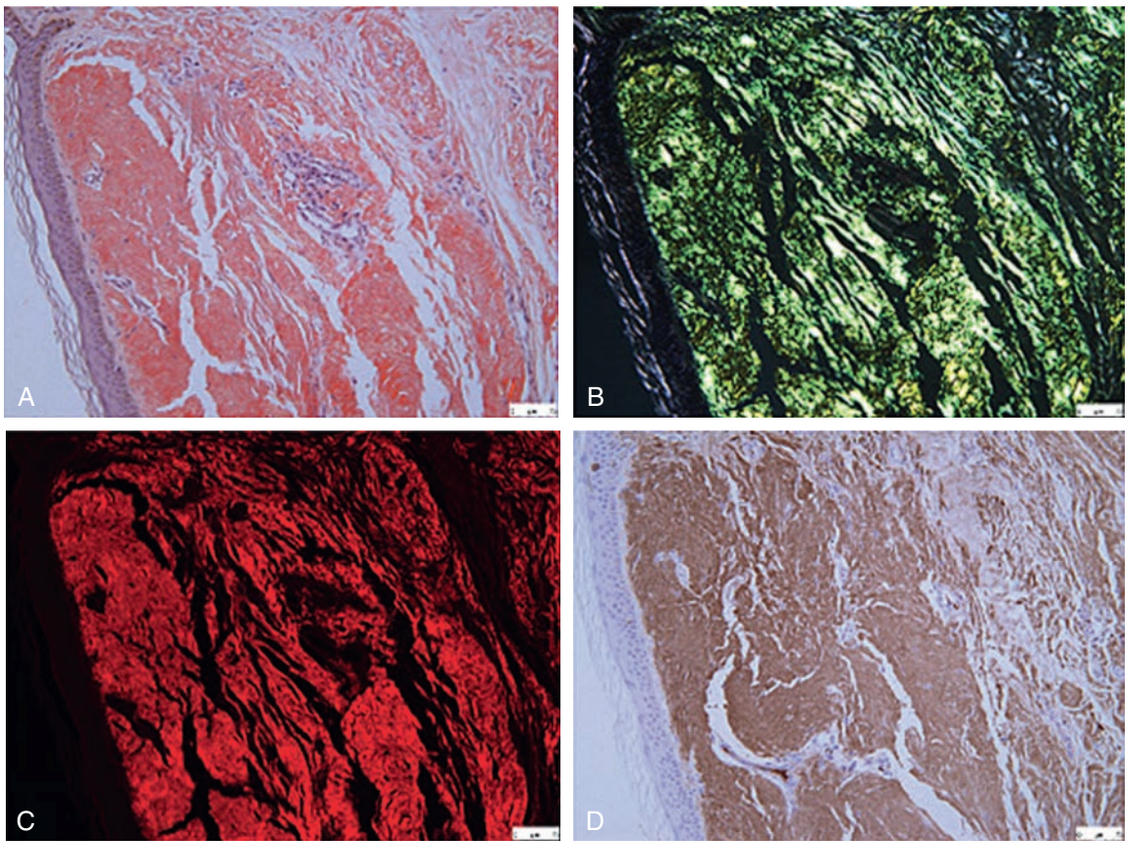

Fig. 21.55. Localized AL amyloid: Skin biopsy. (Courtesy of JA Gilbertson and Professor PN Hawkins, National Amyloidosis Centre, Royal Free Hospital, London.)

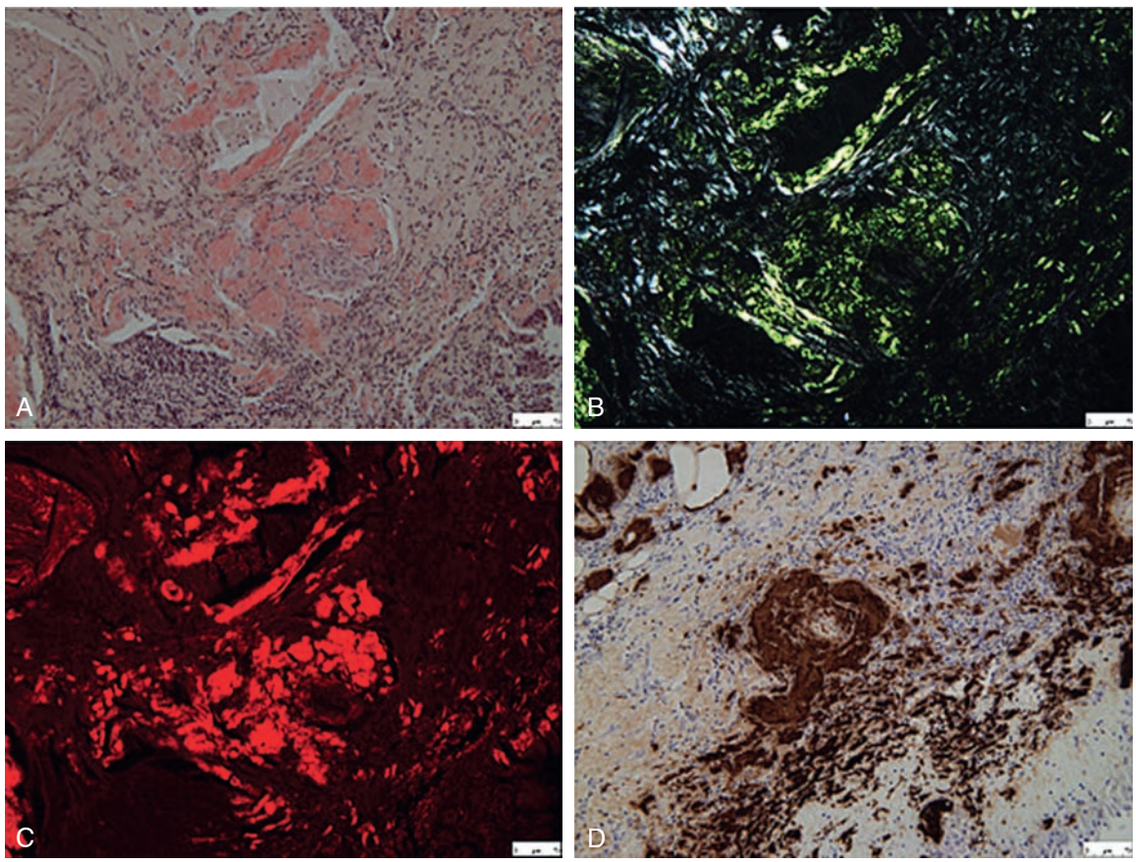

Fig. 21.56. Immunohistochemistry of a bladder deposit. **A,** Congo red staining. **B,** Congo red staining viewed by cross polar lighting. **C,** Congo red staining viewed by fluorescent light. **D,** Anti-SAA staining. (Courtesy of J Gilbertson and Professor PN Hawkins, National Amyloidosis Centre, Royal Free Hospital, London.)

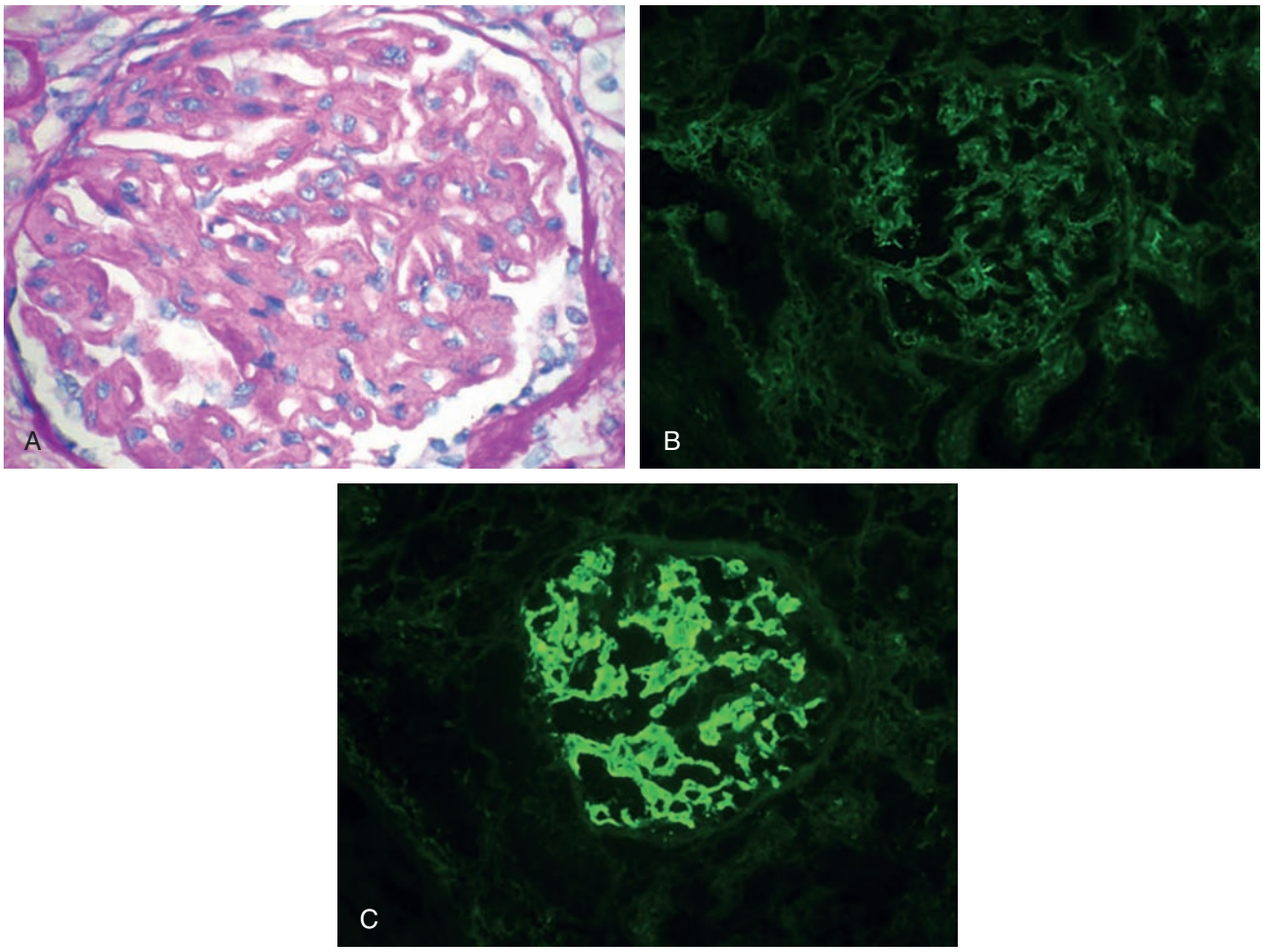

Fig. 21.57. Light chain deposition disease. **A,** The glomerulus exhibits mesangial and capillary wall deposition, which was completely negative for Congo red stain (periodic acid–Schiff PAS; magnification, x600). There is monotypic λchain deposition by immunofluorescence, in absence of other immunoglobulins of complement components **(B)** κ chain and **(C)** λ chain (magnification x200). (Courtesy of Dr. A Garcia-Herrera, Hospital Clinic of Barcelona, Barcelona, Spain.)

CHAPTER

PERIPHERAL T- AND NK-CELL NEOPLASMS

22

MATURE T- AND NK-CELL NEOPLASMS

T-cell and natural killer (NK) cell neoplasms differ, as do B-cell tumors, in terms of the maturation stage from which they arise. However, there is also a greater degree of subdivision into different topographic populations (e.g. cutaneous T cells associated with the skin lymphomas; T cells associated with the gastrointestinal tract with enteric lymphomas). The World Health Organization Classification of these neoplasms is shown in Table 22.1. For some not well-understood reason there is a greater frequency of some of these tumors in Eastern Asia and Native American populations than in Europe and the USA, where they account for less than 20% of non-Hodgkin lymphomas. T-cell neoplasms presenting as leukemias (T-cell prolymphocytic leukemia, T-cell large granular lymphocytic leukemia leukemia, aggressive NK-cell leukemia, adult T-cell leukemia/lymphoma) are discussed in Chapter 18. In this chapter, we discuss peripheral T- and NK-cell lymphomas (PTCL) mainly presenting in extranodal and nodal sites, including the heterogeneous group of primary skin T-cell lymphomas (Table 22.1). The phenotypes of the principal T- and NK-cell lymphomas presented here are summarized in Table 22.2.

TABLE 22.1. THE 2016 REVISED WORLD HEALTH ORGANIZATION CLASSIFICATION OF THE MATURE T- AND NK-CELL NEOPLASMS

Mature T and NK neoplasms
T-cell prolymphocytic leukemia
T-cell large granular lymphocytic leukemia
Chronic lymphoproliferative disorder of NK cells
Aggressive NK-cell leukemia
Systemic EBV+ T-cell lymphoma of childhood
Hydroa vacciniforme-like lymphoproliferative disorder
Adult T-cell leukemia/lymphoma
Extranodal NK-/T-cell lymphoma, nasal type
Enteropathy-associated T-cell lymphoma
Monomorphic epitheliotropic intestinal T-cell lymphoma
Indolent T-cell lymphoproliferative disorder of the gastrointestinal tract
Hepatosplenic T-cell lymphoma
Subcutaneous panniculitis-like T-cell lymphoma
Mycosis fungoides
Sézary síndrome
Primary cutaneous CD30+ T-cell lymphoproliferative disorders • Lymphomatoid papulosis • Primary cutaneous anaplastic large cell lymphoma
Primary cutaneous γδ T-cell lymphoma
Primary cutaneous CD8+ aggressive epidermotropic cytotoxic T-cell lymphoma
Primary cutaneous acral CD8+ T-cell lymphoma
Primary cutaneous CD4+ small/medium T-cell lymphoproliferative disorder
Peripheral T-cell lymphoma, NOS
Angioimmunoblastic T-cell lymphoma
Follicular T-cell lymphoma
Nodal peripheral T-cell lymphoma with TFH phenotype
Anaplastic large-cell lymphoma, ALK^+
Anaplastic large-cell lymphoma, ALK^-
Breast implant–associated anaplastic large-cell lymphoma

Source:Swerdlow SH, et al. Blood 2016;127:2375–2390. Reproduced with permission of *Blood: Journal of the American Society of Hematology*.

EPSTEIN–BARR VIRUS POSITIVE T-CELL LYMPHOPROLIFERATIVE DISEASES OF CHILDHOOD

Epstein–Barr virus (EBV) associated T- and NK-cell lymphoproliferative disorders (LPD) in children and young adults can occur in two major clinicopathologic situations: chronic active EBV infection (CAEBV) and systemic EBV+ T-cell lymphoma of childhood. These situations are more common in Asian and Native American populations.

CHRONIC ACTIVE EBV INFECTION: HYDROA VACCINIFORME-LIKE LYMPHOPROLIFERATIVE DISORDER

CAEBV is characterized by a proliferation of T or NK cells with different clinical manifestations that vary from local and relatively indolent forms such as hydroa vacciniforme-like LPD and severe mosquito bite allergy to the systemic form of CAEBV characterized by fever, hepatosplenomegaly, and lymphadenopathy, with or without cutaneous manifestations. Some patients

Color Atlas of Clinical Hematology: Molecular and Cellular Basis of Disease, Fifth Edition. A. Victor Hoffbrand, Paresh Vyas, Elías Campo, Torsten Haferlach, and Keith Gomez

TABLE 22.2. IMMUNOHISTOLOGIC MARKERS AND POSTULATED NORMAL COUNTERPART OF COMMON T-CELL NEOPLASMS

Neoplasm	CD3 (S;C)	CD5	CD7	CD4	CD8	CD30	CXCL13	CD56	TCR	NK (16, 56)	Cytotoxic granules[a]	EBV
Extranodal NK/T-cell lymphoma	–; +	–	–/+	–	–	–	–	+	–	NA, +	+	+
Hepatosplenic T-cell lymphoma	+	–	+	–	–/+	–	–	+/–	γδ > αβ	+, –/+	+	–
Enteropathy-type T-cell lymphoma	+	–	+	–	–/+	+/–	–	–	αβ > γδ	–	+	–
Mycosis fungoides/Sezary syndrome	+	+	–/+	+	–	–	–	–	αβ	–	–	–
Subcutaneous panniculitis-like T-cell lymphoma	+	+/–	+/–	–	+	–	–	–	αβ	–	+	–
Primary cutaneous γδ T-cell lymphoma	+	–	+/–	–	+/–	–/+	–	+	γδ	–, +/–	+	–
PTCL, NOS	+/–	+/–	+/–	+/–	–/+	–/+	–	–	αβ > γδ	–/+	–/+	–/+
Angioimmunoblastic T-cell lymphoma	+	+	+	+/–	–/+	–	+	–	αβ	–	NA	+/–
ALK+ ALCL	+/–	+/–	NA	–/+	–/+	+	–	–	αβ	–	+	–

+, >90% positive; +/-, >50% positive; -/+, <50% positive; -, <10% positive.
ALCL, anaplastic large cell lymphoma; ALK, anaplastic lymphoid kinase; C, cytoplasmic; EBV, Epstein–Barr virus; G, NA, not available; NK, natural killer; PTCL, NOS, peripheral T-cell lymphoma, not otherwise specified; S, surface; TCR, T-cell receptor gene.
[a] Cytotoxic granules = TIA-1, perforin, and/or granzyme.

develop CAEBV after a clear episode of infectious mononucleosis. The clinical severity of this systemic form of CAEBV is variable among patients apparently related to the host response to EBV infection.

Hydroa vacciniforme-like LPD is a rare chronic disease in children that can progress to an EBV+ T-cell lymphoma mainly reported in native populations of Central and South America, Mexico, and Far East Asian countries. This disorder occurs on sun-exposed skin of the face and extremities and also on covered skin, with edema, blistering, and ulceration similar to the benign form of hydroa vacciniforme (Fig. 22.1 A). The clinical manifestations are very variable from indolent and self-limited lesions to lesions that relapse and eventually progress to an overt lymphoma. In some patients there is associated fever, wasting, lymphadenopathy, anemia, and leukopenia. Skin biopsies (Fig. 22.1 B–F) show superficial and deep perivascular and periappendageal lymphoid infiltrates that often extend into subcutaneous fat. There is ballooning degeneration of the overlying epidermis. The neoplastic cells are predominantly cytotoxic T cells positive for CD3 with cytotoxic granules, and EBV-positive, mainly CD4, with some cases having a CD8 or NK phenotype. There is a monoclonal rearrangement of the T-cell receptor gene. The lesions are morphologic and phenotypically similar in all clinical situations and are not specific aspects that predict the evolution to overt lymphoma.

SYSTEMIC EBV+ T-CELL LYMPHOMA OF CHILDHOOD

This extremely rare, fulminant, and fatal lymphoproliferative disease associated with active EBV infection is characterized by hepatosplenomegaly, often without significant lymphadenopathy, fever, liver failure, pancytopenia, and a hemophagocytic syndrome. The disease occurs shortly after a primary EBV infection or in the context of CAEBV infection. The neoplastic cells have a T-cell phenotype, usually CD8 when the disease occurs after primary EBV infection or CD4 in the context of CAEBV.

EXTRANODAL NK-/T-CELL LYMPHOMA, NASAL TYPE

As other EBV-related T and NK lymphoproliferative disorders this lymphoma is uncommon in the USA and Europe, but is much more common in Far East and Native American populations. It often involves the nose, palate, and skin, but other tissues, including the gut, are also involved. There is a tendency to invade the walls of blood vessels, accompanied in many cases by blockage of vessels by lymphoma cells, often associated with ischemic necrosis of normal and neoplastic tissue (Fig. 22.2). Cutaneous infiltration is usually dermal and can also involve subcutaneous tissue. The neoplastic cells are variable in size with irregular or oval nuclei, and there is typically necrosis (Fig. 22.3). The cell morphology is highly variable, and admixed inflammatory cells can cause difficulty in diagnosing early cases. The neoplastic cells are most commonly of NK rather than T cell in origin: surface CD3 is absent in many cases (although cytoplasmic CD3ε chain is present) and CD56 is often expressed (Fig. 22.4). The cytotoxic proteins granzyme B, perforin, and TIA-1 are also positive. EBV is almost always present in the neoplastic cells (Fig. 22.5). The most frequently found cytogenetic abnormalities are del(6) (q21;q25) and inv(6)(p10). Recurrent mutations have been found in *DDX3X* and JAK/STAT signaling pathway (*STAT3*, *STAT5B*, *JAK3*), among others.

The cutaneous form is an aggressive tumor with a poor prognosis and a median survival less than 1 year. In some cases there is an associated hemophagocytic syndrome. This lymphoma is closely related to aggressive NK-cell leukemia which can also have extensive cutaneous involvement. Nasal disease can have a more protracted course.

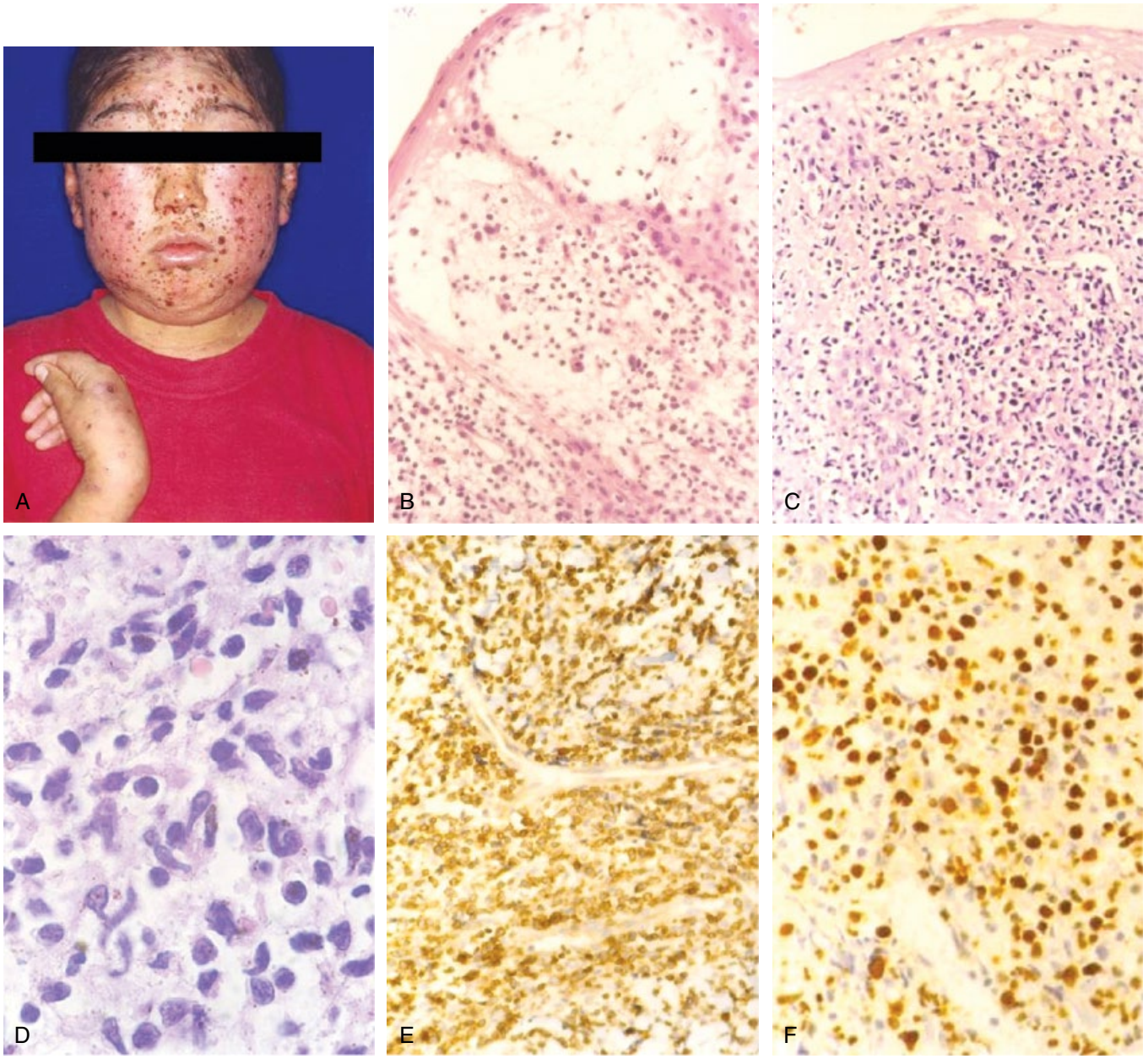

Fig. 22.1 Hydroa vacciniforme-like T-cell lymphoproliferative disorder. **A,** Typical vacciniform skin eruptions in an 8-year-old Peruvian boy. **B,** Skin biopsy showing blisters; **C,** an atypical dermal infiltrate with epidermotrophism and spongiosis; **D,** cytologic detail of pleomorphic neoplastic cells; and **E,** immunopositivity for CD3 and **F,** EBER. (*A–F,* Courtesy of Dr. C Barrionuevo.)

ENTEROPATHY-ASSOCIATED T-CELL LYMPHOMA

Small intestinal lymphomas have long been recognized as a complication of gluten-induced enteropathy (celiac disease). Enteropathy-associated T-cell lymphoma (EATL) is a neoplasm of intraepithelial T cells that occurs in individuals with celiac disease. This complication occurs in patients with known celiac disease or as a de novo manifestation with malabsorption and diarrhea. In some patients, a period of refractory celiac disease is associated with small bowel ulcerations. Most patients have HLA DQA1*0501, DQB1*0201 characteristic of celiac disease. Morphologically, these tumors have a spectrum of cellular pleomorphism with frequent associated inflammatory cells and areas of necrosis. Intraepithelial neoplastic lymphocytes can be very abundant but also scarce. The adjacent mucosa can have typical histologic features of celiac disease but can be absent. Typical histologic appearances are shown in Figs. 22.6–22.8. The neoplastic cells express CD3 and CD7 but are usually negative for CD5, CD4, CD8, and cytotoxic granules. Some cases are CD8 positive. CD30 is frequently positive in the larger cells. An association with EBV has been found in some cases, especially in South and Central America. TCRβ and γ genes are clonally rearranged. The clinical outlook is poor because the neoplasm is frequently multifocal. This neoplasm has to be distinguished from another intestinal T-cell lymphoma called monomorphic epitheliotropic intestinal T-cell lymphoma that is not associated with celiac disease. The tumor cells tend to infiltrate the epithelium and express CD3, CD8 CD56, and MATK.

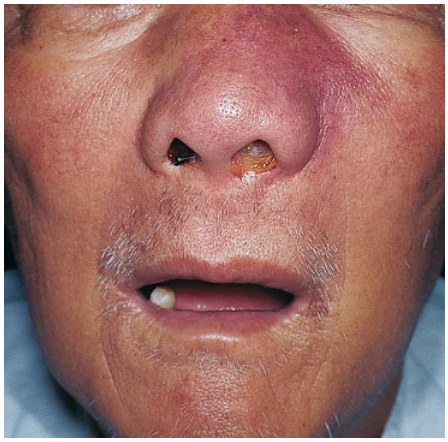

Fig. 22.2 T/NK nasal type (angiocentric) lymphoma: Midline nasal swelling. (Courtesy of Professor R Liang.)

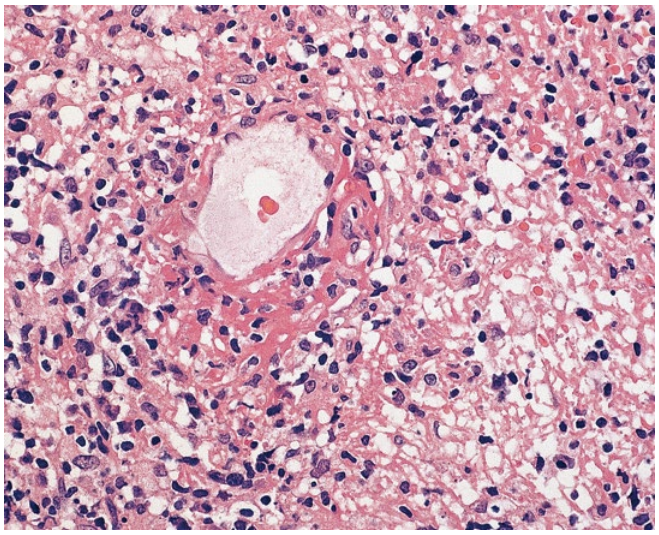

Fig. 22.3 T/NK nasal type (angiocentric) lymphoma: Typical lesion with angiocentricity and marked necrosis. (Courtesy of Professor R Liang.)

HEPATOSPLENIC T-CELL LYMPHOMA

This rare form of lymphoma, representing less than 5% of all T-cell neoplasms, is predominantly a disease of young adults and has a male predominance. There is an increased incidence in immunosuppressed patients following organ transplantation and patients, especially children, treated with azathioprine and infliximab for Crohn disease. The tumor is derived from cytotoxic T cells usually of the γ/δT-cell receptor subtype. Marked sinusoidal infiltration of the spleen (Fig. 22.9), liver, and bone marrow are characteristic features. The neoplastic cells are medium-sized lymphocytes with a high nuclear : cytoplasm ratio. Patients have hepatosplenomegaly with no peripheral lymphadenopathy. There is usually anemia, thrombocytopenia, and leukocytosis. The atypical T cells are occasionally seen in the blood (Fig. 22.10), especially in the later stages of the disease. Infiltration of bone marrow can be seen in aspirates (Fig. 22.11) and trephine biopsies. The immunophenotype is usually CD3 and TCRδ1 positive, CD56 +/–, and CD4, CD5, and CD8 negative. The cells express the cytotoxic protein TIA1, but perforin is usually negative. There is rearrangement of the TCRγ/δ genes. Isochromosome 7q is almost always present. There is no

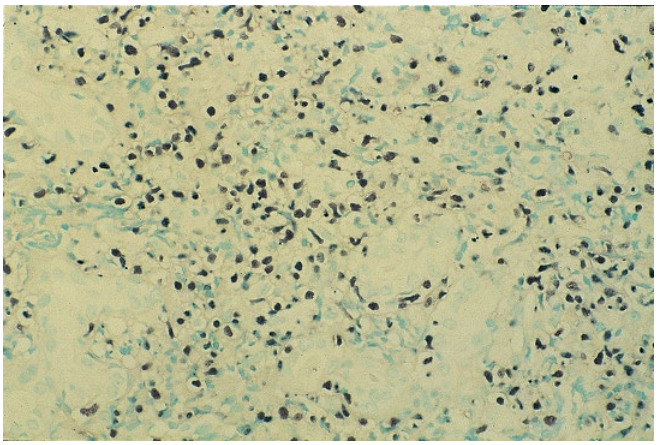

Fig. 22.4 T/NK nasal type (angiocentric) lymphoma: Positive in situ hybridization for EBER. (Courtesy of Professor R Liang.)

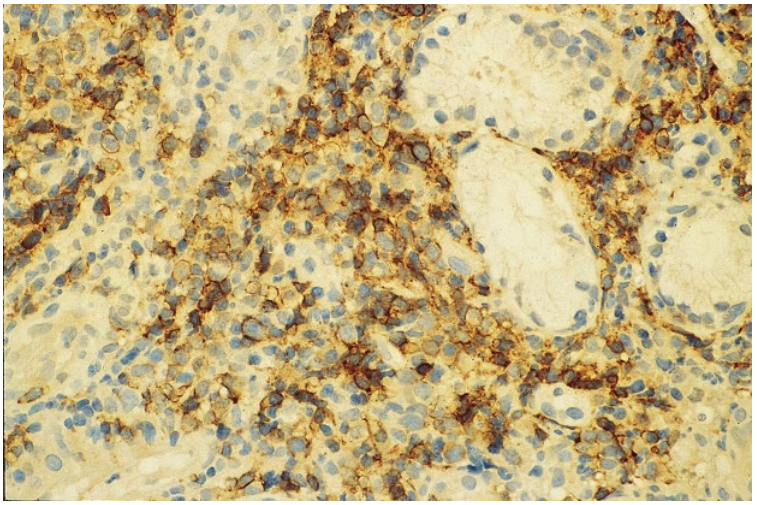

Fig. 22.5 T/NK nasal type (angiocentric) lymphoma: Positive immunoperoxidase stain for CD56. (Courtesy of Professor R Liang.)

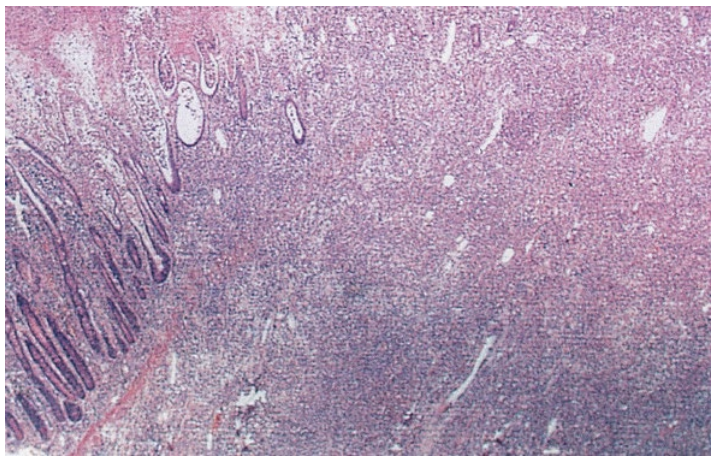

Fig. 22.6 Enteropathy-associated T-cell lymphoma: Ulceration of small intestinal mucosa and infiltration into the smooth muscle below.

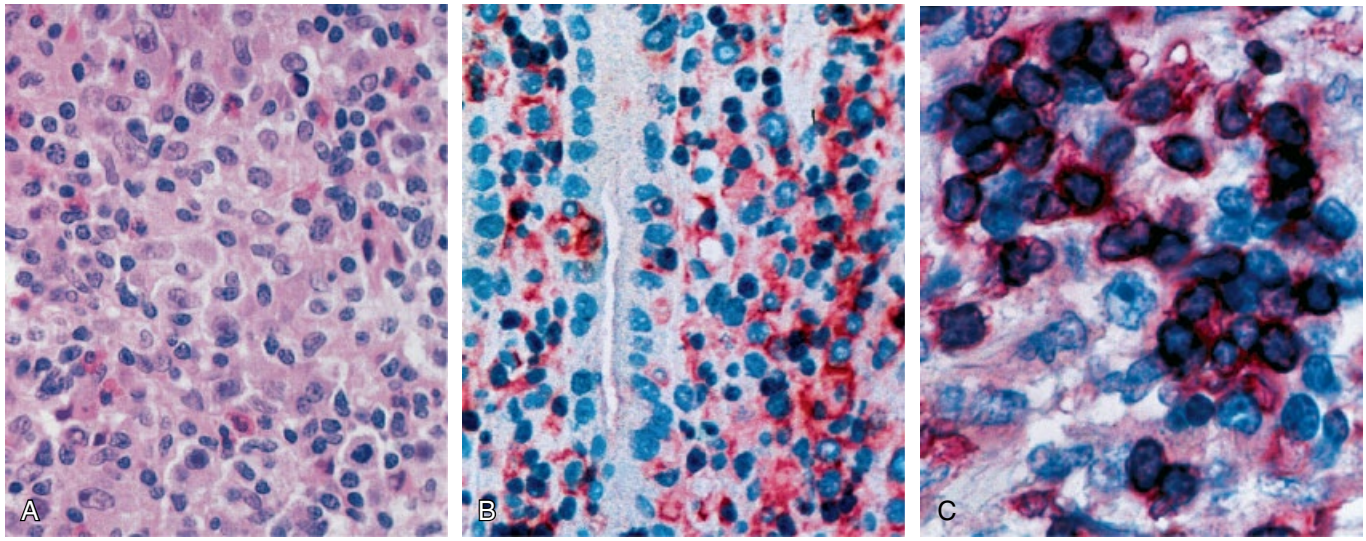

Fig. 22.7 Enteropathy-associated T-cell lymphoma. **A,** High-power view showing pleomorphic and polymorphic infiltration of lymphoid cells. **B, C,** APAAP immunoalkaline phosphatase stain shows that some but not all of the neoplastic cells express CD3.

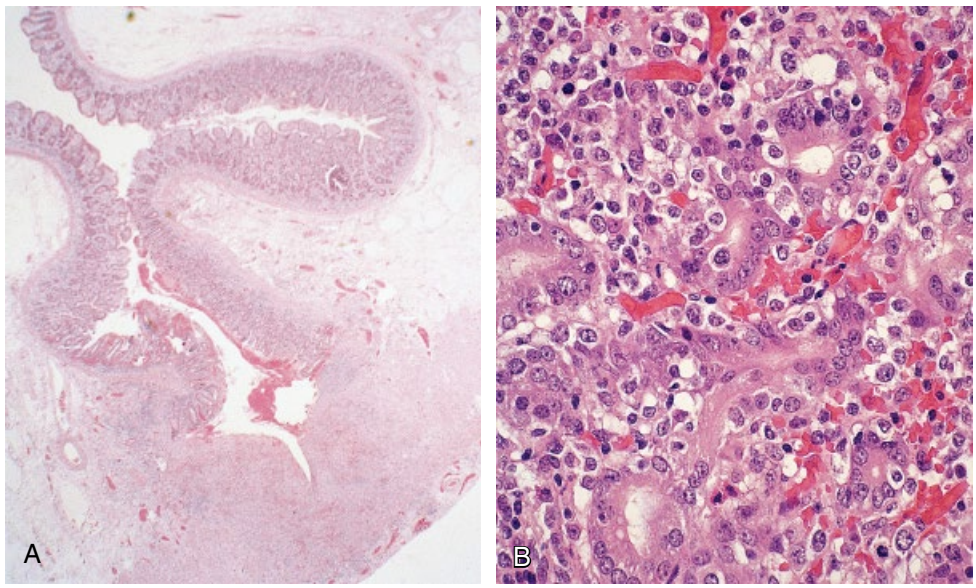

Fig. 22.8 Enteropathy-associated T-cell lymphoma. **A,** Deep fissure formation and a flat, small intestinal mucosa. **B,** Infiltration of small intestinal crypts by neoplastic cells.

evidence of EBV involvement. Less commonly, variant cases express the αβ T-cell receptor (Fig. 22.12). Activating mutations of *STAT5B* and, more rarely, of *STAT3* have been found in 40% of cases. These lymphomas are aggressive, with a median survival of less than 2 years.

PRIMARY CUTANEOUS T-CELL LYMPHOMAS

The T-cell lymphomas that occur in the skin (Table 22.1) are a heterogeneous group with clinical and biologic features different from systemic T-cell lymphomas. Mycosis fungoides and Sézary syndrome are well known and make up over 60% of all cutaneous T-cell lymphomas. Some of the more recently recognized conditions are classified as provisional entities as they are rare tumors and their clinical and biologic behavior is not yet well established. Correct diagnosis of cutaneous T-cell lymphomas requires close correlation between clinical, histologic, and phenotypic features.

SUBCUTANEOUS PANNICULITIS-LIKE T-CELL LYMPHOMA

This tumor is a neoplasms of T-cytotxic cells that preferentially involve the subcutaneous tissue. Subcutaneous nodules up to several centimeters in diameter are the usual presenting features of this rare lymphoma. Histologically, the subcutaneous tissue is infiltrate by atypical lymphocytes with hyperchromatic nuclei. The cells surround or "rim" individual fat cells, and there are often foci of apoptotic and necrotic cells (Fig. 22.13). The neoplastic cell population has an αβ cytotoxic T-cell phenotype with positivity for CD8 and cytotoxic granule molecules granzyme B, perforin, and

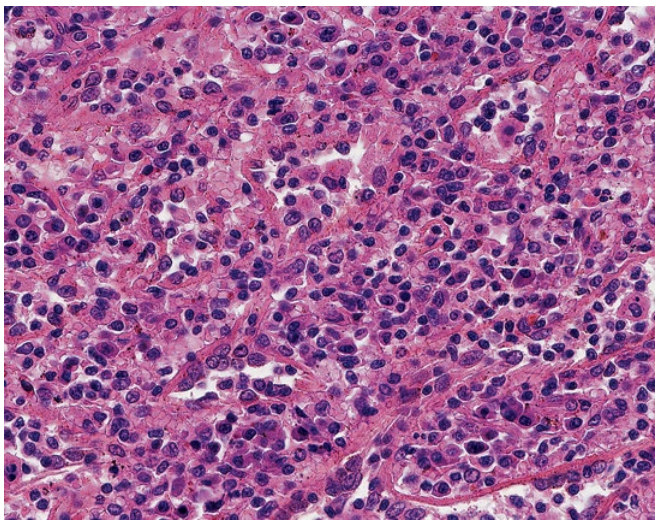

Fig. 22.9 Hepatosplenic γδ T-cell lymphoma: Infiltration of splenic pulp cords by medium-sized lymphoma cells. The cells showed clonal T-cell receptor γ and δ rearrangements.

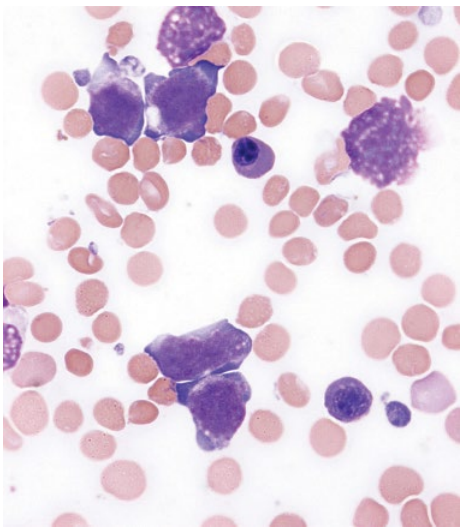

Fig. 22.11 Hepatosplenic T-cell lymphoma: Bone marrow aspirate in same patient as Fig. 22.12. The four large lymphoma cells show a vesicular chromatin pattern, nucleoli, and basophilic cytoplasm. (Courtesy of Dr. W Erber.)

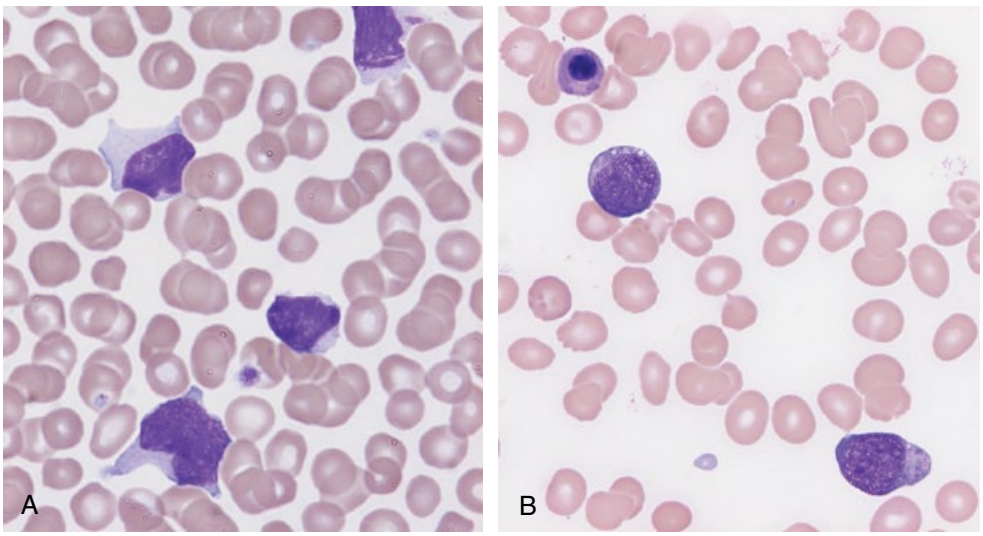

Fig. 22.10 Hepatosplenic T-cell lymphoma: Peripheral blood film. **A,** The atypical lymphocytes show large nuclei and abundant cytoplasm. **B,** In another patient the cells are more blastic in appearance with basophilic cytoplasm. (Courtesy of Dr. W Erber.)

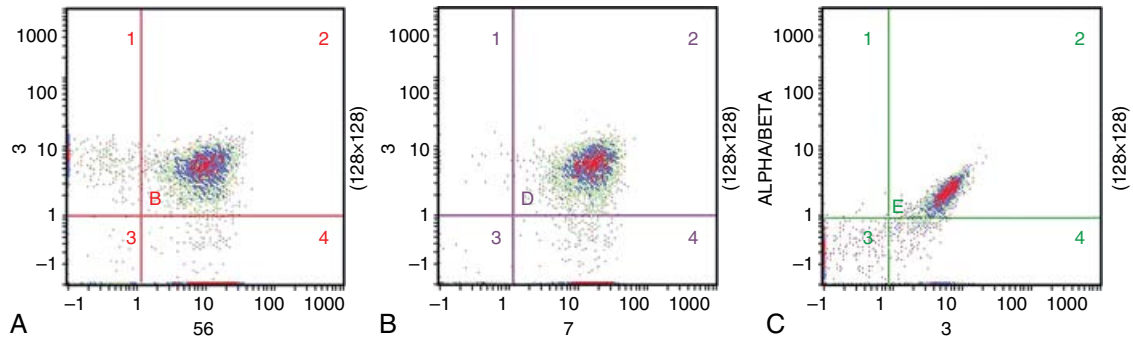

Fig. 22.12 Hepatosplenic T-cell lymphoma: Flow cytometry. A, CD3/CD56; B, CD3/CD7; **and C,** αβ/CD3] shows the neoplastic T-cells are positive for CD3, CD7, and CD56 and express the αβ T-cell receptor. (Courtesy of Dr. W Erber.)

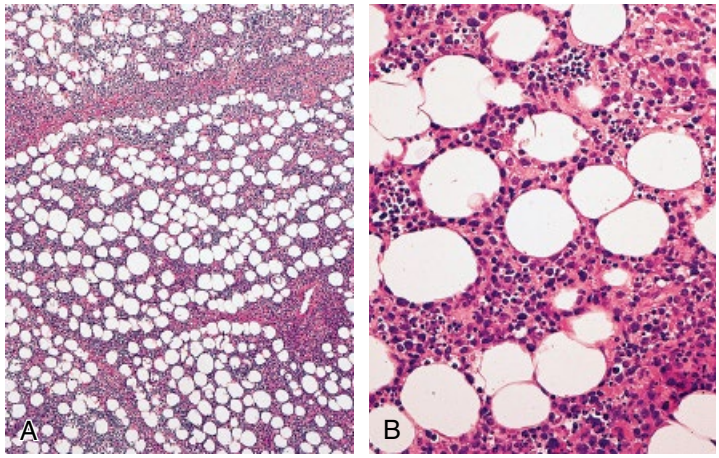

Fig. 22.13 Subcutaneous panniculitis-like T-cell lymphoma. **A,** Low-power view showing lymphomatous infiltration between fat cells. **B,** Lymphomatous infiltration between fat cells with areas of apoptosis by lymphoma cells.

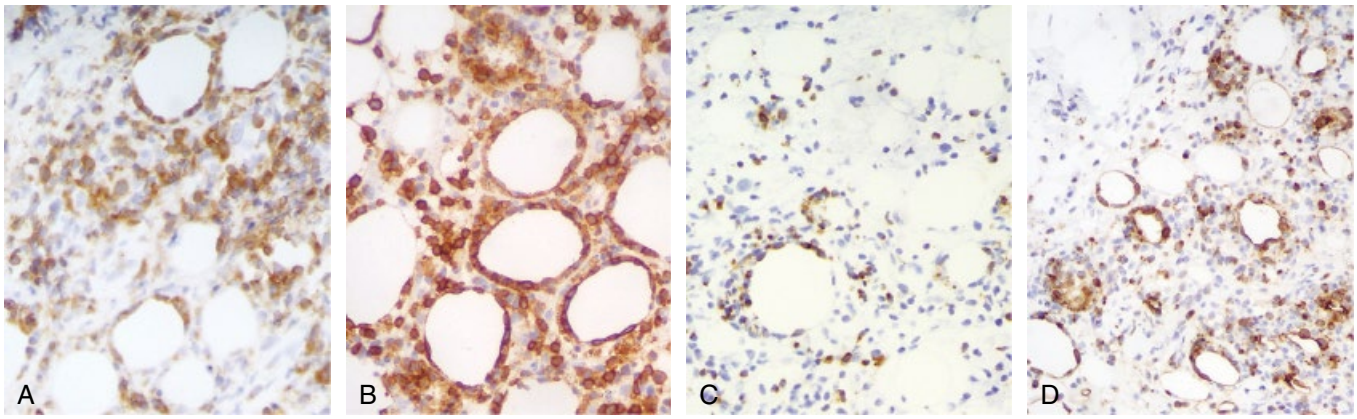

Fig. 22.14 Subcutaneous panniculitis-like T-cell lymphoma: Immunoperoxidase staining. **A,** CD3. **B,** CD8. **C,** Granzyme B. **D,** Perforin. (Courtesy of Dr. G Taylor.)

TIA-1 but negative for CD56 (Fig. 22.14). T-cell receptor genes are rearranged, and there is no evidence of involvement by EBV. The disease has an indolent course in most cases. Dissemination to regional lymph nodes and other organs is unusual but can occur late in the disease. Release of cytokines and chemokines can produce a hemophagocytic syndrome with fever, pancytopenia, and hepatosplenomegaly, and it is associated with more aggressive clinical evolution.

MYCOSIS FUNGOIDES

The classic form of mycosis fungoides is the most common primary cutaneous T-cell lymphoma. Most patients are elderly, and there is a male predominance. The disease usually has a long natural history and evolves through three stages:

1. The first stage is a premycotic stage with lesions similar to eczema or psoriasis (Fig. 22.15).

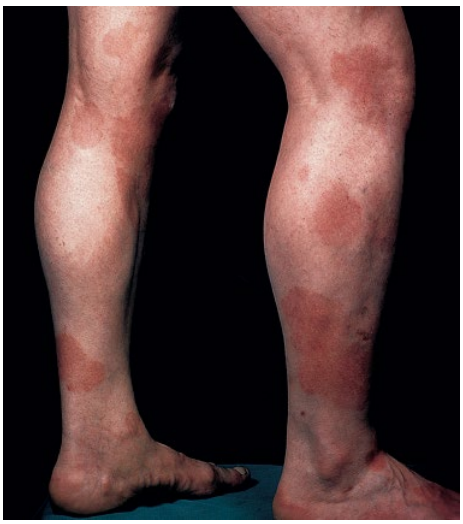

Fig. 22.15 Mycosis fungoides: Typical eczematoid lesions at presentation.

2. The second stage is an infiltrative or plaque stage (Fig. 22.16).
3. The third stage is a nodular or tumor stage associated with deeper invasion by the tumor (Fig. 22.17) and infiltration of lymph nodes and other organs (e.g. liver, spleen, and lungs). Bone marrow involvement is rare.

The skin lesions show dermal and epidermotropic infiltrates of small to medium-sized cells with convoluted or cerebriform nuclei (Fig. 22.18). Localized pockets of these cells in the epidermis (Pautrier microabscesses, Fig. 22.19) are characteristic but are not seen in all cases. The cells express pan T-cell antigens (Fig. 22.20) and are usually positive for CD2, CD3, CD5, and TCRβ. The T-cell receptor genes are rearranged in most patients. There are no specific cytogenetic abnormalities, but patients with advanced disease can have complex karyotypes.

FOLLICULOTROPHIC MYCOSIS FUNGOIDES (MYCOSIS FUNGOIDES-ASSOCIATED FOLLICULAR MUCINOSIS)

This variant of mycosis fungoides is characterized by a follicular infiltrate, often with sparing of the epidermis. Most cases show mucinous degeneration of the hair follicles (Fig. 22.21). There is preferential involvement of the head and neck. The immunophenotype is similar to classic mycosis fungoides. Isolated CD30-positive blast cells can be seen.

PAGETOID RETICULOSIS

In this localized variant of mycosis fungoides, patients have a slowly progressive, solitary psoriaform or hyperkeratotic plaque usually on the arms or legs. There is epidermal hyperplasia with a Pagetoid infiltration of atypical cells with convoluted nuclei (Fig. 22.22). The neoplastic cells canbe positive for either CD3 and CD4 or more commonly CD3 and CD8 with variable expression of CD30. Extracutaneous dissemination and progression of this form have not been reported.

GRANULOMATOUS SLACK SKIN DISEASE

Granulomatous slack skin disease is an extremely rare cutaneous T-cell lymphoma characterized by the development of laxity in the major skin folds and granulomatous infiltrates of neoplastic T cells (Fig. 22.23).

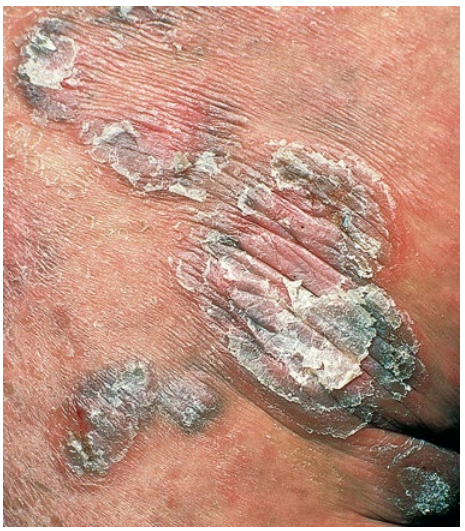

Fig. 22.16 Mycosis fungoides. These psoriasiform plaques appeared 6 months later (same patient as shown in Fig. 22.15).

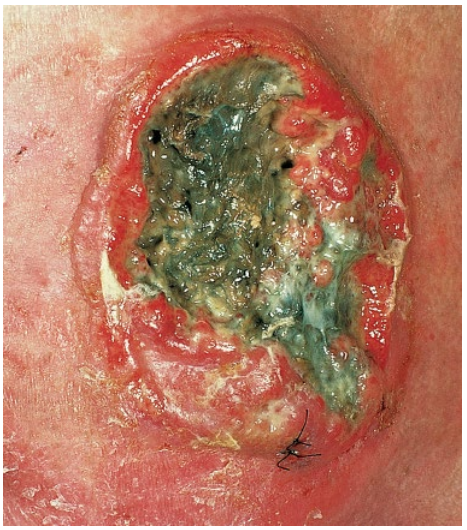

Fig. 22.17 Mycosis fungoides. Extensive ulceration of the abdominal skin indicative of the invasive tumor stage.

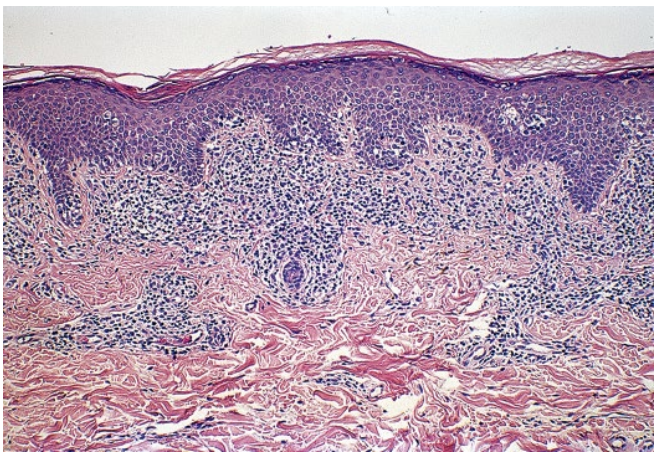

Fig. 22.18 Mycosis fungoides. There is a bandlike dermal infiltrate with atypical lymphocytes in the basal epidermis. (Courtesy of Dr. D Weedon and Dr. G Strutton.)

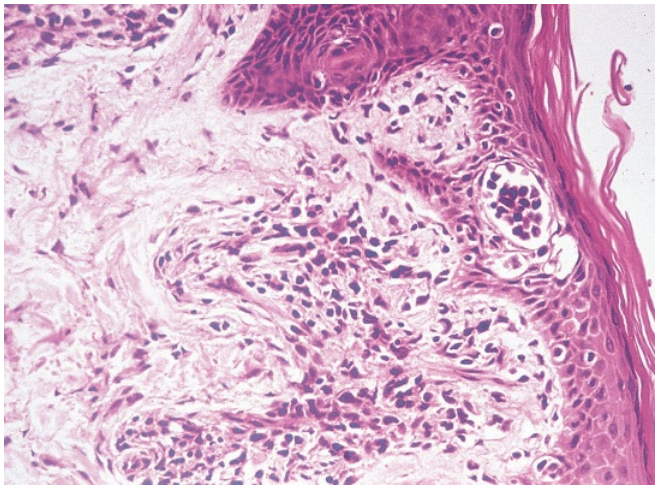

Fig. 22.19 Mycosis fungoides. Typical histologic pattern, showing a focal intraepidermal collection of abnormal lymphoid cells (Pautrier abscess) and similar groups of tumor cells in the papillary dermis.

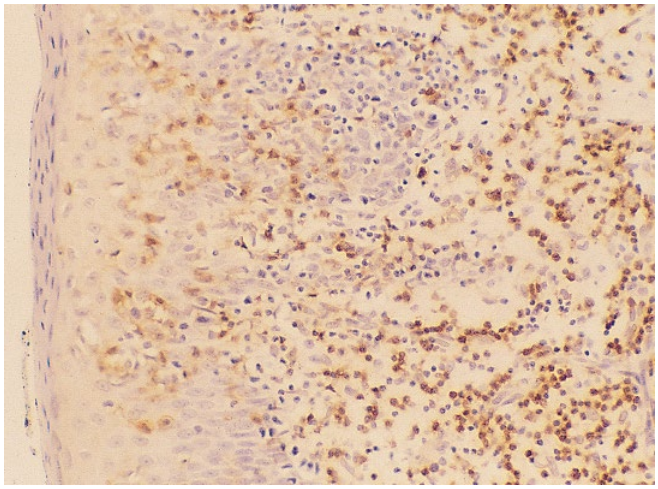

Fig. 22.20 Mycosis fungoides. Malignant lymphoid cells in a skin biopsy show cytoplasmic positivity for the T-cell marker CD45RO (antibody UCHL1). (Courtesy of Dr. JE McLaughlin.)

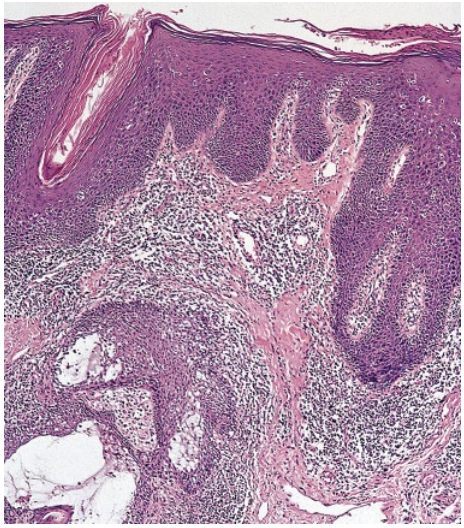

Fig. 22.21 Folliculotrophic mycosis fungoides (follicular mucinosis). There is a folliculotrophic infiltrate of neoplastic lymphocytes and mucinous degeneration of the hair follicle. (Courtesy of Dr. D Weedon and Dr. G Strutton.)

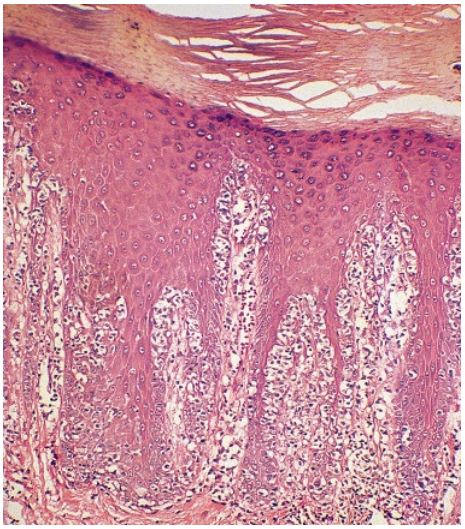

Fig. 22.22 Pagetoid reticulosis. There is a marked epidermotrophism of atypical lymphocytes. (Courtesy of Dr. D Weedon and Dr. G Strutton.)

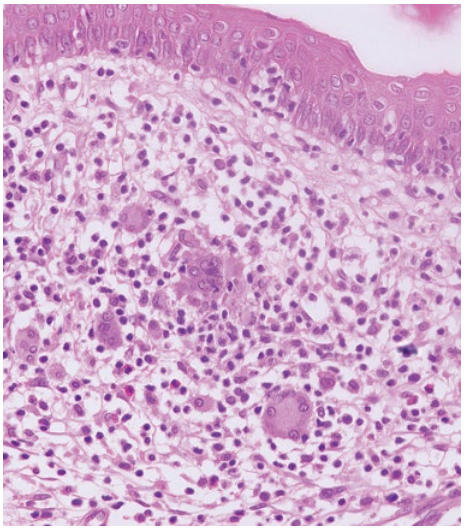

Fig. 22.23 Granulomatous slack skin disease. There is an intraepidermal and dermal lymphoid infiltrate and characteristic multinucleated histiocytic giant cells. Elastophagocytosis was present in other fields of the biopsy.

SÉZARY SYNDROME

In Sézary syndrome there is erythroderma, generalized lymphadenopathy, and characteristic neoplastic T cells (Sézary cells) in blood, skin, and lymph nodes. In addition, one or more of the following criteria are required for a diagnosis of Sézary syndrome: An absolute blood count of Sézary cells of 1.0×10^9/L; an expanded CD4+ T-cell population resulting in a CD4:CD8 ratio of more than 10; and/or loss of one or more T-cell antigens. Traditionally, this rare disease of adults has been considered to be a leukemic and aggressive variant of mycosis fungoides but they correspond to separate entities. The erythroderma (Fig. 22.24) is often associated with exfoliation and intense pruritus. The atypical cells in the blood have markedly convoluted nuclei and may be small (Lutzner cells) or large (classic Sézary cells) (Figs. 22.25 and 22.26). The cytoplasm can show periodic acid–Schiff (PAS) positive granules (Fig. 22.27), and electron microscopy defines

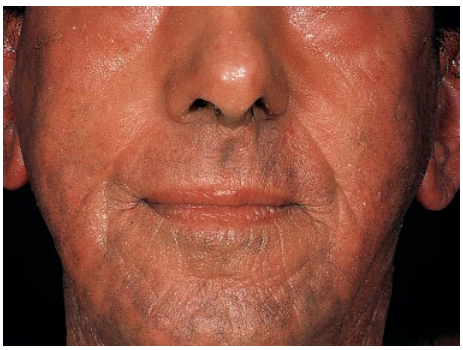

Fig. 22.24 Sézary syndrome. Erythroderma in advanced disease.

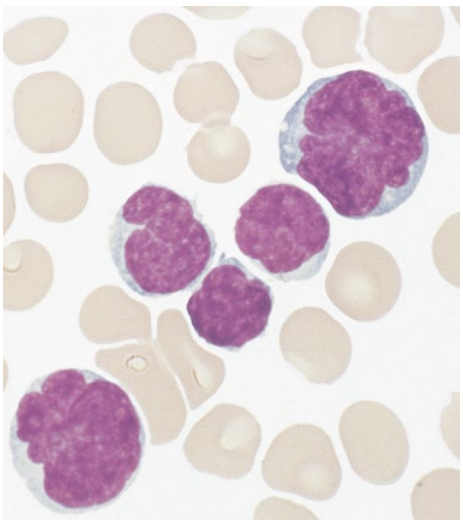

Fig. 22.25 Sézary syndrome. Abnormal cells in the peripheral blood have characteristic, cerebriform, large, and clefted nuclei with fine chromatin pattern and scanty cytoplasm. (Courtesy of Professor D Catovsky.)

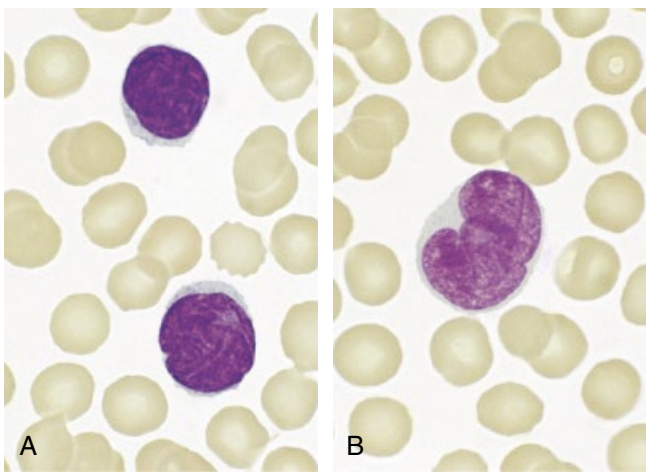

Fig. 22.26 Sézary syndrome. **A,** Small cell type (Lutzner cell). The cells show grooved nuclear chromatin with a high nuclear:cytoplasm (N:C) ratio. **B,** Large cell type with grooved nuclear pattern, densely clumped chromatin, and lower N:C ratio. (Courtesy of Professor D Catovsky.)

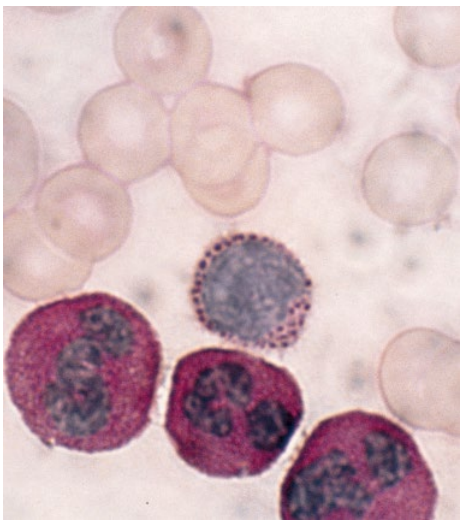

Fig. 22.27 Sézary syndrome. PAS-positive granules surrounding the nucleus in a lymphocyte with convoluted nucleus. (Courtesy of Dr. PM Canfield.)

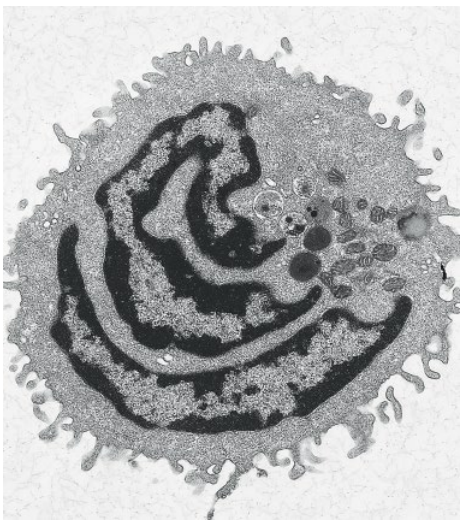

Fig. 22.28 Mycosis fungoides–Sézary syndrome. Electron micrograph of an abnormal T lymphocyte from the peripheral blood shows a deeply clefted nucleus (×8000). (Courtesy of Dr. E Matutes and Professor D Catovsky.)

the deeply clefted cerebriform nuclei (Fig. 22.28). Lymphoid marker studies show positivity for CD2, CD3, TCRβ, and CD5, and in most cases CD4. The skin lesions are similar to those of mycosis fungoides with epidermal and dermal infiltrates of convoluted lymphocytes.

PRIMARY CUTANEOUS CD30+ T-CELL LYMPHOPROLIFERATIVE DISORDERS

This group of diseases constitutes a spectrum of relatively common lesions that include lymphomatoid papulosis, primary cutaneous anaplastic large cell lymphoma, and some lesions with intermediate features between both of them. These lesions show overlapping histopathologic, phenotypic, and genetic features and therefore the diagnosis requires the integration of the clinical and pathologic features.

LYMPHOMATOID PAPULOSIS

This chronic recurrent atypical lymphoproliferative disorder is characterized by the appearance and spontaneous regression of multiple skin papules, some of which show ulceration. In most patients the condition has a benign course over many years, but a late evolution to systemic lymphoma occurs in 5% of patients. Biopsy shows dermal infiltrates of atypical neoplastic lymphocytes (Fig. 22.29) sometimes resembling Reed–Sternberg cells (Fig. 22.28 B). CD30, CD4, and cytotoxic granule proteins are positive in most cases. There is usually a variable associated population of inflammatory cells (type A). In less than 10% of cases (type B), the infiltrate is epidermotropic with predominantly cerebriform cells similar to mycosis fungoides. The cells in this subgroup are CD3 and CD4 positive and CD30 positive or negative. Some cases are composed of sheets of large atypical CD30-positive cells (type C). These histologic types do not have clinical or biologic differences. Clonal rearrangement of T-cell receptor genes is demonstrated in approximately 70% of cases.

PRIMARY CUTANEOUS ANAPLASTIC LARGE CELL LYMPHOMA

The usual presenting features are solitary skin nodules or tumors. Multifocal cutaneous lesions are seen in only 20% of cases. The lesions have a tendency for partial or complete spontaneous regression with frequent relapses. Late involvement of regional nodes occurs only in a minority of patients. Skin biopsies show an extensive dermal infiltrate of atypical lymphoid cells (Fig. 22.30 A). The cytologic features are similar to nodal or systemic anaplastic large cell lymphoma, but multinucleated giant cells are often more conspicuous (Fig. 22.30 B). Strong positivity for CD30 is seen in most of the neoplastic cells (Fig. 22.30 C). CD4 and cytotoxic granule-associated proteins (granzyme B, perforin, TIA-1) are usually positive. In contrast to nodal and systemic anaplastic T-cell tumors, the primary cutaneous tumors are negative for epithelial membrane antigen (EMA) and ALK protein. TCR genes are clonally rearranged. Rearrangements of *DUSP22-IRF4* on 6q25.3 are seen in some cases and also in lymphomatoid papulosis.

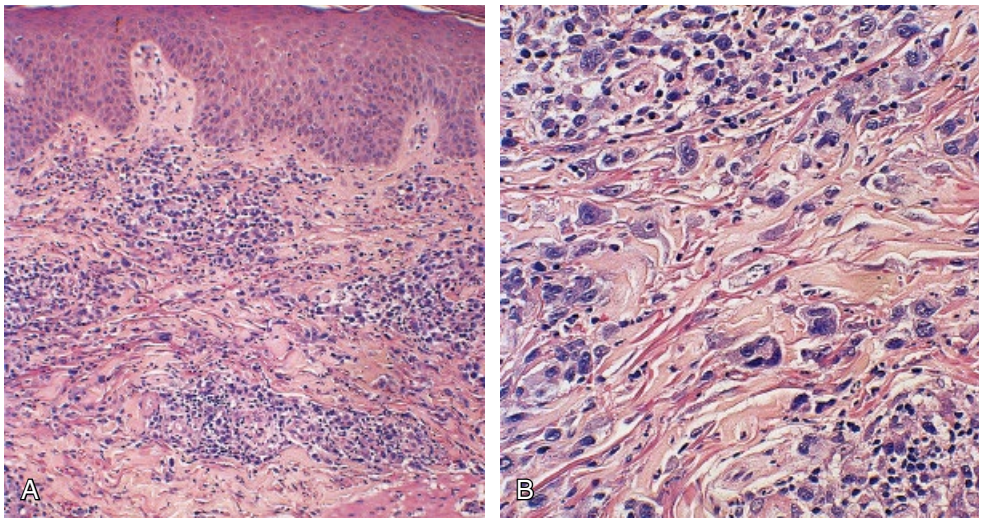

Fig. 22.29 Lymphomatoid papulosis. The dermal infiltrates **(A)** at higher magnification **(B)** are a mixture of small lymphocytes and atypical large cells similar to those seen in anaplastic large cell lymphoma. Some cells are multinucleated and others resemble Reed–Sternberg cells. (Courtesy of Dr. D Weedon and Dr. G Strutton.)

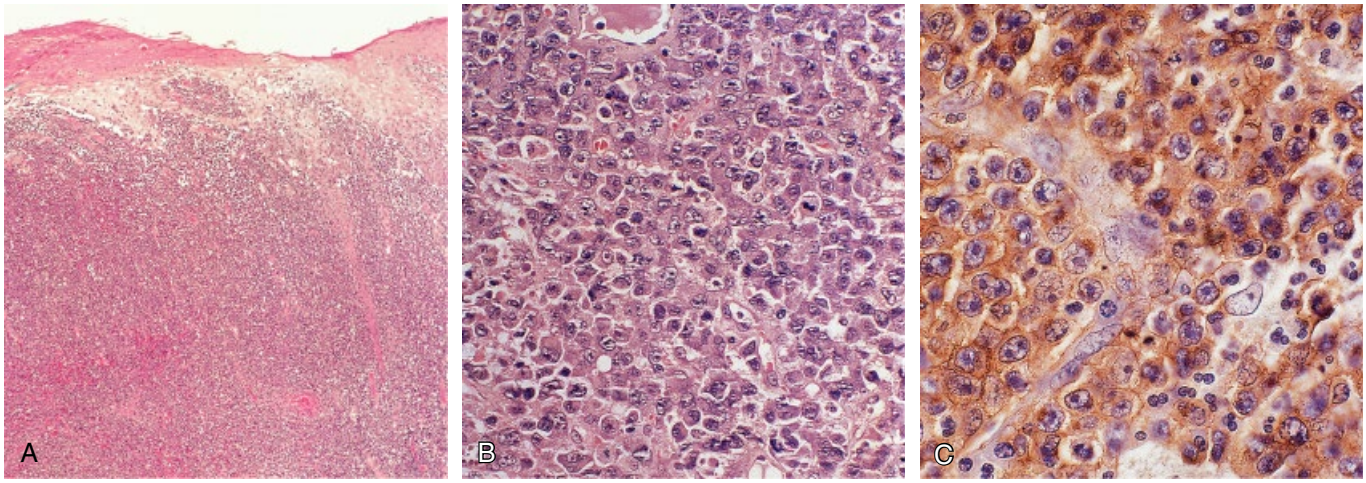

Fig. 22.30 Primary cutaneous anaplastic large cell lymphoma: Skin biopsy. **A,** An extensive dermal infiltrate of atypical lymphoid cells. **B,** The infiltrating large neoplastic cells are pleomorphic with prominent nucleoli. **C,** Immunostaining for CD30 shows positive cytoplasmic and Golgi zone staining. (*A,* Courtesy of Dr. S McDowell. *B* and *C,* Courtesy of Dr. D Weedon and Dr. G Strutton.)

PRIMARY CUTANEOUS γδ T-CELL LYMPHOMA

In this rare tumor there is a clonal proliferation of mature activated γδ T cells, CD56-positive, with a cytotoxic phenotype. Patients usually have disseminated plaques or ulcerated nodules or tumors. There can be involvement of mucosal and other extranodal sites, and occasionally there is a hemophagocytic syndrome. Pleomorphic small to large cells infiltrate the subcutaneous tissue and dermis (Fig. 22.31). The cells are TCRδ and/or TCRγ positive and negative TCRβ (βF1). Most patients have aggressive disease resistant to therapy, and the median survival is about 15 months.

PRIMARY CUTANEOUS AGGRESSIVE EPIDERMOTROPHIC CD8+ T-CELL LYMPHOMA (PROVISIONAL CATEGORY)

These lymphomas usually manifest as disseminated eruptive papules, nodules, and tumors showing central ulceration or as hyperkeratotic plaques. Occasionally, there is involvement of the oral mucosa. Histologically, the tumor cells are epidermotropic (Fig. 22.32); invasion and destruction of adnexal structures, angiocentricity, and angioinvasion can be present. The tumor cells vary in size with pleomorphic or blastic nuclei. Immunohistology shows positivity for βF1, CD3, CD8, granzyme B, perforin, TIA1, and CD45RA. EBV is usually negative.

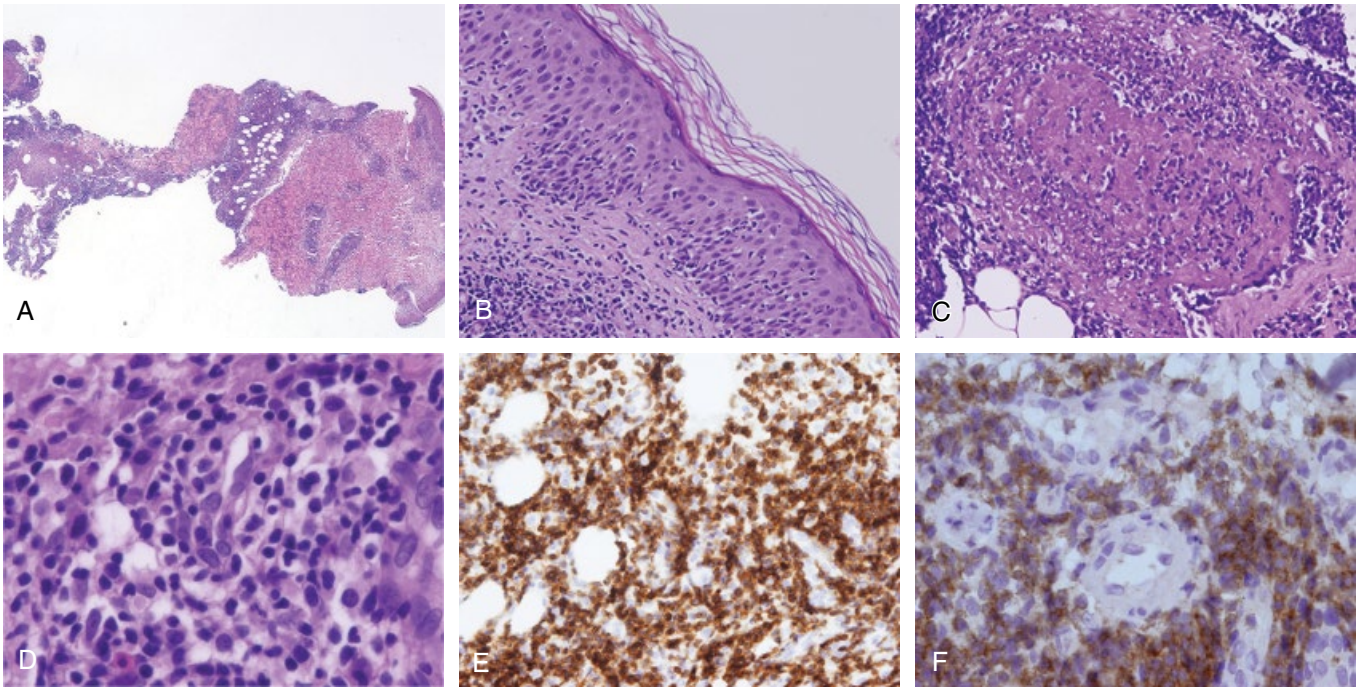

Fig. 22.31 Cutaneous γδ T-cell lymphoma. **A,** Infiltrates of neoplastic lymphoid cells involve both the dermis and subcutaneous fat. **B,** Focal collections of atypical lymphocytes also involve the epidermis and **C,** there is angiocentricity and angiodestruction. **D,** At higher magnification the cells are predominantly small and medium-sized lymphocytes. The neoplastic cells show immunoreactivity for **E,** CD3 and **F,** TCRδ1.

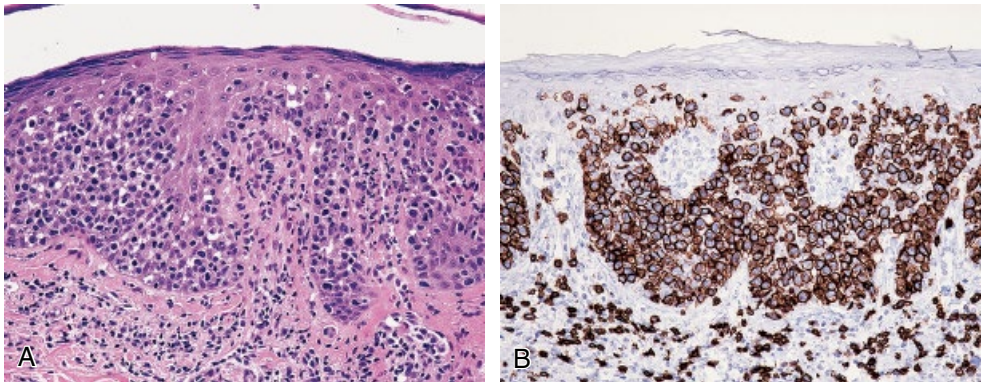

Fig. 22.32 Primary cutaneous aggressive epidermotrophic CD8+ T-cell lymphoma: skin biopsy. **A,** The infiltrate of atypical cells is almost wholly intraepidermal. **B,** The lymphoma cells express CD8. (Courtesy of Dr. P McKee.)

Systemic dissemination occurs and the prognosis is poor with a medium survival of less than 3 years.

PRIMARY CUTANEOUS SMALL/MEDIUM CD4+ T-CELL LYMPHOPROLIFERATIVE DISORDER (PROVISIONAL CATEGORY)

This lesion usually presents as solitary plaque or tumor on the face, neck, or upper trunk with an indolent slow growth pattern. Occasionally, there are multiple lesions, but systemic dissemination is rare. The benign course of these lesions has led to substitute the term "lymphoma" by lymphoproliferative disorder for this entity in the updated 2016 WHO classification (Table 22.1). The small to medium-sized lymphocytes infiltrate the dermis and sometimes the upper subcutaneous tissues (Fig. 22.33). Large cells are sometimes seen but they are always less than 30% of the population. Occasionally, there is focal epidermotrophism. The immunophenotype is CD3+ and CD4+. PD1 is positive in a variable number of cells. CD8, CD30, and the cytotoxic proteins are not expressed. The prognosis is favorable. Demonstration of TCR gene rearrangement and an abnormal T-cell phenotype are useful in excluding pseudo-T-cell lymphomas.

PERIPHERAL T-CELL LYMPHOMA, NOT OTHERWISE SPECIFIED

Although a number of well-defined categories of T-cell neoplasia have come to be recognized over the years (e.g. mycosis fungoides and those described previously), many T-cell lymphomas have features that do not match these entities. The WHO classification recognizes the category of "peripheral T-cell lymphoma, not otherwise specified (NOS)" to include cases that do not fulfill the criteria of other well-defined entities. These tumors make up half of all T-cell lymphomas seen in Western countries. Most patients are adults with lymphadenopathy, but often there is generalized disease with involvement of bone marrow, liver, spleen, and skin.

These neoplasms typically show diffuse infiltrates with replacement of normal lymph node architecture. The neoplastic cells can be very heterogeneous from small to large pleomorphic cells, often with irregular nuclei. Clear cells (Fig. 22.34) and Reed–Sternberg-like cells are often present. There can be a marked infiltration of non-neoplastic cells, including macrophages and eosinophils. Rare variant morphologic patterns are recognized. In the lymphoepithelioid variant (Lennert lymphoma) clusters of epithelioid histiocytes are seen (Fig. 22.35). In some cases the tumor cells infiltrate the interfollicular with preservation or even hyperplasia of follicles (Fig. 22.36). These morphologic variants do not appear to have any specific clinical

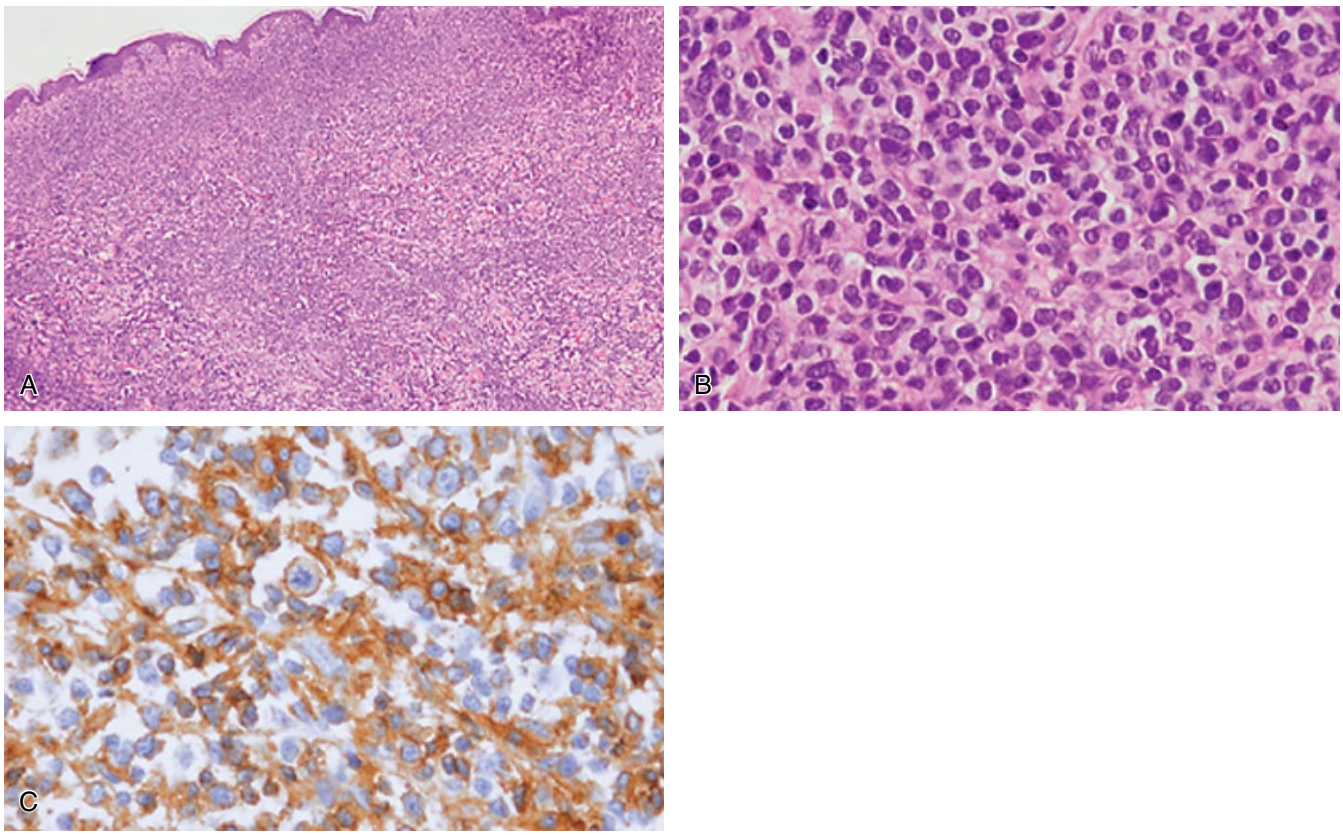

Fig. 22.33 Primary cutaneous small/medium CD4+ T-cell lymphoproliferative disorder. **A,** There is a dense diffuse lymphoid infiltrate throughout the entire dermis. **B,** At higher magnification the cells are predominantly small and medium-sized lymphocytes with positivity for CD4 **(C).**

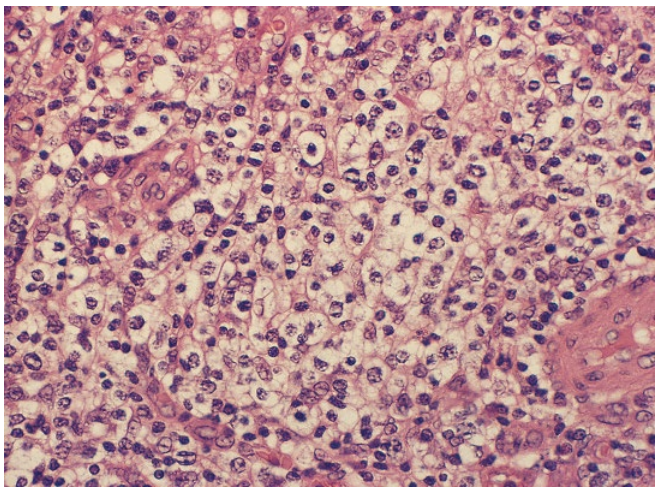

Fig. 22.34 Peripheral T-cell lymphoma, NOS. High-power view of a peripheral T-cell lymphoma of clear type showing a focus of neoplastic T cells with water-clear cytoplasm, which are commonly encountered in malignant lymphomas of peripheral T-cell lineage.

features. A variety of patterns of T-cell antigen expression are found (Figs. 22.37 and 22.38). Loss of one or more mature T-cell markers, mainly CD7, is seen. CD4 is more frequently positive than CD8. CD30 can be expressed in large cell tumors. Positivity for cytotoxic granules is rare in nodal disease, and EBV is usually not present in tumor cells. TCR genes are clonally rearranged in most cases. Complex karyotypes are often found. These tumors can infiltrate many organs and tissues. Involvement of skeletal muscle is shown in Fig. 22.39. Positron emission tomography is useful in detecting sites of involvement and the effectiveness of therapy (Fig. 22.40). The prognosis of these unspecified T-cell lymphomas is highly variable.

ANGIOIMMUNOBLASTIC T-CELL LYMPHOMA

Angioimmunoblastic T-cell lymphoma is characterized by a proliferation of neoplastic T-follicular helper cells (TFH) that are usually associated with a complex histologic picture that includes proliferating vessels, epithelioid histiocytes, plasma

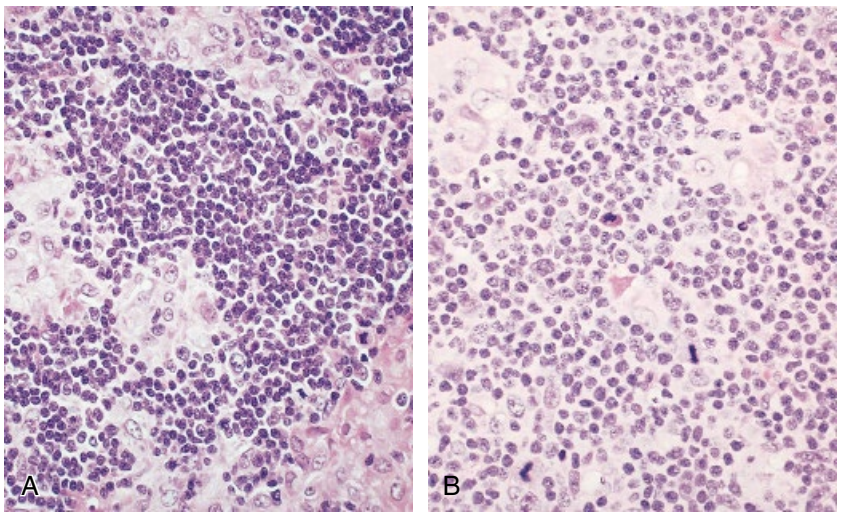

Fig. 22.35 Peripheral T-cell lymphoma, NOS, showing nodular accumulations of macrophages. **A, B,** This appearance corresponds to the lymphoepithelioid morphological variant of these lymphoma, although no evidence indicates that this variant has clinical differences from other PTCL, NOS. Clumps of epithelioid cells are interspersed with a mixed population of small and large lymphocytes with occasional mitoses and large atypical cells that resemble Reed–Sternberg cells. The small cells show irregular angular nuclei. The tumor T cells are thought to produce lymphokines that cause epithelioid cell formation from histiocytes. (Courtesy of Dr. JE McLaughlin.)

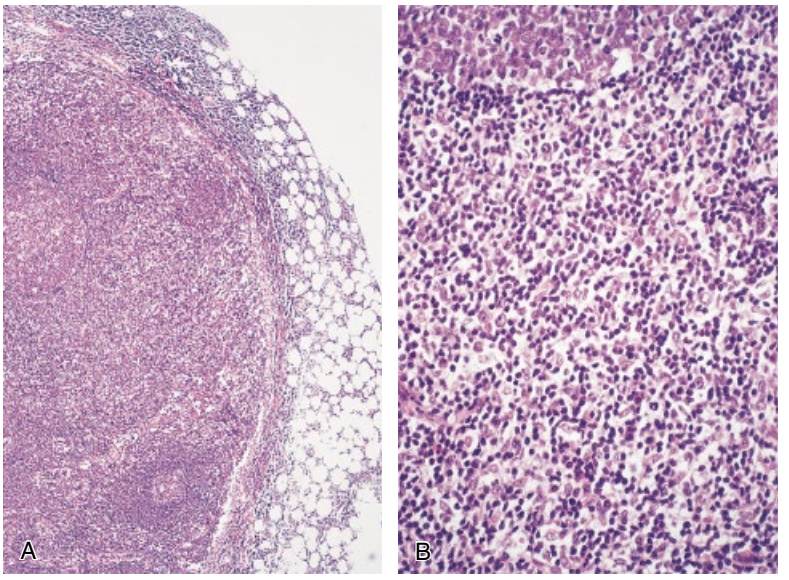

Fig. 22.36 Peripheral T-cell lymphoma, NOS. **A,** Expansion of paracortical region with wide separation of reactive follicles. **B,** High power shows many T lymphocytes with clear cytoplasm, eosinophils, and prominent venules. (Courtesy of Dr. JE McLaughlin.)

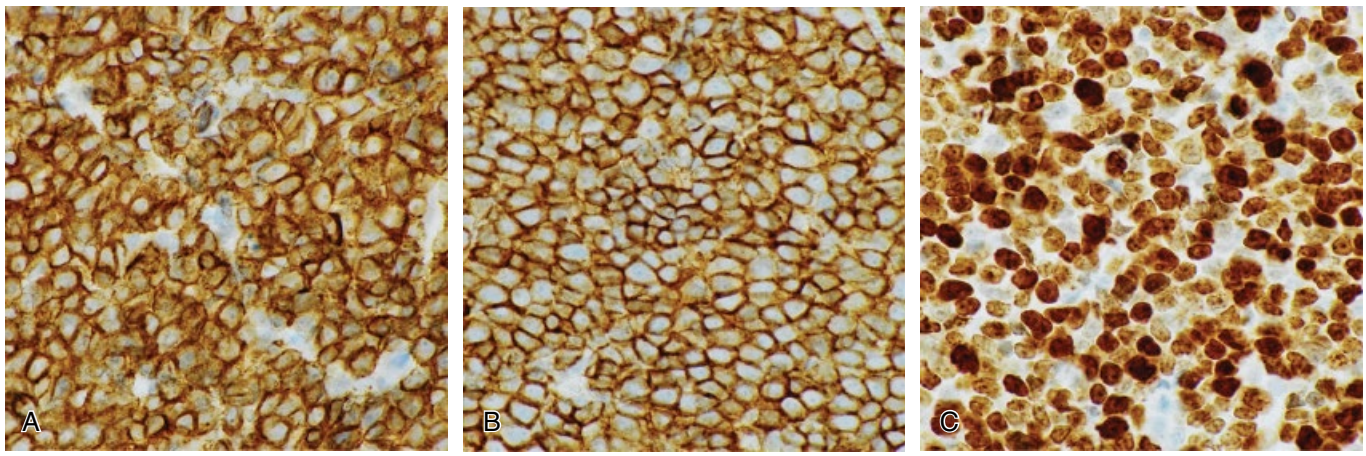

Fig. 22.37 Peripheral T-cell lymphoma, NOS. Immunoperoxidase stains showing positivity for CD3 **(A)** and CD5 **(B).** A high proliferation rate is indicated with Ki-67 **(C).**

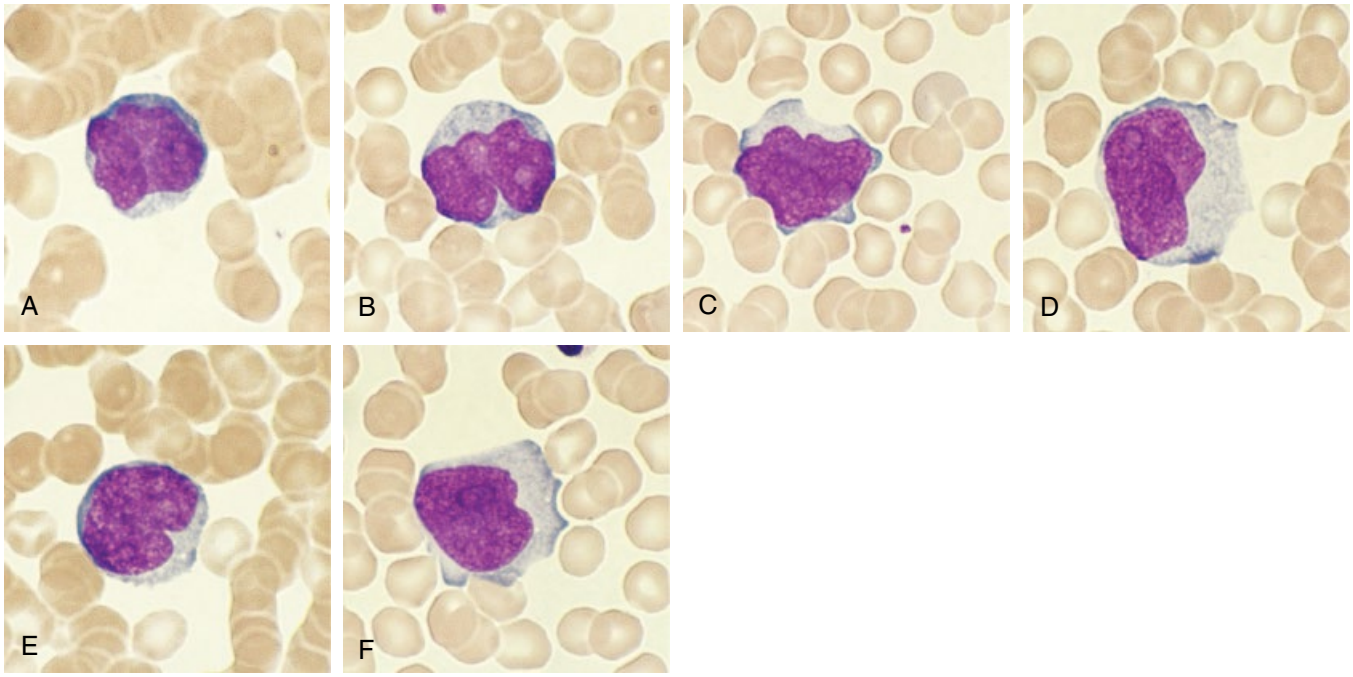

Fig. 22.38 Peripheral T-cell lymphoma, NOS. Peripheral blood film in same case as Fig. 22.37 showing selected atypical lymphoma cells.

cells, eosinophils, and hyperplastic clusters of follicular dendritic cells (Fig. 22.41). The neoplastic cells are of variable morphology and include atypical "clear" cells with indented nuclei and abundant pale cytoplasm. Immunohistology shows positivity for the T-cell markers CD3 and CD4 (Fig. 22.42). The tumor cells express the TFH markers PD1, CXCL13, CD10, BCL6, and ICOS. Hyperplastic clusters of follicular dendritic cells (CD35 and CD21+) may be prominent (Fig. 22.42C). EBV-positive B cells are frequently positive and recognized by EBER positivity (Fig. 22.42D). T-cell receptor genes are rearranged in 75% of cases. The most frequent cytogenetic abnormalities are trisomy 3, trisomy 5, and an additional X chromosome. Recurrent mutations have been identified in *IDH2* (20–30%), *TET2* (50–80%), *DNMT3A* (20–30%), and *RHOA* (60–70%). There is frequently involvement of bone marrow (Fig. 22.43), and occasionally the neoplastic T cells are seen in blood films (Fig. 22.44).

The disease is most frequent among the elderly and can manifest at multiple extranodal sites. Patients often have systemic symptoms such as weight loss, fever, skin rash (Fig. 22.45), and a polyclonal hypergammaglobulinemia. The disease is moderately aggressive; patients may die from infective complications, and a high-grade lymphoma (usually of T-cell but occasionally of B-cell type) may emerge. The median survival is less than 3 years.

ANAPLASTIC LARGE CELL LYMPHOMA, ALK POSITIVE

Anaplastic large cell lymphoma (ALCL), anaplastic lymphoma kinase (ALK) positive is a T-cell lymphoma usually composed of large atypical lymphoid cells with abundant cytoplasm and pleomorphic nuclei, and CD30 expression that carry a chromosomal

translocation involving the *ALK* gene that leads to its overexpression. These neoplasms tend to share unusual morphologic features with cohesive "pseudo-carcinomatous" growth pattern and sinusoidal invasion of the tumor cells that can mimic a metastatic carcinoma. The tumor cells can be large bizarre with abundant cytoplasm, and pleomorphic, often horseshoe-shaped nuclei. The most common translocation activating *ALK* in these tumors is the t(2;5)(q23;q35) that creates the *NPM-ALK* fusion gene, encoding a hybrid tyrosine kinase. Other variant translocations in which *ALK* can be fused to other gene partners can be found: the t(1;2) (*TPM3-ALK*), t(2,3) (*TFG-ALK*), and t(2;17) (*CLTC-ALK*) translocation, among others. All these translocation have the same effect of activating the expression of ALK.

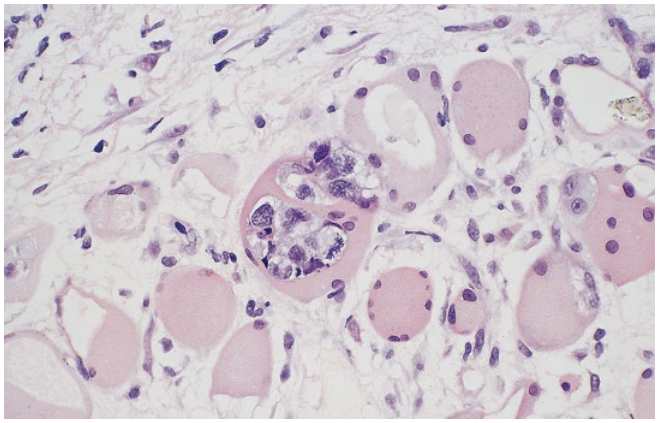

Fig. 22.39 Peripheral T-cell lymphoma, NOS. Neoplastic cells are invading striated muscle.

Typical biopsy appearances are shown in Fig. 22.46. The tumor cells are positive for CD30 on the cell membrane and in the Golgi region (Fig. 22.47 A) and their distribution is often perivascular (Fig. 22.46 B). ALK staining is usually both cytoplasmic and nuclear (Fig. 22.47 C). One or more T-cell antigens, EMA, and the cytotoxic-associated antigens granzyme B, perforin, and TIA-1 are positive in the great majority of cases (Fig. 22.47 D and *E*). CD3 is negative in most cases. Approximately 90% of these tumors show clonal rearrangement of the T-cell receptor. EBV sequences are absent.

ALCL is most frequent in the first three decades of life. It accounts for approximately 3% of adult non-Hodgkin lymphomas and up to 30% of childhood lymphomas. The disease involves both lymph nodes and extranodal sites. Bone marrow involvement (Figs. 22.48–22.50) is present in up to 30% of cases if immunostaining for CD30, EMA, and ALK is employed. In occasional patients, large neoplastic T cells are seen in blood films (Fig. 22.51). Chemotherapy is often curative, particularly in children. The overall 5-year survival rate in ALK-positive ALCL is close to 80%.

ANAPLASTIC LARGE CELL LYMPHOMA, ALK NEGATIVE

ALK-negative cases of ALCL are less well characterized. Patients are generally older, and the disease has a more aggressive course and less favorable prognosis. The histologic appearances are similar to ALK-positive disease, and the neoplastic cells are generally larger and more pleomorphic. There are no differences in phenotypic or molecular markers other than the ALK negativity.

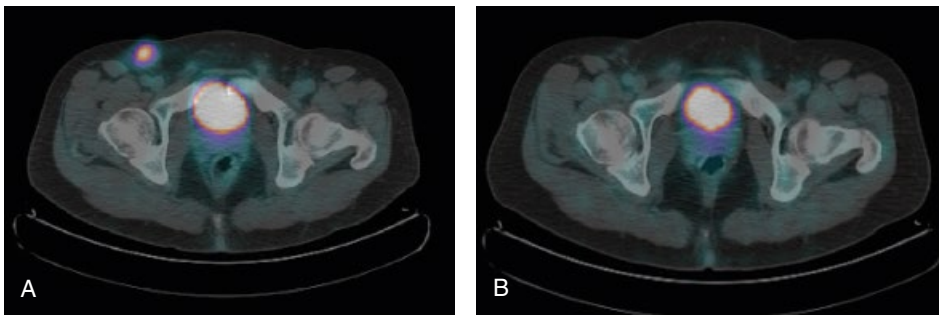

Fig. 22.40 Peripheral T-cell lymphoma, NOS. **A,** Right groin disease is indicated by axial fused FDG PET/CT. **B,** Following chemotherapy the corresponding image shows a complete metabolic response. (Courtesy of Dr. G Cook.)

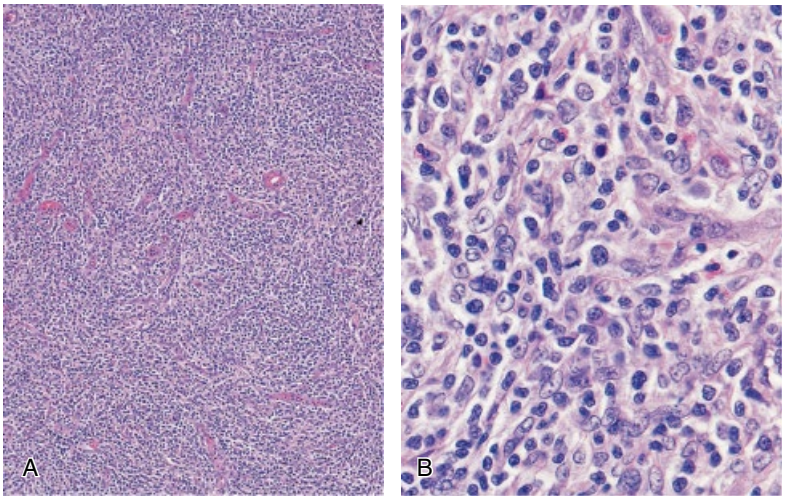

Fig. 22.41 Angioimmunoblastic T-cell lymphoma: **A,** Low-power view showing prominent arborizing vascular pattern. **B,** High-power view showing clear cell cytology of the neoplastic T cells.

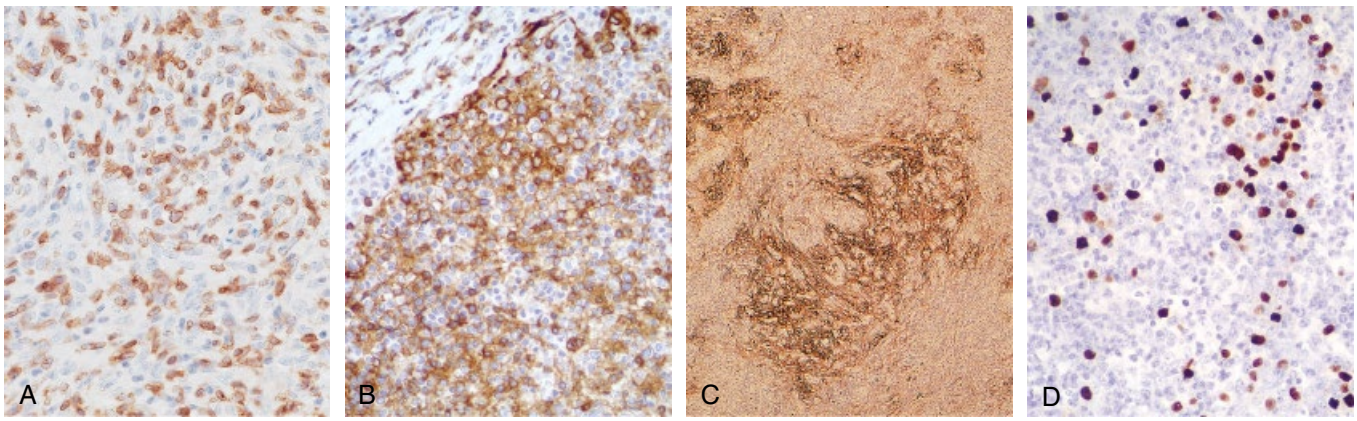

Fig. 22.42 Angioimmunoblastic T-cell lymphoma: Immunoperoxidase staining. The neoplastic T-cells show positive staining for **A,** CD3 and **B,** CD4. **C,** CD21 positivity identifies perivascular proliferation of follicular dendritic cells. **D,** Numerous cells are positive for EBER. By double staining most of these EBER positive cells are CD20 positive B cells. (**B, D,** Courtesy of Dr. G Taylor.)

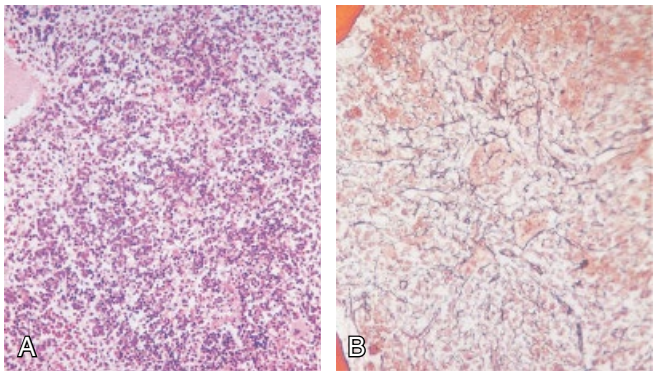

Fig. 22.43 Angioimmunoblastic T-cell lymphoma: Bone marrow trephine biopsy. **A,** Extensive replacement of hemopoietic cells by abnormal lymphoid tissue. **B,** Silver impregnation staining outlines the characteristic arborizing vascular pattern of the condition.

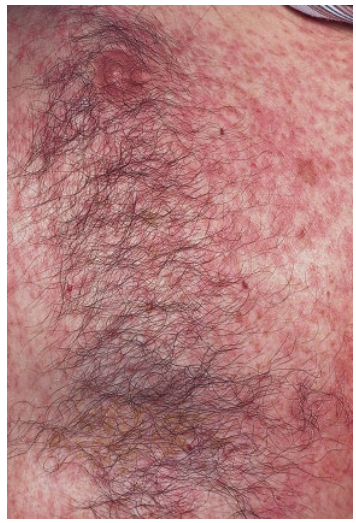

Fig. 22.45 Angioimmunoblastic T-cell lymphoma. Skin appearances of a 65-year-old man with fever, an erythematous rash, and lymphadenopathy. He subsequently died of a high-grade lymphoma.

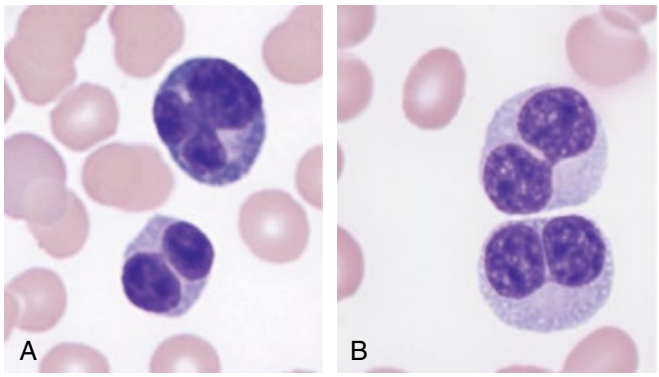

Fig. 22.44 Angioimmunoblastic T-cell lymphoma: Peripheral blood film. **A** and **B,** The atypical lymphoid cells show nuclear lobation and segmentation. (Courtesy of Dr. W Erber.)

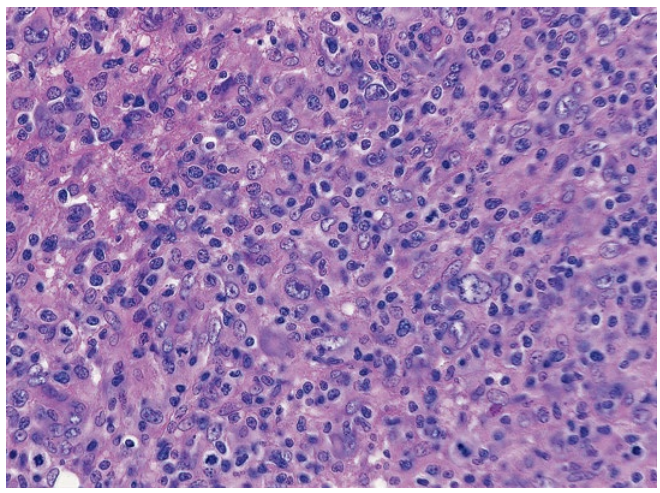

Fig. 22.46 Anaplastic large cell lymphoma. High-power view showing typical cytologic features with large cells with prominent nucleoli, abundant cytoplasm, and prominent Golgi zones.

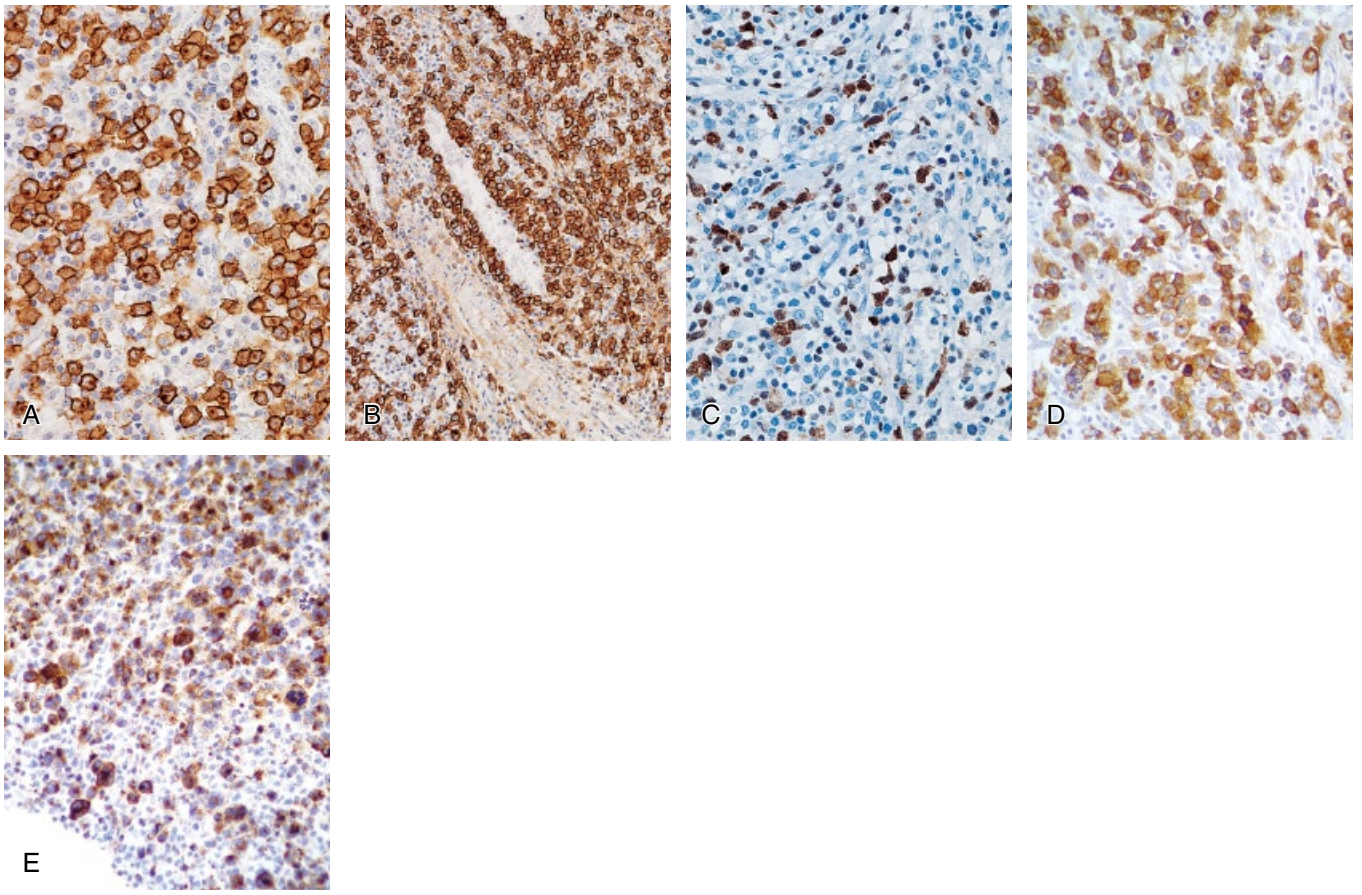

Fig. 22.47 Anaplastic large cell lymphoma: Immunoperoxidase staining. **A,** Positive cell membrane and Golgi zone staining for CD30. **B,** CD30 positivity showing perivascular accumulation of tumor cells. **C,** The neoplastic cells show nuclear and cytoplasmic positivity for ALK. **D,** The cells are also positive for EMA. **E,** Positivity for granzyme B. (*D* and *E,* Courtesy of Dr. G Taylor.)

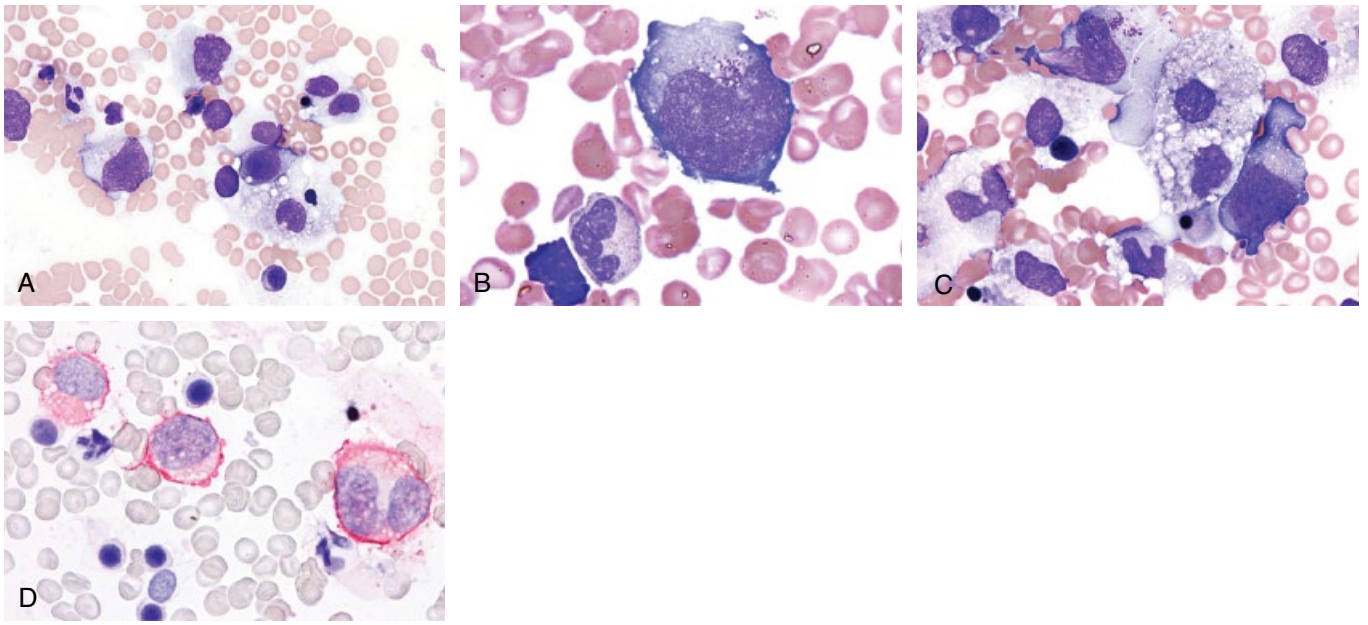

Fig. 22.48 Anaplastic large cell lymphoma: bone marrow aspirate. **A–C,** MGG stain. The tumor cells are large and pleomorphic with prominent nucleoli and pale cytoplasm. The two large vacuolated cells are histiocytes. **D,** Immunoperoxidase staining shows membrane positivity for CD30 in the large neoplastic cells. (Courtesy of Dr. W Erber.)

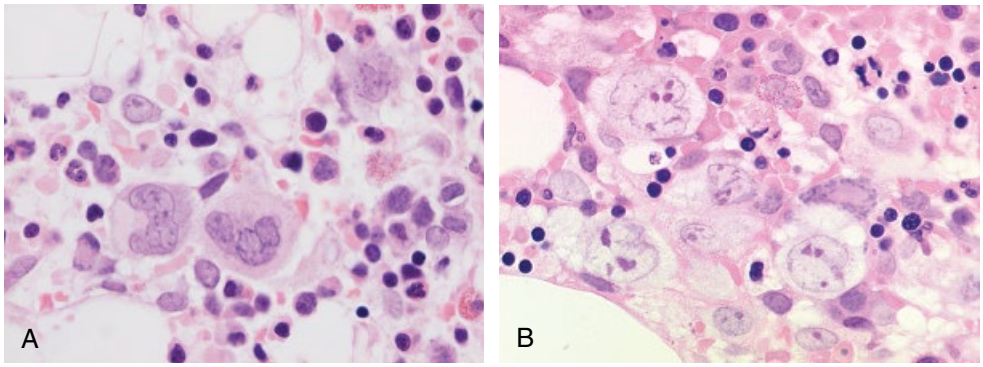

Fig. 22.49 Anaplastic large cell lymphoma: Bone marrow trephine biopsy. **A,** The lymphoma cells are large with prominent nucleoli and abundant agranular cytoplasm. **B,** In this patient there was an associated hemophagocytic syndrome. The large lymphoma cells show cytoplasm with prominent large vacuoles. (Courtesy of Dr. W Erber.)

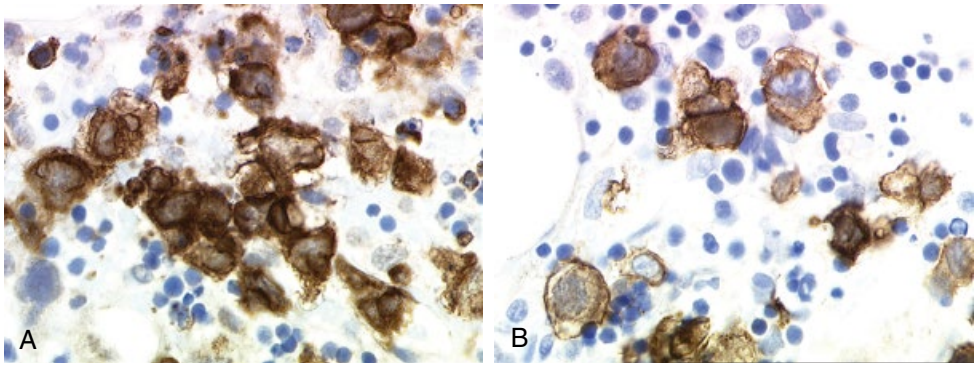

Fig. 22.50 Anaplastic large cell lymphoma: Immunoperoxidase staining, same case as Fig. 22.49, *B*. **A,** Positive staining for CD3. **B,** Positive staining for CD30. (Courtesy of Dr. W Erber.)

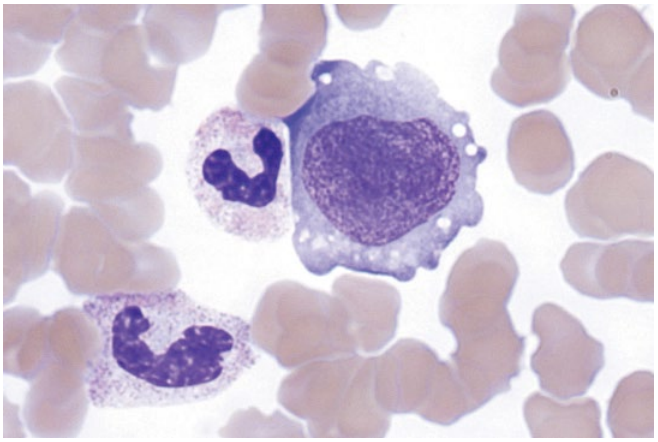

Fig. 22.51 Anaplastic large cell lymphoma. Peripheral blood film showing two band form neutrophils and a very large atypical lymphoma cell with multiple nucleoli, a vesicular nuclear chromatin pattern, and abundant pale vacuolated cytoplasm. (Courtesy of Dr. W Erber.)

CHAPTER

23

HODGKIN LYMPHOMA

Hodgkin lymphoma is one of the most common categories of lymphoid neoplasia that frequently affects the lymph nodes and rarely extranodal sites.

PRESENTATION AND EVOLUTION

In many patients, at presentation the disease is localized to a single peripheral lymph node region, and studies of its natural history indicate that its subsequent progression is initially by direct contiguity within the lymphatic system.

With advanced disease, dissemination involves nonlymphatic tissue. The disease affects all age groups, but is particularly common in young and middle-aged adults. Most patients have a painless, asymmetric, firm, and discrete enlargement of the superficial lymph nodes (Figs. 23.1 and 23.2). Mediastinal disease, occasionally accompanied by an obstructed superior vena cava (Fig. 23.3) and involvement of retroperitoneal lymph nodes can be detected during staging procedures. Clinical splenomegaly occurs during the course of the disease in 50% of patients. Rarely, patients have lymphatic obstruction (Fig. 23.4).

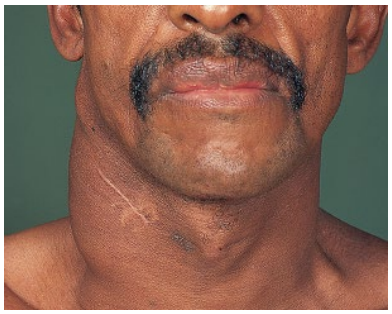

Fig. 23.1. Hodgkin lymphoma. Right-sided cervical lymphadenopathy. The scar of previous biopsy incision is well healed.

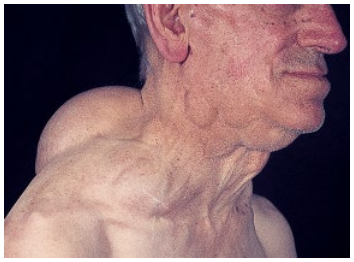

Fig. 23.2. Hodgkin lymphoma. Massive cervical lymphadenopathy in a 73-year-old man with extensive disease.

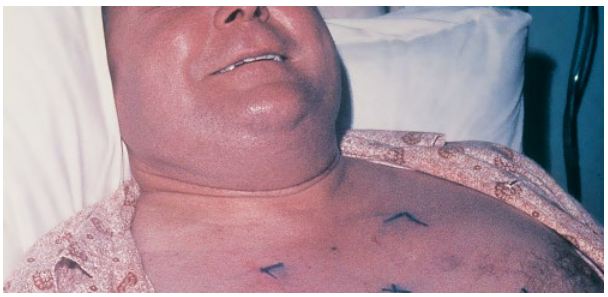

Fig. 23.3. Hodgkin lymphoma. Cyanosis and edema of the face, neck, and upper trunk result from superior vena cava obstruction caused by mediastinal node involvement. The skin markings over the anterior chest indicate the field of radiotherapy.

The disease involves the liver, very rarely the skin (Fig. 23.5), and other organs, for example, the gastrointestinal tract or brain and, in rare patients, the retina (Fig. 23.6). Depressed cell-mediated immunity is also present and is associated with an increased incidence of infections, particularly herpes zoster (Fig. 23.7), fungal diseases, and tuberculosis.

Occasionally, the first indication of Hodgkin lymphoma follows fine-needle aspiration of enlarged nodes (Figs. 23.8 and 23.9). The diagnosis is usually made from histologic examination of excised lymph nodes. The affected nodes are enlarged and show pale translucent cut surfaces (Fig. 23.10). Initially the nodes remain discrete, but later in the disease they become matted together and can invade surrounding tissues. Hodgkin tissue in other organs has a similar pale, flesh-like appearance (Fig. 23.11).

HISTOLOGY

Hodgkin lymphoma is characterized by the presence of Reed–Sternberg cells, which are multinucleated cells, typically with prominent nucleoli and abundant violaceous cytoplasm (as seen in routine H&E staining; Figs. 23.12–23.14). The diagnosis of Hodgkin lymphoma is made when Reed–Sternberg cells are found against a proper background usually composed of a variable amount of of lymphocytes, histiocytes, neutrophils, and eosinophils (Figs. 23.13 and 23.14), which distinguishes the disease from other conditions (occasional viral infections, drug reactions, non-Hodgkin lymphomas) in which cells with cytologic features resembling Reed–Sternberg cells are found.

Color Atlas of Clinical Hematology: Molecular and Cellular Basis of Disease, Fifth Edition. A. Victor Hoffbrand, Paresh Vyas, Elías Campo, Torsten Haferlach, and Keith Gomez

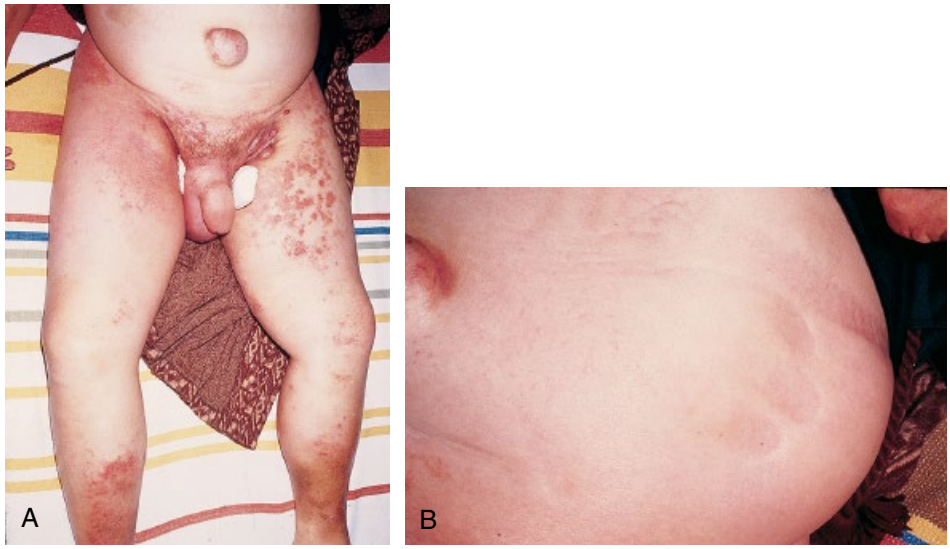

Fig. 23.4. Hodgkin lymphoma. **A**, Gross edema of the legs, genitals, and lower abdominal wall with umbilical herniation caused by lymphatic obstruction that resulted from extensive involvement of the inguinal and pelvic lymph nodes. A staphylococcal infection in the skin folds of the groin is present. **B,** A close-up view of "pitting" edema of the abdominal wall is shown.

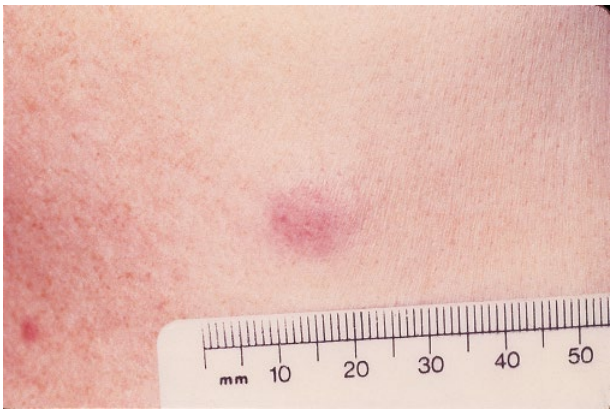

Fig. 23.5. Hodgkin lymphoma. A skin deposit approximately 1 cm in diameter is shown.

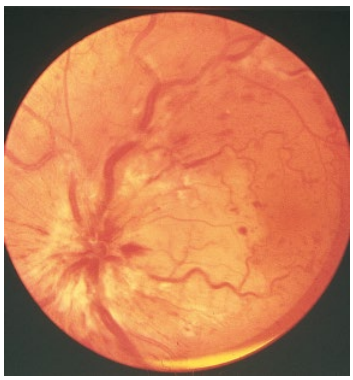

Fig. 23.6. Hodgkin lymphoma. Extensive infiltration of the optic disc and surrounding retina.

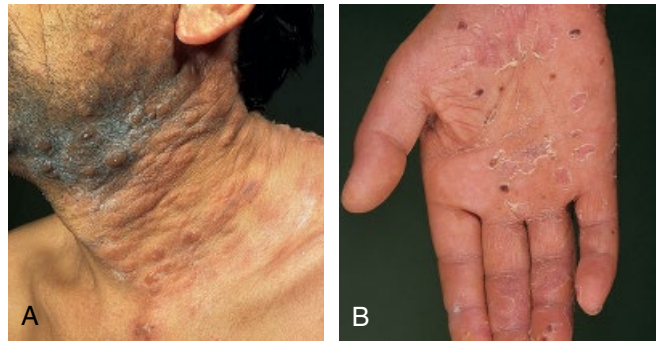

Fig. 23.7. Hodgkin lymphoma. **A,** Vesicular cutaneous eruption of the neck caused by herpes zoster. **B,** Atypical herpetic eruption of the palmar surface of the hand.

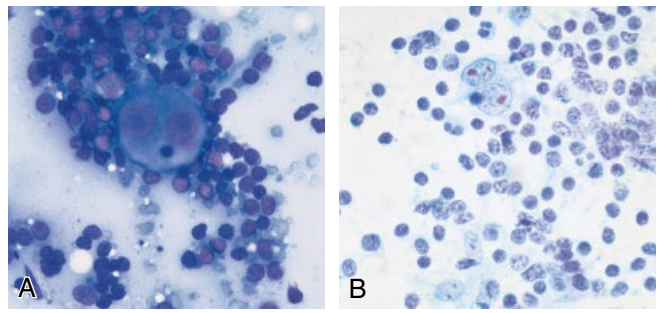

Fig. 23.8. Hodgkin lymphoma. Fine-needle aspirates of involved lymph nodes showing Reed–Sternberg cells stained by **(A)** May-Grünwald–Giemsa and **(B)** Papanicolaou techniques.

HODGKIN REED–STERNBERG CELL

The Reed–Sternberg cells of classic Hodgkin lymphoma have a unique phenotype, usually being positive for both CD15 and CD30 (Fig. 23.15). They do not show phenotypes found in normal lymphocytes. Molecular studies relying on single-cell micromanipulation and amplification of RNA and genomic DNA by polymerase chain reaction (PCR) have established a B-cell origin for Reed–Sternberg cells. Recurrent mutations involving genes of the I κB family are usually present. In most patients the Reed–Sternberg cells have clonal rearrangement of the V, D, and J segments of the immunoglobulin heavy chain locus similar to mature B cells of germinal center or postgerminal center origin. However, in most cases the neoplastic Reed–Sternberg cells lose the phenotypic features of normal germinal center cells

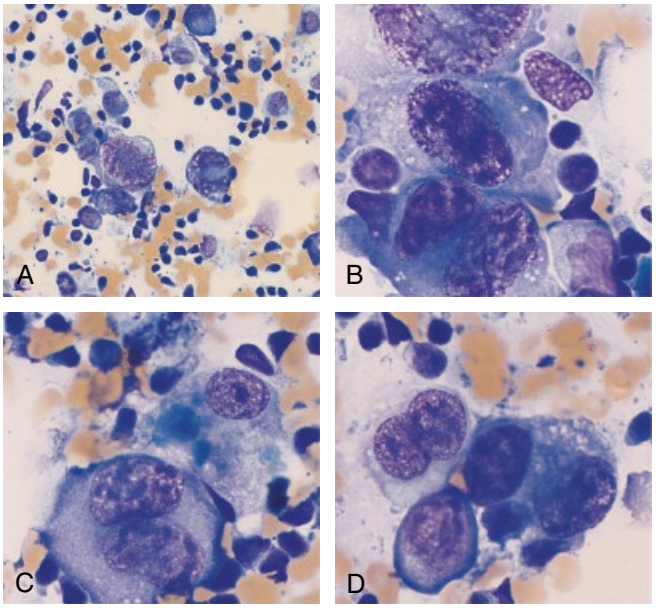

Fig. 23.9. Hodgkin lymphoma. **A,** Fine-needle aspirate of lymph node showing Reed–Sternberg cells, a mitotic figure, histiocytes, and lymphoid cells. **B–D,** At higher magnification, further Reed–Sternberg cells from the same fine-needle aspirate.

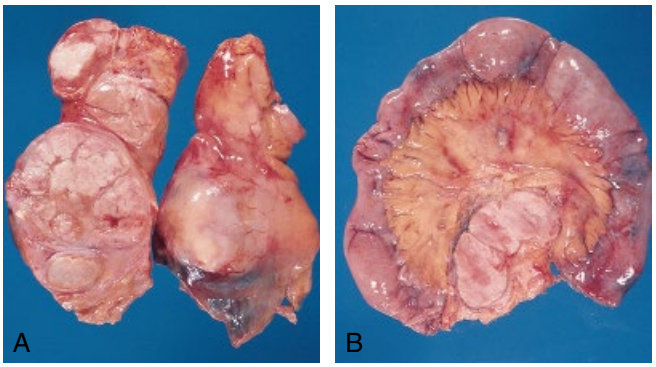

Fig. 23.10. Hodgkin lymphoma. **A,** Matted block of resected involved cervical nodes showing a cross-section of the pale, translucent, fleshy tumor tissue with areas of fibrosis and necrosis. **B,** Mesenteric lymph nodes removed at necropsy showing in cross-section the typical moist "fish flesh" appearance of this tumor.

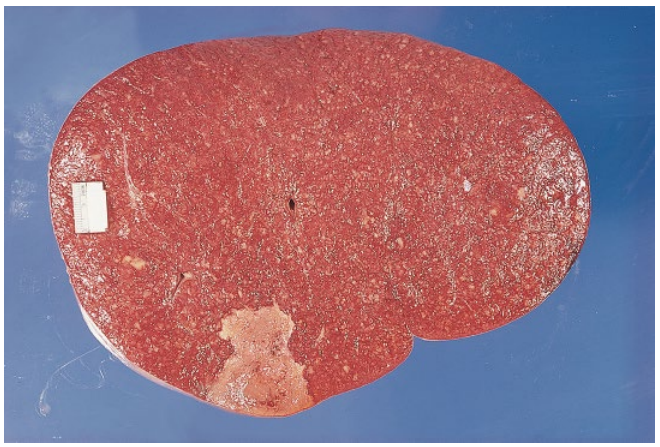

Fig. 23.11. Hodgkin lymphoma. Cross section of a spleen removed at laparotomy shows an ischemic necrosis adjacent to the capsule. Numerous scattered focal grayish-yellow areas up to 4 mm in diameter are also present.

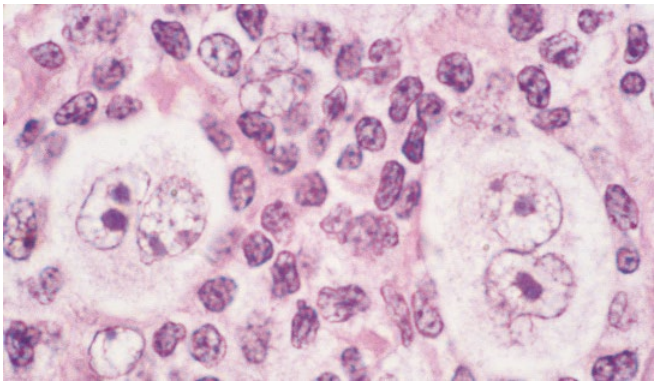

Fig. 23.12. Hodgkin lymphoma. High-power view of lymph node biopsy showing two typical multinucleate Reed–Sternberg cells surrounded by lymphocytes.

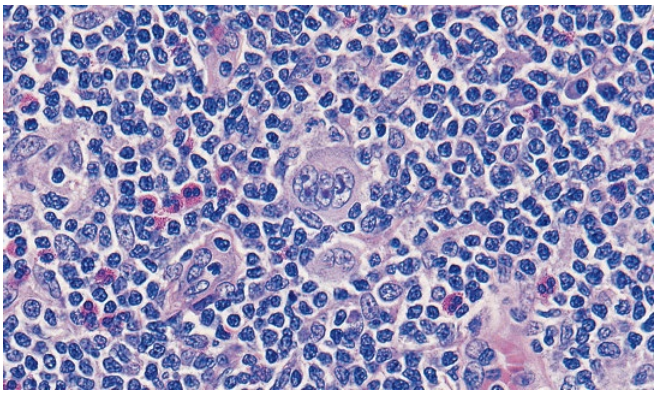

Fig. 23.13. Hodgkin lymphoma. Lymph node biopsy showing multinucleate Reed–Sternberg cells surrounded by lymphocytes, histiocytes, neutrophils, and eosinophils.

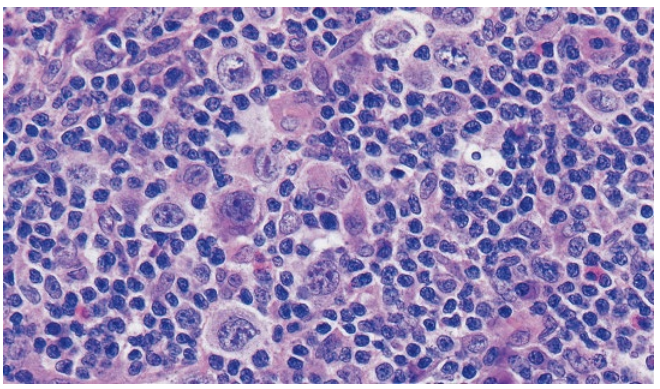

Fig. 23.14. Hodgkin lymphoma. Lymph node biopsy showing multiple Reed–Sternberg cells surrounded by lymphocytes and other mononuclear cells in mixed cellularity disease.

such as BCL-6 and only a minority show CD20. The B-cell transcription factor PAX5 is weakly expressed in virtually all cases. Somatic hypermutation usually results in a crippled cell with nonfunctioning immunoglobulin variable regions and failure to transcribe RNA for immunoglobulin. The absence of immunoglobulin gene expression can result from impaired activation of the immunoglobulin promotors and enhancers because of lack of expression of B-cell transcription factors (e.g. Oct2, BOB.1).

It appears likely that activation of the nuclear factor κB (NFκB) transcription factor signaling pathway is a reason for the growth

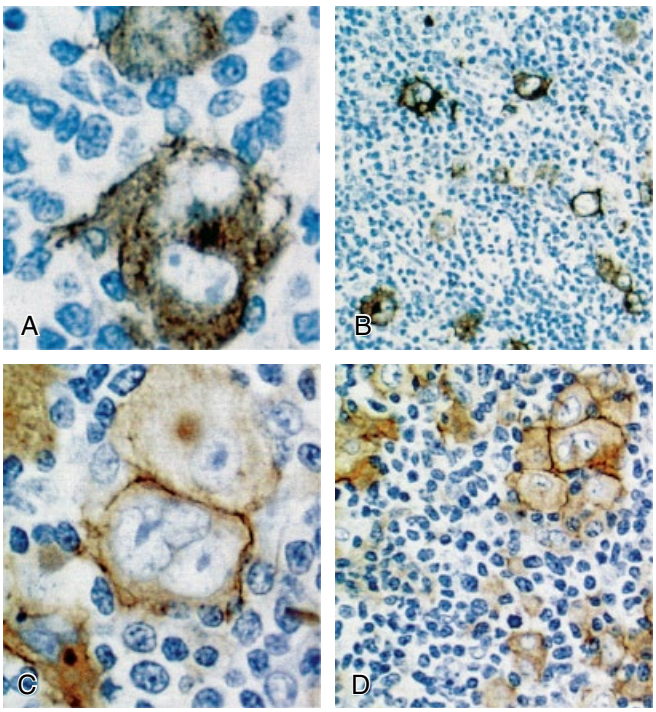

Fig. 23.15. Hodgkin lymphoma. Abnormal mononuclear Hodgkin cells and binucleate Reed–Sternberg cells are positively labeled for **(A,B)** CD 15 and **(C,D)** CD30. (*A–D,* Immunoperoxidase stain.)

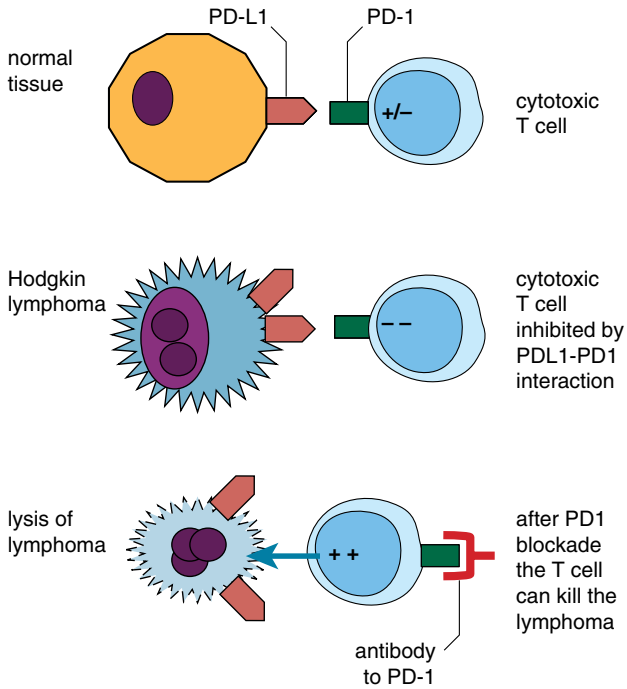

Fig. 23.16. Potential mechanism whereby Hodgkin lymphoma is controlled after treatment with antibodies to block PD-1. PD-1 and PD-L1 are natural molecules that limit the attack of normal tisssues by cytotoxic T cells. Hodgkin lymphoma overexpresses PD-L1 due to gene amplification or effects of EBV infection. This delivers a strong negative signal to the T cells around the tumor. If antibody-mediated blockade of PD-1 is used, the T cells can then recognize and kill the tumor. Source: Hoffbrand AV, et al. eds. *Postgraduate Haematology*, 7th edn. John Wiley & Sons, Ltd. 2016. Reproduced with permission of John Wiley and Sons.

and survival of the Reed–Sternberg cells of classic Hodgkin lymphoma. Epstein–Barr virus (EBV) present in most cases of mixed cellularity and lymphocyte depletion subtypes contribute to NFκB activation. The antiapoptotic action of NFκB may help prevent these crippled cells from being negatively selected for apoptosis. The Reed–Sternberg cells express high levels of the ligand PD-L1. This links to PD-1 on T cells which prevents the T cells from killing the neoplastic cells (Fig. 23.16). Anti-PD-1 antibodies block the inhibitory molecule PD-1 and so allow the T cells to destroy the Hodgkin lymphoma.

The presence of EBV in Reed–Sternberg cells varies from 75% in the mixed cellularity subtype to as low as 10–40% in nodular sclerosis Hodgkin lymphoma. In human immunodeficiency virus (HIV) infected patients and those living in developing countries, positivity for EBV approaches 100%.

In Hodgkin lymphoma there are variable but nonspecific cytogenetic abnormalities. Aneuploidy and hypertetraploidy reflect the multinuclearity of the Reed–Sternberg cells. Many cases show 14q abnormalities, and fluorescence in situ hybridization (FISH) analysis has shown abnormalities in chromosome number in most cases. Intraclonal variability reflects chromosome instability.

CLASSIFICATION OF HODGKIN LYMPHOMA

The World Health Organization (WHO) histologic classification of Hodgkin lymphoma is shown in Table 23.1.

NODULAR SCLEROSING HODGKIN LYMPHOMA

In nodular sclerosing Hodgkin lymphoma, normal lymph nodal architecture is replaced by a nodular proliferation of tumor surrounded by birefringent collagen. This subtype accounts

TABLE 23.1 HODGKIN LYMPHOMA: WORLD HEALTH ORGANIZATION HISTOLOGIC CLASSIFICATION

Type	Features
Nodular lymphocyte predominance Hodgkin lymphoma	Lymphocyte proliferation of irregular nodules that contain abnormal polymorphic B cells (LP or "popcorn" cells) Reed–Sternberg cells are absent
Classic Hodgkin lymphoma	
Nodular sclerosis	Tumor nodules surrounded by collagen bands extending from nodal capsule
Grades I and II (see text)	Characteristic "lacunar cell" variant of Reed–Sternberg cell often seen
Mixed cellularity	Numerous Reed–Sternberg cells seen No sclerosis or fibrosis Intermediate numbers of lymphocytes
Lymphocyte rich	Scanty Reed–Sternberg cells; multiple small lymphocytes with few eosinophils and plasma cells; nodular and diffuse types
Lymphocyte depleted	"Reticular" pattern with predominant Reed–Sternberg cells and sparse lymphocytes or "diffuse fibrosis" with disordered connective tissue, few lymphocytes, and infrequent Reed–Sternberg cells This subtype is very rarely diagnosed currently

for about 70% of all cases of classic disease. The median age of presentation is 28 years, and the incidence is equal in males and females. Mediastinal involvement is present in 80% of cases and in over 50% there are large tumors. Most patients present with stage II disease, and B symptoms are present in approximately 40%.

Lymph node histology reveals classic Hodgkin lymphoma with a nodular growth pattern. Broad collagen bands surround the tumor (Fig. 23.17), and there is usually a fibrous thickening of the nodal capsule. The nodules contain variable numbers of Reed–Sternberg cells, small lymphocytes, and other non-neoplastic inflammatory cells, including eosinophils and neutrophils. A further diagnostic feature is the presence of the lacunar cells, which are Reed–Sternberg cell variants with friable cytoplasmic processes that open up into a "lake-like" appearance when subjected to routine processing (Fig. 23.18).

When Reed–Sternberg cells are particularly numerous, cohesive, or pleomorphic (the criteria are subjective but about >25% of the node or cells should be affected), the condition is believed to carry a worse prognosis and is graded by the British National Lymphoma Investigation group and WHO as Grade II. All other nodular sclerosis cases are Grade I. This grading is controversial, and many oncologists fail to find it of any prognostic value.

Reed–Sternberg cells show the classic Hodgkin lymphoma phenotype with positivity for CD15 and CD30 (Fig. 23.15). EBV encoded latent membrane protein 1 (LMP1) is less frequently positive (10–40%) than in other subtypes.

MIXED CELLULARITY HODGKIN LYMPHOMA

This subtype makes up 20–25% of classic Hodgkin lymphoma. There is a 70% male predominance, and an increased prevalence in HIV-infected patients and in developing countries. Mixed cellularity disease is often stage III or IV at presentation.

Histology of involved nodes show typical Reed–Sternberg cells in a diffuse or partly nodular mixed inflammatory background of lymphocytes, and variable numbers of eosinophils, neutrophils, histiocytes, and plasma cells (Fig. 23.19). There can be small granulomatous clusters of epithelioid histiocytes.

Reed–Sternberg cells show classic CD15 and CD30 phenotype. In 70% of patients, the EBV encoded LMP1 is positive (Fig. 23.20).

LYMPHOCYTE-RICH CLASSIC HODGKIN LYMPHOMA

The term "*lymphocyte-rich classic Hodgkin lymphoma*" is applied to morphologic variants characterized by an abundance of small lymphocytes with relatively scanty Reed–Sternberg cells and very few eosinophils and plasma cells. This variant makes up only 5–10% of all cases of Hodgkin lymphoma, peripheral lymph nodes are usually involved, and most patients have stage I or II disease without B symptoms. In the more common nodular variant there is expansion of tumor in the mantle zones and attenuation of surrounding T zones (Fig. 23.21, *A–C*). The sparsely distributed

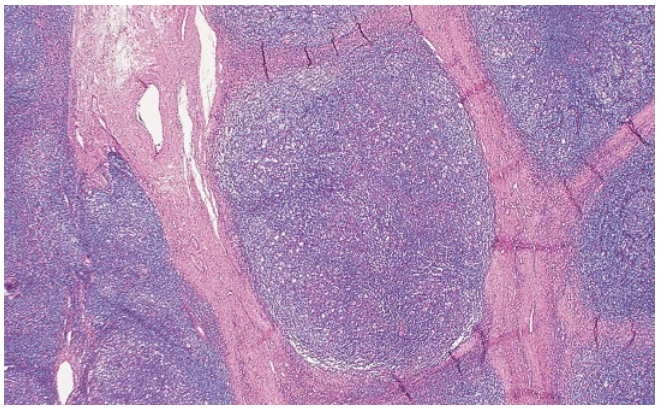

Fig. 23.17. Hodgkin lymphoma. Lymph node biopsy showing abundant bands of collagenous connective tissue separating areas of abnormal Hodgkin tissue in the nodular sclerosis type.

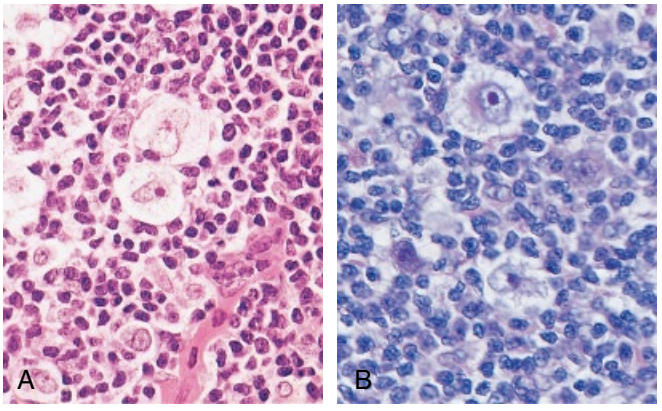

Fig. 23.18. Hodgkin lymphoma. **A,B,** High-power views of "lacunar" variants of Reed–Sternberg cells.

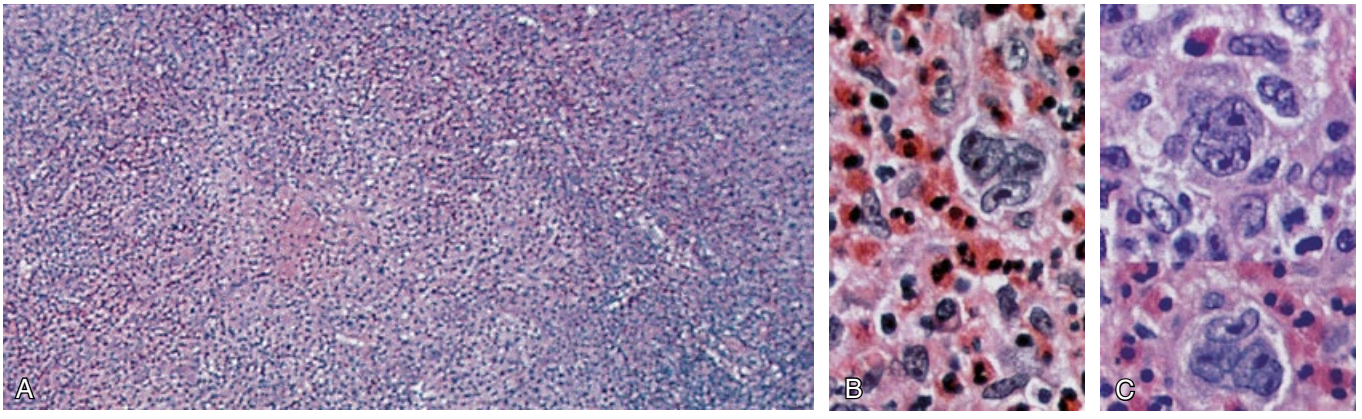

Fig. 23.19. Hodgkin lymphoma. Mixed cellularity disease showing Reed–Sternberg cells surrounded by a mixed population of lymphocytes and eosinophils. **A,** Low power. **B,C,** Higher powers.

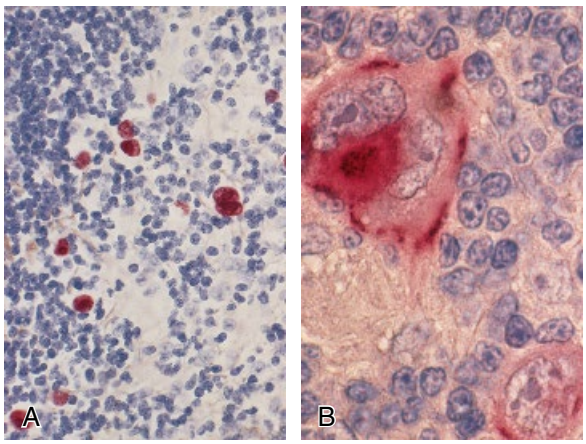

Fig. 23.20. Mixed cellularity Hodgkin lymphoma. **A,** In situ hybridization for EBV-encoded small nuclear RNAs (EBER1 and 2). Note the strong selective staining of the Hodgkin and Reed–Sternberg cells. **B,** Immunoalkaline phosphatase (APAAP) staining for the EBV-encoded latent membrane protein. Note the strong selective staining of the two Reed–Sternberg cells. (Courtesy of Professor H Stein.)

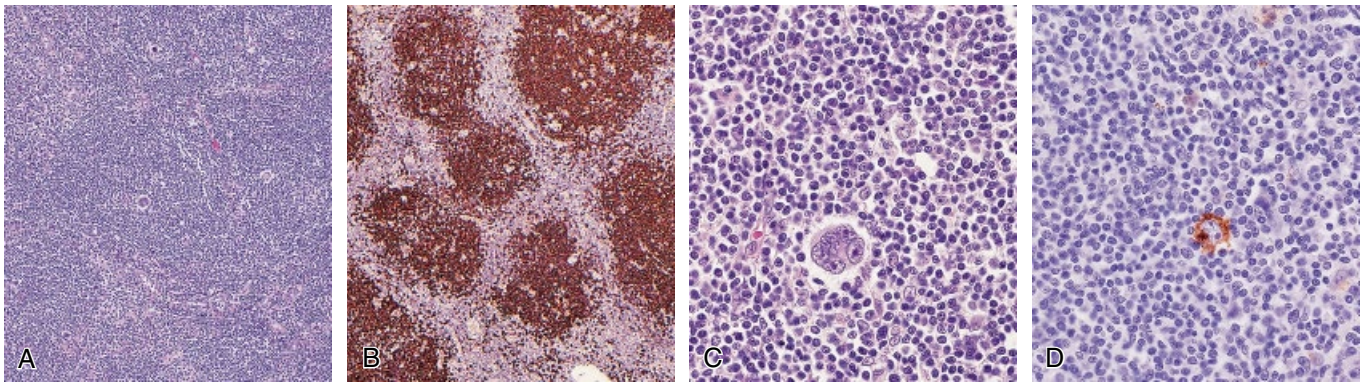

Fig. 23.21. Lymphocyte-rich classic Hodgkin lymphoma. **A,** Low-power view showing nodular growth pattern. **B,** Immunostain for CD20 shows that the nodules are composed of small B cells. **C,D,** Diffuse growth pattern. A high-power view **(C)** shows a single Reed–Sternberg cell in a sea of small lymphoid cells, and **(D)** immunostaining for CD30 highlights Hodgkin and Reed–Sternberg cells.

Reed–Sternberg cells show positivity for CD30 (Fig. 23.21, *D*) and CD15 similar to that found in other subtypes of classic Hodgkin lymphoma. In the rarer diffuse variant there is no evidence of involvement of germinal centers, and isolated Reed–Sternberg cells can be surrounded by lymphocytes and histiocytes. The prognosis with modern therapy is better than that in other forms of classic Hodgkin lymphoma, and survival is similar to that of nodular lymphocyte-predominant Hodgkin lymphoma.

LYMPHOCYTE-DEPLETED HODGKIN LYMPHOMA

In lymphocyte-depleted Hodgkin lymphoma, Reed–Sternberg cells are present as sheets or clusters within a fibrous stroma containing small numbers of lymphocytes with no surrounding inflammatory cells (Fig. 23.22). In a fibrotic variant the fibrous stroma is dominant with only small numbers of Reed–Sternberg cells (Fig. 23.30). These lymphocyte-depleted Hodgkin lymphomas are rarely diagnosed in current clinical practice and make up less than 5% of all Hodgkin lymphomas. Most lymphoma pathology groups that have reviewed their cases of this subtype and have applied immunostaining criteria have reclassified them as large B-cell lymphomas or anaplastic large cell lymphoma. Lymphocyte-depleted Hodgkin lymphoma usually occurs in those over 50 years of age, with a high frequency of advanced disease, abdominal and bone marrow involvement, and B-category symptoms. It is often now associated with HIV infection, and there is a low complete remission rate and poor survival.

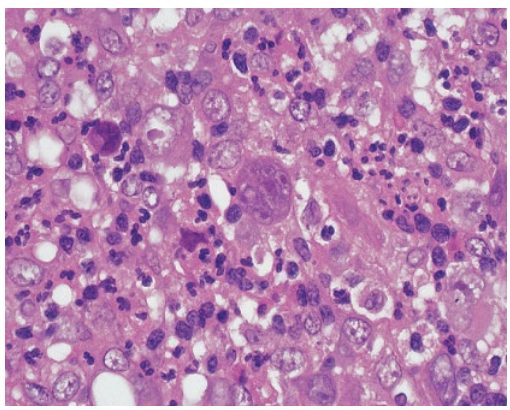

Fig. 23.22. Hodgkin lymphoma: Lymphocyte depleted. Frequent Reed–Sternberg and mononuclear cells are present with a paucity of inflammatory cells.

The Reed–Sternberg cells show a similar immunophenotype to other forms of classic Hodgkin lymphoma. The majority of HIV-positive patients are EBV infected, and immunostains for LMP1 are positive.

NODULAR LYMPHOCYTE-PREDOMINANT HODGKIN LYMPHOMA

Nodular lymphocyte-predominant Hodgkin lymphoma (NLPHL) is a distinct entity from classic Hodgkin lymphoma. It has always been recognized as quite separate from other types

of Hodgkin lymphoma in view of its good prognosis, with or without treatment, and its unique histology (especially the lack of Reed–Sternberg cells). It usually manifests in older patients as stage I disease.

The lymph node histology shows replacement of normal architecture by a nodular or nodular and diffuse population of small lymphocytes, epithelioid histiocytes, and intermingling foci of atypical large neoplastic cells known as lymphocyte-predominant (LP) cells. These cells usually have a single nucleolus and scanty cytoplasm (Fig. 23.23, *A* and *C*). The nuclei of the largest cells are often polylobated to such an extent as to be called "popcorn" cells. The nucleoli of these giant cells are often multiple but smaller than those of classic Hodgkin lymphoma (Figs. 23.23, *C;* 23.32; and 23.33).

Unlike the Reed–Sternberg cell of classic Hodgkin lymphoma, the neoplastic cells of NLPHL show immunopositivity for the B-cell associated antigens CD19, CD20, CD22, CD79a, and intense PAX5 (Figs. 23.23, *B* and *D;* and 23.34, *A* and *B*); J chain and CD45 are demonstrated in most cases and EMA (Fig. 23.23, *A*) in over 50%. They also express the nuclear protein encoded by *BCL6*. Immunostaining shows expression of the transcription factor Oct2 (Fig. 23.24, *B*). The cells also express the Oct2 cofactor BOB.1 (Fig. 23.24, *C*) but are negative for both CD30 and CD15. Surrounding the neoplastic LP cells there is usually a corona of T cells, positive for CD3 (Fig. 23.23, *E*) , PD1 and CD57.

Sensitive PCR techniques of isolated LP cells show rearranged and hypermutated immunoglobulin heavy chain genes (VH) and ongoing mutations. In most cases the rearrangements are functional and immunoglobulin mRNA transcripts are detectable. Nonspecific cytogenetic abnormalities in chromosome number similar to those found in classic Hodgkin lymphoma and other variable mutations are present in most cases studied.

The genetic, immunophenotypic, and cytologic features support a B-cell tumor arising from proliferating centroblasts of the germinal center.

Significant morphologic and phenotypic differences between Reed–Sternberg cells and the LP neoplastic cells of NLPHL are shown in Table 23.2.

STAGING TECHNIQUES

The prognosis and selection of the optimum treatment depends on accurate staging of the disease (Table 23.3). After thorough clinical examination, a number of laboratory and radiologic

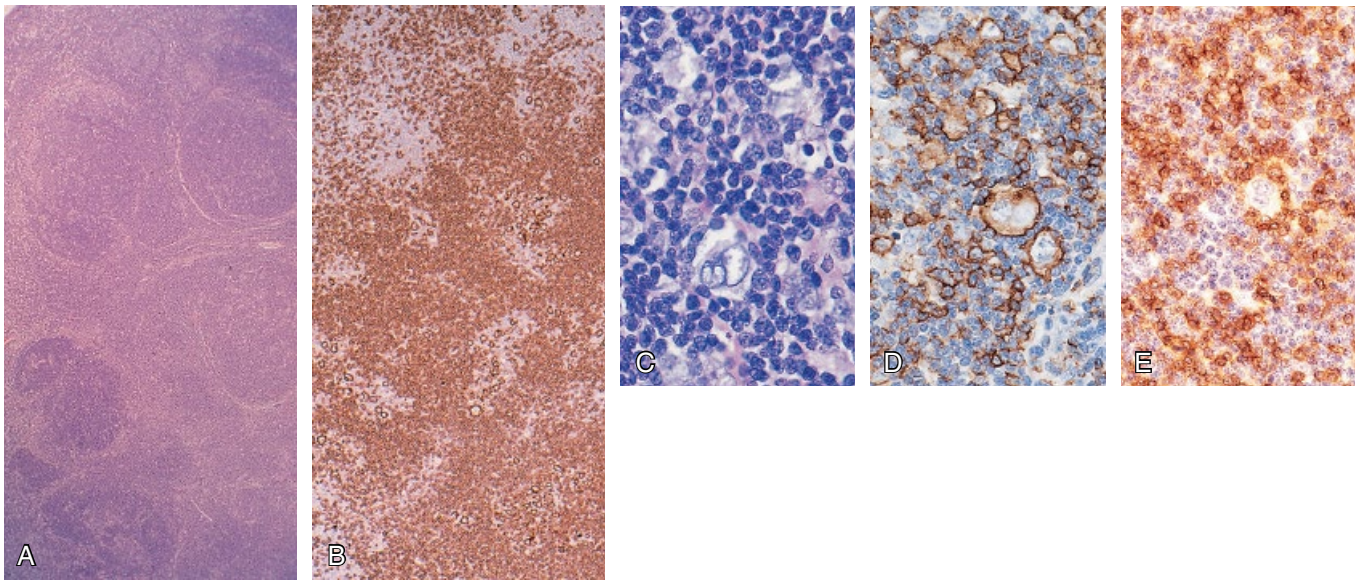

Fig. 23.23. Hodgkin lymphoma: Nodular lymphocyte predominant. **A,** Low-power view showing macronodular pattern. **B,** Immunoperoxidase stain for CD20 showing B-cell-rich nodules; the larger LP cells stand out in a corona of unstained T cells. **C,** LP cells show large lobulated nuclei. **D,** LP cells showing strong CD20 membrane in immunostaining. **E,** Immunoperoxidase stain for CD3 showing corona of T cells surrounding LP cells.

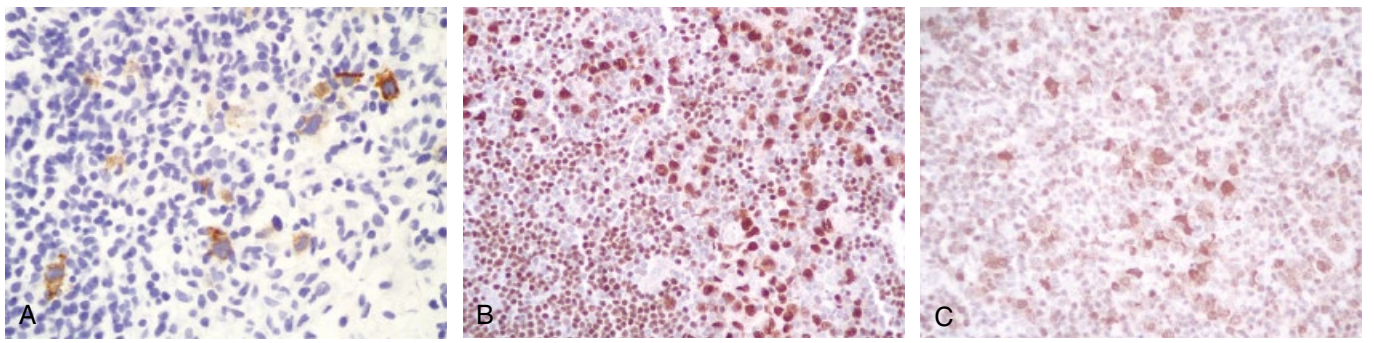

Fig. 23.24. Nodular lymphocyte-predominant Hodgkin lymphoma. Immunostaining showing popcorn cell positivity for epithelial membrane antigen **(A).** There is also strong positive staining in popcorn cells for Oct2 **(B)** and BOB.1 **(C)** with weaker staining of the bystander B lymphocytes. (Courtesy of Dr. G Taylor.)

TABLE 23.2. HODGKIN LYMPHOMA: COMPARISON OF CLASSIC REED–STERNBERG CELLS WITH TYPICAL NEOPLASTIC CELLS OF THE NODULAR LYMPHOCYTE-PREDOMINANT SUBTYPE

	Classic Hodgkin lymphoma	Nodular LPHL
Neoplastic cells	Reed–Sternberg cells, mononuclear and lacunar cells	LP cells with vesicular polylobated nuclei – "popcorn" cells
Associated cells	Lymphocytes, histiocytes, plasma cells, eosinophils	Lymphocytes and histiocytes
Sclerosis	Common	Rare
CD30, CD15	+	–
CD20	–/+	+
PAX5	Weak	Strong
CD45, EMA, Oct2, BOB.1	–	+
J chain	–	+
Ig	Negative or positive polytypic (κ and λ) from passive absorption of tissue fluid Ig	Negative or monotypic
EBV	Reed–Sternberg cells positive in over 50%	Infrequently positive
Associated lymphocytes	Predominantly T cells	Predominantly B cells
Ig genes (single-cell PCR)	Rearranged, clonal crippled	Rearranged, clonal, hypermutated, ongoing mutations

Ig, immunoglobulin; LP, lymphocyte predominant; LPHL, lymphocyte-predominant Hodgkin lymphoma; PCR, polymerase chain reaction.

TABLE 23.3. HODGKIN LYMPHOMA: ANN ARBOR STAGING, AND LATER COTSWOLD AMENDMENTS

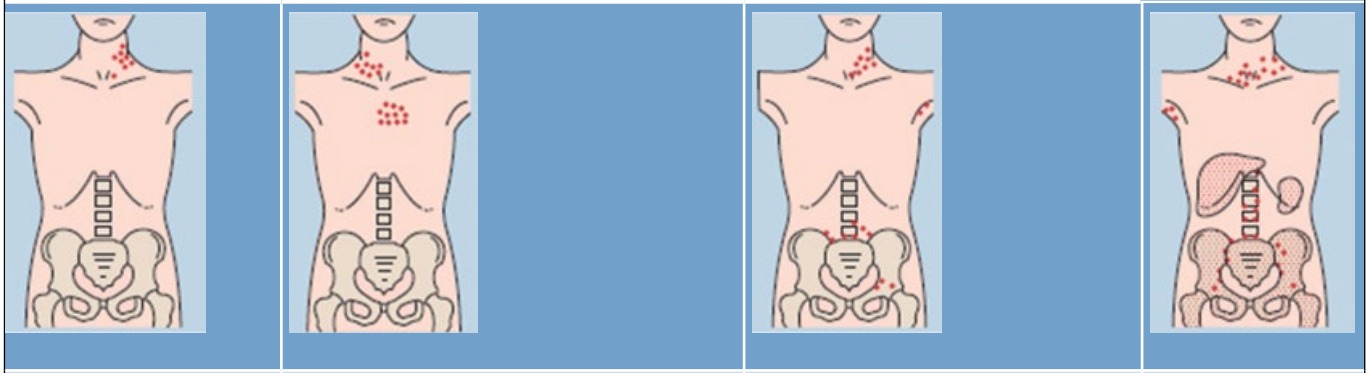

Stage I	Stage II	Stage III	Stage IV
Involvement of single lymph node region or single extralymphatic site (I_E)	Involvement of two or more lymph node regions on same side of diaphragm; may include localized extralymphatic involvement on same side of diaphragm (II_E)	Involvement of lymph node regions on both sides of the diaphragm; may include spleen (III_S) or localized extranodal disease (III_E)	Diffuse extralymphatic disease (e.g. in liver, bone marrow, lung, skin)

NB: if unexplained weight loss of >10% body weight in preceding 6 months and/or fevers of >38°C and night sweats, classified as B; if absent, A.

Stage I: Single lymph node region or lymphoid structure involvement (e.g. spleen, thymus, Waldeyer ring). Stage II: Two or more lymph node regions or lymphoid structures confined to one side of diaphragm. Stage III: Lymph node regions or lymphoid structures above and below diaphragm (splenic involvement is included in this classification because it is often a prelude to widespread hematogenous spread). Stage IV: Extranodal areas, including bone marrow and liver. The stage number is followed by either "A" (absence) or "B" (presence), referring to unexplained fever above 38°C (100.4°F), night sweats, and loss of more than 10% of body weight within 6 months. The subscript "E" indicates localized extranodal extension from a nodal mass; for example, IE describes mediastinal disease with contiguous spread to the lung or spinal theca. In the Cotswold classification Stage III is divided into Stage III1, "Involvement of splenic, celiac or portal nodes" and Stage III2, "Involvement of para-aortic, iliac or mesenteric nodes." The definition of bulk is nodal mass >10 cm diameter and mediastinal mass greater than one-third maximum diameter of chest. Source:Hoffbrand AV Pettit JE. *Essential Haematology*, 3rd edn. Blackwell Scientific, 1993. Reproduced with permission of John Wiley & Sons.

procedures are employed in the initial assessment (Table 23.4). Many patients have a normochromic normocytic anemia with a leukocytosis and/or eosinophilia, and bone marrow aspirates and trephine biopsies provide diagnostic material (Figs. 23.25–23.34).

Mediastinal, hilar node, or lung involvement can be detected by chest radiography (Figs. 23.35 and 23.36), liver involvement by percutaneous biopsy, and para-aortic or pelvic lymph node involvement by abdominal radiography (Fig. 23.37). Computed tomography (CT) scanning (Fig. 23.38) and magnetic resonance imaging (MRI) are used in the search for thoracic, abdominal, and pelvic lymph node and organ involvement. Positron emission tomography (PET) scans also detect areas of involvement. They are particularly sensitive at detecting small areas of tumor and are able to distinguish active areas of disease from scar tissue following therapy (Figs. 23.39–23.42).

TABLE 23.4. HODGKIN LYMPHOMA: LABORATORY AND RADIOLOGIC TECHNIQUES FOR STAGING PATIENTS

Laboratory	Full blood count Erythrocyte sedimentation rate Bone marrow aspirate and trephine biopsy Liver function Lactate dehydrogenase C-reactive protein
Radiology	Chest radiography Computed tomography (thorax, abdomen, pelvis, neck)
Special tests	Magnetic resonance imaging Bone scan Positron-emission tomography

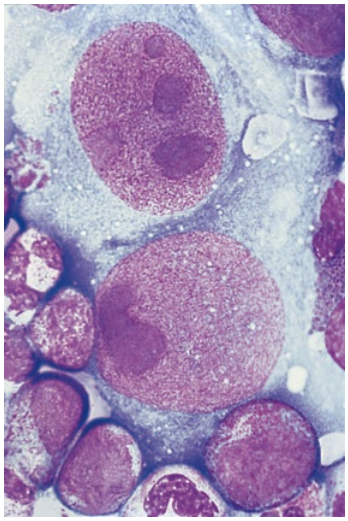

Fig. 23.25. Hodgkin lymphoma. High-power view of bone marrow aspirate, showing a Reed–Sternberg cell.

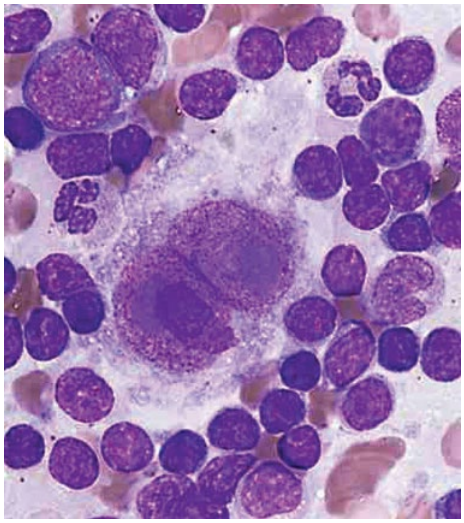

Fig. 23.26. Hodgkin lymphoma. Bone marrow aspirate squash preparation showing a typical binucleate Reed–Sternberg cell surrounded by lymphoid cells, neutrophils, and monocytes. (Courtesy of Dr. W Erber.)

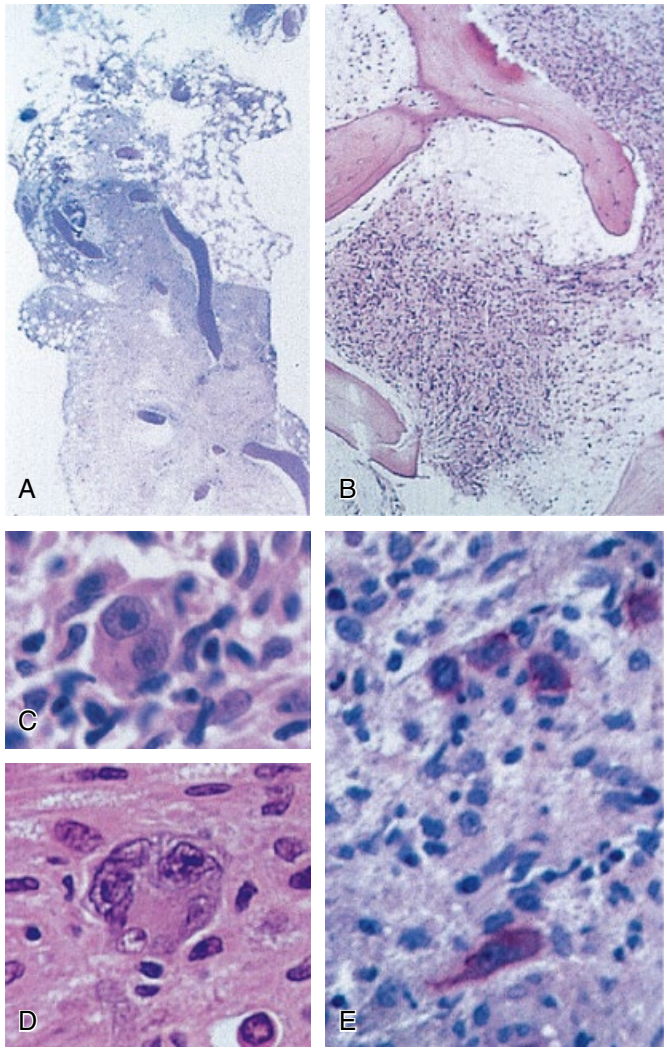

Fig. 23.27. Hodgkin lymphoma: Trephine biopsy. **(A,B)** Hodgkin tissue replacing normal hematopoietic elements. **(C,D)** Higher power view showing fibrosis and Reed–Sternberg cells, which show immunopositivity for CD30 **(E).**

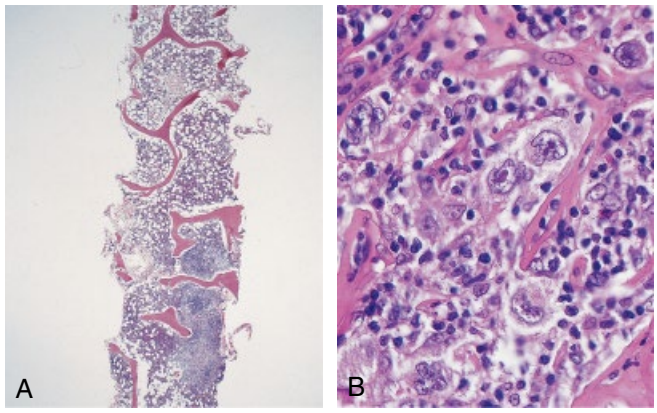

Fig. 23.28. Hodgkin lymphoma: Bone marrow trephine biopsy. **A,** Low-power view showing focal involvement. **B,** High-power view showing mononuclear Hodgkin cells.

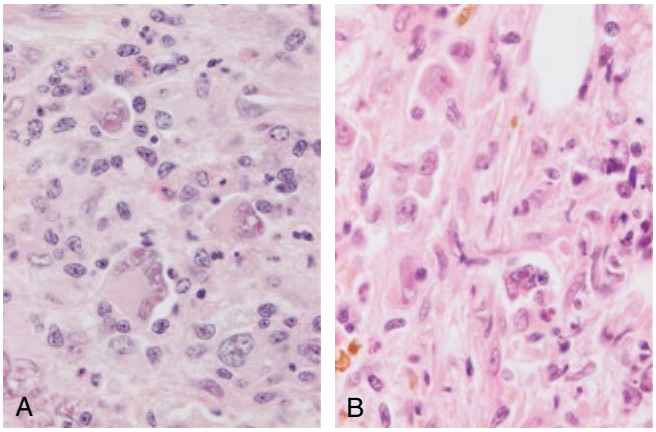

Fig. 23.29. Hodgkin lymphoma. Bone marrow trephine biopsy in two patients **(A)** and **(B)** showing Reed–Sternberg and mononuclear Hodgkin cells with scattered lymphocytes and eosinophils and neutrophils in **(A).** (Courtesy of Dr.W Erber.)

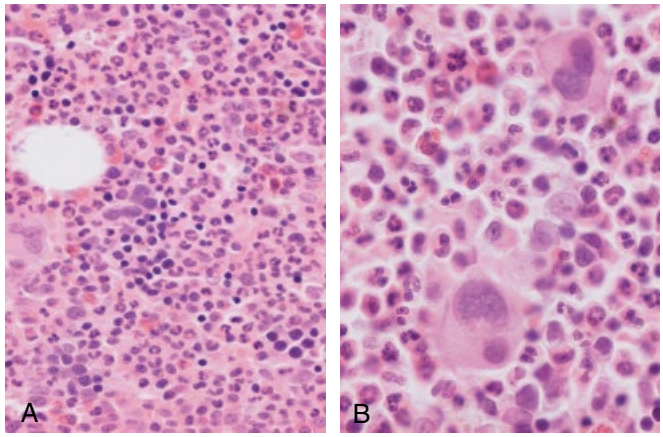

Fig. 23.31. Hodgkin lymphoma. **A,** Bone marrow trephine biopsy showing reactive hyperplasia of granulopoiesis with prominent neutrophils and eosinophils. No Reed–Sternberg cells were seen. **B,** At higher magnification the large polylobated cells are megakaryocytes. (Courtesy of Dr.W Erber.)

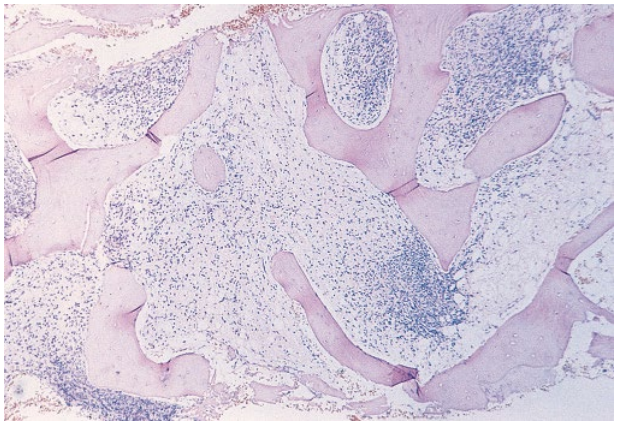

Fig. 23.30. Hodgkin lymphoma. Trephine biopsy in the fibrotic variant of lymphocyte-depleted disease, showing almost complete replacement of hematopoietic tissue by Hodgkin deposits, along with abundant fibrous tissue in the intertrabecular space.

DEAUVILLE SCORE

This is used to standardize the reporting of PET scans especially in Hodgkin lymphoma but also in other lymphomas. It is based on visual interpretation of FDG uptake. It takes advantage of two reference points of the individual patient, which have demonstrated relatively constant uptake on serial imaging. The two reference organs are the mediastinum (blood pool) and the liver.

The scale ranges from 1 to 5, where 1 is best and 5 is the worst. Each FDG-avid (or previously FDG-avid) lesion is rated independently.

1. No uptake or no residual uptake (when used interim).
2. Slight uptake, but below blood pool (mediastinum).
3. Uptake above mediastinal, but below or equal to uptake in the liver.
4. Uptake slightly to moderately higher than liver.
5. Markedly increased uptake or any new lesion (on response evaluation).

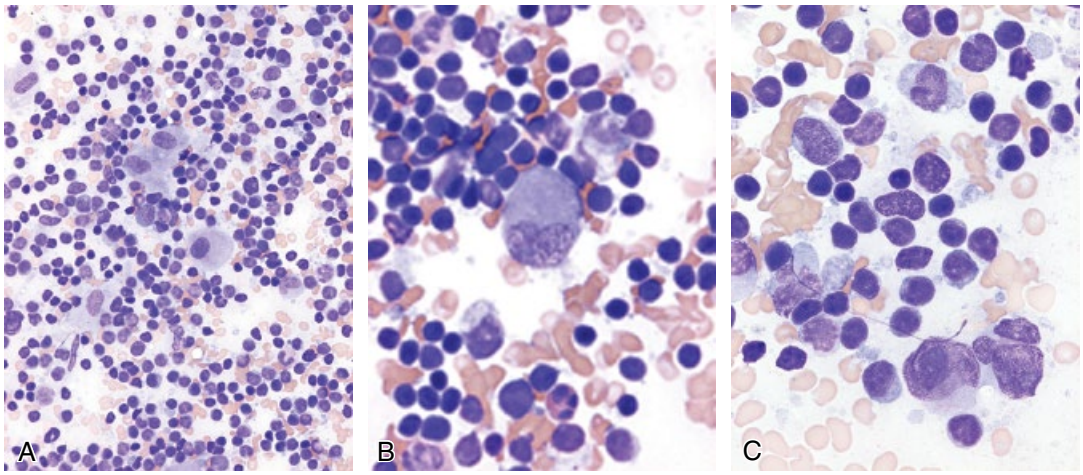

Fig. 23.32. Nodular lymphocyte predominant Hodgkin lymphoma. **A,** Bone marrow aspirate showing lymphoctye predominant (LP) cells surrounded by large numbers of lymphocytes. **B,C,** At higher magnification, the characteristic vesicular polylobated nuclei of the larger LP or popcorn cells are evident. (Courtesy of Dr.W Erber.)

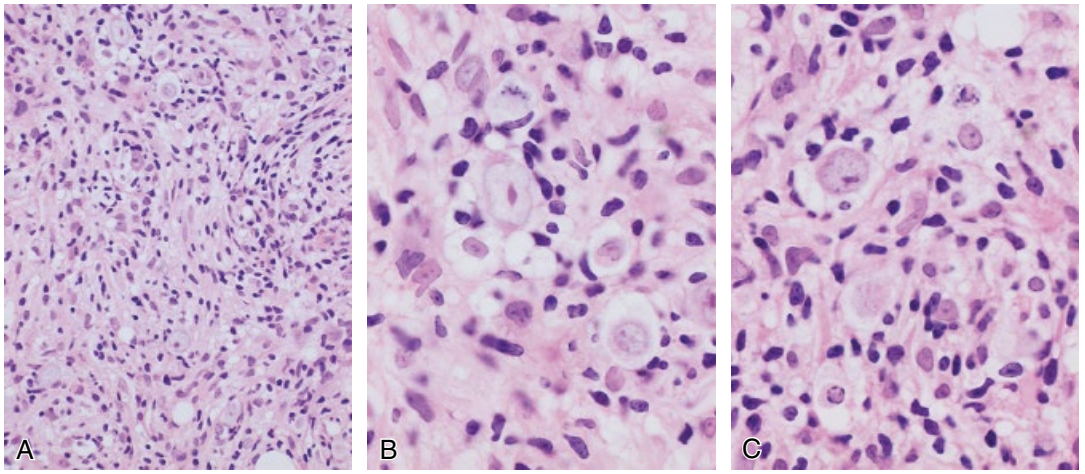

Fig. 23.33. Nodular lymphocyte-predominant Hodgkin lymphoma. **A,** Bone marrow trephine biopsy showing LP cells and lymphocytes supported by a delicate fibrous stroma. **B, C,** At higher magnification, the large vesicular nuclei and relatively small nucleoli of the LP cells are evident. (Courtesy of Dr. W Erber.)

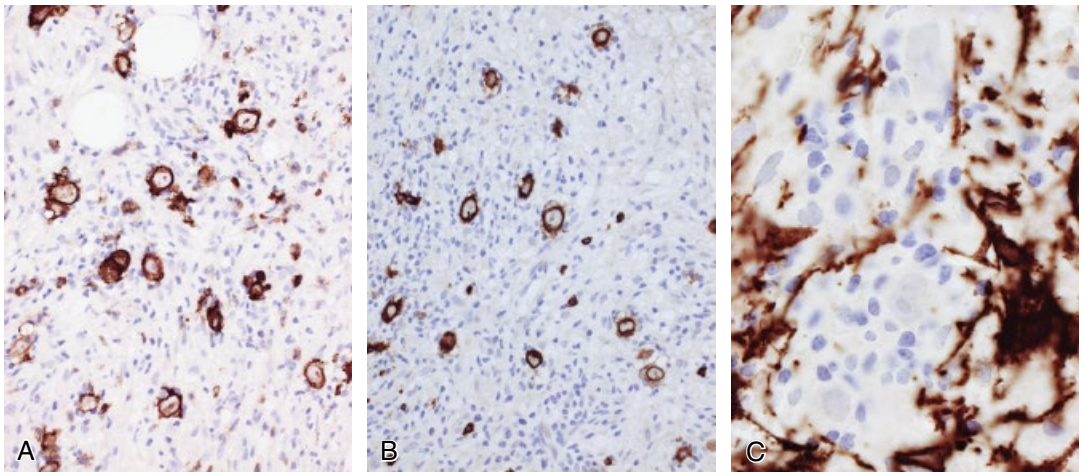

Fig. 23.34. Nodular lymphocyte-predominant Hodgkin lymphoma. Bone marrow trephine biopsy. Immunostaining for CD20 **(A)** and CD 79a **(B)** shows strong positivity in the LP cells. With immunostaining for CD10 **(C)** the LP cells are negative but the supporting stroma is positive. (Courtesy of Dr. W Erber.)

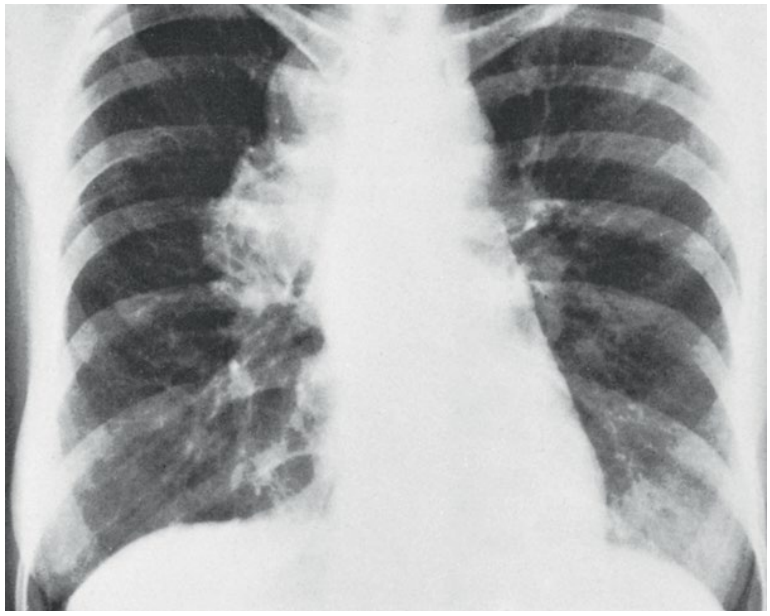

Fig. 23.35. Hodgkin lymphoma. Chest radiograph showing prominent right paratracheal and hilar lymph node enlargement. The enlargement of the anterior mediastinal, subcarinal, and left hilar nodes is less marked and the proximal regions of both major bronchi are significantly narrowed. Contrast material in the apical lymph node on the left is from previous lymphangiography.

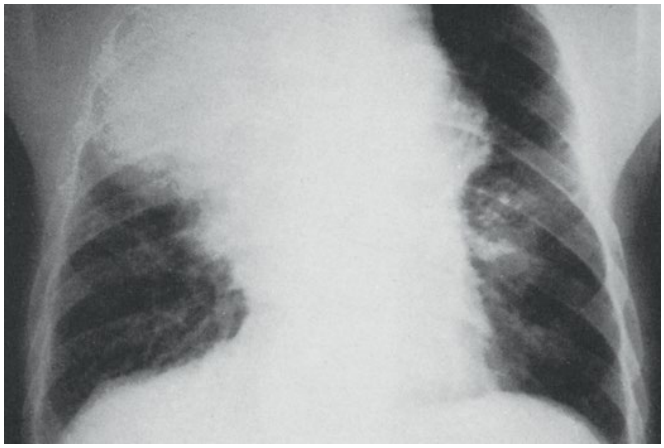

Fig. 23.36. Hodgkin lymphoma. Chest radiograph showing widespread enlargement of hilar and mediastinal lymph nodes with associated collapse of the right upper lobe and infiltration or possibly pneumonic changes in the midzone of the left lung.

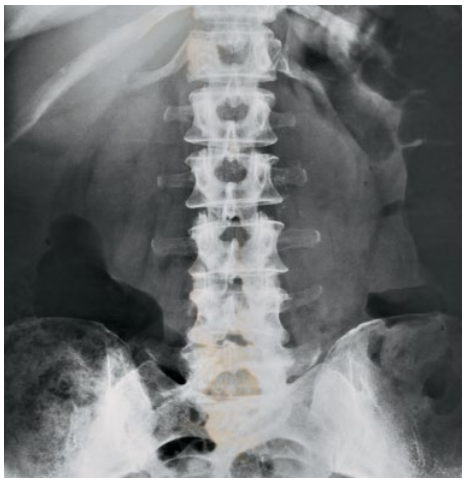

Fig. 23.37. Hodgkin lymphoma. Plain abdominal radiograph showing bilateral massive para-aortic lymph node enlargement. (Courtesy of Dr. D Nag.)

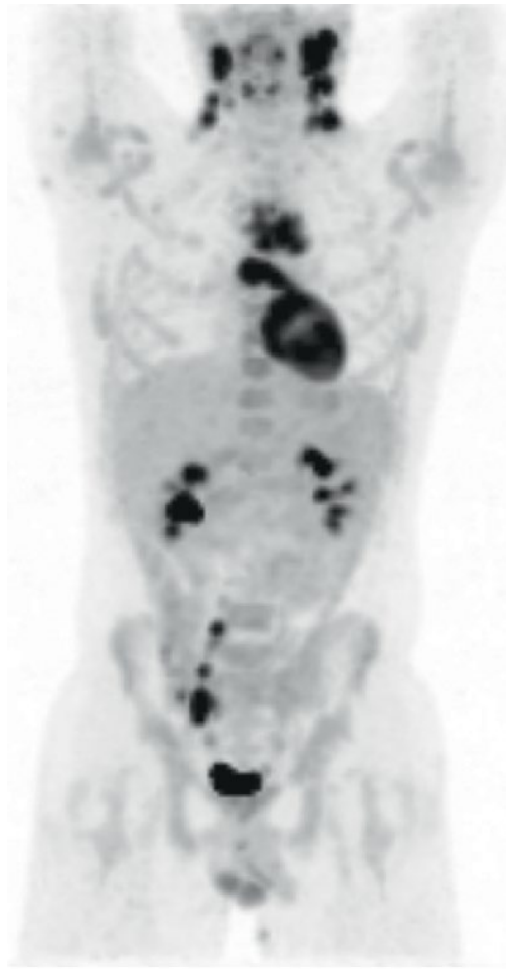

Fig. 23.39. Hodgkin lymphoma. Fluorodeoxyglucose (FDG) PET maximum projection intensity (MIP) image of a 14-year-old boy with recurrent Hodgkin lymphoma indicating relapse of nodal disease in the neck, mediastinum, and right pelvis. (Courtesy of Dr. G Cook.)

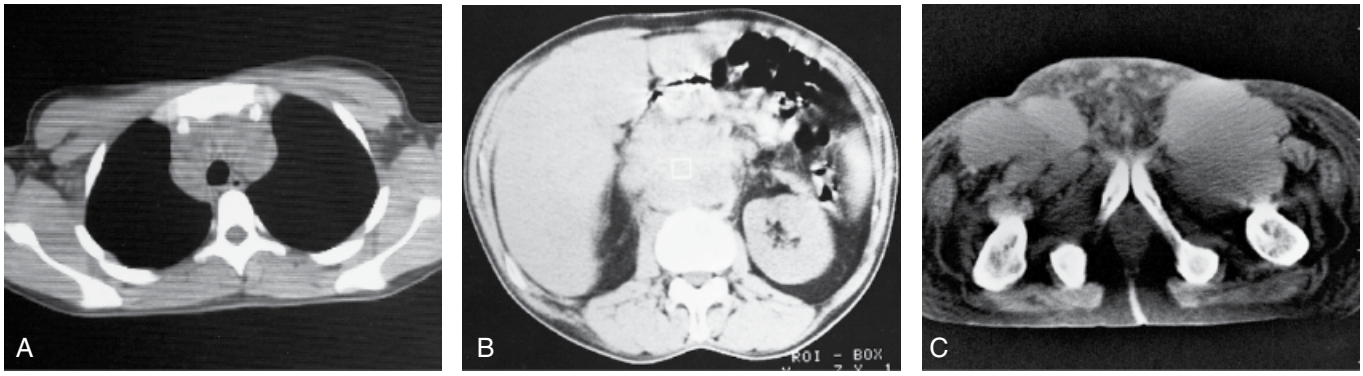

Fig. 23.38. Hodgkin lymphoma. **A,** CT scans of chest showing paratracheal and anterior mediastinal lymph node enlargement. **B,** Abdomen showing massive para-aortic lymph node enlargement displacing the pancreas forward. **C,** Pelvis showing massive bilateral inguinal and pelvic lymphadenopathy with marked edema of the lower abdominal wall (same patient as Fig. 23.34).

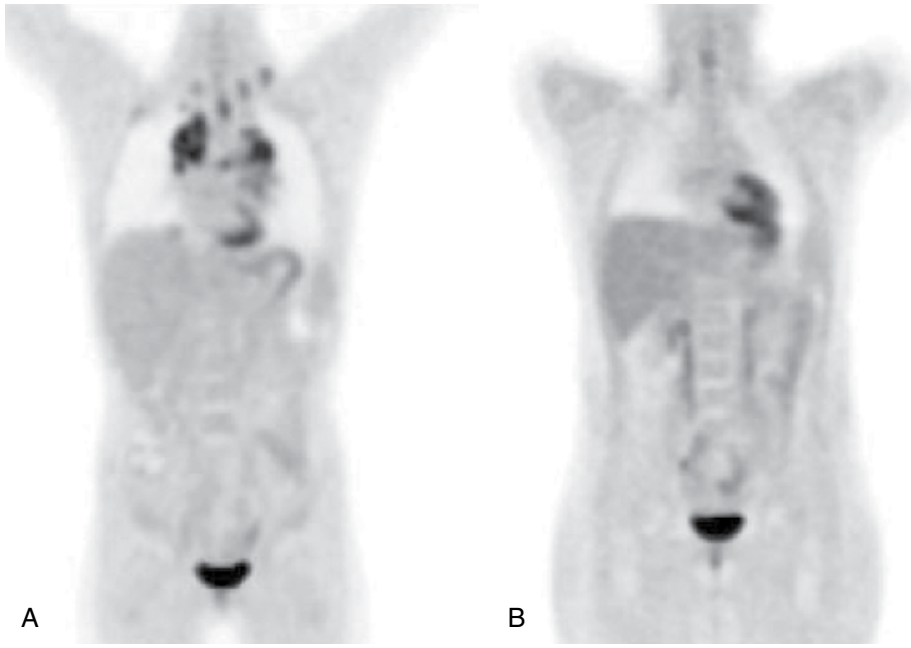

Fig. 23.40. Hodgkin lymphoma. FDG PET MIP image showing Hodgkin's disease before chemotherapy **(A)** and after two cycles of chemotherapy **(B)** showing a complete response and chemosensitivity. (Courtesy of Dr. G Cook.)

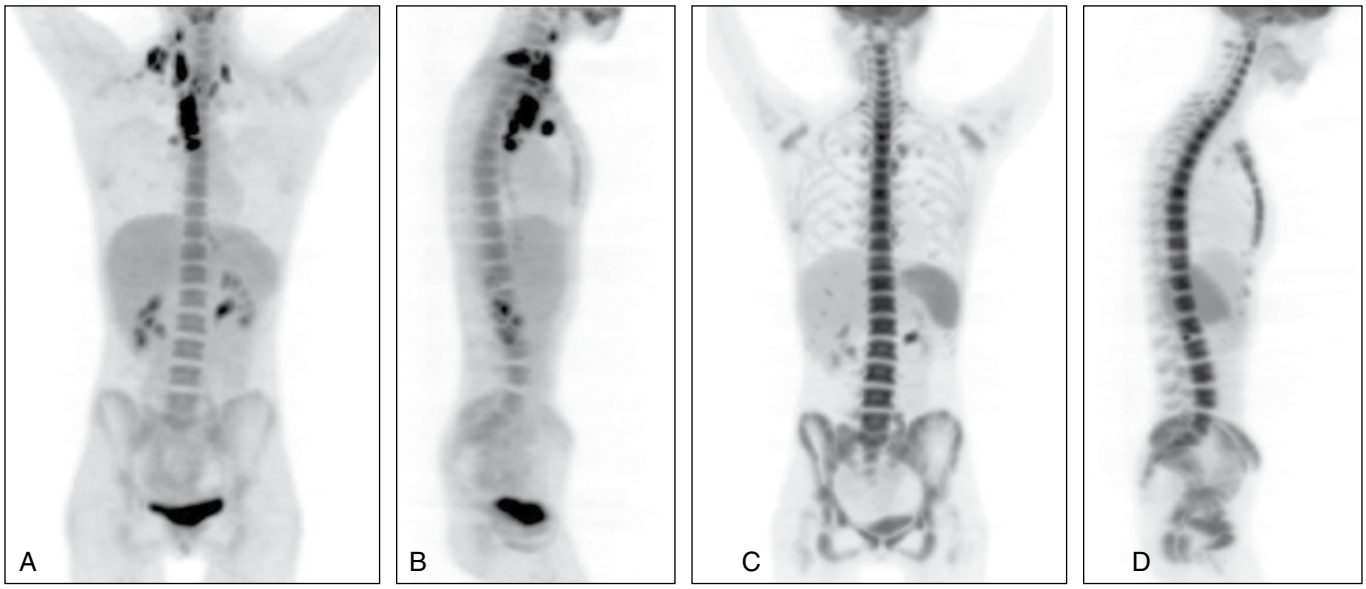

Fig. 23.41. Hodgkin lymphoma. FDG PET MIP coronal **(A)** and sagittal **(B)** images showing extensive cervical and mediastinal nodal involvement. Following chemotherapy, corresponding images **(C** and **D)** show no residual disease. Uptake in the skeleton reflects regeneration or rebound of bone marrow after chemotherapy. (Courtesy of Dr. H Fraser.)

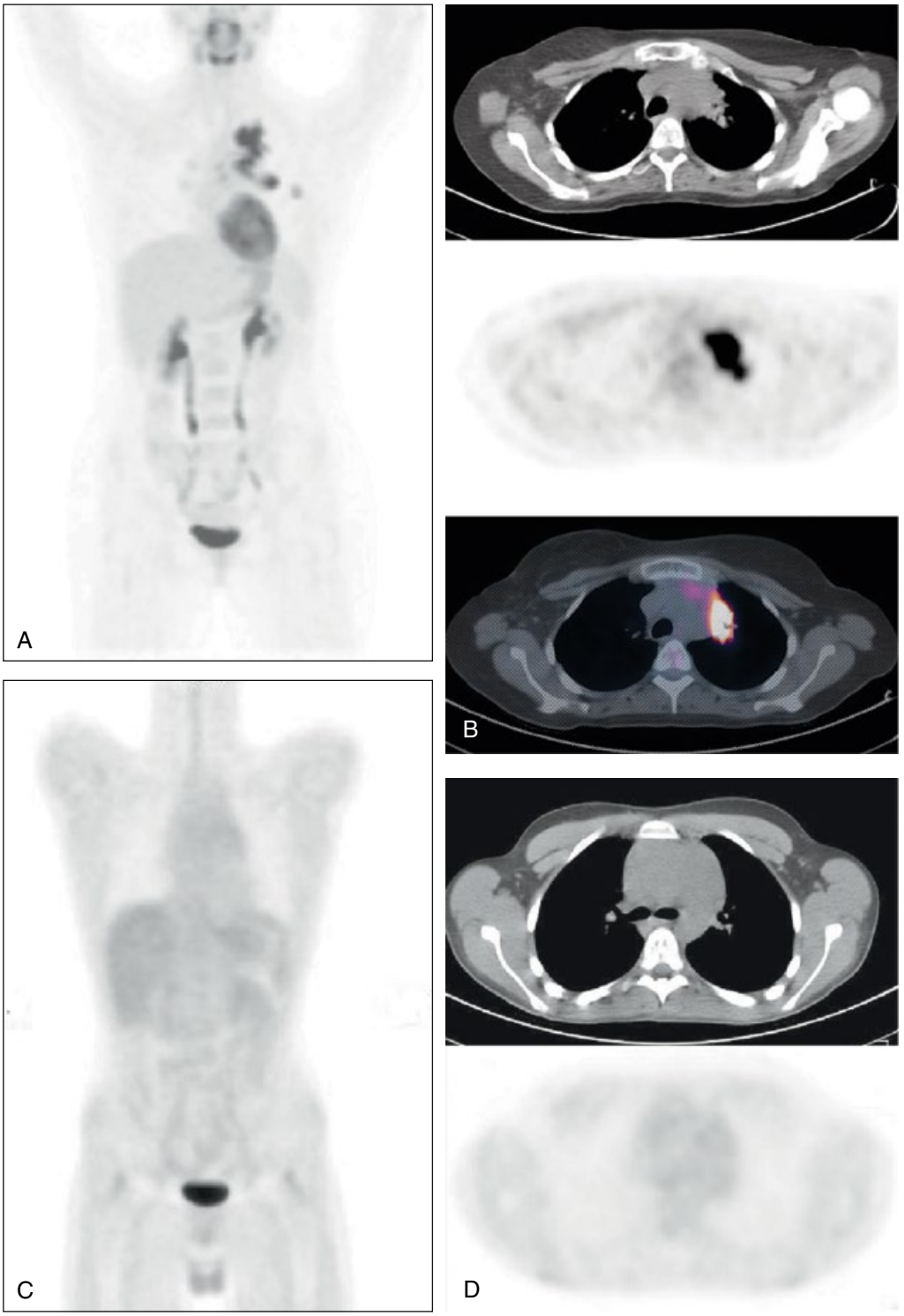

Fig. 23.42. Hodgkin lymphoma. **A,** FDG PET MIP image. **B,** CT, FDG PET, and fused axial slices through the mediastinum following chemotherapy showing persistent abnormal uptake in an anterior mediastinal mass indicating residual disease activity. Following more chemotherapy, FDG PET MIP image **(C)** and CT and FDG PET components of the PET/CT acquisition **(D)** show no abnormal uptake in an anterior mediastinal mass indicating scar tissue and no residual active Hodgkin lymphoma. (Courtesy of Dr. G Cook.)

Some authors also use X for any lesion not overtly attributable to lymphoma.

Previously used staging techniques such as lymphangiography (Figs. 23.43 and 23.44), other contrast X-ray methods (Figs. 23.45 and 23.46), gallium tomography (Fig. 23.47), and laparotomy with abdominal node and liver biopsy and splenectomy are very rarely employed today.

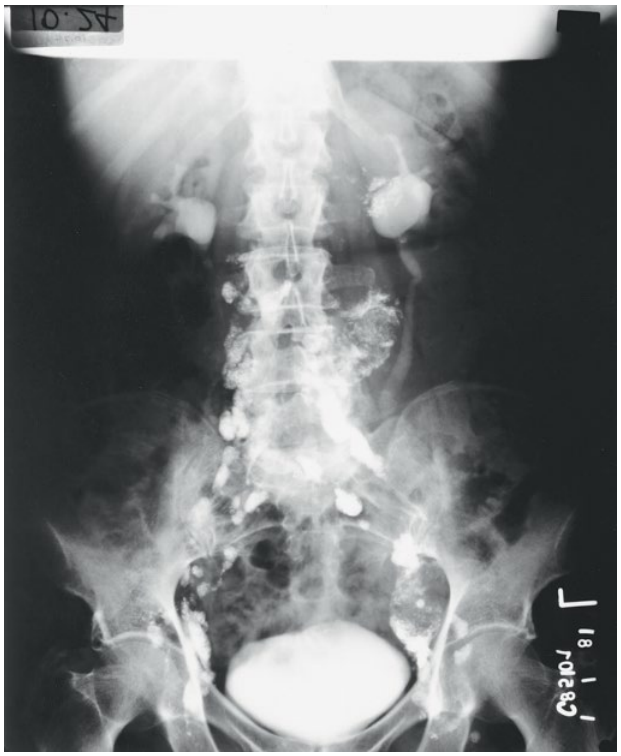

Fig. 23.43. Hodgkin lymphoma. Lymphangiogram with intravenous pyelogram shows enlarged para-aortic lymph nodes (particularly on the left and lower left pelvis) with displacement of the ureter.

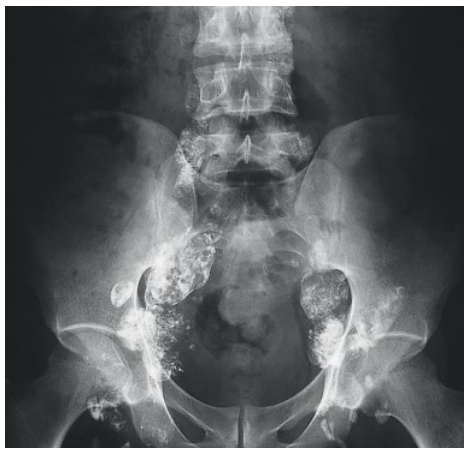

Fig. 23.44. Hodgkin lymphoma. Lymphangiogram showing bilateral external iliac and lower para-aortic lymph node enlargement and filling defects.

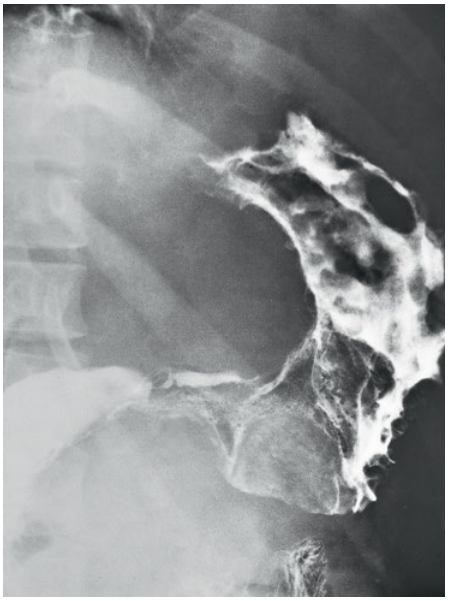

Fig. 23.45. Hodgkin lymphoma. Barium meal demonstrating extensive mucosal and gastric wall involvement of the body and pylorus of the stomach. (Courtesy of Dr. D Nag.)

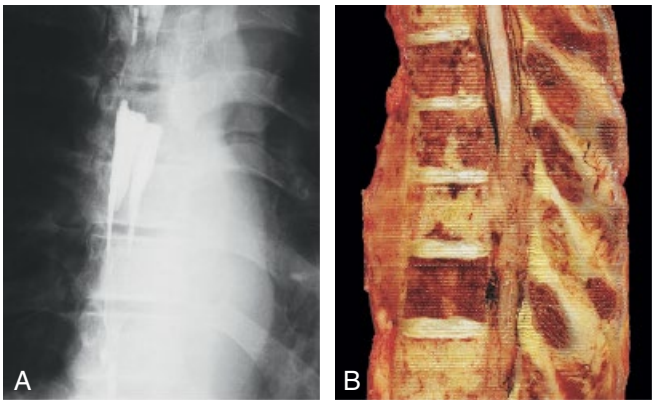

Fig. 23.46. Hodgkin lymphoma. **A,** Sisternogram showing partial block of contrast at the T4 level and a complete block at the lower part of T6. **B,** Sagittal section postmortem shows extradural extension of tumor from the body of T4 (uppermost) and more extensive cordal involvement at T7 and T9. There is patchy involvement of other vertebral bodies and spinous processes. Extensive paravertebral tumor is seen anteriorly below the T5 level.

PROGNOSTIC FACTORS

Based on the analysis of large numbers of patients, a number of prognostic indices have been published for patients with Hodgkin lymphoma. For patients with localized disease, the European Organization for Research and Treatment of Cancer

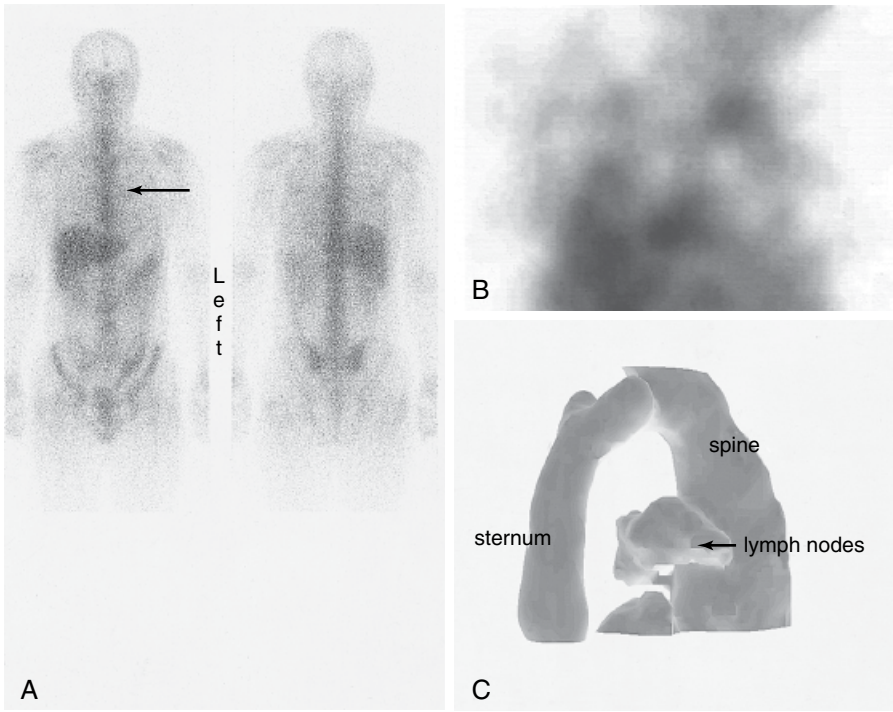

Fig. 23.47. Non-Hodgkin lymphoma: Stage IIb. Postchemotherapy with residual mediastinal mass see on CT scan. **A,** Whole body scan 48 hours after injection of gallium-67 citrate, with subtle increased uptake in the mediastinum (arrow). **B,** Tomographic image shows uptake in mediastinum. **C,** Surface rendered tomographic image confirms presence of active disease in hilar lymph nodes. (Courtesy of Dr. AJW Hilson.)

TABLE 23.5. HODGKIN LYMPHOMA: EUROPEAN ORGANIZATION FOR RESEARCH AND TREATMENT OF CANCER (EORTC) RISK FACTORS FOR LOCALIZED HODGKIN LYMPHOMA

Favorable
Patients must have all of the following features: • Clinical stage I and II • Maximum of three nodal areas involved • Age <50 years • ESR <50 mm/h without B symptoms or ESR <30 mm/h with B symptoms • Mediastinal : thoracic ratio <0.35
Unfavorable
Patients have any of the following features: • Clinical stage II with involvement of at least four nodal areas • Age >50 years • ESR >50 mm/h if asymptomatic or ESR >30 mm/h if B symptoms • Mediastinal: thoracic ratio >0.35

ESR, erythrocyte sedimentation rate.

TABLE 23.6. HODGKIN LYMPHOMA: INTERNATIONAL PROGNOSTIC INDEX (HANSCLEVER INDEX) FOR ADVANCED HODGKIN LYMPHOMA

Age >45 years
Male gender
Serum albumin <40 g/dL
Hemoglobin level <10.5 g/dL
Stage IV disease
Leukocytosis (white cell count ≥15 × 10^9/L)
Lymphopenia (<0.6 × 10^9/L or <8% of the white cell count)

The presence of each of the seven factors is associated with a reduction of five-year freedom from progression by about 8%.
Source: Hasenclever D, Diehl V. *N Engl J Med* 1998;339:1506–1514. Reproduced with permission of Massachusetts Medical Society: The New England Journal of Medicine.

(EORTC) Index based on factors shown in Table 23.5 has been useful. For patients with advanced disease, the International Prognostic Score or Hansclever Index is widely used. In this latter index seven factors were identified (Table 23.6), each of which was associated with an 8% reduction in the predicted 5-year disease-free progression rate.

CHAPTER

24

HISTIOCYTIC DISORDERS

WRITTEN WITH STEFANO A. PILERI

This chapter includes discussion of both reactive proliferative conditions and the histiocytic and dendritic cell neoplasms.

HEMOPHAGOCYTIC LYMPHOHISTIOCYTOSIS (HEMOPHAGOCYTIC SYNDROME)

Hemophagocytic lymphohistiocytosis (HLH) is the most frequently seen proliferative disorder of macrophages and is more common than malignant tumors of histiocytes. The syndrome occurs in a familial primary form with a recessive inheritance pattern that affects infants and young children and in an acquired secondary form. Sporadic cases are seen in association with the genetic immunodeficiencies Chédiak–Higashi, Griscelli, and X-linked lymphoproliferative syndromes.

HLH is not a clonal or neoplastic disease but is probably a reactive proliferative disorder related to an excessive production of monocyte-stimulating cytokines (e.g. interleukins 1, 2, and 10), tumor necrosis factor α and interferon γ, and chemokines (e.g. MIP-1a, Mig, and IP-10). Infection with Epstein–Barr virus or another virus is frequently the initiating event. There is uncontrolled macrophage activation and enhanced phagocytic activity.

Defects of perforin and other proteins of the cytolytic pathway have been associated with defective T-cell function and the hemophagocytic syndrome. In the primary inherited form, mutations in the perforin gene at locus 10q24 and defects in perforin synthesis have been found in up to 40% of affected patients. Similar defects have also been found in patients treated later in life with presumed acquired disease. Less common mutations in primary inherited hemophagocytic syndrome include those of the *UNC13D* gene at locus 17q25 and the *STX11* gene at locus 6q24. and of *STXBP2*. These mutations cause impaired cytotoxic function and an uncontrolled inflammatory response with expansion and activation of interferon γ producing T cells. This leads to macrophage activation and overproduction of proinflammatory cytokines. An external cause (e.g. infection) is probably necessary to initiate or trigger the activation of the disease.

The acquired form is precipitated by viral, bacterial, fungal, or protozoan infections, and is also seen in immunocompromised patients, in connective tissue or autoimmune disorders, and in patients with lymphoma or leukemia. It is likely that many adult patients with HLH have an underlying genetic predisposition. Although most patients previously diagnosed with malignant histiocytosis would now be classified as having large cell malignant lymphoma, many had features identical to the hemophagocytic syndrome.

Patients with HLH have fever, pancytopenia, liver dysfunction, or neurologic symptoms. Guidelines for the diagnosis are listed in Table 24.1. Phagocytosis of red cells by monocytes can be seen in the blood film (Fig. 24.1). Fibrinogen levels are usually low, and prolongation of the activated partial thromboplastin time (APTT) indicate an associated coagulopathy. Serum ferritin and triglyceride levels are elevated. Special studies show low or absent natural killer (NK) cell activity. Bone marrow aspirates show histiocytic hyperplasia and hemophagocytosis (Figs. 24.2–24.4). Trephine biopsies show extensive replacement of other hematopoietic cells by sheets of hyperplastic histiocytes (Fig. 24.5). The bone marrow features in a patient with virus-associated hemophagocytic syndrome are illustrated in Fig. 24.6. Liver biopsy show hemophagocytosis, histiocytic infiltration, and areas of

TABLE 24.1. DIAGNOSTIC GUIDELINES FOR HEMOPHAGOCYTIC LYMPHOHISTIOCYTOSIS (HLH)

Guidelines
The diagnosis of HLH requires a molecular diagnosis consistent with HLH or five of eight of these criteria:
1. Fever
2. Splenomegaly
3. Cytopenias affecting ≥2 lineages a. Hemoglobin <9 g/dL b. Platelets $<100 \times 10^9$/L c. Neutrophils $<1.0 \times 10^9$/L
4. Hypertriglyceridemia and/or hypofibrinogenemia a. Triglycerides ≥265 mg/dL b. Fibrinogen ≤150 mg/dL
5. Hemophagocytosis in bone marrow, spleen, or lymph nodes
6. Low or absent NK cell activity
7. Ferritin ≥500 μg/L
8. sCD25 (i.e., sIL2R) ≥2400 U/mL

Source: Schram AM, Berliner N. *Blood* 2015;125:2908–2914. http://www.bloodjournal.org/content/125/19/2908/tab-article-info?sso-checked=true

Color Atlas of Clinical Hematology: Molecular and Cellular Basis of Disease, Fifth Edition. A. Victor Hoffbrand, Paresh Vyas, Elías Campo, Torsten Haferlach, and Keith Gomez

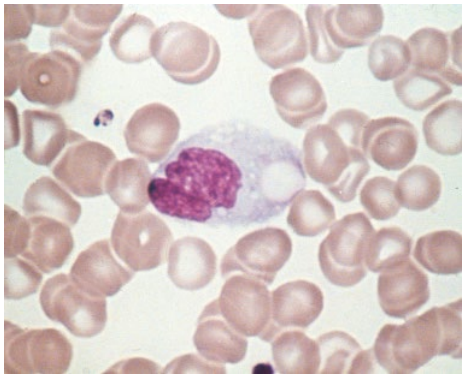

Fig. 24.1. Hemophagocytic lymphohistiocytosis syndrome. Blood film showing a phagocytosed red cell inside a monocyte.

necrosis (Fig. 24.7). Histiocytic proliferation also occurs in the spleen, lymph nodes, and other tissues. In the familial form, there is often central nervous system involvement (Fig. 24.8).

XANTHOGRANULOMA

Xanthogranuloma is an uncommon histiocytic "tumor" arising in the first 5 years of life. Yellowish to reddish nodular "tumors" measuring up to several centimeters in diameter are usually solitary and are most frequent in the skin of the head and neck region, although other skin regions, mucous membranes, or almost any site in the body can be involved. Less commonly there are multiple tumors. Systemic spread from the primary site is rarely seen. Xanthogranuloma is most probably a reactive proliferation and there is usually a spontaneous involution. Histologically, the skin "tumors" show intradermal collections of histiocytes with eosinophilic or vacuolated cytoplasm with variable numbers of Touton-type giant cells (Figs. 24.9 and 24.10). Some lesions show small numbers of neutrophils, eosinophils, lymphocytes, or plasma cells. In established lesions, lipid accumulation (Fig. 24.11) and xanthoma cells are prominent. The histiocytes show positivity for CD45, CD68, CD4, and HLA-DR, and are negative for CD1a.

ROSAI–DORFMAN DISEASE

Rosai–Dorfman disease, or sinus histiocytosis with massive lymphadenopathy, is a rare condition seen most frequently in young black people. It is characterized by lymphadenopathy, fever, leukocytosis, and hypergammaglobulinemia. Although Rosai–Dorfman disease has been considered a reactive process (possibly sustained by a viral infection), the recent demonstration of somatic mutation in some cases, including *KRAS* K117N, challenged this hypothesis. Furthermore, Rosai–Dorfman disease can occur in individuals with germline mutations of the *SLC29A3* gene (Faisalabad histiocytosis/familial Rosai–Dorfman disease) and in autoimmune lymphoproliferative syndrome type Ia, associated with *TNFRSF6* mutations. The cervical nodes are usually involved (Fig. 24.12). Histologically, the nodes

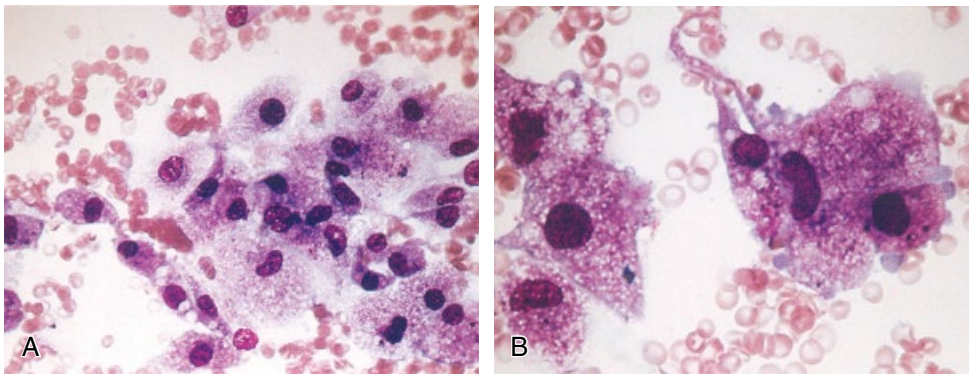

Fig. 24.2. Hemophagocytic lymphohistiocytosis syndrome. **A,** Bone marrow aspirate in a 64-year-old man with pancytopenia, hepatomegaly, and splenomegaly showing abnormal histiocytes in the cell trail. **B,** At high power the cells show considerable nuclear pleomorphism and abundant vacuolated cytoplasm.

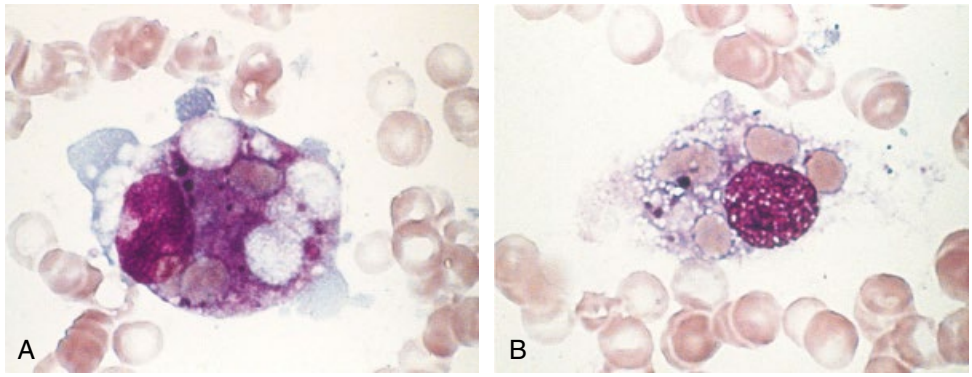

Fig. 24.3. Hemophagocytic lymphohistiocytosis syndrome. **A** and **B,** Bone marrow aspirate images showing prominent red cell phagocytosis in abnormal histiocytes.

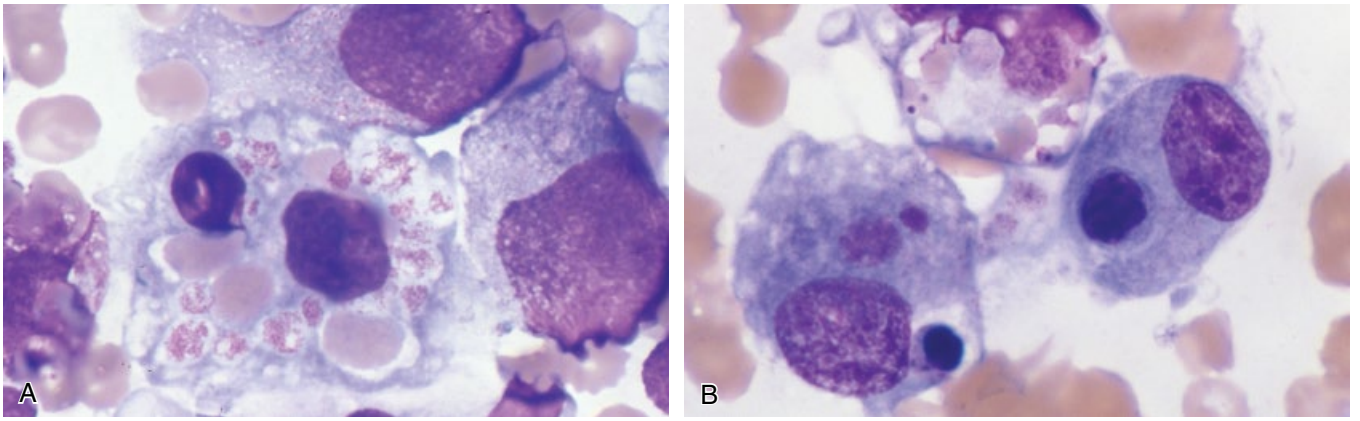

Fig. 24.4. Famialial hemophagocytic lymphohistiocytosis syndrome. **A** and **B,** Bone marrow aspirate images showing two abnormal histiocytes with phagocytosed red cells, platelets, and lymphocytes. (Courtesy of Dr. S Imashuku.)

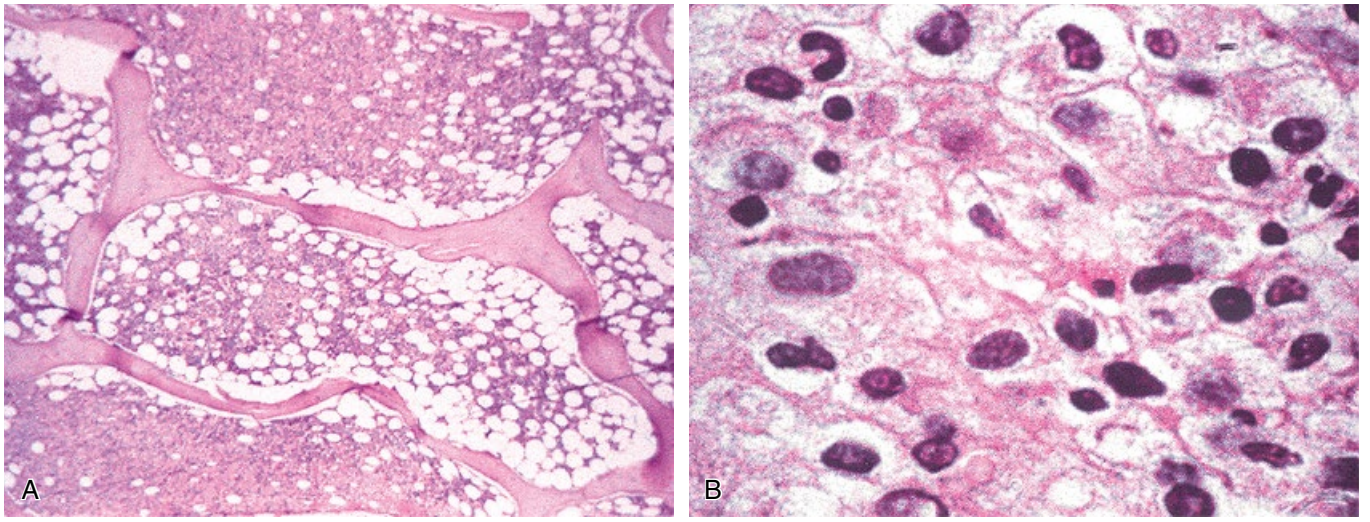

Fig. 24.5. Hemophagocytic lymphohistiocytosis syndrome: trephine biopsy in the same case shown in Fig. 24.2. **A,** There is extensive replacement of normal intertrabecular hematopoietic tissue by sheets of abnormal histiocytes. **B,** At higher magnification the cells are pleomorphic with hyperchromatic nuclei and abundant vacuolated cytoplasm.

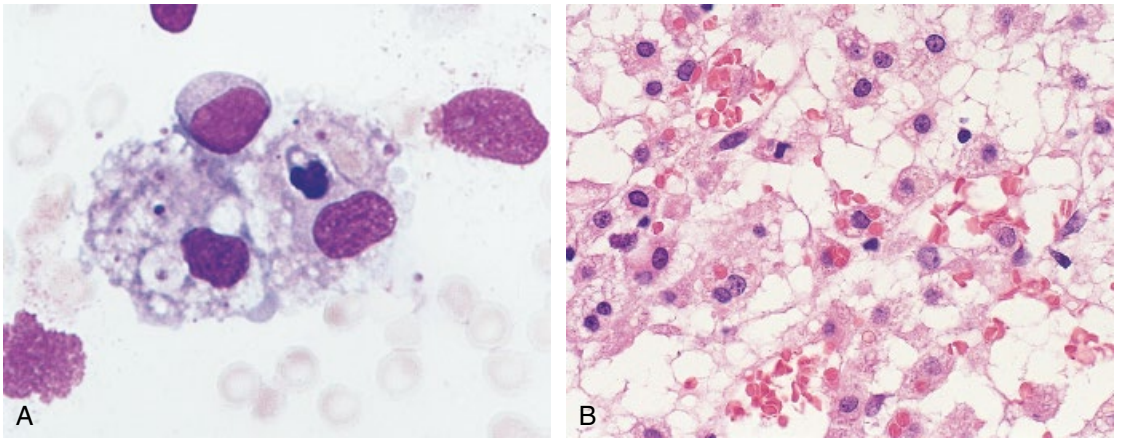

Fig. 24.6. Virus-associated hemophagocytic lymphohistiocytosis syndrome. **A,** Bone marrow aspirate showing two histiocytes that have engulfed red cells and erythroblasts. **B,** Bone marrow trephine biopsy showing replacement of normal architecture by erythrophagocytic histiocytes. (*A*, Courtesy of Dr. S Knowles. *B*, Courtesy of Professor KA MacLennan.)

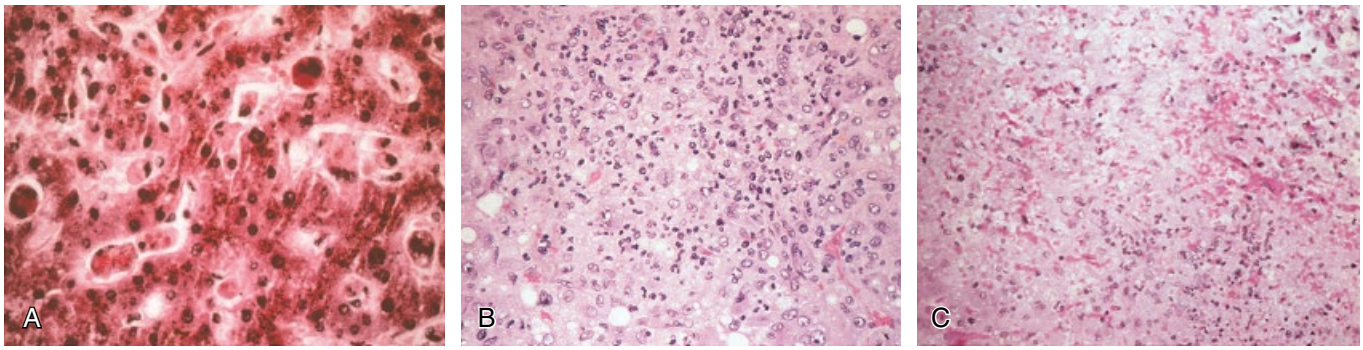

Fig. 24.7. Hemophagocytic syndrome: Liver biopsies in different patients. **A,** Sinusoidal Küpffer cell erythrophagocytosis. **B,** Infiltration of parenchymal cells by abnormal histiocytes. **C,** Associated areas of liver cell necrosis.

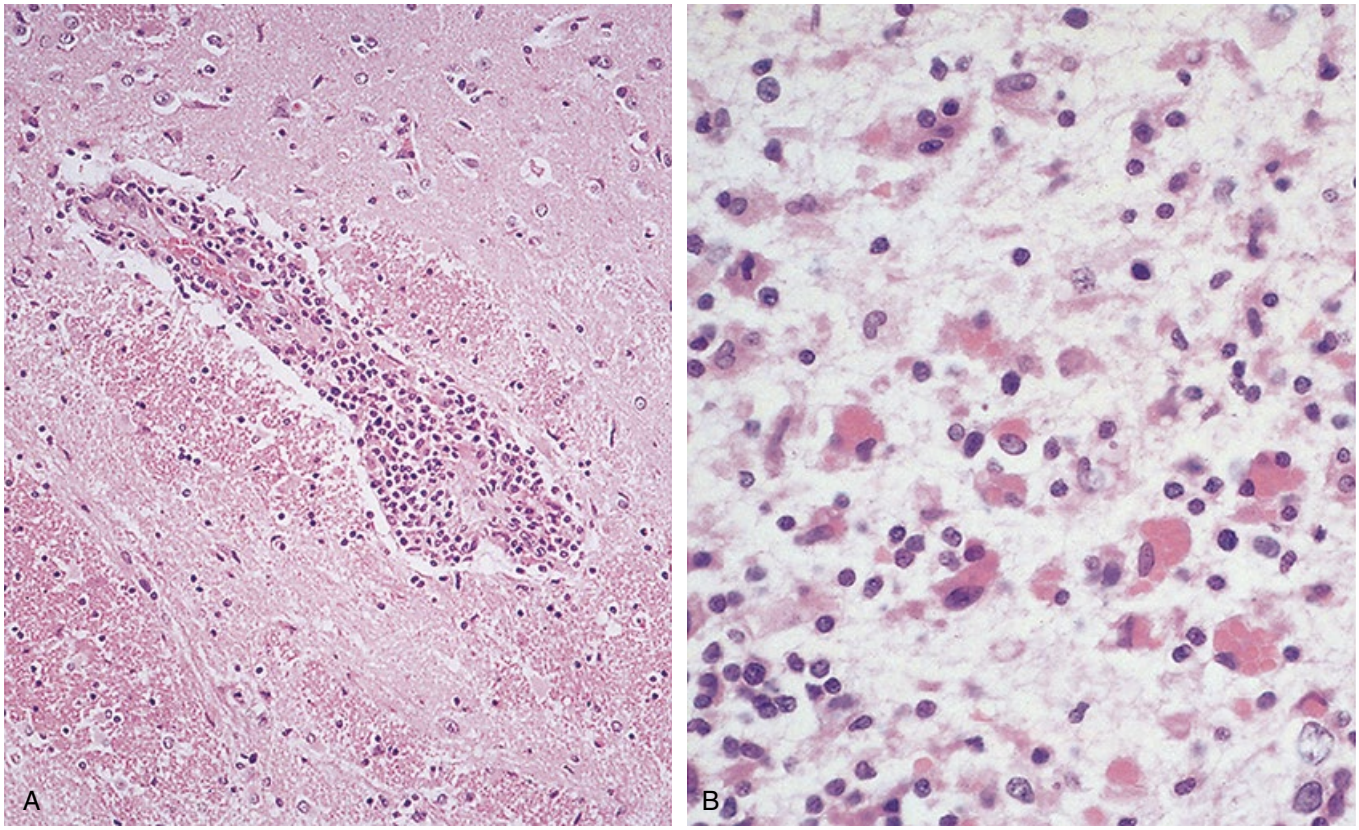

Fig. 24.8. Familial hemophagocytic syndrome. **A,** Section of brain at necropsy showing a collection of lymphocytes in the perivascular (Virchow–Robin) space. **B,** Higher magnification shows histiocytes that contain both red cells (erythrophagocytosis) and lymphocytes (lymphophagocytosis). (*A* and *B*, Courtesy of Dr. JE McLaughlin.)

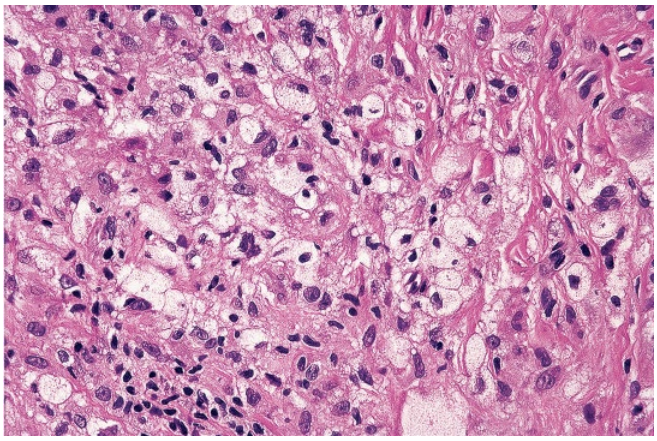

Fig. 24.9. Xanthogranuloma. Skin biopsy showing an established lesion consisting of histiocytes, lymphocytes, and xanthoma cells. (Courtesy of Professor PH McKee.)

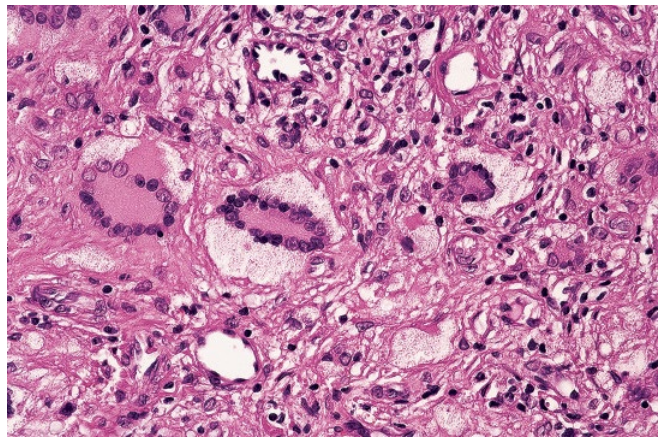

Fig. 24.10. Xanthogranuloma. Skin biopsy showing multinucleated giant cells, which are a characteristic feature. (Courtesy of Professor PH McKee.)

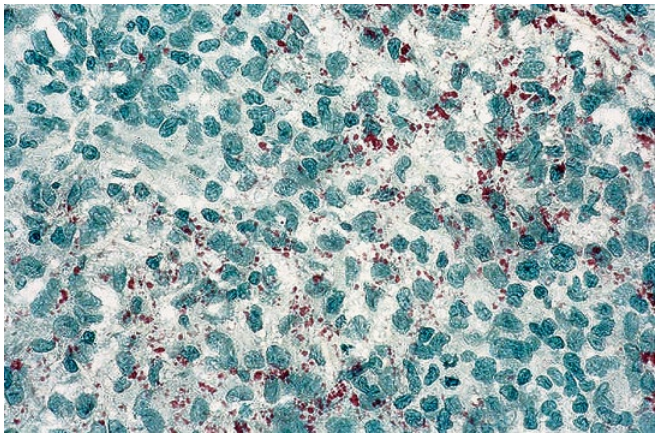

Fig. 24.11. Xanthogranuloma: skin biopsy. The presence of lipid can be identified in frozen sections stained with oil red O. (Courtesy of Professor PH McKee.)

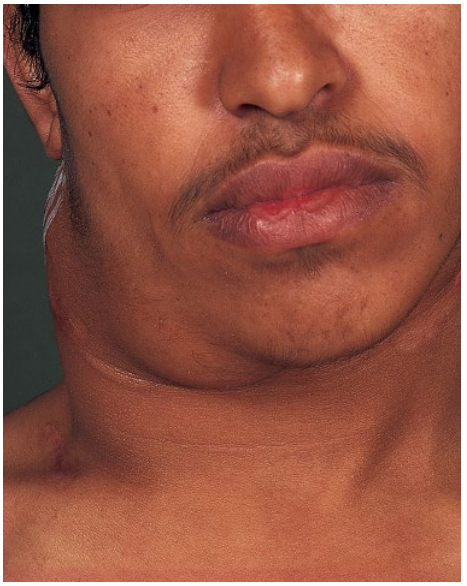

Fig. 24.12. Rosai–Dorfman disease. Massive painless cervical lymphadenopathy in a teenager from the Middle East. This resolved spontaneously over a 2-year period.

show marked sinusoidal dilatation by macrophages with foamy cytoplasm (Fig. 24.13) and plasma cells. There is often evidence of engulfment of lymphocytes by hyperplastic histiocytes (Fig. 24.14). Immunohistologic staining demonstrates strong positivity for S-100 (Fig. 24.15). Although the disease can follow a protracted course, recovery is usually spontaneous and total.

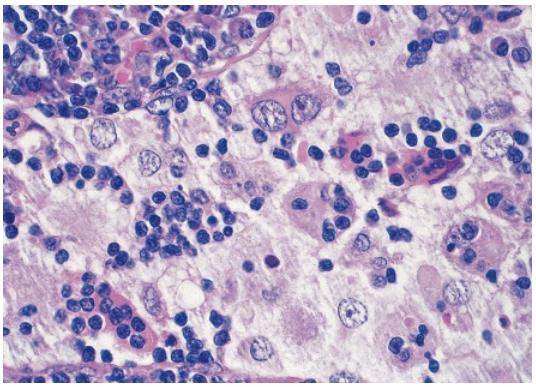

Fig. 24.14. Rosai–Dorfman disease: Lymph node biopsy. High-power view showing characteristic histiocytes with engulfment of lymphocytes. (Courtesy of Professor KA MacLennan.)

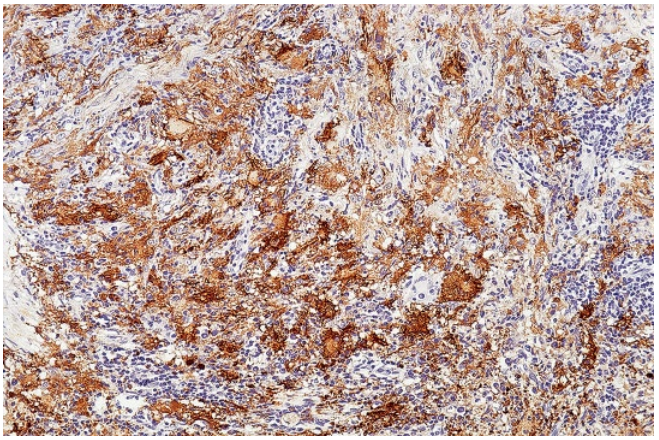

Fig. 24.15. Rosai–Dorfman disease: Lymph node biopsy. The histiocytes are S-100 positive. (Courtesy of Professor PH McKee.)

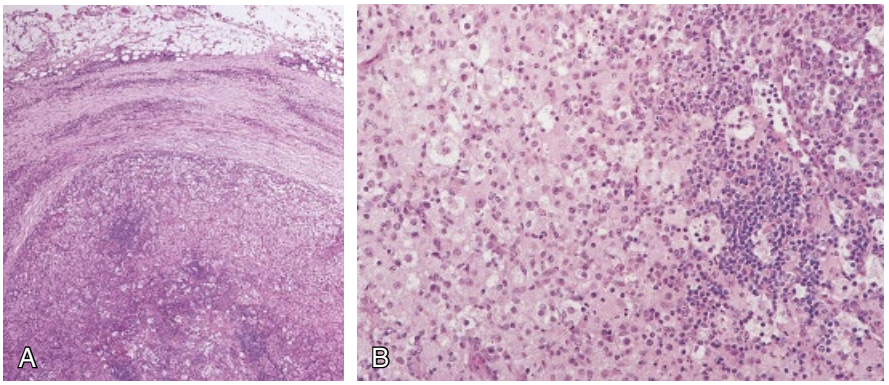

Fig. 24.13. Rosai–Dorfman disease. **A,** Lymph node biopsy showing marked capsular and pericapsular fibrosis. The sinuses are distended by a proliferation of histiocytes. This condition may occasionally be confused with a histiocytic lymphoma. **B,** Higher-power view shows a confluent mass of histiocytes with abundant vacuolated cytoplasm. There is a focal collection of lymphocytes and residual medullary cords.

HISTIOCYTIC AND DENDRITIC CELL NEOPLASMS

The 2016 Revised fourth edition of the World Health Organization (WHO) classification of histiocytic and dendritic cell tumors is shown in Table 24.2. Table 24.3 lists the characteristic immunophenotypic marker patterns of histiocytes and accessory dendritic cells that help to identify the tumor type.

The cellular counterparts of this group of neoplasms consist of myeloid-derived macrophages, myeloid-derived dendritic cells, and stromal-derived dendritic cells, whose genealogy is summarized in Fig. 24.16. The myeloid-derived macrophages and dendritic cells constitute divergent lines of differentiation from bone marrow precursors, although transdifferentiation or hybrid differentiation states likely occur. Follicular dendritic stem cells form a mesenchymal precursor, which also gives rise to fibroblastic reticulum cells contributing to the maintenance of lymphoid integrity and cytokine production and transport. Histiocytic and dendritic cell neoplasms (HDCN) tend to reproduce the morphologic, phenotypic, and ultrastructural characteristics of terminally differentiated elements. In line with this, in the WHO Classification, blastic plasmacytoid dendritic cell neoplasm was excluded from the HDCN chapter and listed autonomously among myeloid neoplasms, because it stems from a cell that acquires terminal differentiation and dendritic appearance following activation.

TABLE 24.2. REVISED WORLD HEALTH ORGANIZATION (2016) CLASSIFICATION OF TUMORS OF HISTIOCYTES AND DENDRITIC CELLS

Histiocytic and dendritic cell neoplasms	
9755/3	Histiocytic sarcoma
9751/1	Langerhans cell histiocytosis
9756/3	Langerhans cell sarcoma
9757/3	Indeterminate dendritic cell tumour
9757/3	Interdigitating dendritic cell sarcoma
9758/3	Follicular dendritic cell sarcoma
9759/3	Fibroblastic reticular cell tumour
0000/0	Disseminated juvenile xanthogranuloma
9750/1	Erdheim–Chester disease

TABLE 24.3. IMMUNOPHENOTYPES OF HISTIOCYTES AND DENDRITIC CELLS ACCORDING TO *WHO (2016) CLASSIFICATION OF TUMOURS OF HAEMATOPOIETIC AND LYMPHOID TISSUES*

Marker	LC	IDC	FDC	PDC	Mø	DIDC
MHC Class II	+c	++s	–	+	+	+/–
Fc receptors	–	–	+	–	+	–
CD1a	++	–	–	–	–	–
CD4	+	+	+	+	+	+/–
CD21	–	–	++	–	–	–
CD35	–	–	++	–	–	–
CD68	+/–	+/–	–	++	++	+
CD123	–	–	–	++	–	–
CD163	–	–	–	–	++	–
Factor XIIa	–	–	+/–	–	–	++
Fascin	–	++	+/++	–	–/+	+
Langerin	++	–	–	–	–	–
Lysozyme	+/–	–	–	–	+	–
S100	++	++	+/–	–	+/–	+/–
TCL1	–	–	–	+	–	–

c, Cytoplasmic; DIDC, dermal/interstitial dendritic cell; FCR, Fc IgG receptors (include CD16, CD32. CD64 on some cells); FDC, follicular dendritic cell; IDC, interdigitating dendritic cell; LC, Langerhans cell; Mø, macrophage; PDC, plasmacytoid dendritic cell; s, surface. Expression is semiquantitatively graded 0 through ++: + present, ++ high, +/– low or varies with cell activity.

HISTIOCYTIC SARCOMA

Histiocytic sarcoma is a rare tumor associated with an aggressive clinical course. Most cases occur in adults. The most common presenting feature is lymphadenopathy, closely followed by gastrointestinal or skin involvement. Fever, weight loss, blood pancytopenia, hepatomegaly, and splenomegaly can be present in cases with systemic involvement through metastatic spread.

Characteristic histologic features of the malignant cells are depicted in Fig. 24.17. The cells are large and polymorphic with round or oval nuclei and abundant eosinophilic or foamy cytoplasm. The neoplastic cells are associated with a dense reticulin fiber network (Fig. 24.18). They must be differentiated from large cell lymphomas by the demonstration of histiocytic markers, such as lysozyme (Fig. 24.19), CD68, CD163, CD11c, or CD14. Images from a further case of histiocytic sarcoma are shown in Fig. 24.20. Clonal *IGVH* or *TCR* rearrangements have been reported in a few cases, which might represent examples of transdifferentiation. *BRAF* mutations have also been occasionally detected.

LANGERHANS CELL HISTIOCYTOSIS

Langerhans cell histiocytosis comprises the diseases previously known as histiocytosis X: Letterer–Siwe disease, Hand–Schuller–Christian disease, and eosinophilic granuloma of bone. Langerhans cells are distinguished on electron microscopy by the presence of Birbeck granules (Fig. 24.21) and by immunohistologic positivity for CD1a, S-100, and CD207. Rearrangement of *IGVH* or *TCR* has been reported in some cases as the results of transdifferentiation. Normal Langerhans cells are antigen-presenting cells, but the neoplastic cells of Langerhans cell histiocytosis are primitive dendritic cells and have lost this function. Small numbers of families have more than one relative affected, and the disease has occurred in several sets of monozygotic and dizygotic twins. Although these family clusters support a role for genetic factors, no chromosomal abnormalities have been established. A number of studies have suggested that, like other pediatric clonal neoplastic proliferations, Langerhans cell histiocytosis may require a two-step mutational process. It has recently been shown that tumor cell proliferation in Langerhans-cell histiocytosis is driven by extracellular signal-regulated kinase (ERK) activation of the MAP kinase pathway, which in about 50% of cases is triggered by *BRAF V600E* mutation, or by activating mutations of *MAP2K1*, *MAP3K1*, *ARAF, NRAS, KRAS, ALK*,

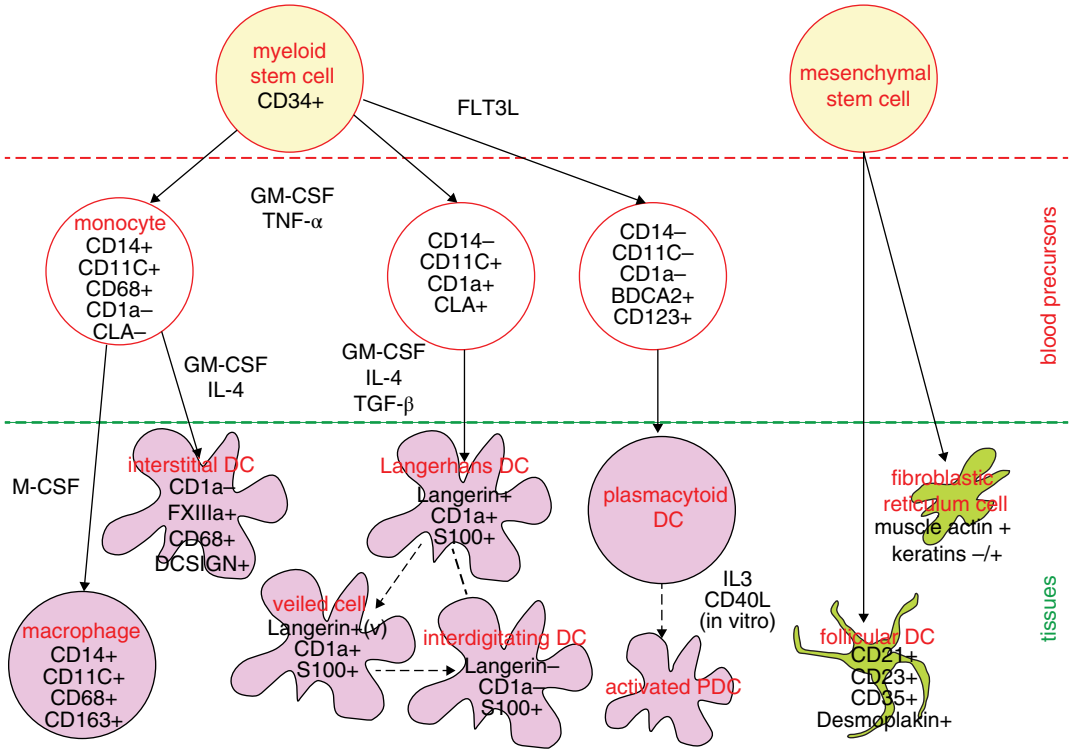

Fig. 24.16. The genealogy and maturation steps of histiocytes and dendritic cells according to the Revised WHO (2016) Classification of Haematopietic and Lymphoid Tissues. CD, cluster of differentiation according to the Leukocyte Differentiation Antigen Classification; CD40L, CD40 ligand; DC, dendritic cell; FLT3L, FMS-like tyrosine kinase 3 ligand; GM-CSF, granulocyte–monocyte colony-stimulating factor; IL, interleukin; M-CSF, monocyte colony-stimulating factor; S-100, protein S-100; TGF-β, transforming growth factor β; TNF-α, tumor necrosis factor α.

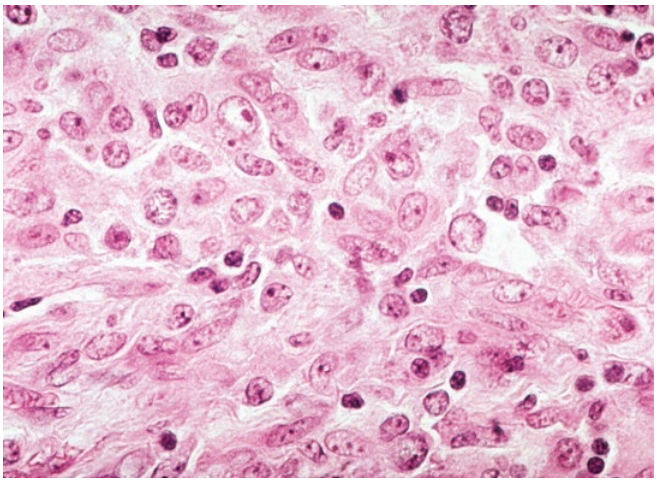

Fig. 24.17. Histiocytic sarcoma. Histologic section of lymph node showing replacement of normal architecture by abnormal histiocytic cells with abundant cytoplasm.

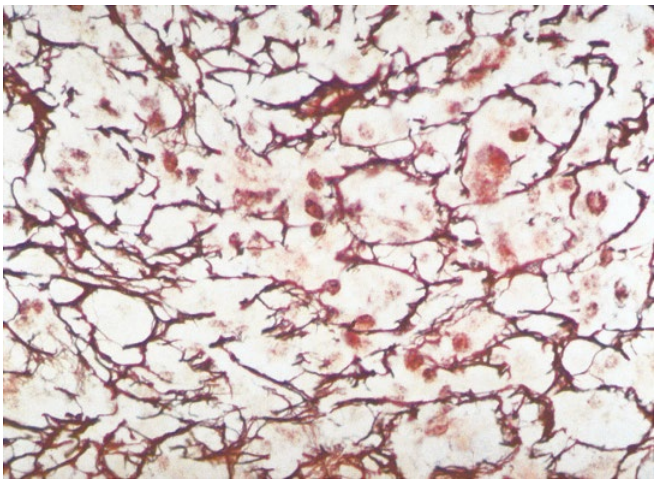

Fig. 24.18. Histiocytic sarcoma. Silver impregnation staining of the case in Fig. 24.17 shows a prominent dense reticulin fiber network surrounding individual tumor cells.

or *NTRK1* in a fraction of *BRAF* wild-type cases. A relationship between stage of maturation of the cell in which the mutational hit occurs and extent of the disease might explain the broad spectrum of clinical manifestations.

In Langerhans cell histiocytosis, the neoplastic cells, sometimes associated with eosinophils, lymphocytes, neutrophils, and macrophages, infiltrate a wide variety of organs, especially the skin, bone, lymph nodes, liver, spleen, and bone marrow. The disease can involve a single or multiple systems. The central nervous system, lungs, and gastrointestinal tract can also become involved. Multisystem disease usually affects children initially in the first 3 years of life, with hepatomegaly, splenomegaly, lymphadenopathy, and eczematoid skin eruptions (Fig. 24.22). Localized lesions occur frequently in the skull (Figs. 24.23–24.25), ribs, and long bones. Involvement of the central nervous system results in degenerative changes in the cerebellum (Fig. 24.26). In familial forms of Langerhans cell histiocytosis, the disease involves white matter of the cerebral hemispheres (Fig. 24.27). Diabetes insipidus can follow disease in the hypothalamus and pituitary stalk (Fig. 24.28). Lung involvement

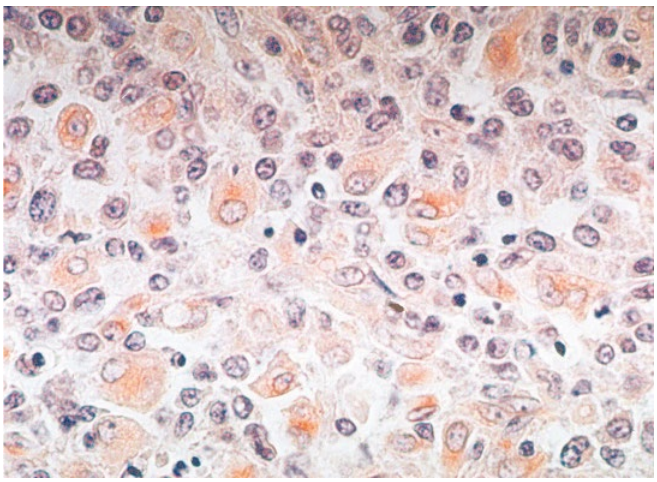

Fig. 24.19. Histiocytic sarcoma. Immunoperoxidase staining for lysozyme of the case in Fig 24.17 shows a proportion of positive cells indicating a monocytic-histiocytic origin. The cells were also positive for α_1-antitrypsin.

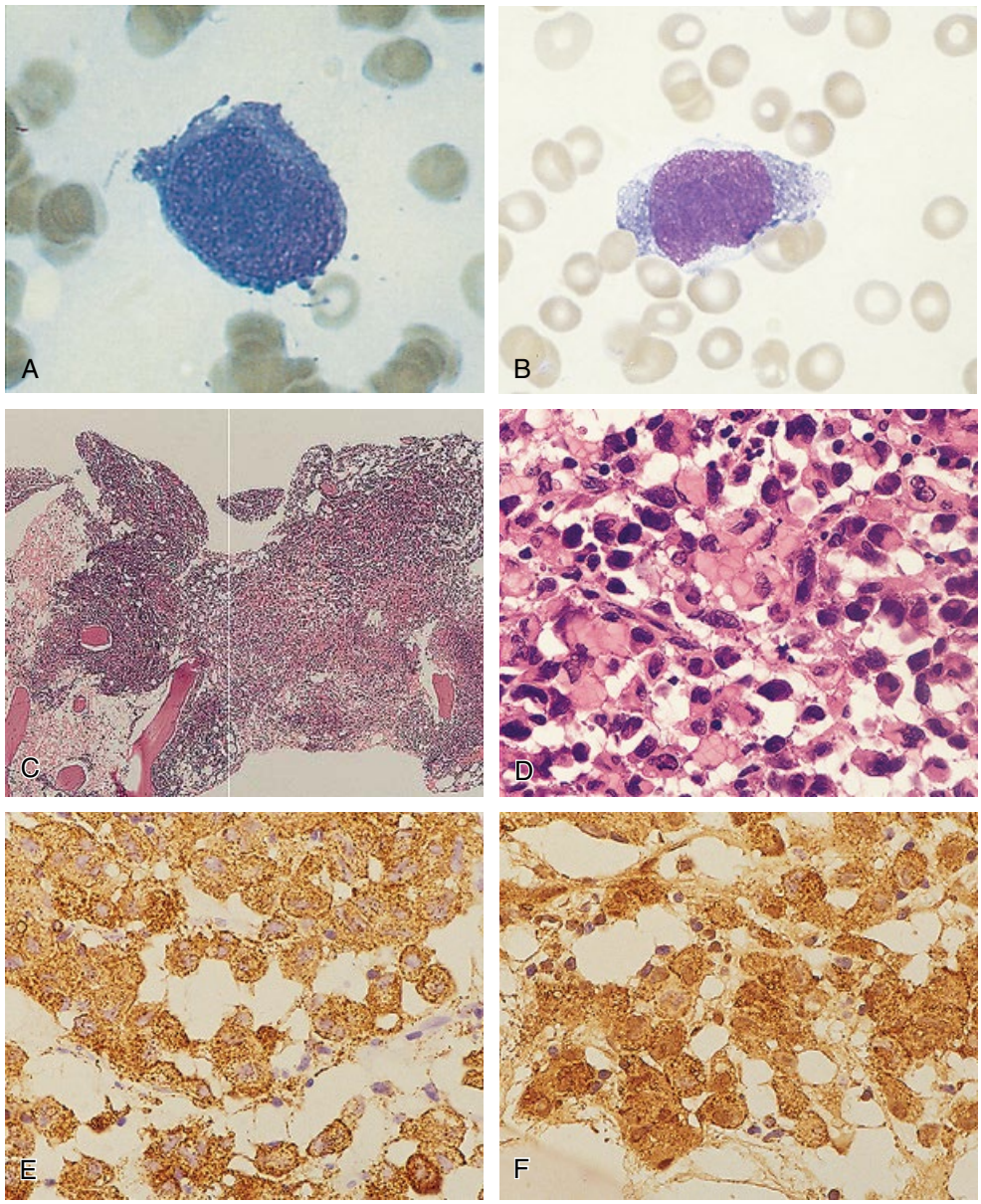

Fig. 24.20. Histiocytic sarcoma. **A** and **B,** Two examples of the large atypical monocytoid cells in peripheral blood. **C,** Trephine biopsy showing extensive replacement of hematopoietic tissue and fat by tumor. **D,** At higher magnification the atypical monocytoid cells are pleomorphic with hyperchromic nuclei and abundant cytoplasm, which in some cells show vacuolation. **E,** Immunoperoxidase staining shows cytoplasmic positivity for CD68 and lysozyme **(F);** the cells are also positive for CD45. (Courtesy of Professor PG Isaacson.)

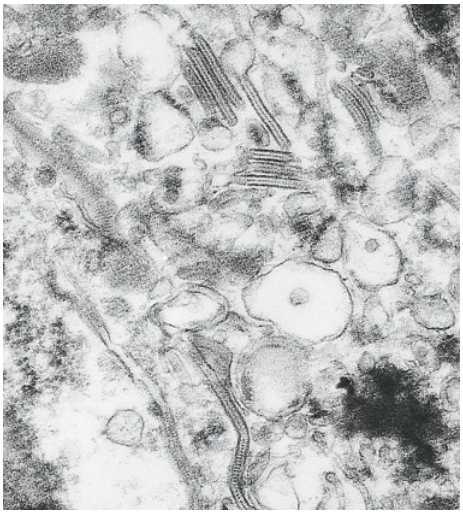

Fig. 24.21. Langerhans cell histiocytosis: Birbeck granules in the cytoplasm. These are rod-shaped structures with a central striated line that terminates in some cases in a vesicular dilation, which gives a tennis racquet appearance. They may arise secondary to receptor-mediated endocytosis and are not present in normal monocytes and non-Langerhans macrophages. (Courtesy of Professor P Lanzkowsky.)

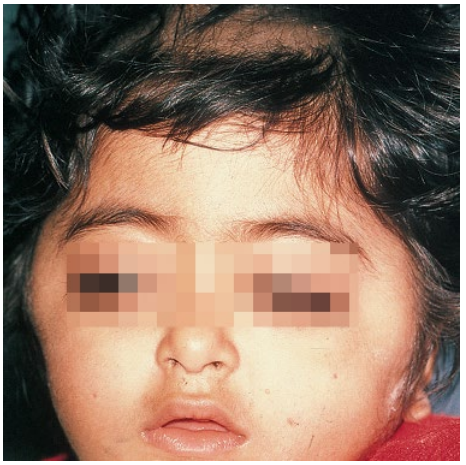

Fig. 24.23. Multisystem Langerhans cell histiocytosis. Prominent bossing of the frontal bone and proptosis in a child with multiple skull deposits. (Courtesy of Dr. U O'Callaghan.)

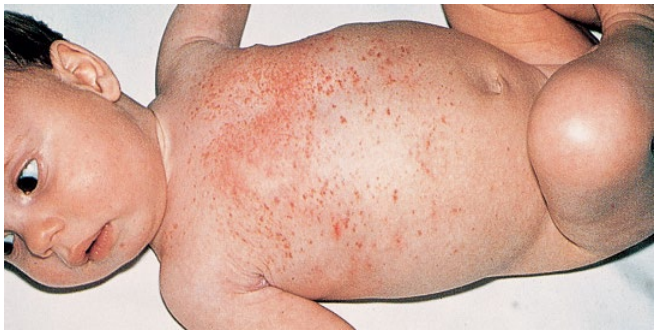

Fig. 24.22. Multisystem Langerhans cell histiocytosis. Typical hemorrhagic eczematoid rash in a 10-month-old child. (Courtesy of Dr. MD Holdaway.)

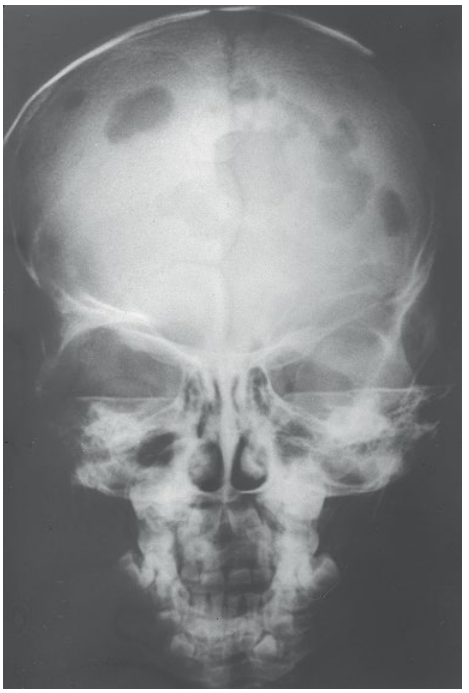

Fig. 24.24. Multisystem Langerhans cell histiocytosis. Skull x-ray showing the presence of numerous osteolytic lesions. (Courtesy of Dr. S Imashuku.)

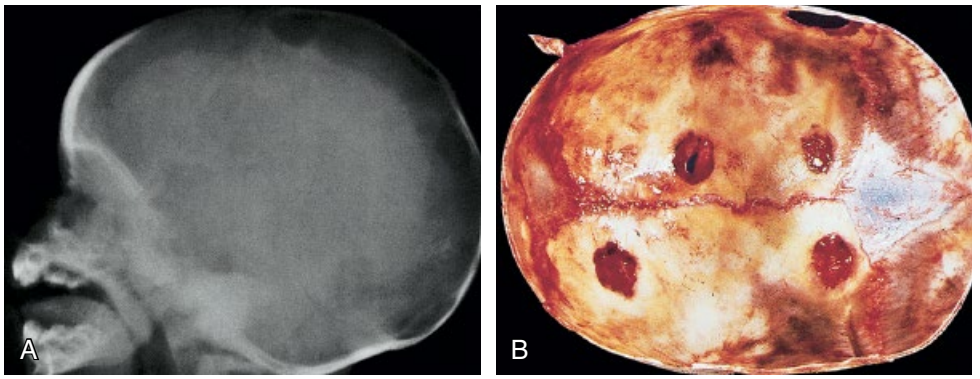

Fig. 24.25. Multisystem Langerhans cell histiocytosis. Skull of an infant seen radiographically **(A)** and at necropsy **(B)** shows the typical osteolytic deposits in the vault.

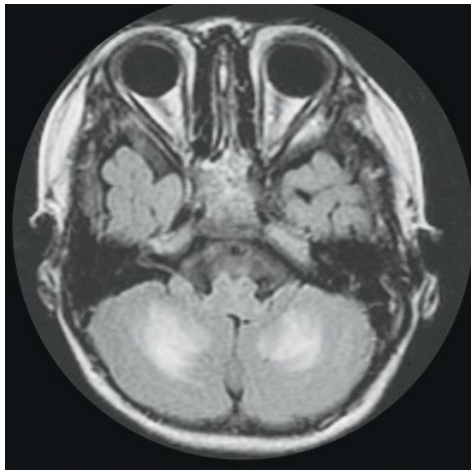

Fig. 24.26. Multisystem Langerhans cell histiocytosis. Magnetic resonance imaging (MRI) scan showing increased signal in the cerebellum indicating cerebellar degeneration. (Courtesy of Dr. S Imashuku.)

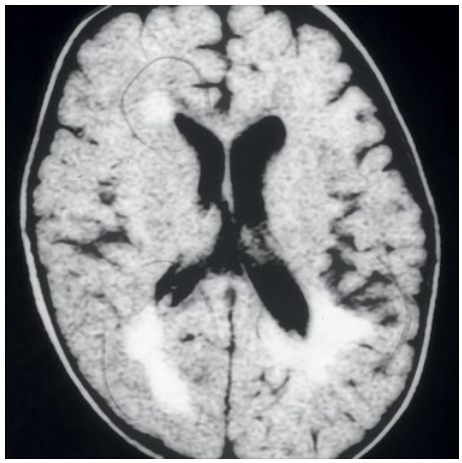

Fig. 24.27. Multisystem Langerhans cell histiocytosis. Magnetic resonance imaging (MRI) scan showing increased signal in the white matter of the occipital and frontal lobes in a patient with the familial form of the disease. (Courtesy of Dr. S Imashuku.)

causes extensive fibrocystic changes resulting in a characteristic radiographic "honeycomb lung" (Fig. 24.29).

Typical histologic features in skin biopsies are shown in Figs. 24.30–24.32. Langerhans cells are recognized by their characteristically grooved, folded, or lobulated nuclei with fine

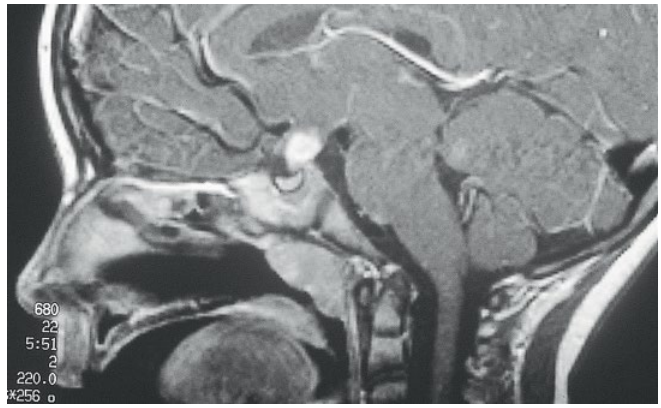

Fig. 24.28. Multisystem Langerhans cell histiocytosis. Magnetic resonance imaging (MRI) showing thickened pituitary stalk with absent posterior pituitary signal on T1-weighted images. (Courtesy of Dr. DKH Webb.)

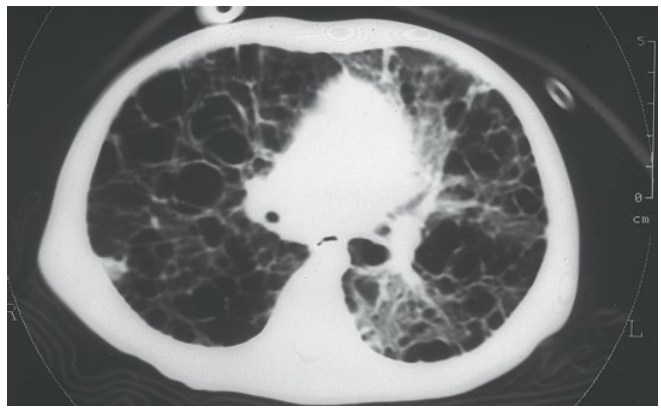

Fig. 24.29. Multisystem Langerhans cell histiocytosis. Magnetic resonance imaging (MRI) scan showing extensive fibrocystic changes in the lungs ("honeycomb lung"). (Courtesy of Dr. S Imashuku.)

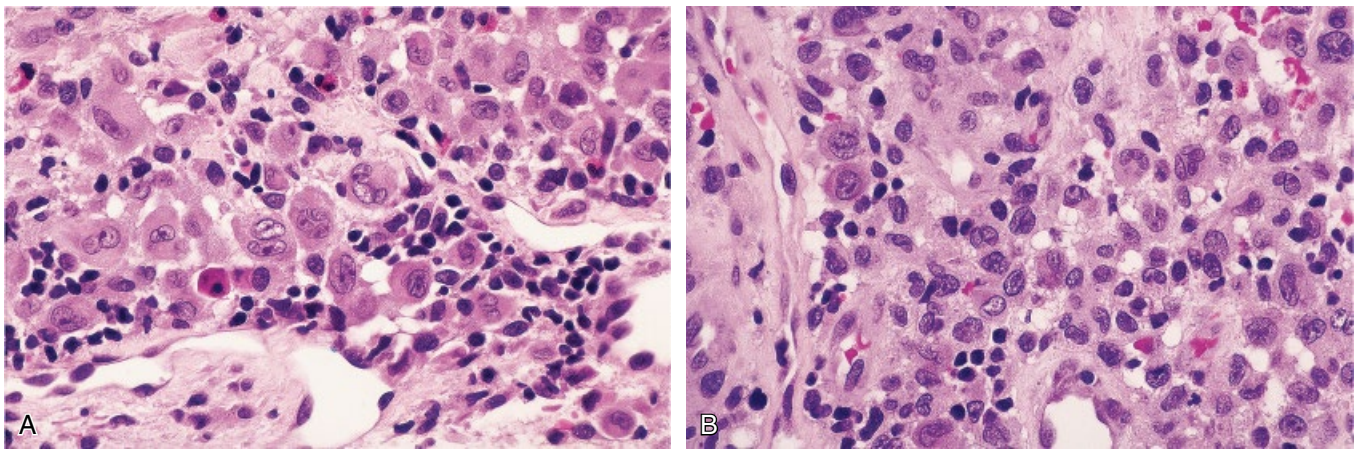

Fig. 24.30. Multisystem Langerhans cell histiocytosis: Skin biopsy. **A,** This field shows typical coffee bean vesicular nuclei. **B,** A nucleus with a nuclear groove is present in the center of the field. (Courtesy of Professor PH McKee.)

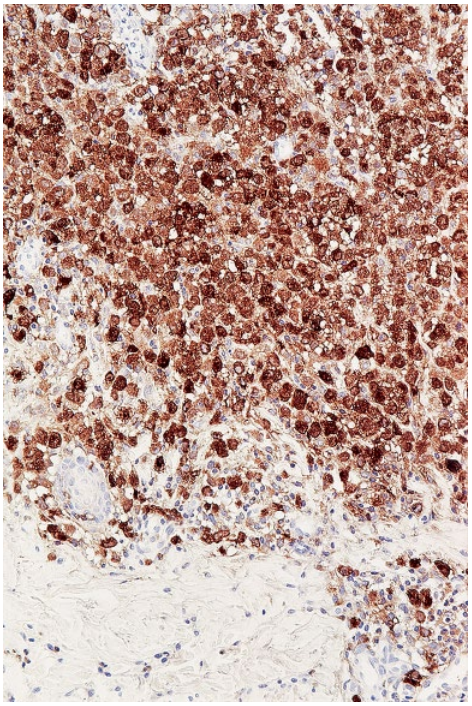

Fig. 24.31. Multisystem Langerhans cell histiocytosis: Skin biopsy. Immunohistologic staining shows a uniform expression of S-100 in tumor cells. (Courtesy of Professor PH McKee.)

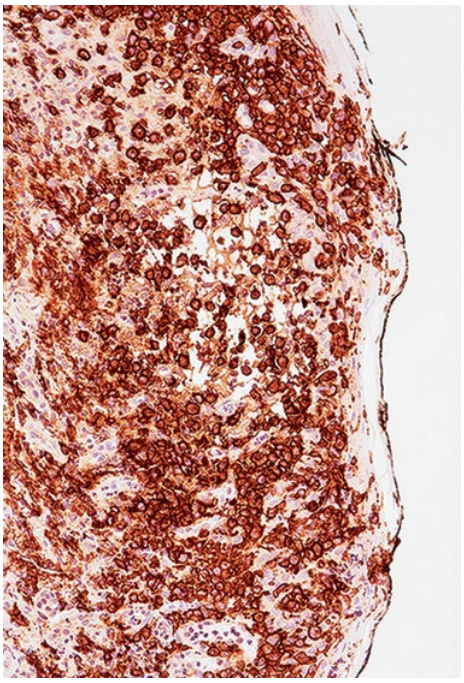

Fig. 24.32. Multisystem Langerhans cell histiocytosis: Skin biopsy. CD1a is also strongly positive. (Courtesy of Professor PH McKee.)

chromatin and inconspicuous nucleoli and moderately abundant cytoplasm. Bone marrow aspirates occasionally show cells with typical Langerhans cell features (Fig. 24.33), but evidence of involvement is more easily seen in trephine biopsies. In localized disease in bone, the Langerhans cells are associated with

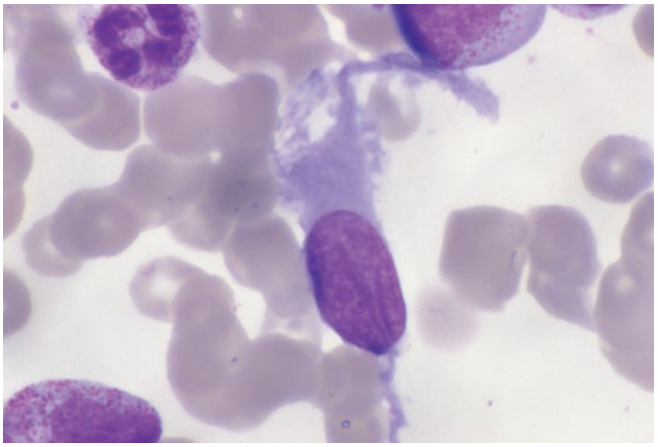

Fig. 24.33. Multisystem Langerhans cell histiocytosis. Bone marrow aspirate showing a Langerhans cell with a central nuclear groove. (Courtesy of Dr. S Imashuku.)

eosinophils (Fig. 24.34). Biopsy of later localized osteolytic bone lesions shows sheets of lipid-laden foam cells (Fig. 24.35).

LANGERHANS CELL SARCOMA

Langerhans cell sarcoma is exceedingly rare. It has been reported in both adults and children. Multisystem involvement includes lymph nodes, liver, spleen, lung, and bone. Histology shows large cells with malignant features including hyperchromatic nuclei and prominent nucleoli (Fig. 24.36). There may be nuclear grooves similar to those found in Langerhans cell histiocytosis, and there is a high mitotic rate. Birbeck granules are present on electron microscopy. Immunohistologic staining shows S-100 and focal CD1a and CD207 positivity and, in some cases, positivity for CD68, CD45, and lysozyme. Genetic aberrations as in Langerhans-cell histiocytosis have been reported.

INDETERMINATE DENDRITIC CELL TUMOR

This very rare tumor is thought to derive from the precursor cells of Langerhans cells. There is a diffuse dermal and subcutaneous infiltrate of neoplastic ovoid and spindle-shaped cells that express S-100 protein and CD1a but lack CD207 and Birbeck granules on electron microscopy.

INTERDIGITATING DENDRITIC CELL SARCOMA

Interdigitating dendritic cell sarcoma is another exceedingly rare tumor. Asymptomatic lymph node involvement is most common, but some cases have involved skin tumors. In some patients, there is an aggressive clinical course with fever, weight loss, hepatomegaly, splenomegaly, and gastrointestinal involvement. Histologic examination of excised lymph nodes shows a paracortical distribution of tumor cells with residual lymphoid follicles (Fig. 24.37, *A*). The neoplastic dendritic cells form fascicles and whorls of oval and spindled cells with areas of more rounded larger cells (Fig. 24.37, *B* and *C*). The tumor cells consistently show S-100 positivity (Fig. 24.37, *D*) and are negative

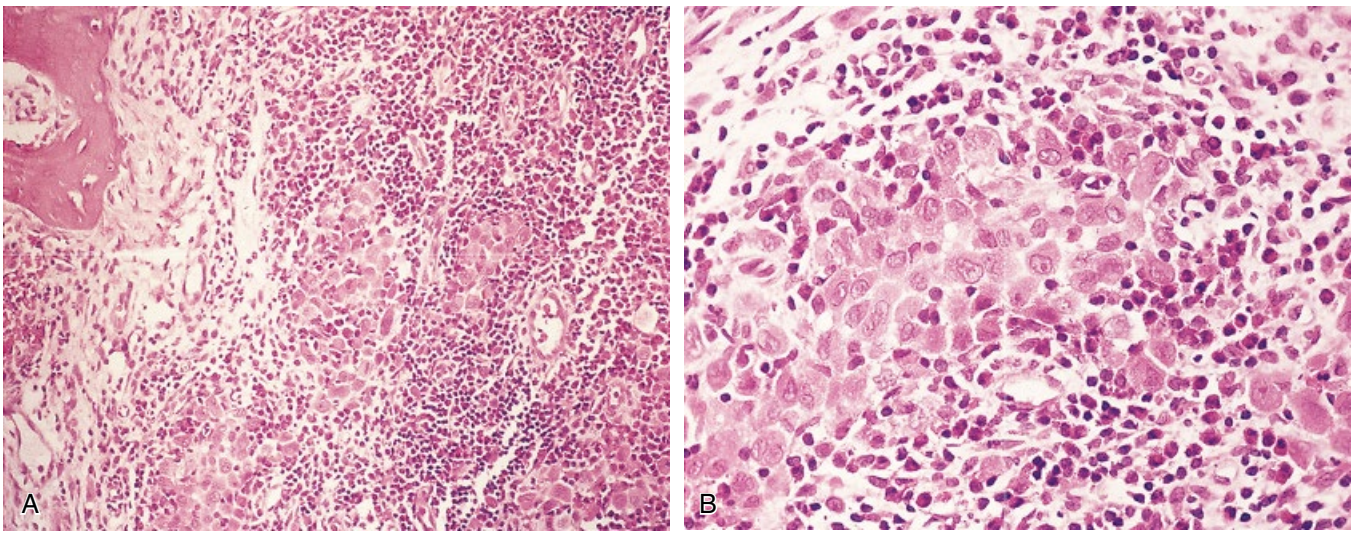

Fig. 24.34. Single-system Langerhans cell histiocytosis. **A,** Trephine biopsy of a 28-year-old man with skeletal lesions shows replacement of normal hematopoietic tissue by sheets of histiocytes and eosinophils. **B,** Higher-power view of the abnormal histiocytes and eosinophils.

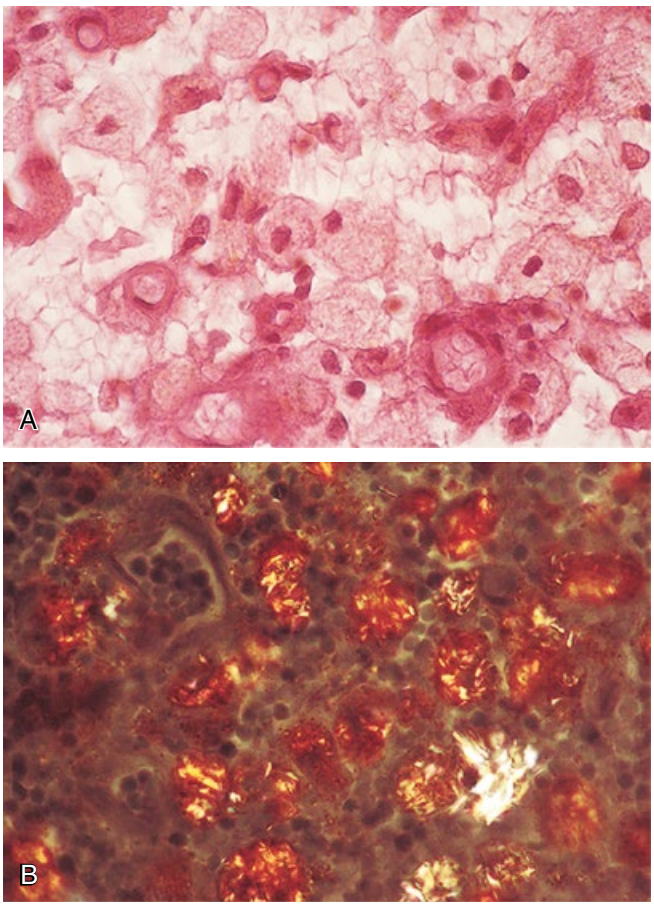

Fig. 24.35. Multisystem Langerhans cell histiocytosis. Frozen sections of a skeletal lesion stained using the Sudan IV technique and viewed under **A,** normal and **B,** polarized light. The staining reaction indicated accumulation in the cytoplasm of neutral fat and cholesterol.

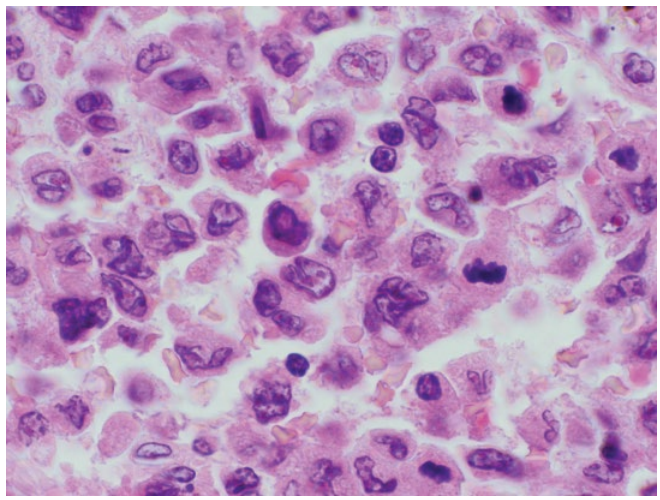

Fig. 24.36. Langerhans cell sarcoma. High-power histologic section showing pleomorphic cells resembling Langerhans cells with nuclear folding and eosinophilic cytoplasm, but also showing malignant features such as nuclear hyperchromatism, prominent nucleoli, and multinuclearity. There are numerous mitoses. (Courtesy of Dr. LM Weiss.)

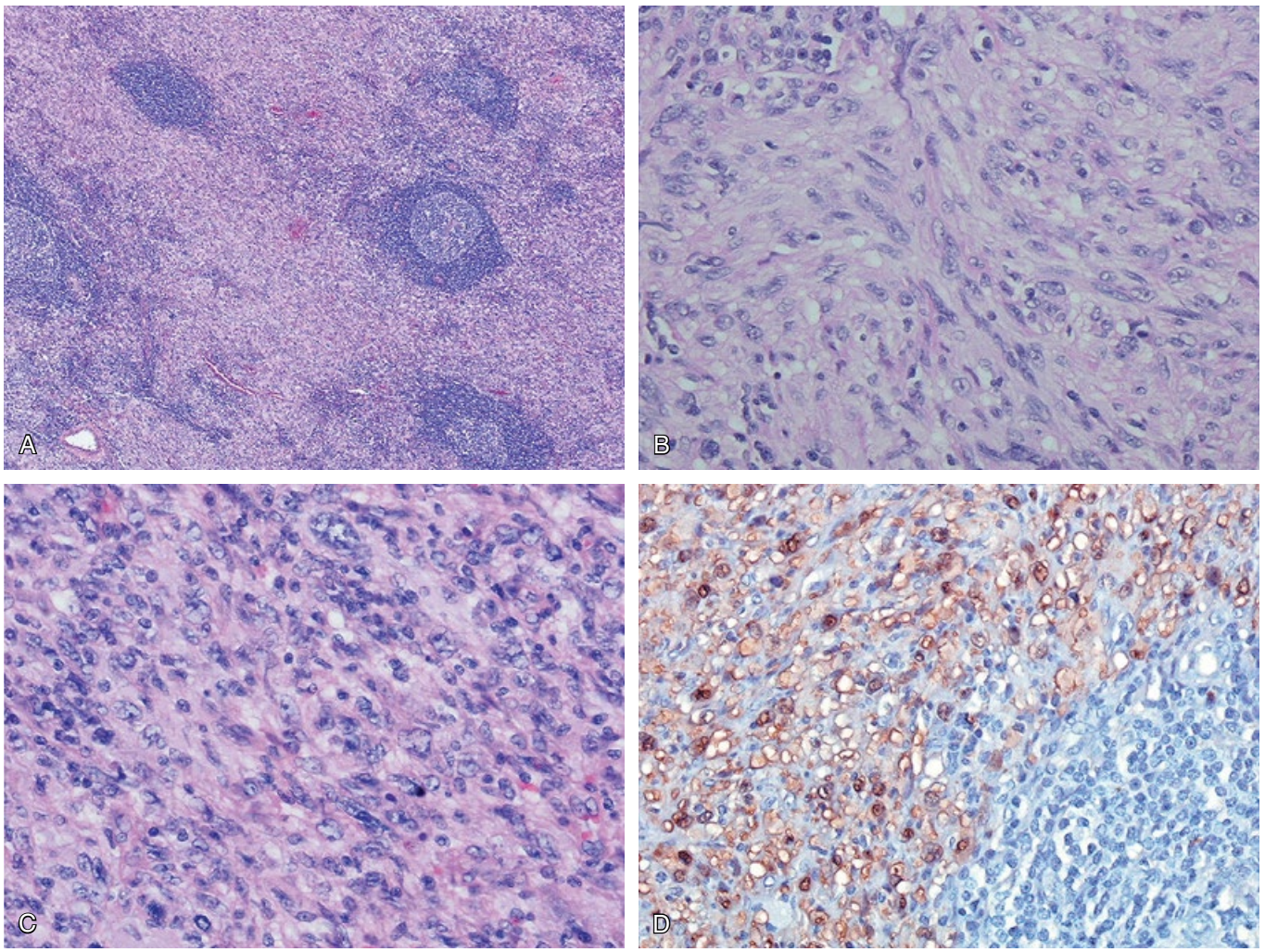

Fig. 24.37. Interdigitating dendritic cell sarcoma: Lymph node biopsy. **A,** A low-power image shows extensive paracortical tumor with residual lymphoid follicles. **B,** At higher power many of the tumor cells are spindle-shaped with indistinct borders and bland nuclei with a vesicular chromatin pattern. **C,** In other areas the tumor cells are rounded and more pleomorphic, and some have single nucleoli. **D,** Immunohistologic staining with S-100 shows positivity for the tumor cells, but there is no labeling of cells in the residual lymphoid follicle on the lower right. (Courtesy of Dr. D Ellis.)

for CD1a and CD207 as well as for the markers used to identify follicular dendritic cells, CD21 and CD35.

FOLLICULAR DENDRITIC CELL SARCOMA

Follicular dendritic cell tumors are also rare. In 10–20% of cases there has been an association with Castleman disease. Conversely to histiocytic sarcoma, Langerhans cell neoplasms, interdigitating cell sarcoma, and indeterminate cell sarcoma, the process does not originate from a myeloid precursor but from a mesenchymal stem cell. In over half of the cases described patients present with asymptomatic lymphadenopathy. Extranodal involvement is recorded in 58%, the most commonly affected sites being the tonsil, spleen, oral cavity, gastrointestinal tract, liver, soft tissues, skin, and breast. Nodal localization is detected in 31% of patients, cervical lymph nodes being the most commonly interested ones with fewer patients having axillary, mesenteric, mediastinal, or retroperitoneal nodal involvement. In about 10% of cases, both nodal and extranodal involvement is observed. Compared with interdigitating dendritic cell sarcomas, follicular dendritic tumors are most often indolent and tend to be localized with a potential for local spread or recurrence with less frequent spread to distant sites.

Histologic examination of involved sites (Fig. 24.38, *A* and *B*) shows neoplastic ovoid and spindle-shaped cells often in fascicles, storiform, or whorling patterns. Residual lymphocytes are scattered throughout the tumor cells or in perivascular locations. Immunohistologic stains show positivity for one or more of the follicular dendritic cell markers CD21, CD23, CD35, CXCL13, clusterin, desmoplakin, podoplanin, claudin 4, vimentin, fascin, and EGFR (Fig. 24.38, *C*). Most if not all cases carry PD-L1, in keeping with the results of recent molecular studies. Aberrant phenotypic expression can be seen, including CD30 positivity. Ultrastructurally, neoplastic cells show long processes connected by scattered desmosomes. A targeted sequencing study revealed recurrent loss-of-function of tumor suppressor genes involved in the negative regulation of NFκB (38%) and cell cycle (31%), including *NFKBIA*, *CYLD*, *CDKN2A*, and *RB1*.

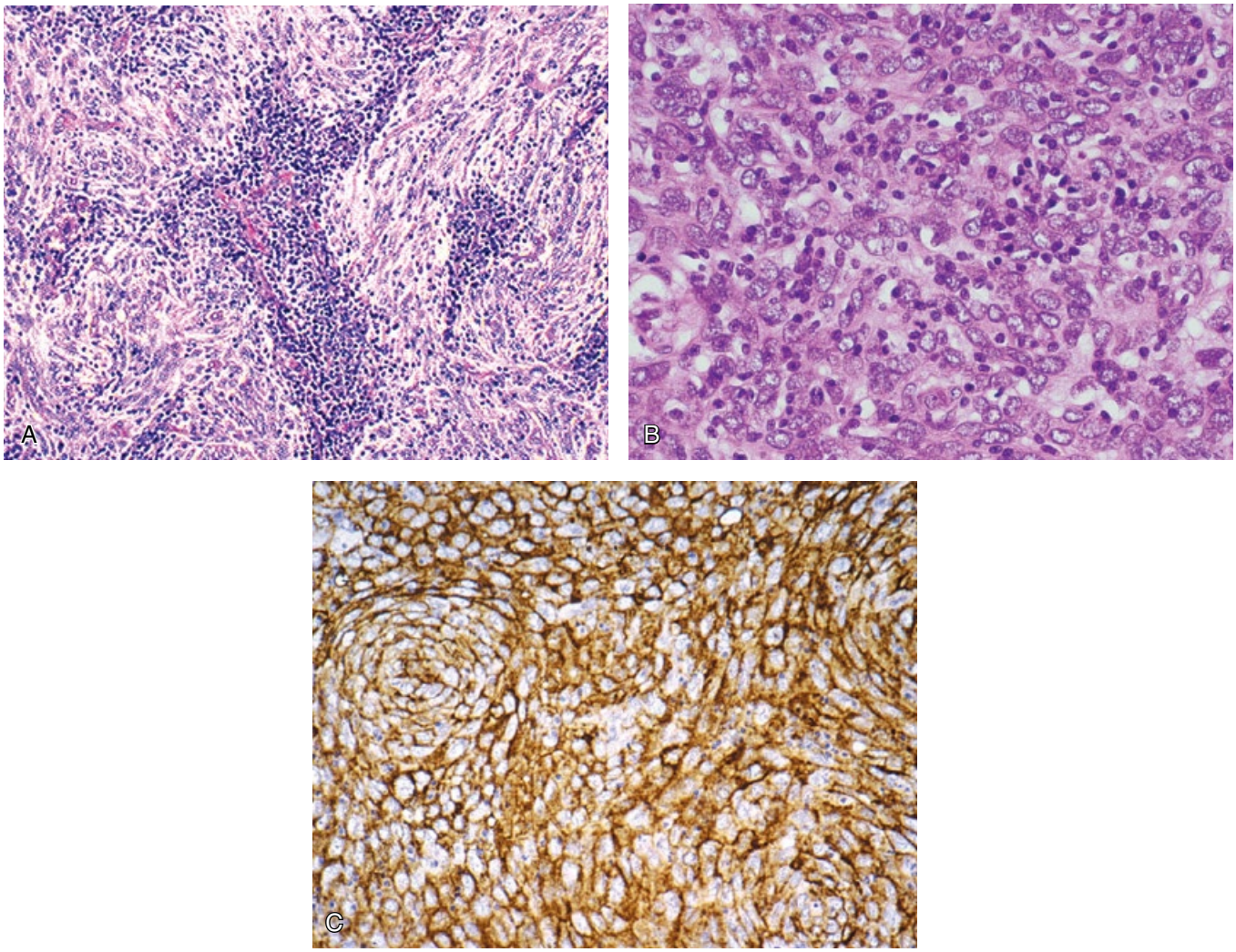

Fig. 24.38. Follicular dendritic cell tumor: Lymph node biopsy. **A,** At low power there are sheets, fascicles, and whorls of spindle and oval tumor cells with perivascular collections of residual lymphocytes. **B,** In a higher-power view the cells show mild atypia with vesicular nuclei and indistinct cytoplasmic outlines. Occasional cells have multiple nuclei. Small numbers of small lymphocytes are scattered within the tumor. **C,** Immunostaining with CD21 shows strong positivity and outlines a prominent whorl of tumor cells on the left. (Courtesy of Dr. LM Weiss.)

FIBROBLASTIC RETICULAR CELL TUMOR

Tumors arising from the fibroblastic reticular (dendritic) stromal support cells of lymph nodes, spleen, and tonsil are very rare (Fig. 24.39). These tumors show a whorled pattern of oval and spindle cells in a collagenous background. Immunostaining shows variable positivity for CD21, CD35, vimentin, desmin, smooth muscle actin, CD68, and cytokeratin.

DISSEMINATED JUVENILE XANTHOGRANULOMA

Disseminated juvenile xanthogranuloma (DJXG) is characterized by a proliferation of histiocytes similar to those of the dermal JXG, commonly having a foamy (xanthomatous) component with Touton-type giant cells. There is evidence for clonality in some instances. Erdheim–Chester disease (ECD) is distinguished from JXG in the current classification of histiocytic neoplasms. The majority of deep, visceral, and disseminated forms occur by age 10 years, half within the first year of life.

ERDHEIM–CHESTER DISEASE

Erdheim–Chester disease (EDC) is a clonal systemic proliferation of histiocytes, commonly having a foamy (xanthomatous) component containing Touton giant cells (Fig. 24.40, *A* and *B*). It was first described by Chester in 1930 and named Erdheim–Chester disease in 1972 to recognize the contribution given to the discovery of the condition by Erdheim, who was Chester's mentor. EDC is a rare adult form with bone and lung involvement, which shares some molecular features with Langerhans-cell histiocytosis, including *BRAF* mutations but represents a distinct entity in the Revised *WHO Classification of Tumours of Haematopoietic and Lymphoid Tissues*. Diagnosis relies on strict correlation between clinical features, imaging, and histology.

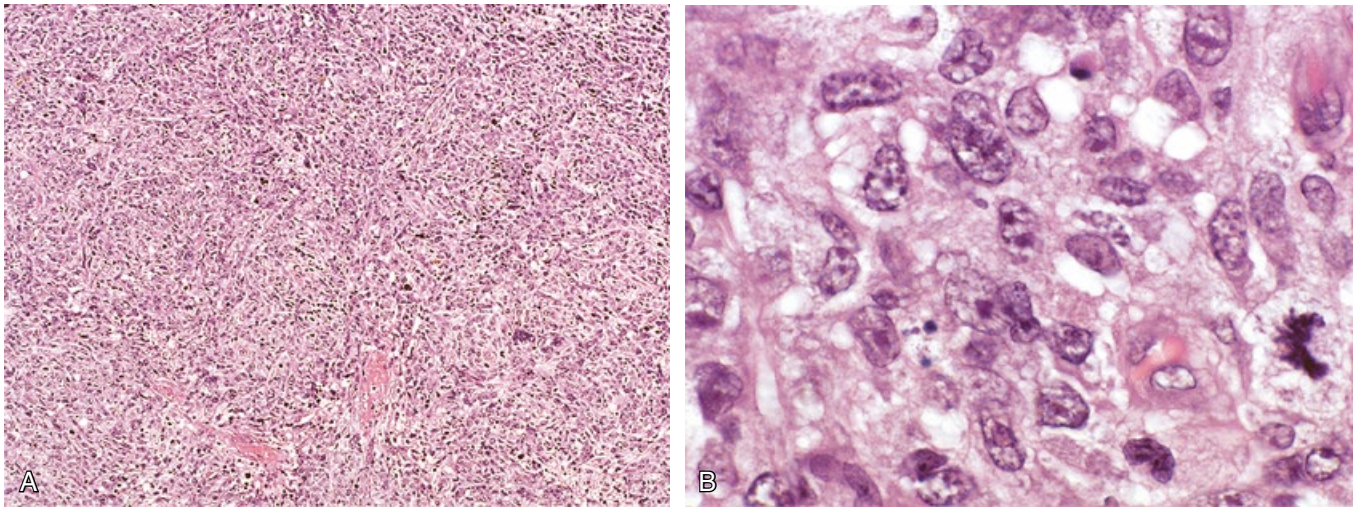

Fig. 24.39. Dendritic cell sarcoma. **A,** Lymph node biopsy showing complete replacement of normal architecture by pleomorphic oval- and spindle-shaped cells with some areas showing a storiform ("cartwheel") appearance. **B,** At higher magnification, the cells show irregular vesicular nuclei and pale cytoplasm within distinct borders. A prominent mitotic figure is seen here. Immunostaining was not carried out.

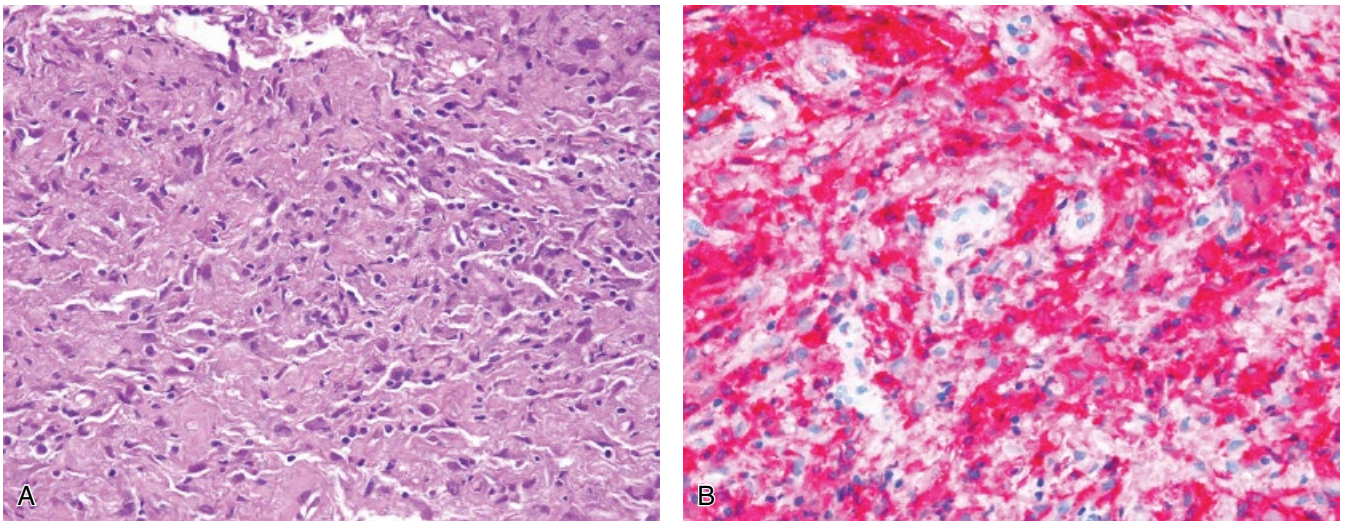

Fig. 24.40. Erdheim–Chester disease: Lung biopsy. **A,** The population consists of fibroblasts and histiocytes, partly showing foamy appearance or corresponding to giant cells. **B,** On immunohistochemistry, the histiocytic population strongly expresses the CD68 molecule as revealed by the PG-M1 monoclonal antibody and an immuno-alkaline-phosphatase technique (Courtesy of Professor SA Pileri.) The cells are also CD163+ but CD1a–.

BLASTIC PLASMACYTOID DENDRITIC CELL NEOPLASM

This tumor, previously known as blastic NK-/T-cell lymphoma and hematodermic dendritic cell tumor (Fig. 24.41), is rare and has an aggressive course. The tumor usually occurs in the skin. In most patients, there is involvement of bone marrow (Fig. 24.42), lymph nodes, and peripheral blood. The skin shows a dermal infiltrate of medium-sized lymphoid cell resembling lymphoblasts. The diagnosis of blastic plasmacytoid dendritic cell neoplasm (BPDCN) requires positivity of CD4 and/or CD56 and at least two of the four plasmacytoid dendritic cell markers (CD123, CD303, TCL1, MXA), with negativity for CD3, CD20, myeloperoxidase, and lysozyme. Recently, the high sensitivity and specificity of an antibody recognizing the master plasmacytoid dendritic cell transcription factor TCF4/E2-2 has been shown. BCL2 is always expressed conversely to what seen in normal plasmacytoid dendritic cells. The primitive hematopoietic marker TdT may be positive (Fig. 24.40). T-cell receptor genes are germline and the tumor cells are negative for Epstein–Barr virus. The mutational profile of BPDCN analyzed by massive parallel sequencing identified *TET2* as the most commonly mutated gene. In addition, mutations of *IKZF3, ZEB2*, *ASXL1*, *NPM1*, and *H-/K-/N-RAS* have been reported. In one study, half of BPDCN cases had mutations affecting either the DNA methylation or chromatin remodeling pathways, which may be provided with therapeutic relevance. Chemotherapy similar to that used in acute myeloid leukemia usually induces

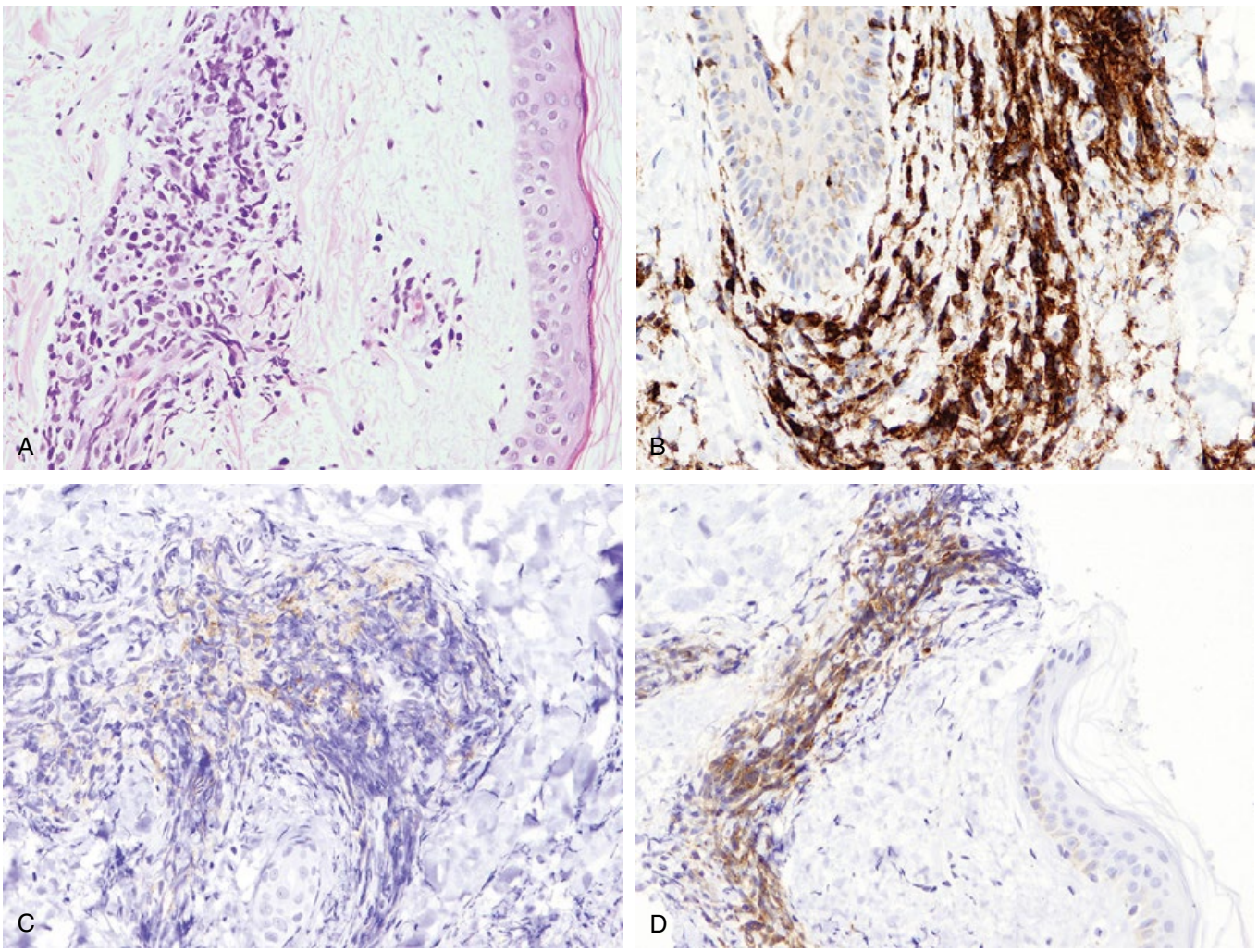

Fig. 24.41. Blastic plasmacytoid dendritic cell neoplasm. There is a dermal infiltrate of medium-sized atypical cells **(A)**. The cells show positivity for CD4 **(B)**, CD56 **(C),** and the primitive hematopoietic cell marker TdT **(D).** (Courtesy of Professor PG Isaacson.)

remission, but relapse and resistance to further chemotherapy is common. The median survival is about 14 months. Better results have been reported with schedules developed for acute lymphoblastic leukemia and aggressive malignant lymphomas, especially in children.

In the Revised WHO (2016) classification, this tumor is listed autonomously among myeloid neoplasms, consistently with the results of gene expression profiling studies showing derivation from the myeloid lineage and, in particular, from resting plasmacytoid dendritic cells.

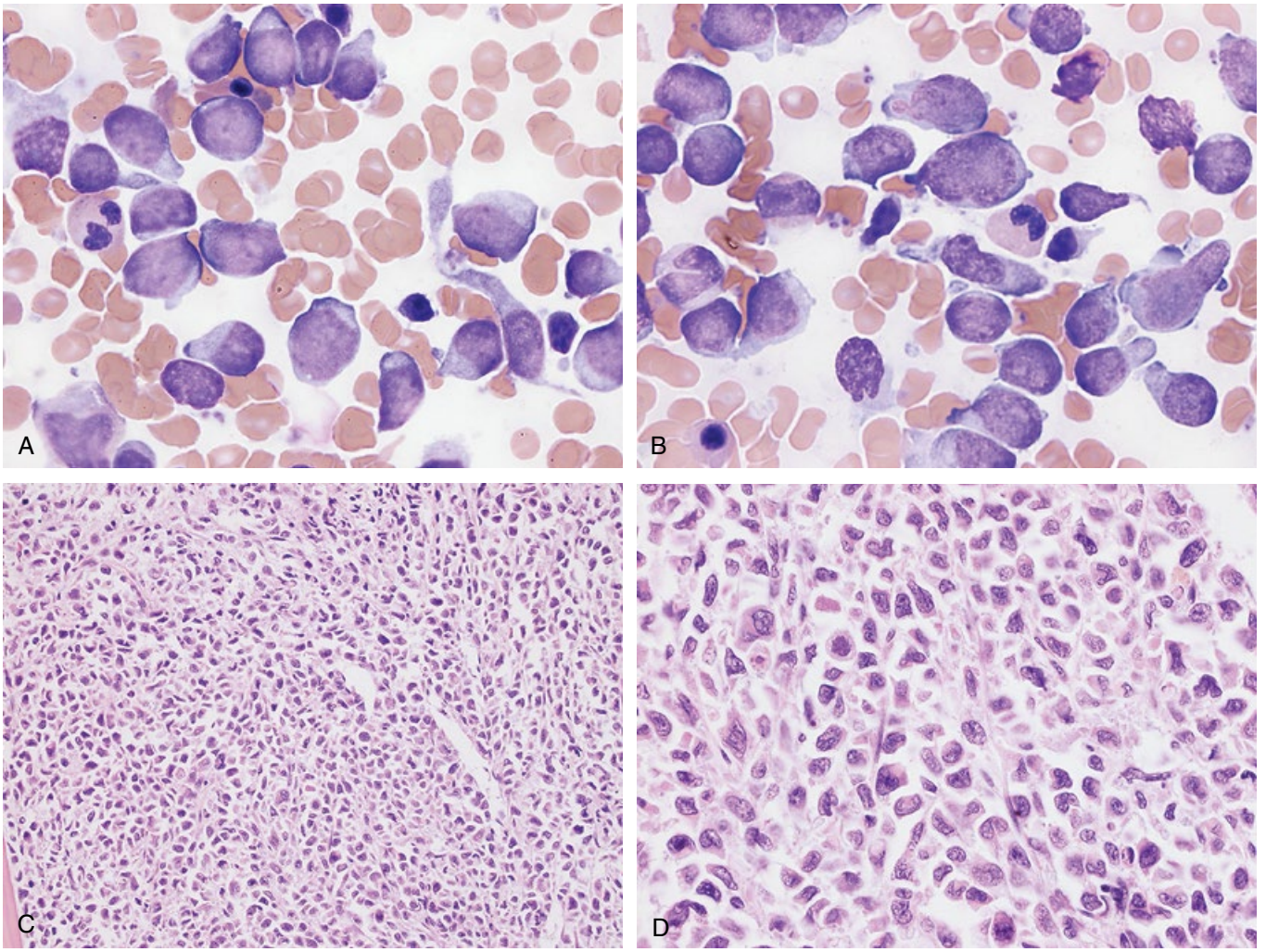

Fig. 24.42. Blastic plasmacytoid dendritic cell neoplasm. The bone marrow aspirate **(A** and **B)** shows numerous blast forms, some of which have plasmacytoid features. The trephine biopsy **(C** and **D)** shows almost complete replacement of normal hematopoietic cells by the neoplastic primitive cells. (Courtesy of Dr. W Erber.)

CHAPTER

STEM CELL TRANSPLANTATION

25

HUMAN LEUKOCYTE ANTIGEN SYSTEM

The short arm of chromosome 6 (6p21) contains a cluster of genes known as the major histocompatibility complex (MHC) or the human leukocyte antigen (HLA) region (Fig. 25.1). Among the genes in this region are those that code for the proteins of the HLAs that are present on the cell membranes of many nucleated cells. As well as having a major role in transplant rejection, these antigens are involved in many aspects of immunologic recognition and reaction.

The MHC proteins are highly polymorphic and classified into three types (Table 25.1). Class I proteins comprise two polypeptides, the larger of which is encoded by the MHC. These larger polypeptides coded for by Class I genes A, B, and C (Fig. 25.2). They are expressed as transmembrane surface glycoproteins. The small component, a β_2-microglobulin, is encoded on chromosome 15. Class II proteins coded for in the D region, divided serologically into DR, DP, and DQ groups, comprise an α and a β chain, both of which are both encoded by the MHC (Fig. 25.2). DRB genes encode for the β chain and DRA genes for the α chain. Class III proteins are the complement components encoded by the MHC region.

Class I and II molecules share a similar structure with four extracellular domains. The two distal domains, for Class I αI and αII, for Class II αand β, contain a cleft for binding to small peptides (e.g. nine amino acids in length). For Class I, the source of the peptide is from intracellular breakdown of self or viral proteins in proteasomes. These are trafficked via the endoplasmic reticulum and Golgi apparatus to the surface. Class II molecules receive peptides derived from breakdown of exogenous proteins (e.g. from microbes or dead cells), in cell endosomes.

Class I proteins act as surface recognition antigens, which can be identified by cytotoxic CD8+ T lymphocytes and by natural killer cells. This recognition results in death of the cell. Class II proteins are involved in cooperation and interaction between T helper CD4+ lymphocytes and antigen-presenting cells. Thus, Class II cells cause proliferation of the CD4+ T lymphocytes and antigen-presenting cells which recognize their peptides and they in turn stimulate proliferation of B lymphocytes which synthesize antibodies directed against the antigenic peptide on the surface of the Class II molecule (see Chapter 11). HLA-A, HLA-B, and HLA-C Class I antigens are present on all nucleated cells and platelets, and those encoded by the D region, HLA-D, Class II antigens are present mainly on antigen-presenting cells such as B lymphocytes, monocytes, macrophages, dendritic cells, and some activated T cells.

HUMAN LEUKOCYTE ANTIGEN NOMENCLATURE

The World Health Organization (WHO) Nomenclature Committee designates HLA alleles by an agreed notation. This involves a letter followed by an asterisk (*) (Table 25.2).

Alleles are numbered after the letter that defines the locus by up to eight digits separated in pairs by a colon. The first two digits indicate the allele group (broadly corresponding to serologic group), the third and fourth list subtypes, and the number is assigned in the order in which the DNA sequences have been determined. The fifth and sixth digits are used to name alleles that differ only by synonymous nucleotide substitutions ("silent" or "noncoding"). The seventh and eighth digits name alleles that differ in either intron or 3′ or 5′ regions of the gene. Finally, an allele can have a suffix indicating aberrant expression: for

Fig. 25.1 Major histocompatibility complex (MHC) polymorphism: The main genes that encode MHC Class I and II molecules. In practice, the genes that encode most of the three main types of the Class IIα and β chains are located at more than one locus and there are additional Class I MHC loci. (Prepared by SGE Marsh.)

Color Atlas of Clinical Hematology: Molecular and Cellular Basis of Disease, Fifth Edition. A. Victor Hoffbrand, Paresh Vyas, Elías Campo, Torsten Haferlach, and Keith Gomez

TABLE 25.1. HUMAN MAJOR HISTOCOMPATIBILITY COMPLEX: GENES

Name	Molecular characteristics
HLA-A	Class I α chain
HLA-B	Class I α chain
HLA-C	Class I α chain
HLA-E	Associated with Class I 6.2 kb Hind III fragment
HLA-F	Associated with Class I 5.4 kb Hind III fragment
HLA-G	Associated with Class I 6.0 kb Hind III fragment
HLA-H	Class I pseudogene associated with 5.4 kb Hind III fragment
HLA-J	Class I pseudogene associated with 5.9 kb Hind III fragment
HLA-K	Class I pseudogene associated with 7.0 kb Hind III fragment
HLA-L	Class I pseudogene associated with 9.2 kb Hind III fragment
HLA-DRA	DR α chain
HLA-DRB1	DR βI chain determining specificities DR1, DR2, DR3, DR4, DR5, etc.
HLA-DRB2	Pseudogene with DR β-like sequences
HLA-DRB3	DR β3 chain determining DR52 and Dw24, Dw25, Dw26 specificities
HLA-DRB4	DR β4 chain determining DR53
HLA-DRB5	DR β5 chain determining DR51
HLA-DRB6	DRB pseudogene found on DR1, DR2, and DR10 haplotypes
HLA-DRB7	DRB pseudogene found on DR4, DR7, and DR9 haplotypes
HLA-DRB8	DRB pseudogene found on DR4, DR7, and DR9 haplotypes
HLA-DRB9	DRB pseudogene, isolated fragment
HLA-DQA1	DQA α chain as expressed
HLA-DQB1	DQA β chain as expressed
HLA-DQA2	DQ α-chain-related sequence, not known to be expressed
HLA-DQB2	DQ β-chain-related sequence, not known to be expressed
HLA-DQB3	DQ β-chain-related sequence, not known to be expressed
HLA-DOA	DO α chain
HLA-DOB	DO β chain
HLA-DMA	DM α chain
HLA-DMB	DM β chain
HLA-DPA1	DP α chain as expressed
HLA-DPB1	DP β chain as expressed
HLA-DPA2	DP α-chain-related pseudogene
HLA-DPB2	DP β-chain-related pseudogene
TAP1	ABC (ATP binding cassette) transporter
TAP2	ABC (ATP binding cassette) transporter
LMP2	Proteasome-related sequence
LMP7	Proteasome-related sequence
MICA	Class I chain-related gene
MICB	Class I chain-related gene
MICC	Class I chain-related pseudogene
MICD	Class I chain-related pseudogene
MICE	Class I chain-related pseudogene

Source: Bodmer JG, et al. *Hum Immunol* 1999;60:361–395. Reproduced with permission of John Wiley and Sons.

example, N for a null allele with no proteins expressed; L for low cell surface expression; and S for an allele only expressed in soluble form. The most recent advances in HLA nomenclature can be found by accessing the IMGT/HLA Sequence Database (www.ebi.ac.uk/imgt/hla).

For Class II, the gene name includes a reference to the specific heavy or light chain locus (e.g. *HLA-DQA1** or *HLA-DQA2** for the first two DQA chain loci). The *DRB1* gene codes for the HLA-DR (1–18) antigens recognized serologically. *DRB3* codes for the DR52 antigens, *DRB4* for the DR53 antigens, and *DRB5* for the DR51 antigens (Fig. 25.3).

TYPING OF HUMAN LEUKOCYTE ANTIGENS

HLA-A, HLA-B, and HLA-C typing is usually carried out on peripheral blood lymphocytes. Originally, antigens of the D system were identified by nonreactivity in mixed lymphocyte culture (lymphocyte reaction proliferation assay) against rare homozygous D-locus cells. Detection of HLA polymorphisms Class I and II is now carried out routinely by dsDNA methods rather than serotyping (Fig. 25.4). Matching is then performed by comparing DNA sequences between recipient and potential donors. It is likely that next generation sequencing will replace methods employing polymerase chain reaction (PCR) techniques with either specific primer or oligonucleotide probes (Fig. 25.5).

OTHER HUMAN LEUKOCYTE ANTIGENS

Human leukocytes carry a variety of antigens (CD), numbering 371 in April 2016, which are recognized by monoclonal antibodies. These various CD antigens are listed electronically including cellular expression, molecular weight, and functions, together with examples of antibodies that detect them. The use of these antibodies to define normal and malignant hematopoietic cell subpopulations is described in other chapters.

For patients undergoing allogeneic transplantation from an HLA-matching sibling, there is still a risk of graft-versus-host disease (GVHD) because of disparity in polymorphisms for proteins coded for outside the MHC region (minor histocompatibility antigens). An example is the presence of antigens (HY) coded for by the Y chromosome in males, absent in females. Multiparous female donors who have had male infants may have been primed against male (HY) antigens. Their T cells can then react against these antigens. Consistent with this, male patients receiving female grafts are particularly liable to GVHD.

STEM CELL TRANSPLANTATION

Stem cell transplantation (SCT) can be carried out between siblings (allogeneic transplantation; Fig. 25.6) who are HLA identical or can be shown to be matching by a number of different techniques of DNA analysis. Syngeneic (identical twin), haploidentical, HLA-matched but unrelated donors, and placental (cord) blood can also be used in appropriate cases (Table 25.3).

The recipient has a malignant marrow disorder (e.g. poor-prognosis acute leukemia, myelodysplasia, chronic myeloid leukemia) myeloma or lymphoma; aplastic anemia; or a genetic abnormality (e.g. thalassemia major) (Table 25.4).

In autologous transplantation, the patient's own stem cells are used to rescue the patient from profound marrow ablation

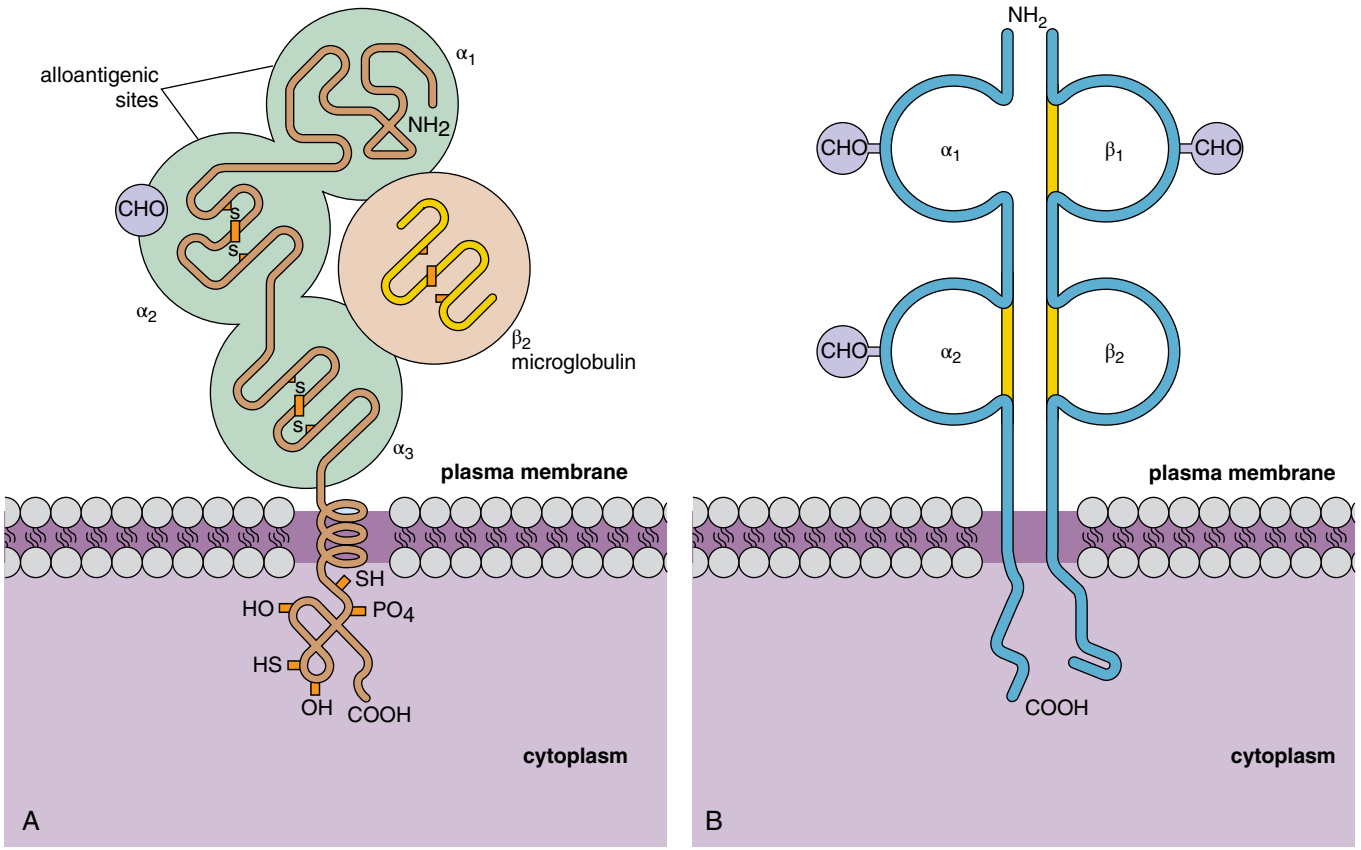

Fig. 25.2 Structure in the plasma membrane: **(A)** Class I and **(B)** Class II HLAs. The Class I MHC-encoded chain has three globular domains α1, α2, and α3. A non-MHC-encoded peptide, β_2-microglobulin, is closely associated with the α3 domain. Alloantigens occur on the α1 and α2 domains. The HLA-DR antigen consists of an α and a β peptide, noncovalently bound together. Each peptide has two globular domains, which are structurally related to immunoglobulin (Ig) domains.

TABLE 25.2 ALLELES: NUMBER AT EACH HUMAN LEUKOCYTE ANTIGEN (HLA) LOCUS, AS ASSIGNED BY THE WHO NOMENCLATURE COMMITTEE FOR FACTORS OF THE HLA SYSTEM, JANUARY 2009

	HLA gene	Alleles (no)	Antigens (no)
Class I	*A*	740	24
	B	1141	50
	C	400	9
Class II	*DRB1*	610	20
	DRB3	50	1
	DRB4	13	1
	DRB5	18	1
	DQA1	34	–
	DQB1	96	7
	DPA1	27	–
	DPB1	133	–

caused by high-dose chemotherapy, with or without total body irradiation, for malignant disease (Fig. 25.7).

Peripheral blood stem cells (PBSCs) can be harvested using a cell separator and used instead of bone marrow both for allogeneic and autologous transplantation. Usually, the patient is given cyclophosphamide and a 4- to 6-day course of granulocyte colony-stimulating factor (G-CSF) to mobilize PBSCs. Normal donors receive G-CSF but not cyclophosphamide. A collection of >2.5× 10^6/kg CD34+ cells is regarded as adequate. Stem cells appear similar to small or medium-sized lymphocytes (Fig. 25.8) and are contained in a CD34-enriched cell population. Recovery of platelets after PBSC transplantation is enhanced compared to the recovery of platelets after bone marrow transplantation.

A typical hematologic chart of a patient having allogeneic SCT for aplastic anemia is shown in Fig. 25.9.

Immediately following SCT, the recipient's blood shows chimerism, the presence of both recipient and donor cells. The degree of chimerism can be determined by DNA analysis at subsequent time points and in different cell lineages (Fig. 25.10, *A*). If there is a sex mismatch between donor and recipient, fluorescence in situ hybridization (FISH) analysis of the proportion of circulating Y-chromosome-containing cells can also be used (Fig. 25.10, *B*).

Failure of engraftment is unusual in well-matched transplants for leukemia but is more common when the recipient has aplastic anemia or when donor and recipient are not fully matched or when T-cell depletion has been carried out.

NONMYELOABLATIVE (REDUCED INTENSITY) TRANSPLANTS

In reduced intensity conditioning (RIC) transplant procedures, the donor is treated with drugs and/or radiotherapy at lower doses than those used used for standard SCT. The aim is to achieve immunosuppression sufficient for donor stem cells to be

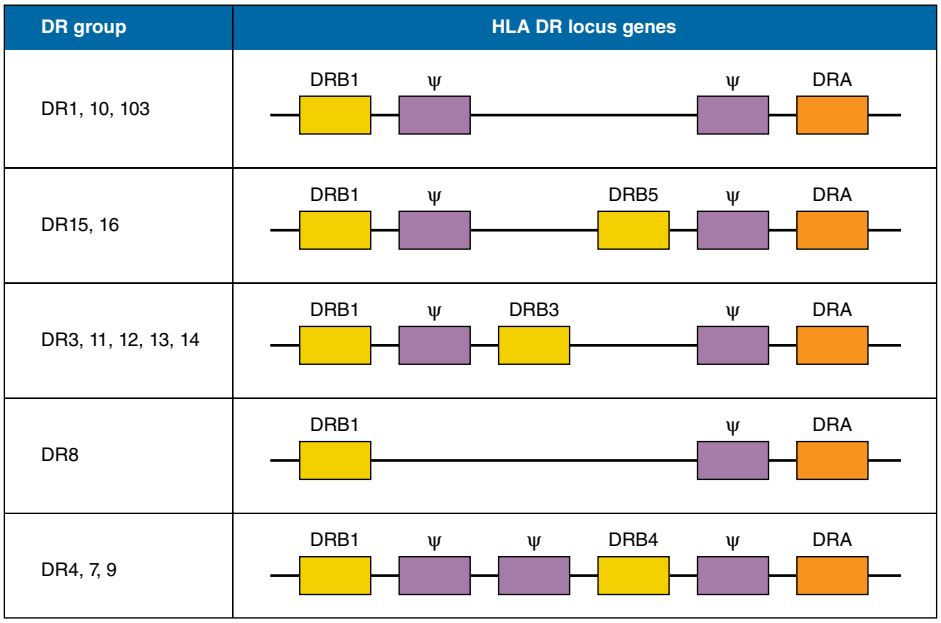

Fig. 25.3 Variable expression of genes according to HLA haplotype. *Yellow boxes*, DRB genes; *orange boxes*, nonpolymorphic DRA genes; *purple boxes*, pseudogenes. Source: Adapted with permission from Mickelson E, Petersdorf EW. *Hematopoietic Cell Transplantation*, 2nd edn. Oxford, Blackwell Science, 1999. Reproduced with permission of John Wiley & Sons.

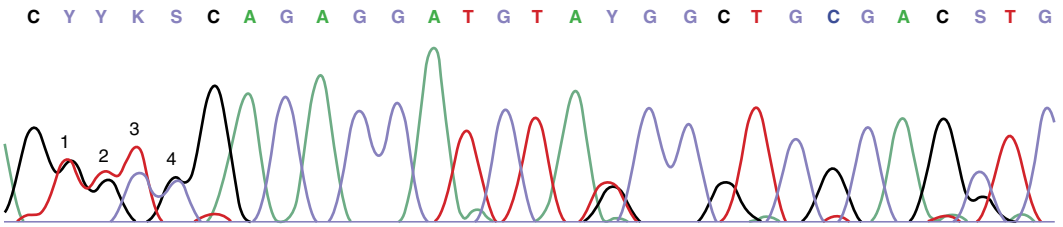

Fig. 25.4 Electropherogram of sequencing results from analysis of a heterozygous locus. The sequence is read from left to right. For this short stretch of nucleotides, many different results are possible. Heterozygous positions are given appropriate IUB codes. First heterozygous position (marked 1): CC or CT, continuing to second heterozygous position (marked 2): CCC or CCT or CTC or CTT, continuing to third heterozygous position (marked 3): CCCG or CCCT or CCTG or CCTT or CTCT or CTCG or CTTT or CTTG, continuing to fourth heterozygous position (marked 4): CCCGG or CCCGC or CCCTG or CCCTC or CCTGG or CCTGC or CCTTG or CCTTC or CTCTG or CTCTC or CTCGG or CTCGC or CTTTG or CTTTC or CTTGG or CTTGC, etc. (Courtesy of ST Cox, the Anthony Nolan Trust.)

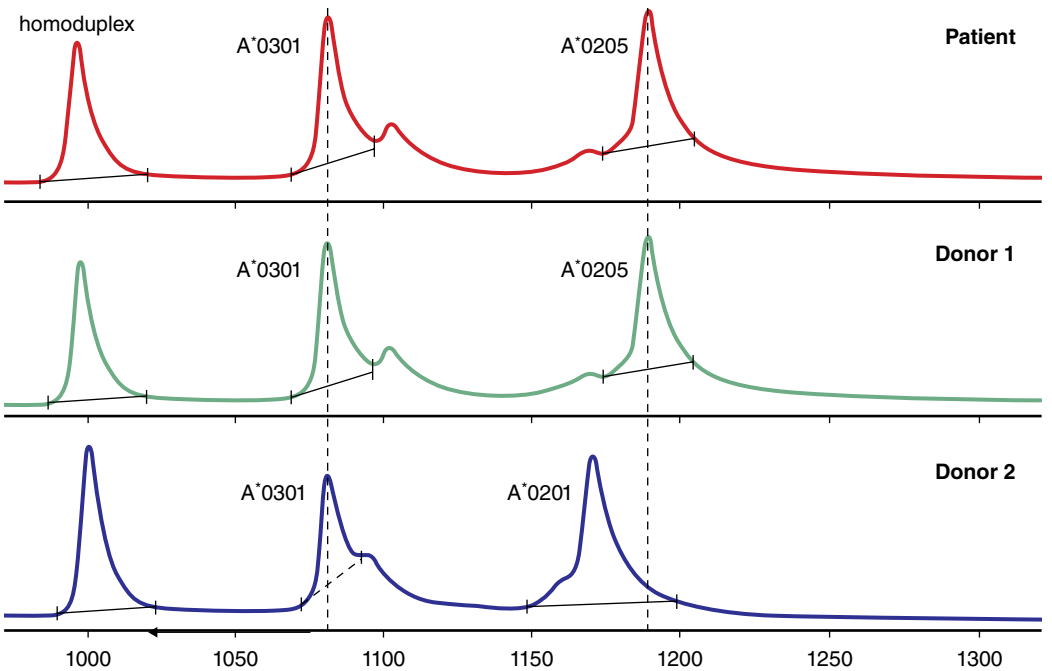

Fig. 25.5 Allogeneic bone marrow transplantation. Electropherogram with results for HLA-A locus matching for a patient and two unrelated bone marrow donors. After electrophoresis the homoduplex peak is assigned an arbitrary value of 1000 on the horizontal scale. The vertical scale represents the homoduplex and heteroduplex peaks detected by laser. The patient and two potential donors were matched by serology for HLA-A2 and HLA-A3. By RSCA analysis, the patient shares allele A*0301 with both potential donors, but only shares the second allele, A*0205, with donor 1. (Courtesy of Professor JA Madrigal.)

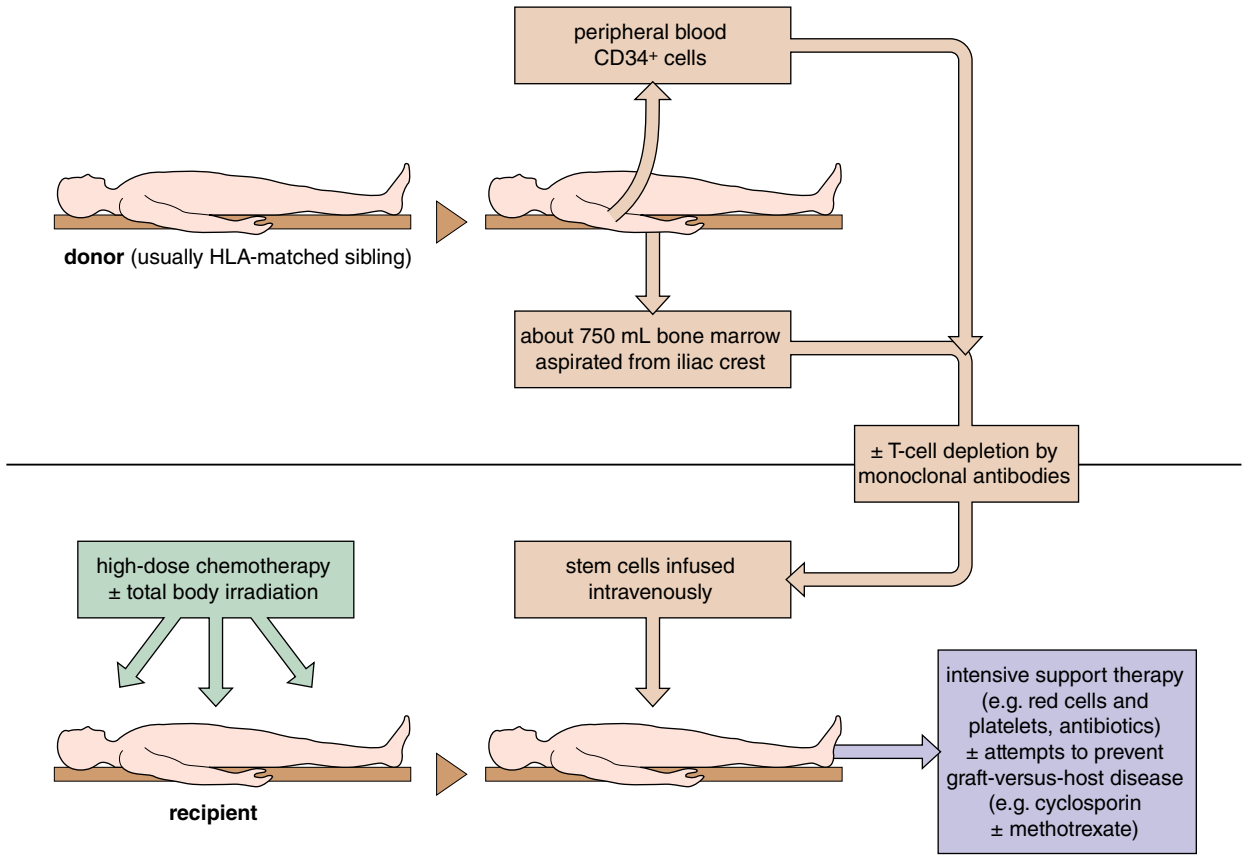

Fig. 25.6 Allogeneic stem cell transplantation. Stem cells can be harvested from peripheral blood or bone marrow.

TABLE 25.3. STEM CELL (BONE MARROW OR PERIPHERAL BLOOD) TRANSPLANTATION: DONORS

Type	Donor
Syngeneic	Identical twin
Allogeneic	HLA-matching brother or sister HLA-matching other family member (e.g. parent, cousin) HLA-matching unrelated volunteer donor (VUD or MUD)
Cord (placental) blood	
Autologous	

MUD, matched unrelated donor; VUD, volunteer unrelated donor.

TABLE 25.4. STEM CELL (BONE MARROW OR PERIPHERAL BLOOD) TRANSPLANTATION: INDICATIONS

Allogeneic (or syngeneic)	
Malignant	**Immunodeficiency**
Acute myeloid leukemia (some cases) Acute lymphoblastic leukemia: • Poor prognosis: first remission • Second remission or subsequently Chronic myeloid leukemia (tyrosine kinase inhibitor failures) Other severe acquired disorders of the marrow, selected cases (e.g. Hodgkin disease, non-Hodgkin lymphoma, myeloma, myelodysplasia, myelofibrosis, chronic lymphocytic leukemia)	Severe combined immunodeficiency Wiscott–Aldrich syndrome **Metabolic storage diseases** Gaucher disease (type II) Mucopolysaccharidosis
Bone marrow disorders	
Aplastic anemia Paroxysmal nocturnal hemoglobinuria Thalassemia major Sickle cell anemia Kostmann syndrome Chronic granulomatous disease Chédiak–Higashi syndrome Adhesion molecule deficiency Glanzmann disease Bernard–Soulier disease Osteoporosis Congenital hemophagocytic syndrome	**Autologous** Malignant lymphoma (Hodgkin or non-Hodgkin) usually post first relapse Myeloma Gene therapy (e.g. adenosine deaminase deficiency, thalassemia major)

accepted into the marrow microenvironment, and to establish a durable graft without total marrow ablation by the conditioning treatment. Drugs used in different regimens include fludarabine, cyclophosphamide, antilymphocytic globulin, alemtuzemab (anti-CD52, Campath), and busulfan. The aim is to establish chimerism between recipient and donor cells (Fig. 25.10) and for the donor immune-competent cells to effect a cure by a graft-versus-leukemia, -myelodysplasia, -myeloma, or -lymphoma effect.

DONOR LEUKOCYTES

Donor leukocytes can be given after allogeneic SCT if residual disease or recurrence of disease is evident. The best results are

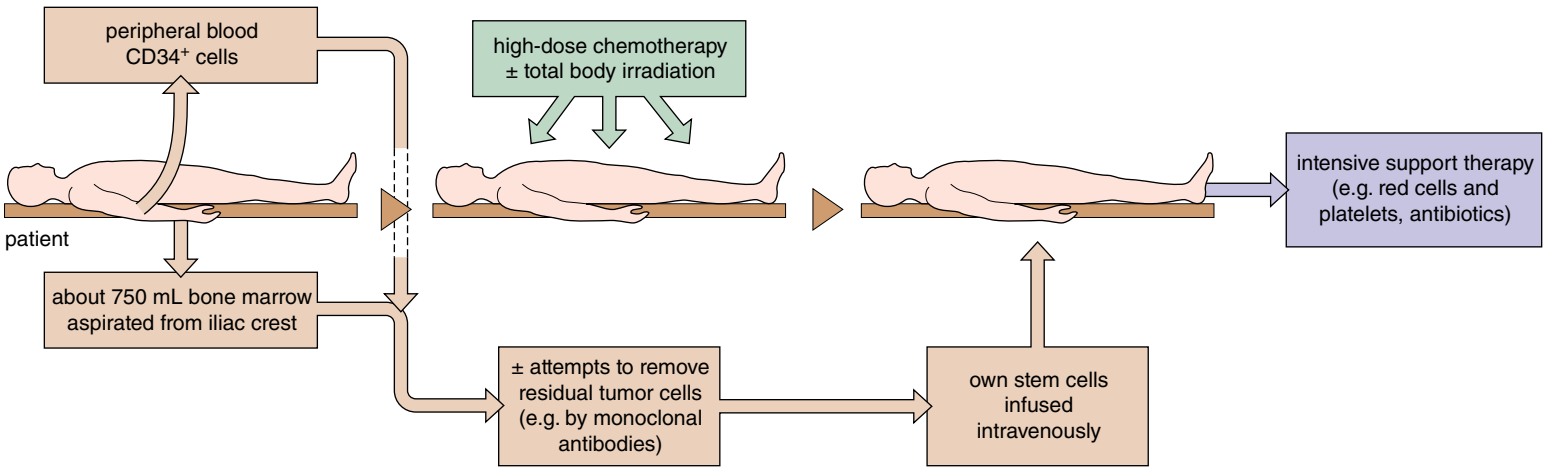

Fig. 25.7 Autologous stem cell transplantation. Stem cells can be harvested from peripheral blood or bone marrow.

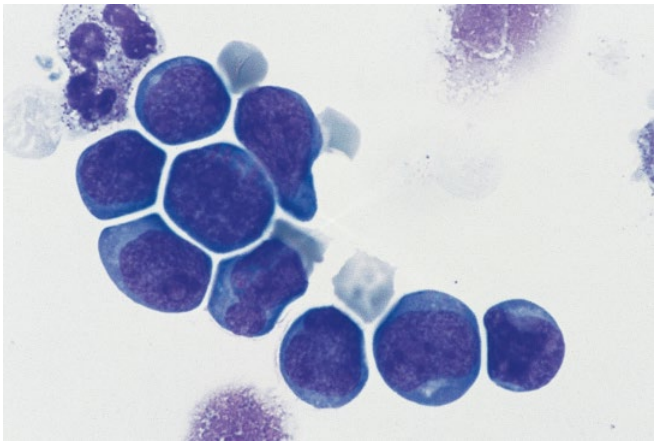

Fig. 25.8 Peripheral blood stem cell collection. Enriched CD34+ cells stained by May-Grunwald–Giemsa. The cells have the appearance of small- and medium-sized lymphocytes. (Courtesy of Dr. M Potter.)

obtained if only minimal disease is present in chronic myeloid leukemia detected by molecular methods or cytogenetics only, rather than from hematologic relapse of the disease (Fig. 25.11). Also, it is important that chimerism is still present (i.e. there is evidence of donor as well as recipient cells in the blood or bone marrow of the recipient). Other factors determine the efficacy and toxicity (e.g. GVHD). Responses are less frequent in diseases other than chronic myeloid leukemia and also the responses may be less durable (e.g. in acute leukemias and myelodysplasia).

COMPLICATIONS OF STEM CELL TRANSPLANTS

The incidence of complications causing death varies according to whether the transplant is autologous, allogeneic from an HLA-matching sibling, or from an unrelated donor (Fig. 25.12).

Full intensity allogeneic transplantation is not usually carried out for patients older than 65 years because of the increased incidence of complications (Table 25.5), but low intensity and autologous transplantation are carried out for patients up to age 70 years. At least 2 weeks of pancytopenia usually follow conditioning before the infused donor pluripotent stem cells, having seeded the recipient's bone marrow, proliferate and differentiate sufficiently to produce new mature red cells, leukocytes, and platelets.

Infections are a major hazard during the post-transplant period (Fig. 25.13). These can be bacterial, fungal, or viral (Figs. 25.14 and 25.15). Hematopoietic growth factors (e.g. G-CSF) are used to enhance granulocyte recovery.

Cytomegalovirus (CMV) infection can result from reactivation of a previous latent infection or from transmission of the virus in blood products, and can result in severe pneumonitis and marrow suppression (Figs. 25.16 and 25.17).

Herpes simplex virus (e.g. HHV6) infection is a frequent complication that tends to become generalized and can cause pneumonia, encephalitis, skin lesions (Fig. 25.18), or marrow suppression. Infection can be prevented by the use of prophylactic intravenous aciclovir. Pneumonia caused by *Pneumocystis jiroveci (carinii)* is another frequent complication of the immunosuppression and neutropenia (Figs. 25.19 and 25.20).

Total body irradiation can cause side effects that involve epithelial structures; damage to the nails and nail beds (Fig. 25.21) and temporary complete alopecia occur (Fig. 25.22). Veno-occlusive disease (VOD) of the liver is an acute complication caused

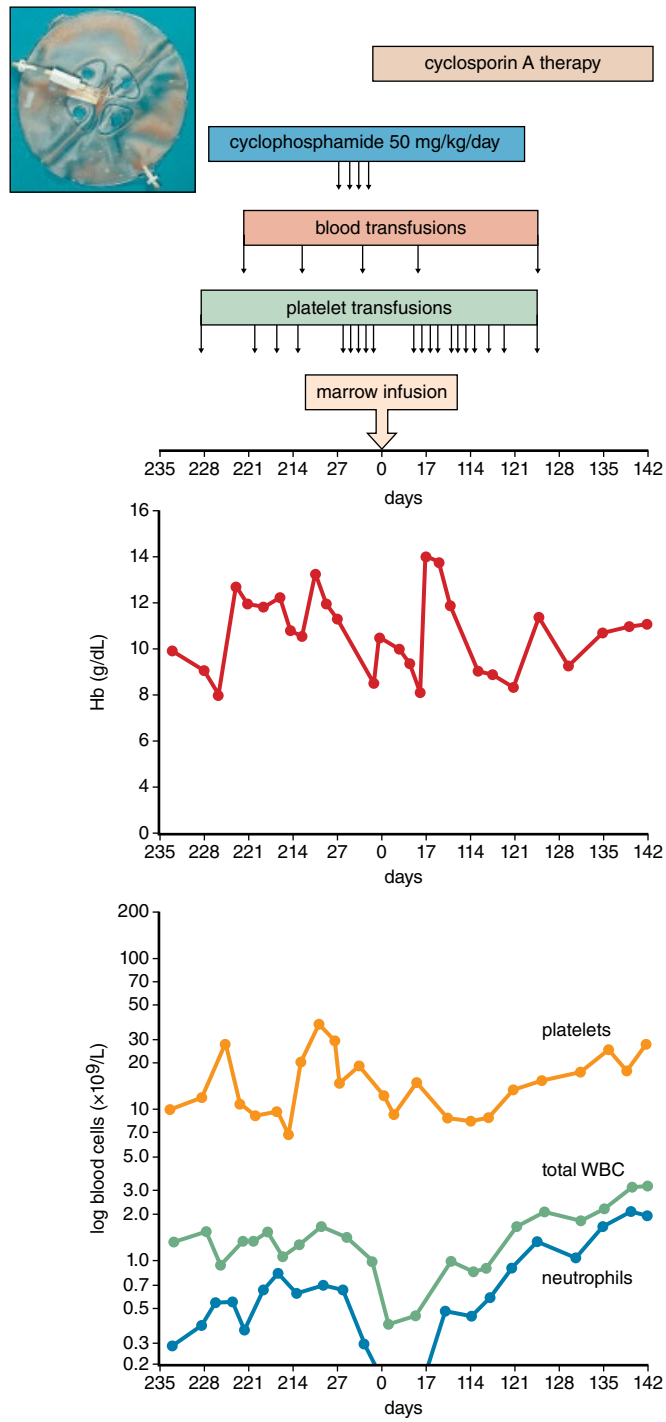

Fig. 25.9 Aplastic anemia: Hematologic response to bone marrow transplantation. Marrow (500–1000 mL) is harvested from the pelvis of the donor. Red cells are removed and in some circumstances T lymphocytes are also eliminated (e.g. by monoclonal antibodies) to prevent graft-versus-host disease (GVHD). Cyclosporin A is used to ameliorate GVHD and to enhance engraftment in aplastic anemia. When the recipient has leukemia, total body irradiation is usually used in addition to chemotherapy in the conditioning. The inset shows donor marrow depleted of red cells and T lymphocytes before infusion into the recipient. (Courtesy of M Gilmore.)

by chemotherapy and radiotherapy (Fig. 25.23). Preceding chemotherapy and abnormal liver function also predispose to VOD. Hemorrhagic cystitis can result from cyclophosphamide metabolites (mesna is given to try to prevent this) or from viral infection (e.g. adenovirus, CMV, or polyoma virus).

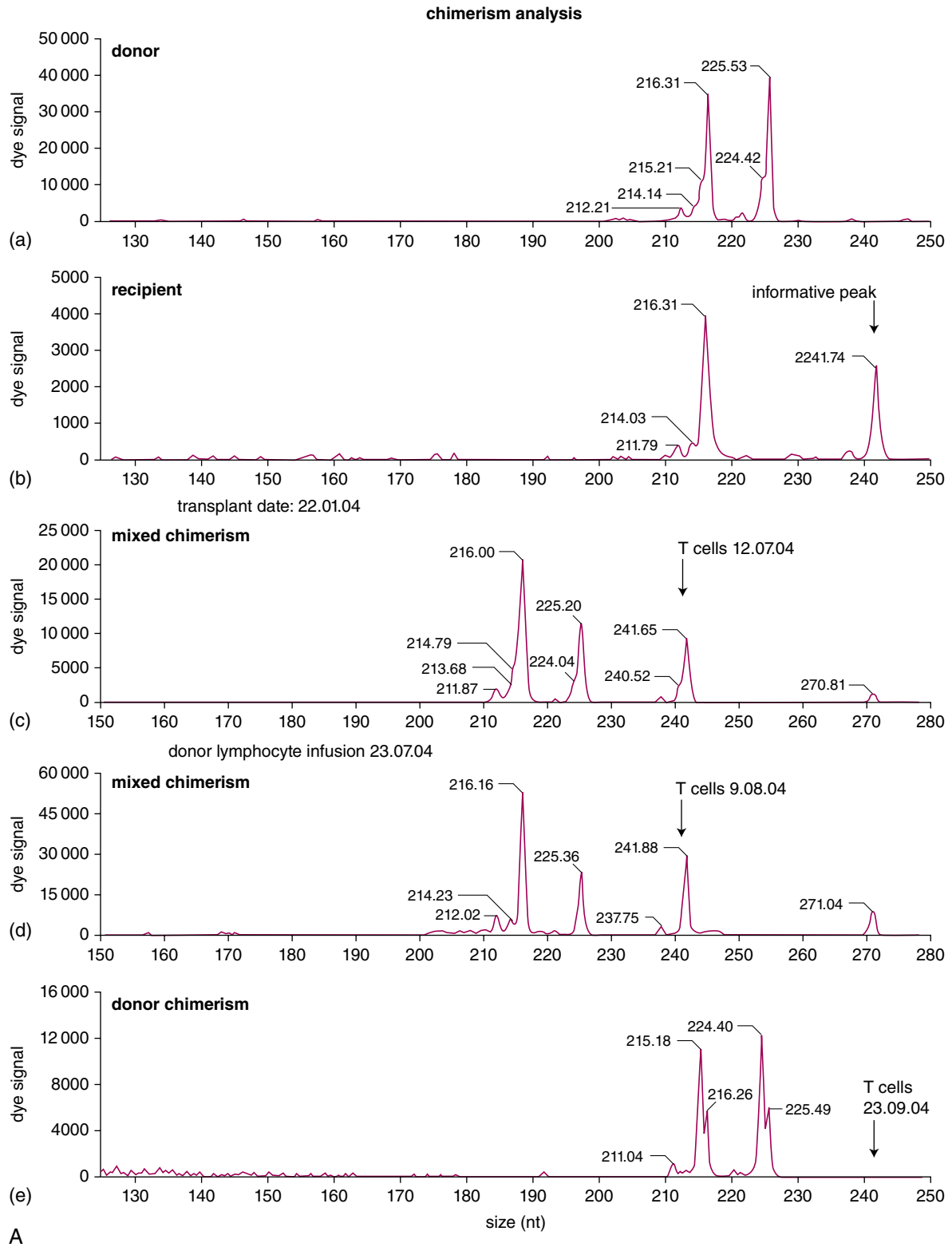

Fig. 25.10 A, Chimerism analysis after stem cell transplantation. Fluorescence polymerase chain reaction (PCR) products are electrophoresed through a capillary matrix and are detected following excitation with a laser. The results are displayed in an electrophoretogram as shown. **(a)** The donor profile. **(b)** The pretransplant recipient profile. Using a microsatellite marker, the donor and recipient are both heterozygous with one common allele. The *red arrow* highlights the informative peak—the presence of which in a post-transplant sample would indicate a mixed chimera. **(c)** The presence of mixed chimerism in the T-cell lineage. A donor lymphocyte infusion (DLI) was administered. **(d)** The persistence of mixed chimerism. Within 2 months after DLI the T cells are showing a full donor chimerism (**e**). More than 2 years after the DLI, the patient remained fully donor in the following lineages: T cells, B cells, granulocytes, and peripheral blood mononuclear cells. **B,** Chimerism analysis after sex-mismatched stem cell transplantation using FISH analysis of peripheral blood leukocytes with probes specific for the centromere regions (CEP) of the X *(red)* and Y *(green)* chromosomes: The upper panel shows normal male signal pattern (*left*) and normal female pattern (*right*). The lower panel shows a mixture of male and female cells in a patient following sex-mismatched stem cell transplantation. (A, Courtesy Professor S Mackinnon.)

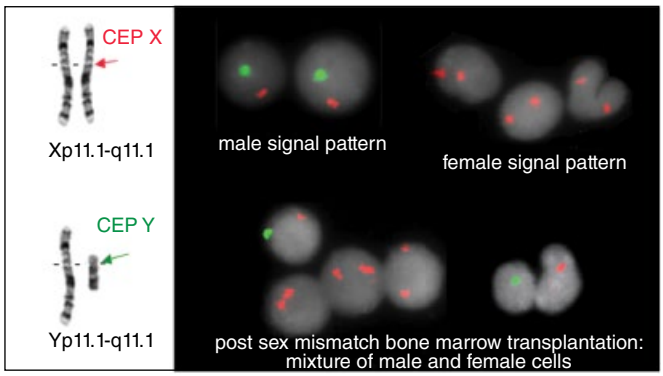

B

Fig. 25.10 (Continued)

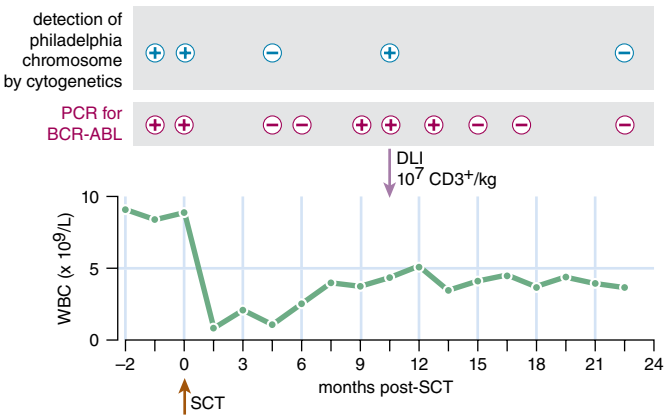

Fig. 25.11 Example of donor leukocyte infusion (DLI) in the treatment of chronic myeloid leukemia (CML) that relapsed following allogeneic stem cell transplantation (SCT). Polymerase chain reaction (PCR) analysis of the blood for the BCR-ABL transcript shows that there was transient loss of the transcript, but molecular and cytogenetic relapse occurred at 10 months. One infusion of donor leukocytes led to re-establishment of a durable complete remission.

GRAFT-VERSUS-HOST DISEASE

A major post-transplant complication is reaction of the immunocompetent cells in the graft against the tissues of the host, causing GVHD, which can be acute (occurring in the first 100 days post-transplant) or chronic (Table 25.6). For acute GVHD, the triad of skin, gut, and liver involvement is classified according to severity into grades I–IV (Table 25.7).

In acute GVHD, an erythematous itchy skin rash is widespread (Fig. 25.22) and tends to be particularly severe on the hands and feet. In severe cases, a bullous eruption and subsequent widespread exfoliation occur (Fig. 25.24).

In chronic GVHD, the lesions tend to be firm, red, and plaque-like (Fig. 25.25) and ultimately, in some patients, form a scleroderma-like picture with contractures and ulceration (Fig. 25.26). The hands and feet can continue to exfoliate (Fig. 25.27).

The mucous membranes are also affected, with formation of lichen planus-like lesions in the mouth and pharynx (Fig. 25.28).

The histologic appearances of GVHD are normally seen after skin or rectal biopsy. In acute GVHD, the skin shows inflammatory changes with death of epidermal cells and a lymphoid infiltrate (Fig. 25.29) leading, in severe cases, to denudation.

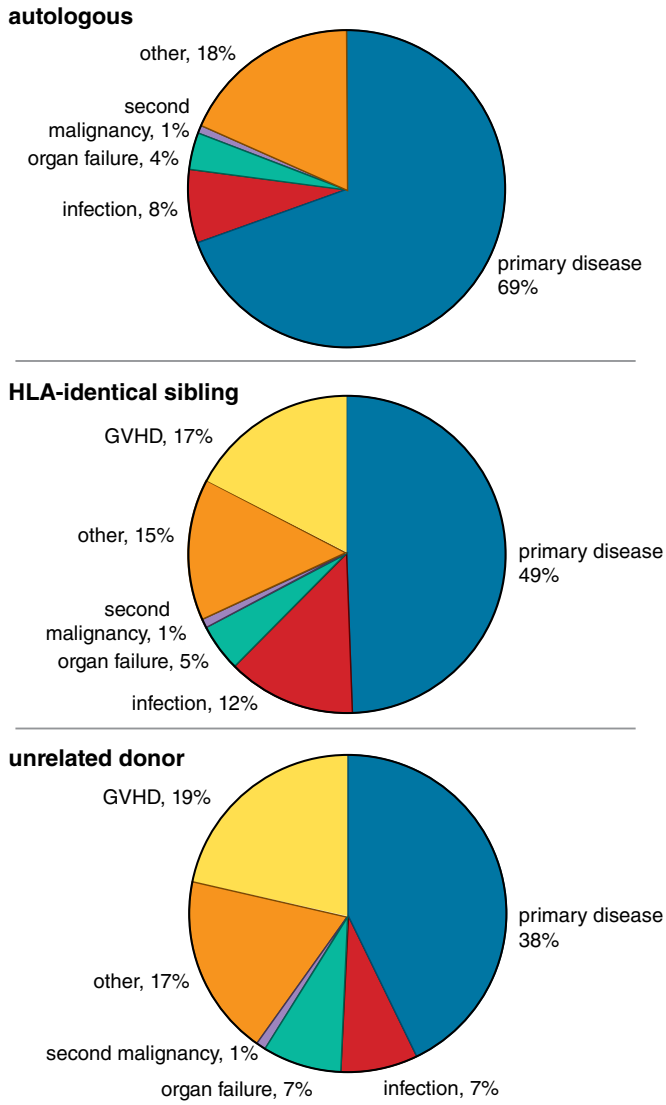

Fig. 25.12 The incidence of the complications causing death differ according to whether the stem cell transplant was autologous, allogeneic form an HLA matching sibling or allogeneic from an unrelated donor. (Courtesy of the International Bone Marrow Transplant Registry.)

TABLE 25.5. ALLOGENEIC STEM CELL TRANSPLANTATION: COMPLICATIONS

Early (<100 days)
Acute graft-versus-host disease
• Skin • Liver • Gut
Infections
• Bacterial • Fungal • Herpes simplex • Cytomegalovirus
Graft failure
Hemorrhagic cystitis
Interstitial pneumonitis

(*Continued*)

TABLE 25.5 (CONTINUED)

Veno-occlusive disease
Cardiac failure
Late (>100 days)
Chronic graft-versus-host disease
• Scleroderma • Sicca syndrome • Arthritis • Hepatitis • Malabsorption • Pulmonary lesions
Chronic pulmonary disease • Bronchiolitis obliterans syndrome (BOS) • Cryptogenic organizing pneumonia (COP) • Late-onset interstitial pneumonitis
Autoimmune disorders
Cataracts
Infertility
Leukoencephalopathy
Secondary malignancy
Cardiac failure
Late-onset infections
Endocrine complications • Hypothyroidism • Osteopenia/osteoporosis • Gonadal failure • Infertility
Osteonecrosis

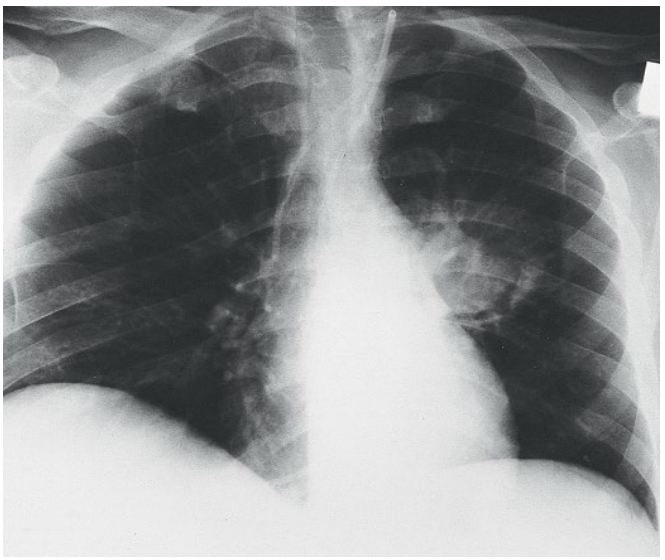

Fig. 25.14 Stem cell transplantation. Chest radiograph showing an opacity in the upper left zone, with a cystic center that contains a dense central zone, caused by aspergillosis.

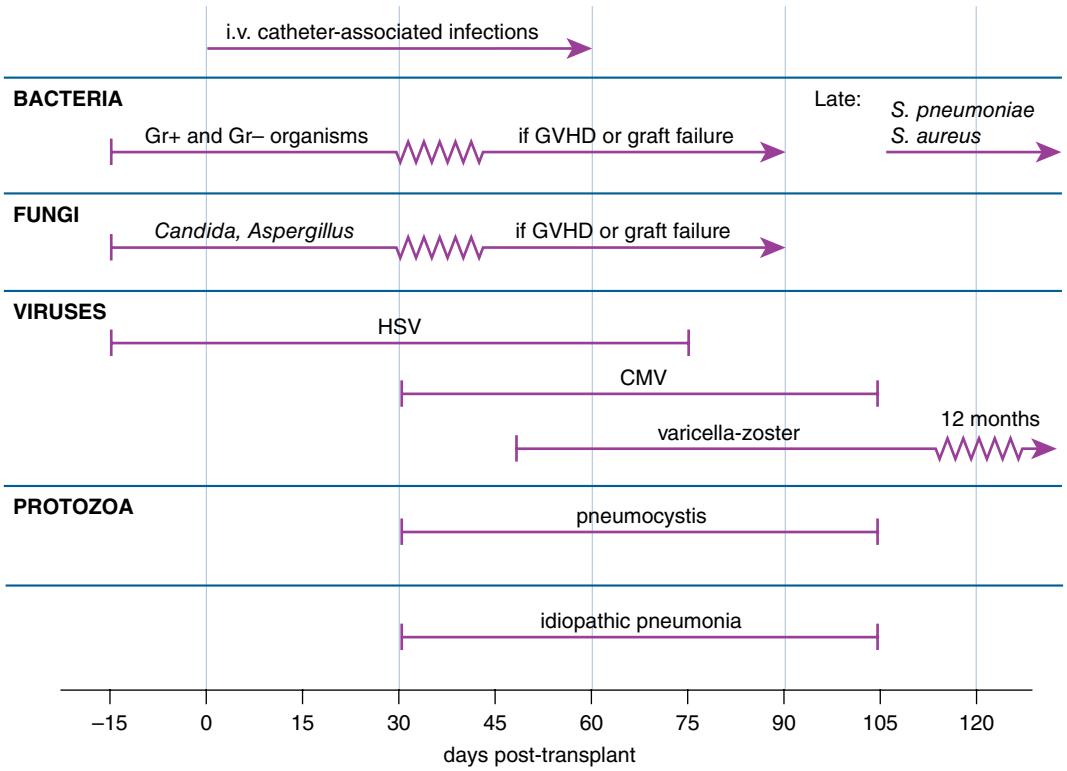

Fig. 25.13 Infections complicating allogeneic stem cell transplantation, according to the typical time sequence of onset. CMV, cytomegalovirus; Gr+, Gr–, Gram-positive or -negative; GVHD, graft-versus-host disease; HSV, herpes simplex virus. Source:Hoffbrand AV and Moss PAH. *Hoffbrand's Essential Haematology*, 7th edn. John Wiley & Sons Ltd., 2016. Reproduced with permission of John Wiley and Sons.

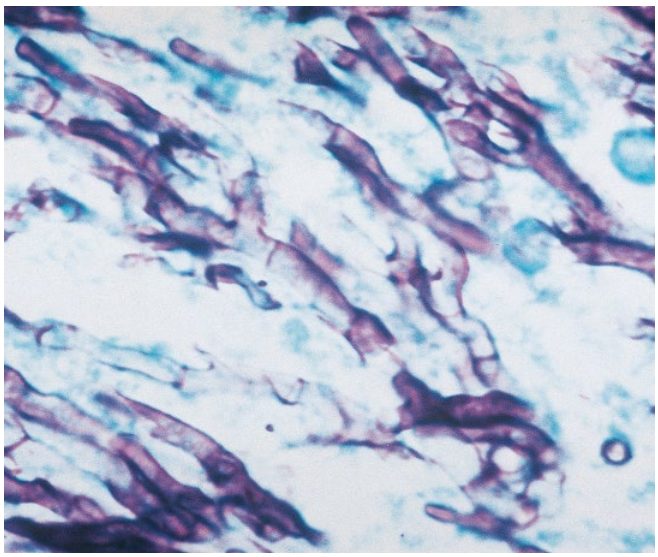

Fig. 25.15 Stem cell transplantation. Cytology of sputum from the case shown in Fig. 25.14 illustrates the typical branching septate hyphae of aspergilli. (Methenamine silver stain.)

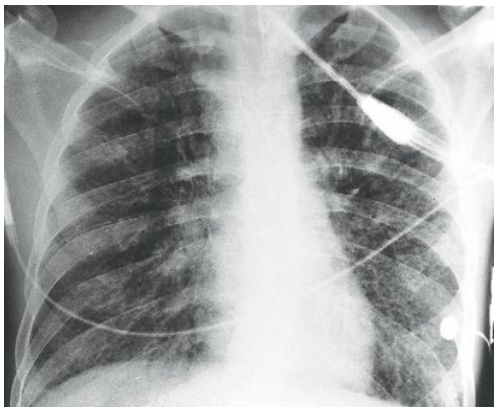

Fig. 25.16 Stem cell transplantation. Chest radiograph showing widespread interstitial pneumonia. Sputum cultures and indirect immunofluorescence showed the presence of cytomegalovirus.

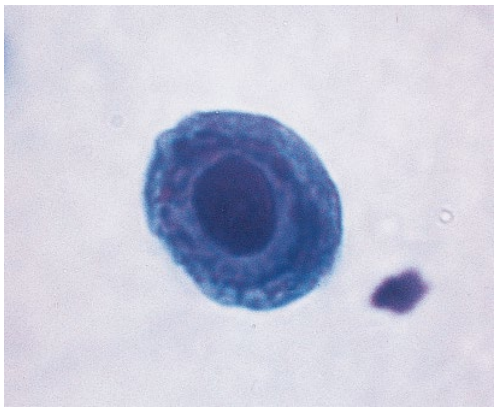

Fig. 25.17 Stem cell transplantation. Sputum cytology shows a pulmonary cell with degenerative changes and a large intranuclear inclusion body typical of cytomegalovirus infection. (Papanicolaou stain.) (Courtesy of Professor YS Erozan.)

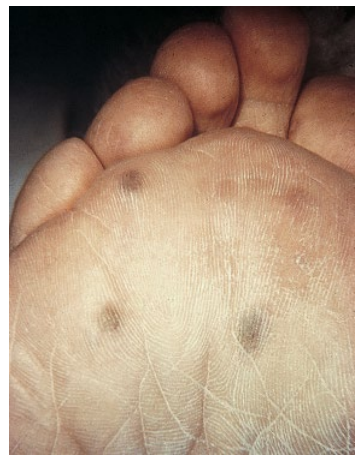

Fig. 25.18 Stem cell transplantation. Herpes simplex virus infection with multiple widespread lesions on the skin of the sole of the foot. (Courtesy of Professor HG Prentice.)

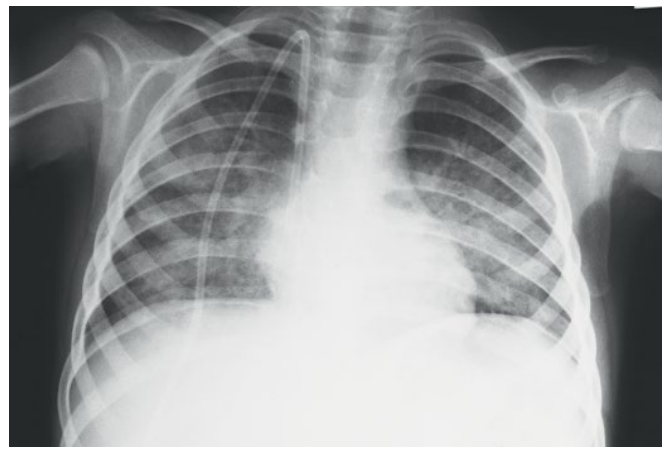

Fig. 25.19 Stem cell transplantation. Chest radiograph showing typical "bat wing" shadowing of both lung fields caused by *Pneumocystis jiroveci carinii*) infection.

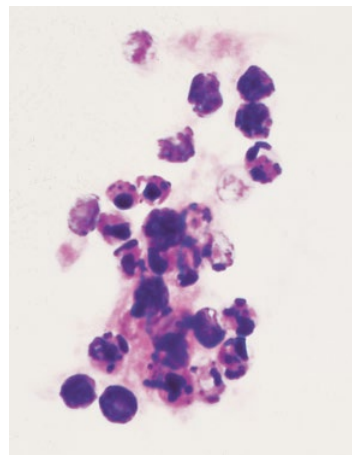

Fig. 25.20 Stem cell transplantation. High-power view of concentrated bronchial washings showing typical appearance of *P. jiroveci*. (Gram–Weigert stain.) (Courtesy of Professor YS Erozan.)

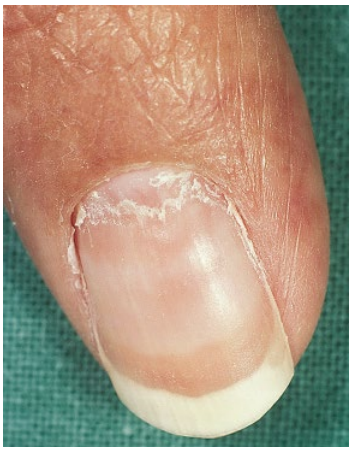

Fig. 25.21 Stem cell transplantation. This nail shows horizontal ridges and atrophy of the nail bed as a result of total body irradiation. (Courtesy of Professor HG Prentice.)

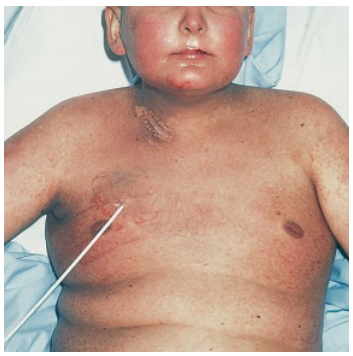

Fig. 25.22 Stem cell transplantation: Acute GVHD. Widespread erythematus skin rash. An indwelling central Hickman catheter is in place. (Courtesy of Professor HG Prentice.)

The rectal mucosa also shows death of epithelial (crypt) cells and inflammatory changes (Fig. 25.30). When severe, there is loss of small and large intestinal mucosa (Fig. 25.31).

Liver function is abnormal in acute and chronic GVHD, except in mild cases. The histologic appearances include damage to bile duct epithelial cells, inflammatory changes, and cholestasis (Fig. 25.32). GVHD can be prevented in HLA-matched allogeneic transplantation if T lymphocytes (or selected T-cell subsets) are completely removed in vitro from donor bone

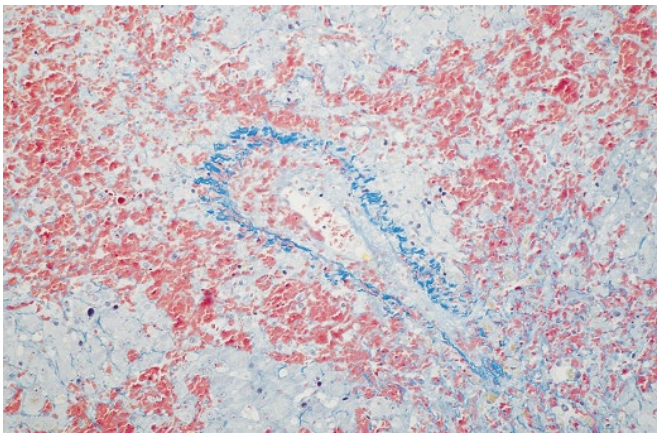

Fig. 25.23 Stem cell transplantation: VOD. Section showing a terminal hepatic venule with marked narrowing of its lumen. The deep-blue staining identifies the collagen of the original venule wall, while the inner paler blue area represents new collagen obstructing the lumen. Note the loss of hepatocytes in the perivenular area and the intense congestion of the sinusoids. (Chromotrope Aniline Blue ×40 stain.) (Courtesy of Dr. M Jarmulowicz.)

TABLE 25.6. CLASSIFICATION OF CHRONIC GRAFT-VERSUS-HOST DISEASE (GVHD)

Limited chronic GVHD
Either or both
Localized skin involvement
Hepatic dysfunction as a result of chronic GVHD
Extensive chronic GVHD
Either
Generalized skin involvement
or
Localized skin involvement and/or hepatic dysfunction as a result of chronic GVHD
plus
Liver histology showing chronic aggressive hepatitis-bridging necrosis or cirrhosis
or
Involvement of eye (Schirmer test with <5 mm wetting)
or
Involvement of minor salivary glands or oral mucosa demonstrated on labial biopsy
or
Involvement of any other target organ

Source: Blume et al. *Thomas' Hematopoietic Stem Cell Transplantation*, 3rd edn. 2004. Reproduced with permission of John Wiley and Sons.

TABLE 25.7. GLUCKSBERG STAGING OF ACUTE GVHD: (A) CLINICAL STAGING; (B) CLINICAL GRADING

(a) Stage	Skin	Liver bilirubin (μmol/L)	Gut
+	Maculopapular rash <25% body surface	34–51	Diarrhea 500–1000 mL/day or persistent nausea
++	Maculopapular rash 25–50% body surface	51–102	Diarrhea 1000–1500 mL/day
+++	Generalized erythroderma	102–255	Diarrhea >1500 mL/day
++++	Desquamation and bullae	>255	Pain ± ileus

(b) Overall grade	Skin	Liver	Gut	Functional impairment
0 (none)	0	0	0	0
I (mild)	+ to ++	0	0	0
II (moderate)	+ to +++	+	+	+
III (severe)	++ to +++	++ to +++	++ to +++	++
IV (life-threatening)	+ to ++++	++ to ++++	++ to ++++	+++

Source: Blume et al. *Thomas' Hematopoietic Stem Cell Transplantation*, 3rd edn. 2004. Reproduced with permission of John Wiley and Sons.

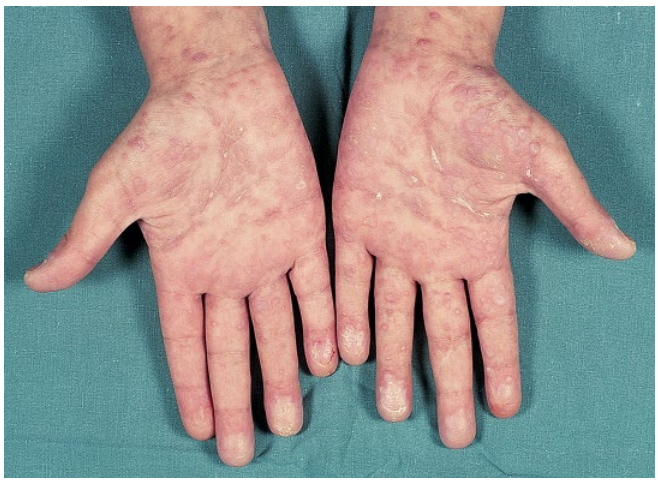

Fig. 25.24 Stem cell transplantation: Acute GVHD. The palmar surfaces of these hands show an erythematus maculopapular eruption with bullous ulceration and denudation. (Courtesy of Professor HG Prentice.)

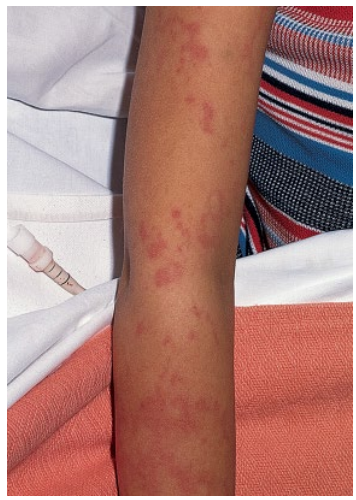

Fig. 25.25 Stem cell transplantation: Chronic GVHD. These patchy raised erythematous skin lesions are characteristic. (Courtesy of Professor HG Prentice.)

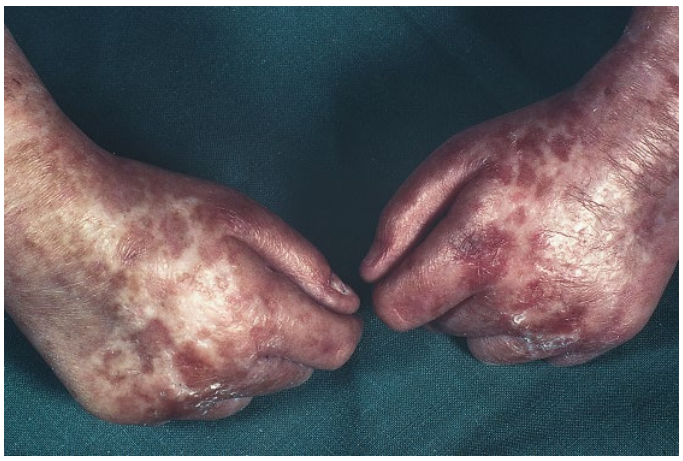

Fig. 25.26 Stem cell transplantation: Chronic GVHD. Scleroderma-like contractions of the hands with thickening of the skin and marked pigmentation. (Courtesy of Professor HG Prentice.)

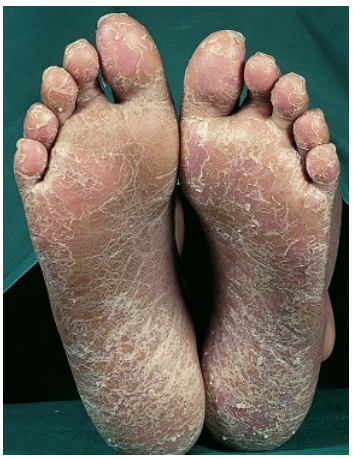

Fig. 25.27 Stem cell transplantation: Chronic GVHD. Erythema and exfoliation of the epidermis of the soles of the feet. (Courtesy of Professor HG Prentice.)

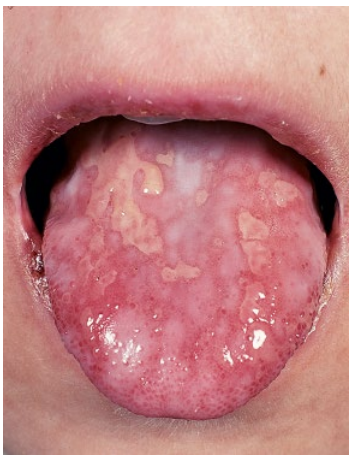

Fig. 25.28 Stem cell transplantation: Chronic GVHD. Lesions of the tongue and lips similar to those of lichen planus. (Courtesy of Professor HG Prentice.)

marrow, but this can increase the risk of graft failure or of leukemic relapse in some situations. Prevention of GVHD is usually carried out with ciclosporin with or without methotrexate; corticosteroids, infliximab, etanercept, sirolimus, and mycophenolate mofetil, are other drugs used for prevention and treatment of GVHD.

A frequent post-transplantation complication is an interstitial pneumonia (Fig. 25.33), which is more common in GVHD but can also be related to lung irradiation and to infection, particularly with CMV.

POST-TRANSPLANT LYMPHOPROLIFERATIVE DISORDERS

Post-transplant lymphoproliferative disorders (PTLDs) are polyclonal or monoclonal lymphoid proliferations or lymphomas that occur in recipients of stem cell or, more frequently, solid organ allografts, as a result of the immunosuppression (Figs. 25.34–25.39). There may be polyclonal Epstein–Barr virus (EBV) driven lymphocytosis and lymphadenopathy resembling

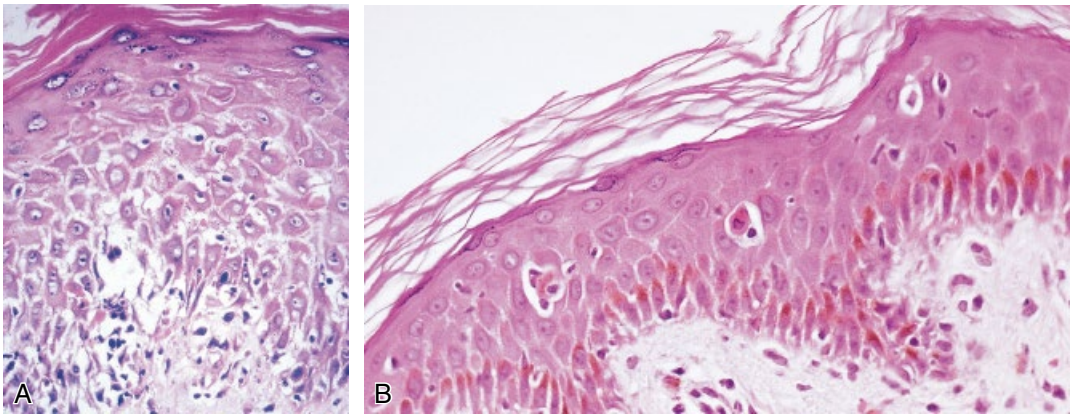

Fig. 25.29 Stem cell transplantation: Acute GVHD. Histologic sections of skin in moderately severe (Grade II) acute GVHD. **A,** Vacuolation of the basal epidermal cells with inflammatory changes in the superficial dermis. **B,** Prominent vacuoles containing necrotic epidermal cells and lymphocytes, from an African patient.

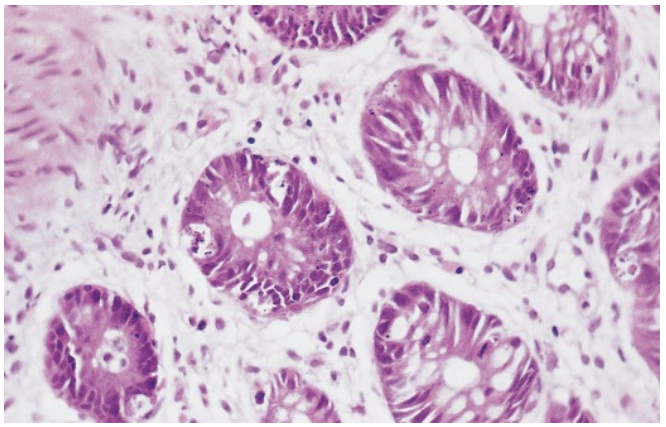

Fig. 25.30 Stem cell transplantation: Acute GVHD. High-power view of rectal biopsy in Grade I acute GVHD showing individual crypt cell necrosis and edema of the lamina propria.

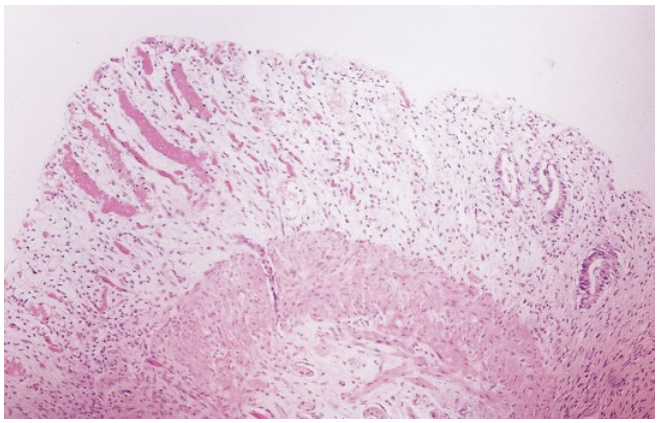

Fig. 25.31 Stem cell transplantation: Acute GVHD. Postmortem section of colon in Grade IV acute GVHD showing almost complete denudation of the epithelium, with edema and lymphocytic infiltration of the submucosa.

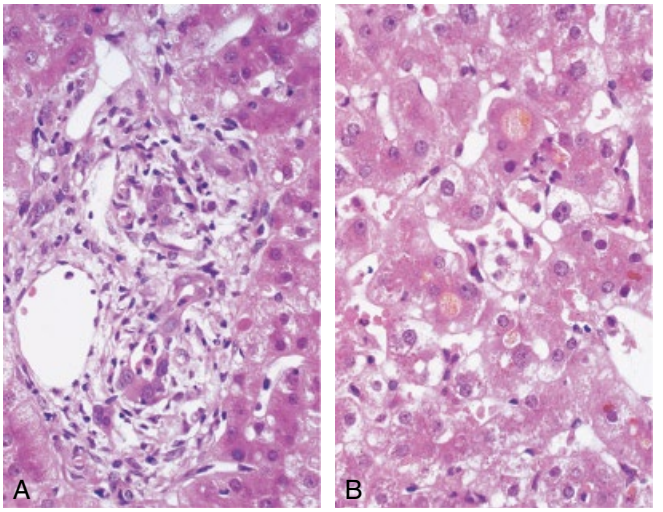

Fig. 25.32 Stem cell transplantation: Acute GVHD. High-power views of liver biopsy. **A,** Damaged, irregular, and elongated bile duct epithelial cells with occasional pyknotic nuclei in the portal tract (there is a moderate infiltration of lymphocytes and neutrophils). **B,** Cholestatic changes include dilated bile canaliculi and pigmented hepatocytes. (*A, B*, Courtesy of Professor PJ Scheuer.)

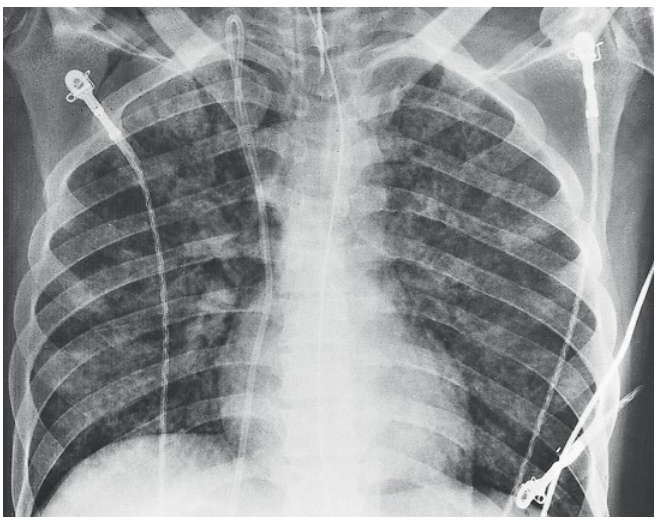

Fig. 25.33 Stem cell transplantation. Chest radiograph of interstitial pneumonitis showing widespread diffuse mottling. The patient had received total body irradiation and had Grade III GVHD. No infective cause of the pneumonitis was identified in this case.

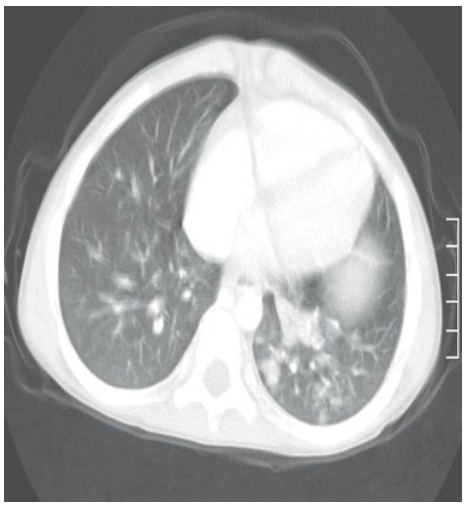

Fig. 25.34 Post-transplant lymphoproliferative disease (PTLD). Lung nodules after liver transplant: a 5-year-old boy 23 months after orthotopic liver transplant had adenotonsillar hypertrophy, pulmonary nodules, and mediastinal adenopathy. Biopsy showed polymorphic, polyclonal hyperplasia with CD20+ EBER+ B cells. He was treated with rituximab with a complete response. (Courtesy of Dr. HE Heslop.)

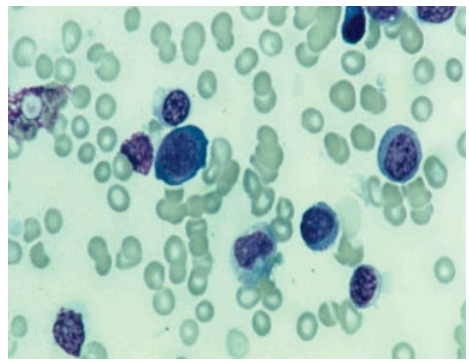

Fig. 25.36 Post-transplant lymphoproliferative disease. Blood film with circulating EBV-transformed lymphoid cells. A 3-year-old girl 64 days following a T-cell-depleted unrelated stem cell transplant had fevers and an EBV DNA greater than 100 000 copies/μL peripheral blood. On examination of a blood film she had circulating B lymphoblasts, which were LMP1 (EBV viral antigen) positive by immunostaining. (Courtesy of Dr. HE Heslop.)

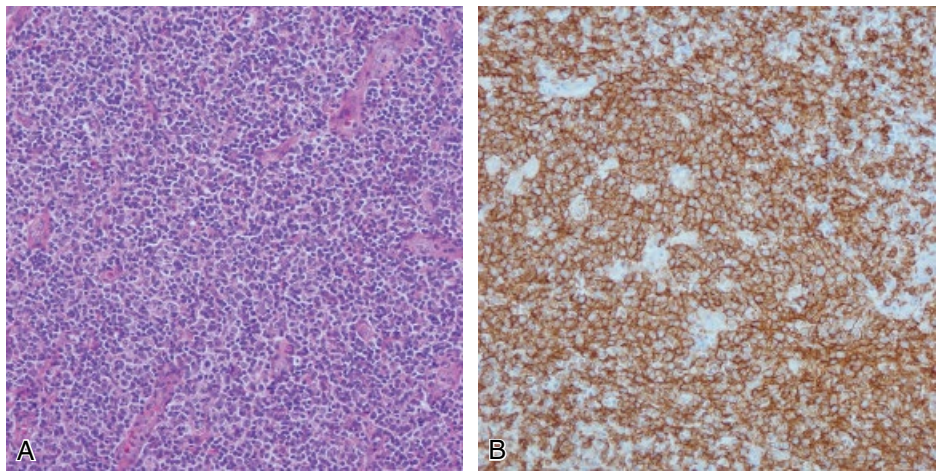

Fig. 25.35 Post-transplant lymphoproliferative disease (PTLD). A 2-year-old girl with tonsillar and pulmonary PTLD 18 months following cardiac transplantation for congenital dilated cardiomyopathy. The cells were EBV positive but polymorphic. (*A*, H&E stain; *B*, CD20 stain.) (Courtesy of Dr. P Amrolia and Dr. N Sabire.)

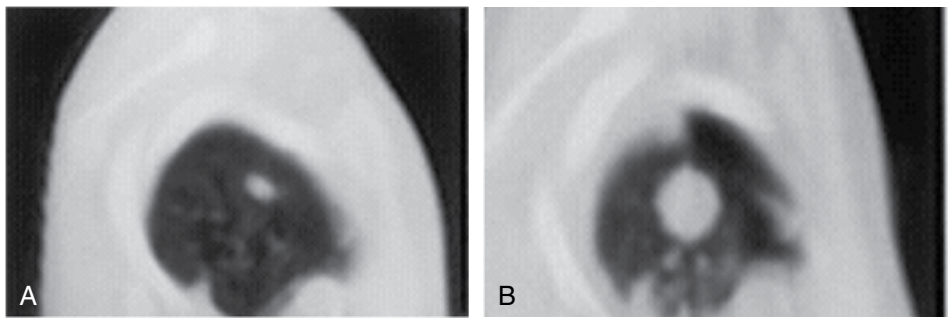

Fig. 25.37 Post-transplant lymphoproliferative disease. Lung nodule after bone marrow transplant (BMT). A 3-year-old boy 8 months after a T-cell-depleted transplant from a mismatch family member had fevers and lymphadenopathy. A computed tomography (CT) scan showed pulmonary nodules, and biopsy confirmed diffuse large B-cell lymphoma, and EBV was detected in the tumor by amplification of viral DNA with the polymerase chain reaction and by immunofluorescence staining for the viral antigen LMP1. He attained complete remission after infusion of donor cells. (Courtesy of Dr. HE Heslop.)

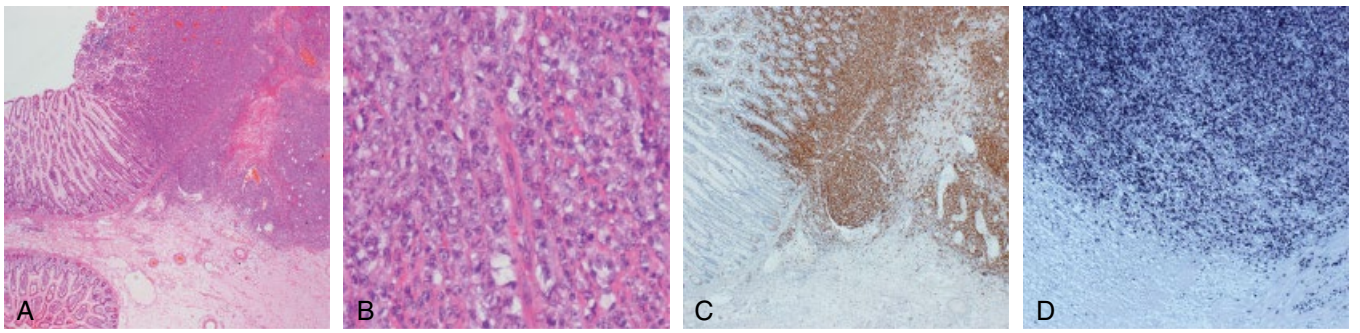

Fig. 25.38 Post-transplant lymphoproliferative disease. Male 17-year-old 5 months after renal transplantation had small bowel perforation caused by diffuse large B-cell lymphoma. **A,** Low-power view of lymphoid mass invading small bowel. **B,** High-power view of lymphoid mass. **C,** Immunostaining for CD20. **D,** EBV-ISH (in situ hybridization) stain showing the tumor cells are positive for EBV. (Courtesy of Dr. P Amrolia and Dr. N Sebire.)

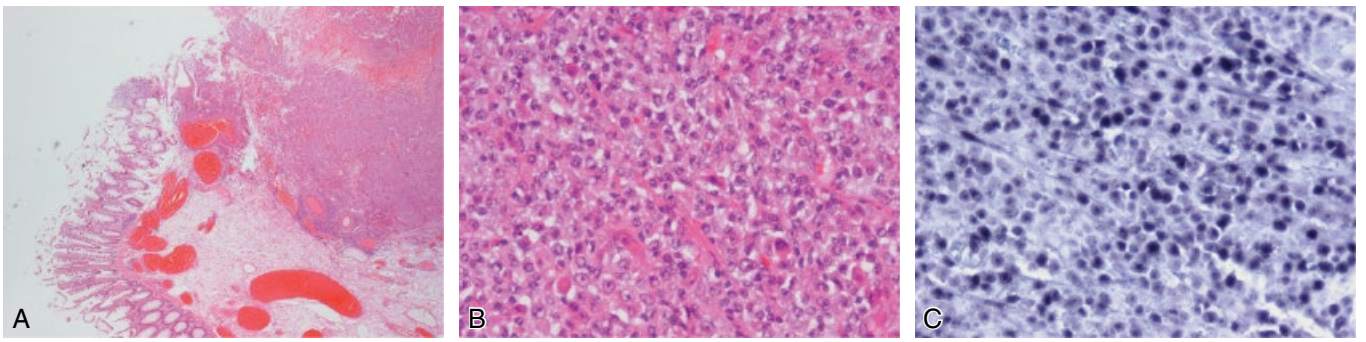

Fig. 25.39 Post-transplant lymphoproliferative disease. A 12-year-old boy 8 months after bilateral lung transplantation for cystic fibrosis had colonic perforation. **A,** Low-power view of tumor invading large bowel. **B,** High-power view of tumor showing diffuse, large cell lymphoblast replacement. **C,** EBV-ISH stain showing the tumor cells are positive for EBV. (Courtesy of Dr. P Amrolia and Dr. N Sebire.)

TABLE 25.8. CATEGORIES OF POST-TRANSPLANT LYMPHOPROLIFERATIVE DISORDER (PTLD)

Non-destructive PTLDs
Plasmacytic hyperplasia
Infectious mononucleosis
Florid follicular hyperplasia
Polymorphic PTLD
Monomorphic PTLDs[a] (classify according to lymphoma they resemble)
B-cell neoplasms:
Diffuse large B-cell lymphoma
Burkitt lymphoma
Plasma cell myeloma
Plasmacytoma
Other[b]
T-cell neoplasms:[a]
Peripheral T-cell lymphoma, NOS
Hepatosplenic T-cell lymphoma
Other
Classic Hodgkin lymphoma PTLD[a]

[a] The ICD-O codes for these lesions are the same as those for the respective lymphoid or plasmacytic neoplasm.
[b] Indolent small B-cell lymphomas arising in transplant recipients are not included among the PTLDs, with the exception of EBV-positive marginal zone lymphomas (see text).
Source: Adapted with permission from Swerdlow SH, et al., eds. *WHO Classification of Tumours of Haematopoietic and Lymphoid Tissues*, revised 4th edn. International Agency for Research on Cancer, 2017.

infectious mononucleosis or EBV-positive or EBV-negative lymphomas, most frequently B cell but occasionally T cell. They are classified by WHO 2016 as shown in Table 25.8, according to the criteria used in Table 25.9.

Treatment of these disorders is with rituximab (anti-CD20), chemotherapy, or specific anti-EBV cytotoxic T lymphocytes (Fig. 25.40). Withdrawal of immunosuppressive therapy is also helpful, particularly when the proliferation is polyclonal.

TABLE 25.9. CRITERIA USED IN THE CATEGORIZATION OF POST-TRANSPLANT LYMPHOPROLIFERATIVE DISORDER (PTLD)

Pathologic type of PTLD	Histopathology		Immunophenotype/in situ hybridization	Genetics	
	Architectural effacement	Major findings		IGH/TR clonal rearrangements	Cytogenetic/oncogene abnormalities
Plasmacytic hyperplasia	Absent	Predominantly small lymphocytes and plasma cells	Pcl B cells and admixed T cells; EBV+	Pcl or very small mcl B-cell population (s)	None
Infectious mononucleosis	Absent	Admixed small lymphocytes, plasma cells, and immunoblasts	Pcl B cells and admixed T cells; EBV+	Pcl or very small mcl B-cell population(s); may have clonal/oligoclonal TR genes	Simple cytogenetic abnormalities rarely present
Florid follicular hyperplasia	Absent	Prominent hyperplastic germinal centres	Pcl B cells and admixed T cells; EBV±	Pcl or very small mcl B-cell population(s)	Nonspecific simple cytogenetic abnormalities rarely present
Polymorphic	Present	Full spectrum of lymphoid maturation seen, not fulfilling criteria for NHL	Pcl ± mcl B cells and admixed T cells; most EBV+	Mcl B cells, non-clonal T cells	Some have *BCL6* somatic hypermutations
Monomorphic	Usually present	Fulfils criteria for an NHL (other than one of the indolent B-cell neoplasms) [a] or plasma cell neoplasm	Varies based on type of neoplasm they resemble; EBV more variable than in other categories	Clonal B cells and/or T cells (except for rare NK-cell cases)	Variably present (see text)
CHL	Present	Fulfils criteria for CHL	Similar to other CHL; EBV+	IGH not easily demonstrated	Unknown

CHL, classic Hodgkin lymphoma; NHL, non-Hodgkin lymphoma; mcl, monoclonal; pcl, polyclonal. Monoclonality and polyclonality are only inferred when finding monotypic or polytypic light chain expression.

[a] EBV-positive MALT lymphomas, at least of skin/subcutaneous tissues, should be considered a type of PTLD.

Source: Adapted with permission fromSwerdlow SH, et al., eds. *WHO Classification of Tumours of Haematopoietic and Lymphoid Tissues*, revised 4th edn. International Agency for Research on Cancer, 2017.

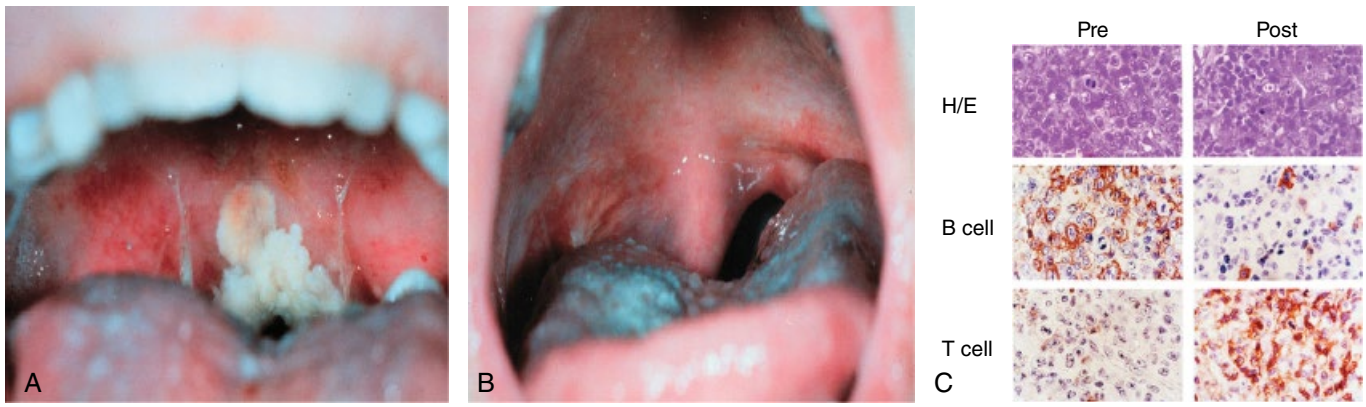

Fig. 25.40 Post-transplant lymphoproliferative disease. **A,** A 12-year-old boy 7 months after HLA-matched unrelated bone marrow transplantation had massive lymphadenopathy and respiratory obstruction. **B,** He was treated with EBV-specific cytotoxic T lymphocytes (CTLs). All symptoms resolved and he remained in remission 4 years later. **C,** Tumor biopsies before and after CTL therapy. (Courtesy of Dr. HE Heslop, with permission, Rooney CM, et al. *Blood* 1998;92:1549–1555. Reproduced with permission of *Blood: Journal of the American Society of Hematology*.)

CHAPTER

26

NORMAL HEMOSTASIS, PLATELET PRODUCTION AND FUNCTION

The purpose of hemostasis is to prevent hemorrhage following vascular injury by rapidly plugging holes in blood vessels. This is achieved through the interaction of endothelium, platelets, and coagulation factors (Fig. 26.1). While the primary purpose is to prevent blood loss, there are effects on inflammation, wound healing, cancer metastasis, and vasculogenesis. The initial arrest of hemorrhage is the result of vasoconstriction and the elastic recoil of severed blood vessels, together with the formation of platelet plugs. At the same time there is activation of blood coagulation factors, which converts soluble fibrinogen in the plasma into an insoluble fibrin clot, reinforcing the sealing effect (Fig. 26.2).

A key function of the intact endothelium is to prevent pathologic thrombosis. A number of endothelial components cause vasodilatation (e.g. nitric oxide), inhibit platelet aggregation (e.g. prostacyclin or epoprostenol), or fibrin clot formation (e.g. thrombomodulin and endothelial protein C receptor), or activate fibrinolysis (e.g. tissue plasminogen activator) (Fig. 26.3). Von Willebrand factor (VWF), the key protein that mediates the platelet–endothelium interaction, is expressed in endothelial cells and stored in their Weibel–Palade bodies (Fig. 26.4). When endothelial cells are disrupted the contents of the Weibel–Palade bodies become exposed to flowing blood (Fig. 26.5). This unravels the highest molecular weight VWF multimers to form long "strings" to which platelets attach. The change of VWF from a globular to an unfolded protein in an extended chain under shear stress exposes binding sites for platelets and collagen and is shown in Fig. 26.6.

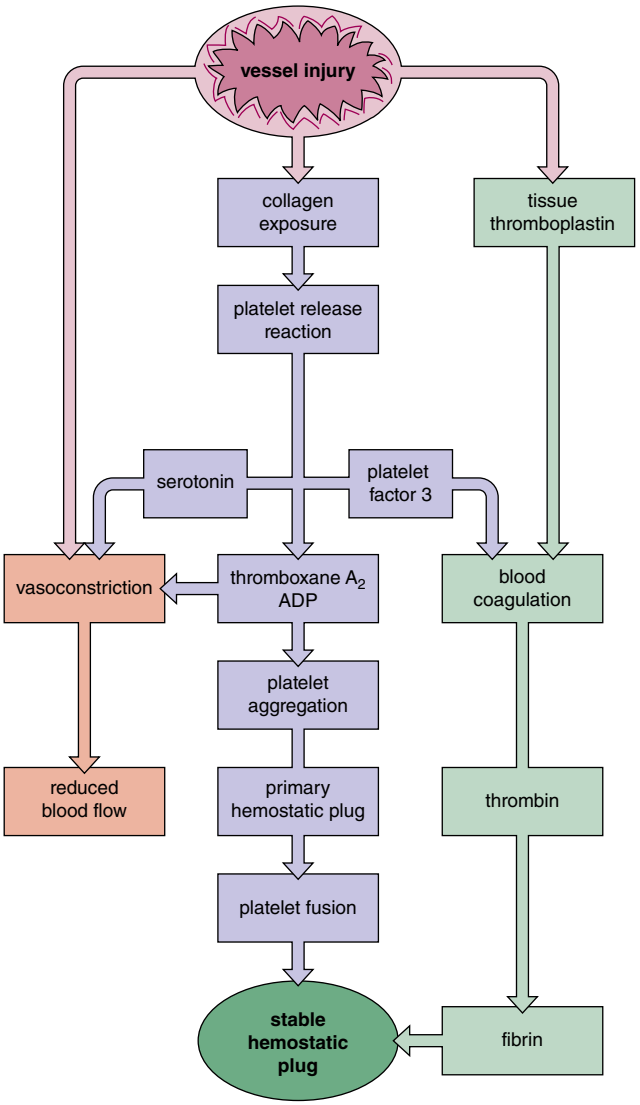

Fig. 26.1. Normal hemostasis mechanisms.

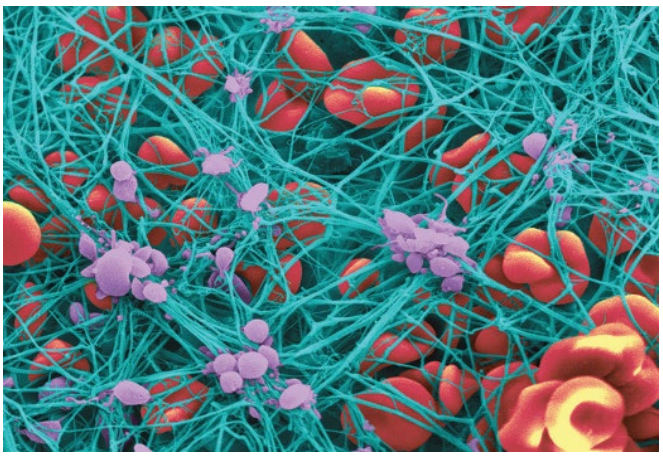

Fig. 26.2. Colorized scanning electron micrograph of a whole blood clot formed in vitro. Platelets are violet, fibrin fibres are light blue, and erythrocytes are red. (Courtesy of Dr. YI Veklich and Dr. JW Weisel, Department of Cell and Developmental Biology, University of Pennsylvania School of Medicine, Philadelphia.)

Color Atlas of Clinical Hematology: Molecular and Cellular Basis of Disease, Fifth Edition. A. Victor Hoffbrand, Paresh Vyas, Elías Campo, Torsten Haferlach, and Keith Gomez

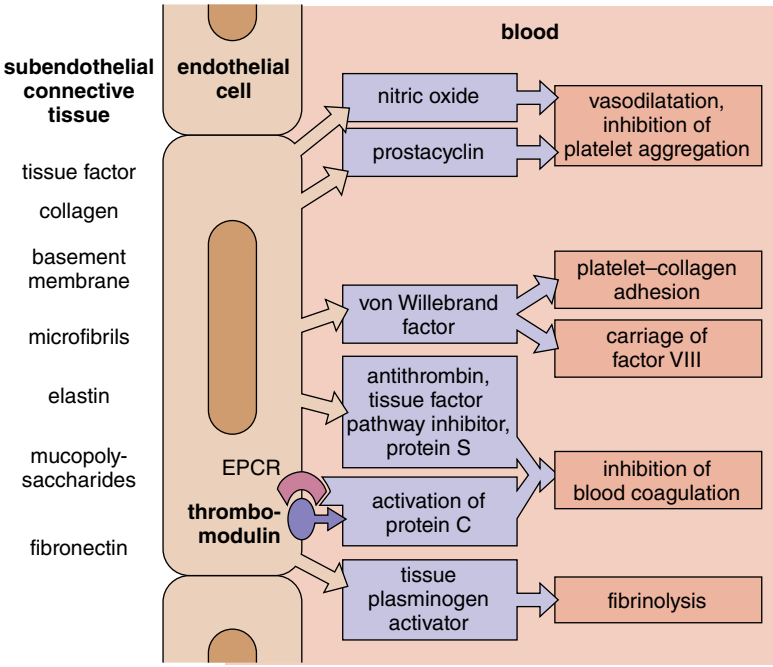

Fig. 26.3. Function of intact vessel wall. The endothelial cell forms a barrier between platelet and plasma clotting factors, and subendothelial connective tissues. Endothelial cells produce a variety of substances that cause vasodilatation, inhibit hemostasis or platelet aggregation, or activate fibrinolysis. EPCR, endothelial protein C receptor.

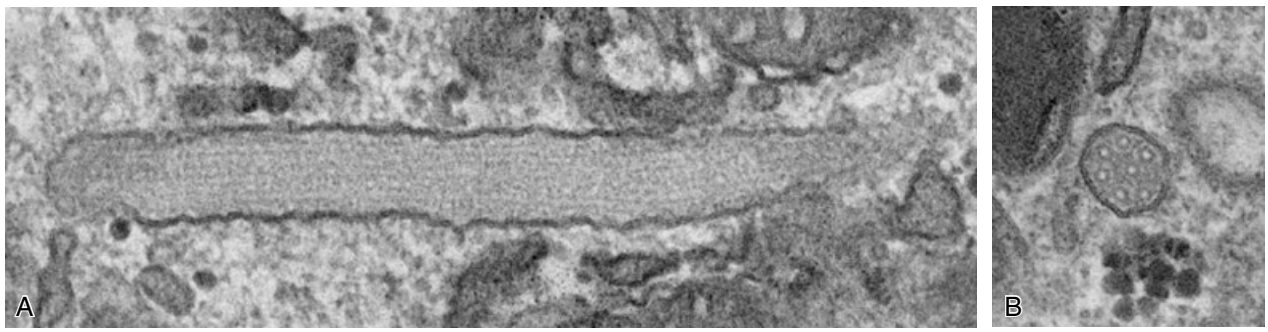

Fig. 26.4. Scanning electron microscopy of Weibel–Palade bodies in **(A)** longitudinal and **(B)** cross-section views. VWF molecules can be seen as tubular structures.

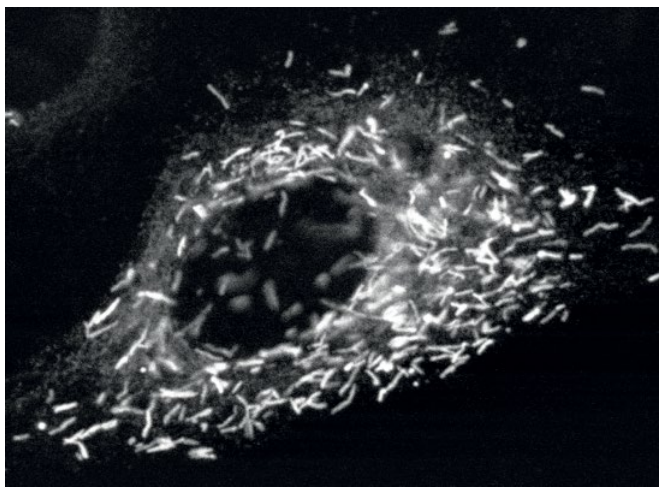

Fig. 26.5. Fluorescence microscopy of human umbilical vein endothelial cell showing release of VWF under shear stress.

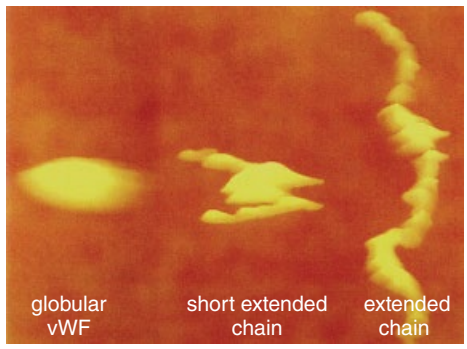

Fig. 26.6. Von Willebrand factor atomic force microscopy (AFM) shows a globular structure under negligible shear; shear forces applied by the AFM probe tip cause protein unfolding, giving VWF a short extended chain information. With a more extended and severe shear stress, VWF has an extended conformation. (Courtesy ofSiedlecki CA, et al. *Blood* 1996;88:2939–2950. Reproduced with permission of *Blood: Journal of the American Society of Hematology*.)

THE COAGULATION CASCADE

The main proteins of the blood coagulation cascade are zymogens and procofactors (Fig. 26.7). The pathway is triggered when disruption of the vessel wall brings factor VII (FVII) into contact with tissue factor (TF) to form the extrinsic tenase complex FVIIa-TF. This is the first in a series of macromolecular complexes formed when zymogens are activated and bound by their activated cofactors. The zymogens are mostly serine proteases that are part of the same protein super family and share common characteristics. This is important for regulation. The small amount of thrombin generated is insufficient for fibrin clot formation but activates the amplification loop in which the remaining enzymes are sequentially activated. This self-perpetuating loop leads to a large burst of thrombin generation and formation of the fibrin clot (Fig. 26.8). These enzymatic reactions require calcium and most take place on negatively charged phospholipid surfaces which are provided by activated platelets. The conversion of soluble fibrinogen to insoluble fibrin clot is only one of several thrombin functions. This key protein amplifies its own production, activates anticoagulant pathways, and subsequently initiates clot breakdown processes which enable vascular remodeling and lead to wound healing. This single enzyme achieves these multiple, seemingly antagonistic functions, through two exosites which switch the protein between pro- and anticoagulant actions (Fig. 26.9).

Measurement of coagulation involves three basic clotting tests: prothrombin time, activated partial thromboplastin time (APTT), and thrombin time (TT). These tests were developed in the mid-twentieth century when the original waterfall hypothesis of coagulation was widely thought to reflect physiologic clot formation. For this reason, understanding which clotting factors these tests are sensitive to is best understood by superimposing them on the original cascade (Fig. 26.10).

REGULATION OF COAGULATION

Control of the coagulation cascade is important in preventing pathologic thrombosis. The first and simplest control mechanism is the physical separation of the triggers: TF and FVII by an intact endothelium. Once initiation has occurred, regulation is achieved through three main anticoagulant proteins: Tissue factor pathway inhibitor (TFPI), the protein C (PC) pathway, and antithrombin (AT). TFPI has assumed greater clinical relevance in recent years as drugs that inhibit TFPI are undergoing clinical trials in hemophilia (see Chapter 28) and those that mimic TFPI are under development as anticoagulants (see Chapter 29). TFPI contains

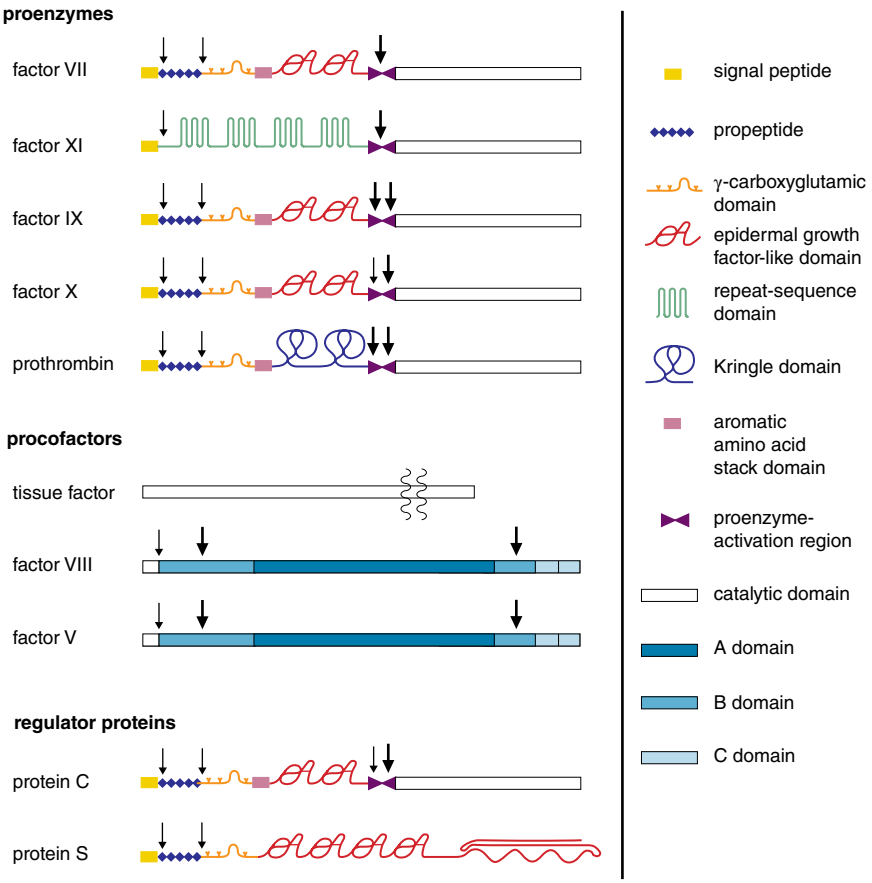

Fig. 26.7. Domains of the enzymes, receptors, and cofactors involved in blood coagulation and regulation. The components are proenzymes, procofactors, and regulatory proteins. The proenzymes, including protein C, contain a catalytic domain, an activation region, and a signal peptide. The vitamin K-dependent proteins include a propeptide and a γ-carboxyglutamic acid domain. Other important domains include the epidermal growth factor-like domain, the Kringle domain, and the repeat-sequence domain. Tissue factor is an integral membrane protein unrelated to other known proteins. Factors V and VIII have marked similarities in structure. Sites of intracellular peptide bonds cleaved during synthesis are indicated by thin arrows, and sites of peptide bonds cleaved during protein activation are indicated by thick arrows. The transmembrane domain of tissue factor is shown within the phospholipid bilayer. (Source: Modified with permission from Furie B, Furie BC. *N Engl J Med* 1992;326:800–806. Reproduced with permission of Massachusetts Medical Society: The New England Journal of Medicine.)

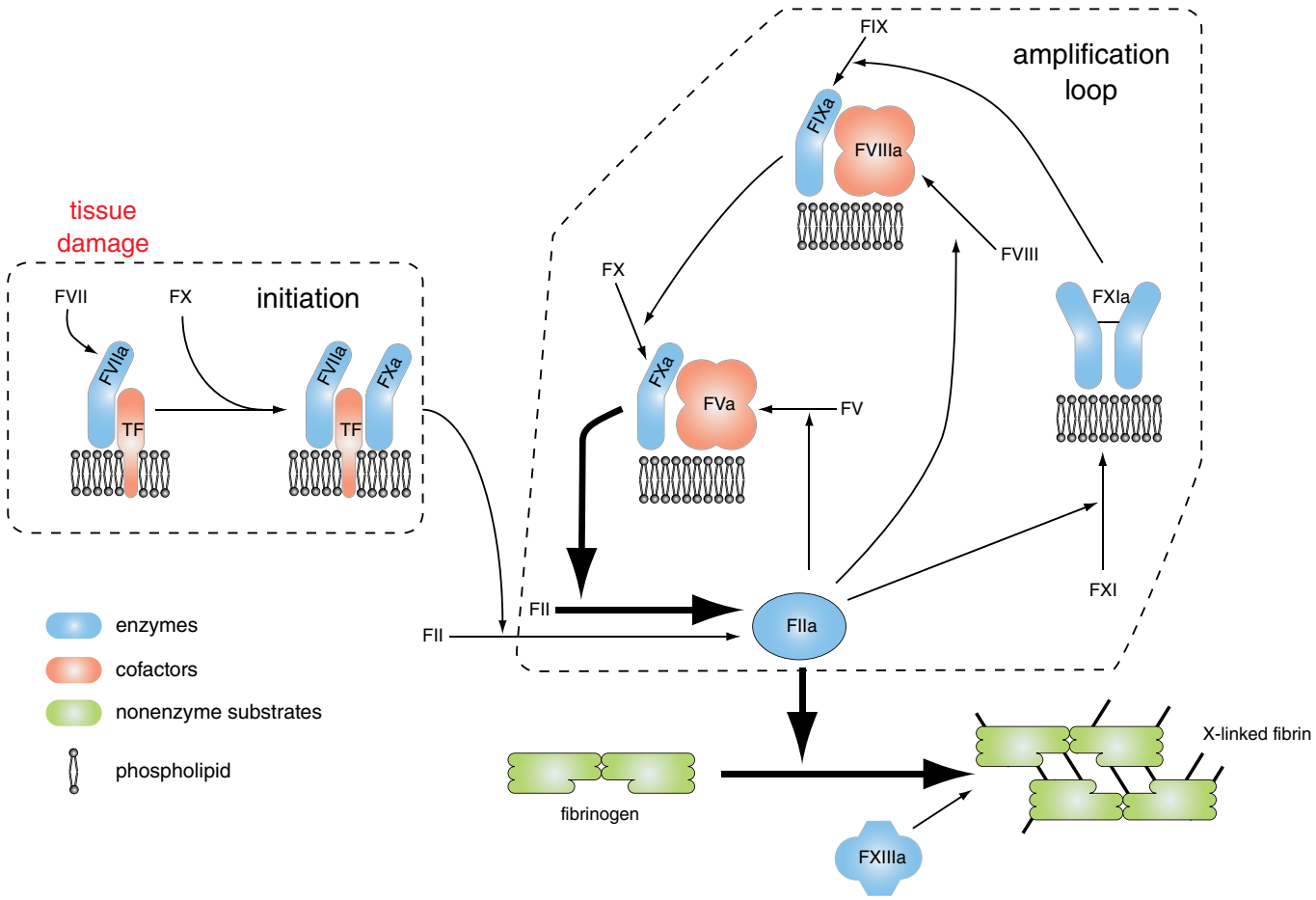

Fig. 26.8. Fibrin clot formation is initiated in vivo by tissue damage exposing tissue factor to factor VII. A small amount of thrombin is formed that is not sufficient to form fibrin clot but activates the amplification loop containing the rest of the coagulation factors. This leads to a large burst of thrombin formation (shown by thick arrows) that converts soluble fibrinogen into insoluble fibrin. Coagulation enzymes are shown as blue shapes and cofactors are in red. The negatively charged phospholipid membrane on which these reactions occur is mostly provided by activated platelets.

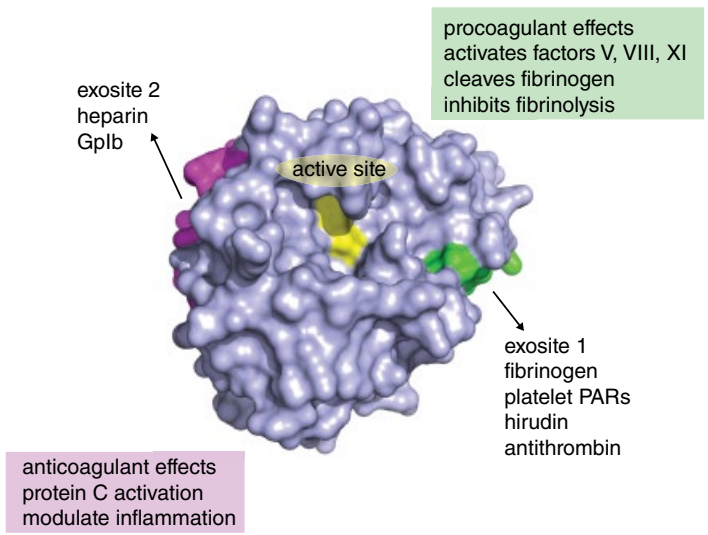

Fig. 26.9. Thrombin is the key protein in coagulation. It has a number of substrates that are both pro- and anticoagulant. Switching between these functions is partly achieved by ligand binding to two exosites (green and magenta) that flank the proteolytic cleft (yellow) that leads to conformational changes that alter substrate specificity.

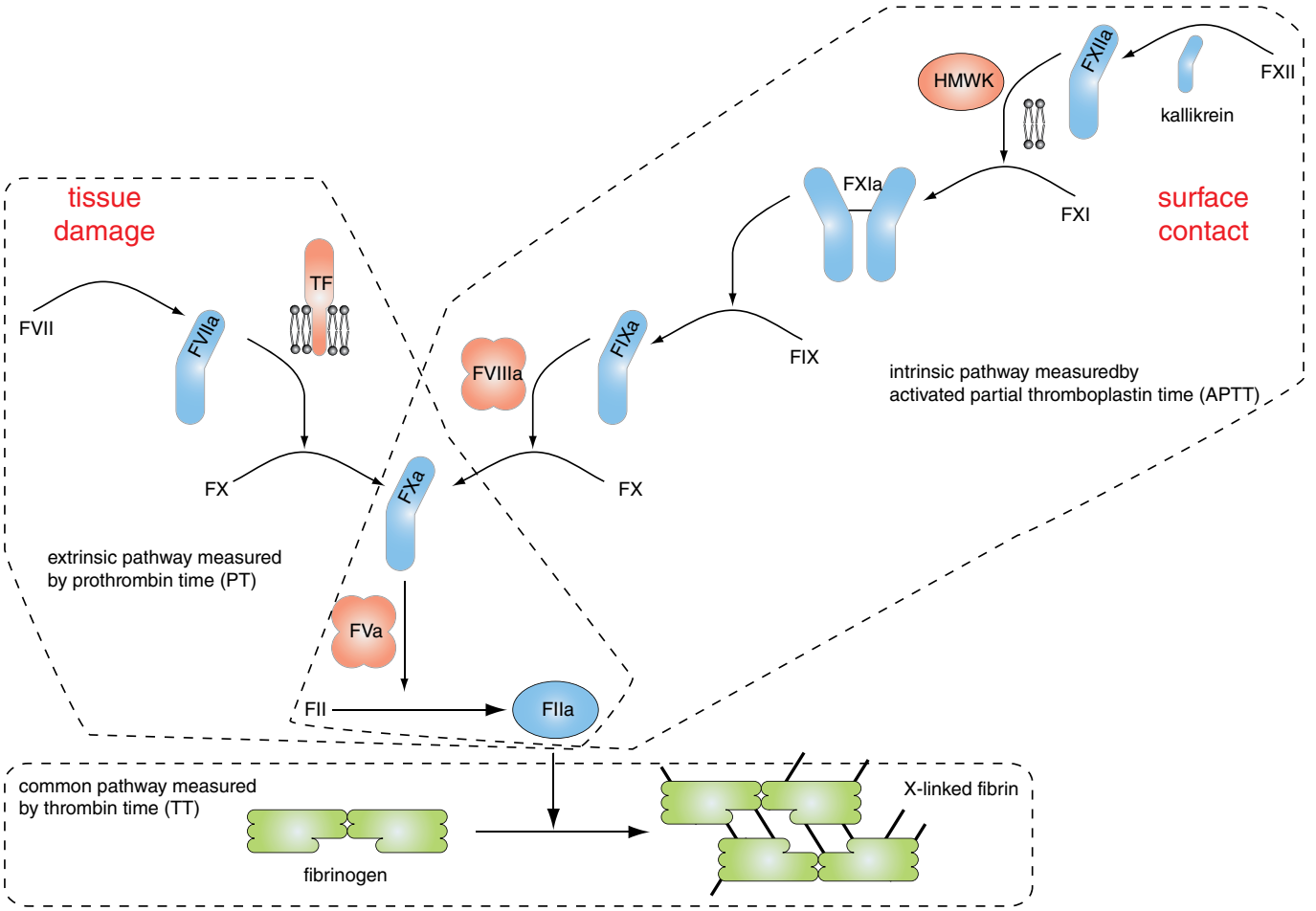

Fig. 26.10. Original waterfall hypothesis of coagulation. It was originally believed that there were two separate pathways of thrombin generation and tests were developed to assess these pathways. The extrinsic pathway was so-called because it involved triggering by tissue factor that was extrinsic to plasma and is measured by the prothrombin time (PT). The intrinsic pathway is initiated by contact factors that are intrinsic components of plasma and is measured by the activated partial thromboplastin time (APTT). It is now established that the contact system is not involved in physiologically important thrombin generation as part of hemostasis. The final common pathway of fibrinogen conversion to fibrin is measured by the thrombin time (TT).

three inhibitory Kunitz domains of which the first two bind to FVIIa and FXa. The function of the third Kunitz domain remained a mystery for many years until it was found to bind protein S (PS), the main cofactor for PC (Fig. 26.11). Note that TFPI only blocks free FXa or FXa in the extrinsic tenase complex. It does not bind FXa in the intrinsic tenase complex formed by FIXa-FVIIIa or in the prothrombinase complex, FXa-FVa. Regulation of this part of the cascade, the amplification loop, is achieved by PC and AT. Thrombin bound to its receptor thrombomodulin is able to activate PC bound to its endothelium receptor (EPCR). Activated PC with its cofactor PS is a potent enzymatic in activator of both activated FVIII and FV. EPCR is predominantly expressed in the endothelium of large vessels demonstrating the importance of this pathway in preventing large vessel thrombosis.

AT is a universal serine protease inhibitor (SERPIN) and is able to inhibit the cascade at a number of points taking advantage of the similar modular structure of several clotting factors (Fig. 26.12). The two key serine proteases that it inhibits are FXa and thrombin with a less important effect on FIXa. Inhibition is achieved through insertion of a reactive center loop into the active site cleft of the serine protease. Cleavage of this loop causes the serine protease to become irreversibly trapped resulting in degradation of both protease and SERPIN (see Chapter 29). The inhibitory function of AT is greatly enhanced by endogenous heparinoids. This is achieved through two mechanisms: first, recognition of a specific pentasaccharide sequence in heparin by a heparin-binding site in AT leads to a conformational change that makes the reactive center loop more accessible to cleavage and, second, larger molecular weight heparinoids are able to envelope both the SERPIN and the serine protease which facilitates the inhibitory reaction. The importance of these two mechanisms is discussed in Chapter 29.

MEGAKARYOCYTE AND PLATELET PRODUCTION

The earliest small progenitor cells of the megakaryocytic line are not easily differentiated from myeloblasts. They can be identified by electron microscopic or immunologic techniques. Megakaryoblasts undergo nuclear and cytoplasmic maturation from progenitor cells (Fig. 26.13). The megakaryocyte matures through endomitotic synchronous nuclear replications, which enlarge the cytoplasmic volume as the number of nuclei increases in multiples of two. These polyploid cells contain the

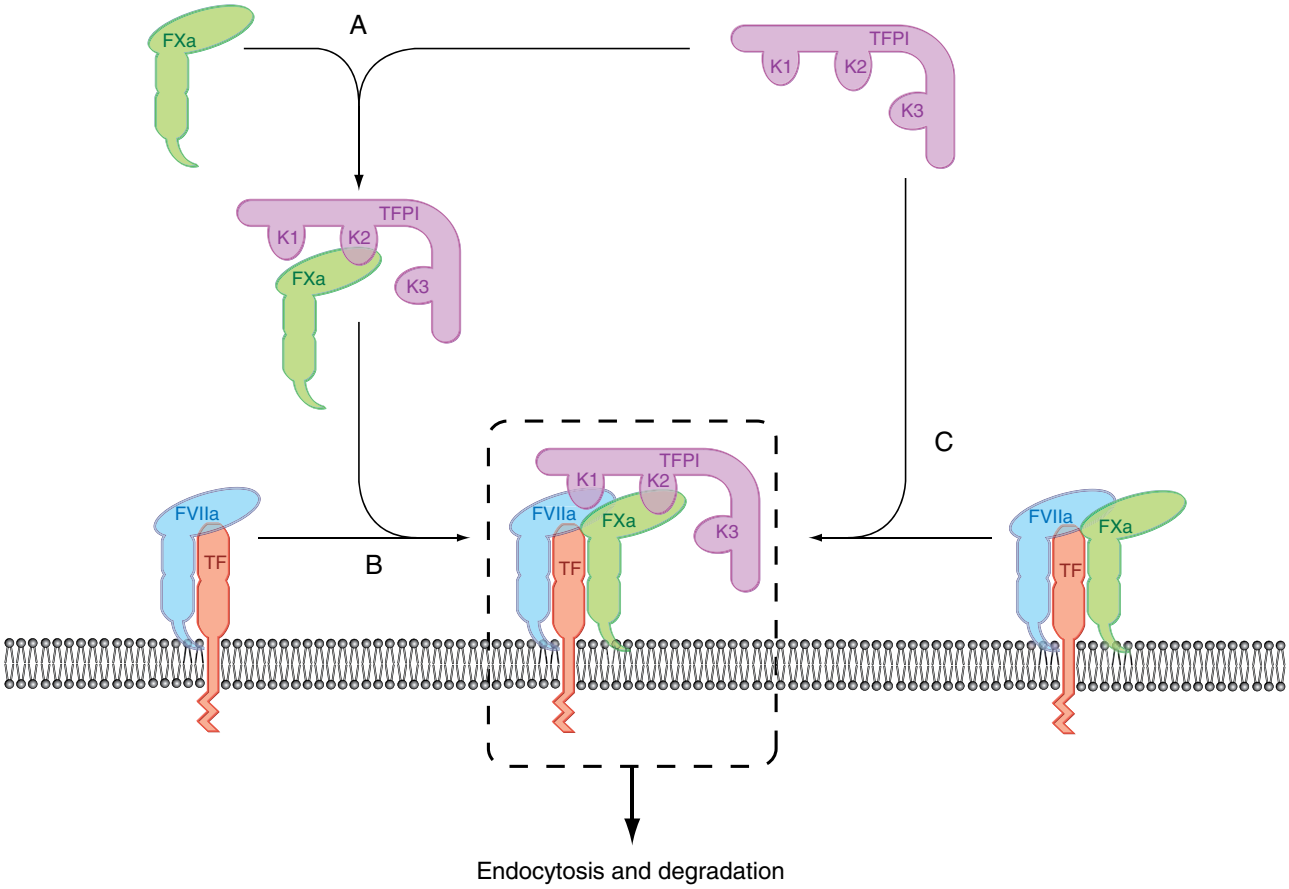

Fig. 26.11. Tissue factor pathway inhibitor (TFPI) regulation of the coagulation trigger. TFPI inhibits FVIIa and FXa through its K1 and K2 domains, respectively. TFPI either binds free FXa first (A) before binding to TF-FVIIa (B) or binds directly to TF-FVIIa·FXa (C). The K3 domain binds protein S and the C-terminus is involved in stabilizing the complex on the membrane. The serine proteases are irreversibly bound in the final TF-FVIIa-FXa-TFPI macromolecular complex which is internalized for degradation.

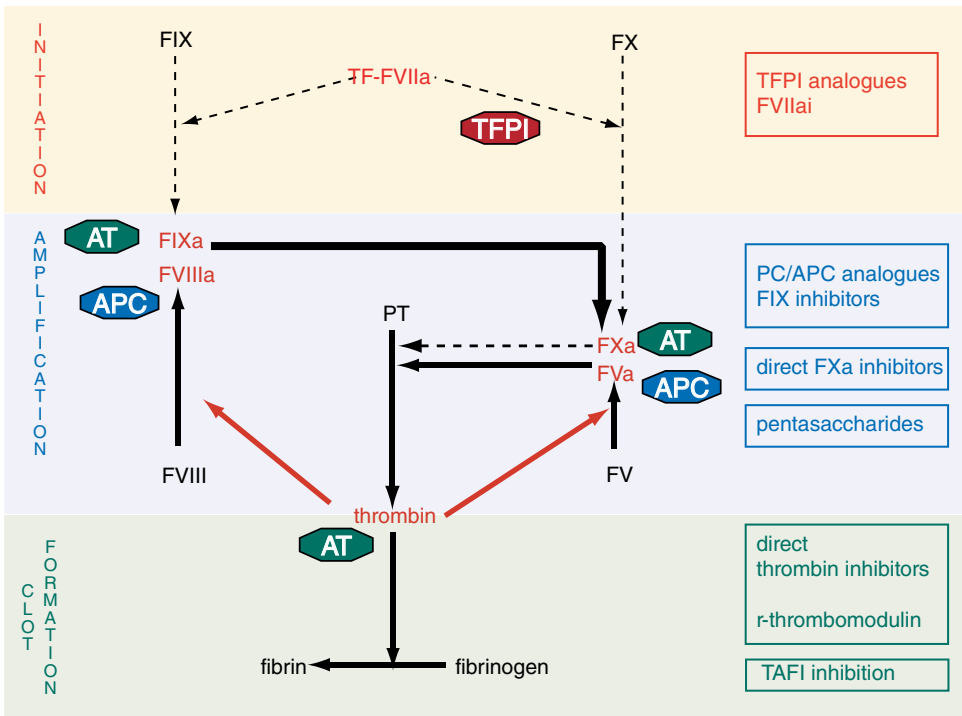

Fig. 26.12. Points of action of endogenous inhibitors of coagulation and the main classes of anticoagulants.

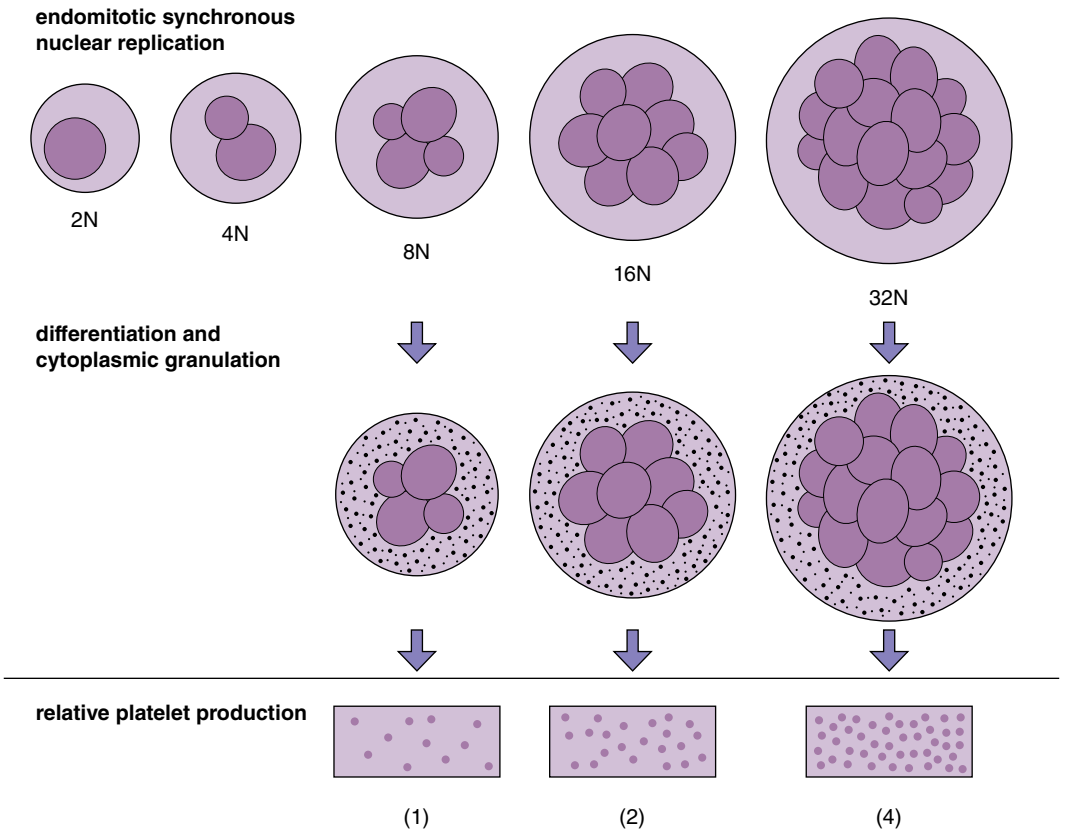

Fig. 26.13. Megakaryocyte development and platelet production. Each nuclear unit has two sets of chromosomes. N, number of sets of chromosomes or "ploidy."

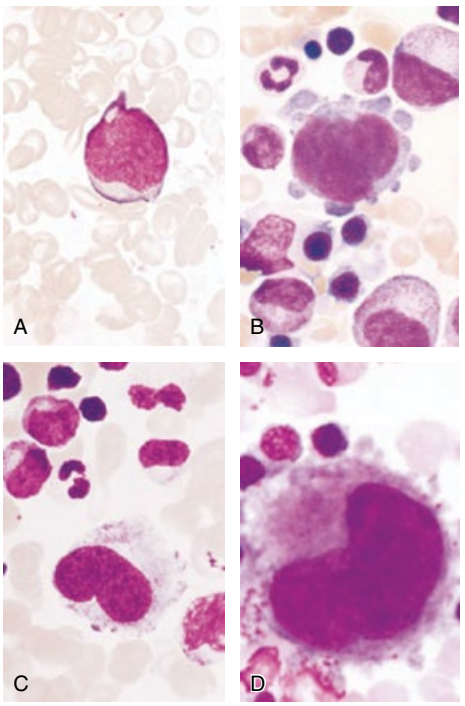

Fig. 26.14. Megakaryocyte development. **A, B,** Megakaryoblasts with nucleoli. **C,** Early bilobed megakaryocyte with no obvious cytoplasmic granulation. **D,** Larger megakaryocyte with obvious early granulation of cytoplasm.

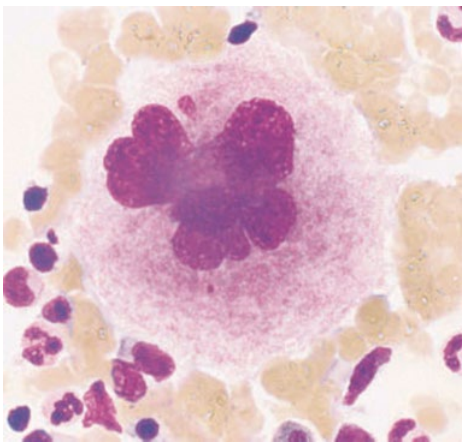

Fig. 26.15. Megakaryocyte. Mature megakaryocyte with many nuclear lobes and pronounced granulation of its cytoplasm.

equivalent of 4, 8, 16, or 32 sets of chromosomes. At a variable stage of development, usually at the 4N, 8N, or 16N stage, further nuclear replication and cell growth cease (Fig. 26.14 and Fig. 26.15), the cytoplasm becomes granular, and platelets are produced. Platelets appear as granular basophilic forms with a diameter of 1–3 µm (Fig. 26.16 and Fig. 26.17). The volume of platelets diminishes as they mature and age in the circulation.

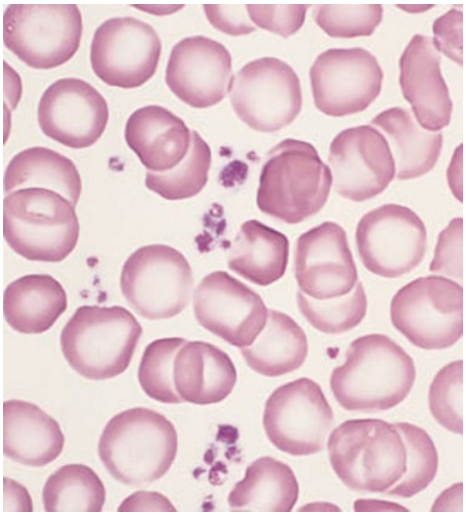

Fig. 26.16. Normal platelets. In this blood film, made from a fingerprick sample, the platelets have agglutinated into small clumps. This is a regular feature of blood films prepared from blood that has not been collected into an anticoagulant.

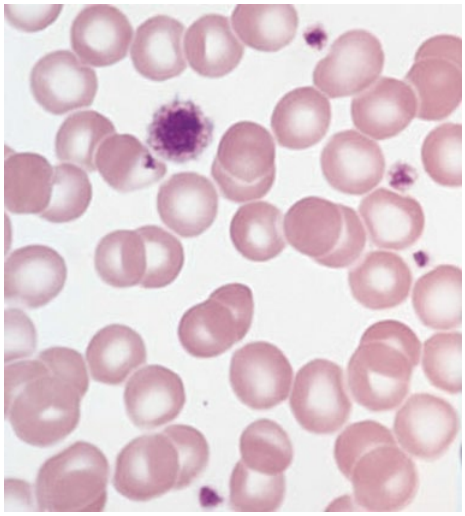

Fig. 26.17. Normal platelets. These platelets show more variation in size than those in Fig. 26.16, the largest measuring approximately 6 μm in diameter. Platelets of this size are seen only rarely in normal blood films.

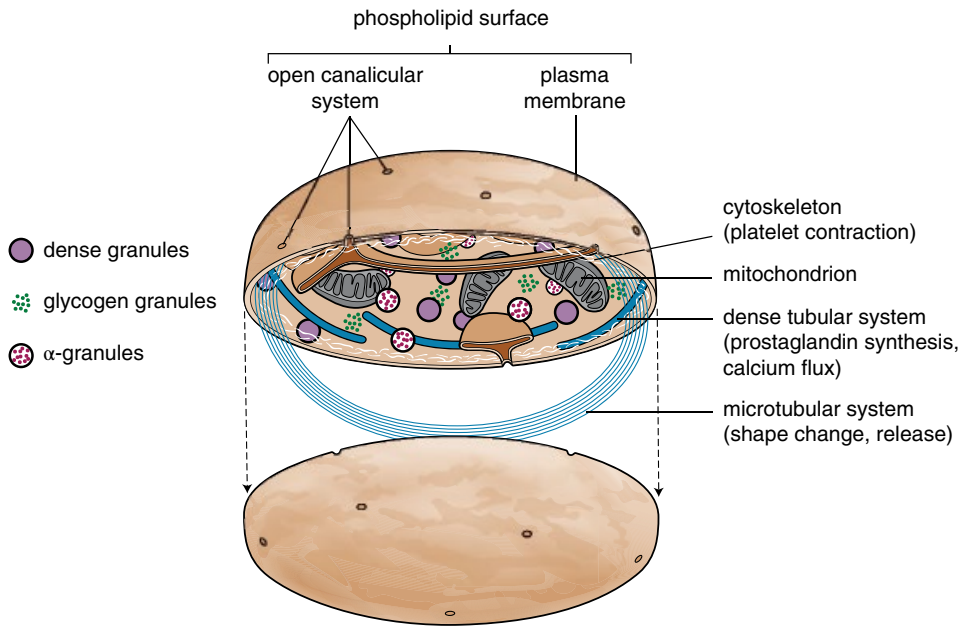

Fig. 26.18. Ultrastructure of a platelet. Electron-dense granules contain adenine nucleotides, calcium, and serotonin; α-granules contain growth factors, for example, PDGF, fibrinogen, factors V, VIII, and von Willebrand factor, fibronectin, β-thromboglobulin (TGF-β), plasminogen, thrombospondin, vascular endothelial growth factor (VEGF) A and C, and chemokines and proteases; lysosomes contain acid hydrolases; the plasma membrane and open canalicular surface provide the negatively charged surface to which activated clotting factors bind.

PLATELET AND VON WILLEBRAND FACTOR FUNCTION

The platelet has a trilamellar surface membrane that invaginates into the cytoplasm to form an open canalicular system, providing a large surface area to which clotting factors adhere (Fig. 26.18). A mucopolysaccharide coat outside the membrane is important in platelet adhesion to the vessel wall and in aggregation and adsorption of clotting factors, especially fibrinogen and FVIII. Glycoproteins (GPs) on the platelet surface include GP Ib-IX-V (defective in Bernard–Soulier syndrome) and GP IIb-IIIa (defective in Glanzmann thrombasthenia). Both ligands, but particularly GP 1b-IX-V, are important in the attachment of platelets to VWF and hence to endothelium. The binding site for GP IIb-IIIa is also the receptor for fibrinogen and, after conformational change, leads to platelet–platelet aggregation.

A submembranous microtubular system maintains the platelet shape. Microfilaments distributed throughout the cytoplasm (including a complex mixture of muscle proteins) are involved in changes in platelet contraction and secretion, and clot retraction.

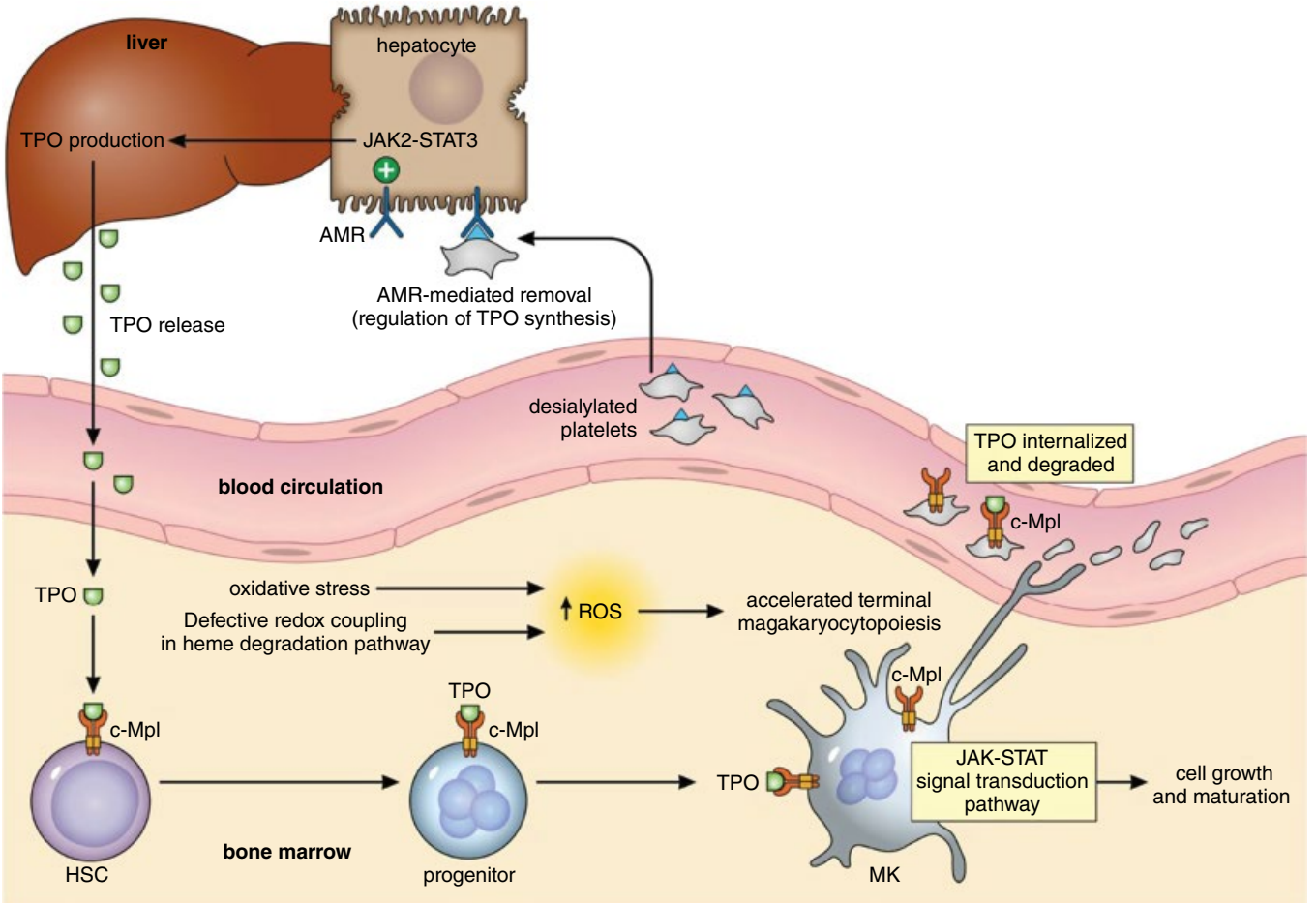

Fig. 26.19. As platelets age they lose sialic acid and bind to Ashwell–Morrell receptors (AMR) in the liver and regulators of platelet production. Aging is accompanied by a change in the ratio of BCL-xl and BAK which mediates apoptosis. MK; megakaryocyte; ROS, reactive oxygen species; TPO, thrombopoietin. (Source: Zhang B, Zehnder JL. *Blood* 2016;128:613–614. https://doi.org/10.1182/blood-2016-06-718544. Reproduced with permission of *Blood: Journal of American Society of Hematology*.)

Platelets have within their cytoplasm three categories of secretory granules all derived from multivesicular bodies. Each platelet has 50–80 α-granules containing a variety of pro- and anticoagulant factors alongside other hemostatic proteins. Dense bodies (δ-granules) number about 10 per platelet and contain calcium, adenine nucleotides, and serotonin. Finally, lysosomes, of which there are about three per platelet, contain acid hydrolases and are ubiquitous, unlike the first two granule types which are platelet-specific. The other key structures in the platelet cytoplasm are mitochondria and a dense tubular system that contains substantial quantities of calcium and can be a site of synthesis of prostaglandins and thromboxane A2.

Platelets are produced by budding of pseudopodial extensions from megakaryocytes (MKs) in the bone marrow, which are themselves derived from hematopoietic stem cells via myeloid and then megakaryocyte–erythroid progenitors. The key feature of MKs that sets them apart from other progenitors is that they undergo endomitosis such that DNA replication occurs without nuclear division. This results in MKs exhibiting polyploidy with many multiples of the normal complement of 46 chromosomes within a single nucleus, although it is now recognized that a proportion of MKs have two separate nuclei. The growth factors that turn stem cells into MKs include thrombopoietin (TPO), IL6, and TGFβ. The transcription factors involved are GATA1, GATA2, NFE2, TAL1/SCL, and FLI1. The most important growth factor is TPO, a hepatic growth factor that binds to the MPL receptor on MK precursors. Recombinant thrombopoietin is now an important drug for treating thrombocytopenia.

The lifespan of the platelet is determined by the relative activity of pro- and antiapoptotic BCL-2 proteins, principally by the ratio of BAK (proapoptotic) and the prosurvival protein BCL-xl. In young platelets, BAK is held in check by BCL-xl, but as the platelet ages in the circulation, there is loss of the less stable Bcl-xl protein and BAK initiates cell death by apoptosis (Fig. 26.19).

The platelet attaches to subendothelial structures of damaged vessels, initially via attachment to VWF (Fig. 26.20), which has binding sites for collagen microfibrils in the exposed subendothelium. The GP Ia-IIa complex attaches to collagen. VWF provides the bridge that anchors activated platelets, with the coagulation cascade developing on their membranes, to the site of vessel wall injury. The VWF monomer contains binding sites for platelet glycoproteins, endothelial structures such as collagen, and coagulation factors such as fibrinogen and FVIII (Fig. 26.21). Monomers are joined via disulfide bonds to form high-molecular-weight multimers that allows binding of multiple ligands simultaneously. At rest the multimers are coiled with binding sites largely hidden. Under high shear stress applied by blood flowing at the rates seen in arteries, the multimers unravel exposing the binding sites and capturing activated platelets as they flow past.

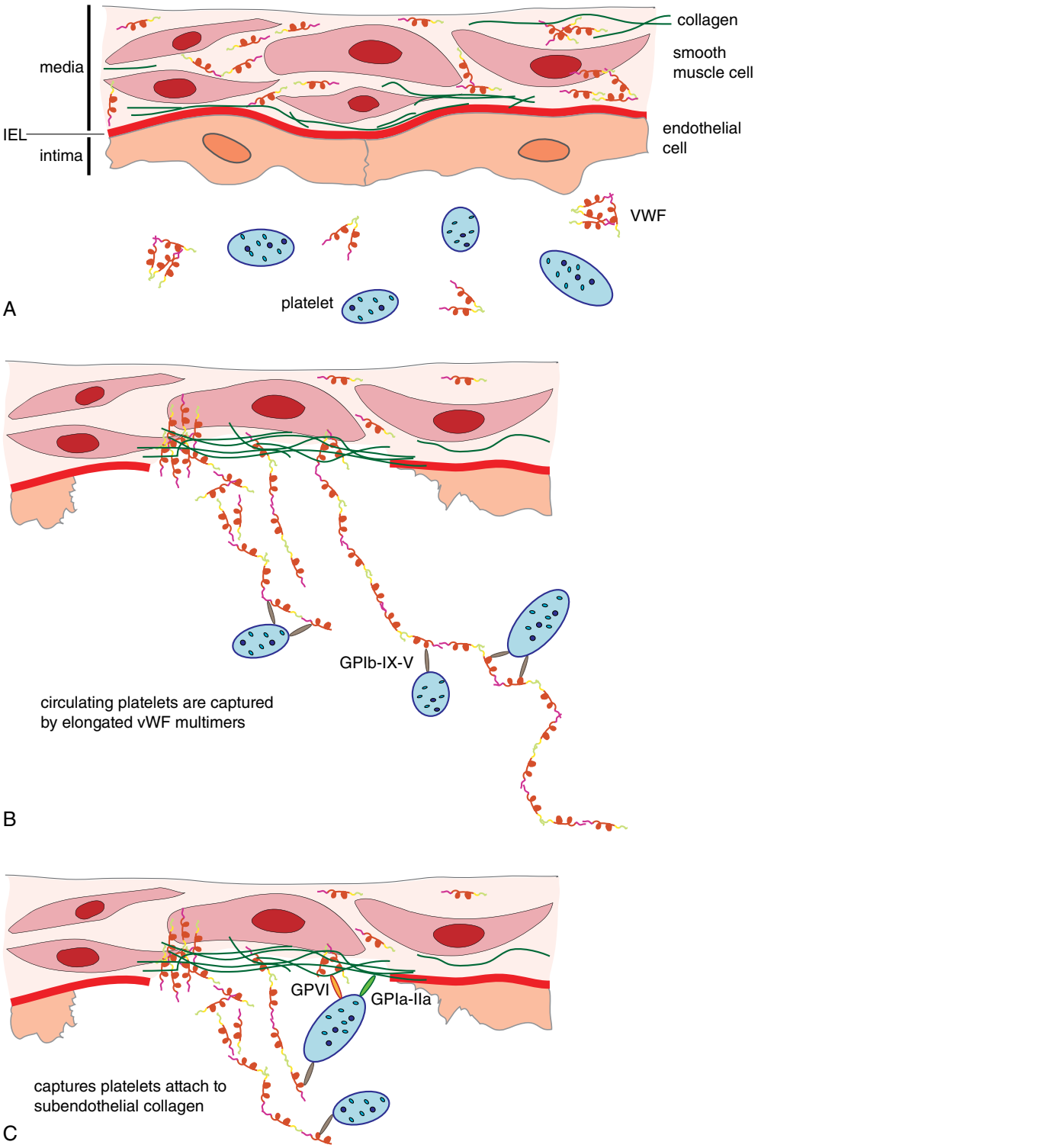

Fig. 26.20. The interaction of platelets with the endothelium via von Willebrand factor (VWF). **A,** The resting condition with the internal elastic lamina (IEL) separating the endothelial layer from subendothelial structures. Platelets are in their resting spherical state and relatively low-molecular weight VWF multimers are in the plasma as the highest molecular weight forms are in the vessel wall. **B,** Disruption of the endothelial layer unravels the high molecular weight VWF exposing the binding sites for collagen and platelets. The key platelet receptor for VWF is GPIb-IX-V. **C,** Platelets captured by VWF become further anchored to the subendothelium via their own collagen receptors, GPVI and GPIa-IIa. **D,** Activated platelets are more discoid in shape and release the contents of their granules providing high concentrations of clotting factors at the site of vessel injury. They aggregate together via GPIIb-IIIa which also binds fibrin clot.

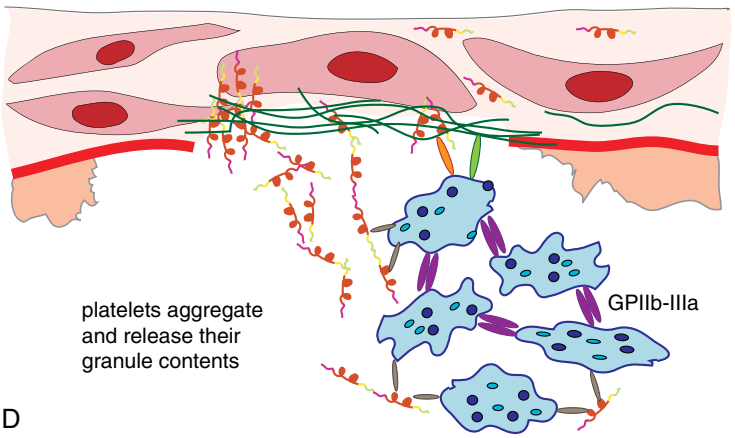

D

Fig. 26.20. (*Continued*)

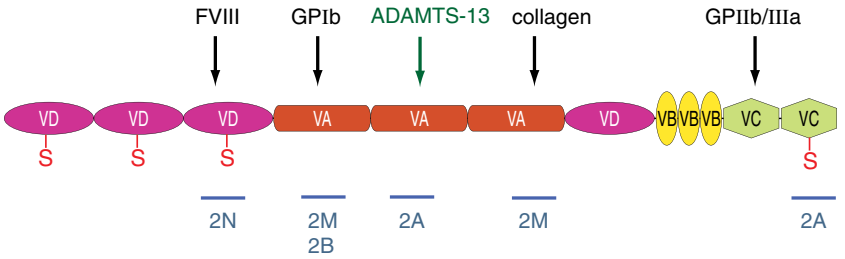

Fig. 26.21. Von Willebrand factor monomer showing sequence of A, B, C, and D domains. The binding sites for key ligands is shown with FVIII binding in the D domains, platelets binding via surface glycoprotein receptors (GPIb) in the A1 domain and C domains and subendothelial collagen binding in the A3 domain. Multimerization is through disulfide bond formation between cysteine residues shown by -S (red). Breakdown of high-molecular-weight multimers is through cleavage by the metalloproteinase ADAMTS-13 which cleaves the scissile bond Tyr1605-Met1606 in the A2 domain. The location of variants associated with different types of type 2 von Willebrand disease is shown by blue bars.

CHAPTER

VASCULAR AND PLATELET BLEEDING DISORDERS

27

Disorders of platelets and small blood vessels manifest as purpuras with pronounced cutaneous and mucosal bleeding, either petechial or multiple small ecchymoses. Prolonged bleeding from superficial cuts and abrasions is a feature of thrombocytopenia and disorders of platelet function. Gastrointestinal bleeding may occur. Menorrhagia is often the dominant clinical problem of women with severe thrombocytopenia or von Willebrand disease. Deep hematomas and hemarthroses are rare. Repeated hemarthroses, deep dissecting hematomas, and serious delayed excessive post-traumatic bleeding are characteristic of severe deficiencies of blood coagulation factors (see Chapter 28). Initial hemostasis, in these cases, can be accomplished by vascular reaction and platelet plugs.

VASCULAR BLEEDING DISORDERS

Disorders associated with vascular bleeding with molecular pathology are listed in Table 27.1. The genetic basis of some of these disorders has now been uncovered. This greatly facilitates diagnosis, prediction of heterogeneous phenotypes, and paves the way for molecular therapy.

HEREDITARY HEMORRHAGIC TELANGIECTASIA (OSLER–WEBER–RENDU SYNDROME)

The small vascular malformations that are the essential lesion in hereditary hemorrhagic telangiectasia can be confused with petechiae. These bright red or purple spots are permanent and most noticeable on the face, nose, lips, and tongue, and on plantar and palmar surfaces (Figs. 27.1 and 27.2). Usually the lesions do not appear until adulthood, becoming more numerous with advancing age. Bleeding from the telangiectasia of the gastrointestinal mucosa produces a state of chronic severe iron deficiency.

Hepatic and splenic arteriovenous shunts, as well as intracranial, aortic, and splenic aneurysms, may develop; pulmonary arteriovenous fistulas (Fig. 27.3) are associated with oxygen desaturation, hemoptysis, and paradoxical emboli to the brain. This form of the disease is caused by an abnormality of the endothelial protein endoglin, the gene being on chromosome 9. Other faults include defects of the gene on chromosome 12q12 coding for the activin receptor-like kinase, a receptor for transforming growth factor β (TGF-β) ligands.

EHLERS–DANLOS SYNDROME

In Ehlers–Danlos syndrome the purpura arises from defective interaction between platelets and the endothelium because of an inherited abnormality of collagen. In some patients there is also evidence of abnormal platelet aggregation. There are several forms of Ehlers–Danlos syndrome (Fig. 27.4) and the clinical manifestations depend on which type of collagen is affected. The main characteristics are joint hypermobility, hyperextensible skin, and fragility of the connective tissues. Abnormalities of several collagen-encoding genes have now been uncovered.

SENILE PURPURA

Relative indolent purpuric ecchymoses are found frequently in the elderly, particularly on areas of skin exposed to sunlight; for example, on the backs of the hands and wrists (Fig. 27.5), the extensor surfaces of the forearms, and the back of the neck. This condition can be caused by atrophy of dermal collagen and loss of subcutaneous fat, weakening the supporting tissue of the small blood vessels of the skin, which then become more susceptible to shear strain.

SCURVY

Petechiae of perifollicular distribution (Fig. 27.6) are a feature of scurvy, probably because of a defect in the microvascular supporting tissue. Disordered platelet function may also be present.

PURPURA ASSOCIATED WITH PROTEIN DEPOSITION

Petechiae and ecchymoses are seen in patients with multiple myeloma, Waldenström macroglobulinemia, benign monoclonal gammopathy, cryoglobulinemia, and cryofibrinogenemia. Many of the proteins involved in these conditions interfere with platelet function and fibrin formation.

Small vessel hemorrhages also result from hyperviscosity of blood or from damage to the vessel on precipitation of these proteins in the cooler parts of the skin. Similarly, patients with amyloidosis show purpura caused by deposition of amyloid in the microcirculation or coagulation factor deficiency because of adsorption of clotting factors on to abnormal fibrils (Fig. 27.7). Some forms of amyloidosis have a genetic basis.

Color Atlas of Clinical Hematology: Molecular and Cellular Basis of Disease, Fifth Edition. A. Victor Hoffbrand, Paresh Vyas, Elías Campo, Torsten Haferlach, and Keith Gomez

TABLE 27.1. ABNORMAL VASCULAR BLEEDING: ASSOCIATED DISORDERS

Hereditary	Gene	Mode of inheritance	Clinical features in addition to bleeding
Hereditary hemorragic telangiectasia	*ENG*	AD	Telangiectasia Arteriovenous malformations
Ehlers–Danlos syndrome	*COL5A2, COL5A1, COL1A1*	AD	Joint hypermobility and dislocations Poor wound healing Vascular malformations
Marfan syndrome	*FBN1*	AD	Tall with long limbs and digits Skeletal deformity Ocular abnormalities Heart valve abnormalities
Ostegoenesis imperfecta	*COL1A1, COL1A2*	AD	Multiple fractures Blue sclerae
Fabry disease	*GLA*	X-linked	Renal failure Cardiac abnormalities Stroke Peripheral neuropathy
Immune-mediated vessel abnormalities	**Pathophysiology**		**Clinical features in addition to bleeding**
Henoch–Schönlein purpura	IgA immune complex deposition		Nephritis Arthritis
Systemic lupus erythematosus	Antibody-mediated multisystem inflammation Genetic factors (e.g. HLA type) Environmental factors (e.g. UV exposure)		Arthritis Rash Lymphadenopathy Neuropsychiatric Nephritis Cardiovascular
Miscellaneous	**Molecular basis**		**Clinical features in addition to bleeding**
Senile purpura	Degeneration of vascular connective tissue		None
Cushing syndrome Corticosteroid therapy	Atrophy of vascular collagen fibres		Hypertension Obesity Psychologic Myopathy Hirsutism
Amyloidosis	Deposition of misfolded proteins (amyloid fibrils) Genetic (e.g. *TTR, FGA, APOA1, GSN*)		Nephrotic syndrome Cardiopathy Neuropathy Hepatomegaly
Scurvy	Vitamin C deficiency impairs post-translational modifications in collagen		Fatigue Bone pain Myalgia Gum disease
Drugs	Platelet dysfunction (e.g. antidepressants, anticonvulsants) Thrombocytopenia (e.g. heparin)		

IMMUNE-MEDIATED VESSEL WALL PURPURAS

The skin lesions in these disorders are more variable. Petechiae and ecchymoses associated with the Henoch–Schönlein syndrome are accompanied by itching, tingling sensations, erythema, and urticarial swelling. The lesions occur most commonly on the buttocks and legs (Fig. 27.8). In this syndrome there is associated submucosal hemorrhage in the intestine (Fig. 27.9), hematuria, and joint pain.

Some allergic drug reactions manifest as erythematous and purpuric skin eruptions (Fig. 27.10). The lesions can be generalized or have a symmetric proximal distribution. Extensive purpuric bleeding can also accompany severe vasculitis, as in systemic lupus erythematosus (SLE; Figs. 27.11 and 27.12) and other connective tissue disorders.

PLATELET BLEEDING DISORDERS

A common cause of abnormal bleeding is a platelet disorder caused by either reduced numbers of platelets (thrombocytopenia) or defective platelet function. Our understanding of platelet dysfunctions is increasing rapidly through discovery of new genetic causes and underlying biochemical mechanisms. Characteristic features are spontaneous skin purpura (Fig. 27.13), mucosal hemorrhage, and prolonged bleeding after trauma (Fig. 27.14).

THROMBOCYTOPENIA

Failure to produce platelets and increased peripheral destruction are the main causes of thrombocytopenia. Drug toxicity

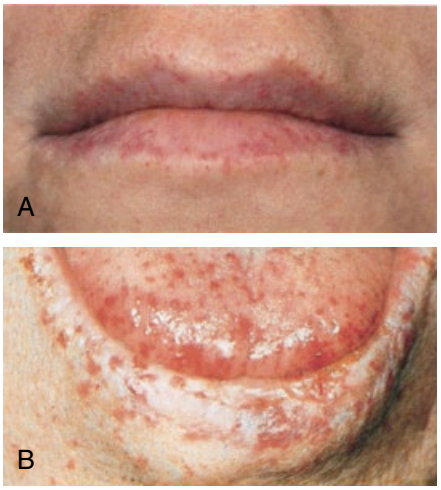

Fig. 27.1. Hereditary hemorrhagic telangiectasia. The characteristic small vascular lesions are obvious on **(A)** lips and **(B)** tongue.

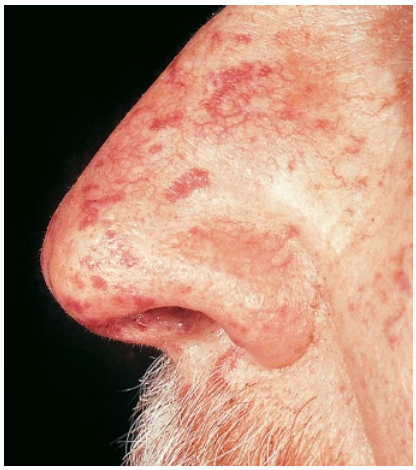

Fig. 27.2. Hereditary hemorrhagic telangiectasia. Characteristic vascular malformations in the skin of the nose.

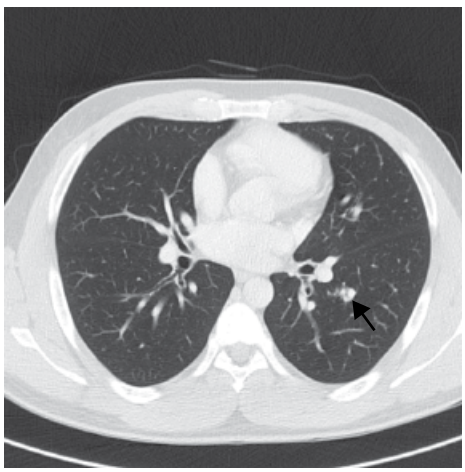

Fig. 27.3. Hereditary hemorrhagic telangiectasia. Arteriovenous fistula in the lung (arrow).

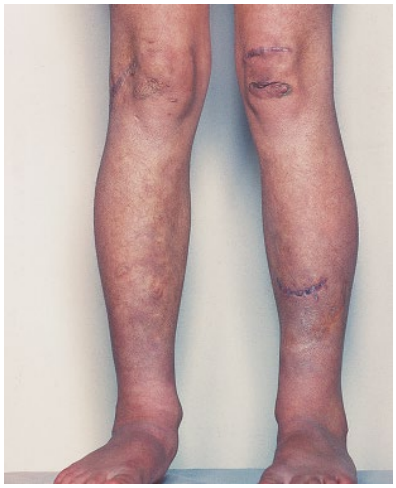

Fig. 27.4. Ehlers–Danlos syndrome. Purpura into scars of the skin, especially around the knees, of a 16-year-old boy who also displayed hyperextensible joints, thin, easily torn skin, and poor healing. The scars are raised into folds by the underlying bulging subcutaneous tissues. (Courtesy of Dr. I Sarkany.)

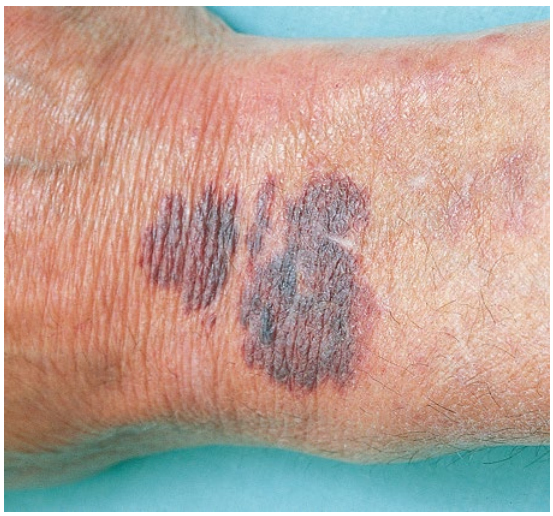

Fig. 27.5. Senile purpura. Typical ecchymoses on the extensor surface of the wrist of an elderly man.

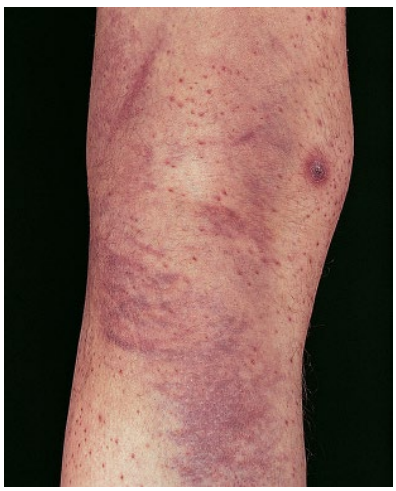

Fig. 27.6. Scurvy. Widespread petechial perifollicular hemorrhages becoming confluent. Deeper hematomas were also present.

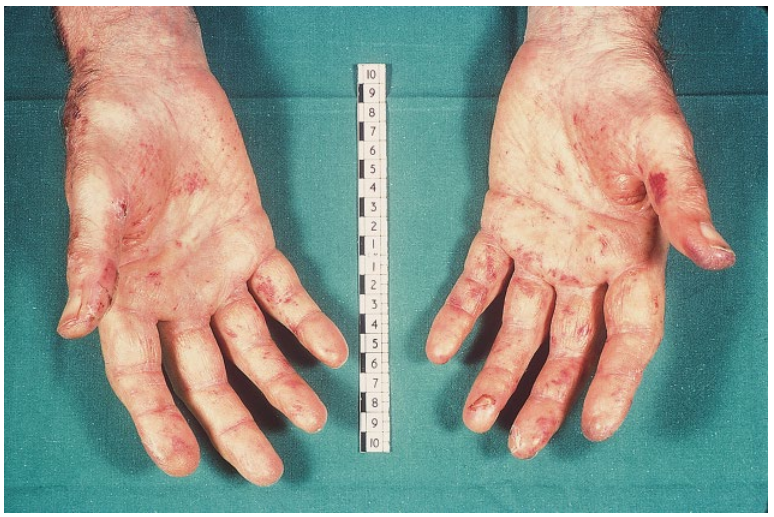

Fig. 27.7. Amyloidosis. Purpura of the skin with characteristic smooth yellowish deposits secondary to multiple myeloma.

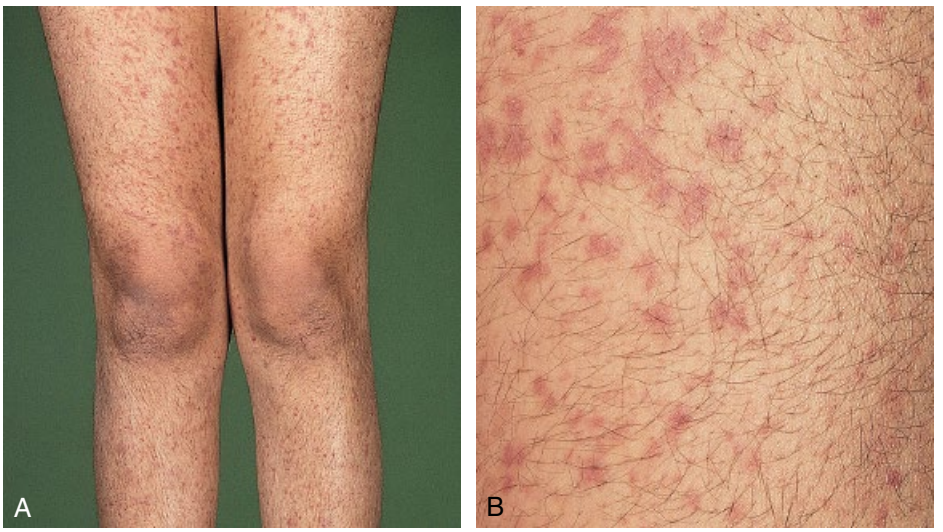

Fig. 27.8. A, Extensive purpura of the skin of the legs in a patient with Henoch–Schönlein syndrome. **B,** The early lesions are more an urticarial erythema than true petechial hemorrhage.

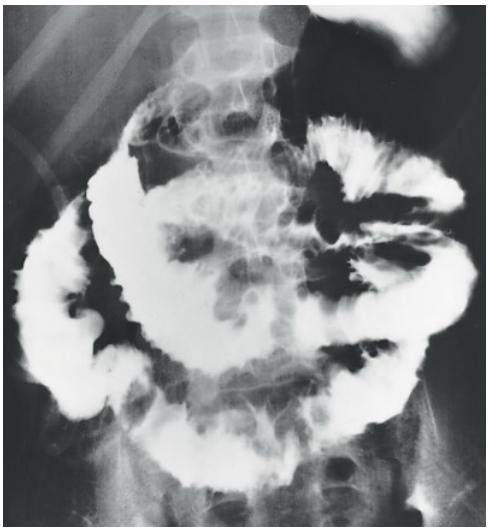

Fig. 27.9. Radiograph of patient with Henoch–Schönlein syndrome with mucosal bleeding in the small intestine, indicated by the characteristic "thumbprint" appearance of the barium pattern.

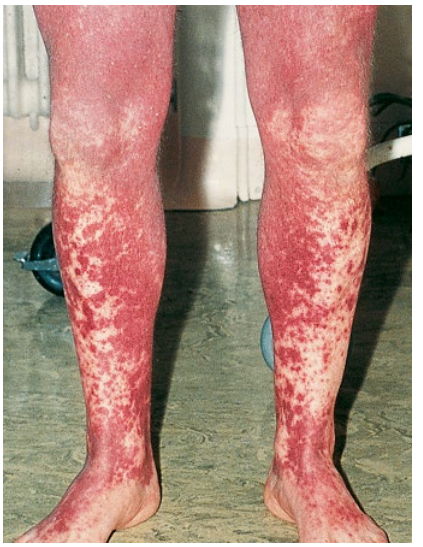

Fig. 27.10. Symmetric widespread erythematous and purpuric eruption as a hypersensitivity reaction to allopurinol.

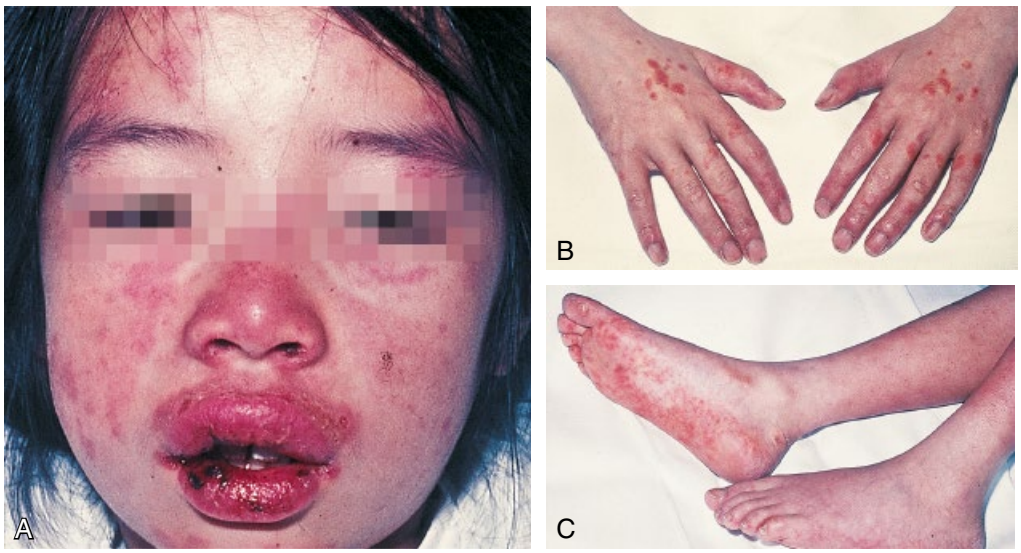

Fig. 27.11. Systemic lupus erythematosus. **A,** Typical fixed erythematous reaction over the "butterfly" area of the face, and mucosal hemorrhage from the petechial lesions of the nasal and oral mucous membranes. **B, C,** Skin of the hands and feet of the same patient shows erythematous and purpuric lesions. (*A, B,* Courtesy of Dr. MD Holdaway.)

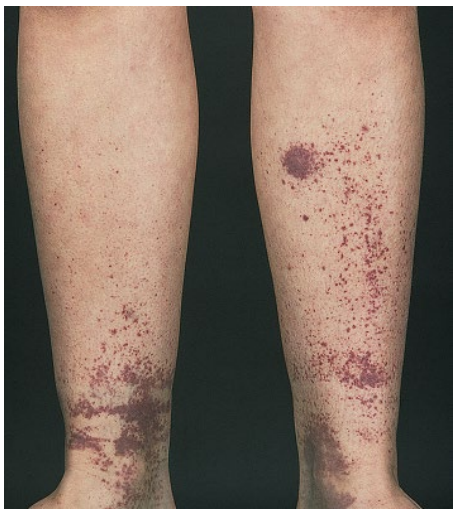

Fig. 27.12. Systemic lupus erythematosus. Purpuric lesions over the shins of a 17-year-old girl (platelet count normal).

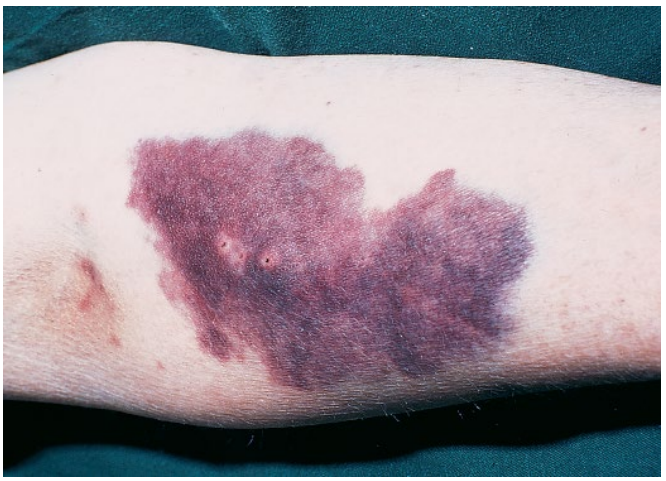

Fig. 27.14. Thrombocytopenia. Large ecchymosis following performance of the Ivy bleeding-time test. The puncture marks of the stylet cutter are clearly seen.

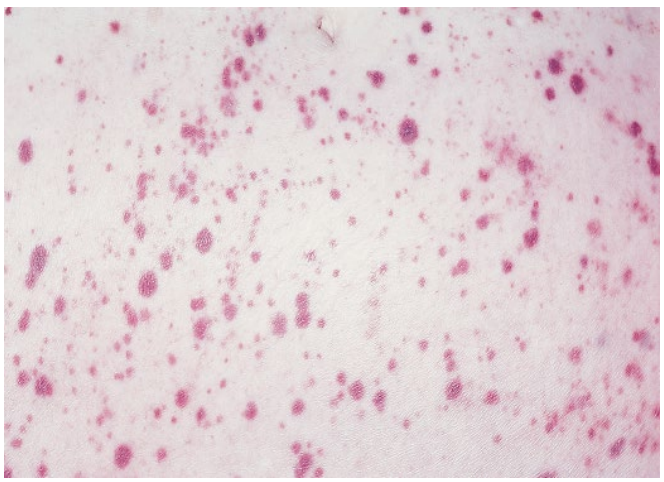

Fig. 27.13. Thrombocytopenia. Abdominal skin purpura in myelodysplastic syndrome. The platelets are often functionally abnormal, as well as reduced in number.

or viral infections result in selective megakaryocyte depression, whereas in aplastic anemia, leukemia, myelofibrosis, cytotoxic chemotherapy, or marrow infiltrations, decreased numbers of megakaryocytes can be part of a generalized bone marrow failure (Figs. 27.15 and 27.16). Congenital deficiency of megakaryocytes can occur, in many cases with associated skeletal, renal, or cardiac malformations – bilateral aplasia of the radii being the most common associated abnormality (Fig. 27.17).

Neonatal thrombocytopenia occurs in newborn infants as a result of intrauterine rubella or other infections, platelet antibodies, disseminated intravascular coagulation (DIC), hereditary thrombocytopenias, giant hemangioma, or congenital absence of megakaryocytes. Among the variety of hereditary thrombocytopenias, in the Wiskott–Aldrich syndrome there is associated immunodeficiency and eczema (Fig. 27.18); in some, such as the Bernard–Soulier syndrome, abnormalities of platelet morphology and function also occur (Fig. 27.30), whereas other syndromes are better known for the associated abnormalities (e.g. May–Hegglin, Chédiak–Higashi; see Chapter 10).

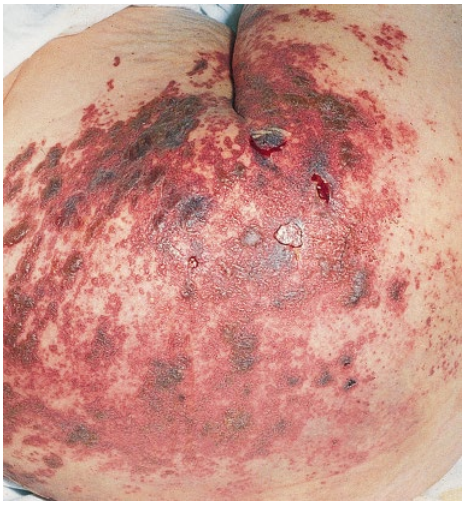

Fig. 27.15. Herpes zoster. Hemorrhagic herpetic skin eruption over the lower back and upper thigh (lateral view) in a patient with acute leukemia.

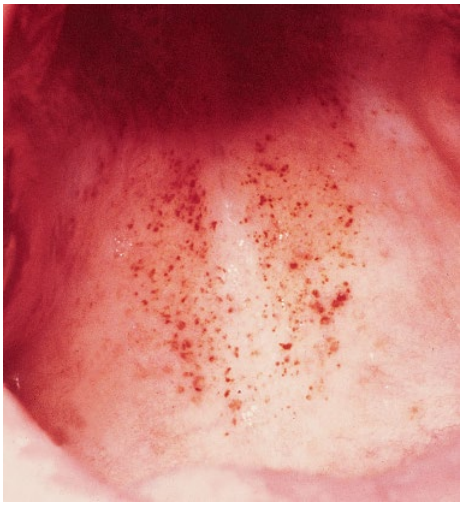

Fig. 27.16. Infectious mononucleosis. Extensive petechiae in the mucosa of the palate.

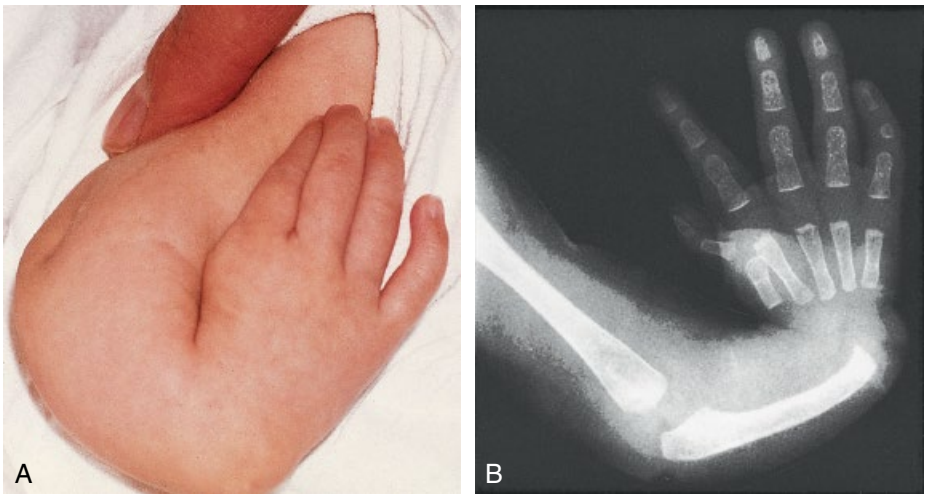

Fig. 27.17. Thrombocytopenia with absent radii syndrome. **A,** The characteristic flexion deformity. **B,** Radiography shows complete absence of the radius.

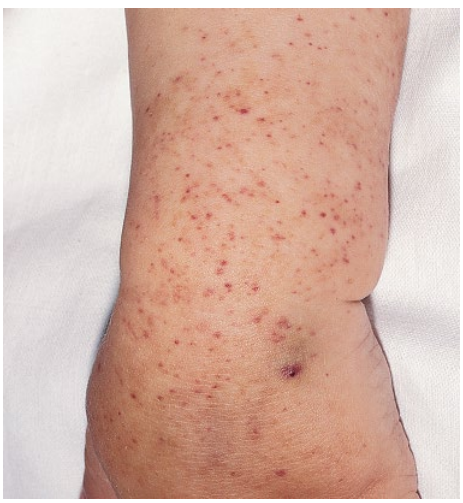

Fig. 27.18. Wiskott–Aldrich syndrome. Eczema and skin purpura in an infant. (Courtesy of Dr. U O'Callaghan.)

Immune Thrombocytopenic Purpura

In immune thrombocytopenic purpura (ITP), a relatively common disorder, platelet sensitization with autoantibodies (usually immunoglobulin G [IgG]) leads to their premature removal from the circulation by cells of the reticuloendothelial system. Megakaryopoiesis can also be impaired; plasma levels of thrombopoietin (TPO) are normal or only slightly increased. Patients have petechial hemorrhage, easy bruising, or menorrhagia. The blood film shows reduced numbers of platelets, which are often large (Fig. 27.19), and the bone marrow has increased numbers of megakaryocytes (Fig. 27.20).

The disease occurs alone (primary) or is accompanied by autoimmune hemolytic anemia (Evans syndrome). ITP can also occur in patients with other diseases, such as SLE (Fig. 27.21), human immunodeficiency virus (HIV) infection, chronic lymphocytic leukemia, and following stem cell transplantation.

Initial treatment is with high-dose corticosteroids. Splenectomy can be performed in patients who do not respond to corticosteroids or who relapse when corticosteroids are withdrawn. Sections of splenic tissue show prominent collections of macrophages

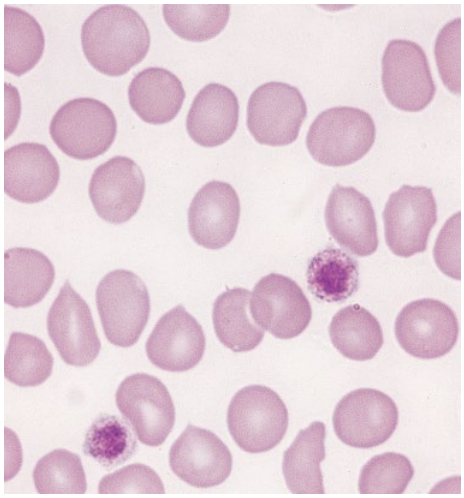

Fig. 27.19. Immune thrombocytopenia. Blood film showing two large platelets.

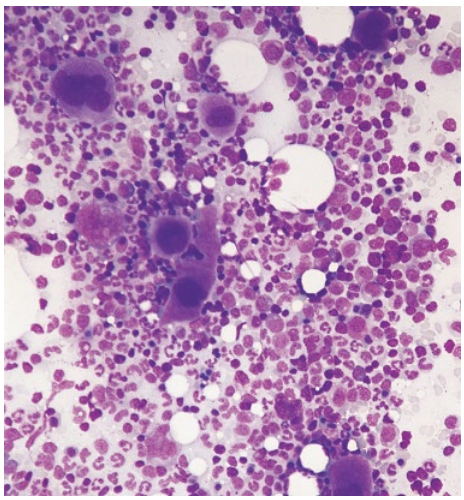

Fig. 27.20. Immune thrombocytopenia. Bone marrow aspirate showing increased numbers of megakaryocytes.

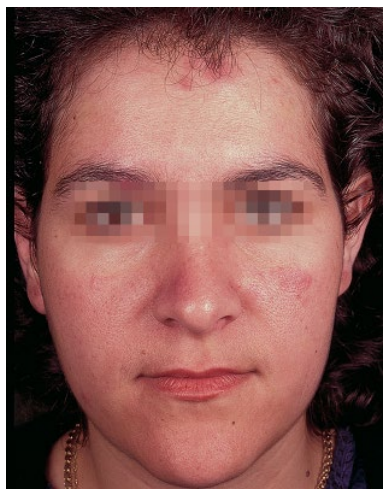

Fig. 27.21. Systemic lupus erythematosus. Typical butterfly rash and frontal alopecia in a woman who also had immune thrombocytopenia.

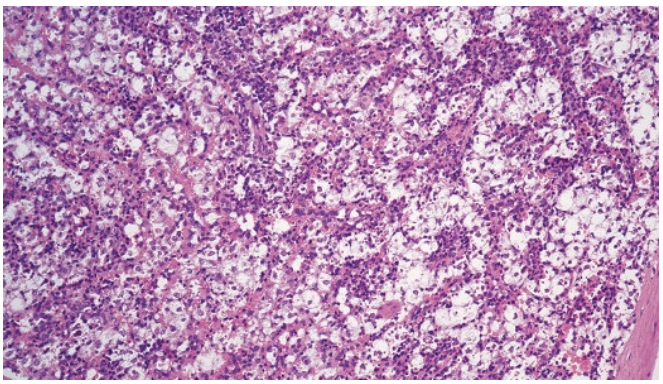

Fig. 27.22. Immune thrombocytopenic purpura. Histologic section of spleen showing prominent collections of lipid-filled macrophages caused by excessive breakdown of platelets in the splenic pulp.

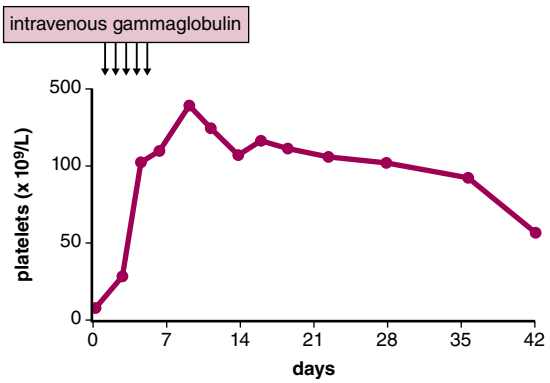

Fig. 27.23. Chronic immune thrombocytopenic purpura. Typical response in platelet count to therapy with intravenous high-dose gammaglobulin (IVG) therapy (5-day course; 0.4 g/kg/day).

with lipid-laden cytoplasm (Fig. 27.22). High-dose intravenous immunoglobulin has produced substantial rises in platelets in about 75% of cases of chronic ITP (Fig. 27.23). This therapy is most useful during the later stages of pregnancy to control acute bleeding episodes or in preparation of the patient for surgery, because the improvement is usually only marked for about 4 weeks. It is often valuable in children and infants. The mechanism of action is either blockage of Fc receptors on macrophages or inhibition of the antiplatelet antibody biosynthesis. Rituximab (anti-CD20), azathiopine, and other immunosuppressive drugs are used in refractory cases.

Thrombopoietin receptor agonists that bind to thrombopoietin receptors and stimulate platelet production are now in clinical trials (Fig. 27.24). These may reduce sensitization with antibody and so peripheral clearance.

Drug-Induced Immune Thrombocytopenia

An allergic mechanism has been demonstrated to be the cause of many drug-induced thrombocytopenias. Rapid removal of platelets from the circulation can result in severe thrombocytopenia, and many patients have mucosal hemorrhage (Fig. 27.25) in addition to skin purpura. Heparin-induced thrombocytopenia (HIT), however, is associated with thrombosis. It is caused by platelet-activating IgG antibodies that recognize complexes of platelet factor 4 and heparin. There are markedly elevated thrombin–antithrombin complexes with in vivo platelet activation of endothelium and monocytes.

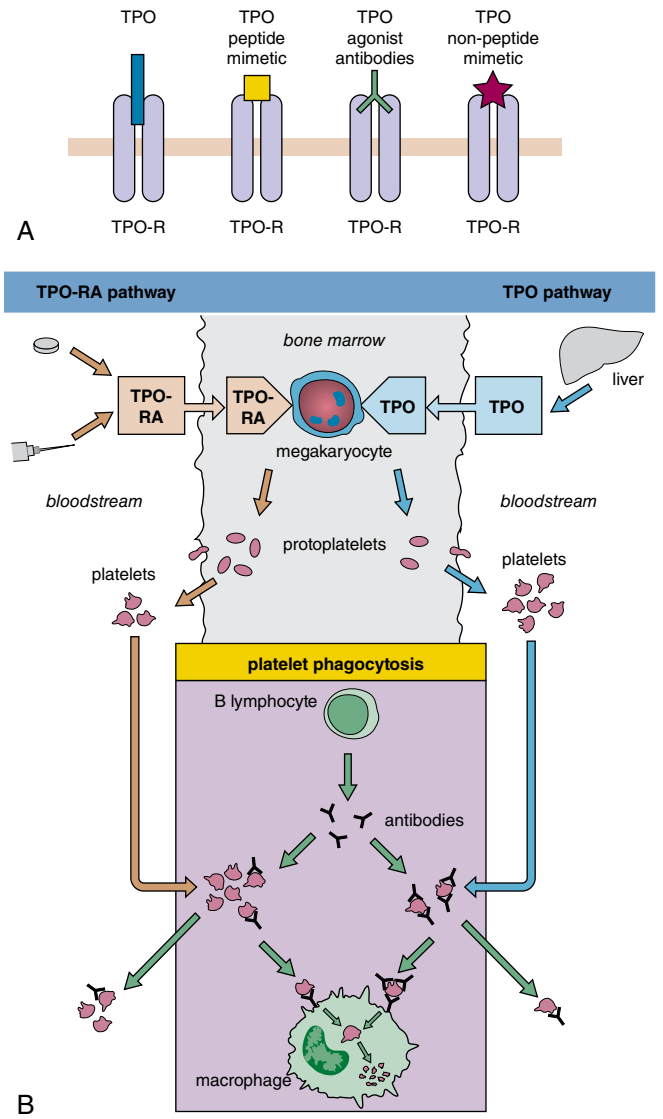

Fig. 27.24. A, Thrombomimetics: Pharmaceuticals that activate the thrombopoietin (TPO) receptor by different mechanisms. **B,** Role of thrombopoietin receptor agonists (RAs) in ITP. Stimulation of megakaryocytes with TPO receptor agonists generates larger numbers of platelets and can overcome antibody destruction of megakaryocytes and reduce peripheral destruction of platelets. (Source: Adapted fromCines DB. *Blood* 2007;109:4591. Reproduced with permission of *Blood: Journal of American Society of Hematology*.)

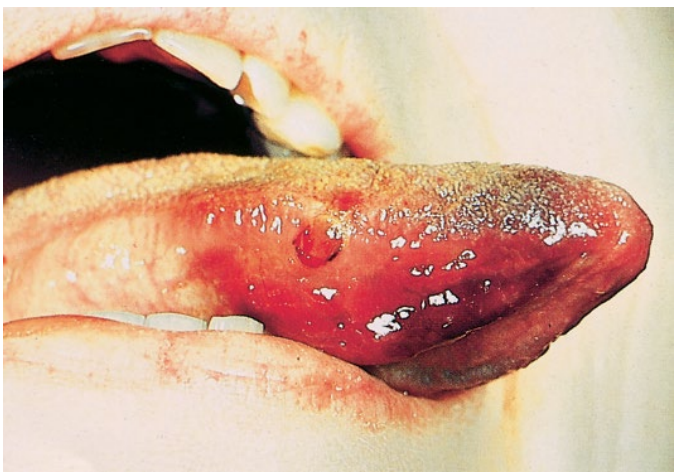

Fig. 27.25. Drug-induced thrombocytopenia. Sublingual mucosal hemorrhage.

Disseminated Intravascular Coagulation, Thrombotic Thrombocytopenic Purpura, and Hemolytic–Uremic Syndrome

In these conditions, thrombocytopenia is the result of increased consumption of platelets. In thrombotic thrombocytopenic purpura (TTP), platelet aggregation and accretion in small blood vessels is widespread (Fig. 27.26), but plasma levels of coagulation factors are normal. The clinical course may be fulminant and fatal, with confluent purpura and ischemic damage to many organs, such as the brain, kidneys, and skin (Figs. 27.27 and 27.28); serum lactate dehydrogenase (LDH) activity is raised, and the majority of patients have an associated microangiopathic hemolytic anemia (see Chapter 8). The acquired form may have no obvious precipitating cause, but some cases follow an infection, occur in pregnancy, or after allogeneic stem cell transplantation, particularly with cyclosporin use. Inhibitory antibodies against ADAMTS-13 (a disintegrin and metalloprotease with thrombospondin type 1 repeats), a protease that cleaves von Willebrand factor (VWF) (Fig. 27.21), occur in the plasma of patients with acute TTP (Fig. 27.29). A familial form of TTP, Upshaw–Schulman syndrome, results from mutations of the *ADAMTS13* gene situated on chromosome 9q34. It is characterized by TTP of neonatal onset with response to fresh plasma infusion. An unusual preponderance of large multimers of VWF occurs in the plasma of

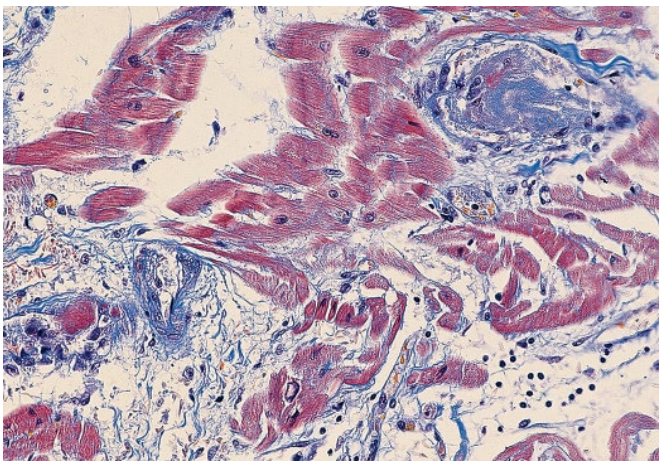

Fig. 27.26. Thrombotic thrombocytopenic purpura. Fibrin thrombus (red) in an arteriole of the heart and microthrombi (purple) of von Willebrand factor aggregate in another vessel. (Martius scarlet blue; Courtesy of Professor S Lucas.)

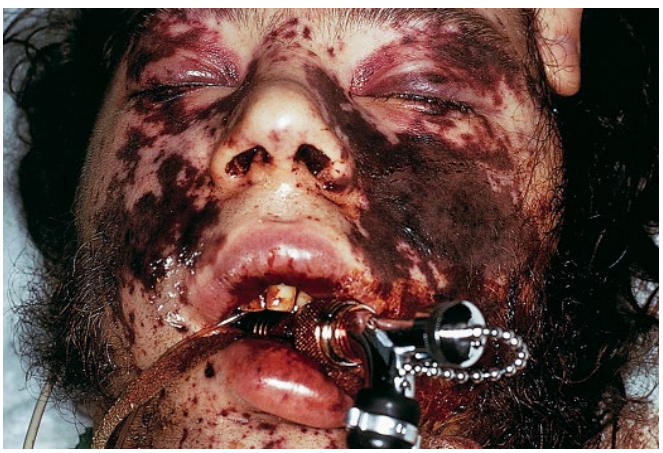

Fig. 27.27. Thrombotic thrombocytopenic purpura. Widespread confluent and necrotic ecchymoses of the facial skin.

patients with TTP and of those with hemolytic–uremic syndrome (HUS). It is likely that the unusual large multimers of VWF cause platelet aggregation in the microcirculation in TTP. Treatment is with plasma exchanges, which remove autoantibodies and multimers of VWF, and provide the necessary ADAMTS-13 protease. Antiplatelet drugs, corticosteroids, vincristine, rituximab, and splenectomy have also been used with varying success.

Although HUS resembles TTP, it occurs mainly in infants and young children and is characterized by acute anemia, thrombocytopenia, and renal failure. Gastrointestinal symptoms include bloody diarrhea and hypotension, and fits may occur. There is an association with infection by verotoxin-producing organisms, especially *Escherichia coli* O157:H57 strain and *Shigella dysenteriae* types 1 and 24. The protease that cleaves VWF is present.

The HELPP syndrome occurs in late pregnancy and consists of hemolysis, elevated liver enzymes, and low platelet count in association with pre-eclampsia; DIC may be present.

DISORDERS OF PLATELET FUNCTION

Many of the conditions associated with abnormal platelet function are listed in Table 24.3. Platelet aggregometry is the key investigation and normal tracings are shown in Fig. 27.30.

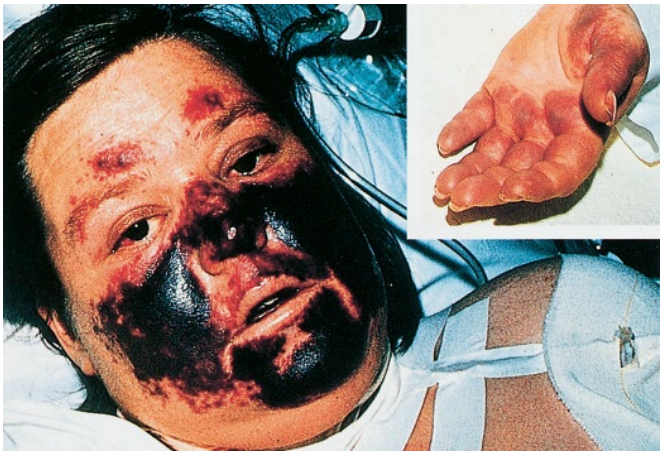

Fig. 27.28. Thrombotic thrombocytopenic purpura. Massive area of hemorrhagic necrosis of the facial skin and extensive confluent ecchymoses on the hand (inset).

Hereditary Disorders

The advent of next generation sequencing has led to the discovery of many genes associated with quantitative (Table 27.2) and qualitative platelet abnormalities. Qualitative abnormalities

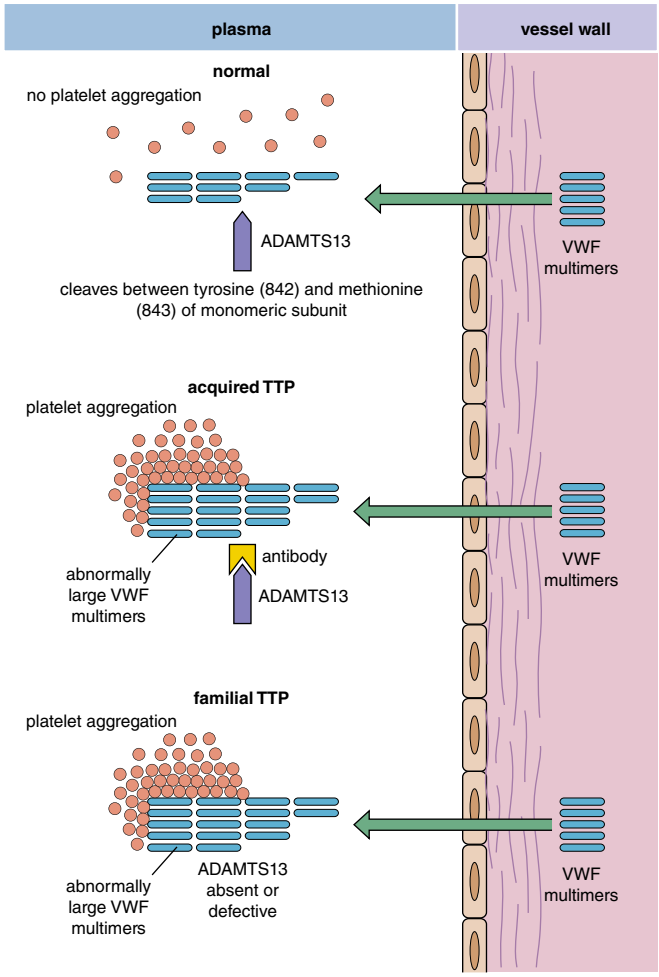

Fig. 27.29. Thrombotic thrombocytopenic purpura. Postulated mechanism of how large von Willebrand factor (VWF) multimers accumulate in plasma because of the lack of protease ADMTS13 as a result of an immune mechanism or a congenital deficiency.

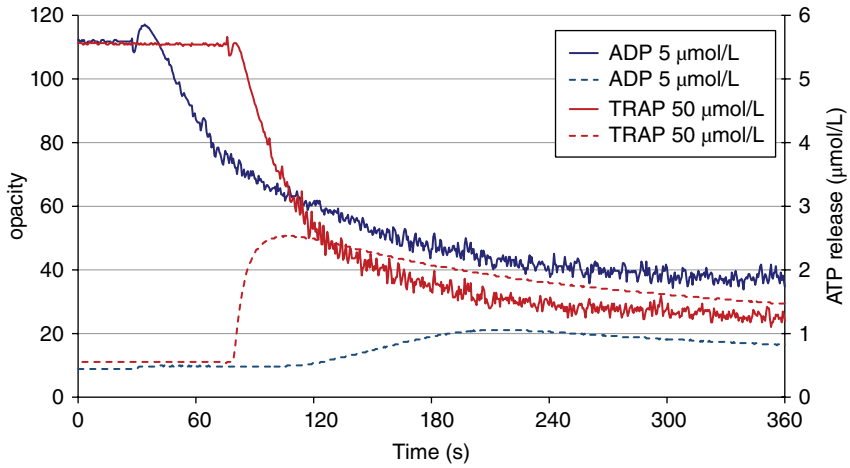

Fig. 27.30. Platelet aggregation in response to two agonists with simultaneous ATP release from granules. The solid line shows aggregation and the dashed line of the same color shows simultaneous ATP release. Note that the ATP released in response to ADP (a weak agonist) is less than that released in response to TRAP (thrombin receptor activating peptide, a strong agonist).

TABLE 27.2. HEREDITABLE CAUSES OF PLATELET DYSFUNCTION AND THROMBOCYTOPENIA

Gene	Disorder	Mode of inheritance	Clinical features in addition to thrombocytopenia
HOXA11, MECOM	Amegakaryocytic thrombocytopenia with radioulnar synostosis	AD	Sensorineural deafness Skeletal abnormalities Panyctopenia
TUBB1, ACTN1	Autosomal dominant macrothrombocytopenia	AD	
MPL	Congenital amegakaryocytic thrombocytopenia (CAMT)	AR	Pancytopenia
THPO	Cyclic thrombocytopenia and thrombocythemia 1	AD	Thrombocythemia
RUNX1	Familial platelet disorder with predisposition to AML	AD	Acute myeloid leukemia
FLNA	Filamin A-related disorders	XR	Mental retardation Cardiac structural anomalies Skeletal abnormalities
RASGRP2	*CalDAG-GEFI* defect	AR	
FERMT3	Leukocyte adhesion deficiency 3	AR	Hepatosplenomegaly Osteopetrosis Leukocytosis and recurrent infections
MYH9	MYH9-related thrombocytopenia (May–Hegglin anomaly, Sebastian, Fechtner, and Epstein syndromes)	AD	Leukocyte inclusions (Döhle body-like) Sensorineural deafness Nephritis Cataracts
FYB	Recessive microthrombocytopenia	AR	
ABCG5; ABCG8	Sitosterolemia with thrombocytopenia	AR	Atherosclerosis Splenomegaly Depressed cholesterol biosynthesis Arthritis Tendinous and tuberous xanthoma
STIM1	Stormorken syndrome	AD (GOF)	Short stature Dysmorphic features Hyposplenism Proximal muscle weakness Learning difficulties
RBM8A	Thrombocytopenia absent radius (TAR) syndrome	AR	Short stature Dysmorphic features Cardiac anomalies Skeletal abnormalities Neurologic abnormalities
DIAPH1	Thrombocytopenia with deafness	AD (GOF)	Sensorineural deafness
ADAMTS13	Thrombotic thrombocytopenic purpura	AR	Neurologic (seizures) Renal impairment Fever Microangiopathic hemolytic anemia
WAS	Wiskott–Aldrich syndrome	XR	Immunodeficiency Inflammatory bowel disease Hemolytic anemia Lymphopenia Abnormal immunoglobulins

A, autosomal; D, dominant; GOF, gain of function; R, recessive; X, X-linked.

can be further subdivided into those that affect platelet structure such as granule content (Table 27.3), surface receptors, or signaling pathways (Table 27.4). For many of these disorders the underlying molecular mechanism remains obscure. Identifying the responsible gene has important prognostic value as many platelet dysfunctions are part of multisystem disorders. These rare inherited disorders are often heterogeneous and can be associated with a wide variety of clinical features. Without knowledge of the underlying genetic abnormality the link between these symptoms and signs and the platelet abnormality may not be recognized. While many of these disorders might present with mild thrombocytopenia and little or no bleeding symptoms, over time there can be more serious manifestations such as leukemic transformation.

Platelet Receptor Defects

In thrombasthenia (Glanzmann disease), primary platelet aggregation fails with all agonists, but platelet count, size, and morphology are normal. There is deficiency of membrane GPIIb-IIIa which is the receptor to which fibrinogen normally attaches during aggregation. In Bernard–Soulier syndrome, the platelets are large (Fig. 27.31) and lack surface GPIb-IX-V which is the main platelet receptor for VWF. Historically, these were generally considered to be autosomal recessive severe bleeding

TABLE 27.3. PLATELET GRANULE DISORDERS

Gene	Disorder	Mode of inheritance	Clinical features in addition to platelet dysfunction
ANKRD26; *CYCS, ETV6, SLFN14*	Autosomal dominant thrombocytopenia	AD	Acute leukemia
GFI1B	Autosomal dominant macrothrombocytopenia with bleeding and platelet dysfunction	AD or AR	Myelofibrosis
VIPAS39; VPS33B	ARC syndrome	AR	Arthrogryposis multiplex congenita Dysmorphic features Cardiac valve abnormalities Cholestasis Nephropathy Developmental delay
LYST	Chediak–Higashi syndrome	AR	Oculocutaneous albinism Hepatosplenomegaly Mental retardation Neuropathy Immunodeficiency
NBEA	Autism and dense granule abnormalities	AD	Autism
NBEAL2	Gray platelet syndrome	AR	Myelofibrosis Splenomegaly
HPS1; *AP3B1*; *HPS3*; *HPS4*; *HPS5*; *HPS6*; *DTNBP1*; *BLOC1S3; AP3D1*	Hermansky–Pudlak syndrome	AR	Oculocutaneous albinism Pulmonary fibrosis Granulomatous colitis Neutropenia
FLI1	Paris–Trousseau thrombocytopenia and Jacobson syndrome	AD (11q deletion) or AR	Skeletal abnormalities Mental retardation
PLAU	Quebec platelet disorder	AD (duplication)	
SRC	Thrombocytopenia with myelofibrosis and bone defects	AD (GOF)	Dysmorphic features Osteopetrosis
GATA1	X-linked macrothrombocytopenia with dyserythropoiesis	XR	Dyserythropoiesis

TABLE 27.4. PLATELET RECEPTOR OR SIGNALING DEFECTS

Gene	Disorder	Mode of inheritance	Clinical features in addition to platelet dysfunction
P2RY12	ADP receptor defect	AR	
GP1BA; *GP1BB*; *GP9*	Bernard–Soulier syndrome	AR or AD	
GP6	Bleeding diathesis due to glycoprotein VI deficiency	AR	
PTGS1; PTGS2	Cyclo-oygenase deficiency	AD	Increased sensitivity to NSAIDs
PLA2G4A	Deficiency of phospholipase A2, group IVA	AR	Gastrointestinal ulceration
ITGA2B; *ITGB3*	Glanzmann thrombasthenia	AR or AD	
GP1BA	Platelet-type von Willebrand disease	AD	Deficiency in von Willebrand factor
ANO6	Scott syndrome	AR	
TBXA2R	Thromboxane A2 receptor defect	AR	

NSAID, nonsteroidal anti-inflammatory drug.

disorders but it is now recognized that milder phenotypes and dominant inheritance patterns can also be seen.

Granule Disorders

Our understanding of the molecular causes of platelet granule deficiency has increased greatly through next generation sequencing projects (Fig. 27.32). In Hermansky–Pudlak syndrome (HPS), the classic features are defective dense granule formation in association with oculocutaneous albinism (Figs. 27.33 and 27.34). In the most severe form of the disease resulting from variants in the *HPS1* or *HPS4* genes, the accumulation of ceroid-like pigment in bone marrow, intestinal, and pulmonary macrophages leads to pulmonary fibrosis and granulomatous colitis (Fig. 27.35). Mutations in at least seven other genes have been described with a generally milder phenotype that may be limited to the classic features only. In the *HPS2* variety, which is associated with neutropenia, there are genetic defects of the protein AP3B1, which encodes the β-subunit of the heterotetrameric AP3 adapter

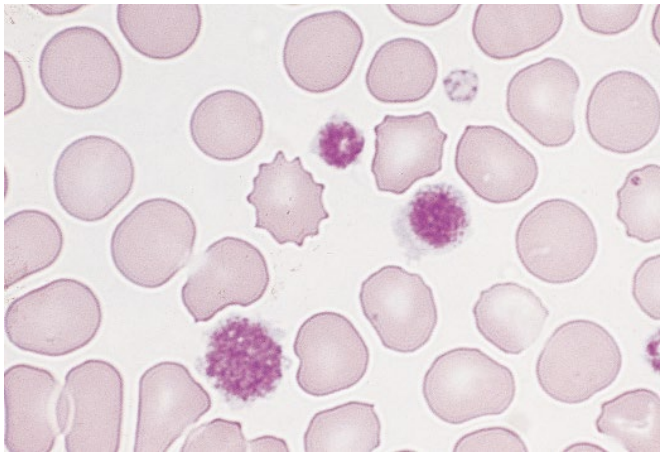

Fig. 27.31. Bernard–Soulier syndrome. Blood film showing abnormally large platelets.

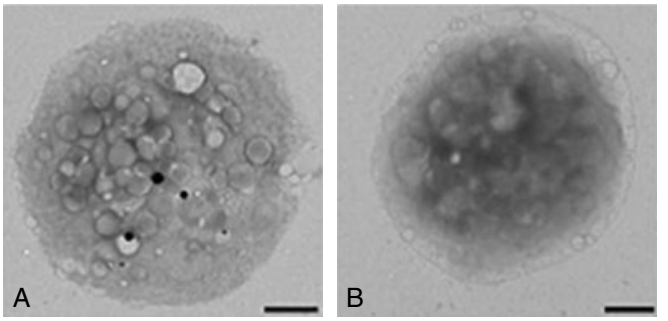

Fig. 27.33. Whole mount electron microscopy of a normal platelet **(A)** and a patient with Hermansky–Pudlak syndrome. Dense granules are labelled and appear as black spots. **B,** Note the absence of black spots in Hermansky–Pudlak syndrome. Scale bars 1μm. (Courtesy of Professor D Cutler, *J Thromb Haemost* 2016;14:839–849.)

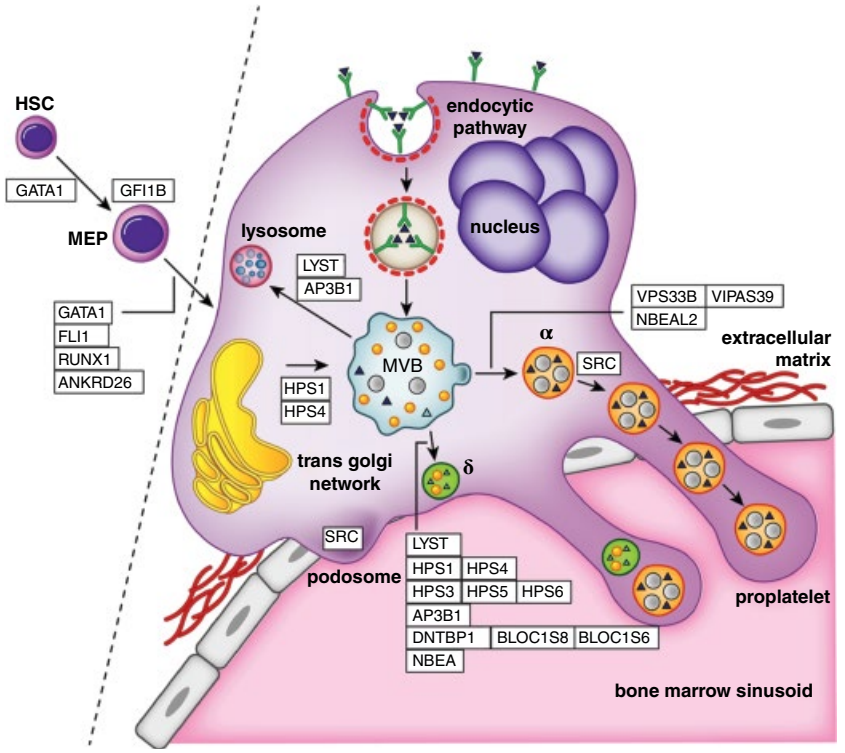

Fig. 27.32. Genetic regulation of granule biogenesis: insights from genomics. The cartoon summarizes the process of granule biogenesis from hematopoietic stem cell (HSC) to megakaryocyte-erythroid precursor (MEP) to megakaryocyte. In the megakaryocyte the dual contribution of the endocytic pathway and the trans Golgi network to the development of the multivesicular body (MVB) is illustrated, and subsequent differentiation into α-, δ-, and lysosomal granules. The point at which specific gene defects impact on granule formation is mapped to their respective molecular pathway (Source: Bariana TK, *et al. Br J Haematol* 2017;176:705–720. Reproduced with permission of John Wiley and Sons.)

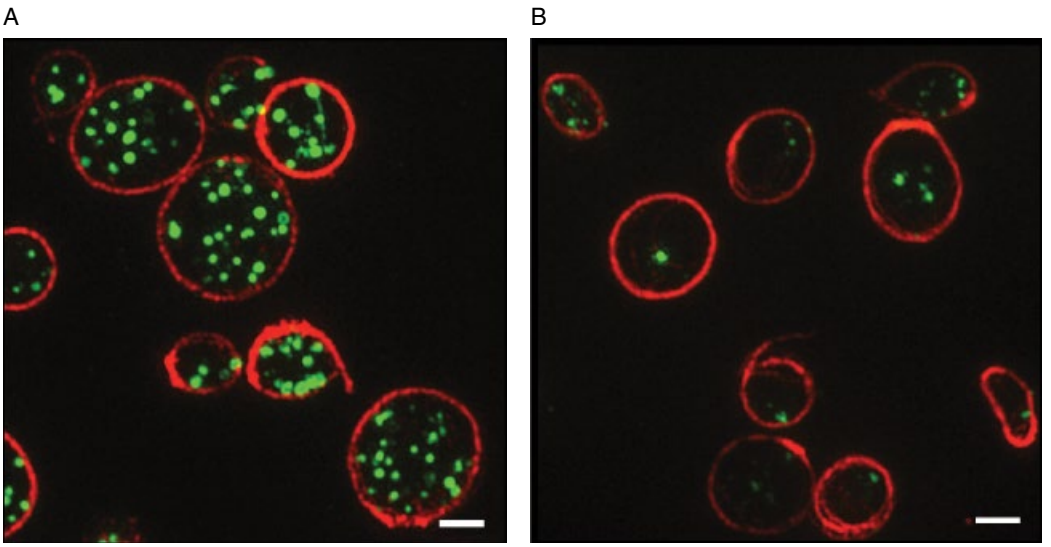

Fig. 27.34. Super resolution structured illumination microscopy of platelets in **(A)** normal and **(B)** Hermansky–Pudlak syndrome. CD63 is a dense granule marker and is labelled here by green fluorescence. Tubulin marks the platelet membrane and is labelled here in red. Note the reduction in CD63 positive structures in Hermansky–Pudlak syndrome. Scale bars 1μm. (Courtesy of Professor Dan Cutler, *J Thromb Haemost* 2016;14:839–849.)

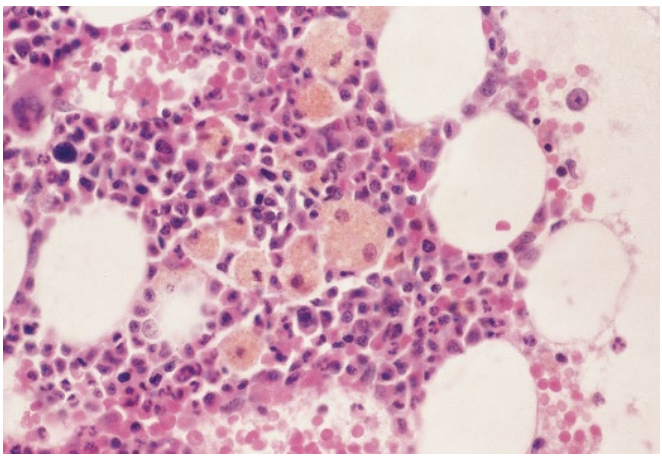

Fig. 27.35. Hermansky–Pudlak syndrome. Bone marrow trephine biopsy showing prominent macrophages with ceroid-like pigment-laden cytoplasm. There is a defective platelet function resulting from a storage pool defect caused by dense body deficiency. (Courtesy of Professor EGD Tuddenham.)

protein complex. AP3 directs post-transitional trafficking of the intraluminal "cargo" proteins from the trans Golgi network to lysosomes. There is defective platelet granule formation and defective platelet aggregation with collagen, ristocetin, and arachidonic acid.

While HPS is a storage pool disorders (SPD) associated with multisystem abnormalities, the majority of SPDs result only in δ-granule deficiency, defective platelet aggregation, and mild bleeding symptoms (Fig. 27.36). In some of the milder cases, platelet aggregation might be normal and the defect is only recognized on direct measurement of platelet nucleotide levels or release from granules (Fig. 27.37). The genetic causes remain largely undiscovered. Although the mode of inheritance appears to be autosomal dominant or recessive in most, most patients are female, as with von Willebrand disease, because these are mucocutaneous bleeding disorders with a predilection for gynecologic and obstetric bleeding. Syndromes with abnormalities in the other main platelet vesicular body (α-granule) have a similar incidence and the best characterized is gray platelet syndrome (Figs. 27.37 and 27.38).

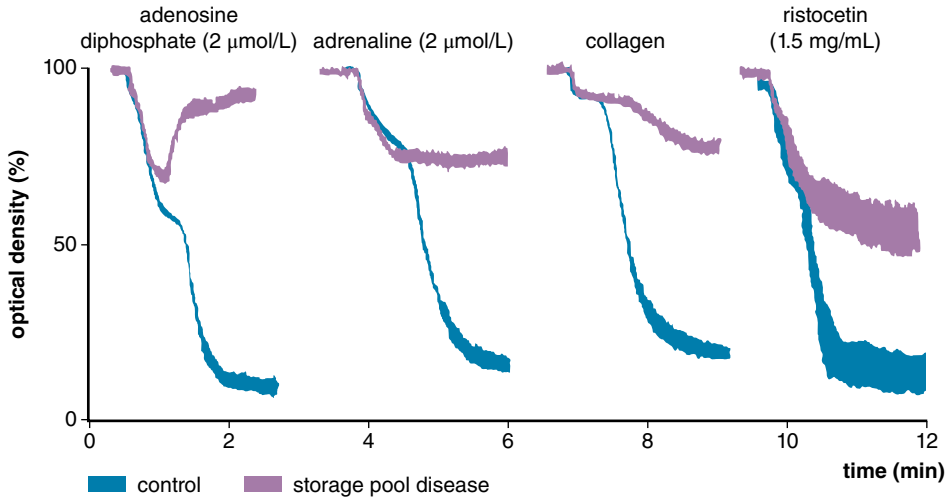

Fig. 27.36. Storage pool disease. Platelet aggregation studies show defective primary and secondary aggregation with adenosine diphosphate, adrenaline, and collagen. (Courtesy of Dr. RA Hutton.)

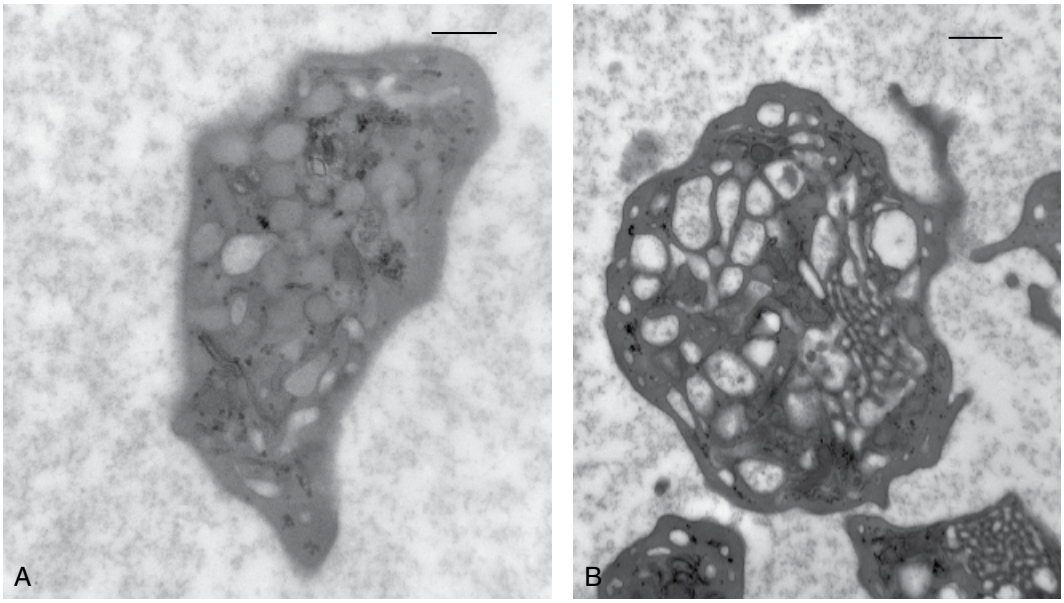

Fig. 27.37. Scanning electron microscopy of platelets from: **(A)** Normal, **(B)** gray platelet syndrome. α Granules appear as circular electron opaque structures in the normal platelet but are replaced by empty vacuoles in the gray platelet syndrome. This explains the "ghost-like" appearance on light microscopy. Note also the scale bars showing that the gray platelets are much larger than normal platelets.

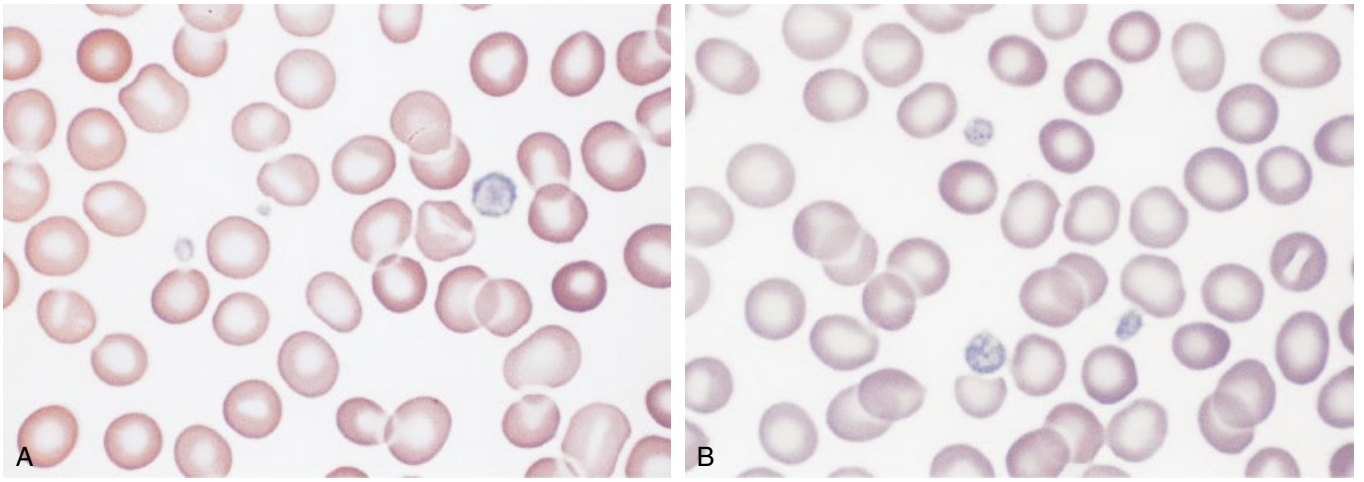

Fig. 27.38. Gray platelet syndrome. **A, B,** Typical large platelets that lack normal α-granules. (*A, B,* Courtesy of Dr. PC Shrivastava.)

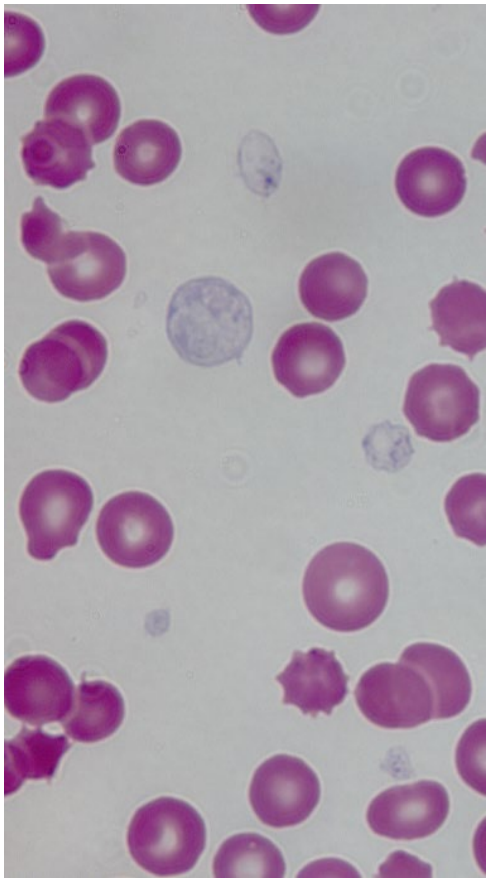

Fig. 27.39. ARC (arthrogryposis, renal dysfunction, and cholestasis) syndrome. Platelets appear large and pale, with aberrant α-granules. (Courtesy of Professor WHA Kahr.)

In ARC syndrome (arthrogryposis, renal dysfunction, and cholestasis), there is defective platelet aggregation with arachidonic acid and ADP (Fig. 27.39). Mutations of *VIPAS39* or *VPS33B* a Secl/Munc 18 protein involved in intracellular vesicle trafficking underlie the syndrome. Platelet α-granules are absent.

Von Willebrand disease is caused by an inherited quantitative deficiency or functional abnormality of VWF (Fig. 27.20). This results in defective platelet adhesion and defective in vitro aggregation activity with ristocetin (Fig. 27.40).

Acquired Disorders

Intrinsic abnormalities of platelet function are found in many patients with essential thrombocythemia and other myeloproliferative diseases, uremia, liver disease, and hyperglobulinemia (Table 27.5). Aspirin and other nonsteroidal anti-inflammatory drugs produce a platelet function defect, which often manifests as abnormal bleeding time; however, spontaneous hemorrhage during therapy, except for gastric mucosal bleeding caused by erosions, is not common. Antiplatelet drugs (usually aspirin or clopidogel) are used in the prevention of thrombosis, which reduces the risk of recurrence of myocardial infarct or of stroke in patients with transient ischemic attacks.

Antiplatelet drugs that block the GPIIa–IIIb receptor (Fig. 29.22) – one of the integrin adhesion molecule receptors – are used in the setting of percutaneous coronary intervention or acute coronary syndrome in patients on aspirin.

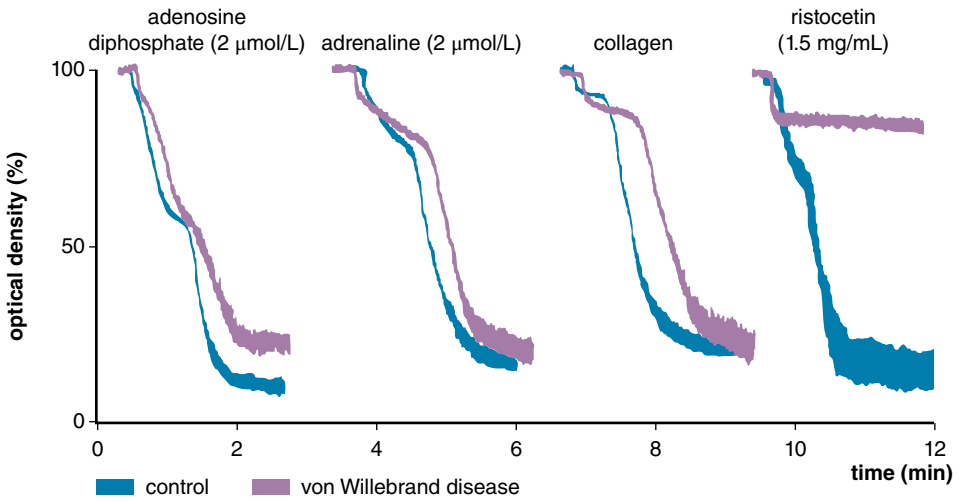

Fig. 27.40. Von Willebrand disease. Platelet aggregation studies show normal aggregation patterns with adenosine diphosphate, adrenaline, and collagen, but no aggregation with ristocetin. (Courtesy of Dr. RA Hutton.)

TABLE 27.5. CAUSES OF ACQUIRED THROMBOCYTOPENIA

Failure of platelet production

Generalized bone marrow failure
- Leukemia; myelodysplasia; aplastic anemia; human immunodeficiency virus (HIV) infection; myelofibrosis; megaloblastic anemia; uremia; multiple myeloma; marrow infiltration (e.g. carcinoma, lymphoma), cytotoxic chemotherapy

Selective megakaryocyte depression
- Drugs; alcohol; chemicals; viral infections

Abnormal distribution of platelets

Splenomegaly

Increased destruction of platelets

Immune
- Alloantibodies – neonatal; post-transfusion
- Autoantibodies – primary; secondary (e.g. systemic lupus erythematosus, chronic lymphocytic leukemia, postinfection, HIV infection, poststem cell transplantation

Drug induced
- Immune or because of platelet aggregation

Disseminated intravascular coagulation

Microangiopathic processes
- Hemolytic–uremic syndrome; thrombotic thrombocytopenic purpura; extracorporeal circulation; HELPP (hemolysis, elevated liver enzymes and low platelet count in association with pre-eclampsia) syndrome; poststem cell transplantation

Giant hemangioma (Kasabach–Merritt syndrome)

Dilutional loss

Massive transfusion of stored blood

CHAPTER

28

INHERITED AND ACQUIRED COAGULATION DISORDERS

HEREDITARY COAGULATION DISORDERS

Most inherited coagulation disorders involve deficiency of a single factor, with deficiencies of factor VIII (hemophilia A) von Willebrand disease being the most frequent. Other hereditary disorders that were previously thought to be rare are now increasingly well recognized. Factor XI and VII deficiency have a higher incidence than hemophilia B (Table 28.1).

HEMOPHILIA

In hemophilia A, plasma factor VIII activity is absent or at a low level (<1% in severe cases, 1–5% in moderate cases, and >5% in mild cases), because of either defective synthesis of the factor VIII molecule or synthesis of a structurally abnormal molecule (Fig. 28.1). The protein consists of three homologous regions, A1, A2, and A3, separated by a long B domain, rich in glycosylation sites and followed by two homologous C regions (Figs. 28.2 and 28.3). The A regions show homology with the copper-binding protein ceruloplasmin. The single-chain mature polypeptide has a molecular weight (MW) of about 267 kDa and is cleaved by thrombin into two calcium-linked polypeptides of MW 90 and 80 kDa. It is in this activated form that it activates factor X. The gene maps to the distal band of the long arm of chromosome X (Xq28). There are over 2000 unique variants described in the *F8* database with >1300 single nucleotide changes, about 500 small insertion-deletions, and 100 copy number variants. Single nucleotide changes can be associated with any disease severity but the other variants that disrupt gene structure to a greater extent are invariably associated with severe disease. The single most common variant is a rearrangement resulting in inversion of the distal part of the gene after intron 22 (Fig. 28.1, *C*). This accounts for almost 50% of severe cases. In about 30% of cases with severe disease and 5% of those with nonsevere disease, patients develop a factor VIII inhibitor in plasma. Molecular analysis has helped uncover the mechanism of various important subtypes of hemophilia such as those associated with assay discrepancy. In this nonsevere type of hemophilia the measured factor VIII activity varies depending on which assay is used to measure the level. Generally, the chromogenic or two-stage assay correlates best with the bleeding phenotype which is more severe than expected from the one-stage assay (Fig. 28.4). The von Willebrand factor (VWF) activity is normal and VWF is present in normal amounts.

In hemophilia B (Christmas disease), either factor IX is absent or the factor IX molecule is structurally abnormal. The inheritance of both hemophilias is sex linked (Fig. 28.3). As factors VIII and IX together form the intrinsic tenase complex (see Chapter 26), the biochemical effect of deficiency of either protein is the same and so the clinical phenotypes are very similar.

Major hemorrhage of the joints is the dominant problem in severe hemophilia A or B and most frequently affects the knees, elbows, ankles, and hips, although other synovial joints are involved. Usually, severe pain is present and the affected joint is tender, warm, and can be grossly distended (Figs. 28.5 and 28.6). Chronic joint hemorrhage results in degenerative joint changes and mechanical derangement of articular surfaces (Figs. 28.7 and 28.8).

TABLE 28.1 NUMBER OF PATIENTS AND RELATIVE FREQUENCY (IN PARENTHESES) OF INHERITED COAGULATION DEFICIENCIES IN THE UK (EXCLUDING VON WILLEBRAND DISEASE)

Defect	Number (%)	Gene location
X-linked		
Factor VIII (hemophilia A)	3554 (76.8)	X
Factor IX (hemophilia B)	762 (16.1)	X
Autosomal recessive		
Fibrinogen	11 (0.2)	4
Prothrombin	1 (0.02)	11
Factor V	28 (0.6)	1
Factor VIII	62 (1.3)	13
Factor V + VIII	18 (0.3)	18 (*LMAN1*)*
		2 (*MCFD2*)*
Factor X	25 (0.5)	13
Factor XI	150 (3.3)	
Factor XIII	26 (0.5)	6 subunit A
		1 subunit B

* *LMAN1s* act as chaperone for factor V and factor VIII; *MCFD2* is a cofactor for *LMAN1*.
Source: Peyvandi F, Mannucci PM. In Hoffbrand AV, et al. eds. *Postgraduate Haematology*, 5th edn, Blackwell, Oxford, 2005, Table 50.2. Reproduced with permission of John Wiley and Sons.

Color Atlas of Clinical Hematology: Molecular and Cellular Basis of Disease, Fifth Edition. A. Victor Hoffbrand, Paresh Vyas, Elías Campo, Torsten Haferlach, and Keith Gomez

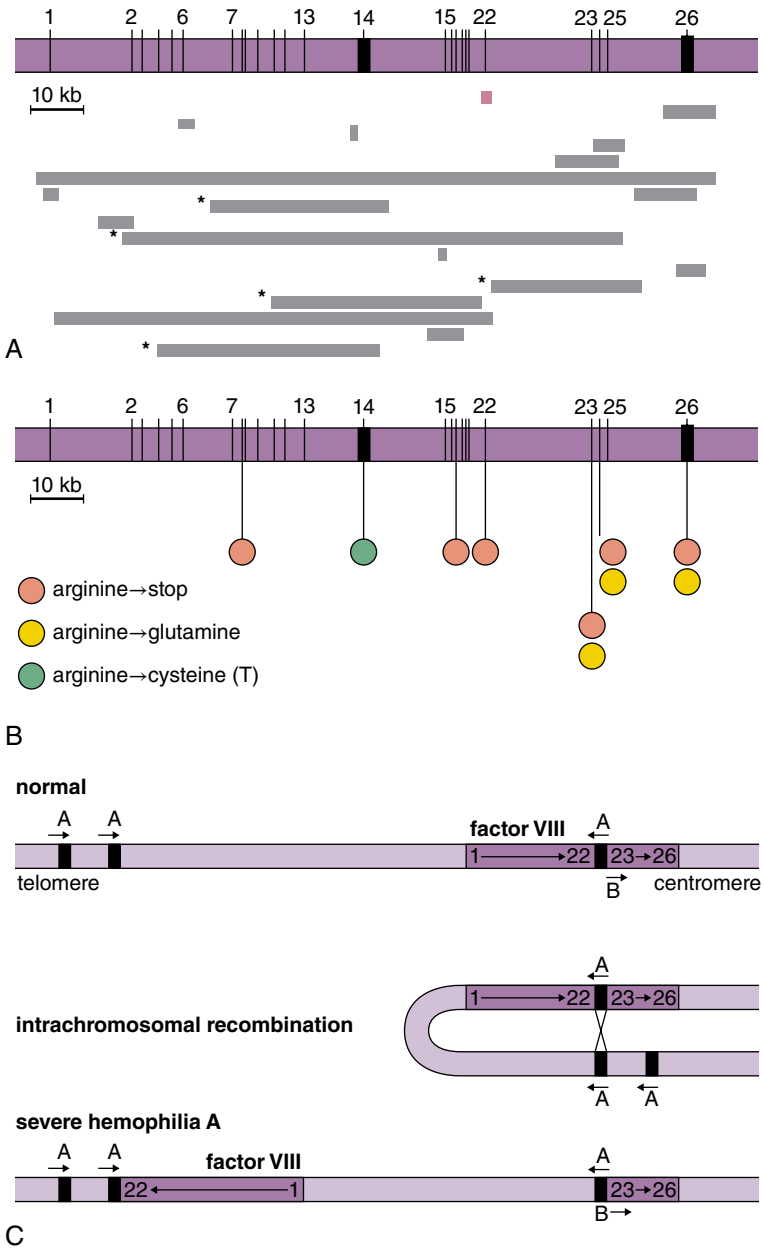

Fig. 28.1. Some of the mutations in the factor VIII gene and the region of chromosome X that contains it. **A,** Examples of deletion mutations. Bars beneath the representation of the factor VIII gene show the approximate size of DNA deletions that lead to hemophilia. The deletion in pink corresponds to a case of mild hemophilia; all other patients have severe disease. The asterisks correspond to gene deletion in hemophiliacs who have developed inhibitor antibodies. **B,** Examples of point mutations. Nonsense (red) and missense (yellow and green) mutations have been discovered in parts of the factor VIII gene that normally encode the amino acid arginine. Many other examples of point mutations and deletions exist. **C,** The region of chromosome X q28 that contains the factor VIII gene. Inversion model of the recombination that accounts for approximately 45% of severe hemophilia A. (*A,* Homologous promoter that is repeated; *B,* second promoter near *A* that is only in intron 22 and when active transcribes exons 23 to 26 – the opposing orientation of *A* sequences allows intrachromosomal homologous recombination.) (*A, B,* Source: Modified with permission from Hoffman R, et al. eds: *Hematology: Basic Principles and Practice,* Churchill Livingstone, New York, 1991, p. 1286. Reproduced with permission of Elsevier. *C,* Courtesy of Professor KJ Pasi.)

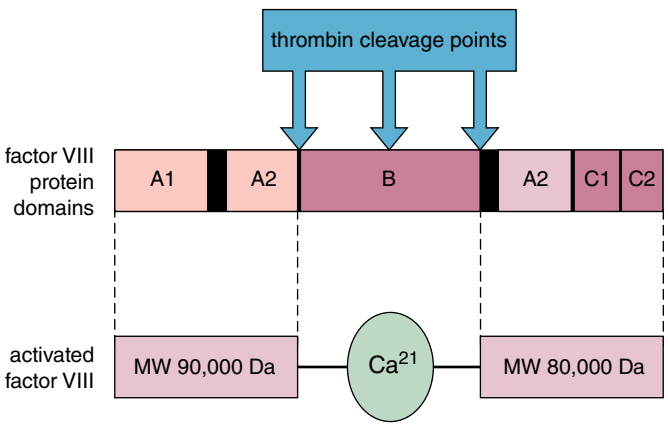

Fig. 28.2. Factor VIII clotting factor: Structure.

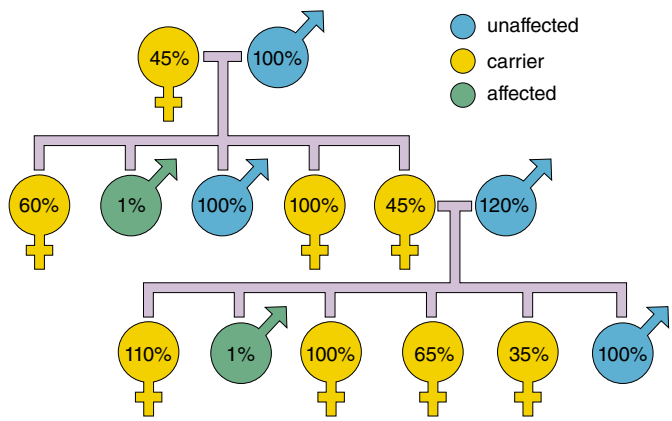

Fig. 28.3. Hemophilia: Pattern of inheritance (family tree).

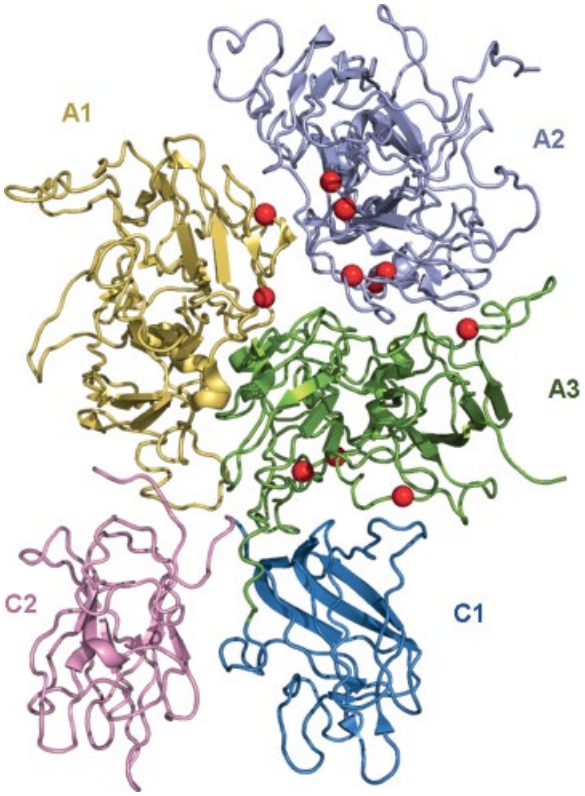

Fig. 28.4. Ribbons diagram of the crystal structure of factor VIII showing the position of variants causing assay discrepancy. The domains are labeled and shown in different colored ribbons. Variants associated with assay discrepancy are shown as red spheres and are seen to cluster at the interdomain boundaries. It is this destabilizing effect that results in variable inactivation of the protein depending on the assay conditions.

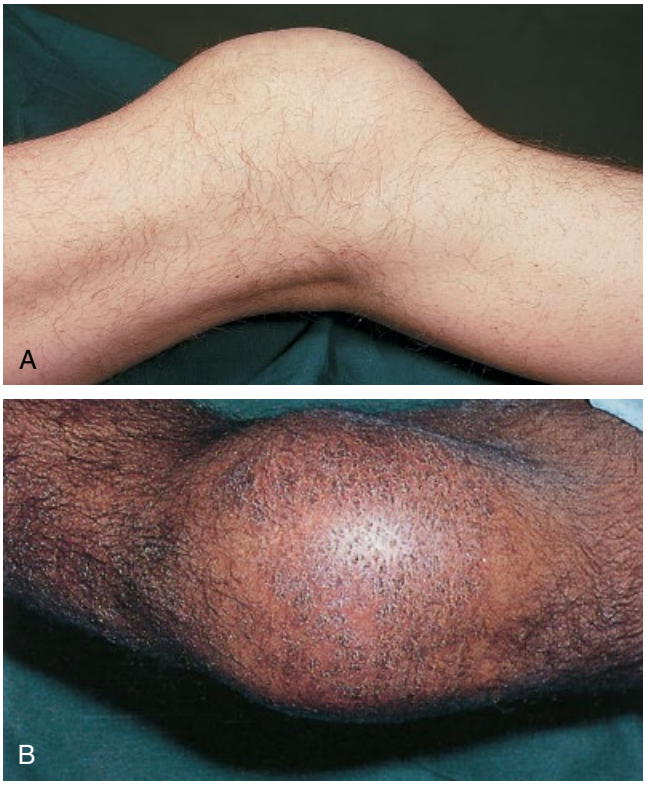

Fig. 28.5. Hemophilia A. **A, B,** Gross swelling from acute hemarthroses of the knee joints.

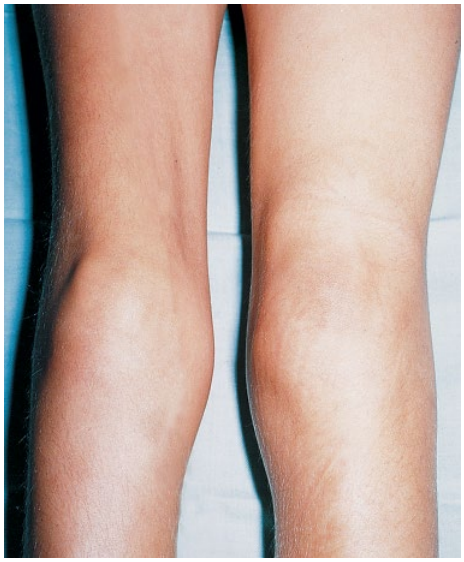

Fig. 28.6. Hemophilia A: Acute hemarthrosis of the left knee joint, with swelling of the suprapatellar area. The quadriceps muscles are wasted, particularly on the patient's right thigh.

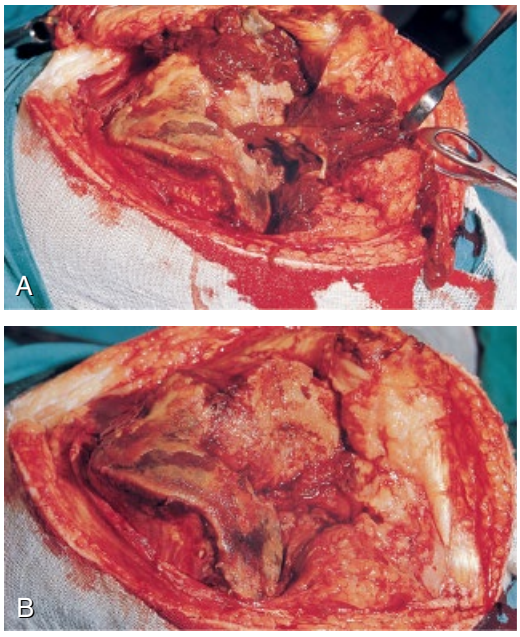

Fig. 28.7. Hemophilia A. **A,** Opened knee joint showing the femoral condyles and hypertrophied hemosiderin-stained synovium. Widespread erosion of the articular cartilage has exposed large areas of hemosiderin-stained bone. **B,** Removal of the synovium of the suprapatellar pouch and of the patella exposes the grossly damaged femoral articular surface.

Demineralization, loss of articular cartilage, bone lipping, and osteophyte formation produce deformity and crippling (Figs. 28.9–28.11). The end result in poorly treated patients is permanent fixation of the affected joint or flexion deformities (Figs. 28.12 and 28.13).

Traumatic and spontaneous soft-tissue hemorrhage is a feature of hemophilia (Figs. 28.14–28.17). Dissecting hematomas can involve large areas of muscle or deep fascial layers (Fig. 28.18). Hemorrhage into retroperitoneal fascial spaces or into the psoas muscle produce considerable problems in differential diagnosis

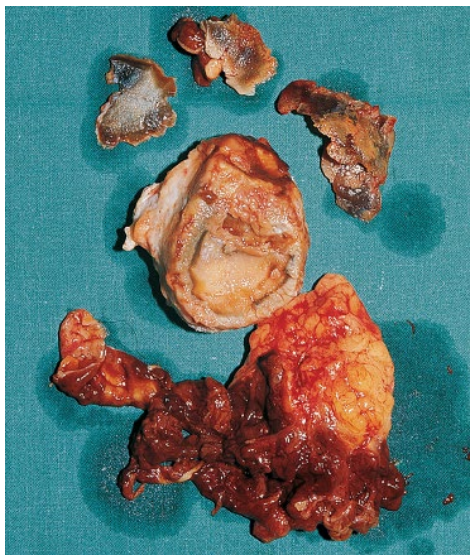

Fig. 28.8. Hemophilia A: Resected material from the knee in Fig. 28.7 included (from top to bottom) osteophytes from the arthritic femoral condyles; the patella, which shows hemosiderin-stained articular cartilage and secondary arthritic changes; and a portion of grossly hemosiderin-stained synovium of the suprapatellar pouch.

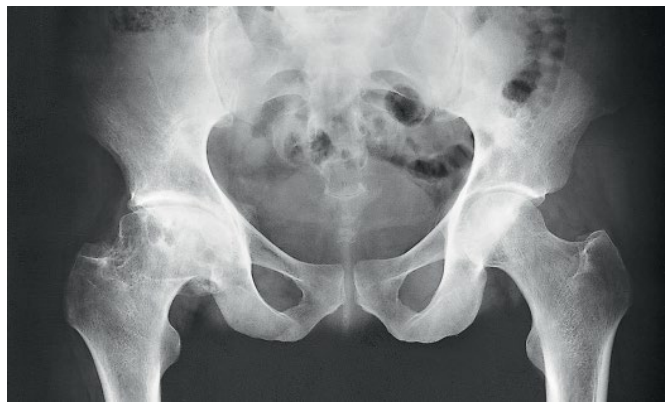

Fig. 28.10. Hemophilia A: Radiograph of the pelvis, showing marked destruction and deformation of the right acetabulum and femoral head. Numerous subchondral cysts are present, and the right femoral neck is shortened and widened.

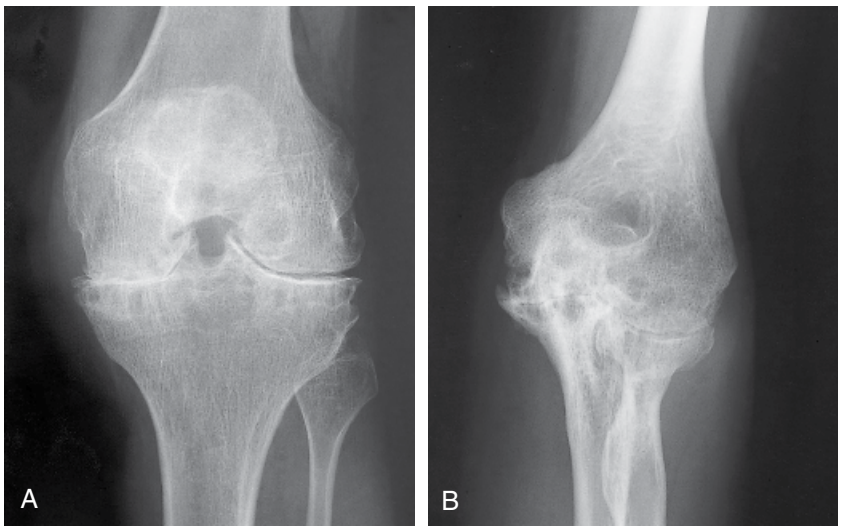

Fig. 28.9. Hemophilia A. **A,** Radiograph of the knee joint, showing marked narrowing of the joint space (particularly medially), a widened intercondylar notch, prominent osteoarthritic changes, and subchondral cyst formation, with erosion of the upper lateral border of the tibial plateau. **B,** Radiograph of the elbow joint, showing marked joint space narrowing, enlargement of the radial head, secondary osteoarthritic features, and subchondral cyst formation.

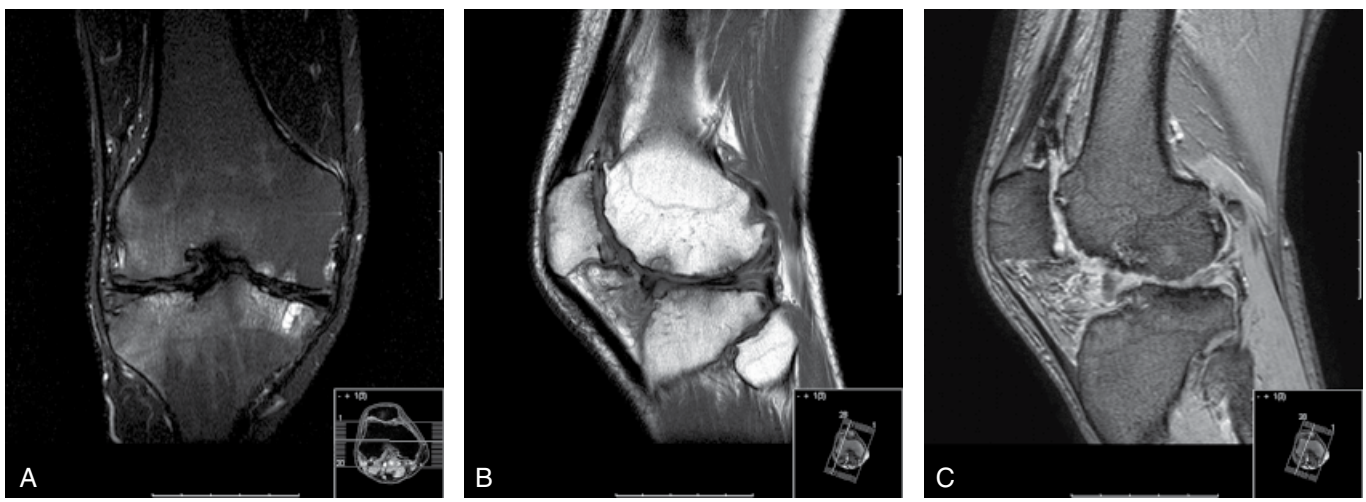

Fig. 28.11. Hemophilia A. **A–C,** Magnetic resonance imaging (MRI) of knee joint. Gross arthritic changes affecting all three compartments of the knee joint with severe articular cartilage thinning and irregularity, prominent subarticular cysts, and flattening and tears of the posterior horns of both medial menisci.

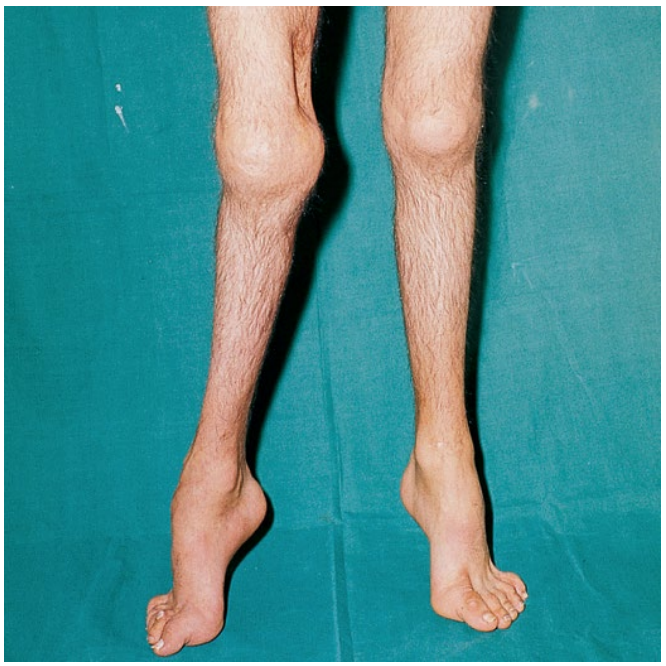

Fig. 28.12. Hemophilia A: Gross crippling. The right knee is swollen, with posterior subluxation of the tibia on the femur. The ankles and feet show residual deformities of talipes equinus and some degree of cavus and associated toe clawing. Generalized muscle wasting is most marked on the right. The scar on the medial side of the right lower thigh is the site of a previously excised "pseudotumor."

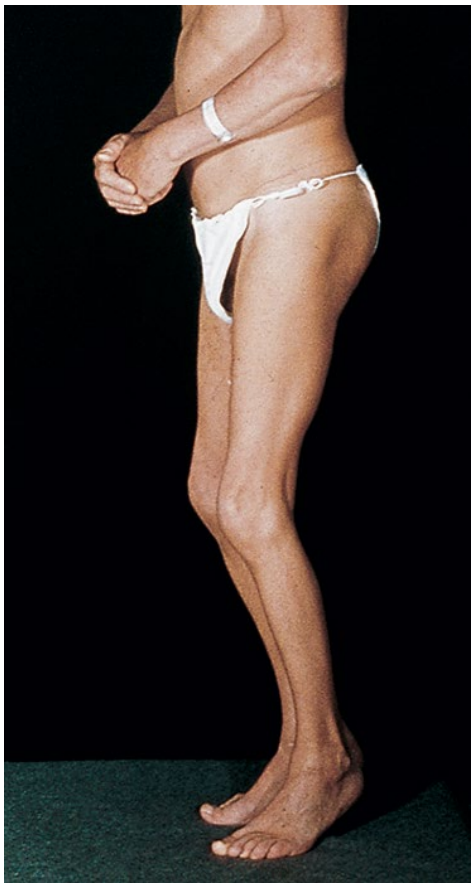

Fig. 28.13. Hemophilia A. Flexion deformities of the elbow, hip, knee, and ankle joints following a 35-year history of multiple hemarthroses.

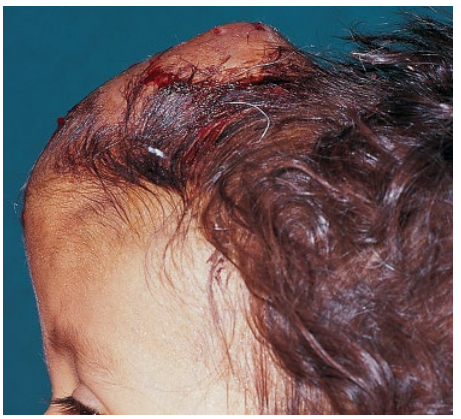

Fig. 28.14. Hemophilia A. Extensive post-traumatic hematoma of the forehead in an infant.

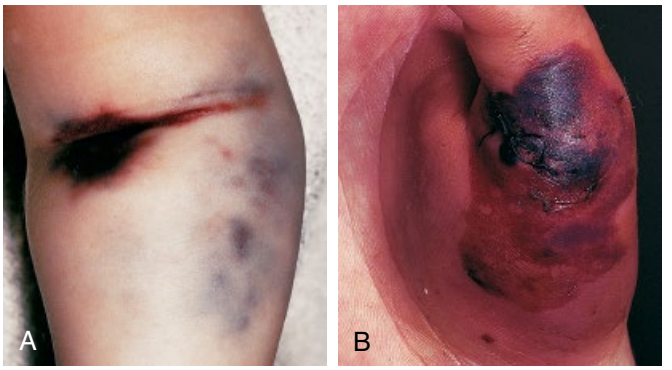

Fig. 28.15. Hemophilia B. **A,** Extensive subcutaneous hemorrhage about the elbow joint of an infant following venipuncture. **B,** Extensive bleeding into the thenar muscles and overlying subcutaneous tissue.

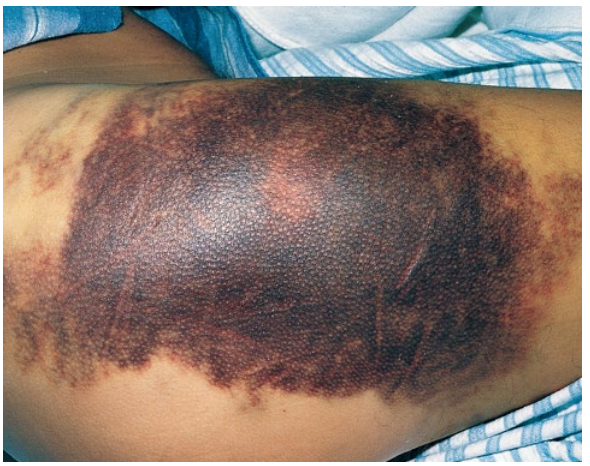

Fig. 28.16. Hemophilia A. Massive hemorrhage in the area of the right buttock, following an intramuscular injection.

(Figs. 28.19–28.21), because associated pain, tenderness, and fever suggest other causes of the acute abdomen.

Hemophilic "pseudotumors" are a serious complication of extensive fascial or subperiosteal hemorrhage. These blood-filled multiloculated cysts cause extensive destruction of both soft tissue (Fig. 28.22) and bone (Figs. 28.23 and 28.24) as they increase in size.

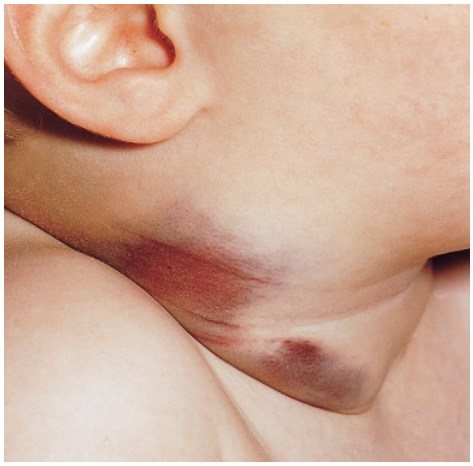

Fig. 28.17. Hemophilia B. Extensive hemorrhage into the soft tissues of the neck following venipuncture of the external jugular vein.

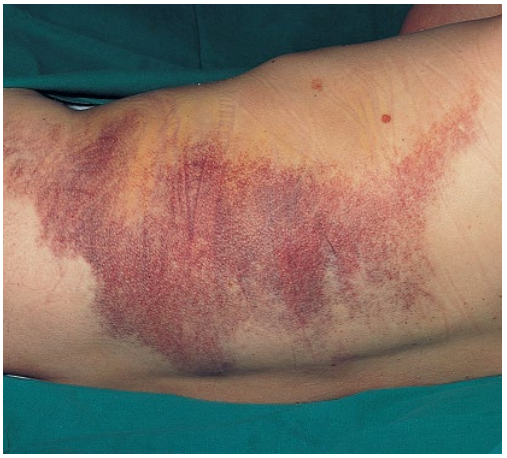

Fig. 28.20. Hemophilia A: Acute retroperitoneal hemorrhage (same patient as shown in Fig. 28.19). The extensive subcutaneous bruising of the left flank appeared 24 hours after presentation.

Fig. 28.18. Hemophilia A. **A,** Marked submandibular swelling resulting from a large hemorrhage in the sublingual tissues. **B,** The most superficial part of the sublingual hemorrhage is clearly visible beneath the mucosa of the floor of the mouth.

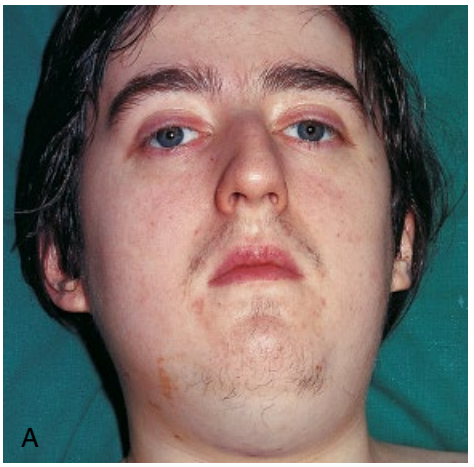

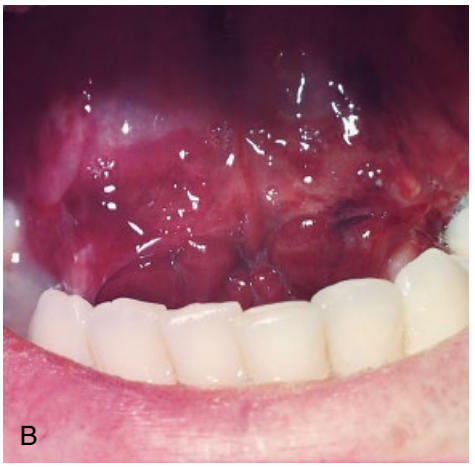

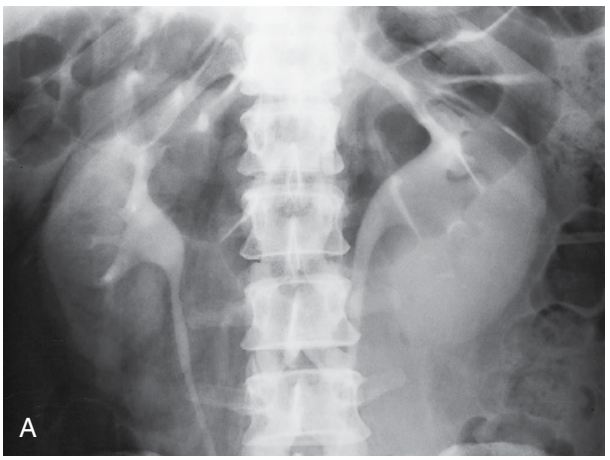

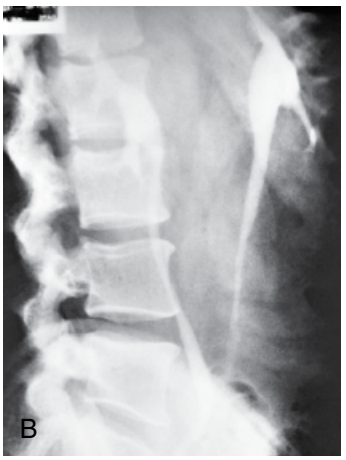

Fig. 28.19. Hemophilia A: Intravenous pyelogram showing acute retroperitoneal hemorrhage. **A,** A soft-tissue mass in the left flank has caused medial rotation of the left kidney and anteromedial displacement of the ureter. **B,** The lateral view confirms the anterior displacement of both the kidney and ureter.

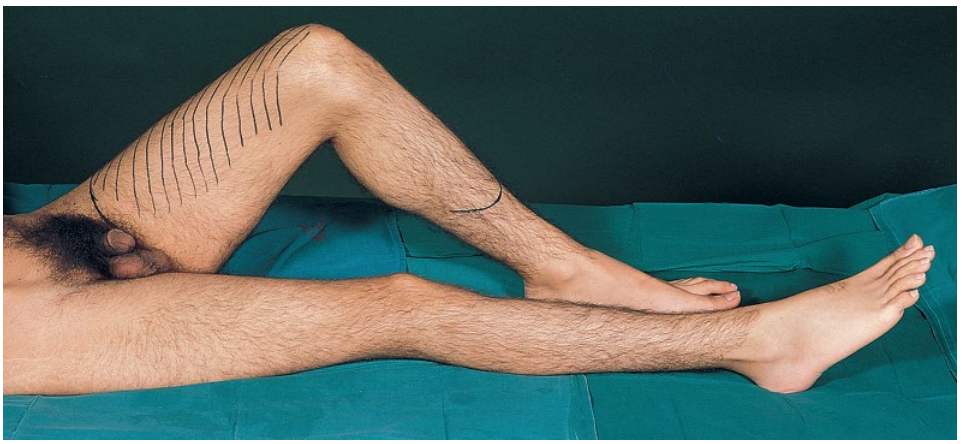

Fig. 28.21. Hemophilia A: Acute retroperitoneal hemorrhage into the left psoas muscle. The lines indicate an area of anesthesia over the distribution of the femoral nerve. There was also weakness of the quadriceps muscle and a flexion contracture at the left hip.

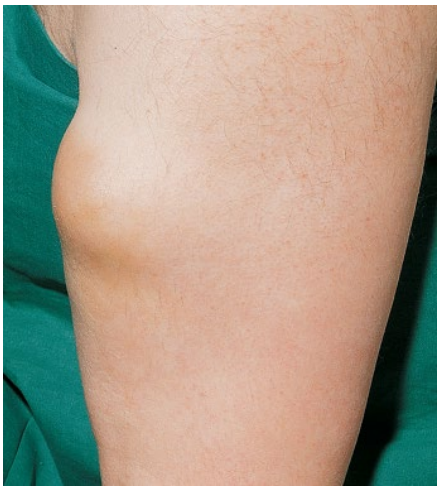

Fig. 28.22. Hemophilia A. "Pseudotumor" of the biceps, in fact a hard residual encapsulated swelling following incomplete resolution and repair of previous muscle hemorrhage.

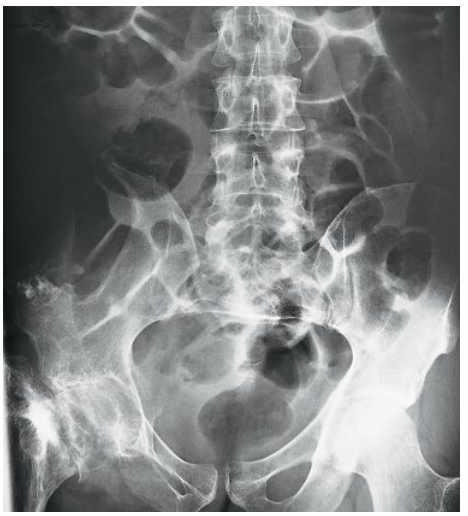

Fig. 28.24. Hemophilia A: Pelvic radiograph (same patient as shown in Fig. 28.23). The pseudotumor destroyed a large area of the wing of the right iliac bone, including the anterior crest. The hip joint space on the right is obliterated and the femoral neck has a disunited fracture, with resultant pseudoarthrosis, gross deformity, and shortening.

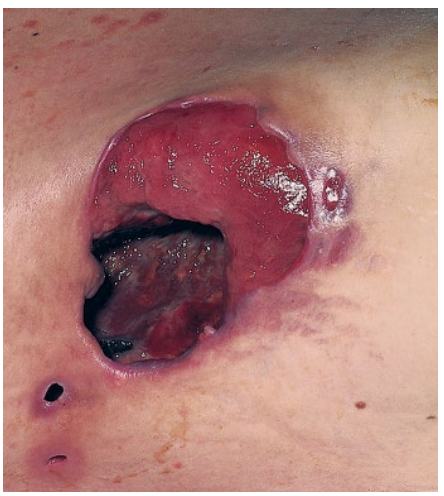

Fig. 28.23. Hemophilia A. Large ulcer overlying the entrance to a multiloculated and cavernous pseudotumor of the right iliac bone and overlying soft tissues.

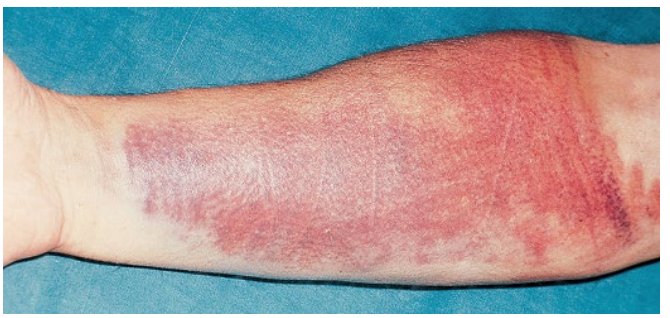

Fig. 28.25. Hemophilia A. Subcutaneous bruising and extensive hemorrhage into the flexor muscles and associated soft tissues of the right forearm.

Ischemic contractures follow extensive hemorrhage into the muscles of the limbs (Fig. 28.25); for example, Volkmann contracture of the forearm (Fig. 28.26). Prolonged bleeding occurs after dental extractions, and operative hemorrhage is life-threatening in both severely and mildly affected patients.

Spontaneous intracranial hemorrhage (Fig. 28.27), although an infrequent cause of bleeding in individuals, remains the most common cause of death in patients with severe hemophilia.

Prior to the introduction of factor replacement therapy in the 1950s, life expectancy for patients with severe disease was about 20 years. Now in the developed world, prophylactic therapy with plasma and recombinant factor concetrates and early treatment of bleeding episodes have reduced the occurrence of hemarthroses and normalized life expectency. In the developing world, access to replacement therapy remains a major challenge and many patients still reach early adulthood with crippling disease. In most patients, replacement therapy with the appropriate coagulation factor concentrates has allowed even major surgical procedures to be undertaken without excessive risk.

In the last few years there has been an explosion in new treatment options with extended half-life products and adjunctive therapies that improve thrombin generation without increasing the factor level. Gene therapy, where normal copies of the gene are introduced using vectors modified from viruses, offers the potential for cure in the foreseeable future (Fig. 28.28).

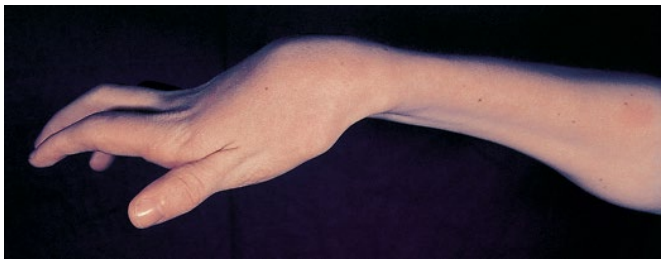

Fig. 28.26. Hemophilia A: Volkmann's contracture. The wasting and flexion deformities are a result of extensive repair and stricture formation in muscles damaged by repeated hematomas.

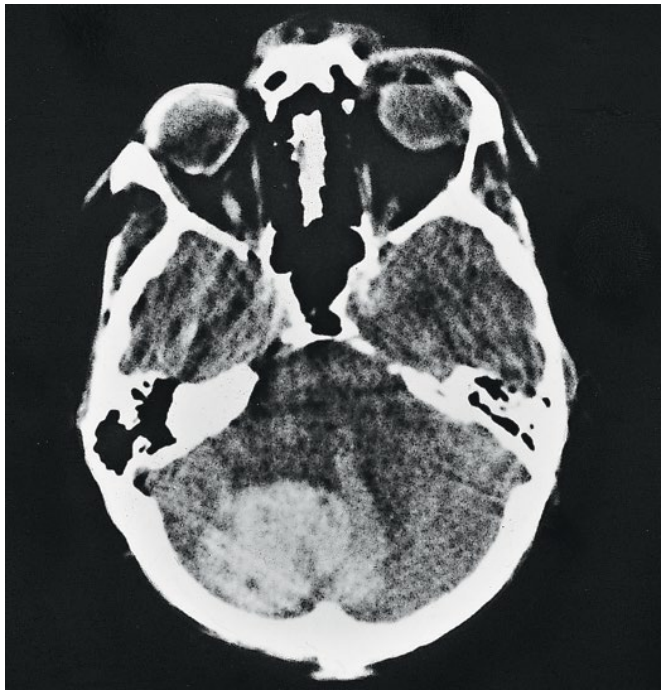

Fig. 28.27. Hemophilia A. Computed tomography (CT) scan showing a large hematoma of the cerebellum.

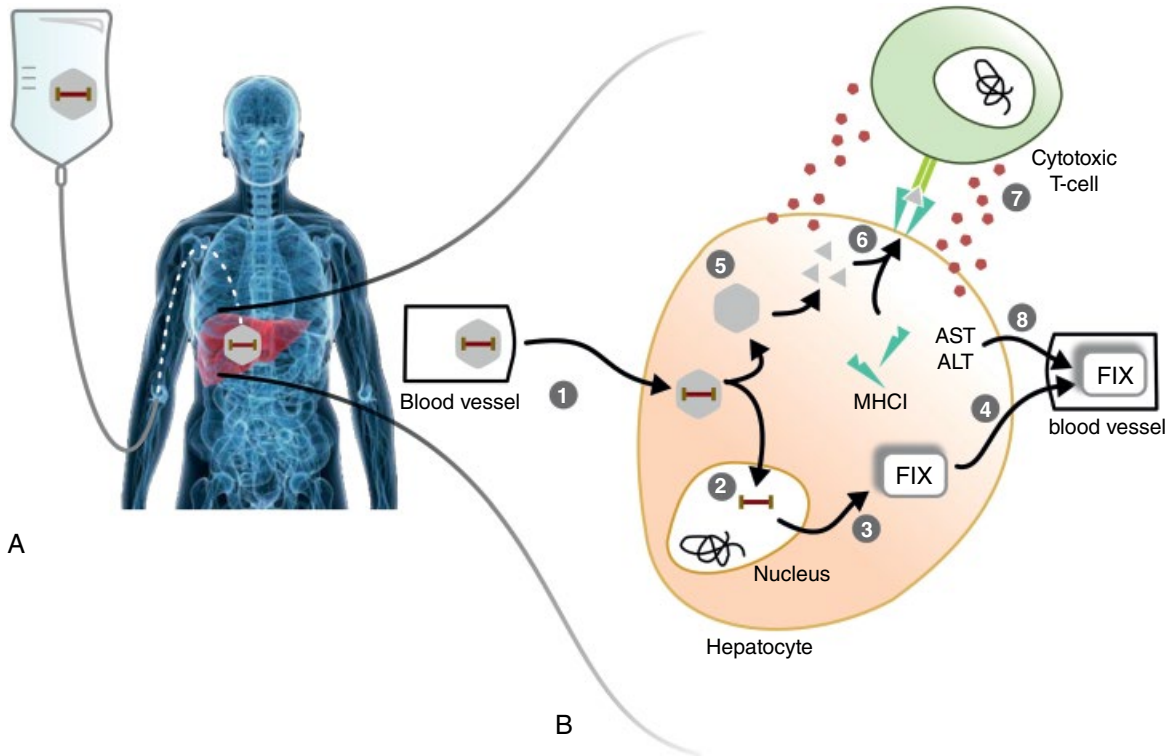

Fig. 28.28. Adeno-associated virus intravenous delivery and liver toxicity. **A,** Schematic representation of peripheral vein administration. **B,** Hepatocyte toxicity: 1, vector endocytosis; 2, vector genome entry into the nucleus; 3, recombinant factor IX (FIX) protein synthesis; 4, recombinant FIX secretion; 5, capsid cleavage; 6, MHC Class I molecules loading with capsid antigens, activation of cytotoxic T-cells; 7, cytokine secretion; 8, permeabilization of hepatocyte membranes, transaminases (ALT, AST) leaks out into the blood circulation. (Source: *Blood Reviews* 2015;29:321–328.)

Carrier Detection and Antenatal Diagnosis

DNA analysis has improved carrier detection and prenatal diagnosis compared with the measurement of factor VIII or IX antigenic and coagulation activity in plasma. Direct detection of the defect is possible using DNA sequencing providing an index case is available to establish the particular mutation present in the family (Figs. 28.29 and 28.29 Fig. 28.30).

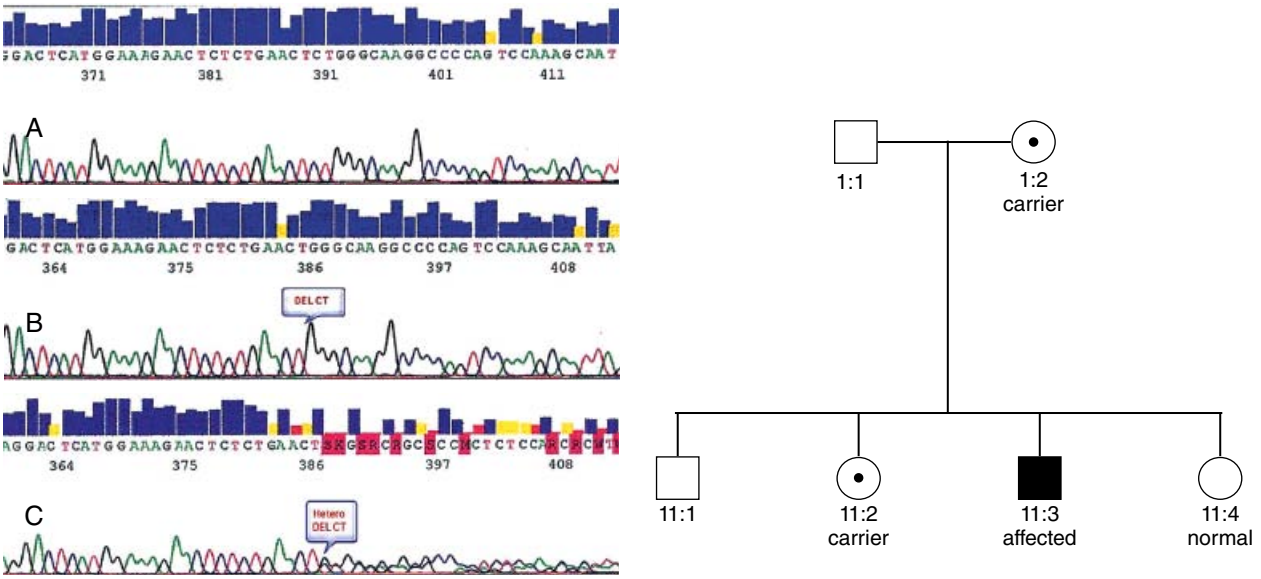

Fig. 28.29. Family 1 Hemophilia A. Carrier detection by DNA analysis of peripheral blood leukocytes. **A,** Normal reference sequence. **B,** Automated dideoxy sequencing of the factor VIII gene has shown the affected son in this family (II-3) to have a 2 basepair (CT) deletion in exon 14, resulting in a frameshift causing the introduction of a premature stop codon. **C,** His mother is shown to be a carrier illustrated by one allele showing normal sequence and the second carrying the 2 basepair deletion. His older sister (II-2) was also a carrier, whereas his younger sister (II-4) was normal. (Courtesy of Haemophilia Centre, Royal Free Hospital.)

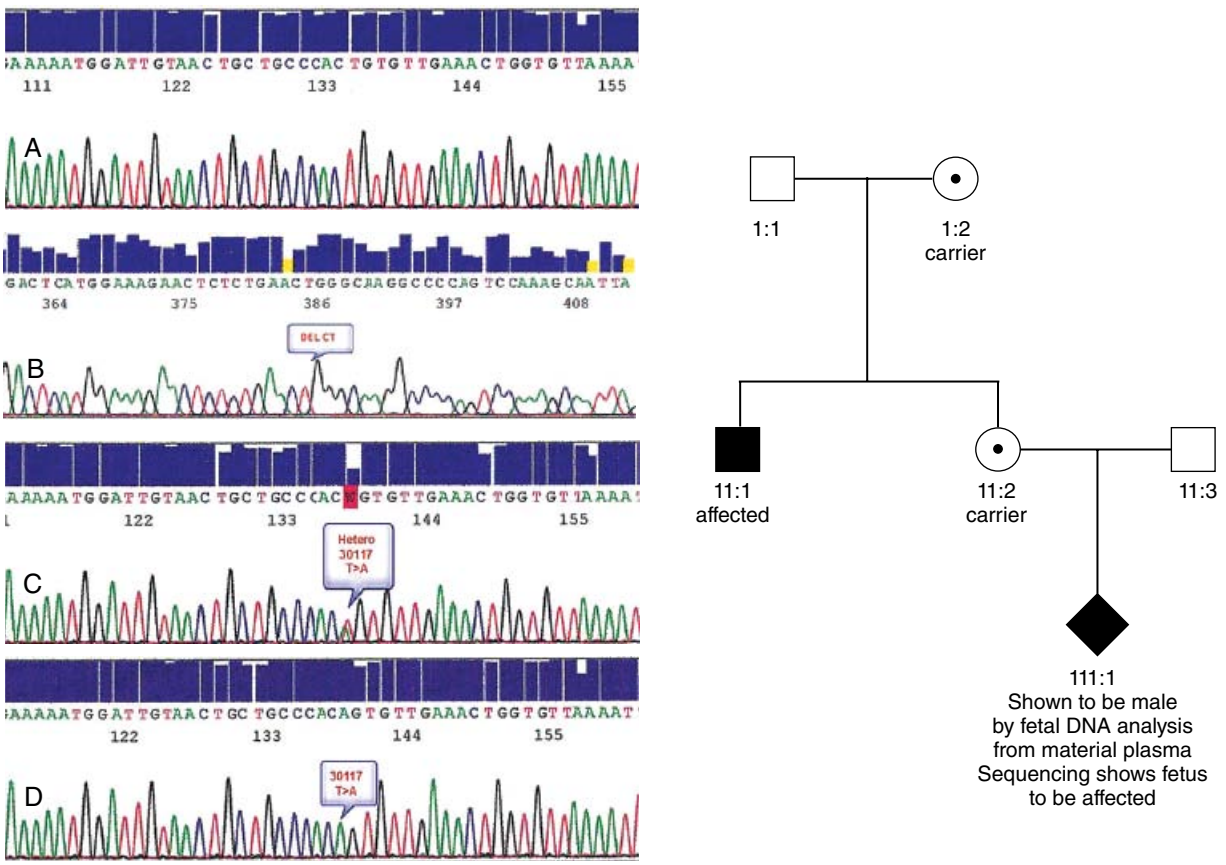

Fig. 28.30. Factor IX deficiency: Antenatal diagnosis. Hemophilia B: Prenatal diagnosis by chorion villus biopsy and direct sequencing. **A,** Normal reference sequence. **B,** Automated dideoxy sequencing of the factor IX gene has shown the affected son in this family (II-1) to have a T>A substitution at nucleotide 30117 in exon 7. This results in a cysteine to serine change at codon 222. **C,** His sister is shown to be a carrier, illustrated by the heterozygous peak at 30117 showing both the T and the A nucleotides. **D,** Direct sequencing shows that her male fetus is affected as he has only the abnormal A at position 30117. (Courtesy of Haemophilia Centre, Royal Free Hospital.)

VON WILLEBRAND DISEASE

Von Willebrand disease is a bleeding disorder caused by inherited defects in the concentration, structure, or function of VWF caused by mutations at the VWF locus and possibly other mutations. This protein is an oligomer of units, each of MW 210 000. It carries factor VIII coagulation factor and is itself essential for the adhesion of platelets to damaged vessel walls. The subunits dimerize "tail to tail" in the endoplasmic reticulum and then form multimers through "head to head" disulfide bonds in the D domains. The multimers are secreted or stored in the Weibel–Palade bodies or in platelets. The fate of secreted VWF multimers depends on their size, interactions with platelets, susceptibility to proteolysis by ADAMTS13, and rate of clearance from the circulation (Fig. 28.31). Under high fluid shear stress, multimers are stretched, bind platelets, and are exposed to cleavage by ADAMT513. Normal blood contains multimers of different sizes with characteristic cleavage products, not found in endothelial VWF. In normal plasma, the largest VWF multimers are smaller than those assembled initially in the endothelial cell (Fig. 28.31). In thrombocytic thrombocytopenic purpura, ultralarge multimers are present in plasma. The pattern of VWF multimer distribution differs in the different types of von Willebrand disease (Fig. 28.32).

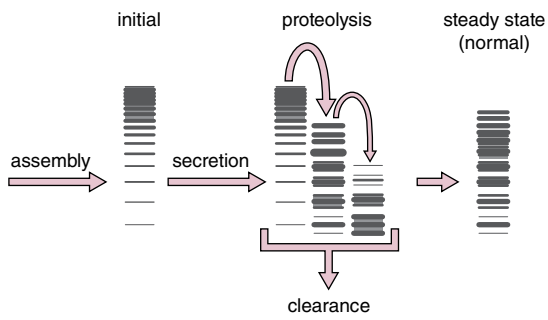

Fig. 28.31. Synthesis and catabolism of VWF multimers. In plasma, VWF is cleaved by ADAMTS13 metalloprotease so that the largest multimers are smaller than those assembled initially. Faint satellite bands flank the smallest bands, reflecting proteolytic remodeling. (Source: Adapted from Sadler et al. *J Thromb Haemost* 2006;4:2103–2114.)

The inheritance pattern of von Willebrand disease found in most patients is autosomal dominant. The disorder is characterized by operative and post-traumatic hemorrhage, mucous membrane bleeding particularly from the oral cavity and genital tract, and excessive blood loss from both superficial cuts and abrasions (Fig. 28.33; Table 28.2). Spontaneous hemarthroses and arthritic changes are particularly rare, and occur only in patients with type 3 disease (Fig. 28.34).

The molecular defects include point mutations or deletions. The disease is divided into three types based on laboratory findings and type 2 is further divided into four subtypes. The results of hemostasis tests in von Willebrand disease and the hemophilias are given in Table 28.3.

OTHER HEREDITARY COAGULATION DISORDERS

Patients with inherited defects of coagulation factors other than VIII or IX (e.g. factor XI) often show easy bruising and spontaneous and excessive post-traumatic bleeding (Fig. 28.35). However, spontaneous hemarthroses and soft-tissue hematomas are most unusual.

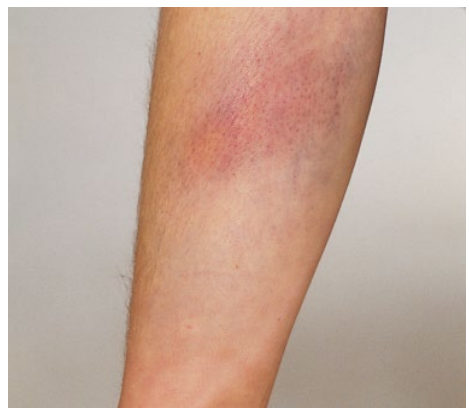

Fig. 28.33. Von Willebrand disease. Subcutaneous bruising overlying hemorrhage into the muscles and soft tissues of the left forearm.

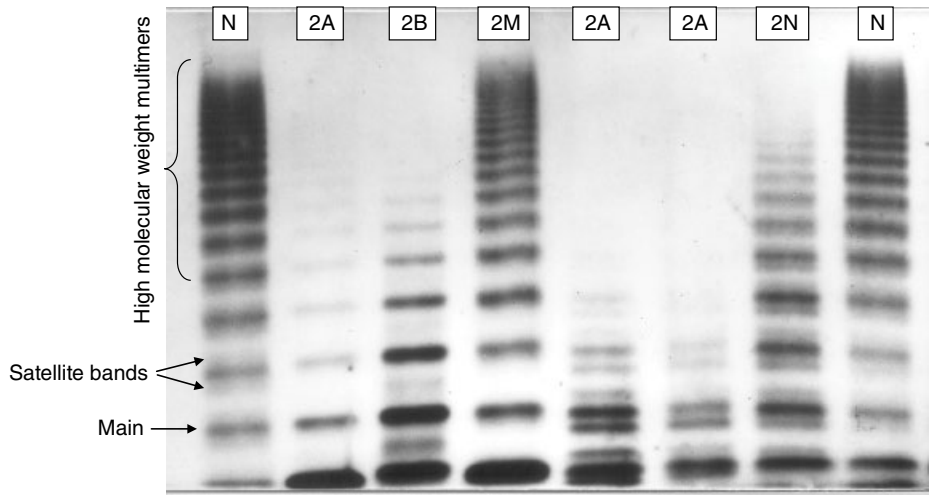

Fig. 28.32. Von Willebrand factor multimers in normal plasma (N) and in patients with different types of von Willebrand disease. Higher molecular weight forms are towards the top of the gel. In the normal lane notice the bands representing multimers of different molecular weight and the satellite bands on either side of the main band forming the triplet pattern. Type 2 von Willebrand disease is characterized by loss of high molecular forms and/or abnormalities of the triplet pattern.

TABLE 28.2. PATHOPHYSIOLOGY AND CLASSIFICATION OF VON WILLEBRAND DISEASE

Type	Description	FVIII:C	VWF:Ag	VWF:RCo	VWF:CB	VWF:FVIIIB	VWF: Multimers	RIPA
1	Partial quantitative deficiency of VWF	Decreased	Decreased	Decreased (concordant)	Decreased (concordant)	Normal	May or may not contain mutant VWF subunits	Reduced
2	Qualitative VWF defects	Decreased	Decreased	Decreased (discordant)	Decreased (discordant)	Normal		Reduced
2A	Decreased VWF-dependent platelet adhesion and a selective deficiency of HMW VWF multimers	Decreased or normal	Decreased or normal	Decreased (discordant)	Decreased (discordant)	Normal	Absent HMW Medium MW multimers	Reduced
2B	Increased affinity for platelet glycoprotein Ib	Decreased or normal	Decreased or normal	Decreased (discordant)	Decreased (discordant)	Normal	Absent HMW multimers 2B Malmo or New York (normal pattern)	Increased with low dose Ristocetin (0.5mg/mL)
2M	Decreased VWF-dependent platelet adhesion without a selective deficiency of HMW VWF multimers	Decreased or normal	Decreased or normal	Decreased (discordant)	Decreased (concordant)	Normal	Normal pattern	Reduced
2N	Markedly decreased binding affinity for FVIII:C	Markedly decreased	Normal	Normal	Normal	Decreased	Normal pattern	Normal
3	Virtually complete deficiency of VWF	Markedly decreased	Markedly decreased	Markedly decreased (concordant)	Markedly decreased (concordant)	Normal	Markedly decreased	Reduced

HMW, high molecular weight; RIPA, ristocetin-induced platelet agglutination; VWF, von Willebrand factor; VWF:Ag, VWF antigen; VWF:CB, VWF collagen binding; VWF:FVIII:B, VWF factor VIII binding; VWF:Rco, VWF ristocetin cofactor. Concordant/discordant refers to a reduction in relation to VWF:Ag.

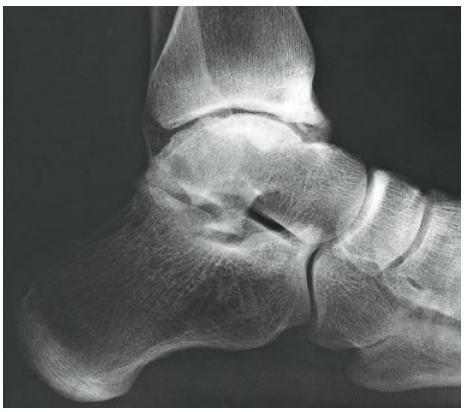

Fig. 28.34. Von Willebrand disease. Lateral radiograph of ankle joint showing loss of joint space, marginal sclerosis, and a small subchondral cyst in the tibial epiphysis.

ACQUIRED COAGULATION DISORDERS

In clinical practice the acquired coagulation disorders (Table 28.4) are seen more often than the inherited disorders. Unlike the inherited diseases, there are usually multiple clotting factor deficiencies. Bleeding episodes that result from vitamin K deficiency, overdosage with oral anticoagulants, or in association with liver disease and with disseminated intravascular coagulation (DIC) are seen most frequently.

TABLE 28.3. HEMOSTASIS TESTS: TYPICAL RESULTS IN HEMOPHILIAS A AND B AND VON WILLEBRAND DISEASE

	Hemophilia A	Hemophilia B	von Willebrand's disease
Bleeding time or PFA-100 test	Normal	Normal	Prolonged
Prothrombin time	Normal	Normal	Normal
Activated partial thromboplastin time	Prolonged	Prolonged	Prolonged
Thrombin clotting time	Normal	Normal	Normal
Factor VIII	Low	Normal	Low or normal
VWF:antigen	Normal	Normal	Low or normal (rarely raised)
VWF: ristocetin cofactor activity	Normal	Normal	Low (or rarely raised)
Factor IX	Normal	Low	Normal

LIVER DISEASE

Liver cell immaturity and lack of vitamin K synthesis in the gut are principal causes of hemorrhagic disease of the newborn. In adults, vitamin K deficiency is the result of obstructive jaundice or pancreatic or small bowel disease. Multiple hemostatic abnormalities contribute

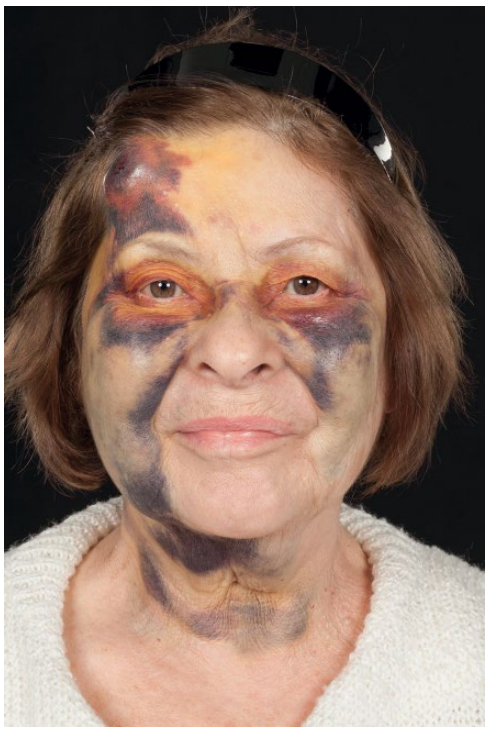

Fig. 28.35. Bleeding into the face of a patient with severe factor XI deficiency who knocked her forehead on a kitchen cabinet.

TABLE 28.4. ACQUIRED COAGULATION DISORDERS

Liver disease
Deficiency of vitamin K-dependent factors
Hemorrhagic disease of the newborn
Biliary obstruction
Malabsorption of vitamin K (e.g. sprue, celiac disease)
Vitamin K-antagonist therapy (e.g. coumarins, indanediones)
Disseminated intravascular coagulation
Inhibition of coagulation
Specific inhibitors (e.g. antibodies against factor VIII components)
Nonspecific inhibitors (e.g. antibodies found in systemic lupus erythematosus, rheumatoid arthritis)
Miscellaneous
Diseases with M-protein production
L-Asparaginase
Therapy with heparin, defibrinating agents, or thrombolytics
Massive transfusion syndrome

to increased surgical bleeding and exacerbate hemorrhage from esophageal varices. Biliary obstruction results in impaired absorption of vitamin K and decreased synthesis of factors II, VII, IX, and X by the liver parenchymal cells. The hypersplenism associated with portal hypertension frequently results in thrombocytopenia. Patients in liver failure have deficiency of factor V and variable abnormalities of platelet function, and often produce functionally abnormal fibrinogen. As well as variceal bleeding and increased loss of blood during surgery, patients with severe liver disease can also develop spontaneous superficial hemorrhage (Figs. 28.36 and 28.37).

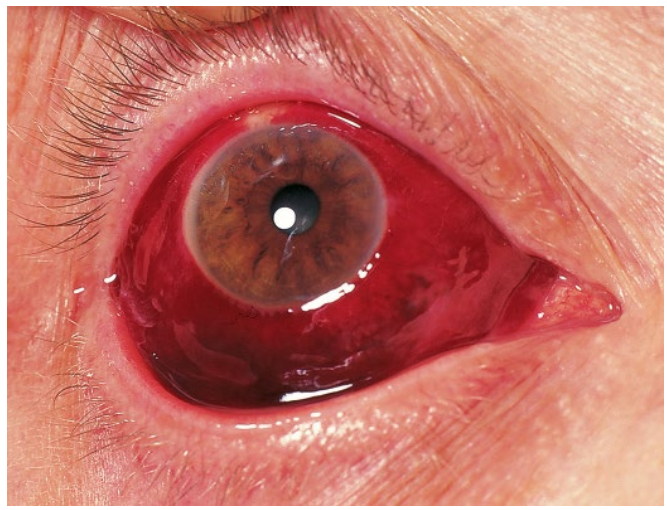

Fig. 28.36. Liver failure: Extensive subconjunctival hemorrhage.

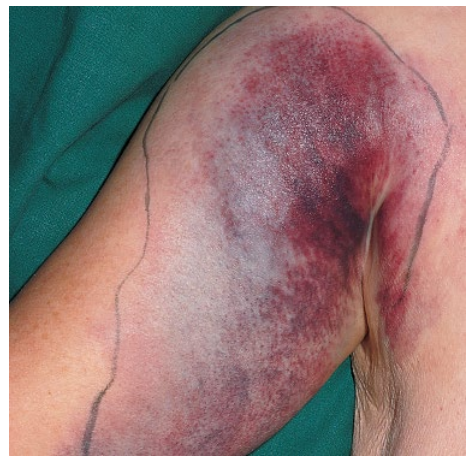

Fig. 28.37. Liver failure. Subcutaneous hemorrhage of the upper arm following minor trauma. Laboratory tests revealed deficiencies of factors II, VII, IX, and X, as well as dysfibrinogenemia.

OVERDOSAGE WITH ANTICOAGULANTS

Overdosage with oral anticoagulants that are vitamin K antagonists results in severe deficiencies of coagulation factors II, VII, IX, and X. Patients can have extensive skin bruising (Fig. 28.38) or severe internal bleeding (Fig. 28.39).

Similar skin lesions to those seen in homozygous protein C deficiency can occur in patients commencing anticoagulant therapy with coumarin drugs (Fig. 28.40). Selective severe protein C deficiency can occur temporarily before the levels of the vitamin K-dependent clotting factors fall (Fig. 28.40).

DISSEMINATED INTRAVASCULAR COAGULATION

A consequence of many disorders, DIC causes widespread endothelial damage, platelet aggregation, or release of procoagulant material into the circulation (Table 28.5). It is associated with widespread intravascular deposition of fibrin and consumption of coagulation factors and platelets (Fig. 28.41). This leads to both abnormal bleeding and widespread thrombosis, which is often fulminant (Figs. 28.42–28.45), although it can run a less severe, chronic course.

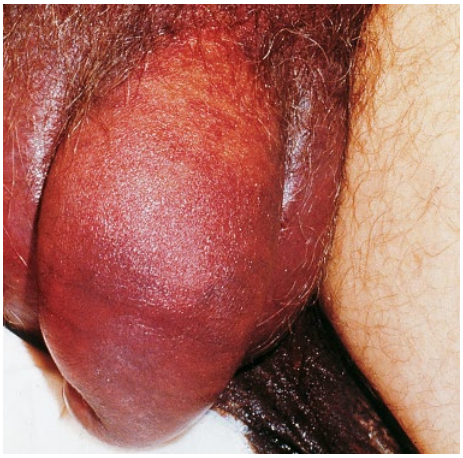

Fig. 28.38. Warfarin overdose. Massive subcutaneous hemorrhage over the penis, scrotal, and pubic areas following sexual intercourse.

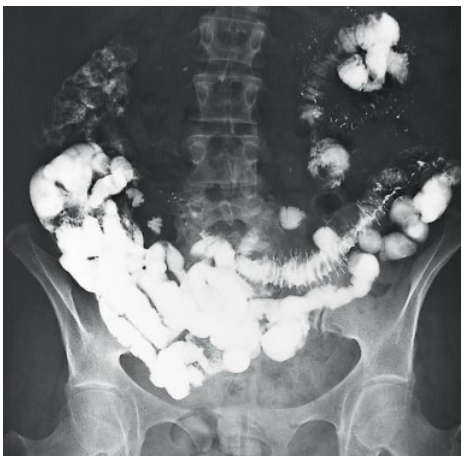

Fig. 28.39. Warfarin overdose. Radiograph shows intramural bleeding in the small intestine with the characteristic "stacked coin" pattern of barium distribution. (Courtesy of Dr. D Nag.)

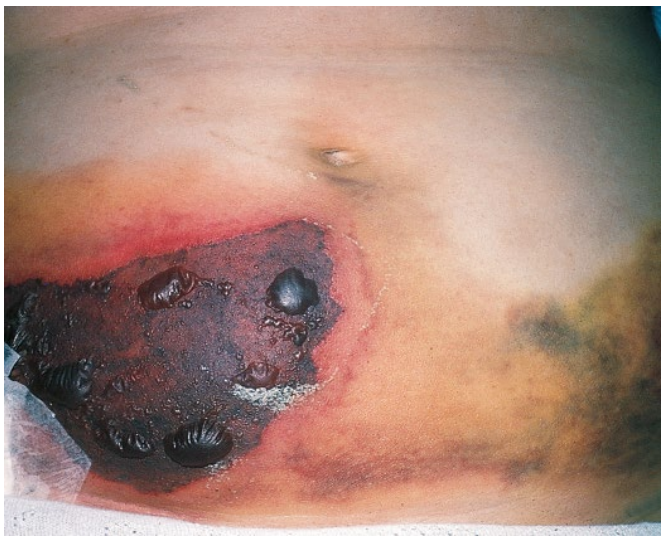

Fig. 28.40. Warfarin skin necrosis. These lesions over the abdomen developed in the first few days of warfarin therapy in a 40-year-old woman. Her protein C level was not measured but, in more recent examples of coumarin-induced skin necrosis, patients have been found to have reduced plasma levels of protein C. (Courtesy of Professor SJ Machin.)

TABLE 28.5. CAUSES OF DISSEMINATED INTRAVASCULAR COAGULATION

Infections	Hypersensitivity reactions
Gram-negative and meningococcal septicemia	Anaphylaxis
Septic abortion and *Clostridium welchii* septicemia	Incompatible blood transfusion
Severe falciparum malaria	**Widespread tissue damage**
Viral infection (purpura fulminans)	Following surgery or trauma
Malignancy	**Miscellaneous**
Widespread mucin-secreting adenocarcroma	Liver failure
Acute promyelocytic leukemia (AML M_3)	Snake and invertebrate venoms
Obstetric complications	Severe burns
Amniotic fluid embolism	Hypothermia
Premature separation of placenta	Heat stroke
Eclampsia; retained placenta	Hypoxia
	Vascular malformations (e.g. Kasabach–Merrit syndrome)

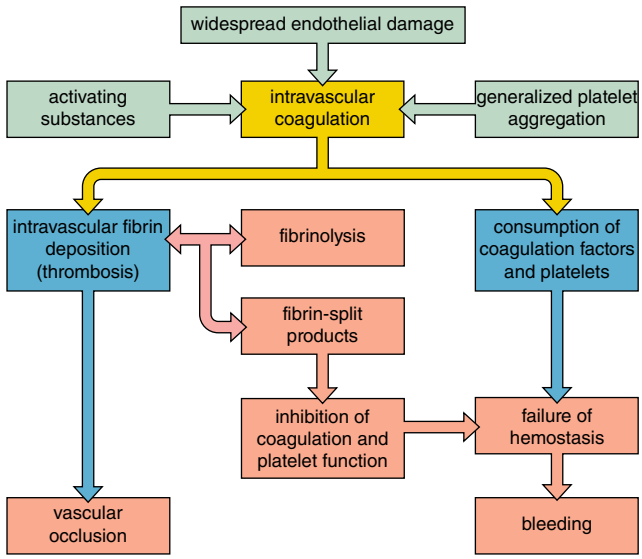

Fig. 28.41. Disseminated intravascular coagulation: Pathogenesis.

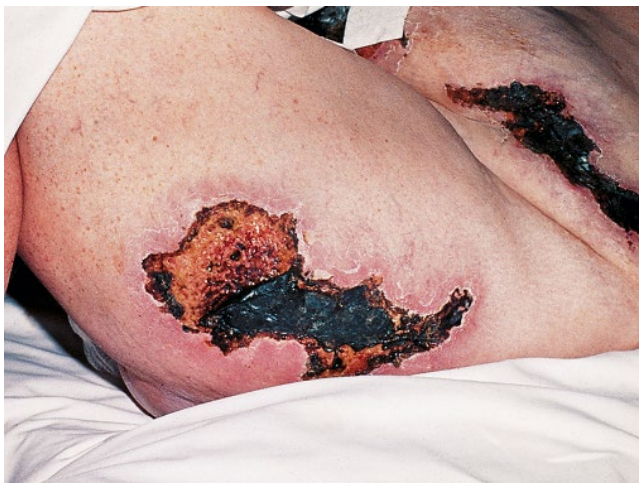

Fig. 28.42. Disseminated intravascular coagulation: Later stages of skin necrosis (same patient as shown in Fig. 28.44). Loss of superficial necrotic tissue over the thigh and lateral abdominal wall has left large, deep, irregular ulcers with hemorrhagic areas of exposed tissue. (Courtesy of Dr. BB Berkeley.)

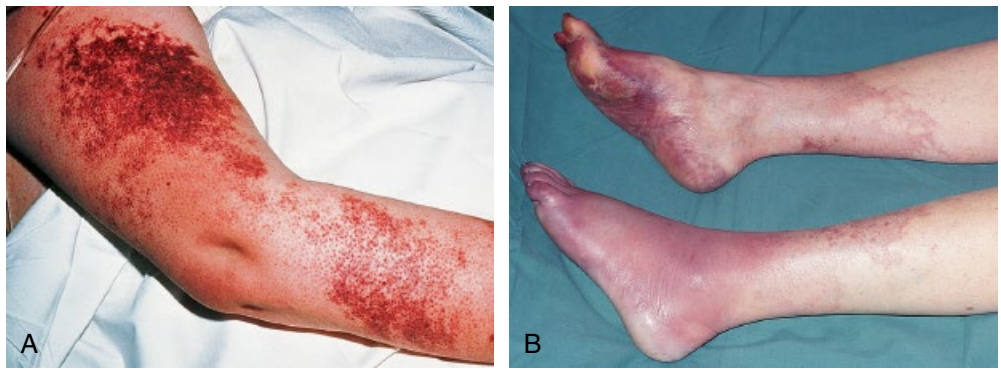

Fig. 28.43. Disseminated intravascular coagulation. **A,** Indurated and confluent purpura of the arm. **B,** Peripheral gangrene with swelling and discoloration of the skin of the feet in fulminant disease.

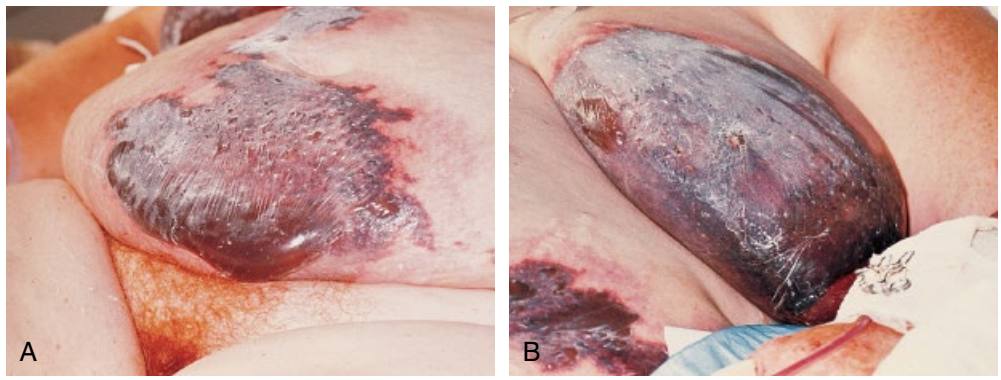

Fig. 28.44. Disseminated intravascular coagulation. Extensive necrosis of the skin and subcutaneous tissues of **(A)** the lower abdominal wall and **(B)** breast in a grossly obese patient (same patient as shown in Fig. 28.42). (*A, B,* Courtesy of Dr. BB Berkeley.)

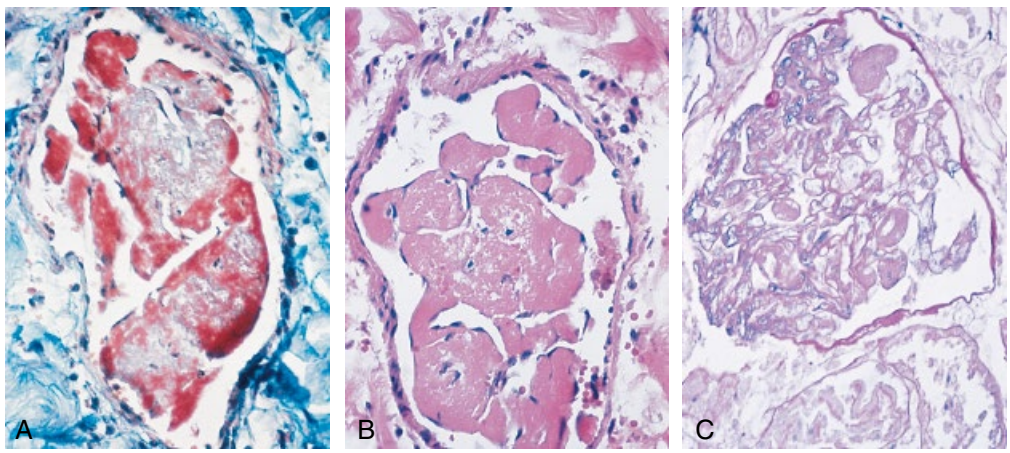

Fig. 28.45. Disseminated intravascular coagulation. **A, B,** Sections through a skin venule deep to an area of necrosis show occlusion by a thrombus composed mainly of fibrin. **C,** Necrosis of the glomerulus and the surrounding tubules with variable amounts of fibrinous material in the glomerular blood vessels. (*A,* Martius scarlet-blue; *B,* H&E; *C,* periodic acid–Schiff stains.)

In Kasabach–Merritt syndrome, a congenital hemangioma is associated with DIC (Fig. 28.46). The stimulus to intravascular coagulation is local, but the enhanced proteolytic activity of both coagulation and fibrinolytic systems probably becomes disseminated throughout the blood.

Meningococcal septicemia (Fig. 28.47) is classically associated with DIC, but purpura associated with other infections may be the result of toxic damage to the endothelium or of immune complex-type hypersensitivity. Necrosis can coexist with bleeding with varicella zoster infection (Fig. 28.48).

ACQUIRED COAGULATION FACTOR INHIBITOR

Occasionally, patients have a bleeding syndrome (Fig. 28.49) caused by circulating antibodies to coagulation factor VIII or to other clotting factors. These antibodies usually occur

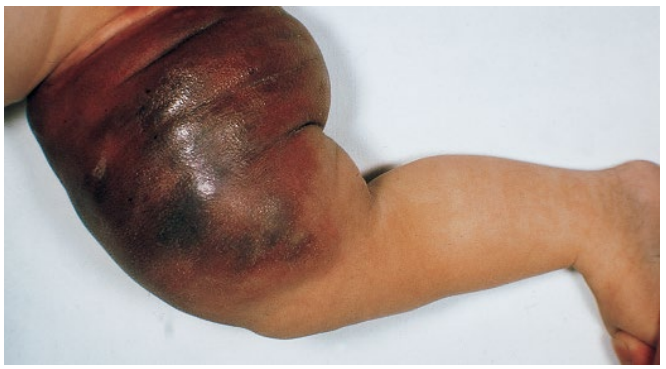

Fig. 28.46. Kasabach–Merritt syndrome. This giant congenital hemangioma of the thigh was associated with disseminated intravascular coagulation.

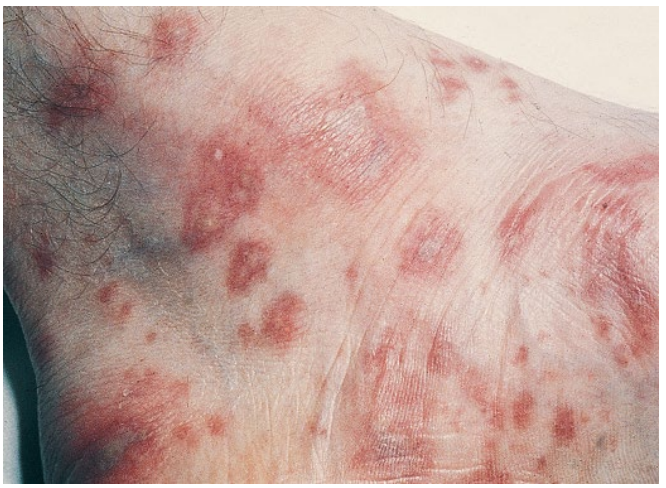

Fig. 28.47. Meningococcal septicemia. Typical purpuric skin lesions around the ankle in acute fulminating disease with disseminated intravascular coagulation.

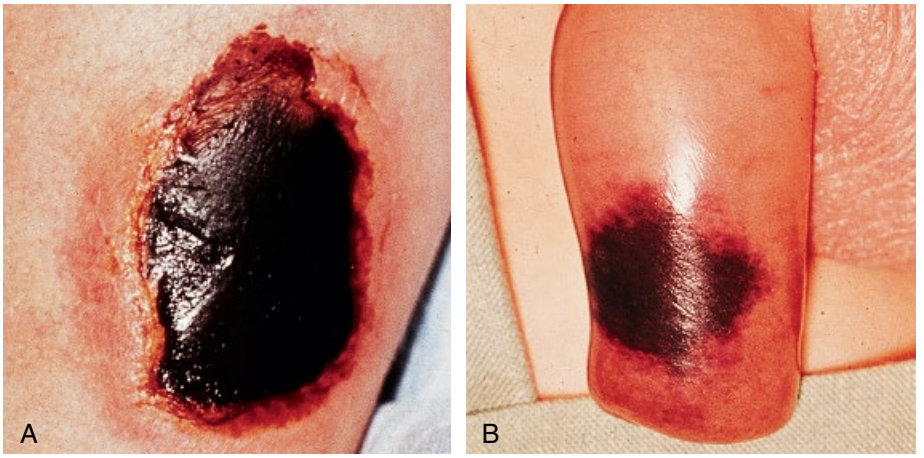

Fig. 28.48. Purpura fulminans. Large necrotic ecchymoses of skin of **(A)** the leg and **(B)** penis of an infant, following varicella infection. (A, B, Courtesy of Dr. MD Holdaway.)

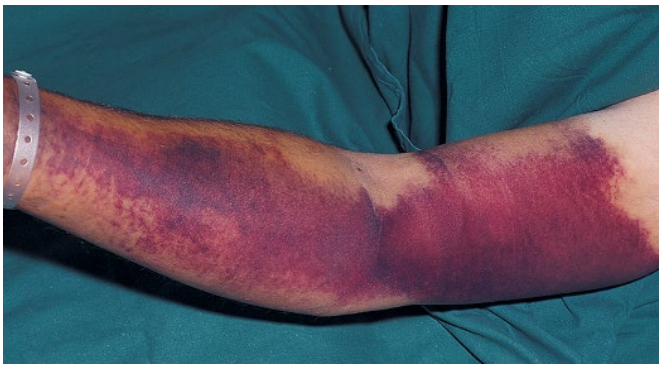

Fig. 28.49. Acquired coagulation factor inhibitor. Extensive subcutaneous and deep soft-tissue hemorrhage in the arm because of circulating autoantibody to factor VIII.

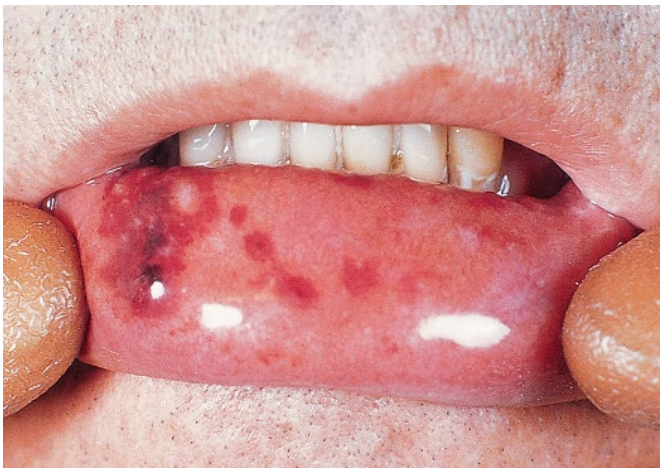

Fig. 28.50. Multiple myeloma: Purpuric haemorrhages in the mucosal surface of the lower lip.

postpartum, in systemic lupus erythematosus (SLE) associated with a malignancy, and in old age.

Patients with SLE, other autoimmune disorders, and, rarely, infections also develop a less specific inhibitor, immunoglobulin G (IgG) or immunoglobulin M (IgM), which is directed against phospholipid and is associated with a prolongation of the partial thromboplastin time not corrected by normal plasma. Paraproteins can also inhibit coagulation factor function (Fig. 28.50). Patients with this "lupus anticoagulant" may have no clinical symptoms, or have thrombosed arteries or veins or experience recurrent spontaneous abortions (see Chapter 29). Results of hemostasis tests in the major acquired coagulation disorders are shown in Table 28.6.

TABLE 28.6. HEMOSTASIS TESTS: TYPICAL RESULTS IN ACQUIRED BLEEDING DISORDERS

	Platelet count	Prothrombin time	Activated partial thromboplastin time	Thrombin time
Liver diseases	Low	Prolonged	Prolonged	Normal (rarely prolonged)
Disseminated intravascular coagulation	Low	Prolonged	Prolonged	Grossly prolonged
Massive transfusion	Low	Prolonged	Prolonged	Prolonged
Heparin	Normal (rarely low)	Mildly prolonged	Prolonged	Prolonged
Circulating anticoagulant	Normal	Normal or prolonged	Prolonged	Normal

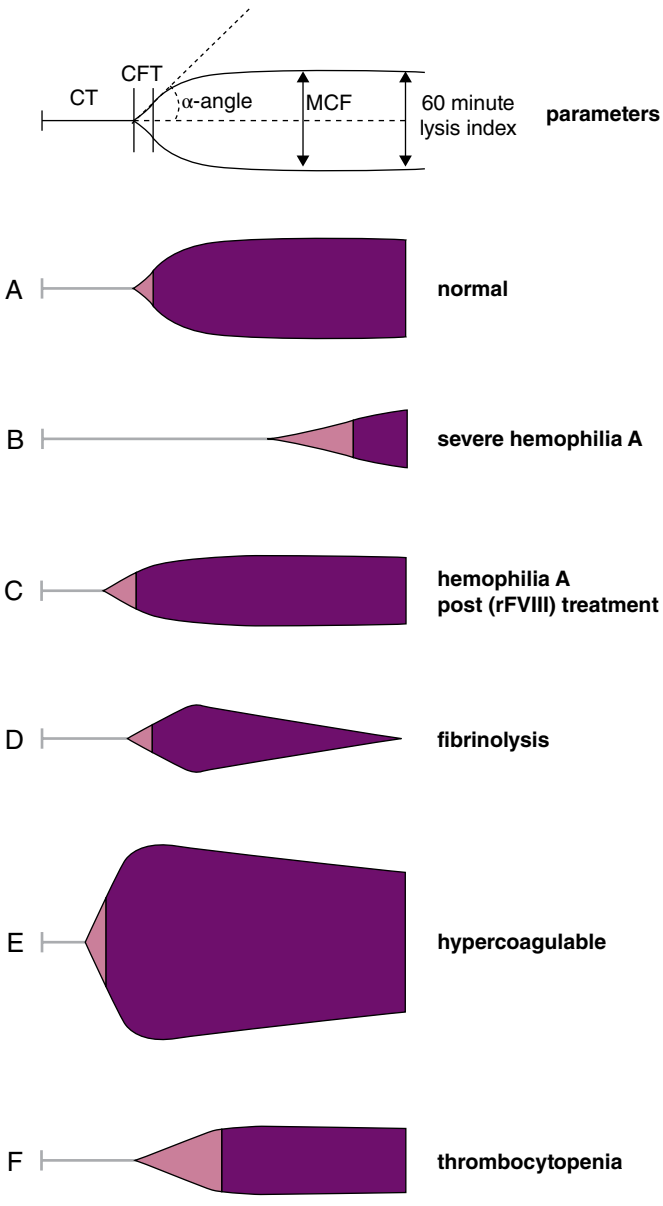

Fig. 28.51. Thromboelastometry (TEM). **(A)** Normal trace and appearance, in hemophilia **(B)** before and **(C)** after factor VIII infusion, **(D)** fibrinolysis (as in disseminated intravascular coagulation), **(E)** hypercoaguable states, and **(F)** thrombocytopenia. Parameter definitions: clotting time (CT), time until 2 mm clot firmness has been activated after the test has been started by the addition of a trigger; clot formation time (CFT), the kinetics of the formation of a stable clot from activated platelets and fibrin and is defined as the time elapsed between 2 and 20 mm clot firmness; alpha angle (°), alpha angle is a tangent to the clotting curve through the 2 mm point and describes the kinetics of clot formation. It is the angle between slope and baseline; clot formation rate (CFR), the tangent at the maximum slope; maximum clot firmness (MCF), the measure for the firmness of the clot and is measured at the maximum amplitude achieved during coagulation before fibrinolysis; lysis index (Ly60), degree of lysis that takes place after 60 minutes of clot time and is calculated as the ratio of the amplitude and the maximum firmness (percentage remaining clot firmness).

THROMBOELASTOMETRY AND THROMBOELASTOGRAPHY

Thromboelastometry (TEM) or thromboelastography (TEG) are used for global assessment of hemostatic function. Freshly drawn blood is placed in a cuvette. In TEM, rotational movement of a pin oscillated via an elastic string is detected by a light-sensitive sensor. The fibrin clot affects movement of the pin. Amplitude 0 mm means unobstructed rotation whereas amplitude 100 mm implies infinite firmness and choking the pin by the clot. The rate of initial fibrin formation, coagulation time, strength of fibrin clot, clot lysis index, or retraction is measured. Typical TEM results in different disorders are shown in Fig. 28.51.

CHAPTER

29 THROMBOSIS AND ANTITHROMBOTIC THERAPY

Intravascular thrombi have a basic structure of platelets and fibrin. Consequential ischemia from vascular obstruction or thrombotic embolism is of great clinical importance. Thrombus formation is the key pathogenic event in deep vein occlusion and pulmonary emboli. Abnormalities of the vessel wall are the main pathology underlying coronary artery, cerebrovascular, and peripheral arterial diseases.

ATHEROTHROMBOSIS

The pathogenesis of arterial atherosclerosis is illustrated in Fig. 29.1. Multiple factors contribute, including endothelial dysfunction, dyslipidemia and oxidation of low-density lipoprotein (LDL), intimal inflammation, platelet adhesion and aggregation, plaque rupture, and thrombosis. Increased endothelial permeability to lipoproteins is mediated by nitric oxide released by endothelial cells, prostacyclin, platelet-derived growth factor (PDGF), angiotensin II, and endothelin.

Oxidation of LDL in the subendothelial space stimulates monocyte chemotaxis, and phagocytosis of lipid by macrophages results in foam cells. Mitochondrial dysfunction, apoptosis, and necrosis of foam cells release cellular lysosomal proteases, inflammatory cytokines, tissue factor, and other prothrombotic factors. Migration of inflammatory cells into the intima is mediated by oxidized LDL, monocyte chemotactic protein I, interleukin 8, PDGF, and macrophage colony-stimulating factor (M-CSF). Following intimal migration and proliferation, smooth muscle cells become laden with lipid. Apoptosis of inflammatory cells and smooth muscle cells stimulates repair processes with increasing fibrous connective tissue contributing to the development of the fibrous cap and the atherosclerotic plaque.

With expansion, the intimal plaque develops its own microvascular network and plaque hemorrhage increases the size of the lesion. Regrowth of endothelium and repair processes at the site of overlying thrombus and its subsequent incorporation into the arterial wall contribute further to arterial thickening and restriction of the arterial lumen. Thinning of the fibrous cap, plaque rupture, and associated thrombosis lead to acute coronary occlusion, myocardial infarction, or stroke.

In addition to local arterial obstruction by the thrombus, emboli of platelet and fibrin thrombi can break from the primary thrombus and occlude distal arteries (e.g. emboli from carotid artery thrombi can cause cerebral thrombosis or transient ischemic attacks; heart valve and heart chamber thrombi can lead to systemic emboli and infarcts). Histology of a left coronary artery in a patient who died a sudden death is shown in Fig. 29.2.

Risk factors for arterial thrombosis and atherosclerosis are listed in Table 29.1. For coronary artery disease, risk profiling based on knowledge of the key modifiable factors has been useful in initiating therapeutic and lifestyle changes aimed at preventing or delaying the onset of clinical disease.

Arterial narrowing, thrombi, and emboli are readily identified by angiography (Figs. 29.3–29.5).

VENOUS THROMBOSIS

Many factors contribute to the pathogenesis of venous and arterial thrombosis, including genetic predisposition and many acquired risk factors. Venous thrombosis occurs most frequently in the calf veins and/or femoral and iliac veins and can be complicated by pulmonary embolism.

In the nineteenth century, Virchow proposed an important triad of factors that were important for thrombosis: reduced blood flow, vessel wall damage, and blood hypercoagulability. In most patients with venous thrombosis, vascular stasis and increased blood coagulability are most important and vessel wall damage is less important than in arterial disease. However, vascular damage can be important in patients with sepsis, trauma, or malignancy or in those with indwelling catheters. Stasis allows completion of blood coagulation at sites where thrombus formation is initiated (e.g. behind valve pockets of the leg veins in immobile patients).

THROMBOPHILIA

Many factors contribute to a genetic predisposition to venous thrombosis (Table 29.2). A hereditary risk factor should be suspected in patients with a first unprovoked venous thrombosis before 40 years of age. A family history of venous thrombosis in first degree relatives before 40 years of age may be relevant. The hereditary predisposition to venous thrombosis is often referred to as thrombophilia and is more common in venous thrombosis occurring in unusual sites such as cerebral venous

Color Atlas of Clinical Hematology: Molecular and Cellular Basis of Disease, Fifth Edition. A. Victor Hoffbrand, Paresh Vyas, Elías Campo, Torsten Haferlach, and Keith Gomez

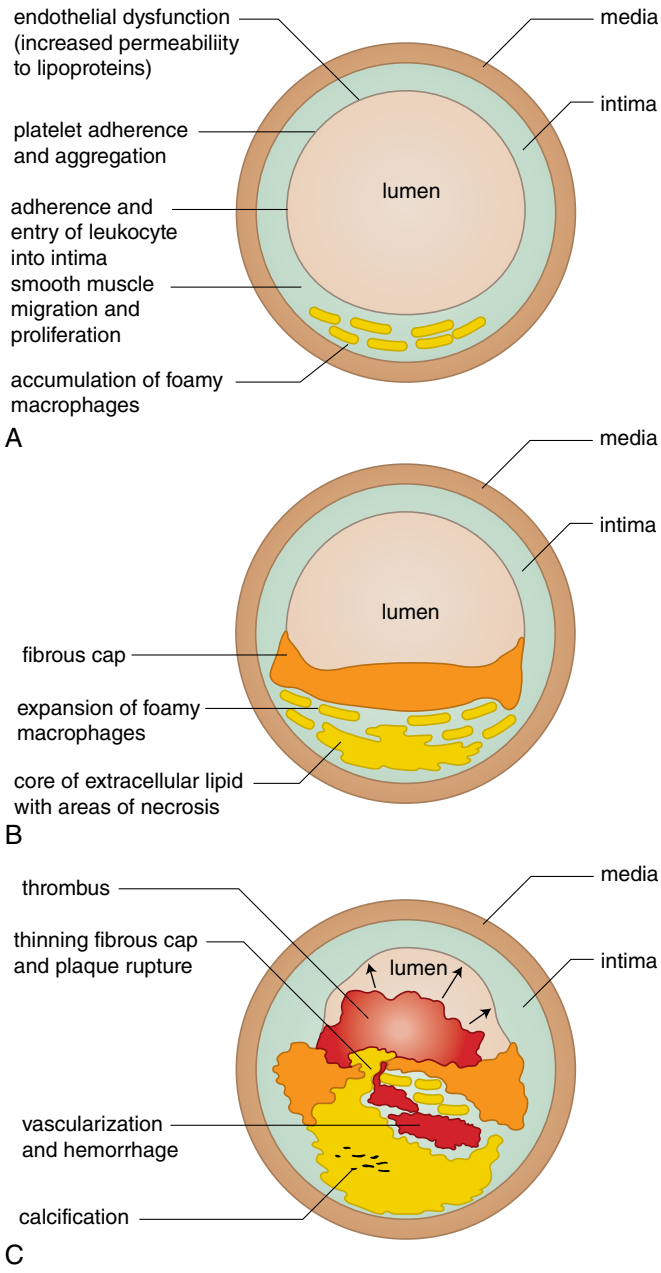

Fig. 29.1. Atherosclerosis: Pathogenesis of arterial lesion. **A,** Fatty streak stage. **B,** Atherosclerotic plaque. **C,** Complicated lesion with thrombosis.

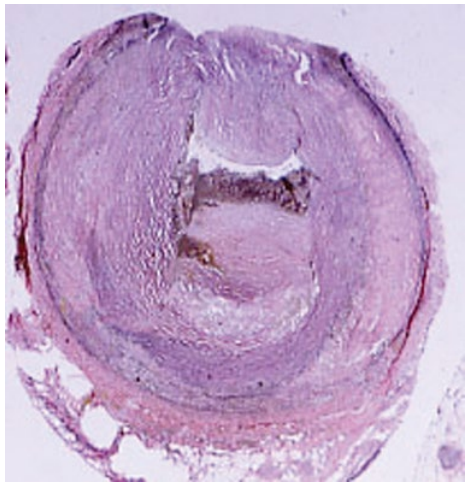

Fig. 29.2. Coronary artery atherosclerosis: Left coronary artery of a 51-year-old man who died suddenly. The lesion is complicated with gross sclerosis and thickening of the intima, plaque hemorrhage, and rupture with overlying thrombus. The lumen is almost completely occluded. (Elastic Van Giesen stain.) (Courtesy of Dr. K Anderson.)

TABLE 29.1. RISK FACTORS FOR ARTERIAL THROMBOSIS

Modifiable
Hypertension
Hyperlipidemia
Diabetes mellitus
Tobacco use
Obesity
Diet high in saturated fats
Physical inactivity
Non-modifiable
Age (>55 for women)
Male gender
Positive family history
Heritable rare disorders (e.g. Fabry disease, homocystinuria)
Acquired thrombotic conditions (e.g. lupus anticoagulant)

sinus thrombosis. It should be noted that there is no good evidence that these conditions are a significant risk factor in arterial thrombosis. The more severe thrombophilias increase the risk of recurrence of venous thrombosis and are an indication for lifelong anticoagulation.

Factor V Leiden

The factor V Leiden variant (R506Q) is the most common cause of thrombophilia and is detected in about 30% of patients with venous thrombosis. The abnormal factor V is resistant to the action of activated protein C.

The mutation occurs at the site at which activated protein C normally cleaves factor Va (Fig. 29.6). Heterozygosity for this disorder is as high as 8% in some white populations. The overall global prevalence is about 3% and different geographic regions are illustrated in Fig. 29.7. The risk of thrombosis in heterozygotes is only modestly increased to about four times greater than that of a control population so that only about 10% of heterozygotes develop a venous thrombosis at some point in their lifetime. In the homozygous form (1 in 5000) of factor V Leiden the risk rises to about 50-fold. There is similarly an increased risk of recurrent miscarriage. The risks are compounded with other risk factors, such as in women taking the contraceptive pill.

Protein C Deficiency

Protein C is a vitamin K-dependent plasma protein synthesized by the liver. Its active form inhibits the active forms of coagulation factors V and VIII, and also increases lysis of clots by inactivating a protein that normally destroys tissue plasminogen activator (tPA). Activation of protein C occurs via thrombin bound to a protein, thrombomodulin, on the surface of the endothelial cell (Fig. 29.8).

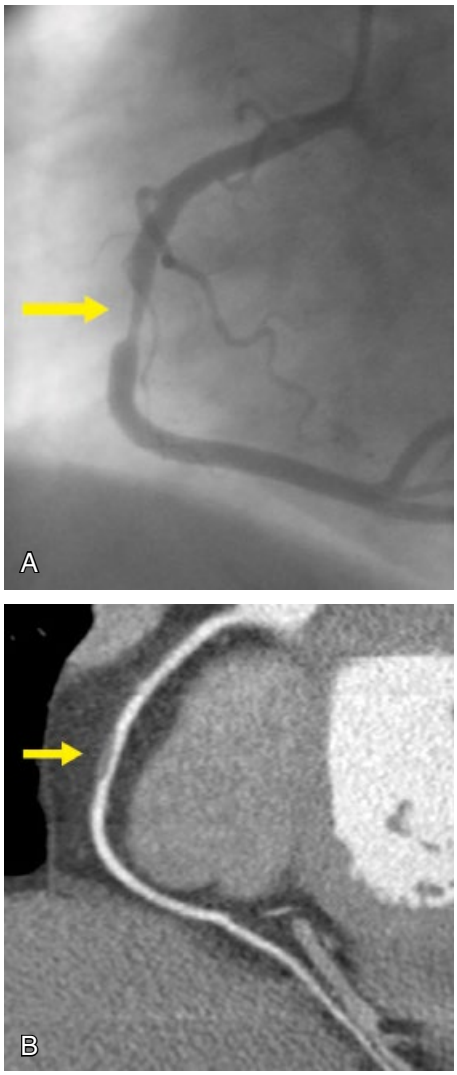

Fig. 29.3. Coronary artery atherosclerosis. A 43-year-old woman who had atypical chest pain and was at low risk for ischemic heart disease. Corresponding images of the right coronary artery from cardiac catheter **(A)** and computed tomography (CT) coronary angiography **(B)** demonstrate a noncalcified plaque resulting in 70% stenosis. (Courtesy of Dr. S MacDonald and Dr. T Young.)

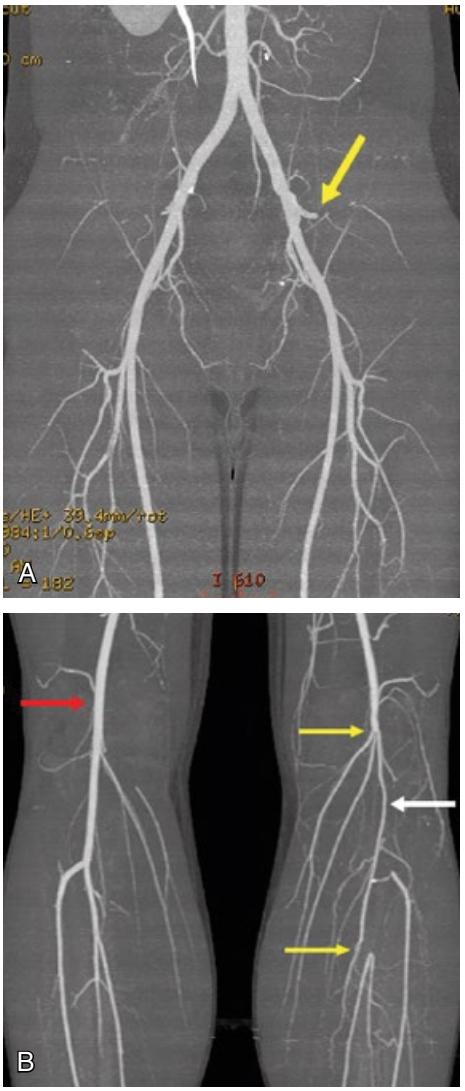

Fig. 29.4. Arterial thrombosis: Computed tomography arteriography. **A,** Embolic occlusion of left superior gluteal artery in a patient with endocarditis. **B,** Thrombotic occlusion of left popliteal artery (between *yellow arrows*) with collateral blood flow in the geniculate artery *(white arrow)* Right popliteal artery is normal *(red arrow)*. (Courtesy of Professor T Buchenham.)

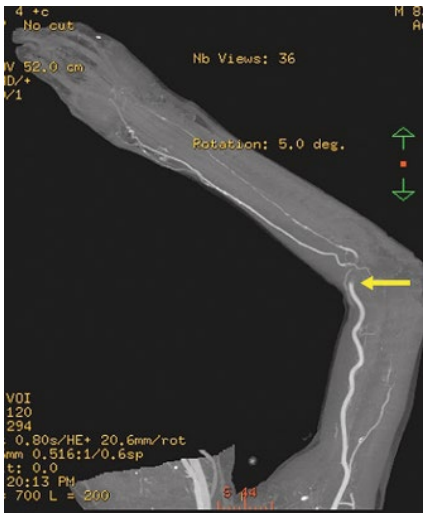

Fig. 29.5. Arterial thrombosis. Computed tomography arteriography showing thrombotic occlusion of the right brachial artery *(yellow arrow)*. (Courtesy of Professor T Buchenham.)

TABLE 29.2. CAUSES OF INHERITED THROMBOPHILIA

Established
Protein C deficiency
Protein S deficiency
Antithrombin deficiency
Activated protein C resistance (factor V Leiden: R506Q)
Elevated prothrombin levels (mutation G20210A)
Weak or unproven association
Dysfibrinogenemia
Elevated factor VIII levels
Heparin cofactor II deficiency
Plasminogen activator inhibitor 1 deficiency
Elevated homocysteine levels

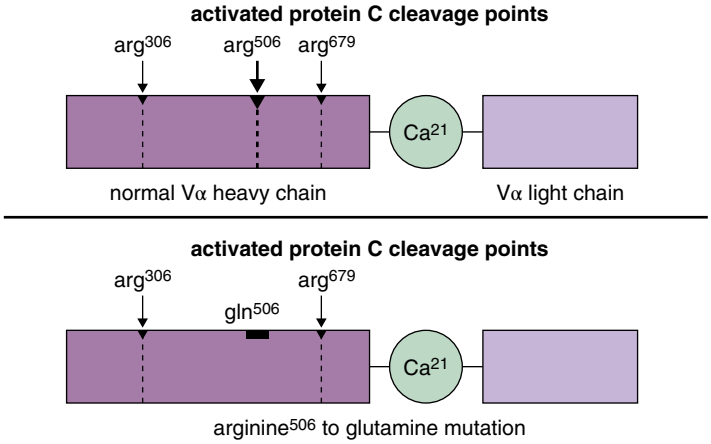

Fig. 29.6. Inactivation of factor Va. Activated protein C inactivates membrane-bound factor Va through proteolytic cleavage at three points in the Va heavy chain. In the factor V Leiden mutation, arginine at position 506 is replaced by glutamine, which renders this position resistant to activated protein C cleavage. The mutant factor V molecule can still be inactivated, but more slowly, at the remaining cleavage sites.

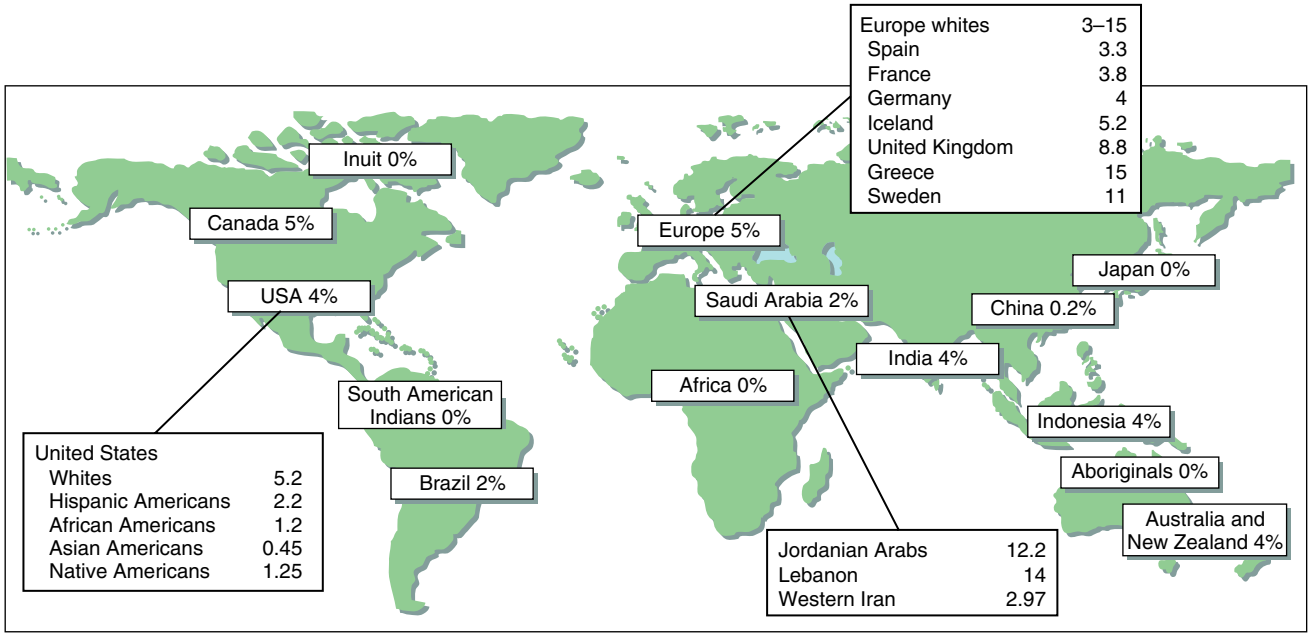

Fig. 29.7. Mutation *FV:R506Q:* Distribution in the world population. (Source: Modified with permission from Axelsson F, Rosén S. *Activated protein C resistance,* product monograph, Mölindal, Sweden, 1997, Chromogenix. Reproduced with permission of Walter Gruyter and Company.)

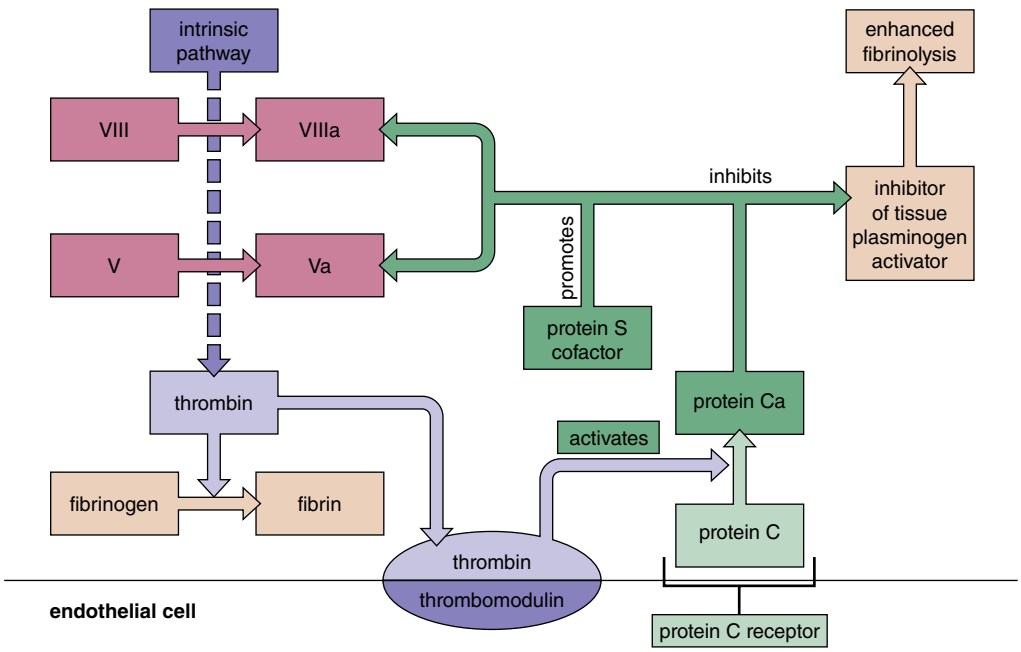

Fig. 29.8. Anticoagulant and fibrinolytic actions of protein C and protein S. a, Activated.

Heterozygous protein C deficiency predisposes affected individuals to recurrent venous thromboses, which tend to manifest at an early age, usually less than 30 years. Homozygous protein C deficiency results in neonatal purpura fulminans, characterized by superficial thromboses. The skin lesions are initially swollen and red or purple; they become blue–black and become necrotic (Fig. 29.9). The blood shows features of disseminated intravascular coagulation (DIC) with low levels of factors V and VIII, antithrombin, fibrinogen, and platelets. Activated protein C concentrate is an effective treatment for severe DIC. Although warfarin reduces levels of the functional form of protein C, it is still an effective long-term treatment for the prevention of thrombosis associated with this condition.

Protein S Deficiency

The anticoagulant activity of protein C requires a cofactor protein S, which is also vitamin K-dependent and exists in plasma as free and bound forms. Protein S deficiency, inherited probably as a dominant, causes recurrent venous thromboses.

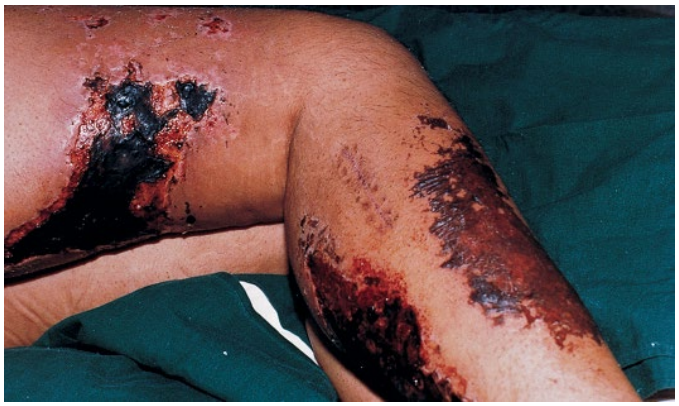

Fig. 29.9. Homozygous protein C deficiency. The patient, a 15-year-old girl, had skin necrosis and multiple venous thrombosis at 2 years of age.

Antithrombin Deficiency

Antithrombin is a potent inhibitor of activated serine proteases particularly factor Xa and thrombin and to a lesser extent factors IXa and XIa. It forms irreversible inactivating macromolecular complexes with these proteins and this action is enhanced by endogenous heparinoids. Deficiency of antithrombin leads to recurrent venous thromboses that tend to be severe and manifest early in the homozygous form. Some patients are resistant to the effect of heparin but treatment with oral anticoagulants is effective. Antithrombin concentrate can be used for short-term risks such as surgery. Reduced antithrombin levels can be seen in nephrotic syndrome.

Hyperhomocysteinemia

Extremely high levels of homocysteine are a contributing factor in thrombosis and vascular disease, including peripheral vascular disease, myocardial infarct, stroke, and venous thrombosis. This is usually only seen with rare genetic variants in the enzymes involved in homocysteine metabolism, such as cystathionine β-synthase, as part of a multisystem disorder associated with learning disabilities and musculoskeletal abnormalities (Fig. 29.10). Mild elevations of homocysteine associated with common variants in the gene for methylene tetrahydrolate reductase (*MTHFR)* are seen in about 5% of the population but extensive studies have shown that these have only a mild effect on the risk of thrombosis. Deficiencies of folate, vitamin B_{12}, and vitamin B_6 also cause mild hyperhomocysteinemia and supplementation with these vitamins can reduce levels but has no effect on the risk of recurrence of thrombosis. The plasma level of homocysteinemia rises with age, is higher in men than in premenopausal women, and is raised after liver or renal transplantation.

Hyperprothrombinemia

A variant in the 3′ untranslated region of the prothrombin gene, *G20210A*, causes mild elevations in prothrombin probably by increasing mRNA stability. This is seen almost exclusively in Caucasian populations where it has a prevalence of about 3% and slightly increases the risk of venous thrombosis.

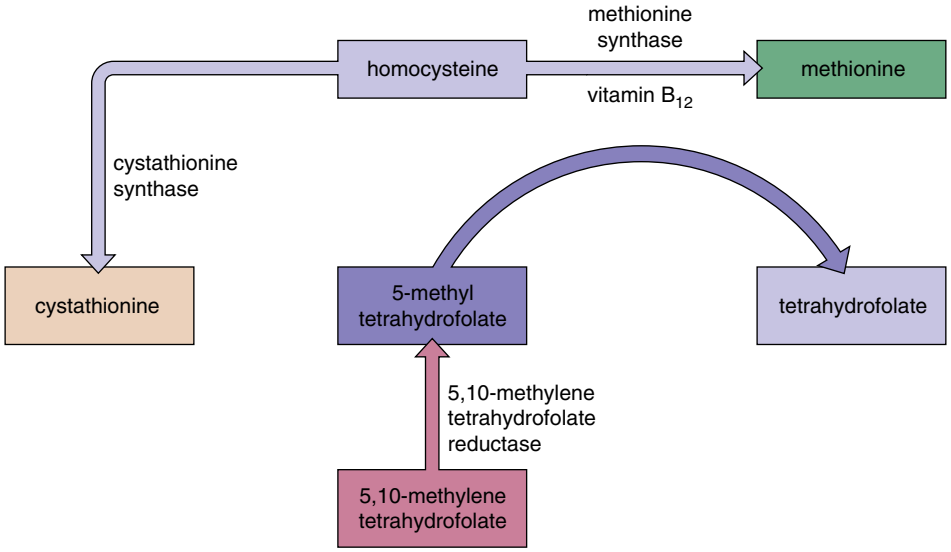

Fig. 29.10. Homocysteine metabolism. The roles of methionine synthase, cystathionine synthase, and 5,10-methylene tetrahydrofolate reductase (see also Chapter 7).

Other Disorders

Although there are associations between thrombotic risk and high factor VIII levels, deficiency of heparin cofactor II and plasminogen, as well as other fibrinolytic defects, the evidence for familial thrombophilia as a result of these conditions is inconclusive. Dysfibrinogenemia is rarely a cause of thrombophilia.

ACQUIRED RISK FACTORS FOR VENOUS THROMBOSIS

Prominent acquired risk factors for venous thrombosis are listed in Table 29.3. These can be responsible for thrombosis in patients without another identifiable risk factor, but thrombosis is more likely if an inherited predisposition is also present.

Venous stasis and immobility are responsible for high rates of venous thrombosis in congestive heart failure, myocardial infarction, and varicose veins. In atrial fibrillation, thrombin generation from accumulated activated coagulation factors can lead to a high risk of systemic embolism. Venous stasis and immobility are also responsible for thrombosis associated with prolonged air, road, or rail travel.

Malignant tumors release tissue factors and a procoagulant that directly activates factor X. Deep vein thrombosis (DVT) is associated particularly with ovarian, pancreatic, and cerebral tumors.

TABLE 29.3. ACQUIRED RISK FACTORS FOR VENOUS THROMBOSIS

Active cancer or cancer treatment
Age over 50
Immobility >3 days
Lupus anticoagulant
Obesity (BMI >30 kg/m^2)
Drugs:
Estrogen therapy (oral contraceptive and hormone replacement therapy)
Acitvated clotting factors
Thalidomide and analogues
Pregnancy and puerperium
Trauma and surgery
Dehydration
Inflammatory conditions
Cardiovascular disease
Varicose veins with phlebitis
Hyperviscosity states
Myeloproliferative disorders
Pelvic obstruction
Heparin-induced thrombocytopenia
Activated coagulation factor concentrates
Glucosylceremide deficiency
Paroxysmal nocturnal hemoglobinuria
Behçet syndrome
Smoking
Flights longer than 3 hours

Postoperative thrombosis is more likely in orthopedic and abdominal surgery and in the obese, the elderly, or those with a previous history or family history of thrombosis.

Thrombosis in inflammation can be related to increased activity of procoagulant factors and is particularly associated with systemic tuberculosis, inflammatory bowel disease, systemic lupus erythematosus (SLE), and Behçet's disease.

Increased viscosity, thrombocytosis, and platelet function defects contribute to a high incidence of thrombosis in patients with myeloproliferative disorders.

Estrogen therapy (particularly high-dose contraceptive or hormone replacement therapy) is associated with increased thrombosis risk. These patients have elevated levels of coagulation factors II, VII, VIII, IX, and X and decreased plasma levels of antithrombin and tPA.

Thrombosis following the administration of activated clotting factors to treat bleeding is particularly seen in patients with liver disease who are unable to clear these activated factors promptly.

ANTIPHOSPHOLIPID SYNDROME

In this syndrome, arterial or venous thrombosis or recurrent miscarriage is associated with laboratory evidence of persistent antiphospholipid antibodies. The "lupus anticoagulant" is identified when prolongation of the activated partial thromboplastin time (APTT) is not corrected by the addition of normal plasma. Other antibodies are anticardiolipin and antibodies to β_2-GPI. The reaction on the platelet surface is thrombogenic, even though coagulation tests such as the APTT appear to show anticoagulation. These antibodies were first described in SLE and other autoimmune disorders. They also occur in lymphoproliferative disorders and with drugs such as phenothiazines, or they may be primary or idiopathic. The most common cause is a transient rise following viral or other infections which is not pathogenic. In addition to thrombosis and recurrent miscarriage, the antiphospholipid antibodies can be associated with persistent or relapsing thrombocytopenia and the skin condition, livedo reticularis.

DIAGNOSIS OF VENOUS THROMBOSIS

CLINICAL PROBABILITY ASSESSMENT

DVT is suspected in patients with calf swelling or tenderness, unilateral pitting edema, and the presence of collateral superficial nonvaricose veins. Previous DVT, immobility, and cancer are important associations. A number of clinical probability assessments have been proposed. The modified Wells score (Table 29.4) is used in acute clinical presentations to predict the likelihood of leg DVT. The diagnosis should be confirmed by imaging such as with Doppler ultrasound scan. In low-probability patients, the median negative predictive value was 96%. Positive predictive values for high-probability patients were less than 75%.

D-Dimer Assay

After the stabilization of fibrin monomer by the action of activated factor XIII, covalent bonds between adjacent D-domains produce cross-linked fibrin. During fibrinolysis proteolytic cleavage of cross-linked fibrin by plasmin produces a heterogeneous group of degradation products, the smallest of which is D-dimer (Fig. 29.11). The immunoassay for D-dimer is

fibrin specific because D-dimer is not found in fibrinogen or in proteolytic fragments of fibrinogen. Elevated levels of D-dimer are almost invariably found when there is recent venous thrombosis or pulmonary embolism. The test has excellent negative predictive value and is most useful to exclude a diagnosis of DVT in patients with equivocal clinical features. In trials a negative D-dimer result in these patients was associated with a median negative predictive value of 99%. D-dimer testing in high-risk patients is not useful because most will have a positive result and will require radiologic imaging regardless of the result.

D-dimer elevation in elderly patients, trauma, postsurgery and delivery, cancer, and inflammation limits its usefulness in hospital patients.

Ultrasound and Radiologic Imaging

Serial compression ultrasound is a reliable and practical method for detecting DVT in the thigh and other sites. The main signs are the absence of flow on color Doppler and an inability to compress the vein (Fig. 29.12). DVT in the popliteal and calf veins can also be detected by contrast computed tomography (CT) scanning (Fig. 29.13). Contrast venography (Figs. 29.14 and 29.15) has been largely replaced by Doppler scanning but remains a very sensitive technique to demonstrate the site, size, and extent of the thrombus. It is often a painful technique and carries a risk of procedure-induced DVT. Both contrast venography and CT scanning have been used in diagnosis of venous thrombosis in other sites (e.g. hepatic) (Figs. 29.16 and 29.17).

A possible diagnostic approach for DVT is shown in Fig. 29.18.

TABLE 29.4. CLINICAL ASSESSMENT OF DEEP VENOUS THROMBOSIS (DVT): THE WELLS SCORE

	Points
Active cancer (treatment ongoing or within previous 6 months or palliative)	1
Paresis or plaster immobilization of lower limb	1
Bedridden for more than 3 days, major surgery within 4 weeks	1
Tenderness along veins	1
Entire leg swollen	1
Calf swelling at least 3 cm larger than asymptomatic side	1
Pitting edema confined to the symptomatic leg	1
Collateral superficial veins (nonvaricose)	1
Previously doucmented DVT	1
Alternative diagnosis at least as likely as DVT	–2
Clinical Probability Score	
DVT likely	2 or more points
DVT unlikely	1 point or less

Source: Wells PS, et al. *N Engl J Med* 2003;349:1227. Reproduced with permission of Massachusetts Medical Society: The New England Journal of Medicine.

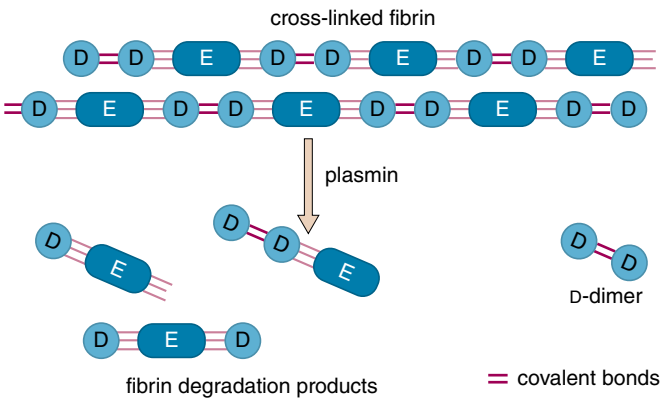

Fig. 29.11. Venous thrombosis: The formation of D-dimer.

DIAGNOSIS OF PULMONARY EMBOLUS

CLINICAL ASSESSMENT

A sudden onset of dyspnea is the usual presenting symptom. Oppressive substernal pain is a feature of massive embolism. Pleuritic chest pain and hemoptysis occur only after infarction has occurred. Physical examination can be deceptively normal. In massive embolism, signs include a palpable lift over the right ventricle at the left sternal edge and right ventricular gallop.

A pleural friction rub and signs of pleural effusion will not be present unless infarction has occurred. Electrocardiography can show evidence of right-sided heart strain in relatively severe cases. Chest x-rays are often normal but can show evidence of pulmonary infarcts or pleural effusion.

CT pulmonary angiography is an accurate and rapid way to diagnose pulmonary embolism and has virtually replaced conventional pulmonary angiography. Patients in whom contrast should be avoided (e.g. pregnant women) can be diagnosed using nuclear medicine ventilation–perfusion scans. Although less sensitive for small emboli, it has been argued that the greater sensitivity of CT pulmonary angiography leads to the diagnosis of clinically insignificant, incidental subsegmental emboli. The emboli are visualized as filling defects within the contrast-filled pulmonary arteries (Figs. 29.19 and 29.20). Gallium-enhanced magnetic resonance imaging (MRI) is a relatively new and expensive technique, but it is accurate.

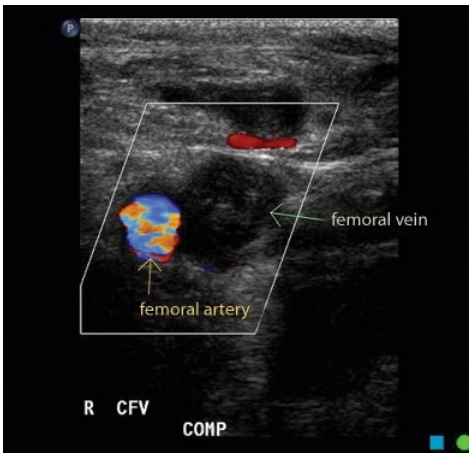

Fig. 29.12. Deep vein thrombosis. Color power Doppler ultrasound of right femoral vessels with compression showing normal flow in the femoral artery but absent flow in the vein because of thrombosis. A normal vein would collapse with compression of the probe. (Courtesy of Dr. T Young.)

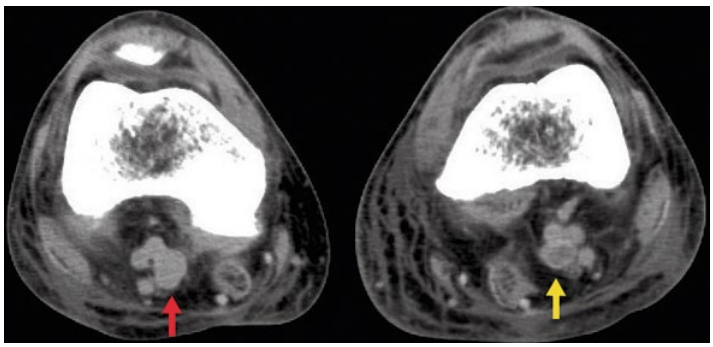

Fig. 29.13. Deep vein thrombosis. Computed tomography scan of the popliteal region following intravenous injection of contrast. There is normal enhancement of veins on the *right (red arrow)*. The *left* image shows a peripheral rim of enhancement surrounding thrombus within the popliteal vein *(yellow arrow)*. (Courtesy of Dr. S MacDonald.)

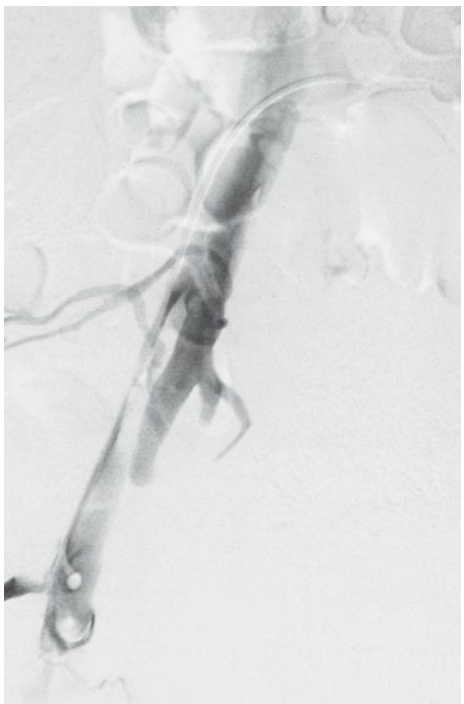

Fig. 29.14. Deep vein thrombosis. A femoral venogram demonstrating extensive thrombus within the right external iliac vein extending into the right common iliac vein. (Courtesy of Dr. IS Francis and Dr. AF Watkinson.)

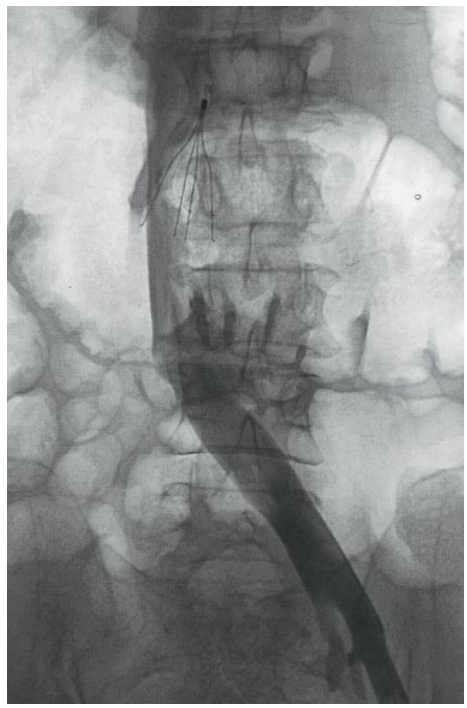

Fig. 29.15. Deep vein thrombosis. A Gunther–Tulip filter positioned within the infrarenal inferior vena cava to prevent pulmonary embolism. Percutaneous access is via either the femoral or internal jugular vein. This particular device has a proximal hook, which permits its removal up to 2 weeks following placement. (Courtesy of Dr. IS Francis and Dr. AF Watkinson.)

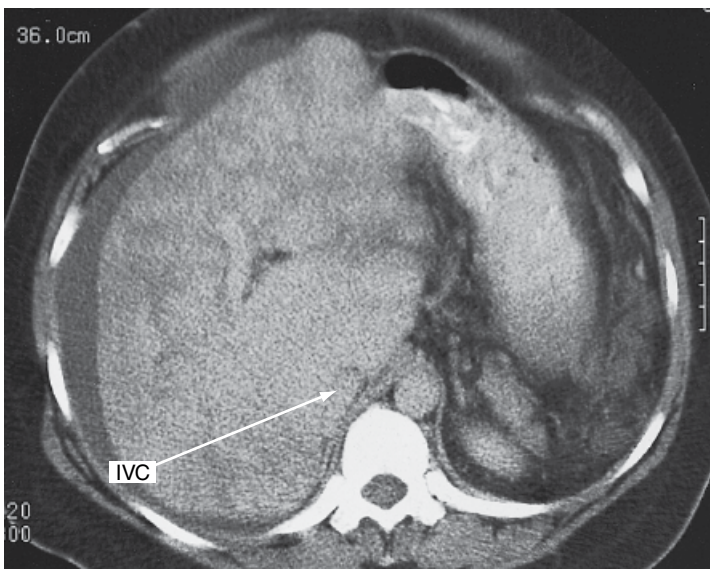

Fig. 29.16. Hepatic veno-occlusive disease (Budd–Chiari syndrome). Dynamic contrast-enhanced computed tomography showing the reticulated mosaic pattern of hepatic parenchymal enhancement with poor visualization of the hepatic veins. Typically, the caudate lobe enhances normally and appears hyperdense relative to the remaining liver parenchyma. Ascites is present, and the inferior vena cava is narrowed. (Courtesy of Dr. IS Francis and Dr. J Tibballs.)

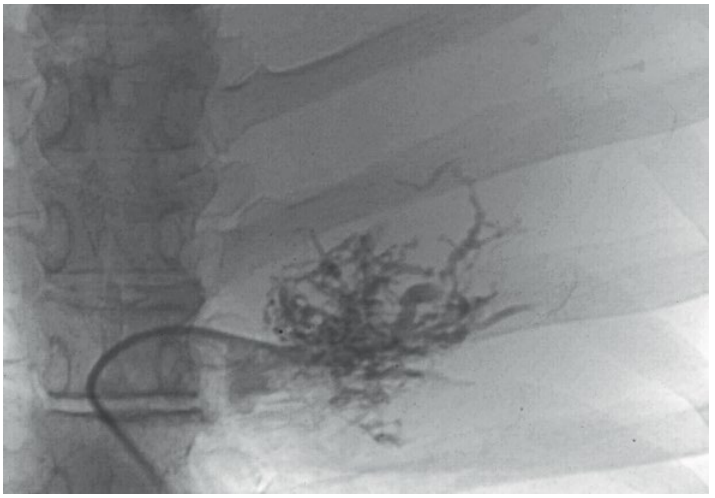

Fig. 29.17. Hepatic veno-occlusive disease (Budd–Chiari syndrome). Using a transjugular approach, a catheter was introduced into the right hepatic vein. Direct injection of contrast shows a characteristic interlacing network of intrahepatic, portal and hepatic veins, with no flow exiting via the hepatic veins. This "spider web" appearance is unique to Budd–Chiari syndrome. (Courtesy of Dr. IS Francis and Dr. J Tibballs.)

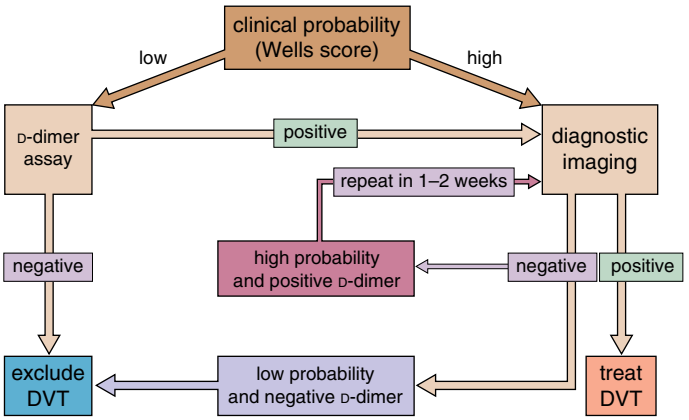

Fig. 29.18. Deep vein thrombosis (DVT): An approach to diagnosis.

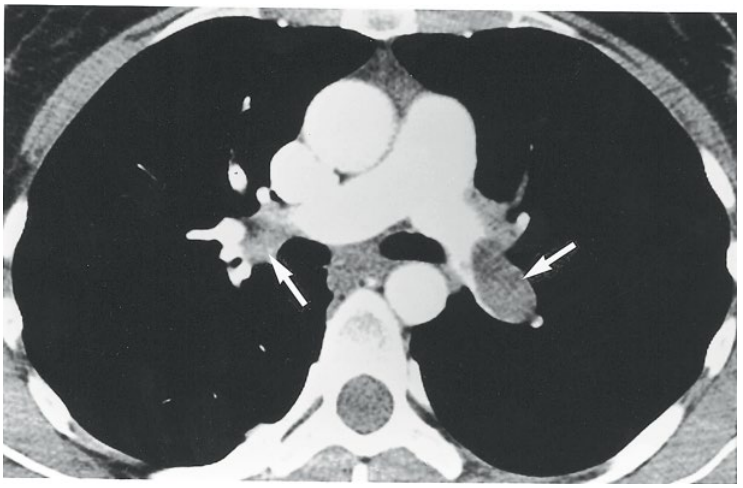

Fig. 29.19. Pulmonary embolus. Contrast-enhanced spiral computed tomography that shows filling defects within both main pulmonary arteries *(arrows)*. These represent large pulmonary emboli. (Courtesy of Professor DM Hansell.)

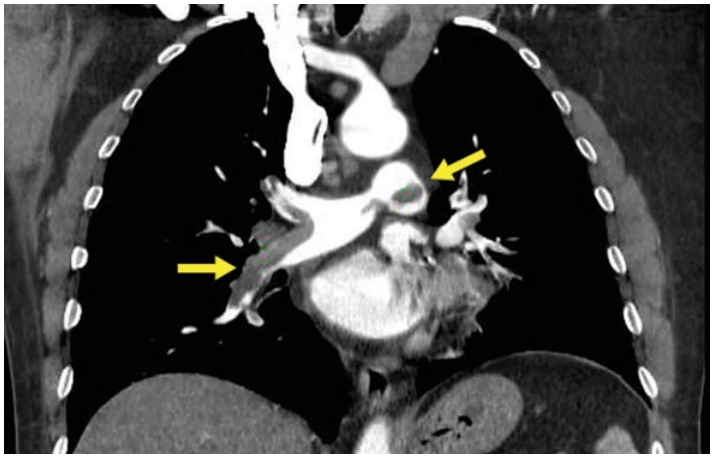

Fig. 29.20. Pulmonary embolus. Computed tomography pulmonary angiography. A coronal image shows bilateral filling defects in the central pulmonary arteries indicating pulmonary emboli *(yellow arrows)*. (Courtesy of Dr. T Young.)

ANTIPLATELET DRUGS

The action of antiplatelet drugs is depicted in Fig. 29.21.

ASPIRIN

Aspirin inhibits platelet cyclo-oxygenase irreversibly, thus reducing the production of platelet thromboxane A2. It has been suggested that vascular endothelial cyclo-oxygenase is less sensitive to aspirin than platelet cyclo-oxygenase. Low-dose therapy (e.g. 75 mg/day) is more effective than standard doses at enhancing the prostacyclin : thromboxane A2 ratio and can have a greater antithrombotic effect. Aspirin is now used widely in the prevention of coronary, cerebrovascular, and peripheral arterial disease, as well as in patients who have a history of these conditions. It is also useful in preventing thrombosis in patients with thrombocytosis.

DIPYRIDAMOLE (PERSANTIN)

This drug is a phosphodiesterase inhibitor thought to elevate cyclic adenosine monophosphate (cAMP) levels in circulating platelets, which decreases their sensitivity to activating stimuli. Dipyridamole has been shown to reduce thromboembolic complications in patients with prosthetic heart valves and to improve the results in coronary bypass operations.

ADP RECEPTOR INHIBITORS

Generally, these are from the thienopyridine class of drugs and the first two agents to gain widespread use were ticlopidine and clopidogrel. Side effects of ticlopidine include neutropenia and thrombocytopenia. It has largely been replaced by clopidogrel except in patients intolerant of clopidogrel. This adenosine diphosphate (ADP) receptor antagonist is an antiplatelet agent in use for reduction of ischemic events in patients with ischemic stroke, myocardial infarction, or peripheral vascular disease. It is used after coronary artery stenting or angioplasty (often in combination with aspirin) and in patients requiring long-term antiplatelet therapy who are intolerant of or allergic to aspirin.

Newer ADP receptor blockers are prasugrel and ticagrelor. Although these seem to have enhanced efficacy in some settings this may be at the risk of more bleeding.

GLYCOPROTEIN IIB/IIIA INHIBITORS

Abciximab, eptifibatide, and tirofiban are monoclonal antibodies that inhibit the platelet GPIIb-IIIa complex, a member

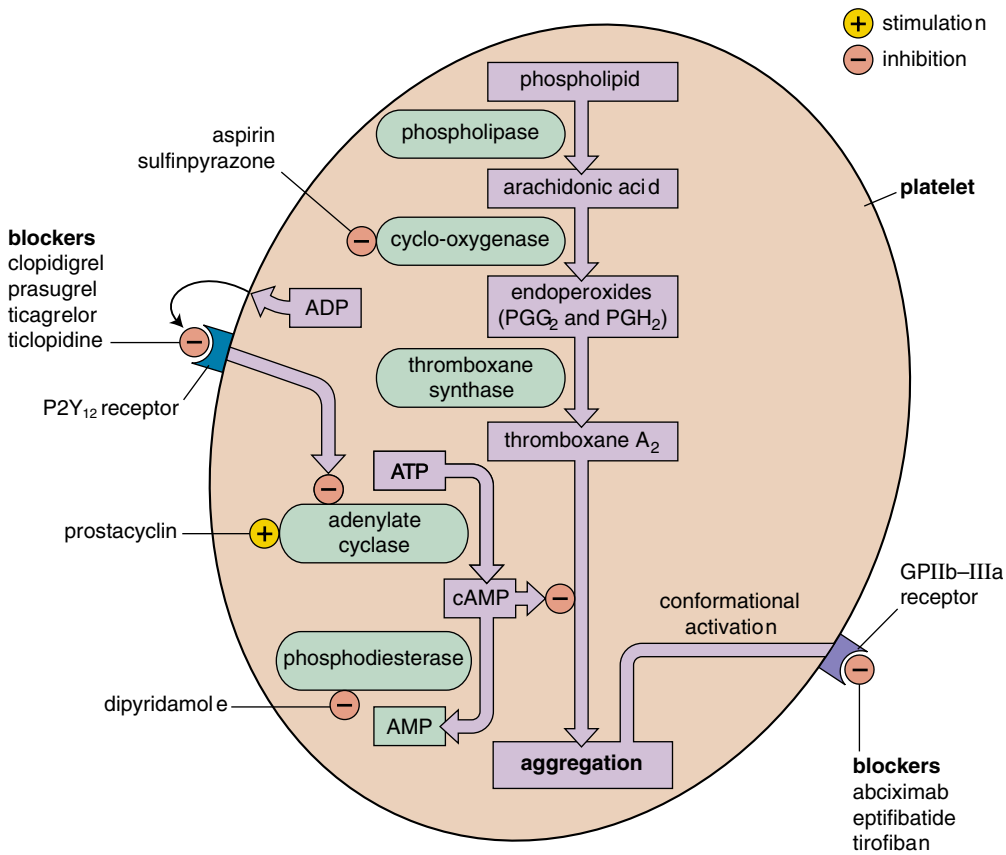

Fig. 29.21. Sites of action of antiplatelet drugs. Aspirin acetylates the enzyme cyclo-oxygenase irreversibly. Sulfinpyrazone inhibits cyclo-oxygenase reversibly. Dipyridamole inhibits phosphodiesterase, increases cyclic adenosine monophosphate (cAMP) levels, and inhibits aggregation. Inhibition of adenosine uptake by red cells allows adenosine accumulation in plasma, which stimulates platelet adenylate cyclase. Prostacyclin stimulates adenylate cyclase. ADP receptor blockers inhibit at the $P2Y_{12}$ receptor thereby limiting the inhibitory effect of ADP on adenylate cyclase. Three GP IIb/IIIa blockers are licensed for human use: abciximab, eptifibatide, and tirofiban. The lipid-soluble β-blockers inhibit phospholipase. Calcium channel antagonists block the influx of free calcium ions across the platelet membrane. Dextrans coat the surface, interfering with adhesion and aggregation. ADP, adenosine diphosphate; ATP, adenosine triphosphate; PG, prostaglandin. (Source: Modified from Hoffbrand AV, Pettit JE. *Essential Hematology,* 3rd edn. Blackwell Scientific, Oxford, 1993. Reproduced with permission of John Wiley and Sons.)

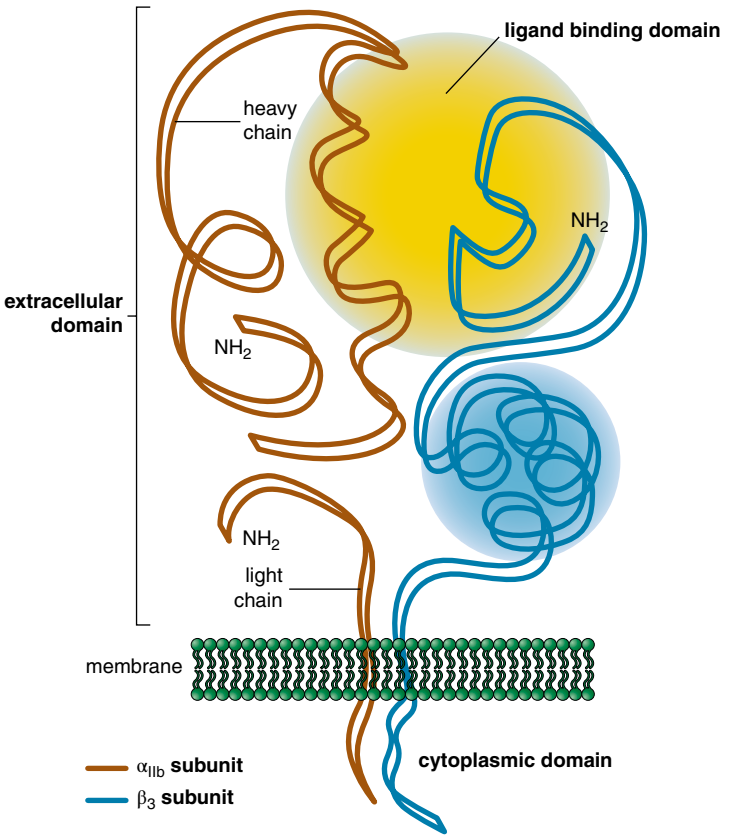

Fig. 29.22. The platelet GPIIb-IIIa complex. (Source: Modified with permission from Topol EJ, et al. *Lancet* 1999;353:227–231. Reproduced with permission of Elsevier.).

of the integrin family of receptors (Fig. 29.22). They are used in conjunction with heparin and aspirin for the prevention of ischemic complications in high-risk patients undergoing percutaneous transluminal coronary angioplasty and in those with an acute coronary syndrome. They can be used once only. A summary of antiplatelet therapy in acute coronary syndromes is tabulated in Table 29.5.

PROSTACYCLIN

Intravenous prostacyclin has been used in clinical trials in patients with peripheral vascular disease and thrombotic thrombocytopenic purpura. It has also reduced arteriovenous shunt blockage in hemodialysis patients.

ANTICOAGULANT THERAPY

HEPARIN

Heparin is a glycosaminoglycan carbohydrate that contains variable repeats of a disaccharide unit. It indirectly inhibits the serine protease coagulation factors by enhancing the action of antithrombin (Fig. 29.23). Preparations are either unfractionated (standard heparin, molecular weight [MW] 15–18 kDa) or fractionated (low-molecular-weight heparin [LMWH], MW 4.5 kDa). LMWH (e.g. dalteparin, enoxaparin) are better able to inhibit factor Xa than thrombin (Fig. 29.24), interact less with platelets, and cause less bleeding. A comparison of the pharmokinetic properties of common therapeutic anticoagulants is shown in Table 29.6. Side effects of heparin include bleeding and thrombocytopenia, either type I within 1 or 2 days because of agglutinates or type II after 5 days or more because of platelet-activating autoantibodies directed against platelet factor 4 complexes (Fig. 29.25). Type II is associated with thrombosis. Rarely, skin necrosis occurs at sites of injection (Fig. 29.26), and osteoporosis is a complication of long-term use.

TABLE 29.5. ANTIPLATELET THERAPY: ANTIPLATELET DRUGS USED IN PATIENTS WITH AN ACUTE CORONARY SYNDROME AND IN THOSE UNDERGOING PERCUTANEOUS CORONARY INTERVENTION (PCI)

Drug	Target/ patient group	Duration
Acute coronary syndrome		
Aspirin	All	Lifelong
ADP receptor inhibitors	All	9–12 months
Glycoprotein IIb-IIa inhibitors:		
Abciximab	None	–
Eptifibatide	High risk	48–72 hours
Tirofiban	High risk	48–72 hours
Patients undergoing PCI		
Aspirin	All	Lifelong
ADP receptor inhibitors	All	9–12 months
Abciximab	High risk	12 hours after PCI
Eptifibatide	High risk	18–24 hours after PCI

Source: Lange RA, Hillis LD. *N Engl J Med* 2004;350:277–280. Reproduced with permission of Massachusetts Medical Society: The New England Journal of Medicine.

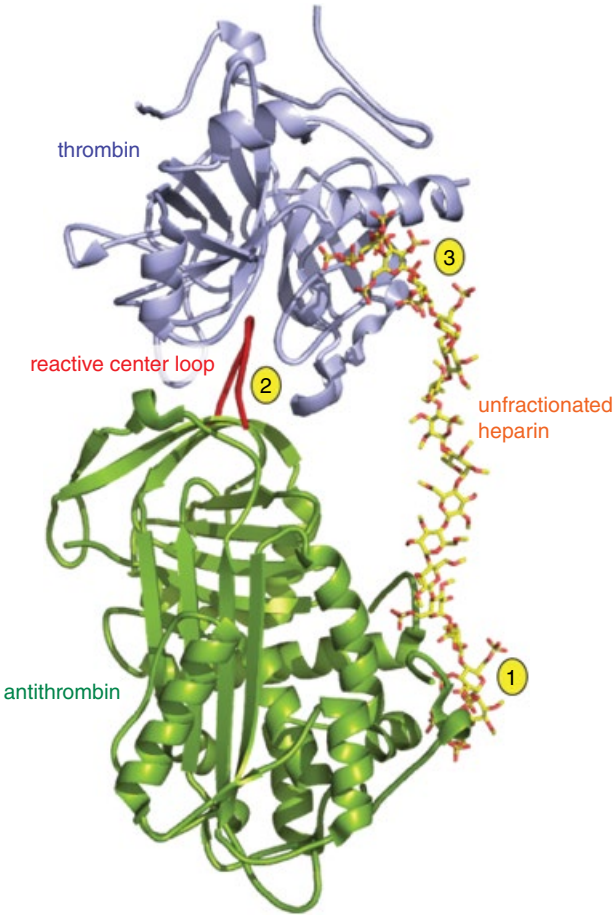

Fig. 29.23. The action of heparin: (1) A specific pentasaccharide sequence binds to the heparin binding site on antithrombin. (2) A conformational change causes the reactive center loop to become exposed and inserted irreversibly into the active site of the serine protease (in this case thrombin). (3) The long heparin chain brackets the thrombin and antithrombin molecules holding them together.

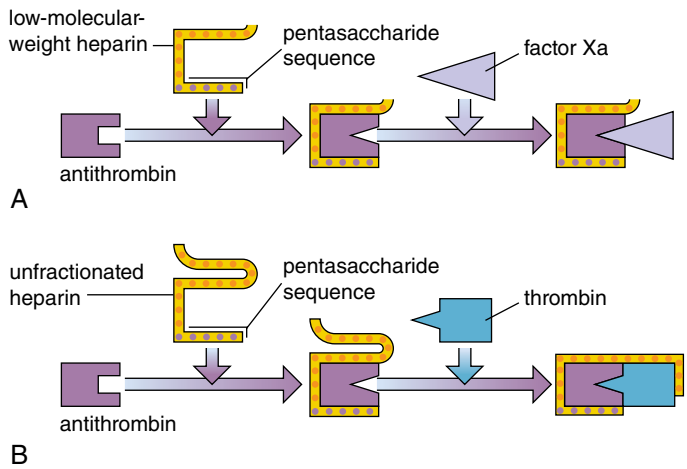

Fig. 29.24. Heparins (unfractionated and of low molecular weight): Catalysis of antithrombin-mediated inactivation of thrombin or factor Xa. **A,** The pentasaccharide sequence of both types of heparin causes a conformational change at the reactive center of antithrombin when bound to it, which accelerates its reaction with factor Xa. **B,** Catalysis of antithrombin-mediated inactivation of thrombin requires the formation of a ternary heparin-antithrombin-thrombin complex, which can be formed only by chains at least 18 saccharide units long. This explains why heparins of low molecular weight have less inhibitory activity against thrombin than unfractionated heparin. (Source: Modified with permission from Weitz JI. *N Engl J Med* 1997;337:688–698. Reproduced with permission of Massachusetts Medical Society: The New England Journal of Medicine.)

TABLE 29.6. COMPARISON OF PHARMACOKINETIC PROPERTIES OF COMMON ANTICOAGULANTS

	Dabigatran	Rivaroxaban	Apixaban	Warfarin	Enoxaparin
Mechanism	Anti-IIa	Anti-Xa	Anti-Xa	Inhibits Vitamin K dependent factors	Anti-Xa, Anti-IIa
Time to peak (hours)	2–3	3	3–4	120	3–5
Bioavailability (%)	6.5	80–100	50	100	92
Half-life (hours)	8–17	7–11	8–15	36–48	4.5
Affected by renal dysfunction	Yes	Yes	Partly	No	Yes
Affected by hepatic dysfunction	No	Yes	Yes	Yes	No
Protein binding (%)	25–30	95	87	99.5	80
Food effect	Absorption delayed	Required for absorption	Not known	Variable	None

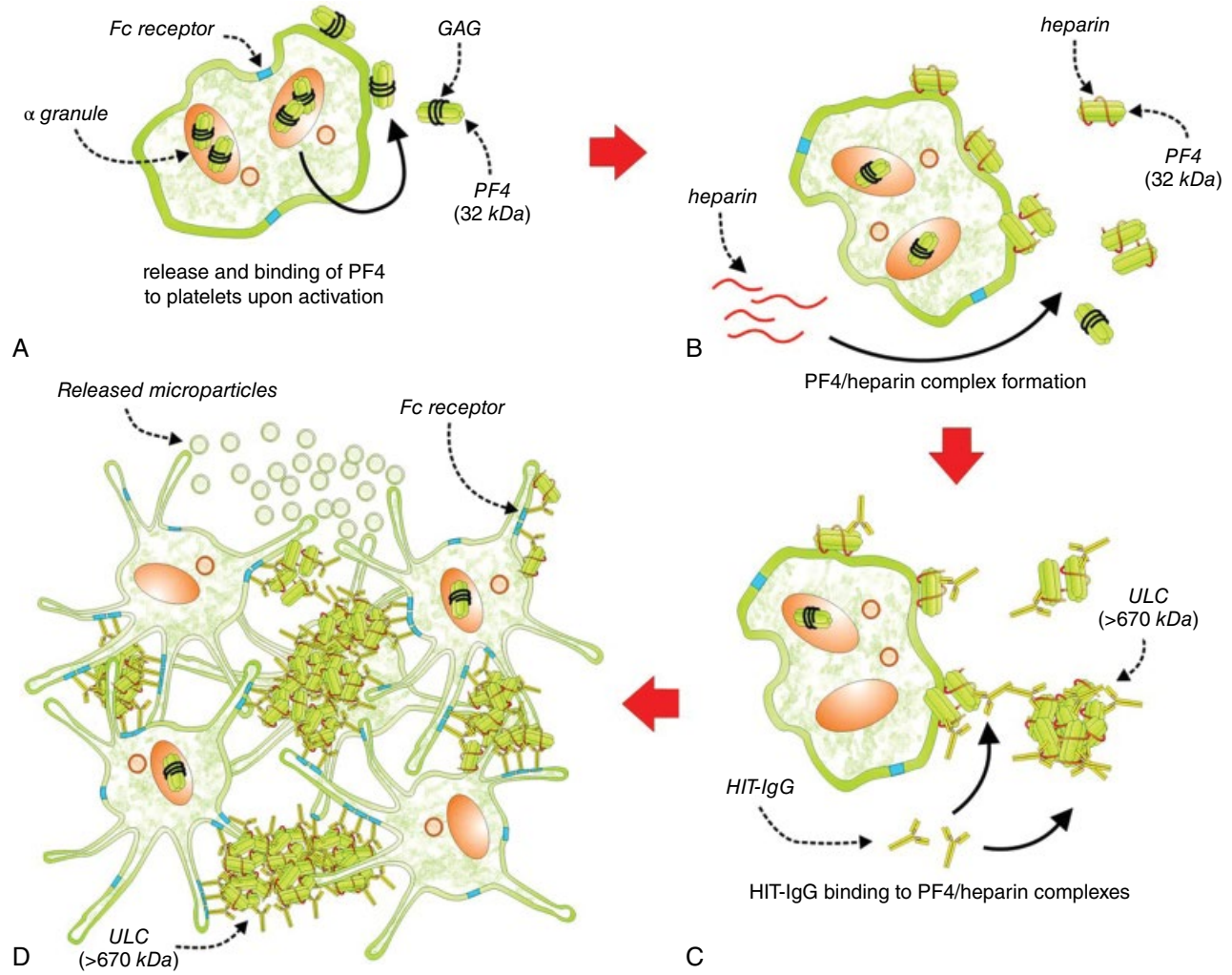

Fig. 29.25. Mechanism of heparin-induced thrombocytopenia (HIT). GAG, glycosaminoglycans; PF4, platelet factor 4; ULC, ultralarge complexes (Source: Kelton *Blood* 2008;112:2607–2616, fig. 5. Reproduced with permission of *Blood: Journal of American Society of Hematology*.)

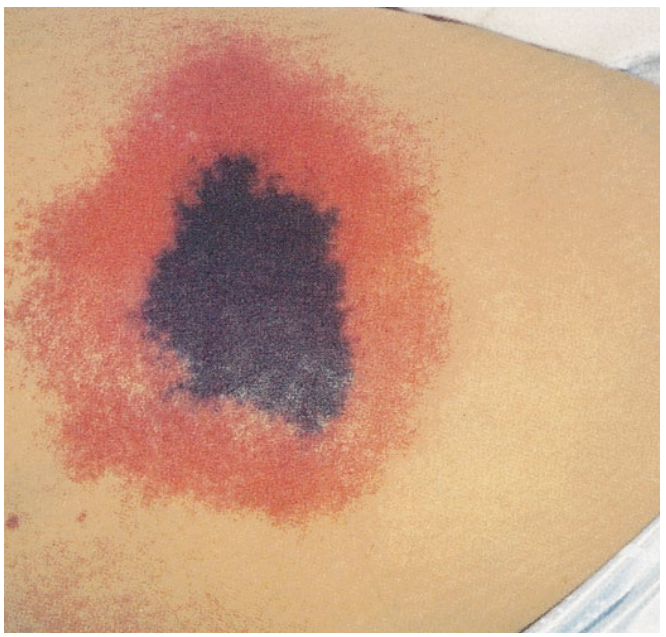

Fig. 29.26. Heparin: Skin necrosis. After local subcutaneous injection of unfractionated heparin.

Danaparoid is a mixture of various heparinoids of relatively low molecular weight. It has very low cross-reactivity rate with heparin-associated antiplatelet antibodies and so is used in place of heparin in heparin-induced thrombocytopenia. It is excreted through the kidney and requires monitoring using a specific anti-Xa.

WARFARIN

The traditional oral anticoagulants are derivatives of coumarin and indanedione. Warfarin, a coumarin derivative, is used most widely. These drugs are vitamin K antagonists, and therapy results in reduced activity of coagulation factors II, VII, IX, and X and also anticoagulant proteins C and S.

The mechanism of action is shown in Fig. 29.27. Therapy is monitored by the international normalized ratio (INR) (Table 29.7). The activity of warfarin can be enhanced or inhibited by a wide variety of drugs (Table 29.8). Warfarin resistance is also caused by variants in the gene that codes the vitamin K epoxide reductase complex *(VKORC1)*. Sensitivity to warfarin can be increased with variants in cytochrome P450 CYP2C9, which are associated with a low dose requirement. A recommended approach to the management of overdose and bleeding complications is outlined in Table 29.9.

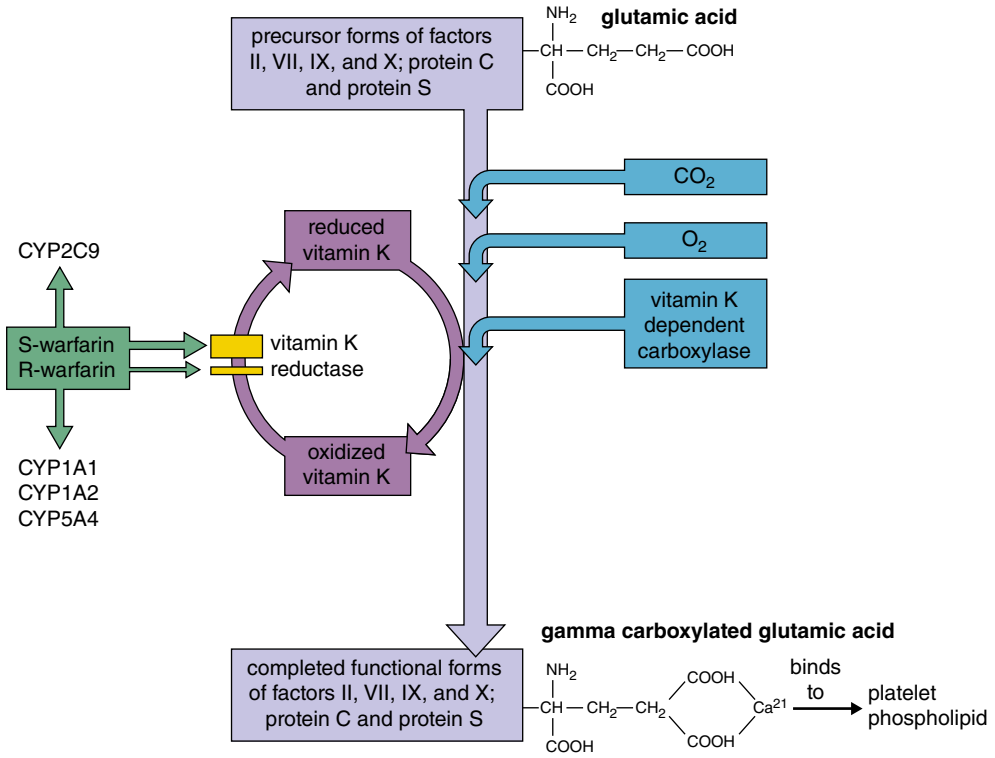

Fig. 29.27. The action of vitamin K in γ-carboxylation of glutamic acid in coagulation factors, which are then able to bind to platelet phospholipid. By inhibiting vitamin K-epoxide reductase, warfarin interferes with the regeneration of the reduced form of vitamin K required for the carboxylation of coagulation factors. Abnormalities in the gene coding for this enzyme (*VKORC1*) result in warfarin resistance. Variants in the cytochrome P450 complex CYP2C9 may result in different warfarin dose requirements. Patients with the variants CYP2C9*2 and CYP2C9*3 eliminate warfarin slowly and require lower doses. Single-nucleotide polymorphisms in vitamin K reductase are also associated with increased sensitivity to warfarin.

TABLE 29.7. WARFARIN THERAPY: RECOMMENDED RANGES FOR INTERNATIONAL NORMALIZED RATIO FOR DIFFERENT CLINICAL INDICATIONS

Target INR	Clinical state
2.5 (2.0–3.0)	Treatment of DVT, pulmonary embolism, atrial fibrillation, recurrent DVT off warfarin; symptomatic inherited thrombophilia, cardiomypothay, mural thrombosis, cardioversion
3.5 (3.0–4.0)	Recurrent DVT while on warfarin, mechanical prosthetic heart valves, antiphospholipid syndrome (some cases)

DVT, deep vein thrombosis; INR, internationl normalized ratio.

INDIRECT FACTOR Xa INHIBITORS

Fondaparinux, a synthetic analog of the antithrombin-binding pentasaccharide of heparin, is an indirect factor Xa inhibitor. Given subcutaneously with a half-life of 17 hours, it does not require laboratory monitoring. Idraparinux, a chemically modified analog of fondaparinux, has a longer half-life, and as a weekly injection in selected patients it may be more convenient than warfarin or LMWH.

DIRECT FACTOR Xa INHIBITORS

Rivaroxaban, apixaban, and edoxaban are small molecules that can be taken orally and directly inhibit factor Xa by binding to the active site of the enzyme. Compared with warfarin, they have a rapid onset of action and a much shorter half-life. Their main advantage is that they have a predictable anticoagulant effect that is little affected by diet and other medications (with some important exceptions). This means that generally they can be used without the need for monitoring of the anticoagulant effect.

DIRECT THROMBIN INHIBITORS

Direct thrombin inhibitors (Table 29.10) are effective against both free thrombin and thrombin bound to fibrin. Hirudin was originally extracted from the salivary glands of the medicinal leech *Hirudo medicinalis*. Bivalirudin and lepirudin are derivatives that are effective anticoagulants but they are rarely used now because of replacement with easier to use alternatives that have fewer side effects such as bleeding. Argatroban is a parental direct thrombin inhibitor that is primarily used in heparin-induced thrombocytopenia. In comparison with danaparoid, the primary route of elimination is through hepatic metabolisation. It is monitored by the APTT.

Dabigatran etexilate is a once daily, orally active direct thrombin inhibitor, approved in the UK for thromboprophylaxis following surgery and in atrial fibrillation, and for treatment of venous thrombosis.

FIBRINOLYTIC AGENTS

Fibrinolytic agents act by enhancing conversion of plasminogen to plasmin, which degrades fibrin by proteolytic cleavage (Fig. 29.28). They are able to lyse fresh thrombi and are widely used in clinical practice. Systemic intravenous therapy is of

TABLE 29.8. WARFARIN THERAPY: DRUG INTERFERENCE WITH CONTROL OF THERAPY

Increase warfarin effect	
Antibiotics	*Cardiac*
Cephalosporins	Amiodarone
Ciprofloxacin	Clofibrate
Clarithromycin	Propanolol
Co-trimoxazole	Propafenone
Erythromycin	Quinidine
Isoniazid	Statins
Metronidazole	Verapamil
Penicillins	*Central nervous system*
Quinolones	Antidepressants
Roxithromycin	Tricyclics
Tetracycline	SSRIs
Antifungals	Valproate
Fluconazole	*Gastrointestinal*
Itraconazole	Cimetidine
Ketoconazole	Cisapride
Miconazole	Omeprazole
Anti-inflammatory	*Others*
Aspririn	Allopurinol
Phenylbutazone	Anabolic steroids
Diclofenac	Danazol
Piroxicam	Disulfiram
Other NSAIDs	Flutamide
Paracetamol	Fosfamide
Sulfinpyrazone	Tamoxifen
	Thyroxine
	Proquanil
	Ritonavir
Decrease warfarin effect	
Aminoglutethimide	Oral contraceptives
Acetretin	Phenytoin
Barbiturates	Primidone
Carbamazepine	Rifampicin
Chlorodiazepoxide	Sucralfate
Cholestyramine	Vitamin K
Griseofulvin	

NSAID, nonsteroidal anti-inflammatory drug; SSRI, selective serontonin reuptake inhibitor.

TABLE 29.9. WARFARIN THERAPY: RECOMMENDATIONS FOR THE MANAGEMENT OF BLEEDING AND EXCESSIVE ANTICOAGULATION

INR above target range but <6.0 No bleeding	Reduce or stop warfarin Restart warfarin when INR in target range
INR 6.0–8.0 No bleeding or minor bleeding	Stop warfarin Repeat INR next day Restart in reduced dose when INR in target range If INR fails to shorten or if reversal required within 24–48 hours give 1 mg oral vitamin K
If INR >8.0 No bleeding or minor bleeding	Stop warfarin, give 1–2 mg oral vitamin K Repeat INR next day; give repeat dose of vitamin K if necessary Restart warfarin in reduced dosage when INR in target range
Major bleeding	Stop warfarin Give vitamin K 1–2 mg intravenously slowly Give prothrombin complex concentrate or fresh frozen plasma

INR, international normalized ratio.

TABLE 29.10. ACTIVATION AND INHIBITION OF BLOOD COAGULATION: SITES OF ACTION OF ANTICOAGULANTS

Sites of action of newer anticoagulants		
	Coagulation pathway	**Anticoagulants**
Initiation		**Tissue factor pathway inhibitors –** TFPI, NAPc2, VIIai
Thrombin generation	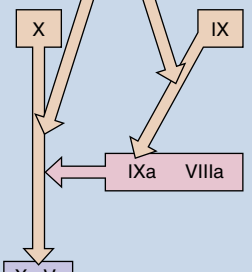	**IXa inhibitors –** IXai, IXa antibody **Direct Xa inhibitors** Apixaban Rivaroxaban Edoxaban **Indirect Xa inhibitors** Low-molecular weight heparin Unfractionated heparin Fondaparinux, idraparinux Danaparoid
Thrombin activity	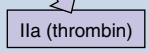	**Direct thrombin (IIa) inhibitors** Dabigatran Argatroban Hirudin, bivalirudin **Indirect thrombin (IIa) inhibitors** Unfractionated heparin

Drugs in clinical use are shown in normal type and those under investigation are shown in italics.

proven benefit for patients with acute myocardial infarction, major pulmonary emboli, or iliofemoral DVT. Local therapy via an indwelling catheter is used in acute peripheral arterial or venous thrombosis.

Streptokinase, a peptide produced by hemolytic streptococci, forms a complex with plasminogen that converts other plasminogen molecules to plasmin. Urokinase is a tPA initially extracted from urine. Second-generation thrombolytic agents include tPA, which is synthesized using recombinant DNA technology. Recombinant tPA (alteplase) is more fibrin specific with less systemic activation of fibrinolysis and bleeding than streptokinase. It is superior to streptokinase, has a lower short-term mortality rate, and is now the agent most commonly used in clinical practice. Other newer agents include single-chain, urokinase-type plasminogen activator and acylated plasminogen streptokinase activator complex. In acute arterial thrombosis, a short burst of thrombolysis is generally used and laboratory tests for monitoring are generally unnecessary. In extensive venous thrombosis, infusions over several hours or days are used and the

fibrinolytic effect should be monitored by measuring fibrinogen levels. The possibility of dangerous hemorrhage or other clinical complications may exclude the use of thrombolytic therapy (Table 29.11).

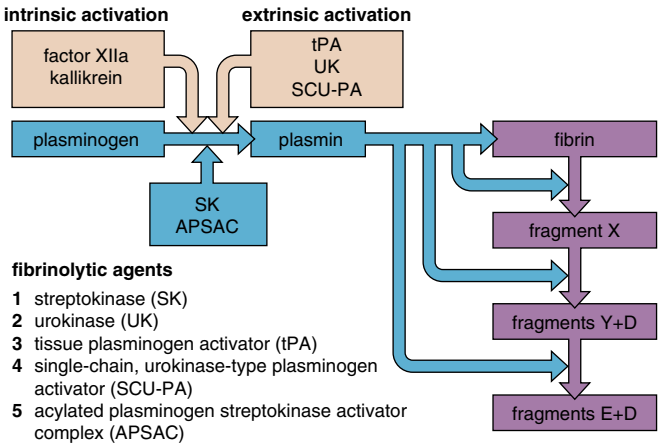

Fig. 29.28. The fibrinolytic system and fibrinolytic agents. (Source: Modified with permission from Hoffbrand AV and Pettit JE. *Essential Hematology,* 3rd edn. Blackwell Scientific, Oxford, 1993. Reproduced with permission of John Wiley and Sons.)

TABLE 29.11. CONTRAINDICATIONS TO THROMBOLYTIC THERAPY

Absolute contraindications
Active gastrointestinal bleeding
Aortic dissection
Head injury or cerebrovascular accident in the past 2 months
Neurosurgery in the past 2 months
Intracranial aneurysm or neoplasm
Proliferative diabetic retinopathy
Relative contraindications
Traumatic cardiopulmonary resuscitation
Major surgery in the past 10 days
Past history of gastrointestinal bleeding
Recent obstetric delivery
Prior arterial puncture
Prior organ biopsy
Serious trauma
Severe arterial hypertension (systolic pressure >200 mmHg, diastolic pressure >110 mmHg)
Bleeding diathesis

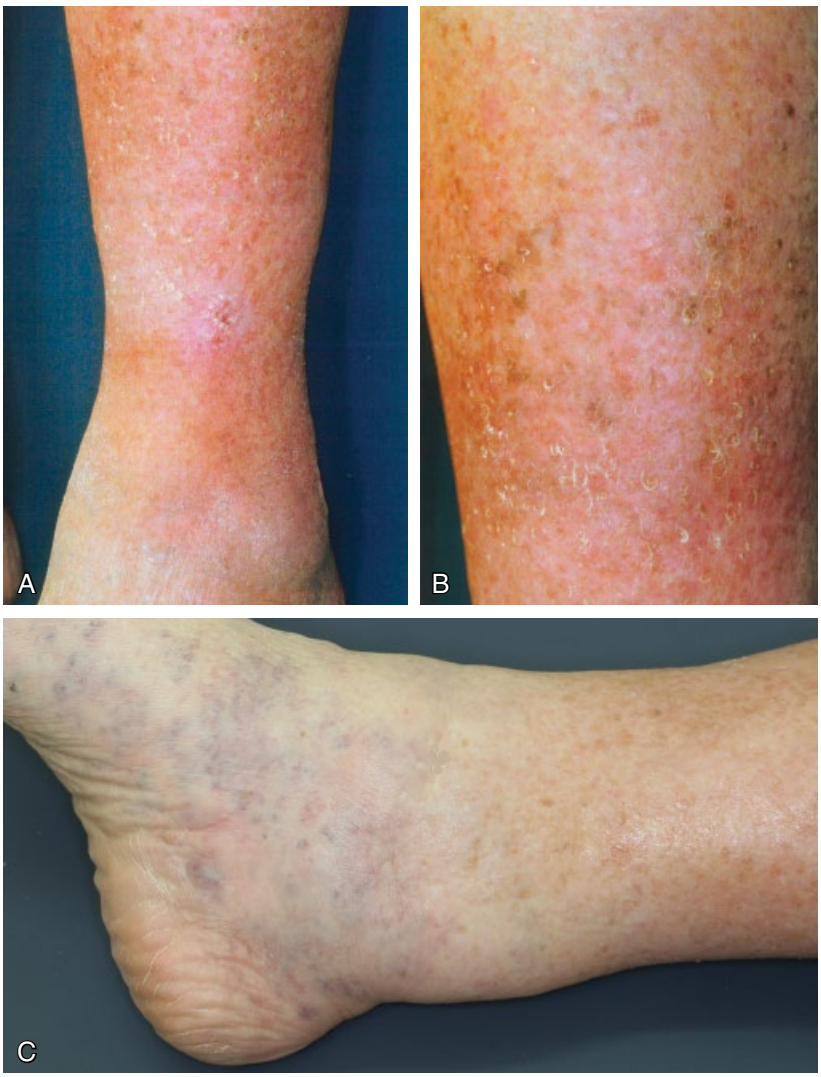

Fig. 29.29. Post-thrombotic syndrome: Skin changes in chronic venous insufficiency. **A,** Lower left leg pigmentation, lipodermatosclerosis, and a small venous ulcer. **B,** A closer view of the same leg showing central atrophy blanche and lateral changes of asteatosis (acquired ichthyosis). **C,** Lower leg and ankle edema in a different patient. (All images courtesy of Dr. K Macdonald.)

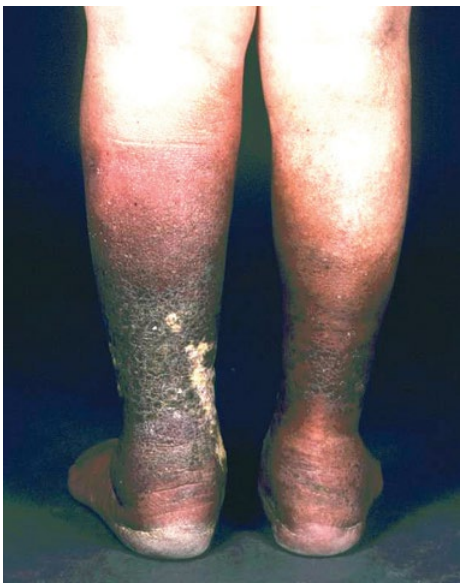

Fig. 29.30. Post-thrombotic syndrome. Both lower legs show marked pigmentation and lipodermatosclerosis. (Courtesy of Professor G Hamilton.)

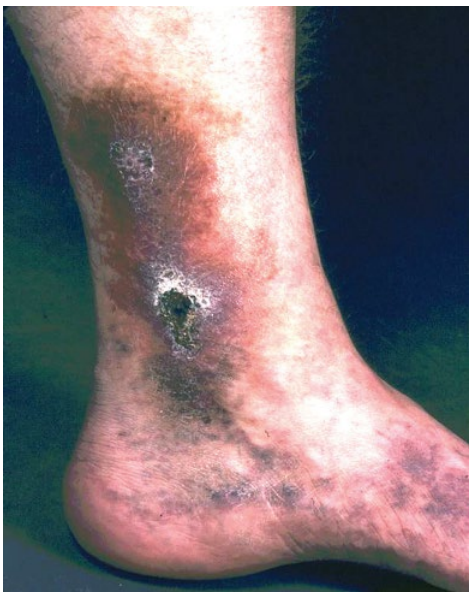

Fig. 29.31. Post-thrombotic syndrome: A healing venous ulcer with surrounding pigmentation. (Courtesy of Professor G Hamilton.)

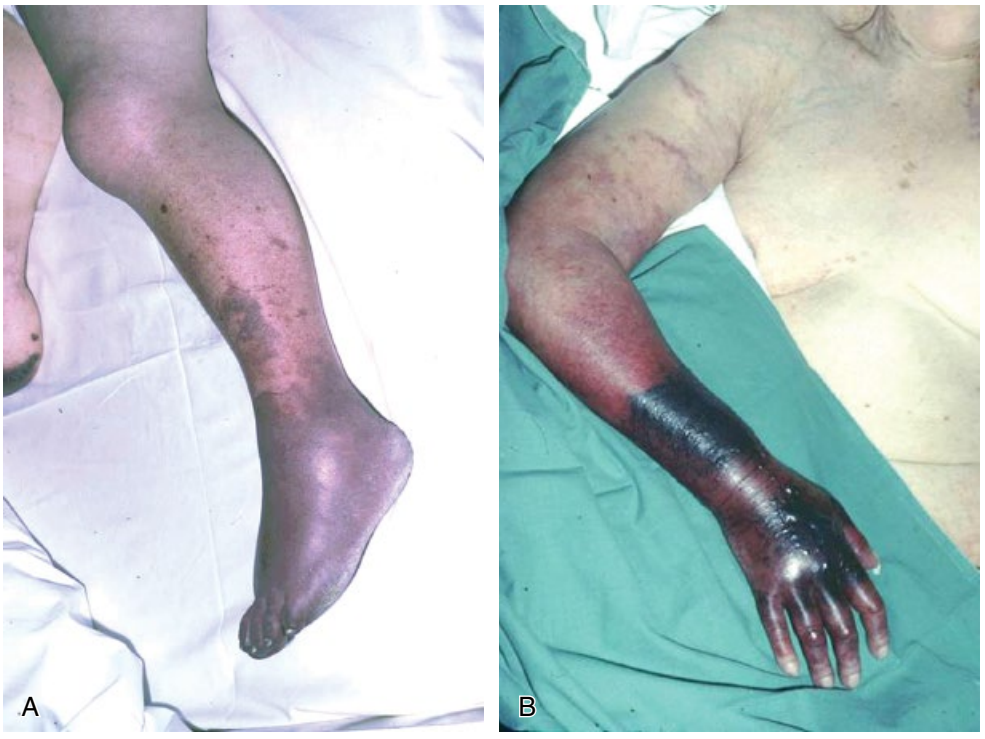

Fig. 29.32. Post-thrombotic syndrome: Phlegmasia cerulea dolens. **A,** Grossly swollen left leg with marked cyanosis and early ischemic changes in the foot. **B,** Swollen right arm with marked cyanosis and early venous gangrene of the hand. (Courtesy of Professor G Hamilton.)

POST-THROMBOTIC SYNDROME

Post-thrombotic or postphlebitic syndrome is the development of chronic venous insufficiency after DVT. Injury to the venous system produces symptoms that include edema, pain, changes in skin pigmentation, and venous ulcers. Trophic skin changes include any of the following: hyperpigmentation, lipodermatosclerosis, asteatosis (acquired ichthyosis), atrophy blanche, and venous ulceration (Figs. 29.29–29.31). In a minority of patients, extensive proximal venous thrombosis is complicated by thrombosis in collateral veins, and this can be associated with phlegmasia. Many patients with this serious complication have widespread cancer. In the milder form of phlegmasia (alba dolens), there is severe edema, pain, and blanching (alba) without cyanosis. In fulminant or progressive disease associated with ischemia (phlegmasia cerulea dolens), there is marked cyanosis in addition to massive edema and, in many patients, venous gangrene (Fig. 29.32). Involvement of the arm occurs in less than 5% of patients. Longstanding untreated venous ulceration can be complicated by the development of squamous cell carcinoma (Fig. 29.33).

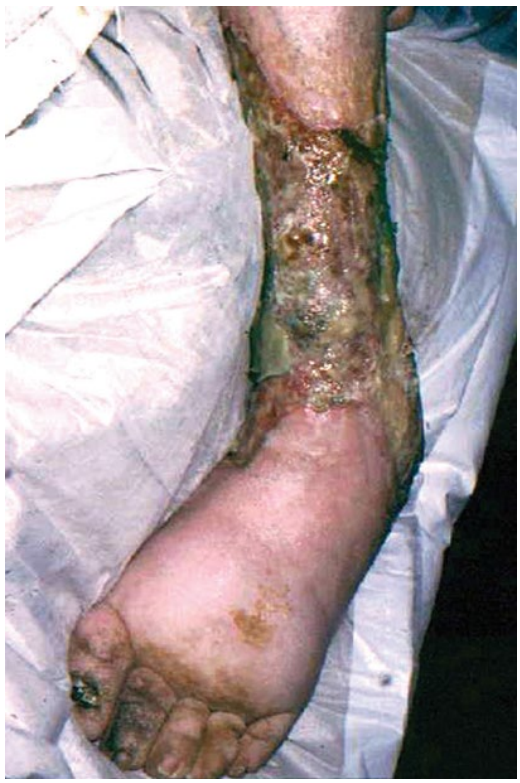

Fig. 29.33. Post-thrombotic syndrome: Marjolin ulcer. Squamous cell carcinoma at the margins of a very extensive and neglected venous ulcer. (Courtesy of Professor G Hamilton.)

CHAPTER

30 HEMATOLOGIC ASPECTS OF SYSTEMIC DISEASES

ANEMIA OF CHRONIC DISORDERS

The anemia of chronic disorders, sometimes referred to as secondary anemia, is found in patients with infections, inflammation, and malignancy (Table 30.1). Less well recognized is its association with severe heart disease, diabetes, severe trauma, and acute and chronic immune activation in some patients. The blood count usually shows a moderate normocytic, normochromic anemia, although occasionally hemoglobin levels can be <8.0 g/dL.

A number of factors contribute to the pathogenesis of this anemia (Fig. 30.1). The dominant problem is reduced red cell production. Hemoglobin production is restricted by reduced release of iron from macrophages with low serum iron levels. Increased hepcidin levels in patients with infections, inflammation, and malignancy have a dominant role in this disturbance of iron metabolism. Erythropoiesis is unable to respond to the anemia despite moderate increases in erythropoietin levels. There can be increased apoptosis of erythroblasts. Inadequate erythropoietin production in response to the anemia can be a minor contributing factor. Cytokine and growth factor release (e.g. IL-1, IL-6, tumor necrosis factor) by the primary condition initiates activation of other cytokines (e.g. interferons β and α), which replicate a similar anemia in animals. A minor factor in the pathogenesis of anemia is some reduction in red cell survival.

The blood film shows mild red cell changes, including anisocytosis and poikilocytosis. There may be obvious rouleaux formation (Fig. 30.2). The reticulocyte count is inappropriately low. The extent of elevation in erythrocyte sedimentation rate (ESR), C-reactive protein, and fibrinogen are determined by the underlying illness. The serum iron and transferrin or total iron-binding capacity are low with a normal or mildly reduced iron saturation. The serum ferritin level is usually normal or elevated but, in this setting, is an inaccurate indicator of iron stores because of its release by inflammatory and necrotic tissue. Serum transferrin receptor levels are not increased.

The bone marrow can show minor changes in erythropoiesis. There may be clusters of erythroblasts in close proximity to macrophages (Fig. 30.3). Iron staining shows normal or increased storage of iron with absent siderotic granulation in erythroblasts (Fig. 30.4).

TABLE 30.1. CONDITIONS ASSOCIATED WITH ANEMIA OF CHRONIC DISORDERS

Chronic inflammatory diseases
Infectious
For example, pulmonary abscess, tuberculosis, osteomyelitis, pneumonia, bacterial endocarditis
Noninfectious
For example, rheumatoid arthritis, systemic lupus erythematosus and other connective tissue diseases, sarcoid, Crohn disease, cirrhosis
Malignant disease
For example, carcinoma, lymphoma, sarcoma, myeloma

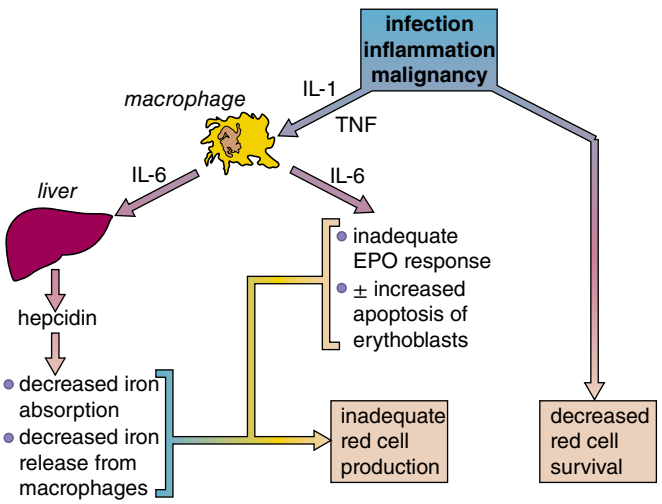

Fig. 30.1. Factors involved in the pathogenesis of anemia of chronic disorders.

Color Atlas of Clinical Hematology: Molecular and Cellular Basis of Disease, Fifth Edition. A. Victor Hoffbrand, Paresh Vyas, Elías Campo, Torsten Haferlach, and Keith Gomez

MALIGNANT DISEASES (OTHER THAN LEUKEMIAS, LYMPHOMAS, HISTIOCYTIC AND MYELOPROLIFERATIVE DISORDERS)

Anemia results from many factors. The anemia of chronic disorders, blood loss, iron deficiency, bone marrow failure from extensive marrow replacement by metastatic disease, folate deficiency, hemolysis, and marrow suppression from chemotherapy or radiotherapy are involved in different malignancies (Table 30.2).

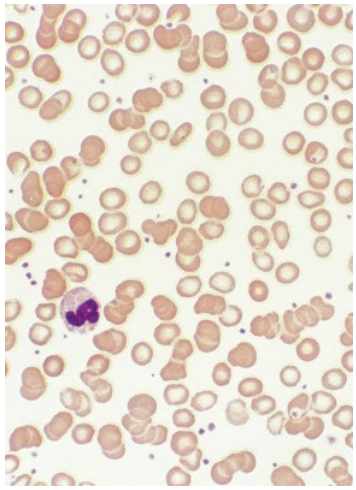

Fig. 30.2. Anemia of chronic disorders. Blood film showing mild red cell anisocytosis, poikilocytosis, and rouleaux formation.

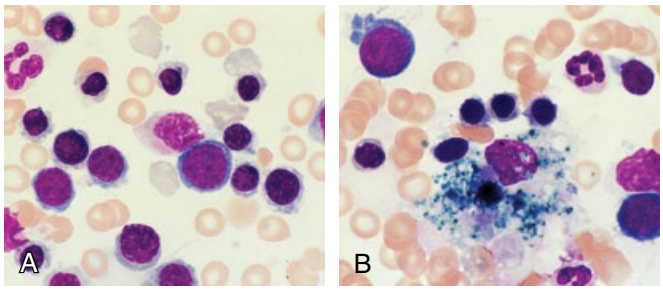

Fig. 30.3. Anemia of chronic disorders: Bone marrow aspirate. **A,** Normoblastic erythroblasts showing minor irregularity. **B,** Erythroblasts in close association with a macrophage.

In the blood film, leukoerythroblastic change (Fig. 30.5) is found when there is extensive metastatic involvement of marrow. Leukemoid changes occur if there is associated inflammation or tumor necrosis.

Microangiopathic hemolysis occurs with mucin-secreting adenocarcinoma such as some tumors of the stomach, lung, or breast (Fig. 30.6). Autoimmune hemolytic anemia occurs in some malignant lymphomas and rarely in other tumors. Primary red cell aplasia has been found in association with thymomas and lymphoma, and myelodysplastic syndrome can follow chemotherapy or radiotherapy. Some cases of carcinoma of the stomach occur in association with pernicious anemia.

Secondary polycythemia (see Chapter 16) is seen in occasional patients with renal, hepatic, cerebellar, and uterine tumors.

Malignancy is associated either with thrombocytosis or thrombocytopenia. Disseminated intravascular coagulation occurs with mucin-secreting adenocarcinoma. There is activation of fibrinolysis in some carcinomas of the prostate.

Venous thromboembolism is most common in tumors of the ovary, brain, pancreas, and colon. It has a high frequency after surgical treatment of any cancer, unless prophylaxis is given.

The bone marrow is involved most commonly by metastatic deposits from carcinomas of the breast (Fig. 30.7), prostate (Fig. 30.8), lung (Fig. 30.9), kidney (Fig. 30.10), and thyroid. Metastatic involvement by carcinomas of the stomach colon (Figs. 30.11 and 30.12) and pancreas occurs less frequently, but virtually any malignant tumor can involve the marrow (Figs. 30.13 and 30.14). Extensive osteoclastic resorption of bone is often found in trephine biopsies (Fig. 30.15). Most tumors provoke some healing and sometimes new bone deposition; osteoblastic activity is most pronounced in metastatic spread from carcinoma of the prostate (Fig. 30.16) and breast.

Occasionally, fragments of epidermis are carried into the marrow cavity by the trephine biopsy (Fig. 30.17), but the well-differentiated nature of such fragments allows easy distinction from metastatic carcinoma.

Metastatic spread of malignant melanoma frequently involves the bone marrow (Fig. 30.18). Occasionally, melanin is found in blood monocytes (Fig. 30.19). Bone marrow examination may detect marrow involvement by other tumors, including metastatic neuroblastoma (Fig. 30.20), medulloblastoma, and Kaposi sarcoma (Fig. 30.21). Metastatic rhabdomyosarcoma

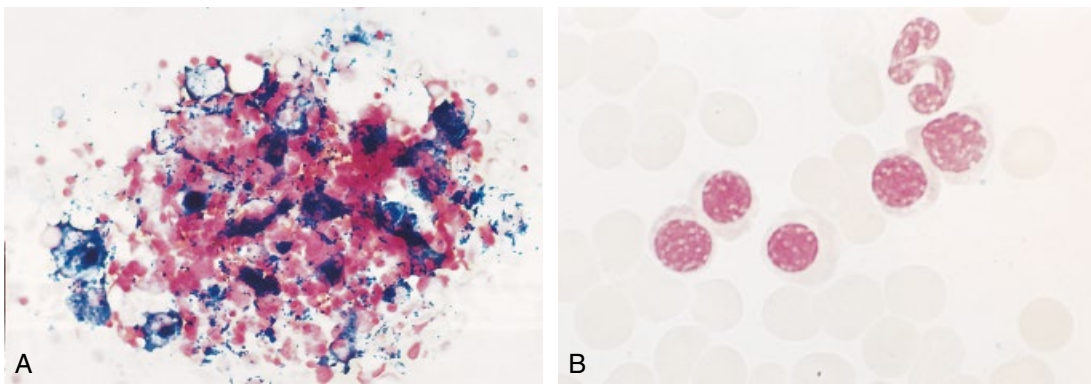

Fig. 30.4. Secondary anemia. Bone marrow aspirate showing fragments containing adequate iron in the reticuloendothelial cells **(A)** and no siderotic granules in the developing erythroblasts **(B).** (Perls stain.)

TABLE 30.2. HEMATOLOGIC ABNORMALITIES IN MALIGNANT DISEASE

Hematologic abnormalities	Tumor or treatment associated
Pancytopenia	
Marrow hypoplasia	Chemotherapy, radiotherapy
Myelodysplasia	Metastases in marrow
Leukoerythroblastic	Folate deficiency
Megaloblastic	B_{12} deficiency (carcinoma of stomach)
Red cells	
Anemia of chronic disorders	Most forms
Iron deficiency anemia	Especially gastrointestinal, uterine
Pure red-cell aplasia	Thymoma
Immune hemolytic anemia	Lymphoma, ovary, other tumors
Microangiopathic hemolytic anemia	Mucin-secreting carcinoma
Polycythemia	Kidney, liver, cerebellum, uterus
White cells	
Neutrophil leukocytosis	Most forms
Leukemoid reaction	Disseminated tumors, those with necrosis
Eosinophilia	Hodgkin lymphoma, others
Monocytosis	Various tumors
Platelets and coagulation	
Thrombocytosis	Gastrointestinal tumors with bleeding, others
Disseminated intravascular coagulation	Mucin-secreting carcinoma, prostate
Activation of fibrinolysis	Prostate
Acquired inhibitors of coagulation	Most forms
Paraprotein interfering with platelet function	Lymphomas, myeloma
Tumor cell procoagulants – tissue factor and cancer procoagulant (direct activation of factor X)	Especially ovarian, pancreas, brain, colon

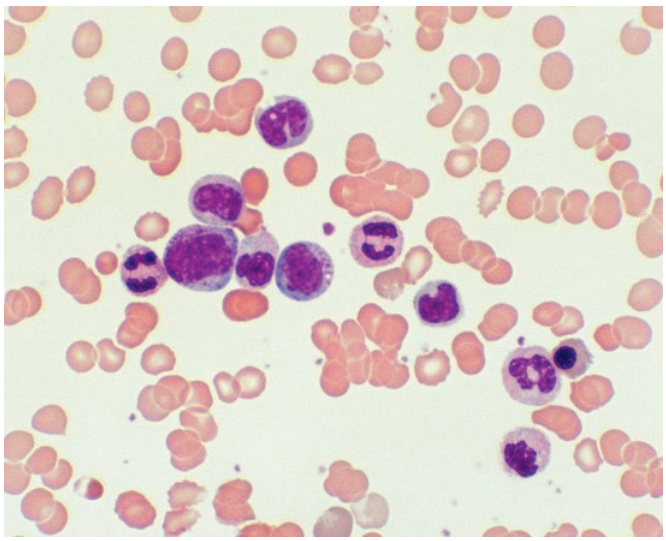

Fig. 30.5. Malignant disease. Blood film in a patient with carcinoma of the breast and metastatic marrow involvement showing leukoerythroblastic features.

(Fig. 30.22) may be confused with other blastic tumors, but immunopositivity with antidesmin (intermediate filaments) is able to confirm a mesodermal origin.

Although most primary bone tumors do not spread to parts of the skeleton distant from their origin, bone marrow examination can reveal evidence of dissemination in Ewing tumor of bone (Fig. 30.23).

Blood and bone marrow involvement by malignant lymphoma and histiocytic proliferations are discussed in Chapters 19, 20 and 24, respectively.

RHEUMATOID ARTHRITIS AND OTHER CONNECTIVE TISSUE DISEASES

In active rheumatoid arthritis, the anemia of chronic disorders is usually present and proportional to the severity of disease. Gastrointestinal hemorrhage related to therapy with aspirin, corticosteroids, and nonsteroidal anti-inflammatory drugs can cause iron deficiency. Gold therapy may be followed by marrow hypoplasia.

Arthritis with associated neutropenia and splenomegaly is found in Felty syndrome (Fig. 30.24).

In systemic lupus erythematosus, the anemia of chronic disorders is complicated by neutropenia and lymphopenia. In severe cases a marked pancytopenia occurs. Some patients develop an autoimmune hemolytic anemia (Fig. 30.25) and there is an autoimmune thrombocytopenia in 5% of cases. Occasional patients have problems related to thrombosis and recurrent miscarriage related to the presence of the "lupus anticoagulant" and other antiphospholipid antibodies (see Chapter 29). The bone marrow stromal tissue in severe disease may show degenerative changes.

The anemia of chronic disorders occurs in other collagen vascular disorders. Patients with polyarthralgia rheumatica and temporal (giant) arteritis have marked elevation of ESR, marked red cell rouleaux in the blood film, and polyclonal increase in immunoglobulins.

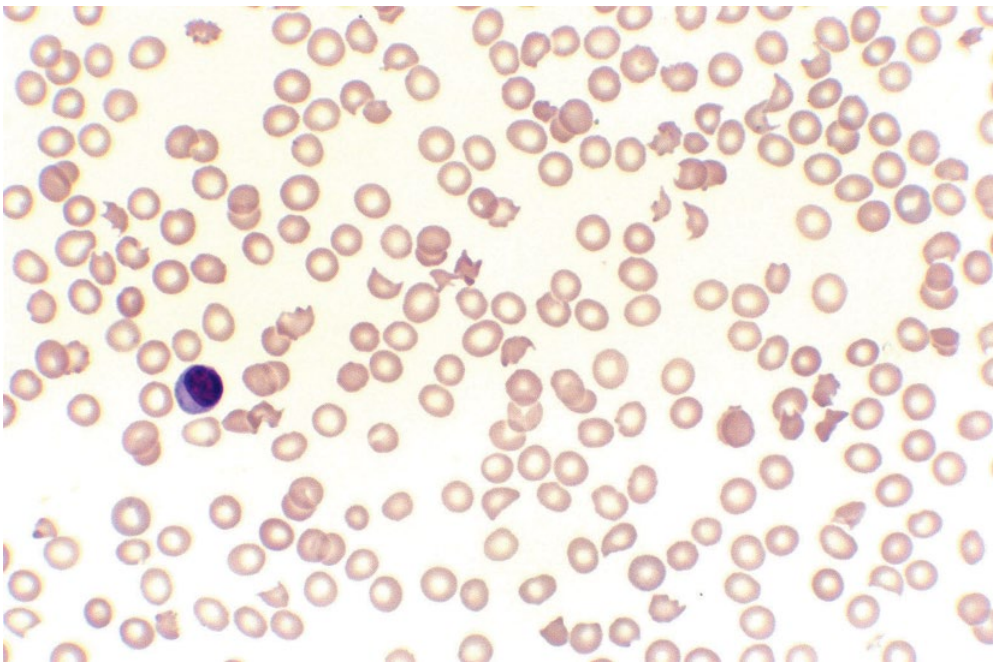

Fig. 30.6. Carcinoma of the stomach. Blood film showing red cell fragmentation and thrombocytopenia.

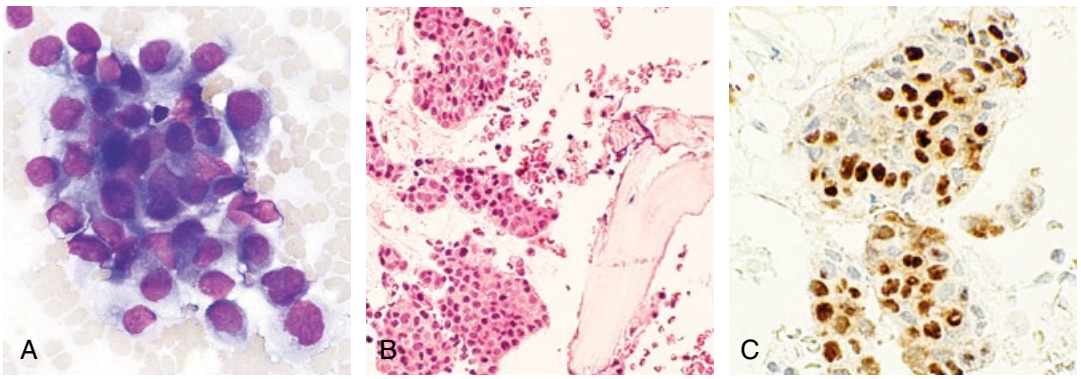

Fig. 30.7. Metastatic carcinoma of the breast. **A,** Marrow aspirate cell trail showing a nest of neoplastic epithelial cells with features of a large undifferentiated carcinoma. **B,** The trephine biopsy also shows sheets and clumps of similar neoplastic epithelial cells. **C,** Immunohistologic staining in the same biopsy showing positivity for estrogen receptor (ER).

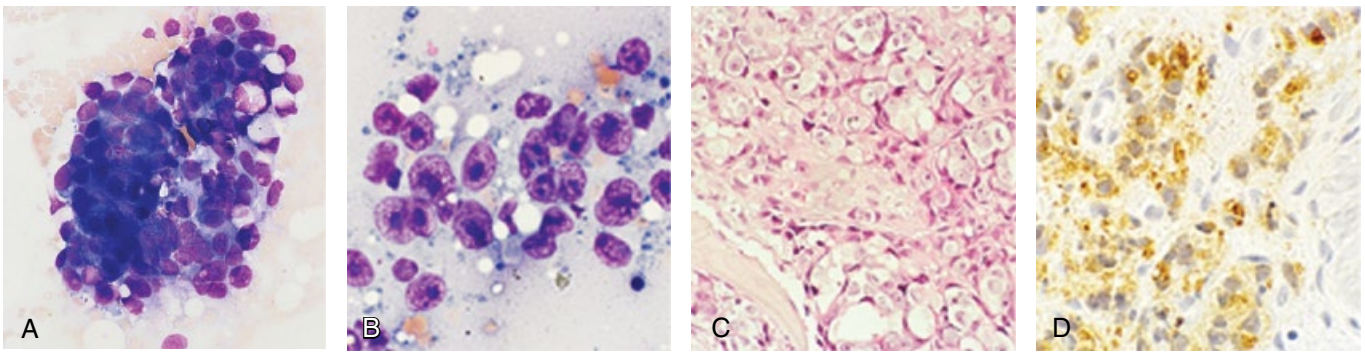

Fig. 30.8. Metastatic carcinoma of the prostate. **A,** Marrow aspirate showing a sheet of neoplastic cells. **B,** A trephine biopsy "roll" in the same patient shows nuclear detail, including prominent nucleoli. **C,** The trephine sections from the same patient show almost complete replacement of hematopoietic cells by sheets of pleomorphic cells from a poorly differentiated adenocarcinoma. **D,** Immunohistologic staining for prostate-specific antigen (PSA) shows strong cytoplasmic positivity in the tumor cells.

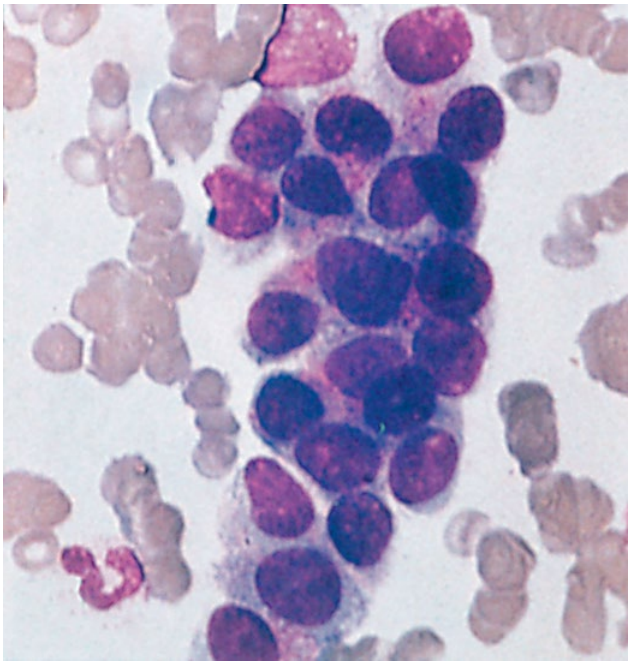

Fig. 30.9. Metastatic carcinoma of the lung. The marrow aspirate shows a loose collection of pleomorphic neoplastic cells.

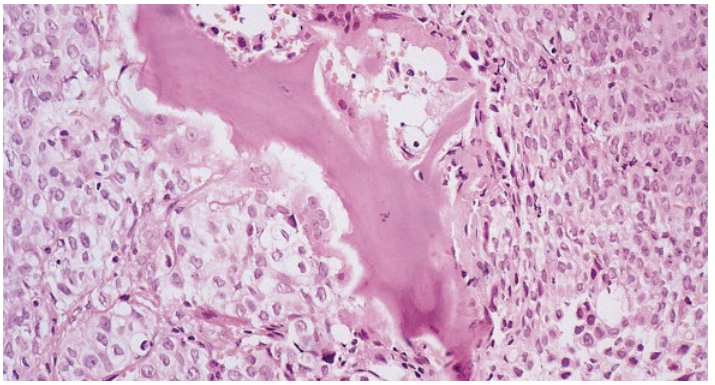

Fig. 30.10. Metastatic carcinoma: Metastatic deposits from a carcinoma of the kidney. Sheets of neoplastic epithelial cell surrounding residual trabecular bone with osteoclasts adjacent to the scalloped edges

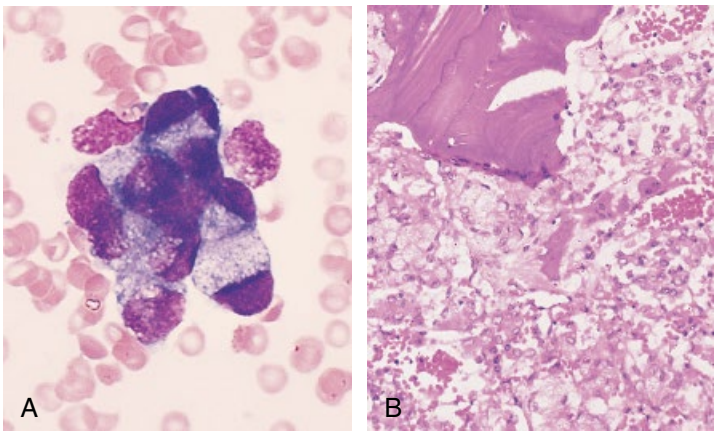

Fig. 30.11. Metastatic carcinoma. **A,** A clump of distended and vacuolated neoplastic epithelial cells in a patient with microangiopathic hemolytic anemia and laboratory evidence of disseminated intravascular coagulation. **B,** Sheets and acini of mucin-secreting adenocarcinoma in the same patient as described in **A,** who had a primary tumor of the stomach.

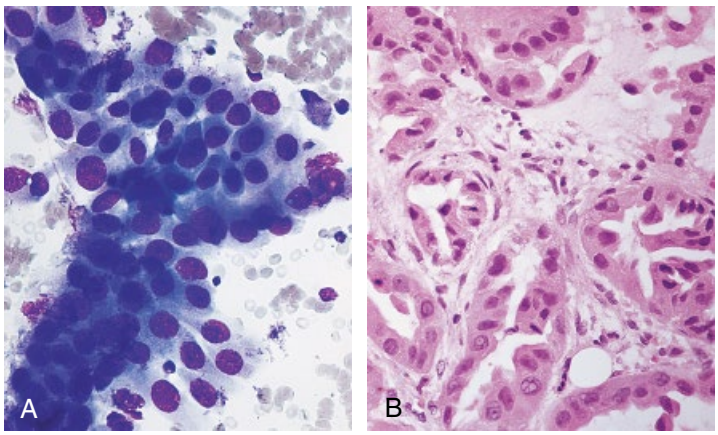

Fig. 30.12. Metastatic carcinoma. **A,** A sheet of neoplastic columnar cells in bone marrow. **B,** Replacement of normal hematopoietic tissue by acini of neoplastic columnar cells in the same patient, who had a primary carcinoma of the ascending colon.

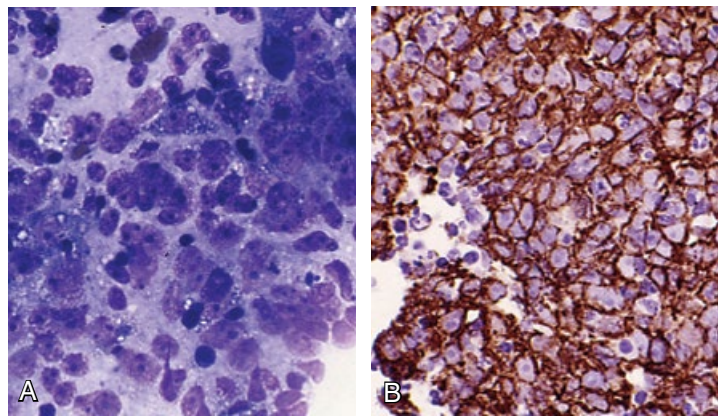

Fig. 30.13. Metastatic carcinoma. Marrow aspirate from a patient with a primary nasopharyngeal carcinoma. **A,** The cell trails contained sheets of neoplastic epithelial cells. **B,** Immunohistologic staining shows strong positivity for anti low-molecular-weight cytokeratin CAM 5.2.

RENAL FAILURE

The hematologic abnormalities found in patients with chronic renal failure (CRF) are listed in Table 30.3. Normochromic anemia is present in most patients with CRF. Generally, there is a 2.0 g/dL fall in hemoglobin level for every 10 mmol/L rise in blood urea. There is impaired red cell production as a result of defective erythropoietin secretion. Variable shortening of red cell lifespan occurs, and in severe uremia the red cells show abnormalities including spicules (spurs) and "burr" cells (Fig. 30.26). Increased red cell 2,3-diphosphoglycerate (2,3-DPG) levels in response to the anemia and hyperphosphatemia result in decreased oxygen affinity and a shift of the hemoglobin oxygen dissociation curve to the right, which is augmented by uremic acidosis. The patient's symptoms are therefore relatively mild for the degree of anemia. Other factors that complicate the anemia of CRF include the anemia of chronic disorders, iron deficiency from blood loss during dialysis or caused by bleeding because of defective platelet function, and folate deficiency in some chronic dialysis patients. Aluminum excess in patients on chronic dialysis also inhibits erythropoiesis. Patients with polycystic kidneys usually have retained erythropoietin production and can have less severe anemia for the degree of renal failure.

The hemolytic–uremic syndrome and thrombotic thrombocytopenic purpura are discussed in Chapter 27.

A bleeding tendency with purpura, gastrointestinal bleeding, or uterine bleeding occurs in 30–50% of patients with CRF and is marked in patients with acute renal failure. The bleeding is out of proportion to the degree of thrombocytopenia and has been associated with abnormal platelet or vascular function, which can be reversed by dialysis.

In CRF there is resistance to the action of vitamin D and a compensatory parathyroid hyperplasia. Characteristic changes are found in bone architecture on trephine biopsy (Fig. 30.27). In mild disease, the lesions are predominantly osteomalacic. Microscopically, the trabeculae are increased in thickness and in number, and the osteoid seams have defective mineralization, similar to the changes seen in vitamin D deficiency. In severe disease, evidence of osteitis fibrosa is also present(Fig. 30.28).

LIVER DISEASE

The hematologic abnormalities in liver disease are listed in Table 30.4. Chronic liver disease is associated with anemia that is mildly macrocytic and often accompanied by target cells, mainly as a result of increased cholesterol in the membrane (Fig. 30.29). Contributing factors to the anemia include blood loss (e.g. bleeding varices) with iron deficiency, dietary folate deficiency, and direct suppression of hematopoiesis by alcohol. Alcohol can have an inhibiting effect on folate metabolism and is occasionally associated with sideroblastic changes. Hemolytic anemia occurs in patients with alcohol intoxication (Zieve syndrome) and in Wilson disease, and autoimmune hemolytic anemia is found in some patients with chronic immune hepatitis. Viral hepatitis (usually non-A, non-B, non-C) is associated with aplastic anemia.

Bleeding results from deficiencies of vitamin K-dependent factors (II, VII, IX, and X) and, in severe disease, of factor V and fibrinogen. Thrombocytopenia results from hypersplenism or from immune complex-mediated platelet destruction. Dysfibrinogenemia with abnormal fibrin polymerization occurs

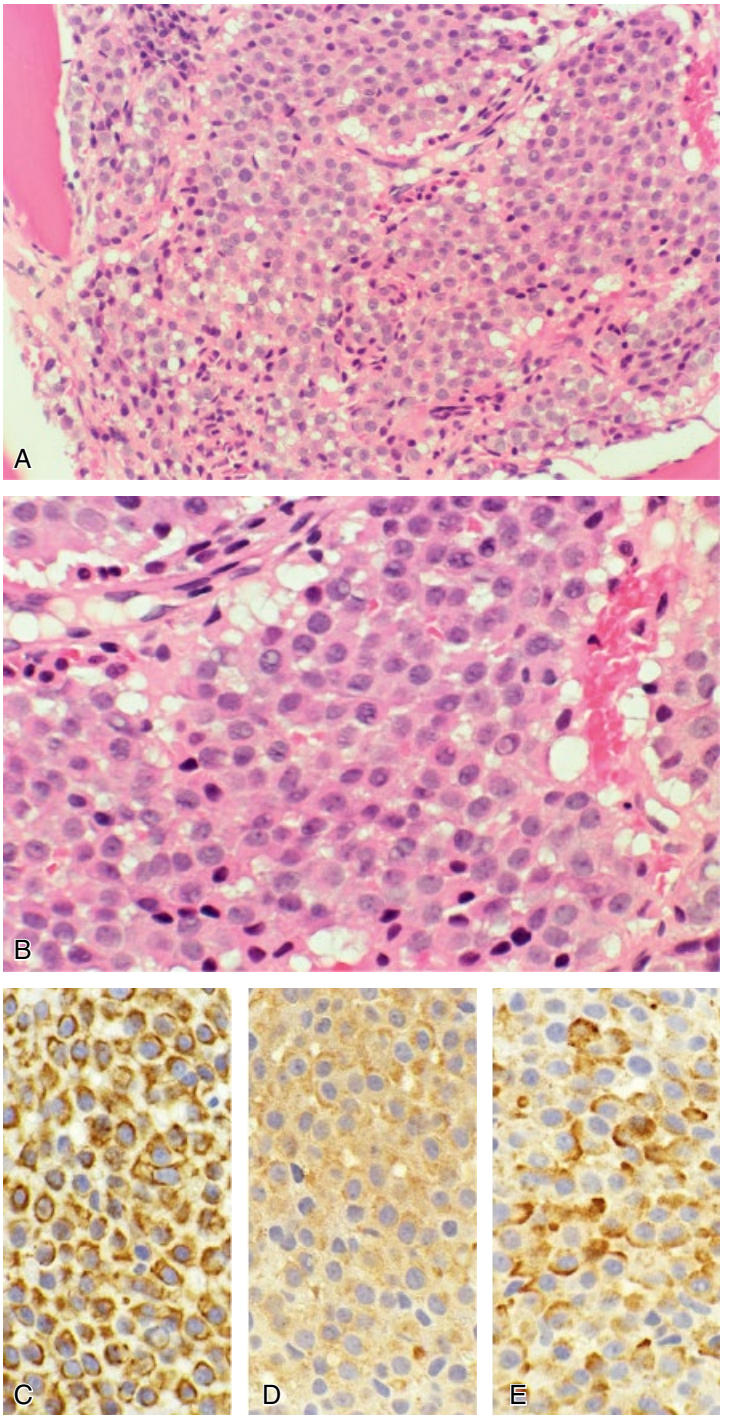

Fig. 30.14. Metastatic neuroendocrine carcinoma. **A,** The trephine section shows almost complete replacement of hematopoietic cells by tumor. **B,** At higher magnification the cells show moderate pleomorphism and sporadic nuclear vacuolation. **C–E,** Immunostaining shows positivity for CAM 5.2 **(C),** Synaptophysin **(D),** and Chromogranin **(E).**

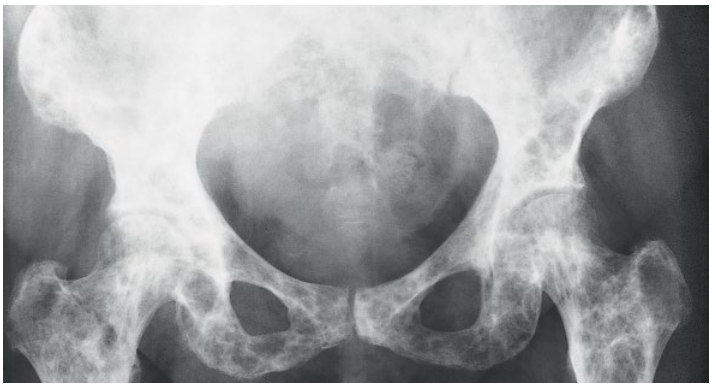

Fig. 30.15. Metastatic carcinoma. Radiograph of the pelvis of a 58-year-old man with carcinoma of the lung. Metastatic deposits of tumor have produced widespread lytic lesions, most marked in the lower pelvis and upper parts of the femurs.

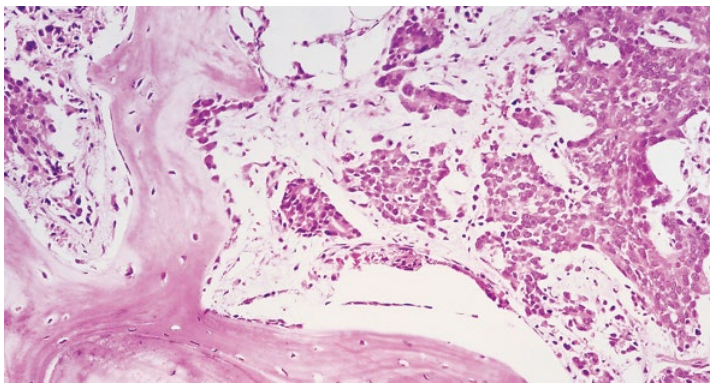

Fig. 30.16. Metastatic carcinoma. There is thickening of medullary trabecular bone, and osteoblasts are prominent along the right-hand margin of the vertical trabecula. The intertrabecular space contains nests of malignant epithelial cells supported by an abundant fibrous stroma. The patient had carcinoma of the prostate.

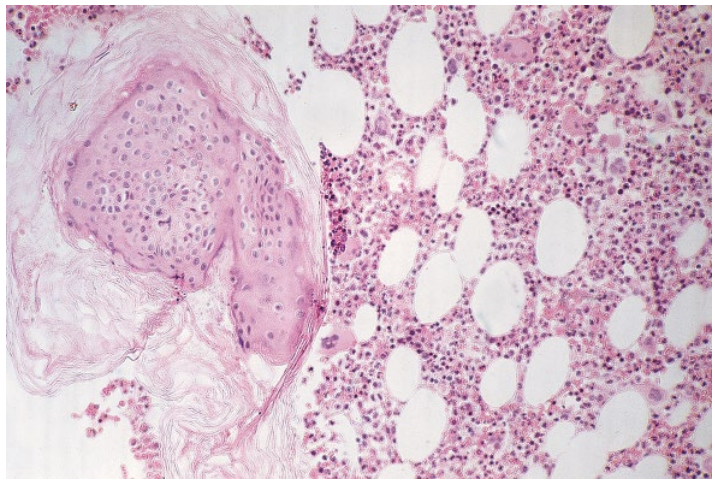

Fig. 30.17. Artifact on trephine biopsy. A small fragment of well-differentiated keratinized squamous epithelium has been carried into the bone marrow cavity. Normal hematopoietic tissue is on the right.

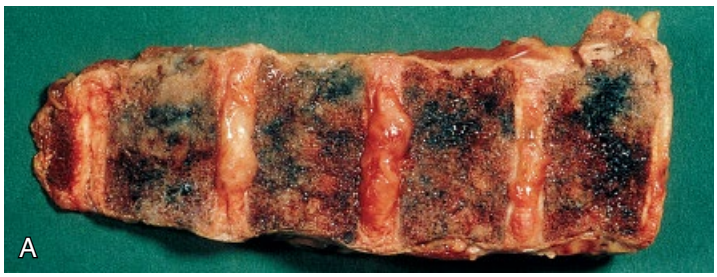

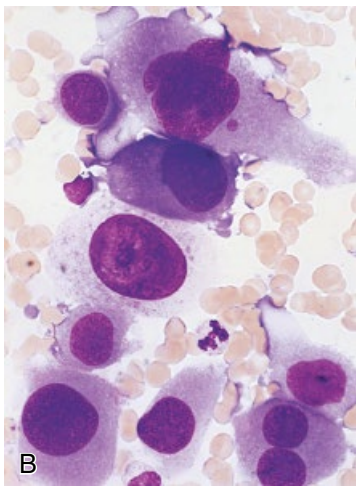

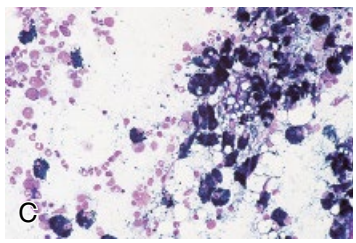

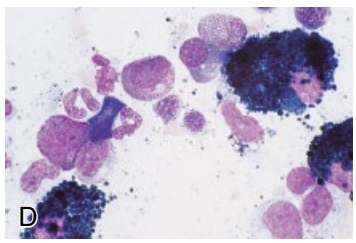

Fig. 30.18. Metastatic malignant melanoma. **A,** Postmortem section of spine showing multiple black deposits. **B,** Large malignant melanoma cells of variable size with primitive chromatin patterns and nucleoli. **C** and **D,** Lower- and higher-power views show no malignant cells, but numerous melanin-filled macrophages are evident. The patient had a malignant melanoma on the skin of the back. (*A,* Courtesy of Dr. R Britt.)

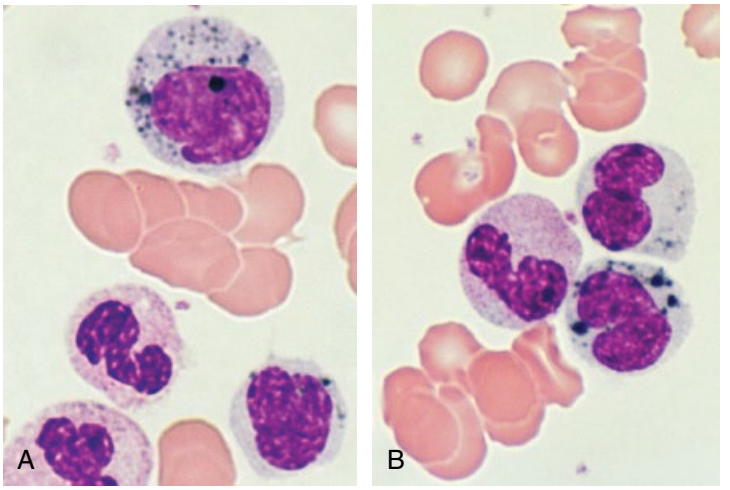

Fig. 30.19. Malignant melanoma. Blood film showing monocytes with inclusions of phagocytosed melanin.

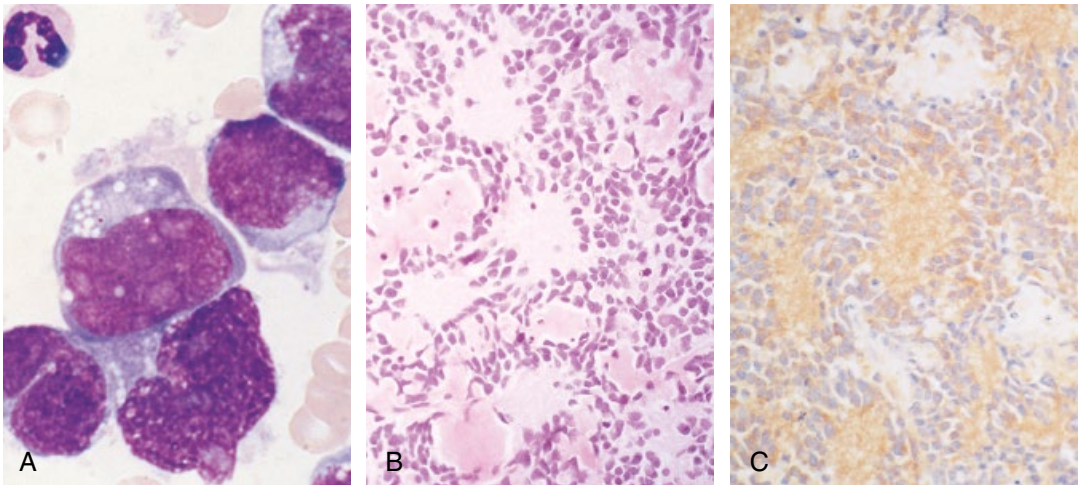

Fig. 30.20. Metastatic neuroblastoma. **A,** Bone marrow from a 3-year-old boy with neuroblastoma in the right thorax shows malignant "neuroblasts," somewhat larger and more pleomorphic than hematopoietic blast cells and with fine chromatin patterns and prominent nucleoli. **B,** Rosettes of neuroblastoma cells, some pyriform or fibrillar, with neurofibrils within amorphous extracellular material. **C,** Staining for neuron-specific enolase, using an immunoperoxidase–avidin biotin complex technique, demonstrates the antigen within the cells and in the neurofibrillary extracellular material. (*B* and *C,* Courtesy of Dr. POG Wilson.)

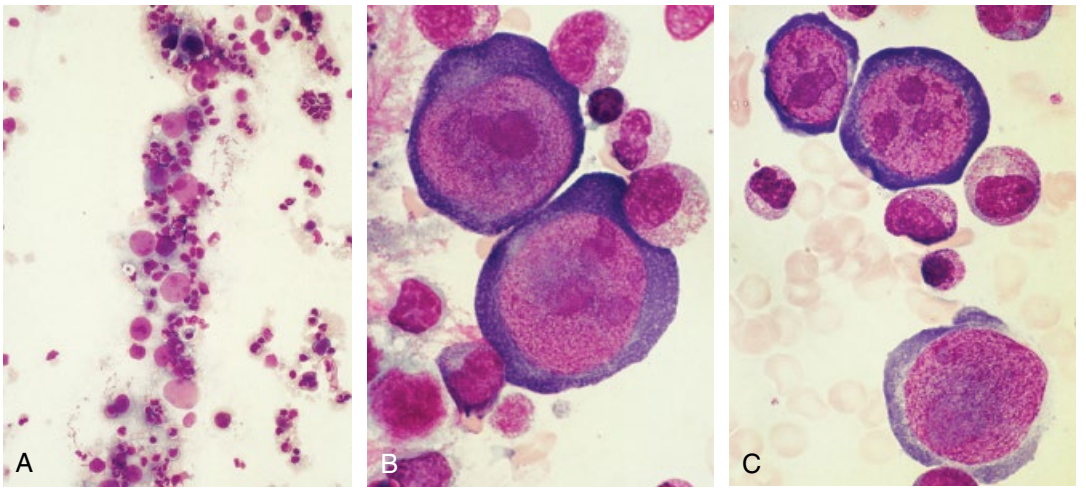

Fig. 30.21. Kaposi sarcoma: Marrow aspirate. **A,** Low-power view of a cell trail showing numerous large pleomorphic cells. **B**, **C,** High-power images showing basophilic cytoplasm and nuclear detail, including large prominent nucleoli.

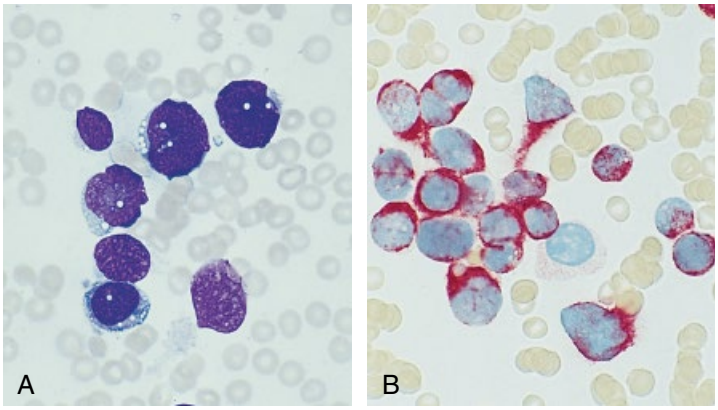

Fig. 30.22. Metastatic rhabdomyosarcoma: **A,** May-Grünwald–Giemsa stain**; B,** anti-desmin antibody (AP-AAP technique). (*A* and *B,* Courtesy of Professor DY Mason.)

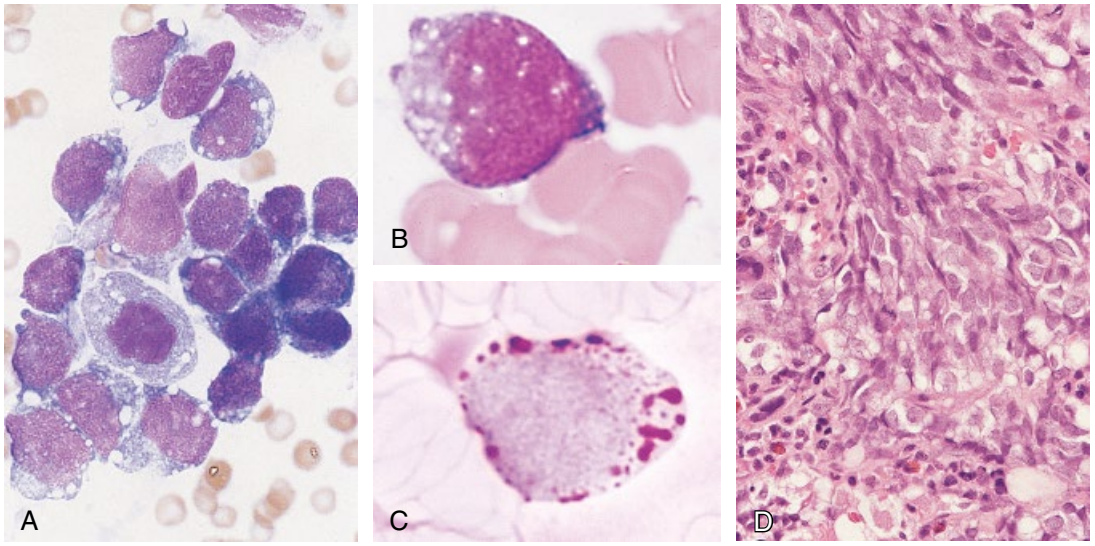

Fig. 30.23. Metastatic Ewing sarcoma. **A,** Bone marrow aspirate showing vacuolated pleomorphic cells, including a cell in mitosis. **B,** At higher magnification a tumor cell shows a fine chromatin pattern and vacuolated basophilic cytoplasm. **C,** Periodic acid–Schiff base (PAS) staining shows coarse blocks of positive material. **D,** A trephine biopsy shows a sheetlike deposit of primitive cells with normal hematopoietic cells below. (*A* and *B,* May-Grünwald–Giemsa; *C,* PAS; *D,* H&E.) (*A* and *D,* Courtesy of Dr. DM Swirsky.)

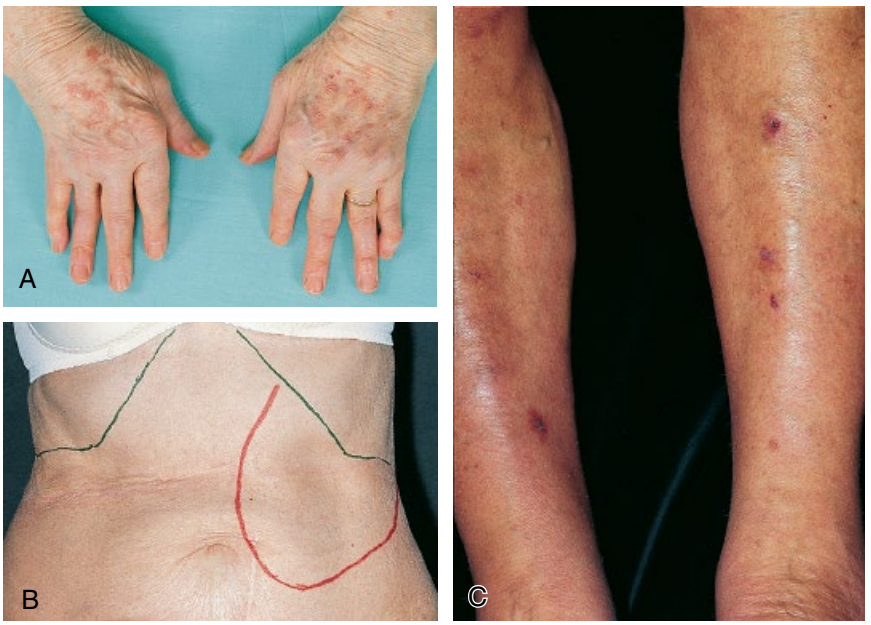

Fig. 30.24. Felty syndrome. **A,** The deformities of rheumatoid arthritis include prominent ulnar styloids, ulnar deviation of the hands, swan-neck deformities (best seen in the right fourth finger and left fourth and fifth fingers), and wasting of the intrinsic muscles. **B,** Splenic enlargement. **C,** Skin ulceration on the anterior surface of the leg.

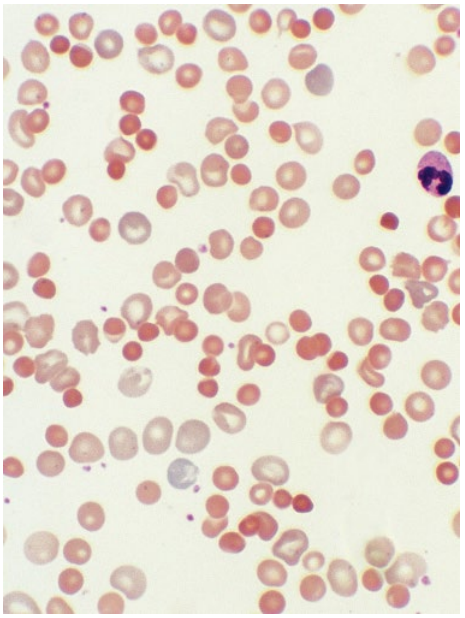

Fig. 30.25. Systemic lupus erythematosus. Blood film in autoimmune hemolytic anemia showing prominent red cell spherocytosis and polychromasia.

TABLE 30.3. HEMATOLOGIC ABNORMALITIES IN RENAL DISEASE

Anemia
Reduced erythropoietin production
Aluminium excess in dialysis patients
Anemia of chronic disorders
Iron deficiency
blood loss (e.g. dialysis, venesection, defective platelet function)
Folate deficiency
chronic hemodialysis without replacement therapy
Abnormal platelet function
Thrombocytopenia
Immune complex-mediated (e.g. systemic lupus erythematosus, polyarteritis nodosa)
Some cases of acute nephritis and following allograft
Hemolytic–uremic sydrome and thrombotic thrombocytopenic purpura
Thrombosis
Some cases of the nephrotic syndrome
Polycythemia
In renal allograft recipients
Rarely, in renal cell carcinoma, cysts, arterial disease

as a result of excess sialic acid in the fibrinogen molecules. These hemostatic defects contribute to major blood loss from bleeding varices caused by portal hypertension.

HYPOTHYROIDISM

A moderate anemia is usual and can be caused by lack of thyroxine. T_3 and T_4 potentiate the action of erythropoietin. The blood film shows mild macrocytosis and acanthocytosis (Fig. 30.30). There is also a reduced oxygen need and thus reduced erythropoietin secretion. Autoimmune thyroid disease, especially myxedema or Hashimoto disease, is associated with pernicious anemia. Iron deficiency can also be present, particularly in women with menorrhagia.

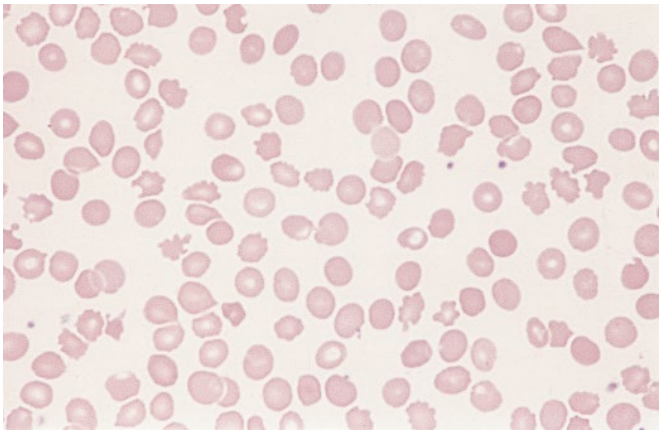

Fig. 30.26. Renal failure. Peripheral blood film showing coarse acanthocytes and "burr" cells.

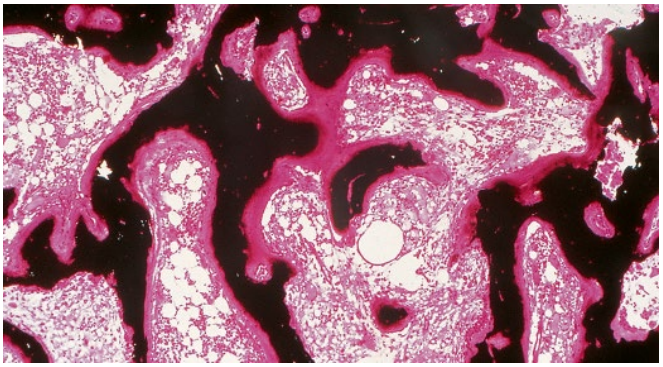

Fig. 30.27. Osteomalacia. Thickened trabeculae with prominent layers of uncalcified osteoid on their outer borders. (Von Kossa stain.) (Source: Courtesy of Bullough PG, Vigorita VJ. *Atlas of Orthopedic Pathology,* Gower Medical Publishing, New York, 1984.)

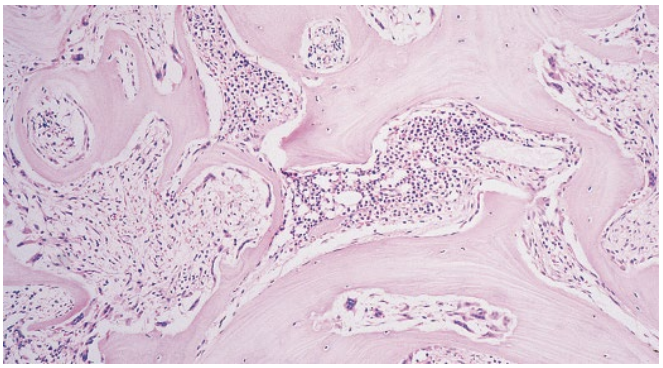

Fig. 30.28. Renal osteodystrophy and osteitis fibrosa cystica. Extensive resorption of bone trabeculae with fibrous replacement. Osteoclasts lie adjacent to areas of active resorption.

TABLE 30.4. HEMATOLOGIC ABNORMALITIES IN LIVER DISEASE

Liver failure ± obstructive jaundice ± portal hypertension
Anemia
Usually mildly macrocytic, often with target cells, may be associated with:
Blood loss and iron deficiency
Alcohol (± ring sideroblastic change)
Folate deficiency
Hemolysis (e.g. Zieve syndrome, Wilson disease, autoimmune, hypersplenism from portal hypertension)
Bleeding tendency
Deficiency of vitamin K-dependent factors; also of factor V and fibrinogen
Thrombocytopenia in hypersplenism, immune, platelet function defects
Functional abnormalities of fibrinogen
Increased fibrinolysis
Portal hypertension – hemorrhage from varices
Viral hepatitis
Aplastic anemia
Tumors
Polycythemia
Neutrophil leukocytosis and leukemoid reactions

INFECTIONS

BACTERIAL INFECTIONS

Blood and bone marrow abnormalities occur in many infections (Table 30.5). Anemia of chronic disorders is found in chronic bacterial infections. Severe hemolytic anemia, sometimes associated with disseminated intravascular coagulation, can occur with bacterial septicemia, particularly those associated with meningococcal and gram-negative organisms. *Clostridium perfringens* organisms produce an α toxin, a lecithinase that produces marked spherocytosis. In children, the hemolytic–uremic syndrome can be associated with infection by *Escherichia coli* with verotoxin 0157 (Fig. 30.31) or with other organisms, for example, *Shigella*. Hemolysis in Oroya fever is caused by direct red cell infection by *Bartonella* organisms. *Mycoplasma pneumoniae* infections are associated with "cold"-type autoimmune hemolytic anemia.

Bacterial infections are the most common causes of neutrophil leukocytosis, and severe infections can be associated with a leukemoid reaction. In tuberculosis, marrow replacement by granulomatous infiltration and fibrosis (Fig. 30.32) associated with miliary disease causes leukoerythroblastic change in blood and increases the severity of the anemia. If left untreated, tuberculosis involving the bone marrow becomes extensive, particularly in the anterior aspects of the vertebral bodies and in the

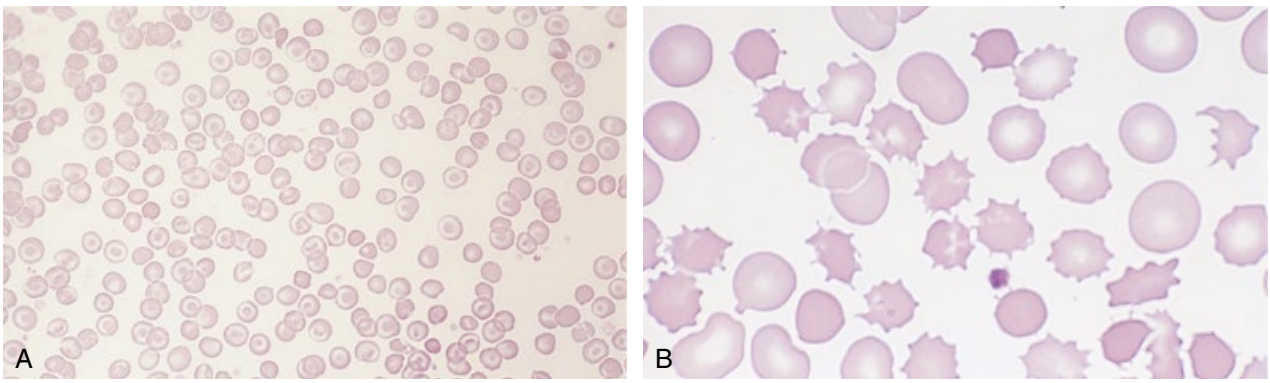

Fig. 30.29. Liver disease. **A,** Peripheral blood films showing marked target cell formation. **B,** At higher magnification, marked red cell acanthocytosis is seen.

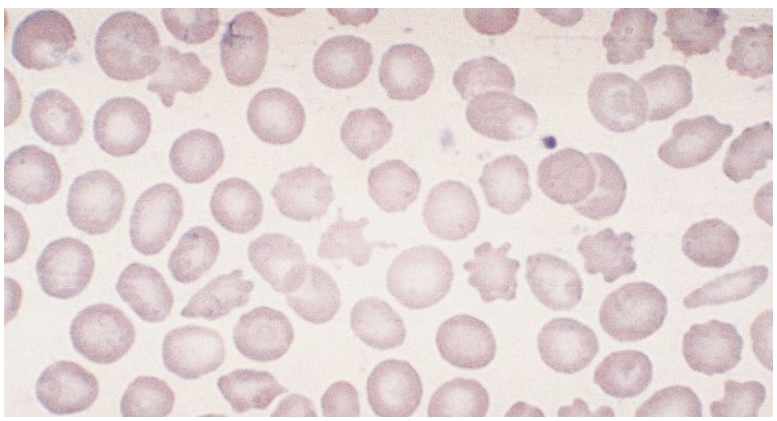

Fig. 30.30. Hypothyroidism. Peripheral blood film showing mild macrocytosis, poikilocytosis, and irregular acanthocytosis.

TABLE 30.5. HEMATOLOGIC ABNORMALITIES IN INFECTIONS

Hematologic abnormality	Infection associated
Anemia	
Anemia of chronic disorders	Chronic infections, especially tuberculosis
Aplastic anemia	Viral hepatitis
Transient red-cell aplasia	Human parvovirus
Marrow fibrosis	Tuberculosis
Immune hemolytic anemia	Infectious mononucleosis, *Mycoplasma pneumoniae*
Direct red-cell damage or microangiopathic	Bacterial septicemia (associated disseminated intravascular coagulation) *Clostridium perfringens*, malaria, bartonellosis
	Viruses – hemolytic–uremic syndrome and thrombotic thrombocytopenic purpura
Hypersplenism	Chronic malaria, tropical splenomegaly syndrome, leishmaniasis, schistosomiasis
White cell changes	
Neutrophil leukocytosis	Acute bacterial infections
Leukemoid reactions	Severe bacterial infections, particularly in infants
	Tuberculosis
Eosinophilia	Parasitic diseases (e.g. hookworm, filariasis, schistosomiasis)
	Recovery from acute infections
Monocytosis	Chronic bacterial infections – tuberculosis, brucellosis, bacterial endocarditis, typhoid
Neutropenia	Viral infections – human immunodeficiency virus, hepatitis, influenza
	Fulminant bacterial infections (e.g. typhoid, miliary tuberculosis)
Lymphocytosis	Infectious mononucleosis, toxoplasmosis, cytomegalovirus, rubella, viral hepatitis, pertussis, tuberculosis, brucellosis
Lymphopenia	Human immunodeficiency virus infection
	Legionella pneumophila
Thrombocytopenia	
Megakaryocytic depression, immune-complex mediated, and direct interaction with platelets	Acute viral infections, particularly in children (e.g. measles, varicella, rubella, malaria, severe bacterial infection)
Prothrombotic state	All with prolonged inflammation

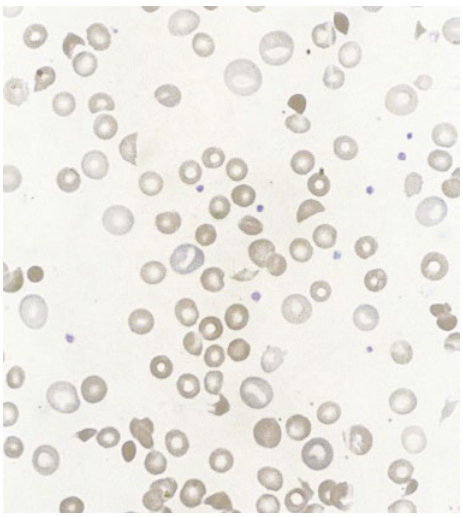

Fig. 30.31. Hemolytic–uremic syndrome: Blood film in a child with *Escherichia coli* septicemia. The red cells show marked fragmentation, polychromasia, and anisocytosis.

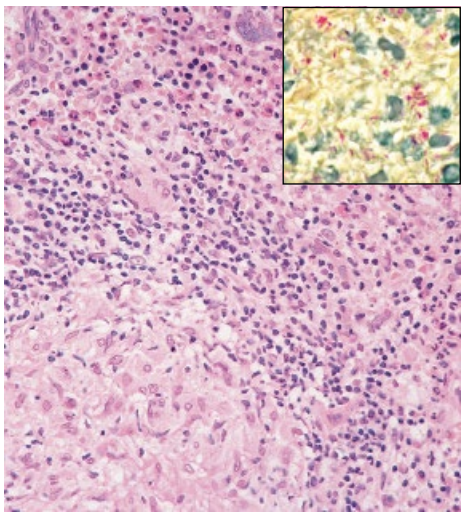

Fig. 30.32. Tuberculosis: A small granuloma surrounded by hyperplastic hematopoietic tissue. The *inset* shows small numbers of acid-fast bacilli. (*Inset,* Ziehl–Neelsen stain.)

metaphyseal regions of long bones, producing cystic areas of osteomyelitis that erode the endplates and can involve nearby joint spaces.

In Whipple disease (infection with *Tropheryma whippelii*), marrow examination shows granulomatous inflammation or other changes (Fig. 30.33).

VIRAL INFECTIONS

Infectious mononucleosis (Epstein–Barr virus [EBV] infection) and human immunodeficiency virus (HIV) infection are associated with a wide range of hematologic changes, and both of these conditions are described and illustrated in Chapter 11.

Acute viral infections are often associated with mild anemia. An immune hemolytic anemia with anti-i autoantibody occurs in infectious mononucleosis, and other viral infections, as well as syphilis, have been associated with paroxysmal cold hemoglobinuria. Viruses have been associated with the hemolytic–uremic syndrome, thrombotic thrombocytopenic purpura, and the hemophagocytic syndrome. Aplastic anemia can follow infection with hepatitis A but is more frequently seen in non-A, non-B, non-C hepatitis. Transient red cell aplasia is associated with parvovirus infection and can cause severe anemia in patients who already have a hemolytic anemia (e.g. hereditary spherocytosis or sickle cell disease).

Many viral infections, including rubella and cytomegalovirus (CMV) infection, are associated with a reactive lymphocytosis with variable numbers of atypical lymphocytes in the blood film. Transient neutropenia is frequently present. CMV transmission by white cells can cause a post-transfusion infectious mononucleosis-like syndrome. In stem cell transplant recipients or other immunosuppressed patients, CMV infections can cause pancytopenia. CMV infections in infants are associated with massive splenomegaly and hepatomegaly.

Acute and transient immune or nonimmune thrombocytopenia can follow viral infection, particularly in children.

Toxoplasmosis

Toxoplasmosis in adults and children is associated with lymphadenopathy and large numbers of atypical lymphocytes in the blood (Fig. 30.34). Newborn infants with congenital disease may be hydropic and have gross hepatomegaly, splenomegaly,

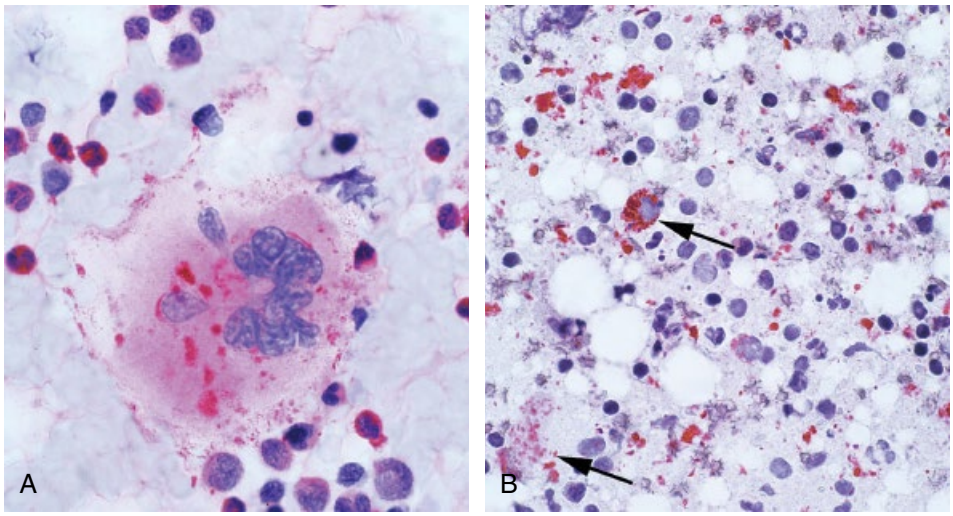

Fig. 30.33. Whipple disease. **A,** Bone marrow aspirate showing a hypersegmented megakaryocyte with strongly periodic acid–Schiff base (PAS) positive staining cytoplasmic inclusions. **B,** Mesenteric lymph node section, diastase-resistant PAS stain. *Left arrow,* Diastase-resistant PAS-positive granular material and bacilliform structures in the extracellular space. *Right arrow,* Granular and rod-shaped inclusions in macrophages. (Courtesy of Dr. R Walter.)

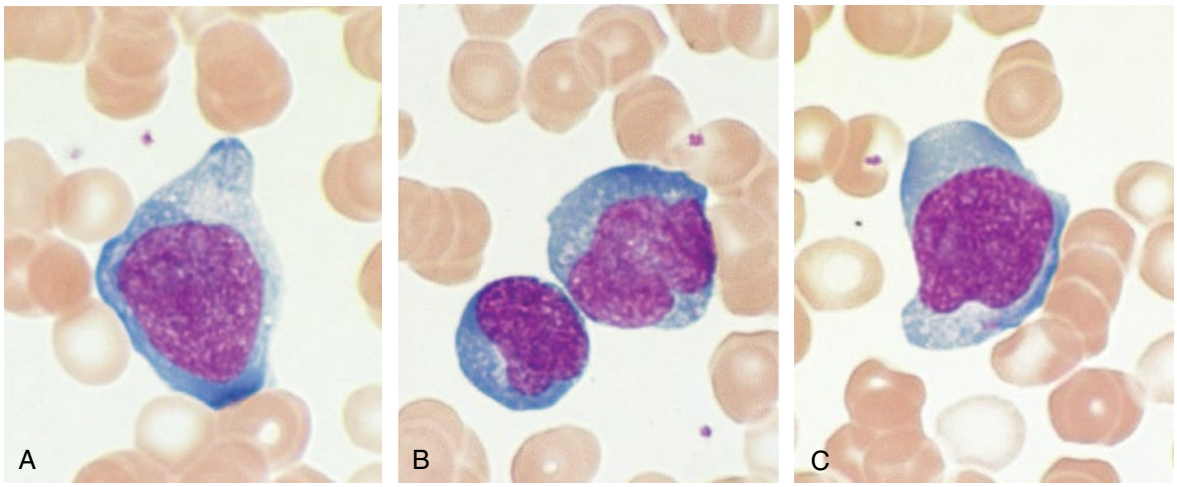

Fig. 30.34. Toxoplasmosis: Blood film showing atypical lymphocytes.

leukoerythroblastic anemia, and thrombocytopenia. Their condition may be mistaken for hydrops fetalis (see Figs. 11.35 and 31.16).

PARASITIC INFECTIONS DIAGNOSED IN BLOOD

Parasitic involvement of blood is discussed separately and in more detail in Chapter 31, which includes descriptions of malaria and other protozoan parasites responsible for trypanosomiasis, babesiosis, and toxoplasmosis; the microfilaria of roundworm infections, filariasis and loaiasis; bacterial infection in bartonellosis; and the spirochetes responsible for borreliosis, or sleeping sickness.

Kala-azar (Visceral Leishmaniasis)

Kala-azar is distributed widely throughout tropical and warm regions of the world. The causal organism, *Leishmania donovani,* is transmitted by the bite of sandflies of the genus *Phlebotomus*. Nonflagellated amastigote forms of the organism are distributed widely through macrophages in the bone marrow, spleen, and liver. Diagnosis is made by examining bone marrow (Fig. 30.35), splenic aspirates, or biopsy specimens. Clinical features include fever, lassitude, weight loss, splenomegaly, hepatomegaly, anemia, neutropenia, and polyclonal increases in immunoglobulin.

MARROW INVOLVEMENT IN OTHER INFECTIONS

Bone marrow examination has little part to play in the diagnosis and management of osteomyelitis, although occasionally initial evidence of a disseminated fungal infection is uncovered (Fig. 30.36).

The bone marrow and spleen can be involved in cases of disseminated histoplasmosis. The *Histoplasma capsulatum* organisms are seen inside macrophages either in marrow aspirates or trephine biopsies (Fig. 30.37).

GRANULOMATOUS INFLAMMATION

Granulomatous inflammation of bone marrow is found in a wide variety of disorders (Table 30.6).

SARCOIDOSIS

This granulomatous disorder of unknown etiology most frequently affects the middle-aged. It is characterized by widespread epithelioid granulomas, depression of delayed hypersensitivity, and lymphoproliferation. Multisystem involvement is characteristic; intrathoracic disease affects 90% of cases, ocular and skin involvement each occur in about 20% of cases, and erythema nodosum occurs in one-third of cases. In different series

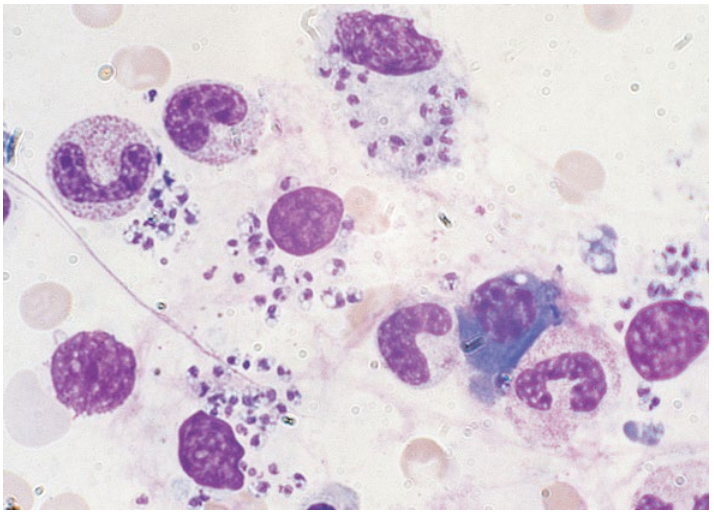

Fig. 30.35. Kala-azar (visceral leishmaniasis): Bone marrow showing macrophages that contain Leishman–Donovan bodies. Also seen are neutrophil metamyelocytes and a plasma cell.

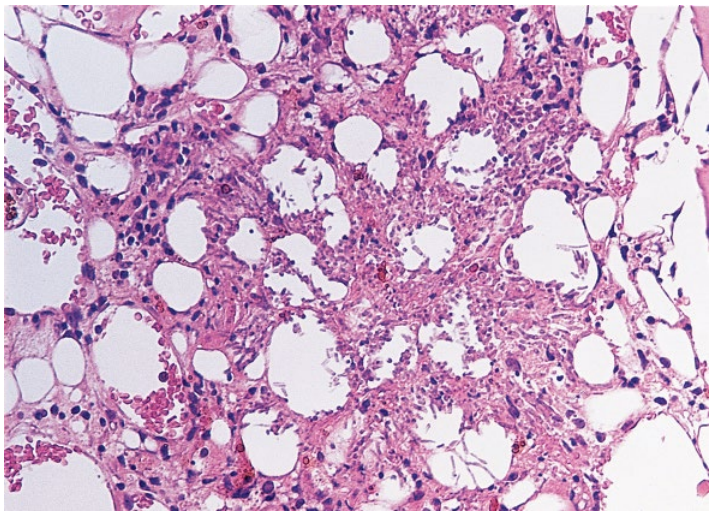

Fig. 30.36. Disseminated aspergillosis. Biopsy taken after bone marrow transplantation showing hyphae of *Aspergillus* in an area of necrosis.

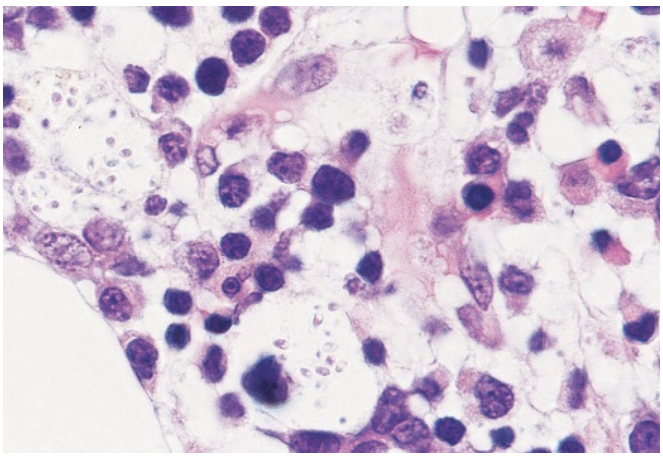

Fig. 30.37. Histoplasmosis: Trephine biopsy. The encapsulated organisms are seen clearly inside the macrophages.

TABLE 30.6. CONDITIONS ASSOCIATED WITH BONE MARROW GRANULOMAS

Infections
Tuberculosis, atypical mycobacterial infection, disseminated bacillus Calmette–Guerin (BCG), leprosy, brucellosis, syphilis, typhoid fever, legionnaire disease, Whipple disease, leishmaniasis, toxoplasmosis, histoplasmosis, cryptococcosis, blastomycosis, coccidiodomycosis, herpes viral infection, and others
Sarcoidosis
Malignancy
Hodgkin lymphoma, non-Hodgkin lymphoma, mycosis fungoides, multiple myeloma, acute lymphoblastic leukemia
Foreign material
Anthracosis, silicosis, berylliosis, talc
Drug hypersensitivity
For example, chlorpropamide, phenylbutazone, phenytoin, sulphasalazine, allopurinol

the reticuloendothelial system has been involved in up to 40% of patients. Evidence of disease can be found during bone marrow examination (Fig. 30.38).

OTHER GRANULOMAS

Evidence of other granulomatous disease can be found during bone marrow examination (Figs. 30.39–30.41). Investigations may reveal a diagnosis, but in many cases no cause is found.

OSTEOPETROSIS (ALBERS–SCHÖNBERG OR MARBLE BONE DISEASE)

Osteopetrosis is group of inherited disorders in which there is defective bone resorption by osteoclasts. This failure of bone resorption and remodeling leads to an increase in density of all bones. The disease is inherited in a severe autosomal recessive form, as an autosomal dominant milder disease, and rarely as an X-linked form. An intermediate form resembles the severe recessive disease but develops later and is milder. Mutations in at least nine genes underlie the disease. Three of the more common genes in which mutations cause osteopetrosis are shown in Fig. 30.42. The most frequently mutated gene is *TC1RG1*, in which more than 60 different mutations have been reported in cases of osteopetrosis. Mutations of this gene have been detected in over 50% of patients. These cause a defect in the osteoclast vacuolar H^+-ATPase proton pump. A second frequently mutated gene is *CLCN7,* which codes for a protein in the osteoclast-specific chloride channel. The third most frequently mutated gene is *CAD11* (Fig. 30.42).

Severe forms of the disease manifest in infancy with anemia and hepatosplenomegaly. These children have little or no bone marrow; hematopoiesis is chiefly extramedullary, and blood transfusions are required to sustain life. The typical radiographic appearances are shown in Figs. 30.43 and 30.44). Characteristic microscopic abnormalities are found in trephine bone biopsies (Figs. 30.45 and 30.46) and leukoerythroblastic changes are seen in the blood. Failure to resorb bone results in optic atrophy, deafness, and hydrocephalus. Allogeneic stem cell transplantation

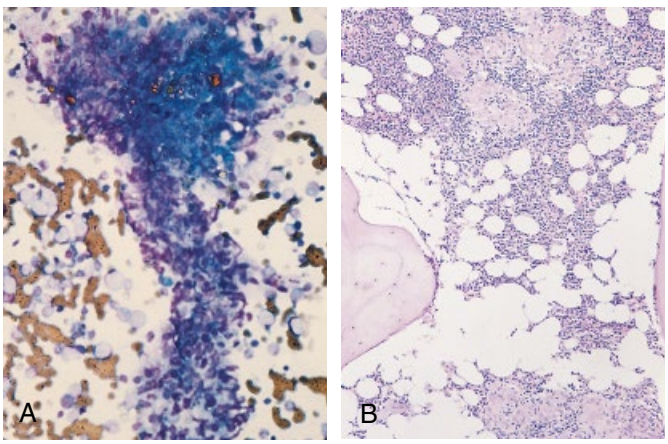

Fig. 30.38. Sarcoidosis. **A,** A sheet of epithelioid histiocytic cells, scattered lymphocytes, and myeloid cells. **B,** Two small granulomas comprising epithelioid cells and lymphocytes.

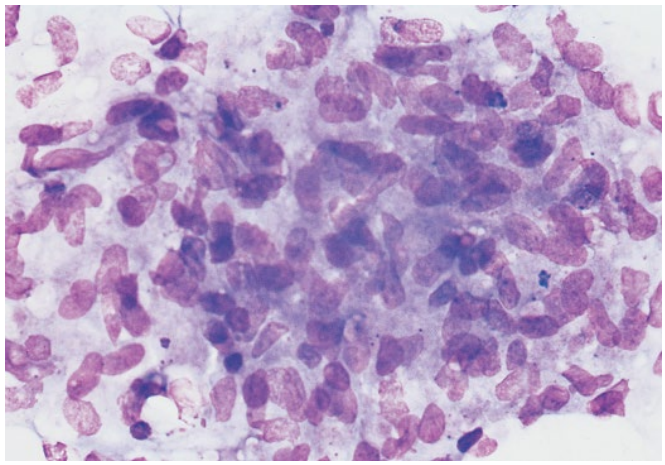

Fig. 30.39. Nonspecific marrow granuloma. This small collection of epithelioid cells was found in a bone marrow cell trail that showed no other abnormality. No specific diagnosis was made.

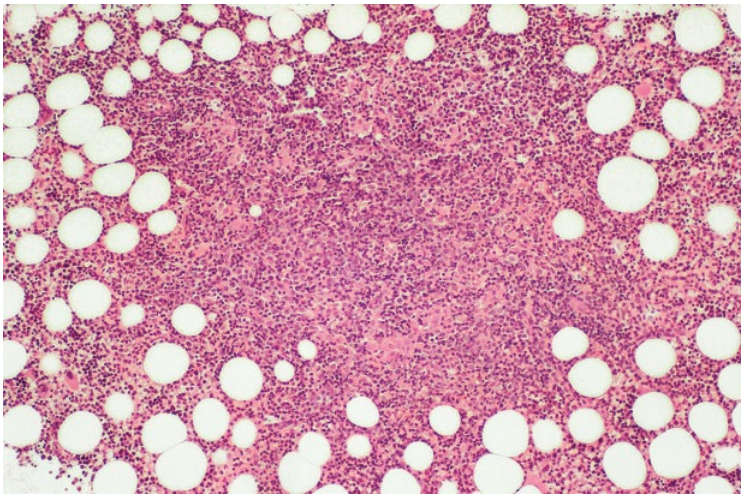

Fig. 30.40. Marrow granuloma. Trephine biopsy in a patient with refractory anemia and concurrent allopurinol hypersensitivity. The intertrabecular space contains a large, loosely formed granuloma of lymphocytes and histiocytes.

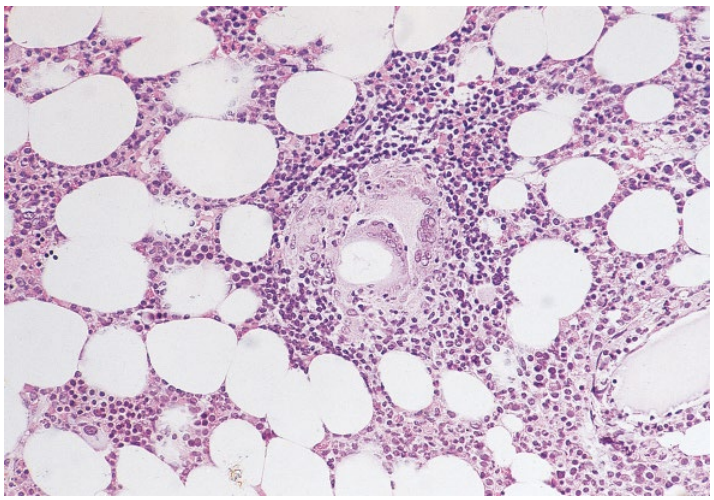

Fig. 30.41. Foreign body granuloma. An isolated granuloma with a central large vacuole that contains a refractile body of uncertain origin surrounded by giant cells.

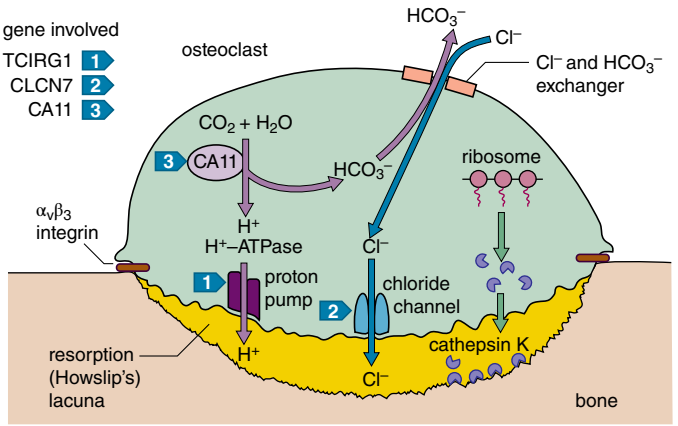

Fig. 30.42. Osteopetrosis: Osteoclast mutations and malfunction. To achieve acidification of the resorption lacunae and demineralization, carbonic anhydrase II (CAD II) generates a proton and bicarbonate from carbon dioxide and water. This proton is passed across the ruffled border membrane through the action of a vacuolar H^+ ATPase "proton pump." A chloride channel coupled to the pump facilitates balancing the ions across the membrane. Excess bicarbonate is removed from the cell by passive exchange with chloride. The organic matrix of bone is removed by cathepsin K and other enzymes. The sites of malfunction caused by the mutations are indicated. (Source: Modified from Tolar J et al. *N Engl J Med* 2004;351:2839–2849. Reproduced with permission of Massachusetts Medical Society: The New England Journal of Medicine.)

may cure the disease. Milder cases manifest later in childhood or in adult life with retarded growth, anemia, and splenomegaly. The dominantly inherited form usually occurs with fractures, scoliosis or with dense bones discovered by chance.

ANOREXIA NERVOSA

These patients have severe deficiency of carbohydrates, fats, and calories, but little protein deficiency. The peripheral blood may reveal mild anemia and thrombocytopenia with acanthocytes; the marrow is hypocellular, with fat cells replaced by acid mucopolysaccharides appearing as pink-staining extracellular material (Fig. 30.47). Similar appearances occur in other causes of malnutrition, such as extensive neoplasia (Fig. 30.48).

CYSTINOSIS

In this recessively inherited disease, cystine crystals are deposited in the reticuloendothelial and corneal tissues. In its more severe form (cystinosis with Fanconi syndrome or the de

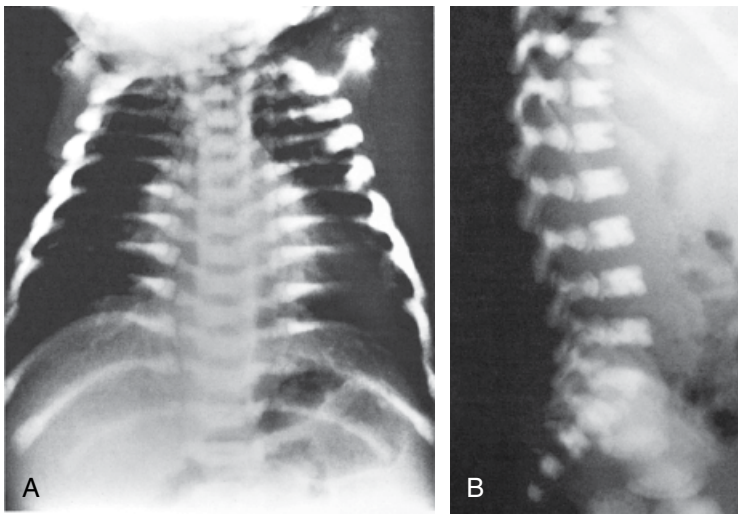

Fig. 30.43. Osteopetrosis. Radiographs of the chest **(A)** and the lower spine **(B)** of an infant with a gross generalized increase in bone density. The changes are most marked at the upper and lower margins of the vertebral bodies. The vertebrae also show the characteristic "bone-in-bone" appearance.

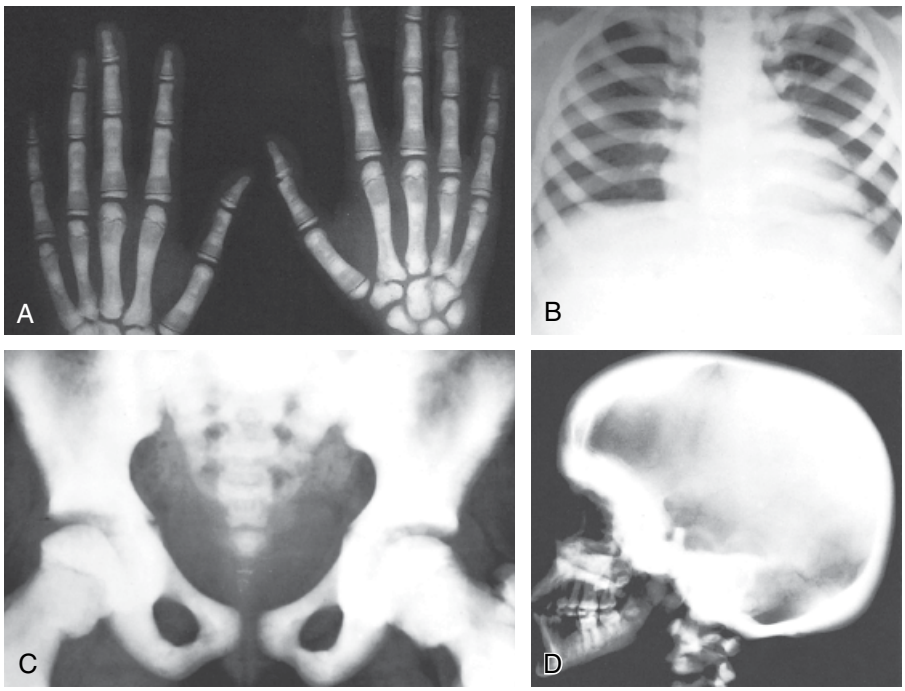

Fig. 30.44. Osteopetrosis. Radiographs of the hands **(A),** the chest **(B),** the pelvis **(C),** and the skull **(D)** of a 14-year-old girl with retarded growth, leukoerythroblastic anemia, and massive splenomegaly. The bones are dense with coarse trabeculation and lack the usual corticomedullary demarcation. The mandible appears normal.

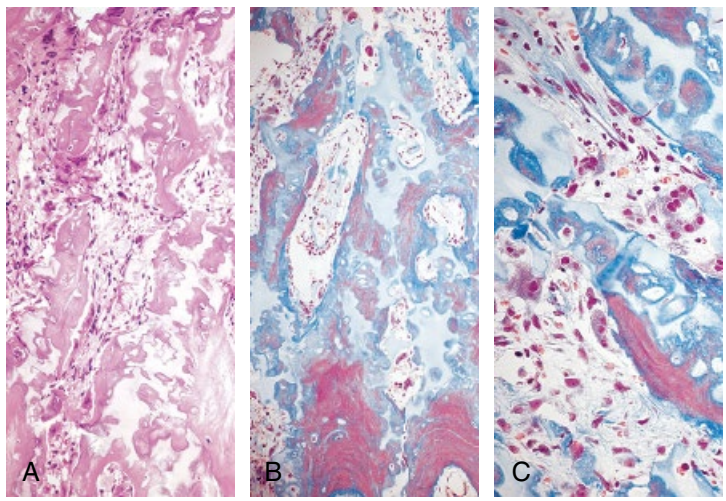

Fig. 30.45. Osteopetrosis. **A,** Compacted intramedullary osseous tissue and relatively little hematopoietic tissue; cores of cartilaginous matrix are bordered by areas of primitive bone. **B** and **C,** Persistence of cartilage, lack of bone modeling, and primitive osseous tissue at the edges of and within the cartilage. (*B* and *C,* Picro-Mallory stain.)

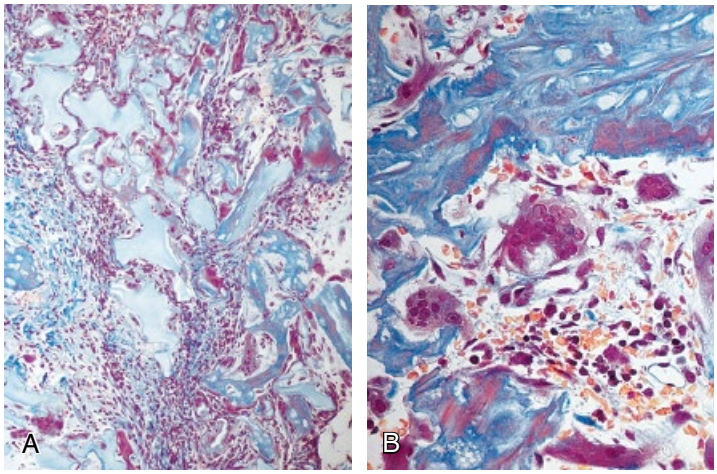

Fig. 30.46. Osteopetrosis: Biopsy (same case as shown in Fig. 30.45). **(A)** showing large numbers of osteoclasts, better seen at high power **(B).** There is little evidence of bone resorption, and no trabeculae or hematopoietic marrow spaces are seen. (*A* and *B,* Picro-Mallory stain.)

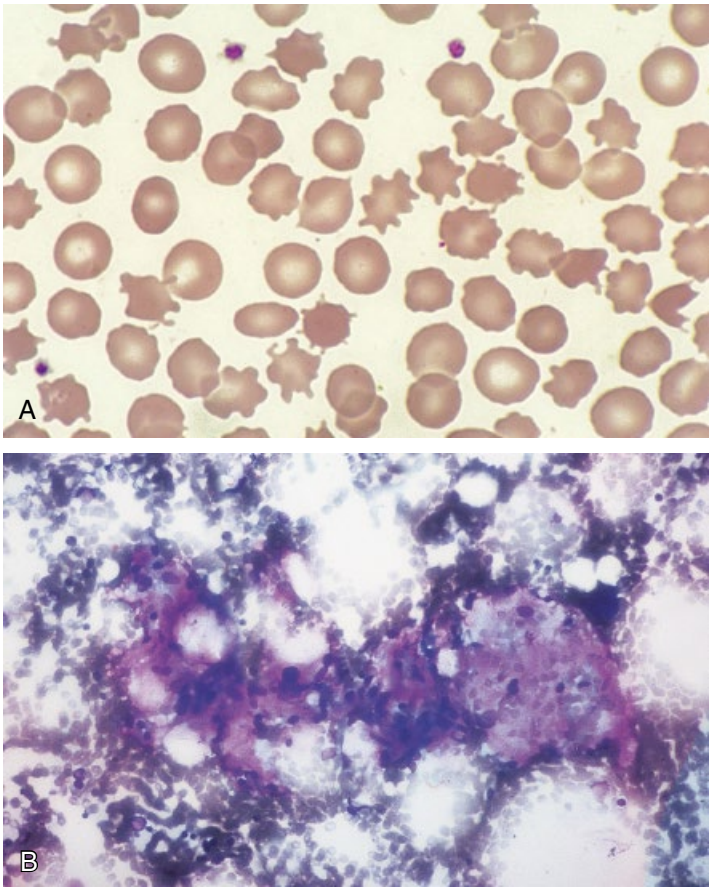

Fig. 30.47. Anorexia nervosa. **A,** Peripheral blood film showing red cell acanthocytosis. **B,** Bone marrow showing extracellular homogeneous pink- and purple-staining material that replaces fat spaces and is composed of acid mucopolysaccharide.

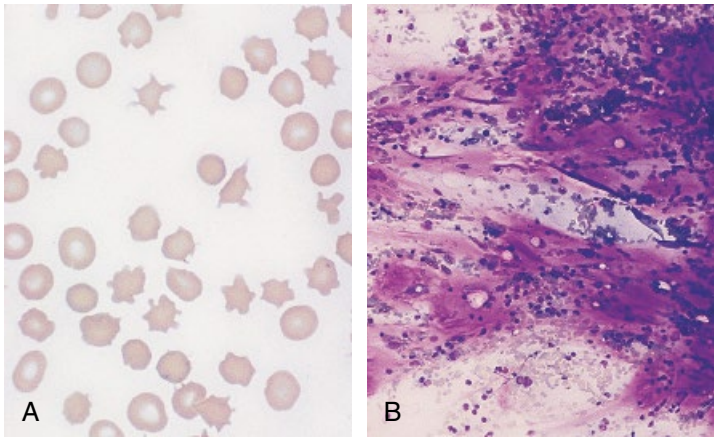

Fig. 30.48. Cachexia caused by carcinomatosis. **A,** Peripheral blood film and bone marrow showing similar appearances to those in Fig. 30.47 **(B).** (*A* and *B,* Courtesy of Dr. D Simpson.)

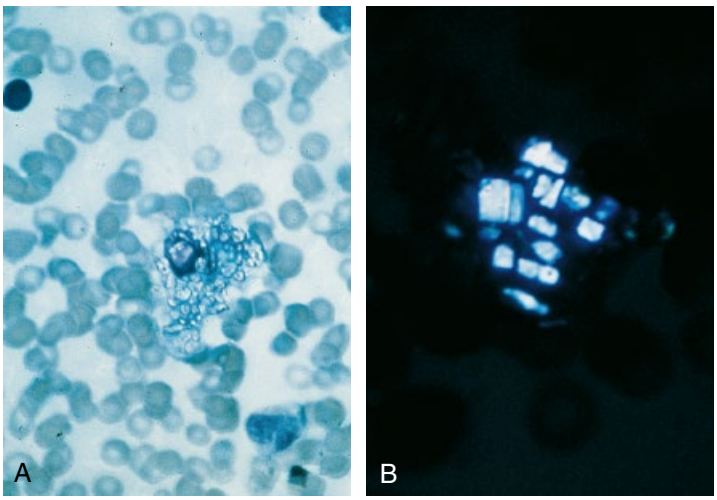

Fig. 30.49. Cystinosis. **A,** Bone marrow containing histiocytic cells, which under polarized light **(B)** show the characteristic birefringence of cystine crystals.

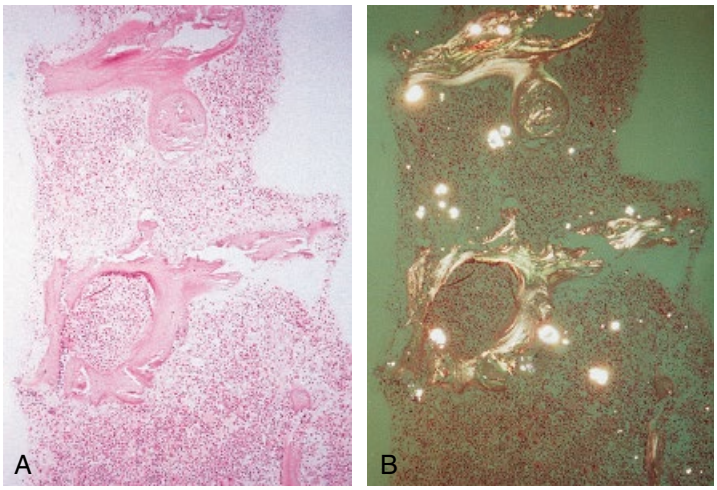

Fig. 30.50. Primary oxaluria. **A,** Normal and **B,** polarizing microscopy showing birefringent calcium oxalate monohydrate crystals (and normal birefringent cortical bone). The patient, a 3-month-old boy, had renal failure. (*A* and *B,* Courtesy of Dr. S Milkins.)

Toni–Fanconi–Lignac syndrome), progressive renal degeneration is fatal during early childhood. Children with this syndrome usually have anorexia, thirst, polyuria, failure to thrive, rickets, or photophobia. Laboratory tests reveal glycosuria, proteinuria, low serum bicarbonate, hypokalemia, or hypophosphatemia. The diagnosis is established by the demonstration of cystine crystals in macrophages in bone marrow aspirates (Fig. 30.49).

PRIMARY OXALURIA

In this fatal autosomal recessive metabolic disorder, there is widespread deposition of calcium oxalate crystals in the kidneys and elsewhere in the body, including the liver, spleen, and bone marrow (Fig. 30.50). A number of different enzyme deficiencies have been implicated as causal factors.

CHAPTER

31

PARASITIC DISORDERS

MALARIA

The protozoal disease malaria has a distribution that is essentially worldwide in tropical and warm temperate regions. Mosquito-borne infection is caused by four species of the genus *Plasmodium: P. vivax* (benign tertian), *P. falciparum* (malignant tertian), *P. malariae* (quartan), and *P. ovale* (ovale tertian). Infections caused by *P. vivax* and *P. falciparum* are the most common, with the latter much more likely to be life threatening.

The malarial life cycle (Fig. 31.1) begins in the female mosquito after ingestion of human blood that contains the sexual forms (gametocytes) of the causal organisms. The resultant conjugate develops into infective forms (sporozoites) within the mosquito, which are transmitted to humans when the

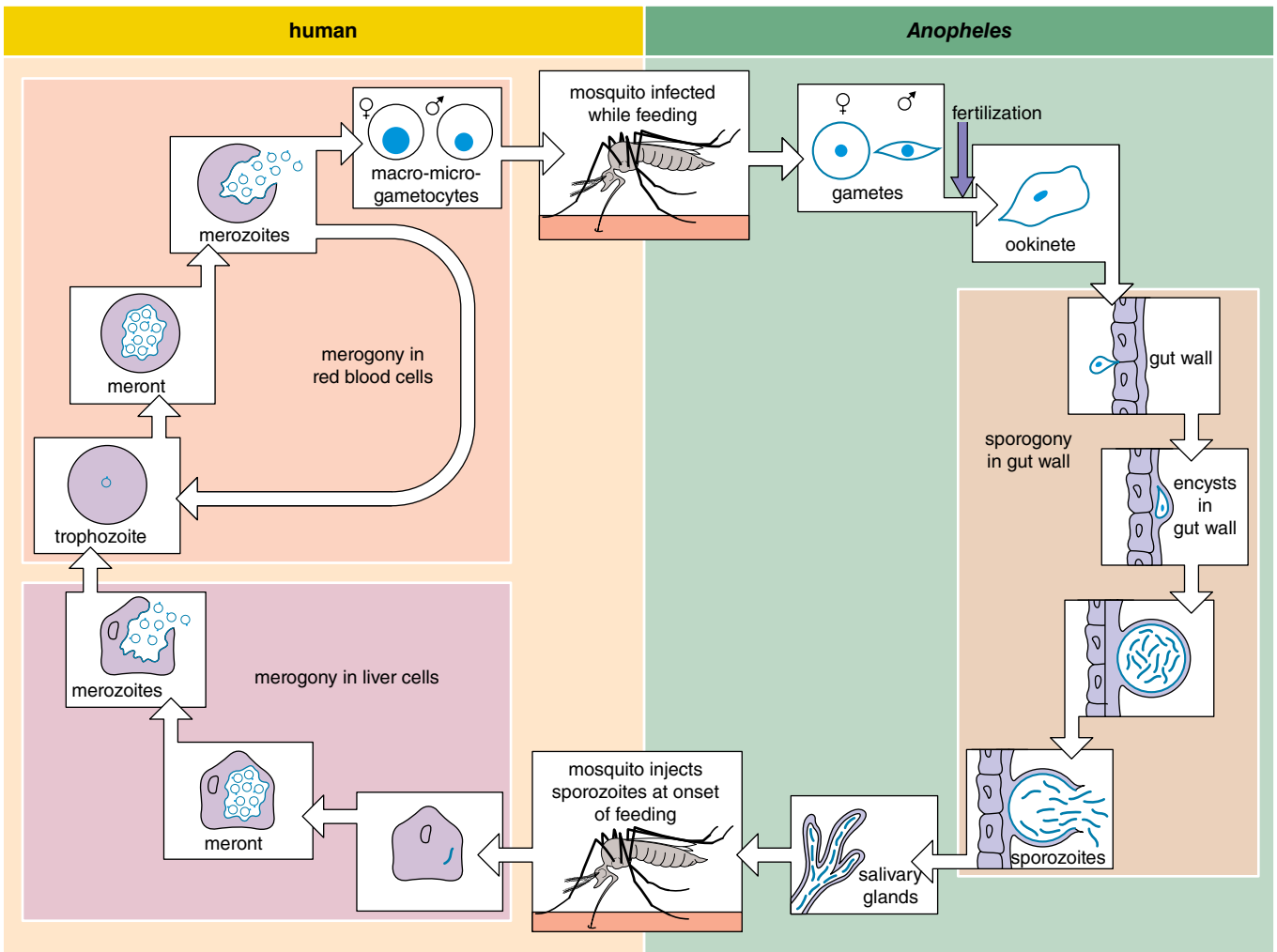

Fig. 31.1. Life cycle of a malarial parasite.

Color Atlas of Clinical Hematology: Molecular and Cellular Basis of Disease, Fifth Edition. A. Victor Hoffbrand, Paresh Vyas, Elías Campo, Torsten Haferlach, and Keith Gomez

TABLE 31.1. IDENTIFICATION OF THE DIFFERENT FORMS OF MALARIA IN THE PERIPHERAL BLOOD

	Plasmodium falciparum	*Plasmodium malariae*	*Plasmodium vivax*	*Plasmodium ovale*
Red blood cells (RBCs)				
Enlargement	None	None	Yes	Yes; oval shape; fimbriated edge
Inclusions (not always present)	Maurer's clefts	Ziemann's dots (rare)	Schüffner's dots (coarse red granules)	Red granules similar to Schüffner's dots
Ring form				
Size	Less than one-third of RBC	Greater than one-third of RBC	Greater than one-third of RBC	Greater than one-third of RBC
Multiple parasites in RBC	Common; often at margins	Rare	Rare	Rare
Shape	Delicate; often double chromatin dot	Tends to be compact; inverted chromatin dot	Rough; single chromatin dot	Rough; single chromatin dot common
Ameboid forms	Absent	Common; often as band across RBC	Common	Common
Meront (schizont)				
Frequency	Very rarely seen	Common; dense, central, yellow–black hemozoin pigment	Common; with hemozoin pigment	Common
Configuration	Random	Daisy head	Random	Daisy head
Merozoite number	8–24	8–12	12–24	8–12
Gametocyte				
	Crescent forms; centrally placed chromatin	Small and round; eccentrically placed chromatin; occupies half to two-thirds of RBC	Large and round; eccentrically placed chromatin; fills RBC	Small and round; eccentrically placed chromatin; occupies half to two-thirds of RBC

Infections with two types of malarial parasite are common.

insects feed. The sporozoites pass through the blood to the parenchymal cells of the liver, where they multiply and divide, producing merozoites in this pre-erythrocytic phase. When the liver cell ruptures, the parasites enter the red cells. In the red cells, the parasites pass from early trophozoite, or ring forms, to actively ameboid forms with malarial pigment (hemozoin), which then undergo chromatin division to form merozoites. The mature parasite is called a meront (schizont). The red cell ruptures, releasing merozoites into the plasma, which may enter other red cells and repeat the cycle or form male and female sexual forms (gametocytes).

The four types of malaria organisms are distinguished by their characteristic appearances within red cells (Table 31.1). In *P. vivax* infection (Fig. 31.2), the red cells are large (because they are young) and Schüffner's dots (degraded red cell microtubules) are present; the ring forms and meronts of the parasites are large, with up to 24 merozoites per meront.

In *P. falciparum* infections (Fig. 31.3), usually a heavy parasitemia with small ring forms occurs, often with double chromatin dots; multiple ring forms are found, some on the margins within individual red cells, and the red cells contain blue-staining Maurer's clefts. The gametocytes have a characteristic crescent shape, and meronts are rarely seen.

As in *P. falciparum* infections, with *P. malariae* (Fig. 31.4) the red cells are not enlarged and do not contain pigment; the ring form tends to have an inverted chromatin dot. Occasionally, dustlike stippling (Ziemann's dots) is seen. The ameboid trophozoites often show band forms, and the merozoites show a "daisy-head" distribution.

P. ovale (Fig. 31.5) infections are distinguished by the parasitized red cells being enlarged and oval-shaped, but with fimbriated edges. The red cells show red granules similar to Schüffner's dots, and the meronts have a daisy-head distribution.

Immunochromatography methods (Fig. 31.6) are able to identify *P. falciparum* and distinguish this infection from other malarial species. These techniques use two antibodies, one specific to the histidine protein-rich protein II of *P. falciparum* and the other specific for an antigen common to all four malarial species.

EFFECTS OF MALARIA ON VARIOUS ORGANS

Malaria affects the structure and function of various organs. The most serious complication is cerebral malaria, which can prove fatal. Parasites in cerebral capillaries (Figs. 31.7 and 31.8) can lead to hemorrhage (Figs. 31.9 and 31.10). The placenta is infested with parasites, but they do not usually cross from the maternal to the fetal circulation (Fig. 31.11).

Anemia is frequent, partly because parasitized red cells are prematurely destroyed and phagocytosed (Fig. 31.12). It may also arise from hypersplenism because frequently there is splenic enlargement, caused by the phagocytosis of infected red cells in splenic macrophages (Fig. 31.13).

COMPARATIVE METHODS FOR MALARIA DIAGNOSIS

In Table 31.2 the sensitivities of the different methods for malaria diagnosis are compared. Thick films improve sensitivity.

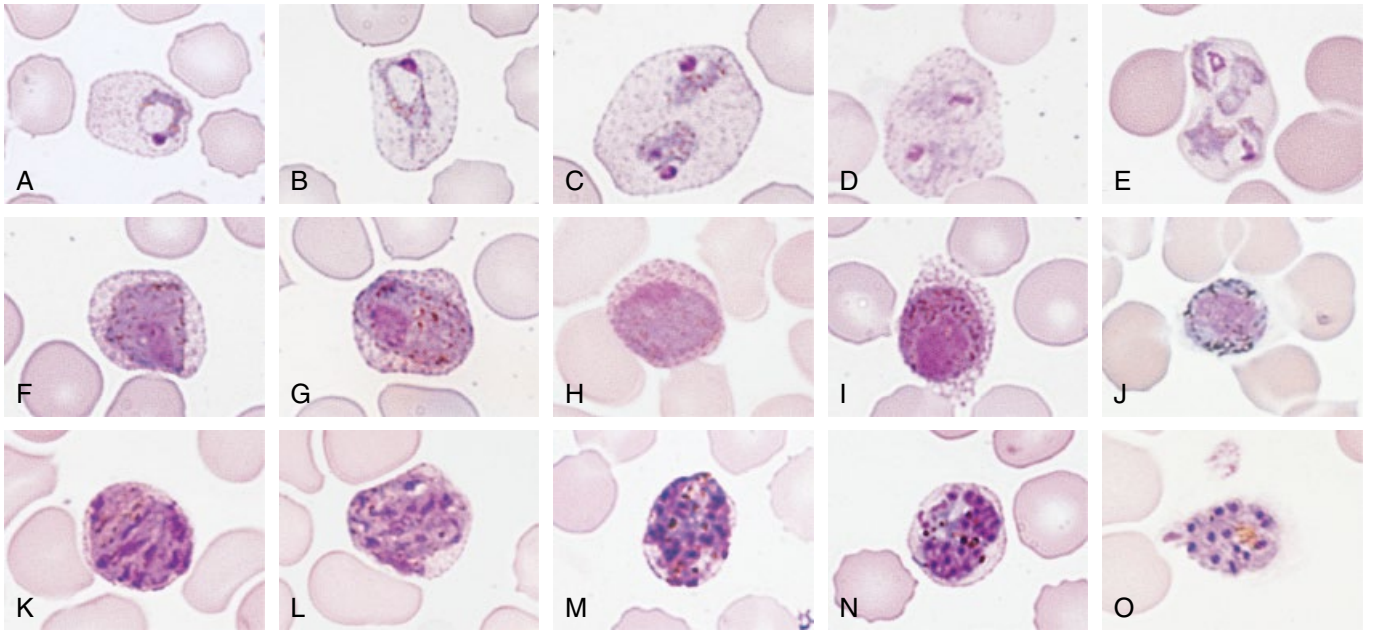

Fig. 31.2. Malaria: Peripheral blood films showing various stages of *Plasmodium vivax*. **A,** Early trophozoite or ring form. **B** and **C,** Young ameboid trophozoites with Schüffner's dots. **D** and **E,** Developing trophozoites after asexual binary fission. **F–H,** Female gametocytes with localized eccentric chromatin. **I** and **J,** Male gametocytes with more diffuse chromatin. **K–O,** Early and later meronts with hemozoin pigment densities and many merozoites randomly distributed.

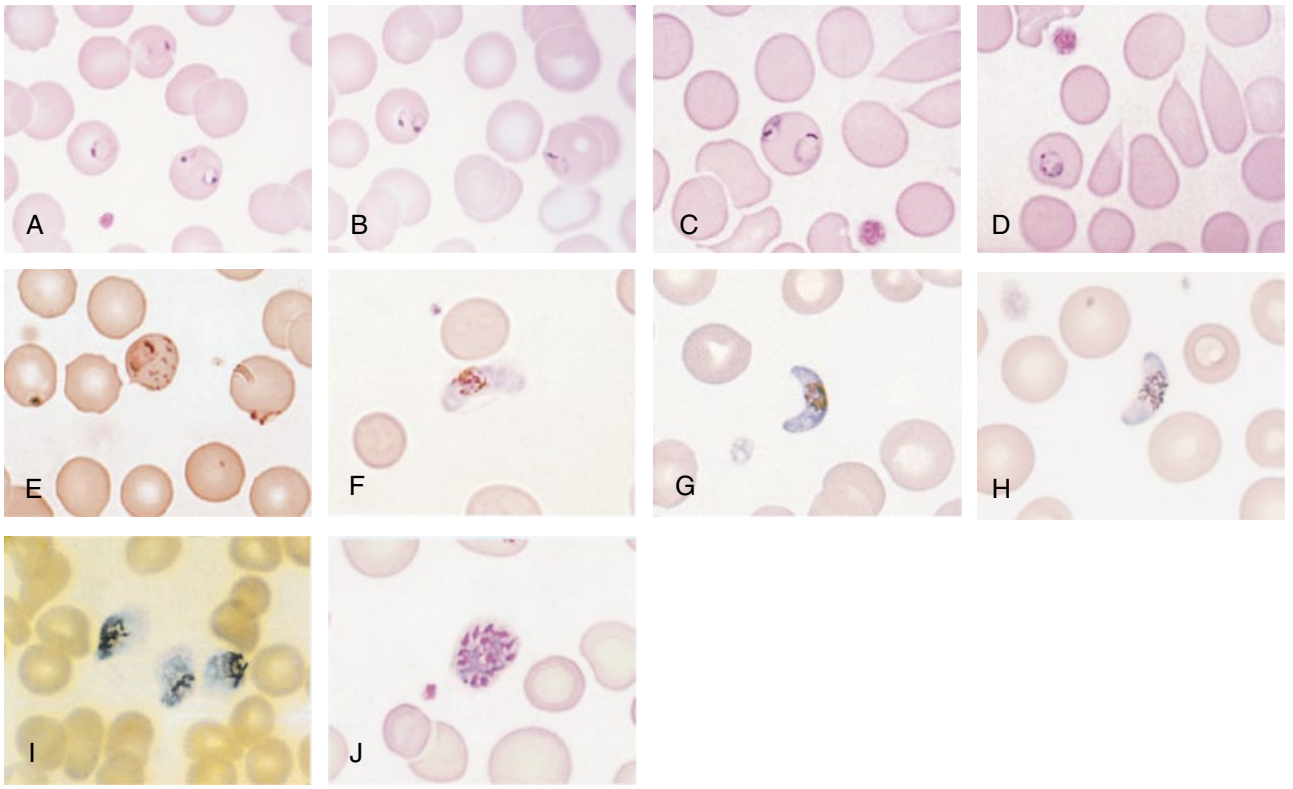

Fig. 31.3. Malaria: Peripheral blood films showing various stages of *Plasmodium falciparum*. **A–D,** Small ring forms. **E,** Small ring form showing Maurer's clefts, denatured red cell microtubules. **F–H,** Crescentic gametocytes with centrally placed chromatin. **I,** Rarely seen rounded "pink flag" gametocytes. **J,** Rarely seen meront with randomly distributed merozoites. (*E,* Courtesy of Dr. S Knowles.)

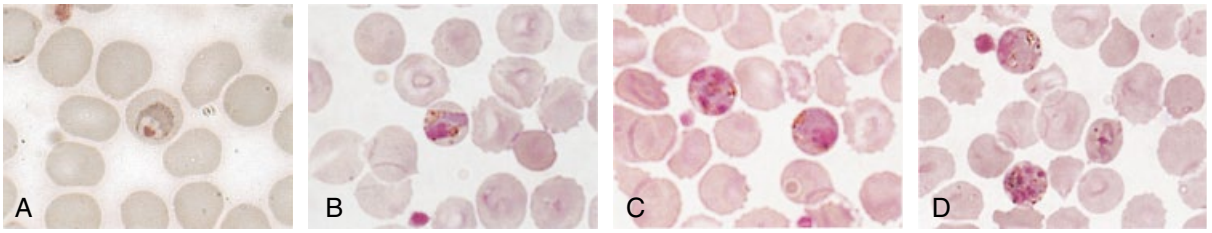

Fig. 31.4. Malaria: Peripheral blood films showing various stages of *Plasmodium malariae*. **A.** Ring form with inverted chromatin dot. **B,** Band-form ameboid trophozoite. **C,** Developing trophozoite and female gametocyte. **D,** From *top left* clockwise: Male gametocyte, ring form, and developing meront with daisy-head merozoite distribution. (*A* and *B,* Courtesy of Dr. S Knowles and J. Griffiths.)

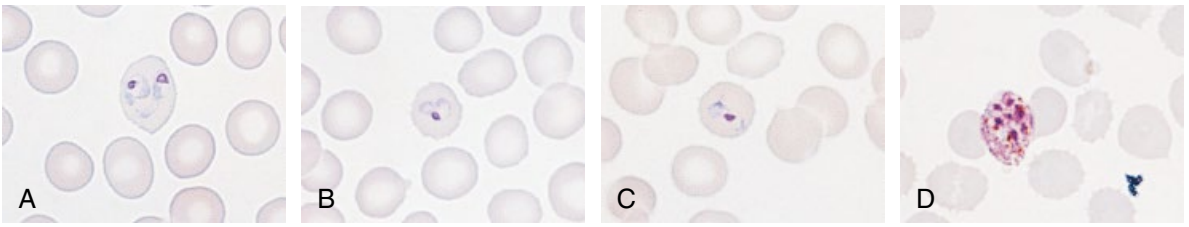

Fig. 31.5. Malaria: Peripheral blood films showing various stages of *Plasmodium ovale*. **A–C,** Ring forms in enlarged red cells with fimbriated margins and faint red granules. **D,** Meront with daisy-head merozoite distribution.

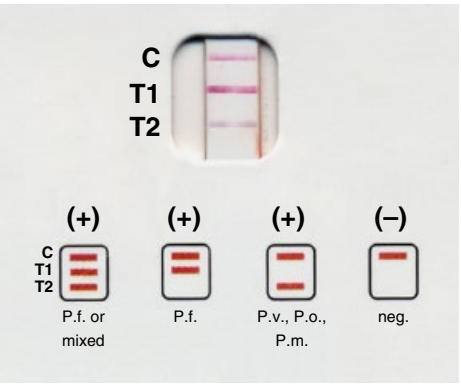

Fig. 31.6. Immunochromatography screening test (Binax Inc.). The result is consistent with *P. falciparum* infection.

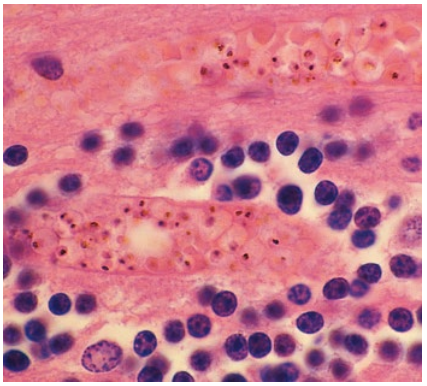

Fig. 31.8. Cerebral malaria: Cerebral capillary. In this histologic preparation, two capillaries are seen with parasitized red cells adherent to the endothelium (sequestration). (Courtesy of Professor S Lucas.)

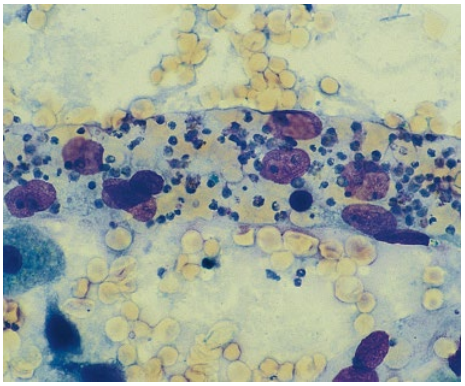

Fig. 31.7. Cerebral malaria: Cerebral capillary. This high-power view shows abundant parasites within red cells. (Squash preparation of white matter stained with Giemsa.) (Courtesy of Professor S Lucas.)

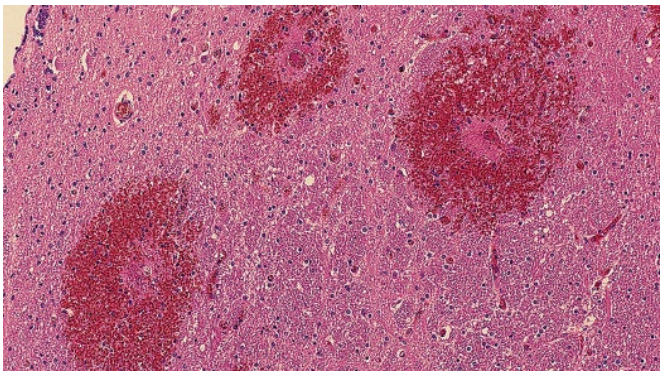

Fig. 31.9. Cerebral malaria: Hemorrhage. Low-power view of brain white matter with three ring hemorrhages caused by obstructed vessels. (Courtesy of Professor S Lucas.)

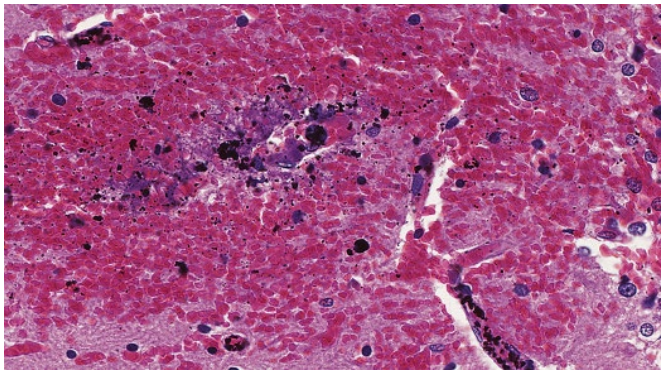

Fig. 31.10. Cerebral malaria: Hemorrhage from vessel rupture by *P. falciparum* malaria. The intense pigmentation within the blood vessel indicates the heavy parasitemia at this site. (Courtesy of Professor S Lucas.)

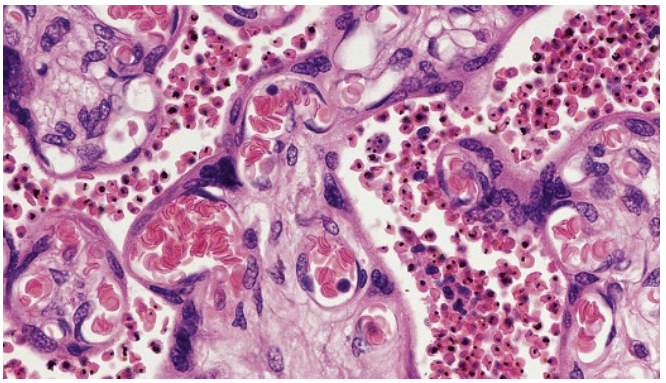

Fig. 31.11. Placental malaria: Placental villi and maternal sinus. Nearly all of the red blood cells in the maternal sinus contain parasites, pigment, or both. Note that the fetal vessels in the villi are not infected. (Courtesy of Professor S Lucas.)

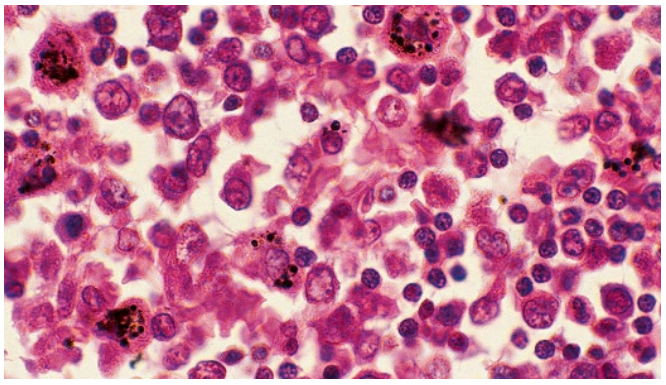

Fig. 31.12. Pediatric malaria: Hypercellular bone marrow. Macrophages that contain brown-colored hemozoin malaria pigment are plentiful. Parasites inside red blood cells are not seen in this field. (Courtesy of Professor S Lucas.)

Red cell lysis is carried out at pH 6.8 in phosphate buffers for 10 minutes. Thick films are made and stained with Giemsa at pH 7.2 for 30 minutes. Fig. 31.14 shows positive films for *P. vivax* and Fig. 31.15 shows a film with a heavy parasite load in *P. falciparum* infection.

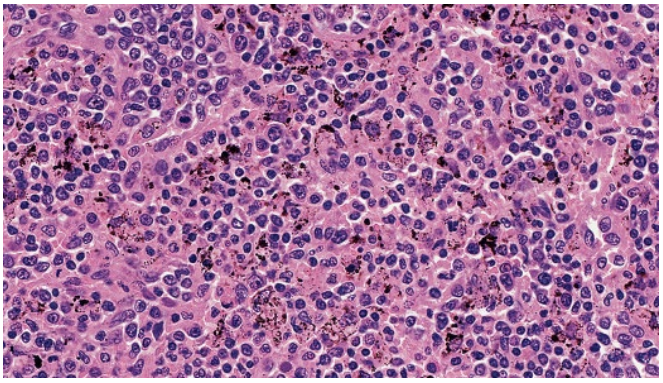

Fig. 31.13. Spleen: Red pulp showing abundant macrophages that contain brown-colored hemozoin malaria pigment. (Courtesy of Professor S Lucas.)

TABLE 31.2. COMPARISON OF METHODS FOR MALARIA DIAGNOSIS

	Limits of detection (parasites/mL)
Thin film	200
Thick film	10
Quantitative buffy coat	20[a]
Histidine-rich protein II antigen detection[b]	50
DNA hybridization	40
Polymerase chain reaction	<5

[a] The quantitative buffy coat method is as sensitive as thick film for *Plasmodium falciparum* but less so for other species.
[b] Histidine-rich protein II antigen is in the red cell membrane and is secreted by red cells infected by *P. falciparum*.
Courtesy of Dr. W Erber.

RESISTANCE TO ANTIMALARIAL THERAPY

A wide range of drugs is available. Artemisinins are the most rapidly acting against *P. falciparum* and the cornerstone of first line combination therapy for this infection. Resistance to artemisinins is determined by mutations in a gene in the parasite, encoding the kelch (K13) propellor domains.

TOXOPLASMOSIS

Toxoplasmosis, a common infection, is caused by the protozoan *Toxoplasma gondii*. Most human infections are acquired from cats. Affected patients are symptomless or have a brief febrile illness with lymphadenopathy and fatigue. Severe infection, most commonly seen in the fetus (congenital toxoplasmosis) or in patients with immunodeficiency, is associated with extensive damage to the brain, eyes, muscle, heart, and lungs. Diagnosis is usually confirmed by positive serology, although a lymph node biopsy may be needed (see Fig. 11.38). Rarely, the trophozoite forms are present in blood monocytes (Fig. 31.16).

BABESIOSIS

Babesiosis is a tick-borne disease caused by protozoan parasites of the genus *Babesia*. Although the disease affects a number of animal species, it is only occasionally transmitted to humans.

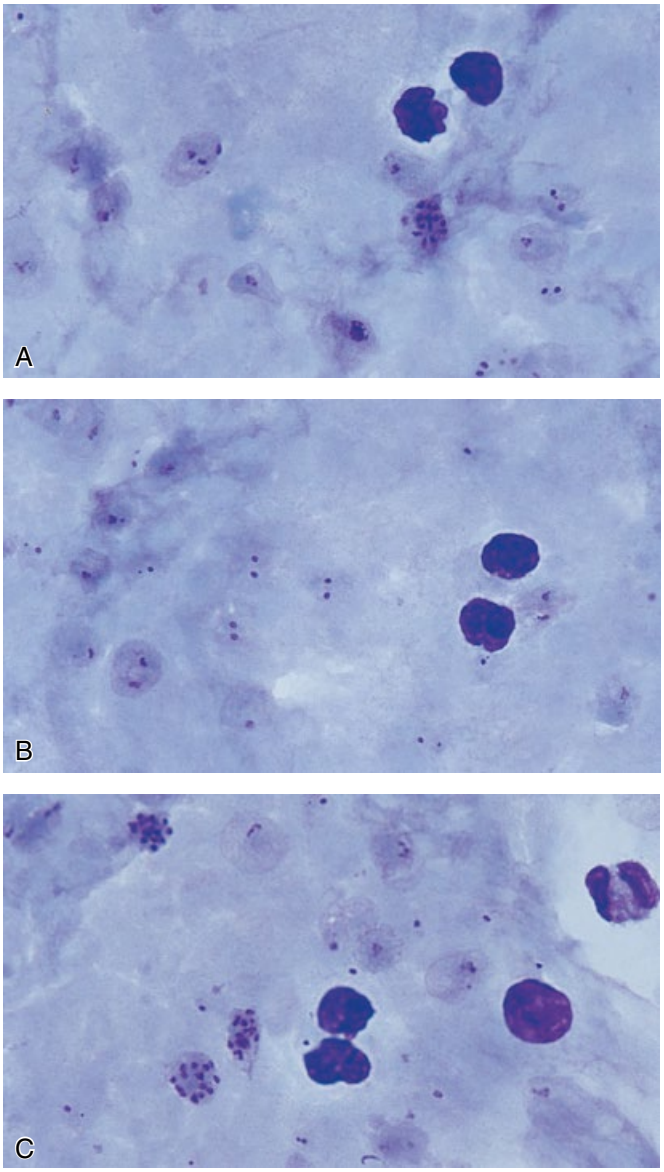

Fig. 31.14. Malaria diagnosis: Thick films. **A,** *P. vivax* trophozoites and schizonts. **B,** *P. vivax* trophozoites. **C,** *P. vivax* trophozoites and schizonts. (Giemsa stain.) (*A–C,* Courtesy of Dr. W Erber.)

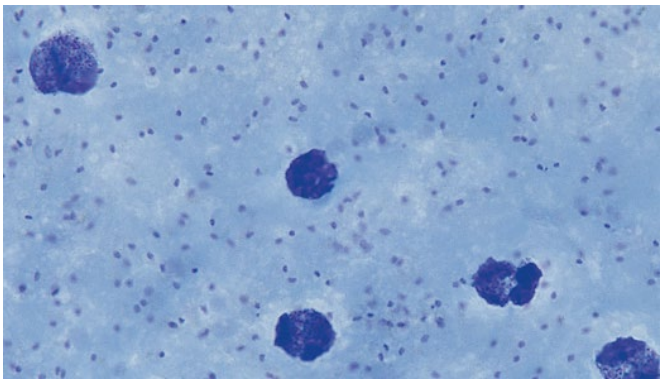

Fig. 31.15. Malaria diagnosis: Thick film of *P. falciparum* (heavy infection). Chromatin dots of *P. falciparum* are easily seen in this thick film. (Giemsa stain.) (Courtesy of Dr. W Erber.)

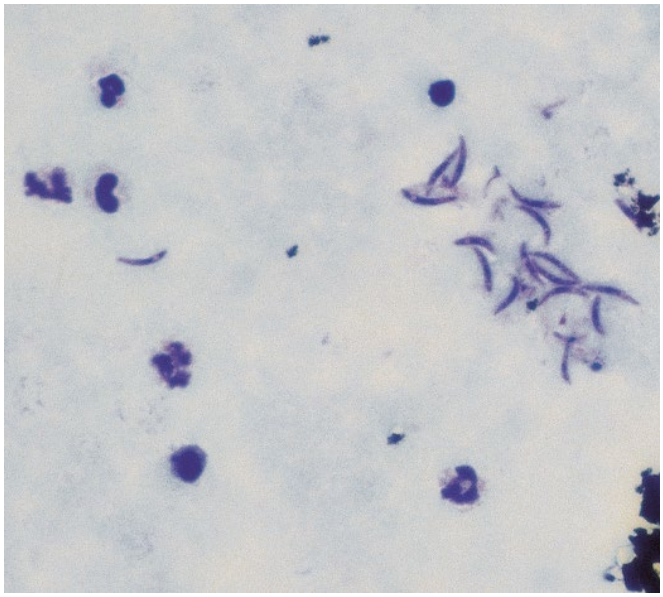

Fig. 31.16. Acute toxoplasmosis: Thick peripheral blood film showing trophozoite forms of *Toxoplasma gondii* from a ruptured monocyte.

In most patients the illness is mild and characterized by fever, malaise, myalgia, mild hepatosplenomegaly, and hemolytic anemia. Occasionally, patients who have had previous splenectomy have developed a more fulminating infection with massive intravascular hemolysis, which has sometimes proved fatal.

Most human infections are caused by *B. microti,* a species that usually infects rodents. Several cases in splenectomized patients result from *B. bovis,* a species associated with red water fever in cattle. Diagnosis is made by finding the trophozoites, which resemble small ring forms of *P. falciparum,* in the red cells (Fig. 31.17).

TRYPANOSOMIASIS

The East and West African variants of trypanosomiasis are caused by *Trypanosoma brucei* and *T. brucei gambiense,* respectively. Both are transmitted by tsetse flies of the genus Glossina. The dominant clinical problems are related to involvement of the central nervous system. In the acute phase of the disease, organisms are found in the blood (Fig. 31.18).

American trypanosomiasis, or Chagas disease, occurs widely in Mexico and in many countries in Central and South America. The causative organism, *T. cruzi,* is transmitted by a triatomid bug. During the acute febrile stage of the illness, flagellated parasites are found in the blood (Fig. 31.19). In the chronic stage, which is associated with myocarditis, megacolon, or megaesophagus; nests of amastigote forms are found within the tissues.

BANCROFTIAN FILARIASIS

Bancroftian filariasis is a widespread disease that occurs throughout the tropical and subtropical regions of the world caused by *Wuchereria bancrofti*. A similar condition is caused by infection with the related *Brugia malayi*.

Both organisms are transmitted by infected mosquitoes. Larvae pass into the lymphatic vessels and lymph nodes, where they mature into adult worms (Fig. 31.20). The fertilized

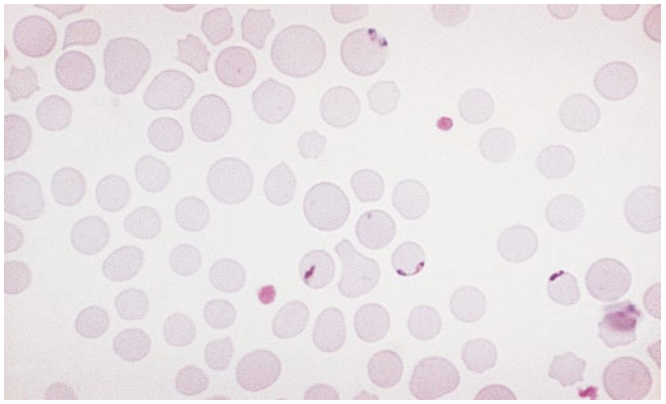

Fig. 31.17. Babesiosis: Peripheral blood film showing red cell infestation with the typical small coccoid and dumbbell-shaped *Babesia* organisms. (Courtesy of PJ Humphries.)

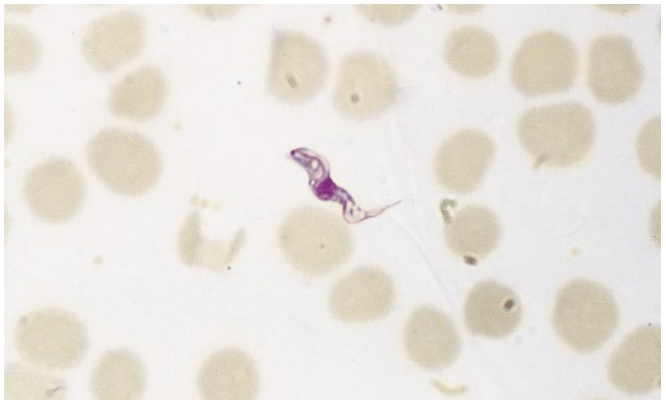

Fig. 31.18. African trypanosomiasis: Peripheral blood film showing *Trypanosoma brucei*.

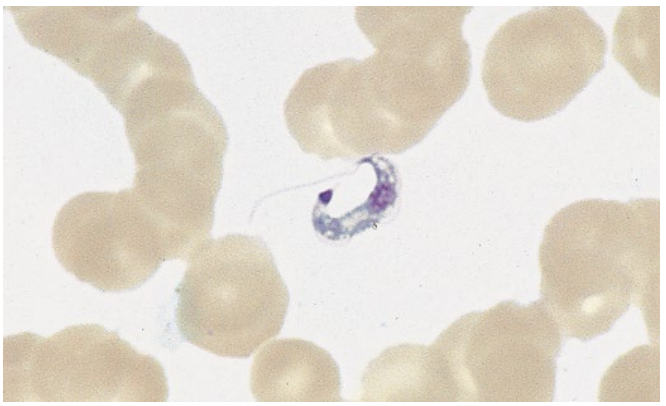

Fig. 31.19. Chagas disease: Peripheral blood film showing the flagellate form of *Trypanosoma cruzi*. (Courtesy of J Williams.)

females release microfilariae via the lymphatic vessels into the bloodstream.

Many patients are asymptomatic, but others develop a febrile illness with headaches, muscle pains, and lymphadenitis. Chronic inflammatory changes in the infected lymphoid system can lead to lymphatic obstruction and elephantiasis of the scrotum or lower extremities. Diagnosis is usually made by demonstrating microfilariae in the blood (Figs. 31.21 and 31.22). Microfilaremia is usually greatest at night.

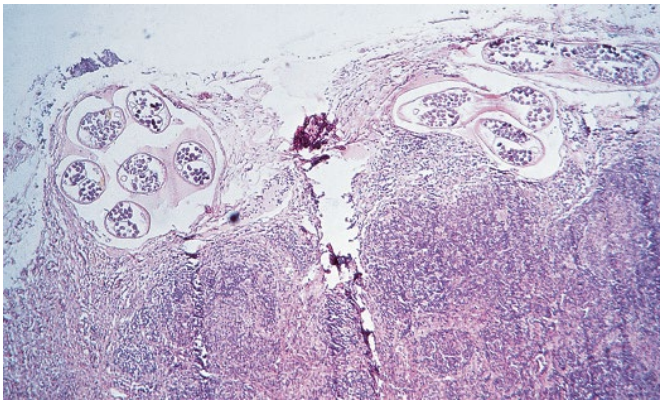

Fig. 31.20. Bancroftian filariasis: Section of lymph node showing adult forms of *Wuchereria bancrofti* in the peripheral sinus area.

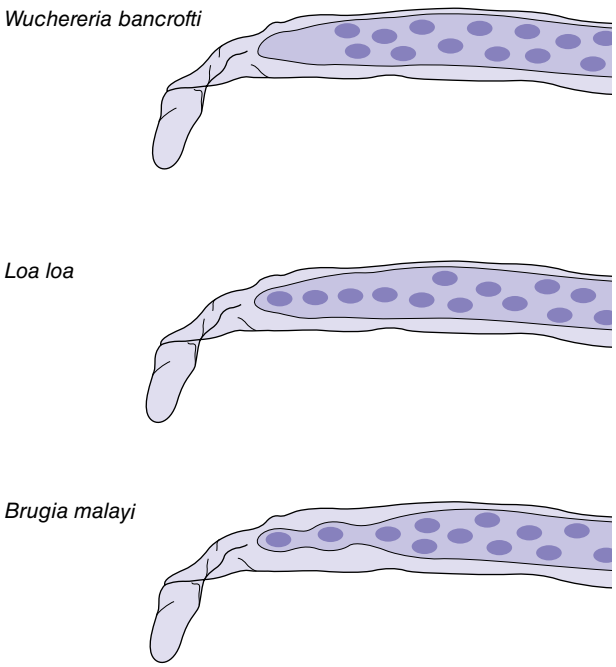

Fig. 31.21. Posterior ends of sheathed microfilariae found in blood. In *W. bancrofti* the nuclei do not extend to the tip of the tail; in *Loa loa* there is a continuous line of nuclei to the end of the tail; in *Brugia malayi* the nuclei are not continuous, with two isolated nuclei at the tip of the tail.

LOIASIS

Infection with *Loa loa* occurs in Central and West Africa. The adult worm causes subcutaneous swellings, but occasionally its passage through the subconjunctival tissues produces local pain and acute conjunctivitis. Microfilariae are found in the blood (Fig. 31.23), and infestation is via tabanid flies.

BARTONELLOSIS

Bartonella bacilliformis causes a severe febrile hemolytic anemia. The disease occurs in inhabitants of the Andes Mountains in Peru, Colombia, and Ecuador. The characteristic rod-shaped coccobacilli are found in red cells (Fig. 31.24). The infection is also known as Oroya fever and Carrión disease and is transmitted by *Phlebotomus* sandflies.

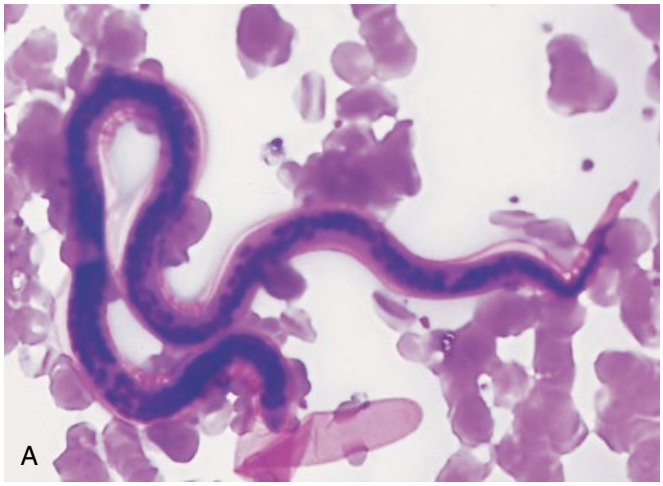

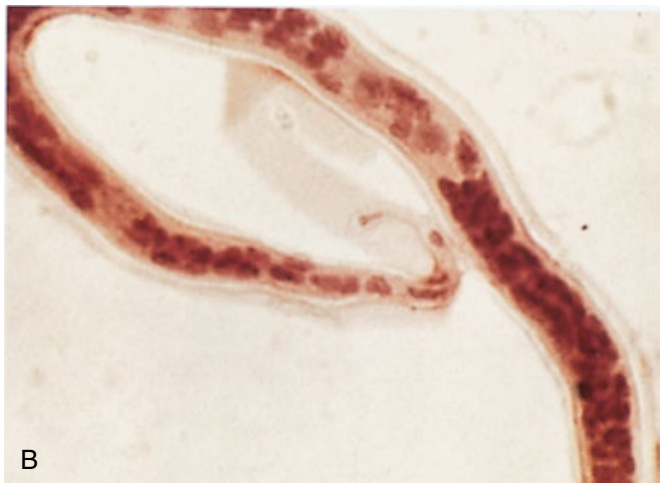

Fig. 31.22. Filariasis: Thick preparations of peripheral blood showing the center and tail portions of the microfilariae of *W. bancrofti* **(A)** and *Br. malayi* **(B).** (*B,* Courtesy of Dr. AE Bianco.)

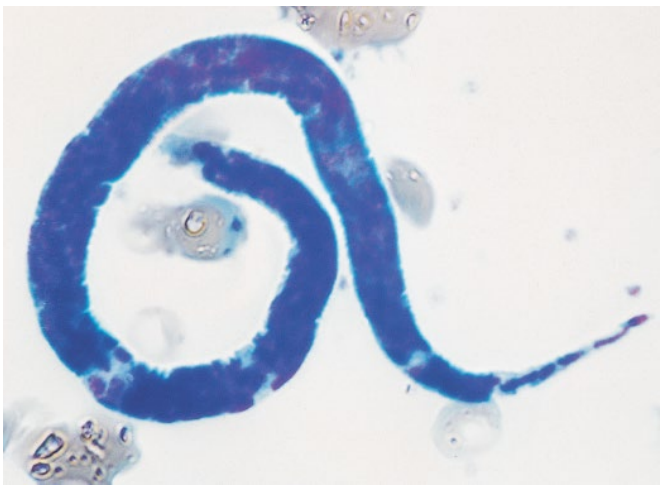

Fig. 31.23. Loiasis: Peripheral blood film with sheathed microfilaria of *L. loa*.

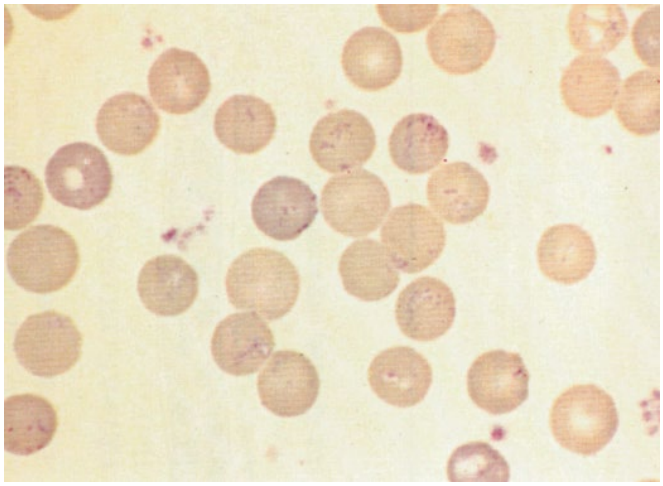

Fig. 31.24. Bartonellosis: Peripheral blood film showing rod-shaped coccobacilli of *Bartonella bacilliformis* in the red cells in Oroya fever. (Courtesy of H Furze.)

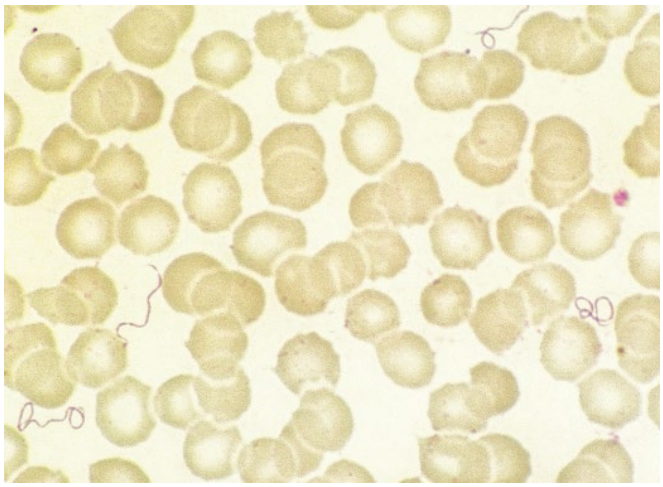

Fig. 31.25. Relapsing fever: Peripheral blood film showing the coiled spirochetes *Borrelia recurrentis*.

RELAPSING FEVER

Various spirochetes of the genus *Borrelia* cause relapsing fever. Louse-borne relapsing fever is a human disease caused only by *Bo. recurrentis,* but tick-borne relapsing fever is a zoonosis caused by a number of different species. It is during the febrile period of the disease that the organisms are present in the blood (Fig. 31.25). With the production of antibodies, the *Borrelia* spirochetes disappear and the patient becomes afebrile. Relapses occur after 7–10 days, with the production of new antigenic variants of the organisms. In louse-borne relapsing fever, a single relapse is usual, whereas in the tick-borne forms of the disease, multiple relapses occur.

CHAPTER

32

BLOOD TRANSFUSION

Blood transfusion involves transfusion of whole blood or a blood component (red cells, platelets, fresh frozen plasma, cryoprecipitate, or white cells) from an individual (the donor) into the recipient. In the case of red cells, autologous (self) transfusion can also be carried out. The major clinical need is for red cells, for which compatibility between donor red cell antigens and the antibodies in the recipient's plasma must be ensured. The reader is referred to chapter 12 Red cell immunohaematology (G Daniels, M Contreras, and S Allard) and chapter 13 Clinical blood transfusion (S Allard and M Contreras) in *Postgraduate Haematology*, 7th edition (2016), John Wiley and Sons, for detailed descriptions of the scientific basis and clinical practice of blood transfusion. This chapter derives Tables 32.1–32.4, 32.6, and 32.10 from those chapters.

RED CELL ANTIGENS

The International Society of Blood Transfusion recognizes 347 red cell surface antigens, 308 belonging to one of 36 blood group systems (Table 32.1). Each system is due to a single gene (32 systems) or two or three closely linked homologous genes. There are

TABLE 32.1. HUMAN BLOOD GROUP SYSTEMS

No.	Name	Symbol[a]	No. of antigens	HGNC gene symbol(s)	Chromosome	Structure	CD number
001	ABO	ABO	4	*ABO*	9	Carbohydrate	
002	MNS	MNS	48	*GYPA, GYPB, GYPE*	4	Glycoprotein	CD235a/b
003	P1PK	P1PK	3	*A4GALT*	22	Carbohydrate	
004	Rh	RH	54	*RHD, RHCE*	1	Protein	CD240D/CE
005	Lutheran	LU	22	*BCAM*	19	Glycoprotein	CD239
006	Kell	KEL	35	*KEL*	7	Glycoprotein	CD238
007	Lewis	LE	6	*FUT3*	19	Carbohydrate	
008	Duffy	FY	5	*DARC*	1	Glycoprotein	CD234
009	Kidd	JK	3	*SLC14A1*	18	Glycoprotein	
010	Diego	DI	22	*SLC4A1*	17	Glycoprotein	CD233
011	Yt	YT	2	*ACHE*	7	Glycoprotein	
012	Xg	XG	2	*XG, CD99*	X/Y	Glycoprotein	CD99[b]
013	Scianna	SC	7	*ERMAP*	1	Glycoprotein	
014	Dombrock	DO	10	*ART4*	12	Glycoprotein	CD297
015	Colton	CO	4	*AQP1*	7	Glycoprotein	
016	Landsteiner–Wiener	LW	3	*ICAM4*	19	Glycoprotein	CD242
017	Chido–Rodgers	CH/RG	9	*C4A, C4B*	6	Glycoprotein	
018	H	H	1	*FUT1*	19	Carbohydrate	
019	Kx	XK	1	*XK*	X	Protein	
020	Gerbich	GE	11	*GYPC*	2	Glycoprotein	CD236
021	Cromer	CROM	18	*CD55*	1	Glycoprotein	CD55
022	Knops	KN	9	*CR1*	1	Glycoprotein	CD35
023	Indian	IN	4	*CD44*	11	Glycoprotein	CD44

(*Continued*)

Color Atlas of Clinical Hematology: Molecular and Cellular Basis of Disease, Fifth Edition. A. Victor Hoffbrand, Paresh Vyas, Elías Campo, Torsten Haferlach, and Keith Gomez

TABLE 32.1. (CONTINUED)

No.	Name	Symbol[a]	No. of antigens	HGNC gene symbol(s)	Chromosome	Structure	CD number
024	Ok	OK	3	*BSG*	19	Glycoprotein	CD147
025	Raph	RAPH	1	*CD151*	11	Glycoprotein	CD151
026	John Milton Hagen	JMH	6	*SEMA7A*	15	Glycoprotein	CD108
027	I	I	1	*GCNT2*	6	Carbohydrate	
028	Globoside	GLOB	2	*B3GALT3*	3	Carbohydrate	
029	Gill	GIL	1	*AQP3*	9	Glycoprotein	
030	RHAG	RHAG	4	*RHAG*	6	Glycoprotein	CD241
031	Forssman	FORS	1	*GBGT1*	9	Carbohydrate	
032	JR	JR	1	*ABCG2*	4	Glycoprotein	
033	Lan	LAN	1	*ABCB6*	2	Glycoprotein	
034	Vel	VEL	1	*SMIM1*	1	Glycoprotein	
035	CD59	CD59	1	*CD59*	11	Glycoprotein	CD59
036	Augustine	AUG	2	*SLC29A1*	6	Glycoprotein	

HGNC, Human Genome Organisation Gene Nomenclature Committee.
[a] ISBT gene name in italics.
[b] Does not include Xg glycoprotein.
Source: Hoffbrand AV, et al. eds. *Postgraduate Haematology*, 7th edn. John Wiley and Sons, 2016. Reproduced with permission of John Wiley and Sons.

also 39 antigens for which there is less genetic evidence. They are inherited in a simple Mendelian fashion and are stable. Blood group polymorphisms may be caused by differences in amino acid sequence as in Rh or Kell antigens or by the differences in oligosaccharide sequences as in the ABO system, in glycoproteins or glycolipids. Environmental factors affect expression of some of the antigens. The proteins are attached to the red cell membrane (see Fig. 8.7) and can cross this once with the amino terminal on the outside (Type 1; e.g. the glycophorins which carry the MNS antigens), or inside (Type 2; e.g. the Kell glycoprotein), or cross several times (Type 3) exposing several extracellular loops, one of which is usually glycosylated (as for ABO, H, and Ii groups). Both the terminal amino acid and carbohydrate domains of these proteins (N-glycans) are usually cytosolic, as for the Rh, band 3, and Kidd glycoproteins. The antigen also resides on membrane microdomains, rich in cholesterol, known as lipid rafts. These are attached to the lipid bilayer by a glycosylphosphatidylinositol (GPI) anchor. There are no Type 4 proteins in the red cell membrane.

Subjects who lack any antigen are likely to make antibodies to that antigen if they are exposed to it. The red cell blood group systems to which red cell antibodies cause a hemolytic reaction are detailed in Table 32.2.

TABLE 32.2. ANTIBODIES ASSOCIATED WITH HEMOLYTIC TRANSFUSION REACTIONS

Blood group system	Antibodies implicated in intravascular hemolysis	Antibodies implicated in extravascular hemolysis
ABO	-A,B; -A; -B	
Hh	-H (Bombay)	
Rh		All
Kell		K, k, Kp^a, Kp^b, Js^a, Js^b
Kidd		Jk^a, Jk^b, Jk^3
Duffy		Fy^a, Fy^b, Fy^3
MNS		M, S, s, U(some)
Lutheran		Lub (some)
Lewis	Le^a, Le^b, Lea^{+b}	
Cartwright		Yt^a (some)
Vel	Vel	Vel (some)
Colton		Co^a,Co^b
Dombrock		Do^a, Do^b

Source: Hoffbrand AV, et al. eds. *Postgraduate Haematology*, 7th edn. John Wiley and Sons, 2016. Reproduced with permission of John Wiley and Sons.

RED CELL ANTIBODIES

There are two types of red cell antibodies: natural and immune. Natural antibodies are a normal occurrence in plasma in the absence of transfusion or pregnancy. They start to appear at 3–6 months of age. Immune antibodies develop in response to exposure to the antigen by transfusion or by exposure to red cells that cross the placenta during pregnancy. Natural antibodies, usually immunoglobulin M (IgM), react best in the cold and include anti-A and anti-B. Immune antibodies, usually immunoglobulin G (IgG), react best at 37°C and include Rhesus (Rh) antibody anti-D. Ig antibodies, but not IgM, cross the placenta.

ABO SYSTEM

The structure of the A, B, and H antigens is shown in Fig. 32.1. The gene is on 9q, which codes the A and B glycosyltransferases. Products of the A and B alleles differ by four amino acids on exon 7, two of which determine whether the sugar transferred to the H antigen is *N*-acetyl-D-galactosamine (group A) or galactosamine (group B).The H antigen has a fucose moiety transferred in mesodermally derived tissues including hematopoietic tissues by an α1,2-fucosyltransferase (FUT1) to the terminal galactose of the H precursor chain. A second enzyme,

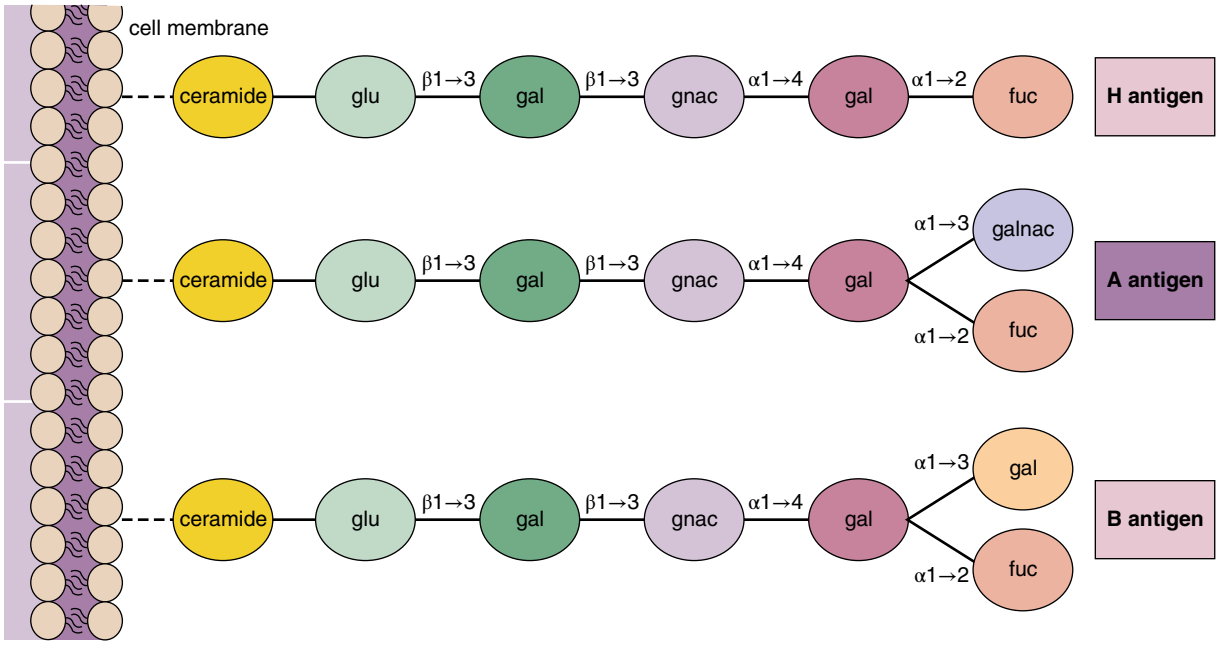

Fig. 32.1. Structure of the ABO blood group antigens: each consists of a chain of sugars, in a or b conformation, linked through different carbon atoms (numbered 1–4). The H antigen of the O blood group has a terminal fucose (fuc). The A antigen has an additional *N*-acetylgalactosamine (galnac), whereas the B antigen has an additional D-galactose (gal). (*glu,* glucose; *gnac, N*-acetyl-D-glucosamine.)

FUT2, is responsible for expression of the H antigen on endodermally derived tissues. The A, B, and H antigens occur in most blood cells, including red cells, leukocytes, and platelets, and in plasma. In secretors (80% of the population), they also occur in other body fluids such as saliva, tears, semen, and sweat. ABH secretory status depends on the *FUT2* gene and if both alleles are inactive, usually due to a nonsense mutation, the subject is a nonsecretor.

The A group is divided into A1 and A2, A2 being for practical purposes a weaker form of A1. An antibody that will agglutinate A1 but not A2 cells is not used routinely as it is not necessary to distinguish A1 from A2 in transfusion practice. The number of antigenic sites for group A is fewer on AB cells than on A cells, so for A2B cells the A antigen can be very weak and missed unless powerful anti-A antibodies are used in testing. The relative incidence in the UK population is shown in Table 32.3. Rare ABO variants (e.g. A3, A end, Ax) are usually detected because an expected ABO antibody is missing.

TABLE 32.3. INCIDENCE OF ABO GROUPS IN SOUTHERN ENGLAND

Phenotype	Frequency (%)	
O		44.9
A_1	30.8	41.1
A_2	10.3	
B		10.1
A_1B	2.7	3.9
A_2B	1.2	

Source: Hoffbrand AV, et al. eds. *Postgraduate Haematology*, 7th edn. John Wiley and Sons, 2016. Reproduced with permission of John Wiley and Sons.

Rh SYSTEM

The Rh system is more complex than the ABO system. There are three closely linked loci with alternative antigens, Cc, D or no D (termed "d," for which there is no antigen), and Ee (Table 32.4). There are only two Rh genes, one coding for D, the other for the Cc and Ee antigens. As Cc and Ee polymorphisms are determined by separate regions of a single gene, the DCE terminology has been retained.

Rh antibodies are immune, and before the introduction of prophylaxis with Rh anti-D after delivery or miscarriage, anti-D was the dominant cause of hemolytic disease of the newborn.

TABLE 32.4. EIGHT Rh HAPLOTYPES AND THEIR FREQUENCIES IN ENGLISH, NIGERIAN, AND HONG KONG CHINESE POPULATIONS

Haplotype		Frequencies (%)		
CDE	Rh-Hr	English	Nigerian	Chinese
DCe	R^1	42	6	73
dce	*R*	39	20	2
DcE	R^2	14	12	19
Dce	R^0	3	59	3
dcE	*r″*	1	Very rare	Very rare
dCe	*r′*	1	3	2
DCE	R^z	Rare	Very rare	Rare
dCE	*r″*	Very rare	Very rare	Rare

Results of testing, with anti-D, -C, -c, -E and -e, red cells from 2000 English donors, 274 Yoruba of Nigeria, and 4648 Cantonese from Hong Kong.

Source: Hoffbrand AV, et al. eds. *Postgraduate Haematology*, 7th edn. John Wiley and Sons, 2016. Reproduced with permission of John Wiley and Sons.

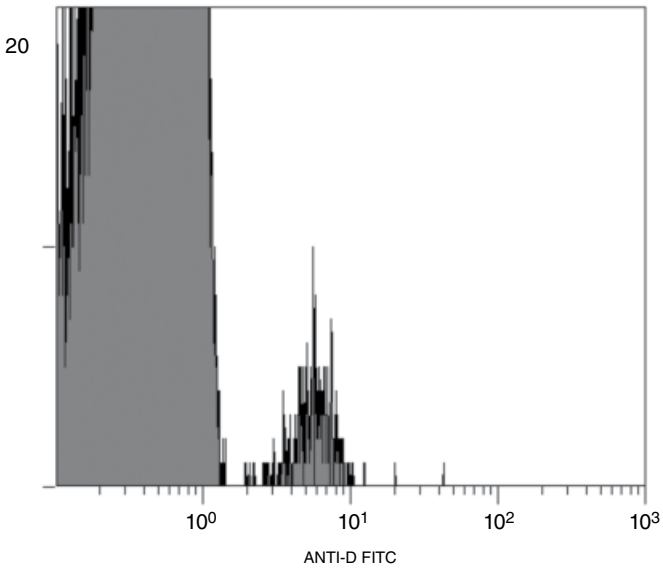

Fig. 32.2. Determination by flow cytometry of the number of RhD fetal cells in the maternal circulation using a fluorescence-labeled antibody to RhD, the mother being Rhdd. (Courtesy of Dr.W Erber.)

The number of fetal cells entering the maternal circulation at delivery or miscarriage can be determined by the Kleihauer technique (Fig. 9.86) or by flow cytometry using a fluorescent-labeled antibody to RhD (Fig. 32.2) or by DNA techniques.

BLOOD GROUPING AND CROSS-MATCHING

Blood grouping and cross-matching are carried out by a tile (Fig. 32.3), microplate (Fig. 32.4), E gel microtube (Fig. 32.5), or IgM agglutination (Fig. 32.6, *A*) technique. Automated techniques are now widely used based on microplate or microcolumn techniques. The patient's cells are mixed with known antisera and the patient's serum is mixed with cells of known A, B, or O type (see Figs. 32.3 and 32.4). An indirect antiglobulin test (IAT) can be used to detect irregular red cell antibodies in the patient's serum (Fig. 32.6, *B*). This technique can also be used to detect antibodies in the serum of the recipient that react against the donor red cells. Agglutination can be enhanced by proteases

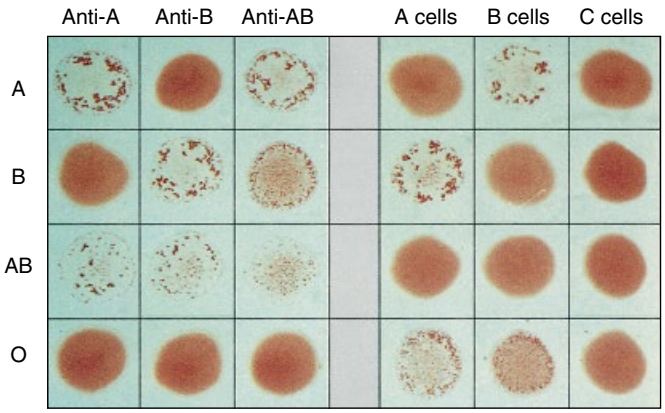

Fig. 32.3. ABO blood group testing: reactions observed. Agglutination denotes reactivity. The three left-hand columns denote patient cells (A, B, AB, or O) mixed with anti-A, anti-B, or anti-AB. The three right-hand columns denote plasma from the patients, mixed with A, B, or O cells.

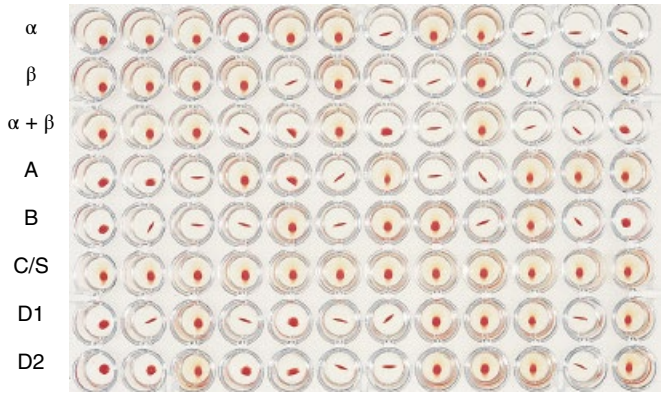

Fig. 32.4. ABO grouping: Standard layout for 96-well microplate blood grouping (12 patients grouped on one plate). Symbols along the vertical side are as follows: α, anti-A; β, anti-B; α+β, anti-A+B; A, B, known A or B cells; C/S, patient cells and serum; D1, D2, two sources of anti-D. Sharp agglutination ("comma-like") shows a positive reaction, and no agglutination shows a negative reaction. (Courtesy of G Hazlehurst.)

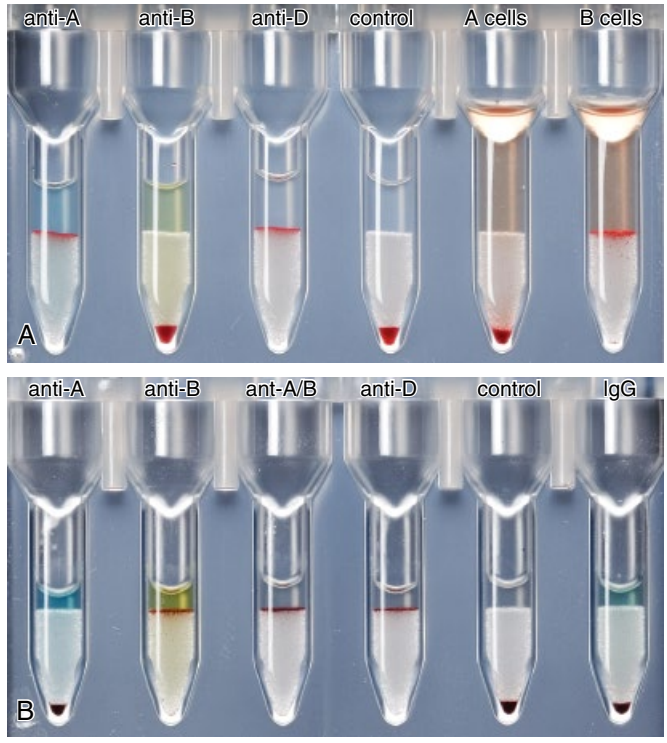

Fig. 32.5. Blood grouping using microcolumn (gel) system. **A,** A Rh(D) positive. The three left hand tubes contain patient cells, the two right hand, patient plasma. Control = patient cells and plasma. **B,** The patient is B Rh(D) positive, with an additional direct antiglobulin test using anti IgG, which is negative. (Courtesy of G Hazlehurst.)

such as papain, by albumin and other colloids, by glycols and by low ionic strength solutions. For patients with antibodies, the selection of red cell units should be based on antigen specificity and clinical significance (Table 32.5).

RED CELL COMPONENTS

Saline–adenine–glucose–mannitol (SAG-M) blood can be provided as leukocyte-depleted red cells (Fig. 32.7) or as a multi-satellite, small volume, red cell pack (e.g. for neonates).

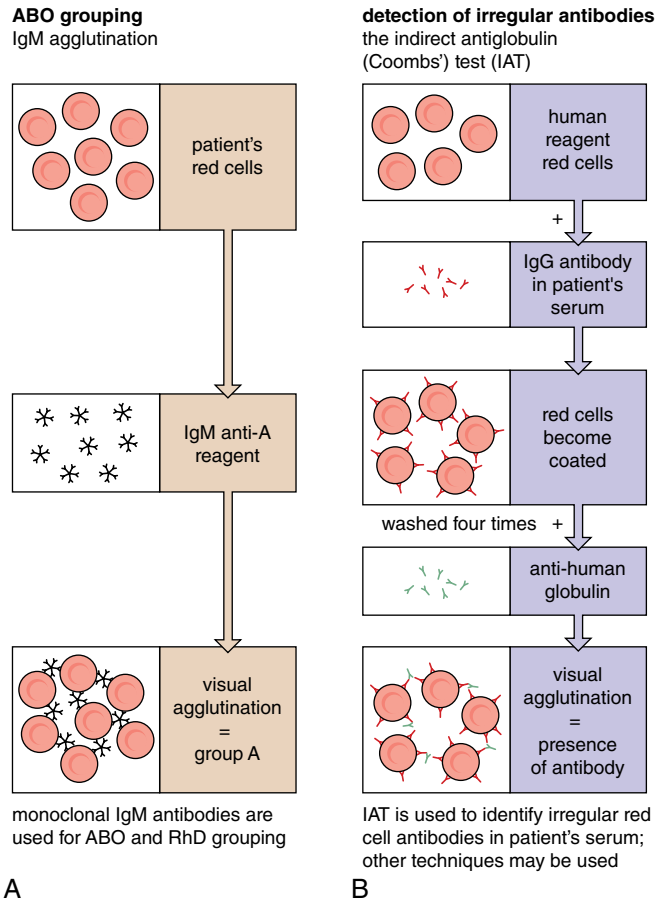

Fig. 32.6. ABO grouping. **A,** IgM agglutination. Monoclonal IgM antibodies are used for ABO and RhD grouping. **B,** The indirect antiglobulin (Coombs) test (IAT). The IAT is used to identify irregular red cell antibodies in the patient's serum. (*A, B,* Courtesy of Professor M Contreras and North London Blood Transfusion Centre.)

TABLE 32.5. RED CELL UNITS: SELECTION BASED ON ANTIGEN SPECIFICITY AND CLINICAL SIGNIFICANCE

Specificity	Clinical significance	Selection of units and compatibility testing
Rh antibodies (reactive in IAT)	Yes	Antigen negative
Kell antibodies	Yes	Antigen negative
Duffy antibodies	Yes	Antigen negative
Kidd antibodies	Yes	Antigen negative
Anti-S, -s	Yes	Antigen negative
Anti-A_1, -P_1, -N	Rarely	IAT cross-match compatible at 37°C
Anti-M	Rarely	IAT cross-match compatible at 37°C
Anti-M IAT reactive at 37°C	Sometimes	Antigen negative
Anti-Le^a, anti-Le^{a+b}	Rarely	IAT cross-match compatible at 37°C
Anti-Le^b	No	Not clinically significant and can be ignored
High-titer low-avidity antibodies	Unlikely	Seek advice from Blood Center
Antibodies against high-frequency antigens	Depends on specificity	Seek advice from Blood Center

Courtesy of British Committee for Standardization in Haematology, 1996.

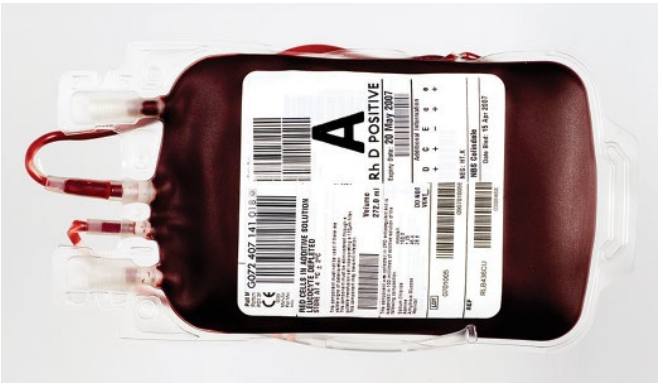

Fig. 32.7. Leukocyte-depleted red cells. The average volume of this product, which contains CPDA-1 (citrate-phosphate-dextrose-adenine) as the anticoagulant, is 280 mL. SAG-M (see text) additive solution (100 mL) is added to give a final hematocrit of 50–70%. The storage temperature of these red cells is 4° ± 2°C and the shelf life is 35 days. Depletion in the white cell content of red cell products to less than 5×10^6/unit reduces the incidence of reactions caused by human leukocyte antigen (HLA) alloimmunization and of transfusion of CMV or prions. (Courtesy of G Hazlehurst.)

CLINICAL BLOOD TRANSFUSION

Hospital transfusion in the UK is governed by the 2005 UK Blood and Quality Regulations based on EU Directives. It is regulated by the Medicines and Healthcare products Regulatory Agency (MHRA). Transfusion management guidelines are given in: *Guidelines for the Blood Transfusion Services in the United Kingdom*, 8th edition (2013). Stationery Office, London and in: *Guidelines on the Administration of Blood Components, British Committee for Standards in Haematology (BCSH)* (2009). The schedule for the normal quantities of blood ordered for different surgical procedures is set at hospital level (Fig. 32.8). In some patients, especially those with sickle cell anemia, exchange transfusion is needed, which can be carried out using a cell separator or manually in infants. For neonatal exchange transfusion, plasma-reduced blood in CPDA1 less than 5 days old, irradiated and CMV negative is used.

COMPLICATIONS OF BLOOD TRANSFUSION

Allergic or pyrogenic reactions to white cells, platelets, or proteins are the most frequently encountered complications (Table 32.6). Complications of blood transfusions also include hemolytic reactions, immediate or delayed as a result of red cell incompatibilities (Fig. 32.9). These are intravascular or extravascular (Table 32.2). A number of other nonimmune reactions occur acutely (e.g. circulatory overload, air embolism, thrombophlebitis), as may complications of massive transfusion (e.g. clotting abnormalities, citrate toxicity, hyperkalemia). Massive transfusion is defined as replacement of one blood volume in 24 hours or of 50% blood volume in 3 hours, or need to replace a rate of loss of 150 mL/minute in adults.

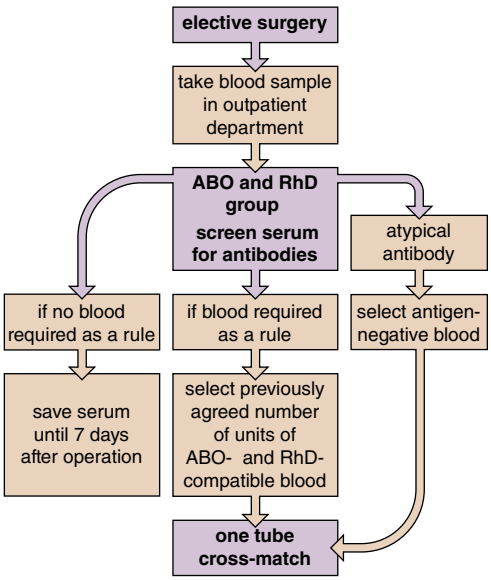

Fig. 32.8. Surgical blood ordering policy.

TABLE 32.6. HAZARDS OF TRANSFUSION

Immediate (hours)
Nonimmune complications
Bacterial: acute sepsis or endotoxic shock
Hypothermia
Hypocalcemia (↓ Ca^{2+}) in infants and massive transfusion
Transfusion-associated circulatory overload (TACO)
Immune complications
Febrile nonhemolytic transfusion reactions
Acute hemolytic transfusion reactions: intravascular (IgM), extravascular (IgG)
Allergic reactions (urticarial)
Anaphylactic reactions (anti-IgA)
Transfusion-related acute lung injury (TRALI)
Delayed (days to years)
Nonimmune complications
HIV, HCV, HBV, CMV
Others: parvovirus B19, HAV, HEV, WNV, dengue, malaria
Chagas disease, brucellosis, syphilis, vCJD
Immune complications
Delayed hemolytic transfusion reactions (due to anamnestic immune responses with red cell alloantibodies)
Post-transfusion purpura
Transfusion-associated graft-versus-host disease

CMV, cytomegalovirus; HAV, hepatitis A virus; HBV, hepatitis B virus; HCV, hepatitis C virus; HEV, hepatitis E virus; Ig, immunoglobulin; vCJD, new variant Creutzfeldt–Jakob disease; WNV,West Nile virus.

Source: Hoffbrand AV, et al. eds. *Postgraduate Haematology*, 7th edn. John Wiley and Sons, 2016. Reproduced with permission of John Wiley and Sons.

INFECTIONS

Immediate shock can occur after transfusion if the blood is infected, and a number of different infectious diseases may be transmitted: bacterial, parasitic (Table 32.7), viral, or prions (Table 32.8).

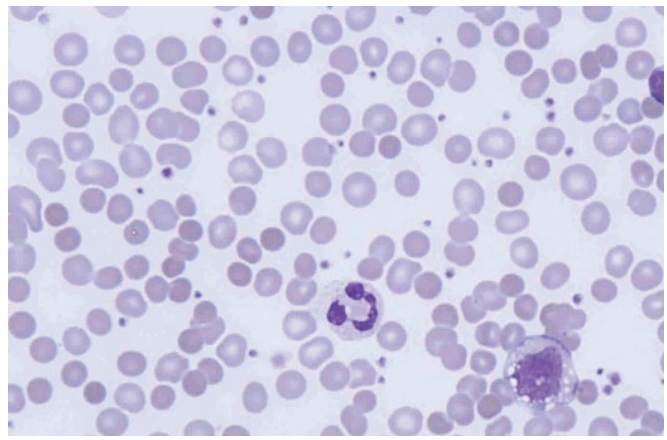

Fig. 32.9. Blood transfusion: Delayed transfusion reaction. Peripheral blood film showing microspherocytes and polychromasia. (Courtesy of Dr. W Erber.)

TABLE 32.7. BLOOD TRANSFUSION: TRANSMISSIBLE BACTERIA AND PARASITES

Bacteria
Occasional bacterial contaminants (e.g. *Staphylococcus* spp, *Klebsiella, Pseudomonas, Salmonella, Sarcina, Micrococcus*)
Treponema pallidum (syphilis)
Yersinia enterocolitica
Brucellosis (donors giving a history are not accepted in the UK)
Borrelia burgdorferi (Lyme disease)
Parasites
Plasmodium spp. (malaria)
Trypanosoma cruzi (Chagas disease) endemic in Latin America, this parasite is present in 75% of seropositive subjects; up to 22% of donors in Latin America may be seropositive
Toxoplasma gondii
Only a risk in granulocytes transfused to immunosuppressed seronegative recipients
Babesia microti (Nantucket fever)
Potential risk in certain areas of North America
Leishmania spp.

Viruses

Viral infections are the most common, so blood donations are tested for these infectious agents (Table 32.9). Hepatitis B (Fig. 32.10, *A*) was frequently transmitted. A typical course of an acute infection is illustrated in Fig. 32.10, *B*. The sequelae are cirrhosis and, in a minority of cases, hepatocellular carcinoma. A similar outcome can occur after hepatitis C infection (see Fig. 9.26). The risk that a donation is positive for human immunodeficiency virus (HIV) is now estimated to be 1 in 4.5 million, the risk that a donation is positive for hepatitis B is 1 in 450 000, and the risk that a donation is positive for hepatitis C is 1 in 20 million.

Prion Disease

Four definite cases of Creutzfeldt–Jakob disease (CJD) have been caused by blood transfusion. The donors have been traced and recipients informed and undergo surveillance. Also, if patients with CJD have received blood, the donors are traced. It is clear that the disease can be transmitted by infectious agents

TABLE 32.8. BLOOD TRANSFUSION: TRANSMISSIBLE VIRUSES; PRIONS ARE ALSO POTENTIALLY TRANSMISSIBLE

Plasma-borne viruses
Hepatitis B
Hepatitis A (rarely)
Hepatitis C
Hepatitis E
Parvovirus B19
HIV-1 and HIV-2
West Nile virus
Dengue
Cell-associated viruses
Cytomegalovirus (CMV)
Epstein–Barr virus (EBV) (more than 95% of adults are immune)
HTLV-1 (causes human T-cell leukemia and tropical spastic paraparesis)
HTLV-11 (clinical relevance not clear, may be more common than HTLV-1 in Western developed countries)
Prions
Transmissible by blood transfusion from asymptomatic donors

TABLE 32.9. BLOOD DONATIONS: MANDATORY TESTING FOR INFECTIOUS AGENTS IN ENGLAND

Hepatitis B	Surface antigen (on pools of 48 samples)
Anti-HCV	
Anti-HIV-1, anti-HIV-2	HIV-1 antigen (on pools of 48 samples)
Anti-HTLV	
Anti-CMV	
Anti-*Treponema pallidum*	
Anti-*Plasmodium falciparum*	
Anti-Chagas disease	

(e.g. in pituitary-derived growth hormone and gonadotropins). The cause of the disease is transmission of an abnormal form of a naturally occurring protein, prion (PrP). In prion disease, it is considered that a natural protein (PrP) is converted into an abnormal form (PrP scrapie or PrPSc). This has the ability to convert the normal protein, which has a multiple helical structure, into the abnormal variant in which much of the backbone is straightened out. The abnormal PrP arises by a random change in a normal protein, which probably accounts for sporadic CJD. In familial CJD, a point mutation occurs in the DNA coding for the protein. Thus, there is the potential for transmission of the disease to recipients of the blood if it is present in the blood of asymptomatic individuals. New variant CJD (nvCJD) is caused by the same prion as bovine spongiform encephalitis (BSE; Figs. 32.11–32.14). Non-UK plasma is now used for fractionation. Potential blood donors who have themselves received blood or blood product transfusion are excluded as donors.

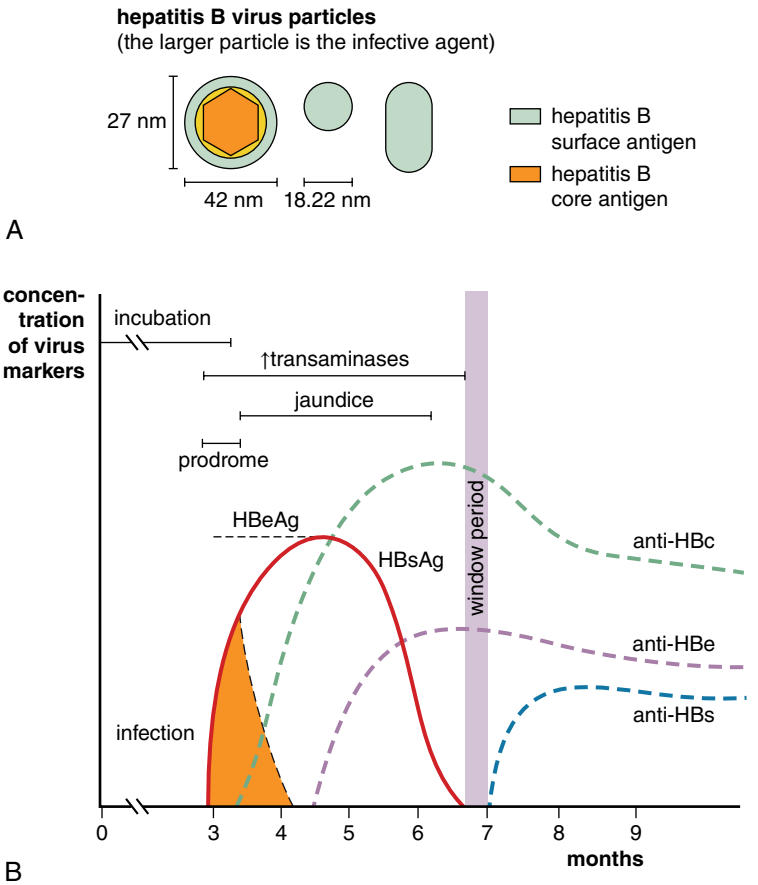

Fig. 32.10. Hepatitis B. **A,** Hepatitis B virus particles (the larger particle is the infective agent). **B,** Typical course of an acute infection with hepatitis B virus (HBV). (HbeAg, hepatitis Be antigen; HbsAg, hepatitis B surface antigen; HBc, hepatitis B core antigen.) (*A, B,* Courtesy of Professor M Contreras and the NHS Blood Transfusion Service.)

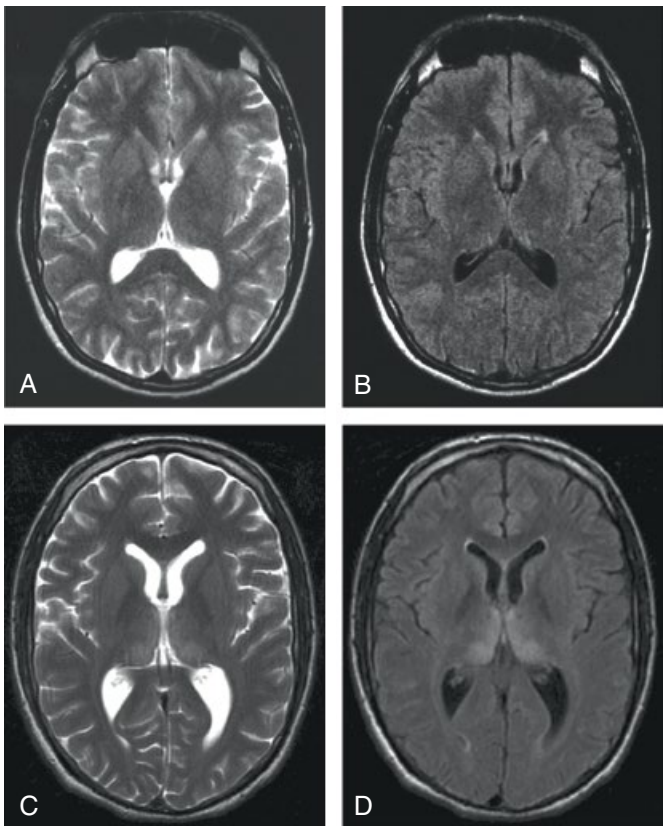

Fig. 32.11. New variant Creutzfeldt–Jakob disease (nvCJD). Magnetic resonance imaging (MRI) appearances late in the clinical course. **A, B,** Normal appearances on T_2 and FLAIR. **C, D,** Abnormal increased T_2 and FLAIR: High signal within the posteromedial thalamus 18 months later. (Source: Wroe SJ, et al. *Lancet* 2006;368: 2061–2067. Courtesy of Professor J Collinge. Reproduced with permission of Elsevier.)

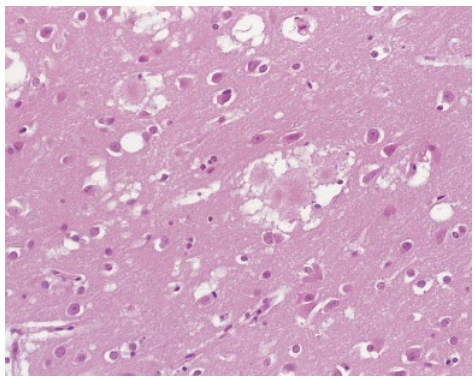

Fig. 32.12. New variant Creutzfeldt–Jakob disease (nvCJD). Frontal cortex from a 22-year-old man with nvCJD showing the characteristic florid plaques (center), which are composed of aggregates of the prion protein. (Courtesy of Dr. JW Ironside.)

IRON OVERLOAD

Iron overload can become a major clinical problem in multitransfused anemic patients. In such cases, iron chelation therapy is required (see Chapters 6 and 9).

TRANSFUSION-RELATED ACUTE LUNG INJURY

Transfusion-related acute lung injury (TRALI) is an acute respiratory distress syndrome, resembling adult respiratory distress syndrome, which occurs within 6 hours (rarely, 1–2 days). It is characterized by dyspnea and hypoxia, with transient pulmonary infiltrates on chest radiography (Fig. 32.15). Oxygen support is needed and mechanical ventilation is needed in more than 50% of patients. It is rare, occurring in about 1 in 5000 transfusions, and patients usually (greater than 90%) recover. The etiology is unclear; it results from a combination of different mechanisms, including reaction of the recipient's neutrophils with human leukocyte antigen (HLA) or neutrophil antibodies in donor plasma, which leads to increased permeability in the pulmonary circulation, or from cell membrane-derived lipids in the donor plasma priming the recipient's neutrophils. The donors are often multiparous women and, once identified as the cause of a reaction, should be removed from the donor panel. All UK fresh frozen plasma (FFP) is now prepared from male donors.

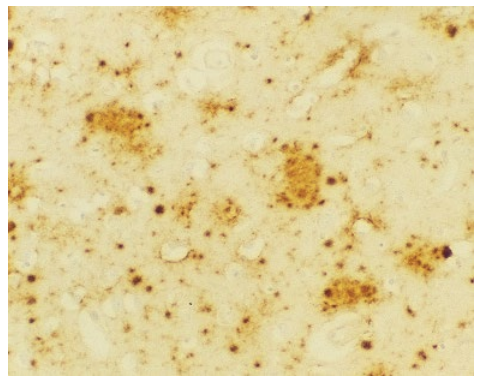

Fig. 32.13. New variant Creutzfeldt–Jakob disease (nvCJD). Immunocytochemistry for PrP in the occipital cortex in nvCJD shows strong staining of individual plaques, with diffuse PrP deposits around neurons and blood vessels (KG9 monoclonal antibody). (Courtesy of Dr. JW Ironside.)

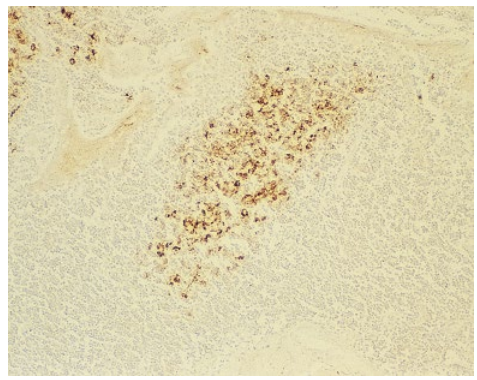

Fig. 32.14. New variant Creutzfeldt–Jakob disease (nvCJD). The tonsil in a 27-year-old woman with nvCJD shows positive staining for PrP within the germinal center in follicular dendritic cells (KG9 monoclonal antibody). (Courtesy of Dr. JW Ironside.)

GRAFT-VERSUS-HOST DISEASE

Transfusion of viable lymphocytes to a heavily immunosuppressed host can result in "grafting" of the lymphocytes, which proliferate in the host and cause a disease similar to graft-versus-host disease (GVHD) in stem cell transplant recipients. Transfusion GVHD is rare, is likely to be associated with marrow aplasia and pancytopenia, and is usually fatal. It is diagnosed by finding lymphocytes in the blood of the recipient that are of the HLA type of the donor, and it is prevented by irradiation of

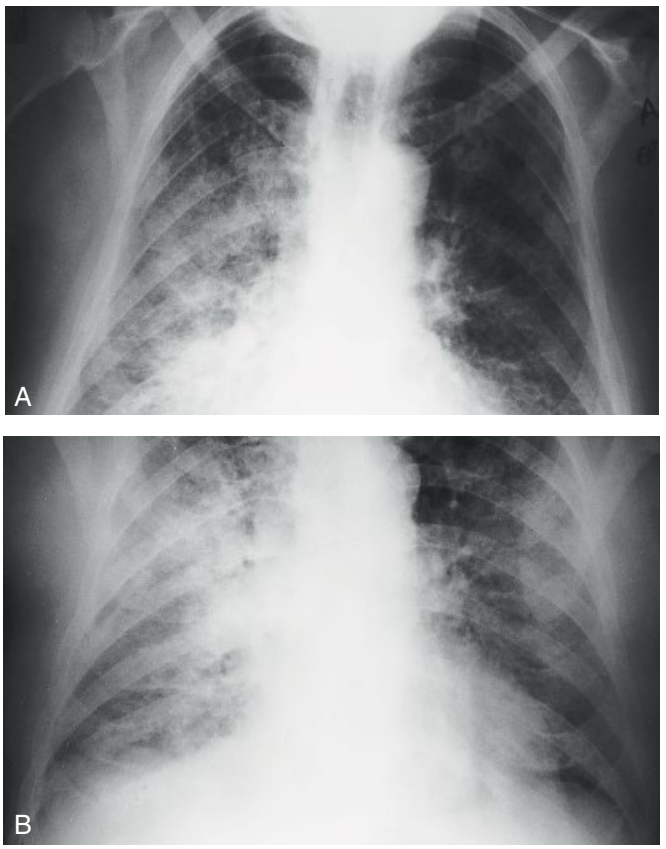

Fig. 32.15. Transfusion-related acute lung injury: Chest radiographs. **A,** 3 hours and **B,** 48 hours after onset of dyspnea in a 55-year-old man receiving chemotherapy for acute myeloid leukemia. The patient had received 1 unit of platelets 12 hours before the onset of symptoms, then 4 units of blood and a further unit of platelets 30 minutes before the onset. The patient was treated with high-dose corticosteroids and made a full recovery, with chest radiographs clear 7 days after onset of symptoms. (*A, B,* Courtesy of Dr. A Virchis.)

all blood products before transfusion into immunosuppressed patients (Table 32.10).

TABLE 32.10. INDICATIONS FOR IRRADIATED CELLULAR BLOOD COMPONENTS[a] IN HEMATO-ONCOLOGY PATIENTS

Patient group	Irradiated blood components
Adults or children with acute leukemia	Not required (except for HLA-matched platelets or donations from first or second degree relatives)
Recipients of allogeneic (donor) HSC transplantation	From the start of conditioning chemoradiotherapy, continue while receiving GVHD prophylaxis
	If chronic GVHD or on immunosuppressive treatment, continue irradiated blood components
Bone marrow and peripheral blood stem cell donors	Provide irradiated cellular components during and for 7 days before the harvest
Bone marrow or peripheral blood HSC harvesting for future autologous reinfusion	Provide irradiated cellular components during and for 7 days before the harvest
Autologous HSC transplant patients	From start of conditioning chemoradiotherapy until 3 months post-transplant (6 months if total body irradiation was used)
Adults and children with Hodgkin lymphoma at any stage of the disease	Irradiated cellular components indefinitely
Patients treated with purine analogs (fludarabine, cladribine, and deoxycoformicin)[b]	Irradiated cellular components indefinitely
Patients treated with alemtuzumab (anti-CD52)[c]	Irradiated cellular components indefinitely

[a] Red cells, platelets, and granulocytes.
[b] Irradiated components are recommended for newer purine analogs and related compounds, such as bendamustine, until further data are available.
[c] Irradiated components are also recommended for solid organ transplant patients receiving alemtuzumab. Patients who have received CAR-T-cell therapy for B-cell neoplasms should be added.
Source: Hoffbrand AV, et al. eds. *Postgraduate Haematology*, 7th edn. John Wiley and Sons, 2016. Reproduced with permission of John Wiley and Sons.

OTHER BLOOD COMPONENTS

The preparation of blood components from whole blood is illustrated in Fig. 32.16.

PLATELET CONCENTRATES

Platelet concentrates are prepared from whole blood donors (Fig. 32.17) or from a single donor apheresis (Fig. 32.18). They are required for patients with severe thrombocytopenia as a result of bone marrow failure (e.g. caused by acute leukemia, myelodysplasia, aplastic anemia, chemotherapy, or radiotherapy). The usual adult therapeutic dose (ATD) is $2.5–3.0 \times 10^{11}$/L platelets. They are used prophylactically because the platelet count is extremely low, less than 5×10^9/L, or likely to fall that low, or is $10–20 \times 10^9$/L and associated with infection; or before minor surgery (e.g. liver biopsy, insertion of indwelling catheter), or in patients with less severe degrees of thrombocytopenia (and established hemorrhage) to raise the platelet count to greater than 50×10^9/L. In some circumstances, the platelet count can be raised by the thrombopoietin receptor agonists, romiplostim and eltrombopag.

Patients with platelet functional defects require platelet support at higher platelet counts. Platelets express only HLA Class I antigens, whereas leukocytes express both HLA Class I and II antigens. Both are required to stimulate the reticuloendothelial system to make HLA antibodies. These antibodies can cause refractoriness to mixed-platelet pools. If this occurs, HLA-compatible platelets are needed, from a special tissue-typed panel of donors.

LEUKOCYTES

Leukocytes are not often used because of the difficulties in obtaining sufficient quantities, their short lifespan in vivo, the lack of data on a beneficial effect, and the danger of transmission of disease (e.g. cytomegalovirus [CMV]). Buffy coat preparations or cells harvested by leukapheresis from patients with chronic myeloid leukemia have a restricted place in therapy, particularly in severely neutropenic patients with local infections.

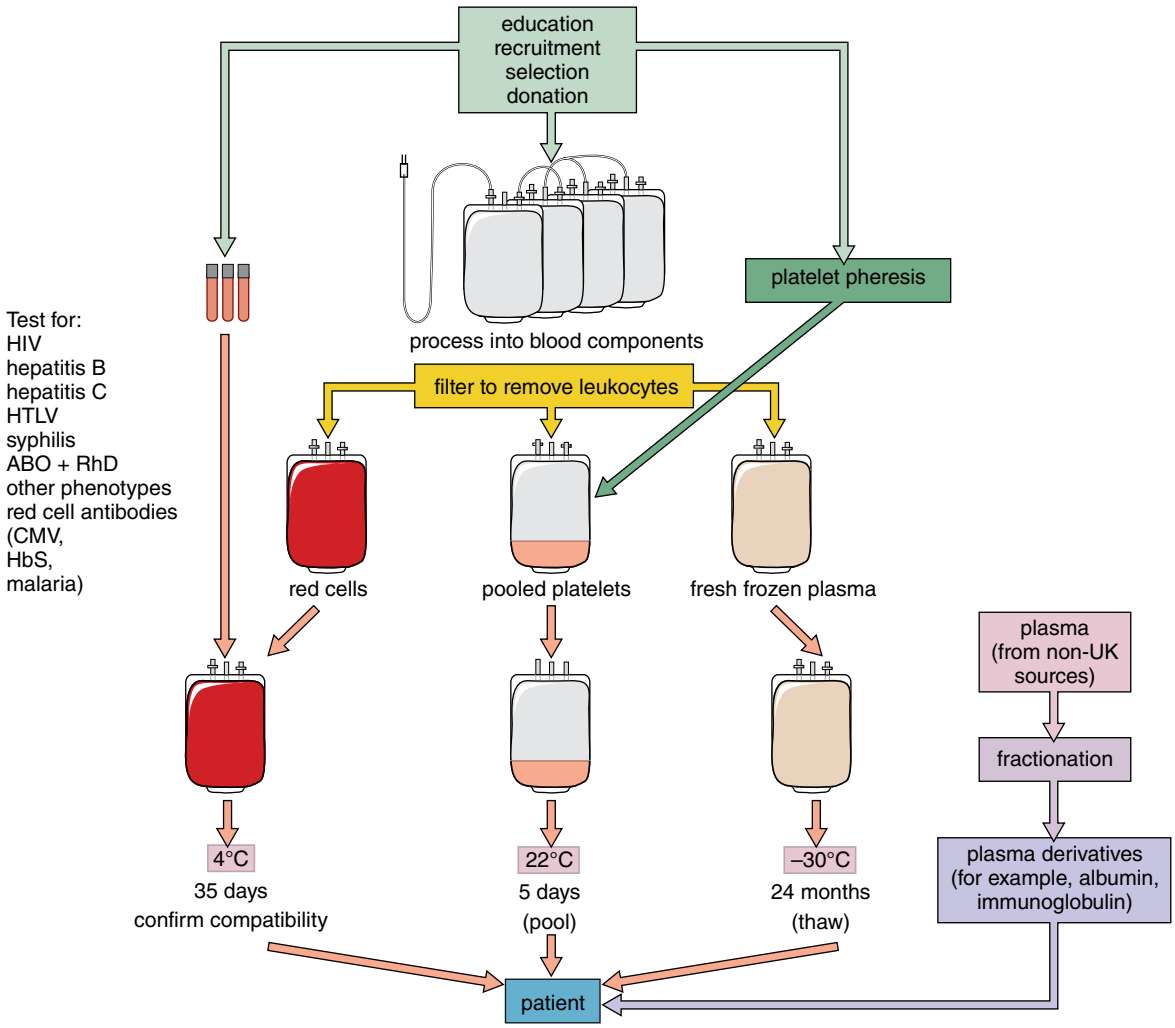

Fig. 32.16. Production of blood components and plasma derivatives: Preparation. (Source: Adapted from McClelland DBL, ed. *Handbook of Transfusion Medicine*, 4th edn, 2007, United Kingdom Blood Services. Reproduced with permission of Elsevier.)

Fig. 32.17. Platelet pool. This may be derived from four to six donors depending on the place of manufacture. When produced by the buffy coat method a pool of platelets contains more than 250×10^9/L platelets per pool.

FRESH FROZEN PLASMA

Fresh frozen plasma (FFP; Fig. 32.19) is provided in doses of 240–300 mL and in pediatric doses of 50 mL. It is used to replace clotting factors, for example, in patients after massive transfusion or cardiopulmonary bypass, in liver disease, or for plasma exchange in thrombotic thrombocytopenic purpura (see Chapter 27). The dose is 15–20 mL/kg body weight, monitored by coagulation factor assays. Prothrombin complex concentrates are now preferred over FFP to reverse a warfarin effect in a bleeding patient.

Cryoprecipitate (Fig. 32.20) is obtained by thawing FFP at 4°C, and is widely used as a replacement for fibrinogen if no concentrate is available.

PLASMA DERIVATIVES

Human albumin solution (4.5%) is used mainly to treat shock. Human albumin solution (20%) is used for patients with severe hypoalbuminemia (e.g. with liver disease or nephrotic syndrome).

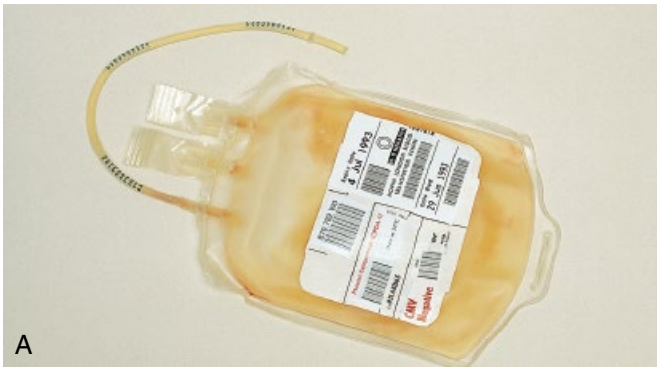

Fig. 32.18. A, Platelet concentrates from a single donor. These platelet concentrates are derived from a single blood donation and are approximately 50 mL in volume. The concentrate is derived from CPDA-1 plasma and contains platelets >55 × 10^9 and leukocytes <0.05 × 10^9 per unit. Platelets should be maintained at 22°C, and they have a shelf life of 5 days. **B,** Platelet concentrates can also be made by apheresis from a single donor. These platelet concentrates are approximately 215 mL in volume and contain about 290 × 10^9 platelets and 0.3 × 10^6 white cells per pack. In addition, they may be HLA-matched or cross-matched to be compatible with recipient serum in cases of refractory patients. (Courtesy of G Hazlehurst.)

Clotting factor concentrates (e.g. factor VIII or IX) and immunoglobulin concentrates can also be made from human plasma. Other concentrates include fibrinogen and prothrombin complex concentrated (which contain zymogen or activated IX, VII, and to a lesser extend X, XI, and thrombin) with or without factor X.

Fig. 32.19. Fresh frozen plasma (FFP). This is provided in 240–300 mL volumes including adult and pediatric doses. It can be supplied from volunteer plasmapheresis donors or recovered from routine blood donations. Illustrated here is a 240 mL FFP pack anticoagulated with CPDA-1. It should be stored at –30°C, and will then keep for up to 2 years. It should not be used as a plasma expander. Its use should be monitored with tests of coagulation when administered to correct a documented coagulation abnormality. (Courtesy of G Hazlehurst.)

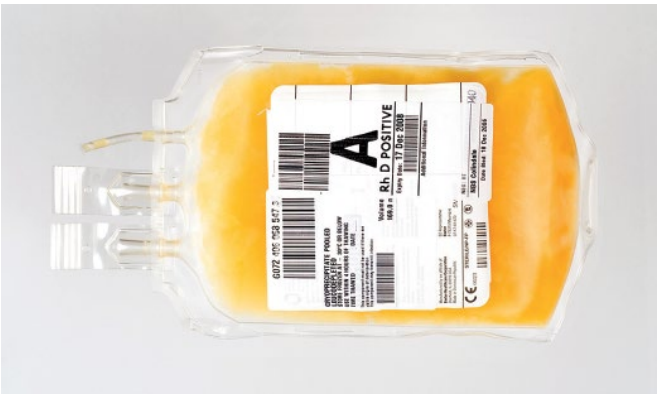

Fig. 32.20. Batched cryoprecipitate. Individual cryoprecipitates from different donors may be batched together in groups of six to represent an adult dose. Each unit contains approximately 20 mL and is derived from CPDA-1 plasma. It contains fibrinogen greater than 140 mg per unit and factor VIII greater than 70 IU per unit. It should be stored at -30°C and has a shelf life of 1 year. In general, group A donors have higher levels of factor VIII than group O donors. (Courtesy of G Hazlehurst.)

2016 WORLD HEALTH ORGANIZATION CLASSIFICATION OF LYMPHOID AND MYELOID NEOPLASMS

Swerdlow SH, et al. *Blood* 2016;127:2375–2390.
Arber DA, et al. *Blood* 2016;127:2391–2405.
Swerdlow SH, et al. eds. *WHO Classification of Tumours of Haematopoietic and Lymphoid Tissues*. International Agency for Research on Cancer, Lyon, 2017.

Myeloproliferative neoplasms	
Chronic myeloid leukemia, *BCR-ABL 1*-positive	9875/3
Chronic neutrophilic leukemia	9963/3
Polycythemia vera	9950/3
Primary myelofibrosis	9961/3
Essential thrombocythemia	9962/3
Chronic eosinophilic leukemia, NOS	9964/3
Myeloproliferative neoplasm, unclassifiable	9975/3
Mastocytosis	
Cutaneous mastocytosis	9740/1
Indolent systemic mastocytosis	9741/1
Systemic mastocytosis with an associated hematologic neoplasm	9741/3
Aggressive systemic mastocytosis	9741/3
Mast cell leukemia	9742/3
Mast cell sarcoma	9740/3
Myeloid/lymphoid neoplasms with eosinophilia and gene rearrangement	
Myeloid/lymphoid neoplasms with *PDGFRA* rearrangement	9965/3
Myeloid/lymphoid neoplasms with *PDGFRB* rearrangement	9966/3
Myeloid/lymphoid neoplasms with *FGFR1* rearrangement	9967/3
Myeloid/lymphoid neoplasms with PCM1-JAK2	9968/3[a]
Myelodysplastic/myeloproliferative neoplasms	
Chronic myelomonocytic leukemia	9945/3
Atypical chronic myeloid leukemia, *BCR-ABL1*-negative	9876/3
Juvenile myelomonocytic leukemia	9946/3
Myelodysplastic/myeloproliferative neoplasm with ring sideroblasts and thrombocytosis	9982/3
Myelodysplastic/myeloproliferative neoplasm, unclassifiable	9975/3
Myelodysplastic syndromes	
Myelodysplastic syndrome with single lineage dysplasia	9980/3
Myelodysplastic syndrome with ring sideroblasts and single lineage dysplasia	9982/3
Myelodysplastic syndrome with ring sideroblasts and multilineage dysplasia	9993/3[a]
Myelodysplastic syndrome with multilineage dysplasia	9985/3
Myelodysplastic syndrome with excess blasts	9983/3
Myelodysplastic syndrome with isolated del(5q)	9986/3
Myelodysplastic syndrome, unclassifiable	9989/3
Refractory cytopenia of childhood	9985/3
Myeloid neoplasms with germline predisposition	
Acute myeloid leukemia with germline *CEBPA* mutation	
Myeloid neoplasms with germline *DDX41* mutation	
Myeloid neoplasms with germline *RUNX1* mutation	
Myeloid neoplasms with germline *ANKRD26* mutation	
Myeloid neoplasms with germline *ETV6* mutation	
Myeloid neoplasms with germline *GATA2* mutation	
Acute myeloid leukemia (AML) and related precursor neoplasms	
AML with recurrent genetic abnormalities	
AML with t(8;21)(q22;q22.1); *RUNX1-RUNX1T1*	9896/3
AML with inv(16)(p13.1q22) or t(16;16)(p13.1;q22); *CBFB-MYH11*	9871/3
Acute promyelocytic leukemia with *PML-RARA*	9866/3
AML with t(9;11)(p21.3;q23.3); *KMT2A-MLLT3*	9897/3
AML with t(6;9)(p23;q34.1); *DEK-NUP214*	9865/3
AML with inv(3)(q21.3q26.2) or t(3;3)(q21.3;q26.2); *GATA2, MECOM*	9869/3
AML (megakaryoblastic) with t(1;22)(p13.3;q13.1); *RBM15-MKL1*	9911/3
AML with BCR-ABL1	9912/3[a]
AML with mutated *NPM1*	9877/3[a]

Color Atlas of Clinical Hematology: Molecular and Cellular Basis of Disease, Fifth Edition. A. Victor Hoffbrand, Paresh Vyas, Elías Campo, Torsten Haferlach, and Keith Gomez

AML with biallelic mutation of *CEBPA*	9878/3[a]
AML with mutated RUNX1	9879/3[a]
AML with myelodysplasia-related changes	9895/3
Therapy-related myeloid neoplasms	9920/3
Acute myeloid leukemia, NOS	9861/3
AML with minimal differentiation	9872/3
AML without maturation	9873/3
AML with maturation	9874/3
Acute myelomonocytic leukemia	9867/3
Acute monoblastic and monocytic leukemia	9891/3
Pure erythroid leukemia	9840/3
Acute megakaryoblastic leukemia	9910/3
Acute basophilic leukemia	9870/3
Acute panmyelosis with myelofibrosis	9931/3
Myeloid sarcoma	9930/3
Myeloid proliferations associated with Down syndrome	
Transient abnormal myelopoiesis associated with Down syndrome	9898/1
Myeloid leukemia associated with Down syndrome	9898/3
Blastic plasmacytoid dendritic cell neoplasm	9727/3
Acute leukemias of ambiguous lineage	
Acute undifferentiated leukemia	9801/3
Mixed-phenotype acute leukemia with t(9;22) (q34.1;q11.2); *BCR-ABL1*	9806/3
Mixed-phenotype acute leukemia with t(v; 11q23.3); *KMT2A*-rearranged	9807/3
Mixed-phenotype acute leukemia, B/myeloid, NOS	9808/3
Mixed-phenotype acute leukemia, T/myeloid, NOS	9809/3
Mixed-phenotype acute leukemia, NOS, rare types	
Acute leukemias of ambiguous lineage, NOS	
Precursor lymphoid neoplasms	
B-lymphoblastic leukemia/lymphoma, NOS	9811/3
B-lymphoblastic leukemia/lymphoma with t(9;22) (q34.1;q11.2); *BCR-ABL 1*	9812/3
B-lymphoblastic leukemia/lymphoma with t(v;11q23.3); *KMT2A*-rearranged	9813/3
B-lymphoblastic leukemia/lymphoma with t(12;21) (p13.2;q22.1); *ETV6-RUNX1*	9814/3
B-lymphoblastic leukemia/lymphoma with hyperdiploidy	9815/3
B-lymphoblastic leukemia/lymphoma with hypodiploidy (hypodiploid ALL)	9816/3
B-lymphoblastic leukemia/lymphoma with t(5;14) (q31.1;q32.1); IGH/IL-3	9817/3
B-lymphoblastic leukemia/lymphoma with t(1;19) (q23;p13.3); *TCF3-PBX1*	9818/3
B-lymphoblastic leukemia/lymphoma, *BCR-ABL 1*-like	9819/3[a]
B-lymphoblastic leukemia/lymphoma with *IAMP21*	9811/3
T-lymphoblastic leukemia/lymphoma	9837/3
Early T-cell precursor lymphoblastic leukemia	9837/3
NK-lymphoblastic leukemia/lymphoma	
Mature B-cell neoplasms	
Chronic lymphocytic leukemia (CLL)/small lymphocytic lymphoma	9823/3
Monoclonal B-cell lymphocytosis, CLL-type	9823/1[a]
Monoclonal B-cell lymphocytosis, non-CLL-type	9591/1[a]
B-cell prolymphocytic leukemia	9833/3
Splenic marginal zone lymphoma	9689/3
Hairy cell leukemia	9940/3
Splenic B-cell lymphoma/leukemia, unclassifiable	9591/3
Splenic diffuse red pulp small B-cell lymphoma	9591/3
Hairy cell leukemia variant	9591/3
Lymphoplasmacytic lymphoma	9671/3
Waldenström macroglobulinemia	9761/3
IgM monoclonal gammopathy of undetermined significance	9761/1[a]
Heavy chain diseases	
μ Heavy chain disease	9762/3
γ Heavy chain disease	9762/3
α Heavy chain disease	9762/3
Plasma cell neoplasms	
Non-IgM monoclonal gammopathy of undetermined significance	9765/1
Plasma cell myeloma	9732/3
Solitary plasmacytoma of bone	9731/3
Extraosseous plasmacytoma	9734/3
Monoclonal immunoglobulin deposition diseases	
Primary amyloidosis	9769/1
Light chain and heavy chain deposition diseases	9769/1
Extranodal marginal zone lymphoma of mucosa-associated lymphoid tissue (MALT lymphoma)	9699/3
Nodal marginal zone lymphoma	9699/3
Pediatric nodal marginal zone lymphoma	9699/3
Follicular lymphoma	9690/3
In situ follicular neoplasia	9695/1[a]
Duodenal-type follicular lymphoma	9695/3
Testicular follicular lymphoma	9690/3
Pediatric-type follicular lymphoma	9690/3
Large B-cell lymphoma with IRF4 rearrangement	9698/3
Primary cutaneous follicle center lymphoma	9597/3
Mantle cell lymphoma	9673/3
In situ mantle cell neoplasia	9673/1[a]
Diffuse large B-cell lymphoma (DLBCL), NOS	9680/3
Germinal centre B-cell subtype	9680/3
Activated B-cell subtype	9680/3
T-cell/histiocyte-rich large B-cell lymphoma	9688/3
Primary DLBCL of the CNS	9680/3
Primary cutaneous DLBCL, leg type	9680/3
EBV-positive DLBCL, NOS	9680/3
EBV-positive mucocutaneous ulcer	9680/1[a]
DLBCL associated with chronic inflammation	9680/3
Fibrin-associated diffuse large B-cell lymphoma	
Lymphomatoid granulomatosis, grade 1, 2	9766/1
Lymphomatoid granulomatosis, grade 3	9766/3[a]
Primary mediastinal (thymic) large B-cell lymphoma	9679/3
Intravascular large B-cell lymphoma	9712/3
ALK-positive large B-cell lymphoma	9737/3
Plasmablastic lymphoma	9735/3
Primary effusion lymphoma	9678/3
Multicentric Castleman disease	

HHV8-positive DLBCL, NOS	9738/3
HHV8-positive germinotropic lymphoproliferative disorder	9738/1[a]
Burkitt lymphoma	9687/3
Burkitt-like lymphoma with 11q aberration	9687/3[a]
High-grade B-cell lymphoma	
High-grade B-cell lymphoma with *MYC* and *BCL2* and/or *BCL6* rearrangements	9680/3
High-grade B-cell lymphoma, NOS	9680/3
B-cell lymphoma, unclassifiable, with features intermediate between DLBCL and classic Hodgkin lymphoma	9596/3
Mature T- and NK-cell neoplasms	
T-cell prolymphocytic leukemia	9834/3
T-cell large granular lymphocytic leukemia	9831/3
Chronic lymphoproliferative disorder of NK cells	9831/3
Aggressive NK-cell leukemia	9948/3
Systemic EBV-positive T-cell lymphoma of childhood	9724/3
Chronic active EBV infection of T- and NK-cell type, systemic form	
Hydroa vacciniforme-like lymphoproliferative disorder	9725/1[a]
Severe mosquito bite allergy	
Adult T-cell leukemia/lymphoma	9827/3
Extranodal NK/T-cell lymphoma, nasal type	9719/3
Enteropathy-associated T-cell lymphoma	9717/3
Monomorphic epitheliotropic intestinal	
Hydroa vacciniforme T-cell lymphoma	9717/3
Intestinal T-cell lymphoma, NOS	9717/3
Indolent T-cell lymphoproliferative disorder of the gastrointestinal tract	9702/1[a]
Hepatosplenic T-cell lymphoma	9716/3
Subcutaneous panniculitis-like T-cell lymphoma	9708/3
Mycosis fungoides	9700/3
Sézary syndrome	9701/3
Primary cutaneous CD30-positive T-cell lymphoproliferative disorders	
Hydroa vacciniforme lymphomatoid papulosis	9718/1[a]
Hydroa vacciniforme primary cutaneous anaplastic large cell lymphoma	9718/3
Primary cutaneous γδT-cell lymphoma	9726/3
Primary cutaneous CD8-positive aggressive epidermotropic cytotoxic T-cell lymphoma	9709/3
Primary cutaneous acral CD8-positive T-cell lymphoma	9709/3[a]
Primary cutaneous CD4-positive small/medium T-cell lymphoproliferative disorder	9709/1
Peripheral T-cell lymphoma, NOS	9702/3
Angioimmunoblastic T-cell lymphoma	9705/3
Follicular T-cell lymphoma	9702/3
Nodal peripheral T-cell lymphoma with T-follicular helper phenotype	9702/3
Anaplastic large cell lymphoma, ALK-positive	9714/3
Anaplastic large cell lymphoma, ALK-negative	9715/3[a]
Breast implant-associated anaplastic large cell lymphoma	9715/3[a]
Hodgkin lymphomas	
Nodular lymphocyte predominant Hodgkin lymphoma	9659/3
Classic Hodgkin lymphoma	9650/3
Nodular sclerosis classic Hodgkin lymphoma	9663/3
Lymphocyte-rich classic Hodgkin lymphoma	9651/3
Mixed cellularity classic Hodgkin lymphoma	9652/3
Lymphocyte-depleted classic Hodgkin lymphoma	9653/3
Immunodeficiency-associated lymphoproliferative disorders	
Post-transplant lymphoproliferative disorders (PTLD)	
Nondestructive PTLD	
Plasmacytic hyperplasia PTLD	
Infectious mononucleosis PTLD	
Florid follicular hyperplasia	
Polymorphic PTLD	9971/1
Monomorphic PTLD	[b]
Classic Hodgkin lymphoma PTLD	9650/3
Other iatrogenic immunodeficiency-associated lymphoproliferative disorders	
Histiocytic and dendritic cell neoplasms	
Histiocytic sarcoma	9755/3
Langerhans cell histiocytosis, NOS	9751/1
Langerhans cell histiocytosis, monostotic	9751/1
Langerhans cell histiocytosis, polystotic	9751/1
Langerhans cell histiocytosis, disseminated	9751/3
Langerhans cell sarcoma	9756/3
Indeterminate dendritic cell tumor	9757/3
Interdigitating dendritic cell sarcoma	9757/3
Follicular dendritic cell sarcoma	9758/3
Fibroblastic reticular cell tumor	9759/3
Disseminated juvenile xanthogranuloma	
Erdheim–Chester disease	9749/3

The morphology codes are from the International Classification of Diseases for Oncology (ICD-O). Behaviour is coded /0 for benign tumors; /1 for unspecified, borderline, or uncertain behavior; /2 for carcinoma in situ and grade III intraepithelial neoplasia; and /3 for malignant tumors. The classification is modified from the previous WHO classification, taking into account changes in our understanding of these lesions.

[a] These new codes were approved by the IARC/WHO Committee for ICD-O.

[b] These lesions are classified according to the lymphoma to which they correspond, and are assigned the respective ICD-O code.

Italics: Provisional tumor entities.

INDEX

Page locators in **bold** indicate tables; page locators in *italics* indicate figures.
Index uses letter-by-letter alphabetization.

Color Atlas of Clinical Hematology: Molecular and Cellular Basis of Disease, Fifth Edition. A. Victor Hoffbrand, Paresh Vyas, Elías Campo, Torsten Haferlach, and Keith Gomez